

N O T I C E

THIS DOCUMENT HAS BEEN REPRODUCED FROM
MICROFICHE. ALTHOUGH IT IS RECOGNIZED THAT
CERTAIN PORTIONS ARE ILLEGIBLE, IT IS BEING RELEASED
IN THE INTEREST OF MAKING AVAILABLE AS MUCH
INFORMATION AS POSSIBLE

JI
NASA Technical Memorandum 82661

Bibliography of Lewis Research Center Technical Publications Announced in 1980

(NASA-TM-82661) BIBLIOGRAPHY OF LEWIS
RESEARCH CENTER TECHNICAL PUBLICATIONS
ANNOUNCED IN 1980 (NASA) 373 P
HC A16/MF A01

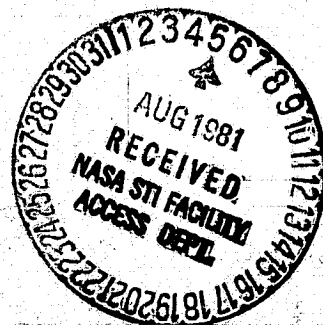
N81-29026

CSCL 05B

Unclas
G3/82 26960

May 1981

NASA



PREFACE

In 1980, Lewis' 1020 research authors published 427 technical publications which were announced to and reached the worldwide scientific community. This number was our typical output even though, once again, we had a slight decrease in staff. In recent years, the trend in Lewis publishing has been that each year the number of technical presentations given at seminars, society symposia, and Lewis-hosted conferences has surpassed the record set the previous year. Lewis authors publish approximately 61 percent of their research contributions in outside publications and the rest as NASA research reports. Lewis authors primarily use society proceedings, seminar presentations, and journal and transactions articles to describe their work.

In 1980 the production of 307 contractor-authored research reports was higher than the previous year's output of 294. In addition, 38 patent applications were filed, and 17 patents were issued, fewer numbers than in recent years.

In 1980, the annual award for Best Lewis Publication was presented to J. Anthony Powell, Anthony J. Strazisar, and Richard G. Seasholtz for their paper "Efficient Laser Anemometer for Intra-Rotor Flow Mapping in Turbomachinery," which describes several innovative features of this anemometer. The paper was presented at the Joint Fluids Engineering Gas Turbine Conference and Products Show, New Orleans, Louisiana, March 10-13, 1980. A description is given in abstract A80-36140 (p. 111) in this bibliography.

Also in 1980, the American Society of Lubrication Engineers presented the "Captain Alfred E. Hunt Memorial Award" for the best paper appearing in one of its publications to L. D. Wedeven. This paper, coauthored with Professor Cristino Cusano, a summer faculty fellow from the University of Illinois, entitled "Elastohydrodynamic Film Thickness Measurements of Artificially Produced Nonsmooth Surfaces," is described in abstract A80-14720 (p. 102).

All the publications in this collection were announced in the 1980 issues of STAR (Scientific and Technical Aerospace Reports) and IAA (International Aerospace Abstracts).

The arrangement of the material is by NASA subject category, as noted in the Contents. The Lewis-authored items are listed first, followed by the contractor items. Within each of these groups is listed report literature, in N-number sequence, followed by the journal and conference presentations, in A-number sequence.

The various indexes will help locate specific publications by subject, author, contractor organization, contract number, and report number.

George Mandel
Chief, Management Services Division

CONTENTS

	Page
AERONAUTICS (GENERAL)	1
AERODYNAMICS	2
AIR TRANSPORTATION AND SAFETY	8
AIRCRAFT COMMUNICATIONS AND NAVIGATION	9
AIRCRAFT DESIGN, TESTING AND PERFORMANCE	10
AIRCRAFT INSTRUMENTATION	11
AIRCRAFT PROPULSION AND POWER	12
AIRCRAFT STABILITY AND CONTROL	46
RESEARCH AND SUPPORT FACILITIES (AIR)	47
ASTRONAUTICS (GENERAL)	48
GROUND SUPPORT SYSTEMS AND FACILITIES (SPACE)	49
LAUNCH VEHICLES AND SPACE VEHICLES	50
SPACE TRANSPORTATION	51
SPACECRAFT COMMUNICATIONS, COMMAND AND TRACKING	52
SPACECRAFT DESIGN, TESTING AND PERFORMANCE	53
SPACECRAFT PROPULSION AND POWER	56
CHEMISTRY AND MATERIALS (GENERAL)	66
COMPOSITE MATERIALS	67
INORGANIC AND PHYSICAL CHEMISTRY	74
METALLIC MATERIALS	76
NONMETALLIC MATERIALS	85
PROPELLANTS AND FUELS	93
ENGINEERING (GENERAL)	96
COMMUNICATIONS	97
ELECTRONICS AND ELECTRICAL ENGINEERING	101
FLUID MECHANICS AND HEAT TRANSFER	104
INSTRUMENTATION AND PHOTOGRAPHY	110
LASERS AND MASERS	113
MECHANICAL ENGINEERING	114
QUALITY ASSURANCE AND RELIABILITY	130
STRUCTURAL MECHANICS	132
GEOSCIENCES (GENERAL)	135
EARTH RESOURCES	136
ENERGY PRODUCTION AND CONVERSION	137
ENVIRONMENT POLLUTION	157
METEOROLOGY AND CLIMATOLOGY	159
LIFE SCIENCES (GENERAL)	160
AEROSPACE MEDICINE	161
COMPUTER OPERATIONS AND HARDWARE	162
COMPUTER PROGRAMMING AND SOFTWARE	163
STATISTICS AND PROBABILITY	164
SYSTEMS ANALYSIS	165
THEORETICAL MATHEMATICS	166
ACOUSTICS	167
ATOMIC AND MOLECULAR PHYSICS	174

	Page
PLASMA PHYSICS	175
SOLID-STATE PHYSICS	178
THERMODYNAMICS AND STATISTICAL PHYSICS	180
ADMINISTRATION AND MANAGEMENT	181
ECONOMICS AND COST ANALYSIS	182
URBAN TECHNOLOGY AND TRANSPORTATION	183
SUBJECT INDEX (KEYWORDS)	A-1
PERSONAL AUTHOR INDEX (INCLUDES LEWIS AND CONTRACTOR AUTHORS)	B-1
CORPORATE SOURCE INDEX (CONTRACTOR ORGANIZATIONS)	C-1
CONTRACT NUMBER INDEX	D-1
REPORT/ACCESSION NUMBER INDEX (INCLUDES PATENTS)	E-1

01 AERONAUTICS (GENERAL)

N80-21271* National Aeronautics and Space Administration.
Lewis Research Center, Cleveland, Ohio.

COMPUTERIZED SYSTEMS ANALYSIS AND OPTIMIZATION OF AIRCRAFT ENGINE PERFORMANCE, WEIGHT, AND LIFE CYCLE COSTS

c07

Laurence H. Fishbach / In AGARD The Use of Computers as a Design Tool Jan. 1980 15 p refs (For primary document see N80-21243 12-01)

Avail: NTIS HC A19/MF A01 CSCL 21E

The computational techniques are described which are utilized at Lewis Research Center to determine the optimum propulsion systems for future aircraft applications and to identify system tradeoffs and technology requirements. Cycle performance, and engine weight can be calculated along with costs and installation effects as opposed to fuel consumption alone. Almost any conceivable turbine engine cycle can be studied. These computer codes are: NNEP, WATE, LIFCYC, INSTAL, and POD DRG. Examples are given to illustrate how these computer techniques can be applied to analyze and optimize propulsion system fuel consumption, weight and cost for representative types of aircraft and missions.

F.O.S.

02 AERODYNAMICS

Includes aerodynamics of bodies, combinations, wings, rotors, and control surfaces; and internal flow in ducts and turbomachinery.

For related information see also 34 *Fluid Mechanics and Heat Transfer*.

N80-10128* National Aeronautics and Space Administration, Lewis Research Center, Cleveland, Ohio.

COANNULAR SUPERSONIC EJECTOR NOZZLES

Allan R Bishop In NASA Ames Res. Center Workshop on Thrust Augmenting Ejectors Sep. 1979 p 385-396 refs (For primary document see N80-10107 01-02)

Avail: NTIS HC A22/MF A01 CSCL 01A

The nozzles described exhibit a flow field which is supersonic except for the initial flow region, and the secondary mass flow is typically about five percent of the primary core flow. The features to improve the accuracy of the performance calculations are discussed. A special calculation is made to get as realistic a sonic line as possible for this geometry, using an analysis developed by Brown. The mixing between the secondary and core flows is treated to account for entrainment of the secondary flow into core. Both of these phenomena directly affect the pressure distribution on the shroud and therefore, the thrust that the nozzle produces. The importance of using a realistic sonic line and a mixing analysis is stressed. M.M.M.

N80-11037* National Aeronautics and Space Administration, Lewis Research Center, Cleveland, Ohio.

EXPERIMENTAL STUDY OF LOW ASPECT RATIO COMPRESSOR BLADING

Lonnie Reid and Royce D. Moore 1979 19 p refs Proposed for presentation at the 25th Ann. Intern. Gas Turbine Conf., New Orleans, La., 9-13 Mar. 1980; sponsored by Am. Soc. of Mech. Engrs.

(NASA-TM-79280; E-217) Avail: NTIS HC A02/MF A01 CSCL 01A

The effects of low aspect ratio blading on aerodynamic performance were examined. Four individual transonic compressor stages, representative of the inlet stage of an advanced high pressure ratio core compressor, are discussed. The flow phenomena for the four stages are investigated. Comparisons of blade element parameters are presented for the two different aspect ratio configurations. Blade loading levels are compared for the near stall conditions and comparisons are made of loss and diffusion factors over the operating range of incidence angles. A.W.H.

N80-14050* National Aeronautics and Space Administration, Lewis Research Center, Cleveland, Ohio.

LASER ANEMOMETER MEASUREMENTS IN A TRANSONIC AXIAL FLOW COMPRESSOR ROTOR

Anthony J. Strazisar and J. Anthony Powell 1979 17 p refs Presented at 25th Ann. Intern. Gas Turbine Conf. and 22d Ann. Fluids Engr. Conf., New Orleans, 9-13 Mar. 1970; sponsored by ASME

(NASA-TM-79323; E-279) Avail: NTIS HC A02/MF A01 CSCL 01A

A laser anemometer system employing an efficient data acquisition technique was used to make measurements upstream, within, and downstream of the compressor rotor. A fluorescent dye technique allowed measurements within endwall boundary layers. Adjustable laser beam orientation minimized shadowed regions and enabled radial velocity measurements outside of the blade row. The flow phenomena investigated include flow variations from passage to passage, the rotor shock system, three-dimensional flows in the blade wake, and the development of the outer endwall boundary layer. Laser anemometer measurements are compared to a numerical solution of the streamfunction equations and to measurements made with conventional instrumentation. Author

N80-14051* National Aeronautics and Space Administration, Lewis Research Center, Cleveland, Ohio.

MODIFICATION OF AXIAL COMPRESSOR STREAMLINE PROGRAM FOR ANALYSIS OF ENGINE TEST DATA

Jeffrey G. Williams Nov. 1979 49 p refs

(NASA-TM-79312; E-268) Avail: NTIS HC A03/MF A01 CSCL 01A

An existing axial compressor streamline analysis computer program to allow input of measured radial pressure and temperature profiles obtained from engine or cascade data is described. The proposed modifications increase the input flexibility and are accomplished without changing the computer program's input format. A.R.H.

N80-15051* National Aeronautics and Space Administration, Lewis Research Center, Cleveland, Ohio.

SUMMARY OF ADVANCED METHODS FOR PREDICTING HIGH SPEED PROPELLER PERFORMANCE

L. A. Bober 1980 14 p refs Presented at 18th Aerospace Sci. Meeting, Pasadena, Calif., 14-16 Jan. 1980; sponsored by AIAA

(NASA-TM-81409) Avail: NTIS HC A02/MF A01 CSCL 01A

Three advanced analyses for predicting aircraft propeller performance at high subsonic speeds are described. Two of these analyses use a lifting line representation for the propeller blades and vortex filaments for the blade wakes but differ in the details of the solution. The third analysis is a finite difference solution of the unsteady, three dimensional Euler equations for the flow between adjacent blades. Analysis results are compared to data for a high speed propeller having eight swept blades integrally designed with the spinner and nacelle. Author

N80-17030* National Aeronautics and Space Administration, Lewis Research Center, Cleveland, Ohio.

PREDICTION METHOD FOR TWO-DIMENSIONAL AERODYNAMIC LOSSES OF COOLED VANES USING INTEGRAL BOUNDARY-LAYER PARAMETERS

Louis J. Goldman and Raymond E. Augler Feb. 1980 43 p refs

(NASA-TP-1623; E-076) Avail: NTIS HC A03/MF A01 CSCL 01A

A generalized analysis to predict the two-dimensional aerodynamic losses of film-cooled vanes by using integral boundary-layer parameters is presented. Heat-transfer and trailing-edge injection effects are included in the method. An approximate solution of the generalized equations is also included to show more clearly the effect of the different boundary-layer and cooling parameters on the losses. The analytical predictions agree well with the experimental results, indicating that available boundary-layer calculations for cooled vanes are of sufficient accuracy to use in the prediction method. Author

N80-21285* National Aeronautics and Space Administration, Lewis Research Center, Cleveland, Ohio.

HIGH SPEED TURBOPROPS FOR EXECUTIVE AIRCRAFT, POTENTIAL AND RECENT TEST RESULTS

Daniel C. Mikkelsen and Glenn A. Mitchell 1980 26 p refs Presented for the Turbine-Powered Executive Meeting, (Phoenix), 9-11 Apr. 1980, sponsored by the Soc. of Automotive Engrs.

(NASA-TM-81482; E-419) Avail: NTIS HC A03/MF A01 CSCL 01A

Four high speed propeller models were designed and tested in an 8x6 foot wind tunnel in order to evaluate the potential of advanced propeller technology. Results from these tests show that the combination of: increased blade number, aerodynamically integrated propeller/nacelles, reduced blade thickness, spinner area ruling, and blade sweep are important in achieving high propeller efficiency at the high cruise speeds. R.E.S.

N80-27284* National Aeronautics and Space Administration, Lewis Research Center, Cleveland, Ohio.

CAS2D: FORTRAN PROGRAM FOR NONROTATING BLADE-TO-BLADE, STEADY, POTENTIAL TRANSONIC CASCADE FLOWS

Djordje S. Dulikravich Jul. 1980 36 p refs
(NASA-TP-1705; E-253) Avail: NTIS HC A03/MF A01 CSCL 01A

An exact, full-potential-equation (FPE) model for the steady, irrotational, homentropic and homoenergetic flow of a compressible, homocompositional, inviscid fluid through two dimensional planar cascades of airfoils was derived, together with its appropriate boundary conditions. A computer program, CAS2D, was developed that numerically solves an artificially time-dependent form of the actual FPE. The governing equation was discretized by using type-dependent, rotated finite differencing and the finite area technique. The flow field was discretized by providing a boundary-fitted, nonuniform computational mesh. The mesh was generated by using a sequence of conforming mapping, nonorthogonal coordinate stretching, and local, isoparametric, bilinear mapping functions. The discretized form of the FPE was solved iteratively by using successive line overrelaxation. The possible isentropic shocks were correctly captured by adding explicitly an artificial viscosity in a conservative form. In addition, a three-level consecutive, mesh refinement feature makes CAS2D a reliable and fast algorithm for the analysis of transonic, two dimensional cascade flows.

Author

N80-27286* National Aeronautics and Space Administration, Lewis Research Center, Cleveland, Ohio.

AN ALTERNATIVE APPROACH TO THE NUMERICAL SIMULATION OF STEADY INVISCID FLOW

Gary M. Johnson Jun. 1980 8 p refs Presented at 7th Intern. Conf. on Numerical Methods in Fluid Dyn., Stanford, Calif., 23-27 Jun. 1980; sponsored by NACA, AFOSR, NSF, and ONR (NASA-TM-81542) Avail: NTIS HC A02/MF A01

A numerical procedure for the efficient simulation of steady inviscid flow is described and its utility demonstrated. Application of the surrogate equation technique allows the formulation of stable, fully conservative, type dependent finite difference equations for use in obtaining numerical solutions to systems of first order partial differential equations, such as the steady state Euler equations or their various approximations. Computational results are presented for the full Euler equations and for the transonic disturbance equations. For the latter case, a computational efficiency greater than that obtained by means of the standard perturbation potential approach is indicated.

E.D.K.

N80-33357* National Aeronautics and Space Administration, Lewis Research Center, Cleveland, Ohio.

WIND: COMPUTER PROGRAM FOR CALCULATION OF THREE DIMENSIONAL POTENTIAL COMPRESSIBLE FLOW ABOUT WIND TURBINE ROTOR BLADES

Djordje S. Dulikravich Oct. 1980 20 p refs
(NASA-TP-1729; E-474) Avail: NTIS HC A02/MF A01 CSCL 01A

A computer program is presented which numerically solves an exact, full potential equation (FPE) for three dimensional, steady, inviscid flow through an isolated wind turbine rotor. The program automatically generates a three dimensional, boundary conforming grid and iteratively solves the FPE while fully accounting for both the rotating cascade and Coriolis effects. The numerical techniques incorporated involve rotated, type dependent finite differencing, a finite volume method, artificial viscosity in conservative form, and a successive line overrelaxation combined with the sequential grid refinement procedure to accelerate the iterative convergence rate. Consequently, the WIND program is capable of accurately analyzing incompressible and compressible flows, including those that are locally transonic and terminated by weak shocks. The program can also be used to analyze the flow around isolated aircraft propellers and helicopter rotors in hover as long as the total relative Mach number of the oncoming flow is subsonic.

A.R.H.

A80-20966 * Summary of advanced methods for predicting high speed propeller performance. L. J. Bober and G. A. Mitchell (NASA, Lewis Research Center, Cleveland, Ohio). *American Institute of Aeronautics and Astronautics, Aerospace Sciences Meeting, 18th, Pasadena, Calif., Jan. 14-16, 1980, Paper 80-0225*, 12 p. 10 refs.

Three advanced analyses for predicting aircraft propeller performance at high subsonic speeds are described. Two of these analyses use a lifting line representation for the propeller blades and vortex filaments for the blade wakes but differ in the details of the solution. The third analysis is a finite difference solution of the unsteady, three-dimensional Euler equations for the flow between adjacent blades. Analysis results are compared to data for a high speed propeller having 8 swept blades integrally designed with the spinner and nacelle. These analyses provide tools for the propeller designer ranging from a short running program for initial design studies to a very long running program for checking final configurations.

(Author)

A80-20967 * Computation of three-dimensional flow in turbofan mixers and comparison with experimental data. L. A. Povinelli, B. H. Anderson, and W. Gerstenmaier (NASA, Lewis Research Center, Cleveland, Ohio). *American Institute of Aeronautics and Astronautics, Aerospace Sciences Meeting, 18th, Pasadena, Calif., Jan. 14-16, 1980, Paper 80-0227*, 10 p. 7 refs.

A three-dimensional, viscous computer code was used to calculate the mixing downstream of a typical turbofan mixer geometry. Experimental data were obtained using pressure and temperature rakes at the lobe and nozzle exit stations. Secondary flow velocities were also obtained. These data were used to validate the computer results. An assessment was also made to determine the relative importance of turbulence in the mixing phenomenon as compared with the streamwise vorticity set up by the secondary flows. The observations suggest that the generation of streamwise vorticity appears to play a significant role in determining the temperature distribution at the nozzle exit plane.

(Author)

A80-20969 * Numerical simulation of supersonic inlets using a three-dimensional viscous flow analysis. B. H. Anderson and C. E. Towne (NASA, Lewis Research Center, Cleveland, Ohio). *American Institute of Aeronautics and Astronautics, Aerospace Sciences Meeting, 18th, Pasadena, Calif., Jan. 14-16, 1980, Paper 80-0384*, 15 p. 20 refs.

A three-dimensional fully viscous computer analysis, which retains the viscous nature of the Navier-Stokes equations, was evaluated to determine its usefulness in the design of supersonic inlets. This procedure takes advantage of physical approximations to limit the high computer time and storage associated with complete Navier-Stokes solutions. Computed results are presented for a Mach 3.0 supersonic inlet with bleed and a Mach 7.4 hypersonic inlet. Good agreement was obtained between theory and data for both inlets. Results of a mesh sensitivity study are also shown.

(Author)

A80-38897 * Comparison between optical measurements and a numerical solution of the flow field within a transonic axial-flow compressor rotor. A. J. Strazisar and R. V. Chima (NASA, Lewis Research Center, Cleveland, Ohio). *AIAA, SAE, and ASME, Joint Propulsion Conference, 16th, Hartford, Conn., June 30-July 2, 1980, AIAA Paper 80-1078*, 10 p. 11 refs.

A comparison between numerical and experimental results is presented for the flowfield within a transonic axial-flow compressor rotor. The rotor was tested at design speed and a wide open throttle discharge condition. The relative tip Mach number was 1.4. A laser anemometer system was used to measure velocity and flow angle upstream, within, and downstream of the rotor. A holographic interferometer was used to visualize the rotor shock system near the tip. The computational procedure solves the full three-dimensional Euler equations using a time-marching technique. Shock location and shape determined from the two optical systems are compared. Calculated relative Mach number and flow angle contours, shock locations, and shock strength are compared to values measured with the laser anemometer.

(Author)

A80-38904 * # An experimental investigation of endwall profiling in a turbine vane cascade. F. C. Kopper, R. Milano (United Technologies Corp., Pratt and Whitney Aircraft Group, East Hartford, Conn.), and M. Vanco (NASA, Lewis Research Center, Cleveland, Ohio). *AIAA, SAE, and ASME, Joint Propulsion Conference, 16th, Hartford, Conn., June 30-July 2, 1980, AIAA Paper 80-1089*. 10 p. 18 refs. Contract No. NAS3-20646.

Measurements of surface static pressures, flow total pressure loss, and exit air angle were obtained for two linear cascades to establish the effects of endwall profiling. Testing was conducted at an isentropic exit Mach number of 0.85. One cascade was fabricated with planar endwalls while the other had one planar and one profiled endwall. Both cascades utilized the same high pressure turbine inlet guide vane section. It was found that in terms of full passage loss the profiled endwall cascade has the superior performance. The secondary loss results obtained are reasonably well predicted by correlations developed from incompressible flow testing of similar configurations. Inviscid flow and boundary layer calculations are compared with the test data, and overall, the agreement is found to be good. Use of the results for design purposes is briefly discussed. (Author)

A80-41203 * # Zero-length, slotted-lip inlet for subsonic military aircraft. E. R. Glasgow, W. E. Beck (Lockheed-California Co., Burbank, Calif.), and R. R. Woollett (NASA, Lewis Research Center, Cleveland, Ohio). *AIAA, SAE, and ASME, Joint Propulsion Conference, 16th, Hartford, Conn., June 30-July 2, 1980, AIAA Paper 80-1245*. 13 p. 24 refs. Contract No. NAS3-21461.

Zero-length, slotted-lip inlet performance and associated fan blade stresses were determined during model tests using a 20-inch diameter fan simulator in the NASA-LeRC 9- by 15-foot low-speed wind tunnel. The model configuration variables consisted of inlet contraction ratio, slot width, circumferential extent of slot fillers, and length of a constant area section between the inlet throat and fan face. Inlet configurations having contraction ratios of 1.2 and 1.3 satisfied all critical low-speed inlet operating requirements for a fixed horizontal nacelle and tilt-nacelle-type subsonic V/STOL aircraft, respectively. Relative to a conventional axisymmetric tilt-nacelle inlet, the zero-length, slotted-lip inlet has a 27-percent smaller inlet lip contraction ratio, an 83-percent shorter total length, and a 5-percent smaller maximum cowl diameter. (Author)

A80-42145 * # Streakline flow visualization study of a horseshoe vortex in a large-scale, two-dimensional turbine stator cascade. R. E. Gaugler and L. M. Russell (NASA, Lewis Research Center, Cleveland, Ohio). *American Society of Mechanical Engineers, Gas Turbine Conference and Products Show, New Orleans, La., Mar. 10-13, 1980, Paper 80-GT-4*. 8 p. 12 refs. Members, \$1.50; nonmembers, \$3.00.

Neutrally buoyant helium-filled bubbles were observed as they followed the streamlines in a horseshoe vortex system around the vane leading edge in a large-scale, two-dimensional, turbine stator cascade. Bubbles were introduced into the endwall boundary layer through a slot upstream of the vane leading edge. The paths of the bubbles were recorded photographically as streaklines on 16-mm movie film. Individual frames from the film have been selected, and overlaid to show the details of the horseshoe vortex around the leading edge. The transport of the vortex across the passage near the leading edge is clearly seen when compared to the streaks formed by bubbles carried in the main stream. Limiting streamlines on the endwall surface were traced by the flow of oil drops. (Author)

A80-44229 * # Numerical calculation of transonic axial turbomachinery flows. D. S. Dulikravich (NASA, Lewis Research Center, Cleveland, Ohio). *U.S. Air Force, NASA, NSF, and U.S. Navy, International Conference on Numerical Methods in Fluid Dynamics, 7th, Stanford University, Stanford, Calif., June 23-27, 1980, Paper. 8* p. 15 refs.

This paper presents a numerical method and the results of a computer program for solving an exact, three-dimensional, full-potential equation that models rotating and nonrotating inviscid,

absolutely irrotational, homentropic flows. Besides calculating the flows through an arbitrarily shaped rotor or stator blade row mounted on an axisymmetric hub and confined in an axisymmetric duct, the computer program is also capable of analysing flow fields about arbitrarily shaped wing-body combinations, propellers, helicopter rotors in hover, and wind turbine rotors. The governing equation is solved numerically in a fully conservative form by using an artificial time concept, a finite volume technique, rotated type-dependent differencing, successive line overrelaxation, and sequential boundary-conforming grid refinement. An artificial viscosity is added in fully conservative form; and an initial guess for the potential field is applied, as determined by a two-dimensional cascade analysis. (Author)

A80-44862 * The effect of finite turbulence spatial scale on the amplification of turbulence by a contracting stream. M. E. Goldstein (NASA, Lewis Research Center, Cleveland, Ohio) and P. A. Durbin (Cambridge University, Cambridge, England). *Journal of Fluid Mechanics*, vol. 98, June 12, 1980, p. 473-508. 23 refs.

The turbulence downstream of a rapid contraction is calculated for the case when the turbulence scale can have the same magnitude as the mean-flow spatial scale. The approach used is based on the formulation of Goldstein (1978) for turbulence downstream of a contraction, with the added assumptions of a parallel mean flow at downstream infinity and turbulence calculated far enough downstream so that the nonuniformity of the mean flow field has decayed, and by treating the inverse contraction ratio as a small parameter. Consideration is given to the large-contraction-ratio and classical rapid-distortion theory limits, and to results at an arbitrary contraction ratio. It is shown that the amplification effect of the contraction is reduced when the spatial scale of the turbulence increases, with the upstream turbulence actually suppressed for a contraction ratio less than five and a turbulence spatial scale greater than three times the transverse dimensions of the downstream channel. A.L.W.

N80-10134*# Douglas Aircraft Co., Inc., Long Beach, Calif. **AN EFFICIENT USER-ORIENTED METHOD FOR CALCULATING COMPRESSIBLE FLOW IN AN ABOUT THREE-DIMENSIONAL INLETS** Final Report, Nov. 1977 - Apr. 1979

John I. Hess, Dun-Pok Mack, and Norbert O. Stockman (NASA, Lewis Res. Center) Apr. 1979 117 p refs

(Contract NAS3-21135)

(NASA-CR-159578; MDC-J7733)

Avail: NTIS

HC A06/MF A01 CSCL 01A

A panel method is used to calculate incompressible flow about arbitrary three-dimensional inlets with or without centerbodies for four fundamental flow conditions: unit onset flows parallel to each of the coordinate axes plus static operation. The computing time is scarcely longer than for a single solution. A linear superposition of these solutions quite rigorously gives incompressible flow about the inlet for any angle of attack, angle of yaw, and mass flow rate. Compressibility is accounted for by applying a well-proven correction to the incompressible flow. Since the computing times for the combination and the compressibility correction are small, flows at a large number of inlet operating conditions are obtained rather cheaply. Geometric input is aided by an automatic generating program. A number of graphical output features are provided to aid the user, including surface streamline tracing and automatic generation of curves of curves of constant pressure, Mach number, and flow inclination

N80-17995*# Cincinnati Univ., Ohio. Dept. of Aerospace Engineering and Applied Mechanics.

A CALCULATION PROCEDURE FOR VISCOUS FLOW IN TURBOMACHINES, VOLUME 2

J. Khalil and W. Tabakoff Jan. 1980 54 p refs

(Contract NAS3-21509; DA Proj. 11-1-61102-AH-45)

(NASA-CR-159636) Avail: NTIS HC A04/MF A01 CSCL 21E

Turbulent flow within turbomachines having arbitrary blade geometries is examined. Effects of turbulence are modeled using two equations, one expressing the development of the turbulence kinetic energy and the other its dissipation rate. To account for complicated blade geometries, the flow equations are formulated in terms of a nonorthogonal boundary fitted coordinate system. The analysis is applied to a radial inflow turbine. The solution obtained indicates the severity of the complex interaction mechanism that occurs between the different flow regimes (i.e., boundary layers, recirculating eddies, separation zones, etc.). Comparison with nonviscous flow solutions tend to justify strongly the inadequacy of using the latter with standard boundary layer techniques to obtain viscous flow details within turbomachine rotors. Capabilities and limitations of the present method of analysis are discussed. M.G.

N80-24263* General Dynamics/Fort Worth, Tex.
EXPERIMENTAL INVESTIGATION OF A 0.15 SCALE MODEL OF A CONFORMAL VARIABLE-RAMP INLET FOR THE F-16 AIRPLANE Final Report
 J. E. Hawkins Mar. 1980 219 p refs Sponsored by NASA (NASA-CR-159640; ERR-FW-2014) Avail: NTIS HC A10/MF A01 CSCL 01A

A 0.15 scale model of a proposed conformal variable-ramp inlet for the Multirole Fighter was tested from Mach 0.8 to 2.2 at a wide range of angles of attack and sideslip. Inlet ramp angle was varied to optimize ramp angle as a function of engine airflow, Mach number, angle of attack, and angle of sideslip. Several inlet configuration options were investigated to study their effects on inlet operation and to establish the final flight configuration. These variations were cowl sidewall cutback, cowl lip bluntness, boundary layer bleed, and first-ramp leading edge shape. Diagnostic and engine face instrumentation were used to evaluate inlet operation at various inlet stations and at the inlet/engine interface. Pressure recovery and stability of the inlet were satisfactory for the proposed application. On the basis of an engine stability audit of the worst-case instantaneous distortion patterns, no inlet/engine compatibility problems are expected for normal operations. Author

N80-26274* Cincinnati Univ., Ohio.
A CALCULATION PROCEDURE FOR VISCOUS FLOW IN TURBOMACHINES, VOLUME 3
 I. Khalil, Y. Sheoran, and W. Tabakoff Jun. 1980 46 p (Contract NAS3-21609)
 (NASA-CR-159864) Avail: NTIS HC A03/MF A01 CSCL 01A

A method for analyzing the nonadiabatic viscous flow through turbomachine blade passages was developed. The field analysis is based upon the numerical integration of the full incompressible Navier-Stokes equations, together with the energy equation on the blade-to-blade surface. A FORTRAN IV computer program was written based on this method. The numerical code used to solve the governing equations employs a nonorthogonal boundary fitted coordinate system. The flow may be axial, radial or mixed and there may be a change in stream channel thickness in the through-flow direction. The inputs required for two FORTRAN IV programs are presented. The first program considers laminar flows and the second can handle turbulent flows. Numerical examples are included to illustrate the use of the program, and to show the results that are obtained. A.R.H.

N80-27288* Pennsylvania State Univ., University Park.
THREE DIMENSIONAL MEAN FLOW AND TURBULENCE CHARACTERISTICS OF THE NEAR WAKE OF A COMPRESSOR ROTOR BLADE Final Report
 A. Ravindranath and B. Lakshminarayana Jun. 1980 298 p refs (Grant NSG-3012)
 (NASA-CR-159518; PSU-TURBO-R-80-4) Avail: NTIS HC A13/MF A01 CSCL 01A

The investigation was carried out using the rotating hot wire technique. Measurements were taken inside the end wall boundary layer to discern the effect of annulus and hub wall boundary

layer, secondary flow, and tip leakage on the wake structure. Static pressure gradients across the wake were measured using a static stagnation pressure probe insensitive to flow direction changes. The axial and the tangential velocity defects, the radial component of velocity, and turbulence intensities were found to be very large as compared to the near and far wake regions. The radial velocities in the trailing edge region exhibited characteristics prevalent in a trailing vortex system. Flow near the blade tips found to be highly complex due to interaction of the end wall boundary layers, secondary flows, and tip leakage flow with the wake. The streamwise curvature was found to be appreciable near the blade trailing edge. Flow properties in the trailing edge region are quite different compared to that in the near and far wake regions with respect to their decay characteristics, similarity, etc. Fourier decomposition of the rotor wake revealed that for a normalized wake only the first three coefficients are dominant. F.D.K.

N80-28302* Atmospheric Science Associates, Bedford, Mass
CALCULATION OF WATER DROP TRAJECTORIES TO AND ABOUT ARBITRARY THREE-DIMENSIONAL BODIES IN POTENTIAL AIRFLOW Final Report

Hillyer G. Normant Washington NASA Aug 1980 83 p refs (Contract NAS3-22199)

(NASA-CR-3291) Avail: NTIS HC A05/MF A01 CSCL 20D
 Calculations can be performed for any atmospheric conditions and for all water drop sizes, from the smallest cloud droplet to large raindrops. Any subsonic, external, non-lifting flow can be accommodated; flow into, but not through, inlets also can be simulated. Experimental water drop drag relations are used in the water drop equations of motion and effects of gravity settling are included. Seven codes are described: (1) a code used to debug and plot body surface description data; (2) a code that processes the body surface data to yield the potential flow field; (3) a code that computes flow velocities at arrays of points in space; (4) a code that computes water drop trajectories from an array of points in space; (5) a code that computes water drop trajectories and fluxes to arbitrary target points; (6) a code that computes water drop trajectories tangent to the body; and (7) a code that produces stereo pair plots which include both the body and trajectories. Code descriptions include operating instructions, card inputs and printouts for example problems, and listing of the FORTRAN codes. Accuracy of the calculations is discussed, and trajectory calculation results are compared with prior calculations and with experimental data. Author

N80-29251* Stanitz (John D.), University Heights, Ohio.
GENERAL DESIGN METHOD FOR THREE-DIMENSIONAL POTENTIAL FLOW FIELDS, 1: THEORY Final Report
 John D. Stanitz Washington, D.C. Aug. 1980 82 p refs (Contract NAS3-21605)

(NASA-CR-3288) Avail: NTIS HC A05/MF A01 CSCL 01A
 A general design method was developed for steady, three dimensional, potential, incompressible or subsonic-compressible flow. In this design method, the flow field, including the shape of its boundary, was determined for arbitrarily specified, continuous distributions of velocity as a function of arc length along the boundary streamlines. The method applied to the design of both internal and external flow fields, including, in both cases, fields with planar symmetry. The analytic problems associated with stagnation points, closure of bodies in external flow fields, and prediction of turning angles in three dimensional ducts were reviewed. R.C.T.

N80-31351* United Technologies Research Center, East Hartford, Conn.
INFLUENCE OF MISTUNING ON BLADE TORSIONAL FLUTTER
 A. V. Srinivasan Aug. 1980 55 p refs (Contract NAS3-21603)
 (NASA-CR-165137; R80-914545-16) Avail: NTIS HC A04/MF A01 CSCL 01A

An analytical technique for the prediction of fan blade flutter was evaluated by utilizing first stage fan flutter data from tests on an advanced high performance engine. The formulation includes both aerodynamic and mechanical coupling among all the blades of the assembly. Mistuning is accounted for in the analysis so that individual blade inertias, frequencies, or damping can be considered. Airfoil stability was predicted by calculating a flutter determinant, the eigenvalues of which indicate the extent of susceptibility to flutter. When blade to blade differences in frequencies are considered, a stable system is predicted for the test points examined. For a tuned system, it was found that torsional flutter can be predicted at a limited number of interblade phase angles. Examination of these phase angles indicated that they were 'close' to the condition of acoustic resonance. For the range of Mach numbers and reduced frequencies considered, the so called subcritical flutter cannot be predicted. The essential influence of mechanical coupling among the blades is to change the frequencies of the system with little or no change in damping; however, aerodynamic coupling together with mechanical coupling could change not only frequencies, but also damping in the system, with a trend toward instability. A.R.H.

N80-32328* Illinois Inst. of Tech., Chicago.
EFFECTS OF AXISYMMETRIC CONTRACTIONS ON TURBULENCE OF VARIOUS SCALES Final Report
 Jimmy Tan-atchat, Hassan M. Nagib, and Robert E. Drubka
 Sep 1980 376 p refs
 (Grant NSG-3220)
 (NASA-CR-165136, R80-1) Avail. NTIS HC A17/MF A01
 CSCI 01A

Digitally acquired and processed results from an experimental investigation of grid generated turbulence of various scales through and downstream of nine matched cubic contour contractions ranging in area ratio from 2 to 36, and in length to inlet diameter ratio from 0.25 to 1.50 are reported. An additional contraction with a fifth order contour was also utilized for studying the shape effect. Thirteen homogeneous and nearly isotropic test flow conditions with a range of turbulence intensities, length scales and Reynolds numbers were generated and used to examine the sensitivity of the contractions to upstream turbulence. The extent to which the turbulence is altered by the contraction depends on the incoming turbulence scales, the total strain experienced by the fluid, as well as the contraction ratio and the strain rate. Varying the turbulence integral scale influences the transverse turbulence components more than the streamwise component. In general, the larger the turbulence scale, the lesser the reduction in the turbulence intensity of the transverse components. Best agreement with rapid distortion theory was obtained for large scale turbulence, where viscous decay over the contraction length was negligible, or when a first order correction for viscous decay was applied to the results. T.M.

A80-18324* Evaluation of a strained-coordinate perturbation procedure - Nonlinear subsonic and transonic flows. S. S. Stahara, A. J. Crisalli (Nielsen Engineering and Research, Inc., Mountain View, Calif.), and J. R. Spreiter (Stanford University, Stanford, Calif.). *American Institute of Aeronautics and Astronautics, Aerospace Sciences Meeting, 18th, Pasadena, Calif., Jan. 14-16, 1980, Paper 80-0339*. 12 p. 9 refs. Contract No. NAS3-20836.

An evaluation is made of a perturbation method devised to obtain highly accurate approximations to families of strongly nonlinear solutions which are either continuous or discontinuous, and which represent variations in some arbitrary parameter. The method first defines a unit perturbation by using two nonlinear solutions which differ from one another by a nominal change in some geometric or flow parameter, then employs this unit perturbation to predict a family of related nonlinear solutions over a range of parameter variation. Coordinate straining is incorporated into this perturbation method for determining the unit perturbation to account for the movement of discontinuities and maxima of high-gradient regions due to the perturbation. Attention is given to transonic and subsonic flows. Comparisons of the perturbation results with the corresponding 'exact' nonlinear solutions show a remarkable accuracy and range of validity of the perturbation method across the spectrum of examples considered. S.D.

A80-20086 // A phenomenological model of the dynamic stall of a helicopter blade profile (Modèle phénoménologique de décrochage dynamique sur profil de pale d'hélicoptère). R. Dat, C. T. Tran, and D. Petot (ONERA, Châtillon-sous-Bagneux, Hauts-de-Seine, France). (*Association Aéronautique et Astronautique de France, Colloque d'Aérodynamique Appliquée, 16th, Lille, France, Nov. 13-15, 1979*). ONERA, TP no. 1979-149, 1979. 43 p. 7 refs. In French.

A phenomenological model developed for the prediction of helicopter blade stall is presented. The model uses a system of procedure for turbulent compressible flow in axisymmetric ducts was used to successfully model the HIMAT duct flow. The analysis technique was further used to estimate the initiation of separation and delineate the steady and unsteady flow regimes in similar S-shaped ducts. (Author)

A80-20748* // Griffith diffusers. T.-T. Yang (Clemson University, Clemson, S.C.) and C. D. Nelson. *ASME, Transactions, Journal of Fluids Engineering*, vol. 101, Dec. 1979, p. 473-477. 13 refs. Research supported by Clemson University; Contracts No. NAS3-13486; No. F33615-74-C-2039; Grant No. NGL-41-001-031.

Contoured wall diffusers are designed by using an inverse method. The prescribed wall velocity distribution(s) was taken from the high lift airfoil designed by A. A. Griffith in 1938; therefore, such diffusers are named Griffith diffusers. First the formulation of the inverse problem and the method of solution are outlined. Then the typical contour of a two-dimensional diffuser and velocity distributions across the flow channel at various stations are presented. For a Griffith diffuser to operate as it is designed, boundary layer suction is necessary. Discussion of the percentage of through-flow required to be removed for the purpose of boundary layer control is given. Finally, reference is made to the latest version of a computer program for a two-dimensional diffuser requiring only area ratio, nondimensional length and suction percentage as inputs. (Author)

A80-38895* // Inlet flow distortion in turbomachinery. I - Comparison of theory and experiment in a transonic fan stage. II - A parameter study. B. S. Seidel, M. D. Matwey (Delaware University, Newark, Del.), and J. J. Adamczyk (NASA, Lewis Research Center, Cleveland, Ohio). *AIAA, SAE, and ASME, Joint Propulsion Conference, 16th, Hartford, Conn., June 30-July 2, 1980, AIAA Paper 80-1076*. 6 p. 7 refs. Grant No. NSG-3189.

In the present paper, a semi-actuator-disk theory is reviewed that was developed previously for the distorted inflow to a single-stage axial-flow compressor. Flow distortion occurs far upstream; it may be a distortion in stagnation temperature, stagnation pressure, or both. Losses, quasi-steady deviation angles, and reference incidence correlations are included in the analysis, and both subsonic and transonic relative Mach numbers are considered. The theory is compared with measurements made in a transonic fan stage, and a parameter study is carried out to determine the influence of solidity on the attenuation of distortions in stagnation pressure and stagnation temperature. V.P.

A80-41601* // A three-dimensional turbulent compressible subsonic duct flow analysis for use with constructed coordinate systems. R. Levy, H. McDonald, W. R. Briley, and J. P. Kreskovsky (Scientific Research Associates, Inc., Glastonbury, Conn.). *American Institute of Aeronautics and Astronautics, Fluid and Plasma Dynamics Conference, 13th, Snowmass, Colo., July 14-16, 1980, Paper 80-1398*. 10 p. 7 refs. Contract No. NAS3-21735.

An approximate analysis, applicable to nonorthogonal coordinate systems having a curved centerline and planar transverse coordinate surfaces normal to the centerline, is presented for computation of three-dimensional subsonic flow in straight and curved diffusers. The formulation is intended to facilitate the use of constructed coordinates in circumstances where it is difficult to maintain smooth behavior in higher derivatives; the use of local Cartesian variables and fluxes leads to governing equations which

require only first derivatives of the coordinate transformation. The analysis is applied to a particular family of duct and diffuser geometries having curved centerlines and superelliptic cross sections. Qualitative agreement with experimental measurements is observed with regard to streamwise vortices and distortion of the primary flow.
J.P.B.

A80-44128 * // An implicit finite-difference code for inviscid and viscous cascade flow. J. L. Steger (Flow Simulations, Inc., Sunnyvale, Calif.), T. H. Pulliam (NASA, Ames Research Center, Moffett Field, Calif.), and R. V. Chima (NASA, Lewis Research Center, Cleveland, Ohio). *American Institute of Aeronautics and Astronautics, Fluid and Plasma Dynamics Conference, 13th, Snowmass, Colo., July 14-16, 1980, Paper 80-1427*. 15 p. 32 refs.

An implicit finite-difference code is developed to solve either inviscid or viscous flow about two-dimensional cascade blade elements. General coordinate transformations are used so that boundaries can coincide with coordinate lines, and an automatic grid generation routine based on elliptic partial differential equations is employed to mesh arbitrary cascade elements. Characteristic combinations of the differential equations are used at inflow and outflow boundaries. Computed results for both inviscid and viscous flow are compared with other existing cascade solutions and experimental data.
(Author)

A80-45841 * Aerodynamic analysis of a supersonic cascade vibrating in a complex mode. J. E. Caruthers (Tennessee, University, Space Institute, Tullahoma, Tenn.) and R. E. Riffel (General Motors Corp., Detroit Allison Div., Indianapolis, Ind.). *Journal of Sound and Vibration*, vol. 71, July 22, 1980, p. 171-183. 10 refs. Contract No. NAS3-20055.

An analysis is presented which has been used to predict the unsteady aerodynamic behavior of a finite supersonic cascade of airfoils forced in harmonic oscillation with airfoil-to-airfoil variations in amplitude. Theoretical predictions are compared with some recent experimental results at a reduced frequency representative of actual fan or compressor flutter cases. The similarity of the experimental situation in the finite cascade to the flutter of a severely mistuned rotor is noted.
(Author)

03 AIR TRANSPORTATION AND SAFETY

Includes passenger and cargo air transport operations;
and aircraft accidents

For related information see also *16 Space Transportation*
and *85 Urban Technology and Transportation*

NSO-15059*# National Aeronautics and Space Administration
Lewis Research Center, Cleveland, Ohio

SIMULTANEOUS CABIN AND AMBIENT OZONE MEASUREMENTS ON TWO BOEING 747 AIRPLANES, VOLUME 1

Porter J. Perkins, J. D. Holdeman, and G. D. Nastrom (Control Data Corp., Minneapolis, Minn.) Jul 1979 826 p refs (NASA-TM-79166, FAA-EE-79-05, E-196) Avail NTIS HC A99/MF A01 CSCL 01C

Measurements of ozone concentrations both outside and in the cabin of an airline operated Boeing 747SP and Boeing 747-100 airliner are presented. Plotted data and the corresponding tables of observations taken at altitude between the departure and destination airports of each flight are arranged chronologically for the two aircraft. Data were taken at five or ten minute intervals by automated instrumentation used in the NACA Global Atmospheric Sampling Program.

M M M

04 AIRCRAFT COMMUNICATIONS AND NAVIGATION

Includes digital and voice communication with aircraft; air navigation systems (satellite and ground based); and air traffic control.

For related information see also 17 *Spacecraft Communications, Command, and Tracking* and 32 *Communications*.

A80-13064 * 17 UHF coplanar-slot antenna for aircraft-to-satellite data communications. R. W. Myhre (NASA, Lewis Research Center, Cleveland, Ohio). *New Mexico State University and U.S. Army, Printed Circuit Antenna Technology Workshop, Las Cruces, N. Mex., Oct. 17-19, 1979, Paper*. 19 p.

The initiative for starting the Aircraft-to-Satellite Data Relay (ASDAR) Program came from a recognition that much of the world's weather originates in the data sparse area of the tropics which are primarily ocean. The ASDAR system consists of (1) a data acquisition and control unit to acquire, store and format these data; (2) a clock to time the data sampling and transmission periods; and (3) a transmitter and low-profile upper hemisphere coverage antenna to relay the formatted data via satellite to the National Weather Service ground stations, as shown schematically. The low-profile antenna is a conformal antenna based on the coplanar-slot approach. The antenna is circular polarized and has an on-axis gain of nearly 2.5 dB and a HPBW greater than 90 deg. The discussion covers antenna design, radiation characteristics, flight testing, and system performance.

S.D.

05 AIRCRAFT DESIGN, TESTING AND PERFORMANCE

Includes aircraft simulation technology.
For related information see also 18 Spacecraft Design, Testing and Performance and 39 Structural Mechanics.

A80-15123 * # Examination of the flap-lag stability of rigid articulated rotor blades. K. R. V. Kaza (NASA, Lewis Research Center, Cleveland; Toledo, University, Toledo, Ohio) and R. G. Kvaternik (NASA, Langley Research Center, Structures and Dynamics Div., Hampton, Va.). *Journal of Aircraft*, vol. 16, Dec. 1979, p. 876-884, 20 refs.

A critical examination of flap-lag stability of a centrally hinged, spring-restrained rigid blade in both hover and forward flight is presented. Several differences in the equations of motion for blade flap-lag stability in the existing literature are identified. A rigorous and systematic development of these equations for a rigid articulated blade in forward flight shows the existence of some linear aerodynamic coupling terms associated with blade steady-state flapping and lagging in the perturbation equations. The differences identified are shown to be associated with whether or not the lag hinge flaps with the blade. The implications of these differences on stability are examined, and it is shown that the pitch-lag coupling terms associated with a hinge arrangement in which the lag hinge flaps with the blade have a marked influence on flap-lag stability, depending on the system parameters. (Author)

A80-28853 * # Measurements of cabin and ambient ozone on B747 airplanes. G. D. Nastrom (Control Data Corp., Minneapolis, Minn.), J. D. Holdeman, and P. J. Perkins (NASA, Lewis Research Center, Combustion and Pollution Research Branch, Cleveland, Ohio). *Journal of Aircraft*, vol. 17, Apr. 1980, p. 246-249. 14 refs. FAA-supported research.

In response to recent concerns over possibly high ozone levels in the cabins of aircraft flying in the stratosphere, simultaneous measurements of the cabin and ambient ozone levels have been made as part of the NASA Global Atmospheric Sampling Program. Examples of the data taken on commercially operated Boeing 747-100 and 747SP airplanes are given for selected flights, together with summary statistics of over 5600 observations. Cabin ozone levels vary with the ambient level and, for unmodified aircraft, are higher on the 747SP than on the 747-100. Modifications to the ventilation system of the 747SP reduced cabin ozone levels by varying amounts up to a factor of 14. (Author)

A80-41193 * # Development of a Kevlar/PMR-15 reduced drag DC-9 nacelle fairing. R. T. Kawai (Douglas Aircraft Co., Long Beach, Calif.) and F. J. Hrach (NASA, Lewis Research Center, Engine Component Improvement Office, Cleveland, Ohio). *AIAA, SAE, and ASME, Joint Propulsion Conference, 16th, Hartford, Conn., June 30-July 2, 1980, AIAA Paper 80-1194*, 9 p. 5 refs.

The paper describes an advanced composite fairing designed to reduce drag on DC-9 nacelles as a part of the NASA Engine Component Improvement Program. This fairing is the aft enclosure for the thrust reverser actuator system on JT8D engine nacelles and is subjected to a 500 F exhaust flow during the reverse thrust. A reduced-drag configuration was developed by using in-flight tuft surveys for flow visualization in order to identify areas with low-quality flow, and then modifying the aerodynamic lines to improve the flow. A fabrication method for molding the part in an autoclave was developed; this material system is suitable for 500 F. The resultant composite fairing reduces the overall aircraft drag 1% with a weight reduction of 40% when compared with a metal component. A.T.

A80-41194 * # Reduced bleed air extraction for DC-10 cabin air conditioning. W. H. Newman, M. R. Viele (Douglas Aircraft Co., Long Beach, Calif.), and F. J. Hrach (NASA, Lewis Research Center, Cleveland, Ohio). *AIAA, SAE, and ASME, Joint Propulsion Conference, 16th, Hartford, Conn., June 30-July 2, 1980, AIAA Paper 80-1197*, 8 p.

It is noted that a significant fuel savings can be achieved by reducing bleed air used for cabin air conditioning. Air in the cabin can be recirculated to maintain comfortable ventilation rates but the quality of the air tends to decrease due to entrainment of smoke and odors. Attention is given to a development system designed and fabricated under the NASA Engine Component Improvement Program to define the recirculation limit for the DC-10. It is shown that with the system, a wide range of bleed air reductions and recirculation rates is possible. A goal of 0.8% fuel savings has been achieved which results from a 50% reduction in bleed extraction from the engine. M.E.P.

N80-18060 * # Massachusetts Inst. of Tech., Cambridge.

AIR POLLUTION FROM AIRCRAFT

John B. Heywood, James A. Fay, and Norman A. Chigier (Sheffield Univ.) Oct. 1979 47 p refs
(Grant NGR-22-009-378)
(NASA-CR-159712) Avail: NTIS HC A03/MF A01 CSCL 21E

A series of fundamental problems related to jet engine air pollution and combustion were examined. These include soot formation and oxidation, nitric oxide and carbon monoxide emissions mechanisms, pollutant dispersion, flow and combustion characteristics of the NASA swirl can combustor, fuel atomization and fuel-air mixing processes, fuel spray drop velocity and size measurement, ignition and blowout. A summary of this work, and a bibliography of 41 theses and publications which describe this work, with abstracts, is included. A.R.H.

N80-32378 * # Douglas Aircraft Co., Inc., Long Beach, Calif.

ENGINE BLEED AIR REDUCTION IN DC-10

W. H. Newman and M. R. Viele Sep. 1980 75 p refs
(Contract NAS3-21763)
(NASA-CR-159846) Avail: NTIS HC A04/MF A01 CSCL 01C

An 0.8 percent fuel savings was achieved by a reduction in engine bleed air through the use of cabin air recirculation. The recirculation system was evaluated in revenue service on a DC-10. The cabin remained comfortable with reductions in cabin fresh air (engine bleed air) as much as 50 percent. Flight test verified the predicted fuel saving of 0.8 percent. R.C.T.

06 AIRCRAFT INSTRUMENTATION

Includes cockpit and cabin display devices; and flight instruments.

For related information see also 19 *Spacecraft Instrumentation* and 35 *Instrumentation and Photography*.

N80-14110* // National Aeronautics and Space Administration. Langley Research Center, Hampton, Va.

WIND-TUNNEL INVESTIGATION OF THE FLOW CORRECTION FOR A MODEL-MOUNTED ANGLE OF ATTACK SENSOR AT ANGLES OF ATTACK FROM -10 DEG TO 110 DEG

Thomas M. Moul Nov. 1979 20 p refs
(NASA-TM-80189) Avail: NTIS HC A02/MF A01 CSCL 01C

A preliminary wind tunnel investigation was undertaken to determine the flow correction for a vane angle of attack sensor over an angle of attack range from -10 deg to 110 deg. The sensor was mounted ahead of the wing on a 1/5 scale model of a general aviation airplane. It was shown that the flow correction was substantial, reaching about 15 deg at an angle of attack of 90 deg. The flow correction was found to increase as the sensor was moved closer to the wing or closer to the fuselage. The system measurements are made using optical transducers which are fixed to the case. Measurements made in this way are the equivalent of those obtained by placing three surface-normal displacement transducers at three positions on each blade of an operational rotor.

M.M.M.

07 AIRCRAFT PROPULSION AND POWER

Includes prime propulsion systems and systems components, e.g., gas turbine engines and compressors; and on-board auxiliary power plants for aircraft.

For related information see also 20 *Spacecraft Propulsion and Power*, 28 *Propellants and Fuels*, and 44 *Energy Production and Conversion*.

N80-10205* National Aeronautics and Space Administration, Lewis Research Center, Cleveland, Ohio.

AEROPROPULSION 1979

1979 464 p Proceedings of conf. held at Cleveland, Ohio, 1-16 May 1979

(NASA-CP-2092; E-079) Avail: NTIS HC A20/MF A01 CSCL 21E

State of the art technology in aeronautical propulsion is assessed. Noise and air pollution control techniques, advances in supersonic propulsion for transport aircraft, and composite materials and structures for reliable engine components are covered along with engine design for improved fuel consumption. For individual titles, see N80-10206 through N80-10219.

N80-10206* National Aeronautics and Space Administration, Lewis Research Center, Cleveland, Ohio.

AIRCRAFT ENERGY EFFICIENCY (ACEE) STATUS REPORT

Donald L. Nored, James F. Dugan, Jr., Neal T. Saunders, and Joseph A. Ziemianski *In its Aeropropulsion* 1979 1979 p 1-58 refs (For primary document see N80-10205 01-07)

Avail: NTIS HC A20/MF A01 CSCL 21E

Fuel efficiency in aeronautics, for fuel conservation in general as well as for its effect on commercial aircraft operating economics is considered. Projects of the Aircraft Energy Efficiency Program related to propulsion are emphasized. These include: (1) engine component improvement, directed at performance improvement and engine diagnostics for prolonged service life; (2) energy efficient engine, directed at proving the technology base for the next generation of turbofan engines; and (3) advanced turboprop, directed at advancing the technology of turboprop powered aircraft to a point suitable for commercial airline service. Progress in these technology areas is reported. J.M.S.

N80-10207* National Aeronautics and Space Administration, Lewis Research Center, Cleveland, Ohio.

EMISSION REDUCTION

Donald A. Petrash, Larry A. Dietrich, Robert E. Jones, and Edward J. Mularz *In its Aeropropulsion* 1979 1979 p 59-84 (For primary document see N80-10205 01-07)

Avail: NTIS HC A20/MF A01 CSCL 21E

Control of the gaseous pollutant emissions of aircraft engines is considered in terms of the emission standards for six classes of aircraft engines. Emphasis is placed on combustor design concepts to significantly reduce emissions levels and lean-burning techniques to lower flame temperature, to reduce the oxides of nitrogen in the gaseous emissions. J.M.S.

N80-10208* National Aeronautics and Space Administration, Lewis Research Center, Cleveland, Ohio.

NOISE REDUCTION

Charles E. Feiler, John F. Groeneweg, Francis J. Montegani, John P. Raney (NASA, Langley Research Center), Edward J. Rice, and James R. Stone *In its Aeropropulsion* 1979 1979 p 85-128 refs (For primary document see N80-10205 01-07)

Avail: NTIS HC A20/MF A01 CSCL 21E

The turbofan engine's noise-producing components are discussed in terms of efficient and economical noise reduction techniques that do not penalize the engine performance or weight significantly. Specific topics covered include fan noise, acoustic suppression, jet noise technology, combustor noise, and aircraft noise prediction. J.M.S.

N80-10209* National Aeronautics and Space Administration, Lewis Research Center, Cleveland, Ohio.

ALTERNATIVE JET AIRCRAFT FUELS

Jack Grobman *In its Aeropropulsion* 1979 1979 p 129-148 refs (For primary document see N80-10205 01-07)

Avail: NTIS HC A20/MF A01 CSCL 21E

Potential changes in jet aircraft fuel specifications due to shifts in supply and quality of refinery feedstocks are discussed with emphasis on the effects these changes would have on the performance and durability of aircraft engines and fuel systems. Combustion characteristics, fuel thermal stability, and fuel pumpability at low temperature are among the factors considered. Combustor and fuel system technology needs for broad specification fuels are reviewed including prevention of fuel system fouling and fuel system technology for fuels with higher freezing points. J.M.S.

N80-10210* National Aeronautics and Space Administration, Lewis Research Center, Cleveland, Ohio.

MATERIALS AND STRUCTURES TECHNOLOGY

Robert A. Signorelli, Thomas K. Glasglow, Gary R. Halford, and Stanley R. Levine *In its Aeropropulsion* 1979 1979 p 149-186 refs (For primary document see N80-10205 01-07)

Avail: NTIS HC A20/MF A01 CSCL 21E

Materials and structures performance limitations, particularly for the hot section of the engine in which these limitations limit the life of components, are considered. Failure modes for components such as blades, vanes, and combustors and how they are affected by the environment for such components are discussed. Methods used to improve the materials used for such components are: (1) application of directional structures to turbine components for high strength at high temperatures; (2) improved coatings to increase oxidation and corrosion resistance; (3) increase strength and stiffness with reduced weight by applying higher specific properties of composite materials; and (4) cost effective processing such as near net shape powder methods applied to disks. Life prediction techniques developed to predict component life accurately in advance of service and progress in improving the intermediate and cold section components of turbine engines are covered. J.M.S.

N80-10211* National Aeronautics and Space Administration, Lewis Research Center, Cleveland, Ohio.

COMPUTATIONAL FLUID MECHANICS OF INTERNAL FLOW

David N. Bowditch, William D. McNally, Bernhard H. Anderson, John J. Adamczyk, and Peter M. Sockol *In its Aeropropulsion* 1979 1979 p 187-230 refs (For primary document see N80-10205 01-07)

Avail: NTIS HC A20/MF A01 CSCL 21E

Major solution techniques for internal computational fluid mechanics are discussed and some examples are presented. The major steps involved in developing a large computer code are then discussed. R.E.S.

N80-10212* National Aeronautics and Space Administration, Lewis Research Center, Cleveland, Ohio.

TURBOMACHINERY TECHNOLOGY

Cavour H. Hauser, Jeffrey E. Haas (U.S. Army Res. and Technol. Labs., Cleveland, Ohio), Lonnie Reid, and Francis S. Stepka *In its Aeropropulsion* 1979 1979 p 231-272 (For primary document see N80-10205 01-07)

Avail: NTIS HC A20/MF A01 CSCL 21E

A technology assessment of turbomachinery is presented. The design of the fan, compressor, and turbine components for future advanced aircraft engines is discussed. Basic flow characteristics in compressors and turbines and the heat transfer phenomena in cooled turbines are also discussed. R.E.S.

N80-10213* National Aeronautics and Space Administration. Lewis Research Center, Cleveland, Ohio.

MECHANICAL COMPONENTS

William J. Anderson, Robert C. Bill, John J. Coy, and David Fleming *In its Aeropropulsion* 1979 1979 p 273-308 ref (For primary document see N80-10205 01-07)

Avail: NTIS HC A20/MF A01 CSCL 21E

Research on bearings, gears, seals, and rotor dynamics (specifically high speed balancing and dampers) is presented. The research pertains to problems in both aircraft turbine engines and helicopter transmissions. R.E.S.

N80-10214* National Aeronautics and Space Administration. Lewis Research Center, Cleveland, Ohio.

INSTRUMENTATION TECHNOLOGY

William C. Nieberding, David R. Englund, Jr., and George E. Glawe *In its Aeropropulsion* 1979 1979 p 309-328 refs (For primary document see N80-10205 01-07)

Avail: NTIS HC A20/MF A01 CSCL 21E

Some of the efforts made in applying technologically new tools to today's propulsion measurement problems are described. They include: (1) a blade-tip clearance system; (2) a pulsed thermocouple system used to measure gas temperature with a thermocouple at temperatures above the melting point of the thermocouple; (3) an optical technique for measuring blade flutter; (4) a probe for dynamic flow and flow angle measurement; and (5) a laser anemometer system for rapidly mapping the flow profiles between the blades of a rotating compressor. R.E.S.

N80-10215* National Aeronautics and Space Administration. Lewis Research Center, Cleveland, Ohio.

CONTROL TECHNOLOGY

John R. Szuch *In its Aeropropulsion* 1979 1979 p 329-344 refs (For primary document see N80-10205 01-07)

Avail: NTIS HC A20/MF A01 CSCL 21E

An overview of engine control technology is presented with emphasis on gas turbine engine controls. The role of the government, and NASA in particular, in advancing this technology is discussed. R.E.S.

N80-10216* National Aeronautics and Space Administration. Lewis Research Center, Cleveland, Ohio.

SUPERSONIC PROPULSION TECHNOLOGY

Albert G. Powers, Robert E. Coltrin, Leonard E. Stitt, Richard J. Weber, and John B. Whitlow, Jr. *In its Aeropropulsion* 1979 1979 p 345-386 (For primary document see N80-10205 01-07)

Avail: NTIS HC A20/MF A01 CSCL 21E

Propulsion concepts for commercial supersonic transports are discussed. It is concluded that variable cycle engines, together with advanced supersonic inlets and low noise coannular nozzles, provide good operating performance for both supersonic and subsonic flight. In addition, they are reasonably quiet during takeoff and landing and have acceptable exhaust emissions. K.L.

N80-10217* National Aeronautics and Space Administration. Lewis Research Center, Cleveland, Ohio.

HYPERSONIC PROPULSION

H. Lee Beach, Jr. *In its Aeropropulsion* 1979 1979 p 387-408 refs (For primary document see N80-10205 01-07)

Avail: NTIS HC A20/MF A01 CSCL 21E

Research on hydrogen fueled scramjet engines for hypersonic flight is reviewed. Component developments, computational methods, and preliminary ground tests of subscale scramjet engine modules at Mach 4 and 7 are emphasized. Airframe integration, structures, and flow diagnostics are also discussed. It is shown that mixed-mode perpendicular and parallel fuel injection controls heat release over a wide Mach range and the fixed geometry inlet gives good performance over a wide range of Mach numbers. K.L.

N80-10218* National Aeronautics and Space Administration. Lewis Research Center, Cleveland, Ohio.

VERTICAL TAKEOFF AND LANDING (VTOL) PROPULSION TECHNOLOGY

Carl C. Ciepluch, John M. Abbott, Royce D. Moore, and James F. Sellers *In its Aeropropulsion* 1979 1979 p 409-444 refs (For primary document see N80-10205 01-07)

Avail: NTIS HC A20/MF A01 CSCL 21E

Propulsion problems and advanced technology requirements of VTOL aircraft are discussed. Specific topics covered include inlets with high angle of attack capability, rapid thrust modulation fans, and propulsion-system/aircraft-control integration. K.L.

N80-10219* National Aeronautics and Space Administration. Lewis Research Center, Cleveland, Ohio.

HIGH-PERFORMANCE-VEHICLE TECHNOLOGY

Louis A. Povinelli *In its Aeropropulsion* 1979 1979 p 445-462 refs (For primary document see N80-10205 01-07)

Avail: NTIS HC A20/MF A01 CSCL 21E

Propulsion needs of high performance military aircraft are discussed. Inlet performance, nozzle performance and cooling, and afterburner performance are covered. It is concluded that nonaxisymmetric nozzles provide cleaner external lines and enhanced maneuverability, but the internal flows are more complex. Swirl afterburners show promise for enhanced performance in the high altitude, low Mach number region. K.L.

N80-11087* National Aeronautics and Space Administration. Lewis Research Center, Cleveland, Ohio.

INFLUENCE OF COOLANT TUBE CURVATURE ON FILM COOLING EFFECTIVENESS AS DETECTED BY INFRARED IMAGERY

S. Stephen Papell, Robert W. Graham, and Richard P. Cagiao Washington Nov. 1979 18 p refs

(NASA-TP-1546; E-066) Avail: NTIS HC A02/MF A01 CSCL 21E

Thermal film cooling footprints observed by infrared imagery from straight, curved, and looped coolant tube geometries are compared. It was hypothesized that the differences in secondary flow and in the turbulence structure of flow through these three tubes should influence the mixing properties between the coolant and the main stream. A flow visualization tunnel, an infrared camera and detector, and a Hilsch tube were employed to test the hypothesis. A.W.H.

N80-12092* National Aeronautics and Space Administration. Lewis Research Center, Cleveland, Ohio.

ENGINE COMPONENT IMPROVEMENT PROGRAM: PERFORMANCE IMPROVEMENT

John E. McAulay 1979 17 p refs Presented at 18th Aerospace Sci. Meeting, Pasadena, Calif., 14-16 Jan. 1980; sponsored by AIAA

(NASA-TM-79304; E-256) Avail: NTIS HC A02/MF A01 CSCL 21E

Fuel consumption of commercial aircraft is considered. Fuel saving and retention components for new production and retrofit of JT9D, JT8D, and CF6 engines are reviewed. The manner in which the performance improvement concepts were selected for development and a summary of the current status of each of the 16 selected concepts are discussed. R.C.T.

N80-13046* National Aeronautics and Space Administration. Lewis Research Center, Cleveland, Ohio.

FLUTTER SPECTRAL MEASUREMENTS USING STATIONARY PRESSURE TRANSDUCERS

A. P. Kurkov 1980 15 p refs Presented at the 25th Annual Intern. Gas Turbine Conf. and the 22d Annual Fluids Eng. Conf., New Orleans, 9-13 Mar. 1980; sponsored by ASME

(NASA-TM-79293; E-237) Avail: NTIS HC A02/MF A01 CSCL 21E

Engine-order sampling was used to eliminate the integral harmonics from the flutter spectra corresponding to a case-mounted static pressure transducer. Using the optical displacement

data, it was demonstrated that the blade-order sampling of pressure data may yield erroneous results due to the interference caused by blade vibration. Two methods are presented which effectively eliminate this interference yielding the blade-pressure-difference spectra. The phase difference between the differential-pressure and the displacement spectra was evaluated. Author

N80-13047* National Aeronautics and Space Administration, Lewis Research Center, Cleveland, Ohio.

ATOMIZING CHARACTERISTICS OF SWIRL CAN COMBUSTOR MODULES WITH SWIRL BLAST FUEL INJECTORS
Robert D. Ingebo 1980 11 p refs Presented at the 25th Annual Intern. Gas Turbine Conf., New Orleans, 9-13 Mar. 1980; sponsored by ASME
(NASA-TM-79297; E-248) Avail: NTIS HC A02/MF A01 CSCL 21E

Cold flow atomization tests of several different designs of swirl can combustor modules were conducted in a 7.6 cm diameter duct at airflow rates (per unit area) of 7.3 to 25.7 g/sq cm sec and water flow rates of 6.3 to 18.9 g/sec. The effect of air and water flow rates on the mean drop size of water sprays produced with the swirl blast fuel injectors were determined. Also, from these data it was possible to determine the effect of design modifications on the atomizing performance of various fuel injector and air swirler configurations. The trend in atomizing performance, as based on the mean drop size, was then compared with the trends in the production of nitrogen oxides obtained in combustion studies with the same swirl can combustors. It was found that the fuel injector design that gave the best combustor performance in terms of a low NOx emission index also gave the best atomizing performance as characterized by a spray of relatively small mean drop diameter. It was also demonstrated that at constant inlet air stream momentum the nitrogen oxides emission index was found to vary inversely with the square of the mean drop diameter of the spray produced by the different swirl blast fuel injectors. Test conditions were inlet air static pressures of 100,000 to 200,000 N/sq m at an inlet air temperature of 293 K. Author

N80-14121* National Aeronautics and Space Administration, Lewis Research Center, Cleveland, Ohio.

STATIC TEST-STAND PERFORMANCE OF THE YF-102 TURBOFAN ENGINE WITH SEVERAL EXHAUST CONFIGURATIONS FOR THE QUIET SHORT-HAUL RESEARCH AIRCRAFT (QSRA)

Jack G. McArdle, Leonard Homyak, and Allan S. Moore Nov. 1979 62 p
(NASA-TP-1556; E-019) Avail: NTIS HC A04/MF A01 CSCL 21E

The performance of a YF-102 turbofan engine was measured in an outdoor test stand with a bellmouth inlet and seven exhaust-system configurations. The configurations consisted of three separate-flow systems of various fan and core nozzle sizes and four confluent-flow systems of various nozzle sizes and shapes. A computer program provided good estimates of the engine performance and of thrust at maximum rating for each exhaust configuration. The internal performance of two different-shaped core nozzles for confluent-flow configurations was determined to be satisfactory. Pressure and temperature surveys were made with a traversing probe in the exhaust-nozzle flow for some confluent-flow configurations. The survey data at the mixing plane, plus the measured flow rates, were used to calculate the static-pressure variation along the exhaust nozzle length. The computed pressures compared well with experimental wall static-pressure data. External-flow surveys were made, for some confluent-flow configurations, with a large fixed rake at various locations in the exhaust plume. A.R.H.

N80-14123* National Aeronautics and Space Administration, Lewis Research Center, Cleveland, Ohio.

DYNAMIC RESPONSE OF A MACH 2.5 AXISYMMETRIC INLET AND TURBOJET ENGINE WITH A POPPET-VALVE CONTROLLED INLET STABILITY BYPASS SYSTEM WHEN

SUBJECTED TO INTERNAL AND EXTERNAL AIRFLOW TRANSIENTS

Bobby W. Sanders Washington Jan. 1980 102 p refs
(NASA-TP-1531; E-9467) Avail: NTIS HC A06/MF A01 CSCL 21E

The throat of a Mach 2.5 inlet that was attached to a turbojet engine was fitted with a poppet-valve-controlled stability bypass system that was designed to provide a large, stable airflow range. Propulsion system response and stability bypass performance were determined for several transient airflow disturbances, both internal and external. Internal airflow disturbances included reductions in overboard bypass airflow, power lever angle, and primary-nozzle area as well as compressor stall. For reference, data are also included for a conventional, fixed-exit bleed system. The poppet valves greatly increased inlet stability and had no adverse effects on propulsion system performance. Limited unstated-inlet bleed performance data are presented. Author

N80-14124* National Aeronautics and Space Administration, Lewis Research Center, Cleveland, Ohio.

TURBOJET-EXHAUST-NOZZLE SECONDARY-AIRFLOW PUMPING AS AN EXIT CONTROL OF AN INLET-STABILITY BYPASS SYSTEM FOR A MACH 2.5 AXISYMMETRIC MIXED-COMPRESSION INLET

Bobby W. Sanders Jan. 1980 82 p refs
(NASA-TP-1532; E-9468) Avail: NTIS HC A05/MF A01 CSCL 21E

The throat of a Mach 2.5 inlet that was attached to a turbojet engine was fitted with large, porous bleed areas to provide a stability bypass system that would allow a large, stable airflow range. Exhaust-nozzle, secondary-airflow pumping was used as the exit control for the stability bypass airflow. Propulsion system response and stability bypass performance were obtained for several transient airflow disturbances, both internal and external. Internal airflow disturbances included reductions in overboard bypass airflow, power lever angle, and primary-nozzle area, as well as compressor stall. Nozzle secondary pumping as a stability bypass exit control can provide the inlet with a large stability margin with no adverse effects on propulsion system performance. Author

N80-14125* National Aeronautics and Space Administration, Lewis Research Center, Cleveland, Ohio.

EFFECT OF DEGREE OF FUEL VAPORIZATION UPON EMISSIONS FOR A PREMIXED PARTIALLY VAPORIZED COMBUSTION SYSTEM

Larry P. Cooper Jan. 1980 25 p refs
(NASA-TP-1582; E-010) Avail: NTIS HC A02/MF A01 CSCL 21E

An experimental and analytical study of the combustion of partially vaporized fuel-air mixtures was performed to assess the impact of the degree of fuel vaporization upon emissions for a premixing-prevaporizing flametube combustor. Data collected in this study showed near linear increases in nitric oxide emissions with decreasing vaporization at equivalence ratios of 0.6. For equivalence ratios of 0.72, the degree of vaporization had very little impact on nitric oxide emissions. A simple mechanism which accounts for the combustion of liquid droplets in partially vaporized mixtures was found to agree with the measured results with fair accuracy with respect to both trends and magnitudes. Author

N80-14126* National Aeronautics and Space Administration, Lewis Research Center, Cleveland, Ohio.

NASA BROAD-SPECIFICATION FUELS COMBUSTION TECHNOLOGY PROGRAM: STATUS AND DESCRIPTION

James S. Fear 1979 14 p refs Presented at 25th Ann. Intern. Gas Turbine Conf., New Orleans, 9-13 Mar. 1980; sponsored by Am. Soc. of Mech. Engr.
(NASA-TM-79315; E-272) Avail: NTIS HC A02/MF A01 CSCL 21E

The program presented is a contracted effort to evolve and demonstrate the technology required to utilize broad-specification fuels in current and next generation commercial Conventional

Takeoff and Landing aircraft engines, and to verify this technology in full-scale engine tests in 1983. The program consists of three phases: Combustor Concept Screening, Combustor Optimization Testing, and Engine Verification Testing. The development and screening of the combustion system designs for the CF6-80 engine and the JT9D-7 engine, respectively, in high-pressure sector test rigs are reported. M.M.M.

N80-14128* National Aeronautics and Space Administration. Lewis Research Center, Cleveland, Ohio.

LASER-OPTICAL BLADE TIP CLEARANCE MEASUREMENT SYSTEM

John P. Barranger and M. John Ford (Pratt and Whitney Aircraft Group, West Palm Beach, Fla.) 13 Mar. 1979 10 p refs Proposed for presentation at 25th Ann. Intern. Gas Turbine Conf. and the 22d Ann. Fluids Engr. Conf., New Orleans, 9-13 Mar. 1980; sponsored by Am. Soc. of Mech. Engr. (NASA-TM-81376) Avail: NTIS HC A02/MF A01 CSCL 21E

A laser-optical measurement system was developed to measure single blade tip clearances and average blade tip clearances between a rotor and its gas path seal in rotating component rigs and complete engines. The system is applicable to fan, compressor and turbine blade tip clearance measurements. The engine mounted probe is particularly suitable for operation in the extreme turbine environment. The measurement system consists of an optical subsystem, an electronic subsystem and a computing and graphic terminal. Bench tests and environmental tests were conducted to confirm operation at temperatures, pressures, and vibration levels typically encountered in an operating gas turbine engine. DOE

N80-15127* National Aeronautics and Space Administration. Lewis Research Center, Cleveland, Ohio.

QUIET POWERED-LIFT PROPULSION

1979 426 p refs Conf. held at Cleveland, Ohio, 14-15 Nov. 1978 (NASA-CP-2077; E-9906) Avail: NTIS HC A19/MF A01 CSCL 21E

Latest results of programs exploring new propulsion technology for powered-lift aircraft systems are presented. Topics discussed include results from the 'quiet clean short-haul experimental engine' program and progress reports on the 'quiet short-haul research aircraft' and 'tilt-rotor research aircraft' programs. In addition to these NASA programs, the Air Force AMST YC 14 and YC 15 programs were reviewed. R.E.S.

N80-15128* National Aeronautics and Space Administration. Lewis Research Center, Cleveland, Ohio.

DIRECT INTEGRATION OF TRANSIENT ROTOR DYNAMICS

Albert F. Kascak Washington Jan. 1980 23 p refs (NASA-TP-1597; AVRADCOM-TR-79-42; E-101) Avail: NTIS HC A02/MF A01 CSCL 21E

An implicit method was developed for integrating the equations of motion for a lumped mass model of a rotor dynamics system. As an aside, a closed form solution to the short bearing theory was also developed for a damper with arbitrary motion. The major conclusions are that the method is numerically stable and that the computation time is proportional to the number of elements in the rotor dynamics model rather than to the cube of the number. This computer code allowed the simulation of a complex rotor bearing system experiencing nonlinear transient motion and displayed the vast amount of results in an easily understood motion picture format - a 10 minute, 16 millimeter, color, sound motion picture supplement. An example problem with 19 mass elements in the rotor dynamics model took 0.7 second of central processing unit time per time step on an IBM 360-67 computer in a time sharing mode. R.C.T.

N80-15132* National Aeronautics and Space Administration. Lewis Research Center, Cleveland, Ohio.

COMPUTER SIMULATION OF ENGINE SYSTEMS

L. H. Fishback 1980 26 p refs Presented at the 18th Aerospace Sci. Meeting, Pasadena, Calif., 14-16 Jan. 1980; sponsored by AIAA (NASA-TM-79290; E-234) Avail: NTIS HC A03/MF A01 CSCL 21E

The use of computerized simulations of the steady state and transient performance of jet engines throughout the flight regime is discussed. In addition, installation effects on thrust and specific fuel consumption is accounted for as well as engine weight, dimensions and cost. The availability throughout the government and industry of analytical methods for calculating these quantities are pointed out. M.M.M.

N80-15133* National Aeronautics and Space Administration. Lewis Research Center, Cleveland, Ohio.

IMPACT OF NEW INSTRUMENTATION ON ADVANCED TURBINE RESEARCH

Robert W. Graham Mar. 1980 25 p refs Proposed for presentation at the 1980 Spring Ann. Meeting, New Orleans, 5-13 Mar. 1980; sponsored by ASME (NASA-TM-79301; E-251) Avail: NTIS HC A02/MF A01 CSCL 21E

A description is presented of an orderly test program that progresses from the simplest stationary geometry to the more complex, three dimensional, rotating turbine stage. The instrumentation requirements for this evolution of testing are described. The heat transfer instrumentation is emphasized. Recent progress made in devising new measurement techniques has greatly improved the development and confirmation of more accurate analytical methods for the prediction of turbine performance and heat transfer. However, there remain challenging requirements for novel measurement techniques that could advance the future research to be done in rotating blade rows of turbomachines. M.M.M.

N80-15134* National Aeronautics and Space Administration. Lewis Research Center, Cleveland, Ohio.

AN ANALYTICAL AND EXPERIMENTAL STUDY OF A SHORT S-SHAPED SUBSONIC DIFFUSER OF A SUPERSONIC INLET

Harvey E. Neumann, Louis A. Povinelli, and Robert E. Coltrin 1980 14 p refs Presented at 18th Aerospace Sci. Meeting, Pasadena, Calif., 14-16 Jan 1980; sponsored by AIAA (NASA-TM-81406; E-320) Avail: NTIS HC A02/MF A01 CSCL 21E

A subscale HIMAT forebody and inlet was investigated over a range of Mach numbers to 1.4. The inlet exhibited a transitory separation within the diffuser but steady state data indicated reattachment at the diffuser exit. A finite difference procedure for turbulent compressible flow in axisymmetric ducts was used to successfully model the HIMAT duct flow. The analysis technique was further used to estimate the initiation of separation and delineate the steady and unsteady flow regimes in similar S-shaped ducts. R.C.T.

N80-17071* National Aeronautics and Space Administration. Lewis Research Center, Cleveland, Ohio.

AERODYNAMIC PERFORMANCES OF THREE FAN STATOR DESIGNS OPERATING WITH ROTOR HAVING TIP SPEED OF 337 METERS PER SECOND AND PRESSURE RATIO OF 1.54. 1: EXPERIMENTAL PERFORMANCE

Thomas F. Gelder Feb. 1980 108 p refs (NASA-TP-1610; E-136) Avail: NTIS HC A06/MF A01 CSCL 21E

The aerodynamic performances of four stator-blade rows are presented and evaluated. The aerodynamic designs of two of these stators were compromised to reduce noise, a third design was not. On a calculated operating line passing through the design point pressure ratio, the best stator had overall pressure-ratio and efficiency decrements of 0.031 and 0.044, respectively, providing a stage pressure ratio of 1.483 and efficiency of 0.865. The other stators showed some correctable deficiencies due partly to the design compromises for noise. In the end-wall regions blade-element losses were significantly less for the shortest chord studied. Author

N80-18039* National Aeronautics and Space Administration. Lewis Research Center, Cleveland, Ohio.

METHOD AND APPARATUS FOR RAPID THRUST INCREASES IN A TURBOFAN ENGINE Patent

Jack E. Cornett (GE, Cincinnati, Ohio), Ralph C. Corley (GE, Cincinnati, Ohio), Thomas O. Fraley (GE, Cincinnati, Ohio), and Andrew A. Saunders, Jr., inventors (to NASA) (GE, Cincinnati, Ohio) Issued 22 Jan. 1980 9 p Filed 9 Dec. 1977 Sponsored by NASA

(NASA-Case-LEW-12971-1; US-Patent-4,184,327 ; US-Patent-Appl-SN-858936; US-Patent-Class-60-240; US-Patent-Class-60-39.03; US-Patent-Class-60-39.27) Avail: US Patent and Trademark Office CSCL 21E

Upon a landing approach, the normal compressor stator schedule of a fan speed controlled turbofan engine is temporarily varied to substantially close the stators to thereby increase the fuel flow and compressor speed in order to maintain fan speed and thrust. This running of the compressor at an off-design speed substantially reduces the time required to subsequently advance the engine speed to the takeoff thrust level by advancing the throttle and opening the compressor stators.

Official Gazette of the U.S. Patent and Trademark Office

N80-18043* National Aeronautics and Space Administration. Lewis Research Center, Cleveland, Ohio.

AEROPROPULSION IN YEAR 2000

Richard J. Weber 1980 18 p refs Proposed for presentation at Global Technol. 2000, the 1980 Intern. Meeting of the Am. Inst. of Aeron. and Astronautics, Baltimore, 5-11 May 1980 21A

A sampling of probable future engine types, such as convertible engines for helicopters, turboprops for fuel-conservative airliners, and variable-cycle engines for supersonic transports are presented. Related technology improvements in propellers, materials, noise suppression, etc. are reviewed R.E.S.

N80-19110* National Aeronautics and Space Administration. Lewis Research Center, Cleveland, Ohio.

PRELIMINARY STUDY OF VTO THRUST REQUIREMENTS FOR A V/STOL AIRCRAFT WITH LIFT PLUS LIFT/CRUISE PROPULSION

George E. Turney and John L. Allen Feb. 1980 23 p refs (NASA-TM-81429; E-351) Avail: NTIS HC A02/MF A01 CSCL 21E

A preliminary assessment was made of the VTO thrust requirements for a supersonic (Type B) aircraft with a Lift plus Lift/Cruise propulsion system. A baseline aircraft with a takeoff gross weight (TOGW) of 13 608 kg (30,000 lb) was assumed. Pitch, roll, and yaw control thrusts (i.e., the thrusts needed for aircraft attitude control in the flight hover mode) were estimated based on a specified set of maneuver acceleration requirements for V/STOL aircraft. Other effects (such as installation losses, suckdown, reingestion, etc.), which add to the thrust requirements for VTO were also estimated. For the baseline aircraft, the excess thrust required for attitude control of the aircraft during VTO and flight hover was estimated to range from 36.9 to 50.9 percent of the TOGW. It was concluded that the total thrust requirements for the aircraft/propulsion system are large and significant. In order to achieve the performance expected of this aircraft/propulsion system, reductions must be made in the excess thrust requirements. J.M.S.

N80-20272* National Aeronautics and Space Administration. Lewis Research Center, Cleveland, Ohio.

EFFECT OF WATER INJECTION AND OFF SCHEDULING OF VARIABLE INLET GUIDE VANES, GAS GENERATOR SPEED AND POWER TURBINE NOZZLE ANGLE ON THE PERFORMANCE OF AN AUTOMOTIVE GAS TURBINE ENGINE

Edward L. Warren Mar. 1980 35 p (Contract EC-77-A-31-1040) (NASA-TM-81415; E-333; DOE/NASA/1040-80/10) Avail: NTIS HC A03/MF A01 CSCL 21E

The Chrysler/ERDA baseline automotive gas turbine engine was used to experimentally determine the power augmentation

and emissions reductions achieved by the effect of variable compressor and power engine geometry, water injection downstream of the compressor, and increases in gas generator speed. Results were dependent on the mode of variable geometry utilization. Over 20 percent increase in power was accompanied by over 5 percent reduction in SFC. A fuel economy improvement of at least 6 percent was estimated for a vehicle with a 75 kW (100 hp) engine which could be augmented to 89 kW (120 hp) relative to an 89 Kw (120 hp) unaugmented engine. Author

N80-20274* National Aeronautics and Space Administration. Lewis Research Center, Cleveland, Ohio.

JT9D-7A (SP) JET ENGINE PERFORMANCE DETERIORATION TRENDS

G. Paul Richter, W. J. Olsson, and N. B. Andersen 1980 24 p ref Presented at the Intern. Aircraft Maintenance Eng. Exhibition and Conf., Dallas, 8-10 Apr. 1980; sponsored by Hamilton Burr Publishing Co. Prepared in cooperation with Pratt and Whitney Aircraft Group, East Hartford, Conn. and Pan American World Airways, Inc., Jamaica, N.Y.

(NASA-TM-81459; E-388) Avail: NTIS HC A02/MF A01 CSCL 21E

The levels, trends, and causes of engine performance deterioration were investigated. A series of installed engine calibrations (both on-the-ground and in-flight) were performed on two new Pan American World Airways 747 SP aircraft. The performance data gathered covered from before the first flight through approximately 1000 flight cycles and 6900 flight hours. To accomplish the calibrations a special instrumentation system for ground testing of installed engines over a broad power range was used along with performing concurrent in-flight engine calibrations under revenue service conditions. Results of the analysis of the data, which provide a better understanding of short and long term performance deterioration of both engines and modules are presented. J.M.S.

N80-20275* National Aeronautics and Space Administration. Lewis Research Center, Cleveland, Ohio.

OPTIMUM SUBSONIC, HIGH-ANGLE-OF-ATTACK NACELLES

Roger W. Luidens, Norbert O. Stockman, and James H. Diedrich [1979] 20 p refs Prepared for the 12th Congr. of the Intern. Council of the Aeron. Sci., Munich, 13-17 Oct. 1980 and the 1980 Aerospace Congr. and Exposition, Los Angeles, 13-16 Oct. 1980; sponsored by the Soc. of Automotive Engr.

(NASA-TM-81491; E-406) Avail: NTIS HC A02/MF A01 CSCL 21E

The optimum design of nacelles that operate over a wide range of aerodynamic conditions and their inlets is described. For low speed operation the optimum internal surface velocity distributions and skin friction distributions are described for three categories of inlets; those with BLC, and those with blow in door slots and retractable slats. At cruise speed the effect of factors that reduce the nacelle external surface area and the local skin friction is illustrated. These factors are cruise Mach number, inlet throat size, fan-face Mach number, and nacelle contour. The interrelation of these cruise speed factors with the design requirements for good low speed performance is discussed. J.M.S.

N80-21323* National Aeronautics and Space Administration. Lewis Research Center, Cleveland, Ohio.

EXPERIMENTAL EVALUATION OF A SPINNING-MODE ACOUSTIC-TREATMENT DESIGN CONCEPT FOR AIRCRAFT INLETS

Laurence J. Heidelberg, Edward J. Rice, and Leonard Homyak Apr. 1980 29 p refs

(NASA-TP-1613; E-185) Avail: NTIS HC A03/MF A01 CSCL 21E

An aircraft-inlet noise suppressor method based on mode cutoff ratio was qualitatively checked by testing a series of liners on a YF-102 turbofan engine. Far-field directivity of the blade passing frequency was used extensively to evaluate the results. The trends and observations of the test data lend much qualitative

support to the design method. The best of the BPF liners attained a suppression at design frequency of 19 dB per unit length-diameter ratio. The best multiple-pure-tone linear attained a remarkable suppression of 65.6 dB per unit length-diameter ratio. Author

N80-21324* National Aeronautics and Space Administration. Lewis Research Center, Cleveland, Ohio.
AERODYNAMIC PERFORMANCES OF THREE FAN STATOR DESIGNS OPERATING WITH ROTOR HAVING TIP SPEED OF 337 METERS PER SECOND AND PRESSURE RATIO OF 1.64. RELATION OF ANALYTICAL CODE CALCULATIONS TO EXPERIMENTAL PERFORMANCE
 Thomas F. Gelder, James F. Schmidt, and Genevieve M. Esqar
 Apr. 1980 53 p refs
 (NASA-TP-1614; E-137) Avail: NTIS HC A04/MF A01 CSCL 21E

A hub-to-shroud and a blade-to-blade internal-flow analysis code, both inviscid and basically subsonic, were used to calculate the flow parameters within four stator-blade rows. The produced ratios of maximum suction-surface velocity to trailing-edge velocity correlated well in the midspan region, with the measured total-parameters over the minimum-loss to near stall operating range for all stators and speeds studied. The potential benefits of a blade designed with the aid of these flow analysis codes are illustrated by a proposed redesign of one of the four stators studied. An overall efficiency improvement of 1.6 points above the peak measured for that stator is predicted for the redesign. Author

N80-21325* National Aeronautics and Space Administration. Lewis Research Center, Cleveland, Ohio.
PERFORMANCE OF SINGLE-STAGE AXIAL-FLOW TRANSONIC COMPRESSOR WITH ROTOR AND STATOR ASPECT RATIOS OF 1.19 AND 1.26 RESPECTIVELY, AND WITH DESIGN PRESSURE RATIO OF 2.05
 Royce D. Moore and Lonnie Reid Washington Apr. 1980 103 p
 (NASA-TP-1659; E-138) Avail: NTIS HC A06/MF A01 CSCL 21E

The overall and blade-element performances of a low-aspect-ratio transonic compressor stage are presented over the stable operating flow range for speeds from 50 to 100 percent of design. At design speed the rotor and stage achieved peak efficiencies of 0.876 and 0.840 at pressure ratios of 2.056 and 2.000, respectively. The stage stall margin at design speed was 10 percent. Author

N80-21326* National Aeronautics and Space Administration. Lewis Research Center, Cleveland, Ohio.
ANALYSIS OF UNCERTAINTIES IN TURBINE METAL TEMPERATURE PREDICTIONS
 Francis S. Stepka Washington Apr. 1980 19 p refs
 (NASA-TP-1593; E-228) Avail: NTIS HC A02/MF A01 CSCL 21E

An analysis was conducted to examine the extent to which various factors influence the accuracy of analytically predicting turbine blade metal temperatures and to determine the uncertainties in these predictions for several accuracies of the influence factors. The advanced turbofan engine gas conditions of 1700 K and 40 atmospheres were considered along with those of a highly instrumented high temperature turbine test rig and a low temperature turbine rig that simulated the engine conditions. The analysis showed that the uncertainty in analytically predicting local blade temperature was as much as 98 K, or 7.6 percent of the metal absolute temperature, with current knowledge of the influence factors. The expected reductions in uncertainties in the influence factors with additional knowledge and tests should reduce the uncertainty in predicting blade metal temperature to 28 K, or 2.1 percent of the metal absolute temperature. Author

N80-21333* National Aeronautics and Space Administration. Lewis Research Center, Cleveland, Ohio.

STEADY-STATE PERFORMANCE OF J85-21 COMPRESSOR AT 100 PERCENT OF DESIGN SPEED WITH AND WITHOUT INTERSTAGE RAKE BLOCKAGE

Roger A. Werner Mar. 1980 36 p refs
 (NASA-TM-81451; E-377) Avail: NTIS HC A03/MF A01 CSCL 21E

Internal compressor instrumentation blockage effects on steady state J85-21 compressor performance at 100 percent of design speed are determined. The blockage was generated by instrumented vanes for the first three compressor stages and by removal rakes for stages 4 to 9. Individual flow passage blockages ranged up to 4.5 percent with the instrumented vanes and up to 22 percent with the removable interstage rakes. At a Reynolds number index of 1.0, pressure ratio and airflow remained unchanged with insertion of the interstage rakes, but efficiency dropped 0.3 percentage point. Compressor exit profiles, compressor stage static pressure rise coefficients, turbine exit temperature, and fuel flow are also presented. J.M.S.

N80-22327* National Aeronautics and Space Administration. Lewis Research Center, Cleveland, Ohio.
GENERAL AVIATION PROPULSION
 Mar 1980 437 p refs Conf held in Cleveland. 28-29 Nov. 1979
 (NASA-CP-2126; E-310) Avail: NTIS HC A19/MF A01 CSCL 21E

Programs exploring and demonstrating new technologies in general aviation propulsion are considered. These programs are the quiet, clean, general aviation turbofan (QCGAT) program, the general aviation turbine engine (GATE) study program, the general aviation propeller technology program, and the advanced rotary, diesel, and reciprocating engine programs. For individual titles, see N80-22328 through N80-22348.

N80-22334* National Aeronautics and Space Administration. Lewis Research Center, Cleveland, Ohio.
SUMMARY OF NASA QCGAT PROGRAM
 Gilbert K. Sievers In its Gen. Aviation Propulsion Mar. 1980 p 189-193 (For primary document see N80-22327 13-07)
 Avail: NTIS HC A19/MF A01 CSCL 21E

The application of large turbofan engine technology to small general aviation turbofan engines to achieve low noise, low emissions, and acceptable fuel consumption is described. R.E.S.

N80-22335* National Aeronautics and Space Administration. Lewis Research Center, Cleveland, Ohio.
NEW OPPORTUNITIES FOR FUTURE, SMALL, GENERAL-AVIATION TURBINE ENGINES (GATE)
 William C. Strack In its Gen. Aviation Propulsion Mar. 1980 p 195-219 refs (For primary document see N80-22327 13-07)
 Avail: NTIS HC A19/MF A01 CSCL 21E

The results of four independent contracted studies to explore the opportunities for future small turbine engines are summarized in a composite overview. Candidate advanced technologies are screened, various cycles and staging arrangements are parametrically evaluated, and optimum conceptual engines are identified for a range of 300 to 600 horsepower applications. Engine improvements of 20 percent in specific fuel consumption and 40 percent in engine cost were forecast using high risk technologies that could be technically demonstrated by 1988. The ensuing economic benefits are in the neighborhood of 20 to 30 percent for twin-engine aircraft currently powered by piston engines. Author

N80-22336* National Aeronautics and Space Administration. Lewis Research Center, Cleveland, Ohio.
AN OVERVIEW OF NASA RESEARCH ON POSITIVE DISPLACEMENT GENERAL-AVIATION ENGINES
 Erwin E. Kempke, Jr. In its Gen. Aviation Propulsion Mar. 1980 p 227-229 (For primary document see N80-22327 13-07)
 Avail: NTIS HC A19/MF A01 CSCL 21E

The research and technology program related to improved

and advanced general aviation engines is described. Current research is directed at the near-term improvement of conventional air-cooled spark-ignition piston engines and at future alternative engine systems based on all-new spark-ignition piston engines, lightweight diesels, and rotary combustion engines that show potential for meeting program goals in the midterm and long-term future. The conventional piston engine activities involve efforts on applying existing technology to improve fuel economy, investigation of key processes to permit leaner operation and reduce drag, and the development of cost effective technology to permit flight at high-altitudes where fuel economy and safety are improved. The advanced engine concepts activities include engine conceptual design studies and enabling technology efforts on the critical or key technology items. R.E.S.

N80-22340* National Aeronautics and Space Administration. Lewis Research Center, Cleveland, Ohio.

POSITIVE DISPLACEMENT TYPE GENERAL-AVIATION ENGINES: SUMMARY AND CONCLUDING REMARKS

Erwin E. Kempke, Jr. *In its Gen. Aviation Propulsion* Mar. 1980 p 313-314 (For primary document see N80-22327 13-07) Avail: NTIS HC A19/MF A01 CSCL 21E

The activities of programs investigating various aspects of aircraft internal combustion engines are briefly described including developments in fuel injection technology, cooling systems and drag reduction, turbocharger technology, and stratified-charge rotary engines. M.G.

N80-22341* National Aeronautics and Space Administration. Lewis Research Center, Cleveland, Ohio.

NASA PROPELLER TECHNOLOGY PROGRAM

Daniel C. Mikkelsen *In its Gen. Aviation Propulsion* Mar. 1980 p 315-325 refs (For primary document see N80-22327 13-07) Avail: NTIS HC A19/MF A01 CSCL 21E

A program on propeller technology applicable to both low and high speed general aviation aircraft is summarized, and the overall program objectives and approach are outlined. M.G.

N80-22344* National Aeronautics and Space Administration. Lewis Research Center, Cleveland, Ohio.

HIGH-SPEED-PROPELLER WIND-TUNNEL AEROACOUSTIC RESULTS

Robert J. Jeracki and James H. Dittmar *In its Gen. Aviation Propulsion* Mar. 1980 p 361-374 refs (For primary document see N80-22327 13-07)

Avail: NTIS HC A19/MF A01 CSCL 21E

Some aerodynamic concepts are presented together with an explanation of how these concepts are applied to advanced propeller design. The unique features of this propulsion system are addressed with emphasis on the design concepts being considered for the high speed turboprop. More particular emphasis is given to the blade sweep, long blade chords, and the large number of blades. R.C.T.

N80-22345* National Aeronautics and Space Administration. Lewis Research Center, Cleveland, Ohio.

ADVANCED PROPELLER AERODYNAMIC ANALYSIS

Lawrence J. Bober *In its Gen. Aviation Propulsion* Mar. 1980 p 375-385 refs (For primary document see N80-22327 13-07) Avail: NTIS HC A19/MF A01 CSCL 21E

The analytical approaches as well as the capabilities of three advanced analyses for predicting propeller aerodynamic performance are presented. It is shown that two of these analyses use a lifting line representation for the propeller blades, and the third uses a lifting surface representation. R.C.T.

N80-22346* National Aeronautics and Space Administration. Lewis Research Center, Cleveland, Ohio.
EFFECT OF THERMAL CYCLING ON ZrO₂-Y₂O₃ THERMAL BARRIER COATINGS

G. McDonald and Robert C. Hendricks 1980 10 p refs Presented at the Intern. Conf. on Met. Coatings, San Diego, Calif., 21-25 Apr. 1980; sponsored by the Am. Vacuum Soc. (NASA-TM-81480; E-416) Avail: NTIS HC A02/MF A01 CSCL 21E

A study was made of the comparative life of plasma sprayed ZrO₂-Y₂O₃ thermal barrier coatings on NiCrAlY bond coats on Rene 41 in short (4 min) and long (57 min) thermal cycles to 1040 C in a 0.3 Mach flame. Short cycles greatly reduced the life of the ceramic coating in terms of time at temperature as compared to longer cycles. Appearance of the failed coating indicated compressive failure. Failure occurred at the bond coat-ceramic coat junction. At heating rates greater than 550 kw/sq m, the calculated coating detachment stress was in the range of literature values of coating adhesive/cohesive strength. Methods are discussed for decreasing the effect of high heating rate by avoiding compressive stress. Author

N80-22350* National Aeronautics and Space Administration. Lewis Research Center, Cleveland, Ohio.

PRELIMINARY STUDY OF ADVANCED TURBOPROP AND TURBOSHAFT ENGINES FOR LIGHT AIRCRAFT

G. Knip, R. M. Plencner, and J. D. Eisenberg Apr. 1980 62 p refs

(NASA-TM-81467; E-397) Avail: NTIS HC A04/MF A01 CSCL 21E

The effects of engine configuration, advanced component technology, compressor pressure ratio and turbine rotor-inlet temperature on such figures of merit as vehicle gross weight, mission fuel, aircraft acquisition cost, operating, cost and life cycle cost are determined for three fixed- and two rotary-wing aircraft. Compared with a current production turboprop, an advanced technology (1988) engine results in a 23 percent decrease in specific fuel consumption. Depending on the figure of merit and the mission, turbine engine cost reductions required to achieve aircraft cost parity with a current spark ignition reciprocating (SIR) engine vary from 0 to 60 percent and from 6 to 74 percent with a hypothetical advanced SIR engine. Compared with a hypothetical turboshaft using currently available technology (1978), an advanced technology (1988) engine installed in a light twin-engine helicopter results in a 16 percent reduction in mission fuel and about 11 percent in most of the other figures of merit. A.R.H.

N80-23310* National Aeronautics and Space Administration. Lewis Research Center, Cleveland, Ohio.

SIGNIFICANCE OF THERMAL CONTACT RESISTANCE IN TWO-LAYER THERMAL-BARRIER-COATED TURBINE VANES

Curt H. Liebert and Raymond E. Gaugler 1980 11 p refs Presented at the Intern. Conf. on Met. Coatings, San Diego, Calif., 21-25 Apr. 1980; sponsored by the Am. Vacuum Soc. (NASA-TM-81483; E-420) Avail: NTIS HC A02/MF A01 CSCL 21E

The importance of thermal contact resistance between layers in heat transfer through two layer, plasma sprayed, thermal barrier coatings applied to turbine vanes was investigated. Results obtained with a system of NiCrAlY bond and yttria stabilized zirconia ceramic show that thermal contact resistance between layers is negligible. These results also verified other studies which showed that thermal contact resistance is negligible for a different coating system of NiCr bond calcia stabilized zirconia ceramic. The zirconia stabilized ceramic thermal conductivity data scatter presented in the literature is ± 20 to ± 10 percent about a curve fit of the data. More accurate predictions of heat transfer and metal wall temperatures are obtained when the thermal conductivity values are used at the ± 20 percent level. E.D.K.

N80-23313* National Aeronautics and Space Administration. Lewis Research Center, Cleveland, Ohio.

DEVELOPMENT OF IMPROVED-DURABILITY PLASMA SPRAYED CERAMIC COATINGS FOR GAS TURBINE ENGINES

Irving E. Sumner and Duane L. Ruckle (Pratt and Whitney Aircraft,

East Hartford, Conn.) 1980 25 p refs. Proposed for presentation at the 16th Joint Propulsion Conf., Hartford, 30 Jun. - 2 Jul. 1980; sponsored by AIAA, ASME and SAE (NASA-TM-81512; E-451) Avail: NTIS HC A02/MF A01 CSCL 21E

As part of a NASA program to reduce fuel consumption of current commercial aircraft engines, methods were investigated for improving the durability of plasma sprayed ceramic coatings for use on vane platforms in the JT9D turbofan engine. Increased durability concepts under evaluation include use of improved strain tolerant microstructures and control of the substrate temperature during coating application. Initial burner rig tests conducted at temperatures of 1010 C (1850 F) indicate that improvements in cyclic life greater than 20:1 over previous ceramic coating systems were achieved. Three plasma sprayed coating systems applied to first stage vane platforms in the high pressure turbine were subjected to a 100-cycle JT9D engine endurance test with only minor damage occurring to the coatings. A.R.H.

N80-23314* National Aeronautics and Space Administration. Lewis Research Center, Cleveland, Ohio.

QCSEE FAN EXHAUST BULK ABSORBER TREATMENT EVALUATION

H. E. Bloomer and Nick E. Samanich 1980 20 p refs. Presented at 6th Aeroacoustics Conf., 4-6 June 1980; sponsored by AIAA (NASA-TM-81498; E-435) Avail: NTIS HC A02/MF A01 CSCL 21E

The acoustic suppression capability of bulk absorber material designed for use in the fan exhaust duct walls of the quiet clean short haul experiment engine (QCSEE UTW) was evaluated. The acoustic suppression to the original design for the engine fan duct which consisted of phased single degree-of-freedom wall treatment was tested with a splitter and also with the splitter removed. Peak suppression was about as predicted with the bulk absorber configuration, however, the broadband characteristics were not attained. Post test inspection revealed surface oil contamination on the bulk material which could have caused the loss in bandwidth suppression. R.C.T.

N80-24315* National Aeronautics and Space Administration. Lewis Research Center, Cleveland, Ohio.

QCSEE UTW ENGINE POWERED-LIFT ACOUSTIC PERFORMANCE

I. J. Loeffler, N. E. Samanich, and H. E. Bloomer 1980 35 p refs. Presented at the 6th Aeroacoustics Conf., Hartford, 4-6 Jun. 1980; sponsored by the AIAA (NASA-TM-81504; E-442) Avail: NTIS HC A03/MF A01 CSCL 21E

Powered-lift acoustic test of the Quiet Clean Short Haul Experimental Engine (QCSEE) under the wing (UTW) engine are reported. Propulsion systems for two powered-lift concepts were designed, fabricated, and tested. In addition to low noise features, the designs included composite structures, gear-driven fans, digital control, and a variable pitch fan (UTW). The UTW engine was tested in a static ground test facility with wing and flap segments to simulate installation on a short haul transport aircraft of the future. Powered-lift acoustic performance of the UTW engine is compared with that of the previously tested and reported QCSEE over-the-wing (OTW) engine. Both engines were slightly above the noise goal but were significantly below current FAA and modern wide-body jet transport levels. The UTW system in the powered-lift mode was penalized by reflected engine noise from the wing and flap system, while the OTW system was benefited by a wing noise shielding effect. J.M.S.

N80-24314* National Aeronautics and Space Administration. Lewis Research Center, Cleveland, Ohio.

COMPARISON OF SEVERAL INFLOW CONTROL DEVICES FOR FLIGHT SIMULATION OF FAN TONE NOISE USING A JT15D-1 ENGINE

J. G. McArdle, W. L. Jones, L. J. Heidelberg, and L. Homyak 1980 45 p refs. Presented at the 6th Aeroacoustics Conf.,

Hartford, 4-6 Jun. 1980; sponsored by AIAA (NASA-TM-81505; E-443) Avail: NTIS HC A02/MF A01 CSCL 21E

To enable accurate simulation of in-flight fan tone noise during ground static tests, four devices intended to reduce inflow disturbances and turbulence were tested with a JT15D-1 turbofan engine. These inflow control devices (ICD's) consisted of honeycomb/screen structures mounted over the engine inlet. The ICD's ranged from 1.6 to 4 fan diameters in size, and differed in shape and fabrication method. All the ICD's significantly reduced the BPF tone in the far-field directivity patterns, but the smallest ICD's apparently introduced propagating modes which could be recognized by additional lobes in the speeds; at supersonic fan tip speed the smallest ICD's had some measurable loss, but the largest had no loss. Data from a typical transducer show that the unsteady inflow distortion modes (turbulence) were eliminated or significantly reduced when either of the ICD's was installed. However, some steady inflow distortion modes remained. A.R.H.

N80-24316* National Aeronautics and Space Administration. Lewis Research Center, Cleveland, Ohio.

ADVANCED COMPONENT TECHNOLOGIES FOR ENERGY-EFFICIENT TURBOFAN ENGINES

Neal T. Saunders 1980 19 p refs. Presented at the 16th Joint Propulsion Conf., Hartford, 30 Jun. - 2 Jul. 1980; cosponsored by AIAA, ASME and SAE (NASA-TM-81507; E-445) Avail: NTIS HC A02/MF A01 CSCL 21E

A cooperative government-industry effort, the Energy Efficient Engine Project, to develop the advanced technology base for future commercial development of a new generation of more fuel conservative turbofan engines for airline use is described. Engine configurations that are dependent upon technology advances in each major engine component are defined and current design and development of the advanced components are included. J.M.S.

N80-25337* National Aeronautics and Space Administration. Lewis Research Center, Cleveland, Ohio.

DESIGN AND COLD-AIR TEST OF SINGLE-STAGE UN-COOLED TURBINE WITH HIGH WORK OUTPUT

Thomas P. Moffitt, Edward M. Szanca, Warren J. Whitney, and Frank P. Behning Jun. 1980 18 p refs (NASA-TP-1680; E-316) Avail: NTIS HC A02/MF A01 CSCL 21E

A solid version of a 50.8 cm single stage core turbine designed for high temperature was tested in cold air over a range of speed and pressure ratio. Design equivalent specific work was 76.84 J/g at an engine turbine tip speed of 579.1 m/sec. At design speed and pressure ratio, the total efficiency of the turbine was 88.5 percent, which is 0.6 point lower than the design value of 89.2 percent. The corresponding mass flow was 4.0 percent greater than design. Author

N80-25338* National Aeronautics and Space Administration. Lewis Research Center, Cleveland, Ohio.

COLD-AIR INVESTIGATION OF A 4 1/2 STAGE TURBINE WITH STAGE-LOADING FACTOR OF 4.66 AND HIGH SPECIFIC WORK OUTPUT. 2: STAGE GROUP PERFORMANCE

Warren J. Whitney, Frank P. Behning, Thomas P. Moffitt, and Glen M. Hotz Jun. 1980 16 p refs (NASA-TP-1688; E-315) Avail: NTIS HC A02/MF A01 CSCL 21E

The stage group performance of a 4 1/2 stage turbine with an average stage loading factor of 4.66 and high specific work output was determined in cold air at design equivalent speed. The four stage turbine configuration produced design equivalent work output with an efficiency of 0.856; a barely discernible difference from the 0.855 obtained for the complete 4 1/2 stage turbine in a previous investigation. The turbine was designed and the procedure embodied the following design features: (1) controlled vortex flow, (2) tailored radial work distribution, and (3) control of the location of the boundary-layer transition point on the airfoil suction surface. The efficiency

forecast for the 4 1/2 stage turbine was 0.886, and the value predicted using a reference method was 0.862. The stage group performance results were used to determine the individual stage efficiencies for the condition at which design 4 1/2 stage work output was obtained. The efficiencies of stages one and four were about 0.020 lower than the predicted value, that of stage two was 0.014 lower, and that of stage three was about equal to the predicted value. Thus all the stages operated reasonably close to their expected performance levels, and the overall (4 1/2 stage) performance was not degraded by any particularly inefficient component. E.R.

N80-25339* National Aeronautics and Space Administration, Lewis Research Center, Cleveland, Ohio.

STATIC AND TRANSIENT PERFORMANCE OF YF-102 ENGINE WITH UP TO 14 PERCENT CORE AIRBLED FOR THE QUIET SHORT-HAUL RESEARCH AIRCRAFT

Jack G. McArdle, Leonard Homyak, and Allan S. Moore Jun. 1980 26 p refs

(NASA-TP-1692) Avail: NTIS HC A02/MF A01 CSCL 21E

An outdoor static test stand was used to measure the steady-state and transient performance of the YF-102 turbofan engine with core airbled. The test configuration included a bellmouth inlet and a confluent-flow exhaust system similar in size to the quiet short-haul research aircraft (QSRA) exhaust system. For the steady-state tests, the engine operated satisfactorily with core bleed up to 14 percent of the core inlet flow. For the transient tests the engine accelerated and decelerated satisfactorily with no core bleed and with core bleed up to 11 percent of the core inlet flow (maximum tested). For some of the tests the core-bleed flow rate was scheduled to vary with fan discharge pressure, to simulate the QSRA bleed requirements. No stability, surge, stall, overtemperature, combustor flameout, or other operating problems were encountered in any of the tests. Steady-state and transient engine performance data are presented in graphs, and fuel-control trajectories for typical transient tests are shown. A.R.H.

N80-26299* National Aeronautics and Space Administration, Lewis Research Center, Cleveland, Ohio.

DURABILITY TESTS OF SOLENOID VALVES FOR DIGITAL ACTUATORS

A. N. Baez Jun. 1980 11 p refs

(NASA-TM-81522; E-466) HC A02/MF A01 CSCL 21E

The durability of various materials used to make solenoid valve poppets and seats was investigated. Six different poppet materials and two seat materials were considered. Each material was tested for over 100 million cycles. Serious damage was found in four kinds of poppet materials tested. Less damage was evident in an aluminum poppet and in graphite composite poppet. The graphite composite poppet in combination with a Vespel seat was considered the most promising combination for use in digital electronic controls for gas turbine engines. E.D.K.

N80-27362* National Aeronautics and Space Administration, Lewis Research Center, Cleveland, Ohio.

COMPOSITE WALL CONCEPT FOR HIGH TEMPERATURE TURBINE SHROUDS: HEAT TRANSFER ANALYSIS

Francis S. Stepka and Lawrence P. Ludwig 1980 17 p refs Presented at Aerospace Congr., Los Angeles, 13-16 Oct. 1980; sponsored by Soc. of Automotive Engr.

(NASA-TM-81539; E-402) Avail: NTIS HC A02/MF A01 CSCL 21E

A heat transfer analysis was made of a composite wall shroud consisting of a ceramic thermal barrier layer bonded to a porous metal layer which, in turn, is bonded to a metal base. The porous metal layer serves to mitigate the strain differences between the ceramic and the metal base. Various combinations of ceramic and porous metal layer thicknesses and of porous metal densities and thermal conductivities were investigated to determine the layer thicknesses required to maintain a limiting temperature in the porous metal layer. Analysis showed that the composite wall offered significant air cooling flow reductions compared to an all impingement air cooled, all metal shroud. Author

N80-27363* National Aeronautics and Space Administration, Lewis Research Center, Cleveland, Ohio.

NUMERICAL CALCULATION OF TRANSONIC AXIAL TURBOMACHINERY FLOWS

Djordje S. Dulikravich 1980 10 p refs Presented at 7th Intern. Conf. on Numerical Methods in Fluid Dyn., Stanford, Calif., 23-27 Jun. 1980; sponsored by NASA, AFOSR, NSF, and ONR (NASA-TM-81544; E-500) Avail: NTIS HC A02/MF A01 CSCL 21E

A numerical method and the results of a computer program are presented for solving an exact, three dimensional, full potential equation that models rotating and nonrotating inviscid, absolutely irrotational, homentropic flows. Besides calculating the flows through an arbitrarily shaped rotor or stator blade row mounted on an axisymmetric hub and confined in an axisymmetric duct, the computer program is also capable of analyzing flow fields about arbitrarily shaped wing body combinations, propellers, helicopter rotors in hover, and wind turbine rotors. The governing equation is solved numerically in a fully conservative form by using an artificial time concept, a finite volume technique, rotated type dependent differencing, successive line overrelaxation, and sequential boundary conforming grid refinement. An artificial viscosity is added in fully conservative form, and an initial guess for the potential field is applied, as determined by a two dimensional cascade analysis. Author

N80-27365* National Aeronautics and Space Administration, Lewis Research Center, Cleveland, Ohio.

LOSS MODEL FOR OFF-DESIGN PERFORMANCE ANALYSIS OF RADIAL TURBINES WITH PIVOTING-VANE, VARIABLE-AREA STATORS

Peter L. Meitner and Arthur J. Glassman 1980 22 p refs Proposed for presentation at the Aerospace Congr., Los Angeles, 13-16 Oct. 1970; sponsored by the Society of Automotive Engineers. Prepared in cooperation with Army Aviation Research and Development Command, Cleveland

(NASA-TM-81532; AVRADCOM-TR-80-C-15; E-455) Avail: NTIS HC A02/MF A01 CSCL 21E

An off-design performance loss model is developed for variable-area (pivoted vane) radial turbines. The variation in stator loss with stator area is determined by a viscous loss model while the variation in rotor loss due to stator area variation (for no stator end-clearance gap) is determined through analytical matching of experimental data. An incidence loss model is also based on matching of the experimental data. A stator vane end-clearance leakage model is developed and sample calculations are made to show the predicted effects of stator vane end-clearance leakage on performance. Author

N80-28352* National Aeronautics and Space Administration, Lewis Research Center, Cleveland, Ohio.

OFF-DESIGN CORRELATION FOR LOSSES DUE TO PART-SPAN DAMPERS ON TRANSONIC ROTORS

William B. Roberts, James E. Crouse, and Donald M. Sandercock Jul. 1980 24 p refs

(NASA-TP-1693; E-309) Avail: NTIS HC A02/MF A01 CSCL 21E

Experimental data from 10 transonic fan rotors were used to correlate losses created by part-span dampers located near the midchord position on the rotor blades. The design tip speed of these rotors varied from 419 to 425 m/sec, and the design pressure ratio varied from 1.6 to 2.0. Additional loss caused by the dampers for operating conditions between 50 and 100 percent of design speed were correlated with relevant aerodynamic and geometric parameters. The resulting correlation predicts the variation of total-pressure-loss coefficient in the damper region to a good approximation. Author

N80-29300* National Aeronautics and Space Administration, Lewis Research Center, Cleveland, Ohio.

AIRCRAFT RESEARCH AND TECHNOLOGY FOR FUTURE FUELS

Jul. 1980 229 p refs Symp. held in Cleveland, Ohio, 16-17 Apr. 1980

(NASA-CP-2146; E-398) Avail: NTIS HC A11/MF A01 CSCL

21E

The potential characteristics of future aviation turbine fuels and the property effects of these fuels on propulsion system components are examined. The topics that are discussed include jet fuel supply and demand trends, the effects of refining variables on fuel properties, shale oil processing, the characteristics of broadened property fuels, the effects of fuel property variations on combustor and fuel system performance, and combustor and fuel system technology for broadened property fuels. For individual titles, see N80-29301 through N80-29330

N80-29301* National Aeronautics and Space Administration, Lewis Research Center, Cleveland, Ohio.

FUTURE AVIATION FUELS OVERVIEW

Gregory M. Reck *In its Aircraft Res. and Technol. for Future Fuels* Jul. 1980 p 1-4 refs (For primary document see N80-29300 20-07)

Avail: NTIS HC A11/MF A01 CSCL 21D

The outlook for aviation fuels through the turn of the century is briefly discussed and the general objectives of the NASA Lewis Alternative Aviation Fuels Research Project are outlined. The NASA program involves the evaluation of potential characteristics of future jet aircraft fuels, the determination of the effects of those fuels on engine and fuel system components, and the development of a component technology to use those fuels.

M.G.

N80-29309* National Aeronautics and Space Administration, Lewis Research Center, Cleveland, Ohio.

FUELS CHARACTERIZATION STUDIES

Gary T. Seng, Albert C. Antoine, and Francisco J. Flores *In its Aircraft Res. and Technol. for Future Fuels* Jul. 1980 p 59-65 refs (For primary document see N80-29300 20-07)

Avail: NTIS HC A11/MF A01 CSCL 21D

Current analytical techniques used in the characterization of broadened properties fuels are briefly described. Included are liquid chromatography, gas chromatography, and nuclear magnetic resonance spectroscopy. High performance liquid chromatographic ground-type methods development is being approached from several directions, including aromatic fraction standards development and the elimination of standards through removal or partial removal of the alkene and aromatic fractions or through the use of whole fuel refractive index values. More sensitive methods for alkene determinations using an ultraviolet-visible detector are also being pursued. Some of the more successful gas chromatographic physical property determinations for petroleum derived fuels are the distillation curve (simulated distillation), heat of combustion, hydrogen content, API gravity, viscosity, flash point, and (to a lesser extent) freezing point.

M.G.

N80-29310* National Aeronautics and Space Administration, Lewis Research Center, Cleveland, Ohio.

COMBUSTION TECHNOLOGY OVERVIEW

Richard W. Niedzwiecki *In its Aircraft Res. and Technol. for Future Fuels* Jul. 1980 p 67-73 refs (For primary document see N80-29300 20-07)

Avail: NTIS HC A11/MF A01 CSCL 21B

An overview of combustor technology developments required for use of broadened property fuels in jet aircraft is presented. The intent of current investigations is to determine the extent to which fuel properties can be varied, to obtain a data base of combustion - fuel quality effects, and to determine the trade-offs associated with broadened property fuels. Subcomponents of in-service combustors such as fuel injectors and liners, as well as air distributions and stoichiometry, are being altered to determine the extent to which fuel flexibility can be extended. Finally, very advanced technology consisting of new combustor concepts is being evolved to optimize the fuel flexibility of gas turbine combustors.

M.G.

N80-29313* National Aeronautics and Space Administration, Lewis Research Center, Cleveland, Ohio.

NASA BROADENED-SPECIFICATION FUELS COMBUS-

TION TECHNOLOGY PROGRAM

James S. Fear *In its Aircraft Res. and Technol. for Future Fuels* Jul. 1980 p 95-98 (For primary document see N80-29300 20-07)

Avail: NTIS HC A11/MF A01 CSCL 21B

The broadened-Specification Fuels Combustion Technology program's purpose is to evolve and demonstrate the technology required to enable current and next generation high-thrust, high-bypass-ratio turbofan engines to use fuels with broadened properties and to verify the evolved technology in full scale engine tests. The three phases of the program are combustor concept screening, combustor optimization testing, and engine verification testing. Constraints for designing combustion systems are outlined and problems to be expected in the use of broadened properties fuels are listed.

E D K

N80-29317* National Aeronautics and Space Administration, Lewis Research Center, Cleveland, Ohio.

FUELS RESEARCH: COMBUSTION EFFECTS OVERVIEW

John B. Haggard, Jr. *In its Aircraft Res. and Technol. for Future Fuels* Jul. 1980 p 115-116 (For primary document see N80-29300 20-07)

Avail: NTIS HC A11/MF A01 CSCL 21B

The effects of broadened property fuels on gas turbine combustors were assessed. Those physical and chemical properties of fuels that affect aviation gas turbine combustion were isolated and identified. Combustion sensitivity to variations in particular fuel properties were determined. Advanced combustion concepts and subcomponents that could lessen the effect of using broadened property fuels were also identified.

R.C.T.

N80-29319* National Aeronautics and Space Administration, Lewis Research Center, Cleveland, Ohio.

ANTIMISTING KEROSENE

Harold W. Schmidt *In its Aircraft Res. and Technol. for Future Fuels* Jul. 1980 p 125-130 (For primary document see N80-29300 20-07)

Avail: NTIS HC A11/MF A01 CSCL 21D

The antimisting additive ((FM-9) was tested in terms of its propulsion systems performance. The effect of the additive on engine operation was evaluated, operating problems were identified, the adaptability of engines to antimisting kerosene was assessed, and the potential viability of this fuel for use in present and future fan jet engines was determined.

R.C.T.

N80-29323* National Aeronautics and Space Administration, Lewis Research Center, Cleveland, Ohio.

PRELIMINARY STUDIES OF COMBUSTOR SENSITIVITY TO ALTERNATIVE FUELS

Francis M. Humanik *In its Aircraft Res. and Technol. for Future Fuels* Jul. 1980 p 153-160 refs (For primary document see N80-29300 20-07)

Avail: NTIS HC A11/MF A01 CSCL 21B

Combustion problems associated with using alternative fuel; ground power and aeropropulsion applications were studied. Rectangular sections designed to simulate large annular combustor test conditions were examined. The effects of using alternative fuels with reduced hydrogen content, increased aromatic content, and a broad variation in fuel property characteristics were also studied. Data of special interest were collected which include: flame radiation characteristics in the various combustor zones; the corresponding increase in liner temperature from increased radiant heat flux; the effect of fuel bound nitrogen on oxides of nitrogen (NO sub x) emissions; and the overall total effect of fuel variations on exhaust emissions.

R.C.T.

N80-29324* National Aeronautics and Space Administration, Lewis Research Center, Cleveland, Ohio.

FUELS RESEARCH: FUEL THERMAL STABILITY OVERVIEW

Stephen M. Cohen *In its Aircraft Res. and Technol. for Future Fuels* Jul. 1980 p 161-168 ref (For primary document see

N80-29300 20-07)
Avail NTIS HC A11/MF A01 CSCL 21B

Alternative fuels or crude supplies are examined with respect to satisfying aviation fuel needs for the next 50 years. The thermal stability of potential future fuels is discussed and the effects of these characteristics on aircraft fuel systems are examined. Advanced fuel system technology and design guidelines for future fuels with lower thermal stability are reported. R.C.T.

N80-29328*# National Aeronautics and Space Administration
Lewis Research Center, Cleveland, Ohio

FUEL SYSTEM TECHNOLOGY OVERVIEW

Robert Friedman / In its Aircraft Res and Technol for Future Fuels Jul 1980 p 195-203 refs (For primary document see N80-29300 20-07)

Avail NTIS HC A11/MF A01 CSCL 21E

Fuel system research and technology studies are being conducted to investigate the correlations and interactions of aircraft fuel system design and environment with applicable characteristics of the fuel. Topics include: (1) analysis of in-flight fuel temperatures; (2) fuel systems for high freezing point fuels; (3) experimental study of low temperature pumpability; (4) full scale fuel tank simulation; and (5) rapid freezing point measurement. E.D.K.

N80-29332*# National Aeronautics and Space Administration
Lewis Research Center, Cleveland, Ohio

INVESTIGATION OF PERFORMANCE DETERIORATION OF THE CF6/JT9D, HIGH-BYPASS RATIO TURBOFAN ENGINES

Joseph A. Ziemianski and Charles M. Mehalic 1980 22 p refs Proposed for presentation at the 56th AGARD Propulsion and Energetics Symp on Turbine Engine Testing, Turin, 29 Sep - 3 Oct 1980 and SAE Aerospace Congr., Los Angeles, 13-16 Oct. 1980

(NASA-TM-81552; E-511) Avail: NTIS HC A02/MF A01 CSCL 21E

The aircraft energy efficiency program within NASA is developing technology required to improve the fuel efficiency of commercial subsonic transport aircraft. One segment of this program includes engine diagnostics which is directed toward determining the sources and causes of performance deterioration in the Pratt and Whitney Aircraft JT9D and General Electric CF6 high-bypass ratio turbofan engines and developing technology for minimizing the performance losses. Results of engine performance deterioration investigations based on historical data, special engine tests, and specific tests to define the influence of flight loads and component clearances on performance are presented. The results of analysis of several damage mechanisms that contribute to performance deterioration such as blade tip rubs, airfoil surface roughness and erosion, and thermal distortion are also included. The significance of these damage mechanisms on component and overall engine performance is discussed. A.R.H.

N80-29333*# National Aeronautics and Space Administration
Lewis Research Center, Cleveland, Ohio

DESCRIPTION OF THE WARM CORE TURBINE FACILITY RECENTLY INSTALLED AT NASA LEWIS RESEARCH CENTER

W. J. Whitney, R. G. Stabe, and T. P. Moffitt 1980 18 p refs Proposed for presentation at Aerospace Congr., Los Angeles, 13-16 Oct. 1980; sponsored by Am. Soc. of Automotive Engrs. (NASA-TM-81562; E-524) Avail: NTIS HC A02/MF A01 CSCL 21E

The two net facilities were installed and operated at their design, or rated conditions. The important feature of both of these facilities is that the ratio of turbine inlet temperature to coolant temperature encountered in high temperature engines can be duplicated at moderate turbine inlet temperature. The limits of the facilities with regard to maximum temperature, maximum pressure, maximum mass flow rate, turbine size, and dynamometer torque-speed characteristics are discussed. Author

N80-29358*# National Aeronautics and Space Administration
Lewis Research Center, Cleveland, Ohio

STATE-OF-THE-ART SIALON MATERIALS

Sunil Dutta / In AGARD Ceram. for Turbine Eng. Appl. Mar. 1980 15 p refs (For primary document see N80-29342 20-07) Avail: NTIS HC A16/MF A01 CSCL 21E

The state of the art of SIALONs is examined. The review includes work on phase relations, crystal structure, synthesis, fabrication, and properties of various SIALONs. The essential features of compositions, fabrication methods, and microstructure are reviewed. High temperature flexure strength, creep, fracture toughness, oxidation, and thermal shock resistance are discussed. These data are compared to those for some currently produced silicon nitride ceramics to assess the potential of SIALON materials for use in advanced gas turbine engines. E.D.K.

N80-31399*# National Aeronautics and Space Administration
Lewis Research Center, Cleveland, Ohio

REVERSE THRUST PERFORMANCE OF THE QCSEE VARIABLE PITCH TURBOFAN ENGINE

N. E. Samanich, D. C. Reemsnyder, and H. E. Blodmer 1980 57 p refs Presented at the Aerospace Congr., Los Angeles, 13-16 Oct. 1980; sponsored by Am. Soc. of Automotive Engr. (NASA-TM-81558; E-519) Avail: NTIS HC A04/MF A01 CSCL 21E

Results of steady state reverse and forward to reverse thrust transient performance tests are presented. The original quiet, clean, short haul, experimental engine four segment variable fan nozzle was retested in reverse and compared with a continuous, 30 deg half angle conical exlet. Data indicated that the significantly more stable, higher pressure recovery flow with the fixed 30 deg exlet resulted in lower engine vibrations, lower fan blade stress, and approximately a 20 percent improvement in reverse thrust. Objective reverse thrust of 35 percent of takeoff thrust was reached. Thrust response of less than 1.5 sec was achieved for the approach and the takeoff to reverse thrust transients. Author

N80-31400*# National Aeronautics and Space Administration
Lewis Research Center, Cleveland, Ohio

AN EXPERIMENTAL EVALUATION OF THE PERFORMANCE DEFICIT OF AN AIRCRAFT ENGINE STARTER TURBINE

Jeffrey E. Hass, Richard J. Roelke, and Paul Hermann (Sunstrand Corp., Rockford, Ill.) 1980 21 p ref Presented at the Aerospace Congr., Los Angeles, 13-16 Oct. 1980; sponsored by Am. Soc. of Automotive Engr.

(NASA-TM-81571; E-539) Avail: NTIS HC A02/MF A01 CSCL 21E

An experimental investigation was made to determine the reasons for the low aerodynamic performance of a 13.5 centimeter tip diameter aircraft engine starter turbine. The investigation consisted of an evaluation of both the stator and the stage. An approximate ten percent improvement in turbine efficiency was obtained when the honeycomb shroud over the rotor blade tips was filled to obtain a solid shroud surface. Author

N80-31401*# National Aeronautics and Space Administration
Lewis Research Center, Cleveland, Ohio

THE NASA HIGH-SPEED TURBOPROP PROGRAM

James F. Dugan, Brent A. Miller, Edwin J. Graber, and David A. Sagerer 1980 48 p refs Presented at the Aerospace Congr., Los Angeles, 13-16 Oct. 1980; sponsored by the Am. Soc. of Automotive Engr.

(NASA-TM-81561; E-452) Avail: NTIS HC A03/MF A01 CSCL 01C

Technology readiness for Mach 0.7 to 0.8 turboprop powered aircraft with the potential for fuel savings and DOC reductions of up to 30 and 15 percent respectively relative to current in-service aircraft is addressed. The areas of propeller aeroacoustics, propeller structures, turboprop installed performance, aircraft cabin environment, and turboprop engine and aircraft studies are emphasized. Large scale propeller characteristics and high speed propeller flight research tests using a modified testbed aircraft are also considered. J.M.S.

N80-31402* National Aeronautics and Space Administration. Lewis Research Center, Cleveland, Ohio.

IMPROVED COMPONENTS FOR ENGINE FUEL SAVINGS
Robert J. Antl and John E. McAulay 1980 33 p refs Presented at the Aerospace Congr., Los Angeles, 13-16 Oct. 1980; sponsored by Am. Soc. of Automotive Engr.
(NASA-TM-81577; E-506) Avail: NTIS HC A03/MF A01 CSCL 21E

The Engine Component Improvement (ECI) Project formulated to address near term improvements for current engines is described with emphasis on the development of component technologies to reduce the fuel consumption of CF6, JT9D, and JT8D engines. The technical and economical acceptability and the fuel saving systems to relate the variation of cost on blade size. Geometries typical of blade designs at 24, 30, 36 and 42 blades per disc were used. The impact of individual process yield factors on costs was also assessed as well as effects of process parameters, raw materials, labor rates and consumable items. A R H

N80-32384* National Aeronautics and Space Administration. Lewis Research Center, Cleveland, Ohio.

PERFORMANCE DETERIORATION OF COMMERCIAL HIGH-BYPASS RATIO TURBOFAN ENGINES

Charles M. Mehlic and Joseph A. Ziemiński 1980 30 p refs Presented at SAE Aerospace Congr., Los Angeles, 13-16 Oct. 1980 and at the 56th AGARD Propulsion and Energetics Symp. on Turbine Engine Testing, Turin, 29 Sep. - 3 Oct. 1980 Revised
(NASA-TM-81552-Rev; E-511-Rev) Avail: NTIS HC A03/MF A01 CSCL 21E

The results of engine performance deterioration investigations based on historical data, special engine tests, and specific tests to define the influence of flight loads and component clearances on performance are presented. The results of analyses of several damage mechanisms that contribute to performance deterioration such as blade tip rubs, airfoil surface roughness and erosion, and thermal distortion are also included. The significance of these damage mechanisms on component and overall engine performance is discussed. E.D.K.

N80-32395* National Aeronautics and Space Administration. Lewis Research Center, Cleveland, Ohio.

THE ENERGY EFFICIENT ENGINE PROJECT Status Report

Lawrence E. Macioce, John W. Schaefer, and Neal T. Saunders 1980 42 p refs Presented at the Aerospace Congr., Los Angeles, 13-16 Oct. 1980
(NASA-TM-81566; E-531) Avail: NTIS HC A03/MF A01 CSCL 21E

The Energy Efficient Engine Project is directed at providing, by 1984, the advanced technologies which could be used for a generation of fuel conservative turbofan engines. The project is conducted through contracts with the General Electric Company and Pratt and Whitney Aircraft. The scope of the entire project and the current status of these efforts are summarized. A description of the preliminary designs of the fully developed engines is included and the potential benefits of these advanced engines, as well as highlights of some of the component technology efforts conducted to date, are discussed. E.D.K.

N80-32396* National Aeronautics and Space Administration. Lewis Research Center, Cleveland, Ohio.

LOW-PRESSURE PERFORMANCE OF ANNULAR, HIGH-PRESSURE (40 ATM) HIGH-TEMPERATURE (2480 K) COMBUSTION SYSTEM

Jerrold D. Wear Washington Sep. 1980 23 p refs
(NASA-TP-1713; E-372) Avail: NTIS HC A02/MF A01 CSCL 21E

Experimental tests were conducted to develop a combustion system for a 40 atmosphere pressure, 2480 K exhaust gas temperature, turbine cooling facility. The tests were conducted in an existing facility with a maximum pressure capability of 10 atmospheres and where inlet air temperatures as high as 894 K could be attained. Exhaust gas temperatures were as high as 2365 K. Combustion efficiencies were about 100 percent

over a fuel air ratio range of 0.016 to 0.056. Combustion efficiency decreased at leaner and richer ratios when the inlet air temperature was 589 K. Data are presented that show the effect of fuel air ratio and inlet air temperature on liner metal temperature. Isothermal system pressure loss as a function of diffuser inlet Mach number is also presented. Data included exhaust gas pattern factors, unburned hydrocarbon, carbon monoxide, and oxides of nitrogen emission index values, and smoke numbers. Author

N80-33410* National Aeronautics and Space Administration. Lewis Research Center, Cleveland, Ohio.

EXPERIMENTAL PERFORMANCE AND ANALYSIS OF 15.04-CENTIMETER-TIP-DIAMETER, RADIAL-INFLOW TURBINE WITH WORK FACTOR OF 1.126 AND THICK BLADING

Kerry L. McLallin and Jeffrey E. Haas Oct 1980 21 p refs Prepared in cooperation with Army Aviation Research and Development Command, St. Louis, Mo.
(NASA-TP-1730; E-391; AVRADCOM-TR-80-09) Avail: NTIS HC A02/MF A01 CSCL 21E

The aerodynamic design, the performance, and an internal loss breakdown were examined for a 15.04 cm tip diameter, radial-inflow turbine. The design application was to drive a two stage, 10 to 1 pressure ratio compressor with a mass flow of 0.952 kg/sec and a rotational speed of 70,000 rpm. The turbine inlet temperature was 1478 K, and the turbine was designed with blades thick enough for internal cooling passages. The rotor tip diameter was limited to 86 percent of optimum in order to obtain a reduced tip speed design. The turbine was fabricated with solid, uncooled blading and tested in air at nominal inlet pressure and temperature of 1.379 x 10000 N/sq m and 322.2 K, respectively. Results indicated the turbine total efficiency to be 5.3 points less than design. Analysis of these results has indicated the deficit in performance to be due to stator secondary flow losses, vaneless space surface friction losses, and trailing edge wake mixing losses. R.C.T.

A80-10033 * Identification and dual adaptive control of a turbojet engine. W. Merrill (NASA, Lewis Research Center, Cleveland, Ohio) and G. Leininger (Toledo, University, Toledo, Ohio), *International Federation of Automatic Control, Symposium on Identification and System Parameter Estimation, 5th, Darmstadt, West Germany, Sept. 24-28, 1979, Paper, 8 p, 14 refs.* Grant No. NGR-36-010-024.

The objective of this paper is to utilize the design methods of modern control theory to realize a 'dual-adaptive' feedback control unit for a highly non-linear single spool airbreathing turbojet engine. Using a very detailed and accurate simulation of the non-linear engine as the data source, linear operating point models of unspecified dimension are identified. Feedback control laws are designed at each operating point for a prespecified set of sampling rates using sampled-data output regulator theory. The control system sampling rate is determined by an adaptive sampling algorithm in correspondence with turbojet engine performance. The result is a 'dual-adaptive' control law that is functionally dependent upon the sampling rate selected and environmental operating conditions. Simulation transients demonstrate the utility of the dual-adaptive design to improve on-board computer utilization while maintaining acceptable levels of engine performance. (Author)

A80-10034 * Turbine engine altitude chamber and flight testing with liquid hydrogen. E. W. Conrad (NASA, Lewis Research Center, Cleveland, Ohio), *Deutsche Gesellschaft für Luft- und Raumfahrt und Deutsche Forschungs- und Versuchsanstalt für Luft- und Raumfahrt, International Symposium on Hydrogen in Air Transportation, Stuttgart, West Germany, Sept. 11-14, 1979, Paper, 20 p, 12 refs.*

In the late fifties the Lewis Research Center evaluated experimentally the use of hydrogen using three different turbojet engines in altitude test chambers. One of these engines was later flown experimentally using liquid hydrogen fuel. This paper is a brief overview of the significant aspects of this exploratory research and

gives a few implications of the results to modern turbine engines. A subsequent contract dealing with a positive displacement pump operating on liquid hydrogen is discussed and some aspects of liquid hydrogen propellant systems, reflected by rocket booster experience are treated briefly. Areas requiring further research and technology effort are delineated. (Author)

A80-17737 * # Preparing aircraft propulsion for a new era in energy and the environment. W. L. Stewart, D. L. Nored, J. S. Grobman, C. E. Feiler, and D. A. Petrash (NASA, Lewis Research Center, Cleveland, Ohio). *Astronautics and Aeronautics*, vol. 18, Jan. 1980, p. 18-31, 37, 22 refs.

Improving fuel efficiency, new sources of jet fuel, and noise and emission control are subjects of NASA's aeronautics program. Projects aimed at attaining a 5% fuel savings for existing engines and a 13-22% savings for the next generation of turbofan engines using advanced components, and establishing a basis for turboprop-powered commercial air transports with 30-40% savings over conventional turbofan aircraft at comparable speeds and altitudes, are discussed. Fuel sources are considered in terms of reduced hydrogen and higher aromatic contents and resultant higher liner temperatures, and attention is given to lean burning, improved fuel atomization, higher freezing-point fuel, and deriving jet fuel from shale oil or coal. Noise sources including the fan, turbine, combustion process, and flow over internal struts, and attenuation using acoustic treatment, are discussed, while near-term reduction of polluting gaseous emissions at both low and high power, and far-term defining of the minimum gaseous-pollutant levels possible from turbine engines are also under study. J.P.B.

A80-18253 * # Computer simulation of engine systems. L. H. Fishbach (NASA, Lewis Research Center, Flight Performance Section, Cleveland, Ohio). *American Institute of Aeronautics and Astronautics, Aerospace Sciences Meeting, 18th, Pasadena, Calif., Jan. 14-16, 1980, Paper 80-0051*, 15 p. 32 refs.

The paper discusses the availability throughout the government and industry of analytical methods for calculating both the steady state and transient performance of an aircraft engine during an entire flight regime. The historical development of some of the analytical tools capable of evaluating installation effects on engine performance is traced and their present status is described. C.F.W.

A80-19300 * # Engine component improvement program - Performance improvement. J. E. McAulay (NASA, Lewis Research Center, Performance Improvement Section, Cleveland, Ohio). *American Institute of Aeronautics and Astronautics, Aerospace Sciences Meeting, 18th, Pasadena, Calif., Jan. 14-16, 1980, Paper 80-0223*, 10 p. 7 refs.

The Engine Component Improvement (ECI) Program is NASA sponsored and is specifically directed at reducing the fuel consumption of commercial aircraft in the near-term. As part of the ECI program, a Performance Improvement (PI) effort aimed at developing fuel saving and retention components for new production and retrofit of JT9D, JT8D, and CF6 engines is underway. This paper reviews the manner in which the PI concepts were selected for development and summarizes the current status of each of the 16 NASA selected concepts. (Author)

A80-20988 * # Scale model performance test investigation of exhaust system mixers for an Energy Efficient Engine (E3) propulsion system. A. P. Kuchar (General Electric Co., Cincinnati, Ohio) and R. Chamberlin (NASA, Lewis Research Center, Energy Conservative Engine Office, Cleveland, Ohio). *American Institute of Aeronautics and Astronautics, Aerospace Sciences Meeting, 18th, Pasadena, Calif., Jan. 14-16, 1980, Paper 80-0229*, 10 p.

A scale model performance test was conducted as part of the NASA Energy Efficient Engine (E3) Program, to investigate the

geometric variables that influence the aerodynamic design of exhaust system mixers for high-bypass, mixed-flow engines. Mixer configuration variables included lobe number, penetration and perimeter, as well as several cutback mixer geometries. Mixing effectiveness and mixer pressure loss were determined using measured thrust and nozzle exit total pressure and temperature surveys. Results provide a data base to aid the analysis and design development of the E3 mixed-flow exhaust system. (Author)

A80-32887 * # Aeropropulsion in year 2000. R. J. Weber (NASA, Lewis Research Center, Cleveland, Ohio). *American Institute of Aeronautics and Astronautics, International Meeting and Technical Display on Global Technology 2000, Baltimore, Md., May 6-8, 1980, Paper 80-0914*, 11 p. 5 refs.

The paper demonstrates that many advances can be anticipated in propulsion systems for aircraft in the next 20 years. A survey is presented of probable future engine types, including convertible engines for helicopters, turboprops for fuel efficient airliners, and variable cycle engines for supersonic transports. Also examined is the use of rotary engines in general aviation aircraft. Finally, a review is given of related technology improvements in propellers, materials, noise suppression, and digital electronic controls. M.E.P.

A80-35101 * # Engine environmental effects on composite behavior. C. C. Chamis and G. T. Smith (NASA, Lewis Research Center, Cleveland, Ohio). In: Structures, Structural Dynamics, and Materials Conference, 21st, Seattle, Wash., May 12-14, 1980, Technical Papers, Part 2. (A80-34993 14-39) New York, American Institute of Aeronautics and Astronautics, Inc., 1980, p. 987-997. 7 refs. (AIAA 80-0695)

The effects of turbojet engine environmental saturation moisture and temperatures up to 300 F on composites were investigated. It was found that epoxy resin composites absorbed the most moisture (2 wt %), while polyimide resin composites absorbed 0.8%. High moisture and 250 F degraded the flexural and interlaminar shear properties, and the environmental and impact conditions severely damaged epoxy composites. The impact damage of fiber composites in moisture-temperature environments can be assessed with finite element and composite mechanics analyses. Engine operation environmental conditions of 0.8% moisture and 140 F had no discernible effect on the fatigue resistance of composite fan exit guide vanes, which can be designed to exceed engine operational requirements using composite materials. A.T.

A80-37482 * # Airbreathing propulsion component technologies. C. Rosen (NASA, Washington, D.C.), B. Koff (General Electric Co., Aircraft Engine Group, Cincinnati, Ohio), and M. Hartmann (NASA, Lewis Research Center, Fluid Systems Components Div., Cleveland, Ohio). *Astronautics and Aeronautics*, vol. 18, June 1980, p. 42-53. 22 refs.

The article suggests that the 1980's will see significant improvements in virtually all gas-turbine engine components and their materials and structural design methods. These improvements will be made possible by improved theoretical models, laser Doppler measurement techniques, advances in rotor-spool technology, the evolution of engine controls, etc. It is suggested that the engine components field should expect broad and steady advances in the technologies of flow, materials, and structures in terms of scope, precision, and tools of design. B.J.

A80-39635 * # Significance of thermal contact resistance in two-layer, thermal-barrier-coated turbine vanes. C. H. Liebert and E. Gaugler (NASA, Lewis Research Center, Cleveland, Ohio). *American Vacuum Society, International Conference on Metallurgical Coatings, San Diego, Calif., Apr. 21-25, 1980, Paper*, 9 p. 11 refs.

The paper studies calculated and measured metal wall temperatures of uncoated vanes and the same vanes coated with a thermal

barrier coating system of NiCrAlY bond and yttria-stabilized zirconia ceramic. It is shown that thermal contact between layers is negligible. The significance of data scatter and of published ceramic thermal conductivity values is discussed.

V.T.

A80-39638 * # Far-field radiation of AFT turbofan noise. E. J. Rice and A. V. Saule (NASA, Lewis Research Center, Cleveland, Ohio). *Acoustical Society of America, Meeting, 99th, Atlanta, Ga., Apr. 21-25, 1980, Paper, 23 p.* 23 refs.

The far-field radiation from the end of an exhaust duct is studied using both approximate and exact methods. Experimental data of narrow-band tone noise from static tests are compared to a multimodal radiation pattern. It is pointed out that possibly the exhaust noise in the far-field is inherently more difficult to attenuate than an inlet noise using duct suppressors.

V.T.

A80-38640 * # Comparison of several inflow control devices for flight simulation of fan tone noise using a JT15D-1 engine. J. G. McArdie, W. L. Jones, L. J. Heidelberg, and L. Homyak (NASA, Lewis Research Center, Cleveland, Ohio). *American Institute of Aeronautics and Astronautics, Aeroacoustics Conference, 6th, Hartford, Conn., June 4-6, 1980, Paper 80-1025, 45 p.* 12 refs.

The paper describes the tests of four devices intended to reduce inflow disturbances and turbulences using a JT15D-1 turbofan engine. The tests were made to simulate the in-flight fan tone noise; the inflow control devices (ICD's) consisted of honeycomb/screen structures mounted over the engine inlet. The ICD's ranged from 1.6 to 4 fan diameters in size, and were made with several fabrication methods. All the ICD's significantly reduced the BPF tone in the far-field directivity patterns, but the smallest ICD's introduced propagating modes which could be recognized by additional lobes in the patterns. The JT15D-1 engine had a tone source which generated a strong propagating mode at fan speeds corresponding to 'approach' power and higher. Data from a typical transducer showed that the unsteady inflow distortion modes were eliminated or reduced when either of the ICD's was installed.

A.T.

A80-38651 * # QCSEE UTW engine powered-lift acoustic performance. I. J. Loeffler, N. E. Samanich, and H. E. Bloomer (NASA, Lewis Research Center, Cleveland, Ohio). *American Institute of Aeronautics and Astronautics, Aeroacoustics Conference, 6th, Hartford, Conn., June 4-6, 1980, Paper 80-1065, 34 p.* 17 refs.

Powered-lift acoustic tests of a quiet clean short-haul experimental engine (QCSEE) under-the-wing (UTW) engine are described. Engine and wing configurations are outlined, along with instrumentation and test facilities. The results of these tests are reported. In addition, the UTW engine powered-lift performance is compared with that of the previously tested QCSEE over-the-wing (OTW) engine.

V.T.

A80-38902 * # Advanced component technologies for energy-efficient turbofan engines. N. T. Saunders (NASA, Lewis Research Center, Cleveland, Ohio). *AIAA, SAE, and ASME, Joint Propulsion Conference, 16th, Hartford, Conn., June 30-July 2, 1980, AIAA Paper 80-1086, 11 p.* 6 refs.

The paper reviews NASA's Energy Efficient Engine Project which was initiated to provide the advanced technology base for a new generation of fuel-conservative engines for introduction into airline service by the late 1980s. Efforts in this project are directed at advancing engine component and systems technologies to a point of demonstrating technology-readiness by 1984. Early results indicate high promise in achieving most of the goals established in the project.

V.P.

A80-38903 * # Experimental evaluation of exhaust mixers for an Energy Efficient Engine. H. Kozlowski (United Technologies

Corp., Pratt and Whitney Aircraft Group, East Hartford, Conn.) and G. Kraft (NASA, Lewis Research Center, Cleveland, Ohio). *AIAA, SAE, and ASME, Joint Propulsion Conference, 16th, Hartford, Conn., June 30-July 2, 1980, AIAA Paper 80-1088, 7 p.*

Static scale model tests were conducted to evaluate exhaust system mixers for a high bypass ratio engine as part of the NASA sponsored Energy Efficient program. Gross thrust coefficients were measured for a series of mixer configurations which included variations in the number of mixer lobes, tailpipe length, mixer penetration, and length. All of these parameters have a significant impact on exhaust system performance. In addition, flow visualization pictures and pressure/temperature traverses were obtained for selected configurations. Parametric performance trends are discussed and the results considered relative to the Energy Efficient Engine program goals.

(Author)

A80-41514 * # CF6-50 Short Core Exhaust Nozzle. D. J. Dusa (General Electric Co., Cincinnati, Ohio) and F. J. Hrach (NASA, Lewis Research Center, Engine Component Improvement Office, Cleveland, Ohio). *AIAA, SAE, and ASME, Joint Propulsion Conference, 16th, Hartford, Conn., June 30-July 2, 1980, AIAA Paper 80-1196, 6 p.*

The General Electric CF6-50 engine nacelle was originally equipped with both fan nozzle and core nozzle thrust reversers. Many airline operators later deactivated the core reverser. Elimination of the core reverser enabled design changes to be made to help improve performance. A reduction in core nozzle length of approximately two feet was possible. This concept, defined as the Short Core Exhaust Nozzle, was evaluated in engine ground tests, including performance, acoustic, and endurance tests under the NASA/Lewis Engine Component Improvement Program. The test results verified the performance predictions from scale model tests. The Short Core Exhaust Nozzle provides an internal cruise SFC reduction of 0.9% without an increase in engine noise. The nozzle hardware successfully completed 1000 flight cycles of endurance testing with no signs of distress.

(Author)

A80-41515 * # Influence of pressure driven secondary flows on the behavior of turbofan forced mixers. B. Anderson, L. Povinelli, and W. Gerstenmaier (NASA, Lewis Research Center, Cleveland, Ohio). *AIAA, SAE, and ASME, Joint Propulsion Conference, 16th, Hartford, Conn., June 30-July 2, 1980, AIAA Paper 80-1198, 27 p.* 12 refs.

An analytical and experimental study was performed to determine the influence of pressure driven secondary flows on the behavior of turbofan forced mixer nozzles. The basic secondary flow structure entering the nozzle was identified experimentally and was composed of a strong vortex system aligned with the radial interface between the fan and core streams. A generic secondary flow vortex structure was constructed for input to the analysis to represent the large scale structure of this inflow condition. Comparison between experiment and analysis at five axial stations showed very good agreement and indicated that this vortex system was convected downstream and dominated the mixing process.

(Author)

A80-42147 * # Experimental study of low aspect ratio compressor blading. L. Reid and R. D. Moore (NASA, Lewis Research Center, Cleveland, Ohio). *American Society of Mechanical Engineers, Gas Turbine Conference and Products Show, New Orleans, La., Mar. 10-13, 1980, Paper 80-GT-6, 8 p.* Members, \$1.50; nonmembers, \$3.00.

The paper presents a study of low aspect blading for the inlet stages of a high pressure ratio, high-speed core compressor. The basic overall design variables were stage pressure ratio and blade aspect ratio; these four stages represent two levels of total pressure ratio, two levels of rotor blade aspect ratio, and two levels of stator vane aspect ratios. Comparisons of the overall performance, radial distributions of performance parameters, diffusion factors at the near-stall conditions, blade element data, and the axial distribution

of rotor tip static pressures yielded the following results: (1) higher peak pressure ratio, high stage and rotor efficiencies, and greater stall margin were obtained with the lower aspect ratio blading, (2) the lower aspect ratio blading showed improved performance over the entire blade span, and (3) the lower aspect ratio rotors operated at higher diffusion factors and higher incidence angles over the entire blade span. A.T.

A80-42154 * # Performance of annular prediffuser-combustor systems. W. B. Wagner, S. Tanrikut (United Technologies Corp., Pratt and Whitney Aircraft Group, East Hartford, Conn.), and D. E. Sokolowski (NASA, Lewis Research Center, Cleveland, Ohio). *American Society of Mechanical Engineers, Gas Turbine Conference and Products Show, New Orleans, La., Mar. 10-13, 1980, Paper 80-GT-15.* 12 p. 19 refs. Members, \$1.50; nonmembers, \$3.00.

Results of an experimental investigation of the aerodynamic performance of several annular prediffuser-combustor systems are presented. Three curved wall, dump prediffusers of different length, area ratio, and turning angle were tested with and without a simulated combustor located downstream of the prediffuser. Performance was significantly influenced by the presence of the combustor. Pressure recovery and flow losses were determined as a function of prediffuser inlet velocity profile, flow extraction at the prediffuser inlet, axial and radial location of the combustor front end, and distribution of the flow in the combustor. Axial location of the combustor was found to be the most significant parameter influencing system performance. (Author)

A80-42164 * # Atomizing characteristics of swirl can combustor modules with swirl blast fuel injectors. R. D. Ingebo (NASA, Lewis Research Center, Cleveland, Ohio). *American Society of Mechanical Engineers, Gas Turbine Conference and Products Show, New Orleans, La., Mar. 10-13, 1980, Paper 80-GT-30.* 7 p. 8 refs. Members, \$1.50; nonmembers, \$3.00.

Cold flow atomization tests of several different designs of swirl can combustor modules were conducted in a 7.6 cm diameter duct at airflow rates (per unit area) of 7.3 to 25.7 g/sq cm sec and water flow rates of 6.3 to 18.9 g/sec. The effect of air and water flow rates on the mean drop size of water sprays produced with the swirl blast fuel injectors were determined. Also, from these data it was possible to determine the effect of design modifications on the atomizing performance of various fuel injector and air swirler configurations. The trend in atomizing performance, as based on the mean drop size, was then compared with the trends in the production of nitrogen oxides obtained in combustion studies with the same swirl can combustors. (Author)

A80-42199 * # Low NO_x/ heavy fuel combustor program. E. Lister (U.S. Department of Energy, Germantown, Md.), R. W. Niedzwiecki, and L. Nichols (NASA, Lewis Research Center, Cleveland, Ohio). *American Society of Mechanical Engineers, Gas Turbine Conference and Products Show, New Orleans, La., Mar. 10-13, 1980, Paper 80-GT-69.* 10 p. Members, \$1.50; nonmembers, \$3.00.

The paper deals with the 'Low NO_x/ Heavy Fuel Combustor Program'. Main program objectives are to generate and demonstrate the technology required to develop durable gas turbine combustors for utility and industrial applications, which are capable of sustained, environmentally acceptable operation with minimally processed petroleum residual fuels. The program will focus on 'dry' reductions of oxides of nitrogen (NO_x), improved combustor durability and satisfactory combustion of minimally processed petroleum residual fuels. Other technology advancements sought include: fuel flexibility for operation with petroleum distillates, blends of petroleum distillates and residual fuels, and synfuels (fuel oils derived from coal or shale); acceptable exhaust emissions of carbon monoxide, unburned hydrocarbons, sulfur oxides and smoke; and retrofit capability to existing engines. (Author)

A80-42258 * # Results from tests on a high work transonic turbine for an energy efficient engine. D. E. Crow, H. Welna, J. D. Singer (United Technologies Corp., Pratt and Whitney Aircraft Group, East Hartford, Conn.), and M. R. Vanco (NASA, Lewis Research Center, Cleveland, Ohio). *American Society of Mechanical Engineers, Gas Turbine Conference and Products Show, New Orleans, La., Mar. 10-13, 1980, Paper 80-GT-146.* 9 p. Members, \$1.50; nonmembers, \$3.00. Contract No. NAS3-20646.

The experimental results of the evaluation of two high work, transonic, single-stage turbines investigated under the Energy Efficient Engine (E3) Program are presented. The objective of the E3 program is to provide an advanced technology base for a new generation of fuel-conservative turbofan engines. A single-stage turbine required fewer cooled airfoils, a reduced number of leakage paths and no interstage seals. These advanced energy efficient engines require high engine pressure ratios resulting in high expansion ratio, transonic, turbine designs which must have high aerodynamic efficiency. The goal of the turbine program is to develop a high pressure turbine that is compatible with the overall engine design and has an uncooled efficiency of 90.8 percent. (Author)

A80-43283 * # A theoretical and experimental investigation of propeller performance methodologies. K. D. Korkan, G. M. Gregorek (Ohio State University, Columbus, Ohio), and D. C. Mikkelsen (NASA, Lewis Research Center, Subsonic Propulsion Section, Cleveland, Ohio). *AIAA, SAE, and ASME, Joint Propulsion Conference, 16th, Hartford, Conn., June 30-July 2, 1980, AIAA Paper 80-1240.* 22 p. 37 refs. Grant No. NSG-3247.

This paper briefly covers aspects related to propeller performance by means of a review of propeller methodologies; presentation of wind tunnel propeller performance data taken in the NASA Lewis Research Center 10 x 10-wind tunnel; discussion of the predominant limitations of existing propeller performance methodologies; and a brief review of airfoil developments appropriate for propeller applications. (Author)

A80-42284 * # CF6 fan performance improvement. R. F. Patt (General Electric Co., Evandale, Ohio) and D. C. Reemsnyder (NASA, Lewis Research Center, Cleveland, Ohio). *American Society of Mechanical Engineers, Gas Turbine Conference and Products Show, New Orleans, La., Mar. 10-13, 1980, Paper 80-GT-178.* 11 p. Members, \$1.50; nonmembers, \$3.00.

A significant portion of the NASA-sponsored Performance Improvement Program for the CF6 engine was the development of an improved fan concept. This involved aerodynamic redesign of the CF6 fan blade to increase fan efficiency while retaining the mechanical integrity, operability, and acoustic characteristics of the existing blade. A further improvement in performance was obtained by adding a fan case stiffener ring to decouple blade-case vibrational characteristics, permitting a significant reduction in running tip clearance. Engine testing was performed to establish the performance, mechanical and acoustic properties of the new design relative to the current fan, and to establish power management characteristics for the CF6-50C2/E2 engine. A significant improvement in cruise power SFC of 1.8 percent was demonstrated in Sea Level testing projected to altitude flight conditions. (Author)

A80-44230 * # JT9D-7A /SP/ jet engine performance deterioration trends. G. P. Richter (NASA, Lewis Research Center, Cleveland, Ohio), W. J. Olsson (United Technologies Corp., Pratt and Whitney Aircraft Group, East Hartford, Conn.), and N. B. Andersen (Pan American World Airways, Inc., Kennedy International Airport, N.Y.). *Hamilton Burr Publishing Co., International Aircraft Maintenance Engineering Exhibition and Conference, Dallas, Tex., Apr. 8-10, 1980, Paper.* 21 p.

It is noted that increasing fuel costs and the decreasing availability of fuel supplies have lead to an increase in the importance of maintaining good specific fuel consumption over the life cycle of jet engines. Attention is given to an engine diagnostics program

sponsored by NASA Lewis Research Center which has the objectives of identifying and quantifying the levels, trends, and causes of engine performance deterioration. It is reported that as part of the program, a series of installed engine calibrations were performed on two new Pan American World Airways 747 SP aircraft. A discussion of this specific test program and the results of the analysis of the data are presented.
M.E.P.

A80-44491 * # Prediction of unsuppressed jet engine exhaust noise in flight from static data. J. R. Stone (NASA, Lewis Research Center, Jet Acoustics Branch, Cleveland, Ohio). *American Institute of Aeronautics and Astronautics, Aeroacoustics Conference, 6th, Hartford, Conn., June 4-6, 1980, Paper 80-1008*. 24 p. 22 refs.

In order to assess the impact of aircraft noise on the environment in the vicinity of an airport, it is essential that a methodology be developed for predicting in-flight exhaust noise from static data. Such a methodology is presented in this paper and is compared with experimental data for several unsuppressed turbojet engines. For each engine, static data over a range of jet velocities are compared with the predicted jet mixing noise and shock-cell noise. The static engine noise over and above the jet and shock noises is identified as 'excess' noise. The excess noise data are then empirically correlated to smooth the spectral and directivity relations and account for variations in test conditions. This excess noise is then projected to flight based on the assumption that the only effects of flight are a Doppler frequency shift and a level change. The effects of flight on jet mixing noise and shock noise are computed by published NASA methods.
(Author)

A80-48013 * # Similarity tests of turbine vanes - Effects of ceramic thermal barrier coatings. H. J. Gladden (NASA, Lewis Research Center, Cleveland, Ohio). *American Society of Mechanical Engineers and American Institute of Chemical Engineers, Joint National Heat Transfer Conference, Orlando, Fla., July 27-30, 1980, ASME Paper 80-HT-24*. 9 p. 12 refs. Members, \$1.50; nonmembers, \$3.00.

The role of material thermal conductivity was analyzed for its effect on the thermal performance of air-cooled gas turbine components coated with a ceramic thermal barrier material when tested at reduced temperatures and pressures. This study shows that the thermal performance can be evaluated reliably at reduced gas and coolant conditions. However, thermal conductivity corrections are required for the data at reduced conditions. These corrections for a ceramic thermal barrier coated vane are significantly different than the corrections for an uncoated vane. Comparison of uncorrected test data, therefore, would show erroneously that the thermal barrier coating was ineffective. When thermal conductivity corrections are applied to the test data these data are then shown to be representative of engine data and also show that the thermal barrier coating increases the vane cooling effectiveness by 12.5 percent.
(Author)

A80-48014 * # Uncertainties in predicting turbine blade metal temperatures. F. S. Stepka (NASA, Lewis Research Center, Cleveland, Ohio). *American Society of Mechanical Engineers and American Institute of Chemical Engineers, Joint National Heat Transfer Conference, Orlando, Fla., July 27-30, 1980, ASME Paper 80-HT-25*. 8 p. 12 refs. Members, \$1.50; nonmembers, \$3.00.

An analysis is presented of the effects of the hot-gas and coolant temperatures, the gas-to-blade and blade-to-coolant heat transfer coefficients, and the thermal conductances of a metal wall and a ceramic thermal-barrier coating on the prediction of local turbine-blade surface temperatures. The analysis was applied to the conditions of an advanced turbofan engine and a 1700 K, 40 atm turbine test rig, and to conditions that simulated the engine at 756 K and 15.6 atm. The results showed that with current information on boundary conditions, geometry, heat-transfer coefficients, and material thermal properties, the uncertainty in predicting and verifying local turbine-blade surface temperatures in an average engine is 98 kelvins or 7.6% of the reference metal absolute temperature for uncoated blades, and 62 kelvins or 5.7% for ceramic-thermal-barrier-

coated blades.

A.T.

N80-10221 * # Pratt and Whitney Aircraft Group, East Hartford, Conn.

EXPERIMENTAL EVALUATION OF A LOW EMISSIONS HIGH PERFORMANCE DUCT BURNER FOR VARIABLE CYCLE ENGINES (VCE) Final Report

R. P. Lohman and R. J. Mador 1979 117 p refs

(Contract NAS3-20602)

(NASA-CR-159694; PWA-5513-32)

Avail: NTIS

HC A05/MF A01 CSCL 21E

A three-stage Vorbix duct burner was evaluated to determine the performance and emissions characteristics of this concept and to refine the configuration to provide acceptable durability and operational characteristics for its use in the VCE Testbed Program. The tests were conducted at representative takeoff, transonic climb and supersonic cruise inlet conditions for the VCE-502B study engine. The carbon monoxide and unburned hydrocarbon emissions were low at all three operating conditions with combustion efficiencies in excess of 99.7 percent, as compared to the goal of 99.0 percent. Nitric oxide emissions were moderate but in excess of the program goal of 1 gm/kg at takeoff. The thrust efficiency exceeded the goal level of 94.5 percent reaching a value of 97 percent at supersonic cruise. Soft ignition, the absence of combustion generated acoustic instabilities and liner temperature levels acceptable for experimental hardware were also demonstrated. The total pressure loss across the duct burner, at 6.76 the loss mechanisms have been identified and, in one configuration 40 percent of this excess loss was eliminated without comprising the emissions or thrust efficiency.
A.R.H.

N80-10222 * # Pratt and Whitney Aircraft, East Hartford, Conn. Chemical Products Div.

VSCE TECHNOLOGY DEFINITION STUDY Final Report

R. A. Howlett and R. B. Hunt Aug. 1979 114 p refs

(Contract NAS3-21389)

(NASA-CR-159730; PWA-5630-11)

Avail: NTIS

HC A06/MF A01 CSCL 21E

Refined design definition of the variable stream control engine (VSCE) concept for advanced supersonic transports is presented. Operating and performance features of the VSCE are discussed, including the engine components, thrust specific fuel consumption, weight, noise, and emission system. A preliminary engine design is presented.
A.W.H.

N80-12091 * # Pratt and Whitney Aircraft Group, East Hartford, Conn.

DESIGN, DURABILITY AND LOW COST PROCESSING TECHNOLOGY FOR COMPOSITE FAN EXIT GUIDE VANES

S. S. Blecherman Aug. 1979 139 p refs

(Contract NAS3-21037)

(NASA-CR-159677; PWA-5570-37)

Avail: NTIS

HC A07/MF A01 CSCL 21E

A lightweight composite fan exit guide vane for high bypass ratio gas turbine engine application was investigated. Eight candidate material/design combinations were evaluated by NASTRAN finite element analyses. A total of four combinations were selected for further analytical evaluation, part fabrication by two vendors, and fatigue test in dry and wet condition. A core and shell vane design was chosen in which the unidirectional graphite core fiber was the same for all candidates. The shell material, fiber orientation, and ply configuration were varied. Material tests were performed on raw material and composite specimens to establish specification requirements. Pre-test and post-test microstructural examination and nondestructive analyses were conducted to determine the effect of material variations on fatigue durability and failure mode. Relevant data were acquired with respect to design analysis, materials properties, inspection standards, improved durability, weight benefits, and part price of the composite fan exit guide vane.
R.C.T.

N80-13041* National Aeronautics and Space Administration. Ames Research Center, Moffett Field, Calif.
FLIGHT TEST OF NAVIGATION AND GUIDANCE SENSOR ERRORS MEASURED ON STOL APPROACHES

David N. Warner and F. J. Moran. Dec. 1979. 42 p.
(NASA-TM-81154, A-8008) Avail. NASA. Ames Res. Center, (Contract NAS3-21238)
(NASA-CR-159693; D180-25481-3-Vol-3) Avail. NTIS HC A18/MF A01 CSCL 21E

A computerized method which utilizes the engine performance data and estimates the installed performance of aircraft gas turbine engines is presented. This installation includes: engine weight and dimensions, inlet and nozzle internal performance and drag, inlet and nacelle weight, and nacelle drag. The use of two data base files to represent the engine and the inlet/nozzle/aftbody performance characteristics is discussed. The existing library of performance characteristics for inlets and nozzle/aftbodies and an example of the 1000 series of engine data tables is presented. A.W.H.

N80-13043* Boeing Co., Seattle, Wash. Advanced Airplane Branch.

COMPUTER CODE FOR ESTIMATING INSTALLED PERFORMANCE OF AIRCRAFT GAS TURBINE ENGINES. VOLUME 1: FINAL REPORT

Edward J. Kowalski. Dec. 1979. 204 p. refs 3 Vol.
(Contract NAS3-21238)
(NASA-CR-159691; D180-25481-1-Vol-1) Avail. NTIS HC A10/MF A01 CSCL 21E

A computerized method which utilizes the engine performance data is described. The method estimates the installed performance of aircraft gas turbine engines. This installation includes: engine weight and dimensions, inlet and nozzle internal performance and drag, inlet and nacelle weight, and nacelle drag. A.W.H.

N80-13044* Boeing Co., Seattle, Wash. Advanced Airplane Branch.

COMPUTER CODE FOR ESTIMATING INSTALLED PERFORMANCE OF AIRCRAFT GAS TURBINE ENGINES. VOLUME 2: USERS MANUAL

Edward J. Kowalski. Dec. 1979. 444 p. 3 Vol.
(Contract NAS3-21238)
(NASA-CR-159692; D180-25481-2-Vol-2) Avail. NTIS HC A19/MF A01 CSCL 21E

A computerized method which utilizes the engine performance data and estimates the installed performance of aircraft gas turbine engines is presented. This installation includes: engine weight and dimensions, inlet and nozzle internal performance and drag, inlet and nacelle weight, and nacelle drag. A user oriented description of the program input requirements, program output, deck setup, and operating instructions is presented. A.W.H.

N80-13048* General Electric Co., Cincinnati, Ohio. Aircraft Engine Group.

ADVANCED CATALYTIC COMBUSTORS FOR LOW POLLUTANT EMISSIONS, PHASE 1 Final Report

W. J. Dodds. Nov. 1979. 159 p. refs. Sponsored in part by Air Force Engineering Services Center, Tyndall AFB, Fla.
(Contract NAS3-20820)
(NASA-CR-159535; CEEDO-TR-79-03) Avail. NTIS HC A08/MF A01 CSCL 21E

The feasibility of employing the known attractive and distinguishing features of catalytic combustion technology to reduce nitric oxide emissions from gas turbine engines during ejector performance. These characteristic points determined which of nine possible ejector configurations provided optimal performance at any given flight and injected gas conditions. Detailed examination of the thermodynamic cycle was made for representative cases and data was presented to illustrate the influence of ejectors upon conventional gas generator performance. The influence of nozzle loss, skin friction and flow separation, incomplete kinetic and thermal mixing, and boundary layer ingestion were taken into consideration in the analysis. Correlation with existing stationary solid and jet-diffuser ejector experiments showed excellent agreement between theory and experiment. It

has been shown that ejectors designed according to the methods described, can provide large improvement in propulsion system performance throughout the entire practical flight regime. GRA

N80-14116* General Electric Co., Cincinnati, Ohio. Aircraft Engine Group.

QUIET CLEAN SHORT-HAUL EXPERIMENTAL ENGINE (QCSEE) ACOUSTIC AND AERODYNAMIC TESTS ON A SCALE MODEL OVER-THE-WING THRUST REVERSER AND FORWARD THRUST NOZZLE

D. L. Stimpert. 18 Jan. 1978. 85 p. refs
(Contract NAS3-18021)
(NASA-CR-135254; R75AEG504) Avail. NTIS HC A05/MF A01 CSCL 21E

An acoustic and aerodynamic test program was conducted on a 1/6.25 scale model of the Quiet, Clean, Short-Haul Experimental Engine (QCSEE) forward thrust over-the-wing (OTW) nozzle and OTW thrust reverser. In reverse thrust, the effect of reverser geometry was studied by parametric variations in blocker spacing, blocker height, lip angle, and lip length. Forward thrust nozzle tests determined the jet noise levels of the cruise and takeoff nozzles, the effect of opening side doors to achieve takeoff thrust, and scrubbing noise of the cruise and takeoff jet on a simulated wing surface. Velocity profiles are presented for both forward and reverse thrust nozzles. An estimate of the reverse thrust was made utilizing the measured centerline turning angle. Author

N80-14116* General Electric Co., Cincinnati, Ohio. Advanced Engineering and Technology Programs Dept.

QUIET CLEAN SHORT-HAUL EXPERIMENTAL ENGINE (QCSEE) UNDER-THE-WING (UTW) ENGINE BOILERPLATE NACELLE TEST REPORT. VOLUME 2: AERODYNAMICS AND PERFORMANCE

31 Dec. 1977. 61 p. refs
(Contract NAS3-18021)
(NASA-CR-135250; R77AEG2122-Vol-2) Avail. NTIS HC A04/MF A01 CSCL 21E

The initial phase of testing of the under the wing engine and boilerplate nacelle components is discussed. The aerodynamics and performance are outlined. M.M.M.

N80-14117* General Electric Co., Cincinnati, Ohio. Aircraft Engine Group.

QUIET, CLEAN, SHORT-HAUL EXPERIMENTAL ENGINE (QCSEE) UNDER-THE-WING (UTW) ENGINE ACOUSTIC DESIGN

H. D. Sowers and W. E. Coward. Jan. 1978. 62 p. refs
(Contract NAS3-18021)
(NASA-CR-135267; R76AEG195) Avail. NTIS HC A04/MF A01 CSCL 21E

The acoustic considerations involved in the low source noise basic engine design and the design procedures followed in the development of the under-the-wing (UTW) engine boilerplate and composite nacelle acoustic treatment designs are presented. Laboratory experiments, component tests, and scale model and engine tests supporting the UTW engine acoustic design are referenced. Acoustic design features include a near-sonic inlet, low fan and core pressure ratios, low fan tip speed, high and low frequency stacked core treatment, multiple thickness treatment, and fan frame and stator vane treatment. R.E.S.

N80-14118* General Electric Co., Cincinnati, Ohio. Aircraft Engine Group.

QUIET, CLEAN, SHORT-HAUL EXPERIMENTAL ENGINE (QCSEE) OVER-THE-WING (OTW) ENGINE ACOUSTIC DESIGN

H. D. Sowers and W. E. Coward. Jun. 1978. 58 p. refs
(Contract NAS3-18021)
(NASA-CR-135268; R76AEG228) Avail. NTIS HC A04/MF A01 CSCL 21E

The acoustic considerations involved in the low source noise basic engine design and the design procedures followed in the development of the over-the-wing (OTW) nacelle acoustic treatment design are presented. Laboratory experiments, component tests, and scale model and engine tests supporting the OTW engine acoustic design are referenced. Acoustic design features include a near-sonic inlet, low fan and core pressure ratios, low fan tip speed, high and low frequency stacked core treatment, multiple thickness treatment, and fan frame and stator vane treatment. R.E.S.

N80-14119* General Electric Co., Cincinnati, Ohio. Advanced Engineering and Technology Programs Dept.
QUIET CLEAN SHORT-HAUL EXPERIMENTAL ENGINE (QCSEE) UNDER-THE-WING (UTW) GRAPHITE/PMR COWL DEVELOPMENT

C. L. Ruggles Jul. 1978 75 p refs
 (Contract NAS3-18021)
 (NASA-CR-135279; R79AEG208) Avail: NTIS
 HC A04/MF A01 CSCL 21E

The PMR process development, tooling concepts, testing conducted to generate materials properties data, and the fabrication of a subscale model of the inner cowl are presented. It was concluded that the materials, processes, and tooling concepts were satisfactory for making an inner cowl with adequate structural integrity. M.M.M.

N80-14120* General Electric Co., Cincinnati, Ohio. Advanced Engineering and Technology Programs Dept.
QUIET CLEAN SHORT-HAUL EXPERIMENTAL ENGINE (QCSEE) OVER-THE-WING (OTW) PROPULSION SYSTEM TEST REPORT. VOLUME 2: AERODYNAMICS AND PERFORMANCE

Jul. 1978 49 p refs
 (Contract NAS3-18021)
 (NASA-CR-135324; R77AEG474-Vol-2) Avail: NTIS
 HC A03/MF A01 CSCL 21E

The design and testing of the over the wing engine, a high bypass, geared turbofan engine, are discussed. The propulsion system performance is examined for uninstalled performance and installed performance. The fan aerodynamic performance and the D nozzle and reverser thrust performance are evaluated. A.W.H.

N80-14122* General Electric Co., Cincinnati, Ohio. Aircraft Engine Group.
FEASIBILITY OF SiC COMPOSITE STRUCTURES FOR 1644 K (2500 F) GAS TURBINE SEAL APPLICATION Final Report, 28 Apr. - 30 May 1979

R. Darolia Nov. 1979 120 p ref
 (Contract NAS3-20082)
 (NASA-CR-159597; R79AEG625) Avail: NTIS
 HC A06/MF A01 CSCL 21E

The silicon carbide composites evaluated consisted of Si/SiC and sintered silicon carbide as substrates, both with attached surface layers containing BN as an additive. A total of twenty-eight candidates with variations in substrate type and density, and layer chemistry, density, microstructure, and thickness were evaluated for abrasability, cold particle erosion resistance, static oxidation resistance, ballistic impact resistance, and fabricability. BN-free layers with variations in density and pore size were later added for evaluation. The most promising candidates were evaluated for Mach 1.0 gas oxidation/erosion resistance from 1477 K (2200 F) to 1644 K (2500 F). The as-fabricated rub layers did not perform satisfactorily in the gas oxidation/erosion tests. However, preoxidation was found to be beneficial in improving the hot gas erosion resistance. Overall, the laboratory and rig test evaluations show that material properties are suitable for 1477 K (2200 F) gas turbine seal applications. Further improvements are needed in hot gas erosion resistance and abrasability to demonstrate feasibility to 1644 K (250 F). A.R.H.

N80-14127* General Electric Co., Cincinnati, Ohio. Aircraft Engine Group.

THE CFB JET ENGINE PERFORMANCE IMPROVEMENT: NEW FRONT MOUNT

W. A. Fasching Dec. 1979 139 p refs
 (Contract NAS3-20629)
 (NASA-CR-159639; R79AEG366) Avail: NTIS
 HC A07/MF A01 CSCL 21E

The New Front Mount was evaluated in component tests including stress, deflection/distortion and fatigue tests. The test results demonstrated a performance improvement of 0.1% in cruise sfc, 16% in compressor stall margin and 10% in compressor stator angle margin. The New Front Mount hardware successfully completed 35,000 simulated flight cycles endurance testing. Author

N80-14128* Detroit Diesel Allison, Indianapolis, Ind.
STUDY OF TURBOPROP SYSTEMS RELIABILITY AND MAINTENANCE COSTS Final Report

Jun. 1978 304 p refs
 (Contract NAS3-20057)
 (NASA-CR-135192; EDR-9132) Avail: NTIS
 HC A14/MF A01 CSCL 21E

The overall reliability and maintenance costs (R&MC's) of past and current turboprop systems were examined. Maintenance cost drivers were found to be scheduled overhaul (40%), lack of modularity particularly in the propeller and reduction gearbox, and lack of inherent durability (reliability) of some parts. Comparisons were made between the 501-D13/54H60 turboprop system and the widely used JT8D turbofan. It was found that the total maintenance cost per flight hour of the turboprop was 75% higher than that of the JT8D turbofan. Part of this difference was due to propeller and gearbox costs being higher than those of the fan and reverser, but most of the difference was in the engine core where the older technology turboprop core maintenance costs were nearly 70 percent higher than for the turbofan. The estimated maintenance cost of both the advanced turboprop and advanced turbofan were less than the JT8D. The conclusion was that an advanced turboprop and an advanced turbofan, using similar cores, will have very competitive maintenance costs per flight hour. J.M.S.

N80-14130* Avco Lycoming Div., Williamsport, Pa.
EXHAUST EMISSION REDUCTION FOR INTERMITTENT COMBUSTION AIRCRAFT ENGINES

R. N. Moffett Oct. 1979 114 p
 (Contract NAS3-19754)
 (NASA-CR-159757) Avail: NTIS HC A06/MF A01 CSCL 21E

Three concepts for optimizing the performance, increasing the fuel economy, and reducing exhaust emission of the piston aircraft engine were investigated. High energy-multiple spark discharge and spark plug tip penetration, ultrasonic fuel vaporization, and variable valve timing were evaluated individually. Ultrasonic fuel vaporization did not demonstrate sufficient improvement in distribution to offset the performance loss caused by the additional manifold restriction. High energy ignition and revised spark plug tip location provided no change in performance or emissions. Variable valve timing provided some performance benefit; however, even greater performance improvement was obtained through induction system tuning which could be accomplished with far less complexity. A.R.H.

N80-14182* Acurex Corp., Mountain View, Calif. Autodata Div.

PHASE-LOCKED TELEMETRY SYSTEM FOR ROTARY INSTRUMENTATION OF TURBOMACHINERY, PHASE 1 Final Report

Alan Adler and Bas Hoeks Sep. 1978 192 p
 (Contract NAS3-20290; Acurex Proj. 6497)
 (NASA-CR-159453; Acurex-78-284) Avail: NTIS
 HC A09/MF A01 CSCL 09F

A telemetry system for use in making strain and temperature measurements on the rotating components of high speed turbomachines employs phase locked transmitters, which offer greater measurement channel capacity and reliability than existing systems which employ L-C carrier oscillators. A prototype

transmitter module was tested at 175 C combined with 40,000 g's acceleration. A.R.H.

N80-15100* General Electric Co., Cincinnati, Ohio. Aircraft Engine Group.
QUIET CLEAN SHORT-HAUL EXPERIMENTAL ENGINE (QCSEE) UNDER-THE-WING (UTW) COMPOSITE NACELLE SUBSYSTEM TEST REPORT
C. L. Stotler, Jr., E. A. Johnston, and D. S. Freeman Jul. 1977 83 p refs
(Contract NAS3-18021)
(NASA-CR-135075; R76AEG420) Avail. NTIS
HC A05/MF A01 CSCL 21E

The element and subcomponent testing conducted to verify the under the wing composite nacelle design is reported. This composite nacelle consists of an inlet, outer cowl doors, inner cowl doors, and a variable fan nozzle. The element tests provided the mechanical properties used in the nacelle design. The subcomponent tests verified that the critical panel and joint areas of the nacelle had adequate structural integrity. J.M.S.

N80-15101* General Electric Co., Cincinnati, Ohio. Advanced Engineering and Technology Programs Dept.
QUIET CLEAN SHORT-HAUL EXPERIMENTAL ENGINE (QCSEE). BALL SPLINE PITCH CHANGE MECHANISM DESIGN REPORT
Apr. 1978 73 p refs
(Contract NAS3-18021)
(NASA-CR-134873; R77AEG327) Avail. NTIS
HC A04/MF A01 CSCL 21E

Detailed design parameters are presented for a variable-pitch change mechanism. The mechanism is a mechanical system containing a ball screw/spline driving two counteracting master bevel gears meshing pinion gears attached to each of 18 fan blades. R.E.S.

N80-15102* General Electric Co., Cincinnati, Ohio.
ACOUSTIC ANALYSIS OF AFT NOISE REDUCTION TECHNIQUES MEASURED ON A SUBSONIC TIP SPEED 50.8 cm (TWENTY INCH) DIAMETER FAN
D. L. Stimpert and A. Clemons Jan. 1977 149 p refs
(Contract NAS3-18021)
(NASA-CR-134891; R75AEG368) Avail. NTIS
HC A07/MF A01 CSCL 21E

Sound data which were obtained during tests of a 50.8 cm diameter, subsonic tip speed, low pressure ratio fan were analyzed. The test matrix was divided into two major investigations: (1) source noise reduction techniques; and (2) aft duct noise reduction with acoustic treatment. Source noise reduction techniques were investigated which include minimizing second harmonic noise by varying vane/blade ratio, variation in spacing, and lowering the Mach number through the vane row to lower fan broadband noise. Treatment in the aft duct which includes flow noise effects, faceplate porosity, rotor OGV treatment, slant cell treatment, and splitter simulation with variable depth on the outer wall and constant thickness treatment on the inner wall was investigated. Variable boundary conditions such as variation in treatment panel thickness and orientation, and mixed porosity combined with variable thickness were examined. Significant results are reported. R.C.T.

N80-15103* Curtiss-Wright Corp., Wood-Ridge, N.J. Power Systems.
QUIET CLEAN SHORT-HAUL EXPERIMENTAL ENGINE (QCSEE) MAIN REDUCTION GEARS TEST PROGRAM Final Report
O. W. Misel Mar. 1977 220 p refs
(Contract NAS3-18021)
(NASA-CR-134669; CW-WR-77-008) Avail. NTIS
HC A10/MF A01 CSCL 21E
Sets of under the wing (UTW) engine reduction gears and sets of over the wing (OTW) engine reduction gears were fabricated for rig testing and subsequent installation in engines. The UTW

engine reduction gears which have a ratio of 2.465:1 and a design rating of 9712 kW at 3157 rpm fan speed were operated at up to 105% speed at 60% torque and 100% speed at 125% torque. The OTW engine reduction gears which have a ratio of 2.062:1 and a design rating of 12,615 kW at 3861 rpm fan speed were operated at up to 95% speed at 50% torque and 80% speed at 109% torque. Satisfactory operation was demonstrated at powers up to 12,172 kW, mechanical efficiency up to 99.1% UTW, and a maximum gear pitch line velocity of 112 m/s (22,300 fpm) with a corresponding star gear spherical roller bearing DN of 850,00 OTW. Oil and star gear bearing temperatures, oil churning, heat rejection, and vibratory characteristics were acceptable for engine installation. R.C.T.

N80-15104* General Electric Co., Cincinnati, Ohio. Advanced Engineering and Technology Programs Dept.
QUIET CLEAN SHORT-HAUL EXPERIMENTAL ENGINE (QCSEE) CLEAN COMBUSTOR TEST REPORT
Oct. 1975 66 p refs
(Contract NAS3-18021)
(NASA-CR-134916; R75AEG449) Avail. NTIS
HC A04/MF A01 CSCL 21E

A component pressure test was conducted on a F101 PFRT combustor to evaluate the emissions levels of this combustor design at selected under the wing and over the wing operating conditions for the quiet clean short haul experimental engine (QCSEE). Emissions reduction techniques were evaluated which included compressor discharge bleed and sector burning in the combustor. The results of this test were utilized to compare the expected QCSEE emissions levels with the emission goals of the QCSEE engine program. R.C.T.

N80-15105* Curtiss-Wright Corp., Wood-Ridge, N.J.
QUIET CLEAN SHORT-HAUL EXPERIMENTAL ENGINE (QCSEE) MAIN REDUCTION GEARS BEARING DEVELOPMENT PROGRAM Final Report
Dec. 1975 40 p
(Contract NAS3-18021)
(NASA-CR-134890) Avail. NTIS HC A03/MF A01 CSCL 21E

The viability of proposed bearing designs to operate at application conditions is described. Heat rejection variables were defined for the test conditions. Results indicate that there is potential for satisfactory operation of spherical roller bearing in the QCSEE main reduction gear application. R.C.T.

N80-15106* Curtiss-Wright Corp., Wood-Ridge, N.J.
QUIET CLEAN SHORT-HAUL EXPERIMENTAL ENGINE (QCSEE) MAIN REDUCTION GEARS DETAILED DESIGN REPORT Final Report
A. Defeo and M. Kulina Jul. 1977 221 p
(Contract NAS3-18021)
(NASA-CR-134872; CW-WR-77-024) Avail. NTIS
HC A10/MF A01 CSCL 21E

Lightweight turbine engines with geared slower speed fans are considered. The design of two similar but different gear ratio, minimum weight, epicyclic star configuration main reduction gears for the under the wing (UTW) and over the wing (OTW) engines is discussed. The UTW engine reduction gear has a ratio of 2.465:1 and a 100% power design rating of 9885 kW (13,256 hp) at 3143 rpm fan speed. The OTW engine reduction gear has a ratio of 2.062:1 and a 100% power design rating of 12813 kW (17183 hp) at 3861 rpm fan speed. Details of configuration, stresses, deflections, and lubrication are presented. J.M.S.

N80-15107* Hamilton Standard, Windsor Locks, Conn. Aircraft Systems Dept.
QUIET CLEAN SHORT-HAUL EXPERIMENTAL ENGINE (QCSEE): HAMILTON STANDARD CAM/HARMONIC DRIVE VARIABLE PITCH FAN ACTUATION SYSTEM DETAIL DESIGN REPORT

Mar. 1976 159 p
(Contract NAS3-18021)
(NASA-CR-134852; HSER-7001) Avail: NTIS
HC A08/MF A01 CSCL 21E

A variable pitch fan actuation system was designed which incorporates a remote nacelle-mounted blade angle regulator. The regulator drives a rotating fan-mounted mechanical actuator through a flexible shaft and differential gear train. The actuator incorporates a high ratio harmonic drive attached to a multitrack spherical cam which changes blade pitch through individual cam follower arms attached to each blade trunnion. Detail design parameters of the actuation system are presented. These include the following: design philosophies, operating limits, mechanical, hydraulic and thermal characteristics, mechanical efficiencies, materials, weights, lubrication, stress analyses, reliability and failure analyses. Author

N80-15108* General Electric Co., Cincinnati, Ohio. Advanced Engineering and Technology Programs Dept.
QUIET CLEAN SHORT-HAUL EXPERIMENTAL ENGINE (QCSEE) UNDER-THE-WING ENGINE COMPOSITE FAN BLADE DESIGN REPORT Final Report
R. Ravenhall and C. T. Salemm Feb. 1977 61 p refs
(Contract NAS3-18021)
(NASA-CR-135046; R77AEG177) Avail: NTIS
HC A04/MF A01 CSCL 21E

A total of 38 quiet clean short haul experimental engine under the wing composite fan blades were manufactured for various component tests, process and tooling, checkout, and use in the QCSEE UTW engine. The component tests included frequency characterization, strain distribution, bench fatigue, platform static load, whirligig high cycle fatigue, whirligig low cycle fatigue, whirligig strain distribution, and whirligig over-speed. All tests were successfully completed. All blades planned for use in the engine were subjected to and passed a whirligig proof spin test. R.C.T.

N80-15109* General Electric Co., Cincinnati, Ohio. Aircraft Engine Group.
QUIET CLEAN SHORT-HAUL EXPERIMENTAL ENGINE (QCSEE): THE AERODYNAMIC AND MECHANICAL DESIGN OF THE QCSEE UNDER-THE-WING FAN
Mar. 1977 144 p
(Contract NAS3-18021)
(NASA-CR-135009; R75AEG484) Avail: NTIS
HC A07/MF A01 CSCL 21E

The design, fabrication, and testing of two experimental high bypass geared turbofan engines and propulsion systems for short haul passenger aircraft are described. The aerodynamic and mechanical design of a variable pitch 1.34 pressure ratio fan for the under the wing (UTW) engine are included. The UTW fan was designed to permit rotation of the 18 composite fan blades into the reverse thrust mode of operation through both flat pitch and stall pitch directions. R.C.T.

N80-15110* General Electric Co., Cincinnati, Ohio.
QUIET CLEAN SHORT-HAUL EXPERIMENTAL ENGINE (QCSEE) COMPOSITE FAN FRAME DESIGN REPORT
S. C. Mitchell Sep. 1978 97 p refs
(Contract NAS3-18021)
(NASA-CR-135278; R77AEG439) Avail: NTIS
HC A04/MF A01 CSCL 21E

An advanced composite frame which is flight-weight and integrates the functions of several structures was developed for the over the wing (OTW) engine and for the under the wing (UTW) engine. The composite material system selected as the basic material for the frame is Type AS graphite fiber in a Hercules 3501 epoxy resin matrix. The frame was analyzed using a finite element digital computer program. This program was used in an iterative fashion to arrive at practical thicknesses and ply orientations to achieve a final design that met all strength and stiffness requirements for critical conditions. Using this information, the detail design of each of the individual parts of the frame was completed and released. On the basis of these designs, the required tooling was designed to fabricate the various

component parts of the frame. To verify the structural integrity of the critical joint areas, a full-scale test was conducted on the frame before engine testing. The testing of the frame established critical spring constants and subjected the frame to three critical load cases. The successful static load test was followed by 153 and 58 hours respectively of successful running on the UTW and OTW engines. J.M.S.

N80-15111* General Electric Co., Cincinnati, Ohio. Advanced Engineering and Technology Programs Dept.
QUIET CLEAN SHORT-HAUL EXPERIMENTAL ENGINE (QCSEE) UTW FAN PRELIMINARY DESIGN
Feb. 1975 107 p
(Contract NAS3-18021)
(NASA-CR-134842; R75AEG213) Avail: NTIS
HC A06/MF A01 CSCL 21E

High bypass geared turbofan engines and propulsion systems designed for short-haul passenger aircraft are described. The propulsion technology required for future externally blown flap aircraft with engines located both under the wing and over the wing is emphasized. The aerodynamic and mechanical preliminary design of the QCSEE under the wing 1.34 pressure ratio fan with variable blade pitch is presented. Design information is given for two pitch change actuation systems which will provide reverse thrust. J.M.S.

N80-15112* General Electric Co., Cincinnati, Ohio. Advanced Engineering and Technology Programs Dept.
QUIET CLEAN SHORT-HAUL EXPERIMENTAL ENGINE (QCSEE): THE AERODYNAMIC AND PRELIMINARY MECHANICAL DESIGN OF THE QCSEE OTW FAN
Feb. 1975 80 p
(Contract NAS3-18021)
(NASA-CR-134841; R75AEG381) Avail: NTIS
HC A05/MF A01 CSCL 21E

The aerodynamic and mechanical preliminary design of the QCSEE over the wing 1.36 pressure ratio fan is presented. Design information is given for both the experimental and flight designs. J.M.S.

N80-15113* General Electric Co., Cincinnati, Ohio. Advanced Engineering and Technology Programs Dept.
QUIET CLEAN SHORT-HAUL EXPERIMENTAL ENGINE (QCSEE) UNDER-THE-WING ENGINE COMPOSITE FAN BLADE DESIGN
May 1975 57 p
(Contract NAS3-18021)
(NASA-CR-134840; R75AEG278) Avail: NTIS
HC A04/MF A01 CSCL 21E

The design and analysis of a composite fan blade for the under the wing (UTW) QCSEE is presented. The blade is designed for a variable pitch, 18 bladed rotor and is constructed from a hybrid composite combination of materials consisting of Kevlar-49, type AS graphite, boron, and S-glass fibers in a PR288 epoxy resin matrix. The blade has an attached platform which is constructed of AS-graphite, PR278 epoxy resin matrix and aluminum honeycomb. The blade is designed to satisfy aerostability and cyclic life and strength requirements with a light weight construction. The attached platform is designed for a fail-safe condition in that it is retainable by the blade, under centrifugal force loading, even in the event of blade to platform bond separation. Details of the blade design and the results of stress, vibration, and impact analysis are included. J.M.S.

N80-15114* General Electric Co., Cincinnati, Ohio. Advanced Engineering and Technology Programs Dept.
QUIET CLEAN SHORT-HAUL EXPERIMENTAL ENGINE (QCSEE) OVER-THE-WING ENGINE AND CONTROL SIMULATION RESULTS
Oct. 1978 107 p refs
(Contract NAS3-18021)
(NASA-CR-135049; R76AEG218) Avail: NTIS
HC A06/MF A01 CSCL 21E

A hybrid-computer simulation of the over the wing turbofan engine was constructed to develop the dynamic design of the control. This engine and control system includes a full authority digital electronic control using compressor stator reset to achieve fast thrust response and a modified Kalman filter to correct for sensor failures. Fast thrust response for powered-lift operations and accurate, fast responding, steady state control of the engine is provided. Simulation results for throttle bursts from 62 to 100 percent takeoff thrust predict that the engine will accelerate from 62 to 95 percent takeoff thrust in one second. J.M.S.

N80-15115* General Electric Co., Cincinnati, Ohio. Aircraft Engine Group
QUIET CLEAN SHORT-HAUL EXPERIMENTAL ENGINE (QCSEE) BALL SPLINE PITCH-CHANGE MECHANISM WHIRLIGIG TEST REPORT
 Sep 1978 64 p refs
 (Contract NAS3-18021)
 (NASA-CR-135354; R77AEG394) Avail: NTIS
 HC A04/MF A01 CSCL 21E

The component testing of a ball spline variable pitch mechanism is described including a whirligig test. The variable pitch actuator successfully completed all planned whirligig tests including a fifty cycle endurance test at actuation rates up to 125 deg per second at up to 102 percent fan speed (3400 rpm). J.M.S.

N80-15116* General Electric Co., Cincinnati, Ohio. Advanced Engineering and Technology Programs Dept.
QUIET CLEAN SHORT-HAUL EXPERIMENTAL ENGINE (QCSEE) UNDER-THE-WING (UTW) BOILER PLATE NACELLE AND CORE EXHAUST NOZZLE DESIGN REPORT
 Oct. 1976 104 p
 (Contract NAS3-18021)
 (NASA-CR-135008; R76AEG222) Avail: NTIS
 HC A06/MF A01 CSCL 21E

The mechanical design of the boiler plate nacelle and core exhaust nozzle for the QCSEE under the wing engine is presented. The nacelle, which features interchangeable hard-wall and acoustic panels, is to be utilized in the initial engine testing to establish acoustic requirements for the subsequent composite nacelle as well as in the QCSEE over the wing engine configuration. J.M.S.

N80-15117* Hamilton Standard, Windsor Locks, Conn.
QUIET CLEAN SHORT-HAUL EXPERIMENTAL ENGINE (QCSEE) WHIRL TEST OF CAM/HARMONIC PITCH CHANGE ACTUATION SYSTEM Contractor Report, 10 Nov. 1975 - 16 Feb. 1976
 Apr. 1976 208 p refs
 (Contract NAS3-18021)
 (NASA-CR-135140; HSER-7002) Avail: NTIS
 HC A10/MF A01 CSCL 21E

A variable pitch fan actuation system, which incorporates a remote nacelle mounted blade angle regulator, was tested. The regulator drives a rotating fan mounted mechanical actuator through a flexible shaft and differential gear train. The actuator incorporates a high ratio harmonic drive attached to a multitrack spherical cam which changes blade pitch through individual cam follower arms attached to each blade trunnion. Testing of the actuator on a whirl rig, is reported. Results of tests conducted to verify that the unit satisfied the design requirements and was structurally adequate for use in an engine test are presented. J.M.S.

N80-15118* General Electric Co., Cincinnati, Ohio.
QUIET CLEAN SHORT-HAUL EXPERIMENTAL ENGINE (QCSEE) OVER-THE-WING (OTW) PROPULSION SYSTEMS TEST REPORT, VOLUME 4: ACOUSTIC PERFORMANCE
 D. L. Stimpert Feb. 1979 144 p refs
 (Contract NAS3-18021)
 (NASA-CR-135326; R77AEG476-Vol-4) Avail: NTIS
 HC A07/MF A01 CSCL 21E

A series of acoustic tests were conducted on the over the wing engine. These tests evaluated the fully suppressed noise levels in forward and reverse thrust operation and provided insight into the component noise sources of the engine plus the suppression achieved by various components. System noise levels using the contract specified calculation procedure indicate that the in-flight noise level on a 152 m sideline at takeoff and approach are 97.2 and 94.6 EPNdB, respectively, compared to a goal of 95.0 EPNdB. In reverse thrust, the system noise level was 106.1 PNdB compared to a goal of 100 PNdB. Baseline source noise levels agreed very well with pretest predictions. Inlet-radiated noise suppression of 14 PNdB was demonstrated with the high throat Mach number inlet at 0.79 throat Mach number. R.E.S.

N80-15119* General Electric Co., Cincinnati, Ohio. Advanced Engineering and Technology Programs Dept.
QUIET CLEAN SHORT-HAUL EXPERIMENTAL ENGINE (QCSEE) UNDER-THE-WING (UTW) COMPOSITE NACELLE Final Design Report
 E. A. Johnston Aug. 1978 128 p
 (Contract NAS3-18021)
 (NASA-CR-135352; R77AEG588) Avail: NTIS
 HC A07/MF A01 CSCL 21E

The detail design of the under the wing experimental composite nacelle components is summarized. Analysis of an inlet, fan bypass duct doors, core cowl doors, and variable fan nozzle are given. The required technology to meet propulsion system performance, weight, and operational characteristics is discussed. The materials, design, and fabrication technology for quiet propulsion systems which will yield installed thrust to weight ratios greater than 3.5 to 1 are described. R.C.T.

N80-15120* General Electric Co., Cincinnati, Ohio. Aircraft Engine Group.
QUIET CLEAN SHORT-HAUL EXPERIMENTAL ENGINE (QCSEE) Final Report
 William S. Willis Aug. 1979 408 p refs
 (Contract NAS3-18021)
 (NASA-CR-159473; R79AEG478) Avail: NTIS
 HC A18/MF A01 CSCL 21E

The design, fabrication, and testing of two experimental propulsion systems for powered lift transport aircraft are given. The under the wing (UTW) engine was intended for installation in an externally blown flap configuration and the over the wing (OTW) engine for use in an upper surface blowing aircraft. The UTW engine included variable pitch composite fan blades, main reduction gear, composite fan frame and nacelle, and a digital control system. The OTW engine included a fixed pitch fan, composite fan frame, boilerplate nacelle, and a full authority digital control. Many acoustic, pollution, performance, and weight goals were demonstrated. R.C.T.

N80-15121* General Electric Co., Cincinnati, Ohio. Advanced Engineering and Technology Programs Dept.
QUIET CLEAN SHORT-HAUL EXPERIMENTAL ENGINE (QCSEE). DOUBLE-ANNULAR CLEAN COMBUSTOR TECHNOLOGY DEVELOPMENT REPORT
 D. W. Bahr, D. L. Burrus, and P. E. Sabla May 1979 149 p refs
 (Contract NAS3-18021)
 (NASA-CR-159483; R79AEG397) Avail: NTIS
 HC A07/MF A01 CSCL 21E

A sector combustor technology development program was conducted to define an advanced double annular dome combustor sized for use in the quiet clean short haul experimental engine (QCSEE). A design which meets the emission goals, and combustor performance goals of the QCSEE engine program was developed. Key design features were identified which resulted in substantial reduction in carbon monoxide and unburned hydrocarbon emission levels at ground idle operating conditions, in addition to very low nitric oxide emission levels at high power operating conditions. Their significant results are reported. R.C.T.

N80-15122* General Electric Co., Cincinnati, Ohio. Aircraft Engine Group

QUIET CLEAN SHORT-HAUL EXPERIMENTAL ENGINE (QCSEE): ACOUSTIC TREATMENT DEVELOPMENT AND DESIGN

Art Clemons. May 1979. 353 p. refs.
(Contract NAS3-18021)
(NASA-CR-135266; R76AEG379-1) Avail. NTIS
HC A16/MF A01 CSCL 21E

Acoustic treatment designs for the quiet clean short-haul experimental engines are defined. The procedures used in the development of each noise-source suppressor device are presented and discussed in detail. A complete description of all treatment concepts considered and the test facilities utilized in obtaining background data used in treatment development are also described. Additional supporting investigations that are complementary to the treatment development work are presented. The expected suppression results for each treatment configuration are given in terms of delta SPL versus frequency and in terms of delta PNdB. R.E.S.

N80-15123* General Electric Co., Cincinnati, Ohio. Advanced Engineering and Technology Programs Dept.

QUIET CLEAN SHORT-HAUL EXPERIMENTAL ENGINE (QCSEE): PRELIMINARY ANALYSES AND DESIGN REPORT, VOLUME 1

Oct. 1974. 372 p.
(Contract NAS3-18021)
(NASA-CR-134838; R74AEG479-Vol-1) Avail. NTIS
HC A16/MF A01 CSCL 21E

The experimental propulsion systems to be built and tested in the 'quiet, clean, short-haul experimental engine' program are presented. The flight propulsion systems are also presented. The following areas are discussed: acoustic design; emissions control; engine cycle and performance; fan aerodynamic design; variable-pitch actuation systems; fan rotor mechanical design; fan frame mechanical design; and reduction gear design. R.E.S.

N80-15124* General Electric Co., Cincinnati, Ohio. Advanced Engineering and Technology Programs Dept.

QUIET CLEAN SHORT-HAUL EXPERIMENTAL ENGINE (QCSEE): PRELIMINARY ANALYSES AND DESIGN REPORT, VOLUME 2

Oct. 1974. 330 p.
(Contract NAS3-18021)
(NASA-CR-134839; R74AEG479-Vol-2) Avail. NTIS
HC A15/MF A01 CSCL 21E

The experimental and flight propulsion systems are presented. The following areas are discussed: engine core and low pressure turbine design; bearings and seals design; controls and accessories design; nacelle aerodynamic design; nacelle mechanical design; weight; and aircraft systems design. R.E.S.

N80-15125* General Electric Co., Cincinnati, Ohio. Advanced Engineering and Technology Programs Dept.

QUIET CLEAN SHORT-HAUL EXPERIMENTAL ENGINE (QCSEE) OVER-THE-WING (OTW) PROPULSION SYSTEM TEST REPORT, VOLUME 1: SUMMARY REPORT

Jan. 1978. 67 p.
(Contract NAS3-18021)
(NASA-CR-135323; R77AEG473-Vol-1) Avail. NTIS
HC A04/MF A01 CSCL 21E

Sea level, static, ground testing of the over-the-wing engine and boilerplate nacelle components was performed. The equipment tested and the test facility are described. Summaries of the instrumentations, the chronological history of the tests, and the test results are presented. R.E.S.

N80-15126* General Electric Co., Cincinnati, Ohio. Advanced Engineering and Technology Programs Dept.

QUIET CLEAN SHORT-HAUL EXPERIMENTAL ENGINE (QCSEE) OVER-THE-WING (OTW) PROPULSION SYSTEM TEST REPORT, VOLUME 3: MECHANICAL PERFOR-

MANCE

Feb. 1978. 121 p.
(Contract NAS3-18021)
(NASA-CR-135325; R77AEG475-Vol-3) Avail. NTIS
HC A06/MF A01 CSCL 21E

The mechanical performance of the over-the-wing engine is described with emphasis on the advanced technology components. The overall dynamic response of the engine was excellent. R.E.S.

N80-15130* Yale Univ., New Haven, Conn. Dept. of Engineering and Applied Science

THEORY OF DEPOSITION OF CONDENSIBLE IMPURITIES ON SURFACES IMMersed IN COMBUSTION GASES. Semiannual Report, 15 Jan. - 14 Jul. 1979

Daniel E. Rosner. 1979. 11 p. refs.
(Grant NSG-3107)
(NASA-CR-159716; SAR-6) Avail. NTIS HC A02/MF A01
CSCL 21E

The components resulting from the deposition of inorganic salts (e.g., Na₂SO₄) and oxides present in the combustion products from gas turbine engines were investigated. Emphasis was placed on the effects of multicomponent vapor transport, thermophoretic transport of vapor and small particles to actively cooled surfaces, variable fluid properties within mass transfer boundary layers, and free stream turbulence. R.C.T.

N80-15131* Yale Univ., New Haven, Conn. High Temperature Chemical Reaction Engineering Lab.

EXPERIMENTAL STUDIES OF THE FORMATION/DEPOSITION OF SODIUM SULFATE IN/FROM COMBUSTION GASES. Semiannual Report, 15 May - 15 Dec. 1979

Daniel E. Rosner. Dec. 1979. 10 p. refs.
(Grant NSG-3169)
(NASA-CR-159753; SAR-4) Avail. NTIS HC A02/MF A01
CSCL 21E

An optical polarization (ellipsometric) technique was developed for measuring rapidly growing and evaporating transparent liquid condensate films (e.g., boric oxide) on solid surfaces exposed to combustion product gases. Results for the B₂O₃ deposition rate from BCl₃-seeded propane/air flames are shown to agree well with the results of earlier interference measurements, and also with theoretical CVD predictions. Evaporation rates (from platinum ribbons into seeded propane air flames) are estimated using the polarization technique. It appears that, compared with the interference method, the polarization technique places less stringent requirements on surface quality, which may justify the added optical components needed for such measurements. It is concluded that the complementary optical methods of polarization (ellipsometry) and interference hold considerable promise for application to the rapid measurement of condensation and evaporation rates in high temperature (e.g., combustion product) environments. A.R.H.

N80-15083* General Electric Co., Washington, D. C. Aircraft Engine Group.

DEMONSTRATION OF SHORT-HAUL AIRCRAFT AFT NOISE REDUCTION TECHNIQUES ON A TWENTY INCH (50.8 cm) DIAMETER FAN, VOLUME 1

D. L. Stimpert and R. A. McFall. May 1975. 131 p. refs.
(Contract NAS3-18021)
(NASA-CR 134849; R75AEG252-Vol-1) Avail. NTIS
HC A07/MF A01 CSCL 21E

Tests of a 20 inch diameter, low tip speed, low pressure ratio fan which investigated aft fan noise reduction techniques are reported. These techniques included source noise reduction features of selection of vane-blade ratio to reduce second harmonic noise, spacing effects, and lowering the Mach number through a vane row. Aft suppression features investigated included porosity effects, variable depth treatment, and treatment regenerated flow noise. Initial results and selected comparisons are presented. J.M.S.

N80-15084* General Electric Co. Washington, D C Aircraft Engine Group

DEMONSTRATION OF SHORT HAUL AIRCRAFT AFT NOISE REDUCTION TECHNIQUES ON A TWENTY INCH (50.8) DIAMETER FAN, VOLUME 2

D L Stimpert Apr 1975 307 p 3 Vol

(Contract NAS3-18021)

(NASA CR 134850, R75AEG252 Vol-2)

Avail NTIS

HC A14/MF A01 CSCL 21E

All fan noise reduction techniques were investigated. The 1/3 octave band sound data were plotted with the following plots included: perceived noise level vs acoustic angle at 2 fan speeds, PWL vs frequency at 2 fan speeds, and sound pressure level vs frequency at 2 aft angles and 2 fan speeds. The source noise plots included: band pass filter sound pressure level vs acoustic angle at 2 fan speeds, and 2nd harmonic SPL acoustic angle at 2 fan speeds. R.C.T.

N80-15085* General Electric Co. Cincinnati, Ohio Aircraft Engine Group

DEMONSTRATION OF SHORT HAUL AIRCRAFT AFT NOISE REDUCTION TECHNIQUES ON A TWENTY INCH (50.8 cm) DIAMETER FAN, VOLUME 3

D L Stimpert Apr 1975 725 p 3 Vol

(Contract NAS3-18021)

(NASA CR 134851, R75AEG252-Vol-3)

Avail NTIS

HC A99/MF A01 CSCL 21E

Tests of a twenty inch diameter, low tip speed, low pressure ratio fan which investigated all fan noise reduction techniques are reported. The 1/3 octave band sound data are presented for all the configurations tested. The model data are presented on 17 foot arc and extrapolated to 200 foot sideline. J.M.S.

N80-15086* General Electric Co. Cincinnati, Ohio Advanced Engineering and Technology Programs Dept.

QUIET CLEAN SHORT-HAUL EXPERIMENTAL ENGINE (QCSEE) OVER THE WING (OTW) DESIGN REPORT Final Report

Jun 1977 530 p

(Contract NAS3-18021)

(NASA CR 134848, R75AEG443)

Avail NTIS

HC A23/MF A01 CSCL 21E

The design, fabrication, and testing of two experimental high bypass geared turbofan engines and propulsion systems for short haul passenger aircraft are described. The propulsion technology required for future externally blown flap aircraft with engines located both under the wing and over the wing is demonstrated. Position are among the parameters investigated. Straight and swept wing configurations were tested across a range of nozzle pressure ratios, lift coefficients, and Mach numbers. F.O.S.

N80-15099* General Electric Co., Cincinnati, Ohio Aircraft Engine Group.

QUIET CLEAN SHORT-HAUL EXPERIMENTAL ENGINE (QCSEE) OVER-THE-WING (OTW) BOILERPLATE NACELLE DESIGN REPORT

May 1977 78 p

(Contract NAS3-18021)

(NASA-CR-135168; R77AEG300)

Avail NTIS

HC A05/MF A01 CSCL 21E

A summary of the mechanical design of the boiler plate nacelle for the QCSEE over the wing (OTW) engine is presented. The nacelle, which features a D-shaped nozzle/thrust reverser and interchangeable hard wall and acoustic panels, is utilized in the engine testing to establish the aerodynamic and acoustic requirements for nozzles and reversers of this type. J.M.S.

N80-15100* General Electric Co., Cincinnati, Ohio Aircraft Engine Group.

QUIET CLEAN SHORT-HAUL EXPERIMENTAL ENGINE (QCSEE) UNDER-THE-WING (UTW) COMPOSITE NACELLE SUBSYSTEM TEST REPORT

C. L. Stoller, Jr., E. A. Johnston, and D. S. Freeman Jul. 1977 83 p refs

(Contract NAS3-18021)

(NASA-CR-135075, R76AEG420)

Avail NTIS

HC A05/MF A01 CSCL 21E

The element and subcomponent testing conducted to verify the under the wing composite nacelle design is reported. This composite nacelle consists of an inlet, outer cowl doors, inner cowl doors, and a variable fan nozzle. The element tests provided the mechanical properties used in the nacelle design. The subcomponent tests verified that the critical panel and joint areas of the nacelle had adequate structural integrity. J.M.S.

N80-15088* General Electric Co., Cincinnati, Ohio Advanced Engineering and Technology Programs Dept.

QUIET CLEAN SHORT-HAUL EXPERIMENTAL ENGINE (QCSEE) PRELIMINARY UNDER THE WING FLIGHT PROPULSION SYSTEM ANALYSIS REPORT

D. F. Howard Feb 1976 261 p refs

(Contract NAS3-18021)

(NASA-CR-134868, R75AEG349)

Avail NTIS

HC A12/MF A01 CSCL 21E

The preliminary design and installation of high bypass, geared turbofan engine with a composite nacelle forming the propulsion system for a short haul passenger aircraft are described. The technology required for externally blown flap aircraft with under the wing (UTW) propulsion system installations for introduction into passenger service in the mid 1980's is included. The design, fabrication, and testing of this UTW experimental engine containing the required technology items for low noise, fuel economy, with composite structure for reduced weight and digital engine control are provided. R.C.T.

N80-15089* General Electric Co., Cincinnati, Ohio Group Engineering Div.

QUIET CLEAN SHORT-HAUL EXPERIMENTAL ENGINE (QCSEE). THE AERODYNAMIC AND MECHANICAL DESIGN OF THE QCSEE OVER-THE-WING FAN

Apr 1976 98 p

(Contract NAS3-18021)

(NASA-CR-134915) Avail: NTIS HC A05/MF A01 CSCL 21E

The aerodynamic and mechanical design of a fixed-pitch 136 pressure ratio fan for the over-the-wing (OTW) engine is presented. The fan has 28 blades. Aerodynamically, the fan blades were designed for a composite blade, but titanium blades were used in the experimental fan as a cost savings measure. R.E.S.

N80-15090* General Electric Co., Cincinnati, Ohio Advanced Engineering and Technology Programs Dept.

QUIET CLEAN SHORT-HAUL EXPERIMENTAL ENGINE (QCSEE) UNDER-THE-WING ENGINE DIGITAL CONTROL SYSTEM DESIGN REPORT

Jan. 1978 321 p refs

(Contract NAS3-18021)

(NASA-CR-134920; R75AEG483)

Avail NTIS

HC A14/MF A01 CSCL 21E

A digital electronic control was combined with conventional hydromechanical components to operate the four controlled variables on the under-the-wing engine: fuel flow, fan blade pitch, fan exhaust area, and core compressor stator angles. The engine and control combination offers improvements in noise, pollution, thrust response, operational monitoring, and pilot workload relative to current engines. R.E.S.

N80-15091* General Electric Co., Cincinnati, Ohio Advanced Engineering and Technology Programs Dept.

QUIET CLEAN SHORT-HAUL EXPERIMENTAL ENGINE (QCSEE) UNDER-THE-WING ENGINE SIMULATION REPORT

Jul. 1977 103 p refs

(Contract NAS3-18021)

(NASA-CR-134914; R75AEG444)

Avail NTIS

HC A06/MF A01 CSCL 21E

Hybrid computer simulations of the under-the-wing engine were constructed to develop the dynamic design of the controls. The engine and control system includes a variable pitch fan and a digital electronic control. Simulation results for throttle bursts from 62 to 100 percent net thrust predict that the engine will accelerate 62 to 95 percent net thrust in one second. R.E.S.

N80-15092* General Electric Co., Cincinnati, Ohio. Advanced Engineering and Technology Programs Dept.
QUIET CLEAN SHORT-HAUL EXPERIMENTAL ENGINE (QCSEE) OVER-THE-WING CONTROL SYSTEM DESIGN REPORT

Dec. 1977 249 p refs
(Contract NAS3-18021)
(NASA-CR-135337; R77AEG664) Avail: NTIS
HC A11/MF A01 CSCL 21E

A control system incorporating a digital electronic control was designed for the over-the-wing engine. The digital electronic control serves as the primary controlling element for engine fuel flow and core compressor stator position. It also includes data monitoring capability, a unique failure indication and corrective action feature, and optional provisions for operating with a new type of servovalve designed to operate in response to a digital-type signal and to fail with its output device hydraulically locked into position. R.E.S.

N80-15093* General Electric Co., Cincinnati, Ohio. Aircraft Engine Group.

QUIET CLEAN SHORT-HAUL EXPERIMENTAL ENGINE (QCSEE), CORE ENGINE NOISE MEASUREMENTS

H. D. Sowers and W. E. Coward Dec. 1977 52 p ref
(Contract NAS3-18021)
(NASA-CR-135160; R75AEG511) Avail: NTIS
HC A04/MF A01 CSCL 21E

Noise measurements were taken on a turbofan engine which uses the same core, with minor modifications, employed on the quiet clean short-haul experimental engine (QCSEE) propulsion systems. Both nearfield and farfield noise measurements were taken in order to determine the core internally generated noise levels. The resulting noise measurements were compared to predicted combustor and turbine noise levels, to verify or improve the predicted QCSEE combustor and turbine noise levels. Author

N80-15094* General Electric Co., Cincinnati, Ohio. Aircraft Engine Engineering Div.

QUIET CLEAN SHORT-HAUL EXPERIMENTAL ENGINE (QCSEE) UNDER-THE-WING (UTW) ENGINE COMPOSITE NACELLE TEST REPORT, VOLUME 1: SUMMARY, AERODYNAMIC AND MECHANICAL PERFORMANCE

Apr. 1979 214 p refs
(Contract NAS3-18021)
(NASA-CR-159471; R78AEG573-Vol-1) Avail: NTIS
HC A10/MF A01 CSCL 21E

The performance test results of the final under-the-wing engine configuration are presented. One hundred and six hours of engine operation were completed, including mechanical and performance checkout, baseline acoustic testing with a bellmouth inlet, reverse thrust testing, acoustic technology tests, and limited controls testing. The engine includes a variable pitch fan having advanced composite fan blades and using a ball-spline pitch actuation system. R.E.S.

N80-15095* General Electric Co., Cincinnati, Ohio. Group Engineering Div.

QUIET CLEAN SHORT-HAUL EXPERIMENTAL ENGINE (QCSEE) PRELIMINARY OVER-THE-WING FLIGHT PROPULSION SYSTEM ANALYSIS REPORT

D. F. Howard Jun. 1977 174 p refs
(Contract NAS3-18021)
(NASA-CR-135296; R77AEG305) Avail: NTIS
HC A08/MF A01 CSCL 21E

The preliminary design of the over-the-wing flight propulsion system installation and nacelle component and systems design features of a short-haul, powered lift aircraft are presented.

Economic studies are also presented and show that high bypass, low pressure ratio turbofan engines have the potential of providing an economical propulsion system for achieving the very quiet aircraft noise level of 95 EPNdB on a 152.4 m sideline. R.E.S.

N80-15096* General Electric Co., Cincinnati, Ohio. Advanced Engineering and Technology Programs Dept.

QUIET CLEAN SHORT-HAUL EXPERIMENTAL ENGINE (QCSEE), UNDER-THE-WING (UTW) ENGINE BOILERPLATE NACELLE TEST REPORT, VOLUME 1 Summary Report

31 Dec. 1977 65 p 3 Vol.
(Contract NAS3-18021)
(NASA-CR-135249; R77AEG2121-Vol-1) Avail: NTIS
HC A04/MF A01 CSCL 21E

The design and testing of high bypass geared turbofan engines with nacelles forming the propulsion system for short haul passenger aircraft are considered. The test results demonstrate the technology required for externally blown flap aircraft for introduction into passenger service in the 1980's. The equipment tested is described along with the test facility and instrumentation. A chronological history of the test and a summary of results are given. J.M.S.

N80-15097* General Electric Co., Cincinnati, Ohio. Advanced Engineering and Technology Programs Dept.

QUIET CLEAN SHORT-HAUL EXPERIMENTAL ENGINE (QCSEE), UNDER-THE-WING (UTW) ENGINE BOILERPLATE NACELLE TEST REPORT, VOLUME 3: MECHANICAL PERFORMANCE

31 Dec. 1977 128 p refs 3 Vol.
(Contract NAS3-18021)
(NASA-CR-135251; R77AEG212-Vol-3) Avail: NTIS
HC A07/MF A01 CSCL 21E

Results of initial tests of the under the wing experimental engine and boilerplate nacelle are presented. The mechanical performance of the engine is reported with emphasis on the advanced technology components. Technology elements of the propulsion system covered include: system dynamics, composite fan blades, reduction gear, lube and accessory drive system, fan frame, inlet, core cowl cooling, fan exhaust nozzle, and digital control system. J.M.S.

N80-15098* General Electric Co., Cincinnati, Ohio.

QUIET CLEAN SHORT-HAUL EXPERIMENTAL ENGINE (QCSEE), COMPOSITE FAN FRAME SUBSYSTEM TEST REPORT

C. L. Stotler, Jr. and J. H. Bowden Sep. 1977 71 p
(Contract NAS3-18021)
(NASA-CR-135010; R76AEG233) Avail: NTIS
HC A04/MF A01 CSCL 21E

The element and subcomponent testing conducted to verify the composite fan frame design of two experimental high bypass geared turbofan engines and propulsion systems for short haul passenger aircraft is described. Emphasis is placed on the propulsion technology required for future externally blown flap aircraft with engines located both under the wing and over the wing, including technology in composite structures and digital engine controls. The element tests confirmed that the processes used in the frame design would produce the predicted mechanical properties. The subcomponent tests verified that the detail Composite structures and digital engine controls are among the topics included. R.C.T.

N80-15099* General Electric Co., Cincinnati, Ohio. Aircraft Engine Group.

QUIET CLEAN SHORT-HAUL EXPERIMENTAL ENGINE (QCSEE) OVER-THE-WING (OTW) BOILERPLATE NACELLE DESIGN REPORT

May 1977 78 p
(Contract NAS3-18021)
(NASA-CR-135168; R77AEG300) Avail: NTIS
HC A05/MF A01 CSCL 21E

A summary of the mechanical design of the boiler plate nacelle for the QCSEE over the wing (OTW) engine is presented. The nacelle, which features a D-shaped nozzle/thrust reverser and interchangeable hard wall and acoustic panels, is utilized in the engine testing to establish the aerodynamic and acoustic requirements for nozzles and reversers of this type. JMS

N80-16061* General Electric Co., Cincinnati, Ohio Aircraft Engine Group
CORE NOISE INVESTIGATION OF THE CF6-50 TURBOFAN ENGINE Data Report, 1978 - 1979
 V. L. Doyle Jan 1980 357 p
 (Contract NAS3-21260)
 (NASA-CR-159598, R79AEG247) Avail NTIS
 HC A16/MF A01 CSCL 21E

Acoustic data obtained during the running of the CF6-50 turbofan engine on an outdoor test stand are presented. The test was conducted to acquire simultaneous internal and far-field measurements to determine the influence of internally generated noise on the far-field measurements. The data includes internal and far-field narrowband and one-third octave band pressure spectra. RES

N80-16062* General Electric Co., Cincinnati, Ohio Aircraft Engine Group
CORE NOISE INVESTIGATION OF THE CF6-50 TURBOFAN ENGINE Final Report
 V. L. Doyle and M. T. Moore Jan 1980 520 p refs
 (Contract NAS3-21260)
 (NASA-CR-159749, R79AEG395) Avail NTIS
 HC A22/MF A01 CSCL 21E

The contribution of the standard production annular combustor to the far-field noise signature of the CF6-50 engine was investigated. Internal source locations were studied. Transfer functions were determined for selected pairs of combustor sensors and from two internal sensors to the air field. The coherent output power was determined in the far-field measurements, and comparisons of measured overall power level were made with component and engine correlating parameters. RES

N80-16063* Pratt and Whitney Aircraft Group, East Hartford, Conn.
EXPANDED STUDY OF FEASIBILITY OF MEASURING IN-FLIGHT 747/JT9D LOADS, PERFORMANCE, CLEARANCE, AND THERMAL DATA
 G. P. Sallee and R. L. Martin (Boeing Commercial Airplane Co., Seattle, Wash.) 4 Feb. 1980 107 p
 (Contract NAS3-20632)
 (NASA-CR-159717, PWA-5512-46) Avail: NTIS
 HC A06/MF A01 CSCL 21E

The JT9D jet engine exhibits a TSFC loss of about 1 percent in the initial 50 flight cycles of a new engine. These early losses are caused by seal-wear induced opening of running clearances in the engine gas path. The causes of this seal wear have been identified as flight induced loads which deflect the engine cases and rotors, causing the rotating blades to rub against the seal surfaces, producing permanent clearance changes. The real level of flight loads encountered during airplane acceptance testing and revenue service and the engine's response in the dynamic flight environment were investigated. The feasibility of direct measurement of these flight loads and their effects by concurrent measurement of 747/JT9D propulsion system aerodynamic and inertia loads and the critical engine clearance and performance changes during 747 flight and ground operations was evaluated. A number of technical options were examined in relation to the total estimated program cost to facilitate selection of the most cost effective option. It is concluded that a flight test program meeting the overall objective of determining the levels of aerodynamic and inertia load levels to which the engine is exposed during the initial flight acceptance test and normal flight maneuvers is feasible and desirable. A specific recommended flight test program, based on the evaluation of cost effectiveness, is defined. A.R.H.

N80-17073* Pratt and Whitney Aircraft Group, West Palm Beach, Fla.
DISTRIBUTION ANALYSIS FOR F100(3) ENGINE Final Report

W. A. Walter and M. Shaw Jan 1980 66 p refs
 (Contract NAS3-20835)
 (NASA-CR-159754, FR-12087) Avail NTIS
 HC A04/MF A01 CSCL 21E

The F100(3) compression system response to inlet circumferential distortion was investigated using an analytical compressor flow model. Compression system response to several types of distortion, including pressure, temperature, and combined pressure/temperature distortions, was investigated. The predicted response trends were used in planning future F100(3) distortion tests. Results show that compression system response to combined temperature and pressure distortions depends upon the relative orientation, as well as the individual amplitudes and circumferential extents of the distortions. Also the usefulness of the analytical predictions in planning engine distortion tests is indicated. JMS

N80-17074* Pratt and Whitney Aircraft, East Hartford, Conn.
EXPERIMENTAL EVALUATION OF A LOW EMISSIONS HIGH PERFORMANCE DUCT BURNER FOR VARIABLE CYCLE ENGINES (VCE) Final Report

R. P. Lohmann and R. J. Mador Oct 1979 118 p refs
 (Contract NAS3-20802)
 (NASA-CR-159694, PWA-5513-32A) Avail: NTIS
 HC A06/MF A01 CSCL 21A

An evaluation was conducted with a three stage Vortex duct burner to determine the performance and emissions characteristics of the concept and to refine the configuration to provide acceptable durability and operational characteristics for its use in the variable cycle engine (VCE) testbed program. The tests were conducted at representative takeoff, transonic climb, and supersonic cruise inlet conditions for the VSCE-502B study engine. The test stand, the emissions sampling and analysis equipment, and the supporting flow visualization rigs are described. The performance parameters including the fuel-air ratio, the combustion efficiency/exist temperature, thrust efficiency, and gaseous emissions calculations are defined. The test procedures are reviewed and the results are discussed. A.W.H.

N80-18040* Little (Arthur D.), Inc., Cambridge, Mass.
STUDY OF RESEARCH AND DEVELOPMENT REQUIREMENTS OF SMALL GAS-TURBINE COMBUSTORS
 E. P. Demetri, R. F. Topping, and R. P. Wilson, Jr. Jan. 1980 69 p refs
 (Contract NAS3-21980)
 (NASA-CR-159798, ADL-83381-2) Avail: NTIS
 HC A04/MF A01 CSCL 21E

A survey is presented of the major small-engine manufacturers and governmental users. A consensus was undertaken regarding small-combustor requirements. The results presented are based on an evaluation of the information obtained in the course of the study. The current status of small-combustor technology is reviewed. The principal problems lie in liner cooling, fuel injection, part-power performance, and ignition. Projections of future engine requirements and their effect on the combustor are discussed. The major changes anticipated are significant increases in operating pressure and temperature levels and greater capability of using heavier alternative fuels. All aspects of combustor design are affected, but the principal impact is on liner durability. An R&D plan which addresses the critical combustor needs is described. The plan consists of 15 recommended programs for achieving necessary advances in the areas of liner thermal design, primary-zone performance, fuel injection, dilution, analytical modeling, and alternative-fuel utilization. M.M.M.

N80-18041* General Electric Co., Cincinnati, Ohio Aircraft Engine Group
INTERNAL COATING OF AIR COOLED GAS TURBINE BLADES Final Report
 P. L. Ahuja Nov. 1979 73 p refs

(Contract NAS3-21038)
(NASA-CR-159701) Avail NTIS HC A04/MF A01 CSCL 21E

Six coating systems were evaluated for internal coating of decent stage (DS) eutectic high pressure turbine blades. Sequential deposition of electroless Ni by the hydrazine process, slurry Cr, and slurry Al, followed by heat treatment provided the coating composition and thickness for internal coating of DS eutectic turbine blades. Both NiCr and NiCrAl coating compositions were evaluated for strain capability and ductile to brittle transition temperature RCT

N80-18042* Vought Corp., Dallas, Tex
LOW SPEED TEST OF THE AFT INLET DESIGNED FOR A TANDEM FAN V/STOL NACELLE

W W Rhodes and A H Ybarra Feb 1980 79 p refs

(Contract NAS3-21468)

(NASA-CR-159752, TR-2-30320/OR-52360) Avail NTIS HC A05/MF A01 CSCL 21E

An approximately 25 scale model of a Tandem Fan nacelle designed for a Type A V/STOL aircraft configuration was tested in a 10-by-10 foot wind tunnel. A 12 inch, tip driven, turbofan simulator was used to provide the suction source for the aft fan inlet. The front fan inlet was faired over for this test entry. Model variables consisted of a long aft inlet cowl, a short aft inlet cowl, a shaft simulator, blow-in door passages and diffuser vortex generators. Inlet pressure recovery, distortion, inlet angle of attack separation limits were evaluated at tunnel velocities from 0 to 240 knots, angles of attack from -10 to 40 degrees and inlet flow rates representative of throat Mach numbers of 0.1 to 0.6. High inlet performance and stable operation was verified at all design forward speed and angle of attack conditions. The short aft inlet configuration provided exceptionally high pressure recovery except at the highest combination of angle of attack and forward speed. The flow quality at the fan face was somewhat degraded by the addition of blow-in door passages to the long aft inlet configuration due to the pressure disturbances generated by the flow entering the diffuser through the auxiliary air passages M M M

N80-19113* Pratt and Whitney Aircraft Group, East Hartford, Conn. Commercial Products Div.

CORE COMPRESSOR EXIT STAGE STUDY. 1: AERODYNAMIC AND MECHANICAL DESIGN

E. A. Burdall, E. Canal, Jr., and K. A. Lyons Sep. 1979 128 p ref

(Contract NAS3-20578)

(NASA-CR-159714; FWA-5561-55)

Avail: NTIS

HC A07/MF A01 CSCL 21E

The effect of aspect ratio on the performance of core compressor exit stages was demonstrated using two three stage, highly loaded, core compressors. Aspect ratio was identified as having a strong influence on compressors endwall loss. Both compressors simulated the last three stages of an advanced eight stage core compressor and were designed with the same 0.915 hub/tip ratio, 4.30 kg/sec (9.47 lbm/sec) inlet corrected flow, and 167 m/sec (547 ft/sec) corrected mean wheel speed. The first compressor had an aspect ratio of 0.81 and an overall pressure ratio of 1.357 at a design adiabatic efficiency of 88.3% with an average diffusion factor of 0.529. The aspect ratio of the second compressor was 1.22 with an overall pressure ratio of 1.324 at a design adiabatic efficiency of 88.7% with an average diffusion factor of 0.491. R.C.T.

N80-20271* Teledyne Continental Motors, Muskegon, Mich.
A 150 AND 300 kW LIGHTWEIGHT DIESEL AIRCRAFT ENGINE DESIGN STUDY Final Report

Alex P. Brouwers Apr. 1980 149 p refs

(Contract NAS3-20830)

(NASA-CR-3280; Rept-756) Avail: NTIS HC A07/MF A01 CSCL 21A

The diesel engine was reinvestigated as an aircraft powerplant through design study conducted to arrive at engine configurations and applicable advanced technologies. Two engines are discussed, a 300 kW six-cylinder engine for twin engine general aviation

aircraft and a 150 kW four-cylinder engine for single engine aircraft. Descriptions of each engine include concept drawings, a performance analysis, stress and weight data, and a cost study. This information was used to develop two airplane concepts, a six-place twin and a four-place single engine aircraft. The aircraft study consists of installation drawings, computer generated performance data, aircraft operating costs, and drawings of the resulting airplanes. The performance data show a vast improvement over current gasoline-powered aircraft. RES

N80-21328* General Electric Co., Cincinnati, Ohio Aircraft Engine Group.

PROGRAM FOR IMPACT TESTING OF SPAR-SHELL FAN BLADES, TEST REPORT

R. Ravenhall and C. T. Salemme Apr. 1978 95 p

(Contract NAS3-20801)

(NASA-CR-135393; R78AEG444)

Avail: NTIS

HC A05/MF A01 CSCL 21E

Six filament-wound, composite spar-shell fan blades were impact tested in a whirling rig relative to foreign object damage resulting from ingestion of birds into the fan blades of a QCSEE-type engine. Four of the blades were tested by injecting a simulated two pound bird into the path of the rotating blade and two were tested by injecting a starling into the path of the blade. RES

N80-21329* Pratt and Whitney Aircraft Group, East Hartford, Conn. Commercial Products Div.

MANUFACTURE OF LOW CARBON ASTROLOGY TURBINE DISK SHAPES BY HOT ISOSTATIC PRESSING, VOLUME 2, PROJECT 1 Final Report

R. D. Eng and D. J. Evans Jan. 1979 10 p

(Contract NAS3-20072)

(NASA-CR-135410; FWA-5574-37)

Avail: NTIS

HC A02/MF A01 CSCL 21E

The performance of a hot isostatic pressed disk installed in an experimental engine and exposed to realistic operating conditions in a 150-hour engine test and a 1000 cycle endurance test is documented. Post test analysis, based on visual, fluorescent penetrant and dimensional inspection, revealed no defects in the disk and indicated that the disk performed satisfactorily. RES

N80-21330* IIT Research Inst., Chicago, Ill.
THERMAL FATIGUE AND OXIDATION DATA FOR DIRECTIONALLY SOLIDIFIED MAR-M 246 TURBINE BLADES

V. L. Hill and V. E. Humphreys Jan. 1980 45 p refs

(Contract NAS3-19696)

(NASA-CR-159798; IITRI-M6003-53)

Avail: NTIS

HC A03/MF A01 CSCL 21E

Thermal fatigue and oxidation data were obtained for 11 plasma spray coated and 13 uncoated directionally solidified and single crystal MAR-M 246 blades. Blade coatings on the airfoil included several metal-oxide thermal barrier layers based on Al₂O₃, Cr₂O₃, or ZrO₂. The 24 turbine blades were tested simultaneously for 3000 cycles in fluidized beds maintained at 950 and 25 C using a symmetrical 360 sec thermal cycle. In 3000 cycles, only uncoated turbine blades exhibited cracking on the trailing edge near the platform; 3 of the 13 uncoated blades did not crack. Cracking occurred over the range 400 to 2750 cycles, with single crystal blades indicating the poorest thermal fatigue resistance. Oxidation of the uncoated blades was limited in 3000 cycles. All coatings indicated microscopically visible spalling at the trailing edge radius after 3000 cycles. Severe general spalling on the airfoil was observed for two multilayered coatings. Author

N80-21331* AiResearch Mfg. Co., Phoenix, Ariz.

AIRESEARCH QCGAT PROGRAM Final Report

R. W. Heldenbrand and W. M. Norgren 10 Jan. 1979 199 p

refs

(Contract NAS3-20585)

(NASA-CR-159758; AIRESEARCH-21-3071) Avail: NTIS

HC A09/MF A01 CSCL 21E

A model TFE731-1 engine was used as a baseline for the NASA quiet clean general aviation turbofan engine and engine/nacelle program designed to demonstrate the applicability of large turbofan engine technology to small general aviation turbofan engines, and to obtain significant reductions in noise and pollutant emissions while reducing or maintaining fuel consumption levels. All new technology design for rotating parts and all items in the engine and nacelle that contributed to the acoustic and pollution characteristics of the engine system were of flight design, weight, and construction. The major noise, emissions, and performance goals were met. Noise levels estimated for the three FAR Part 36 conditions, are 10 to 15 ENPD below FAA requirements; emission values are considerably reduced below that of current technology engines; and the engine performance represents a TSFC improvement of approximately 9 percent over other turbofan engines. A.R.H.

N80-21332*# Pratt and Whitney Aircraft Group, East Hartford, Conn.**DEVELOPMENT OF IMPROVED HIGH PRESSURE TURBINE OUTER GAS PATH SEAL COMPONENTS Progress Report, Dec. 1976 - Oct. 1979**

Lawrence T. Shiembob Jan. 1980 80 p

(Contract NAS3-20590)

(NASA-CR-159801; PWA-5568)

Avail: NTIS

HC A05/MF A01 CSCL 21E

A plasma sprayed graded layered ceramic/metallic (ZrO₂/CoCrAlY) seal was evaluated for JT9D turbine application by rig and engine tests. Four cyclic thermal shock rig tests were conducted during the program. Three completed 1000 simulated engine thermal cycle tests and the fourth completed 500 cycles without severe cracking or spalling. Three ceramic seals were installed in a JT9D experimental engine to evaluate the effect of the engine thermal environment on the seals. All three seals completed the test successfully without severe cracking or spalling. The three seals did have slight laminar cracks at the 85/15-40/60 ZrO₂/CoCrAlY interface. The second engine test evaluated the rub capabilities of the seal. Six ceramic seals were installed in the engine with fourteen abrasive tip blades. Three of the six seals rubbed to a depth of 24 mils. Eight of the fourteen abrasive tip blades showed evidence of wear. Three of the eight blades wore a maximum of five mils. Engine rub test results demonstrated the potential of reducing turbine clearances and thereby improving engine performance by use of sprayed ceramic seals. J.M.S.

N80-21334*# Pratt and Whitney Aircraft Group, West Palm Beach, Fla.**DATA ANALYSIS OF P SUB T/P SUB S NOSEBOOM PROBE TESTING ON F100 ENGINE P80072 AT NASA LEWIS RESEARCH CENTER Final Report**

C. H. Foote Mar. 1980 23 p

(Contract NAS3-19442)

(NASA-CR-159816; PWA-FR-12540)

Avail: NTIS

HC A02/MF A01 CSCL 21E

Results from the altitude testing of a P sub T/P sub S noseboom probe on the F100 engine are discussed. The results are consistent with sea level test results. The F100 engine altitude test verified automatic downmatch with the engine pressure ratio control, and backup control inlet case static pressure demonstrated sufficient accuracy for backup control fuel flow scheduling. The production P6 probe measured Station 6 pressures accurately for both undistorted and distorted inlet airflows. M.G.

N80-22323*# Massachusetts Inst. of Tech., Cambridge. Aeroelastic and Structures Research Lab.**TWO-DIMENSIONAL FINITE-ELEMENT ANALYSES OF SIMULATED ROTOR-FRAGMENT IMPACTS AGAINST RINGS AND BEAMS COMPARED WITH EXPERIMENTS**

Thomas R. Stagliano, Emmett A. Witmer, and Jose J. A. Rodal Dec. 1979 363 p refs

(Grant NGR-22-009-339)

(NASA CR-159645; ASRL-TR-154-13)

Avail: NTIS

HC A16/MF A01 CSCL 21E

Finite element modeling alternatives as well as the utility

and limitations of the two dimensional structural response computer code CIVM-JET 4B for predicting the transient, large deflection, elastic plastic, structural responses of two dimensional beam and/or ring structures which are subjected to rigid fragment impact were investigated. The applicability of the CIVM-JET 4B analysis and code for the prediction of steel containment ring response to impact by complex deformable fragments from a trihub burst of a T58 turbine rotor was studied. Dimensional analysis considerations were used in a parametric examination of data from engine rotor burst containment experiments and data from sphere beam impact experiments. The use of the CIVM-JET 4B computer code for making parametric structural response studies on both fragment-containment structure and fragment-deflector structure was illustrated. Modifications to the analysis/computation procedure were developed to alleviate restrictions. E.D.K.

N80-22324*# Pratt and Whitney Aircraft Group, East Hartford, Conn.**PERFORMANCE DETERIORATION BASED ON EXISTING (HISTORICAL) DATA; JT9D JET ENGINE DIAGNOSTICS PROGRAM**

G. Phil Sallee 20 Apr. 1978 228 p refs

(Contract NAS3-20632)

(NASA-CR-135448; PWA-5512-21)

Avail: NTIS

HC A11/MF A01 CSCL 21E

The results of the collection and analysis of historical data pertaining to the deterioration of JT9D engine performance are presented. The results of analyses of prerepair and postrepair engine test stand performance data from a number of airlines to establish the individual as well as average losses in engine performance with respect to service use are included. Analysis of the changes in mechanical condition of parts, obtained by inspection of used gas-path parts of varying age, allowed preliminary assessments of component performance deterioration levels and identification of the causative factors. These component performance estimates, refined by data from special engine back-to-back testing related to module performance restoration, permitted the development of preliminary models of engine component/module performance deterioration with respect to usage. The preliminary assessment of the causes of module performance deterioration and the trends with usage are explained, along with the role each module plays in overall engine performance deterioration. Preliminary recommendations with respect to operating and maintenance practices which could be adopted to control the level of performance deterioration are presented. The needs for additional component sensitivity testing as well as outstanding issues are discussed. J.M.S.

N80-22325*# Solar Turbines International, San Diego, Calif. ADVANCED CERAMIC MATERIAL FOR HIGH TEMPERATURE TURBINE TIP SEALS Final Report, Feb. 1976 - May 1979

J. W. Vogan, N. G. Solomon, and A. R. Stetson Jan. 1980 97 p refs

(Contract NAS3-20081)

(NASA-CR-159774; SR79-R-4482-43; RDR-1831-43)

Avail: NTIS HC A05/MF A01 CSCL 11A

Forty-one material systems were evaluated for potential use in turbine blade tip seal applications at 1370 C. Both ceramic blade tip inserts and abradable ceramic tip shoes were tested. Hot gas erosion, impact resistance, thermal stability, and dynamic rub performance were the criteria used in rating the various materials. Silicon carbide and silicon nitride were used, both as blade tips and abradables. The blade tip inserts were fabricated by hot pressing while low density and honeycomb abradables were sintered or reaction bonded. Author

N80-22326*# Teledyne Continental Motors, Muskegon, Mich. DESIGN STUDY: A 186 kW LIGHTWEIGHT DIESEL AIRCRAFT ENGINE Final Report

Alex P. Brouwers Apr. 1980 24 p

(Contract NAS3-20830)

(NASA-CR-3261) Avail: NTIS HC A02/MF A01 CSCL 21E

The design of an aircraft engine capable of developing 186 kW shaft power at a 7620 m altitude is described. The 186 kW design takes into account expected new developments in aircraft designs resulting in a reassessment of the power requirements at the cruise mode operation. Based on the results of this analysis a three phase technology development program is projected resulting in production dates of 1985, 1992, and 2000. R.E.S.

N80-22333*# Avco Lycoming Div., Stratford, Conn.
AVCO LYCOMING QUIET CLEAN GENERAL AVIATION TURBOFAN ENGINE

Craig A. Wilson / In NASA, Lewis Res. Center Gen. Aviation Propulsion Mar. 1980 p 155-187 refs (For primary document see N80-22327 13-07)

Avail: NTIS HC A19/MF A01 CSCL 21E

A fan module was developed using an existing turboshaft engine. The fan was designed using the latest in large engine noise control technology. A mixer was added to reduce the already low exhaust gas velocity. A nacelle incorporating sound treatment was provided for the test engine. A noise prediction model was used through the design process to evaluate the various design alternatives. Acoustic tests were then made to development of advances in combustion systems, electronics, materials and control systems. R.E.S.

N80-23309*# General Electric Co., Cincinnati, Ohio.
CF6 JET ENGINE PERFORMANCE IMPROVEMENT: NEW FAN

W. A. Fasching May 1980 202 p

(Contract NAS3-20629)

(NASA-CR-159699; R79AEG413)

Avail: NTIS

HC A10/MF A01 CSCL 21E

As part of the NASA sponsored engine component improvement program, and fan package was developed to reduce fuel consumption in current CF6 turbofan aircraft engine. The new fan package consist of an improved fan blade, reduced fan tip clearance due to a fan case stiffener, and a smooth fan casing tip shroud. CF6 engine performance and acoustic tests demonstrated the predicted 1.8% improvement in cruise sfc without an increase in engine noise. Power management thrust/fan speed characteristics were defined. Mechanical and structural integrity was demonstrated in model fan rotor photoelastic stress tests, full-size fan blade bench fatigue tests, and CF6 engine bird ingestion, crosswind, and cyclic endurance tests. The fan was certified in the CF6-500c2/E2 engines and is in commercial service on the Boeing 747-200, Douglas DC-10-30, and Airbus Industrie A300B aircraft. A.R.H.

N80-23311*# Hamilton Standard, Windsor Locks, Conn.
ACOUSTIC TEST AND ANALYSES OF THREE ADVANCED TURBOPROP MODELS Final Report

Bennett M. Brooks and F. B. Metzger Jan. 1980 245 p refs (Contract NAS3-20614)

(NASA-CR-159667) Avail: NTIS HC A11/MF A01 CSCL 21E

Results of acoustic tests of three 62.2 cm (24.5 inch) diameter models of the prop-fan (a small diameter, highly loaded, multi-bladed variable pitch advanced turboprop) are presented. Results show that there is little difference in the noise produced by unswept and slightly swept designs. However, the model designed for noise reduction produces substantially less noise at test conditions simulating 0.8 Mach number cruise speed or at conditions simulating takeoff and landing. In the near field at cruise conditions the acoustically designed. In the far field at takeoff and landing conditions the acoustically designed model is 5 db quieter than unswept or slightly swept designs. Correlation between noise measurement and theoretical predictions as well as comparisons between measured and predicted acoustic pressure pulses generated by the prop-fan blades are discussed. The general characteristics of the pulses are predicted. Shadowgraph measurements were obtained which showed the location of bow and trailing waves. R.C.T.

N80-23312*# Pratt and Whitney Aircraft Group, East Hartford, Conn.

CORE COMPRESSOR EXIT STAGE STUDY, 2 Final Report

R. F. Behlke, E. A. Burdall, E. Canal, Jr., and N. D. Korn Oct. 1979 90 p refs

(Contract NAS3-20578)

(NASA-CR-159812; PWA-5561-66)

Avail: NTIS

HC A05/MF A01 CSCL 21E

A total of two three-stage compressors were designed and tested to determine the effects of aspect ratio on compressor performance. The first compressor was designed with an aspect ratio of 0.81; the other, with an aspect ratio of 1.22. Both compressors had a hub-tip ratio of 0.915, representative of the rear stages of a core compressor, and both were designed to achieve a 15.0% surge margin at design pressure ratios of 1.357 and 1.324, respectively, at a mean wheel speed of 167 m/sec. At design speed the 0.81 aspect ratio compressor achieved a pressure ratio of 1.346 at a corrected flow of 4.28 kg/sec and an adiabatic efficiency of 86.1%. The 1.22 aspect ratio design achieved a pressure ratio of 1.314 at 4.35 kg/sec flow and 87.0% adiabatic efficiency. Surge margin to peak efficiency was 24.0% with the lower aspect ratio blading, compared with 12.4% with the higher aspect ratio blading.

R.C.T.

N80-23315*# Williams Research Corp., Walled Lake, Mich.
CONCEPTUAL DESIGN STUDY OF AN IMPROVED GAS TURBINE POWERTRAIN Final Report

W. I. Chapman Mar. 1980 294 p refs

(Contracts DEN3-12; EC-77-A-31-1040)

(NASA-CR-159852; DOE/NASA/0013-80/1; WRC-78-182)

Avail: NTIS HC A13/MF A01 CSCL 21E

The conceptual design for an improved gas turbine (IGT) powertrain and vehicle was investigated. Cycle parameters, rotor systems, and component technology were reviewed and a dual rotor gas turbine concept was selected and optimized for best vehicle fuel economy. The engine had a two stage centrifugal compressor with a design pressure ratio of 5.28, two axial turbine stages with advanced high temperature alloy integral wheels, variable power turbine nozzle for turbine temperature and output torque control, catalytic combustor, and annular ceramic recuperator. The engine was rated at 54.81 kW, using water injection on hot days to maintain vehicle acceleration. The estimated vehicle fuel economy was 11.9 km/l in the combined driving cycle, 43 percent over the 1976 compact automobile. The estimated IGT production vehicle selling price was 10 percent over the comparable piston engine vehicle, but the improved fuel economy and reduced maintenance and repair resulted in a 9 percent reduction in life cycle cost. R.C.T.

N80-23316*# General Electric Co., Cincinnati, Ohio. Aircraft Engine Group.

CF6-6D ENGINE SHORT-TERM PERFORMANCE DETERIORATION

W. H. Kramer, J. E. Paas, J. J. Smith, and R. H. Wulf Apr. 1980 154 p

(Contract NAS3-20631)

(NASA-CR-159830; R80AEG374)

Avail: NTIS

HC A08/MF A01

Studies conducted as part of the NASA-Lewis CF6 jet engine diagnostics program are summarized. An 82-engine sample of DC-10-10 aircraft engine checkout data that were gathered to define the extent and magnitude of CF6-6D short term performance deterioration were analyzed. These data are substantiated by the performance testing and analytical teardown of CF6-6D short term deterioration engine serial number (ESN) 451507. R.C.T.

N80-25332*# Pratt and Whitney Aircraft Group, East Hartford, Conn. Commercial Products Div.

ENGINE COMPONENT IMPROVEMENT: PERFORMANCE IMPROVEMENT, JT9D-7 3.8 AR FAN Progress Report, Jan. 1978 - Feb. 1979

W. O. Gaffin 12 Jun. 1980 57 p ref

(Contract NAS3-20630)
(NASA-CR-159806; PWA-5515-114) Avail: NTIS
HC A04/MFA01 CSCL 21E

A redesigned, fuel efficient fan for the JT9D-7 engine was tested. Tests were conducted to determine the effect of the 3.8 AR fan on performance, stability, operational characteristics, and noise of the JT9D-7 engine relative to the current 4.6 AR Bill-of-Material fan. The 3.8 AR fan provides increased fan efficiency due to a more advanced blade airfoil with increased chord, eliminating one part span shroud and reducing the number of fan blades and fan exit guide vanes. Engine testing at simulated cruise conditions demonstrated the predicted 1.3 percent improvement in specific fuel consumption with the redesigned 3.8 AR fan. Flight testing and sea level stand engine testing demonstrated exhaust gas temperature margins, fan and low pressure compressor stability, operational suitability, and noise levels comparable to the Bill-of-Material fan. Author

N80-25333* Pratt and Whitney Aircraft, East Hartford, Conn. Commercial Products Div.

STUDY OF BLADE ASPECT RATIO ON A COMPRESSOR FRONT STAGE Final Report, 28 Oct. 1977 - 28 May 1979
R. F. Behlke, J. D. Brooky, and E. Canal, Jr. Nov. 1980 261 p refs

(Contract NAS3-20809)
(NASA-CR-159556; PWA-5583-58) Avail: NTIS
HC A12/MF A01 CSCL 21E

A single stage, low aspect ratio, compressor with a 442.0 m/sec (1450 ft/sec) tip speed and a 0.597 hub/tip ratio typical of an advanced core compressor front stage was tested. The test stage incorporated an inlet duct which was representative of an engine transition duct between fan and high pressure compressors. At design speed, the rotor stator stage achieved a peak adiabatic efficiency of 86.6 percent at a flow of 44.35 kg/sec (97.8 lbm/sec) and a pressure ratio of 1.8. Surge margin was 12.5 percent from the peak stage efficiency point. Author

N80-25335* Detroit Diesel Allison, Indianapolis, Ind.
EXPERIMENTAL DETERMINATION OF UNSTEADY BLADE ELEMENT AERODYNAMICS IN CASCADES. VOLUME 1: TORSION MODE CASCADE Final Report

R. E. Riffel and M. D. Rothrock Jun. 1980 305 p
(Contract NAS3-20055)
(NASA-CR-159831; EDR-10119-Vol-1) Avail: NTIS
HC A14/MF A01 CSCL 21E

A two dimensional cascade of harmonically oscillating airfoils was designed to model a near tip section from a rotor which was known to have experienced supersonic torsional flutter. This five bladed cascade had a solidity of 1.17 and a setting angle of 1.07 rad. Graphite epoxy airfoils were fabricated to achieve the realistically high reduced frequency level of 0.44. The cascade was tested over a range of static pressure ratios approximating the blade element operating conditions of the rotor along a constant speed line which penetrated the flutter boundary. The time-steady and time-unsteady flow field surrounding the center cascade airfoil were investigated. The effects of reduced solidity and decreased setting angle on the flow field were also evaluated. Author

N80-25340* Pratt and Whitney Aircraft Group, East Hartford, Conn. Commercial Products Div.
PERFORMANCE DETERIORATION BASED ON IN-SERVICE ENGINE DATA: JT9D JET ENGINE DIAGNOSTICS PROGRAM

G. P. Sallee 27 Apr. 1979 185 p refs
(Contract NAS3-20632)
(NASA-CR-159525; PWA-5512-35) Avail: NTIS
HC A09/MF A01 CSCL 21E

Results of analyses of engine performance deterioration trends and levels with respect to service usage are presented. Thirty-two JT9D-7A engines were selected for this purpose. The selection of this engine fleet provided the opportunity of obtaining engine performance data starting before the first flight through initial service such that the trend and levels of engine deterioration related to both short and long term deterioration could be more

carefully defined. The performance data collected and analyzed included in-flight, on wing (ground), and test stand prerepair and postrepair performance calibrations with expanded instrumentation where feasible. The results of the analyses of these data were used to: (1) close gaps in previously obtained historical data as well as augment the historical data with more carefully obtained data; (2) refine preliminary models of performance deterioration with respect to usage; (3) establish an understanding of the relationships between ground and altitude performance deterioration trends; (4) refine preliminary recommendations concerning means to reduce and control deterioration; and (5) identify areas where additional effort is required to develop an understanding of complex deterioration issues. E.R.

N80-26300* Pratt and Whitney Aircraft Group, East Hartford, Conn. Commercial, Products Div.

EXPERIMENTAL AERODYNAMIC AND ACOUSTIC MODEL TESTING OF THE VARIABLE CYCLE ENGINE (VCE) TESTBED COANNULAR EXHAUST NOZZLE SYSTEM

D. P. Nelson and P. M. Morris 15 Jun. 1980 83 p
(Contract NAS3-20061)
(NASA-CR-159710; PWA-5550-31) Avail: NTIS
HC A05/MF A01 CSCL 21E

Aerodynamic performance and jet noise characteristics of a one sixth scale model of the variable cycle engine testbed exhaust system were obtained in a series of static tests over a range of simulated engine operating conditions. Model acoustic data were acquired. Data were compared to predictions of coannular model nozzle performance. The model, tested with and without a hardwall ejector, had a total flow area equivalent to a 0.127 meter (5 inch) diameter conical nozzle with a 0.65 fan to primary nozzle area ratio and a 0.82 fan nozzle radius ratio. Fan stream temperatures and velocities were varied from 422 K to 1089 K (760 R to 1960 R) and 434 to 755 meters per second (1423 to 2477 feet per second). Primary stream properties were varied from 589 to 1089 K (1060 R to 1960 R) and 353 to 600 meters per second (1158 to 1968 feet per second). Exhaust plume velocity surveys were conducted at one operating condition with and without the ejector installed. Thirty aerodynamic performance data points were obtained with an unheated air supply. Fan nozzle pressure ratio was varied from 1.8 to 3.2 at a constant primary pressure ratio of 1.6; primary pressure ratio was varied from 1.4 to 2.4 while holding fan pressure ratio constant at 2.4. Operation with the ejector increased nozzle thrust coefficient 0.2 to 0.4 percent. B.D.

N80-26301* Pratt and Whitney Aircraft Group, East Hartford, Conn. Commercial Products Div.

EXPERIMENTAL AERODYNAMIC AND ACOUSTIC MODEL TESTING OF THE VARIABLE CYCLE ENGINE (VCE) TESTBED COANNULAR EXHAUST NOZZLE SYSTEM: COMPREHENSIVE DATA REPORT

D. P. Nelson and P. M. Morris Jun. 1980 225 p
(Contract NAS3-20061)
(NASA-CR-159711; PWA-5550-40) Avail: NTIS
HC A10/MF A01 CSCL 21E

The component detail design drawings of the one sixth scale model of the variable cycle engine testbed demonstrator exhaust system tested are presented. Also provided are the basic acoustic and aerodynamic data acquired during the experimental model tests. The model drawings, an index to the acoustic data, an index to the aerodynamic data, tabulated and graphical acoustic data, and the tabulated aerodynamic data and graphs are discussed. B.D.

N80-26302* General Electric Co., Cincinnati, Ohio. Aircraft Engine Group.

CF6 JET ENGINE PERFORMANCE IMPROVEMENT PROGRAM: HIGH PRESSURE TURBINE AERODYNAMIC PERFORMANCE IMPROVEMENT

W. A. Fasching Jul. 1980 156 p refs
(Contract NAS3-20629)
(NASA-CR-159832) Avail: NTIS HC A08/MF A01 CSCL 21E

The improved single shank high pressure turbine design was evaluated in component tests consisting of performance, heat transfer and mechanical tests, and in core engine tests. The instrumented core engine test verified the thermal, mechanical, and aeromechanical characteristics of the improved turbine design. An endurance test subjected the improved single shank turbine to 1000 simulated flight cycles, the equivalent of approximately 3000 hours of typical airline service. Initial back-to-back engine tests demonstrated an improvement in cruise sfc of 1.3% and a reduction in exhaust gas temperature of 10 C. An additional improvement of 0.3% in cruise sfc and 6 C in EGT is projected for long service engines. Author

N80-27361* Curtiss-Wright Corp., Wood-Ridge, N.J.
PERFORMANCE, EMISSIONS, AND PHYSICAL CHARACTERISTICS OF A ROTATING COMBUSTION AIRCRAFT ENGINE, SUPPLEMENT A
 R. K. Lamping, I. Manning, D. Myers, and B. Tjoa May 1980
 74 p
 (Contract NAS3-20808)
 (NASA-CR-135119; CW-WR-76-028.3) Avail: NTIS
 HC A04/MF A01 CSCL 21E

Testing was conducted using the basic RC2-75 engine, to which several modifications were incorporated which were designed to reduce the hydrocarbon emissions and reduce the specific fuel consumption. The modifications included close-in surface gap spark plugs, increased compression ratio rotors, and provisions for utilizing either side or peripheral intake ports, or a combination of the two if required. The proposed EPA emissions requirements were met using the normal peripheral porting. The specific fuel economy demonstrated for the modified RC2-75 was 283 g/kW-hr at 75% power and 101 brake mean effective pressure (BMEP) and 272.5 g/kW-hr at 75% power and 111 BMEP. The latter would result from rating the engine for takeoff at 285 hp and 5500 rpm, instead of 6000 rpm. E.D.K.

N80-27364* General Electric Co., Cincinnati, Ohio. Aircraft Engine Group.
CF6-6D ENGINE PERFORMANCE DETERIORATION
 Ray H. Wulf, W. H. Kramer, J. E. Pass, and J. J. Smith Jan. 1980 286 p refs
 (Contract NAS3-20631)
 (NASA-CR-159786; R80AEG218) Avail: NTIS
 HC A13/MF A01 CSCL 21E

Cruise cockpit recordings and test cell performance data in conjunction with hardware inspection data from airline overhaul shops were analyzed to define the extent and magnitude of performance deterioration of the General Electric CF6-6D model engine. These studies successfully isolated short-term deterioration from the longer term, and defined areas where a significant reduction in aircraft energy requirements for the 1980's can be realized. Unrestored losses which remain after engine refurbishment represent over 70% of the loss at engine shop visit. Sixty-three percent of the unrestored losses are cost-effective to restore which could reduce fuel consumed by CF6-6D engines in 1980 by 10.9 million gallons. Author

N80-29302* Department of Energy, Washington, D. C.
OUTLOOK FOR ALTERNATIVE ENERGY SOURCES
 Michael E. Card In NASA. Lewis Res. Center Aircraft Res. and Technol. for Future Fuels Jul. 1980 p 5-9 (For primary document see N80-29300 20-07)
 Avail: NTIS HC A11/MF A01 CSCL 21D

Predictions are made concerning the development of alternative energy sources in the light of the present national energy situation. Particular emphasis is given to the impact of alternative fuels development on aviation fuels. The future outlook for aircraft fuels is that for the near term, there possibly will be no major fuel changes, but minor specification changes may be possible if supplies decrease. In the midterm, a broad cut fuel may be used if current development efforts are successful. As synfuel production levels increase beyond the 1990's there may be some mixtures of petroleum-based and synfuel products with the possibility of some shale distillate and indirect coal liquefaction products near the year 2000. M.G.

N80-29303* United Air Lines, Inc., Chicago, Ill.

CURRENT JET FUEL TRENDS

Paul P. Campbell In NASA. Lewis Res. Center Aircraft Res. and Technol. for Future Fuels Jul. 1980 p 11-14 (For primary document see N80-29300 20-07)

Avail: NTIS HC A11/MF A01 CSCL 21D

Data concerning the properties of commercial jet fuels during the period between 1974 and 1979 are discussed. During this period the average aromatics content of fuels increased from 16% to 17.5%. It is evident that the arrival of Alaska North Slope crude in 1977 had a significant impact upon the aromatics content of jet fuel supply at West Coast points with less effect upon the entire United States domestic market. This increase in aromatics has not been accompanied by a corresponding reduction in burning quality as measured by smoke point. There has been a reduction of .6 smoke point on the average. Looking at hydrogen content as a measure of burning quality, the all refinery average calculated hydrogen for 1978 was approximately 13.7%. The relationship between hydrogen content and aromatics content shows a slope of .043% reduction in hydrogen for 1% increase in aromatics. M.G.

N80-29304* Boeing Commercial Airplane Co., Seattle, Wash.
AVIATION FUELS OUTLOOK

Albert M. Momeny In NASA. Lewis Res. Center Aircraft Res. and Technol. for Future Fuels Jul. 1980 p 15-24 (For primary document see N80-29300 20-07)

Avail: NTIS HC A11/MF A01 CSCL 21D

Options for satisfying the future demand for commercial jet fuels are analyzed. It is concluded that the most effective means to this end are to attract more refiners to the jet fuel market and encourage development of processes to convert oil shale and coal to transportation fuels. Furthermore, changing the U.S. refineries fuel specification would not significantly alter jet fuel availability. M.G.

N80-29305* California Univ. at Los Angeles. School of Engineering and Applied Science.

A METHODOLOGY FOR LONG-RANGE PREDICTION OF AIR TRANSPORTATION

Mohammad B. Ayati and J. Morley English In NASA. Lewis Res. Center Aircraft Res. and Technol. for Future Fuels Jul. 1980 p 25-30 refs Presented at the SAE Intern. Air Transportation Meeting, Cincinnati, 20-22 May 1980 (For primary document see N80-29300 20-07)

Avail: NTIS HC A11/MF A01 CSCL 01C

A framework and methodology for long term projection of demand for aviation fuels is presented. The approach taken includes two basic components. The first was a new technique for establishing the socio-economic environment within which the future aviation industry is embedded. The concept utilized was a definition of an overall societal objective for the very long run future. Within a framework so defined, a set of scenarios by which the future will unfold are then written. These scenarios provide the determinants of the air transport industry operations and accordingly provide an assessment of future fuel requirements. The second part was the modeling of the industry in terms of an abstracted set of variables to represent the overall industry performance on a macro scale. The model was validated by testing the desired output variables from the model with historical data over the past decades. M.G.

N80-29306* Exxon Research and Engineering Co., Linden, N.J.

EFFECT OF REFINING VARIABLES ON THE PROPERTIES AND COMPOSITION OF JP-5

Martin Lieberman and William F. Taylor In NASA. Lewis Res. Center Aircraft Res. and Technol. for Future Fuels Jul. 1980 p 31-39 (For primary document see N80-29300 20-07) (Contract N00140-78-C-1491)

Avail: NTIS HC A11/MF A01 CSCL 21D

Potential future problem areas that could arise from changes in the composition, properties, and potential availability of JP-5 produced in the near future are identified. Potential fuel problems

concerning thermal stability, lubricity, low temperature flow, combustion, and the effect of the use of specific additives on fuel properties and performance are discussed. An assessment of available crudes and refinery capabilities is given. M.G.

N80-29307* Douglas Aircraft Co., Inc., Santa Monica, Calif.
FUEL/ENGINE/AIRFRAME TRADEOFF STUDY, PHASE 1
A. T. Peacock *In* NASA. Lewis Res. Center Aircraft Res. and Technol. for Future Fuels Jul. 1980 p 41-47 Sponsored by AF (For primary document see N80-29300 20-07)
Avail: NTIS HC A11/MF A01 CSCL 21E

The effects of broadening the specifications for JP-4 and JP-8 fuel on the performance and cost of all USAF aircraft presently using JP-4 as well as those expected to be introduced into the force structure by 1983 are investigated. Test results indicated that there was no impact on engine performance, turbine durability, and coking, however there was a small maintenance cost increase as a result of a small combustor life decrease. Using JP-4 as standard fuel will avoid the use of high demand middle distillate fuels and give producers flexibility. Extensive use of JP-8 in the United States will increase middle distillate demand and cause a slight increase in engine hot-section maintenance. It is also concluded that the maximum allowable freeze point of JP-4 or JP-8 cannot be increased without degrading system performance and safety as critical conditions are approached. M.G.

N80-29308* Air Force Aero Propulsion Lab., Wright-Patterson AFB, Ohio.

MILITARY JET FUEL FROM SHALE OIL

Edward N. Coppola *In* NASA. Lewis Res. Center Aircraft Res. and Technol. for Future Fuels Jul. 1980 p 49-57 refs (For primary document see N80-29300 20-07)
Avail: NTIS HC A11/MF A01 CSCL 21D

Investigations leading to a specification for aviation turbine fuel produced from whole crude shale oil are described. Refining methods involving hydrocracking, hydrotreating, and extraction processes are briefly examined and their production capabilities are assessed. M.G.

N80-29311* General Electric Co., Fairfield, Conn.
EXPERIMENTAL COMBUSTOR STUDY PROGRAM

John M. Kasper and Edward E. Ekstedt *In* NASA. Lewis Res. Center Aircraft Res. and Technol. for Future Fuels Jul. 1980 p 75-82 (For primary document see N80-29300 20-07)
Avail: NTIS HC A11/MF A01 CSCL 21E

Advanced combustor concepts are evaluated as a means of accommodating possible future broad specification fuels. The three advanced double annular combustor concepts consisted of (1) a concept employing high pressure drop fuel nozzles for improved atomization, (2) a concept with premixing tubes in the main stage, and (3) a concept with the pilot stage on the inside and the main stage on the sideout, which is the reverse of the other two concepts. All of the advanced concepts show promise for reduced sensitivity to fuel hydrogen content. Some hardware problems were encountered, but these problems could be quickly resolved if refinement tests were conducted. The design with the premixing main stage was selected for a parametric test because of its low NOx emissions level, carbon free dome, and very low dome temperatures which were essentially independent of fuel type. The other advanced designs also had low dome temperatures. The premixing dome design liner temperatures exhibited less sensitivity to fuel type than did the base-line combustor, although more sensitivity than observed for concept 1. The inner liner hot spot and the observed smoke results for the premixing design suggest that the fuel-air mixture was not as uniform as desired. M.G.

N80-29312* Air Force Aero Propulsion Lab., Wright-Patterson AFB, Ohio.

FUEL CHARACTER EFFECTS ON THE J79 AND F101 ENGINE COMBUSTION SYSTEMS

Thomas A. Jackson *In* NASA. Lewis Res. Center Aircraft

Res. and Technol. for Future Fuels Jul. 1980 p 83-93 (For primary document see N80-29300 20-07)
Avail: NTIS HC A11/MF A01 CSCL 21E

The effects of select fuel property variations on two major engine classifications are summarized. Thirteen refined and blended fuels were used which exhibited significant variations in hydrogen content, aromatic type, initial boiling point, final boiling point, and viscosity. Trends were very similar but the degree of fuel sensitivity was not constant. For both systems the dominant fuel property during high pressure operation was found to be fuel hydrogen content. For operation at low pressure test points the fuel volatility and viscosity became the dominant fuel properties for both systems. Aromatic type and final boiling point did not significantly affect combustion data. Correlations of other fuel properties with these and other performance parameters are presented. E.D.K.

N80-29314* Air Force Aero Propulsion Lab., Wright-Patterson AFB, Ohio.

AIR FORCE FUEL MAINBURNER/TURBINE EFFECTS PROGRAMS

Thomas A. Jackson *In* NASA. Lewis Res. Center Aircraft Res. and Technol. for Future Fuels Jul. 1980 p 99-103 (For primary document see N80-29300 20-07)
Avail: NTIS HC A11/MF A01 CSCL 21E

A program for the determination of fuel property effects on aircraft gas turbine engine mainburners and turbines is discussed. The six engines selected as test candidates are the J79, J85, J57, TF30, TF39, and F100. Fuels election is the responsibility of the contractors with two fuels as exceptions. The petroleum JP-4 is to be used as a baseline in all tests. The shale JP-4 is to be used in nearly all tests. Fuel properties are to be correlated with combustion system performance parameters. In addition, life predictions are to be made for combustor and turbine hardware. These predictions are to be based on a typical mission for each system, measured metal temperatures and temperature gradients, and oxidation/corrosion effects. E.D.K.

N80-29315* Pratt and Whitney Aircraft Group, East Hartford, Conn. Commercial Products Div.

THE BROADENED-SPECIFICATION FUELS COMBUSTION TECHNOLOGY PROGRAM AT PRATT AND WHITNEY AIRCRAFT

Robert P. Lohmann *In* NASA. Lewis Res. Center Aircraft Res. and Technol. for Future Fuels Jul. 1980 p 105-108 (For primary document see N80-29300 20-07)
Avail: NTIS HC A11/MF A01 CSCL 21B

The impact of the use of broadened specification fuels on combustor design was investigated. Particular emphasis was placed on establishing the viability of various combustor modifications to permit the use of broadened specification fuels while meeting exhaust emissions and performance specifications and maintaining acceptable combustor operational and durability characteristics. Three different combustor concepts will be evaluated. Various design modifications on the operating capability of each of the combustor concepts with experimental referee broadened specification fuels and modifications that were evaluated included perturbation of the combustor airflow schedules to alter local stoichiometry and residence time histories revisions to the fuel injectors and variations in liner cooling including the use of thermal barrier coatings and/or advanced cooling concepts. R.C.T.

N80-29316* General Electric Co., Cincinnati, Ohio. Aircraft Engine Group.

NASA/GENERAL ELECTRIC BROAD-SPECIFICATION FUELS COMBUSTION TECHNOLOGY PROGRAM, PHASE 1

Willard J. Dodds *In* NASA. Lewis Res. Center Aircraft Res. and Technol. for Future Fuels Jul. 1980 p 109-113 (For primary document see N80-29300 20-07)
Avail: NTIS HC A11/MF A01 CSCL 21D

The use of broad specification fuels in aircraft turbine engine combustion systems was examined. Three different

combustor design concepts were evaluated for their ability to use broad specification fuels while meeting several specific emissions, performance, and durability goals. These combustor concepts covered a range from those having limited complexity and relatively low technical risk to those having high potential for achieving all of the program goals at the expense of increased technical risk. R.C.T.

N80-29318* Purdue Univ., Lafayette, Ind.
ATOMIZATION OF BROAD SPECIFICATION AIRCRAFT FUELS

J. G. Skifstad and A. H. Lefebvre /In NASA, Lewis Res. Center Aircraft Res. and Technol. for Future Fuels Jul. 1980 p 117-124 (For primary document see N80-29300 20-07)

Avail: NTIS HC A11/MF A01 CSCL 21D

The atomization properties of liquid fuels for the potential use in aircraft gas turbine engines are discussed. The significance of these properties are addressed with respect to the ignition and subsequent combustion behavior of the fuel spray/air mixture. It is shown that the fuel properties which affect the atomization behavior (viscosity, surface tension, and density) are less favorable for the broad specification fuels as compared to with those for conventional fuels. R.C.T.

N80-29320* Massachusetts Inst. of Tech., Cambridge.
SOOT FORMATION AND BURNOUT IN FLAMES

B. Prado, J. D. Bittner, K. Neoh, and J. B. Howard /In NASA, Lewis Res. Center Aircraft Res. and Technol. for Future Fuels Jul. 1980 p 131-137 refs (For primary document see N80-29300 20-07)

Avail: NTIS HC A11/MF A01 CSCL 21B

The amount of soot formed when burning a benzene/hexane mixture in a turbulent combustor was examined. Soot concentration profiles in the same combustor for kerosene fuel are given. The chemistry of the formation of soot precursors, the nucleation, growth and subsequent burnout of soot particles, and the effect of mixing on the previous steps were considered. R.C.T.

N80-29321* Exxon Research and Engineering Co., Linden, N.J.
FUEL PROPERTY EFFECTS IN STIRRED COMBUSTORS

/In NASA, Lewis Res. Center Aircraft Res. and Technol. for Future Fuels Jul. 1980 p 139-146 Sponsored by DOE (For primary document see N80-29300 20-07)

Avail: NTIS HC A11/MF A01 CSCL 21E

Soot formation in strongly backmixed combustion was investigated using the jet-stirred combustor (JSC). This device provided a combustion volume in which temperature and combustion were uniform. It simulated the recirculating characteristics of the gas turbine primary zone; it was in this zone where mixture conditions were sufficiently rich to produce soot. Results indicate that the JSC allows study of soot formation in an aerodynamic situation relevant to gas turbines. R.C.T.

N80-29322* Southwest Research Inst., San Antonio, Tex.
EFFECT OF FUEL MOLECULAR STRUCTURE ON SOOT FORMATION IN GAS TURBINE COMBUSTION

D. W. Naegeli and C. A. Moses /In NASA, Lewis Res. Center Aircraft Res. and Technol. for Future Fuels Jul. 1980 p 147-152 (For primary document see N80-29300 20-07)

Avail: NTIS HC A11/MF A01 CSCL 21B

The effect of fuel variations at the same hydrogen content on the formation of soot in a gas turbine combustor was studied. Six fuels were burned to a combustor over a matrix of about 50 test conditions with test conditions ranging over 500-1800 kPa (5-18 atm) pressure and 500-1000 K burner inlet temperature; fuel-air ratios were varied from 0.008-0.024. Flame radiation measurements were made through a sapphire window toward the end of the primary zone. The hydrogen content of the six test fuels ranged from 12.80 to 12.88%. Five fuels emphasized hydrocarbon types: (mono, di, and tricyclic), naphthenes (decalin) and partially hydrogenated aromatics (tetralin); the sixth fuel emphasized final boiling point. R.C.T.

N80-29325* United Technologies Research Center, East Hartford, Conn.

EXPERIMENTAL STUDY OF TURBINE FUEL THERMAL STABILITY IN AN AIRCRAFT FUEL SYSTEM SIMULATOR
Alexander Vranos and Pierre J. Marteney /In NASA, Lewis Res. Center Aircraft Res. and Technol. for Future Fuels Jul. 1980 p 169-179 ref (For primary document see N80-29300 20-07)

(Contract NAS3-21593)

Avail: NTIS HC A11/MF A01 CSCL 21D

The thermal stability of aircraft gas turbines fuels was investigated. The objectives were: (1) to design and build an aircraft fuel system simulator; (2) to establish criteria for quantitative assessment of fuel thermal degradation; and (3) to measure the thermal degradation of Jet A and an alternative fuel. Accordingly, an aircraft fuel system simulator was built and the coking tendencies of Jet A and a model alternative fuel (No. 2 heating oil) were measured over a range of temperatures, pressures, flows, and fuel inlet conditions. R.C.T.

N80-29326* Naval Air Propulsion Test Center, Trenton, N.J.
DETERMINATION OF JET FUEL THERMAL DEPOSIT RATE USING A MODIFIED JFTOT

C. J. Nowack and R. J. Delfosse /In NASA, Lewis Res. Center Aircraft Res. and Technol. for Future Fuels Jul. 1980 p 181-184 (For primary document see N80-29300 20-07)

Avail: NTIS HC A11/MF A01 CSCL 21D

Three fuels having different breakpoint temperatures were studied in the modified jet fuel thermal oxidation tester. The lower stability fuel with a breakpoint of 240 C was first stressed at a constant temperature. After repeating this procedure at several different temperatures, an Arrhenius plot was drawn from the data. The correlation coefficient and the energy of activation were calculated to be 0.97 and 8 kcal/mole respectively. Two other fuels having breakpoint temperatures of 271 C and 285 C were also studied in a similar manner. A straight line was drawn through the data at a slope equivalent to the slope of the lower stability fuel. The deposit formation rates for the three fuels were determined at 260 C, and a relative deposit formation rate at this temperature was calculated and plotted as a function of the individual fuel's breakpoint temperatures. R.C.T.

N80-29327* Colorado School of Mines, Golden.
MECHANISMS OF NITROGEN HETEROCYCLE INFLUENCE ON TURBINE FUEL STABILITY

Stephen R. Daniel and Jonathan H. Worstell /In NASA, Lewis Res. Center Aircraft Res. and Technol. for Future Fuels Jul. 1980 p 185-193 (For primary document see N80-29300 20-07) (Contract NSG-3122)

Avail: NTIS HC A11/MF A01 CSCL 21D

Lewis bases were extracted from a Utah COED syncrude via ligand exchange. Addition of this extract to Jet A at levels as low as 5 ppm N produced deterioration of stability in both JFTOT and accelerated storage tests (7 days at 394 K with 13:1 air to fuel ratio). Comparable effects on Jet A stability were obtained by addition of pyridine and quinoline, while pyrrole and indole were less detrimental at the same concentration level. The weight of deposit produced accelerated storage tests was found to be proportional to the concentration of added nitrogen compound. Over the narrow temperature range accessible with the experimental method, Arrhenius plots obtained by assuming specific rate to be proportional to the weight of material deposited in seven days exhibit greater slopes in the presence of those nitrogen compounds producing the greater deposition rates. It is shown that despite variation in appearance the elemental composition and spectral characteristics of the deposits are unaffected by addition of the nitrogen compounds. The linearity of the Arrhenius plots and of a plot of Arrhenius slope versus intercept for all the compounds suggests a constancy of mechanism over the range of temperature and heterocycles studied. R.C.T.

N80-29329* Boeing Military Airplane Development, Seattle.

Wash.

HIGH-FREEZING-POINT FUEL STUDIES

Frederick F. Tolle / In NASA. Lewis Res. Center Aircraft Res. and Technol. for Future Fuels Jul. 1980 p 205-219 refs (For primary document see N80-29300 20-07)

Avail: NTIS HC A11/MF A01 CSCL 21D

Considerable progress in developing the experimental and analytical techniques needed to design airplanes to accommodate fuels with less stringent low temperature specifications is reported. A computer technique for calculating fuel temperature profiles in full tanks was developed. The computer program is being extended to include the case of partially empty tanks. Ultimately, the completed package is to be incorporated into an aircraft fuel tank thermal analyzer code to permit the designer to fly various thermal exposure patterns, study fuel temperatures versus time, and determine holdup. E.D.K.

N80-29297* General Electric Co., Cincinnati, Ohio. Advanced Engineering and Technology Programs Dept.

QUIET CLEAN SHORT-HAUL EXPERIMENTAL ENGINE (QCSEE) UNDER-THE-WING (UTW) COMPOSITE NACELLE TEST REPORT, VOLUME 2: ACOUSTIC PERFORMANCE

D. L. Stimpert Nov. 1979 124 p refs 2 Vol.

(Contract NAS3-18021)

(NASA-CR-159472; R78AEG-574-Vol-2)

Avail: NTIS

HC A06/MF A01 CSCL 21E

High bypass geared turbofan engines with nacelles forming the propulsion system for short-haul passenger aircraft were tested for use in externally blown flap-type aircraft. System noise levels for a four-engine, UTW-powered aircraft operating in the powered lift mode were calculated to be 97.2 and 95.7 EPNdB at takeoff and approach, respectively, on a 152.4 m (500 ft) sideline compared to a goal of 95.0 EPNdB. A.R.H.

N80-29298* General Electric Co., Cincinnati, Ohio. Advanced Engineering and Technology Programs Dept.

QUIET CLEAN SHORT-HAUL EXPERIMENTAL ENGINE (QCSEE) UNDER-THE-WING ENGINE COMPOSITE FAN BLADE: PRELIMINARY DESIGN TEST REPORT

May 1975 63 p

(Contract NAS3-18021)

(NASA-CR-134846; R75AEG411)

Avail: NTIS

HC A04/MF A01 CSCL 21E

Results of tests conducted on preliminary design polymeric-composite fan blade for the under the wing (UTW) QCSEE engine are presented. During this phase of the program a total of 17 preliminary QCSEE UTW composite fan blades were manufactured for various component tests including frequency characteristics, strain distribution, bench fatigue, dovetail pull, whirligig overspeed and whirligig impact. All tests were successfully completed with the exception of whirligig impact tests. Improvements in local impact capability are being evaluated for the QCSEE blade under other NASA and related programs. Author

N80-29299* General Electric Co., Cincinnati, Ohio.

ACOUSTIC PERFORMANCE OF A 50.8-cm (20-INCH) DIAMETER VARIABLE-PITCH FAN AND INLET. VOLUME 2: ACOUSTIC DATA Final Report

K. R. Bilwakesh, A. Clemons, and D. L. Stimpert Nov. 1979 495 p refs 2 Vol.

(NASA-CR-135118; R77AEG229-Vol-2)

Avail: NTIS

HC A21/MF A01 CSCL 21E

Results from acoustic tests on a 50.8 cm (20 inch) QCSEE Under-the-Wing (UTW) engine, variable pitch fan and inlet simulator are tabulated. Tests were run in both forward and reverse thrust modes with a bellmouth inlet, five accelerating inlets (one hardwall and four treated), and four low Mach number inlets (one hardwall and three treated). The 1/3 octave-band acoustic data are presented for the model size on the measured 5.2 m (17.0 ft) arc and also data scaled to full QCSEE size 71:20 on a 152.4 m (500 ft) sideline. A.R.H.

N80-29330* Lockheed-California Co., Burbank.

LOW TEMPERATURE FUEL BEHAVIOR STUDIES

Francis J. Stockemer / In NASA. Lewis Res. Center Aircraft Res. and Technol. for Future Fuels Jul. 1980 p 221-233 refs (For primary document see N80-29300 20-07)

(Contract NAS3-20814)

Avail: NTIS HC A11/MF A01 CSCL 21E

Aircraft fuels at low temperatures near the freezing point. The principal objective was an improved understanding of the flowability and pumpability of the fuels in a facility that simulated the heat transfer and temperature profiles encountered during flight in the long range commercial wing tanks. R.C.T.

N80-29331* TRW, Inc., Cleveland, Ohio.

TUNGSTEN WIRE/FIBER MATRIX TURBINE BLADE FABRICATION STUDY

P. Melnyk and J. N. Fleck Dec. 1979 99 p refs

(Contract NAS3-20391)

(NASA-CR-159788; TRW-ER-8101)

Avail: NTIS

HC A05/MF A01 CSCL 21E

The objective was to establish a viable FRS monotape technology base to fabricate a complex, advanced turbine blade. All elements of monotape fabrication were addressed. A new process for incorporation of the matrix, including bi-alloy matrices, was developed. Bonding, cleaning, cutting, sizing, and forming parameters were established. These monotapes were then used to fabricate a 48 ply solid JT9D-7F 1st stage turbine blade. Core technology was then developed and first a 12 ply and then a 7 ply shell hollow airfoil was fabricated. As the fabrication technology advanced, additional airfoils incorporated further elements of sophistication, by introducing in sequence bonded root blocks, cross-plying, bi-metallic matrix, tip cap, trailing edge slots, and impingement inserts. Author

N80-30310* General Electric Co., Cincinnati, Ohio. Aircraft Business Group.

ENGINE CYCLE STUDIES PROGRAM Final Report, Sep. 1978 - Oct. 1979

R. D. Allan, J. E. Johnson, W. Joy, R. H. Brown, and H. J. Barriar Aug. 1980 176 p refs

(Contract NAS3-21388)

(NASA-CR-159500; R80AEG428)

Avail: NTIS

HC A09/MF A01 CSCL 21E

The double bypass, variable cycle engine (VCE) used as the propulsion system for a Mach 2.4 cruise supersonic commercial transport was examined in the following areas: (1) the acoustic and performance payoffs of the high flow mode of the double bypass VCE; (2) possible cycle improvements for noise; (3) manufacturing cost, reliability and maintainability of the VCE compared to other engine concepts; (4) an assessment of the performance and economic payoffs of the features used in the double bypass VCE. The high flow capability of the double bypass VCE did show acoustic and performance payoffs both with unsuppressed and with mechanically suppressed coannular exhaust systems. At lower noise goals, changes to the baseline VCE cycle improved takeoff gross weight for a design version by up to 4%. The double bypass feature of the VCE provided performance and acoustic flexibility that resulted in lower takeoff gross weight for all noise levels, utilizing unsuppressed coannular nozzle, suppressed coannular nozzle, and single stream fully suppressed nozzle. The manufacturing cost, reliability, and maintainability of the double bypass VCE compares favorably with the simpler concepts studied (within 1 to 5.5%). L.F.M.

N80-31398* TRW, Inc., Cleveland, Ohio. Materials Technology.

COST ANALYSIS OF COMPOSITE FAN BLADE MANUFACTURING PROCESSES Final Report

T. S. Stelson and C. F. Barth Jun. 1980 87 p refs

(Contract NAS3-21352)

(NASA-CR-159876; TRW-ER-8064)

Avail: NTIS

HCA05/MFA01 CSCL 21E

The relative manufacturing costs were estimated for large high technology fan blades prepared by advanced composite fabrication methods using seven candidate materials/process

systems. These systems were identified as laminated resin matrix composite, filament wound resin matrix composite, superhybrid solid laminate, superhybrid spar/shell, metal matrix composite, metal matrix composite with a spar and shell, and hollow titanium. The costs were calculated utilizing analytical process models and all cost data are presented as normalized relative values where 100 was the cost of a conventionally forged solid titanium fan blade whose geometry corresponded to a size typical of 42 blades per disc. Four costs were calculated for each of the seven candidate systems to relate the variation of cost on blade size. Geometries typical of blade designs at 24, 30, 36 and 42 blades per disc were used. The impact of individual process yield factors on costs was also assessed as well as effects of process parameters, raw materials, labor rates and consumable items. A.R.H.

N80-33408* # General Electric Co., Cincinnati, Ohio. Aircraft Engine Group.

ENERGY EFFICIENT ENGINE

D. Burrus, P. E. Sabla, and D. W. Bahr Jun. 1980 118 p refs

(Contract NAS3-20643)

(NASA-CR-159685; R79AEG562)

Avail: NTIS

HC A06/MF A01 CSCL 21E

The feasibility of meeting or closely approaching the emissions goals established for the Energy Efficient Engine (E3) Project with an advanced design, single annular combustor was determined. A total of nine sector combustor configurations and one full-annular-combustor configuration were evaluated. Acceptable levels of carbon monoxide and hydrocarbon emissions were obtained with several of the sector combustor configurations tested, and several of the configurations tested demonstrated reduced levels of nitrogen oxides compared to conventional, single annular designs. None of the configurations tested demonstrated nitrogen oxide emission levels that meet the goal of the E3 Project. Author

A80-27737 * # Laser anemometer measurements at the exit of a T63 combustor. D. R. Zimmerman (General Motors Corp., Detroit Diesel Allison Div., Indianapolis, Ind.). In: Flow in primary, non-rotating passages in turbomachines; Proceedings of the Winter Annual Meeting, New York, N.Y., December 2-7, 1979. (A80-27732 10-02) New York, American Society of Mechanical Engineers, 1979, p. 57-62. 9 refs. Research supported by the General Motors Corp.; Contract No. NAS3-21267.

In the first practical application of laser anemometry to an actual gas turbine engine combustor, the mean velocity and turbulent intensity profiles were measured in a steady-flow combustion rig across an annulus simulating a turbine inlet; to establish a basis for comparison with similar measurements to be made in an operating engine and to confirm current turbine aerodynamics and heat transfer design assumptions. It was necessary to develop a new experimental technique for traversing the annulus due to differential thermal expansion of the cantilevered combustion rig and a new computer-graphics analysis technique for analyzing the velocity histograms due to the high background light intensity. The axial mean velocity and turbulent intensity were uniform across the annulus under all operating conditions and the flow had little or no swirl component. The isothermal mean velocity was doubled by the burning of fuel, however, the isothermal turbulent intensity was relatively unaffected. (Author)

A80-35958 * # Acoustic measurements of three Prop-Fan models. B. M. Brooks (United Technologies Corp., Hamilton Standard Div., Windsor Locks, Conn.). *American Institute of Aeronautics and Astronautics, Aeroacoustics Conference, 6th, Hartford, Conn., June 4-6, 1980, Paper 80-0995.* 13 p. 16 refs. Contract No. NAS3-20614.

Results of NASA sponsored acoustic tests of three 2 ft. diameter models of the Prop-Fan (a small diameter, highly loaded, many-bladed variable pitch advanced turboprop) are presented. The highly swept model designed for noise reduction produces substantially less near field noise at simulated 0.8 Mach number cruise conditions than

the unswept or slightly swept models. It also produces less far field noise at conditions simulating takeoff and landing. The noise reduction mechanism is discussed. Correlation between harmonic noise measurements and theoretical predictions and between measured and predicted acoustic pressure pulses is good. Shadowgraph measurements which show the location of blade associated wave patterns were obtained. Predicted and measured wave locations show good general agreement. Full scale near and far field noise is predicted. (Author)

A80-38982 * # Multifuel rotary aircraft engine. C. Jones and M. Berkowitz (Curtiss-Wright Corp., Wood-Ridge, N.J.). *AIAA, SAE, and ASME, Joint Propulsion Conference, 16th, Hartford, Conn., June 30-July 2, 1980, AIAA Paper 80-1237.* 15 p. 17 refs. Contract No. NAS3-21285.

The broad objectives of this paper are the following: (1) to summarize the Curtiss-Wright design, development and field testing background in the area of rotary aircraft engines; (2) to briefly summarize past activity and update development work in the area of stratified charge rotary combustion engines; and (3) to discuss the development of a high-performance direct injected unthrottled stratified charge rotary combustion aircraft engine. Efficiency improvements through turbocharging are also discussed. S.D.

A80-41506 * # Fuel conservation through active control of rotor clearances. R. S. Beitler, A. A. Saunders, and R. P. Wanger (General Electric Co., Aircraft Engine Group, Evendale, Ohio). *AIAA, SAE, and ASME, Joint Propulsion Conference, 16th, Hartford, Conn., June 30-July 2, 1980, AIAA Paper 80-1087.* 8 p. Contract No. NAS3-20643.

Under the NASA-sponsored Energy Efficient Engine (EEE) Project, technology is being developed which will significantly reduce the fuel consumption of turbofan engines for subsonic transport aircraft. One technology concept being pursued is active control of rotor tip clearances. Attention is given to rotor tip clearance considerations and an overview of preliminary study results as well as the General Electric EEE clearance control approach is presented. Finally, potential fuel savings with active control of rotor clearances for a typical EEE mission are predicted. M.E.P.

A80-50191 * # An acoustic sensitivity study of general aviation propellers. K. D. Korkan, G. M. Gregorek (Ohio State University, Columbus, Ohio), and I. Keiter (Cessna Aircraft Co., Vandalia, Ohio). *American Institute of Aeronautics and Astronautics, Aircraft Systems Meeting, Anaheim, Calif., Aug. 4-6, 1980, Paper 80-1871.* 32 p. 22 refs. Contract No. NAS3-21719.

This paper describes the results of a study in which a systematic approach has been taken in studying the effect of selected propeller parameters on the character and magnitude of propeller noise. Four general aviation aircraft were chosen, i.e., a Cessna 172, Cessna 210, Cessna 441, and a 19 passenger commuter concept, to provide a range in flight velocity, engine horsepower, and gross weight. The propeller parameters selected for examination consisted of number of blades, rpm reduction, thickness/chord reduction, activity factor reduction, proplets, airfoil improvement, sweep, position of maximum blade loading, and diameter reduction. (Author)

08 AIRCRAFT STABILITY AND CONTROL

Includes aircraft handling qualities, piloting, flight controls, and autopilots

N80-29369* // National Aeronautics and Space Administration
Lewis Research Center, Cleveland, Ohio.

SINGLE-STAGE ELECTROHYDRAULIC SERVOSYSTEM FOR ACTUATING ON AIRFLOW VALVE WITH FREQUENCIES TO 500 HERTZ

John A. Webb, Jr., Oral Mehmed, and Carl F. Lorenzo Aug
1980 35 p refs
(NASA TP-1678, E-252) Avail. NTIS HC A03/MF A01 CSCL
01C

An airflow valve and its electrohydraulic actuation servosystem are described. The servosystem uses a high-power, single-stage servovalve to obtain a dynamic response beyond that of systems designed with conventional two-stage servovalves. The electrohydraulic servosystem is analyzed and the limitations imposed on system performance by such nonlinearities as signal saturations and power limitations are discussed. Descriptions of the mechanical design concepts and developmental considerations are included. Dynamic data, in the form of sweep-frequency test results, are presented and comparison with analytical results obtained with an analog computer model is made. R.K.G.

09 RESEARCH AND SUPPORT FACILITIES (AIR)

Includes airports, hangars and runways; aircraft repair and overhaul facilities; wind tunnels; shock tube facilities; and engine test blocks.

For related information see also *14 Ground Support Systems and Facilities (Space)*.

N80-32404* Southampton Univ. (England). Dept. of Aeronautics and Astronautics.

SELECTED DATA FROM A TRANSONIC FLEXIBLE WALLED TEST SECTION Semiannual Progress Report

S. W. D. Wolf Sep. 1980 108 p refs

(Grant NsG-7172)

(NASA-CR-159360) Avail: NTIS HC A06/MF A01 CSCL
14B

Twenty four test runs of the Transonic Self-Streamlining Wind Tunnel were performed with the flexible walls 'streamlined' around a two dimensional section of four inch chord, over the Mach number range 0.3 to 0.89. Relevant wall and model data for the streamlined cases are presented. L.F.M.

12 ASTRONAUTICS (GENERAL)

For extraterrestrial exploration see 91 *Lunar and Planetary Exploration*

A80-20961 * # Cost-effective technology advancement directions for electric propulsion transportation systems in earth-orbital missions. J. D. Regetz, Jr. (NASA, Lewis Research Center, Cleveland, Ohio) and C. H. Terwilliger, Jr. (Boeing Aerospace Co., Seattle, Wash.), *Princeton University, AIAA, and DGLR, International Electric Propulsion Conference, 14th, Princeton, N.J., Oct. 30-Nov. 1, 1979, AIAA Paper 79-2043*. 19 p.

This paper presents the results of a study to determine the directions that electric propulsion technology should take to meet the primary propulsion requirements for earth-orbital missions of the next three decades in the most cost-effective manner. Discussed are the mission set requirements, state-of-the-art electric propulsion technology and the baseline system characterized by it, adequacy of the baseline system to meet the mission set requirements, cost-optimum electric propulsion system characteristics for the mission set, and sensitivities of mission costs and design points to system-level electric propulsion parameters. It is found that the efficiency-specific impulse characteristic generally has a more significant impact on overall costs than specific masses or costs of propulsion and power systems. (Author)

A80-35504 * # LeRC reduced gravity fluid management technology program. J. C. Aydelott and E. P. Symons (NASA, Lewis Research Center, Cleveland, Ohio). *Joint Army-Navy-NASA-Air Force Interagency Propulsion Committee, Propulsion Meeting, Monterey, Calif., Mar. 11-13, 1980, Paper*. 18 p. 38 refs.

The program reviewed in the present paper has provided information of the reduced-gravity behavior of fluids, thermal control of cryogenic tankage, and fluid management system design. The studies are currently shifting from the utilization of in-house experimental facilities to the development of Spacelab experiments. The cryogenic fluid management experiment, currently undergoing detailed design, is expected to provide an orbital evaluation of a subcritical liquid hydrogen storage and supply system, as part of the Shuttle/Spacelab program. Efforts are continuing to develop computer techniques for simulating reduced-gravity fluid dynamic processes. V.P.

N80-31423*# General Dynamics/Convair, San Diego, Calif. **CONCEPTUAL DESIGN OF AN ORBITAL PROPELLANT TRANSFER EXPERIMENT. VOLUME 2: STUDY RESULTS** G. L. Drake, C. E. Bossett, F. Merino, L. E. Siden, R. E. Bradley, E. J. Carr, and R. E. Parker Aug. 1980 196 p refs (Contract NAS3-21935) (NASA-CR-165150; GDC-ASP-80-013-Vol-2) Avail: NTIS HC A09/MF A01 CSCL 22A

The OTV configurations, operations and requirements planned for the period from the 1980's to the 1990's were reviewed and a propellant transfer experiment was designed that would support the needs of these advanced OTV operational concepts. An overall integrated propellant management technology plan for all NASA centers was developed. The preliminary cost estimate (for planning purposes only) is \$56.7 M, of which approximately \$31.8 M is for shuttle user costs. R.K.G.

N80-32412*# General Dynamics/Convair, San Diego, Calif. **COMPARATIVE THERMAL ANALYSIS OF ALTERNATE CRYOGENIC FLUID MANAGEMENT EXPERIMENT (CFME) CONFIGURATIONS** F. Merino and R. F. O'Neill Jul. 1980 66 p refs (Contract NAS3-21935) (NASA-CR-165151; GDC-CRAD-80-014) Avail: NTIS HC A04/MF A01 CSCL 22A

The Cryogenic Fluid Management Experiment (CFME) was analyzed to assess the feasibility and advisability of deleting the vapor cooled shield (VCS) from the baseline CFME insulation and pressure control system. Two alternate concepts of CFME insulation and pressure control, neither of which incorporated the VCS, were investigated. The first concept employed a thermodynamic vent system (TVS) to throttle the flow through an internal wall mounted heat exchanger (HX) within the pressure vessel to decrease boiloff and pressure rise rate, while the second concept utilized a TVS without an internal heat exchanger. Only the first concept was viable. Its performance was assessed for a seven day mission and found to be satisfactory. It was also concluded that VCS development costs would be greater than for an internal HX installation. Based upon the above comparisons, the HX was recommended as a replacement for the VCS. A R H

14 GROUND SUPPORT SYSTEMS AND FACILITIES (SPACE)

Includes launch complexes, research and production facilities, ground support equipment, mobile transporters, and simulators.

For related information see also 09 Research Support Facilities (Air).

A80-13308 * # An electric propulsion long term test facility. G. Trump, E. James (Xerox Electro-Optical Systems, Pasadena, Calif.), R. Vetrone, and R. Bechtel (NASA, Lewis Research Center, Cleveland, Ohio). *Princeton University, AIAA, and DGLR, International Electric Propulsion Conference, 14th, Princeton, N.J., Oct. 30-Nov. 1, 1979, AIAA Paper 79-2080*. 8 p. Contract No. NAS3-20399.

An existing test facility was modified to provide for extended testing of multiple electric propulsion thruster subsystems. A program to document thruster subsystem characteristics as a function of time is currently in progress. The facility is capable of simultaneously operating three 2.7-kW, 30-cm mercury ion thrusters and their power processing units. Each thruster is installed via a separate air lock so that it can be extended into the 7m x 10m main chamber without violating vacuum integrity. The thrusters exhaust into a 3m x 5m frozen mercury target. An array of cryopanel collect sputtered target material. Power processor units are tested in an adjacent 1.5m x 2m vacuum chamber or accompanying forced convection enclosure. The thruster subsystems and the test facility are designed for automatic unattended operation with thruster operation computer controlled. Test data are recorded by a central data collection system scanning 200 channels of data a second every two minutes. Results of the Systems Demonstration Test, a short shakedown test of 500 hours, and facility performance during the first year of testing are presented. (Author)

N80-27403* # General Dynamics/Convair, San Diego, Calif. **CONCEPTUAL DESIGN OF TWO-PHASE FLUID MECHANICS AND HEAT TRANSFER FACILITY FOR SPACELAB**

B. F. North and M. E. Hill Jun. 1980 190 p refs

(Contract NAS3-21750)

(NASA-CR-159810; GDC-CRAD-80-002)

Avail: NTIS

HC A09/MF A01 CSCL 14B

Five specific experiments were analyzed to provide definition of experiments designed to evaluate two phase fluid behavior in low gravity. The conceptual design represents a fluid mechanics and heat transfer facility for a double rack in Spacelab. The five experiments are two phase flow patterns and pressure drop, flow boiling, liquid reorientation, and interface bubble dynamics. Hardware was sized, instrumentation and data recording requirements defined, and the five experiments were installed as an integrated experimental package. Applicable available hardware was selected in the experiment design and total experiment program costs were defined. Author

15 LAUNCH VEHICLES AND SPACE VEHICLES

Includes boosters, manned orbital laboratories, reusable vehicles and space stations

N80-25357* General Electric Co., Philadelphia, Pa. Space Div

STUDY OF ADVANCED COMMUNICATIONS SATELLITE SYSTEMS BASED ON SS-FDMA

John Kiesling May 1980 359 p

(Contract NAS3-21745)

(NASA-CR-159778, DOC-80SDS4217)

Avail: NTIS

HC A16/MF A01 CSCL 22B

A satellite communication system based on the use of a multiple, contiguous beam satellite antenna and frequency division multiple access (FDMA) is studied. Emphasis is on the evaluation of the feasibility of SS (satellite switching) FDMA technology, particularly the multiple, contiguous beam antenna, the onboard switch and channelization, and on methods to overcome the effects of severe Ka band fading caused by precipitation. This technology is evaluated and plans for technology development and evaluation are given. The application of SS-FDMA to domestic satellite communications is also evaluated. Due to the potentially low cost Earth stations, SS-FDMA is particularly attractive for thin route applications up to several hundred kilobits per second, and offers the potential for competing with terrestrial facilities at low data rates and over short routes. The onboard switch also provides added route flexibility for heavy route systems. The key beneficial SS-FDMA strategy is to simplify and thus reduce the cost of the direct access Earth station at the expense of increased satellite complexity. E.D.K.

A80-35329 * Concepts for 20/30 GHz satcom systems for direct-to-user applications. R. Jorasch, R. Davies, and M. Baker (Ford Aerospace and Communications Corp., Palo Alto, Calif.). In: Communications Satellite Systems Conference, 8th, Orlando, Fla., April 20-24, 1980, Technical Papers. Conference sponsored by the American Institute of Aeronautics and Astronautics, New York, American Institute of Aeronautics and Astronautics, Inc., 1980, 8 p. Contract No. NAS3-21362. (AIAA 80-0582)

A baseline technique is described for implementing a direct-to-user (DTU) satcom communications system at 20/30 GHz transmission frequency. The purpose of this application is to utilize the high capacity frequency spectrum at K(A) band for communications among thousands of small terminals located at or close to a customer's facility. The baseline DTU system utilizes a TDMA method of communications with QPSK modulation. Twenty-five coverage beams from a geosynchronous orbit spacecraft provide full coverage of CONUS. Low cost terminals are limited to less than 4.5 meters diameter. The impact of rain attenuation on communications availability is examined. Other techniques including satellite switched antenna beams are outlined and critical K(A)-band technology developments are identified. (Author)

16 SPACE TRANSPORTATION

Includes passenger and cargo space transportation e.g. shuttle operations, and rescue techniques.

For related information see also 03 Air Transportation and Safety and 85 Urban Technology and Transportation.

NSO-20304* National Aeronautics and Space Administration
Lewis Research Center, Cleveland, Ohio

LeRC REDUCED GRAVITY FLUID MANAGEMENT TECHNOLOGY PROGRAM

John C. Aydelott and E. Patrick Symons (1980) 19 p refs
Prepared for the 1980 JANNAF Propulsion Meeting, Monterey, Calif., 11-13 Mar. 1980

(NASA-TM-81460, E-371) Avail: NTIS HC A02/MF A01 CSCL 22A

A survey of the reduced gravity fluid management technology program is presented. Information on reduced gravity fluid behavior, techniques for thermal control of cryogenic tankage, and design for fluid management systems are discussed. The development of Spacelab experiments, propellant management systems for orbit transfer vehicles, and computer techniques for simulating reduced gravity fluid dynamic processes is reported.

A.W.H.

A80-10032 * Communications technology satellite - United States experiments and disaster communications applications. P. L. Donoughe, H. R. Hunczak, and G. S. Gurski (NASA, Lewis Research Center, Cleveland, Ohio). *United Nations, Regional Seminar on the Use of Satellite Technology for Disaster Applications, São José dos Campos, São Paulo, Brazil, Oct. 2-13, 1978, Paper*, 43 p. 22 refs.

The experimental Communications Technology Satellite (CTS), also called Hermes, uses a high-power transmitter and 12- and 14 GHz frequencies for wideband (two- and one-way television) and narrowband (voice, data) communications. In the joint program, both Canada and the United States have conducted a variety of communications experiments. This report concentrates on U.S. CTS experiments and miniexperiments that use ground antennas from 0.6 to 5 meters in diameter. The U.S. CTS experiments program is synopsized in this report. The use of CTS for simulated and actual disasters is summarized.

(Author)

17 SPACECRAFT COMMUNICATIONS, COMMAND AND TRACKING

Includes telemetry; space communications networks; astronavigation; and radio blackout.

For related information see also 04 Aircraft Communications and Navigation and 32 Communications.

N80-21412* National Aeronautics and Space Administration. Lewis Research Center, Cleveland, Ohio.

A DIGITALLY IMPLEMENTED COMMUNICATIONS EXPERIMENT UTILIZING THE COMMUNICATIONS TECHNOLOGY SATELLITE, HERMES

H D Jackson and J. Fiala Mar. 1980 19 p refs
(NASA-TM-81452, E-379) Avail: NTIS HC A02/MF A01 CSCL 17B

Developments which will reduce the costs associated with the distribution of satellite services are considered with emphasis on digital communication link implementation. A digitally implemented communications experiment (DICE) which demonstrates the flexibility and efficiency of digital transmission of television video and audio, telephone voice, and high-bit-rate data is described. The utilization of the DICE system in a full duplex teleconferencing mode is addressed. Demonstration teleconferencing results obtained during the conduct of two sessions of the 7th AIAA Communication Satellite Systems Conference are discussed. Finally, the results of link characterization tests conducted to determine (1) relationships between the Hermes channel 1 EIRP and DICE model performance and (2) channel spacing criteria for acceptable multichannel operation, are presented.

J.M.S.

18 SPACECRAFT DESIGN, TESTING AND PERFORMANCE

Includes spacecraft thermal and environmental control; and attitude control.

For life support systems see 54 *Man/System Technology and Life Support*. For related information see also 05 *Aircraft Design, Testing and Performance* and 39 *Structural Mechanics*.

N80-15200* National Aeronautics and Space Administration. Lewis Research Center, Cleveland, Ohio.

CONFIGURATION EFFECTS ON SATELLITE CHARGING RESPONSE

C. K. Purvis 1980 20 p refs Presented at 18th Aerospace Sci. Meeting, Pasadena, Calif., 14-16 Jan. 1980; sponsored by AIAA (NASA-TM-81397; E-307) Avail: NTIS HC A02/MF A01 CSCL 22B

The response of various spacecraft configurations to a charging environment in sunlight was studied using the NASA Charging Analyzer Program code. The configuration features geometry, type of stabilization, and overall size. Results indicate that sunlight charging response is dominated by differential charging effects. Shaded insulation charges negatively result in the formation of

N80-16093* National Aeronautics and Space Administration. Lewis Research Center, Cleveland, Ohio.

EFFECTS OF SECONDARY YIELD PARAMETER VARIATION ON PREDICTED EQUILIBRIUM POTENTIAL OF AN OBJECT IN A CHARGING ENVIRONMENT

Carolyn K. Purvis 1979 21 p refs Presented at the Ann. Conf. on Nucl. and Space Radiation Effects, Santa Cruz, Calif., 16-20 Jul. 1979; sponsored by IEEE (NASA-TM-79299; E-117) Avail: NTIS HC A02/MF A01 CSCL 22B

The sensitivity of predicted equilibrium potential to changes in secondary electron yield parameters was investigated using MATCHG, a simple charging code which incorporates the NASCAP material property formulations. The equilibrium potential was found to be a sensitive function of one of the two parameters specifying secondary electron yield due to proton impact and of essentially all the parameters specifying yield due to electron impact. The information on the electron generated secondary yield parameters was discovered to be obtainable from monoenergetic beam charging data if charging rates as well as equilibrium potentials are accurately recorded. A.W.H.

N80-16094* National Aeronautics and Space Administration. Lewis Research Center, Cleveland, Ohio.

COMPUTED VOLTAGE DISTRIBUTIONS AROUND SOLAR ELECTRIC PROPULSION SPACECRAFT

N. John Stevens 1979 20 p refs Presented at 14th Intern. Conf. on Elec. Propulsion, Princeton, N.J., 30 Oct. - 1 Nov. 1979; sponsored by AIAA and DGLR (NASA-TM-79286; E-225) Avail: NTIS HC A02/MF A01 CSCL 22B

The NASA Charging Analyzer Program is used to conduct preliminary computations of the voltage distributions around such large spacecraft in geomagnetic substorm environments at geosynchronous altitudes. Both a standard operating voltage (+ or - 150 volts on solar arrays) and direct-drive (+1200 volts on arrays) configurations are considered. Thruster-off simulations are computed for both operating voltage configurations while the effect of simulated thruster-on conditions are evaluated only for direct-drive configuration. These simulated thruster-on conditions are evaluated only for direct-drive configuration. These simulated thruster operations appear to alleviate surface charging. M.M.H.

N80-18095* National Aeronautics and Space Administration. Lewis Research Center, Cleveland, Ohio.

NASCAP MODELLING COMPUTATIONS ON LARGE OPTICS SPACECRAFT IN GEOSYNCHRONOUS SUBSTORM ENVIRONMENTS

N. John Stevens and Carolyn K. Purvis 1980 20 p refs Presented at Soc. of Photo-Optical Instrumentation Engineers, Los Angeles Technical Symp., North Hollywood, Calif., 4-7 Feb. 1980

(NASA-TM-81395; E-305) Avail: NTIS HC A02/MF A01 CSCL 22B

The NASA Charging Analyzer Program (NASCAP) is used to evaluate qualitatively the possibility of such enhanced spacecraft contamination on a conceptual version of a large satellite. The evaluation is made by computing surface voltages on the satellite due to encounters with substorm environments and then computing charged particle trajectories in the electric fields around the satellite. Particular attention is paid to the possibility of contaminants reaching a mirror surface inside a dielectric tube because this mirror represents a shielded optical surface in the satellite model used. Deposition of low energy charged particles from other parts of the spacecraft onto the mirror was found to be possible in the assumed moderate substorm environment condition. In the assumed severe substorm environment condition, however, voltage build up on the inside and edges of the dielectric tube in which the mirror is located prevents contaminants from reaching the mirror surface. J.M.S.

N80-32428* National Aeronautics and Space Administration. Lewis Research Center, Cleveland, Ohio.

MODELLING OF ENVIRONMENTALLY INDUCED DISCHARGES IN GEOSYNCHRONOUS SATELLITES

N. John Stevens 1980 9 p refs Presented at the Ann. Conf. on Nucl. and Space Radiation Effects, Ithaca, N.Y., 15-18 Jul. 1980; sponsored by IEEE (NASA-TM-81598; E-581) Avail: NTIS HC A02/MF A01 CSCL 22B

The NASCAP computer code was used to compute the charging and discharging characteristics of a typical communications satellite in geosynchronous orbit. For the case of a severe substorm satellite surface differential charging in sunlight was found to be substantially less than that required to produce discharges in ground simulation studies. A discharge process was postulated involving discharges triggered at edges (or imperfection) followed by discharges to space. The characteristics of such discharges was parametrically varied to evaluate the possible effects on the satellite. Results indicated that discharge characteristics inferred from satellite monitors could be caused by predicted space discharges, that single cell discharges to space can reduce surface potential over entire satellite, and that low density electron trajectory computations indicate that discharge generated electrons do not return to the satellite by long trajectories. Current transients predicted do not agree with available ground simulation results indicating that additional work must be done both analytically and experimentally to understand and fully explain these discrepancies. R.C.T.

A80-19773* Photoelectron charge density and transport near differentially charged spacecraft. M. J. Mandell, I. Katz, G. W. Schnuelle (Systems, Science and Software, La Jolla, Calif.), and J. C. Roche (NASA, Lewis Research Center, Cleveland, Ohio). (IEEE, U.S. Defense Nuclear Agency, and Jet Propulsion Laboratory, Annual Conference on Nuclear and Space Radiation Effects, 16th, Santa Cruz, Calif., July 17-20, 1979.) IEEE Transactions on Nuclear Science, vol. NS-26, Dec. 1979, p. 5107-5111. 5 refs. USAF-supported research; Contract No. NAS3-21762.

The effects of photoelectron space charge and current density on differentially charged spacecraft are studied. The steady-state potentials of a sunlit cylinder are calculated using a two-dimensional computer code with a fully self-consistent treatment of space charge and an effective surface conductivity treatment of photoelectron currents. It is found that under conditions of strong differential charging the results do not differ greatly from NASCAP results, which neglect photosheath space charge and currents. (Author)

A80-19774 * NASCAP modelling of environmental charging-induced discharges in satellites. N. J. Stevens and J. C. Roche (NASA, Lewis Research Center, Cleveland, Ohio). (*IEEE, U.S. Defense Nuclear Agency, and Jet Propulsion Laboratory, Annual Conference on Nuclear and Space Radiation Effects, 16th, Santa Cruz, Calif., July 17-20, 1979.*) *IEEE Transactions on Nuclear Science*, vol. NS-26, Dec. 1979, p. 5112-5120. 22 refs.

A study of the charging and discharging characteristics of a typical geosynchronous satellite experiencing time-varying geomagnetic substorms, in sunlight, is conducted. The NASA Charging Analyzer Program (NASCAP) is used. An electric field criteria of 1.5×10 to the 5th volts/cm to initiate discharges and transfer of 67% of the stored charge is used in this study, based on ground test results. The substorm characteristics are arbitrarily chosen to evaluate effects of electron temperature and particle density (which is equivalent to current density). It has been found that while there is a minimum electron temperature for discharges to occur, the rate of discharges is dependent on particle density and duration times of the encounter. Hence, it is important to define the temporal variations in the substorm environments. (Author)

A80-29750 * # Computed voltage distribution around Solar Electric Propulsion spacecraft. N. J. Stevens (NASA, Lewis Research Center, Cleveland, Ohio). *American Institute of Aeronautics and Astronautics and Deutsche Gesellschaft für Luft- und Raumfahrt, International Conference on Electric Propulsion, 14th, Princeton, N.J., Oct. 30-Nov. 1, 1979, AIAA Paper 79-2104.* 18 p. 31 refs.

The paper uses the NASCAP computer code to compute voltage distributions around a Solar Electric Propulsion (SEP) spacecraft as it encounters an idealized geomagnetic substorm environment. Consideration is given to both a standard operating voltage and direct-drive voltage configuration. The computations are presented without thruster operations as well as with a simplified, simulated thruster-on representation for direct-drive configuration only. Finally, it is stressed that the computations seeking possible areas of concern in the spacecraft design are exploratory. M.E.P.

A80-29751 * # Initial comparison of SSPM ground test results and flight data to NASCAP simulations. N. J. Stevens, J. V. Staskus, J. C. Roche (NASA, Lewis Research Center, Cleveland, Ohio), and P. F. Mize (Aerospace Corp., Space Sciences Laboratory, Los Angeles, Calif.). *American Institute of Aeronautics and Astronautics, Aerospace Sciences Meeting, 18th, Pasadena, Calif., Jan. 14-16, 1980, Paper 80-0336.* 16 p. 23 refs.

The satellite surface potential monitor (SSPM) has been developed for the P78-2 SCATHA (Spacecraft Charging At The High Altitudes) satellite to determine the response of selected spacecraft materials to charged-particle environmental fluxes. Since the monitor infers total surface voltages from a single point on the interior side of insulators, a ground simulation program was undertaken to develop analytical techniques to model the monitors and to obtain an experimental calibration of the relationship between the flight measurement techniques and actual measurements. The experimental testing was conducted using monoenergetic electron beams irradiating samples in the dark. An analytical computer model was developed in the NASCAP (NASA Charging Analyzer Program) code. The analytical model material properties for Kapton that controlled backscatter and secondary yield were adjusted to obtain a single set of values that produced reasonable fits for both voltages and currents. The analytical techniques developed in the ground technology investigation have been applied to space flight conditions. Predictions were compared with limited flight data. The agreement is very good indicating that the technique, and NASCAP, can be used to predict spacecraft material charging behavior. Details of the testing, the analytical modelling technique and flight data comparisons are presented. (Author)

A80-32829 * # NASCAP modelling computations on large optics spacecraft in geosynchronous substorm environments. N. J.

Stevens and C. K. Purvis (NASA, Lewis Research Center, Cleveland, Ohio). *Society of Photo-Optical Instrumentation Engineers, Los Angeles Technical Symposium, North Hollywood, Calif., Feb. 4-7, 1980, Paper.* 18 p. 20 refs.

Satellites in geosynchronous orbits have been found to be charged to significant negative voltages during encounters with geomagnetic substorms. When satellite surfaces are charged, there is a probability of enhanced contamination from charged particles attracted back to the satellite by electrostatic forces. This could be particularly disturbing to large satellites using sensitive optical systems. In this study the NASA Charging Analyzer Program (NASCAP) is used to evaluate qualitatively the possibility of such enhanced contamination on a conceptual version of a large satellite. The evaluation is made by computing surface voltages on the satellite due to encounters with substorm environments and then computing charged-particle trajectories in the electric fields around the satellite. Particular attention is paid to the possibility of contaminants reaching a mirror surface inside a dielectric tube because this mirror represents a shielded optical surface in the satellite model used. Deposition of low energy charged particles from other parts of the spacecraft onto the mirror was found to be possible in the assumed moderate substorm environment condition. In the assumed severe substorm environment condition, however, voltage build up on the inside and edges of the dielectric tube in which the mirror is located prevents contaminants from reaching the mirror surface. (Author)

A80-38909 * # A liquid hydrogen experiment as a Shuttle payload. R. N. Eberhardt, D. A. Fester (Martin Marietta Aerospace, Denver, Colo.), and J. C. Aydelott (NASA, Lewis Research Center, Cleveland, Ohio). *AIAA, SAE, and ASME, Joint Propulsion Conference, 16th, Hartford, Conn., June 30-July 2, 1980, AIAA Paper 80-1096.* 17 p. 18 refs. Contract No. NAS3-21591.

The paper describes the cryogenic fluid management experiment (CFME) as a Shuttle payload. The experiment includes a liquid hydrogen tank containing a fine-mesh screen acquisition device, and a thermal control system consisting of a thermodynamic vent system to intercept heat leak to the hydrogen tank and control tank pressure. Engineering data obtained will be used to establish design criteria for subcritical cryogenic storage and supply tankage. V.T.

A80-41897 * # Orbital transfer of large space structures with nuclear electric rockets. T. H. Silva (Aerospace Corp., El Segundo, Calif.) and D. C. Byers (NASA, Lewis Research Center, Electric Thruster Section, Cleveland, Ohio). *American Astronautical Society, Goddard Memorial Symposium, 18th, Washington, D.C., Mar. 27, 28, 1980, Paper 80-083.* 13 p. 17 refs.

This paper discusses the potential application of electric propulsion for orbit transfer of a large spacecraft structure from low earth orbit to geosynchronous altitude in a deployed configuration. The electric power was provided by the spacecraft nuclear reactor space power system on a shared basis during transfer operations. Factors considered with respect to system effectiveness included nuclear power source sizing, electric propulsion thruster concept, spacecraft deployment constraints, and orbital operations and safety. It is shown that the favorable total impulse capability inherent in electric propulsion provides a potential economic advantage over chemical propulsion orbit transfer vehicles by reducing the number of Space Shuttle flights in ground-to-orbit transportation requirements. (Author)

A80-44238 * # Effects of secondary yield parameter variation on predicted equilibrium potential of an object in a charging environment. C. K. Purvis (NASA, Lewis Research Center, Cleveland, Ohio). *Institute of Electrical and Electronics Engineers, Annual Conference on Nuclear and Space Radiation Effects, Santa Cruz, Calif., July 16-20, 1979, Paper.* 19 p.

A study is presented in which the sensitivity of predicted equilibrium potential to changes in secondary electron yield parameters is investigated using MATCHG, a simple charging code which

incorporates the NASCAP material property formulations. It is found that equilibrium potential is a sensitive function of one of the two parameters specifying secondary electron yield due to proton impact and of essentially all the parameters specifying yield due to electron impact. In addition, it is found that information on the electron generated secondary yield parameters can be obtained from monoenergetic beam charging data if charging rates as well as equilibrium potentials are accurately recorded. M.E.P.

A80-45809 * **First results of material charging in the space environment.** P. F. Mizera, H. C. Koons, E. R. Schnauss, D. R. Croley, Jr., H. K. A. Ken, M. S. Leung (Aerospace Corp., El Segundo, Calif.), N. J. Stevens, F. Berkopec, J. Staskus (NASA, Lewis Research Center, Cleveland, Ohio), and W. L. Lehn (USAF, Materials Laboratory, Wright-Patterson AFB, Ohio). *Applied Physics Letters*, vol. 37, Aug. 1, 1980, p. 276-279, 5 refs. Contract No. F04701-79-C-0080.

A satellite experiment, designed to measure potential charging of typical thermal-control materials at near-geosynchronous altitude, was flown as part of the Spacecraft Charging at High Altitudes program. Direct observations of charging of typical satellite materials in a natural charging event (greater than or equal to 5 keV) are presented. The results show some features which differ significantly from previous laboratory simulations of the environment. (Author)

A80-46890 * **Active control of spacecraft charging.** C. K. Purvis (NASA, Lewis Research Center, Cleveland, Ohio) and R. O. Bartlett (NASA, Goddard Space Flight Center, Greenbelt, Md.). In: *Space systems and their interactions with earth's space environment*. (A80-46879 20-18) New York, American Institute of Aeronautics and Astronautics, Inc., 1980, p. 299-317, 23 refs.

The concept of active control of spacecraft charging by charged particle emission is described. Active potential control experiments using the ATS-5 and ATS-6 geostationary spacecraft are discussed, and results of these experiments are presented. Previously reported results are summarized, and a guide to reports on these data are provided. Experimental evidence presented indicates that emission of electrons only is not effective in maintaining spacecraft potential near plasma potential for spacecraft with electrically insulating surfaces. Emission of a low energy plasma, however, is effective for this purpose. (Author)

A80-46891 * **A three-dimensional spacecraft-charging computer code.** A. G. Rubin (USAF, Geophysics Laboratory, Bedford, Mass.), I. Katz, M. Mandell, G. Schnuelle, P. Steen, D. Parks, J. Cassidy (Systems Science and Software, Inc., La Jolla, Calif.), and J. Roche (NASA, Lewis Research Center, Cleveland, Ohio). In: *Space systems and their interactions with earth's space environment*. (A80-46879 20-18) New York, American Institute of Aeronautics and Astronautics, Inc., 1980, p. 318-336, 9 refs.

A computer code is described which simulates the interaction of the space environment with a satellite at geosynchronous altitude. Employing finite elements, a three-dimensional satellite model has been constructed with more than 1000 surface cells and 15 different surface materials. Free space around the satellite is modeled by nesting grids within grids. Applications of this NASA Spacecraft Charging Analyzer Program (NASCAP) code to the study of a satellite photosheath and the differential charging of the SCATHA (satellite charging at high altitudes) satellite in eclipse and in sunlight are discussed. In order to understand detector response when the satellite is charged, the code is used to trace the trajectories of particles reaching the SCATHA detectors. Particle trajectories from positive and negative emitters on SCATHA also are traced to determine the location of returning particles, to estimate the escaping flux, and to simulate active control of satellite potentials. (Author)

A80-46897 * **Space environmental interactions with biased spacecraft surfaces.** N. J. Stevens (NASA, Lewis Research Center, Spacecraft Environment Section, Cleveland, Ohio). In: *Space systems and their interactions with earth's space environment*. (A80-46879 20-18) New York, American Institute of Aeronautics and Astronautics, Inc., 1980, p. 455-476, 31 refs.

Large, high-voltage space power systems are being proposed for future space missions. These systems must operate in the charged-particle environment of space, and interactions between this environment and the high-voltage surfaces are possible. Ground simulation testing has indicated that dielectric surfaces that usually surround biased conductors can influence these interactions. For positive voltages greater than 100 V, it has been found that the dielectrics contribute to discharges. Using these experimental results a large, high-voltage power system operating in geosynchronous orbit was analyzed with the NASCAP code. Results of this analysis indicated that very strong electric fields exist in these power systems. A technology investigation is required to understand the interactions and develop techniques to alleviate any impact on power system performance. (Author)

A80-13301 * **Evaluation of particle transport for the P80-1 spacecraft.** J. M. Sellen, Jr. and G. K. Komatsu (TRW Defense and Space Systems Group, Redondo Beach, Calif.). *Princeton University, AIAA, and DGLR, International Electric Propulsion Conference, 14th, Princeton, N.J., Oct. 30-Nov. 1, 1979, AIAA Paper 79-2047*, 7 p. Contract No. NAS3-21047.

Charged and neutral particle transport from an 8-cm mercury ion thruster to the surfaces of the P80-1 spacecraft, the Teal Ruby sensor and the ECOM-501 sensor was examined. Evaluation of particle transport modes utilized both laboratory measurements and analysis. Line-of-sight particle transport considered deposition of Group II (high energy-high angle mercury charge exchange) ions and neutral mercury on solar array surfaces. Nonline-of-sight transport modes studied were recirculation/reinterception of mercury ions in magnetic fields and refraction of low energy mercury charge exchange (Group IV) ions by local electric fields. (Author)

A80-18249 * **Plasma collection by high voltage spacecraft at low earth orbit.** I. Katz, M. J. Mandell, G. W. Schnuelle, D. E. Parks, and P. G. Steen (Systems, Science and Software, La Jolla, Calif.). *American Institute of Aeronautics and Astronautics, Aerospace Sciences Meeting, 18th, Pasadena, Calif., Jan. 14-16, 1980, Paper 80-0042*, 7 p. 11 refs. USAF-supported research; Contract No. NAS3-21762.

A computer model of the three-dimensional sheath formation and plasma current collection by high voltage spacecraft has been developed. By using new space charge density and plasma collection algorithms, it is practical to perform calculations for large, complex spacecraft. The model uses NASCAP compatible objects and geometries. Results indicate that ion focusing observed in the laboratory during high voltage collection experiments is probably due to voltage gradients on the collecting surfaces. (Author)

20 SPACECRAFT PROPULSION AND POWER

Includes main propulsion systems and components e.g., rocket engines, and spacecraft auxiliary power sources.

For related information see also 07 Aircraft Propulsion, 28 Propellants and Fuels, and 44 Energy Production and Conversion.

N80-13159* National Aeronautics and Space Administration, Lewis Research Center, Cleveland, Ohio.

Hg ION THRUSTER COMPONENT TESTING

M. A. Mantieniks 1979 15 p refs Presented at 14th Intern. Conf. on Elec. Propulsion, Princeton, N. J., 30 Oct - 1 Nov. 1979; sponsored by AIAA and DGLR (NASA-TM-79287; E-230) Avail: NTIS HC A02/MF A01 CSCL 21C

Electron bombardment thrusters, under development to provide both auxiliary and primary propulsion functions for a large variety of space missions are tested. Thruster design verification which requires life tests of durations of the order of the time anticipated in space applications, are discussed. The life time and reliability of an electron bombardment thruster is dependent upon the performance of several critical components including cathodes, vaporizers, and isolators. The performances of the cathode, vaporizer, and propellant isolators during fatigue analyses are examined. A.W.H.

N80-13163* National Aeronautics and Space Administration, Lewis Research Center, Cleveland, Ohio.

DESIGN AND EVALUATION OF HIGH PERFORMANCE ROCKET ENGINE INJECTORS FOR USE WITH HYDROCARBON FUELS

A. J. Pavli 1979 20 p refs Presented at the 16th JANNAF Combustion Conf., Monterey, Calif., 10-14 Sep. 1979 (NASA-TM-79319; E-275) Avail: NTIS HC A02/MF A01 CSCL

The feasibility of using a heavy hydrocarbon fuel as a rocket propellant is examined. A method of predicting performance of a heavy hydrocarbon in terms of vaporization effectiveness is described and compared to other fuels and to experimental test results. Experiments were done at a chamber pressure of 4137 KN/sq M (600 psia) with RP-1, JP-10, and liquefied natural gas as fuels, and liquid oxygen as the oxidizer. Combustion length effects were explored over a range of 21.6 cm (8 1/2 in) to 55.9 cm (22 in). Four injector types were tested, each over a range of mixture ratios. Further configuration modifications were obtained by reaming each injector several times to provide test data over a range of injector pressure drop. J.M.S.

N80-14188* National Aeronautics and Space Administration, Lewis Research Center, Cleveland, Ohio.

SUPERCHARGED TOPPING ROCKET PROPELLANT FEED SYSTEM Patent

Warner L. Stewart, Ambrose Ginsburg, and Melvin J. Hartmann, inventors (to NASA) Issued 23 Oct. 1979 6 p Filed 21 Apr. 1966

(NASA-Case-XLE-02062-1; US-Patent-4,171,615; US-Patent-Appl-SN-545793; US-Patent-Class-60-203; US-Patent-Class-60-259) Avail: US Patent and Trademark Office CSCL 21H

A rocket propellant feed system utilizing a bleed turbopump to supercharge a topping turbopump is presented. The bleed turbopump is of a low pressure type to meet the cavitation requirements imposed by the propellant storage tanks. The topping turbopump is of a high pressure type and develops 60 to 70 percent of the pressure rise in the propellant.

Official Gazette of the U.S. Patent and Trademark Office

N80-15204* National Aeronautics and Space Administration, Lewis Research Center, Cleveland, Ohio.

ANALYSIS OF GaAs AND Si SOLAR CELL ARRAYS FOR EARTH ORBITAL AND ORBIT TRANSFER MISSIONS

Kent D. Jeffries 1980 9 p refs Presented at 14th Photovoltaic Specialists Conf., San Diego, Calif., 7-10 Jan. 1980, sponsored by IEEE

(NASA-TM-81383; E-291) Avail: NTIS HC A02/MF A01 CSCL 21C

Silicon and gallium arsenide arrays were studied and compared for low earth orbit (LE), geosynchronous orbit (GEO), and LEO to GEO electric propulsion orbit transfer missions. The sensitivities of total cost to parameters such as mission duration, array cost, cover glass thickness, and concentration ratio were determined along with cost tradeoffs between silicon and gallium arsenide arrays for selected mission classes. Results indicate that development of the technology for low cost, light weight concentrators should be increased and that cost reduction efforts for gallium arsenide cells be pursued R.C.T.

N80-16097* National Aeronautics and Space Administration, Lewis Research Center, Cleveland, Ohio.

UPPER STAGES UTILIZING ELECTRIC PROPULSION

David C. Byers 1980 21 p refs Presented at the JANNAF Propulsion Meeting, Monterey, Calif., 11-13 Mar. 1980

(NASA-TM-81412; E-330) Avail: NTIS HC A02/MF A01 CSCL 21C

The payload characteristics of geocentric missions which utilize electron bombardment ion thruster systems are discussed. A baseline LEO to GEO orbit transfer mission was selected to describe the payload capabilities. The impacts on payloads of both mission parameters and electric propulsion technology options were evaluated. The characteristics of the electric propulsion thrust system and the power requirements were specified in order to predict payload mass. This was completed by utilizing a previously developed methodology which provides a detailed thrust system description after the final mass on orbit, the thrusting time, and the specific impulse are specified. The impact on payloads of total mass in LEO, thrusting time, propellant type, specific impulse, and power source characteristics was evaluated. A.W.H.

N80-17138* National Aeronautics and Space Administration, Lewis Research Center, Cleveland, Ohio.

ANALYTICAL INVESTIGATION OF TWO HYDROGEN OXYGEN ROCKET ENGINE SYSTEMS FOR LOW-THRUST APPLICATION

Dean D. Scheer 1980 17 p refs Presented at JANNAF Propulsion Meeting, Monterey, Calif., 11-13 Mar. 1980

(NASA-TM-81420; E-343) Avail: NTIS HC A02/MF A01 CSCL 21H

Two hydrogen oxygen rocket engine system concepts were analyzed parametrically over a thrust range from 100 to 1000 pounds and a chamber pressure range from 175 to 1000 psia. Both concepts were regeneratively cooled with hydrogen and were pump fed by electric motor driven positive displacement pumps. Electric power was provided by either a turboalternator (turboalternator concept) or some means external to the engine system (auxiliary power concept). The turboalternator concept is discussed. The computer program used to conduct the analyses along with the design characteristics of the major engine system components is described. The feasible design range of the systems over the parametric range of thrust is discussed in terms of allowable chamber pressure. Engine system estimated performance, mass, and dimensional envelope parametric data within the feasible design range are presented. A.W.H.

N80-18098* National Aeronautics and Space Administration, Lewis Research Center, Cleveland, Ohio.

ECONOMIC ANALYSIS OF THE DESIGN AND FABRICATION OF A SPACE QUALIFIED POWER SYSTEM

Gregory Ruselowski Jan. 1980 25 p refs (NASA-TM-81418; E-339) Avail: NTIS HC A02/MF A01 CSCL 10B

An economic analysis was performed to determine the cost

of the design and fabrication of a low Earth orbit, 2 kW photovoltaic/battery, space qualified power system. A commercially available computer program called PRICE (programmed review of information for costing and evaluation) was used to conduct the analysis. The sensitivity of the various cost factors to the assumptions used is discussed. Total cost of the power system was found to be \$2.46 million with the solar array accounting for 70.5%. Using the assumption that the prototype becomes the flight system, 77.3% of the total cost is associated with manufacturing. Results will be used to establish whether the cost of space qualified hardware can be reduced by the incorporation of commercial design, fabrication, and quality assurance methods.
J.M.S.

N80-23365* National Aeronautics and Space Administration. Lewis Research Center, Cleveland, Ohio.

COOLING OF HIGH PRESSURE ROCKET THRUST CHAMBERS WITH LIQUID OXYGEN

H. G. Price 1980 15 p refs Proposed for presentation at the 16th Joint Propulsion Conf., Hartford, 30 Jun. - 2 Jul. 1980; cosponsored by AIAA, ASME and SAE (NASA-TM-81503; E-441) Avail: NTIS HC A02/MF A01 CSCL 21H

An experimental program using hydrogen and oxygen as the propellants and supercritical liquid oxygen (LOX) as the coolant was conducted at 4.14 and 8.274 MN/square meters (600 and 1200 psia) chamber pressure. Data on the following are presented: the effect of LOX leaking into the combustion region through small cracks in the chamber wall; and verification of the supercritical oxygen heat transfer correlation developed from heated tube experiments; A total of four thrust chambers with throat diameters of 0.066 m were tested. Of these, three were cyclically tested to 4.14 MN/square meters (600 psia) chamber pressure until a crack developed. One had 23 additional hot cycles accumulated with no apparent metal burning or distress. The fourth chamber was operated at 8.274 MN/square meters (1200 psia) pressure to obtain steady state heat transfer data. Wall temperature measurements confirmed the heat transfer correlation.
R.C.T.

N80-30382* National Aeronautics and Space Administration. Lewis Research Center, Cleveland, Ohio.

ANALYTICAL INVESTIGATION OF TWO HYDROGEN-OXYGEN ROCKET ENGINE SYSTEMS FOR LOW-THRUST APPLICATION

Dean D. Scheer *In APL The 1980 JANNAF Propulsion Meeting*, Vol. 5 Mar. 1980 p 1-20 refs (For primary document see N80-30381 21-20)

Avail: Issuing Activity CSCL 21H

Two hydrogen-oxygen rocket engine system concepts were analyzed parametrically over a thrust range from 100 to 1000 pounds and a chamber pressure range from 175 to 1000 psia. Both concepts were regeneratively cooled with hydrogen and were pump fed by electric motor driven positive displacement pumps. Electric power was provided by either a turboalternator (turboalternator concept) or some means external to the engine system (auxiliary power concept). The computer program used to conduct the analyses along with the design characteristics of the major engine system components are briefly described. The feasible design range of the systems over the parametric range of thrust is discussed in terms of allowable chamber pressure considering the constraints of thrust chamber cooling and cycle power. Engine system estimated performance, mass, and dimensional envelope parametric data within the feasible design range are presented.
Author

N80-30383* National Aeronautics and Space Administration. Lewis Research Center, Cleveland, Ohio.

LARC REDUCED GRAVITY FLUID MANAGEMENT TECHNOLOGY PROGRAM

J. C. Aydelott and E. P. Symons *In APL The 1980 JANNAF Propulsion Meeting*, Vol. 5 Mar. 1980 p 21-34 refs (For primary document see N80-30381 21-20)

Avail: Issuing Activity CSCL 21H

An overview of studies addressing reduced gravity fluid

management problems using scale model propellant tanks in drop towers that provided up to five seconds of reduced gravity test time is given. The Cryogen Fluid Management Experiment designed to provide an orbital evaluation of a subcritical liquid hydrogen storage and supply as part of the shuttle/Spacelab program is described. An experiment to study orbital transfer of liquids and a Spacelab facility capable of housing multiple fluid dynamic and heat transfer experiments are also discussed. Progress in the analytical evaluation of propellant management systems for both low and high thrust orbit transfer propulsion systems and the development of computer techniques for simulating reduced gravity fluid dynamic processes is reported.
J.M.S.

N80-30386* National Aeronautics and Space Administration. Lewis Research Center, Cleveland, Ohio.

UPPER STAGES UTILIZING ELECTRIC PROPULSION

David C. Byers *In APL The 1980 JANNAF Propulsion Meeting*, Vol. 5 Mar. 1980 p 69-84 refs (For primary document see N80-30381 21-20)

Avail: Issuing Activity CSCL 21H

The payload capabilities of upper stages using electric propulsion for a LEO to GEO orbit transfer mission are presented. The impact on payloads of total mass in LEO, thrusting (trip) time, propellant type, specific impulse, and power source characteristics was evaluated. Dependent upon detailed assumptions, electric stages were found capable of delivering payloads in thrusting time less than 50 days with payloads always initially increasing rapidly with increasing thrusting times. For the shorter thrusting (trip) times the payloads increased with increasing propellant mass and decreasing specific impulse. At very long trip times, however, the payload increased with decreasing propellant mass and increasing specific impulse. Variation of the specific mass of the power source between 5 and 30 kg/kW caused the minimum trip times to vary about a factor of three and at short trip times strongly affected the electric stage payload capabilities.
J.M.S.

N80-31449* National Aeronautics and Space Administration. Lewis Research Center, Cleveland, Ohio.

LARGE SPACE SYSTEMS/LOW-THRUST PROPULSION TECHNOLOGY

Jul. 1980 347 p refs Meeting held at Cleveland, 20-21 May 1980

(NASA-CP-2144; E-510) Avail: NTIS HC A15/MF A01 CSCL 21H

The potentially critical interactions that occur between propulsion, structures and materials, and controls for large spacecraft are considered, the technology impacts within these fields are defined and the net effect on large systems and the resulting missions is determined. Topical areas are systems/mission analysis, LSS static and dynamic characterization, and propulsion systems characterization. For individual titles, see N80-31450 through N80-31471.

N80-31452* National Aeronautics and Space Administration. Lewis Research Center, Cleveland, Ohio.

ELECTRIC PROPULSION TECHNOLOGY

Robert C. Finke *In its Large Space Systems/Low-Thrust Propulsion Technol.* Jul. 1980 p 23-30 (For primary document see N80-31449 22-20)

Avail: NTIS HC A15/MF A01 CSCL 21H

The advanced electric propulsion program is directed towards lowering the specific impulse and increasing the thrust per unit of ion thruster systems. In addition, electrothermal and electromagnetic propulsion technologies are being developed to attempt to fill the gap between the conventional ion thruster and chemical rocket systems. Most of these new concepts are exogenous and are represented by rail accelerators, ablative Teflon thrusters, MPD arcs, Free Radicals, etc. Endogenous systems such as metallic hydrogen offer great promise and are also being pursued.
A.R.H.

N80-31453* National Aeronautics and Space Administration. Lewis Research Center, Cleveland, Ohio.

CHEMICAL PROPULSION TECHNOLOGY

Richard J. Priem. *In its Large Space Systems/Low-Thrust Propulsion Technol.* Jul. 1980 p 31-36 (For primary document see N80-31449 22-20)

Avail: NTIS HC A15/MF A01 CSCL 21H

An overview of NASA's low thrust liquid chemical propulsion program is presented with particular emphasis on thrust system technology in the ten to one thousand pound thrust range. Key technology issues include high performance of cooled low thrust engines, small cryogenic pumps; multiple starts-shutdowns (10) with slow ramps (approximately 10 seconds); thrust variation - 4/1 in flight and 20/1 between flights; long life (100 hours); improved system weight and size, and propellant selection.

A.R.H.

N80-31454* National Aeronautics and Space Administration. Lewis Research Center, Cleveland, Ohio.

LSS/PROPULSION INTERACTIONS STUDIES

Omer F. Spurlock. *In its Large Space Systems/Low-Thrust Propulsion Technol.* Jul. 1980 p 37-52 (For primary document see N80-31449 22-20)

Avail: NTIS HC A15/MF A01 CSCL 21H

Interactions between the LSS and the propulsion system are large, significant, interrelated, and complex. Issues and problems in interfacing include the effects on the structure from static, dynamic, and launch loads, control, thrust distribution, throttling, and the environment. Control interaction, the disposal of debris/obsolete spacecraft, and the constraints of launch to low Earth orbit must also be considered.

A.R.H.

N80-31457* National Aeronautics and Space Administration. Lewis Research Center, Cleveland, Ohio.

LOW-THRUST VEHICLE CONCEPT STUDIES

George R. Smolak. *In its Large Space Systems/Low-Thrust Propulsion Technol.* Jul. 1980 p 97-106 (For primary document see N80-31449 22-20)

Avail: NTIS HC A15/MF A01 CSCL 21H

Part of NASA's orbit transfer vehicle propulsion program is devoted to the development of analytical tools to define propulsion system performance, weight, size, and other parameters, and to develop packing concepts for LSS mission propulsion and payload systems. Packing studies discussed relate to shuttle cargo bay constraints; low thrust engine profile and performance; large space frame concept and weight; low thrust vehicles stowed in shuttle, LSS payload capability, and weight distribution. Further study is needed to determine interactions among propulsion system, payload structures, and shuttle. Low thrust-to-weight ratios are desirable to maximize payload weights and deployed areas.

A.R.H.

N80-31471* National Aeronautics and Space Administration. Lewis Research Center, Cleveland, Ohio.

ADVANCED CONCEPTS

Bruce A. Banks. *In its Large Space Systems/Low-Thrust Propulsion Technol.* Jul. 1980 p 337-342 (For primary document see N80-31449 22-20)

Avail: NTIS HC A15/MF A01 CSCL 21H

The relative strengths of those interactions which enable propulsive forces are listed as well as the specific impulse of various propellants. Graphics show the linear synchronous motor of the mass driver, the principle of the direct current electromagnetic launcher, and the characteristics of the rail gun.

A.R.H.

N80-33465* National Aeronautics and Space Administration. Lewis Research Center, Cleveland, Ohio.

SYNCHRONOUS ENERGY TECHNOLOGY

Sep. 1980 144 p Symp. held in Cleveland, 29-30 Apr. 1980 (NASA-CP-2154; E-469) Avail: NTIS HC A07/MF A01 CSCL 21H

The synchronous technology requirements for large space power systems are summarized. A variety of technology areas

including photovoltaics, thermal management, and energy storage, and power management are addressed. For individual titles, see N80-33466 through N80-33475.

N80-33466* National Aeronautics and Space Administration. Lewis Research Center, Cleveland, Ohio.

SYNCHRONOUS ENERGY TECHNOLOGY PROGRAM

Robert C. Finke. *In its Synchronous Energy Technol.* Sep. 1980 p 1-7 (For primary document see N80-33465 24-20)

Avail: NTIS HC A07/MF A01 CSCL 10B

The power program in NASA and DOD are discussed with emphasis on the technology for future large space power systems. The structure of the synchronous energy technology program is described and the technologies required for future geosynchronous power stations are defined. The output of the program is to be a series of design data documents to provide design information and to transfer the technology to the involved community. R.C.T.

N80-33470* National Aeronautics and Space Administration. Lewis Research Center, Cleveland, Ohio.

PHOTOVOLTAIC TECHNOLOGY DEVELOPMENT FOR SYNCHRONOUS ORBIT

Henry W. Brandhorst. *In its Synchronous Energy Technol.* Sep. 1980 p 45-56 (For primary document see N80-33465 24-20)

Avail: NTIS HC A07/MF A01 CSCL 10A

Accomplishments and expected benefits are summarized for the following efforts: (1) achieving silicon solar cell efficiency of 18% at 200 micron m to 250 micron m thickness; (2) reducing silicon cell radiation damage in geosynchronous orbit after 10 years to less than 15%; (3) demonstrating coplanar back contact 50 micron m thick silicon solar cells with efficiency of 14%; (4) demonstrating the feasibility of a radiation tolerant GaAs concentrator cell; (5) achieving 30% efficient photo conversion in the laboratory; (6) defining candidate concepts for 50% efficient electromagnetic conversion; and (7) demonstrating the technology for protecting arrays capable of > 300W/kg after 10 years in geosynchronous orbit.

A.R.H.

A80-10376 * Characteristics of primary electric propulsion systems. D. C. Byers (NASA, Lewis Research Center, Electric Thruster Section, Cleveland, Ohio). *Princeton University, AIAA, and DGLR, International Electric Propulsion Conference, 14th, Princeton, N.J., Oct. 30-Nov. 1, 1979, AIAA Paper 79-2041*, 13 p, 21 refs.

The use of advanced electric propulsion systems will provide cost and performance benefits for future energetic space missions. A methodology to predict the characteristics of advanced electric propulsion systems was developed and programmed for computer calculations to allow evaluation of a broad set of technology and mission assumptions. The impact on overall thrust system characteristics was assessed for variations of propellant type, total accelerating voltage, thruster area, specific impulse, and power system approach. The data may be used both to provide direction to technology emphasis and allow for preliminary estimates of electric propulsion system properties for a wide variety of application. (Author)

A80-10384 * Sputtering in mercury ion thrusters. M. A. Mantieniks and V. K. Rawlin (NASA, Lewis Research Center, Cleveland, Ohio). *Princeton University, AIAA, and DGLR, International Electric Propulsion Conference, 14th, Princeton, N.J., Oct. 30-Nov. 1, 1979, AIAA Paper 79-2061*, 13 p, 48 refs.

Ground-based tests of Hg ion thrusters have identified sputter erosion of thruster components as one of the main life limiting phenomena. Subsequent measurements have revealed that sputtering rates can be affected by background gases at pressures as low as 10 to the -10th torr. With the recent interest in thin film technology, sputtering in the presence of reactive gases has been studied in great detail. This paper presents the results of many of those studies and applies them to the sputtering of electric thrusters. A model, which assumes that chemisorption is the dominant mechanism, is applied to the sputtering rate measurements of the screen grid of a 30-cm thruster in the presence of nitrogen. The model utilizes inputs from a

variety of experimental and analytical sources. The model of environmental effects on sputtering was applied to thruster conditions of low discharge voltage and a discussion of the comparison of theory and experiment is presented. (Author)

A80-10386 * # SERT II 1979 extended flight thruster system performance. W. R. Kerslake and L. R. Ignaczak (NASA, Lewis Research Center, Cleveland, Ohio). *Princeton University, AIAA, and DGLR, International Electric Propulsion Conference, 14th, Princeton, N.J., Oct. 30-Nov. 1, 1979, AIAA Paper 79-2063*. 13 p. 9 refs.

The SERT II spacecraft, launched in 1970, has been maintained in an operational, but intermittently active status since 1971. Periodic thruster status has been reported while waiting for normal orbit precession to return the spacecraft to continuous sunlight in 1979. Now, the thruster has been operated for 600 hours in the first quarter of 1979. Thruster startup and operation in 1979 is unchanged after 9 years in space. The ion thruster was gimbaled and used to maintain spin stabilization of the spacecraft. Minor components of the spacecraft have failed, but have not interfered with the functional status of the spacecraft. (Author)

A80-10387 * # Neutralization tests on the SERT II spacecraft. W. R. Kerslake and S. Domitz (NASA, Lewis Research Center, Cleveland, Ohio). *Princeton University, AIAA, and DGLR, International Electric Propulsion Conference, 14th, Princeton, N.J., Oct. 30-Nov. 1, 1979, AIAA Paper 79-2064*. 15 p. 11 refs.

Orbit precession returned the SERT II spacecraft to continuous sunlight in January 1979 for the first time since early 1972, and new experiments were planned and conducted. Neutralization of an ion beam was accomplished by a second neutralizer cathode located 1 meter away. Plasma potential measurements were made of the plasma surrounding the ion beam and connecting the beam to the second neutralizer. When the density of the connecting plasma was increased by turning on the main discharge of a neighboring ion thruster, the neutralization of the ion beam occurred with improved (lower) coupling voltage. These and other tests reported should aid in the future design of spacecraft using electric thruster systems. Data taken indicate that cross neutralization of ion thrusters in a multiple thruster array should occur readily. (Author)

A80-10392 * # Reduced power processor requirements for the 30-cm diameter Hg ion thruster. V. K. Rawlin (NASA, Lewis Research Center, Cleveland, Ohio). *Princeton University, AIAA, and DGLR, International Electric Propulsion Conference, 14th, Princeton, N.J., Oct. 30-Nov. 1, 1979, AIAA Paper 79-2081*. 10 p. 25 refs.

The characteristics of power processors strongly impact the overall performance and cost of electric propulsion systems. A program was initiated to evaluate simplifications of the thruster-power processor interface requirements. The power processor requirements are mission dependent with major differences arising for those missions which require a nearly constant thruster operating point (typical of geocentric and some inbound planetary missions) and those requiring operation over a large range of input power (such as outbound planetary missions). This paper describes the results of tests which have indicated that as many as seven of the twelve power supplies may be eliminated from the present Functional Model Power Processor used with 30-cm diameter Hg ion thrusters. (Author)

A80-20957 * # Design and evaluation of high performance rocket engine injectors for use with hydrocarbon fuels. A. J. Pavli (NASA, Lewis Research Center, Cleveland, Ohio). *Joint-Army-Navy-NASA-Air Force Interagency Propulsion Committee, Combustion Conference, 16th, Monterey, Calif., Sept. 10-14, 1979, Paper*. 13 p.

An experimental program to determine the feasibility of using a heavy hydrocarbon fuel as a rocket propellant is reported herein. A method of predicting performance of a heavy hydrocarbon in terms of vaporization effectiveness is described and compared to other

fuels and to experimental test results. The work was done at a chamber pressure of 4137 KN/sq M (600 psia) with RP-1, JP-10, and liquefied natural gas as fuels, and liquid oxygen as the oxidizer. Combustion length effects were explored over a range of 21.6 cm (8 1/2 in.) to 55.9 cm (22 in.). Four injector types were tested, each over a range of mixture ratios. Further configuration modifications were obtained by 'reaming' each injector several times to provide test data over a range of injector pressure drop. (Author)

A80-20959 * # HG ion thruster component testing. M. A. Mantenjeks (NASA, Lewis Research Center, Cleveland, Ohio). *Princeton University, AIAA, and DGLR, International Electric Propulsion Conference, 14th, Princeton, N.J., Oct. 30-Nov. 1, 1979, AIAA Paper 79-2116*. 13 p. 20 refs.

Cathodes, isolators, and vaporizers are critical components in determining the performance and lifetime of mercury ion thrusters. The results of life tests of several of these components are reported. A 30-cm thruster CIV test in a bell jar has successfully accumulated over 26,000 hours. The cathode has undergone 65 restarts during the life test without requiring any appreciable increases in starting power. Recently, all restarts have been achieved with only the 44 volt keeper supply with no change required in the starting power. Another ongoing 30-cm Hg thruster cathode test has successfully passed the 10,000 hour mark. A solid-insert, 8-cm thruster cathode has accumulated over 4,000 hours of thruster operation. All starts have been achieved without the use of a high voltage ignitor. The results of this test indicate that the solid impregnated insert is a viable neutralizer cathode for the 8-cm thruster. (Author)

A80-29989 * # Upper stages utilizing electric propulsion. D. C. Byers (NASA, Lewis Research Center, Cleveland, Ohio). *Joint Army-Navy-NASA-Air Force Interagency Propulsion Committee, Propulsion Meeting, Monterey, Calif., Mar. 11-13, 1980, Paper*. 19 p. 23 refs.

The payload capabilities of upper stages using electric propulsion for a LEO to GEO orbit transfer mission are discussed. Payloads are calculated using an established methodology which employs assumptions concerning state-of-the-art electric propulsion technology. The effects on payloads are examined for variations of total mass in LEO (MLEO), thrusting (trip) times, propellant type, specific impulse, and power source specific mass. It is found that the ratios of payload masses to total mass in LEO are insensitive to MLEO, which allows a highly condensed presentation of the overall payload capability. Electric stages are shown capable of delivering payloads in thrusting times less than 50 days with the payloads increasing rapidly with increase in thrusting times. Payload capabilities exceeding those attainable with chemical propulsion are possible using state-of-the-art electric propulsion technology. L.M.

A80-32886 * # Electric propulsion, circa 2000. W. R. Hudson (NASA, Washington, D.C.) and R. C. Finke (NASA, Lewis Research Center, Cleveland, Ohio). *American Institute of Aeronautics and Astronautics, International Meeting and Technical Display on Global Technology 2000, Baltimore, Md., May 6-8, 1980, Paper 80-0912*. 6 p.

This paper discusses the future of electric propulsion, circa 2000. Starting with the first generation Solar Electric Propulsion (SEP) technology as the first step toward the next century's advanced propulsion systems, the current status and future trends of other systems such as the magnetoplasmadynamic accelerator, the mass driver, the laser propulsion system, and the rail gun are described. (Author)

A80-33850 * Origin of reverse annealing in radiation-damaged silicon solar cells. I. Weinberg and C. K. Swartz (NASA, Lewis Research Center, Cleveland, Ohio). *Applied Physics Letters*, vol. 36, Apr. 15, 1980, p. 693-695. 12 refs.

The paper employs relative defect concentrations, energy levels, capture cross sections, and minority carrier diffusion lengths in order to identify the defect responsible for the reverse annealing observed in a radiation damaged $n(+)/p$ silicon solar cell. It is reported that the responsible defect, with the energy level at +0.30 eV, has been tentatively identified as boron-oxygen-vacancy complex. In conclusion, it is shown that removal of this defect could result in significant cell recovery when annealing at temperatures well below the currently required 400 C. M.E.P.

A80-35503 * # Analytical investigation of two hydrogen-oxygen rocket engine systems for low-thrust application. D. D. Scheer (NASA, Lewis Research Center, Cleveland, Ohio). *Joint Army-Navy-NASA-Air Force Interagency Propulsion Committee, Propulsion Meeting, Monterey, Calif., Mar. 11-13, 1980, Paper*, 15 p. 11 refs.

Two hydrogen-oxygen rocket engine system concepts were analyzed parametrically over a thrust range from 100 to 1000 pounds and a chamber pressure range from 175 to 1000 psia. Both concepts were regeneratively cooled with hydrogen and were pumped by electric motor driven positive displacement pumps. Electric power was provided by either a turboalternator (turboalternator concept) or some means external to the engine system (auxiliary power concept). The computer program used to conduct the analyses along with the design characteristics of the major engine system components are briefly described. The feasible design range of the systems over the parametric range of thrust is discussed in terms of allowable chamber pressure considering the constraints of thrust chamber cooling and cycle power. Engine system estimated performance, mass, and dimensional envelope parametric data within the feasible design range are presented. (Author)

A80-38908 * # Capillary device refilling. M. H. Blatt, F. Merino (General Dynamics Corp., Convair Div., San Diego, Calif.), and E. P. Symons (NASA, Lewis Research Center, Cleveland, Ohio). *AIAA, SAE, and ASME, Joint Propulsion Conference, 16th, Hartford, Conn., June 30-July 2, 1980, AIAA Paper 80-1095*, 8 p. Contract No. NAS3-20092.

An analytical and experimental study was conducted dealing with refilling start baskets (capillary devices) with settled fluid. A computer program was written to include dynamic pressure, screen wicking, multiple-screen barriers, standpipe screens, variable vehicle mass for computing vehicle acceleration, and calculation of tank outflow rate and vapor pullthrough height. An experimental apparatus was fabricated and tested to provide data for correlation with the analytical model; the test program was conducted in normal gravity using a scale-model capillary device and ethanol as the test fluid. The test data correlated with the analytical model; the model is a versatile and apparently accurate tool for predicting start basket refilling under actual mission conditions. A.T.

A80-38975 * # Nuclear electric propulsion system utilization for earth orbit transfer of large spacecraft structures. T. H. Silva (Aerospace Corp., El Segundo, Calif.) and D. C. Byers (NASA, Lewis Research Center, Cleveland, Ohio). *AIAA, SAE, and ASME, Joint Propulsion Conference, 16th, Hartford, Conn., June 30-July 2, 1980, AIAA Paper 80-1223*, 13 p. 17 refs.

The paper discusses a potential application of electric propulsion to perform orbit transfer of a large spacecraft structure to geosynchronous orbit (GEO) from LEO, utilizing a nuclear reactor space power source in the spacecraft on a shared basis. The discussions include spacecraft, thrust system, and nuclear reactor space power system concepts. Emphasis is placed on orbiter payload arrangements, spacecraft launch constraints, and spacecraft LEO assembly and deployment sequences. V.T.

A80-38992 * # Cooling of high pressure rocket thrust cham-

bers with liquid oxygen. H. G. Price (NASA, Lewis Research Center, Cleveland, Ohio). *AIAA, SAE, and ASME, Joint Propulsion Conference, 16th, Hartford, Conn., June 30-July 2, 1980, AIAA Paper 80-1260*, 10 p. 9 refs.

An experimental program using hydrogen and oxygen as the propellants and supercritical liquid oxygen (LOX) as the coolant was conducted at 4.14 and 8.274 MN/sq m chamber pressure. It was aimed to demonstrate the effect of LOX leaking into the combustion region through small cracks in the chamber wall, and to verify the supercritical oxygen heat transfer correlation developed from heated tube experiments. Four thrust chambers with throat diameters of 0.066 m were tested; three of these were cyclically tested to 4.14 MN/sq m chamber pressure until a crack developed; the fourth chamber was operated at 8.274 MN/sq m pressure to obtain steady state heat transfer data. Wall temperature measurements confirmed the heat transfer correlation. A.T.

A80-38994 * # Advanced cooling techniques for high-pressure, hydrocarbon-fueled rocket engines. R. T. Cook (Rockwell International Corp., Canoga Park, Calif.) and R. J. Quentzler (NASA, Lewis Research Center, Cleveland, Ohio). *AIAA, SAE, and ASME, Joint Propulsion Conference, 16th, Hartford, Conn., June 30-July 2, 1980, AIAA Paper 80-1266*, 11 p. 7 refs. Contract No. NAS3-21381.

The regenerative cooling limits (maximum chamber pressure) are defined for oxygen/hydrocarbon (Methane, Propane, and RP-1) rocket engines over a thrust range of 20,000 to 600,000 lbf for a reusable life of 250 missions. Chamber pressure limits are first defined without a hot-gas wall carbon layer (unenriched designs). Cooling enhancement chamber pressure limits are then established for seven thermal barriers (carbon layer, ceramic coating, graphite liner, film cooling, zoned combustion, transpiration cooling, and a combination of two of the above). The maximum regenerative-cooled chamber pressure is attained with the oxygen/methane propellant combination. (Author)

A80-48357 * # Power management for multi-100 KWe space systems. J. W. Mildice (General Dynamics Corp., Convair Div., San Diego, Calif.) and M. E. Valgora (NASA, Lewis Research Center, Cleveland, Ohio). In: *Energy to the 21st century; Proceedings of the Fifteenth Intersociety Energy Conversion Engineering Conference, Seattle, Wash., August 18-22, 1980, Volume 2*. (A80-48165 21-44) New York, American Institute of Aeronautics and Astronautics, Inc., 1980, p. 1401-1405. Contract No. NAS3-21757.

This paper examines mid to late 1980s power management technology needs to support development of a general-purpose space platform, capable of supplying 100 to 250 KWe to a variety of users in LEO. To that end, a typical Shuttle-assembled and supplied space platform is described, along with a group of payloads which might reasonably be expected to use such a facility. Examination of platform and user power needs yields a set of power system requirements used to evaluate power management options for life cycle cost effectiveness. The most cost-effective AC/DC and DC systems are evaluated, specifically to develop system details which lead to technology goals including array and transmission voltage, best frequency for AC power transmission, and advantages and disadvantages of AC and DC systems for this application. Finally, system and component requirements are compared with the state of the art to identify areas where technology development is required. (Author)

N80-11137* # TRW Defense and Space Systems Group, Redondo Beach, Calif.
SPECIFIC SPACECRAFT EVALUATION: SPECIAL REPORT
Special Report, 1 Nov. 1977 - 1 Jun. 1978
J. M. Sellen, Jr. 1 Nov. 1978 211 p
(Contract NAS3-21047)
(NASA-CR-159420) Avail: NTIS HC A10/MF A01 CSCL 21H

Charged and neutral particle transport from an 8 cm mercury ion thruster to the surfaces of the P 80-1 spacecraft and to the

Teal Ruby sensor and the ECOM 501 sensor of that spacecraft were investigated. Laboratory measurements and analyses were used to examine line-of-sight and nonline of sight particle transport modes. The recirculation of Hg^{+} ions in the magnetic field of the earth was analyzed for spacecraft velocity and Earth magnetic field vector configurations which are expected to occur in near Earth, circular, high inclination orbits. For these magnetic field and orbit conditions and for expected ion release distribution functions, in both angles and energies, the recirculation/re-interception of ions on spacecraft surfaces was evaluated. The refraction of weakly energetic ions in the electric fields of the thruster plasma plume and in the electric fields between this plasma plume and the material boundaries of the thruster, the thruster sputter shield, and the various spacecraft surfaces were examined. The neutral particle transport modes of interest were identified as sputtered metal atoms from the thruster beam shield. Results, conclusions, and future considerations are presented.

R.C.T.

N80-13158* Hughes Research Labs., Malibu, Calif.
PRIMARY ELECTRIC PROPULSION TECHNOLOGY STUDY
Final Report, 13 Sep. 1977 - 13 Jun. 1979
 R. L. Poeschel and J. R. Beattie Nov. 1979 186 p refs
 (Contract NAS3-21040)
 (NASA-CR-159688) Avail: NTIS HC A09/MF A01 CSCL 01C

An investigation of the 30-cm engineering-model-thruster technology with emphasis placed on the development of models for understanding and predicting the operational characteristics and wear-out mechanisms of the thruster as a function of operating or design parameters is presented. The task studies include: (1) the wear mechanisms and wear rates that determine the useful lifetime of the thruster discharge chamber; (2) cathode lifetime as determined by the depletion of barium from the barium-aluminate-impregnated-porous-tungsten insert that serves as a barium reservoir; (3) accelerator-grid-system technology; (4) a verification of the high-voltage propellant-flow-electrical-isolator design developed under NASA contract NAS3-20395 for operation at 10-kV applied voltage and 10-A equivalent propellant flow with mercury and argon propellants. A model was formulated for predicting performance. M.M.M.

N80-13164* Tennessee Technological Univ., Cookeville. Dept. of Engineering Science.
ANALYSIS OF COMBUSTION INSTABILITY IN LIQUID FUEL ROCKET MOTORS Ph.D. Thesis
 Kin-Wing Wong and M. Ventrice Nov. 1979 119 p refs
 (Grant NGR-43-003-015)
 (NASA-CR-159733) Avail: NTIS HC A06/MF A01 CSCL 21H

The development of a technique to be used in the solution of nonlinear velocity-sensitive combustion instability problems is described. The orthogonal collocation method was investigated. It found that the results are heavily dependent on the location of the collocation points and characteristics of the equations, so the method was rejected as unreliable. The Galerkin method, which has proved to be very successful in analysis of the pressure sensitive combustion instability was found to work very well. It was found that the pressure wave forms exhibit a strong second harmonic distortion and a variety of behaviors are possible depending on the nature of the combustion process and the parametric values involved. A one-dimensional model provides further insight into the problem by allowing a comparison of Galerkin solutions with more exact finite-difference computations. A.R.H.

N80-13165* Tennessee Technological Univ., Cookeville.
STABILITY ANALYSIS OF A LIQUID FUEL ANNULAR COMBUSTION CHAMBER M.S. Thesis
 G. H. McDonald Nov. 1978 151 p refs
 (Grant NGR-43-003-015)
 (NASA-CR-159734) Avail: NTIS HC A08/MF A01 CSCL 21H

High frequency combustion instability problems in a liquid fuel annular combustion chamber are examined. A modified

Galerkin method was used to produce a set of modal amplitude equations from the general nonlinear partial differential acoustic wave equation in order to analyze the problem of instability. From these modal amplitude equations, the two variable perturbation method was used to develop a set of approximate equations of a given order of magnitude. These equations were modeled to show the effects of velocity sensitive combustion instabilities by evaluating the effects of certain parameters in the given set of equations. A.W.H.

N80-14189* Aerojet Liquid Rocket Co., Sacramento, Calif.
PERFORMANCE OF A TRANSPIRATION-REGENERATIVE COOLED ROCKET THRUST CHAMBER Final Report
 H. W. Valler Sep 1979 414 p refs
 (Contract NAS3-21029)
 (NASA-CR-159742) Avail: NTIS HC A18/MF A01 CSCL 21H

The analysis, design, fabrication, and testing of a liquid rocket engine thrust chamber which is gas transpiration cooled in the high heat flux convergent portion of the chamber and water jacket cooled (simulated regenerative) in the barrel and divergent sections of the chamber are described. The engine burns LOX-hydrogen propellants at a chamber pressure of 600 psia. Various transpiration coolant flow rates were tested with resultant local hot gas wall temperatures in the 800 F to 1400 F range. The feasibility of transpiration cooling with hydrogen and helium, and the use of photo-etched copper platelets for heat transfer and coolant metering was successfully demonstrated. A.R.H.

N80-17137* Colorado State Univ., Fort Collins. Dept. of Mechanical Engineering.
PHYSICAL PHENOMENA IN MERCURY ION THRUSTERS
Annual Report, 1 Dec. 1978 - 1 Dec. 1979
 Paul J. Wilbur Dec. 1979 146 p refs
 (Grant NGR-06-002-112)
 (NASA-CR-159784) Avail: NTIS HC A07/MF A01 CSCL 21C

Experimental tests results demonstrating that reductions in screen grid thickness enhance the performance of ion thruster grids are presented. Shaping of the screen hole cross section is shown on the other hand not to affect performance substantially. The effect of the magnetic field in the vicinity of the hollow cathode on cathode performance is studied and test results are presented that show reductions in keeper voltages of a few volts can be realized by judicious applications of fields on the order of 100 gauss. The plasma downstream of a SERT 2 thruster operating without high voltage is studied. A model describing electron escape from the thruster under these conditions is discussed. A model defining the performance of the baffle aperture of an ion thruster is refined and experimental verification of the model is undertaken. Author

N80-17141* Rocketdyne, Canoga Park, Calif.
ADVANCED COOLING TECHNIQUES FOR HIGH-PRESSURE HYDROCARBON-FUELED ENGINES Final Report, Aug. 1978 - Oct. 1979
 R. T. Cook Oct. 1979 230 p refs
 (Contract NAS3-21381)
 (NASA-CR-159790; RI/RD79-310) Avail: NTIS HC A11/MF A01 CSCL 21H

The regenerative cooling limits (maximum chamber pressure) for O₂/hydrocarbon gas generator and staged combustion cycle rocket engines over a thrust range of 89,000 N (20,000 lbf) to 2,669,000 N (600,000 lbf) for a reusable life of 250 missions were defined. Maximum chamber pressure limits were first determined for the three propellant combinations (O₂/CH₄, O₂/C₃H₈, and O₂/RP-1 without a carbon layer (unenhanced designs). Chamber pressure cooling enhancement limits were then established for seven thermal barriers. The thermal barriers evaluated for these designs were: carbon layer, ceramic coating, graphite liner, film cooling, transpiration cooling, zoned combustion, and a combination of two of the above. All fluid barriers were assessed a 3 percent performance loss. Sensitivity studies were then conducted to determine the influence of cycle life

and RP-1 decomposition temperature on chamber pressure limits. Chamber and nozzle design parameters are presented for the unenhanced and enhanced designs. The maximum regenerative cooled chamber pressure limits were attained with the O₂/CH₄ propellant combination. The O₂/RP-1 designs relied on a carbon layer and liquid gas injection chamber contours, short chamber, to be competitive with the other two propellant combinations. This was attributed to the low decomposition temperature of RP-1. RCT

N80-15202* Rocketdyne, Canoga Park, Calif.
LIQUID OXYGEN/LIQUID HYDROGEN AUXILIARY POWER SYSTEM THRUSTER INVESTIGATION Final Report, Oct. 1976 - Feb. 1979

E. E. Eberle and L. Kusak Dec 1979 186 p refs
 (Contract NAS3-20373)
 (NASA CR 159674, RI/RD79-217) Avail NTIS
 HC A09/MF A01 CSCL 21H

The design, fabrication, and demonstration of a 111 newton (25 lb) thrust, integrated auxiliary propulsion system (IAPS) thruster for use with LH₂/LO₂ propellants is described. Hydrogen was supplied at a temperature range of 22 to 33 K (40 to 60 R), and oxygen from 89 to 122 K (160 to 220 R). The thruster was designed to operate in both pulse mode and steady-state modes for vehicle attitude control, space maneuvering, and as an abort backup in the event of failure of the main propulsion system. A dual sleeve, tri axial injection system was designed that utilizes a primary injector/combustor where 100 percent of the oxygen and 8 percent of the hydrogen is introduced, a secondary injector/combustor where 45 percent of the hydrogen is introduced to mix with the primary combustor gases, and a boundary layer injector that uses the remaining 45 percent of the hydrogen to cool the thrust throat/nozzle design. Hot-fire evaluation of this thruster with a BLC injection distance of 2.79 cm (1.10 in.) indicated that a specific impulse value of 390 sec can be attained using a coated molybdenum thrust chamber. Pulse mode tests indicated that a chamber pressure buildup to 90 percent thrust can be achieved in a time on the order of 48 msec. Some problems were encountered in achieving ignition of each pulse during pulse trains. This was interpreted to indicate that a higher delivered spark energy level (~ 100 mJ) would be required to maintain ignition reliability of the plasma torch ignition system under the extra 'cold' conditions resulting during pulsing. Author

N80-16096* Boeing Aerospace Co., Seattle, Wash.
ELECTRIC PROPULSION FOR NEAR-EARTH SPACE MISSIONS Final Report, Feb. 1978 - Apr. 1979

C. H. Terwilliger and W. W. Smith Jan 1980 206 p
 (Contract NAS3-21346)
 (NASA-CR-159735, D180-25475-1) Avail NTIS
 HC A10/MF A01 CSCL 21C

A set of missions was postulated that was considered to be representative of those likely to be desirable/feasible over the next three decades. The characteristics of these missions, and their payloads, that most impact the choice/design of the requisite propulsion system were determined. A system-level model of the near-Earth transportation process was constructed, which incorporated these mission/system characteristics, as well as the fundamental parameters describing the technology/performance of an ion bombardment based electric propulsion system. The model was used for sensitivity studies to determine the interactions between the technology descriptors and program costs, and to establish the most cost-effective directions for technology advancement. The most important factor was seen to be the costs associated with the duration of the mission, and this in turn makes the development of advanced electric propulsion systems having moderate to high efficiencies (> 50 percent) at intermediate ranges of specific impulse (approximately 1000 seconds) very desirable. Author

N80-19185* General Dynamics/Convair, San Diego, Calif.
CAPILLARY ACQUISITION DEVICES FOR HIGH-PERFORMANCE VEHICLES: EXECUTIVE SUMMARY
 M. H. Blatt, R. D. Bradshaw, and J. A. Risberg Feb. 1980

103 p refs
 (Contract NAS3-20092)
 (NASA CR 159658, GDC-CRAD-80 003) Avail NTIS
 HC A06/MF A01 CSCL 21H

Technology areas critical to the development of cryogenic capillary devices were studied. Passive cooling of capillary devices was investigated with an analytical and experimental study of wicking flow. Capillary device refilling with settled fluid was studied using an analytical and experimental program that resulted in successful correlation of a versatile computer program with test data. The program was used to predict Centaur D-1S LO₂ and LH₂ start basket refilling. Comparisons were made between the baseline Centaur D-1S propellant feed system and feed system alternatives including systems using capillary devices. The preferred concepts from the Centaur D-1S study were examined for APOTV and POTV vehicles for delivery and round trip transfer of payloads between LEO and GEO. Mission profiles were determined to provide propellant usage timelines and the payload partials were defined. A.W.H.

N80-24362* Colorado State Univ., Fort Collins, Dept. Of Mechanical Engineering

INERT GAS THRUSTERS Annual Report
 Harold R. Kaufman and Raymond S. Robinson Nov. 1979
 113 p refs
 (Grant NSG-3011)
 (NASA-CR-159813) Avail: NTIS HC A06/MF A01 CSCL 21C

Inert gas thrusters considered for space propulsion systems were investigated. Electron diffusion across a magnetic field was examined utilizing a basic model. The production of doubly charged ions was correlated using only overall performance parameters. The use of this correlation is therefore possible in the design stage of large gas thrusters, where detailed plasma properties are not available. Argon hollow cathode performance was investigated over a range of emission currents, with the positions of the inert, keeper, and anode varied. A general trend observed was that the maximum ratio of emission to flow rate increased at higher propellant flow rates. It was also found that an enclosed keeper enhances maximum cathode emission at high flow rates. The maximum cathode emission at a given flow rate was associated with a noisy high voltage mode. Although this mode has some similarities to the plume mode found at low flows and emissions, it is encountered by being initially in the spot mode and increasing emission. A detailed analysis of large, inert-gas thruster performance was carried out. For maximum thruster efficiency, the optimum beam diameter increases from less than a meter at under 2000 sec specific impulse to several meters at 10,000 sec. The corresponding range in input power ranges from several kilowatts to megawatts. J.M.S.

N80-27424* Xerox Electro-Optical Systems, Pasadena, Calif.
INERT GAS ION THRUSTER DEVELOPMENT Interim Report, Apr. 1978 - Feb. 1979

William D. Ramsey Mar. 1980 99 p refs
 (Contract NAS3-21345)
 (NASA-CR-159805, XEOS-2372; IR-1) Avail: NTIS
 HC A05/MF A01 CSCL 21C

Two 12 cm magneto-electrostatic containment (MESC) ion thrusters were performance mapped with argon and xenon. The first, hexagonal, thruster produced optimized performance of 48.5 to 79 percent argon mass utilization efficiencies at discharge energies of 240 to 425 eV/ion, respectively. Xenon mass utilization efficiencies of 78 to 95 percent were observed at discharge energies of 220 to 290 eV/ion with the same optimized hexagonal thruster. Changes to the cathode baffle reduced the discharge anode potential during xenon operation from approximately 40 volts to about 30 volts. Preliminary tests conducted with the second, hemispherical, MESC thruster showed a nonuniform anode magnetic field adversely affected thruster performance. This performance degradation was partially overcome by changes in the boundary anode placement. Conclusions drawn from the hemispherical thruster tests gave insights into the plasma processes in the MESC discharge that will aid in the design of future thrusters. Author

N80-30384* Rocketdyne, Canoga Park, Calif.

LEO-TO-GEO LOW THRUST CHEMICAL PROPULSION

J. M. Shoji *In* APL The 1980 JANNAF Propulsion Meeting, Vol 5 Mar. 1980 p 35-51 refs (For primary document see N80-30381 21-20)

(Contract NAS3-21941)

Avail: Issuing Activity CSCL 21H

One approach being considered for transporting large space structures from low Earth orbit (LEO) to geosynchronous equatorial orbit (GEO) is the use of low thrust chemical propulsion systems. A variety of chemical rocket engine cycles evaluated for this application for oxygen/hydrogen and oxygen/hydrocarbon propellants (oxygen/methane and oxygen/RP-1) are discussed. These cycles include conventional propellant turbine drives, turboalternator/electric motor pump drive, and fuel cell/electric motor pump drive as well as pressure fed engines. Thrust chamber cooling analysis results are presented for regenerative/radiation and film/radiation cooling.

J.M.S.

N80-31455* Martin Marietta Corp., Bethesda, Md.

DOD LOW-THRUST MISSION STUDIES

William E Pipes *In* NASA, Lewis Research Center Large Space Systems/Low-Thrust Propulsion Technol. Jul. 1980 p 53-71 (For primary document see N80-31449 22-20) (Contract F04611-79-C-0032)

Avail: NTIS HC A15/MF A01 CSCL 21H

The space transportation system (STS) will be the principal means of launching USAF spacecraft beginning in the 1980's. Since it is manned and reusable it provides new opportunities for unique approaches for cost effective utilization of its capabilities. The STS also places additional requirements and constraints on advanced spacecraft deployment systems that did not previously exist for expandable launch vehicles. To fully utilize these new capabilities designers must be prepared by having cost effective technologies available. Advanced propulsion technology that would provide flexibility, performance, and economic benefits to future Air Force missions was identified. Both electric and chemical propulsion systems are discussed. An LO2/LH2 stage with a torus LO2 tank and 500 lbf pump fed engine is high on the list of propulsion technology.

A.R.H.

N80-31456* General Dynamics Corp., San Diego, Calif.

LOW-THRUST VEHICLES CONCEPT STUDIES

William J. Ketchum *In* NASA, Lewis Research Center Large Space Systems/Low-Thrust Propulsion Technol. Jul. 1980 p 73-96 (For primary document see N80-31449 22-20)

Avail: NTIS HC A15/MF A01 CSCL 21H

Low thrust chemical (hydrogen-oxygen) propulsion systems configured specifically for low acceleration orbit transfer of large space systems were studied in order to provide the required additional data to better compare new, low thrust chemical propulsion systems with other propulsion approaches such as advanced electric systems. Study results indicate that it is cost-effective and least risk to combine the low thrust OTV and stowed spacecraft in a single 65 K shuttle. Mission analysis indicates that there are 25 such missions, starting in 1987. Multiple shuttles (LSS in one, OTV in another) result in a 20% increase in LSS (SBR) diameter over single shuttle launches. Synthesis and optimization of the LSS characteristics and OTV capability resulted in determination of the optimum thrust-to-weight and thrust level. For the space based radar with radial truss arms (center thrust application), the optimum thrust-to-weight (maximum) is 0.1, giving a thrust of 2000 lb. For the annular truss (edge-on thrust application) the structure is not as sensitive, and thrust of 1000 lb appears optimum. For the geoplatform, optimum T/W is .15 (3000 lb thrust). The effects of LSS structure material, weight distribution, and unit area density were evaluated, as were the OTV engine thrust transient and number of burns.

A.R.H.

N80-31457* Aerojet Liquid Rocket Co., Sacramento, Calif.

LOW-THRUST CHEMICAL ROCKET ENGINE STUDY

Joseph A. Mellish *In* NASA, Lewis Research Center Large Space Systems/Low-Thrust Propulsion Technol. Jul. 1980 p 237-261 (For primary document see N80-31449 22-20)

(Contract NAS3-21940)

Avail: NTIS HC A15/MF A01 CSCL 21H

Parametric data and preliminary designs on liquid rocket engines for low thrust cargo orbit-transfer-vehicles are described and those items where technology is required to enhance the designs are identified. The results of film cooling studies to establish the upper chamber pressure limit are given. The study showed that regen cooling with RP-1 was not feasible over the entire thrust and chamber pressure ranges. The thermal data showed that the RP-1 bulk temperature exceeded the study coking temperature limit of 1010 R. Based upon the results presented, O2/H2 and O2/CH4 regen engine systems and O2/H2 film cooled engines were selected for further study in the system analysis. Six engine design concepts are examined.

M.G.

N80-31458* Martin Marietta Corp., Bethesda, Md.

PRIMARY PROPULSION/LARGE SPACE SYSTEM INTER-ACTIONS Progress Report, 20 Sep. 1979 - 20 Sep. 1980

Ralph H. Dergance *In* NASA, Lewis Research Center Large Space Systems/Low-Thrust Propulsion Technol. Jul. 1980 p 107-128 (For primary document see N80-31449 22-20) (Contract NAS3-21955)

Avail: NTIS HC A15/MF A01 CSCL 21H

Three generic types of structural concepts and nonstructural surface densities were selected and combined to represent potential LSS applications. The design characteristics of various classes of large space systems that are impacted by primary propulsion thrust required to effect orbit transfer were identified. The effects of propulsion system thrust-to-mass ratio, thrust transients, and performance on the mass, area, and orbit transfer characteristics of large space systems were determined.

A.R.H.

N80-31459* Boeing Aerospace Co., Seattle, Wash.

AUXILIARY CONTROL OF LSS Progress Report, 28 Aug. 1979 - 27 Nov. 1980

William Smith *In* NASA, Lewis Research Center Large Space Systems/Low-Thrust Propulsion Technol. Jul. 1980 p 129-141 (For primary document see N80-31449 22-20) (Contract NAS3-21952)

Avail: NTIS HC A15/MF A01 CSCL 21H

Seven classes of large space structures were identified and idealized into simple geometric shapes which could be easily modelled. Scaling laws were generated which allowed the seven ideal structures to be continuously scaled as to size and mass properties over their respective size ranges. Relevant sources of disturbances were determined and their effects on LSS were compared. These disturbances were applied over the range of scaling parameters to generate control force and torque requirements. Important auxiliary propulsion system (APS) characteristics were identified and an APS characteristic sensitivity matrix was established.

A.R.H.

N80-31460* Rockwell International Corp., Pittsburgh, Pa.

LOW-THRUST CHEMICAL PROPULSION

James M. Shoji *In* NASA, Lewis Research Center Large Space Systems/Low-Thrust Propulsion Technol. Jul. 1980 p 263-286 (For primary document see N80-31449 22-20)

Avail: NTIS HC A15/MF A01 CSCL 21H

Results from investigations leading to the definition of low thrust chemical engine concepts are described. From the thrust chamber cooling analyses, regenerative/radiation-cooled LO2/H2 thrust chambers offered the largest thrust and chamber pressure operational envelope primarily due to the superior cooling capability of hydrogen and its low critical pressure. Regenerative/radiation-cooled LO2/CH4 offered the next largest operational envelope. The maximum chamber pressure for film/radiation-cooling was significantly lower than for regenerative/radiation-cooling. As in regeneration-cooling, LO2/H2 thrust chambers achieved the highest maximum chamber pressure. LO2/CH4 film/radiation-cooling was found not feasible and LO2/RP-1 film/radiation-cooling was extremely limited. In the engine cycle/configuration evaluation, the engine cycle matrix was defined through the incorporation of the heat transfer results. Engine cycle limits were established with the fuel-cell power cycle achieving the highest chamber pressure; however, the fuel cell

system weights were excessive. The staged combustion cycle achieved the next highest chamber pressure but the preburner operational feasibility was in question. M G

N80-31469* Martin Marietta Corp., Bethesda, Md.
LOW-THRUST CHEMICAL ORBIT TO ORBIT PROPULSION SYSTEM PROPELLANT MANAGEMENT STUDY Progress Report, 14 Sep. 1979 - 14 Nov. 1980
Ralph H. Dergance / In NASA Lewis Research Center Large Space Systems/Low-Thrust Propulsion Technol. Jul 1980 p 287-310 refs (For primary document see N80-31449 22-20) (Contract NAS3-21954)
Avail NTIS HC A15/MF A01 CSCL 21H

Propellant requirements, tankage configurations, preferred propellant management techniques, propulsion systems weights, and technology deficiencies for low thrust expendable propulsion systems are examined. A computer program was utilized which provided a complete propellant inventory (including boil-off for cryogenic cases), pressurant and propellant tank dimensions for a given ullage, pressurant requirements, insulation requirements, and miscellaneous masses. The output also includes the masses of all tanks, the mass of the insulation, engines and other components, total wet system and burnout mass; system mass fraction; total impulse and burn time. M G

N80-31470* Rockwell International Corp., Pittsburgh, Pa.
SOLAR ROCKET SYSTEM CONCEPT ANALYSIS Final Report
Jack A. Boddy / In NASA Lewis Research Center Large Space Systems/Low-Thrust Propulsion Technol. Jul 1980 p 311-336 (For primary document see N80-31449 22-20) (Contract F04611-79-C-0007)
Avail NTIS HC A15/MF A01 CSCL 21H

The use of solar energy to heat propellant for application to Earth orbital/planetary propulsion systems is of interest because of its performance capabilities. The achievable specific impulse values are approximately double those delivered by a chemical rocket system, and the thrust is at least an order of magnitude greater than that produced by a mercury bombardment ion propulsion thruster. The primary advantage the solar heater thruster has over a mercury ion bombardment system is that its significantly higher thrust permits a marked reduction in mission trip time. The development of the space transportation system, offers the opportunity to utilize the full performance potential of the solar rocket. The requirements for transfer from low Earth orbit (LEO) to geosynchronous equatorial orbit (GEO) was examined as the return trip, GEO to LEO, both with and without payload. Payload weights considered ranged from 2000 to 100,000 pounds. The performance of the solar rocket was compared with that provided by LO2-LH2, N2O4-MMH, and mercury ion bombardment systems. A.R.H.

N80-33474* Air Force Aero Propulsion Lab., Wright-Patterson AFB, Ohio
STATUS OF NICKEL-HYDROGEN CELL TECHNOLOGY
Don R. Warnock / In NASA Lewis Space Flight Center Synchronous Energy Technol. Sep. 1980 p 97-105 (For primary document see N80-33465 24-20)
Avail NTIS HC A07/MF A01 CSCL 10C

Nickel hydrogen cell technology has been developed which solves the problems of thermal management, oxygen management, electrolyte management, and electrical and mechanical design peculiar to this new type of battery. This technology was weight optimized for low orbit operation using computer modeling programs but is near optimum for other orbits. Cells ranging in capacity up to about 70 ampere-hours can be made from components of a single standard size and are available from two manufacturers. The knowledge gained is now being applied to the development of two extensions to the basic design: a second set of larger standard components that will cover the capacity range up to 150 ampere-hours; and the development of multicell common pressure vessel modules to reduce volume, cost and weight. A manufacturing technology program is planned to optimize the producibility of the cell design and reduce cost. The most important areas for further improvement are life and

reliability which are governed by electrode and separator technology. A.R.H.

N80-33476* Colorado State Univ., Fort Collins Dept. of Mechanical Engineering
BAFFLE APERTURE DESIGN STUDY OF HOLLOW CATHODE EQUIPPED ION THRUSTERS M.S. Thesis Technical Report, 1 Dec. 1979 - 1 Oct. 1980
John R. Brophy, Jr. and Paul J. Wilbur Oct 1980 78 p refs (Grant NGR-06-002-112)
(NASA-CR 165164) Avail NTIS HC A05/MF A01 CSCL 21C

A simple theoretical model which can be used as an aid in the design of the baffle aperture region of a hollow cathode equipped ion thruster was developed. An analysis of the ion and electron currents in both the main and cathode discharge chambers is presented. From this analysis a model of current flow through the aperture, which is required as an input to the design model, was developed. This model was verified experimentally. The dominant force driving electrons through the aperture was the force due to the electrical potential gradient. The diffusion process was modeled according to the Boltzmann diffusion theory. A number of simplifications were made to limit the amount of detailed plasma information required as input to the model to facilitate the use of the model in thruster design. This simplified model gave remarkably consistent results with experimental results obtained with a given thruster geometry over substantial changes in operating conditions. The model was uncertain to about a factor of two for different thruster cathode region geometries. The design usefulness was limited by this factor of two uncertainty and by the accuracy to which the plasma parameters required as inputs to the model were specified. T.M.

A80-13311 * 8-cm Engineering Model Thruster technology. A review of recent developments. W. S. Williamson, C. R. Dulgoff, R. L. Williams (Hughes Research Laboratories, Malibu, Calif.), and J. R. Bayless (U.S. Defense Advanced Research Projects Agency, Washington, D.C.). Princeton University, AIAA, and DGLR, International Electric Propulsion Conference, 14th, Princeton, N.J., Oct. 30-Nov. 1, 1979, AIAA Paper 79-2103. 9 p. 5 refs. Contract No. NAS3-21358.

Recent testing of the NASA Lewis Research Center/Hughes 8-cm Engineering Model Thruster (EMT) and Power Processing Unit has centered on two primary areas of investigation: integration of porous-tungsten dispenser-type cathode inserts into the thruster (replacing previous inserts of rolled-tantalum-foil design) and characterization of thruster operation with the new inserts. Characterization testing of the EMT and of the new cathodes has demonstrated acceptable thruster performance and cathode ignition parameters; the only perceived change in thruster performance has been that a small amount of cathode heater power is required to maintain nominal keeper voltages. Thermal modeling of the cathode structures has facilitated design revisions which reduce this power requirement. (Author)

A80-20962 * A model for predicting the wearout lifetime of the LeRC/Hughes 30-cm mercury ion thruster. J. R. Beattie (Hughes Research Laboratories, Malibu, Calif.). Princeton University, AIAA, and DGLR, International Electric Propulsion Conference, 14th, Princeton, N.J., Oct. 30-Nov. 1, 1979, AIAA Paper 79-2079. 16 p. 23 refs. Contract No. NAS3-21040.

An investigation of parameters that affect the erosion rates of 30-cm-diameter mercury-ion-thruster components is described. A sputter-erosion model is formulated in terms of the design, operational, and material characteristics of the thruster. The erosion model is applied to the screen electrode, which is assumed to be the life-limiting component of the 30-cm thruster, resulting in a model of wearout lifetime. Results of short-term erosion-rate tests are presented that illustrate the dependence of component wear rates on variables such as discharge voltage, accelerator-grid open-area fraction, ion energy, electrode material, and the partial pressure of

facility residual gases such as nitrogen. Test results are compared with wearout rates predicted by the sputter-erosion model. (Author)

A80-23941 * # Computation of three-dimensional viscous supersonic flow in inlets. R. C. Buggeln, H. McDonald, J. P. Kreskovsky, and R. Levy (Scientific Research Associates, Inc., Glastonbury, Conn.). *American Institute of Aeronautics and Astronautics, Aerospace Sciences Meeting, 18th, Pasadena, Calif., Jan. 14-16, 1980, Paper 80-0194*. 12 p. 30 refs. Contract No. NAS3-21003.

A new approach has been developed for the computation of the three-dimensional viscous supersonic flow with embedded subsonic regions adjacent to solid boundaries and is applied to a mixed-compression supersonic inlet typical of current designs. The approach uses a reduced form of the three-dimensional Navier-Stokes equations so that the resultant equations can be treated as an initial boundary value problem and thus be solved by non-iterative forward marching in space. The numerical procedure utilizes an efficient consistently-split linearized block implicit technique to solve the finite difference analogues to the set of governing partial differential equations. (Author)

A80-46301 * # Torquing and electrostatic deformation of the solar sail. R. E. LaQuey (Maya Development Corp., San Diego, Calif.), S. E. DeForest, and M. Douglas. In: *Space systems and their interactions with earth's space environment*. (A80-46879 20-18) New York, American Institute of Aeronautics and Astronautics, Inc., 1980, p. 662-679, Contract No. NAS3-20119.

The impact of natural sources of electrical-mechanical oscillations induced by the environment on the solar sail system is evaluated. The study indicates that, to the level of accuracy (first order) of the analysis, none of the natural sources studied, which range from plasma wave interactions to $E \times B$ forces, will have a significant impact on the proposed solar sail design. The study is not intended as an exhaustive analysis, and further analysis, particularly in the area of artificially induced oscillations, is needed. (Author)

A80-48265 * # Power processing technology for spacecraft primary ion propulsion. J. J. Biess, L. Y. Inouye (TRW Defense and Space Systems Group, Redondo Beach, Calif.), and R. J. Frye (NASA, Lewis Research Center, Cleveland, Ohio). In: *Energy to the 21st century; Proceedings of the Fifteenth Intersociety Energy Conversion Engineering Conference, Seattle, Wash., August 18-22, 1980. Volume 1*. (A80-48165 21-44) New York, American Institute of Aeronautics and Astronautics, Inc., 1980, p. 782-787. 13 refs. Contracts No. NAS12-2183; No. NAS3-14383; No. NAS3-18924; No. NAS3-20403; No. NAS3-21372; No. NAS3-21746.

Advanced technologies developed in support of Ion Propulsion power processing, including the power circuitry portion of the Series L-C Resonant Inverter, Beam Supply, power components, packaging and heat pipe cooling of the 30 cm Ion Engine Power Processor are described. Both the transistorized and SCR versions of the Series L-C Resonant Inverter Beam Supply are discussed. A BIMOD Ion Thruster/Power Processor Prototype Assembly is undergoing environmental and life testing. These advanced technologies can be applied advantageously to other applications of future high power space power processing equipment. (Author)

A80-48356 * # Design, performance and life cycle cost relationships for a 500kW space solar array. P. W. Richardson, F. Q. Miller, and M. N. White (PRC Systems Services Co., Huntsville, Ala.). In: *Energy to the 21st century; Proceedings of the Fifteenth Intersociety Energy Conversion Engineering Conference, Seattle, Wash., August 18-22, 1980. Volume 2*. (A80-48165 21-44) New York, American Institute of Aeronautics and Astronautics, Inc., 1980, p. 1396-1400. Contract No. NAS3-21926.

The effects on life cycle costs of a number of technology areas

are examined for a LEO, 500kW space solar array. A baseline system conceptual design is developed and the life cycle costs estimated in detail. The baseline system requirements and design technologies are then varied and their relationships to life cycle costs quantified. For example, the thermal characteristics of the baseline design are determined by the array materials and masses. The thermal characteristics in turn determine configuration, performance and hence life cycle cost. (Author)

23 CHEMISTRY AND MATERIALS (GENERAL)

Includes biochemistry and organic chemistry.

different response with no MNGC's formation, minimal to no capsule formation, and sample coverage by a uniform cell layer.
R.C.T.

A80-25900 * " Investigation into the effect of plasma pre-treatment on the adhesion of parylene to various substrates. T. Riley, T. C. Mahuson, and K. Seibert (NASA, Lewis Research Center, Cleveland, Ohio). *Society for the Advancement of Material and Process Engineering, Seminar on Cleaning, Finishing and Coating Processes, Los Angeles, Calif., Feb. 5, 6, 1980, Paper.* 18 p. 13 refs.

An experimental effort has been undertaken to examine the effect of plasma pretreatment of various substrate materials coated with a polymer in the parylene family. This report describes the procedure and discusses initial data which indicate using plasmas of argon and oxygen to promote adhesion of parylene coatings upon many difficult-to-bond substrates. Substrates investigated were gold, nickel, kovar, teflon (FEP), kapton, silicon, tantalum, titanium, and tungsten. Without plasma treatment, 180 deg peel tests yield a few g/cm (oz/in) strengths. With dc plasma treatment in the deposition chamber, followed by coating, peel strengths are increased by one to two orders of magnitude. (Author)

A80-28894 * Modeling and analysis of Power Processing Systems. Y. Yu (TRW Defense and Space Systems Group, Redondo Beach, Calif.), F. C. Y. Lee (Virginia Polytechnic Institute and State University, Blacksburg, Va.), and J. Kolecki (NASA, Lewis Research Center, Cleveland, Ohio). In: PESC '79; Power Electronics Specialists Conference, San Diego, Calif., June 18-22, 1979, Record. (A80-28892 10-33) Piscataway, N.J., Institute of Electrical and Electronics Engineers, Inc., 1979, p. 11-24, 20 refs, Contract No. NAS3-19690.

The paper deals with a NASA-sponsored, computer-based program - Modeling and Analysis of Power Processing Systems (MAPPS). Three major MAPPS subprograms, Design Optimization, Control Design, and Performance Analysis are considered. The program makes it possible to reduce the design, analysis, and development time, and thus the cost, in achieving the required performance for power processing equipment and systems. V.T.

N80-33478*# Applied Medical Technology, Cleveland Heights, Ohio

TISSUE RESPONSE TO PERITONEAL IMPLANTS Final Report

George J. Picha Jun. 1980 73 p refs
(NASA Order C-33350-D)

(NASA-CR-159817) Avail. NTIS HC A04/MF A01 CSCL 06P

Peritoneal implants were fabricated from poly 2-OH, ethyl methacrylate (HEMA), polyetherurethane (polytetramethylene glycol 1000 MW, 1,4 methylene diisocyanate, and ethyl diamine), and untreated and sputter treated polytetrafluoroethylene (PTFE). The sputter treated PTFE implants were produced by an 8 cm diameter argon ion source. The treated samples consisted of ion beam sputter polished samples, sputter etched samples (to produce a microscopic surface cone texture) and surface pitted samples (produced by ion beam sputtering to result in 50 microns wide by 100 microns deep square pits). These materials were implanted in rats for periods ranging from 30 minutes to 14 days. The results were evaluated with regard to cell type and attachment kinetics onto the different materials. Scanning electron microscopy and histological sections were also evaluated. In general the smooth hydrophobic surfaces attracted less cells than the ion etched PTFE or the HEMA samples. The ion etching was observed to enhance cell attachment, multinucleated giant cell (MNGC) formation, cell to cell contact, and fibrous capsule formation. The cell responded in the case of ion etched PTFE to an altered surface morphology. However, equally interesting was the similar attachment kinetics of HEMA verses the ion etched PTFE. However, HEMA resulted in a markedly

24 COMPOSITE MATERIALS

Includes laminates.

N80-11142* National Aeronautics and Space Administration. Lewis Research Center, Cleveland, Ohio.

CORROSION RESISTANT THERMAL BARRIER COATING Patent Application

S. R. Levine, R. A. Miller, and P. E. Hodge, inventors (to NASA) Filed 31 Oct. 1979 8 p (NASA-Case-LEW-13088-1; US-Patent-Appl-SN-089779) Avail: NTIS HC A02/MF A01 CSCL 11D

A thermal barrier coating system was developed to protect the surfaces of metal components, gas turbines, and other heat engine parts that are exposed to fuels contaminated with metallic impurities which are normally corrosive to previously known metallic coatings. The coating system includes a metal alloy bond coating, the alloy containing nickel, cobalt, iron, or a combination of these metals. The system also includes a corrosion resistant thermal barrier oxide coating containing at least one alkaline earth silicate. The preferred oxides are calcium silicate, barium silicate, magnesium silicate, or a combination of these silicates.

NASA

N80-11143* National Aeronautics and Space Administration. Lewis Research Center, Cleveland, Ohio.

MICROMECHANICS OF INTRAPLY HYBRID COMPOSITES: ELASTIC AND THERMAL PROPERTIES

C. C. Chamis and J. H. Sinclair Washington 1979 19 p refs Presented at the Winter Ann. Meeting of the Am. Soc. of Mech. Engr., New York, 2-7 Dec. 1979 (NASA-TM-79253; E-164) Avail: NTIS HC A02/MF A01 CSCL 11D

Composite micromechanics are used to derive equations for predicting the elastic and thermal properties of unidirectional intraply hybrid composites. The results predicted using these equations are compared with those predicted using approximate equations based on the rule of mixtures, linear laminate theory, finite element analysis and limited experimental data. The comparisons for three different intraply hybrids indicate that all four methods predict approximately the same elastic properties and are in good agreement with measured data. The micromechanics equations and linear laminate theory predict about the same values for thermal expansion coefficients. The micromechanics equations predict through-the-thickness properties which are in good agreement with the finite element results.

Author

N80-11144* National Aeronautics and Space Administration. Lewis Research Center, Cleveland, Ohio.

TENSILE AND FLEXURAL STRENGTH OF NON-GRAPHITIC SUPERHYBRID COMPOSITES: PREDICTIONS AND COMPARISONS

C. C. Chamis, J. H. Sinclair, and R. F. Lark 1979 27 p refs Presented at 11th Natl. Tech. Conf., Boston, Mass., 13-15 Nov. 1979; sponsored by Soc. for the Advancement of Material and Process Engr. (NASA-TM-79276; E-203) Avail: NTIS HC A03/MF A01 CSCL 11D

Equations are presented and described which can be used to predict bounds on the tensile and flexural strengths of nongraphitic superhybrid (NGSH) composites. These equations are derived by taking into account the measured stress-strain behavior, the lamination residual stresses and the sequence of events leading to fracture. The required input for using these equations includes constituents, properties (elastic and strength), NGSH elastic properties, cure temperature, and ply stress influence coefficients. Results predicted by these equations are in reasonably good agreement with measured data for strength and for the apparent knees in the nonlinear stress-strain curve. The lower bound values are conservative compared to measured data. These equations are relatively simple and are suitable for use in the preliminary design and initial sizing of structural components made from NGSH composites.

Author

N80-11145* National Aeronautics and Space Administration. Lewis Research Center, Cleveland, Ohio.

DYNAMIC RESPONSE OF DAMAGED ANGLEPLYED FIBER COMPOSITES

C. C. Chamis, J. H. Sinclair, and R. F. Lark 1979 17 p refs Presented at the Winter Ann. Meeting of the Am. Soc. of Mech. Engr., New York, 2-7 Dec. 1979 (NASA-TM-79281; E-182) Avail: NTIS HC A02/MF A01 CSCL 11D

The effects of low level damage induced by monotonic load, cyclic load and/or residual stresses on the vibration frequencies and damping factors of fiber composite angleplied laminates were investigated. Two different composite systems were studied - low modulus fiber and ultra high modulus fiber composites. The results obtained show that the frequencies and damping factors of angleplied laminates made from low modulus fiber composites are sensitive to low level damage while those made from ultra high modulus composites are not. Vibration tests may not be sufficiently sensitive to assess concentrated local damage in angleplied laminates. Dynamic response determined from low-velocity impact coupled with the Fast Fourier Transform and packaged in a minicomputer can be a convenient procedure for assessing low-level damage.

A.R.H.

N80-12120* National Aeronautics and Space Administration. Lewis Research Center, Cleveland, Ohio.

MECHANICAL PROPERTY CHARACTERIZATION OF INTRAPLY HYBRID COMPOSITES

C. C. Chamis, R. F. Lark, and J. H. Sinclair 1979 26 p refs Presented at the Am. Soc. for Testing and Materials Symp., Dearborn, Mich., 2-3 Oct. 1979 (NASA-TM-79306; E-261) Avail: NTIS HC A03/MF A01 CSCL 11D

An investigation was conducted to characterize the mechanical properties of intraply hybrids made from graphite fiber/epoxy matrix (primary composites) hybridized with varying amounts of secondary composites made from S-glass or Kevlar 49 fibers. The tests were conducted using thin laminates having the same thickness. The specimens for these tests were instrumented with strain gages to determine stress-strain behavior. Significant results are included.

R.C.T.

N80-13171* National Aeronautics and Space Administration. Lewis Research Center, Cleveland, Ohio.

IMPROVED FIBER RETENTION BY THE USE OF FILLERS IN GRAPHITE FIBER/RESIN MATRIX COMPOSITES

R. E. Gluyas and K. J. Bowles 1980 12 p refs Proposed for presentation at the 35th Ann. Conf. of the Reinforced Plastics/Composites Inst., New Orleans, 4-8 Feb. 1980; sponsored by Soc. of Plastics Ind. (NASA-TM-79288; E-231) Avail: NTIS HC A02/MF A01 CSCL 11D

A variety of matrix fillers were tested for their ability to prevent loss of fiber from graphite fiber/PMR polyimide and graphite fiber/epoxy composites in a fire. The fillers tested included powders of boron, boron carbide lime glass, lead glass, and aluminum. Boron was the most effective and prevented any loss of graphite fiber during burning. Mechanical properties of composites containing boron filler were measured and compared to those of composites containing no filler.

K.L.

N80-14196* National Aeronautics and Space Administration. Lewis Research Center, Cleveland, Ohio.

BURNING CHARACTERISTICS AND FIBER RETENTION OF GRAPHITE/RESIN MATRIX COMPOSITES

Kenneth J. Bowles 8 Feb. 1980 14 p refs Proposed for Presentation at the 35th Ann. Conf. of the Reinforced Plastics/Composites Inst., New Orleans, 4-8 Feb. 1980; sponsored by Soc. of Plastics Ind. (NASA-TM-79314; E-271) Avail: NTIS HC A02/MF A01 CSCL 11D

Graphite fiber reinforced resin matrix composites were subjected to controlled burning conditions to determine their burning characteristics and fiber retention properties. Small samples were

burned with a natural gas fired torch to study the effects of fiber orientation and structural flaws such as holes and slits that were machined into the laminates. Larger laminate samples were burned in a modified heat release rate calorimeter. Unidirectional epoxy/graphite and polyimide/graphite composites and boron powder filled samples of each of the two composite systems were burn tested. The composites were exposed to a thermal radiation of 5.3 Btu/sq ft-sec in air. Samples of each of the unfilled composite were decomposed anaerobically in the calorimeter. Weight loss data were recorded for burning and decomposition times up to thirty-five minutes. The effects of fiber orientation, flaws, and boron filler additives to the resins were evaluated. A high char forming polyimide resin was no more effective in retaining graphite fibers than a low char forming epoxy resin when burned in air. Boron powder additions to both the polyimide and the epoxy resins stabilized the chars and effectively controlled the fiber release. A.R.H.

N80-16102* National Aeronautics and Space Administration
Lewis Research Center, Cleveland, Ohio.
**FRACTURE MODES OF HIGH MODULUS GRAPHITE/
EPOXY ANGLEPLIED LAMINATES SUBJECTED TO OFF-
AXIS TENSILE LOADS**

J. H. Sinclair 1980 22 p refs Presented at 35th Ann. Conf. of the Reinforced Plastics/Composites Inst., New Orleans, 4-8 Feb. 1980, sponsored by Soc. of Plastics Ind. (NASA-TM-81405, E-319) Avail. NTIS HC A02/MF A01 CSCL 11D

Angleplied laminates of high modulus graphite fiber/epoxy were studied in several ply configurations at various tensile loading angles to the zero ply direction in order to determine the effects of ply orientations on tensile properties, fracture modes, and fracture surface characteristics of the various plies. It was found that fracture modes in the plies of angleplied laminates can be characterized by scanning electron microscope observation. The characteristics for a given fracture mode are similar to those for the same fracture mode in unidirectional specimens. However, no simple load angle range can be associated with a given fracture mode. Author

N80-16107* National Aeronautics and Space Administration
Lewis Research Center, Cleveland, Ohio.
**PREDICTION OF FIBER COMPOSITE MECHANICAL
BEHAVIOR MADE SIMPLE**

C. C. Chamis 1980 26 p refs Presented at the 35th Ann. Conf. of the Reinforced Plastics/Composites Inst., New Orleans, 4-8 Feb. 1980; sponsored by the Soc. of Plastics Ind. (NASA-TM-81404; E-331) Avail. NTIS HC A03/MF A01 CSCL 11D

The elastic properties and failure stresses of angleplied fiber composite laminates were determined using a pocket calculator. The procedure uses simple equations and appropriate graphs of elastic properties versus angle plies, and can handle all types of fiber composites including hybrids. The versatility and generality of the method is illustrated in several step-by-step numerical examples. A.R.H.

N80-16106* National Aeronautics and Space Administration.
Lewis Research Center, Cleveland, Ohio.
**APPLICATION OF COMPOSITE MATERIALS TO TURBOFAN
ENGINE FAN EXIT GUIDE VANES**

G. T. Smith 1980 19 p refs Presented at 35th Ann. Conf. of the Reinforced Plastics/Composite Inst., New Orleans, 4-8 Feb. 1980; sponsored by Soc. of Plastics Industries (NASA-TM-81432; E-356) Avail. NTIS HC A02/MF A01 CSCL 11D

A program was conducted by NASA with the JT9D engine manufacturer to develop a lightweight, cost effective, composite material fan exit guide vane design having satisfactory structural durability for commercial engine use. Based on the results of a previous company supported program, eight graphite/epoxy and graphite-glass/epoxy guide vane designs were evaluated and four were selected for fabrication and testing. Two commercial fabricators each fabricated 13 vanes. Fatigue tests were used to qualify the selected design configurations under nominally

dry, 38 C (100 F) and fully wet and 60 C (140 F) environmental conditions. Cost estimates for a production rate of 1000 vanes per month ranged from 1.7 to 2.6 times the cost of an all aluminum vane. This cost is 50 to 80 percent less than the initial program target cost ratio which was 3 times the cost of an aluminum vane. Application to the JT9D commercial engine is projected to provide a weight savings of 236 N (53 lb) per engine. Author

N80-18107* National Aeronautics and Space Administration.
Lewis Research Center, Cleveland, Ohio.
**FIRE TEST METHOD FOR GRAPHITE FIBER REINFORCED
PLASTICS**

Kenneth J. Bowles 1980 13 p refs Presented at 5th Intern. Conf. on Fire Safety, Millbrae, Calif., 14-18 Jan. 1980 (NASA-TM-81436; E-360) Avail. NTIS HC A02/MF A01 CSCL 11D

A potential problem in the use of graphite fiber reinforced resin matrix composites is the dispersal of graphite fibers during accidental fires. Airborne, electrically conductive fibers originating from the burning composites could enter and cause shorting in electrical equipment located in surrounding areas. A test method for assessing the burning characteristics of graphite fiber reinforced composites and the effectiveness of the composites in retaining the graphite fibers has been developed. The method utilizes a modified rate of heat release apparatus. The equipment and the testing procedure are described. The application of the test method to the assessment of composite materials is illustrated for two resin matrix/graphite composite systems. A.R.H.

N80-20313* National Aeronautics and Space Administration.
Lewis Research Center, Cleveland, Ohio.
**DYNAMIC MODULUS AND DAMPING OF BORON, SILICON
CARBIDE, AND ALUMINA FIBERS**

J. A. DiCarlo and W. Williams [1980] 44 p refs Presented at the 4th Ann. Conf. on Composites and Advanced Mater., Cocoa Beach, Fla. 20-24 Jan. 1980; sponsored by the Am. (NASA-TM-81422; E-345) Avail. NTIS HC A03/MF A01 CSCL 11D

The dynamic modulus and damping capacity for boron, silicon carbide, and silicon carbide coated boron fibers were measured from -190 to 800 C. The single fiber vibration test also allowed measurement of transverse thermal conductivity for the silicon carbide fibers. Temperature dependent damping capacity data for alumina fibers were calculated from axial damping results for alumina-aluminum composites. The dynamics fiber data indicate essentially elastic behavior for both the silicon carbide and alumina fibers. In contrast, the boron based fibers are strongly anelastic, displaying frequency dependent moduli and very high microstructural damping. The single fiber damping results were compared with composite damping data in order to investigate the practical and basic effects of employing the four fiber types as reinforcement for aluminum and titanium matrices. K.L.

N80-20314* National Aeronautics and Space Administration.
Lewis Research Center, Cleveland, Ohio.
**CALCULATION OF RESIDUAL PRINCIPAL STRESSES IN
CVD BORON ON CARBON FILAMENTS**

Donald R. Behrendt [1980] 15 p refs Prepared for the 4th Ann. Conf. on Composites and Advanced Mater., Cocoa Beach, Fla., 21-24 Jan. 1980; sponsored by the Am. Ceram. Soc. (NASA-TM-81456; E-386) Avail. NTIS HC A02/MF A01 CSCL 11D

A three-dimensional finite element model of the chemical vapor deposition of boron on a carbon substrate (B/C) is developed. The model includes an expansion of the boron after deposition due to atomic rearrangement and includes creep of the boron and carbon. Curves are presented showing the variation of the principal residual stresses and the filament elongation with the parameters defining deposition strain and creep. The calculated results are compared with experimental axial residual stress and elongation measurements made on B/C filaments. For good agreement between calculated and experimental results, the deposited boron must continue to expand after deposition,

and the build up of residual stresses must be limited by significant boron and carbon creep rates. K.L.

N80-21452* National Aeronautics and Space Administration. Lewis Research Center, Cleveland, Ohio.

PREDICTING THE TIME-TEMPERATURE DEPENDENT AXIAL FAILURE OF B/A1 COMPOSITES

James A. DiCarlo 1980 28 p refs Presented at Symp. on Failure Modes in Composites, Las Vegas, Nev., 25-26 Feb. 1980, sponsored by Metallurgical Soc. of the Am. Inst. of Mining, Metallurgical and Petroleum Engr. (NASA-TM-81474; E-408) Avail: NTIS HC A03/MF A01 CSCL 11D

Experimental and theoretical studies were conducted in order to understand and predict the effects of time, temperature, and stress on the axial failure modes of boron fibers and B/A1 composites. Due to the anelastic nature of boron fiber deformation, it was possible to determine simple creep functions which can be employed to accurately describe creep and fracture stress of as-produced fibers. Analysis of damping and strength data for B/6061 Al composites indicates that fiber creep effects of creep on fiber fracture are measurably reduced by the composite fabrication process. The creep function appropriate for fibers with B/A1 composites was also determined. A fracture theory is presented for predicting the time-temperature dependence of the axial tensile strength for metal matrix composites in general and B/A1 composites in particular. Author

N80-23370* National Aeronautics and Space Administration. Lewis Research Center, Cleveland, Ohio.

ENGINE ENVIRONMENTAL EFFECTS ON COMPOSITE BEHAVIOR

C. C. Chamis and G. T. Smith 1980 20 p refs Presented at the 21st Struct., Structural Dyn. and Mater. Conf., Seattle, 12-14 May 1980; sponsored by AIAA, ASME, ASCE, and AHS (NASA-TM-81508; E-446) Avail: NTIS HC A02/MF A01 CSCL 11D

A series of programs were conducted to investigate and develop the application of composite materials to turbojet engines. A significant part of that effort was directed to establishing the impact resistance and defect growth characteristics of composite materials over the wide range of environmental conditions found in commercial turbojet engine operations. Both analytical and empirical efforts were involved. The experimental programs and the analytical methodology development as well as an evaluation program for the use of composite materials as fan exit guide vanes are summarized. R.C.T.

N80-26389* National Aeronautics and Space Administration. Lewis Research Center, Cleveland, Ohio.

A SILICON-SLURRY/ALUMINIDE COATING Patent Application

D. L. Deadmore and S. G. Young, inventors (to NASA) Filed 20 Jun. 1980 11 p (NASA-Case-LEW-13343-1; US-Patent-Appl-SN-161254) Avail: NTIS HC A02/MF A01 CSCL 11D

A low cost coating is disclosed which protects metallic base system substrates from high temperatures, high gas velocity oxidation, thermal fatigue and hot corrosion. The coating is particularly useful for protecting vanes and blades in aircraft and land based gas turbine engines. A lacquer slurry comprising cellulose nitrate containing high purity silicon powder is sprayed onto the superalloy substrates. The silicon layer is then aluminized to complete the coating. The Si-Al coating is less costly to produce than advanced aluminides and protects the substrate from oxidation and thermal fatigue for a much longer period of time than the conventional aluminide coatings. While more expensive Pt-Al coatings and physical vapor deposited MCrAlY coatings on certain superalloys in high gas velocity oxidation and thermal fatigue. Also, the Si-Al coating increased the resistance of certain superalloys to hot corrosion. NASA

N80-27429* National Aeronautics and Space Administration.

Lewis Research Center, Cleveland, Ohio.

FEASIBILITY OF KEVLAR 49/PMR-15 POLYIMIDE FOR HIGH TEMPERATURE APPLICATIONS

Morgan P. Hanson 1980 16 p refs Proposed for presentation at the 12th Natl. SAMPE Tech. Conf., Seattle, 7-9 Oct. 1980 (NASA-TM-81560; E-521) Avail: NTIS HC A02/MF A01 CSCL 11D

Kevlar 49 aramid organic fiber reinforced PMR-15 polyimide laminates were characterized to determine the applicability of the material to high temperature aerospace structures. Kevlar 49/3501-6 epoxy laminates were fabricated and characterized for comparison with the Kevlar 49/PMR-15 polyimide material. Flexural strengths and moduli and interlaminar shear strengths were determined from 75 F to 600 F for the PMR-15 and from 75 F to 450 F for the Kevlar/3501-6 epoxy material. The effects of hydrothermal and long-term elevated temperature exposures on the flexural strengths and moduli and the interlaminar shear strengths were also studied. Author

N80-28444* National Aeronautics and Space Administration. Lewis Research Center, Cleveland, Ohio.

PROPERTIES OF PMR POLYIMIDE COMPOSITES MADE WITH IMPROVED HIGH STRENGTH GRAPHITE FIBERS

Raymond D. Vannucci 1980 18 p refs Proposed for presentation at 12th Natl. SAMPE Tech. Conf., Seattle, 7-9 Oct. 1980 (NASA-TM-81557; E-518) Avail: NTIS HC A02/MF A01 CSCL 11D

High strength, intermediate modulus graphite fibers were obtained from various commercial suppliers, and were used to fabricate PMR-15 and PMR-2 polyimide composites. The effects of the improved high strength graphite fibers on composite properties after exposure in air at 600 F were investigated. Two of the improved fibers were found to have an adverse effect on the long term performance of PMR composites. The influence of various factors such as fiber physical properties, surface morphology and chemical composition were also examined. R.C.T.

N80-29431* National Aeronautics and Space Administration. Lewis Research Center, Cleveland, Ohio.

POTENTIAL RELEASE OF FIBERS FROM BURNING CARBON COMPOSITES

Vernon L. Bell Jul. 1980 52 p refs (NASA-TM-80214) Avail: NTIS HC A04/MF A01 CSCL 11D

A comprehensive experimental carbon fiber source program was conducted to determine the potential for the release of conductive carbon fibers from burning composites. Laboratory testing determined the relative importance of several parameters influencing the amounts of single fibers released, while large-scale aviation jet fuel pool fires provided realistic confirmation of the laboratory data. The dimensions and size distributions of fire-released carbon fibers were determined, not only for those of concern in an electrical sense, but also for those of potential interest from a health and environmental standpoint. Fire plume and chemistry studies were performed with large pool fires to provide an experimental input into an analytical modeling of simulated aircraft crash fires. A study of a high voltage spark system resulted in a promising device for the detection, counting, and sizing of electrically conductive fibers, for both active and passive modes of operation. Author

N80-29433* National Aeronautics and Space Administration. Lewis Research Center, Cleveland, Ohio.

INFLUENCE OF EXCESS DIAMINE ON PROPERTIES OF PMR POLYIMIDE RESINS AND COMPOSITES

Francis I. Hurwitz 1980 15 p refs Proposed for presentation at 12th Natl. SAMPE Tech. Conf., Seattle, 7-9 Oct. 1980 (NASA-TM-81580; E-550) Avail: NTIS HC A02/MF A01 CSCL 11D

By varying the stoichiometry of the reactants in the preparation of PMR polyimide resin, changes occur in molecular weight distribution which influence the rheological properties and thus the processability of the resin, as well as the mechanical properties of the composite. The influence of 1-10 percent molar

excess MDA on the molecular weight distribution and rheological properties of an imidized PMR system were exposed. Molecular weight distribution is characterized by gel permeation chromatography of the imidized molding compound, shear viscosity is related to changes in average molecular weight. The thermo-oxidative stability at 600 F, glass transition temperature, flexural and interlaminar shear properties of PMR polyimide/Celion 6000 graphite fiber composites are compared as a function of the percent excess MDA in the monomer reactant mixture.

A.R.H.

N80-33482* National Aeronautics and Space Administration. Lewis Research Center, Cleveland, Ohio.

METHOD OF MAKING BEARING MATERIAL Patent

Harold E. Sliney, inventor (to NASA). Issued 29 Jul. 1980. 7 p. Filed 31 Jan. 1977. Supersedes N77-32249 (15 - 23, p. 3050). Division of abandoned US Patent Appl. SN-616528, filed 25 Sep. 1975, which is a division of US Patent Appl. SN-513611, filed 10 Oct. 1974.

(NASA Case-LEW-11930-3; US-Patent-4,214,905.

US-Patent-Appl-SN-764245, US-Patent-Class-75-200.

US-Patent-Class-75-222.

US-Patent-Appl-SN-616528.

US-Patent-Appl-SN-513611) Avail. US Patent and Trademark Office. CSCL 11D.

A composite material is described which will provide low friction surfaces for materials in rolling or sliding contact and is self lubricating and oxidation resistant up to and in excess of about 930 C. The composite is comprised of a metal component which lends strength and elasticity to the structure, a fluoride salt component which provides lubrication and, lastly, a glass component which not only provides oxidation protection to the metal but may also enhance the lubrication qualities of the composite.

Official Gazette of the U.S. Patent and Trademark Office

A80-10036 * Fatigue behavior of SiC reinforced titanium composites. R. T. Bhatt and H. H. Grimes (NASA, Lewis Research Center, Cleveland, Ohio). *American Society for Testing and Materials, Symposium on Fatigue of Fibrous Composite Materials, San Francisco, Calif., May 22, 23, 1979, Paper*. 18 p. 12 refs.

The low cycle axial fatigue properties of 25 and 44 fiber volume percent SiC/Ti(6Al-4V) composites were measured at room temperature and at 650 C. At room temperature, the S-N curves for the composites showed no anticipated improvement over bulk matrix behavior. Although axial and transverse tensile strength results suggest a degradation in SiC fiber strength during composite fabrication, it appears that the poor fatigue life of the composites was caused by a reduced fatigue resistance of the reinforced Ti(6Al-4V) matrix. Microstructural studies indicate that the reduced matrix behavior was due, in part, to the presence of flawed and fractured fibers created near the specimen surfaces by preparation techniques. Another possible contributing factor is the large residual tensile stresses that can exist in fiber-reinforced matrices. These effects, as well as the effects of fatigue testing at high temperature, are discussed.

(Author)

A80-20954 * Mechanical property characterization of intraply hybrid composites. C. C. Chamis, R. F. Lark, and J. H. Sinclair (NASA, Lewis Research Center, Cleveland, Ohio). *American Society for Testing and Materials, Symposium, Dearborn, Mich., Oct. 2, 3, 1979, Paper*. 24 p. 5 refs.

An investigation of the mechanical properties of intraply hybrids made from graphite fiber/epoxy matrix hybridized with secondary S-glass or Kevlar 49 fiber composites is presented. The specimen stress-strain behavior was determined, showing that mechanical properties of intraply hybrid composites can be measured with available methods such as the ten-degree off-axis test for intralaminar shear, and conventional tests for tensile, flexure, and Izod impact properties. The results also showed that combinations of high modulus graphite/S-glass/epoxy matrix composites exist which yield intraply hybrid laminates with the best 'balanced' properties, and that the translation efficiency of mechanical properties from the

constituent composites to intraply hybrids may be assessed with a simple equation.

A.T.

A80-27982 * Dynamic response of damaged angleply fiber composites. C. C. Chamis, J. H. Sinclair, and R. F. Lark (NASA, Lewis Research Center, Cleveland, Ohio). In: *Modern developments in composite materials and structures; Proceedings of the Winter Annual Meeting, New York, N.Y., December 2-7, 1979, (A80-27979 10-39)* New York, American Society of Mechanical Engineers, 1979, p. 31-61.

An investigation was conducted to determine the effects of low level damage induced by monotonic load, cyclic load and/or residual stresses on the vibration frequencies and damping factors of fiber composite angleply laminates. Two different composite systems were studied - low modulus fiber and ultra high modulus fiber composites. The results obtained showed that the frequencies and damping factors of angleply laminates made from low modulus fiber composites are sensitive to low level damage while those made from ultra high modulus composites are not. Also, vibration tests may not be sufficiently sensitive to assess concentrated local damage in angleply laminates. And furthermore, dynamic response determined from low-velocity impact coupled with the Fast Fourier Transform and packaged in a minicomputer can be a convenient procedure for assessing low-level damage in fiber composite angleply laminates.

(Author)

A80-27994 * Micromechanics of intraply hybrid composites: Elastic and thermal properties. C. C. Chamis and J. H. Sinclair (NASA, Lewis Research Center, Cleveland, Ohio). In: *Modern developments in composite materials and structures; Proceedings of the Winter Annual Meeting, New York, N.Y., December 2-7, 1979, (A80-27979 10-39)* New York, American Society of Mechanical Engineers, 1979, p. 253-267.

Composite micromechanics are used to derive equations for predicting the elastic and thermal properties of unidirectional intraply hybrid composites. The results predicted using these equations are compared with those predicted using approximate equations based on the rule of mixtures, linear laminate theory, finite element analysis and limited experimental data. The comparisons for three different intraply hybrids indicate that all four methods predict approximately the same elastic properties and are in good agreement with measured data. The micromechanics equations and linear laminate theory predict about the same values for thermal expansion coefficients. The micromechanics equations predict through-the-thickness properties which are in good agreement with the finite element results.

(Author)

A80-31169 * Fire test method for graphite fiber reinforced plastics. K. J. Bowles (NASA, Lewis Research Center, Cleveland, Ohio). *International Conference on Fire Safety, 5th, Millbrae, Calif., Jan. 14-18, 1980, Paper*. 11 p. 12 refs.

A potential problem in the use of graphite fiber reinforced resin matrix composites is the dispersal of graphite fibers during accidental fires. Airborne, electrically conductive fibers originating from the burning composites could enter and cause shorting in electrical equipment located in surrounding areas. A test method for assessing the burning characteristics of graphite fiber reinforced composites and the effectiveness of the composites in retaining the graphite fibers has been developed. The method utilizes a modified Ohio State University Rate of Heat Release apparatus. The equipment and the testing procedure are described. The application of the test method to the assessment of composite materials is illustrated for two resin matrix/graphite composite systems.

(Author)

A80-32062 * Burning characteristics and fiber retention of graphite/resin matrix composites. K. J. Bowles (NASA, Lewis Research Center, Cleveland, Ohio). In: *Rising to the challenge of the*

'80s; Annual Conference and Exhibit, 35th, New Orleans, La., February 4-8, 1980, Preprints. (A80-32058 12-24) New York, Society of the Plastics Industry, Inc., 1980, p. 11-B 1 to 11-B 5. 8 refs.

Graphite fiber reinforced resin matrix composites were subjected to controlled burning conditions to determine their burning characteristics and fiber retention properties. Two types of burning equipment were used. Small samples were burned with a natural gas fired torch to study the effects of fiber orientation and structural flaws such as holes and slits that were machined into the laminates. Larger laminate samples were burned in a Heat Release Rate Calorimeter. Unidirectional epoxy/graphite and polyimide/graphite composites and boron powder filled sample; of each of the two composite systems were burn tested and exposed to a thermal radiation. The effects of fiber orientation, flaws, and boron filler additives to the resins were evaluated. A high char forming polyimide resin was no more effective in retaining graphite fibers than a low char forming epoxy resin when burning in air. (Author)

A80-32066 * # Improved fiber retention by the use of fillers in graphite fiber/resin matrix composites. R. E. Gluyas and K. J. Bowles (NASA, Lewis Research Center, Cleveland, Ohio). In: Rising to the challenge of the '80s; Annual Conference and Exhibit, 35th, New Orleans, La., February 4-8, 1980, Preprints. (A80-32058 12-24) New York, Society of the Plastics Industry, Inc., 1980, p. 11-F 1 to 11-F 4. 5 refs.

A potential problem in the use of graphite fiber reinforced resin matrix composites is the dispersal of graphite fiber during accidental fires. Airborne electrically conductive fibers originating from burning composites could enter and cause shorting in electrical equipment located in surrounding areas. A variety of matrix fillers have been tested for their ability to prevent loss of fiber from graphite fiber/PMR polyimide and graphite fiber/epoxy composites in a fire. The fillers tested included powders of boron, boron carbide (B₄C), lime glass, lead glass, and aluminum. Of these fillers, boron was the most effective and prevented any loss of graphite fiber during burning. Mechanical properties of composites containing boron filler were measured and compared to those of composite containing no filler. (Author)

A80-32069 * # Fracture modes of high modulus graphite/epoxy angleplied laminates subjected to off-axis tensile loads. J. H. Sinclair (NASA, Lewis Research Center, Cleveland, Ohio). In: Rising to the challenge of the '80s; Annual Conference and Exhibit, 35th, New Orleans, La., February 4-8, 1980, Preprints. (A80-32058 12-24) New York, Society of the Plastics Industry, Inc., 1980, p. 12-C 1 to 12-C 8. 6 refs.

Angleplied laminates of high modulus graphite fiber/epoxy were examined in several ply configurations at various tensile loading angles to the zero ply direction to determine the effects of ply orientations on tensile properties, fracture modes, and fracture surface characteristics of the various plies. Experimental results consist of stress-strain data, selected plots, fracture stresses and strains, and scanning electron microscope (SEM) photographs of fracture surfaces. It was found that the stress-strain curves were linear to fracture, and that although fracture surface characteristics for a given fracture mode are similar to those for the same fracture mode in uniaxial specimens, no simple load angle range can be associated with a given fracture mode. It was also concluded that SEM results must be supplemented with ply stress calculations in order to identify ranges of fracture modes occurring as a function of ply orientation with respect to the load direction. J.P.B.

A80-32632 * Preparation of cast aluminum alloy-mica particle composites. Mr. Deonath (Banaras Hindu University, Varanasi, India), R. T. Bhat (NASA, Lewis Research Center, Cleveland, Ohio), and P. K. Rohatgi (Indian Institute of Science, Bangalore, India). *Journal of Materials Science*, vol. 15, May 1980, p. 1241-1251. 17 refs.

A method for making aluminum-mica particle composites is presented in which mica particles are stirred in molten aluminum alloys followed by casting in permanent molds. Magnesium is added either as an alloying element or in the form of pieces to the surface of the alloy melts to disperse up to 3 wt% mica powders in the melts and to obtain high recoveries of mica in the castings. The mechanical properties of the aluminum alloy-mica composite decrease with increasing mica content; however, even at 2.2% it has a tensile strength of 14.22 kg/sq mm with 1.1% elongation, a compression strength of 42.61 kg/sq mm, and an impact strength of 0.30 kgm/sq cm. Cryogenic and self-lubricating bearing are mentioned applications. L.M.

A80-34764 * A review of issues and strategies in nondestructive evaluation of fiber reinforced structural composites. A. Vary (NASA, Lewis Research Center, Materials and Structures Div., Cleveland, Ohio). In: New horizons - Materials and processes for the eighties; Proceedings of the Eleventh National Conference, Boston, Mass., November 13-15, 1979. (A80-34751 14-23) Azusa, Calif., Society for the Advancement of Material and Process Engineering, 1979, p. 166-177. 12 refs.

The need for advanced nondestructive evaluation (NDE) techniques for quantitative assessment of the mechanical strength and integrity of fiber composites during manufacture and service and following repair operations is stressed. The discussion covers problems and different approaches in regard to acceptance criteria, calibration standards, and methods for NDE of composites in strength critical applications. Finally, it is concluded that acousto-ultrasonic techniques provide the 'methods of choice' in this area. M.E.P.

A80-34789 * High char imide-modified epoxy matrix resins. T. T. Serafini, P. Delvigs, and R. D. Vannucci (NASA, Lewis Research Center, Cleveland, Ohio). In: New horizons - Materials and processes for the eighties; Proceedings of the Eleventh National Conference, Boston, Mass., November 13-15, 1979. (A80-34751 14-23) Azusa, Calif., Society for the Advancement of Material and Process Engineering, 1979, p. 564-573.

Studies were performed to synthesize a novel class of bis (imide-amine) curing agents for epoxy matrix resins. Glass transition temperatures and char yield data of an epoxy cured with various bis (imide-amines) are presented. The room temperature and 350 F mechanical properties, and char yields of unidirectional graphite fiber laminates prepared with conventional epoxy and imide-modified epoxy resins are presented. (Author)

A80-35494 * # Predicting the time-temperature dependent axial failure of B/Al composites. J. A. DiCarlo (NASA, Lewis Research Center, Cleveland, Ohio). *Metallurgical Society of AIME, Symposium on Fracture Modes in Metal Matrix Composites, Las Vegas, Nev., Feb. 25-28, 1980, Paper*. 26 p. 21 refs.

Theoretical and experimental studies are reviewed whose objective was to gain insight into and predict the effects of time, temperature, and stress on the axial failure modes of boron fibers and B/Al composites. Owing to the inelastic nature of boron fiber deformation, it proved possible to develop simple creep functions which can be used to describe accurately the creep and fracture stress of as-produced fibers. Analysis of damping and stress data for B/6061 Al composites indicates that fiber creep and the effects of creep of fiber fracture are measurably reduced by the composite fabrication process. V.P.

A80-44236 * # Dynamic modulus and damping of boron, silicon carbide, and alumina fibers. J. A. DiCarlo (NASA, Lewis Research Center, Cleveland, Ohio) and W. Williams (Lincoln University, Lincoln University, Pa.). *American Ceramic Society, Annual Conference on Composites and Advanced Materials, 4th, Cocoa*

Beach, Fla., Jan. 21-24, 1980, Paper. 42 p. 19 refs.

The dynamic modulus and damping capacity for boron, silicon carbide, and silicon carbide-coated boron fibers were measured from -190 to 800 C. The single fiber vibration test also allowed measurement of transverse thermal conductivity for the silicon carbide fibers. Temperature-dependent damping capacity data for alumina fibers were calculated from axial damping results for alumina-aluminum composites. The dynamic fiber data indicate essentially elastic behavior for both the silicon carbide and alumina fibers. In contrast, the boron-based fibers are strongly anelastic, displaying frequency-dependent moduli and very high microstructural damping. The single fiber damping results were compared with composite damping data in order to investigate the practical and basic effects of employing the four fiber types as reinforcement for aluminum and titanium matrices. (Author)

A80-44237 * # Calculation of residual principal stresses in CVD boron on carbon filaments. D. R. Behrendt (NASA, Lewis Research Center, Cleveland, Ohio). *American Ceramic Society, Annual Conference on Composites and Advanced Materials, 4th, Cocoa Beach, Fla., Jan. 21-24, 1980, Paper*. 13 p. 5 refs.

A three-dimensional finite element model of the chemical vapor deposition (CVD) of boron on a carbon substrate (B/C) is developed. The model includes an expansion of the boron after deposition due to atomic rearrangement and includes creep of the boron and carbon. Curves are presented to show how the principal residual stresses and the filament elongation vary as the parameters defining deposition strain and creep are varied. The calculated results are compared with experimental axial residual stress and elongation measurements made on B/C filaments. This comparison requires that for good agreement between calculated and experimental results, the deposited boron must continue to expand after deposition, and that the build-up of residual stresses is limited by significant boron and carbon creep rates. (Author)

N80-10318* # Avco Systems Div., Wilmington, Mass.
IMPROVING THE STRESS RUPTURE AND CREEP OF SILICON NITRIDE Final Report
T. Vasilos, R. M. Cannon, Jr., and B. J. Wuensch 30 Mar. 1979 68 p refs
(Contract NAS3-20088)
(NASA-CR-159585) Avail: NTIS HC A04/MF A01 CSCL 11D

Yttria-stabilized zirconium oxide (Zyttrite) additions to purified silicon nitride markedly improved the high temperature strength, stress rupture and creep properties of hot pressed samples. Room temperature bend strengths, however, of four (4) compositions evaluated were each about one-third lower than the NC-132 silicon nitride composition. This difference decreased with increasing temperature until at 1200 C, there was reasonable equivalence between most of the zyttrite containing compositions and NC-132 in terms of short time bend strength measurements. At 1370 C, the 10 and 20 wt. % containing zyttrite compositions showed bend strengths as much as double the NC-132 material. Bend stress rupture results for 10 and 20 wt. % zyttrite containing compositions showed a strong stress sensitivity at the 176 MN/sq m (40 Kpsi) level above 1200 C. Creep in bending measurements showed that at 1370 C, zyttrite containing compositions exhibited creep rates that were about two orders of magnitude lower than NC-132 material samples. All compositions appeared to follow deformation kinetics related to a visco-elastic mechanism, i.e., glassy phase diffusional creep or grain boundary sliding. A.R.H.

N80-10319* # United Technologies Research Center, East Hartford, Conn.
DEVELOPMENT OF SILICON NITRIDE OF IMPROVED TOUGHNESS Final Report
J. J. Brennan 2 Oct. 1979 111 p refs
(Contract NAS3-21375)
(NASA-CR-159676; R79-914364-12) Avail: NTIS HC A06/MF A01 CSCL 11D

The application of reaction sintered Si₂N₄ energy absorbing surface layers to hot-pressed Si₃N₄ was investigated. The surface layer was formed by in-place nitridation of silicon powder. It was found that reaction sintered Si₃N₄ layers of 1 mm thickness, fabricated from either -100, +200, -200, or -325 mesh Si powder and nitrided in 96% N₂/4% H₂ so that approximately 20-25 vol % unnitrided Si remained in the layer, resulted in a sevenfold increase in ballistic impact resistance of a 0.64 cm thick hot-pressed Si₃N₄ substrate from RT 1370 C. Both NC-132 Si₃N₄, with MgO additive, and NCX-34 Si₃N₄, with Y₂O₃ additive, were evaluated as substrate material. The finer grain size -200 and -325 mesh nitrided Si layers were for their in N₂/H₂ mixtures, rather than pure N₂, resulted in a microstructure that did not substantially degrade the strength of the hot pressed Si₃N₄ substrate. Thermal cycling tests on the RSSN/HPSN combinations from 200 C to 1370 C for 75 cycles in air did not degrade the impact resistance nor the interfacial bonding, although a large amount of internal silica formation occurred within the RSSN layer. Mach 0.8, 5 hr, hot gas erosion tests showed no surface recession of RSSN layers at 1200 C and slight surface recession at 1370 C. M.M.M.

N80-12118* # TRW Equipment Labs., Cleveland, Ohio.
SECOND GENERATION PMR POLYIMIDE/FIBER COMPOSITES
P. J. Cavano 26 Oct. 1979 144 p refs
(Contract NAS3-21349)
(NASA-CR-159666; ER-7989F) Avail: NTIS HC A07/MF A01 CSCL 11D

A second generation polymerization monomeric reactants (PMR) polyimides matrix system (PMR 2) was characterized in both neat resin and composite form with two different graphite fiber reinforcements. Three different formulated molecular weight levels of laboratory prepared PMR 2 were examined, in addition to a purchased experimental fully formulated PMR 2 precursor solution. Isothermal aging of graphite fibers, neat resin samples and composite specimens in air at 316 C were investigated. Humidity exposures at 65 C and 97 percent relative humidity were conducted for both neat resin and composites for eight day periods. Anaerobic char of neat resin and fire testing of composites were conducted with PMR 15, PMR 2, and an epoxy system. Composites were fire tested on a burner rig developed for this program. Results indicate that neat PMR 2 resins exhibit excellent isothermal resistance and that PMR 2 composite properties appear to be influenced by the thermo-oxidative stability of the reinforcing fiber. R.C.T.

N80-22407* # Westinghouse Research and Development Center, Pittsburgh, Pa.
SILICONE MODIFIED RESINS FOR GRAPHITE FIBER LAMINATES Final Report
L. W. Frost and G. M. Bower 28 Sep. 1979 75 p refs
(Contract NAS3-21373)
(NASA-CR-159750; FR-79-9b7-SICOP-R1) Avail: NTIS HC A04/MF A01 CSCL 11D

The development of silicon modified resins for graphite fiber laminates which will prevent the dispersal of graphite fibers when the composites are burned is discussed. Eighty-five silicone modified resins were synthesized and evaluated including unsaturated polyesters, thermosetting methacrylates, epoxies, polyimides, and phenolics. Neat resins were judged in terms of Si content, homogeneity, hardness, Char formation, and thermal stability. Char formation was estimated by thermogravimetry to 1,000 C in air and in N₂. Thermal stability was evaluated by isothermal weight loss measurements for 200 hrs in air at three temperatures. Four silicone modified epoxies were selected for evaluation in unidirectional filament wound graphite laminates. Neat samples of these resins had 1,000 C char residues of 25 to 50%. The highest flexural values measured for the laminates were a strength of 140 kpsi and a modulus of 10 Mpsi. The highest interlaminar shear strength was 5.3 kpsi. M.G.

N80-25382* # Hamilton Standard, Windsor Locks, Conn.
DIFFUSION BONDED BORON/ALUMINUM SPAR-SHELL

FAN BLADE Final Report, Jun. 1977 - May 1978

C. E. K. Carlson, J. L. Cutler, W. J. Fisher, and J. V. W. Memmott
Jun. 1980 114 p refs

(Contract NAS3-20407)

(NASA-CR-159571; HSER-7968)

Avail: NTIS

HC A08/MF A01 CSCL 11D

Design and process development tasks intended to demonstrate composite blade application in large high by-pass ratio turbofan engines are described. Studies on a 3.0 aspect ratio space and shell construction fan blade indicate a potential weight savings for a first stage fan rotor of 39% when a hollow titanium spar is employed. An alternate design which featured substantial blade internal volume filled with titanium honeycomb inserts achieved a 14% potential weight savings over the B/M rotor system. This second configuration requires a smaller development effort and entails less risk to translate a design into a successful product. The feasibility of metal joining large subsonic spar and shell fan blades was demonstrated. Initial aluminum alloy screening indicates a distinct preference for AA6061 aluminum alloy for use as a joint material. The simulated airfoil pressings established the necessity of rigid air surfaces when joining materials of different compressive rigidities. The two aluminum alloy matrix choices both were successfully formed into blade shells. A.R.H.

N80-26383* Lehigh Univ., Bethlehem, Pa. Inst. of Fracture and Solid Mechanics.

SUDDEN STRETCHING OF A FOUR LAYERED COMPOSITE PLATE Interim Report

G. C. Sih and E. P. Chen Mar. 1980 42 p refs

(Grant NSG-3197)

(NASA-CR-159870; IFSM-80-102)

Avail: NTIS

HC A03/MF A01 CSCL 11D

An approximate theory of laminated plates is developed by assuming that the extensorial and thickness mode of vibration are coupled. The mixed boundary value crack problem of a four layered composite plate is solved. Dynamic stress intensity factors for a crack subjected to suddenly applied stress are found to vary as a function of time and depend on the material properties of the laminate. Stress intensification in the region near the crack front can be reduced by having the shear modulus of the inner layers to be larger than that of the outer layers. Author

N80-26384* Lehigh Univ., Bethlehem, Pa. Inst. of Fracture and Solid Mechanics.

SUDDEN BENDING OF CRACKED LAMINATES Interim Report

G. C. Sih and E. P. Chen Feb. 1980 53 p refs

(Contract NSG-3197)

(NASA-CR-159860; IFSM-80-103)

Avail: NTIS

HC A04/MF A01 CSCL 11D

A dynamic approximate laminated plate theory is developed with emphasis placed on obtaining effective solution for the crack configuration where the $1/\text{square root of } r$ stress singularity and the condition of plane strain are preserved. The radial distance r is measured from the crack edge. The results obtained show that the crack moment intensity tends to decrease as the crack length to laminate plate thickness is increased. Hence, a laminated plate has the desirable feature of stabilizing a through crack as it increases its length at constant load. Also, the level of the average load intensity transmitted to a through crack can be reduced by making the inner layers to be stiffer than the outer layers. The present theory, although approximate, is useful for analyzing laminate failure to crack propagation under dynamic load conditions. Author

N80-29430* Fiber Materials, Inc., Biddeford, Maine.

FABRICATION AND EVALUATION OF LOW FIBER CONTENT ALUMINA FIBER/ALUMINUM COMPOSITES Final Report

J. E. Hack and G. C. Strempek 18 Jun. 1980 72 p refs

(Contract NAS3-21371)

(NASA-CR-159517; AMDL-0001)

Avail: NTIS

HC A04/MF A01 CSCL 11D

The mechanical fabrication of low volume percent fiber,

polycrystalline alumina fiber reinforced aluminum composites was accomplished. Wire preform material was prepared by liquid-metal infiltration of alumina fiber bundles. The wires were subsequently encapsulated with aluminum foil and fabricated into bulk composite material by hot-drawing. Extensive mechanical, thermal and chemical testing was conducted on preform and bulk material to develop a process and material data base. In addition, a preliminary investigation of mechanical forming of bulk alumina fiber reinforced aluminum composite material was conducted. Author

N80-29432* George Washington Univ., Washington, D. C. School of Engineering and Applied Science

STATISTICAL ASPECTS OF CARBON FIBER RISK ASSESSMENT MODELING

Donald Gross, Douglas R. Miller, and Richard M. Soland Jul 1980 127 p refs

(Contract NSG-1556)

(NASA-CR-159318) Avail: NTIS HC A07/MF A01 CSCL 11D

The probabilistic and statistical aspects of the carbon fiber risk assessment modeling of fire accidents involving commercial aircraft are examined. Three major sources of uncertainty in the modeling effort are identified. These are: (1) imprecise knowledge in establishing the model; (2) parameter estimation; and (3) Monte Carlo sampling error. All three sources of uncertainty are treated and statistical procedures are utilized and/or developed to control them wherever possible. A.R.H.

A80-32063 * Fiber release characteristics of graphite hybrid composites. J. Henshaw (Avco Corp., Lowell, Mass.), In: Rising to the challenge of the '80s; Annual Conference and Exhibit, 35th, New Orleans, La., February 4-8, 1980, Preprints. (A80-32058 12-24) New York, Society of the Plastics Industry, Inc., 1980, p. 11-C 1 to 11-C 8. Contract No. NAS3-21385.

The paper considers different material concepts that can be fabricated of hybridized composites which demonstrate improved graphite fiber retention capability in a severe fire without significant reduction to the composite properties. More than 30 panels were fabricated for mechanical and fire tests, the details and results of which are presented. Methods of composite hybridization investigated included the addition of oxidation resistant fillers to the resin, mechanically interlocking the graphite fibers by the use of woven fabrics, and the addition of glass fibers and glass additives designed to melt and fuse the graphite fibers together. It is concluded that a woven fabric with a serving of glass around each graphite tow is by far the superior of those evaluated: not only is there a coalescing effect in each graphite layer, but there is also a definite adhesion of each layer to its neighbor. J.P.B.

A80-32064 * Hybrid composites that retain graphite fibers on burning. E. E. House (Boeing Aerospace Co., Seattle, Wash.), In: Rising to the challenge of the '80s; Annual Conference and Exhibit, 35th, New Orleans, La., February 4-8, 1980, Preprints. (A80-32058 12-24) New York, Society of the Plastics Industry, Inc., 1980, p. 11-D 1 to 11-D 8. Contract No. NAS3-21383.

A laboratory scale program was conducted to determine fiber release tendencies of graphite reinforced/resinous matrix composites currently used or projected for use in civil aircraft. In the event of an aircraft crash and burn situation, there is concern that graphite fibers will be released from the composites once the resin matrix is thermally decomposed. Hybridizing concepts aimed at preventing fiber release on burning were postulated and their effectiveness evaluated under fire, impact, and air flow during an aircraft crash.

(Author)

25 INORGANIC AND PHYSICAL CHEMISTRY

Includes chemical analysis, e.g. chromatography, combustion theory, electrochemistry, and photochemistry

For related information see also 77 *Thermodynamics and Statistical Physics*

N80-24386* # National Aeronautics and Space Administration, Lewis Research Center, Cleveland, Ohio.

AN INTERACTIVE MODULAR DESIGN FOR COMPUTERIZED PHOTOMETRY IN SPECTROCHEMICAL ANALYSIS

Virginia L. Bair 1980 17 p. Presented at the Pittsburgh Conf. on Anal. Chem. and Appl. Spectry., Atlantic City, 10-14 Mar. 1980, cosponsored by the Soc. for Anal. Chemists of Pittsburgh and the Spectry. Soc. of Pittsburgh (NASA-TM-81521; E-465) Avail: NTIS HC A02/MF A01 CSCL 07D

A general functional description of totally automatic photometry of emission spectra is not available for an operating environment in which the sample compositions and analysis procedures are low-volume and non-routine. The advantages of using an interactive approach to computer control in such an operating environment are demonstrated. This approach includes modular subroutines selected at multiple-option, menu-style decision points. This style of programming is used to trace elemental determinations, including the automated reading of spectrographic plates produced by a 3.4 m Ebert mount spectrograph using a dc-arc in an argon atmosphere. The simplified control logic and modular subroutine approach facilitates innovative research and program development, yet is easily adapted to routine tasks. Operator confidence and control are increased by the built-in options including degree of automation, amount of intermediate data printed out, amount of user prompting, and multidirectional decision points. A.R.H.

A80-10041 * # The chemistry of sodium chloride involvement in processes related to hot corrosion. C. A. Stearns, F. J. Kohl, and G. C. Fryburg (NASA, Lewis Research Center, Cleveland, Ohio), U.S. Department of Energy, and Electric Power Research Institute, Conference on Advanced Materials for Alternate Fuel Capable Directly Fired Heat Engines, Castine, Me., July 30-Aug. 3, 1979, Paper, 30 p, 47 refs.

Sodium chloride is one of the primary contaminants that enter gas turbine engines and contribute, either directly or indirectly, to the hot corrosion degradation of hot-gas-path components. The paper surveys the results of laboratory experiments along with thermodynamic and mass transport calculations, intended for elucidating the behavior of sodium chloride in combustion environments. It is shown that besides being a source of sodium for the formation of corrosive liquid Na₂SO₄, the NaCl itself contributes in other indirect ways to the material degradation associated with the high-temperature environmental attack. In addition, the experimental results lend credence to the conceptual scheme presented schematically (behavior of NaCl in a turbine engine combustion gas environment) and resolve conflicting aspects of relevant NaCl misconceptions. S.D.

A80-13070 * # Decay of the zincate concentration gradient at an alkaline zinc cathode after charging. H. E. Kautz and C. E. May (NASA, Lewis Research Center, Cleveland, Ohio), *Electrochemical Society, Meeting, Los Angeles, Calif., Oct. 14-19, 1979, Paper*, 19 p, 9 refs.

The study was carried out by observing the decay of the zincate concentration gradient at a horizontal zinc cathode after charging. This decay was found to approximate first order kinetics as expected from a proposed boundary layer model. The decay half life was

shown to be a linear function of the thickness of porous zinc deposit on the cathode indicating a very rapid transport of zincate through porous zinc metal. The rapid transport is attributed to an electrochemical mechanism. The data also indicated a relatively sharp transition between the diffusion and convection transport regions. The diffusion of zincate ion through asbestos submerged in alkaline electrolyte was shown to be comparable with that predicted from the bulk diffusion coefficient of the zincate ion in alkali. (Author)

A80-20955 * # Combustion of solid carbon rods in zero and normal gravity. C. M. Spuckler, F. J. Kohl, R. A. Miller, C. A. Stearns (NASA, Lewis Research Center, Cleveland, Ohio), and K. J. De Witt (Toledo, University, Toledo, Ohio), *American Institute of Chemical Engineers, Annual Meeting, 72nd, San Francisco, Calif., Nov. 25-29, 1979, Paper*, 30 p, 11 refs.

In order to investigate the mechanism of carbon combustion, normal and zero gravity experiments were conducted in which spectroscopic carbon rods were resistance ignited and burned in an oxygen environment. Direct mass spectrometric sampling was used in the normal gravity tests to measure gas phase concentrations. The gas sampling probe was positioned near the circumference of the horizontally mounted carbon rods, either at the top or at angles of 45 or 90 deg from the top, and yielded concentration profiles of CO₂, CO, and O₂ as a function of distance from the carbon surface. The experimental concentrations were compared to those predicted by a stagnant film model. Zero gravity droptower tests were conducted in order to assess the effect of convection on the normal gravity combustion process. The ratio of flame diameter to rod diameter as a function of time for oxygen pressures of 5, 10, 15, and 20 psia was obtained for three different diameter rods. It was found that this ratio was inversely proportional to both the oxygen pressure and the rod diameter. (Author)

A80-35881 * Durability testing of advanced catalysts and catalyst supports for gas turbine engine combustors. R. M. Heck, M. Chang, H. W. Hess (Engelhard Industries, Inc., Edison, N.J.), and T. S. Mroz (NASA, Lewis Research Center, Cleveland, Ohio), *AIChE Symposium Series*, vol. 75, no. 188 1979, p. 83-94, 9 refs.

The paper presents new information on the durability of a CATCOM catalyst operating at low-emission combustion temperatures (about 1527 K) with a liquid fuel, No. 2 diesel. Information on the activity of No. 2 diesel after 1000 hr of aging is given. In addition, a unique in situ activity test developed for monitoring the subtle changes in the catalyst activity of the CATCOM catalyst is also detailed. The study demonstrated the feasibility of using a CATCOM catalyst in catalytically supported thermal combustion for extended operating periods. S.D.

A80-39640 * # An interactive modular design for computerized photometry in spectrochemical analysis. V. L. Bair (NASA, Lewis Research Center, Cleveland, Ohio), *Society for Analytical Chemists of Pittsburgh and Spectroscopy Society of Pittsburgh, Pittsburgh Conference on Analytical Chemistry and Applied Spectroscopy, Atlantic City, N.J., Mar. 10-14, 1980, Paper*, 15 p.

An interactive, top-down structured program design is described which produces a general flexible description of totally automatic photometry of emission spectra in an operating environment in which sample compositions and analysis procedures are low-volume and nonroutine. The use of this type of programming is illustrated by a project to computerize trace elemental determinations including the automated reading of spectrographic plates produced by a 3.4-m Ebert mount spectrograph using a dc-arc in an argon atmosphere. V.T.

A80-42190 * # An analytical study of nitrogen oxides and carbon monoxide emissions in hydrocarbon combustion with added nitrogen - Preliminary results. D. A. Bittker (NASA, Lewis Research Center, Cleveland, Ohio), *American Society of Mechanical Engineers, Gas Turbine Conference and Products Show, New Orleans, La., Mar.*

10-13, 1980, Paper 80-GT-60. 11 p. 19 refs. Members, \$1.50; nonmembers, \$3.00.

The influence of ground-based gas turbine combustor operating conditions and fuel-bound nitrogen (FBN) found in coal-derived liquid fuels on the formation of nitrogen oxides and carbon monoxide is investigated. Analytical predictions of NO_x and CO concentrations are obtained for a two-stage, adiabatic, perfectly-stirred reactor operating on a propane-air mixture, with primary equivalence ratios from 0.5 to 1.7, secondary equivalence ratios of 0.5 or 0.7, primary stage residence times from 12 to 20 msec, secondary stage residence times of 1, 2 and 3 msec and fuel nitrogen contents of 0.5, 1.0 and 2.0 wt %. Minimum nitrogen oxide but maximum carbon monoxide formation is obtained at primary zone equivalence ratios between 1.4 and 1.5, with percentage conversion of FBN to NO_x decreasing with increased fuel nitrogen content. Additional secondary dilution is observed to reduce final pollutant concentrations, with NO_x concentration independent of secondary residence time and CO decreasing with secondary residence time; primary zone residence time is not observed to affect final NO_x and CO concentrations significantly. Finally, comparison of computed results with experimental values shows a good semiquantitative agreement.

A.L.W.

N80-12142* Pennsylvania State Univ., University Park.
INVESTIGATION OF CRITICAL BURNING OF FUEL DROPLETS Final Report, 1 Sep. 1966 - 30 Jun. 1979

G. M. Faeth Jul 1979 87 p refs

(Grant NGR-39-009-077)

(NASA-CR-159697) Avail. NTIS HC A04/MF A01 CSCL 21B

The general problem of spray combustion was investigated. The combustion of bipropellant droplets; combustion of hydrozine fuels; and combustion of sprays were studied. A model was developed to predict mean velocities and temperatures in a combustor gas jet.

R.C.T.

N80-13193* Tennessee Technological Univ., Cookeville. Dept. of Mechanical Engineering.

AMPLIFICATION OF REYNOLDS NUMBER DEPENDENT PROCESSES BY WAVE DISTORTION Final Report, 1 Jan. 1972 - 31 Oct. 1979

M. Ventrone Nov. 1979 59 p refs

(Grant NGR-43-003-015)

(NASA-CR-159732) Avail. NTIS HC A04/MF A01 CSCL 21B

The amplification of a Reynolds number dependent process by wave distortion and the possibility of applying the results to other similar Reynolds number dependent processes were investigated. The process investigated was that associated with the operation of a constant-temperature hot-wire anemometer. The application of vaporization limited combustion, the type of combustion typically associated with liquid propellant rocket engines, was studied. A series of experiments were carried out to determine the effect of wave distortion on a Reynolds number dependent process and to establish the analogy between the anemometer process and the combustion process. Parametric trends, behavior common to different chamber geometries, and stability boundaries were identified. The results indicate a high degree of similarity between the two processes and the possibility of using the anemometer system to investigate combustion instability. The nonlinear aspects of a Reynolds number dependent process appear to be the dominant mechanisms controlling instability.

J.M.S.

A80-11754 * Symposium /International/ on Combustion, 17th, Leeds University, Leeds, England, August 20-25, 1978. Proceedings. Symposium sponsored by NASA, NSF, U.S. Navy, U.S. Army, U.S. Air Force, ERDA, et al.; NSF Grant No. ENG-78-18544; Contracts No. N00014-78-M-0053; No. NAS3-21311; No. ET-78-G-01-3642; Grant No. DAAK11-78-M-0007. Pittsburgh, Pa., Combustion Institute, 1979. 1491 p. \$66. (For individual items see A80-11755 to A80-11824)

The Symposium focused on deflagration to detonation transition, coal combustion, turbulent combustion interactions, kinetics, furnace combustion, inhibition and ignition, flame structure and chemistry, combustion studies, measurement techniques, fire and explosion, engine combustion, soot, and propellants and explosives. Papers were presented on numerical modeling of the deflagration to detonation transition, the interaction between turbulence and combustion, turbulent flame propagation in premixed gases, spray evaporation in recirculating flow, dissociation of nitric oxide in shock waves, pollutant emissions from partially mixed turbulent flames, energy transfer and quenching rates of laser-pumped electronically excited alkalis in flames, a study of flammability limits using counterflow flames, the unified theory of explosions with fuel consumption, and the dynamics and radiant intensity of large hydrogen flames.

A.T.

A80-35908 * CATCOM catalyst 5 atm 1000 hour aging study using No. 2 fuel oil. I. T. Osgerby, B. A. Olson, and H. C. Lee (Engelhard Minerals and Chemicals Corp., Edison, N.J.). U.S. Environmental Protection Agency, Workshop on Catalytic Combustion, 4th, Cincinnati, Ohio, May 14, 15, 1980, Paper. 44 p. 45 refs. Contract No. NAS3-19416.

The durability of the CATCOM catalyst for use in catalytically supported thermal combustion has been demonstrated at 5 atm, complementing a previous 1000 hour durability study at 1 atm. Both of these studies were conducted at about 640 K air preheat temperature at a reference velocity of about 14 m/s; the adiabatic flame temperature of the fuel/air mixture was about 1530 K. The catalyst proved to be capable of low emissions operations after 1000 hours of diesel fuel aging. However, more severe deactivation occurred in the 5 atm test; this was attributed to a loss in kinetic (ignition) activity.

B.I.

26 METALLIC MATERIALS

Includes physical, chemical, and mechanical properties of metals, e.g., corrosion, and metallurgy

N80-10344* National Aeronautics and Space Administration, Lewis Research Center, Cleveland, Ohio.

ANALYSIS OF THE RESPONSE OF A THERMAL BARRIER COATING TO SODIUM AND VANADIUM DOPED COMBUSTION GASES

Robert A. Miller 1979 23 p refs Presented at 8th Midwest High Temperature Chemistry Conf., Milwaukee, Wis., 4-6 Jun 1979. Sponsored in part by DOE.

(Contract EF-77-A-01-2593)

(NASA-TM-79205, DOE/NASA/2593-79/7, E-090) Avail: NTIS HC A02/MF A01 CSCL 11F

Published data on the behavior of zirconia-based thermal barrier coatings exposed to combustion gases doped with sodium and vanadium were analyzed with respect to calculated condensate dew points and melting points. Coating temperatures, failure locations, and depths were reasonably well correlated. Author

N80-11188* National Aeronautics and Space Administration, Lewis Research Center, Cleveland, Ohio.

MECHANICAL PROPERTIES AND OXIDATION AND CORROSION RESISTANCE OF REDUCED-CHROMIUM 304 STAINLESS STEEL ALLOYS

Joseph R. Stephens, Charles A. Barrett, and Charles A. Gyorgak Washington Nov 1979 22 p refs

(NASA-TP-1557, E-065) Avail: NTIS HC A02/MF A01 CSCL 11F

An experimental program was undertaken to identify effective substitutes for part of the Cr in 304 stainless steel as a method of conserving the strategic element Cr. Although special emphasis was placed on tensile properties, oxidation and corrosion resistance were also examined. Results indicate that over the temperature range of -196 C to 540 C the yield stress of experimental austenitic alloys with only 12 percent Cr compare favorably with the 18 percent Cr in 304 stainless steel. Oxidation resistance and in most cases corrosion resistance for the experimental alloys were comparable to the commercial alloy. Effective substitutes for Cr included Al, Mo, Si, Ti, and V, while Ni and Mn contents were increased to maintain an austenitic structure. R.C.T.

N80-11189* National Aeronautics and Space Administration, Lewis Research Center, Cleveland, Ohio.

EFFECT OF THERMALLY INDUCED POROSITY ON AN AS-HIP POWDER METALLURGY SUPERALLOY

R. L. Dreshfield and R. V. Miner, Jr. Washington 1979 20 p refs To be presented at Ann. Meeting of the Am. Inst. of Mining, Met. and Petrol. Engr., Las Vegas, Nev., 24-28 Feb. 1980

(NASA-TM-79263, E-178) Avail: NTIS HC A02/MF A01 CSCL 11F

The impact of thermally induced porosity on the mechanical properties of an as-hot-isostatically-pressed and heat treated pressing made from low carbon Astroloy was determined. Porosity in the disk-shape pressing studied ranged from 2.6 percent at the bore to 1.4 percent at the rim. Tensile, yield strength, ductility, and rupture life of the rim of the porous pressing was only slightly inferior to the rim of sound pressings. The strength, ductility, and rupture life of the bore of the porous pressing was severely degraded compared to sound pressings. At strain ranges typical of commercial jet engine designs, the rim of the porous pressing had slightly inferior fatigue life to sound pressings. A.R.H.

N80-14232* National Aeronautics and Space Administration, Lewis Research Center, Cleveland, Ohio.

IMPROVED REFRACTORY COATINGS AND METHOD OF

PRODUCING THE SAME Patent Application

W. A. Brainard and D. R. Wheeler, inventors (to NASA) Filed 12 Jul 1979 7 p

(NASA-Case-LEW-13124-1, US-Patent-Appl-SN-102003) Avail: NTIS HC A02/MF A01 CSCL 11F

A thin sputtered film that exhibits improved adherence to a substrate and has improved friction and wear characteristics is described. These improvements are achieved by coating the substrate by rf sputtering with a film of titanium carbide using an argon sputtering plasma. A small nitrogen partial pressure from about 0.5% to 2.5% is added in the initial stages of the deposition during which the interface is formed. The improvements in adhesion of the titanium carbide coating to the substrate results from the presence of both titanium nitride and a nitride of the substrate in the interfacial region. NASA

N80-14234* National Aeronautics and Space Administration, Lewis Research Center, Cleveland, Ohio.

CORROSION RESISTANCE OF SODIUM SULFATE COATED COBALT-CHROMIUM-ALUMINUM ALLOYS AT 900 C, 1000 C, AND 1100 C

G. J. Santoro Nov. 1979 28 p refs

(NASA-TM-79311, E-267) Avail: NTIS HC A03/MF A01 CSCL 11F

The corrosion of sodium sulfate coated cobalt alloys was measured and the results compared to the cyclic oxidation of alloys with the same composition, and to the hot corrosion of compositionally equivalent nickel-base alloys. Cobalt alloys with sufficient aluminum content to form aluminum containing scales corrode less than their nickel-base counterparts. The cobalt alloys with lower aluminum levels form CoO scales and corrode more than their nickel-base counterparts which form NiO scales. M.G.

N80-15234* National Aeronautics and Space Administration, Lewis Research Center, Cleveland, Ohio.

ADHESION AND FRICTION OF IRON-BASE BINARY ALLOYS IN CONTACT WITH SILICON CARBIDE IN VACUUM

Kazuhisa Miyoshi and Donald H. Buckley Jan. 1980 13 p refs

(NASA-TP-1604, E-126) Avail: NTIS HC A02/MF A01 CSCL 11F

Single pass sliding friction experiments were conducted with various iron base binary alloys (alloying elements were Ti, Cr, Mn, Ni, Rh, and W) in contact with a single crystal silicon carbide (0001) surface in vacuum. Results indicate that atomic size and concentration of alloying elements play an important role in controlling adhesion and friction properties of iron base binary alloys. The coefficient of friction generally increases with an increase in solute concentration. The coefficient of friction increases linearly as the solute to iron atomic radius ratio increases or decreases from unity. The chemical activity of the alloying elements was also an important parameter in controlling adhesion and friction of alloys, as these latter properties are highly dependent upon the d bond character of the elements. R.C.T.

N80-15235* National Aeronautics and Space Administration, Lewis Research Center, Cleveland, Ohio.

EFFECT OF SODIUM, POTASSIUM, MAGNESIUM, CALCIUM, AND CHLORINE ON THE HIGH TEMPERATURE CORROSION OF IN-100, U-700, IN-792, AND MAR M-509

Carl E. Lowell, Steven M. Sidik, and Daniel L. Deadmore 1980 28 p refs Proposed for presentation at 25th Ann. Intern. Gas Turbine Conf., New Orleans, 9-13 Mar. 1980; sponsored by the ASME

(Contract EF-77-A-01-2593)

(NASA-TM-79309, E-265; DOE/NASA/2593-79/12) Avail: NTIS HC A03/MF A01 CSCL 07D

The effects of potential impurities such as Na, K, Mg, Ca, and Cl, in coal-derived liquid fuels on accelerated corrosion of IN-100, U-700, IN-792, and Mar M-509 were investigated using a Mach 0.3 burner rig for times to 200 hours in one hour cycles. These impurities were injected in combination as aqueous

solutions into the combustor. Other variables were time, temperature, and fuel-to-air ratio. The experimental matrix was a central composite fractional factorial design divided into blocks to allow modification of the design as data was gathered. The extent of corrosion was determined by metal consumption. The time exponent was near 1.0 for the least corrosion resistant alloys, U-700 and IN-100, near 0.8 for the moderately resistant IN-792, and close to Mar-M-509, the most corrosion resistant alloy. As anticipated, corrosion rapidly increased with increasing temperature as well as Na and K concentrations, while corrosion decreased somewhat as the Ca concentration increased for all alloys. Mg was beneficial for the Ni-base alloys but had little effect on the Co-base alloy. Surprisingly, the effect of increasing Cl was to decrease the corrosion of all alloys. Little interaction among the dopants was noted. A R H

N80-16141* National Aeronautics and Space Administration, Lewis Research Center, Cleveland, Ohio.

SCANNING-ELECTRON-MICROSCOPE STUDY OF NORMAL-IMPINGEMENT EROSION OF DUCTILE METALS

William A. Brainard and Joshua Salik. Jan. 1980. 11 p. refs. (NASA-TP-1609, E-085) Avail: NTIS HC A02/MF A01 CSCL 11F

Scanning electron microscopy was used to characterize the erosion of annealed copper and aluminum surfaces produced by both single- and multiple-particle impacts. Macroscopic 3.2 mm diameter steel balls and microscopic, brittle erodant particles were projected by a gas gun system so as to impact at normal incidence at speeds up to 140 m/sec. During the impacts by the brittle erodant particles, at lower speeds the erosion behavior was similar to that observed for the larger steel balls. At higher velocities, particle fragmentation and the subsequent cutting by the radial wash of debris created a marked change in the erosion mechanism. Author

N80-16143* National Aeronautics and Space Administration, Lewis Research Center, Cleveland, Ohio.

SOME CONSIDERATIONS OF THE PERFORMANCE OF TWO HONEYCOMB GAS PATH SEAL MATERIAL SYSTEMS

Robert C. Bill and Lawrence T. Shiembob. 1980. 29 p. refs. To be presented at the Ann. Meeting of the Am. Soc. of Lubrication Engr., Anaheim, Calif., 5-8 May 1980. Prepared in cooperation with Army Aviation Research and Development Command, Cleveland, and Pratt and Whitney Aircraft Group, East Hartford, Conn. (NASA-TM-81398, AVRAM-TR-79-33, E-032) Avail: NTIS HC A03/MF A01 CSCL 11F

A standard Hastelloy-X honeycomb material and a pack aluminide coated honeycomb material were evaluated as to their performance as labyrinth seal materials for aircraft gas turbine engines. Consideration from published literature was given to the fluid sealing characteristics of two honeycomb materials in labyrinth seal applications, and their rub characteristics, erosion resistance, and oxidation resistance were evaluated. The increased temperature potential of the coated honeycomb material compared to the uncoated standard could be achieved without compromising the honeycomb material's rub tolerance, although there was some penalty in terms of reduced erosion resistance. Author

N80-17199* National Aeronautics and Space Administration, Lewis Research Center, Cleveland, Ohio.

CHEMICAL PROCESSES INVOLVED IN THE INITIATION OF HOT CORROSION OF B-1900 AND NASA-TW VIA

George C. Fryburg, Fred J. Kohl, and Carl A. Stearns. 1979. 49 p. refs. Presented at 165th Meeting of the Electrochem. Soc., Los Angeles, 14-19 Oct. 1979. (NASA-TM-81399, E-308) Avail: NTIS HC A03/MF A01 CSCL 11F

Sodium sulfate induced hot corrosion of B-1900 and NASA-TW VIA at 900 C was studied with special emphasis on the chemical reactions occurring during and immediately after the induction period. Thermogravimetric tests were run for set periods of time after which the samples were washed with water and water soluble metal salts and/or residual sulfates were

analyzed chemically. Element distributions within the oxide layer were obtained from electron microprobe X-ray micrographs. A third set of samples were subjected to surface analysis by X-ray photoelectron spectroscopy. Evolution of SO₂ was monitored throughout many of the hot corrosion tests. Results are interpreted in terms of acid-base fluxing mechanisms. F L

N80-17200* National Aeronautics and Space Administration, Lewis Research Center, Cleveland, Ohio.

ANISOTROPY OF NICKEL-BASE SUPERALLOY SINGLE CRYSTALS

Rebecca A. MacKay (Case Western Reserve Univ., Cleveland), Robert L. Dreshfield, and Richard D. Maier (Case Western Reserve Univ., Cleveland). 1980. 17 p. refs. Prepared for Presentation at 4th Intern. Symp. on Superalloys, Champion, Pa., 21-25 Sep 1980. (NASA-TM-81437, E-327) Avail: NTIS HC A02/MF A01 CSCL 11F

The influence of orientation on the tensile and stress rupture behavior of 52 Mar-M247 single crystals was studied. Tensile tests were performed at temperatures between 23 and 1093 C. stress rupture behavior was examined between 760 and 1038 C. The mechanical behavior of the single crystals was rationalized on the basis of the Schmid factor contours for the operative slip systems and the lattice rotations which the crystals underwent during deformation. The tensile properties correlated well with the appropriate Schmid factor contours. The stress rupture lives at lower testing temperatures were greatly influenced by the lattice rotations required to produce cross slip. A unified analysis was attained for the stress rupture life data generated for the Mar-M247 single crystals at 760 and 774 C under a stress of 724 MPa and the data reported for Mar-M200 single crystals tested at 760 C under a stress of 689 MPa. Based on this analysis, the stereographic triangle was divided into several regions which were rank ordered according to stress rupture life for this temperature regime. Author

N80-18156* National Aeronautics and Space Administration, Lewis Research Center, Cleveland, Ohio.

PRELIMINARY STUDY OF A SOLAR SELECTIVE COATING SYSTEM USING BLACK COBALT OXIDE FOR HIGH TEMPERATURE SOLAR COLLECTORS

G. McDonald. 1980. 16 p. refs. Proposed for presentation at Intern. Conf. on Metal Coatings, San Diego, Calif., 21-25 Apr. 1980; Sponsored by Am. Vacuum Soc. (NASA-TM-81385, E-293) Avail: NTIS HC A02/MF A01 CSCL 10A

Black cobalt oxide coatings (high solar absorptance layer) were deposited on thin layers of silver or gold (low emittance layer) which had been previously deposited on oxidized (diffusion barrier layer) stainless steel substrates. The reflectance properties of these coatings were measured at various thicknesses of cobalt for integrated values of the solar and infrared spectrum. The values of absorptance and emittance were calculated from the measured reflectance values, before and after exposure in air at 650 C for approximately 1000 hours. Absorptance and emittance were interdependent functions of the weight of cobalt oxide. Also, these cobalt oxide/noble metal/oxide diffusion barrier coatings have absorptances greater than 0.90 and emittances of approximately 0.20 even after about 1000 hours at 650 C. Author

N80-18157* National Aeronautics and Space Administration, Lewis Research Center, Cleveland, Ohio.

EFFECTS OF IMPURITIES IN COAL-DERIVED LIQUIDS ON ACCELERATED HOT CORROSION OF SUPERALLOYS Final Report

Daniel L. Deadmore and Carl E. Lowell. Mar. 1980. 30 p. refs. (Contract EF-77-A-01-2593) (NASA-TM-81384; DOE/NASA/2593-79/13; E-292) Avail: NTIS HC A03/MF A01 CSCL 11F

A Mach 0.3 burner rig was used to determine the effects of potential coal derived liquid fuel impurity combustion products on hot corrosion in IN-100, IN-792, IN-738, U-700, Mar-M-509,

and 304 stainless steel. The impurities, added as aqueous solutions to the combustor, were salts of sodium, potassium, vanadium, molybdenum, tungsten, phosphorus, and lead. Extent of attack was determined by metal consumption and compared to the effects of sodium alone. Vanadium, molybdenum, tungsten, phosphorus, and lead in combination with sodium all resulted in increased attack as compared with sodium alone at some temperatures, apparently due in large part to the extension of the formation of liquid deposits. Varying the sodium-potassium ratio had little effect for ratios less than 1:3 for which reduced, but measurable, attack was observed. K.L.

N80-20370* National Aeronautics and Space Administration Lewis Research Center, Cleveland, Ohio
AN EXPERIMENTAL, LOW-COST, SILICON-ALUMINIDE HIGH TEMPERATURE COATING FOR SUPERALLOYS
 Stanley G. Young and Daniel L. Deadmore. 1980. 16 p. refs. To be presented at the Intern. Conf. on Metal Coatings, San Diego, Calif., 21-25 Apr. 1980. Sponsored by the Am. Vacuum Soc. (NASA-TM-81455, E-385) Avail. NTIS HC A02/MF A01 CSCL 11F

An evaluation of a duplex silicon slurry/aluminide coating is presented. The coating is cyclically tested in Mach 1 combustion gases for oxidation and thermal fatigue resistance at 1093 C and in Mach 0.3 gases for hot-corrosion resistance at 900 C. The base metal superalloys are V1A and B-1900. The coated B-1900 specimens performed much better in oxidation than similar specimens coated with aluminides and almost as well as the more expensive Pt-Al and MCrAlY (where M is Ni and/or Co) coatings deposited by the physical vapor deposition process. The coating also provided good hot corrosion protection. Metallographic, X-ray, and electron microprobe studies are used to characterize the coating, determine failure mechanisms, and study some of the changes due to exposure. M.G.

N80-21488* National Aeronautics and Space Administration Lewis Research Center, Cleveland, Ohio
APPLICATION OF SUPERALLOY POWDER METALLURGY FOR AIRCRAFT ENGINES
 R. L. Dreshfield and R. V. Miner, Jr. 1980. 21 p. refs. Proposed for presentation at Intern. Powder Met. Conf., Washington, D.C., 22-27 Jun. 1980. (NASA-TM-81466, E-395) Avail. NTIS HC A02/MF A01 CSCL 11F

In the last decade, Government/Industry programs have advanced powder metallurgy-near net shape technology to permit the use of hot isostatic pressed (HIP) turbine disks in the commercial aircraft fleet. These disks offer a 30% savings of input weight and an 8% savings in cost compared in cast-and-wrought disks. Similar savings were demonstrated for other rotating engine components. A compressor rotor fabricated from hot-die-forged-HIP superalloy billets revealed input weight savings of 54% and cost savings of 35% compared to cast-and-wrought parts. Engine components can be produced from compositions such as Rene 95 and Astroloy by conventional casting and forging, by forging of HIP powder billets, or by direct consolidation of powder by HIP. However, each process produces differences in microstructure or introduces different defects in the parts. As a result, their mechanical properties are not necessarily identical. Acceptance methods should be developed which recognize and account for the differences. A.R.H.

N80-21489* National Aeronautics and Space Administration Lewis Research Center, Cleveland, Ohio
AN INVESTIGATION INTO THE ROLE OF ADHESION IN THE EROSION OF DUCTILE METALS
 William A. Brainard and Joshua Salik. 1980. 20 p. refs. Presented at the 35th Ann. Meeting of the Am. Soc. of Lubrication Engr., Anaheim, Calif., 5-8 May 1980. (NASA-TM-81458, E-028) Avail. NTIS HC A02/MF A01 CSCL 11F

Existing theories of erosion of ductile metals based on cutting and deformation mechanisms predict no material removal at normal incidence which is contradictory to experience. Thus, other

mechanisms may be involved. The possible role of adhesive material transfer during erosion is investigated by both single particle impingement experiments and erosion by streams of particles. Examination of the rebounding particles as well as the eroded surface yields evidence of a significant adhesive mechanism for the ductile metals investigated. Author

N80-21490* National Aeronautics and Space Administration Lewis Research Center, Cleveland, Ohio
TRIBOLOGICAL PROPERTIES OF SPUTTERED MoS₂ SUB 2 FILMS IN RELATION TO FILM MORPHOLOGY
 Talivaldis Spalvins. Mar. 1980. 17 p. refs. Presented at the Intern. Conf. on Met. Coatings, San Diego, 21-25 Apr. 1980. Sponsored by the Am. Vacuum Soc. (NASA-TM-81465, E-394) Avail. NTIS HC A02/MF A01 CSCL 11F

Thin sputter deposited MoS₂ films in the 2000 to 6000 Å thickness range have shown excellent lubricating properties, when sputtering parameters and substrate conditions are properly selected and precisely controlled. The lubricating properties of sputtered MoS₂ films are strongly influenced by their crystalline-amorphous structure, morphology and composition. The coefficient of friction can range from 0.04 which is effective lubrication to 0.4 which reflects an absence of lubricating properties. Visual screening and slight wiping of the as-sputtered MoS₂ film can identify the integrity of the film. An acceptable film displays a black sooty surface appearance whereas an unacceptable film has a highly reflective, gray surface and the film is hard and brittle. Author

N80-21492* National Aeronautics and Space Administration Lewis Research Center, Cleveland, Ohio
FOULING AND THE INHIBITION OF SALT CORROSION
 Final Report
 Daniel L. Deadmore and Carl E. Lowell. Apr. 1980. 16 p. refs. (Contract EF-77-A-01-2593) (NASA-TM-81469, DOE/NASA/2593-80, E-401) Avail. NTIS HC A02/MF A01 CSCL 11F

In an attempt to reduce fouling while retaining the beneficial effects of alkaline earth inhibitors on the hot corrosion of superalloys, the use of both additives and the intermittent application of the inhibitors were evaluated. Additions of alkaline earth compounds to combustion gases containing sodium sulfate were shown to inhibit hot corrosion. However, sulfate deposits can lead to turbine fouling in service. For that reason, dual additives and intermittent inhibitor applications were evaluated to reduce such deposit formation. Silicon in conjunction with vanadium showed some promise. Total deposition was apparently reduced while the inhibition of hot corrosion by barium was unimpaired. The intermittent application of the inhibitor was found to be more effective and controllable. Author

N80-21493* National Aeronautics and Space Administration Lewis Research Center, Cleveland, Ohio
EFFECTS OF FINE POROSITY ON THE FATIGUE BEHAVIOR OF A POWDER METALLURGY SUPERALLOY
 R. V. Miner, Jr. and R. L. Dreshfield. 1980. 25 p. refs. Presented at Ann. Meeting of the Am. Inst. of Mining, Met. and Petroleum Engr., Las Vegas, Nev., 24-28 Feb. 1980. (NASA-TM-81448, E-367) Avail. NTIS HC A02/MF A01 CSCL 11F

Hot isostatically pressed powder metallurgy Astroloy was obtained which contained 1.4 percent fine porosity at the grain boundaries produced by argon entering the powder container during pressing. This material was tested at 650 C in fatigue, creep fatigue, tension, and stress-rupture and the results compared with previous data on sound Astroloy. The pores averaged about 2 micrometers diameter and 20 micrometers spacing. They did influence fatigue crack initiation and produced a more intergranular mode of propagation. However, fatigue life was not drastically reduced. A large 25 micrometers pore in one specimen resulting from a hollow particle did not reduce life by 60 percent. Fatigue behavior of the porous material showed typical correlation with tensile behavior. The plastic strain range life relation was reduced proportionately with the reduction in tensile ductility.

but the elastic strain range-life relation was little changed reflecting the small reduction in σ_{sub}/E for the porous material
R C T

N80-22464* National Aeronautics and Space Administration
Lewis Research Center, Cleveland, Ohio
EFFECTS OF YTTRIUM, ALUMINUM AND CHROMIUM CONCENTRATIONS IN BOND COATINGS ON THE PERFORMANCE OF ZIRCONIA-YTTRIA THERMAL BARRIERS
Stephan Stecura 1980 12 p refs Presented at Intern Conf on Metallurgical Coatings, San Diego, Calif., 21-25 Apr 1980 (NASA-TM-81485, E-423) Avail NTIS HC A02/MF A01 CSCL 11F

A cyclic furnace study was conducted on thermal barrier systems to evaluate the effects of yttrium, chromium, and aluminum in nickel base alloy bond coatings and the effect of bond coating thickness on yttria-stabilized zirconia thermal barrier coating life. Without yttrium in the bond coatings, the zirconia coatings failed very rapidly. Increasing chromium and aluminum in the Ni-Cr-Al-Y bond coatings increased total coating life. This effect was not as great as that due to yttrium. Increased bond coat thickness was also found to increase life
Author

N80-23430* National Aeronautics and Space Administration
Lewis Research Center, Cleveland, Ohio
PRACTICAL APPLICATIONS OF SURFACE ANALYTIC TOOLS IN TRIBOLOGY
John Ferrante 1980 45 p refs Presented at the Intern. Lubrication Conf., San Francisco, 18-21 Aug. 1980, sponsored by ASME and ASLE (NASA-TM-81484, E-422) Avail NTIS HC A03/MF A01 CSCL 20K

A brief description of many of the widely used tools is presented. Of this list, those which have the highest applicability for giving elemental and/or compound analysis for problems of interest in tribology along with being truly surface sensitive (that is less than 10 atomic layers) are presented. The latter group is critiqued in detail in terms of strengths and weaknesses. Emphasis is placed on post facto analysis of experiments performed under real conditions (e.g., in air with lubricants). It is further indicated that such equipment could be used for screening and quality control.
R C T

N80-26426* National Aeronautics and Space Administration
Lewis Research Center, Cleveland, Ohio
IMPROVED PFB OPERATIONS: 400-HOUR TURBINE TEST RESULTS
R. J. Rollbuhler, S. M. Benford, and G. R. Zellars 1980 23 p refs Presented at 6th Intern. Conf. on Fluidized Bed Combust., Atlanta, 9-11 Apr. 1980; sponsored by DOE, Elec. Power Res. Inst., EPA and TVA (NASA-TM-81511, E-260) Avail: NTIS HC A02/MF A01 CSCL 11F

A pressurized fluidized bed (PFB) coal-burning reactor was used to provide hot effluent gases for operation of a small gas turbine. Preliminary tests determined the optimum operating conditions that would result in minimum bed particle carryover in the combustion gases. Solids were removed from the gases before they could be transported into the test turbine by use of a modified two stage cyclone separator. Design changes and refined operation procedures resulted in a significant decrease in particle carryover, from 2800 to 93 ppm (1.5 to 0.05 grains/std cu ft), with minimal drop in gas temperature and pressure. The achievement of stable burn conditions and low solids loadings made possible a 400 hr test of small superalloy rotor, 15 cm (6 in.) in diameter, operating in the effluent. Blades removed and examined metallographically after 200 hr exhibited accelerated oxidation over most of the blade surface, with subsurface alumina penetration to 20 micron m. After 400 hours, average erosion loss was about 25 micron m (1 mil). Sulfide particles, indicating hot corrosion, were present in depletion zones, and their presence corresponded in general to the areas of adherent solids deposit. Sulfidation appears to be a materials problem equal in importance to erosion.
A.R.H.

N80-26433* National Aeronautics and Space Administration
Lewis Research Center, Cleveland, Ohio
THREE DIMENSIONAL FINITE-ELEMENT ELASTIC ANALYSIS OF A THERMALLY CYCLED DOUBLE-EDGE WEDGE GEOMETRY SPECIMEN Final Report, 1 Jun. 1977 - 1 Jan. 1979
Sandra K. Drake, Richard J. Hill, Peter T. Bizon, Jeffrey L. Kladden, and Bruce P. Williams Mar. 1980 49 p refs Prepared in cooperation with AF Wright Aeronautical Labs., Wright-Patterson AFB, Ohio (AF Proj. 3066)
(NASA-TM-81480, AD-A083245, AFWAL-TR-80-2013) Avail NTIS HC A03/MF A01 CSCL 11/6

An elastic stress analysis was performed on a wedge specimen (prismatic bar with double-edge wedge cross-section) subjected to thermal cycles in fluidized beds. Five alloys (IN 100, Mar-M 200, Mar-M 302, NASA TAZ-8A, and Rene 80) subjected to the same thermal cycling condition were analyzed. This condition was alternate 3 minute immersions in fluidized beds maintained at 316 C and 1088 C (600 and 1990 F). The analyses were performed as a joint effort of two laboratories using different models and computer programs (NASTRAN and ISO3DQ). Stress, strain, and temperature results are presented
GRA

N80-31527* National Aeronautics and Space Administration
Lewis Research Center, Cleveland, Ohio
ADHERENCE OF ION BEAM SPUTTER DEPOSITED METAL FILMS ON H-13 STEEL
Michael J. Mirtich 1980 17 p refs Presented at the 27th Natl. Am. Vacuum Soc. Symp., Detroit, 14-17 Oct. 1980 (NASA-TM-81585, E-562) Avail NTIS HC A02/MF A01 CSCL 11F

An electron bombardment argon ion source was used to sputter deposit 17 different metal and metal oxide films ranging in thickness from 1 to 8 micrometers on H-13 steel substrates. The film adherence to the substrate surface was measured using a tensile test apparatus. Comparisons in bond strength were made between ion beam, ion plating, and RF deposited films. A protective coating to prevent heat checking in H-13 steel dies used for aluminum die casting was studied. The results of exposing the coated substrates to temperatures up to 700 degrees are presented.
R K G

N80-32484* National Aeronautics and Space Administration
Lewis Research Center, Cleveland, Ohio
HIGH TOUGHNESS-HIGH STRENGTH IRON ALLOY Patent
Joseph R. Stephens and Walter R. Witzke, inventors (to NASA) Issued 29 Jul. 1980 4 p Filed 25 Jan. 1979 Supersedes N79-19145 (17 - 10, p 1255) Continuation-in-part of abandoned US Patent Appl. SN-803822, filed 6 Jun. 1977 (NASA-Case-LEW-12542-3, US-Patent-4,214,902, US-Patent-Appl-SN-007083, US-Patent-Class-75-124, US-Patent-Appl-SN-803822) Avail: US Patent and Trademark Office CSCL 11F

An iron alloy is provided which exhibits strength and toughness characteristics at cryogenic temperatures. The alloy consists essentially of about 10 to 16 percent by weight nickel, about 0.1 to 1.0 percent by weight aluminum, and 0 to about 3 percent by weight copper, with the balance being essentially iron. The iron alloy is produced by a process which includes cold rolling at room temperature and subsequent heat treatment. Official Gazette of the U.S. Patent and Trademark Office

N80-32486* National Aeronautics and Space Administration
Lewis Research Center, Cleveland, Ohio
FRACTURE TOUGHNESS OF BRITTLE MATERIALS DETERMINED WITH CHEVRON NOTCH SPECIMENS
J. L. Shannon, Jr., R. T. Bursey, D. Munz (Karlsruhe Univ.), and W. S. Pierce [1980] 17 p refs Proposed for presentation at the 5th Intern. Conf. on Fracture, Cannes, France, 29 Mar - 3 Apr. 1981; sponsored by the International Congress on Fracture (NASA-TM-81607, E-600) Avail: NTIS HC A02/MF A01 CSCL 11F

The use of chevron-notch specimens for determining the plane strain fracture toughness ($K_{sub Ic}$) of brittle materials is discussed. Three chevron-notch specimens were investigated: short bar, short rod, and four-point-bend. The dimensionless stress intensity coefficient used in computing $K_{sub Ic}$ is derived for the short bar specimen from the superposition of ligament-dependent and ligament-independent solutions for the straight through crack, and also from experimental compliance calibrations. Coefficients for the four-point-bend specimen were developed by the same superposition procedure, and with additional refinement using the slice model of Bluhm. Short rod specimen stress intensity coefficients were determined only by experimental compliance calibration. Performance of the three chevron-notch specimens and their stress intensity factor relations were evaluated by tests on hot-pressed silicon nitride and sintered aluminum oxide. Results obtained with the short bar and the four-point-bend specimens on silicon nitride are in good agreement and relatively free of specimen geometry and size effects within the range investigated. Results on aluminum oxide were affected by specimen size and chevron-notch geometry, believed due to a rising crack growth resistance curve for the material. Only the results for the short bar specimen are presented in detail. M.G.

N80-32487* National Aeronautics and Space Administration. Lewis Research Center, Cleveland, Ohio.

PERFORMANCE OF TWO-LAYER THERMAL BARRIER SYSTEMS ON DIRECTIONALLY SOLIDIFIED Ni-Al-Mo AND COMPARATIVE EFFECTS OF ALLOY THERMAL EXPANSION ON SYSTEM LIFE

Stephan Secura Washington Oct. 1980 35 p refs
(NASA-TM-81604; E-453) Avail: NTIS HC A03/MF A01 CSCL 11F

A promising two-layer thermal barrier coating system (TBS), Ni-16.4Cr-5.1Al-0.15Y/ZrO₂-6.1Y₂O₃ (all in weight percent), was identified for directionally solidified Ni-Al-Mo (γ/γ' alpha). In cyclic furnace tests at 1095 C this system on γ/γ' alpha was better than Ni-16.4Cr-5.1Al-0.15Y/ZrO₂-7.8Y₂O₃ by about 50 percent. In natural gas - oxygen torch rig tests at 1250 C the ZrO₂-6.1Y₂O₃ coating was better than the ZrO₂-7.8Y₂O₃ coating by 95 percent, on MAR-M509 substrates and by 60 percent on γ/γ' alpha substrates. Decreasing the coefficient of thermal expansion of the substrate material from 17-18x10 to the -6 power/C (MAR-M200 + Hf and MAR-M509) to 11x10 to the -6 power/C (γ/γ' alpha) also resulted in improved TBS life. For example, in natural gas - oxygen torch rig tests at 1250 C, the life of Ni-16.4Cr-5.1Al-0.15Y/ZrO₂-6.1Y₂O₃ was about 30 percent better on γ/γ' alpha than on MAR-M509 substrates. Thus compositional changes in the bond and thermal barrier coatings were shown to have a greater effect on TBS life than does the coefficient of thermal expansion. Author

N80-32488* National Aeronautics and Space Administration. Lewis Research Center, Cleveland, Ohio.

CREEP-RUPTURE BEHAVIOR OF SEVEN IRON-BASE ALLOYS AFTER LONG TERM AGING AT 760 DEG IN LOW PRESSURE HYDROGEN Final Report

Walter R. Witzke and Joseph R. Stephens Aug. 1980 40 p refs
(Contract EC-77-A-31-1040)
(NASA-TM-81534; DOE/NASA/1040-15; E-486) Avail: NTIS HC A03/MF A01 CSCL 11F

Seven candidate iron-base alloys for heater tube application in the Stirling automotive engine were aged for 3500 hours at 760 C in argon and hydrogen. Aging degraded the tensile and creep-rupture properties. The presence of hydrogen during aging caused additional degradation of the rupture strength in fine grain alloys. Based on current design criteria for the Mod 1 Stirling engine, N-155 and 19-9DL are considered the only alloys in this study with strengths adequate for heater tube service at 760 C. Author

N80-32489* National Aeronautics and Space Administration. Lewis Research Center, Cleveland, Ohio.

LONG-TIME CREEP BEHAVIOR OF THE TANTALUM ALLOY

ASTAR 811C

William D. Klopp, Robert H. Titran, and Keith D. Sheffler (Pratt and Whitney Aircraft, East Hartford, Conn.) Sep. 1980 21 p refs

(NASA-TP-1691; E-041) Avail: NTIS CSCL 11F

The high vacuum creep behavior of Astar 811C (Ta-8W-1Re-0.7Hf-0.025C) was studied over the temperature range 800 C to 1700 C as a function of stress, temperature, and grain size in order to develop a relation for predicting long term creep. Primary creep strain was related to time by the Garofalo exponential function, and a second exponential term was developed to describe the tertiary creep portion of the creep curve. No significant periods of secondary (linear) creep were observed. The creep curves were well expressed by a relation that includes terms for primary and tertiary creep. The initial and tertiary creep rates were obtained by differentiating the respective terms from the strain time relation and can be related to temperature by using a dual activation energy to account for lattice and dislocation core diffusion. The strain parameters were determined as power functions of the applied stress. A.R.H.

N80-33555* National Aeronautics and Space Administration. Lewis Research Center, Cleveland, Ohio.

LONG-TIME CREEP BEHAVIOR OF THE NIOBIUM ALLOY C-103

Robert H. Titran and William D. Klopp Oct. 1980 12 p refs
(NASA-TP-1727; E-224) Avail: NTIS HC A02/MF A01 CSCL 11F

The creep behavior of C-103 was studied as a function of stress, temperature, and grain size for test times to 19000 hr. Over the temperature range 827 to 1204 C and the stress range 6.89 to 138 MPa, only tertiary (accelerating) creep was observed. The creep strain epsilon can be related to time t by an exponential relation $\epsilon = \epsilon(0) + K e^{st}$ raised to power (st) - 1, where epsilon (0) is initial creep strain, K is the tertiary creep strain parameter, and s is the tertiary creep rate parameter. The observed stress exponent 2.87 is similar to the three power law generally observed for secondary (linear) creep of Class I solid solutions. The apparent activation energy 374 kJ/g mol is close to that observed for self diffusion of pure niobium. The initial tertiary creep rate was slightly faster for fine grained than for coarse-grained material. The strain parameter K can be expressed as a combination of power functions of stress and grain size and an exponential function of temperature. Strain time curves generated by using calculated values for K and s showed reasonable agreement with observed curves to strains of at least 4 percent. The time to 1 percent strain was related to stress, temperature, and grain size in a similar manner as the initial tertiary creep rate. R.K.G.

N80-33556* National Aeronautics and Space Administration. Lewis Research Center, Cleveland, Ohio.

IMPROVED BOND COATINGS FOR USE WITH THERMAL BARRIER COATINGS Final Report

Michael A. Gedwill Sep. 1980 45 p refs
(Contract EF-77-A-01-2593)
(NASA-TM-81567; DOE/NASA/2593-18; E-532) Avail: NTIS HC A03/MF A01 CSCL 11F

The potential for improving the durability of thermal barrier coatings (TBC's) being developed for coal derived fuel fired gas turbines was studied. Furnace oxidation behavior of plasma deposited bond coatings was improved by increasing the thickness from 0.010 cm to 0.015 cm and by depositing the coatings at 20 kW with argon 3.5 vol % hydrogen arc gas rather than at 11 kW with argon. The most oxidation resistant plasma deposited bond coatings were Ni-14, 1Cr-13.4Al-0.10Zr, Ni-14.3Cr-14.4Al, 0.16Y, and Ni-15.8Cr-12.8Al-0.36Y on B-1900 + Hf and Ni-30.9Cr-11.1Al-0.48Y on MAR-M-509. The oxidation resistant bond coatings improved TBC life when the coatings were deposited on the specimens supported on a nail bed fixture during coating. Author

A80-10043 * The erosion/corrosion of small superalloy turbine rotors operating in the effluent of a PFB coal combustor. G.

R. Zellars, S. M. Benford, A. P. Rowe, and C. E. Lowell (NASA, Lewis Research Center, Cleveland, Ohio). *U.S. Department of Energy and Electric Power Research Institute, Conference on Advanced Materials for Alternate Fuel Capable Directly Fired Heat Engines, Castine, Me., July 30-Aug. 3, 1979, Paper, 25 p.*, 10 refs.

The operation of a turbine in the effluent of a pressurized fluidized bed (PFB) coal combustor presents serious materials problems. Synergistic erosion/corrosion and deposition/corrosion interactions may favor the growth of erosion-resistant oxides on blade surfaces, but brittle cracking of these oxides may be an important source of damage along heavy particle paths. Integrally cast alloy 713LC and IN792 + Hf superalloy turbine rotors in a single-stage turbine with 6% partial admittance have been operated in the effluent of a PFB coal combustor for up to 164 hr. The rotor erosion pattern exhibits heavy particle separation with severe erosion at the leading edge, pressure side center, and suction side trailing edge at the tip. The erosion distribution pattern gives a spectrum of erosion/oxidation/deposition as a function of blade position. The data suggest that preferential degradation paths may exist even under the targeted lower loadings (less than 20 ppm). S.D.

A80-10391 * # Preliminary results of the mission profile life test of a 30 cm Hg bombardment thruster. R. T. Bechtel (NASA, Lewis Research Center, Solar Electric Propulsion Office, Cleveland, Ohio) and E. L. James (Xerox Electro-Optical Systems, Pasadena, Calif.). *Princeton University, AIAA, and DGLR, International Electric Propulsion Conference, 14th, Princeton, N.J., Oct. 30-Nov. 1, 1979, AIAA Paper 79-2078, 14 p.*, 14 refs.

The paper deals with some preliminary results of the Mission Profile Life Test planned to conduct a program of long-term test segments of 30-cm diameter thrusters and power processing units under computer control. Thruster performance data and other operational characteristics taken at various times during a test segment are compared and the results are evaluated in light of the life-timing mechanisms. Thruster control algorithms are also presented. The first test segment completed 2700 hr of a planned 4000 hr test with a J-series 30-cm thruster. The last 1600 hr used a functional model power processing unit (PPU) operated in vacuum. The thruster-PPU was controlled by a computer with software developed to control start-ups, throttling, and variety of off-normal conditions. V.T.

A80-13067 * # Metal-dielectric interactions. D. H. Buckley (NASA, Lewis Research Center, Cleveland, Ohio). *National Research Council, Conference on Electrical Insulation and Dielectric Phenomena, Whitehaven, Pa., Oct. 21-25, 1979, Paper, 22 p.*, 15 refs.

There is a wide variety of situations wherein metals are in solid state contact with dielectric materials. The paper reviews some of the factors that influence solid state interactions for metals in contact with dielectric surfaces. Since surfaces play an important part in these reactions, the use of analytical tools in characterizing surfaces is discussed. Adhesion, friction, and wear are utilized as indicators of the nature of interfacial bonding between metals and dielectrics can be effectively determined with adhesion and friction force measurements. Films present on the surface, such as oxygen or water vapor, markedly alter adhesive bond strength which in turn affects friction force and interfacial fracture when attempts are made to separate the contact regions. Analytical surface tools such as the field ion microscope, Auger emission spectroscopy, and X-ray photoelectron spectroscopy are very effective in providing insight into the effect of contact on the surfaces of metals and dielectrics. S.D.

A80-13071 * # Some TEM observations of Al₂O₃ scales formed on NiCrAl alloys. J. Smialek (NASA, Lewis Research Center, Cleveland, Ohio) and R. Gibala (NASA, Lewis Research Center; Case Western Reserve University, Cleveland, Ohio). *Gordon Research Conference on Corrosion, New London, N.H., July 23-27, 1979, Paper, 32 p.*, 26 refs.

The microstructural development of Al₂O₃ scales on NiCrAl

alloys has been examined by transmission electron microscopy. Voids have been observed within grains in scales formed on a pure NiCrAl alloy. Both voids and oxide grains grew measurably with oxidation time at 1100 C. The size and amount of porosity decreased towards the oxide-metal growth interface. It was postulated that the voids resulted from an excess number of oxygen vacancies near the oxide-metal interface. Short-circuit diffusion paths were discussed in reference to current growth stress models for oxide scales. Transient oxidations of pure, Y-doped, and Zr-doped NiCrAl was also examined. Oriented alpha-(Al,Cr)₂O₃ and Ni(Al,Cr)₂O₄ scales often coexisted in layered structures on all three alloys. Close-packed oxygen planes and directions in the corundum and spinel layers were parallel. The close relationships between oxide layers provided a gradual transition from initial transient scales to steady state Al₂O₃ growth. (Author)

A80-13277 * # Elevated temperature flow strength, creep resistance and diffusion welding characteristics of Ti-6Al-2Nb-1Ta-0.8Mo. J. D. Whittenberger and T. J. Moore (NASA, Lewis Research Center, Materials and Structures Div., Cleveland, Ohio). *Metallurgical Transactions A - Physical Metallurgy and Materials Science*, vol. 10A, Nov. 1979, p. 1597-1605, 10 refs.

A study of the flow strength, creep resistance and diffusion welding characteristics of the titanium alloy Ti-6Al-2Nb-1Ta-0.8Mo has been conducted. Two mill-processed forms of this alloy were examined. The forged material had been processed above the beta transus (approximately 1275 K) while the rolled form had been subjected to work below the beta transus. Between 1150 and 1250 K, the forged material was stronger and more creep resistant than the rolled alloy. Both forms exhibit superplastic characteristics in this temperature range. Strain measurements during diffusion welding experiments at 1200 K reveal that weld interfaces have no measurable effect on the overall creep deformation. Significant deformation appears to be necessary to produce a quality diffusion weld between superplastic materials. A 'soft' interlayer inserted between faying surfaces would seemingly allow manufacture of quality diffusion welds with little overall deformation. (Author)

A80-14445 * Hot corrosion of four superalloys - HA-188, S-57, IN-617, and TD-NiCrAl. G. J. Santoro (NASA, Lewis Research Center, Cleveland, Ohio). *Oxidation of Metals*, vol. 13, Oct. 1979, p. 405-435, 18 refs.

Cyclic oxidation and hot corrosion tests of two cobalt-base and two nickel-base alloys are reported. The alloys were exposed to maximum temperatures of 900 and 1000 C in a Mach 0.3 burner rig whose flame was doped with various concentrations of sea salt and sodium sulfate for hot corrosion tests. The test data were subjected to a regression analysis for the development of model equations relating corrosion to temperature and for the effects of salt concentration and composition on corrosion. The corrosion resistance varied with temperature, sea salt concentration, and salt composition, concluding that the S-57 cobalt-base alloy was the most hot corrosion-resistant alloy, and the TD-NiCrAl nickel-base alloy was the least resistant. However, under straight oxidation conditions, the TD-NiCrAl was most resistant, while S-57 was the least resistant alloy. A.T.

A80-25274 * Improved adhesion of sputtered refractory carbides to metal substrates. D. R. Wheeler and W. A. Brainard (NASA, Lewis Research Center, Cleveland, Ohio). *Wear*, vol. 58, Feb. 1980, p. 341-358, 18 refs.

Sputtered coatings of the refractory metal carbides are of great interest for applications where hard wear-resistant materials are desired. The usefulness of sputtered refractory carbides is often limited in practice by spalling or interfacial separation. In this work improvements in the adherence of refractory carbides on iron, nickel and titanium base alloys were obtained by using oxidation, reactive sputtering or sputtered interlayers to alter the coating-substrate interfacial region. X-ray photoelectron spectroscopy and argon ion

etching were used to characterize the interfacial regions, and an attempt was made to correlate adherence as measured in wear tests with the chemical nature of the interface. (Author)

A80-26465 * The effect of zirconium on the isothermal oxidation of nominal Ni-14Cr-24Al alloys. A. S. Kahn, C. E. Lowell, and C. A. Barrett (NASA, Lewis Research Center, Cleveland, Ohio). *Electrochemical Society, Journal*, vol. 127, Mar. 1980, p. 670-679. 20 refs.

The isothermal oxidation of Ni-14Cr-24Al-xZr-type alloys was performed in still air at 1100, 1150, and 1200 C for times up to 200 hr. The zirconium content of the alloys varied from 0.063 atom percent (a/o). The oxidized surfaces were studied by optical microscopy, X-ray diffraction, and scanning electron microscopy. The base alloy was an alumina former with the zirconium-containing alloys also developing some ZrO₂. The addition of zirconium above 0.066 a/o increased the rate of weight gain relative to the base alloy. Due to oxide penetration, the weight gain increased with Zr content; however, the scale thickness did not increase. The Zr did increase the adherence of the oxide, particularly at 1200 C. The delta W/A vs. time data fit the parabolic model of oxidation. The specific diffusion mechanism operative could not be identified by analysis of the calculated activation energies. Measurements of the Al₂O₃ scale lattice constants yielded the same values for all alloys. (Author)

A80-29990 * # Effects of thermally induced porosity on an as-HIP powder metallurgy superalloy. R. L. Dreshfield and R. V. Miner, Jr. (NASA, Lewis Research Center, Cleveland, Ohio). *American Institute of Mining, Metallurgical and Petroleum Engineers, Annual Meeting, Las Vegas, Nev., Feb. 24-28, 1980, Paper*. 18 p.

The effect of thermally induced porosity on the mechanical properties of an as-hot-isostatically pressed and heat-treated pressing made from low carbon Astroloy is examined. Tensile, stress-rupture, creep, and low cycle fatigue tests were performed and the results were compared with industrial acceptance criteria. It is shown that the porous pressing has a porosity gradient from the rim to the bore with the bore having 1-1/2% greater porosity. Mechanical properties of the test ring below acceptance level are tensile reduction in area at room temperature and 538 C and time for 0.1% creep at 704 C. It is also found that the strength, ductility, and rupture life of the rim are slightly inferior to those of the rim of the sound pressings, while those of the bore are generally below the acceptable level. At strain ranges typical of commercial aircraft engines, the low cycle fatigue life of the rim of the porous pressings is slightly lower than that of the sound pressings. L.M.

A80-35495 * # Effects of fine porosity on the fatigue behavior of a powder metallurgy superalloy. R. V. Miner and R. L. Dreshfield (NASA, Lewis Research Center, Cleveland, Ohio). *American Institute of Mining, Metallurgical and Petroleum Engineers, Annual Meeting, 109th, Las Vegas, Nev., Feb. 25-28, 1980, Paper*. 23 p. 14 refs.

Hot-isostatically-pressed powder-metallurgy Astroloy was obtained which contained 1.4 percent porosity at the grain boundaries produced by argon entering the powder container during pressing. This material was tested at 650 C in fatigue, creep-fatigue, tension, and stress-rupture and the results compared with data on sound Astroloy. They influenced fatigue crack initiation and produced a more intergranular mode of propagation but fatigue life was not drastically reduced. Fatigue behavior of the porous material showed typical correlation with tensile behavior. The plastic strain range-life relation was reduced proportionately with the reduction in tensile ductility, but the elastic strain range-life relation was changed little. (Author)

A80-35500 * # Preliminary study of a solar selective coating system using black cobalt oxide for high temperature solar collectors. G. McDonald (NASA, Lewis Research Center, Cleveland, Ohio).

American Vacuum Society, International Conference on Metallurgical Coatings, San Diego, Calif., Apr. 21-25, 1980, Paper. 14 p. 8 refs.

Black cobalt oxide coatings were deposited on thin layers of silver or gold which had been deposited on oxidized stainless steel substrates. The reflectance properties of these coatings were measured at various thicknesses of cobalt oxide for integrated values of the solar and infrared spectrum. The values of absorptance and emittance were calculated from the measured reflectance values before and after exposure in air at 650 C for 1000 hours. Also, these cobalt oxide/noble metal/oxide diffusion barrier coatings have absorptances greater than 0.90 and emittances of approximately 0.20 even after about 1000 hours at 650 C. (Author)

A80-35501 * # An experimental, low-cost, silicon-aluminide high-temperature coating for superalloys. S. G. Young and D. L. Deadmore (NASA, Lewis Research Center, Cleveland, Ohio). *American Vacuum Society, International Conference on Metallurgical Coatings, San Diego, Calif., Apr. 21-25, 1980, Paper*. 14 p. 19 refs.

A duplex silicon-slurry/aluminide coating has been developed and cyclically tested in Mach 1 combustion gases for oxidation and thermal fatigue resistance at 1093 C and Mach 0.3 gases and hot-corrosion resistance at 900 C. The base-metal superalloys were V1A and B-1900. The coated B-1900 specimens were found to perform much better in oxidation than similar specimens coated with aluminides, and almost as well as the more expensive Pt-Al and MCrAlY (where M is Ni and/or Co) coatings deposited by the physical vapor deposition process. The coatings also provided good hot-corrosion protection. V.P.

A80-35900 * # Effects of yttrium, aluminum and chromium concentrations in bond coatings on the performance of zirconia-yttria thermal barriers. S. Stecura (NASA, Lewis Research Center, Cleveland, Ohio). *American Vacuum Society, International Conference on Metallurgical Coatings, San Diego, Calif., Apr. 21-25, 1980, Paper*. 10 p. 5 refs.

A cyclic furnace study was conducted on thermal barrier systems to evaluate the effects of yttrium, chromium and aluminum in nickel-base alloy bond coatings and the effect of bond coating thickness on yttria-stabilized zirconia thermal barrier coating life. Without yttrium in the bond coatings, the zirconia coatings failed very rapidly. Increasing chromium and aluminum in the Ni-Cr-Al-Y bond coatings increased total coating life. This effect was not as great as that due to yttrium. Increased bond coat thickness was also found to increase life. (Author)

A80-40962 * Stability of several oxide dispersion strengthened alloys and a directionally solidified gamma/gamma prime-alpha eutectic alloy in a thermal gradient. G. Staniek (Deutsche Forschungs- und Versuchsanstalt für Luft- und Raumfahrt, Cologne, West Germany) and J. D. Whittenberger (NASA, Lewis Research Center, Cleveland, Ohio). *Zeitschrift für Werkstofftechnik*, vol. 11, June 1980, p. 197-205. 16 refs. Research supported by the Alexander von Humboldt-Stiftung and Bundesministerium für Forschung und Technologie.

Thermal gradient testing of three oxide dispersion strengthened alloys (two Ni-base alloys, MA 754 and MA 6000 E, and the Fe-base MA 956) and the directionally solidified eutectic alloy, gamma/gamma prime-alpha, have been conducted. Experiments were carried out with maximum temperatures up to 1200 C and thermal gradients on the order of 100 C/mm. The oxide dispersion strengthened alloys were difficult to test because the thermal stresses promoted crack nucleation and growth; thus the ability of these alloys to maintain a thermal gradient may be limited. The stability of individual fibers in gamma/gamma prime-alpha was excellent; however, microstructural changes were observed in the vicinity of grain boundaries. Similar structures were also observed in isothermally annealed material; therefore thermal gradients do not affect the microstructure of gamma/gamma prime-alpha in any significant manner. (Author)

A80-42262 * # Effect of sodium, potassium, magnesium, calcium, and chlorine on the high temperature corrosion of IN-100, U-700, IN-792, and MAR M-609. C. E. Lowell, S. M. Sidik, and D. L. Deadmore (NASA, Lewis Research Center, Cleveland, Ohio). *American Society of Mechanical Engineers, Gas Turbine Conference and Products Show, New Orleans, La., Mar. 10-13, 1980, Paper 80-GT-150*. 18 p. 15 refs. Members, \$1.50; nonmembers, \$3.00.

A80-51573 * # Anisotropy of nickel-base superalloy single crystals. R. A. MacKay, R. D. Maier (Case Western Reserve University, Cleveland, Ohio), and R. L. Dreshfield (NASA, Lewis Research Center, Cleveland, Ohio). *International Symposium on Superalloys, 4th, Champion, Pa., Sept. 21-25, 1980, Paper*. 15 p. 6 refs. Grant No. NSG-3246.

The effects of crystal orientation on the mechanical properties of single crystals of the nickel-based superalloy Mar-M247 are investigated. Tensile tests at temperatures from 23 to 1093 C and stress rupture tests at temperatures from 760 to 1038 C were performed for 52 single crystals at various orientations. During tensile testing between 23 and 760 C, single crystals with high Schmid factors were found to be favorably oriented for slip and to exhibit lower strength and higher ductility than those with low Schmid factors. Crystals which required large rotations to become oriented for cross slip were observed to have the shortest stress rupture lives at 760 C, while those which required little or no rotation had the longest lives. In addition, stereographic triangles obtained for Mar-M247 and Mar-M200 single crystals reveal that crystals with orientations near the -111 had the highest lives, those near the 001 had high lives, and those near the 011 had low lives.

A.L.W.

N80-13218 * # Inco Research and Development Center, Suffern, N. Y.

CHARACTERIZATION OF AN OXIDE DISPERSION STRENGTHENED SUPERALLOY, MA-6000E, FOR TURBINE BLADE APPLICATIONS Final Report

Y. G. Kim and H. F. Merrick May 1979 37 p refs

(Contract NAS3-20093)

(NASA-CR-159493) Avail: NTIS HC A03/MF A01 CSCL 11F

Alloy MA 6000E was developed by the mechanical alloying process for turbine blade applications. The nominal composition of the experimental alloy is Ni-15Cr-2Mo-4W-4.5Al-2.5Ti-2Ta-1.5Zr-0.5C-0.1B-1.1Y2O3. The 1000 hour rupture strength in the longitudinal direction is about 145 MPa at 1093 C and about 483 MPa at 760 C. The alloy displays normal three-stage creep behavior. Typically the creep elongation is 3.5% at 760 C and 2% at 1093 C. The alloy is notch ductile (K sub 1 = 3.5). The rupture properties of the alloy are not significantly degraded by thermal cycling or prior stress isothermal exposure. The alloy also has excellent longitudinal high and low cycle fatigue resistance. Limited testing indicates that MA 6000E possesses good off-axis mechanical properties. The transverse tensile elongation at 760 C is about 3%. The 100 hour transverse rupture strength is 331 MPa at 760 C and about 55 MPa at 1093 C.

A.R.H.

N80-14235 * # AiResearch Mfg. Co., Phoenix, Ariz.
ABRADABLE COMPRESSOR AND TURBINE SEALS, VOLUME 1

D. V. Sundberg, R. E. Dennis, and L. G. Hurst May 1979 178 p

(Contract NAS3-20073)

(NASA-CR-159600; AiResearch-21-3213-1) Avail: NTIS HC A09/MF A01 CSCL 11A

The application and advantages of abradable coatings as gas-path seals in a general aviation turbine engine were evaluated for use on the high-pressure compressor, the high-pressure turbine, and the low-pressure turbine shrouds. Topics covered include: (1) the initial selection of candidate materials for interim full-scale engine testing; (2) interim engine testing of the initially selected materials and additional candidate materials; (3) the design of the component required to adapt the hardware to permit full-scale

engine testing of the most promising materials; (4) finalization of the fabrication methods used in the manufacture of engine test hardware; and (5) the manufacture of the hardware necessary to support the final full-scale engine tests.

A.R.H.

N80-15233 * # Pittsburgh Univ. Pa Dept of Metallurgical and Materials Engineering

AN INVESTIGATION OF THE INITIATION STAGE OF HOT CORROSION IN Ni-BASE ALLOYS Semiannual Report, 1 Mar. 1979 - 31 Aug. 1979

T T Huang and G H Meier 1979 70047 p refs

(Grant NSG 3214)

(NASA CR 159718. SETEC MME 79 61. SAR 2) Avail NTIS HC A03/MF A01 CSCL 11F

The commercial nickel base alloy, IN-738, and high purity laboratory alloys were prepared to simulate the effects of the major elements in IN-738. Results indicate that the initiation of hot corrosion attack of IN-738 and other similar alloys is the result of local penetration of molten salt through the protective oxide scale.

R.C.T.

N80-16142 * # National Aeronautics and Space Administration, Marshall Space Flight Center, Huntsville, Ala.

STRESS CORROSION CRACKING EVALUATION OF MARTENSITIC PRECIPITATION HARDENING STAINLESS STEELS

T. S. Humphries and E. E. Nelson Jan. 1980 34 p refs

(NASA-TM-78257) Avail: NTIS HC A03/MF A01 CSCL 11F

The resistance of the martensitic precipitation hardening stainless steels PH13-8Mo, 15-5PH, and 17-4PH to stress corrosion cracking was investigated. Round tensile and c-ring type specimens taken from several heats of the three alloys were stressed up to 100 percent of their yield strengths and exposed to alternate immersion in salt water, to salt spray, and to a seacoast environment. The results indicate that 15-5PH is highly resistant to stress corrosion cracking in conditions H1000 and H1050 and is moderately resistant in condition H900. The stress corrosion cracking resistance of PH13-8Mo and 17-4PH stainless steels in conditions H1000 and H1050 was sensitive to mill heats and ranged from low to high among the several heats included in the tests. Based on a comparison with data from seacoast environmental tests, it is apparent that alternate immersion in 3.5 percent salt water is not a suitable medium for accelerated stress corrosion testing of these pH stainless steels.

A.R.H.

N80-18155 * # United Technologies Research Center, East Hartford, Conn.

STUDY OF THE EFFECTS OF GASEOUS ENVIRONMENTS ON THE HOT CORROSION OF SUPERALLOY MATERIALS Final Report

John G. Smeggil and N. S. Bornstein 5 Feb. 1980 93 p

(Contract NAS3-21376)

(NASA-CR-159747; R79-914387-4)

Avail: NTIS

HC A05/MF A01 CSCL 11F

The effect of the gaseous corrodent NaCl on the high temperature oxidation and sodium sulfate induced hot corrosion behavior of alumina formers, chromia formers, and the superalloy B-1900 was examined. Isothermal experiments were conducted at 900 C and 1050 C in air in the presence and absence of NaCl vapors. Microstructural changes in oxide morphology and increased rates of oxidation were observed when NaCl(g) was present. It is hypothesized that the accelerated rates of oxidation are the result of removal of aluminum from the scale substrate interface and the weakening of the scale substrate bonds. The aluminum removed was redeposited on the surfaces in the form of alumina whiskers. For the superalloy B-1900, alumina whiskers are also formed, and the alloy oxidizes at catastrophic rates. In the case of Ni-25Cr alloy, NaCl vapors interact with the scale depleting it of chromium.

R.C.T.

N80-26416* IIT Research Inst., Chicago, Ill. Materials Technology Div.

THERMAL FATIGUE AND OXIDATION DATA OF OXIDE DISPERSION-STRENGTHENED ALLOYS

K. E. Hofer, V. L. Hill, and V. E. Humphreys Mar. 1980 42 p refs

(Contract NAS3-17787)

(NASA-CR-159842; IITRI-M6001-82)

Avail: NTIS

HC A03/MF A01 CSCL 11F

Thermal fatigue and oxidation data were obtained on 24 specimens representing 9 discrete oxide dispersion-strengthened alloy compositions or fabricating techniques. Double edge wedge specimens, both bare metal and coated for each system, were cycled between fluidized beds maintained at 1130 C with a three minute immersion in each bed. The systems included alloys identified as 262 in hardness of HRC 38; 264 in hardness of HRC 38, 40 and 43; 265 HRC 39, 266 of HRC 37 and 40; 754; and 956. Specimens in the bare condition of 265 HRC 39 and 266 HRC 37 survived 6000 cycles without cracking on the small radius of the double edge wedge specimen. A coated specimen of 262 HRC 38, 266 HRC 37 and 266 HRC40 also survived 6000 cycles without cracking. A duplicate coated specimen of 262 HRC 38 alloy survived 5250 cycles before cracks appeared. All the alloys showed little weight change compared compared to alloys tested in prior programs. Author

N80-26427* Pittsburgh Univ., Pa. Dept. of Metallurgical and Materials Engineering.

HOT CORROSION OF Co-Cr, Co-Cr-Al, AND Ni-Cr ALLOYS IN THE TEMPERATURE RANGE OF 700-750 DEG C
Semiannual Report, 1 Sep. 1979 - 29 Feb. 1980

K. T. Chiang and G. H. Meier Jun. 1980 29 p

(Grant NSG-3214)

(NASA-CR-159689; SAR-3) Avail: NTIS HC A03/MF A01 CSCL 11F

The effect of SO₃ pressure in the gas phase on the Na₂SO₄ induced hot corrosion of Co-Cr, Ni-Cr, and Co-Cr-Al alloys was studied in the temperature range 700 to 750 C. The degradation of the Co-Cr and Ni-Cr alloys was found to be associated with the formation of liquid mixed sulfates (CoSO₄-Na₂SO₄ or NiSO₄-Na₂SO₄) which provided a selective dissolution of the Co or Ni and a subsequent sulfidation oxidation mode of attack which prevented the maintenance of a protective Cr₂O₃ film. A clear mechanism was not developed for the degradation of Co-Cr-Al alloys. A pitting corrosion morphology was induced by a number of different mechanisms. B.D.

N80-28499* General Electric Co., Cincinnati, Ohio. Aircraft Engine Group.

MATERIALS FOR ADVANCED TURBINE ENGINES. VOLUME 1: POWER METALLURGY RENE 95 ROTATING TURBINE ENGINE PARTS Final Report

W. R. Pfouts, C. E. Shamblen, J. S. Mosier, R. E. Peebles, and R. W. Gorsler Jun. 1979 358 p 2 Vol.

(Contract NAS3-20074)

(NASA-CR-159802; R79AEG416-Vol-1)

Avail: NTIS

HC A16/MF A01 CSCL 11F

An attempt was made to improve methods for producing powder metallurgy aircraft gas turbine engine parts from the nickel base superalloy known as Rene 95. The parts produced were the high pressure turbine aft shaft for the CF6-50 engine and the stages 5 through 9 compressor disk forgings for the CFM56/F101 engines. A 50% cost reduction was achieved as compared to conventional cast and wrought processing practices. An integrated effort involving several powder producers and a major forging source were included. R.C.T.

N80-30482* Pratt and Whitney Aircraft Group, West Palm Beach, Fla.

EVALUATION OF THE CYCLIC BEHAVIOR OF AIRCRAFT TURBINE DISK ALLOYS, PART 2 Contractor Report, Jul. 1978 - Mar. 1980

B. A. Cowles and J. R. Warren Jul. 1980 196 p refs

(Contract NAS3-21379)

(NASA-CR-165123; PWA-FR-13153-Pt-2)

Avail: NTIS

HC A09/MF A01 CSCL 11F

Several nickel-base aircraft turbine disk superalloys were evaluated at 650 C for resistance to fatigue crack initiation and propagation under cyclic and cyclic/dwell conditions. Controlled strain low cycle fatigue (LCF) and controlled load crack propagation tests were performed and results utilized to provide a direct comparison among the alloys. Tests were performed on selected alloys to evaluate the effects of hold times, mean stresses, stress-dwell cycle types, inert environment, and contractor test methods. At the lower total strain ranges of interest, the alloys exhibited generally increasing initiation life with increasing tensile strength for both cyclic (0.33 Hz) and cyclic/dwell (900-sec hold per cycle) conditions. Rank order of the alloys by LCF initiation life changed substantially at higher strain ranges, approaching the rank order expected from monotonic tensile ductilities. The effect of the 900 sec (15 min) hold time fatigue life varied significantly from alloy to alloy. Generally, the higher-strength, finer-grained alloys exhibited more significant reductions in fatigue life due to the dwell. The effects of mean strain were found to be negligible and the effects of mean stress were pronounced. At high strain ranges the mean stress was near zero and did not contribute to reduction in life. At low strain ranges, however, mean stresses were large and significant reductions in LCF lives occurred. L.F.M.

A80-44108 * Development of a high strength hot isostatically pressed (HIP) disk alloy, MERL 76. D. J. Evans and R. D. Eng (United Technologies Corp., Pratt and Whitney Aircraft Group, East Hartford, Conn.). *Metal Powder Industries Federation and American Powder Institute, International Powder Metallurgy Conference and Exhibition, Washington, D.C., June 22-27, 1980, Paper. 13 p.* Contract No. NAS3-20072.

A nickel based powder metal disk alloy developed for use in advanced commercial gas turbines is described. Consideration is given to final alloy chemistry modifications made to achieve a desirable balance between tensile strength and stress rupture life and ductility. The effects of post-consolidation heat treatment are discussed, the preliminary mechanical properties obtained from full-scale turbine disks are presented. V.T.

A80-45825 * Development of exothermically cast single-crystal Mar-M 247 and derivative alloys. T. E. Strangman, G. S. Hoppin, III (AiResearch Manufacturing Company of Arizona, Phoenix, Ariz.), C. M. Phipps (Jetshapes, Inc., Rockleigh, N.J.), K. Harris, and R. E. Schwer (Cannon-Muskegon Corp., Muskegon, Mich.). *Metallurgical Society of AIME and American Society for Metals, International Symposium on Superalloys, 4th, Champion, Pa., Sept. 21-25, 1980, Paper. 14 p. 11 refs.* Contract No. NAS3-20073. (AIRESARCH-21-3469)

A low-cost, exothermic directional-solidification (DS) process was developed to produce single-crystal (SC) Mar-M 247 high-pressure turbine blades. Stress-rupture data indicated that SC Mar-M 247 provides only marginal improvements in longitudinal strength relative to the columnar grained DS material. Removal of grain boundary strengthening elements (B, C, Zr, Hf) from the Mar-M 247 composition (which are also melting point depressants) permitted the alloy to be solutioned at significantly higher temperatures. An order of magnitude improvement in rupture life relative to SC Mar-M 247 was observed for several derivative alloys at 103.5 MPa (15 KSI) and 1093 C. Rupture lives of the modified SC alloys were significantly affected by both alloy purity and heat treatment. Critical aspects of vacuum induction refining, exothermic casting technology, alloy development and heat treatment, which contributed to this new class of turbine blades, are reviewed. (Author)

27 NONMETALLIC MATERIALS

Includes physical, chemical, and mechanical properties of plastics, elastomers, lubricants, polymers, textiles, adhesives, and ceramic materials.

N80-13254* National Aeronautics and Space Administration, Lewis Research Center, Cleveland, Ohio.

CHARACTERIZATION AND PROPERTIES OF CONTROLLED NUCLEATION THERMOCHEMICAL DEPOSITED (CNTD) SILICON CARBIDE

Sunil Dutta, Roy W. Rice (Naval Res. Lab., Washington, D.C.), Henry C. Graham (AFML, Wright-Patterson AFB, Ohio), and Madan C. Mendiratta (Systems Res. Lab., Dayton, Ohio) 1978 24 p refs Presented at 80th Annual Meeting of the Basic Sci. Div. of the Am. Ceramic Soc., Detroit, 6-11 May 1978 (NASA-TM-79277; E-210) Avail: NTIS HC A02/MF A01 CSCL 11G

The microstructure of controlled nucleation thermochemical deposition (CNTD) - SiC material was studied and the room temperature and high temperature bend strength and oxidation resistance was evaluated. Utilizing the CNTD process, ultrafine grained (0.01-0.1 mm) SiC was deposited on W - wires (0.5 mm diameter by 20 cm long) as substrates. The deposited SiC rods had superior surface smoothness and were without any macrocolumnar growth commonly found in conventional CVD material. At both room and high temperature (1200 - 1380 C), the CNTD - SiC exhibited bend strength approximately 200,000 psi (1380 MPa), several times higher than that of hot pressed, sintered, or CVD SiC. The excellent retention of strength at high temperature was attributed to the high purity and fine grain size of the SiC deposit and the apparent absence of grain growth at elevated temperatures. The rates of weight change for CNTD - SiC during oxidation were lower than for NC-203 (hot pressed SiC), higher than for GE's CVD - SiC, and considerably below those for HS-130 (hot pressed Si₃N₄). The high purity, fully dense, and stable grain size CNTD - SiC material shows potential for high temperature structural applications; however problem areas might include: scaling the process to make larger parts, deposition on removable substrates, and the possible residual tensile stress. J.M.S.

N80-13256* National Aeronautics and Space Administration, Lewis Research Center, Cleveland, Ohio.

REACTIONS OF CALCIUM ORTHOSILICATE AND BARIUM ZIRCONATE WITH OXIDES AND SULFATES OF VARIOUS ELEMENTS

Isidor Zaplatynsky Oct. 1979 16 p refs Prepared for DOE (NASA-TM-79272; E-192; DOE/NASA/2593-79/9) Avail: NTIS HC A02/MF A01 CSCL 11G

Calcium orthosilicate and barium zirconate were evaluated as the insulation layer of thermal barrier coatings for air cooled gas turbine components. Their reactions with various oxides and sulfates were studied at 1100 C and 1300 C for times ranging up to 400 and 200 hours, respectively. These oxides and sulfates represent potential impurities or additives in gas turbine fuels and in turbine combustion air, as well as elements of potential bond coat alloys. The phase compositions of the reaction products were determined by X-ray diffraction analysis. BaZrO₃ and 2CaO-SiO₂ both reacted with P₂O₅, V₂O₅, Cr₂O₃, Al₂O₃, and SiO₂. In addition, 2CaO-SiO₂ reacted with Na₂O, BaO, MgO, and CoO and BaZrO₃ reacted with Fe₂O₃. K.L.

N80-14249* National Aeronautics and Space Administration, Lewis Research Center, Cleveland, Ohio.

FRICTION AND WEAR OF PLASMA-SPRAYED COATINGS CONTAINING COBALT ALLOYS FROM 25 DEG TO 650 DEG IN AIR

Harold E. Sliney and Thomas P. Jacobson 1979 20 p refs (NASA-TM-79316; E-189) Avail: NTIS HC A02/MF A01 CSCL 11F

Four different compositions of self-lubricating, plasma-sprayed, composite coatings with calcium fluoride dispersed throughout

cobalt alloy-silver matrices were evaluated on a friction and wear apparatus. In addition, coatings of the cobalt alloys alone and one coating with a nickel alloy-silver matrix were evaluated for comparison. The wear specimens consisted of two, diametrically opposed, flat rub shoes sliding on the coated, cylindrical surface of a rotating disk. Two of the cobalt composite coatings gave a friction coefficient of about 0.25 and low wear at room temperature, 400 and 650 C. Wear rates were lower than those of the cobalt alloys alone or the nickel alloy composite coating. However, oxidation limited the maximum useful temperature of the cobalt composite coating to about 650 C compared to about 900 C for the nickel composite coating.

Author

N80-16165* National Aeronautics and Space Administration, Lewis Research Center, Cleveland, Ohio.

MECHANISMS OF LUBRICATION AND WEAR OF A BONDED SOLID LUBRICANT FILM

Robert L. Fusaro 1980 40 p refs Proposed for presentation at 35th Ann. Meeting of the Am. Soc. of Lubrication Engr., Anaheim, Calif., 5-8 May 1980 (NASA-TM-81396; E-296) Avail: NTIS HC A03/MF A01 CSCL 11H

To obtain a better understanding of how bonded solid lubricant films lubricate and wear (in general), the tribological properties of polyimide-bonded graphite fluoride films were studied (in specific). A pin-on-disk type of testing apparatus was used; but in addition to sliding a hemispherically tipped rider, a rider with a 0.95 mm diameter flat area was slid against the film. This was done so that a lower, less variable contact stress could be achieved. Two stages of lubrication occurred. In the first, the film supported the load. The lubricating mechanism consisted of the shear of a thin surface layer (of the film) between the rider and the bulk of the film. The second occurred after the bonded film had worn to the substrate, and consisted of the shear of very thin lubricant films between the rider and flat plateaus generated on the metallic substrate asperities. The film wear mechanism was strongly dependent on contact stress. M.M.M.

N80-17220* National Aeronautics and Space Administration, Lewis Research Center, Cleveland, Ohio.

LUBRICATION AND WEAR MECHANISMS OF POLYIMIDE-BONDED GRAPHITE FLUORIDE FILMS SUBJECTED TO LOW CONTACT STRESS

Robert L. Fusaro Jan. 1980 27 p refs (NASA-TP-1584; E-9990) Avail: NTIS HC A03/MF A01 CSCL 11H

The tribological properties of polyimide-bonded graphite fluoride films were studied with a pin-on-disk friction apparatus. A 440 C HT stainless steel rider with a 0.95 millimeter diameter flat area was slid against the film in order to achieve a light, closely controlled contact stress. A 1 kilogram load was applied to this flat to give a projected contact stress of 14 megapascals. Two stages of lubrication were operating. In the first stage, the film supported the load and the lubricating mechanism appeared to be the shear of a thin surface layer of the film between the rider and the bulk of the film. The second stage began after the original film was worn away, and the lubricating mechanism appeared to be the shear of very thin lubricant layers between the flat area on the rider and flat plateaus generated on the sandblasted asperities of the metallic substrate. The major difference between the lubricating mechanisms of the hemispherical and flat riders was that the flat wore through the film much more slowly than did the hemisphere. K.L.

N80-18178* National Aeronautics and Space Administration, Lewis Research Center, Cleveland, Ohio.

WEAR PARTICLES OF SINGLE-CRYSTAL SILICON CARBIDE IN VACUUM

Kazuhiro Miyoshi and Donald H. Buckley Feb. 1980 24 p refs Submitted for publication (NASA-TP-1624; E-077) Avail: NTIS HC A02/MF A01 CSCL 20B

Sliding friction experiments, conducted in vacuum with silicon

carbide /000/ surface in contact with iron based binary alloys are described. Multiangular and spherical wear particles of silicon carbide are observed as a result of multipass sliding. The multiangular particles are produced by primary and secondary cracking of cleavage planes /000/, /10(-1)0/, and /11(-2)0/ under the Hertzian stress field or local inelastic deformation zone. The spherical particles may be produced by two mechanisms: (1) a penny shaped fracture along the circular stress trajectories under the local inelastic deformation zone, and (2) attrition of wear particles. M.G.

N80-18181* National Aeronautics and Space Administration, Lewis Research Center, Cleveland, Ohio.

REACTION BONDED SILICON NITRIDE PREPARED FROM WET ATTRITION-MILLED SILICON

Thomas P. Herball, Thomas K. Glasgow, and Nancy J. Shaw 1980 20 p refs. Presented at the 4th Ann. Conf. on Composites and Advan. Mater., Cocoa Beach, Fla., 20-24 Jan. 1980, sponsored by the Am. Ceram. Soc. (NASA-TM-81428, E-329) Avail: NTIS HC A02/MF A01 CSCL 11G

Silicon powder wet milled in heptane was dried, compacted into test bar shape, helium-sintered, and then reaction bonded in nitrogen-4 volume percent hydrogen. As-nitrided bend strengths averaged approximately 290 MPa at both room temperature and 1400 C. Fracture initiation appeared to be associated with subsurface flaws in high strength specimens and both subsurface and surface flaws in low strength specimens. Author

N80-18183* National Aeronautics and Space Administration, Lewis Research Center, Cleveland, Ohio.

COMPARISON OF THE WEIGHT LOSS AND ADHERENCE OF NINE DIFFERENT POLYIMIDE FILMS THERMALLY AGED AT 315 C AND 350 C IN AIR

Robert L. Fusaro Mar. 1980 34 p refs. (NASA-TM-81381, E-286) Avail: NTIS HC A03/MF A01 CSCL 07D

Thermal exposure experiments at 315 and 350 C were performed in air on nine different types of polyimides applied to thin 304 stainless steel foils. The tests were conducted to determine which polyimide was the most thermally stable and adherent when subjected to long exposure times at elevated temperatures. One polyimide designated PIC-7 was found to be more thermally stable than the others; however, it did not possess the adherent properties of PIC-2 and PIC-5. It was concluded that as far as thermal stability and adherence are concerned, five of the polyimides are more suitable for high temperature applications than the other four. K.L.

N80-19263* National Aeronautics and Space Administration, Lewis Research Center, Cleveland, Ohio.

COMPARISON OF THE TRIBOLOGICAL PROPERTIES AT 25 C OF SEVEN DIFFERENT POLYIMIDE FILMS BONDED TO 301 STAINLESS STEEL

Robert L. Fusaro Feb. 1980 25 p refs. (NASA-TM-81413, E-328) Avail: NTIS HC A02/MF A01 CSCL 11G

A pin-on-disk type of friction and wear apparatus was used to study the tribological properties of seven different polyimide films bonded to AISI 301 stainless steel disks at 25 C. It was found that the substrate material was extremely influential in determining the lubricating ability of the polyimide films. All seven films spalled in less than 1000 cycles of sliding. This was believed to be caused by poor adherence to the 301 stainless steel or the inability of the films to withstand the high localized tensile stresses imparted by the deformation of the soft substrate under sliding conditions. The friction coefficients obtained for six of the polyimides varied between 0.21 to 0.32 while one varied between 0.32 to 0.39. K.L.

N80-20398* National Aeronautics and Space Administration, Lewis Research Center, Cleveland, Ohio.

COMPOSITE WALL CONCEPT FOR HIGH TEMPERATURE TURBINE SHROUDS: SURVEY OF LOW MODULUS STRAIN ISOLATOR MATERIALS

Robert C. Bill, Gordon P. Allen, and Donald W. Wisander Mar. 1980 27 p refs. Presented at the 25th Ann. Intern. Gas Turbine Conf., New Orleans, 9-13 Mar. 1980, sponsored by ASME. Prepared in cooperation with Army Aviation Research and Development Command, Cleveland. (NASA-TM-81443, AVRADCOM-TR-80-C-7, E-363) Avail: NTIS HC A03/MF A01 CSCL 11A

Plasma sprayed yttria stabilized zirconium oxide turbine seal specimens, incorporating various low modulus porous metal strain isolator pads between the zirconium oxide and a dense metal substrate, were subjected to cyclic thermal shock testing. Specimens that had a low modulus pad composed of sintered FeNiCrAlY fibermetal survived 1000 thermal shock cycles without spalling of the ceramic. A figure of merit for the low modulus pad materials taking into consideration the elastic modulus, thermal conductivity, strength, and oxidation resistance of the pad was proposed, and showed reasonable agreement with the thermal shock results. A potential surface distress problem on the zirconium oxide, associated with nonuniform temperature distribution and rapid stress relaxation was identified. One approach to solving the surface distress problem through application of laser surface fusion of the zirconium oxide layer showed some promise, but improvements in the laser surface fusion process are necessary to prevent process associated damage to the ceramic. K.L.

N80-21532* National Aeronautics and Space Administration, Lewis Research Center, Cleveland, Ohio.

EFFECTS OF OXIDE ADDITIONS AND TEMPERATURE ON SINTERABILITY OF MILLED SILICON NITRIDE

Alan Arias Apr. 1980 21 p refs. (NASA-TP-1644, E-243) Avail: NTIS HC A02/MF A01 CSCL 11D

Specimens of milled alpha-Si₃N₄ with 0 to 5.07 equivalent percent of oxide additions were pressureless sintered at 1650 to 1820 C for 4 hours in nitrogen while covered with powdered Si₃N₄ + SiO₂. Densities of less than or equal to 97.5 percent resulted with approximately 2.5 equivalent percent of MgO, CeO₂, Y₂O₃, and three mixtures involving these oxides. Densities of greater than or equal to 94 percent were obtained with approximately 0.62 equivalent percent of the same additives. At most temperatures, best sinterability (density maximal) was obtained with 1.2 to 2.5 equivalent percent additive. J.M.S.

N80-21534* National Aeronautics and Space Administration, Lewis Research Center, Cleveland, Ohio.

ADHESION, FRICTION, AND WEAR OF BINARY ALLOYS IN CONTACT WITH SINGLE-CRYSTAL SILICON CARBIDE

Kazuhisa Miyoshi and Donald H. Buckley 1980 24 p refs. Prepared for the Intern. Joint Lubrication Conf., San Francisco, 18-21 Aug. 1980; cosponsored by ASME and the Am. Soc. of Lubrication Engrs.

(NASA-TM-79282, E-221) Avail: NTIS HC A02/MF A01 CSCL 11F

Sliding friction experiments, conducted with various iron base alloys (alloying elements are Ti, Cr, Mn, Ni, Rh and W) in contact with a single crystal silicon carbide /0001/ surface in vacuum are discussed. Results indicate atomic size misfit and concentration of alloying elements play a dominant role in controlling adhesion, friction, and wear properties of iron-base binary alloys. The controlling mechanism of the alloy properties is as an intrinsic effect involving the resistance to shear fracture of cohesive bonding in the alloy. The coefficient of friction generally increases with an increase in solute concentration. The coefficient of friction increases as the solute-to-iron atomic radius ratio increases or decreases from unity. Alloys having higher solute concentration produce more transfer to silicon carbide than do alloys having low solute concentrations. The chemical activity of the alloying element is also an important parameter in controlling adhesion and friction of alloys. M.G.

N80-22493* National Aeronautics and Space Administration
Lewis Research Center, Cleveland, Ohio.

STEADY-STATE WEAR AND FRICTION IN BOUNDARY LUBRICATION STUDIES

William R. Loomis and William R. Jones, Jr. May 1980 11 p
refs
(NASA-TP-1658; E-129) Avail: NTIS HC A02/MF A01 CSCL 11G

A friction and wear study was made at 20 C to obtain improved reproducibility and reliability in boundary lubrication testing. Ester-base and C-ether-base fluids were used to lubricate a pure iron rider in sliding contact with a rotating M-50 steel disk in a friction and wear apparatus. Conditions included loads of 1/2 and 1 kg and sliding velocities of 3.6 to 18.2 m/min in a dry air atmosphere and stepwise time intervals from 1 to 250 min for wear measurements. The wear rate results were compared with those from previous studies where a single 25 min test period was used. Satisfactory test conditions for studying friction and wear in boundary lubrication for this apparatus were found to be 1 kg load; sliding velocities of 7.1 to 9.1 m/min (50 rpm disk speed), and use of a time stepwise test procedure. Highly reproducible steady-state wear rates and steady-state friction coefficients were determined under boundary conditions. Wear ratios and coefficients of friction were constant following initially high values during run-in periods. Author

N80-22494* National Aeronautics and Space Administration
Lewis Research Center, Cleveland, Ohio.

FRICTION AND WEAR OF IRON-BASE BINARY ALLOYS IN SLIDING CONTACT WITH SILICON CARBIDE IN VACUUM

Kazuhisa Miyoshi and Donald H. Buckley May 1980 11 p
refs
(NASA-TP-1612; E-260) Avail: NTIS HC A02/MF A01 CSCL 11F

Multipass sliding friction experiments were conducted with various iron base binary alloys in contact with a single crystal silicon carbide surface in vacuum. Results indicate that the atomic size and concentration of alloy elements play important roles in controlling the transfer and friction properties of iron base binary alloys. Alloys having high solute concentration produce more transfer than do alloys having low solute concentration. The coefficient of friction during multipass sliding generally increases with an increase in the concentration of alloying element. The change of friction with succeeding passes after the initial pass also increases as the solute to iron, atomic radius ratio increases or decreases from unity. Author

N80-23453* National Aeronautics and Space Administration
Lewis Research Center, Cleveland, Ohio.

PRELIMINARY STUDY OF METHOD FOR PROVIDING THERMAL SHOCK RESISTANCE TO PLASMA-SPRAYED CERAMIC GAS-PATH SEALS

Robert C. Bill (AVRADCOM Res. and Technol. Labs.), Donald W. Wisander, and David E. Brews (AVRADCOM Res. and Technol. Labs.) May 1980 24 p
refs
(NASA-TP-1561; E-9941; AVRADCOM-TR-79-28) Avail: NTIS HC A02/MF A01 CSCL 11G

The cyclic thermal shock resistance of several outer air, gas path seal systems for high pressure turbines was evaluated. In all these systems, plasma sprayed, yttria stabilized ZrO₂ was the ceramic constituent. The most promising approaches were those that had a porous-metal, low modulus pad as a strain isolator between the ceramic layer and the dense metal substrate. Cooling pins extending into the low modulus pad significantly reduced the oxidation rate of the porous metal and the extended seal life. The thermal shock resistance of ceramic layer was improved by increasing its porosity and by precracking it before thermal shock testing. Microstructural and probe studies suggested that the long term durability of the high-pressure turbine seal systems would be adversely affected if the metal ceramic interfaces exceeded about 800 C because some metallic species would rapidly diffuse. Author

N80-23456* National Aeronautics and Space Administration
Lewis Research Center, Cleveland, Ohio.

FORMATION OF POROUS SURFACE LAYERS IN REACTION BONDED SILICON NITRIDE DURING PROCESSING

N. J. Shaw and T. K. Glasgow 1979 24 p
refs Presented at the Fall Meeting of the Basic Sci. and Nucl. Div. of the Am. Ceramic Soc., New Orleans, 14-17 Oct. 1979
(NASA-TM-81493; E-431) Avail: NTIS HC A02/MF A01

An effort was undertaken to determine if the formation of the generally observed layer of large porosity adjacent to the as-nitride surfaces of reaction bonded silicon nitrides could be prevented during processing. Isostatically pressed test bars were prepared from wet vibratory milled Si powder. Sintering and nitriding were each done under three different conditions: (1) bars directly exposed to the furnace atmosphere; (2) bars packed in Si powder; (3) bars packed in Si₃N₄ powder. Packing the bars in either Si or Si₃N₄ powder during sintering retarded formation of the layer of large porosity. Only packing the bars in Si prevented formation of the layer during nitridation. The strongest bars (316 MPa) were those sintered in Si and nitrided in Si₃N₄ despite their having a layer of large surface porosity; failure initiated at very large pores and inclusions. The alpha/beta ratio was found to be directly proportional to the oxygen content; a possible explanation for this relationship is discussed. R.C.T.

N80-24437* National Aeronautics and Space Administration
Lewis Research Center, Cleveland, Ohio.

MODIFICATION OF THE ELECTRICAL AND OPTICAL PROPERTIES OF POLYMERS Patent

Michael J. Mirtich and James S. Sovey, inventors (to NASA)
Issued 22 Apr. 1980 4 p Filed 7 Nov. 1978 Supersedes N70-11216 (17 - 02, p 0164)
(NASA-Case-LEW-13027-1; US-Patent-4,199,650;
US-Patent-Appl-SN-958575; US-Patent-Class-428-421;
US-Patent-Class-427-38; US-Patent-Class-427-40;
US-Patent-Class-427-164; US-Patent-Class-428-474) Avail: US Patent and Trademark Office CSCL 11G

An electron bombardment argon ion source is used to form textured surfaces on polyimide and fluorinated ethylene propylene polymers. This treatment improves the optical and electrical properties so that these polymers may be used in industrial and space applications.

Official Gazette of the U.S. Patent and Trademark Office

N80-26447* National Aeronautics and Space Administration
Lewis Research Center, Cleveland, Ohio.

LOW TEMPERATURE CROSS LINKING POLYIMIDES Patent Application

Tito T. Serafini and Peter Delviss, inventors (to NASA) Filed 20 Jun. 1980 14 p
(NASA-Case-LEW-12876-1; US-Patent-Appl-SN-161253) Avail: NTIS HC A02/MF A01 CSCL 07C

A way of forming a prepolymer polyimide which can be cross-linked at a relatively low temperature is disclosed. Usually a polyimide is formed by cross linking a prepolymer formed by reacting a polyfunctional ester, a polyfunctional amine, and an end-capping unit. By providing a styrene derivative end-capping unit, the prepolymer is curable at a temperature of about 175 to 245 C. NASA

N80-27483* National Aeronautics and Space Administration
Lewis Research Center, Cleveland, Ohio.

EFFECT OF W AND WC ON THE OXIDATION RESISTANCE OF YTTRIA-DOPED SILICON NITRIDE

Susan Schuon 30 Apr. 1980 12 p
refs Presented at the Annual Meeting of the Am. Ceramic Soc., Chicago, 28-30 Apr. 1980

(NASA-TM-81528; E-9744) Avail: NTIS HC A02/MF A01 CSCL 07C

The effect of W and WC contamination on the oxidation and cracking in air of sintered Si₃N₄ - 8 w/o Y₂O₃ ceramics at 500, 750, and 1350 C is examined. A mixture of Si₃N₄ - 8Y₂O₃, milled with alumina balls, was divided into four portions. Three portions were doped with 2 w/o WC W, and 4 w/o W

respectively, in order to simulate contamination during milling. The fourth portion was undoped and used on a control. The addition of W or WC did not affect the phase relationships in the system, as all bars with or without additions contained melilite as the major Si-Y-O-N phase after sintering. At 750 C, instability (rapid oxidation and cracking) of W-doped bars appears to have occurred as a result of oxidation of the tungsten containing melilite phase. No intermediate temperature instability was observed in bars containing 2 w/o WC or in bars with no additive. Specimens exposed at 1350 C had good oxidation resistance due to the formation of a protective siliceous oxide layer. A specimen containing 4 w/o W which was preoxidized at 1350 C had improved oxidation resistance at 750 C. The tendency towards oxidation and cracking of Si₃N₄ - 8 Y₂O₃ at 750 C is concluded to be related to tungsten content of the sintered bars. M G

N80-77484* National Aeronautics and Space Administration. Lewis Research Center, Cleveland, Ohio.

EFFECT OF STARTING POWDER CHARACTERISTICS ON DENSITY, MICROSTRUCTURE AND LOW TEMPERATURE OXIDATION BEHAVIOR OF A Si₃N₄W/o Y₂O₃ CERAMIC
Susan Schuon and Sunil Dutta 1980 23 p refs Presented at the Ann. Meeting of the Am. Ceramic Soc., Chicago, 28-30 Apr. 1980
(NASA-TM-81536; E-490) Avail: NTIS HC A02/MF A01 CSCL 07D

The densification and oxidation behavior of Si₃N₄ - 8w/oY₂O₃ prepared from three commercial starting powders were studied. Bars of SN 402, SN 502, and CP 85/15 were sintered for 3 to 4.5 hours at 1750 C. A second set was hot pressed for 2 hours at 1750 C. The microstructures were studied by transmission electron microscopy and scanning electron microscopy, densities were determined, and the phase compositions were determined by X-ray diffraction. Densification and microstructure were greatly influenced by the starting powder morphology and impurity content. Although SN 402 exhibited the maximum weight loss, the highest sintered and hot pressed densities were obtained with this powder. All powders had both equiaxed and elongated grains. Sintered bars were composed of beta silicon nitride and n-melilite. In contrast, hot pressed bars contained beta silicon nitride, H-phase, and J-phase, but no melilite. Yttria distribution in sintered bars was related to the presence of cation impurities such as Ca, Fe, and Mg. A limited oxidation study at 750 C in air showed no instability in these Si₃N₄ - 8 w/oY₂O₃ specimens, regardless of starting powder. Author

N80-28524* National Aeronautics and Space Administration. Lewis Research Center, Cleveland, Ohio.

CHARACTERIZATION OF PMR-15 POLYIMIDE COMPOSITION IN THERMO-OXIDATIVELY EXPOSED GRAPHITE FIBER COMPOSITES

William B. Alston 1980 19 p refs Proposed for Presentation at 12th Natl. SAMPE Tech. Conf., Seattle, 7-9 Oct. 1980
(NASA-TM-81565; AVRADCOM-TR-80-C-10; E-527) Avail: NTIS HC A02/MF A01 CSCL 09C

The contributions of individual resin components to total resin weight loss in 600 F air aged Celion 6000/PMR-15 polyimide composites were determined from the overall resin weight loss in the composite by chemically separating the PMR-15 matrix resin into its monomeric components. The individual resin components were also analyzed by spectroscopic techniques in order to elucidate curing and degradation mechanisms of the PMR-15 matrix resin. The isothermal weight loss of the individual resin components during prolonged 600 F thermo-oxidative aging of the composite was correlated to the changes observed in the Fourier Transform infrared spectra and Fourier Transform nuclear magnetic resonance spectra of the individual resin components. The correlation was used to identify the molecular site of the thermo-oxidative changes in PMR-15 polyimide matrix resin during 600 F curing the prolonged 600 F thermo-oxidative aging. Author

N80-29496* National Aeronautics and Space Administration. Lewis Research Center, Cleveland, Ohio.

CASTABLE HIGH TEMPERATURE REFRACTORY MATERI-

ALS Patent Application

I Zaplatynsky, inventor (to NASA) Filed 30 Jul 1980 5 p (NASA-Case-LEW-13080 1, US-Patent-Appl-SN-173521) Avail: NTIS HC A02/MF A01 CSCL 07D

A method is disclosed for fabricating chemically inert ceramic bodies that are both highly refractory and porous. A paste is formed by mixing alumina grain having uniform particle size with colloidal silica that is stabilized with ammonia. After drying, the cast body has sufficient green strength to be handled, and it is transferred to a furnace for curing. A green body prepared in this fashion does not undergo shrinkage during curing nor during prolonged subsequent heating. NASA

N80-32516* National Aeronautics and Space Administration. Lewis Research Center, Cleveland, Ohio.

METHOD OF CROSS-LINKING POLYVINYL ALCOHOL AND OTHER WATER SOLUBLE RESINS Patent

Warren H. Philipp, Charles E. May, Li-Chen Hsu, and Dean W. Sheibley, inventors (to NASA) Issued 19 Aug. 1980 4 p Filed 20 Dec. 1978 Supersedes N79-14172 (17 - 05, p 0571)
(NASA-Case-LEW-13103-1; US-Patent-4,218,280; US-Patent-Appl-SN-971596; US-Patent-Class-156-272; US-Patent-Class-156-292; US-Patent-Class-264-22; US-Patent-Class-264-212; US-Patent-Class-204-159.11; US-Patent-Class-204-159.14; US-Patent-Class-427-44; US-Patent-Class-428-500; US-Patent-Class-429-139) Avail: US Patent and Trademark Office CSCL 07C

A self supporting sheet structure comprising a water soluble, noncrosslinked polymer such as polyvinyl alcohol which is capable of being crosslinked by reaction with hydrogen atom radicals and hydroxyl molecule radicals is contacted with an aqueous solution having a pH of less than 8 and containing a dissolved salt in an amount sufficient to prevent substantial dissolution of the noncrosslinked polymer in the aqueous solution. The aqueous solution is then irradiated with ionizing radiation to form hydrogen atom radicals and hydroxyl molecule radicals and the irradiation is continued for a time sufficient to effect crosslinking of the water soluble polymer to produce a water insoluble polymer sheet structure. The method has particular application in the production of battery separators and electrode envelopes for alkaline batteries.

Official Gazette of the U.S. Patent and Trademark Office

A80-12089* Boundary lubrication, thermal and oxidative stability of a fluorinated polyether and a perfluoropolyether triazine, W. R. Jones, Jr. (NASA, Lewis Research Center, Cleveland, Ohio) and C. E. Snyder, Jr. (NASA, Lewis Research Center, Cleveland; USAF, Materials Laboratory, Wright-Patterson AFB, Ohio). *American Society of Lubrication Engineers, Annual Meeting, 34th, St. Louis, Mo., Apr. 30-May 3, 1979, Preprint 79-AM-1B-1*, 8 p. 25 refs.

Boundary lubricating characteristics, thermal stability and oxidation-corrosion stability were determined for a fluorinated polyether and a perfluoropolyether triazine. A ball-on-disk apparatus, a tensimeter and oxidation-corrosion apparatus were used. Results were compared to data for a polyphenyl ether and a C-ether. The polyether and triazine yielded better boundary lubricating characteristics than either the polyphenyl ether or C-ether. The polyphenyl ether had the greatest thermal stability (443 C) while the other fluids had stabilities in the range 389 to 397 C. Oxidation-corrosion results indicated the following order of stabilities: perfluoropolyether triazine greater than polyphenylether greater than C-ether greater than fluorinated polyether. (Author)

A80-12094* Effect of thermal aging on the tribological properties of polyimide films and polyimide-bonded graphite fluoride films. R. L. Fusaro (NASA, Lewis Research Center, Cleveland, Ohio). *American Society of Lubrication Engineers, Annual Meeting, 34th, St. Louis, Mo., Apr. 30-May 3, 1979, Preprint 79-AM-3B-1*, 10 p. 10 refs.

The effect of thermal aging on the weight loss, adherence, friction and wear of polyimide films and polyimide-bonded graphite fluoride films applied to 440C-HT stainless steel disks and to 304

stainless steel thin foils was studied. The films were exposed at temperatures of 315, 345, 370 or 400 C for 100 hours or more and then evaluated at temperatures of 25, 315 or 345 C in atmospheres of dry or moist air. Polyimide films were found to be brittle after thermal exposure; but polyimide bonded graphite fluoride films possessed good adherence and gave low friction and wear results. Thus, polyimide-bonded graphite fluoride films appear to be good candidates for solid lubrication applications where long thermal soaks are prevalent. (Author)

A80-13063 * # Characterization and properties of controlled nucleation thermochemical deposited (CNTD) silicon carbide. S. Dutta (NASA, Lewis Research Center, Cleveland, Ohio), R. W. Rice (U.S. Navy, Naval Research Laboratory, Washington, D.C.), H. C. Graham (USAF, Materials Laboratory, Wright-Patterson AFB, Ohio), and M. C. Mendiratta (Systems Research Laboratories, Inc., Dayton, Ohio). *American Ceramic Society, Annual Meeting, 18th, Detroit, Mich., May 6-11, 1978, Paper, 22 p.* 10 refs.

Results are presented for an investigation designed to characterize the microstructure of controlled nucleation thermomechanical deposition (CNTD) produced SiC material with respect to grain structure, stoichiometry, phase analysis, etc., and to evaluate the room-temperature and high-temperature fracture and oxidation behavior. By using the CNTD process, ultrafine-grained SiC is deposited on tungsten wires as substrates, with superior surface smoothness and without the macrocolumnar growth commonly observed in conventional CVD materials. The results suggest that the high-purity, fully dense, and stable grain size SiC material produced by CNTD shows potential for high-temperature structural applications, provided that pertinent problems are resolved. S.D.

A80-13065 * # Mechanical and chemical effects of in-texturing biomedical polymers. A. J. Weigand and M. A. Cenkus (NASA, Lewis Research Center, Cleveland, Ohio). *Alliance for Engineering in Medicine, Annual Conference of Engineering in Medicine and Biology, 32nd, Denver, Colo., Oct. 6-10, 1979, Paper, 27 p.* 17 refs.

A80-18303 * # Thermal barrier coatings for aircraft gas turbines. R. A. Miller, S. R. Levine, and S. Stecura (NASA, Lewis Research Center, Cleveland, Ohio). *American Institute of Aeronautics and Astronautics, Aerospace Sciences Meeting, 18th, Pasadena, Calif., Jan. 14-16, 1980, Paper 80-0302.* 6 p. 13 refs.

Improvements in gas turbine performance are approaching the limits imposed by alloy properties and excessive cooling air requirements. Thin ceramic coatings can increase the difference between gas temperature and metal temperature by several hundred degrees. Thus, they are potentially a major step forward in surface protection. These coatings offer the potential to reduce fuel consumption by permitting reduced coolant flow or higher turbine inlet temperature or to improve durability by reducing metal temperatures and transient thermal stresses. At NASA Lewis, in-house and contractual programs are in place to bring this promising technology to engine readiness in the early 1980's. Progress towards this goal is summarized in this paper. (Author)

A80-32086 * # Liquid chromatographic characterization of PMR-15 resin and prepreg. K. E. Reed (NASA, Lewis Research Center, Cleveland, Ohio). In: *Rising to the challenge of the '80s: Annual Conference and Exhibit, 35th, New Orleans, La., February 4-8, 1980, Preprints. (A80-32058 12-24)* New York, Society of the Plastics Industry, Inc., 1980, p. 26-E 1 to 26-E 4. 6 refs.

A liquid chromatographic method has been developed capable of providing a chemical fingerprint of PMR-15 resin solutions and prepreg. The amounts of two of the monomers can be quantified so their experimentally determined molar ratio can be compared to the formulated one. Only the monomers were detected in fresh resin solution, whereas several additional components, resulting from an

association or reaction between the norbornenyl endcap and the amine, were detected in a resin solution aged for three days. Two commercial prepreps exhibited fingerprints similar to that of laboratory material, but three others contained additional components corresponding to higher esters and nadimides. (Author)

A80-32828 * # Reaction bonded silicon nitride prepared from wet attrition-milled silicon. T. P. Herbell, T. K. Glasgow, and N. J. Shaw (NASA, Lewis Research Center, Cleveland, Ohio). *American Ceramic Society, Annual Conference on Composites and Advanced Materials, 4th, Cocoa Beach, Fla., Jan. 20-24, 1980, Paper, 19 p.* 8 refs.

Silicon powder wet milled in heptane was dried, compacted into test bar shape, helium-sintered, and then reaction bonded in nitrogen-4 vol% hydrogen. As-nitrided bend strengths averaged approximately 290 MPa at both room temperature and 1400 C. Fracture initiation appeared to be associated with subsurface flaws in high-strength specimens and both subsurface and surface flaws in low-strength specimens. (Author)

A80-35502 * # Tribological properties of sputtered MoS₂ films in relation to film morphology. T. Spalvin (NASA, Lewis Research Center, Cleveland, Ohio). *American Vacuum Society, International Conference on Metallurgical Coatings, San Diego, Calif., Apr. 21-25, 1980, Paper, 14 p.* 8 refs.

Thin sputter-deposited MoS₂ films with thicknesses ranging from 2000 to 6000 Å have shown excellent lubricating properties when sputtering parameters and substrate conditions are properly selected and controlled. The lubricating properties are strongly influenced by the crystalline-amorphous structure, morphology, and composition of the films. The coefficient of friction can range from 0.04 (which is effective lubrication) to 0.4 (no lubricating action). V.P.

A80-35899 * # Effect of thermal cycling on ZrO₂-Y₂O₃ thermal barrier coatings. G. McDonald and R. C. Hendricks (NASA, Lewis Research Center, Cleveland, Ohio). *American Vacuum Society, International Conference on Metallurgical Coatings, San Diego, Calif., Apr. 21-25, 1980, Paper, 7 p.* 13 refs.

The paper studies the comparative life of plasma-sprayed ZrO₂-Y₂O₃ thermal barrier coatings on NiCrAlY bond coats on René 41 in short (4 min) and long (57 min) thermal cycles at 1040 C in a 0.3-Mach flame. Attention is given to determining the effect of short- and long-duration cycles on ZrO₂-Y₂O₃ coatings, the cause of any cycle frequency effects, and methods to improve tolerance to thermal stress. Short cycles greatly reduced the life of the ceramic coating in terms of time at temperatures as compared to longer cycles, the failed coating indicating compressive failure. The experiments and stress calculations show that repeatedly subjecting a ceramic coating to high rates of initial heating has a more destructive influence on the coating than sustained operation at temperature. The effect of such thermal compressive stresses might be minimized through coating deposition and thickness control and by turbine cycle measurement to keep starting heating rates below critical values. S.D.

A80-38963 * # Development of improved-durability plasma sprayed ceramic coatings for gas turbine engines. I. E. Sumner (NASA, Lewis Research Center, Engine Component Improvement Office, Cleveland, Ohio) and D. L. Ruckle (United Technologies Corp., Pratt and Whitney Aircraft Group, East Hartford, Conn.). *AIAA, SAE, and ASME, Joint Propulsion Conference, 16th, Hartford, Conn., June 30-July 2, 1980, AIAA Paper 80-1193.* 14 p. 6 refs.

An investigation is reported of improving the durability of plasma sprayed ceramic coatings for the vane platforms in the JT9D turbofan engine. The program aims for reduced fuel consumption of commercial aircraft engines; the use of improved strain tolerant

microstructures and control of the substrate temperature during coating application are being evaluated. The initial burner rig tests at temperatures up to 1010 C indicated that improvements in cyclic life greater than 20:1 over previous ceramic coatings were achieved. Three plasma sprayed coating systems applied to first stage vane platforms in the high pressure turbine were subjected to a 1000-cycle JT9D engine endurance test with only minor damage occurring to the coatings. A.T.

A80-42085 * **Fracture toughness determination of Al₂O₃ using four-point-bend specimens with straight-through and chevron notches.** D. Munz, R. T. Bubsey, and J. L. Shannon, Jr. (NASA, Lewis Research Center, Strength of Materials Section, Cleveland, Ohio). *American Ceramic Society, Journal*, vol. 63, May-June 1980, p. 300-305, 28 refs.

A80-46099 * # **Effect of W and WC on the oxidation resistance of yttria-doped silicon nitride.** S. Schuon (NASA, Lewis Research Center, Cleveland, Ohio). *American Ceramic Society, Annual Meeting, Chicago, Ill., Apr. 28-30, 1980, Paper*, 10 p. 8 refs.

The effect of tungsten and tungsten carbide contamination on the oxidation and cracking in air of yttria-doped silicon nitride ceramics is investigated. Silicon nitride powder containing 8 wt % Y₂O₃ was doped with 2 wt % W, 4 wt % W, 2 wt % WC or left undoped, and sintered in order to simulate contamination during milling, and specimens were exposed in air to 500, 750 and 1350 C for various lengths of time. Scanning electron and optical microscopy and X-ray diffraction of the specimens in the as-sintered state reveals that the addition of W or WC does not affect the phase relationships in the system, composed of alpha and beta Si₃N₄, melilite and an amorphous phase. Catastrophic oxidation is observed at 750 C in specimens containing 2 and 4 wt % W, accompanied by the disappearance of alpha Si₃N₄ and melilite from the structure. At 1350 C, the formation of a protective glassy oxide layer was observed on all specimens without catastrophic oxidation, and it is found that pre-oxidation at 1350 C also improved the oxidation resistance at 750 C of bars doped with 4 wt % W. It is suggested that tungsten contamination from WC grinding balls may be the major cause of the intermediate-temperature cracking and instability frequently observed in Si₃N₄-8Y₂O₃. A.L.W.

A80-46100 * # **Effect of starting powder characteristics on density, microstructure and low temperature oxidation behavior of a Si₃N₄ - 8 w/o Y₂O₃ ceramic.** S. Schuon and S. Dutta (NASA, Lewis Research Center, Cleveland, Ohio). *American Ceramic Society, Annual Meeting, Chicago, Ill., Apr. 28-30, 1980, Paper*, 21 p. 7 refs.

A80-46153 **Sliding friction of some metallic glasses.** J. K. A. Amuzu (International Centre for Theoretical Physics, Trieste, Italy). *Journal of Physics D - Applied Physics*, vol. 13, July 14, 1980, p. L127-L129, 8 refs.

The coefficients of friction have been determined for some metallic glasses using a simple sliding friction rig. Calculated values of the coefficients have also been obtained from consideration of the simple adhesion model which predicts that the coefficient of friction is the ratio of the shear strength and the yield pressure of the contacting materials. Comparisons of the calculated and measured coefficients reveal large discrepancies, in marked contrast to the good agreement obtained for polymers. (Author)

A80-50696 * **Performance of Chevron-notch short bar specimens in determining the fracture toughness of silicon nitride and aluminum oxide.** D. Munz (Deutsche Forschungs- und Versuchsanstalt für Luft- und Raumfahrt, Cologne, West Germany), R. T. Bubsey, and J. L. Shannon, Jr. (NASA, Lewis Research Center, Strength of Materials Section, Cleveland, Ohio). *Journal of Testing and Evaluation*, vol. 8, May 1980, p. 103-107, 10 refs.

Ease of preparation and testing are advantages unique to the chevron-notch specimen used for the determination of the plane

strain fracture toughness of extremely brittle materials. During testing, a crack develops at the notch tip and extends stably as the load is increased. For a given specimen and notch configuration, maximum load always occurs at the same relative crack length independent of the material. Fracture toughness is determined from the maximum load with no need for crack length measurement. Chevron notch acuity is relatively unimportant since a crack is produced during specimen loading. In this paper, the authors use their previously determined stress intensity factor relationship for the chevron-notch short bar specimen to examine the performance of that specimen in determining the plane strain fracture toughness of silicon nitride and aluminum oxide. (Author)

A80-51574 * # **Formation of porous surface layers in reaction bonded silicon nitride during processing.** N. J. Shaw and T. K. Glasgow (NASA, Lewis Research Center, Cleveland, Ohio). *American Ceramic Society, Fall Meeting, New Orleans, La., Oct. 14-17, 1979, Paper*, 22 p. 12 refs.

Microstructural examination of reaction bonded silicon nitride (RBSN) has shown that there is often a region adjacent to the as-nitrified surfaces that is even more porous than the interior of this already quite porous material. Because this layer of large porosity is considered detrimental to both the strength and oxidation resistance of RBSN, a study was undertaken to determine if its formation could be prevented during processing. All test bars studied were made from a single batch of Si powder which was milled for 4 hours in heptane in a vibratory mill using high density alumina cylinders as the grinding media. After air drying the powder, bars were compacted in a single acting die and hydropressed. (Author)

N80-13257*# Acurex Corp., Mountain View, Calif. Aerospace Systems Div.

SYNTHESIS OF IMPROVED POLYESTER RESINS Final Report

A. H. McLeod and C. B. Delano 5 Jul. 1979 83 p refs

(Contract NAS3-21374)

(NASA-CR-159665; FR-79-13/AS)

Avail: NTIS

HC A05/MF A01 CSCL 11G

Eighteen aromatic unsaturated polyester prepolymers prepared by a modified interfacial condensation technique were investigated for their solubility in vinyl monomers and ability to provide high char yield forming unsaturated polyester resins. The best resin system contained a polyester prepolymer of phthalic, fumaric and diphenic acids reacted with 2,7-naphthalene diol and 9,9-bis(4-hydroxyphenyl)fluorene. This prepolymer is very soluble in styrene, divinyl benzene, triallyl cyanurate, diallyl isophthalate and methylvinylpyridine. It provided anaerobic char yields as high as 41 percent at 800 C. The combination of good solubility and char yield represents a significant improvement over state-of-the-art unsaturated polyester resins. The majority of the other prepolymers had only low or no solubility in vinyl monomers. Graphite composites from this prepolymer with styrene were investigated. The cause for the observed low shear strengths of the composites was not determined, however 12-week aging of the composites at 82 C showed that essentially no changes in the composites had occurred. Author

N80-15263*# General Electric Co., Philadelphia, Pa. Space Sciences Lab

SINTERED SILICON NITRIDE RECUPERATOR FABRICATION Final Report

A. Gatti, W. S. Chiu, and L. R. McCreight Jan. 1980 40 p refs

(Contract DEN3-54)

(NASA-CR-159706; DOE/NASA/0054-79/1) Avail: NTIS

HC A03/MF A01 CSCL 11B

The preliminary design and a demonstration of the feasibility of fabricating submodules of an automotive Stirling engine recuperator for waste heat recovery at 370 C are described. Sinterable silicon nitride (Sialon) tubing and plates were fabricated by extrusion and hydrostatic pressing, respectively, suitable for demonstrating a potential method of constructing ceramic recuperator-type heat exchangers. These components were fired in nitrogen atmosphere to 1800 C without significant scale

formation so that they can be used in the as fired condition. A refractory glass composition ($\text{Al}_2\text{O}_3 \times 4.5 \text{ CaO MgO} \times 11\text{SiO}_2$) was used to join and seal component parts by a brazing technique which formed strong recuperator submodules capable of withstanding repeated thermal cycling to 1370 C. The corrosion resistance of these materials to Na_2SO_4 - NaCl carbon mixtures was also assessed in atmospheres of air, hydrogen and CO_2 - N_2 - H_2O mixtures at both 870 C and 1370 C for times to 1000 hours. No significant reaction was observed under any of these test conditions. M M M

N80-15264* TRW Defense and Space Systems Group, Redondo Beach, Calif.

ANALYSES OF MOISTURE IN POLYMERS AND COMPOSITES

L E Ryan and R W Vaughan 11 Jan 1980 99 p refs (Contract NAS3-20406) (NASA-CR-159745, TRW-31782-6082-RU 00) Avail: NTIS HC A05/MF A01 CSCL 07C

A suitable method for the direct measurement of moisture concentrations after humidity/thermal exposure on state of the art epoxy and polyimide resins and their graphite and glass fiber reinforcements was investigated. Methods for the determination of moisture concentration profiles, moisture diffusion modeling and moisture induced chemical changes were examined. Carefully fabricated, precharacterized epoxy and polyimide neat resins and their AS graphite and S glass reinforced composites were exposed to humid conditions using heavy water (D_2O) at ambient and elevated temperatures. These specimens were fixtured to theoretically limit the D_2O permeation to a unidirectional penetration axis. The analytical techniques evaluated were (1) laser pyrolysis gas chromatography mass spectrometry, (2) solids probe mass spectrometry, (3) laser pyrolysis conventional infrared spectroscopy, and (4) infrared imaging thermovision. The most reproducible and sensitive technique was solids probe mass spectrometry. The fabricated exposed specimens were analyzed for D_2O profiling after humidity/thermal conditioning at three exposure time durations. R C T

N80-17221* Aerotherm Acurex Corp., Mountain View, Calif. Aerospace Systems Div.

SYNTHESIS OF IMPROVED PHENOLIC RESINS Final Report

C B Delano and A H McLeod 4 Sep 1979 115 p refs (Contract NAS3-21368) (NASA-CR-159724, FR-79-25/AS) Avail: NTIS HC A06/MF A01 CSCL 11G

Twenty seven addition cured phenolic resin compositions were prepared and tested for their ability to give char residues comparable to state-of-the-art phenolic resins. Cyanate, epoxy, allyl, acrylate, methacrylate and ethynyl derivatized phenolic oligomers were investigated. The novolac-cyanate and propargyl-novolac resins provided anaerobic char yields at 800 C of 58 percent. A 59 percent char yield was obtained from modified epoxy novolacs. A phosphonitrilic derivative was found to be effective as an additive for increasing char yields. The novolac-cyanate, epoxy-novolac and methacrylate-epoxy-novolac systems were investigated as composite matrices with Thornel 300 graphite fiber. All three resins showed good potential as composite matrices. The free radical cured methacrylate-epoxy-novolac graphite composite provided short beam shear strengths at room temperature of 93.3 MPa (13.5 ksi). The novolac-cyanate graphite composite produced a short beam shear strength of 74 MPa (10.7 ksi) and flexural strength of 1302 MPa (189 ksi) at 177 C. Air heat aging of the novolac-cyanate and epoxy novolac based composites for 12 weeks at 204 C showed good property retention. Author

N80-26448* Mechanical Technology, Inc., Latham, N. Y. **HIGH TEMPERATURE SELF-LUBRICATING COATINGS FOR AIR LUBRICATED FOIL BEARINGS FOR THE AUTOMOTIVE GAS TURBINE ENGINE Final Report**

Bharat Bhushan 1 Jul 1980 232 p refs (Contracts DEN3-43; EC-77-A-31-1040) (NASA-CR-159842; DOE/NASA/0043-2) Avail: NTIS

HC A11/MF A01 CSCL 13I

Coating combinations were developed for compliant surface bearings and journals to be used in an automotive gas turbine engine. The coatings were able to withstand the sliding start/stops during rotor liftoff and touchdown and occasional short time, high speed rubs under representative loading of the engine. Some dozen coating variations of CdO-graphite, Cr_2O_3 (by sputtering) and CaF_2 (plasma sprayed) were identified. The coatings were optimized and they were examined for stoichiometry, metallurgical condition, and adhesion. Sputtered Cr_2O_3 was most adherent when optimum parameters were used and it was applied on an annealed (soft) substrate. Metallic binders and interlayers were used to improve the ductility and the adherence. R C T

N80-31552* AiResearch Mfg. Co., Phoenix, Ariz. **THE 3500 HOUR DURABILITY TESTING OF COMMERCIAL CERAMIC MATERIALS Interim Report**

W D Carruthers, D W Richerson, and K W Benn Jul 1980 237 p refs

(Contracts DEN3-27, EC-77-A-31-1040) (NASA-CR-159785; DOE/NASA/0027-80/1, AiResearch-31-3575A) Avail: NTIS HC A11/MF A01 CSCL 11B

A two year durability testing program to evaluate four commercially available ceramic materials under simulated automotive gas turbine combustor discharge conditions was conducted. Conditions included extended cyclic thermal exposures up to 2500 F and 3500 hours. Selected for evaluation were Norton NCX-34 hot pressed silicon nitride, AiResearch RBN 101 reaction bonded silicon nitride, Carborundum pressureless sintered d-siC and British Nuclear Fuels, Ltd. Retel reaction sintered silicon carbide marketed by Pure Carbon Co. These materials initially were exposed to 350 hours/1750 cycles at 1200 and 1270 C (2200 and 2500 F). Subsequent exposure to 1050, 2100, and 3500 hours were performed on the materials maintaining 50 percent of baseline strength after the initial exposure. Additional evaluations of exposed bars included dimension changes, weight changes, dye penetrant, specific damping capacity changes, scanning electron microscope fractography and X-ray diffraction. S.F.

A80-10042 * Thick ceramic coating development for industrial gas turbines - A program plan. J. W. Vogan and A. R. Stetson (Solar Turbines International, San Diego, Calif.). U.S. Department of Energy and Electric Power Research Institute, Conference on Advanced Materials for Alternate Fuel Capable Directly Fired Heat Engines, Castine, Me., July 30-Aug. 3, 1979, Paper. 29 p. 42 refs. Contract No. DEN3-109. (SR79-M-4702-05)

A program plan on a NASA-Lewis funded program is presented, in which effectiveness of thick ceramic coatings in preventing hot corrosion and in providing thermal insulation to gas turbine engine components are to be investigated. Preliminary analysis of the benefit of the thermal insulating effect of this coating on decreasing cooling air and simplifying component design appears very encouraging. The program is in the preliminary stages of obtaining starting materials and establishing procedures. Numerous graphs, tables and photographs are included. S.D.

A80-13066 * State-of-the-art of SIALON materials. S. Dutta (NASA, Lewis Research Center, Cleveland, Ohio), NATO, AGARD, Specialist Meeting on Ceramics for Turbine Engine Applications, Cologne, West Germany, Oct. 7-12, 1979, Paper. 21 p. 41 refs.

The state of the art of 'SIALONS' is reviewed, noting that the term has become a generic one applied to Si_3N_4 based materials. Attention is given to work on phase relations, crystal structure, synthesis, fabrication, and properties of various SIALONS. Also discussed are the essential features of compositions, fabrication methods, and microstructures. In addition, consideration is given to high temperature flexure strength, creep, fracture toughness, oxidation, and thermal shock resistance. Finally, these data are compared to those for some currently produced silicon nitride ceramics to assess the potential of SIALON materials for use in advanced gas turbine engines. M.E.P.

A80-15720 * # The effects of strain and temperature on the dynamic properties of elastomers M. S. Darlow and A. J. Smalley (Mechanical Technology, Inc., Machinery Dynamics Section, Latham, N.Y.). *American Society of Mechanical Engineers, Design Engineering Technical Conference, St. Louis, Mo., Sept. 10-12, 1979, Paper 79-DET-57*, 9 p, 8 refs. Members, \$1.50, nonmembers, \$3.00. Contract No. NAS3-18546.

This paper presents the results of a program of analysis and tests to determine the dynamic properties of elastomers as a function of strain and ambient temperature. Measurements were also made to determine the temperature distribution in the elastomer samples during the tests. These measured properties were compared with analytical predictions based on a visco elastic model designed to take into account the self heating of the materials as a function of strain. The test method used was well established Base Excitation Resonant Mass Technique. The specimens tested were two cylindrical button compression specimens and a shear specimen. Strain was shown to be an important parameter in determining the dynamic properties of the elastomers. In general, these properties were much more sensitive to strain than to frequency. The self heating effect was found to account for a portion of the strain sensitivity of these properties.

(Author)

A80-35575 * # 3500-hour durability testing of ceramic materials for automotive gas turbine engines. W. D. Carruthers, D. W. Richerson, and K. W. Benn (AiResearch Manufacturing Company of Arizona, Phoenix, Ariz.). *U.S. Department of Energy and NASA, International Automotive Propulsion Systems Symposium, 5th, Dearborn, Mich., Apr. 14-18, 1980, Paper. 27*, p. 7 refs. Contract No. DEN3-27. (AIResearch-31-3542)

A two-year durability program was performed by AiResearch Phoenix to evaluate four commercially available ceramic materials under simulated automotive gas turbine combustor discharge conditions. These conditions included extended cyclic thermal exposures up to 2500 F and 3500 hr. The four materials selected for evaluation were Norton NCX-34 hot pressed silicon nitride, AiResearch RBN 101 reaction bonded silicon nitride, Carborundum pressureless sintered alpha-SiC and Pure Carbon Co. (British Nuclear Fuels, Ltd.) Refel reaction sintered silicon carbide. These materials were initially exposed to 350 hr/1750 cycles at 1200 and 1370 C. Subsequent exposures to 1050, 2100 and 3500 hr were performed on those materials maintaining 50% of baseline strength after the initial exposure. Additional evaluations of exposed bars included dimensional and weight changes, dye penetrant, specific damping capacity changes, SEM fractography, and X-ray diffraction.

(Author)

A80-39637 * # Evaluation of present-day thermal barrier coatings for industrial/utility applications. R. J. Bratton, S. K. Lau, and S. Y. Lee (Westinghouse Research and Development Center, Pittsburgh, Pa.). *American Vacuum Society, International Conference on Metallurgical Coatings, San Diego, Calif., Apr. 21-25, 1980, Paper. 22*, p. 12 refs. Research sponsored by the Electric Power Research Institute; Contract No. NAS3-21377.

Atmospheric burner rig tests have been conducted to evaluate the corrosion resistance of present-day thermal barrier coatings. The coatings are primarily plasma-sprayed and zirconia-based. Both duplex and graded coating systems were tested at a gas temperature of 2100 F and metal temperatures that range from 1475 F to 1650 F. The fuels ranged from clean GT No. 2 to that doped with impurity levels which simulate water-washed residual fuels. Results to date suggest that liquid sulfate condensates play an important role in the coating degradation mechanisms, whereas the role of vanadium and its salts is less clear.

(Author)

28 PROPELLANTS AND FUELS

Includes rocket propellants, igniters, and oxidizers, storage and handling, and aircraft fuels

For related information see also 07 Aircraft Propulsion and Power, 20 Spacecraft Propulsion and Power, and 44 Energy Production and Conversion

N80-13268* National Aeronautics and Space Administration Lewis Research Center, Cleveland, Ohio
TEMPERATURE AND FLOW MEASUREMENTS ON NEAR-FREEZING AVIATION FUELS IN A WING-TANK MODEL
 Robert Friedman and Francis J Stockemer 1980 18 p refs
 To be presented at the 25th Intern Gas Turbine Conf., New Orleans, 9-13 Mar 1980, sponsored by ASME
 (NASA-TM-79285, E-156) Avail NTIS HC A02/MF A01 CSCL 21D

Freezing behavior, pumpability, and temperature profiles for aviation turbine fuels were measured in a 190-liter tank chilled to simulate internal temperature gradients encountered in commercial airplane wing tanks. When the bulk of the fuel was above the specification freezing point, pumpout of the fuel removed all fuel except a layer adhering to the bottom chilled surfaces, and the unpumpable fraction depended on the fuel temperature near these surfaces. When the bulk of the fuel was at or below the freezing point, pumpout ceased when solids blocked the pump inlet, and the unpumpable fraction depended on the overall average temperature. K L

N80-18265* National Aeronautics and Space Administration, Lewis Research Center, Cleveland, Ohio.
INITIAL CHARACTERIZATION OF AN EXPERIMENTAL REFERENCE BROADENED-SPECIFICATION (ERBS) AVIATION TURBINE FUEL
 George M. Prok and Gary T. Seng Jan. 1980 10 p refs
 (NASA-TM-81440, E-206) Avail: NTIS HC A02/MF A01 CSCL 21D

Characterization data and a hydrocarbon compositional analysis are presented for a research test fuel designated as an experimental reference broadened-specification aviation turbine fuel. This research fuel, which is a special blend of kerosene and hydrotreated catalytic gas oil, is a hypothetical representation of a future fuel should it become necessary to broaden current kerojet specifications. It is used as a reference fuel in research investigations into the effects of fuel property variations on the performance and durability of jet aircraft components, including combustors and fuel systems. J.M.S.

N80-20402* National Aeronautics and Space Administration, Lewis Research Center, Cleveland, Ohio.
ATOMIC HYDROGEN STORAGE Patent
 John A. Woolam, inventor (to NASA) Issued 18 Mar. 1980 3 p Filed 29 Sep. 1977 Supersedes N78-19907 (16 - 10, p 1365) Division of U.S. Patent Appl. SN-67432, filed 13 Apr. 1976, US Patent-4,077,788
 (NASA-Case-LEW-12081-2; US-Patent-4,193,827; US-Patent-Appl-SN-837794; US-Patent-Class-149-1; US-Patent-Class-423-648R; US-Patent-Appl-SN-676432) Avail: US Patent and Trademark Office CSCL 21D

Atomic hydrogen, for use as a fuel or as an explosive, is stored in the presence of a strong magnetic field in exfoliated layered compounds such as molybdenum disulfide or an elemental layer material such as graphite. The compound is maintained at liquid temperatures and the atomic hydrogen is collected on the surfaces of the layered compound which are exposed during delamination (exfoliation). The strong magnetic field and the low temperature combine to prevent the atoms of hydrogen from recombining to form molecules.

Official Gazette of the U.S. Patent and Trademark Office

N80-21551* National Aeronautics and Space Administration Lewis Research Center, Cleveland, Ohio
MECHANICAL IMPACT TESTS OF MATERIALS IN OXYGEN EFFECTS OF CONTAMINATION
 Paul M. Ordin Washington Apr 1980 36 p refs
 (NASA-TP-1571; E-047) Avail: NTIS HC A03/MF A01 CSCL 20K

The effect of contaminants on the mechanical impact sensitivity of Teflon, stainless steel, and aluminum in a high-pressure oxygen environment was investigated. Uncontaminated Teflon did not ignite under the test conditions. The liquid contaminants - cutting oil, motor lubricating oil, and toolmaker dye - caused Teflon to ignite. Raising the temperature lowered the impact energy required for ignition. Stainless steel was insensitive to ignition under the test conditions with the contaminants used. Aluminum appeared to react without contaminants under certain test conditions; however, contamination with cutting oil, motor lubricating oil, and toolmakers dye increased the sensitivity of aluminum to mechanical impact. The grit contaminants silicon dioxide and copper powder did not conclusively affect the sensitivity of aluminum. A.R.H.

N80-23472* National Aeronautics and Space Administration Lewis Research Center, Cleveland, Ohio
THE IMPACT OF FUELS ON AIRCRAFT TECHNOLOGY THROUGH THE YEAR 2000
 Jack Grobman and Gregory M. Reck 1980 26 p refs Presented at the Intern Meeting and Tech Display, Global Technol 2000, Baltimore, 5-11 May 1980, sponsored by AIAA
 (NASA-TM-81492, E-429) Avail: NTIS HC A03/MF A01 CSCL 21D

The impact that the supply, quality, and processing costs of future fuels may have on aircraft technology is assessed. The potential range of properties for future jet fuels is discussed along with the establishment of a data base of fuel property effects on propulsion system components. Also, the evolution and evaluation of advanced component technology that would permit the use of broader property fuels and the identification of technical and economic trade-offs within the overall fuel production-air transportation system associated with variations in fuel properties are examined. M G

N80-25454* National Aeronautics and Space Administration, Lewis Research Center, Cleveland, Ohio.
ANALYTICAL AND EXPERIMENTAL EVALUATIONS OF THE EFFECT OF BROAD PROPERTY FUELS ON COMBUSTORS FOR COMMERCIAL AIRCRAFT GAS TURBINE ENGINES
 A. L. Smith Jun. 1980 20 p refs Presented at 16th Joint Propulsion Conf., Hartford, Conn., 30 Jun. - 2 Jul. 1980; sponsored by AIAA, ASME, and SAE
 (NASA-TM-81496, E-433) Avail: NTIS HC A02/MF A01 CSCL 21D

The impacts of broad property fuels on the design, performance, durability, emissions, and operational characteristics of current and advanced combustors for commercial aircraft gas turbine engines were studied. The effect of fuel thermal stability on engine and airframe fuel system was evaluated. Tradeoffs between fuel properties, exhaust emissions, and combustor life were also investigated. Results indicate major impacts of broad property fuels on allowable metal temperatures in fuel manifolds and injector support, combustor cyclic durability, and somewhat lesser impacts on starting characteristics, lightoff, emissions, and smoke. E.D.K.

N80-27509* National Aeronautics and Space Administration, Lewis Research Center, Cleveland, Ohio.
USE OF PETROLEUM-BASED CORRELATIONS AND ESTIMATION METHODS FOR SYNTHETIC FUELS
 A. C. Antoine Jun. 1980 23 p refs
 (NASA-TM-81533; E-485) Avail: NTIS HC A02/MF A01 CSCL 21D

Correlations of hydrogen content with aromatics content, heat of combustion, and smoke point are derived for some synthetic fuels prepared from oil and coal syncrudes. Comparing the results

of the aromatics content with correlations derived for petroleum fuels shows that the shale derived fuels fit the petroleum-based correlations, but the coal derived fuels do not. The correlations derived for heat of combustion and smoke point are comparable to some found for petroleum-based correlations. Calculated values of hydrogen content and of heat of combustion are obtained for the synthetic fuels by use of ASTM estimation methods. Comparisons of the measured and calculated values show bases for the equations that exceed the critical statistics values.

Comparison of the measured hydrogen content by the standard ASTM combustion method with that by a nuclear magnetic resonance (NMR) method shows a decided bias. The comparison of the calculated and measured NMR hydrogen contents shows a difference similar to that found with petroleum fuels. Author

N80-27510* National Aeronautics and Space Administration. Lewis Research Center, Cleveland, Ohio.

ADVANCED FUEL SYSTEM TECHNOLOGY FOR UTILIZING BROADENED PROPERTY AIRCRAFT FUELS

G M Reck Jun. 1980 23 p refs Proposed for presentation at 12th Congr. of the Intern. Council of the Aeron. Sci., Munich, 13-17 Oct. 1980 (NASA-TM-81538, E-492) Avail: NTIS HC A02/MF A01 CSCL 21D

Possible changes in fuel properties are identified based on current trends and projections. The effect of those changes with respect to the aircraft fuel system are examined and some technological approaches to utilizing those fuels are described.

R.C.T.

N80-29502* National Aeronautics and Space Administration. Lewis Research Center, Cleveland, Ohio.

SOME ADVANTAGES OF METHANE IN AN AIRCRAFT GAS TURBINE

Robert W. Graham and Arthur J. Glassman 1980 18 p refs Proposed for presentation at Aerospace Congr., Los Angeles, 13-16 Oct. 1980; sponsored by ASAE (NASA-TM-81559, E-520) Avail: NTIS HC A02/MF A01 CSCL 21D

Liquid methane, which can be manufactured from any of the hydrocarbon sources such as coal, shale biomass, and organic waste considered as a petroleum replacement for aircraft fuels. A simple cycle analysis is carried out for a turboprop engine flying a Mach 0.8 and 10, 688 meters (35,000 ft.) altitude. Cycle performance comparisons are rendered for four cases in which the turbine cooling air is cooled or not cooled by the methane fuel. The advantages and disadvantages of involving the fuel in the turbine cooling system are discussed. Methane combustion characteristics are appreciably different from Jet A and will require different combustor designs. Although a number of similar difficult technical problems exist, a highly fuel efficient turboprop engine burning methane appear to be feasible. A.R.H.

N80-31621* National Aeronautics and Space Administration. Lewis Research Center, Cleveland, Ohio.

DESIGN AND EVALUATION OF HIGH PERFORMANCE ROCKET ENGINE INJECTORS FOR USE WITH HYDROCARBON FUELS

A. J. Pavli In APL The 16th JANNAF Combust. Meeting, Vol. 2 Dec. 1979 p 617-643 refs (For primary document see N80-31588 22-28)

Avail: Issuing Activity CSCL 21/9

An experimental program to determine the feasibility of using a heavy hydrocarbon fuel as a rocket propellant is reported. A method of predicting performance of a heavy hydrocarbon in terms of experimental test results. Combustion length effects were explored over a range of 21.6 cm. to 55.9 cm. Four injector types were tested, each over a range of mixture ratios. Further configuration modifications were obtained by reaming each injector several times to provide test data over a range of injector pressure drop. E.D.K.

A80-42193 * # Temperature and flow measurements on near-freezing aviation fuels in a wing-tank model. R. Friedman (NASA, Lewis Research Center, Cleveland, Ohio) and F. J. Stockemer (Lockheed-California Co., Burbank, Calif.). *American Society of Mechanical Engineers, Gas Turbine Conference and Products Show, New Orleans, La., Mar. 10-13, 1980, Paper 80-GT-63*, 12 p. 15 refs. Members, \$1.50; nonmembers, \$3.00.

Freezing behavior, pumpability, and temperature profiles for aviation turbine fuels were measured in a 190-liter tank, to simulate internal temperature gradients encountered in commercial airplane wing tanks. Two low-temperature situations were observed. Where the bulk of the fuel is above the specification freezing point, pumpout of the fuel removes all fuel except a layer adhering to the bottom chilled surfaces, and the unpumpable fraction depends on the fuel temperature near these surfaces. Where the bulk of the fuel is at or below the freezing point, pumpout ceases when solids block the pump inlet, and the unpumpable fraction depends on the overall average temperature. (Author)

A80-42195 * # NASA Broad-Specification Fuels Combustion Technology Program - Status and description. J. S. Fear (NASA, Lewis Research Center, Cleveland, Ohio). *American Society of Mechanical Engineers, Gas Turbine Conference and Products Show, New Orleans, La., Mar. 10-13, 1980, Paper 80-GT-65*, 10 p. 8 refs. Members, \$1.50; nonmembers, \$3.00.

The use of 'broad-specification' fuels in aircraft gas turbine engines can be a significant factor in offsetting anticipated shortages of current-specification jet fuel in the latter part of the century. The changes in fuel properties accompanying the use of broad-specification fuels will tend to cause numerous emissions, performance, and durability problems in currently-designed combustion systems. The NASA Broad-Specification Fuels Combustion Technology Program is a contracted effort to evolve and demonstrate the technology required to utilize broad-specification fuels in current and next generation commercial Conventional Takeoff and Landing (CTOL) aircraft engines, and to verify this technology in full-scale engine tests in 1983. The program consists of three phases: Combustor Concept Screening, Combustor Optimization Testing, and Engine Verification Testing. (Author)

A80-41516 * # Analytical and experimental evaluations of the effect of broad property fuels on combustors for commercial aircraft gas turbine engines. A. L. Smith (NASA, Lewis Research Center, Cleveland, Ohio). *AIAA, SAE, and ASME, Joint Propulsion Conference, 16th, Hartford, Conn., June 30-July 2, 1980, AIAA Paper 80-1204*, 19 p. 9 refs. NASA-supported research.

Analytical and experimental studies were conducted in three contract activities funded by the National Aeronautics and Space Administration, Lewis Research Center, to assess the impacts of broad property fuels on the design, performance, durability, emissions and operational characteristics of current and advanced combustors for commercial aircraft gas turbine engines. The effect of fuel thermal stability on engine and airframe fuel system was evaluated. Trade-offs between fuel properties, exhaust emissions and combustor life were also investigated. Results indicate major impacts of broad property fuels on allowable metal temperatures in fuel manifolds and injector support, combustor cyclic durability and somewhat lesser impacts on starting characteristics, lightoff, emissions and smoke. (Author)

N80-19284* Southwest Research Inst., San Antonio, Tex. Mobile Energy Div. **FUEL QUALITY COMBUSTION ANALYSIS Final Report. 6 Oct. 1978 - Jul. 1979** D. W. Naegeli and C. A. Moses May 1979 50 p refs (Contract NAS3-21587) (NASA-CR-162822; MFD113) Avail: NTIS HC A03/MF A01 CSCL 21D

A high pressure research combustor operating over a wide range of burner inlet conditions was used to determine the effects

of fuel molecular structure on soot formation. Six test fuels with equal hydrogen content (12.8%) were blended to stress different molecular components and final boiling points. The fuels containing high concentrations (20%) of polycyclic aromatics and partially saturated polycyclic structures such as tetralin, produced more soot than would be expected from a hydrogen content correlation for typical petroleum based fuels. Fuels containing naphthenes such as decalin agreed with the hydrogen content correlation. The contribution of polycyclic aromatics to soot formation was equivalent to a reduction in fuel hydrogen content of about one percent. The fuel sensitivity to soot formation due to the polycyclic aromatic contribution decreased as burner inlet pressure and fuel/air ratio increased. R.C.T.

N80-22509* Massachusetts Inst. of Tech., Cambridge, Dept. of Mechanical Engineering.

LABORATORY MEASUREMENTS IN A TURBULENT, SWIRLING FLOW Final Report

David P. Hoult Nov. 1979 52 p refs
(Grant NSG-3076)

(NASA-CR-159723) Avail: NTIS HC A04/MF A01 CSCL 21D

Measurements of soot inside a flame-tube burner using a special water-flushed probe are discussed. The soot is measured at a series of points at each burner, and upon occasion gaseous constituents NO, CO, hydrocarbons, etc., were also measured. Four geometries of flame-tube burners were studied, as well as a variety of different fuels. The role of upstream geometry on the downstream pollutant formation was studied. It was found that the amount of soot formed in particularly sensitive to how aerodynamically clean the configuration of the burner is upstream of the injector swirl vanes. The effect of pressure on soot formation was also studied. It was found that beyond a certain Reynolds number, the peak amount of soot formed in the burner is constant. F.O.S.

N80-25453* United Technologies Corp., East Hartford, Conn. **EXTERNAL FUEL VAPORIZATION STUDY, PHASE 1**

E. J. Szetela and L. Chiappetta Jun. 1980 133 p refs
(Contract NAS3-21971)

(NASA-CR-159850; UTRC-R80-914607-12) Avail: NTIS HC A07/MF A01 CSCL 21D

A conceptual design study was conducted to devise and evaluate techniques for the external vaporization of fuel for use in an aircraft gas turbine with characteristics similar to the Energy Efficient Engine (E3). Three vaporizer concepts were selected and they were analyzed from the standpoint of fuel thermal stability, integration of the vaporizer system into the aircraft engine, engine and vaporizer dynamic response, startup and altitude restart, engine performance, control requirements, safety, and maintenance. One of the concepts was found to improve the performance of the baseline E3 engine without seriously compromising engine startup and power change response. Increased maintenance is required because of the need for frequent pyrolytic cleaning of the surfaces in contact with hot fuel. R.C.T.

N80-30535* United Technologies Research Center, East Hartford, Conn.

AUTOIGNITION CHARACTERISTICS OF AIRCRAFT-TYPE FUELS

Louis J. Spadaccini and John A. TeVelde Jun. 1980 88 p refs

(Contract NAS3-20066)

(NASA-CR-159886; R80-914617-1)

Avail: NTIS HC A05/MF A01 CSCL 21D

The ignition delay characteristics of Jet A, JP 4, no. 2 diesel, cetane and an experimental referee broad specification (ERBS) fuel in air at inlet temperatures up to 1000 K, pressures of 10, 15, 20, 25 and 30 atm, and fuel air equivalence ratios of 0.3, 0.5, 0.7 and 1.0 were mapped. Ignition delay times in the range of 1 to 50 msec at freestream flow velocities ranging from 20 to 100 m/sec were obtained using a continuous flow test apparatus which permitted independent variation and evaluation of the effect of temperature, pressure, flow rate, and

fuel/air ratio. The ignition delay times for all fuels tested appeared to correlate with the inverse of pressure and the inverse exponent of temperature. With the exception of pure cetane, which had the shortest ignition delay times, the differences between the fuels tested did not appear to be significant. The apparent global activation energies for the typical gas turbine fuels ranged from 38 to 40 kcal/mole, while the activation energy determined for cetane was 50 kcal/mole. In addition, the data indicate that for lean mixtures, ignition delay times decrease with increasing equivalence ratio. It was also noted that physical (apparatus dependent) phenomena, such as mixing (i.e., length and number of injection sites) and airstream cooling (due to fuel heating, vaporization and convective heat loss) can have an important effect on the ignition delay. R.K.G.

N80-31619* Hersh Acoustical Engineering, Chatsworth, Calif. **EFFECT OF GRAZING FLOW ON THE NONLINEAR ACOUSTIC BEHAVIOR OF HELMHOLTZ RESONATORS**

A. S. Hersh In APL The 16th JANNAF Combust. Meeting, Vol. 2 Dec. 1979 p 579-603 refs (For primary document see N80-31588 22-28)

(Contract NAS3-19745)

Avail: Issuing Activity CSCL 21/9

A semi empirical fluid mechanical model is derived of the acoustic behavior of thin walled single orifice Helmholtz resonators in a grazing flow environment. The model assumes that the flow field incident to a resonator orifice consists of a spherical sound particle velocity field superimposed upon a mean grazing flow. The incident and cavity sound fields are connected in terms of an orifice discharge coefficient whose values are determined experimentally using the two microphone method. With regard to its application to rocket motor interiors, the most important finding of this study is that the acoustic impedance of Helmholtz resonators is affected by grazing flow when the product of the amplitude of the sound pressure incident to the resonator orifice and the rocket motor interior mean grazing flow speed are less than 0.5. For values greater than 0.5, the acoustic impedance is independent of the grazing flow. E.D.K.

A80-42192 * Effect of fuel molecular structure on soot formation in gas turbine engines. D. W. Naegeli and C. A. Moses (Southwest Research Institute, San Antonio, Tex.). *American Society of Mechanical Engineers, Gas Turbine Conference and Products Show, New Orleans, La., Mar. 10-13, 1980, Paper 80-GT-62.* 8 p. 19 refs. Members, \$1.50; nonmembers, \$3.00. Contract No. NAS3-21587.

A high-pressure research combustor operating over a wide range of burner inlet conditions was used to determine the effects of fuel molecular structure on soot formation. Six test fuels with equal hydrogen content (12.8 percent) were blended to stress different molecular components and final boiling points. The fuels containing high concentrations (20 percent) of poly-cyclic aromatics and partially saturated polycyclic structures such as tetralin, produced more soot than would be expected from a hydrogen content correlation for typical petroleum based fuels. However, fuels containing naphthenes, such as decalin, agreed with the hydrogen content correlation. The contribution of polycyclic aromatics to soot formation was equivalent to a reduction in fuel hydrogen content of about 1%. The fuel sensitivity to soot formation due to the polycyclic aromatic contribution decreased as burner inlet pressure and fuel/air ratio increased. (Author)

31 ENGINEERING (GENERAL)

Includes vacuum technology; control engineering; display engineering; and cryogenics.

N80-13317* National Aeronautics and Space Administration. Lewis Research Center, Cleveland, Ohio.

EVALUATION OF CLEANERS FOR PHOTOVOLTAIC MODULES EXPOSED IN AN OUTDOOR ENVIRONMENT

Final Report

W. D. Knapp Oct 1979 17 p refs
(Contract DE-A101-79ET-20485)

(NASA-TM-79248, E-204, DOE/NASA/20485-79/5) Avail: NTIS HC A02/MF A01 CSCL 13H

Power recovery of silicone encapsulated and glass covered photovoltaic modules, exposed for two years to a suburban environment, was measured after washing with a variety of cleaners including detergents, abrasive soap, and hydrocarbon solvents. Silicone encapsulated modules in operating environments may experience significant power losses or require extensive periodic cleaning. Glass front-faced modules in similar situations are much less affected. Organic hydrocarbon solvents or abrasives were found to be about five times more effective than mild detergents in cleaning encapsulated modules. Author

N80-16232* National Aeronautics and Space Administration. Lewis Research Center, Cleveland, Ohio.

HOMOGENEOUS ALIGNMENT OF NEMATIC LIQUID CRYSTALS BY ION BEAM ETCHED SURFACES

E. G. Wintucky, R. Mahmood, and D. L. Johnson 19 Oct. 1979 19 p refs Presented at 156th Meeting of the Electrochem. Soc., Los Angeles, 15-19 Oct. 1979

(NASA-TM-81378; E-283) Avail: NTIS HC A02/MF A01 CSCL 20L

A wide range of ion beam etch parameters capable of producing uniform homogeneous alignment of nematic liquid crystals on SiO₂ films are discussed. The alignment surfaces were generated by obliquely incident (angles of 5 to 25 deg) argon ions with energies in the range of 0.5 to 2.0 KeV, ion current densities of 0.1 to 0.6 mA sq cm and etch times of 1 to 9 min. A smaller range of ion beam parameters (2.0 KeV, 0.2 mA sq cm, 5 to 10 deg and 1 to 5 min.) were also investigated with ZrO₂ films and found suitable for homogeneous alignment. Extinction ratios were very high (1000), twist angles were small (< or = 3 deg) and tilt-bias angles very small (< or = 1 deg). Preliminary scanning electron microscopy results indicate a parallel oriented surface structure on the ion beam etched surfaces which may determine alignment. Author

A80-25096 * Oxygen-enriched air for MHD power plants. R. W. Ebeling, Jr., J. C. Cutting (Gilbert Associates, Inc., Reading, Pa.), and J. A. Burkhardt (NASA, Lewis Research Center, Cleveland, Ohio). In: Symposium on the Engineering Aspects of Magnetohydrodynamics, 18th, Butte, Mont., June 18-20, 1979, Preprints. (A80-25061 09-31) Bozeman, Mont., Montana State University, 1979, p. G.1.1-G.1.9. 16 refs. Research supported by the U.S. Department of Energy.

Cryogenic air-separation process cycle variations and compression schemes are examined. They are designed to minimize net system power required to supply pressurized, oxygen-enriched air to the combustor of an MHD power plant with a coal input of 2000 MWt. Power requirements and capital costs for oxygen production and enriched air compression for enrichment levels from 13 to 50% are determined. The results are presented as curves from which total compression power requirements can be estimated for any desired enrichment level at any delivery pressure. It is found that oxygen enrichment and recuperative heating of MHD combustor air to 1400 F yields near-term power plant efficiencies in excess of 45%. A minimum power compression system requires 167 MW to supply 330 lb of oxygen per second and costs roughly 100 million dollars.

Preliminary studies show MHD/steam power plants to be competitive with plants using high-temperature air preheaters burning gas. L.M.

N80-15300* Massachusetts Inst. of Tech., Cambridge. Dept. of Materials Science and Engineering.

DIRECTIONAL SOLIDIFICATION AT ULTRA-HIGH THERMAL GRADIENT Final Report

M. C. Flemings, D. S. Lee, and M. A. Neff Jan. 1980 34 p refs

(Grant NsG-3046)

(NASA-CR-159797) Avail: NTIS HC A03/MF A01 CSCL 13H

A high gradient controlled solidification (HGC) furnace was designed and operated at gradients up to 1800 C/cm to continuously produce aluminum alloys. Rubber 'O' rings for the water cooling chamber were eliminated, while still maintaining water cooling directly onto the solidified metal. An HGC unit for high temperature ferrous alloys was also designed. Successful runs were made with cast iron, at thermal gradients up to 500 C/cm. K.L.

N80-16210* Southwest Research Inst., San Antonio, Tex. **PREDICTION OF FRAGMENT VELOCITIES AND TRAJECTORIES** c37

J. J. Kulesz, L. M. Vargas, and P. K. Moseley In Shock and Vibration Inform. Center The Shock and Vibration Bull., Pt. 1 Sep. 1979 p 171-187 refs (For primary document see N80-16198 07-31)

(Contract NAS3-20497)

Avail: NTIS HC A09/MF A01 CSCL 20K

Analytical techniques are described which predict: (1) the velocities of two unequal fragments from bursting cylindrical pressure vessels; (2) the velocity and range of portions of vessels containing a fluid which, when the vessel ruptures, causes the fragment to accelerate as the fluid changes from the liquid to the gaseous phase; and (3) the ranges of fragments subjected to drag and lift forces during flight. Numerous computer runs were made with various initial conditions in an effort to generalize the results for maximum range in plots of dimensionless range versus dimensionless velocity. R.E.S.

32 COMMUNICATIONS

Includes land and global communications, communications theory, and optical communications.

For related information see also 04 Aircraft Communications and Navigation and 17 Spacecraft Communications, Command and Tracking.

N80-32610*# National Aeronautics and Space Administration. Lewis Research Center, Cleveland, Ohio.

A QUANTITATIVE ANALYSIS OF INTER-ISLAND TELEPHONY TRAFFIC IN THE PACIFIC BASIN REGION (PBR)

David D. Evans and Clifford H. Arth. Washington. Sep. 1980. 20 p. refs.

(NASA-TM-81587; E-566) Avail: NTIS HC A02/MF A01 CSCL 17B

As part of NASA's continuing assessment of future communication satellite requirements, a study was conducted to quantitatively scope current and future telecommunication traffic demand in the South Pacific Archipelagos. This demand was then converted to equivalent satellite transponder capacities. Only inter-island telephony traffic for the Pacific Basin Region was included. The results show that if all this traffic were carried by a satellite system, one-third of a satellite transponder would be needed to satisfy the base-year (1976-1977) requirement and about two-thirds of a satellite transponder would be needed to satisfy the forecasted 1985 requirement. Author

A80-25916*# NASA advanced communications systems analysis. J. J. Ward (NASA, Lewis Research Center, Cleveland, Ohio). In: ICC '79; International Conference on Communications, Boston, Mass., June 10-14, 1979, Conference Record, Volume 1. (A80-25901 09-32) Piscataway, N.J., Institute of Electrical and Electronics Engineers, Inc., 1979, p. 15.2.1-15.2.5.

The purpose of the paper is to investigate and study in-depth market and system analysis for improving satellite communications. The analyses fall into two categories: the broad, scoping efforts intended to screen potential candidates and studies to develop viable operational system configurations and identify critical technology elements. To illustrate the approach, the results of 30/20 GHz study efforts which have been under way in the past few years are reviewed in detail. C.F.W.

A80-25917*# 30/20 GHz wideband technology verification program. D. L. Wright (NASA, Lewis Research Center, Cleveland, Ohio). In: ICC '79; International Conference on Communications, Boston, Mass., June 10-14, 1979, Conference Record, Volume 1. (A80-25901 09-32) Piscataway, N.J., Institute of Electrical and Electronics Engineers, Inc., 1979, p. 15.3.1-15.3.4.

This paper discusses various aspects of the 30/20 GHz wideband technology verification activities of NASA. The discussion considers the objectives, approach, system requirements, possible experiment configuration and payload, and the supporting research and technology elements. (Author)

A80-25920*# NASA communications technology research and development. A. F. Durham (NASA, Goddard Space Flight Center, Greenbelt, Md.) and N. Stankiewicz (NASA, Lewis Research Center, Cleveland, Ohio). In: ICC '79; International Conference on Communications, Boston, Mass., June 10-14, 1979, Conference Record, Volume 1. (A80-25901 09-32) Piscataway, N.J., Institute of Electrical and Electronics Engineers, Inc., 1979, p. 15.6.1-15.6.5.

The development of a 1978 NASA study to identify technology requirements is surveyed, and its principal conclusions, recommendations, and priorities are summarized. In addition, antenna, traveling wave tube, and solid state amplifier developments representing selected items from the current communications technology development programs at the NASA Lewis Research and Goddard Space

Flight Centers are described.

M.E.P.

A80-26795*# National Aeronautics and Space Administration plans for space communication technology. R. E. Alexovich (NASA, Lewis Research Center, Cleveland, Ohio). In: EASCON '79; Electronics and Aerospace Systems Conference, Arlington, Va., October 9-11, 1979, Conference Record, Volume 2. (A80-26776 09-32) New York, Institute of Electrical and Electronics Engineers, Inc., 1979, p. 273-278, 10 refs.

A program plan is presented for a space communications application utilizing the 30/20 GHz frequency bands (30 GHz uplink and 20 GHz downlink). Results of market demand studies and spacecraft systems studies which significantly affect the supporting research and technology program are also presented, along with the scheduled activities of the program plan. C.F.W.

A80-28712* NASA's program in communication satellites. J. N. Sivo (NASA, Lewis Research Center, Communications and Applications Div., Cleveland, Ohio). In: Space Shuttle: Dawn of an era; Proceedings of the Twenty-sixth Annual Conference, Los Angeles, Calif., October 29-November 1, 1979. Part 2. (A80-28696 10-16) San Diego, Calif., American Astronautical Society; Univelt, Inc., 1980, p. 659-675. (AAS 79-247)

It is noted that NASA is currently proceeding with a revitalized R&D program aimed at the development and demonstration of advanced communication satellite system concepts and the related enabling technologies. The paper reviews the important elements of this program thrust, the approach NASA is taking to assure proper involvement of both the system supplier industry and the service supplier industry and the specific technology focus in the near term. Finally, highlights of the current NASA and industry activities related to opening up the 30/20 GHz frequency band for both commercial and military use are presented. M.E.P.

N80-10415*# TRW, Inc., Redondo Beach, Calif. Space Systems Div.

THE 30/20 GHz MIXED USER ARCHITECTURE DEVELOPMENT STUDY: Final Report

Oct. 1979. 216 p. refs.

(Contract NAS3-21933)

(NASA-CR-159686) Avail: NTIS HC A10/MF A01 CSCL 17B

A mixed-user system is described which provides cost-effective communications services to a wide range of user terminal classes, ranging from one or two voice channel support in a direct-to-user mode, to multiple 500 mbps trunking channel support. Advanced satellite capabilities are utilized to minimize the cost of small terminals. In a system with thousands of small terminals, this approach results in minimum system cost. Author

N80-10416*# TRW, Inc., Redondo Beach, Calif. Space Systems Div.

THE 30/20 GHz MIXED USER ARCHITECTURE DEVELOPMENT STUDY: EXECUTIVE SUMMARY

Sep. 1979. 24 p.

(Contract NAS3-21933)

(NASA-CR-159687) Avail: NTIS HC A02/MF A01 CSCL 17B

The baseline 30/30 GHz satellite communication system, designed for cost-effective communications in the years 1990 to 2000, incorporates on-board satellite demodulation and routing of individual 64 kbps digital voice-grade circuits. This level of routing flexibility is necessary to provide efficient communications to the large number of direct-to-user terminals (DTU) projected. The circuit interfacing hardware is distributed among all the DTU and master control stations. The switching circuitry which provides full interconnectivity between 30 to 45 thousand circuits is in the satellite. The DTU terminal cost, perhaps the largest element in the system cost, represents the largest economic value element of the system because it avoids using terrestrial signal distribution

and routing and the charges associated with these functions. Satellite baseline design and power requirements for the system are examined
A.R.H.

N80-11277* Ford Aerospace and Communications Corp., Palo Alto, Calif.

CONCEPTS FOR 18/30 GHz SATELLITE COMMUNICATION SYSTEM, VOLUME 1 Final Report

R. Jorasch, M. Baker, R. Davies, L. Cuccia, and C. Mitchell
1 Nov. 1979 169 p 3 Vol.

(Contract NAS3-21362)

(NASA-CR-159625-Vol-1; WDL-TR8457-Vol-1) Avail: NTIS HC A08/MF A01 CSCL 17B

Concepts for 18/30 GHz satellite communication systems are presented. Major terminal trunking as well as direct-to-user configurations were evaluated. Critical technologies in support of millimeter wave satellite communications were determined.

M.M.M.

N80-11278* Ford Aerospace and Communications Corp., Palo Alto, Calif.

CONCEPTS FOR 18/30 GHz SATELLITE COMMUNICATION SYSTEM, VOLUME 1A: APPENDIX Final Report

R. Jorasch, M. Baker, R. Davies, L. Cuccia, and C. Mitchell
1 Nov. 1979 181 p refs 3 Vol.

(Contract NAS3-21362)

(NASA-CR-159625-Vol-1A; WDL-TR8457-Vol-1A) Avail: NTIS HC A09/MF A01 CSCL 17B

The following are appended: (1) Propagation phenomena and attenuation models; (2) Models and measurements of rainfall patterns in the U.S.; (3) Millimeter wave propagation experiments; (4) Comparison of theory and experiment; (5) A practical rain attenuation model for CONUS; (6) Space diversity; (7) Values of attenuation for selected U.S. cities; and (8) Additional considerations.

M.M.M.

N80-11279* Ford Aerospace and Communications Corp., Palo Alto, Calif.

CONCEPTS FOR 18/30 GHz SATELLITE COMMUNICATION SYSTEM STUDY. EXECUTIVE SUMMARY

M. Baker, R. Davies, L. Cuccia, and C. Mitchell 1 Nov. 1979 36 p 3 Vol.

(Contract NAS3-21362)

(NASA-CR-159680; WDL-TR8457) Avail: NTIS HC A03/MF A01 CSCL 17B

An examination of a multiplicity of interconnected parameters ranging from specific technology details to total system economic costs for satellite communication systems at the 18/30 GHz transmission bands are presented. It was determined that K sub A band systems can incur a small communications outage during very heavy rainfall periods and that reducing the outage to zero would lead to prohibitive system costs. On the other hand, the economics of scale, ie, one spacecraft accommodating 2.5 GHz of bandwidth coupled with multiple beam frequency reuse, leads

N80-12259* Case Western Reserve Univ., Cleveland, Ohio. Dept. of Electrical Engineering and Applied Physics.

LOW SIDELobe LEVEL LOW-COST EARTH STATION ANTENNAS FOR THE 12 GHz BROADCASTING SATELLITE SERVICE

R. E. Collin and L. R. Gabel Sep. 1979 117 p refs

(Contract NAS3-21365)

(NASA-CR-159703) Avail: NTIS HC A06/MF A01 CSCL 17B

An experimental investigation of the performance of 1.22 m and 1.83 m diameter paraboloid antennas with an f/D ratio of 0.38 and using a feed developed by Kumar is reported. It is found that sidelobes below 30 dB can be obtained only if the paraboloids are relatively free of surface errors. A theoretical analysis of clam shell distortion shows that this is a limiting factor in achieving low sidelobe levels with many commercially available low cost paraboloids. The use of absorbing pads and small reflecting plates for sidelobe reduction is also considered.

Author

N80-12260* Mitre Corp., Bedford, Mass.
APPLICATION OF ADVANCED ON-BOARD PROCESSING CONCEPTS TO FUTURE SATELLITE COMMUNICATIONS SYSTEMS

J. L. Katz, M. Hoffman, S. L. Kota, J. M. Ruddy, and B. F. White Jun. 1979 408 p refs 2 Vol.

(Contract F19628-79-C-0001; AF Proj. 8680)

(NASA-CR-159682; MTR-3787-Vol-1) Avail: NTIS HC A18/MF A01 CSCL 17B

An initial definition of on-board processing requirements for an advanced satellite communications system to service domestic markets in the 1990's is presented. An exemplar system architecture with both RF on-board switching and demodulation/remodulation baseband processing was used to identify important issues related to system implementation, cost, and technology development.

R.C.T.

N80-12261* Mitre Corp., Bedford, Mass.
APPLICATION OF ADVANCED ON-BOARD PROCESSING CONCEPTS TO FUTURE SATELLITE COMMUNICATIONS SYSTEMS: BIBLIOGRAPHY

R. L. Edelman and J. L. Katz Jun. 1979 109 p 2 Vol.

(Contract F19628-79-C-0001; AF Proj. 8680)

(NASA-CR-159684; MTR-3787-Vol-2) Avail: NTIS HC A06/MF A01 CSCL 17B

Abstracts are presented of a literature survey of reports concerning the application of signal processing concepts. Approximately 300 references are included.

R.C.T.

N80-18262* International Telephone and Telegraph Corp., New York.

THE 30/20 GHz FIXED COMMUNICATIONS SYSTEMS SERVICE DEMAND ASSESSMENT. VOLUME 1: EXECUTIVE SUMMARY

R. B. Gamble, H. R. Seltzer, K. M. Speter, and M. Westheimer Aug. 1979 50 p 3 Vol.

(Contract NAS3-21366)

(NASA-CR-159619) Avail: NTIS HC A03/MF A01 CSCL 17B

Demand for telecommunications services is forecasted for the period 1980-2000, with particular reference to that portion of the demand associated with satellite communications. Overall demand for telecommunications is predicted to increase by a factor of five over the period studied and the satellite portion of demand will increase even more rapidly. Traffic demand is separately estimated for voice, video, and data services and is also described as a function of distance traveled and city size. The satellite component of projected demand is compared with the capacity available in the C and Ku satellite bands and it is projected that new satellite technology and the implementation of Ka band transmission will be needed in the decade of the 1990's.

Author

N80-18263* International Telephone and Telegraph Corp., New York.

THE 30/20 GHz FIXED COMMUNICATIONS SYSTEMS SERVICE DEMAND ASSESSMENT. VOLUME 2: MAIN REPORT

R. B. Gamble, H. R. Seltzer, K. M. Speter, and M. Westheimer Aug. 1979 309 p refs 3 Vol.

(Contract NAS3-21366)

(NASA-CR-159620) Avail: NTIS HC A14/MF A01 CSCL 17B

A forecast of demand for telecommunications services through the year 2000 is presented with particular reference to demand for satellite communications. Estimates of demand are provided for voice, video, and data services and for various subcategories of these services. The results are converted to a common digital measure in terms of terabits per year and aggregated to obtain total demand projections.

J.M.S.

N80-18264* # International Telephone and Telegraph Corp., New York.

THE 30/20 GHz FIXED COMMUNICATIONS SYSTEMS SERVICE DEMAND ASSESSMENT. VOLUME 3: ANNEX
R. B. Gamble, H. R. Seltzer, K. M. Speter, and M. Westheimer
Aug. 1979 63 p 3 Vol.
(Contract NAS3-21366)
(NASA-CR-159621) Avail: NTIS HC A04/MF A01 CSCL 17B

A review of studies forecasting the communication market in the United States is given. The applicability of these forecasts to assessment of demand for the 30/20 GHz fixed communications system is analyzed. Costs for the 30/20 satellite trunking systems are presented and compared with the cost of terrestrial communications.
J.M.S.

N80-22547* # Western Union Telegraph Co., Upper Saddle River, N.J.

THE 18/30 GHz FIXED COMMUNICATIONS SYSTEM SERVICE DEMAND ASSESSMENT. VOLUME 1: EXECUTIVE SUMMARY

t. Gabriszeski, P. Reiner, J. Rogers, and W. Terbo Jun. 1979 32 p 3 Vol.

(Contract NAS3-21359)
(NASA-CR-159546) Avail: NTIS HC A03/MF A01 CSCL 17D

The total demand for voice, video, and data communications services, and satellite transmission services at the 4/6 GHz, 12/14 GHz, and 18/30 GHz frequencies is discussed. Major study objectives, overall methodology, results, and general observations about a satellite systems market characteristics and trends are summarized.
M.G.

N80-22548* # Western Union Telegraph Co., Upper Saddle River, N.J.

THE 18/30 GHz FIXED COMMUNICATIONS SYSTEM SERVICE DEMAND ASSESSMENT. VOLUME 2: MAIN TEXT

T. Gabriszeski, P. Reiner, J. Rogers, and W. Terbo Jun. 1979 328 p refs 3 Vol.

(Contract NAS3-21359)
(NASA-CR-159547) Avail: NTIS HC A15/MF A01 CSCL 17B

The total demand for communications services, and satellite transmission services at the 4/6 GHz, 12/14 GHz, and 18/30 GHz frequencies is assessed. The services are voice, video, and data services. Traffic demand, by service, is distributed by geographical regions, population density, and distance between serving points. Further distribution of traffic is made among four major end user groups: business, government, institutions and private individuals. A traffic demand analysis is performed on a typical metropolitan city to examine service distribution trends. The projected cost of C and Ku band satellite systems are compared on an individual service basis to projected terrestrial rates. Separation of traffic between transmission systems, including 18/30 GHz systems, is based on cost, user, and technical considerations.
M.G.

N80-22549* # Western Union Telegraph Co., Upper Saddle River, N.J.

THE 30/20 GHz FIXED COMMUNICATIONS SYSTEMS SERVICE DEMAND ASSESSMENT. VOLUME 3: APPENDICES

T. Gabriszeski, P. Reiner, J. Rogers, and W. Terbo Jun. 1979 200 p refs 3 Vol.

(Contract NAS3-21359)
(NASA-CR-159548) Avail: NTIS HC A09/MF A01 CSCL 17B

The market analysis of voice, video, and data 18/30 GHz communications systems services and satellite transmission services is discussed. Detail calculations, computer displays of traffic, survey questionnaires, and detailed service forecasts are presented.
M.G.

N80-24514* # Mitre Corp., Bedford, Mass.

ON-BOARD PROCESSING CONCEPTS FOR FUTURE SATELLITE COMMUNICATIONS SYSTEMS

William T. Brandon, ed. and Brian E. White, ed. May 1980 39 p refs

(Contract F19628-80-C-0001)
(NASA-CR-159683; MTR-3543) Avail: NTIS HC A03/MF A01 CSCL 17B

The initial definition of on-board processing for an advanced satellite communications system to service domestic markets in the 1990's is discussed. An exemplar system with both RF on-board switching and demodulation/remodulation baseband processing is used to identify important issues related to system implementation, cost, and technology development. Analyses of spectrum-efficient modulation, coding, and system control techniques are summarized. Implementations for an RF switch and baseband processor are described. Among the major conclusions listed is the need for high gain satellites capable of handling tens of simultaneous beams for the efficient reuse of the 2.5 GHz 30/20 frequency band. Several scanning beams are recommended in addition to the fixed beams. Low power solid state 20 GHz GaAs FET power amplifiers in the 5W range and a general purpose digital baseband processor with gigahertz logic speeds and megabits of memory are also recommended.
A.R.H.

A80-29544 * # An advanced mixed user domestic satellite system architecture. H. G. Raymond (TRW Systems Engineering Laboratory, Redondo Beach, Calif.) and W. M. Holmes, Jr. (TRW Defense and Space Systems Group, Redondo Beach, Calif.). In: Communications Satellite Systems Conference, 8th, Orlando, Fla., April 20-24, 1980, Technical Papers. (A80-29526 11-32) New York, American Institute of Aeronautics and Astronautics, Inc., 1980, p. 148-153. Contract No. NAS3-21933. (AIAA 80-0494)

A domestic satellite system architecture that can efficiently and economically accommodate a wide variety of disparate user classes is described and a baseline system configuration identified. With such a technique, both the efficiency of TDMA operation and the operational terminal flexibility of FDMA can be simultaneously achieved.
V.T.

A80-29574 * # Packet communications in satellites with multiple-beam antennas and signal processing. R. Davies, F. Chethik, and M. Penick (Ford Aerospace and Communications Corp., Palo Alto, Calif.). In: Communications Satellite Systems Conference, 8th, Orlando, Fla., April 20-24, 1980, Technical Papers. (A80-29526 11-32) New York, American Institute of Aeronautics and Astronautics, Inc., 1980, p. 378-385. Contract No. NAS3-21364. (AIAA 80-0537)

A communication satellite with a multiple-beam antenna and onboard signal processing is considered for use in a 'message-switched' data relay system. The signal processor may incorporate demodulation, routing, storage, and remodulation of the data. A system user model is established and key functional elements for the signal processing are identified. With the throughput and delay requirements as the controlled variables, the hardware complexity, operational discipline, occupied bandwidth, and overall user end-to-end cost are estimated for (1) random-access packet switching; and (2) reservation-access packet switching. Other aspects of this network (eg, the adaptability to channel switched traffic requirements) are examined. For the given requirements and constraints, the reservation system appears to be the most attractive protocol. (Author)

A80-29588 * # Ka-band, multibeam, contiguous coverage satellite antenna for the USA. P. Foldes (General Electric Co., Space Div., Philadelphia, Pa.) In: Communications Satellite Systems Conference, 8th, Orlando, Fla., April 20-24, 1980, Technical Papers. (A80-29526 11-32) New York, American Institute of Aeronautics and Astronautics, Inc., 1980, p. 490-499. Contract No. NAS3-21745. (AIAA 80-0557)

The behavior of a multibeam antenna is determined by three

major characteristics: beam topology, realizable radiation characteristics, and realizable beamforming network architecture. Eight canonical topology plans have been developed and analyzed: angular separation between identical frequency cells, angular separation between orthogonally polarized identical frequency cells, number and configuration of cells forming coverage areas, and crossover level between nonidentical frequency band cells. A general topology plan is developed for the continental United States for 100-deg W synchronous satellite longitude.

B.J.

A80-29605 * # Multigigabit satellite on-board signal processing. W. M. Holmes, Jr. (TRW, Inc., Space Systems Div., Redondo Beach, Calif.). In: Communications Satellite Systems Conference, 8th, Orlando, Fla., April 20-24, 1980, Technical Papers (A80-29526 11-32) New York, American Institute of Aeronautics and Astronautics, Inc., 1980, p. 623-626. Contract No. NAS3-21933. (AIAA 80-0583)

The satellite communication system described provides communications for very small and very large (trunking) users. Independent combinations of FDMA and TDMA are used in the uplink and downlink designs to minimize terminal costs. Signal routing for small users is accomplished by a digital store-and-forward technique which greatly simplifies the terminal receiver, compared to satellite-switched TDMA. Different processing techniques are used for very high data rate users, but complete interconnectivity between all users is maintained. This avoids double-hop routing with excessive transmission delays.

(Author)

A80-52479 * System analysis for millimeter-wave communication satellites. L. D. Holland, N. B. Hilsen, J. J. Gallagher (Georgia Institute of Technology, Atlanta, Ga.), and G. Stevens (NASA, Lewis Research Center, Cleveland, Ohio). *Microwave Journal*, vol. 23, Oct. 1980, p. 43-45, 93, 10 refs.

Research and development needs for millimeter-wave space communication systems are presented. Assumed propagation fade statistics are investigated along with high data rate diversity link and storage. The development of reliable ferrite switches, and high performance receivers and transmitters is discussed, in addition to improved tolerance of dish and lens fabrication for the antennas. The typical cost for using a simplex voice channel via a high capacity 40/50 GHz satellite is presented.

R.C.

33 ELECTRONICS AND ELECTRICAL ENGINEERING

Includes test equipment and maintainability; components, e.g., tunnel diodes and transistors; microminiaturization; and integrated circuitry.

For related information see also 60 Computer Operations and Hardware and 76 Solid-State Physics.

N80-11327* National Aeronautics and Space Administration. Lewis Research Center, Cleveland, Ohio.

HEAT PIPE COOLING OF POWER PROCESSING MAGNETICS

Irving G. Hansen and Morris Chester (TRW Corp., Redondo Beach, Calif.) 1979 10 p refs Presented at the 14th Intern. Conf. on Elec. Propulsion, Princeton, N. J., 30 Oct. - 2 Nov. 1979; Sponsored by AIAA and Deut. Ges. für Luft- und Raumfahrt (NASA-TM-79270; E-223) Avail: NTIS HC A02/MF A01 CSCL 09C

A heat pipe cooled transformer and input filter were developed for the 2.4 kW beam supply of a 30 cm ion thruster system. This development yielded a mass reduction of 40% (1.76 kg)

N80-13361* National Aeronautics and Space Administration. Lewis Research Center, Cleveland, Ohio.

PERFORMANCE OF 22.4-kW NONLAMINATED-FRAME dc SERIES MOTOR WITH CHOPPER CONTROLLER Final Report

John R. Schwab Sep. 1979 25 p refs (Contract EC-77-A-31-1044)

(NASA-TM-79252; DOE/NASA/1044-79/4; E-163) Avail: NTIS HC A02/MF A01 CSCL 09C

Performance data obtained through experimental testing of a 22.4 kW traction motor using two types of excitation are presented. Ripple free dc from a motor-generator set for baseline data and pulse width modulated dc as supplied by a battery pack and chopper controller were used for excitation. For the same average values of input voltage and current, the motor power output was independent of the type of excitation. However, at the same speeds, the motor efficiency at low power output (corresponding to low duty cycle of the controller) was 5 to 10 percentage points lower on chopped dc than on ripple free dc. The chopped dc locked rotor torque was approximately 1 to 3 percent greater than the ripple free dc torque for the same average current. J.M.S.

N80-18300* National Aeronautics and Space Administration. Lewis Research Center, Cleveland, Ohio.

LIQUID METAL SLIP RING Patent Application

Frank D. Berkopec, Robert R. Lovell, and David H. Culp, inventors (to NASA) Filed 21 Dec. 1979 11 p (NASA-Case-LEW-12277-3; US-Patent-Appl-SN-106190) Avail: NTIS HC A02/MF A01 CSCL 09A

The liquid metal slip ring described comprises a rotor in the form of a ring about an axis and a stator, the rotor being rotatable relative to the stator. The rotor has a channel in which the liquid metal is retained during operation by surface tension. The stator comprises a brush or probe which is partially immersed in the metal in the channel and is bidirectionally symmetrical so that whichever direction the rotor turns the probe presents the same physical resistance and affords the same electrical conductivity as a connection between the probe and the rotor. Author

N80-18302* National Aeronautics and Space Administration. Lewis Research Center, Cleveland, Ohio.

THERMIONIC CATHODE LIFE TEST STUDIES

Ralph Forman and Paul Elmer (Watkins-Johnson, Palo Alto, Calif.) 1980 11 p refs Proposed for presentation at the Tri-Services

Cathode Workshop, New York, 15-17 Apr. 1980, sponsored by Dept. of the Air Force (NASA-TM-81441; E-317) Avail: NTIS HC A02/MF A01 CSCL 09A

An update on the life testing of commercial, high current density impregnated tungsten cathodes is presented. The B-type cathodes, operated at a current density of 2 A/cm² and a cathode temperature of 1100 C have now been run satisfactorily for more than four years. The M-cathode, at the same current density but at an operating temperature of only 1010 C, have been tested for more than three years. The M-cathodes show no degradation in current over their present operating life whereas the current from the B-cathodes degrade about 6 percent after four years of operation. R.E.S.

N80-19425* National Aeronautics and Space Administration. Lewis Research Center, Cleveland, Ohio.

COUPLED CAVITY TRAVELING WAVE TUBE WITH VELOCITY TAPERING Patent Application

Denis J. Connolly, inventor (to NASA) Filed 20 Feb. 1980 16 p (NASA-Case-LEW-12296-1; US-Patent-Appl-SN-122966) Avail: NTIS HC A02/MF A01 CSCL 09A

A coupled cavity traveling wave tube is described which has a velocity taper, i.e., gradual velocity reduction, which affords beam wave resynchronization and thereby enhances efficiency. The required wave velocity reduction is achieved by reducing the resonant frequencies of the individual resonant cavities as a function of the distance from the electron gun through changes in the internal cavity dimensions. The required changes in cavity dimensions are accomplished, for example, by gradually increasing the cavity radius or decreasing the gap length from cavity to cavity. NASA

N80-20487* National Aeronautics and Space Administration. Lewis Research Center, Cleveland, Ohio.

CATALYST SURFACES FOR THE CHROMOUS/CHROMIC REDOX COUPLE Patent

Jose D. Giner (Giner, Inc.) and Kathleen J. Cahill, inventor (to NASA) (Giner, Inc.) Issued 11 Mar. 1980 8 p Filed 29 Nov. 1978 Supersedes N79-14538 (17 - 05, p 0618) Sponsored by NASA

(NASA-Case-LEW-13148-1; US-Patent-4,192,910; US-Patent-Appl-SN-964754; US-Patent-Class-429-101; US-Patent-Class-429-105; US-Patent-Class-429-107; US-Patent-Class-429-109) Avail: US Patent and Trademark Office CSCL 09A

An electricity producing cell of the reduction-oxidation (REDOX) type is described. The cell is divided into two compartments by a membrane, each compartment containing a solid inert electrode. A ferrous/ferric couple in a chloride solution serves as a cathode fluid which is circulated through one of the compartments to produce a positive electric potential disposed therein. A chromic/chromous couple in a chloride solution serves as an anode fluid which is circulated through the second compartment to produce a negative potential on an electrode disposed therein. The electrode is an electrically conductive, inert material plated with copper, silver or gold. A thin layer of lead plates onto the copper, silver or gold layer when the cell is being charged, the lead ions being available from lead chloride which was added to the anode fluid. If the REDOX cell is then discharged, the current flows between the electrodes causing the lead to deplate from the negative electrode and the metal coating on the electrode will act as a catalyst to cause increased current density.

Official Gazette of the U.S. Patent and Trademark Office

N80-21669* National Aeronautics and Space Administration. Lewis Research Center, Cleveland, Ohio.

MULTISTAGE DEPRESSED COLLECTOR WITH EFFICIENCY OF 90 TO 94 PERCENT FOR OPERATION OF A DUAL-MODE TRAVELING WAVE TUBE IN THE LINEAR REGION

Peter Ramins and Thomas A. Fox Washington Apr. 1980 16 p refs

(NASA-TP-1670; E-9375) Avail: NTIS HC A02/MF A01 CSCL 09A

An axisymmetric, multistage, depressed collector of fixed geometric design was evaluated in conjunction with an octave bandwidth, dual mode traveling wave tube (TWT). The TWT was operated over a wide range of conditions to simulate different applications. The collector performance was optimized (within the constraint of fixed geometric design) over the range of TWT operating conditions covered. For operation of the TWT in the linear, low distortion range, 90 percent and greater collector efficiencies were obtained leading to TWT overall efficiencies of 20 to 35 percent, as compared with 2 to 5 percent with an undepressed collector. With collectors of this efficiency and minimized beam interception losses, it becomes practical to design dual mode TWT's such that the low mode can represent operation well below saturation. Consequently, the required pulse up in beam current can be reduced or eliminated, and this mitigates beam control and dual mode TWT circuit design problems. For operation of the dual mode TWT at saturation, average collector efficiencies in excess of 85 percent were obtained for both the low and high modes across an octave bandwidth, leading to a three to fourfold increase in the TWT overall efficiency. Author

N80-22598* // National Aeronautics and Space Administration, Lewis Research Center, Cleveland, Ohio.

IMPROVED TRAVELING WAVE TUBES

Erik Buck 1980 15 p refs Presented at Western Region Electronic Warfare Tech. Meeting, White Sands Missile Range, N. Mex., 21-24 Apr. 1980; sponsored by Assoc. of Old Crows (NASA-TM-81479; E-415) Avail: NTIS HC A02/MF A01 CSCL 09A

After a brief description of how a typical TWT works, multi-stage depressed collectors (MDC) are discussed. A quick method for computing the expected efficiency of a well engineered TWT is outlined to aid in estimating power supply needs. Applications of improved TWTs and a new power supply are suggested. E.D.K.

A80-13902* // Analytical prediction and experimental verification of TWT and depressed collector performance using multidimensional computer programs. J. A. Dayton, Jr., H. G. Kosmahl, P. Ramins, and N. Stankiewicz (NASA, Lewis Research Center, Cleveland, Ohio). *IEEE Transactions on Electron Devices*, vol. ED-26, Oct. 1979, p. 1589-1598, 14 refs.

A80-13903* // A matrix solution for the simulation of magnetic fields with ideal current loops. N. Stankiewicz (NASA, Lewis Research Center, Cleveland, Ohio). *IEEE Transactions on Electron Devices*, vol. ED-26, Oct. 1979, p. 1598-1601, 5 refs.

A matrix formulation is presented for describing axisymmetric magnetic field data with ideal current loops. A computer program written in APL is used to invert the matrix and hence to solve for the coil strengths which are used to represent the field data. Examples are given of the coil representation for (1) measured magnetic data, (2) refocusing fields, and (3) PPM focusing fields. (Author)

A80-13909* // 90- to 93-percent efficient collector for operation of a dual-mode traveling-wave tube in the linear region. P. Ramins and T. A. Fox (NASA, Lewis Research Center, Cleveland, Ohio). *IEEE Transactions on Electron Devices*, vol. ED-26, Oct. 1979, p. 1662-1664, 8 refs.

An axisymmetric multistage depressed collector was evaluated in conjunction with a dual-mode TWT. Collector performance optimizations for the TWT operation in the linear range were stressed. Measured collector efficiencies in excess of 90 percent led to dramatic improvements in TWT overall efficiency. (Author)

A80-14720* Elastohydrodynamic film thickness measurements of artificially-produced nonsmooth surfaces. C. Cusano (Illinois, University, Urbana, Ill.) and L. D. Wedeven (NASA, Lewis Research Center, Cleveland, Ohio). *American Society of Lubrication Engineers and American Society of Mechanical Engineers, Lubrication Conference, Dayton, Ohio, Oct. 16-18, 1979, ASLE Preprint 79-LC-1A-3*, 13 p. 19 refs.

Optical interferometry is used to measure the elastohydrodynamic (EHD) film thickness associated with artificially produced, nonsmooth surfaces. The nonsmooth surfaces are produced by modifying the surfaces of highly-polished balls with irregularities in the form of multiple grooves and dents. By closely spacing these irregularities, it is possible not only to produce depressions on the surface of the balls but also to generate pseudo asperities. The average roughness wavelength of this artificially-produced, nonsmooth surface approximates the average fundamental roughness wavelength found on surfaces of some mechanical elements operating under concentrated contact. By comparing the measured film thickness profiles to the stylus traces of the irregularities, it is possible to observe the local deformations associated with micro-EHD pressure generation. In both pure rolling and pure sliding conditions, the artificially-produced 'asperities' are deformed and complete separation exists between them and the mating surface. Such findings demonstrate the importance of local surface topography and resulting micro-EHD effects on the film thickness between rough surfaces in concentrated contact. In addition, sliding data are presented which demonstrate a severe constriction, caused by the irregularities, at the exit of the Hertzian region. (Author)

A80-18232* // Two-dimensional representations of axisymmetric fields for computer calculations. N. Stankiewicz (NASA, Lewis Research Center, Cleveland, Ohio). *IEEE Transactions on Electron Devices*, vol. ED-26, Nov. 1979, p. 1790-1795.

An accurate representation of axisymmetric fields has been devised by extending the method of ideal current loops to off-axis fields. It is assumed that the data to be simulated are available through measurements or through a solution of a boundary value problem. The method provides an algebraic expression for the fields throughout a two-dimensional region of interest and eliminates the need for the axial expansion formula in approximating off-axis fields. The use of Gaussian and other functions as alternatives to the coil function is proposed. Examples of the technique in simulating a periodic permanent magnet (PPM) focusing field are presented and compared with a Fourier analysis of the problem. (Author)

A80-31759* // How to quickly predict the overall TWT and the multistage depressed collector efficiency. H. G. Kosmahl (NASA, Lewis Research Center, Cleveland, Ohio). *IEEE Transactions on Electron Devices*, vol. ED-27, Mar. 1980, p. 526-529, 6 refs.

The study deals with an empirical, simple formula extracted from a three-dimensional helical-TWT computer program that expresses the lowest energy in a spent beam in terms of beam perveance and electronic efficiency. The formula has a general validity down to 4 - 5 dB below saturation and gives 1 - delta V/V with less than 20% error down to 10 dB below saturation. V.T.

A80-44235* // Improved traveling wave tubes. E. Buck (NASA, Lewis Research Center, Cleveland, Ohio). *Association of Old Crows, Western Region Electronic Warfare Technical Meeting, White Sands Missile Range, N. Mex., Apr. 21-24, 1980, Paper*, 13 p. 7 refs.

Techniques, pioneered by NASA, which will allow substantial improvements in traveling wave tube (TWT) amplifier efficiency, are described. It is shown that using design techniques developed at the Lewis Research Center, it is possible to approximately double the efficiency of the critical amplifier TWT. Attention is given to a quick method of computing the expected improvement to an ECM TWT. The benefits of such improvements such as less input power, a smaller and lighter power supply, and easier cooling are surveyed, and it is noted that it is now possible to build efficient TWT's which

rather than operating at saturation, can be very linear amplifiers. Finally, a new approach to power supplies is also covered. M.E.P.

A80-45122 * Life test studies on tungsten impregnated cathodes. R. Forman (NASA, Lewis Research Center, Cleveland, Ohio) and P. Elmer (Watkins-Johnson Co., Palo-Alto, Calif.). *IEEE Transactions on Electron Devices*, vol. ED-27, July 1980, p. 1309, 1310.

NASA-Lewis Research Center has conducted an ongoing life test program on commercial impregnated tungsten cathodes since 1971. This brief is an update of the information as of December 1979. B-type cathodes, operated at 1100 C have been run in simulated microwave tubes at 2 A/sq cm for more than four years with about 6-percent degradation in current at a constant reference anode voltage. M-type cathodes have been operated for 30,000 h at a cathode temperature of 1010 C and 2 A/sq cm with no degradation in current as a constant reference anode voltage. (Author)

N80-11328 # Hughes Research Labs., Malibu, Calif.
SOLID-STATE X-BAND COMBINER STUDY Final Report
O. Pitzalis, Jr. and K. J. Russell Aug. 1979 79 p refs Prepared for JPL
(Contracts NAS7-100; JPL-955223)
(NASA-CR-162432) Avail: NTIS HC A05/MF A01 CSCL 09C

The feasibility of developing solid-state amplifiers at 4 and 10 GHz for application in spacecraft altimeters was studied. Bipolar-transistor, field-effect-transistor, and Impatt-diode amplifier designs based on 1980 solid-state technology are investigated. Several output power levels of the pulsed, low-duty-factor amplifiers are considered at each frequency. Proposed transistor and diode amplifier designs are illustrated in block diagrams. Projections of size, weight, and primary power requirements are given for each design. R.C.T.

N80-13362 # TRW Defense and Space Systems Group, Redondo Beach, Calif. Power Conversion Electronics Dept.
HEAT PIPE COOLED POWER MAGNETICS Final Report
M. S. Chester Dec. 1979 176 p Revised
(NASA-CR-159659; TRW-33572-6001-RU-00) Avail: NTIS HC A09/MF A01 CSCL 09A

A high frequency, high power, low specific weight (0.57 kg/kW) transformer developed for space use was re-designed with heat pipe cooling allowing both a reduction in weight and a lower internal temperature rise. The specific weight of the heat pipe cooled transformer was reduced to 0.4 kg/kW and the highest winding temperature rise was reduced from 40 C to 20 C in spite of 10 watts additional loss. The design loss/weight tradeoff was 18 W/kg. Additionally, allowing the same 40 C winding temperature rise as in the original design, the KVA rating is increased to 4.2 KVA, demonstrating a specific weight of 0.28 kg/kW with the internal loss increased by 50W. This space environment tested heat pipe cooled design performed as well electrically as the original conventional design, thus demonstrating the advantages of heat pipes integrated into a high power, high voltage magnetic. Another heat pipe cooled magnetic, a 3.7 kW, 20A input filter inductor was designed, developed, built, tested, and described. The heat pipe cooled magnetics are designed to be Earth operated in any orientation. Author

N80-24550 # Three E Vehicles, San Diego, Calif.
THE PERFORMANCE AND EFFICIENCY OF FOUR MOTOR/CONTROLLER/BATTERY SYSTEMS FOR THE SIMPLER ELECTRIC VEHICLES Final Report
Paul R. Shippo May 1980 88 p refs
(Contracts DEN3-130; EC-77-A-31-1044)
(NASA-CR-159776; DOE/NASA/0130-80/1) Avail: NTIS HC A05/MF A01 CSCL 09C

A test and analysis program performed on four complete propulsion systems for an urban electric vehicle (EV) is described and results given. A dc series motor and a permanent magnet

(PM) motor were tested, each powered by an EV battery pack and controlled by (1) a series/parallel voltage-switching (V-switch) system; and (2) a system using a pulse width modulation, 400 Hz transistorized chopper. Dynamometer tests were first performed, followed by eV performance predictions and data correlating road tests. During dynamometer tests using chopper control; current, voltage, and power were measured on both the battery and motor sides of the chopper, using three types of instrumentation. Conventional dc instruments provided adequate accuracy for eV power and energy measurements, when used on the battery side of the controller. When using the chopper controller, the addition of a small choke inductor improved system efficiency in the lower duty cycle range (some 8% increase at 50% duty cycle) with both types of motors. Overall system efficiency rankings during road tests were: (1) series motor with V-switch; (2) PM motor with V-switch; (3) series motor with chopper; and (4) PM motor with chopper. Chopper control of the eV was smoother and required less driver skill than V-switch control. M.G.

A80-28167 * An adaptive-control switching buck regulator - Implementation, analysis, and design. F. C. Lee (Virginia Polytechnic Institute and State University, Blacksburg, Va.) and Y. Yu (TRW Defense and Space Systems Group, Redondo Beach, Calif.). *IEEE Transactions on Aerospace and Electronic Systems*, vol. AES-16, Jan. 1980, p. 84-99, 13 refs. Contracts No. NAS3-20102; No. NAS3-21051.

Describing-function techniques and averaging methods have been employed to characterize a multiloop switching buck regulator by three functional blocks: power stage, analog signal processor, and pulse modulator. The model is employed to explore possible forms of pole-zero cancellation and the adaptive nature of the control to filter parameter changes. Analysis-based design guidelines are provided including a suggested additional RC-compensation loop to optimize regulator performances such as stability, audiosusceptibility, output impedance, and load transient response. (Author)

34 FLUID MECHANICS AND HEAT TRANSFER

Includes boundary layers, hydrodynamics, fluidics; mass transfer; and ablation cooling.

For related information see also 02 Aerodynamics and 77 Thermodynamics and Statistical Physics.

N80-11376* National Aeronautics and Space Administration, Lewis Research Center, Cleveland, Ohio.

STREAKLINE FLOW VISUALIZATION STUDY OF A HORSESHOE VORTEX IN A LARGE-SCALE, TWO-DIMENSIONAL TURBINE STATOR CASCADE

Raymond E. Gaugler and Louis M. Russell 1979 20 p refs Proposed for presentation at 25th Intern. Gas Turbine Conf. and Products Show, New Orleans, La., 9-13 Mar. 1980; sponsored by ASME (NASA-TM-79274; E-201) Avail: NTIS HC A02/MF A01 CSCL 20D

Neutrally bouyant helium-filled bubbles were observed as they followed the streamlines in a horseshoe vortex system around the vane leading edge in a large scale, two dimensional, turbine stator cascade. Inlet Reynolds number, based on true chord, ranged between 100,000 to 300,000. Bubbles were introduced into the endwall boundary layer through a slot upstream of the vane leading edge. The paths of the bubbles were recorded photographically as streaklines on 16 mm movie film. Individual frames from the film were selected, and overlayed to show the details of the horseshoe vortex around the leading edge. The transport of the vortex across the passage near the leading edge is clearly seen when compared to the streaks formed by bubbles carried in the main stream. Limiting streamlines on the endwall surface were traced by the flow of oil drops. Author

N80-13403* National Aeronautics and Space Administration, Lewis Research Center, Cleveland, Ohio.

MARANGONI BUBBLE MOTION IN ZERO GRAVITY

Robert L. Thompson and Kenneth J. DeWitt (Toledo Univ.) 1979 38 p refs Presented at the 72nd Ann. Meeting of the AICE, San Francisco, 25-29 Nov. 1979 (NASA-TM-79250; E-160) Avail: NTIS HC A03/MF A01 CSCL 20D

It was shown experimentally that the Marangoni phenomenon is a primary mechanism for the movement of a gas bubble in a nonisothermal liquid in a low gravity environment. A mathematical model consisting of the Navier-Stokes and thermal energy equations, together with the appropriate boundary conditions for both media, is presented. Parameter perturbation theory is used to solve this boundary value problem; the expansion parameter is the Marangoni number. The zeroth, first, and second order approximations for the velocity, temperature and pressure distributions in the liquid and in the bubble, and the deformation and terminal velocity of the bubble are determined. Experimental zero gravity data for a nitrogen bubble in ethylene glycol, ethanol, and silicone oil subjected to a linear temperature gradient were obtained using the NASA Lewis zero gravity drop tower. Comparison of the zeroth order analytical results for the bubble terminal velocity showed good agreement with the experimental measurements. The first and second order solutions for the bubble deformation and bubble terminal velocity are valid for liquids having Prandtl numbers on the order of one, but there is a lack of appropriate data to test the theory fully. K.L.

N80-13404* National Aeronautics and Space Administration, Lewis Research Center, Cleveland, Ohio.

COMBUSTION OF SOLID CARBON RODS IN ZERO AND NORMAL GRAVITY

C. M. Spuckler, F. J. Kohl, R. A. Miller, C. A. Stearns, and K. J. DeWitt (Toledo Univ.) 1979 32 p refs Presented at the 72nd Ann. AICE Meeting, San Francisco, 25-29 Nov. 1979 (NASA-TM-79303; E-255) Avail: NTIS HC A03/MF A01 CSCL 21B

In order to investigate the mechanism of carbon combustion, spectroscopic carbon rods were resistance ignited and burned in an oxygen environment in normal and zero gravity. Direct mass spectrometric sampling was used in the normal gravity tests to obtain concentration profiles of CO₂, CO, and O₂ as a function of distance from the carbon surface. The experimental concentrations were compared to those predicted by a stagnant film model. Zero gravity droptower tests were conducted in order to assess the effect of convection on the normal gravity combustion process. The ratio of flame diameter to rod diameter as a function of time for oxygen pressures of 5, 10, 15, and 20 psia was obtained for three different diameter rods. It was found that this ratio was inversely proportional to both the oxygen pressure and the rod diameter. K.L.

N80-15361* National Aeronautics and Space Administration, Lewis Research Center, Cleveland, Ohio.

COMPUTER PROGRAM FOR GENERATING INPUT FOR ANALYSIS OF IMPINGEMENT-COOLED, AXIAL-FLOW TURBINE BLADE

David Rosenbaum Jan. 1980 57 p refs Prepared in cooperation with Army Aviation Research and Development Command, Cleveland, Ohio

(NASA-TP-1603; AVRADCOM-TR-79-34) Avail: NTIS HC A04/MF A01 CSCL 20D

A computer program, TACTGRID, was developed to generate the geometrical input for the TACTI program, a program that calculates transient and steady state temperatures, pressures, and cooling flows in an impingement cooled turbine blade. Using spline curves, the TACTGRID program constructs the blade internal geometry from the previously designed external blade surface and newly selected wall and channel thicknesses. The TACTGRID program generates the TACTI calculational grid, calculates arc length between grid points required by TACTI as input, and prepares the namelist input data set used by TACTI for the blade geometry. In addition, TACTGRID produces a scaled computer plot of each blade slice, detailing the grid and calculational stations, and thus eliminates the need for intermediate drafting J.M.S.

N80-15364* National Aeronautics and Space Administration, Lewis Research Center, Cleveland, Ohio.

COMPUTATION OF THREE-DIMENSIONAL FLOW IN TURBOFAN MIXERS AND COMPARISON WITH EXPERIMENTAL DATA

L. A. Povinelli, B. H. Anderson, and W. Gerstenmaier Jan. 1980 12 p refs Presented at the AIAA Aerospace Sciences Meeting, Pasadena, Calif., 14-16 Jan. 1980 (NASA-TM-81410; E-324) Avail: NTIS HC A02/MF A01 CSCL 20D

A three dimensional, viscous computer code was used to calculate the mixing downstream of a typical turbopan mixer geometry. Experimental data obtained using pressure and temperature rakes at the lobe and nozzle exit stations were used to validate the computer results. The relative importance of turbulence in the mixing phenomenon as compared with the streamwise vorticity set up by the secondary flows was determined. The observations suggest that the generation of streamwise vorticity plays a significant role in determining the temperature distribution at the nozzle exit plane. K.L.

N80-15365* National Aeronautics and Space Administration, Lewis Research Center, Cleveland, Ohio.

NUMERICAL SIMULATION OF SUPERSONIC INLETS USING A THREE-DIMENSIONAL VISCOUS FLOW ANALYSIS

B. H. Anderson and C. E. Towne Jan. 1980 17 p refs Presented at 18th Aerospace Sci. Meeting, Pasadena, Calif., 14-16 Jan. 1980; sponsored by AIAA (NASA-TM-81411; E-325) Avail: NTIS HC A02/MF A01 CSCL 20D

A three dimensional fully viscous computer analysis was evaluated to determine its usefulness in the design of supersonic inlets. This procedure takes advantage of physical approximations

to limit the high computer time and storage associated with complete Navier-Stokes solutions. Computed results are presented for a Mach 3.0 supersonic inlet with bleed and a Mach 7.4 hypersonic inlet. Good agreement was obtained between theory and data for both cases. Results of a mesh sensitivity study are also shown. K.L.

N80-17397* National Aeronautics and Space Administration, Lewis Research Center, Cleveland, Ohio.

EFFECTS OF A CERAMIC COATING ON METAL TEMPERATURES OF AN AIR-COOLED TURBINE VANE

Herbert J. Gladden and Curt H. Liebert Feb 1980 29 p refs (NASA-TP-1598; E-167) Avail: NTIS HC A03/MF A01 CSCL 20D

The metal temperatures of air cooled turbine vanes both uncoated and coated with the NASA thermal barrier system were studied experimentally. Current and advanced gas turbine engine conditions were simulated at reduced temperatures and pressures. Airfoil metal temperatures were significantly reduced, both locally and on the average, by use of the the coating. However, at low gas Reynolds number, the ceramic coating tripped a laminar boundary layer on the suction surface, and the resulting higher heat flux increased the metal temperatures. Simulated coating loss was also investigated and shown to increase local metal temperatures. However, the metal temperatures in the leading edge region remained below those of the uncoated vane tested at similar conditions. Metal temperatures in the trailing edge region exceeded those of the uncoated vane. K.L.

N80-17398* National Aeronautics and Space Administration, Lewis Research Center, Cleveland, Ohio.

VOLUME-ENERGY PARAMETERS AND TURBULENT-FLOW DENSITY FLUCTUATIONS

Robert C. Hendricks Jan. 1980 28 p refs (NASA-TP-1585; E-127) Avail: NTIS HC A03/MF A01 CSCL 20D

Volume-energy relations determined from an equation of state were used to group many sets of heat transfer data for liquids and gases, including the near-critical region. The volume - Gibbs energy parameter grouped these data better than did such other parameters as enthalpy, temperature, or internal energy. K.L.

N80-20532* National Aeronautics and Space Administration, Lewis Research Center, Cleveland, Ohio.

FACTORS AFFECTING CLEANUP OF EXHAUST GASES FROM A PRESSURIZED, FLUIDIZED-BED COAL COMBUSTOR

R. James Rollbuhler and John A. Kobak Mar. 1980 .37 p refs (NASA-TM-81439; E-382) Avail: NTIS HC A03/MF A01 CSCL 20D

The cleanup of effluent gases from the fluidized-bed combustion of coal is examined. Testing conditions include the type and feed rate of the coal and the sulfur sorbent, the coal-sorbent ratio, the coal-combustion air ratio, the depth of the reactor fluidizing bed, and the technique used to physically remove fly ash from the reactor effluent gases. Tests reveal that the particulate loading matter in the effluent gases is a function not only of the reactor-bed surface gas velocity, but also of the type of coal being burnt and the time the bed is operating. At least 95 percent of the fly ash particles in the effluent gas are removed by using a gas-solids separator under controlled operating conditions. Gaseous pollutants in the effluent (nitrogen and sulfur oxides) are held within the proposed Federal limits by controlling the reactor operating conditions and the type and quantity of sorbent material. M.G.

N80-21706* National Aeronautics and Space Administration, Lewis Research Center, Cleveland, Ohio.

SIMILARITY TESTS OF TURBINE VANES, EFFECTS OF CERAMIC THERMAL BARRIER COATINGS

Herbert J. Gladden 1980 14 p refs Proposed for Presentation at 1980 Natl. Heat Transfer Conf., Orlando, Fla., 27-30 Jul.

1980; sponsored by Heat Transfer and Gas Turbine Div. of ASME (NASA-TM-81473; E-407) Avail: NTIS HC A02/MF A01 CSCL 20D

The role of material thermal conductivity was analyzed for its effect on the thermal performance of air-cooled gas turbine components coated with a ceramic thermal barrier material when tested at reduced temperatures and pressures. It is shown that the thermal performance can be evaluated reliably at reduced gas and coolant conditions; however, thermal conductivity corrections are required for the data at reduced conditions. Corrections for a ceramic thermal barrier coated vane are significantly different than for an uncoated vane. Comparison of uncorrected test data, therefore, would show erroneously that the thermal barrier coating was ineffective. When thermal conductivity corrections are applied to the test data these data are then shown to be representative of engine data and also show that the thermal barrier coating increases the vane cooling effectiveness by 12.5 percent. A.R.H.

N80-24573* National Aeronautics and Space Administration, Lewis Research Center, Cleveland, Ohio.

HEAT EXCHANGER AND METHOD OF MAKING Patent

Anthony Fortini and John M. Kazaroff, inventors (to NASA) Issued 29 Apr. 1980 6 p Filed 30 Nov. 1977 Supersedes N79-21313 (17 - 02, p 0164) Div. of US Patent Appl. SN-559846, filed 19 Mar. 1975, US Patent No. 4,108,241

(NASA-Case-LEW-12441-2, US-Patent-4,199,937; US-Patent-Appl-SN-856462; US-Patent-Class-60-267; US-Patent-Class-239-127.1; US-Patent-Appl-SN-559846) Avail: US Patent and Trademark Office CSCL 20D

A heat exchange of increased effectiveness is disclosed. A porous metal matrix is disposed in a metal chamber or between walls through which a heat-transfer fluid is directed. The porous metal matrix has internal bonds and is bonded to the chamber in order to remove all thermal contact resistance within the composite structure. Utilization of the invention in a rocket chamber is disclosed as a specific use. Also disclosed is a method of constructing the heat exchanger.

Official Gazette of the U.S. Patent and Trademark Office

N80-24577* National Aeronautics and Space Administration, Lewis Research Center, Cleveland, Ohio.

EXTENSION OF SIMILARITY TEST PROCEDURES TO COOLED ENGINE COMPONENTS WITH INSULATING CERAMIC COATINGS

Herbert J. Gladden May 1980 16 p refs (NASA-TP-1615; E-337) Avail: NTIS HC A02/MF A01 CSCL 20D

Material thermal conductivity was analyzed for its effect on the thermal performance of air cooled gas turbine components, both with and without a ceramic thermal-barrier material, tested at reduced temperatures and pressures. The analysis shows that neglecting the material thermal conductivity can contribute significant errors when metal-wall-temperature test data taken on a turbine vane are extrapolated to engine conditions. This error in metal temperature for an uncoated vane is of opposite sign from that for a ceramic-coated vane. A correction technique is developed for both ceramic-coated and uncoated components. Author

N80-27632* National Aeronautics and Space Administration, Lewis Research Center, Cleveland, Ohio.

INFLUENCE OF PRESSURE DRIVEN SECONDARY FLOWS ON THE BEHAVIOR OF TURBOFAN FORCED MIXERS

B. Anderson, L. Povinelli, and W. Gerstenmaier Jul. 1980 28 p refs Presented at 16th Joint Prop. Conf., Hartford, Conn., 30 Jun. - 2 Jul. 1980; sponsored by AIAA, ACME, and SAE (NASA-TM-81541; E-493) Avail: NTIS HC A03/MF A01 CSCL 20C

A finite difference procedure was developed to analyze the three dimensional subsonic turbulent flows in turbofan forced mixer nozzles. The method is based on a decomposition of the velocity field into primary and secondary flow components which are determined by solution of the equations governing primary

momentum, secondary vorticity, thermal energy, and continuity. Experimentally, a strong secondary flow pattern was identified which is associated with the radial inflow and outflow characteristics of the core and fan streams and forms a very strong vortex system aligned with the radial interface between the core and fan regions. A procedure was developed to generate a similar generic secondary flow pattern in terms of two constants representing the average radial outflow or inflow in the core and fan streams as a percentage of the local streamwise velocity. This description of the initial secondary flow gave excellent agreement with experimental data. By identifying the nature of large scale secondary flow structure and associating it with characteristic mixer nozzle behavior, it is felt that the cause and effect relationship between lobe design and nozzle performance can be understood. E.D.K.

N80-23623* National Aeronautics and Space Administration, Lewis Research Center, Cleveland, Ohio

TOWARD THE USE OF SIMILARITY THEORY IN TWO-PHASE CHOKED FLOWS

R. C. Hendricks, J. V. Sengers (Maryland Univ., College Park), and R. J. Simoneau 1980 12 p refs Proposed for presentation at Winter Ann. Meeting of the ASME, Chicago 16-21 Nov. 1980

(NASA-TM-81568) Avail: NTIS HC A02/MF A01 CSCL 20D

Comparison of two phase choked flows in normalized coordinates were made between pure components and available data using a reference fluid to compute the thermophysical properties. The results are favorable. Solution of the governing equations for two LNG mixtures show some possible similarities between the normalized choked flows of the two mixtures, but the departures from the pure component loci are significant.

Author

N80-29624* National Aeronautics and Space Administration, Lewis Research Center, Cleveland, Ohio

PRELIMINARY RESULTS FROM A FOUR-WORKING SPACE, DOUBLE-ACTING PISTON, STIRLING ENGINE CONTROLS MODEL

Carl J. Daniele and Carl F. Lorenzo 1980 17 p refs Presented at the 15th Intersoc. Energy Conversion Eng. Conf., Seattle, 18-22 Aug 1980

(Contract EC-77-A-31-1040)

(NASA-TM-81569, DOE/NASA/1040-17; E-534) Avail: NTIS HC A02/MF A01 CSCL 20D

A four working space, double acting piston, Stirling engine simulation is being developed for controls studies. The development method is to construct two simulations, one for detailed fluid behavior, and a second model with simple fluid behaviour but containing the four working space aspects and engine inertias, validate these models separately, then upgrade the four working space model by incorporating the detailed fluid behaviour model for all four working spaces. The single working space (SWS) model contains the detailed fluid dynamics. It has seven control volumes in which continuity, energy, and pressure loss effects are simulated. Comparison of the SWS model with experimental data shows reasonable agreement in net power versus speed characteristics for various mean pressure levels in the working space. The four working space (FWS) model was built to observe the behaviour of the whole engine. The drive dynamics and vehicle inertia effects are simulated. To reduce calculation time, only three volumes are used in each working space and the gas temperature are fixed (no energy equation). Comparison of the FWS model predicted power with experimental data shows reasonable agreement. Since all four working spaces are simulated, the unique capabilities of the model are exercised to look at working fluid supply transients, short circuit transients, and piston ring leakage effects. Author

N80-32689* National Aeronautics and Space Administration, Lewis Research Center, Cleveland, Ohio

WIND TUNNEL INVESTIGATION OF THE TITAN FORWARD SKIRT COMPARTMENT VENT FROM A FREE-STREAM MACH NUMBER OF 0.80 TO 1.96

Albert L. Johns Washington Sep 1980 42 p refs (NASA-TM-81572, E-541) Avail: NTIS HC A03/MF A01 CSCL 20D

A test was conducted to determine the flow characteristics of the Titan forward skirt compartment vent over a free stream Mach number range of 0.80 to 1.96. The vent was mounted in a flat plate and the plate was flush mounted to the tunnel side wall with coinciding center lines. Air was discharged from a duct, located on the tunnel side wall behind the plate, through a canted aft 30 deg honeycomb vent into the free stream. Data for the analysis of the Titan forward skirt compartment venting during ascent through the atmosphere are provided. Full scale simulated flight hardware, such as the honeycomb vent, duct corrugations and field joint ring were used. Boundary layer thicknesses were used to vary boundary height. The highest vent discharge coefficient for any given Mach number and vent pressure ratio generally occurred at the maximum displacement thickness. With no vent flow the static pressure in the vent region was generally less than the free stream static pressure. With vent flow, the static pressures upstream of the vent increased, and those downstream of the vent decreased. R.K.G.

A80-10030 * Some aspects of a free jet phenomena to 105 L/D in a constant area duct. R. C. Hendricks (NASA, Lewis Research Center, Cleveland, Ohio). *International Institute of Refrigeration, International Congress of Refrigeration, 15th, Venice, Italy, Sept. 23-29, 1979, Paper, 39 p.* 7 refs.

The paper examines major constraints involved in the Borda tube free jet phenomena. Under certain conditions, inlets with a Borda type geometry show sufficiently strong separation effects to permit the working fluid to flow through the duct as if it were a 'free jet'. Mass limiting flow data and associated pressure profiles for tubes with L/D's ranging from 14 to 105 with a Borda type inlet were considered to determine bounds of the 'free jet' phenomena using fluid nitrogen. For a given tube roughness, the limits appear to be one dimensional and dependent only on inlet stagnation conditions. For smooth tubes, the upper L/D boundary is defined by an equation relating reduced pressure to reduced temperature, and the lower boundary represents saturation conditions at the inlet. Similar 'free jet' effects were found for fluid hydrogen indicating that fluid jetting may be common to all fluids. A.T.

A80-10031 * Critical mass flux through short Borda type inlets of various cross sections. R. C. Hendricks (NASA, Lewis Research Center, Cleveland, Ohio) and N. P. Poolos (Lake Ridge Academy, North Ridgeville, Ohio). *International Institute of Refrigeration, International Congress of Refrigeration, 15th, Venice, Italy, Sept. 23-29, 1979, Paper, 24 p.* 10 refs.

Mass flux measurements associated with choked flows through four Borda-type inlet geometries: circular, square, triangular, and rectangular (two-dimensional) and two sharp-edged geometries are discussed for a wide range of inlet stagnation conditions. The results obtained indicate that the mass flux is independent of the inlet cross-section geometry, while it is dependent on the inlet stagnation conditions. The results also suggest that parallel surfaces as found in seals, dampers, bearings, and heat exchanger tubes of rectangular cross section with Borda-type inlet configurations are subject to large forces. It is noted that the reduced mass flux is independent of working fluid. V.T.

A80-10037 * Free jet phenomena in a 90 deg-sharp edge inlet geometry. R. C. Hendricks (NASA, Lewis Research Center, Cleveland, Ohio). *National Bureau of Standards, International Cryogenic Engineering Conference and International Cryogenic Materials Conference, Madison, Wis., Aug. 21-24, 1979, Paper, 28 p.* 9 refs.

The effects of free-jet phenomena, jetting, in a 90-deg-sharp-edge inlet tube are analyzed. Mass-limiting flow data and associated pressure profiles for tubes of 53, 64, 73 and 105 L/D with a 90 deg-sharp-edge or orifice-type inlet are compared to Borda-type inlet data to determine bounds of the free-jet phenomena. For smooth

tubes the limits appear to be one-dimensional and dependent only on inlet stagnation conditions. The upper L/D boundary is related by stagnation characteristics and the lower bound appears to be saturation conditions at the inlet. It is noted that similar free-jet effects were found for fluid hydrogen indicating that fluid jetting might be common to all fluids flowing through 90 deg-sharp-edge inlet geometries. V.T.

A80-10038 * # A reduced volumetric expansion factor plot. R. C. Hendricks (NASA, Lewis Research Center, Cleveland, Ohio). *National Bureau of Standards, International Cryogenic Engineering Conference and International Cryogenic Materials Conference, Madison, Wis., Aug. 21-24, 1979, Paper, 27 p.* 7 refs.

A reduced volumetric expansion factor plot has been constructed for simple fluids which is suitable for engineering computations in heat transfer. Volumetric expansion factors have been found useful in correlating heat transfer data over a wide range of operating conditions including liquids, gases and the near critical region. (Author)

A80-10039 * # Application of the principle of similarity fluid mechanics. R. C. Hendricks (NASA, Lewis Research Center, Cleveland, Ohio) and J. V. Sengers (Maryland, University, College Park, Md.). *International Association for Properties of Steam, International Conference on the Properties of Steam, 9th, Munich, West Germany, Sept. 8-14, 1979, Paper, 47 p.* 90 refs. Grant No. NGR-21-002-344.

Possible applications of the principle of similarity to fluid mechanics is described and illustrated. In correlating thermophysical properties of fluids, the similarity principle transcends the traditional corresponding states principle. In fluid mechanics the similarity principle is useful in correlating flow processes that can be modeled adequately with one independent variable (i.e., one-dimensional flows). In this paper we explore the concept of transforming the conservation equations by combining similarity principles for thermophysical properties with those for fluid flow. We illustrate the usefulness of the procedure by applying such a transformation to calculate two phase critical mass flow through a nozzle. (Author)

A80-14660 * Evolution of a rotating flow in the vicinity of a surface. R. G. Deissler (NASA, Lewis Research Center, Fundamental Heat Transfer Branch, Cleveland, Ohio). In: *Studies in heat transfer: A Festschrift for E. R. G. Eckert.* (A80-14655 03-34) Washington, Hemisphere Publishing Corp.; New York, McGraw-Hill Book Co., 1979, p. 83-93 6 refs.

Evolution of a rotating flow in a body of fluid bounded by a stationary flat surface is discussed. The calculated results show that the radial pressure gradient is substantially reduced in the region close to the surface, so that letting that gradient be independent of distance from the surface would be expected to give only rough or qualitative estimates. However, the reduced rotation near the stationary surface is still large enough to cause an inflow near the surface and to set up a recirculation pattern. The concentration of vorticity by the radial inflow is not great enough to increase the tangential velocities near the center of rotation. V.T.

A80-18538 * # Coolant tube curvature effects on film cooling as detected by infrared imagery. S. S. Papell and R. W. Graham (NASA, Lewis Research Center, Cleveland, Ohio). *American Society of Mechanical Engineers, Winter Annual Meeting, New York, N.Y., Dec. 2-7, 1979, Paper 79-WA/GT-7.* 5 p. 6 refs. Members, \$1.50; nonmembers, \$3.00.

Reported herein are comparative thermal film cooling footprints observed by infrared imagery from straight, curved and looped coolant tube geometries. It was hypothesized that the difference in secondary flow and turbulence structure of flow through these three tubes should influence the mixing properties between the coolant and mainstream. The coolant was injected across an adiabatic plate through a hole angled at 30 deg to the surface in line with the free

stream flow. The data cover a range of blowing rates from 0.37 to 1.25 (mass flow per unit area of coolant divided by free stream). Average temperature difference between coolant and tunnel air was 25 C. Data comparisons confirmed that coolant tube curvature significantly influences film cooling effectiveness. (Author)

A80-20958 * # Marangoni bubble motion in zero gravity. R. L. Thompson (NASA, Lewis Research Center, Cleveland, Ohio) and K. J. De Witt (Toledo, University, Toledo, Ohio). *American Institute of Chemical Engineers, Annual Meeting, 72nd, San Francisco, Calif., Nov. 25-29, 1979, Paper, 36 p.* 10 refs.

It is shown experimentally that the Marangoni phenomenon is a primary mechanism for the movement of a gas bubble in a nonisothermal liquid in a low-gravity environment. In such two-phase flow systems, local variations in bubble surface tension are caused by a temperature gradient in the liquid. Shearing stresses thus generated at the bubble surface lead to convection in both media, as a result of which the bubble begins to move. A mathematical model consisting of the Navier Stokes equations and the thermal energy equations, along with the appropriate boundary conditions for both media, is proposed. V.P.

A80-20960 * # Heat pipe cooling of power processing magnetics. I. G. Hansen (NASA, Lewis Research Center, Cleveland, Ohio) and M. Chester (TRW, Inc., Redondo Beach, Calif.). *Princeton University, AIAA, and DGLR, International Electric Propulsion Conference, 14th, Princeton, N.J., Oct. 30 - Nov. 1, 1979, AIAA Paper 79-2082.* 9 p.

The constant demand for increased power and reduced mass has raised the internal temperature of conventionally cooled power magnetics toward the upper limit of acceptability. The conflicting demands of electrical isolation, mechanical integrity, and thermal conductivity preclude significant further advancements using conventional approaches. However, the size and mass of multikilowatt power processing systems may be further reduced by the incorporation of heat pipe cooling directly into the power magnetics. Additionally, by maintaining lower more constant temperatures, the life and reliability of the magnetic devices will be improved. A heat pipe cooled transformer and input filter have been developed for the 2.4 kW beam supply of a 30-cm ion thruster system. This development yielded a mass reduction of 40% (1.76 kg) and a lower mean winding temperature (20 C lower). While these improvements are significant, preliminary designs predict even greater benefits to be realized at higher power. This paper presents the design details along with the results of thermal vacuum operation and the component performance in a 3 kW breadboard power processor. (Author)

A80-28419 * # Effect of temperature on surface noise. W. Olsen and C. Wasserbauer (NASA, Lewis Research Center, Cleveland, Ohio). *AIAA Journal*, vol. 18, Mar. 1980, p. 339, 340. 8 refs.

An experimental work is discussed whose objective was to obtain data that show the effect of temperature and temperature fluctuations on surface noise. This was accomplished experimentally by immersing a small chord airfoil in the turbulent airstream of a hot jet. The theory and experiment reported by Olsen (1976) provided a guide for designing and validating the hot jet experiment and for interpreting the data. It is shown that increased temperature causes a small decrease in the sound levels; at the same time it causes a shift in the spectra that is smaller but similar to the shift observed with subsonic hot jet noise. S.D.

A80-44228 * # An alternative approach to the numerical simulation of steady inviscid flow. G. M. Johnson (NASA, Lewis Research Center, Cleveland, Ohio). *U.S. Air Force, NASA, NSF, and U.S. Navy, International Conference on Numerical Methods in Fluid Dynamics, 7th, Stanford University, Stanford, Calif., June 23-27, 1980, Paper.* 6 p. 9 refs.

A numerical procedure for the efficient simulation of steady inviscid flow is described and its utility is demonstrated. The method is uniformly valid for application in the subsonic, transonic and supersonic flow regimes. It does not rely on the introduction of additional assumptions beyond those necessary to obtain the Euler equations from the Navier-Stokes equations, nor does it make use of a time-asymptotic solution of the unsteady equations of motion. Application of the herein-defined surrogate equation technique allows the formulation of stable, fully-conservative, type-dependent finite difference equations for use in obtaining numerical solutions to systems of first-order partial differential equations, such as the steady-state Euler equations or their various approximations. Computational results are presented for the full Euler equations used to simulate rotational subsonic flow and for the transonic small disturbance equations. For the latter case, a computational efficiency greater than that obtained by means of the standard perturbation potential approach is indicated. (Author)

N80-10460* Battelle Columbus Labs., Ohio.
SPRAY NOZZLE DESIGNS FOR AGRICULTURAL AVIATION APPLICATIONS Final Report, Oct. 1978 - Sep. 1979
 K. W. Lee, A. A. Putnam, J. A. Gieseke, M. N. Golovin, and J. A. Hale 18 Sep 1979 105 p refs
 (Contract NAS3-21581)
 (NASA-CR-159702) Avail: NTIS HC A06/MF A01 CSCL 20D

Techniques of generating monodisperse sprays and information concerning chemical liquids used in agricultural aviation are surveyed. The periodic dispersion of liquid jet, the spinning disk method, and ultrasonic atomization are the techniques discussed. Conceptually designed spray nozzles for generating monodisperse sprays are assessed. These are based on the classification of the drops using centrifugal force, on using two opposing liquid laden air jets, and on operating a spinning disk at an overloaded flow. Performance requirements for the designs are described and estimates of the operational characteristics are presented. A.W.H.

N80-14356* Scientific Research Associates, Inc., Glastonbury, Conn.
DEVELOPMENT OF A THREE-DIMENSIONAL SUPERSONIC INLET FLOW ANALYSIS Final Report
 R. C. Buggein, H. McDonald, R. Levy, and J. P. Kreskovsky Jan. 1980 122 p refs
 (Contract NAS3-21003)
 (NASA-CR-3218) Avail: NTIS HC A06/MF A01 CSCL 20D
 A method for computing three dimensional flow in supersonic inlets is described. An approximate set of governing equations is given for viscous flows which have a primary flow direction. The governing equations are written in general orthogonal coordinates. These equations are modified in the subsonic region of the flow to prevent the phenomenon of branching. Results are presented for the two sample cases: a Mach number equals 2.5 flow in a square duct, and a Mach number equals 3.0 flow in a research jet engine inlet. In the latter case the computed results are compared with the experimental data. A users' manual is included. Author

N80-19450* FWG Associates, Inc., Tullahoma, Tenn.
MONODISPERSE ATOMIZERS FOR AGRICULTURAL AVIATION APPLICATIONS Final Report
 Larry S. Christensen and Sidney L. Stealy Feb. 1980 81 p refs
 (Contract NAS3-21582)
 (NASA-CR-159777) Avail: NTIS HC A05/MF A01 CSCL 20D

Conceptual designs of two monodisperse spray nozzles are described and the rationale used in each design is discussed. The nozzles were designed to eliminate present problems in agricultural aviation applications, such as ineffective plant coverage, drift due to small droplets present in the spray being dispersed, and nonuniform swath coverages. Monodisperse atomization techniques are reviewed and a synopsis of the

information obtained concerning agricultural aviation spray applications is presented. A.W.H.

N80-23599* Sigma Research, Inc., Richland, Wash.
TWO-PHASE WORKING FLUIDS FOR THE TEMPERATURE RANGE OF 50 TO 350 DEG, PHASE 2 Final Report
 E. W. Saaski and J. H. Hartl Mar. 1980 57 p refs
 (Contract NAS3-21202)
 (NASA-CR-159847) Avail: NTIS HC A04/MF A01 CSCL 20D

Several two phase heat transfer fluids were tested in aluminum and carbon steel reflux capsules for over 25,000 hours at temperatures up to 300 C. Several fluids showed very good stability and would be useful for long duration heat transfer applications over the range 100 to 350 C. Instrumentation for the measurement of surface tension and viscosity were constructed for use with heat transfer fluids over the temperature range 0 to 300 C and with pressures from 0 to 10 atmospheres. The surface tension measuring device constructed requires less than a 1.0 cc sample and displays an accuracy of about 5 percent in preliminary tests, while the viscometer constructed for this program requires a 0.05 cc sample and shows an accuracy of about 5 percent in initial tests. E.D.K.

N80-32688* TRW Defense and Space Systems Group, Redondo Beach, Calif.
DEPRIMING OF ARTERIAL HEAT PIPES: AN INVESTIGATION OF CTS THERMAL EXCURSIONS Final Report, Sept. 1978 - Aug. 1980
 D. Antoniuk and D. K. Edwards 20 Aug 1980 214 p refs
 (Contract NAS3-21740)
 (NASA-CR-185153; TRW-34129-6001-UT-00) Avail: NTIS HC A10/MF A01 CSCL 20D

Four thermal excursions of the Transmitter Experiment Package (TEP) were the result of the depriming of the arteries in all three heat pipes in the Variable Conductance Heat Pipe System which cooled the TEP. The determined cause of the depriming of the heat pipes was the formation of bubbles of the nitrogen/helium control gas mixture in the arteries during the thaw portion of a freeze/thaw cycle of the inactive region of the condenser section of the heat pipe. Conditions such as suction freezeout or heat pipe turn-on, which moved these bubbles into the active region of the heat pipe, contributed to the depriming mechanism. Methods for precluding, or reducing the probability of, this type of failure mechanism in future applications of arterial heat pipes are included. Author

A80-42176 * Full-coverage film cooling. I - Comparison of heat transfer data for three injection angles. M. E. Crawford (MIT, Cambridge, Mass.), W. M. Kays, and R. J. Moffat (Stanford University, Stanford, Calif.). *American Society of Mechanical Engineers, Gas Turbine Conference and Products Show, New Orleans, La., Mar. 10-13, 1980, Paper 80-GT-43.* 6 p. 15 refs. Members, \$1.50; nonmembers, \$3.00. Contract No. NAS3-14336.

Wind tunnel experiments were carried out at Stanford between 1971 and 1977 to study the heat transfer characteristics of full-coverage film cooled surfaces with three geometries; normal-, 30 deg slant-, and 30 deg x 45 deg compound-angled injection. A flat full-coverage section and downstream recovery section comprised the heat transfer system. The experimental objectives were to determine, for each geometry, the effects on surface heat flux of injection blowing ratio, injection temperature ratio, and upstream initial conditions. Spanwise-averaged Stanton numbers were measured for blowing ratios from 0 to 1.3, and for two values of injection temperature at each blowing ratio. The heat transfer coefficient was defined on the basis of a mainstream-to-wall temperature difference. Initial momentum and enthalpy thickness Reynolds numbers were varied from 500 to about 3000. (Author)

A80-42177 * # Full-coverage film cooling. II - Heat transfer data and numerical simulation. M. E. Crawford (MIT, Cambridge, Mass.), W. M. Kays, and R. J. Moffat (Stanford University, Stanford, Calif.). *American Society of Mechanical Engineers, Gas Turbine Conference and Products Show, New Orleans, La., Mar. 10-13, 1980, Paper 80-GT-44*. 7 p. 13 refs. Members, \$1.50; nonmembers, \$3.00. Contract No, NAS3-14336.

Experimental research into heat transfer from full-coverage film-cooled surfaces with three injection geometries was described in Part I. This part has two objectives. The first is to present a simple numerical procedure for simulation of heat transfer with full-coverage film cooling. The second objective is to present some of the Stanton number data that was used in Part I of the paper. The data chosen for presentation are the low-Reynolds number, heated-starting-length data for the three injection geometries with five-diameter hole spacing. Sample data sets with high blowing ratio and with ten-diameter hole spacing are also presented. The numerical procedure has been successfully applied to the Stanton number data sets.

(Author)

35 INSTRUMENTATION AND PHOTOGRAPHY

Includes remote sensors; measuring instruments and gages, detectors, cameras and photographic supplies; and holography

For aerial photography see 43 *Earth Resources*. For related information see also 06 *Aircraft Instrumentation*, and 19 *Spacecraft Instrumentation*.

N80-14374* National Aeronautics and Space Administration, Lewis Research Center, Cleveland, Ohio.

TEMPERATURE AND PRESSURE MEASUREMENT TECHNIQUES FOR AN ADVANCED TURBINE TEST FACILITY

Frank G. Pollack and Reeves P. Cochran 1980 12 p refs
Proposed for presentation at the Intern. Gas Turbine Conf. and Ann. Fluids Engr. Conf., New Orleans, 9-13 Mar. 1980; sponsored by Am. Soc. Mech. Engr.
(NASA-TM-79278; E-212) Avail: NTIS HC A02/MF A01 CSCL 14B

A high pressure, high-temperature turbine test facility constructed for use in turbine cooling research is described. Several recently developed temperature and pressure measuring techniques are used in this facility. The measurement techniques, their status, previous applications and some results are discussed. Noncontact surface temperature measurements are made by optical methods. Radiation pyrometry principles combined with photoelectric scanning are used for rotating components and infrared photography for stationary components. Contact (direct) temperature and pressure measurements on rotating components are expected to be handled with an 80 channel rotary data package which mounts on and rotates with the turbine shaft at speeds up to 17,500 rpm. The data channels are time-division multiplexed and converted to digital words in the data package. A rotary transformer couples power and digital data to and from the shaft.
M.M.M.

N80-17422* National Aeronautics and Space Administration, Lewis Research Center, Cleveland, Ohio.

FATIGUE STRENGTH TESTING EMPLOYED FOR EVALUATION AND ACCEPTANCE OF JET-ENGINE INSTRUMENTATION PROBES

Everett C. Armentrout 1980 25 p refs Presented at 25th Ann. Intern. Gas Turbine Conf., New Orleans, 9-13 Mar. 1980; sponsored by ASME
(NASA-TM-81402; E-313) Avail: NTIS HC A02/MF A01 CSCL 14B

The fatigue type testing performed on instrumentation rakes and probes intended for use in the air flow passages of jet engines during full scale engine tests is outlined. A discussion of each type of test performed, the results that may be derived and means of inspection is included.
R.E.S.

N80-17423* National Aeronautics and Space Administration, Lewis Research Center, Cleveland, Ohio.

OPTICAL SENSORS FOR AERONAUTICS AND SPACE

R. J. Baumbick, J. Alexander (NASA Johnson Space Center), R. Katz (Naval Avionics Center, Indianapolis, Ind.), and J. Terry (Army Applied Technology Labs., Ft. Eustis, Va.) Jan. 1980 16 p
(NASA-TM-81407; E-321) Avail: NTIS HC A02/MF A01 CSCL 14B

A review of some NASA and DOD programs to develop optical sensors with fiberoptics for instrumentation and control is presented. Fiber optic systems offer some distinct advantages. Noise immunity is one important asset. Fiber optic systems do not conduct electricity and therefore can be used in and near areas that contain explosive or flammable materials. One objective of these programs is to produce more reliable sensors and to improve the safety and operating economy of future aircraft and space vehicles.
Author

N80-18363* National Aeronautics and Space Administration, Lewis Research Center, Cleveland, Ohio.

FIBER OPTIC SENSORS FOR MEASURING ANGULAR POSITION AND ROTATIONAL SPEED

Robert J. Baumbick Mar. 1980 13 p
(NASA-TM-81454; E-381) Avail: NTIS HC A02/MF A01 CSCL 20F

Two optical sensors, a 360 deg rotary encoder and a tachometer, were built for operation with the light source and detectors located remotely from the sensors. The source and detectors were coupled to the passive sensing heads through 3.65 meter fiber optic cables. The rotary encoder and tachometer were subjected to limited environmental testing. They were installed on an air breathing engine during recent altitude tests. Over 100 hours of engine operation were accumulated without any failure of either device.
K.L.

N80-24595* National Aeronautics and Space Administration, Lewis Research Center, Cleveland, Ohio.

DYNAMIC BEHAVIOR OF A BEAM DRAG-FORCE ANEMOMETER

Gustave C. Fralick Washington May 1980 16 p refs
(NASA-TP-1687; E-340) Avail: NTIS HC A02/MF A01 CSCL 14B

A cantilevered beam with strain gages attached to the fixed ends and the minimax technique were used in an experiment conducted to determine the dynamic behavior of a drag-force anemometer in high frequency, unsteady flow. In steady flow the output of the anemometer is proportional to stream velocity head and flow angle. Fluid mechanics suggests that, in unsteady flow, the output would also be proportional to the rate of change of fluid velocity. It was determined that effects due to the rate of change of fluid velocity are negligible for the probe geometry and frequencies involved.
A.R.H.

N80-25635* National Aeronautics and Space Administration, Lewis Research Center, Cleveland, Ohio.

COMPUTERIZED VIDEO DENSITOMETRY METHOD FOR RAPID ANALYSIS OF INFRARED PHOTOGRAPHIC IMAGES

Ernest Roberts, Jr., Frederick D. Calfo, and Frank G. Pollack Jun. 1980 13 p refs
(NASA-TP-1686; E-354) Avail: NTIS HC A02/MF A01 CSCL 14E

A computerized video densitometry method is described which is approximately 50 times faster than a corresponding manual method of analysis, with no apparent sacrifice of accuracy. The object of the technique is to determine the temperature distribution across a heated surface. Infrared photographs of the heated surfaces provide the raw data. A video based, computer operated image analysis system provides the equipment. Infrared photographic pyrometry using a flat bed microdensitometer forms the basis of the technique. The procedure is illustrated on a thermally cycled aircraft gas turbine blade.
A.R.H.

A80-12630 * Measuring unsteady pressure on rotating compressor blades. D. R. Englund (NASA, Lewis Research Center, Cleveland, Ohio), H. P. Grant, and G. A. Lanati (United Technologies Corp., Pratt and Whitney Aircraft Group, East Hartford, Conn.). In: International Instrumentation Symposium, 25th, Anaheim, Calif., May 7-10, 1979, Proceedings. Part 2. (A80-12601 02-35) Pittsburgh, Pa., Instrument Society of America, 1979, p. 413-426. 7 refs.

The capability for accurate measurement of unsteady pressure on the surface of compressor and fan blades during engine operation was established. Tests were run on miniature semiconductor strain gage pressure transducers mounted in several arrangements. Both surface mountings and recessed flush mountings were tested. Test parameters included mounting arrangement, blade material, temperature, local strain in the blade, acceleration normal to the transducer diaphragm, centripetal acceleration, and pressure. Test results showed no failures of transducers or mountings and indicated an uncertainty of unsteady pressure measurement of approximately + or - 6%, plus 0.1 kPa for a typical application.
V.T.

A80-34546 * **Apparatus for trapping and thermal detection of atomic hydrogen in high magnetic fields at low temperatures.** J. A. Woollam (NASA, Lewis Research Center, Cleveland, Ohio). *Review of Scientific Instruments*, vol. 51, May 1980, p. 602-604. 12 refs.

An apparatus is described in which hydrogen atoms were trapped at temperatures down to 1.1 K in the 11 T field of a large volume superconducting magnet. A high sensitivity thermal detector was used to study trapping and recombination of atoms on the detector surface. The apparatus permits the application of extremely high steady state magnetic fields to study the potential effects of electron spin polarization on the stabilization of hydrogen atoms.

(Author)

A80-36127 * // **The measuring and growing of advanced gas turbines.** M. J. Hartmann (NASA, Lewis Research Center, Cleveland, Ohio). In: *Measurement methods in rotating components of turbomachinery; Proceedings of the Joint Fluids Engineering Gas Turbine Conference and Products Show*, New Orleans, La., March 10-13, 1980. (A80-36126 14-35) New York, American Society of Mechanical Engineers, 1980, p. 1-4.

Advances in the gas turbine technology level and the corresponding advances in measurement instruments and technique are reviewed for each of the past decades, starting with the forties. The review provides a picture of the gradual development from the earlier, relatively simple systems, to the present sophisticated machines. A look in the future indicates that continued advances in gas turbine technology will be needed, used, and supported and that substantial changes are underway as to how these advances will be achieved. Some projections of the type of advances and in technology and measurements to be expected in the decade of the eighties are presented.

V.P.

A80-36137 * // **Laser-optical blade tip clearance measurement system.** J. P. Barranger (NASA, Lewis Research Center, Cleveland, Ohio) and M. J. Ford (United Technologies Corp., Pratt and Whitney Aircraft Group, West Palm Beach, Fla.). In: *Measurement methods in rotating components of turbomachinery; Proceedings of the Joint Fluids Engineering Gas Turbine Conference and Products Show*, New Orleans, La., March 10-13, 1980. (A80-36126 14-35) New York, American Society of Mechanical Engineers, 1980, p. 127-131.

The need for blade tip clearance instrumentation has been intensified recently by advances in technology of gas turbine engines. A new laser-optical measurement system has been developed to measure single blade tip clearances and average blade tip clearances between a rotor and its gas path seal in rotating component rigs and complete engines. The system is applicable to fan, compressor and turbine blade tip clearance measurements. The engine mounted probe is particularly suitable for operation in the extreme turbine environment. The measurement system consists of an optical subsystem, an electronic subsystem and a computing and graphic terminal. Bench tests and environmental tests were conducted to confirm operation at temperatures, pressures, and vibration levels typically encountered in an operating gas turbine engine. (Author)

A80-36140 * // **Efficient laser anemometer for intra-rotor flow mapping in turbomachinery.** J. A. Powell, A. J. Strazisar, and R. G. Seasholtz (NASA, Lewis Research Center, Cleveland, Ohio). In: *Measurement methods in rotating components of turbomachinery; Proceedings of the Joint Fluids Engineering Gas Turbine Conference and Products Show*, New Orleans, La., March 10-13, 1980. (A80-36126 14-35) New York, American Society of Mechanical Engineers, 1980, p. 157-164. 10 refs.

Innovative features of the anemometer include: (1) a rapid and efficient data acquisition process, (2) a detailed real-time graphic display of the data being accumulated, and (3) input laser beam positioning that maximizes the size of the intra-rotor region being mapped. Results demonstrate the anemometer's capability in flow mapping within a transonic axial-flow compressor rotor. The use of fluorescent seed particles allows flow measurements near the rotor hub and the casing window. (Author)

A80-36141 * // **Laser anemometer measurements in a transonic axial flow compressor rotor.** A. J. Strazisar and J. A. Powell (NASA, Lewis Research Center, Cleveland, Ohio). In: *Measurement methods in rotating components of turbomachinery; Proceedings of the Joint Fluids Engineering Gas Turbine Conference and Products Show*, New Orleans, La., March 10-13, 1980. (A80-36126 14-35) New York, American Society of Mechanical Engineers, 1980, p. 165-176. 11 refs.

A laser anemometer system employing an efficient data acquisition technique has been used to make measurements upstream, within, and downstream of the compressor rotor. A fluorescent dye technique allowed measurements within endwall boundary layers. Adjustable laser beam orientation minimized shadowed regions and enabled radial velocity measurements outside of the blade row. The flow phenomena investigated include flow variations from passage to passage, the rotor shock system, three-dimensional flows in the blade wake, and the development of the outer endwall boundary layer. Laser anemometer measurements are compared to a numerical solution of the streamfunction equations and to measurements made with conventional instrumentation. (Author)

A80-36145 * // **Fluid and structural measurements to advance gas turbine technology.** M. J. Hartmann (NASA, Lewis Research Center, Cleveland, Ohio). In: *Measurement methods in rotating components of turbomachinery; Proceedings of the Joint Fluids Engineering Gas Turbine Conference and Products Show*, New Orleans, La., March 10-13, 1980. (A80-36126 14-35) New York, American Society of Mechanical Engineers, 1980, p. 209-213.

In the present paper, the current status of fluid and structural measurements is reviewed, and some potential improvements in gas turbine machinery, directly associated with the new measuring capability are discussed. Some considerations concerning the impact of the new capability on the methods and approaches that will be used in the further development of advanced technology, in general, and to aeropropulsion gas turbine machinery, in particular, are presented.

V.P.

A80-36147 * // **Flutter spectral measurements using stationary pressure transducers.** A. P. Kurkov (NASA, Lewis Research Center, Cleveland, Ohio). In: *Measurement methods in rotating components of turbomachinery; Proceedings of the Joint Fluids Engineering Gas Turbine Conference and Products Show*, New Orleans, La., March 10-13, 1980. (A80-36126 14-35) New York, American Society of Mechanical Engineers, 1980, p. 225-233. 6 refs.

The paper deals with an analysis procedure, based on engine-order sampling, which eliminates effectively the engine harmonics from the overall flutter spectra obtained with a case-mounted static pressure transducer. Qualitative spectral analyses of pressure data, performed on the basis of blade order sampling, are examined. The interference of blade motion with the pressure signal in the steep gradient portion of the blade passage is demonstrated, using optimal displacement spectra. Two methods which remove the contribution of blade motion from the blade-pressure-difference spectra are described.

V.P.

A80-36151 * // **Digital system for dynamic turbine engine blade displacement measurements.** L. J. Kiraly (NASA, Lewis Research Center, Cleveland, Ohio). In: *Measurement methods in rotating components of turbomachinery; Proceedings of the Joint Fluids Engineering Gas Turbine Conference and Products Show*, New Orleans, La., March 10-13, 1980. (A80-36126 14-35) New York, American Society of Mechanical Engineers, 1980, p. 255-262.

The paper presents a technique for measuring blade tip displacements which employs optical probes and an array of microcomputers. A system directly digitizing a minimum of a 2048-point time-deflection history for each of the three measurement locations on each blade is described.

V.T.

A80-36155 * # Impact of new instrumentation on advanced turbine research. R. W. Graham (NASA, Lewis Research Center, Cleveland, Ohio). In: Measurement methods in rotating components of turbomachinery; Proceedings of the Joint Fluids Engineering Gas Turbine Conference and Products Show, New Orleans, La., March 10-13, 1980. (A80-36126 14-35) New York, American Society of Mechanical Engineers, 1980, p. 289-302, 23 refs.

The progression of experimental programs is discussed from the simplest two-dimensional stationary geometry to the highly complex three-dimensional flow in a rotating blade row. Experimental methods and instrumentation techniques are described. Emphasis is placed on rotating blade row measurements. V.T.

A80-36157 * # Temperature and pressure measurement techniques for an advanced turbine test facility. F. G. Pollack and R. P. Cochran (NASA, Lewis Research Center, Cleveland, Ohio). In: Measurement methods in rotating components of turbomachinery; Proceedings of the Joint Fluids Engineering Gas Turbine Conference and Products Show, New Orleans, La., March 10-13, 1980. (A80-36126 14-35) New York, American Society of Mechanical Engineers, 1980, p. 319-326, 13 refs.

A high pressure, high-temperature turbine test facility is being constructed at the NASA Lewis Research Center for use in turbine cooling research. Several recently developed temperature and pressure measuring techniques will be used in this facility. This paper describes these measurement techniques, their status, previous applications and some results. Noncontact surface temperature measurements will be made by optical methods. Radiation pyrometry principles combined with photoelectric scanning will be used for rotating components and infrared photography for stationary components. Contact (direct) temperature and pressure measurements on rotating components will be handled with an 80-channel rotary data package which mounts on and rotates with the turbine shaft at speeds up to 17,500 rpm. The data channels are time-division multiplexed and converted to digital words in the data package. A rotary transformer couples power and digital data to and from the shaft. (Author)

A80-42291 * # Fatigue strength testing employed for evaluation and acceptance of jet-engine instrumentation probes. E. C. Armentrout (NASA, Lewis Research Center, Cleveland, Ohio). *American Society of Mechanical Engineers, Gas Turbine Conference and Products Show, New Orleans, La., Mar. 10-13, 1980, Paper. 23* p. 15 refs. Members, \$1.50; nonmembers, \$3.00.

This report outlines the fatigue type testing performed on instrumentation rakes and probes intended for use in the air flow passages of jet-engines during full-scale engine tests at Lewis Research Center. Included is a discussion of each type of test performed, the results that may be derived and means of inspection. A design and testing sequence outlines the procedures and considerations involved in the generation of suitable instrument probes. (Author)

A80-44233 * # Simulation of transducer-couplant effects on broadband ultrasonic signals. A. Vary (NASA, Lewis Research Center, Cleveland, Ohio). *American Society for Nondestructive Testing, Spring Meeting, Philadelphia, Pa., Mar. 24-27, 1980, Paper. 34* p. 9 refs.

The increasing use of broadband, pulse-echo ultrasonics in nondestructive evaluation of flaws and material properties has generated a need for improved understanding of the way signals are modified by coupled and bonded thin-layer interfaces associated with transducers. This understanding is most important when using frequency spectrum analyses for characterizing material properties. In this type of application, signals emanating from material specimens can be strongly influenced by couplant and bond-layers in the acoustic path. Computer synthesized waveforms were used to simulate a range of interface conditions encountered in ultrasonic transducer systems operating in the 20- to 80-MHz regime. The adverse effects of thin-layer multiple reflections associated with various acoustic impedance conditions are demonstrated. The infor-

mation presented is relevant to ultrasonic transducer design, specimen preparation, and couplant selection. (Author)

N80-14375* # National Aeronautics and Space Administration, Lewis Research Center, Cleveland, Ohio.
EFFICIENT LASER ANEMOMETER FOR INTRA-ROTOR FLOW MAPPING IN TURBOMACHINERY
J. Anthony Powell, Anthony J. Strazisar, and Richard G. Seasholtz 1979 11 p refs Proposed for presentation at the ASME 25th Ann. Intern. Gas Turbine Conf., and the 22nd Ann. Fluids Eng. Conf., New Orleans, 9-13 Mar. 1980
(NASA-TM-79320; E-276) Avail: NTIS HC A02/MF A01 CSCL 14B

A fringe type laser anemometer is described. Features of the anemometer include: a rapid and efficient data acquisition process; a detailed real time graphic display of the data being accumulated; and input laser beam positioning that maximizes the size of the intrarotor region being mapped. Results are presented that demonstrate the anemometer's capability in flow mapping within a transonic axial flow compressor rotor. A velocity profile, derived from 30,000 measurements along 1000 sequential circumferential positions covering 20 blade passages, was obtained in 30 seconds. The use of fluorescent seed particles allowed flow measurements near the rotor hub and the casing window. R.C.T.

N80-17425* # Pratt and Whitney Aircraft, East Hartford, Conn.
THIN FILM TEMPERATURE SENSOR
H. P. Grant and J. S. Przybyszewski 15 Feb. 1980 61 p refs
(Contract NAS3-20768)
(NASA-CR-159782; PWA-5526-31) Avail: NTIS HC A04/MF A01 CSCL 14B

Thin film surface temperature sensors were developed. The sensors were made of platinum-platinum/10 percent rhodium thermocouples with associated thin film-to-lead wire connections and sputtered on aluminum oxide coated simulated turbine blades for testing. Tests included exposure to vibration, low velocity hydrocarbon hot gas flow to 1250 K, and furnace calibrations. Thermal electromotive force was typically two percent below standard type S thermocouples. Mean time to failure was 42 hours at a hot gas flow temperature of 1250 K and an average of 15 cycles to room temperature. Failures were mainly due to separation of the platinum thin film from the aluminum oxide surface. Several techniques to improve the adhesion of the platinum are discussed. R.E.S.

N80-31777* # United Technologies Research Center, East Hartford, Conn.
DESIGN, FABRICATION AND TESTING OF AN OPTICAL TEMPERATURE SENSOR
W. W. Morey, W. H. Glenn, R. O. Decker, and W. C. McClurg Jul. 1980 54 p refs
(Contract NAS3-21841)
(NASA-CR-165125; R80-924624-11) Avail: NTIS HC A04/MF A01 CSCL 14B

The laboratory breadboard optical temperature sensor based on the temperature dependent absorptive characteristics of a rare earth (europium) doped optical fiber. The principles of operation, materials characterization, fiber and optical component design, design and fabrication of an electrooptic interface unit, signal processing, and initial test results are discussed. Initial tests indicated that, after a brief warmup period, the output of the sensor was stable to approximately 1 C at room temperature or approximately + or - 0.3 percent of point (K). This exceeds the goal of 1 percent of point. Recommendations are presented for further performance improvement. L.F.M.

36 LASERS AND MASERS

Includes parametric amplifiers.

N80-14386* # Rasor Associates, Inc., Sunnyvale, Calif.
A CESIUM TELEC EXPERIMENT AT LEWIS RESEARCH CENTER Final Report
E. J. Britt Sep. 1979 59 p refs
(Contract NAS3-21149)
(NASA-CR-159729; NSR-8-1) Avail: NTIS HC A04/MF A01
CSCL 20E

The thermoelectronic laser energy converter (TELEC), was studied as a method of converting a 10.6 mm CO₂ laser beam into electric power. The calculated characteristics of a TELEC seem to be well matched to the requirements of a spacecraft laser energy conversion system. The TELEC is a high power density plasma device which absorbs an intense laser beam by inverse bremsstrahlung with the plasma electrons. In the TELEC process, electromagnetic radiation is absorbed directly in the plasma electrons producing a high electron temperature. The energetic electrons diffuse out of the plasma striking two electrodes which are in contact with the plasma at the boundaries. These two electrodes have different areas: the larger one is designated as the collector, the smaller one is designated as the emitter. The smaller electrode functions as an electron emitter to provide continuity of the current. Waste heat is rejected from the collector electrode. An experiment was carried out with a high power laser using a cesium vapor TELEC cell with 30 cm active length. Laser supported plasma was produced in the TELEC device during a number of laser runs over a period of several days. Electric power from the TELEC was observed with currents in the range of several amperes and output potentials of less than 1 volt. The magnitudes of these electric outputs were smaller

37 MECHANICAL ENGINEERING

Includes auxiliary systems (non-power); machine elements and processes; and mechanical equipment.

N80-12414* National Aeronautics and Space Administration. Lewis Research Center, Cleveland, Ohio.

MODIFIED FACE SEAL FOR POSITIVE FILM STIFFNESS **Patent Application**

Izhak Etsion (Technion-Israel Inst. of Technol., Haifa) and Abraham Lipshitz, inventors (to NASA) (Technion-Israel Inst. of Technol., Haifa) Filed 7 Nov. 1979 7 p. Sponsored by NASA (NASA-Case-LEW-12989-1; US-Patent-Appl-SN-092145) Avail: NTIS HC A02/MF A01 CSCL 11A

An invention to improve the film stiffness of a face seal without increasing the sealing and dam area is described. The improved sealing apparatus has a primary seal ring in the form of a nose piece. A spring forces a sealing surface on the seal ring into sealing contact with a seat to form a face seal. A circumferential clearance seal is formed in series with this face by a lip on the nose piece. The width of the surface of the lip is substantially the same as the width of the sealing surface on the face seal. Also, the clearance between the surface on the lip and the shaft is substantially the same as the spacing between the face sealing surfaces on the face seal when the shaft is rotating. The circumferential clearance seal restricts the flow of fluid from a main cavity to an intermediate cavity with a resulting pressure drop. The hydrostatic opening is strongly dependent on the face seal clearance, and the desired axial stiffness is achieved.

NASA

N80-13473* National Aeronautics and Space Administration. Lewis Research Center, Cleveland, Ohio.

INVESTIGATION INTO THE EFFECT OF PLASMA PRE-TREATMENT ON THE ADHESION OF PARYLENE TO VARIOUS SUBSTRATES

T. Riley, T. Cobo Mahuson, and K. Seibert 1979 20 p refs Presented at the Seminar of Cleaning, Finishing and Coating Processes, Los Angeles, 5-6 Feb. 1979; sponsored by the Soc. for the Advan. of Mater. and Process Eng.

(NASA-TM-79224; E-119) Avail: NTIS HC A02/MF A01 CSCL 11A

A procedure is described for using argon and oxygen plasmas to promote adhesion of parylene coatings upon many difficult-to-bond substrates. Substrates investigated were gold, nickel, kovar, teflon (FEP), kapton, silicon, tantalum, titanium, and tungsten. Without plasma treatment, 180 deg peel tests yield a few g/cm (oz/in) strengths. With dc plasma treatment in the deposition chamber, followed by coating, peel strengths are increased by one to two orders of magnitude.

A.R.H.

N80-14403* National Aeronautics and Space Administration. Lewis Research Center, Cleveland, Ohio.

SELF-ACTING LIFT-PAD GEOMETRY FOR CIRCUMFERENTIAL SEALS: A NONCONTACTING CONCEPT

Gordon P. Allen Jan. 1980 11 p refs

(NASA-TP-1583; E-154) Avail: NTIS HC A02/MF A01 CSCL 11A

A segmented circumferential seal with lift pads for hydrodynamic action was analyzed over ranges of speed and sealed pressure. Performance predictions, which predicted noncontact operation for speeds as high as 600 revolutions per second at sealed pressures to 86 N/sq cm, are discussed. Performance tests were performed on the seals and compared with the performance predictions.

A.W.H.

N80-15410* National Aeronautics and Space Administration. Lewis Research Center, Cleveland, Ohio.

COMPARISON OF PREDICTED AND EXPERIMENTAL PERFORMANCE OF LARGE-BORE ROLLER BEARING OPERATING TO 3.0 MILLION DN

Harold H. Coe and Frederick T. Huller Jan. 1980 20 p refs (NASA-TP-1599; E-083) Avail: NTIS HC A02/MF A01 CSCL 13I

Bearing inner and outer race temperatures and the amount of heat transferred to the lubricant were calculated by using the computer program CYBEAN. The results obtained were compared with previously reported experimental data for a 118 mm bore roller bearing that operated at shaft speeds to 25,500 rpm, radial loads to 8,900 N (2000 lb), and total lubricant flow rates to 0.0102 cu m/min (2.7 gal/min). The calculated results compared well with the experimental data.

Author

N80-16340* National Aeronautics and Space Administration. Lewis Research Center, Cleveland, Ohio.

TRIBOLOGICAL PROPERTIES OF SILICON CARBIDE IN METAL REMOVAL PROCESS

Kazuhisa Miyoshi and Donald H. Buckley 1980 18 p refs To be presented at Intern. Symp. on Metal Working Lubrication, San Francisco, 18-19 Aug. 1980; sponsored by ASME (NASA-TM-79238) Avail: NTIS HC A02/MF A01 CSCL 13H

Material properties are considered as they relate to adhesion, friction, and wear of single crystal silicon carbide in contact with metals and alloys that are likely to be involved in a metal removal process such as grinding. Metal removal from adhesion between sliding surfaces in contact and metal removal as a result of the silicon carbide sliding against a metal, indenting into it, and plowing a series of grooves or furrows are discussed. Fracture and deformation characteristics of the silicon carbide surface are also covered. The adhesion, friction, and metal transfer to silicon carbide is related to the relative chemical activity of the metals. The more active the metal, the higher the adhesion and friction, and the greater the metal transfer to silicon carbide. Atomic size and content of alloying elements play a dominant role in controlling adhesion, friction, and abrasive wear properties of alloys. The friction and abrasive wear (metal removal) decrease linearly as the shear strength of the bulk metal increases. They decrease as the solute to solvent atomic radius ratio increases or decreases linearly from unity, and with an increase of solute content. The surface fracture of silicon carbide is due to cleavages of 0001, 10(-1)0, and/or 11(-2)0 planes.

J.M.S.

N80-16341* National Aeronautics and Space Administration. Lewis Research Center, Cleveland, Ohio.

ANALYSIS OF WEAR-DEBRIS FROM FULL-SCALE BEARING FATIGUE TESTS USING THE FERROGRAPH

William R. Jones and Stuart H. Loewenthal 1980 22 p refs Prepared for presentation at the Ann. Meeting of the Am. Soc. of Lubrication Engr., Anaheim, Calif., 5-8 May 1980

(NASA-TM-81403; E-9827) Avail: NTIS HC A02/MF A01 CSCL 13H

The ferrograph was used to determine the types and quantities of wear particles generated during full-scale bearing fatigue tests. Deep-groove ball bearings made from AISI 52100 steel were used. A MIL-L-23699 tetraester lubricant was used in a recirculating lubrication system containing a 49 mm absolute filter. Test conditions included a maximum Hertz stress of 2.4 GPa, a shaft speed of 15,000 rpm, and a lubricant supply temperature of 74 C (165 F). Four fatigue failures were detected by accelerometers in this test set. In general, the ferrograph was more sensitive (up to 23 hr) in detecting spall initiation than either accelerometers or the normal spectrographic oil analysis. Four particle types were observed: normal rubbing wear particles, spheres, nonferrous particles, and severe wear (spall) fragments.

Author

N80-16342* National Aeronautics and Space Administration. Lewis Research Center, Cleveland, Ohio.

PERFORMANCE OF COMPUTER-OPTIMIZED TAPERED-ROLLER BEARINGS TO 2.4 MILLION DN

R. J. Parker, S. I. Pinel (Industrial Tectonics, Inc., Compton, Calif.), and H. R. Signer (Industrial Tectonics, Inc., Compton, Calif.) 1980 29 p refs Proposed for presentation at the Intern. Lubrication Conf., San Francisco, 16-21 Aug. 1980; sponsored by ASME and the Am. Soc. of Lubrication Engr.

(NASA-TM-81414; E-332) Avail: NTIS HC A03/MF A01 CSCL 131

The performance of 120.65 mm bore high speed design tapered roller bearings was investigated at shaft speeds to 20,000 rpm under combined thrust and radial load. The test bearing design was computer optimized for high speed operation. Temperature distribution and bearing heat generation were determined as a function of shaft speed, radial and thrust loads, lubricant flow rates, and lubricant inlet temperature. The roller bearing operated successfully at shaft speeds up to 20,000 rpm under heavy thrust and radial loads. Cup cooling was effective in decreasing the high cup temperatures to levels equal to the cone temperature. K.L.

N80-17466* National Aeronautics and Space Administration. Lewis Research Center, Cleveland, Ohio.

SPUR-GEAR-SYSTEM EFFICIENCY AT PART AND FULL LOAD

Neil E. Anderson and Stuart H. Loewenthal Feb. 1980 42 p refs Prepared in cooperation with Army Aviation Res. and Develop. Command, Cleveland

(NASA-TP-1622; AVRADCOM-TR-79-46; E-061) Avail: NTIS HC A03/MF A01 CSCL 131

A simple method for predicting the part- and full-load power loss of a steel spur gearset of arbitrary geometry supported by ball bearings is described. The analysis algebraically accounts for losses due to gear sliding, rolling traction, and windage in addition to support-ball-bearing losses. The analysis compares favorably with test data. A theoretical comparison of the component losses indicates that losses due to gear rolling traction, windage, and support bearings are significant and should be included along with gear sliding loss in a calculation of gear-system power loss. M.G.

N80-17467* National Aeronautics and Space Administration. Lewis Research Center, Cleveland, Ohio.

PERFORMANCE SENSITIVITY ANALYSIS OF DEPARTMENT OF ENERGY-CHRYSLER UPGRADED AUTOMOTIVE GAS TURBINE ENGINE, S/N 5-4 Final Report

Roy L. Johnsen Dec. 1979 37 p refs (Contract EC-77-A-31-1040)

(NASA-TM-79242; DOE/NASA/1040-79/9; E-147) Avail: NTIS HC A03/MF A01 CSCL 21A

The performance sensitivity of a two-shaft automotive gas turbine engine to changes in component performance and cycle operating parameters was examined. Sensitivities were determined for changes in turbomachinery efficiency, compressor inlet temperature, power turbine discharge temperature, regenerator effectiveness, regenerator pressure drop, and several gas flow and heat leaks. Compressor efficiency was found to have the greatest effect on system performance. K.L.

N80-17469* National Aeronautics and Space Administration. Lewis Research Center, Cleveland, Ohio.

SIMPLIFIED FATIGUE LIFE ANALYSIS FOR TRACTION DRIVE CONTACTS

Douglas A. Rohn, Stuart H. Loewenthal, and John J. Coy 1980 30 p refs Proposed for presentation at 3d Intern. Power Transmission and Gearing Conf., San Francisco, 18-22 Aug. 1980; sponsored by ASME Prepared in cooperation with Army Aviation Res. and Develop. Command, Cleveland

(NASA-TM-79199; AVRADCOM-TR-80-C-4; E-355) Avail: NTIS HC A03/MF A01 CSCL 131

A simplified fatigue life analysis for traction drive contacts of arbitrary geometry is presented. The analysis is based on the Lundberg-Palmgren theory used for rolling-element bearings. The effects of torque, element size, speed, contact ellipse ratio, and the influence of traction coefficient are shown. The analysis shows that within the limits of the available traction coefficient, traction contacts exhibit longest life at high speeds. Multiple, load-sharing roller arrangements have an advantageous effect on system life, torque capacity, power-to-weight ratio and size. Author

N80-18400* National Aeronautics and Space Administration. Lewis Research Center, Cleveland, Ohio.

GAS PATH SEAL Patent Application

Robert C. Bill and Robert D. Johnson, inventors (to NASA) Filed 20 Nov. 1979 8 p

(NASA-Case-NPO-12131-3; US-Patent-Appl-SN-096255) Avail: NTIS HC A02/MF A01 CSCL 20A

A gas path seal suitable for use with a turbine engine or compressor is described. A shroud wearable or abradable by the abrasion of the rotor blades of the turbine or compressor shrouds the rotor blades. A compliant backing surrounds the shroud. The backing is a yielding deformable porous material covered with a thin ductile layer. A mounting fixture surrounds the backing. NASA

N80-18401* National Aeronautics and Space Administration. Lewis Research Center, Cleveland, Ohio.

CIRCUMFERENTIAL SHAFT SEAL Patent Application

L. P. Ludwig, inventor (to NASA) Filed 7 Dec. 1979 8 p

(NASA-Case-LEW-12119-2; US-Patent-Appl-SN-102004) Avail: NTIS HC A02/MF A01 CSCL 20A

A circumferential shaft seal in which the seal elements are capable of adequate response to shaft motion is described. The seal is comprised of two sealing rings held to a rotating shaft by means of a surrounding elastomeric band. The rings are segmented and have an inner diameter dimensioned so that the segments can slidably and sealably engage the shaft. Alternative embodiments of the seal concept are described and suggestions for component materials are given. M.G.

N80-18403* National Aeronautics and Space Administration. Lewis Research Center, Cleveland, Ohio.

ANALYTICAL AND EXPERIMENTAL SPUR GEAR TOOTH TEMPERATURE AS AFFECTED BY OPERATING VARIABLES

Dennis P. Townsend and Lee S. Akin (Western Gear Corp., Industry, Calif.) 1980 29 p refs Presented at 3d Intern. Power Transmission and Gearing Conf., San Francisco, Calif., 18-22 Aug. 1980; sponsored by Am. Soc. of Mech. Engr. (NASA-TM-81419; E-342) Avail: NTIS HC A03/MF A01 CSCL 131

A gear tooth temperature analysis was performed using a finite element method combined with a calculated heat input, calculated oil jet impingement depth, and estimated heat transfer coefficients. Experimental measurements of gear tooth average surface temperatures and instantaneous surface temperatures were made with a fast response infrared radiometric microscope. Increased oil jet pressure had a significant effect on both average and peak surface temperatures at both high load and speeds. Increasing the speed at constant load and increasing the load at constant speed causes a significant rise in average and peak surface temperatures of gear teeth. The oil jet pressure required for adequate cooling at high speed and load conditions must be high enough to get full depth penetration of the teeth. Calculated and experimental results were in good agreement with high oil jet penetration but showed poor agreement with low oil jet penetration depth. Author

N80-18404* National Aeronautics and Space Administration. Lewis Research Center, Cleveland, Ohio.

EVALUATION OF A HIGH PERFORMANCE FIXED-RATIO TRACTION DRIVE

Stuart H. Loewenthal, Neil E. Anderson, and Douglas A. Rohn 1980 32 p refs Proposed for presentation at 3d Intern. Power Transmission and Gearing Conf., San Francisco, Calif., 18-22 Aug. 1980; sponsored by Am. Soc. of Mech. Engr. (NASA-TM-81425; E-349) Avail: NTIS HC A03/MF A01 CSCL 131

The results of a test program to evaluate a compact, high performance, fixed ratio traction drive are presented. This transmission, the Nasvytis Multiroller Traction Drive, is a fixed ratio, single stage planetary with two rows of stepped planet rollers. Two versions of the drive were parametrically tested back-to-back at speeds to 73,000 rpm and power levels to 180 kW (240 hp). Parametric tests were also conducted with

the Nasvytis drive retrofitted to an automotive gas turbine engine. The drives exhibited good performance, with a nominal peak efficiency of 94 to 96 percent and a maximum speed loss due to creep of approximately 3.5 percent. Author

N80-18405* National Aeronautics and Space Administration. Lewis Research Center, Cleveland, Ohio.
ENDURANCE AND FAILURE CHARACTERISTICS OF MODIFIED VASCO X-2, CBS 600 AND AISI 9310 SPUR GEARS

Dennis P. Townsend and E. V. Zaretsky 1980 28 p refs Proposed for presentation at 3d Intern. Power Transmission and Gearing Conf., San Francisco, Calif., 18-22 Aug. 1980; sponsored by Am. Soc. of Mech. Engr. (NASA-TM-81421; E-344) Avail: NTIS HC A03/MF A01 CSCL 131

Gear endurance tests and rolling-element fatigue tests were conducted to compare the performance of spur gears made from AISI 9310, CBS 600 and modified Vasco X-2 and to compare the pitting fatigue lives of these three materials. Gears manufactured from CBS 600 exhibited lives longer than those manufactured from AISI 9310. However, rolling-element fatigue tests resulted in statistically equivalent lives. Modified Vasco X-2 exhibited statistically equivalent lives to AISI 9310, CBS 600 and modified Vasco X-2 gears exhibited the potential of tooth fracture occurring at a tooth surface fatigue pit. Case carburization of all gear surfaces for the modified Vasco X-2 gears results in fracture at the tips of the gears. Author

N80-18406* National Aeronautics and Space Administration. Lewis Research Center, Cleveland, Ohio.
EFFECT OF GEOMETRY AND OPERATING CONDITIONS ON SPUR GEAR SYSTEM POWER LOSS

Neil E. Anderson and Stuart H. Loewenthal 1980 31 p refs Proposed for presentation at 3d Intern. Power Transmission and Gearing Conf., San Francisco, Calif., 18-22 Aug. 1980; sponsored by Am. Soc. of Mech. Engr. (NASA-TM-81426; E-350; AVRADCOM-TR-80-C-2) Avail: NTIS HC A03/MF A01 CSCL 201

The results of an analysis of the effects of spur gear size, pitch, width, and ratio on total mesh power loss for a wide range of speeds, torques, and oil viscosities are presented. The analysis uses simple algebraic expressions to determine gear sliding, rolling, and windage losses and also incorporates an approximate ball bearing power loss expression. The analysis shows good agreement with published data. Large diameter and fine pitched gears had higher peak efficiencies but low part load efficiency. Gear efficiencies were generally greater than 98 percent except at very low torque levels. Tare (no-load) losses are generally a significant percentage of the full load loss except at low speeds. Author

N80-18407* National Aeronautics and Space Administration. Lewis Research Center, Cleveland, Ohio.
CONSTRAINED FATIGUE LIFE OPTIMIZATION OF A NASVYTIS MULTIROLLER TRACTION DRIVE

John J. Coy, Douglas A. Rohn, and Stuart H. Loewenthal 1980 20 p refs Proposed for presentation at 3d Intern. Power Transmission and Gearing Conf., San Francisco, Calif., 18-22 Aug. 1980; sponsored by Am. Soc. of Mech. Engr. (NASA-TM-81447; AVRADCOM-TR-80-C-6; E-214) Avail: NTIS HC A02/MF A01 CSCL 131

A contact fatigue life analysis method for multiroller traction drives is presented. The method is based on the Lundberg-Palmgren analysis method for rolling element bearing life prediction, and also uses life adjustment factors for materials, processing, lubrication, and effect of traction. The analysis method is applied in an optimization study to the multiroller traction drive, consisting of a single-stage planetary configuration with two rows of stepped planet rollers of five rollers per row. The drive was approximately 25 centimeters in diameter by 11 centimeters long, having a nominal ratio of 15:1. The theoretically predicted drive life was 2510 hours at a nominal continuous power and speed of 74.6 kW (100 hp) and 7500 rpm. Author

N80-18408* National Aeronautics and Space Administration. Lewis Research Center, Cleveland, Ohio.

ANALYSIS AND DESIGN OF A UNIFORM-CLEARANCE, PUMPING-RING ROD SEAL FOR THE STIRLING ENGINE
 I. Etsion Mar. 1980 30 p refs
 (NASA-TM-81463; E-080) Avail: NTIS HC A03/MF A01 CSCL 11A

A uniform clearance pumping ring, as opposed to the conventional taper clearance one, is described. The uniform clearance concept eliminates complex elastohydrodynamic problems and enables a simple analytical treatment to be made. An analytical expression is derived for the pumping rate showing the effect of various design parameters on the pumping ring's performance. An optimum clearance is found by which the pumping rate is maximized and a numerical example is presented to demonstrate the potential of the uniform clearance design. Author

N80-18409* National Aeronautics and Space Administration. Lewis Research Center, Cleveland, Ohio.

SOME LIMITATIONS IN APPLYING CLASSICAL EHD FILM-THICKNESS FORMULAE TO A HIGH-SPEED BEARING

John J. Coy and Erwin V. Zaretsky 1980 32 p refs Proposed for presentation at Intern. Lubrication Conf., San Francisco, 18-21 Aug. 1980; sponsored by Am. Soc. of Mech. Engr. and Am. Soc. of Lubrication Engr. (NASA-TM-81431; AVRADCOM-TR-80-C-3; E-198) Avail: NTIS HC A03/MF A01 CSCL 131

Elastohydrodynamic film thickness was measured for a 20 mm ball bearing using the capacitance technique. The bearing was thrust loaded to 90, 448, and 778 N. The corresponding maximum stresses on the inner race were 1.28, 2.09, and 2.45 GPa. Test speeds ranged from 400 to 14,000 rpm. Film thickness measurements were taken with four different lubricants: (1) synthetic paraffinic; (2) synthetic paraffinic with additives; (3) neopentylpolyol (tetra) ester; and (4) synthetic cycloaliphatic hydrocarbon traction fluid. The test bearing was mist lubricated. Test temperatures were 300, 338, and 393 K. The measured results were compared to theoretical predictions and are presented. A.W.H.

N80-18495* National Aeronautics and Space Administration. Lewis Research Center, Cleveland, Ohio.

DAMPING IN TAPERED ANNULAR SEALS FOR AN INCOMPRESSIBLE FLUID

David P. Fleming Apr. 1980 22 p refs
 (NASA-TP-1646; E-124) Avail: NTIS HC A02/MF A01 CSCL 11A

Damping in annular seals is calculated for an incompressible fluid. Results show that damping in tapered seals optimized for stiffness is considerably less than that in straight seals for the same minimum clearance. Damping in rotating seals can promote fractional frequency whirl. Neglecting fluid acceleration makes solution much easier, but leads to errors in calculated damping of up to 16 percent. K.L.

N80-18496* National Aeronautics and Space Administration. Lewis Research Center, Cleveland, Ohio.

CALCULATED AND EXPERIMENTAL DATA FOR A 118-mm BORE ROLLER BEARING TO 3 MILLION DN

Harold H. Coa and Frederick T. Schuller 1980 37 p refs Proposed for presentation at Intern. Lubrication Conf., San Francisco, 18-21 Aug. 1980; sponsored by ASME and the Am. Soc. of Lubrication Engr. (NASA-TM-81427; E-063) Avail: NTIS HC A03/MF A01 CSCL 131

The operating characteristics for 118 mm bore cylindrical roller bearing are examined using the computer program CYBEAN. The predicted results of inner and outer-race temperatures and heat transferred to the lubricant generally compared well with experimental data for shaft speeds to 3 million DN (25,000 rpm), radial loads to 8900 N (2000 lb), and total lubricant flow rates to 0.0102 cu m/min (2.7 gal/min). M.G.

N80-19497* National Aeronautics and Space Administration, Lewis Research Center, Cleveland, Ohio.
FERROGRAPHIC AND SPECTROGRAPHIC ANALYSIS OF OIL SAMPLED BEFORE AND AFTER FAILURE OF A JET ENGINE

William R. Jones, Jr. Feb. 1980 20 p refs
(NASA-TM-81430; E-353) Avail: NTIS HC A02/MF A01 CSCL 21E

An experimental gas turbine engine was destroyed as a result of the combustion of its titanium components. Several engine oil samples (before and after the failure) were analyzed with a Ferrograph as well as plasma, atomic absorption, and emission spectrometers. The analyses indicated that a lubrication system failure was not a causative factor in the engine failure. Neither an abnormal wear mechanism, nor a high level of wear debris was detected in the oil sample from the engine just prior to the test in which the failure occurred. However, low concentrations of titanium were evident in this sample and samples taken earlier. After the failure, higher titanium concentrations were detected in oil samples taken from different engine locations. Ferrographic analysis indicated that most of the titanium was contained in spherical metallic debris after the failure. K.L.

N80-19498* National Aeronautics and Space Administration, Lewis Research Center, Cleveland, Ohio.
IDEAL SPIRAL BEVEL GEARS: A NEW APPROACH TO SURFACE GEOMETRY

R. L. Huston (Cincinnati Univ., Ohio) and J. J. Coy 1980 22 p refs Proposed for presentation at 3d Intern. Power Transmission and Gearing Conf., San Francisco, 18-22 Aug. 1980; sponsored by ASME
(NASA-TM-81446; E-366; AVRADCOM-TR-80-C-5) Avail: NTIS HC A02/MF A01 CSCL 13I

The fundamental geometrical characteristics of spiral bevel gear tooth surfaces are discussed. The parametric representation of an ideal spiral bevel tooth is developed based on the elements of involute geometry, differential geometry, and fundamental gearing kinematics. A foundation is provided for the study of nonideal gears and the effects of deviations from ideal geometry on the contact stresses, lubrication, wear, fatigue life, and gearing kinematics. M.G.

N80-20591* National Aeronautics and Space Administration, Lewis Research Center, Cleveland, Ohio.

LUBRICATION OF ROLLING-ELEMENT BEARINGS

Richard J. Parker [1980] 26 p refs Proposed for presentation at Intern. Lubrication Conf., San Francisco, 18-21 Aug. 1980; sponsored by ASME and the Am. Soc. of Lubrication Engr.
(NASA-TM-81449; E-370) Avail: NTIS HC A03/MF A01 CSCL 13I

The lubrication of rolling element bearings is surveyed. Emphasis is on the critical design aspects related to speed, temperature, and ambient pressure environment. Types of lubrication including grease, jets, mist, wick, and through the race are discussed. The historical development, present state of technology, and the future problems of rolling element bearing lubrication are discussed. A.W.H.

N80-21753* National Aeronautics and Space Administration, Lewis Research Center, Cleveland, Ohio.

OPERATING CHARACTERISTICS OF HIGH-SPEED, JET-LUBRICATED 35-MILLIMETER-BORE BALL BEARING WITH A SINGLE-OUTER-LAND-GUIDED CAGE

Fredrick T. Schuller, Stanley I. Pinel (Industrial Tectonics, Inc.), and Hans R. Signer (Industrial Tectonics, Inc.) Washington Apr. 1980 16 p refs

(NASA-TP-1657; E-220) Avail: NTIS HC A02/MF A01 CSCL 13I

Parametric tests of a 35 mm bore, angular contact ball bearing with a single outer land guided cage were conducted on a high temperature, high speed bearing tester. Provisions were made for jet lubrication of the bearing and for outer ring cooling. Test conditions included two different thrust loads and a combined thrust and radial load. Nominal shaft speeds were 28,000 to 72,000 rpm, with an oil-in temperature of 394 K (250 F). The bearing was successfully operated to 2.5 million

DN at a maximum thrust load of 1334 N (300 lb) and at a combined 667 N (150-lb) thrust and 222 N (50-lb) radial load. Bearing temperatures increased with shaft speed and decreased with increasing lubricant flow rate. Inner-ring temperature was generally lower than outer ring temperature. Lower operating temperatures resulted from cooling the outer ring. Bearing power loss increased as the lubricant flow rate, speed, or load was increased. The increase in percent cage slip with increasing lubricant flow rate was minimal for all speed and load conditions tested. Percent cage slip decreased significantly when the thrust load was doubled, but it increased appreciably with speed.

Author

N80-21754* National Aeronautics and Space Administration, Lewis Research Center, Cleveland, Ohio.

PARAMETRIC TESTS OF A TRACTION DRIVE RETROFITTED TO AN AUTOMOTIVE GAS TURBINE

Douglas A. Rohn, Stuart H. Lowenthal, and Neil E. Anderson 1980 21 p refs Presented at the 5th Intern. Automotive Propulsion Systems Symp., Dearborn, Mich., 14-18 Apr. 1980 Prepared in cooperation with Army Aviation Research and Development Command, Cleveland, Ohio
(Contract EF-77-A-31-1011)

(NASA-TM-81457; AVRADCOM-TR-80-8; DOE/NASA/1011-80/4) Avail: NTIS HC A02/MF A01 CSCL 13I

The results of a test program to retrofit a high performance fixed ratio Nasvytis Multiroller Traction Drive in place of a helical gear set to a gas turbine engine are presented. Parametric tests up to a maximum engine power turbine speed of 45,500 rpm and to a power level of 11 kW were conducted. Comparisons were made to similar drives that were parametrically tested on a back-to-back test stand. The drive showed good compatibility with the gas turbine engine. Specific fuel consumption of the engine with the traction drive speed reducer installed was comparable to the original helical gears equipped engine.

Author

N80-22701* National Aeronautics and Space Administration, Lewis Research Center, Cleveland, Ohio.

DYNAMIC RESPONSE TO ROTATING-SEAT RUNOUT IN NON-CONTACTING FACE SEALS

I. Etsion Apr. 1980 25 p refs
(NASA-TM-81490; E-392) Avail: NTIS HC A02/MF A01 CSCL 11A

The dynamic response of a flexibly mounted ring to runout of the rotating seat in mechanical face seals is analyzed assuming small perturbations. It is found that tracking ability of the stator depends only on its dynamic characteristics and operating conditions and is not affected by the amount of runout. Three different modes of dynamic response are shown and the condition for parallel tracking is presented.

Author

N80-24619* National Aeronautics and Space Administration, Lewis Research Center, Cleveland, Ohio.

FULLY PLASMA-SPRAYED COMPLIANT BACKED CERAMIC TURBINE SEAL Patent Application

R. C. Bill, inventor (to NASA) Filed 30 Apr. 1980 7 p
(NASA-Case-LEW-13268-1; US-Patent-Appl-SN-145209) Avail: NTIS HC A02/MF A01 CSCL 11A

To maintain the minimum operating clearances between the blade tips and the lining of a high pressure turbine, a low temperature easily decomposable material, such as a polymer, in powder form is blended with a high temperature oxidation resistant metal powder. The two materials are simultaneously deposited on a substrate formed by the turbine casing. Alternately, the polymer powder may be added to the metal powder during plasma spraying. A ceramic layer is then deposited directly onto the metal-polymer composite. The polymer additive mixed with the metal is then completely volatilized to provide a porous layer between the ceramic layer and the substrate. Thermal stresses are reduced by virtue of the resulting porous structure which affords a cushion effect. By using plasma spraying for depositing both the powders of the metal and polymer material, as well as the ceramic powder, no brazing is required. NASA

N80-26658* National Aeronautics and Space Administration. Lewis Research Center, Cleveland, Ohio.

COMPOSITE SEAL FOR TURBOMACHINERY Patent
Robert C. Bill and Lawrence P. Ludwig, inventors (to NASA)
Issued 10 Jun 1980 4 p Filed 4 Aug. 1978 Supersedes
N78-31103 (16 - 22, p 2897) Division of US Patent Appl.
SN-801290, filed 27 May 1977, US Patent-4,135,851
(NASA-CASE-LEW-12131-2; US-Patent-4,207,024;
US-Patent-Appl-SN-931090; US-Patent-Class-415-174;
US-Patent-Class-415-196; US-Patent-Appl-SN-801290;
US-Patent-4,135,851) Avail. US Patent and Trademark Office
CSCL 11A

A gas path seal suitable for use with a turbine engine or compressor is provided. A shroud wearable or abradable by the abrasion of the rotor blades of the turbine or compressor shrouds the rotor blades. A compliant backing surrounds the shroud. The backing is a compliant material covered with a thin ductile layer. A mounting fixture surrounds the backing.

Official Gazette of the U.S. Patent and Trademark Office

N80-26659* National Aeronautics and Space Administration. Lewis Research Center, Cleveland, Ohio.

DIESEL ENGINE CATALYTIC COMBUSTOR SYSTEM Patent Application

Lloyd W. Ream, inventor (to NASA) Filed 6 Jun. 1980 10 p
(NASA-Case-Law-12995-1; US-Patent-Appl-SN-157150) Avail.
NTIS HC A02/MF A01 CSCL 21A

A low compression turbocharged diesel engine is described in which the turbocharger can be operated independently of the engine to power auxiliary equipment. Fuel and air are burned in a catalytic combustor to drive the turbine wheel of the turbine section which is initially caused to rotate by the starter motor. By opening a flapper valve, compressed air from the blower section is directed to the catalytic combustor when it is heated and expanded, serving to drive the turbine wheel and also to heat the catalytic element. To start the engine, one valve is closed, combustion is terminated in the catalytic combustor, and another valve is then opened to utilize air from the blower for the air driven motor. When the engine starts, the constituents in its exhaust gas react in the catalytic element and the heat generated provides additional energy for the turbine section.

NASA

N80-27695* National Aeronautics and Space Administration. Lewis Research Center, Cleveland, Ohio.

DYNAMIC ANALYSIS OF NONCONTACTING FACE SEALS

I. Etsion May 1980 40 p refs
(NASA-TM-79294; E-458) Avail. NTIS HC A03/MF A01 CSCL 11A

The dynamic behavior of a noncontacting coned face seal is analyzed taking into account various design parameters and operating conditions. The primary seal ring motion is expressed by a set of nonlinear equations for three degrees of freedom. These equations, which are solved numerically, allow identification of two dimensionless groups of parameters that affect the seal dynamic behavior. Stability maps for various seals are presented. These maps contain a stable-to-unstable transition region in which the ring wobbles at half the shaft frequency. The effect of various parameters on seal stability is discussed and an empirical expression for critical stability is offered.

Author

N80-27696* National Aeronautics and Space Administration. Lewis Research Center, Cleveland, Ohio.

THE RESPONSE OF TURBINE ENGINE ROTORS TO INTERFERENCE RUBS

Albert F. Kascak 1980 18 p refs Presented at Army Sci. Conf., West Point, N. Y., 17-19 Jun. 1980 Film Supplement number C-294 to this report is available on request from Chief, Management Services Division (5-5), National Aeronautics and Space Administration, Lewis Research Center, 21000 Brookpark Road, Cleveland, Ohio 44135
(NASA-TM-81518; AVRADCOM-TR-80-C-14; E-462) Avail.
NTIS HC A02/MF A01 CSCL 21D

A method was developed for the direct integration of a

rotor dynamics system experiencing a blade loss induced rotor rub. Both blade loss and rotor rub were simulated on a rotor typical of a small gas turbine. A small change in the coefficient of friction (from 0.1 to 0.2) caused the rotor to change from forward to backward whirl and to theoretically destroy itself in a few rotations. This method provides an analytical capability to study the susceptibility of rotors to rub induced backward whirl problems.

L.F.M.

N80-27697* National Aeronautics and Space Administration. Lewis Research Center, Cleveland, Ohio.

STRESSES AND DEFORMATIONS IN ELLIPTICAL CONTACTS

Bernard J. Hamrock 1980 19 p refs Lecture presented at Lulea Univ., Sweden, 24 Jul. - 16 Aug. 1980
(NASA-TM-81535; E-488) Avail. NTIS HC A02/MF A01 CSCL 131

Topics presented deal with defining conformal and nonconformal surfaces, curvature sum and difference, and surface and subsurface stresses in elliptical contacts. Load-deflection relationships for nonconformal contacts are developed. The deformation within the contact is, among other things, a function of the ellipticity parameter and elliptic integrals of the first and second kinds. Simplified expressions that allow quick calculations of the deformation to be made simply from a knowledge of the applied load, the material properties, and the geometry of the contacting elements are presented.

L.F.M.

N80-27698* National Aeronautics and Space Administration. Lewis Research Center, Cleveland, Ohio.

FULLY FLOODED ELASTOHYDRODYNAMIC LUBRICATED ELLIPTICAL CONTACTS

Bernard J. Hamrock 1980 27 p refs Lecture presented at Lulea Univ., Sweden, 24 Jul. - 16 Aug. 1980
(NASA-TM-81543; E-497) Avail. NTIS HC A03/MF A01 CSCL 131

Emphasis is on fully flooded, elastohydrodynamic lubricated, elliptical contacts. A fully flooded conjunction is one in which the film thickness is not significantly changed when the amount of lubricant is increased. A brief description of the relevant equations used in the elastohydrodynamic lubrication of elliptical contacts is given. The most important practical aspect of the elastohydrodynamic theory is the determination of the minimum film thickness within the contact. The maintenance of a fluid film of adequate magnitude is an essential feature of the correct operation of lubricated machine elements. The results presented show the influence of contact geometry on minimum film thickness as expressed by the ellipticity parameter and the dimensionless speed, load, and materials parameters. Film thickness equations are developed for materials of high elastic modulus, such as metal, and for materials of low elastic modulus, such as rubber. In addition to the film thickness equations that are developed, plots of pressure and film thickness are presented. These theoretical solutions for film thickness have all the essential features of previously reported experimental observations based on optical interferometry. Correlation between theory and experiments is also presented.

L.F.M.

N80-27699* National Aeronautics and Space Administration. Lewis Research Center, Cleveland, Ohio.

STARVED ELASTOHYDRODYNAMIC LUBRICATED ELLIPTICAL CONTACTS

Bernard J. Hamrock 1980 23 p refs Lecture presented at Lulea Univ., Sweden, 24 Jul. - 16 Aug. 1980
(NASA-TM-81549; E-507) Avail. NTIS HC A02/MF A01 CSCL 131

A theoretical study of the influence of lubricant starvation on film thickness and pressure in hard and soft elliptical elastohydrodynamic contacts is presented. From the results for both hard and soft EHL contacts a simple and important dimensionless inlet boundary distance is specified. This inlet boundary defines whether a fully flooded or a starved condition exists in the contact. Furthermore it is found that the film thickness for a starved condition could be written in dimensionless terms

as a function of the inlet distance parameter and the film thickness for a fully flooded condition. Contour plots of pressure and film thickness in and around the contact are shown for fully flooded and starved conditions. The theoretical findings are compared directly with results obtained experimentally. Author

N80-28711* National Aeronautics and Space Administration, Lewis Research Center, Cleveland, Ohio.

CIRCUMFERENTIAL SHAFT SEAL Patent

Lawrence P. Ludwig, inventor (to NASA) Issued 15 Jul. 1980 4 p Filed 31 Mar. 1976 Supersedes N76-20488 (14-11, p 1394)

(NASA-Case-LEW-12119-1; US-Patent-4,212,477; US-Patent-Appl-SN-672219; US-Patent-Class-277-193; US-Patent-Class-277-153; US-Patent-Class-277-224) Avail: US Patent and Trademark Office CSCL 11A

A circumferential shaft seal is described which comprises two sealing rings held to a rotating shaft by means of a surrounding elastomeric band. The rings are segmented and are of a rigid sealing material such as carbon or a polyimide and graphite fiber composite.

Official Gazette of the U.S. Patent and Trademark Office

N80-28716* National Aeronautics and Space Administration, Lewis Research Center, Cleveland, Ohio.

KINEMATIC CORRECTION FOR ROLLER SKEWING

Michael Savage (Akron Univ.) and Stuart H. Loewenthal Oct. 1980 46 p refs Proposed for presentation at 16th Bien. Mech. Conf., Beverly Hills, Calif., 29 Sep. - 1 Oct. 1980; sponsored by ASME

(NASA-TM-81564; E-526) Avail: NTIS HC A03/MF A01 CSCL 131

A theory of kinematic stabilization of rolling cylinders is developed for high-speed cylindrical roller bearings. This stabilization requires race and roller crowning to product changes in the rolling geometry as the roller shifts axially. These changes put a reverse skew in the rolling elements by changing the rolling taper. Twelve basic possible bearing modifications are identified in this paper. Four have single transverse convex curvature in the rollers while eight have rollers with compound transverse curvature composed of a central cylindrical band of constant radius surrounded by symmetric bands with both slope and transverse curvature. Author

N80-29706* National Aeronautics and Space Administration, Lewis Research Center, Cleveland, Ohio.

ROTORDYNAMIC INSTABILITY PROBLEMS IN HIGH-PERFORMANCE TURBOMACHINERY

1980 463 p refs Conf. held at College Station, 12-14 May 1980; sponsored by Texas A and M Univ., Louisville Univ., and AROD

(NASA-CP-2133; E-413) Avail: NTIS HC A20/MF A01 CSCL 131

Diagnostic and remedial methods concerning rotordynamic instability problems in high performance turbomachinery are discussed. Instabilities due to seal forces and work-fluid forces are identified along with those induced by rotor bearing systems. Several methods of rotordynamic control are described including active feedback methods, the use of elastomeric elements, and the use of hydrodynamic journal bearings and supports. For individual titles, see N80-29707 through N80-29733.

N80-29716* National Aeronautics and Space Administration, Lewis Research Center, Cleveland, Ohio.

DAMPING IN RING SEALS FOR COMPRESSIBLE FLUIDS

David P. Fleming In its Rotordyn. Instability Probl. in High-Performance Turbomachinery 1980 p 169-188 refs (For primary document see N80-29706 20-37)

Avail: NTIS HC A20/MF A01 CSCL 131

An analysis is presented to calculate damping in ring seals for a compressible fluid. Results show that damping in tapered ring seals (optimized for stiffness) is less than that in straight

bore ring seals for the same minimum clearance. Damping in ring seals can promote fractional frequency whirl and can, thus, be detrimental. Thus, tapered seals can benefit rotor and seal stability by having lower damping as well as higher stiffness. Use of incompressible results leads to large errors. Author

N80-29734* National Aeronautics and Space Administration, Lewis Research Center, Cleveland, Ohio.

LUBRICATION OF OPTIMIZED-DESIGN TAPERED-ROLLER BEARINGS TO 2.4 MILLION DN

Richard J. Parker and Stanley I. Pinel Aug. 1980 18 p refs Sponsored in part by Industrial Tectonics, Inc., Compton, Calif. (NASA-TP-1714; E-270) Avail: NTIS HC A02/MF A01 CSCL 131

The performance of 120.65 mm (4.75 in.) bore high speed design, tapered roller bearings was investigated at shaft speeds to 20,000 rpm (2.4 million DN) under combined thrust and radial load. The test bearing design was computer optimized for high speed operation. Temperature distribution bearing heat generation were determined as a function of shaft speed, radial and thrust loads, lubricant flow rates, and lubricant inlet temperature. The high speed design, tapered roller bearing operated successfully at shaft speeds up to 20,000 rpm under heavy thrust and radial loads. Bearing temperatures and heat generation with the high speed design bearing were significantly less than those of a modified standard bearing tested previously. Cup cooling was effective in decreasing the high cup temperatures to levels equal to the cone temperature. Author

N80-29735* National Aeronautics and Space Administration, Lewis Research Center, Cleveland, Ohio.

FILM THICKNESS FOR DIFFERENT REGIMES OF FLUID-FILM LUBRICATION

Bernard J. Hamrock 1980 14 p refs Presented at lecture series at Lulea, Sweden, 24 Jul. - 16 Aug. 1980

(NASA-TM-81550; E-508) Avail: NTIS HC A02/MF A01 CSCL 11H

Film thickness equations are provided for four fluid-film lubrication regimes found in elliptical contacts. These regimes are isoviscous-rigid; viscous-rigid; elastohydrodynamic lubrication of low-elastic-modulus materials (soft EHL), or isoviscous-elastic; and elastohydrodynamic lubrication of high-elastic-modulus materials (hard EHL), or viscous-elastic. The influence or lack of influence of elastic and viscous effects is the factor that distinguishes these regimes. The results are presented as a map of the lubrication regimes, with film thickness contours on a log-log grid of the viscosity and elasticity for three values of the ellipticity parameter. E.D.K.

N80-31790* National Aeronautics and Space Administration, Lewis Research Center, Cleveland, Ohio.

FREE-PISTON REGENERATIVE HOT GAS HYDRAULIC ENGINE Patent

Donald G. Beremand, inventor (to NASA) Issued 5 Aug. 1980 7 p Filed 12 Oct. 1978 Supersedes N79-10426 (17 - 12, p 0057)

(NASA-Case-LEW-12274-1; US-Patent-4,215,548;

US-Patent-Appl-SN-950876; US-Patent-Class-60-520;

US-Patent-Class-417-383) Avail: US Patent and Trademark Office CSCL 131

A displacer piston which is driven pneumatically by a high-pressure or low-pressure gas is included in a free-piston regenerative hydraulic engine. Actuation of the displacer piston circulates the working fluid through a heater, a regenerator and a cooler. The present invention includes an inertial mass such as a piston or a hydraulic fluid column to effectively store and supply energy during portions of the cycle. Power is transmitted from the working fluid to a hydraulic fluid across a diaphragm or lightweight piston to achieve a hydraulic power out-put. The displacer piston of the present invention may be driven pneumatically, hydraulically or electromagnetically. In addition, the displacer piston and the inertial mass of the present invention may be positioned on the same side of the diaphragm member or may be separated by the diaphragm member.

Official Gazette of the U.S. Patent and Trademark Office

**N80-31787*# National Aeronautics and Space Administration
Lewis Research Center, Cleveland, Ohio
SIMULATION AND VISUALIZATION OF FACE SEAL
MOTION STABILITY BY MEANS OF COMPUTER GENER-
ATED MOVIES**

I. Etsion and B. M. Auer 1980 19 p refs Proposed for presentation at the Fluid Sealing Conf., Leeuwenhorst, Holland, 1-3 Apr. 1980; sponsored by the British Hydrodynamic Research Assoc.

(NASA-TM-81581; E-554) Avail: NTIS HC A02/MF A01 CSCL 131

A computer aided design method for mechanical face seals is described. Based on computer simulation, the actual motion of the flexibly mounted element of the seal can be visualized. This is achieved by solving the equations of motion of this element, calculating the displacements in its various degrees of freedom vs. time, and displaying the transient behavior in the form of a motion picture. Incorporating such a method in the design phase allows one to detect instabilities and to correct undesirable behavior of the seal. A theoretical background is presented. Details of the motion display technique are described, and the usefulness of the method is demonstrated by an example of a noncontacting conical face seal. M.G.

**N80-31788*# National Aeronautics and Space Administration
Lewis Research Center, Cleveland, Ohio**

**OBSERVATION OF PRESSURE VARIATION IN THE
CAVITATION REGION OF SUBMERGED JOURNAL
BEARINGS**

I. Etsion and L. P. Ludwig 1980 27 p refs Proposed for presentation at the Lubrication Conf., New Orleans, 11-14 Oct. 1981; sponsored by the ASME

(NASA-TM-81582; E-555) Avail: NTIS HC A03/MF A01 CSCL 131

Visual observations and pressure measurements in the cavitation zone of a submerged journal bearing are described. Tests were performed at various shaft speeds and ambient pressure levels. Some photographs of the cavitation region are presented showing strong reverse flow at the downstream end of the region. Pressure profiles are presented showing significant pressure variations inside the cavitation zone, contrary to common assumptions of constant cavitation pressure. Author

**N80-33749*# National Aeronautics and Space Administration
Lewis Research Center, Cleveland, Ohio**

**EFFECT OF CAGE DESIGN ON CHARACTERISTICS OF
HIGH-SPEED-JET-LUBRICATED 35-MILLIMETER-BORE
BALL BEARING**

Fredrick T. Schuller, Stanley I. Pinel (Industrial Tectonics, Compton, Calif.), and Hans R. Signer (Industrial Tectonics, Compton, Calif.) Oct. 1980 13 p refs

(NASA-TP-1732; E-289) Avail: NTIS HC A02/MF A01 CSCL 131

Parametric tests were conducted with a 35 mm bore angular contact ball bearing with a double outer land guided cage. Provisions were made for jet lubrication and outer-ring cooling of the bearing. Test conditions included a combined thrust and radial load at nominal shaft speeds of 48,000 rpm, and an oil-in temperature of 394 K (250 F). Successful operation of the test bearing was accomplished up to 2.5 million DN. Test results were compared with those obtained with similar bearing having a single outer land guided cage. Higher temperatures were generated with the double outer land guided cage bearing, and bearing power loss and cage slip were greater. Cooling the outer ring resulted in a decrease in overall bearing operating temperature. Author

**A80-10040*# Survey of ion plating sources. T. Spalvins
(NASA, Lewis Research Center, Cleveland, Ohio), *American Vacuum
Society, National Vacuum Symposium, 26th, New York, N.Y., Oct.
2-5, 1979, Paper, 23 p, 35 refs.***

Ion plating is a plasma deposition technique where ions of the gas and the evaporant have a decisive role in the formation of a coating in terms of adherence, coherence, and morphological growth. The range of materials that can be ion plated is predominantly

determined by the selection of the evaporation source. Based on the type of evaporation source, gaseous media and mode of transport, the following will be discussed: resistance, electron beam sputtering, reactive and ion beam evaporation. Ionization efficiencies and ion energies in the glow discharge determine the percentage of atoms which are ionized under typical ion plating conditions. The plating flux consists of a small number of energetic ions and a large number of energetic neutrals. The energy distribution ranges from thermal energies up to a maximum energy of the discharge. The various reaction mechanisms which contribute to the exceptionally strong adherence - formation of a graded substrate/coating interface are not fully understood, however the controlling factors are evaluated. The influence of process variables on the nucleation and growth characteristics are illustrated in terms of morphological changes which affect the mechanical and tribological properties of the coating. (Author)

**A80-13068*# NASA gear research and its probable effect on
rotorcraft transmission design. E. V. Zaretsky, D. P. Townsend, and
J. J. Coy (NASA, Lewis Research Center, Cleveland, Ohio). *American Helicopter Society, Meeting on Helicopter Propulsion
Systems, Williamsburg, Va., Nov. 6-8, 1979, Paper, 17 p, 42 refs.***

The NASA Lewis Research Center devised a comprehensive gear technology research program beginning in 1969, the results of which are being integrated into the NASA civilian Helicopter Transmission System Technology Program. Attention is given to the results of this gear research and those programs which are presently being undertaken. In addition, research programs studying pitting fatigue, gear steels and processing, life prediction methods, gear design and dynamics, elastohydrodynamic lubrication, lubrication methods and gear noise are presented. Finally, the impact of advanced gear research technology on rotorcraft transmission design is discussed.

M.E.P.

**A80-14727* Some flow characteristics of conventional and
tapered high-pressure-drop simulated seals. R. C. Hendricks (NASA,
Lewis Research Center, Cleveland, Ohio). *American Society of
Lubrication Engineers and American Society of Mechanical Engi-
neers, Lubrication Conference, Dayton, Ohio, Oct. 16-18, 1979,
ASLE Preprint 79-LC-3B-2, 6 p, 11 refs.***

The leak rates through shaft seals with large pressure drops were simulated using gaseous hydrogen, or nitrogen flowing through an annulus with a nonrotating centerbody. The flows were choked. For concentric or eccentric position of the rotor and parallel or convergent tapered flow passages, data and analysis revealed that mass flux or leak rate can be determined from a relation whose normalizing parameters depend on the thermodynamic critical constants of the working fluid and an average flow area expressed in terms of the inlet and exit cross-sectional areas. Using these normalized relations, the flow data for parallel and three convergent, tapered, shaft-seal configurations are in good agreement. Generalization to any simple gas or gas mixtures is implied and demonstrated in part. (Author)

**A80-14734* The friction and wear of metals and binary
alloys in contact with an abrasive grit of single-crystal silicon carbide.
K. Miyoshi and D. H. Buckley (NASA, Lewis Research Center,
Cleveland, Ohio). *American Society of Lubrication Engineers and
American Society of Mechanical Engineers, Lubrication Conference,
Dayton, Ohio, Oct. 16-18, 1979, ASLE Preprint 79-LC-5C-1, 10 p,
19 refs.***

Sliding friction experiments were conducted with various metals and iron-base binary alloys (alloying elements Ti, Cr, Mn, Ni, Rh, and W) in contact with single-crystal silicon carbide riders. Results indicate that the coefficient of friction and groove height (corresponding to the wear volume) decrease linearly as the shear strength of the bulk metal increases. The coefficient of friction and groove height generally decrease with an increase in solute content of binary alloys. A separate correlation exists between the solute to iron

atomic radius ratio and the decreasing rates of change of coefficient of friction and groove height with increasing solute content. These rates of change are minimum at a solute to iron radius ratio of unity. They increase as the atomic ratio increases or decreases linearly from unity. The correlations indicate that atomic size is an important parameter in controlling friction and wear of alloys. (Author)

A80-15736 * // Design of elastomer dampers for a high-speed flexible rotor. J. A. Tecza, A. J. Smalley (Mechanical Technology, Inc., Latham, N.Y.), M. S. Darlow, and R. E. Cunningham (NASA, Lewis Research Center, Cleveland, Ohio). *American Society of Mechanical Engineers, Design Engineering Technical Conference, St. Louis, Mo., Sept. 10-12, 1979, Paper 79-DET-88* 8 p. 26 refs. Members, \$1.50; nonmembers, \$3.00. NASA-sponsored research.

This paper describes a method used to design elastomerically damped supports for high-speed, flexible rotor-bearing systems. The procedure consists of using a damped natural frequency analysis to identify stiffness and damping requirements for the supports over the speed range. Optimum values for these coefficients are found and unbalance response analysis is used to calculate expected rotor behavior. Equations for calculating the shear and compressive stiffness and damping of button-type elastomer mounts are given, as is a procedure for their application to the design of the elastomeric mounts. These techniques were successfully applied to the design of damped elastomeric supports for a high-speed rotor, which traverses two bending critical speeds. Results of the testing showed that the rotor was well behaved and showed linear response to unbalance. Measured modal damping exceeded expectations and tests were conducted with both high- and low-loss elastomers, enabling the exploration of the practical range of elastomer damping capability. (Author)

A80-24002 * // Dynamic properties of elastomer cartridge specimens under a rotating load. M. S. Darlow, A. J. Smalley (Mechanical Technology, Inc., Latham, N.Y.), and R. E. Cunningham (NASA, Lewis Research Center, Cleveland, Ohio). In: *World Congress on the Theory of Machines and Mechanisms, 5th, Montreal, Canada, July 8-13, 1979, Proceedings, Volume 2*. (A80-23976 08-37) New York, American Society of Mechanical Engineers, 1979, p. 1599-1602.

This paper presents the results of a program of analysis and test to determine the dynamic properties of elastomer cartridges operating under a rotating load. These measured properties were compared to predictions based on results of unidirectional tests with the same elastomer material. The test method for the dynamic stiffness and damping measurements was essentially the same as the Base Excitation Resonant Mass Method. The primary difference is that the exciting force used for these most recent tests was exerted by rotating unbalance in a rotational test rig rather than a shake table. The specimens tested were: two rectangular cross-section, continuous ring cartridges of different cross-section and three cylindrical button cartridges of different button thickness. Tests were performed for strains from about 0.0001 to about 0.01 (double amplitude). Material properties and prediction equations determined from reciprocating tests were used to make numerical predictions of stiffness, damping, and loss coefficient for the test elements, with encouraging results. Strain was shown to be an important parameter in determining these dynamic properties, particularly damping and loss coefficient. (Author)

A80-28010 * Wear of seal materials used in aircraft propulsion systems. R. C. Bill (U.S. Army, Army Aviation Research and Development Center, Cleveland, Ohio) and L. P. Ludwig (NASA, Lewis Research Center, Cleveland, Ohio). (*U.S. Navy, Workshop on Thermal Deformation, Annapolis, Md., June 19, 20, 1979*) *Wear*, vol. 59, Mar. 1, 1980, p. 165-189, 23 refs.

A review of various types of seal locations in a gas turbine engine and the significance of wear for each type are presented. Material selection guidelines and the PV (contact pressure times

sliding velocity) criteria for seal materials are discussed, and examples of wear mechanisms in positive contact seals are given. It is suggested that improved wear, erosion, and oxidation resistant materials will be required for improved seal durability; finally, a correlation is proposed between wear characteristics and a factor that includes material strength, ductility, specific heat and hot-working temperature to attain low porosity metallic gas path seal materials. A.T.

A80-31961 * Rolling-element bearings. W. J. Anderson (NASA, Lewis Research Center, Mechanical Components Branch, Cleveland, Ohio). In: *Tribology: Friction, lubrication, and wear*. (A80-39154 12-37) Washington, D.C., Hemisphere Publishing Corp., 1980, p. 397-426, 16 refs.

In contrast to hydrodynamic bearings, which depend for low-friction characteristics on a fluid film between the journal and the bearing surfaces, roller-element bearings employ a number of balls or rollers that roll in an annular space. The paper briefly outlines the advantages and disadvantages of roller-element bearings as compared to hydrodynamic bearings. The discussion covers bearing types, rolling friction, friction losses in rolling bearings, contact stresses, deformations, kinematics (normal and high speeds), bearing dynamics including elastohydrodynamics, load distribution, lubrication (grease, solid oil, oil-air mist), specific dynamic capacity and life, specific static capacity, and fatigue or wearout (elastohydrodynamics, wear). Rolling bearing wear factor as a function of operating environment is plotted and discussed. S.D.

A80-42256 * // Balancing of a power-transmission shaft with the application of axial torque. E. S. Zorzi (Mechanical Technology, Inc., Latham, N.Y.) and D. Flemming (NASA, Lewis Research Center, Cleveland, Ohio). *American Society of Mechanical Engineers, Gas Turbine Conference and Products Show, New Orleans, La., Mar. 10-13, 1980, Paper 80-GT-143*. 5 p. 6 refs. Members, \$1.50; nonmembers, \$3.00. NASA-supported research.

Evaluation of power transmission shafting for high-speed balancing has shown that when axial torque is applied, the imbalance response is altered. An increase in synchronous excitation always occurs if the axial torque level is altered from the value used during balancing; this was the case even when the shaft was balanced with torque applied. The twisting of the long slender shaft produces a change in the imbalance distribution sufficient to disrupt the balanced state. This paper presents a review of the analytic development of a weighted least squares approach to influence coefficient balancing and a review of experimental results. The analytic approach takes advantage of the fact that the past testing has shown that the influence coefficients are not significantly affected by the application of axial torque. The 3.60-m (12-ft) long aluminum shaft, 7.62 cm (3 in.) in diameter was run through the first flexural critical speed at torque levels ranging from zero-torque to 903.8 N-M (8000 lb-in.) in 112.9 N-M (1000 lb-in.) increments. Good comparison was achieved between predicted and experimental results. (Author)

A80-42272 * // Elastomer damper performance - A comparison with a squeeze film for a supercritical power transmission shaft. E. S. Zorzi, G. Burgess (Mechanical Technology, Inc., Latham, N.Y.), and R. Cunningham (NASA, Lewis Research Center, Latham, N.Y.). *American Society of Mechanical Engineers, Gas Turbine Conference and Products Show, New Orleans, La., Mar. 10-13, 1980, Paper 80-GT-162*. 7 p. 7 refs. Members, \$1.50; nonmembers, \$3.00.

This paper describes the design and testing of an elastomer damper on a super-critical power transmission shaft. The elastomers were designed to provide acceptable operation through the fourth bending mode and to control synchronous as well as nonsynchronous vibration throughout the operating range. The design of the elastomer was such that it could be incorporated into the system as a replacement for a squeeze-film damper without a reassembly, which could have altered the imbalance of the shaft. This provided a direct comparison of the elastomer and squeeze-film dampers without having to assess the effect of shaft imbalance changes. (Author)

A80-43159 * An investigation into the role of adhesion in the erosion of ductile metals. W. A. Brainard and J. Salik (NASA, Lewis Research Center, Cleveland, Ohio). *American Society of Lubrication Engineers, Annual Meeting, 35th, Anaheim, Calif., May 5-8, 1980, Preprint 80-AM-3E-3*. 5 p. 20 refs.

Existing theories of erosion of ductile metals based on cutting and deformation mechanisms predict no material removal at normal incidence which is contradictory to experience. Thus, other mechanisms may be involved. The possible role of adhesive material transfer during erosion is investigated by both single-particle impingement experiments and erosion by streams of particles. Examination of the rebounding particles as well as the eroded surfaces yields evidence of a significant adhesive mechanism for the ductile metals investigated. (Author)

A80-43163 * Mechanisms of lubrication and wear of a bonded solid-lubricant film. R. L. Fusaro (NASA, Lewis Research Center, Cleveland, Ohio). *American Society of Lubrication Engineers, Annual Meeting, 35th, Anaheim, Calif., May 5-8, 1980, Preprint 80-AM-3E-1*. 12 p. 6 refs.

The tribological properties of polyimide-bonded graphite fluoride films were investigated. A pin-on-disk type of testing apparatus was used; in addition to sliding a hemispherically tipped rider, a rider with a 0.95-mm-diameter flat area was slid against the film so that a lower, less variable contact stress could be achieved. Two stages of lubrication occurred: in the first, the film supported the load and the lubricating mechanism consisted of the shear of a thin surface layer between the rider and the bulk of the film. The second occurred after the bonded film had worn to the substrate, and consisted of the shear of very thin lubricant films between the rider and flat plateaus generated on the metallic substrate asperities. The film wear mechanism was strongly dependent on contact stress. (Author)

A80-43167 * Analysis of wear debris from full-scale bearing fatigue tests using the Ferrograph. W. R. Jones, Jr. and S. H. Loewenthal (NASA, Lewis Research Center, Cleveland, Ohio). *American Society of Lubrication Engineers, Annual Meeting, 35th, Anaheim, Calif., May 5-8, 1980, Preprint 80-AM-3E-2*. 7 p. 16 refs.

The Ferrograph was used to determine the types of quantities of wear particles generated during full-scale bearing fatigue tests. Deep-groove ball bearings made from AISI 52100 steel were used. A MIL-L-23699 tetraester lubricant was used in a recirculating lubrication system containing a 49-micron absolute filter. Test conditions included a maximum Hertz stress of 2.4 GPa, a shaft speed of 15,000 rpm and a lubricant supply temperature of 74 C (165 F). Four fatigue failures were detected by accelerometers in this test set. In general, the Ferrograph was more sensitive (up to 23 h) in detecting spall initiation than either accelerometers or the normal spectrographic oil analysis (SOAP). Four particle types were observed: normal rubbing wear particles, spheres, nonferrous particles, and severe wear (spall) fragments. (Author)

A80-43176 * Friction and wear of plasma-sprayed coatings containing cobalt alloys from 25 deg to 650 deg in air. H. E. Sliney and T. P. Jacobson (NASA, Lewis Research Center, Cleveland, Ohio). *American Society of Lubrication Engineers, Annual Meeting, 35th, Anaheim, Calif., May 5-8, 1980, Preprint 80-AM-6C-2*. 6 p. 13 refs.

Four different compositions of self-lubricating, plasma-sprayed, composite coatings with calcium fluoride dispersed throughout cobalt alloy-silver matrices were evaluated on a friction and wear apparatus. In addition, coatings of the cobalt alloys alone and of one coating with a nickel alloy-silver matrix were evaluated for comparison. The wear specimens consisted of two, diametrically opposed, flat rub shoes sliding on the coated, cylindrical surface of a rotating disk. Two of the cobalt composite coatings gave a friction coefficient of about 0.25 and low wear at room temperature, 400 and 650 C. Wear rates were lower than those of the cobalt alloys alone or the nickel alloy composite coating. However, oxidation limited the maximum useful temperature of the cobalt composite coating to about 650 C compared to about 900 C for the nickel composite

coating.

(Author)

A80-44240 * # Application of superalloy powder metallurgy for aircraft engines. R. L. Dreshfield and R. V. Miner, Jr. (NASA, Lewis Research Center, Cleveland, Ohio). *Metal Powder Industries Federation and American Powder Metallurgy Institute, International Powder Metallurgy Conference, Washington, D.C., June 22-27, 1980, Paper*. 19 p. 8 refs.

The results of the Materials for Advanced Turbine Engines (MATE) program initiated by NASA are presented. Mechanical properties comparisons are made for superalloy parts produced by as-HIP powder consolidation and by forging of HIP consolidated billets. The effect of various defects on the mechanical properties of powder parts are shown. V.T.

A80-46407 * # Constrained fatigue life optimization of a NASVYTIS multiroller traction drive. J. J. Coy (U.S. Army, Propulsion Laboratory, Cleveland, Ohio), D. A. Rohn, and S. H. Loewenthal (NASA, Lewis Research Center, Cleveland, Ohio). *American Society of Mechanical Engineers, International Power Transmission and Gearing Conference, 3rd, San Francisco, Calif., Aug. 18-22, 1980, Paper*. 18 p. 15 refs.

A contact fatigue life analysis method for multiroller traction drives is presented. The method is based on the Lundberg-Palmgren analysis method for rolling element bearing life prediction, and also uses life adjustment factors for materials, processing, lubrication, and effect of traction. The analysis method is applied in an optimization study to the multiroller traction drive, consisting of a single-stage planetary configuration with two rows of stepped planet rollers of five rollers per row. The drive was approximately 25 centimeters in diameter by 11 centimeters long, having a nominal ratio of 15:1. The theoretically predicted drive life was 2510 hours at a nominal continuous power and speed of 74.6 kW (100 hp) and 75,000 rpm. (Author)

A80-46409 * # Effect of geometry and operating conditions on spur gear system power loss. N. E. Anderson (U.S. Army, Propulsion Laboratory, Cleveland, Ohio) and S. H. Loewenthal (NASA, Lewis Research Center, Cleveland, Ohio). *American Society of Mechanical Engineers, International Power Transmission and Gearing Conference, 3rd, San Francisco, Calif., Aug. 18-22, 1980, Paper*. 29 p. 13 refs.

The results of an analysis of the effects of spur gear size, pitch, width and ratio on total mesh power loss for a wide range of speeds, torques and oil viscosities are presented. The analysis uses simple algebraic expressions to determine gear sliding, rolling and windage losses and also incorporates an approximate ball bearing power loss expression. The analysis shows good agreement with published data. Large diameter and fine-pitched gears had higher peak efficiencies but lower part-load efficiency. Gear efficiencies were generally greater than 98 percent except at very low torque levels. Tare (no-load) losses are generally a significant percentage of the full-load loss except at low speeds. (Author)

A80-46410 * # Evaluation of a high performance fixed-ratio traction drive. S. H. Loewenthal, D. A. Rohn (NASA, Lewis Research Center, Cleveland, Ohio), and N. E. Anderson (U.S. Army, Propulsion Laboratory, Cleveland, Ohio). *American Society of Mechanical Engineers, International Power Transmission and Gearing Conference, 3rd, San Francisco, Calif., Aug. 18-22, 1980, Paper*. 30 p. 21 refs.

The results of a test program to evaluate a compact, high performance, fixed-ratio traction drive are presented. This transmission, the Nasvytis Multiroller Traction Drive, is a fixed-ratio, single-stage planetary with two rows of stepped planet-rollers. Two versions of the drive were parametrically tested back-to-back at speeds to 73,000 rpm and power levels to 180 kW (240 hp). Parametric tests were also conducted with the Nasvytis drive

retrofitted to an automotive gas turbine engine. The drives exhibited good performance, with a nominal peak efficiency of 94 to 96 percent and a maximum speed loss due to creep of approximately 3.5 percent. (Author)

A80-46411 * # Endurance and failure characteristics of modified Vasco X-2, CBS 600 and AISI 9310 spur gears. D. P. Townsend and E. V. Zaretsky (NASA, Lewis Research Center, Cleveland, Ohio). *American Society of Mechanical Engineers, International Power Transmission and Gearing Conference, 3rd, San Francisco, Calif., Aug. 18-22, 1980, Paper, 27 p, 15 refs.*

Gear endurance tests and rolling-element fatigue tests were conducted to compare the performance of spur gears made from AISI 9310, CBS 600 and modified Vasco X-2 and to compare the pitting fatigue lives of these three materials. Gears manufactured from CBS 600 exhibited lives longer than those manufactured from AISI 9310. However, rolling-element fatigue tests resulted in statistically equivalent lives. Modified Vasco X-2 exhibited statistically equivalent lives to AISI 9310. CBS 600 and modified Vasco X-2 gears exhibited the potential of tooth fracture occurring at a tooth surface fatigue pit. Case carburization of all gear surfaces for the modified Vasco X-2 gears results in fracture at the tips of the gears. (Author)

A80-46412 * # Analytical and experimental spur gear tooth temperature as affected by operating variables. D. P. Townsend (NASA, Lewis Research Center, Cleveland, Ohio) and L. S. Akin (Western Gear Corp., Lynwood, Calif.). *American Society of Mechanical Engineers, International Power Transmission and Gearing Conference, 3rd, San Francisco, Calif., Aug. 18-22, 1980, Paper, 27 p, 11 refs.*

A gear tooth temperature analysis was performed using a finite element method combined with a calculated heat input, calculated oil jet impingement depth, and estimated heat transfer coefficients. Experimental measurements of gear tooth average surface temperatures and instantaneous surface temperatures were made with a fast response infrared radiometric microscope. Increased oil jet pressure had a significant effect on both average and peak surface temperatures at both high load and speeds. Increasing the speed at constant load and increasing the load at constant speed causes a significant rise in average and peak surface temperatures of gear teeth. The oil jet pressure required for adequate cooling at high speed and load conditions must be high enough to get full depth penetration of the teeth. Calculated and experimental results were in good agreement with high oil jet penetration but showed poor agreement with low oil jet penetration depth. (Author)

A80-46413 * # Simplified fatigue life analysis for traction drive contacts. D. A. Rohn, S. H. Loewenthal (NASA, Lewis Research Center, Cleveland, Ohio), and J. J. Coy (U.S. Army, Propulsion Laboratory, Cleveland, Ohio). *American Society of Mechanical Engineers, International Power Transmission and Gearing Conference, 3rd, San Francisco, Calif., Aug. 18-22, 1980, Paper, 28 p, 19 refs.*

A simplified fatigue life analysis for traction drive contacts of arbitrary geometry is presented. The analysis is based on the Lundberg-Palmgren theory used for rolling-element bearings. The effects of torque, element size, speed, contact ellipse ratio, and the influence of traction coefficient are shown. The analysis shows that within the limits of the available traction coefficient, traction contacts exhibit longest life at high speeds. Multiple, load-sharing roller arrangements have an advantageous effect on system life, torque capacity, power-to-weight ratio and size. (Author)

N80-13474* # General Electric Co., Cincinnati, Ohio. Aircraft Engine Group. **FEASIBILITY OF SiC COMPOSITE STRUCTURES FOR 1644 DEG GAS TURBINE SEAL APPLICATIONS** Final Report.

28 Apr. - 30 May 1979

R. Darolia May 1979 109 p ref

(Contract NAS3-20082)

(NASA-CR-159597; R79AEG625)

Avail: NTIS

HC A06/MF A01 CSCL 11A

The feasibility of silicon carbide composite structures was evaluated for 1644 K gas turbine seal applications. The silicon carbide composites evaluated consisted of Si/SiC Silcomp (Trademark) - and sintered silicon carbide as substrates, both with attached surface layers containing BN as an additive. A total of twenty-eight candidates with variations in substrate type and density, and layer chemistry, density, microstructure, and thickness were evaluated for abrasability, cold particle erosion resistance, static oxidation resistance, ballistic impact resistance, and fabricability. The BN-free layers with variations in density and pore size were later added for evaluation. The most promising candidates were evaluated for Mach 1.0 gas oxidation/erosion resistance from 1477 K to 1644 K. The as-fabricated rub layers did not perform satisfactorily in the gas oxidation/erosion tests. However, preoxidation was found to be beneficial in improving the hot gas erosion resistance. Overall, the laboratory and rig test evaluations show that material properties are suitable for 1477 K gas turbine seal applications. J.M.S.

N80-15411* # Detroit Diesel Allison, Indianapolis, Ind. **PLASMA-SPRAYED DUAL DENSITY CERAMIC TURBINE SEAL SYSTEM** Final Report

D. L. Clingman, B. Schechter, K. R. Cross, and J. R. Cavanagh

Oct. 1979 67 p refs

(Contract NAS3-21263)

(NASA-CR-159739; EDR-10085)

Avail: NTIS

HC A04/MF A01 CSCL 11A

Dual density, plasma sprayed ceramic coating systems were investigated for possible application as abrasable turbine tip seal systems in small gas turbine engines. Abrasability, erosion resistance, internal leakage, and microstructural characterization were investigated for polyester and cenosphere filled zirconium oxide composites. Results indicate the polyester system is more abrasable but displays significantly less erosion resistance than the cenosphere system. It is also stated that the absence of significant blade tip damage during abrasability testing of both systems suggests additional effort may result in a more nearly optimum balance of abrasability and erosion resistance. M.G.

N80-16338* # General Electric Co., Cincinnati, Ohio. Materials and Process Technology Labs.

PROGRAM TO DEVELOP SPRAYED, PLASTICALLY DEFORMABLE COMPRESSOR SHROUD SEAL MATERIALS Interim Technical Progress Report, 29 Jun. 1976 - 28 Feb. 1979

R. C. Schwab Nov. 1979 78 p refs

(Contract NAS3-20054)

(NASA-CR-159741; ITPR-1) Avail: NTIS HC A05/MF A01 CSCL 11A

A study of fundamental rub behavior for ten dense sprayed materials and eight current compressor clearance materials has been conducted. A literature survey of a wide variety of metallurgical and thermophysical properties was conducted and correlated to rub behavior. Based on these results, the most promising dense rub material was Cu-9Al. Additional studies on the effects of porosity, incursion rate, blade solidity and ambient temperature were carried out on aluminum bronze (Cu-9Al-1Fe) with and without a 515B Feltmetal underlayer. Author

N80-17470* # Chrysler Corp., Detroit, Mich. **MATERIALS REVIEW FOR IMPROVED AUTOMOTIVE GAS TURBINE ENGINE** Final Report

C. Belleau, W. L. Ehlers, and F. A. Hagen Apr. 1978 101 p

refs Sponsored by NASA

(Contract EY-76-C-02-2749.A011)

(NASA-CR-159673; DOE/NASA/2749-79/4 Vol-4) Avail:

NTIS HC A06/MF A01 CSCL 21A

The potential role of superalloys, refractory alloys, and ceramics in the hottest sections of engines operating with turbine

inlet temperatures as high as 1370 C is examined. The conventional superalloys, directionally solidified eutectics, oxide dispersion strengthened alloys, and tungsten fiber reinforced superalloys are reviewed and compared on the basis of maximum turbine blade temperature capability. Improved high temperature protective coatings and special fabrication techniques for these advanced alloys are discussed. Chromium, columbium, molybdenum, tantalum, and tungsten alloys are also reviewed. Molybdenum alloys are found to be the most suitable for mass produced turbine wheels. Various forms and fabrication processes for silicon nitride, silicon carbide, and SiALON's are investigated for use in highstress and medium stress high temperature environments.

K.L.

N80-18402* National Aeronautics and Space Administration, Langley Research Center, Langley Station, Va.

IMPROVED TIRE/WHEEL CONCEPT Patent Application
Philip M. Harper, Sr., inventor (to NASA) (Boeing Commercial Airplane Co., Seattle, Wash.) Filed 12 Dec. 1979 12 p
Sponsored by NASA
(NASA-Case-LAR-11695-2; US-Patent-Appl-SN-103836) Avail:
NTIS HC A02/MF A01 CSCL 01C

A tire and wheel assembly is described which consists of a low profile pneumatic tire with sidewalls that deflect inwardly under a load and a wheel having a narrow central channel and extended rim flanges. The extended rim flanges support the tire sidewalls under static and dynamic loading conditions to produce a combination particularly suited to aircraft applications. NASA

N80-22700* Boeing Commercial Airplane Co., Seattle, Wash.
TESTING OF RECIPROCATING SEALS FOR APPLICATION IN A STIRLING CYCLE ENGINE

J. F. Curulla and T. L. Beck Feb. 1980 76 p refs
(Contract NAS3-20612)

(NASA-CR-159820; DOE/NASA/0612-80/1;
BCAC-D6-48915) Avail: NTIS HC A05/MF A01 CSCL 11A

Six single stage reciprocating seal configurations to the requirements of the Stirling cycle engine were evaluated. The seals tested were: the Boeing Footseal, NASA Chevron polyimide seal, Bell seal, Quad seal, Tetraseal, and Dynabak seal. None of these seal configurations met the leakage goals of .002 cc/sec at helium gas pressure of 1.22×10 to the 7th power PA, rod speed of 7.19 m/sec peak, and seal environmental temperature of 408 K for 1500 hours. Most seals failed due to high temperatures. Catastrophic failures were observed for a minimum number of test runs characterized by extremely high leakage rates and large temperature rises. The Bell seal attained 63 hours of run time at significantly lowered test conditions.

E.D.K.

N80-22702* Kumm (Emerson L.), Tempe, Ariz.
DESIGN STUDY OF FLAT BELT CVT FOR ELECTRIC VEHICLES

Emerson L. Kumm Mar. 1980 159 p refs

(Contract DEN3-114; Contract EC-77-A-31-1044)

(NASA-CR-159822; P-1006) Avail: NTIS HC A08/MF A01 CSCL 131

A continuously variable transmission (CVT) was studied, using a novel flat belt pulley arrangement which couples the high speed output shaft of an energy storage flywheel to the drive train of an electric vehicle. A specific CVT arrangement was recommended and its components were selected and sized, based on the design requirements of a 1700 KG vehicle. A design layout was prepared and engineering calculations made of component efficiencies and operating life. The transmission efficiency was calculated to be significantly over 90% with the expected vehicle operation. A design consistent with automotive practice for low future production costs was considered, together with maintainability. The technology advancements required to develop the flat belt CVT were identified and an estimate was made of how the size of the flat belt CVT scales to larger and smaller design output torques. The suitability of the flat belt CVT for alternate application to an electric vehicle powered by an electric motor without flywheel and to a hybrid electric vehicle powered by an electric motor with an internal combustion engine was studied.

E.D.K.

N80-25661* AiResearch Mfg. Co., Torrance, Calif.

DESIGN STUDY OF TOROIDAL TRACTION CVT FOR ELECTRIC VEHICLES Final Report

A. E. Raynard, James Kraus, and Daniel D. Bell Jan. 1980 161 p refs

(Contracts DEN3-117; EC-77-A-31-1044)

(NASA-CR-159803; DOE/NASA/0117-80/1; Rept-80-16762)

Avail: NTIS HC A08/MF A01 CSCL 131

The development, evaluation, and optimization of a preliminary design concept for a continuously variable transmission (CVT) to couple the high-speed output shaft of an energy storage flywheel to the drive train of an electric vehicle is discussed. An existing computer simulation program was modified and used to compare the performance of five CVT design configurations. Based on this analysis, a dual-cavity full-toroidal drive with regenerative gearing is selected for the CVT design configuration. Three areas are identified that will require some technological development: the ratio control system, the traction fluid properties, and evaluation of the traction contact performance. Finally, the suitability of the selected CVT design concept for alternate electric and hybrid vehicle applications and alternate vehicle sizes and maximum output torques is determined. In all cases the toroidal traction drive design concept is applicable to the vehicle system. The regenerative gearing could be eliminated in the electric powered vehicle because of the reduced ratio range requirements. In other cases the CVT with regenerative gearing would meet the design requirements after appropriate adjustments in size and reduction gearing ratio.

M.G.

N80-24620* Chrysler Corp., Detroit, Mich.

BASLINE AUTOMOTIVE GAS TURBINE ENGINE DEVELOPMENT PROGRAM Final Report

C. E. Wagner, ed. and R. C. Pampreen, ed. Apr. 1979 182 p refs Sponsored by NASA

(Contracts EY-76-C-02-2749; EC-77-A-31-1040)

(NASA-CR-159670; DOE/NASA/2749-79/1-Vol-1;

COO-2749-42) Avail: NTIS HC A09/MF A01 CSCL 21A

Tests results on a baseline engine are presented to document the automotive gas turbine state-of-the-art at the start of the program. The performance characteristics of the engine and of a vehicle powered by this engine are defined. Component improvement concepts in the baseline engine were evaluated on engine dynamometer tests in the complete vehicle on a chassis dynamometer and on road tests. The concepts included advanced combustors, ceramic regenerators, an integrated control system, low cost turbine material, a continuously variable transmission, power-turbine-driven accessories, power augmentation, and linerless insulation in the engine housing.

R.E.S.

N80-24621* Chrysler Corp., Detroit, Mich.

CONCEPTUAL DESIGN STUDY OF AN IMPROVED AUTOMOTIVE GAS TURBINE POWERTRAIN Final Report

C. E. Wagner, ed. and R. C. Pampreen, ed. Jun. 1979 196 p refs

(Contracts DE-AC02-76CS-52749)

(NASA-CR-159672; DOE/NASA/2749-79/3-Vol-3;

COO-2749-40) Avail: NTIS HC A09/MF A01 CSCL 21A

Automotive gas turbine concepts with significant technological advantages over the spark ignition (SI) engine were assessed. Possible design concepts were rated with respect to fuel economy and near-term application. A program plan which outlines the development of the improved gas turbine (IGT) concept that best met the goals and objectives of the study identifies the research and development work needed to meet the goal of entering a production engineering phase by 1983. The fuel economy goal is to show at least a 20% improvement over a conventional 1976 SI engine/vehicle system. On the basis of achieving the fuel economy goal, of overall suitability to mechanical design, and of automotive mass production cost, the powertrain selected was a single-shaft engine with a radial turbine and a continuously variable transmission (CVT). Design turbine inlet temperature was 1150 C. Reflecting near-term technology, the turbine rotor would be made of an advanced superalloy, and the transmission would be a hydromechanical CVT. With successful progress in long-lead R&D in ceramic technology and the belt-drive CVT, the turbine inlet temperature would be

1350 C to achieve near-maximum fuel economy.

A.R.H.

N80-26662* Rocketdyne, Canoga Park, Calif.
SMALL, HIGH PRESSURE LIQUID HYDROGEN TURBOPUMP Final Report, 7 Jun. 1977 - 26 Oct. 1979
A. Csomor and D. J. Warren 23 May 1980 234 p refs
(Contract NAS3-21008)
(NASA-CR-159821; RI/RD79-322) Avail: NTIS
HC A11/MF A01 CSCL 13K

A high pressure, low capacity, liquid hydrogen turbopump was designed, fabricated, and tested. The design configuration of the turbopump is summarized and the results of the analytical and test efforts are presented. Approaches used to pin point the cause of poor suction performance with the original design are described and performance data are included with an axial inlet design which results in excellent suction capability. E.D.K.

N80-29707* Phillips Petroleum Co. Europe-Africa, London (England).

FIELD EXPERIENCES WITH ROTORDYNAMIC INSTABILITY IN HIGH-PERFORMANCE TURBOMACHINERY

H. E. Doyle /in NASA, Lewis Res. Center Rotordyn. Instability Probl. in High-Performance Turbomachinery 1980 p 3-13 (For primary document see N80-29706 20-37)
Avail: NTIS HC A20/MF A01 CSCL 13I

Two field situations illustrate the consequences of rotordynamic instability in centrifugal compressors. One involves the reinjection of produced gas into a North Sea oil formation for the temporary extraction of crude. The other describes on-shore compressors used to deliver natural gas from off-shore wells. The problems which developed and the remedies attempted in each case are discussed. Instability problems resulted in lost production, extended construction periods and costs, and heavy maintenance expenditures. The need for effective methods to properly identify the problem in the field and in the compressor design stage is emphasized. M.G.

N80-29706* Southwest Research Inst., San Antonio, Tex.
FIELD VERIFICATION OF LATERAL-TORSIONAL COUPLING EFFECTS ON ROTOR INSTABILITIES IN CENTRIFUGAL COMPRESSORS

J. C. Wachel and F. R. Szenasi /in NASA, Lewis Res. Center Rotordyn. Instability Probl. in High-Performance Turbomachinery 1980 p 15-34 refs (For primary document see N80-29706 20-37)

Avail: NTIS HC A20/MF A01 CSCL 13I

Lateral and torsional vibration data obtained on a centrifugal compressor train which had shaft instabilities and gear failures is examined. The field data verifies that the stability of centrifugal compressors can be adversely affected by coincidence of torsional natural frequencies with lateral instability frequencies. The data also indicates that excitation energy from gear boxes can reduce stability margins if energy is transmitted either laterally or torsionally to the compressors. The lateral and torsional coupling mechanisms of shaft systems is discussed. The coupling mechanisms in a large industrial compressor train are documented and the potential effect on rotor stability is demonstrated. Guidelines are set forth to eliminate these potential problems by minimizing the interaction of torsional and lateral responses and their effect on rotor stability. M.G.

N80-29709* Mechanical Technology, Inc., Latham, N. Y.
PRACTICAL EXPERIENCE WITH UNSTABLE COMPRESSORS

Stqan B. Malanoski /in NASA, Lewis Res. Center Rotordyn. Instability Probl. in High-Performance Turbomachinery 1980 p 35-43 refs (For primary document see N80-29706 20-37)
Avail: NTIS HC A20/MF A01

Using analytical mathematical modeling techniques for the system components, an attempt is made to gauge the destabilizing effects in a number of compressor designs. In particular the overhung (or cantilevered) compressor designs and the straddle-mounted (or simply supported) compressor designs are examined.

Recommendations are made, based on experiences with stable and unstable compressors, which can be used as guides in future designs. High and low pressure compressors which operate well above their fundamental rotor-bearing lateral natural frequencies can suffer from destructive subsynchronous vibration. Usually the elements in the system design which contribute to this vibration, other than the shafting and the bearings, are the seals (both gas labyrinth and oil breakdown bushings) and the aerodynamic components. M.G.

N80-29710* Ingersoll-Rand Co., Easton, Pa.
ANALYSIS AND IDENTIFICATION OF SUBSYNCHRONOUS VIBRATION FOR A HIGH PRESSURE PARALLEL FLOW CENTRIFUGAL COMPRESSOR

R. G. Kirk, J. C. Nicholas, G. H. Donald, and R. C. Murphy /in NASA, Lewis Res. Center Rotordyn. Instability Probl. in High-Performance Turbomachinery 1980 p 45-63 refs (For primary document see N80-29706 20-37)
Avail: NTIS HC A20/MF A01 CSCL 13I

The summary of a complete analytical design evaluation of an existing parallel flow compressor is presented and a field vibration problem that manifested itself as a subsynchronous vibration that tracked at approximately 2/3 of compressor speed is reviewed. The comparison of predicted and observed peak response speeds, frequency spectrum content, and the performance of the bearing-seal systems are presented as the events of the field problem are reviewed. Conclusions and recommendations are made as to the degree of accuracy of the analytical techniques used to evaluate the compressor design. M.G.

N80-29711* Allis-Chalmers Mfg. Co., Milwaukee, Wis.
SUBSYNCHRONOUS INSTABILITY OF A GEARED CENTRIFUGAL COMPRESSOR OF OVERHUNG DESIGN

J. H. Hudson and L. J. Wittman /in NASA, Lewis Res. Center Rotordyn. Instability Probl. in High-Performance Turbomachinery 1980 p 67-83 refs (For primary document see N80-29706 20-37)

Avail: NTIS HC A20/MF A01 CSCL 13I

The original design analysis and shop test data are presented for a three stage (poster) air compressor with impellers mounted on the extensions of a twin pinion gear, and driven by an 8000 hp synchronous motor. Also included are field test data, subsequent rotor dynamics analysis, modifications, and final rotor behavior. A subsynchronous instability existed on a geared, overhung rotor. State-of-the-art rotor dynamics analysis techniques provided a reasonable analytical model of the rotor. A bearing modification arrived at analytically eliminated the instability. M.G.

N80-29712* Bently Nevada Corp., Minden.
THE PARAMETERS AND MEASUREMENTS OF THE DESTABILIZING ACTIONS OF ROTATING MACHINES, AND THE ASSUMPTIONS OF THE 1950'S

Donald E. Bently /in NASA, Lewis Res. Center Rotordyn. Instability Probl. in High-Performance Turbomachinery 1980 p 95-106 (For primary document see N80-29706 20-37)
Avail: NTIS HC A20/MF A01 CSCL 13I

The measurability of destabilizing actions is demonstrated for a rotor built to produce a forward circular, self excited malfunction (gas whip). It is argued that the continued use of past modeling techniques is unfortunate in that it has led to the use of inappropriate words to express what is happening and a lack of full understanding of the category of forward circular whip instability mechanisms. M.G.

N80-29713* Kobe Steel Ltd. (Japan).
ASYNCHRONOUS VIBRATION PROBLEM OF CENTRIFUGAL COMPRESSOR

Takeshi Fujikawa, Naotsugi Ishiguro, and Mitsuhiro Ito /in NASA, Lewis Res. Center Rotordyn. Instability Probl. in High-Performance Turbomachinery 1980 p 109-118 refs (For primary document see N80-29706 20-37)

Avail: NTIS HC A20/MF A01 CSCL 13I

An unstable asynchronous vibration problem in a high pressure centrifugal compressor and the remedial actions against it are described. Asynchronous vibration of the compressor took place when the discharge pressure (Pd) was increased, after the rotor was already at full speed. The typical spectral data of the shaft vibration indicate that as the pressure Pd increases, pre-unstable vibration appears and becomes larger, and large unstable asynchronous vibration occurs suddenly (Pd = 5.49MPa). A computer program was used which calculated the logarithmic decrement and the damped natural frequency of the rotor bearing systems. The analysis of the log-decrement is concluded to be effective in preventing unstable vibration in both the design stage and remedial actions. M.G.

N80-29714* Louisville Univ., Ky. Mechanical Engineering Dept.

TESTING OF TURBULENT SEALS FOR ROTODYNAMIC COEFFICIENTS

Dara W. Childs, John B. Dressman and S. Bart Childs /in NASA, Lewis Res. Center Rotordyn. Instability Probl. in High-Performance Turbomachinery 1980 p 121-138 refs Prepared in cooperation with Texas A and M Univ., College Station (For primary document see N80-29706 20-37) (Grant NsG-3200)

Avail: NTIS HC A20/MF A01 CSCL 131

A test program developed for dynamic testing of straight and convergent-tapered seals, with the capability of separately determining both direct and cross-coupled stiffness, damping, and added mass coefficients is described. The test apparatus causes the seal journal to execute small-eccentricity centered circular orbits within its bearings. Dynamic measurements are made and recorded of the seal-displacement-vector components, and of the pressure field. The pressure field is integrated to yield seal reaction force components. The displacement and force vector components are analyzed via a generalized Newton-Raphson procedure to yield the desired seal dynamic coefficients. Representative test data are provided and discussed. M.G.

N80-29715* Kobe Univ. (Japan). Engineering Dept.
EVALUATION OF INSTABILITY FORCES OF LABYRINTH SEALS IN TURBINES OR COMPRESSORS

Tkuakuzo Iwatsubo /in NASA, Lewis Res. Center Rotordyn. Instability Probl. in High-Performance Turbomachinery 1980 p 139-167 refs (For primary document see N80-29706 20-37) Avail: NTIS HC A20/MF A01 CSCL 131

The effects of a force induced by the labyrinth seal on the stability of rotor systems and the factors of the seal which affect the stability are investigated. In the analysis, it is assumed that the fluid in the seal is steady and that the rotor is set vertically in order to avoid the effects of gravity force. The force induced by the seal is expressed in terms proportional to the velocity and displacement of the rotor and is deduced to that expression for the oil film force in journal bearings. That force is taken into account in the equations of motion; then the stability of the system is discussed by energy concept. The force induced by the labyrinth seal always makes the rotor system unstable, and the tendency is marked when seal leakages are small. The resonance point of the rotor system is also affected by the labyrinth seal (the resonance point of the rotor system is removed by the seal leakages). The force induced by the labyrinth seal was measured by using a water-tunnel experimental system which was designed to measure the labyrinth seal force by using the similarity between gas and liquid flow theory. M.G.

N80-29717* Stuttgart Univ. (West Germany). Institut fuer Thermische Stromungsmaschinen.

FLOW INDUCED SPRING COEFFICIENTS OF LABYRINTH SEALS FOR APPLICATION IN ROTOR DYNAMICS

H. Benckert and J. Wachter /in NASA, Lewis Res. Center Rotordyn. Instability Probl. in High-Performance Turbomachinery 1980 p 189-212 refs (For primary document see N80-29706 20-37)

Avail: NTIS HC A20/MF A01 CSCL 131

Flow induced aerodynamic spring coefficients of labyrinth seals are discussed and the restoring force in the deflection plane of the rotor and the lateral force acting perpendicularly to it are also considered. The effects of operational conditions on the spring characteristics of these components are examined, such as differential pressure, speed, inlet flow conditions, and the geometry of the labyrinth seals. Estimation formulas for the lateral forces due to shaft rotation and inlet swirl, which are developed through experiments, are presented. The utilization of the investigations is explained and results of stability calculations, especially for high pressure centrifugal compressors, are added. Suggestions are made concerning the avoidance of exciting forces in labyrinths. M.G.

N80-29718* Hitachi Ltd., Tsuchiura (Japan). Mechanical Engineering Research Lab.

HYDRAULIC FORCES CAUSED BY ANNULAR PRESSURE SEALS IN CENTRIFUGAL PUMPS

T. Iino and H. Kaneko /in NASA, Lewis Res. Center Rotordyn. Instability Probl. in High-Performance Turbomachinery 1980 p 213-225 refs (For primary document see N80-29706 20-37) Avail: NTIS HC A20/MF A01 CSCL 131

The hydraulic forces caused by annular pressure seals were investigated. The measured inlet and exit loss coefficients of the flow through the seals were much smaller than the conventional values. The results indicate that the damping coefficient and the inertia coefficient of the fluid film in the seal are not affected much by the rotational speed or the eccentricity of the rotor, though the stiffness coefficient seemed to be influenced by the eccentricity. R.C.T.

N80-29719* California Inst. of Tech., Pasadena.
A TEST PROGRAM TO MEASURE FLUID MECHANICAL WHIRL-EXCITATION FORCES IN CENTRIFUGAL PUMPS

C. E. Brennen, A. J. Acosta, and T. K. Caughey /in NASA, Lewis Res. Center Rotordyn. Instability Probl. in High-Performance Turbomachinery 1980 p 229-247 refs (For primary document see N80-29706 20-37) (Contract NAS8-33108)

Avail: NTIS HC A20/MF A01 CSCL 131

The details of a test program for the measurement of the unsteady forces on centrifugal impellers are discussed. Various hydrodynamic flows are identified as possible contributors to these destabilizing forces. R.C.T.

N80-29720* Technical Univ. of Denmark, Copenhagen.
EFFECT OF FLUID FORCES ON ROTOR STABILITY OF CENTRIFUGAL COMPRESSORS AND PUMPS

Jorgen Colding-Jorgensen /in NASA, Lewis Res. Center Rotordyn. Instability Probl. in High-Performance Turbomachinery 1980 p 249-265 refs (For primary document see N80-29706 20-37) Avail: NTIS HC A20/MF A01 CSCL 131

A simple two dimensional model for calculating the rotordynamic effects of the impeller force in centrifugal compressors and pumps is presented. It is based on potential flow theory with singularities. Equivalent stiffness and damping coefficients are calculated for a machine with a vaneless volute formed as a logarithmic spiral. It is shown that for certain operating conditions, the impeller force has a destabilizing effect on the rotor. R.C.T.

N80-29721* Cornell Univ., Ithaca, N. Y.
NON-SYNCHRONOUS WHIRLING DUE TO FLUID-DYNAMIC FORCES IN AXIAL TURBO-MACHINERY ROTORS

Shan Fu Shen and Vinod G. Mingle /in NASA, Lewis Res. Center Rotordyn. Instability Probl. in High-Performance Turbomachinery 1980 p 267-284 refs (For primary document see N80-29706 20-37)

Avail: NTIS HC A20/MF A01 CSCL 131

The role of fluid forces acting on the blades of an axial turborotor with regards to whirling was analyzed. The dynamic

equations were formulated for the coning mode of an overhung rotor. The exciting forces due to the motion were defined through a set of rotor stability derivatives, and analytical expressions of the aerodynamic contributions were found for the case of small mean stream deflection, high solidity and equivalent flat plate cascade. For a typical case, only backward whirl was indicated when the phase shifting of the rotor wake effect was ignored. A parametric study of the dynamic stability boundary reveals that a reduction in blade stagger angle, mass flow rate, fluid density and an increase in stiffness and external damping are all conducive for improved stability. R.C.T.

N80-29722*# Turbo Research, Inc., Lionville, Pa.
VIBRATION EXCITING MECHANISMS INDUCED BY FLOW IN TURBOMACHINE STAGES

William E. Thompson /in NASA. Lewis Res. Center Rotordyn. Instability Probl. in High-Performance Turbomachinery 1980 p 285-302 refs (For primary document see N80-29706 20-37)
 Avail: NTIS HC A20/MF A01 CSCL 131

The quasisteady computer analysis of the perturbed centrifugal impeller passage flow was reviewed. A total of 115 stage calculations were used to define the fluid damping coefficient, delta sub fluid. Results indicate that the average total damping coefficient per stage needed for stability is delta sub total > 1.85. R.C.T.

N80-29723*# Technische Universitaet, Munich (West Germany).
 Institut fuer Thermische Kraftanlagen.

SELF-EXCITED ROTOR WHIRL DUE TO TIP-SEAL LEAKAGE FORCES

B. Leie and H.-J. Thomas /in NASA. Lewis Res. Center Rotordyn. Instability Probl. in High-Performance Turbomachinery 1980 p 303-316 refs (For primary document see N80-29706 20-37)
 Avail: NTIS HC A20/MF A01 CSCL 131

The limitations in the performance of turbomachines which arise as a result of self-excited vibration were investigated. Bearing forces, elastic hysteresis, and forces from fluid flow through clearances were considered as possible origins. A theoretical evaluation was made to determine the dependence of the forces from the leakage losses and from rotating flow in radial gaps. R.C.T.

N80-29724*# Tokyo Univ. (Japan).
FLUID FORCES ON ROTATING CENTRIFUGAL IMPELLER WITH WHIRLING MOTION

Hideobu Shoji and Hideo Ohashi /in NASA. Lewis Res. Center Rotordyn. Instability Probl. in High-Performance Turbomachinery 1980 p 317-328 refs Sponsored in part by the Japanese Ministry of Education and by Hitachi Ltd. (For primary document see N80-29706 20-37)

Avail: NTIS HC A20/MF A01 CSCL 131

Fluid forces on a centrifugal impeller, whose rotating axis whirls with a constant speed, were calculated by using unsteady potential theory. Calculations were performed for various values of whirl speed, number of impeller blades and angle of blades. Specific examples as well as significant results are given. R.C.T.

N80-29725*# Heriott-Watt Univ., Edinburgh (Scotland),
 Mechanical Engineering Dept.

LIMIT CYCLES OF A FLEXIBLE SHAFT WITH HYDRODYNAMIC JOURNAL BEARINGS IN UNSTABLE REGIMES

R. David Brown and Henry F. Black /in NASA. Lewis Res. Center Rotordyn. Instability Probl. in High-Performance Turbomachinery 1980 p 331-343 refs (For primary document see N80-29706 20-37)

Avail: NTIS HC A20/MF A01 CSCL 131

A symmetric 3 mass rotor supported on hydrodynamic bearings is described. An approximate method of representing finite bearings is used to calculate bearing forces. As the method sums forces from a number of independent circular lobes lemon 3 and 4 lobe bearings are taken into account. The calculations are based on an axial groove bearing. Linear analysis precedes nonlinear simulation of some unstable conditions. The demonstra-

tion of small limit cycles suggests that necessarily flexible rotors e.g., helicopter tail rotors, may be practical without either tilt pad bearings or external dampers. R.C.T.

N80-29726*# Sussex Univ., Brighton (England). School of
 Engineering and Applied Sciences.

ON THE ROLE OF OIL-FILM BEARINGS IN PROMOTING SHAFT INSTABILITY: SOME EXPERIMENTAL OBSERVATIONS

R. Holmes /in NASA. Lewis Res. Center Rotordyn. Instability Probl. in High-Performance Turbomachinery 1980 p 345-357 refs (For primary document see N80-29706 20-37)
 Avail: NTIS HC A20/MF A01 CSCL 131

The occurrence of oil whirl instability in rigid and flexible rotor systems was investigated. The effect of various bearing parameters on the oil whirl frequency and amplitude of rigid and flexible shafts supported on fluid film bearings was also studied. R.C.T.

N80-29727*# Texas A&M Univ., College Station, Dept. of
 Mechanical Engineering.

EXPERIMENTAL RESULTS CONCERNING CENTRIFUGAL IMPELLER EXCITATIONS

J. M. Vance and F. J. Landadio /in NASA. Lewis Res. Center Rotordyn. Instability Probl. in High-Performance Turbomachinery 1980 p 361-367 refs (For primary document see N80-29706 20-37)

Avail: NTIS HC A20/MF A01 CSCL 131

The effect of working fluid on the dynamics of an impeller with radial vanes was investigated. The impeller was supported vertically from a very flexible quill shaft in order to produce a low critical speed, and to allow the fluid dynamic effects on the impeller to predominate. The shaft was supported from ball bearings, so that there was no possibility of oil whip from fluid film bearings as a destabilizing influence. The impeller was run both in the atmosphere, and submerged in working fluids contained in a cylindrical housing, open at the top. Variable speed was obtained with a dc gearmotor drive unit. The speed was measured with a proximity probe pulse tachometer and electronic digital counter. R.C.T.

N80-29728*# Massachusetts Inst. of Tech., Cambridge.
PHYSICAL EXPLANATIONS OF THE DESTABILIZING EFFECT OF DAMPING IN ROTATING PARTS

Stephen H. Crandall /in NASA. Lewis Res. Center Rotordyn. Instability Probl. in High-Performance Turbomachinery 1980 p 369-382 refs (For primary document see N80-29706 20-37)
 Avail: NTIS HC A20/MF A01 CSCL 131

The destabilizing effect of rotating damping was investigated. When the rotation was faster than the whirl, rotating damping drags the orbiting particle forward. When stationary damping was also present, the stability borderline was readily determined by balancing the backward and forward drags. A key notion was that a forward whirl at rate omega a sub n with respect to stationary axes appears to be a backward whirl at rate Omega - omega a sub n with respect to a system rotating supercritically at rate Omega. The growth rate of unstable whirls (or the decay rate of stable whirls) was readily estimated by a simple energy balance. R.C.T.

N80-29729*# Politechnika Lodzka (Poland).
PARAMETRIC INSTABILITIES OF ROTOR-SUPPORT SYSTEMS WITH APPLICATION TO INDUSTRIAL VENTILATORS

Zdzisław Parszewski, Tanusz Krodkiemski, and Krzysztof Marynowski /in NASA. Lewis Res. Center Rotordyn. Instability Probl. in High-Performance Turbomachinery 1980 p 383-400 refs (For primary document see N80-29706 20-37)
 Avail: NTIS HC A20/MF A01 CSCL 131

Rotor support systems interaction with parametric excitation is considered for both unequal principal shaft stiffness (generators) and offset disc rotors (ventilators). Instability regions and types of instability are computed in the first case, and parametric

resonances in the second case. Computed and experimental results are compared for laboratory machine models. A field case study of parametric vibrations in industrial ventilators is reported. Computed parametric resonances are confirmed in field measurements, and some industrial failures are explained. Also the dynamic influence and gyroscopic effect of supporting structures are shown and computed. R.C.T.

N80-29730* Virginia Univ., Charlottesville. Dept. of Mechanical and Aerospace Engineering.
INSTABILITY THRESHOLDS FOR FLEXIBLE ROTORS IN HYDRODYNAMIC BEARINGS

Paul E. Allaire and Ronald D. Flack /in NASA. Lewis Res. Center Rotordyn. Instability Probl. in High-Performance Turbomachinery 1980 p 403-427 refs (For primary document see N80-29706 20-37)

(Grant NsG-3177; Contract DE-AC01-79ET-13151; Grant RC-A-77-6C)

Avail: NTIS HC A20/MF A01 CSCL 131

Two types of fixed pad hydrodynamic bearings (multilobe and pressure dam) were considered. Optimum and nonoptimum geometric configurations were tested. The optimum geometric configurations were determined by using a theoretical analysis and then the bearings were constructed for a flexible rotor test rig. It was found that optimizing bearings using this technique produces a 100% or greater increase in rotor stability. It is shown that this increase in rotor stability is carried out in the absence of certain types of instability mechanisms such as aerodynamic crosscoupling. However, the increase in rotor stability should greatly improve rotating machinery performance in the presence of such forces as well. R.C.T.

N80-29731* Virginia Univ., Charlottesville. Dept. of Mechanical and Aerospace Engineering.
STABILIZATION OF AERODYNAMICALLY EXCITED TURBOMACHINERY WITH HYDRODYNAMIC JOURNAL BEARINGS AND SUPPORTS

Lloyd E. Barrett and Edgar J. Gunter /in NASA. Lewis Res. Center Rotordyn. Instability Probl. in High-Performance Turbomachinery 1980 p 429-452 refs (For primary document see N80-29706 20-37)

(Grant NsG-3105; Contracts DAAG29-77-C-0009; EF-76-S-01-2479)

Avail: NTIS HC A20/MF A01 CSCL 131

A method of analyzing the first mode stability and unbalance response of multimass flexible rotors is presented whereby the multimass system is modeled as an equivalent single mass modal model including the effects of rotor flexibility, general linearized hydrodynamic journal bearings, squeeze film bearing supports and rotor aerodynamic cross coupling. Expressions for optimum bearing and support damping are presented for both stability and unbalance response. The method is intended to be used as a preliminary design tool to quickly ascertain the effects of bearing and support changes on rotor-bearing system performance. R.C.T.

N80-29732* Mechanical Technology, Inc., Latham, N. Y.
USE OF ELASTOMERIC ELEMENTS IN CONTROL OF ROTOR INSTABILITY

Anthony J. Smalley /in NASA. Lewis Res. Center Rotordyn. Instability Probl. in High-Performance Turbomachinery 1980 p 453-465 refs (For primary document see N80-29706 20-37)

Avail: NTIS HC A20/MF A01 CSCL 131

The dynamic characteristics of elastomeric supports are discussed. Stiffness and damping characteristics for elastomers of various geometries including O-rings, buttons loaded in compression, and rectangular elements loaded in shear are presented. The effects of frequency, temperature, and amplitude are illustrated, as well as the effects of material and geometry. Empirical design methods are illustrated, and several examples are presented where elastomers have successfully controlled both synchronous and nonsynchronous vibrations. R.C.T.

N80-29733* Virginia Univ., Charlottesville.
FEASIBILITY OF ACTIVE FEEDBACK CONTROL OF ROTORDYNAMIC INSTABILITY

James W. Moore, David W. Lewis, and John Heinzman /in NASA. Lewis Res. Center Rotordyn. Instability Probl. in High-Performance Turbomachinery 1980 p 467-476 (For primary document see N80-29706 20-37)

(Contract DE-AC01-79ET-13151)

Avail: NTIS HC A20/MF A01 CSCL 131

Some of the considerations involved in the use of feedback control as a means of eliminating or alleviating rotordynamic instability are discussed. A simple model of a mass on a flexible shaft is used to illustrate the application of feedback control concepts. R.C.T.

N80-31795* Eaton Corp., Southfield, Mich. Engineering and Research Center.
SMALL PASSENGER CAR TRANSMISSION TEST; FORD C4 TRANSMISSION Final Report

M. P. Bujold Jun. 1980 383 p

(Contracts DEN3-124; EC-77-A-31-1044)

(NASA-CR-159881; ERC-LIB-8060; DOE/NASA/O124-2) Avail:

NTIS HC A17/MF A01 CSCL 131

A 1979 Ford C4 automatic transmission was tested per a passenger car automatic transmission test code (SAE J651b) which required drive performance, coast performance, and no load test conditions. Under these test conditions, the transmission attained maximum efficiencies in the mid-eighty percent range for both drive performance tests and coast performance tests. The major results of this test (torque, speed, and efficiency curves) are presented. Graphs map the complete performance characteristics for the Ford C4 transmission. A.R.H.

N80-31796* Eaton Corp., Southfield, Mich. Engineering and Research Center.
SMALL PASSENGER CAR TRANSMISSION TEST; CHEVROLET LUV TRANSMISSION Final Report

M. P. Bujold Jun. 1980 428 p

(Contract DEN3-124; EC-77-A-31-1044)

(NASA-CR-159882; ERC-LIB-80121; DOE/NASA/O124-3)

Avail: NTIS HC A19/MF A01 CSCL 131

A 1978 Chevrolet LUV manual transmission tested per the applicable portions of a passenger car automatic transmission test code (SAE J651b) which required drive performance, coast performance, and no load test conditions. Under these test conditions, the transmission attained maximum efficiencies in the upper ninety percent range for both drive performance tests and coast performance tests. The major results of this test (torque, speed, and efficiency curves) are presented. Graphs map the complete performance characteristics for the Chevrolet LUV transmission. A.R.H.

N80-32718* Mechanical Technology, Inc., Latham, N. Y.
DEVELOPMENT OF PROCEDURES FOR CALCULATING STIFFNESS AND DAMPING OF ELASTOMERS IN ENGINEERING APPLICATIONS, PART 7

A. Rieger and E. Zorzi Sep. 1980 85 p refs

(Contract NAS3-21623)

(NASA-CR-165138; Rept-80TR63)

Avail: NTIS

HC A05/MF A01 CSCL 131

An elastomer shear damper was designed, tested, and compared with the performance of the T 55 power turbine supported on the production engine roller bearing support. The Viton 70 shear damper was designed so that the elastomer damper could be interchanged with the production T 55 power turbine roller bearing support. The results show that the elastomer shear dampener permitted stable operation of the power turbine to the maximum operating speed of 16,000 rpm. Author

N80-32719* Chrysler Corp., Detroit, Mich.
UPGRADED AUTOMOTIVE GAS TURBINE ENGINE DESIGN AND DEVELOPMENT PROGRAM, VOLUME 2 Final Report

C. E. Wagner, ed. and R. C. Pamphreen, ed. Jun. 1979 348 p

refs Sponsored by NASA
(Contracts EY-76-C-02-2749; EC-77-A-31-1040)
(NASA-CR-159671; DOE/NASA/2749-79/2-Vol-2;
COO-2749-43-Vol-2) Avail: NTIS HC A15/MF A01 CSCL
131

Results are presented for the design and development of an upgraded engine. The design incorporated technology advancements which resulted from development testing on the Baseline Engine. The final engine performance with all retro-fitted components from the development program showed a value of 91 HP at design speed in contrast to the design value of 104 HP. The design speed SFC was 0.53 versus the goal value of 0.44. The miss in power was primarily due to missing the efficiency targets of small size turbomachinery. Most of the SFC deficit was attributed to missed goals in the heat recovery system relative to regenerator effectiveness and expected values of heat loss. Vehicular fuel consumption, as measured on a chassis dynamometer, for a vehicle inertia weight of 3500 lbs., was 15 MPG for combined urban and highway driving cycles. The baseline engine achieved 8 MPG with a 4500 lb. vehicle. Even though the goal of 18.3 MPG was not achieved with the upgraded engine, there was an improvement in fuel economy of 46% over the baseline engine, for comparable vehicle inertia weight.

Author

N80-32720* # Rochester Inst. of Tech., N. Y.
**DEVELOPMENT OF FLEXIBLE ROTOR BALANCING
CRITERIA Final Report**
Wayne W. Walter and Neville F. Rieger Mar. 1979 115 p
refs
(Grant NsG-3072)
(NASA-CR-159506) Avail: NTIS HC A06/MF A01 CSCL
131

Several studies in which analytical procedures were used to obtain balancing criteria for flexible rotors are described. General response data for a uniform rotor in damped flexible supports were first obtained for plain cylindrical bearings, tilting pad bearings, axial groove bearings, and partial arc bearings. These data formed the basis for the flexible rotor balance criteria presented. A procedure by which a practical rotor in bearings could be reduced to an equivalent uniform rotor was developed and tested. It was found that the equivalent rotor response always exceeded to practical rotor response by more than sixty percent for the cases tested. The equivalent rotor procedure was then tested against six practical rotor configurations for which data was available. It was found that the equivalent rotor method offered a procedure by which balance criteria could be selected for practical flexible rotors, using the charts given for the uniform rotor.

A.R.H.

A80-14739 * # Phase change in liquid face seals. II - Isothermal and adiabatic bounds with real fluids. W. F. Hughes and N. H. Chao (Carnegie-Mellon University, Pittsburgh, Pa.). *American Society of Mechanical Engineers and American Society of Lubrication Engineers, Lubrication Conference, Dayton, Ohio, Oct. 16-18, 1979, ASME Paper 79-Lub-4*, 8 p. Members, \$1.50; nonmembers, \$3.00. Grant No. NsG-3023.

Analytical studies of phase change effects in parallel and tapered liquid face seals are presented. An isothermal and adiabatic model of low Reynolds number flow are considered by numerical integration of the descriptive equations for a real fluid, and its thermodynamic properties are calculated for each step, using a computer program for the steam tables or fluid thermodynamic properties. It was shown that for low leakage rate the isothermal model is more accurate and for high leakage rates the adiabatic model is more accurate; that both models yield the same conclusions regarding stability; and that the transient of collapse is described by the adiabatic model which predicts a catastrophic collapse and then either failure or explosive return to a larger film thickness value. Finally, it is shown that converging seals may become unstable and the mass leakage rate is reduced significantly below the all liquid value when boiling occurs.

A.T.

A80-14760 * # Load support system analysis high speed input pinion configuration. S. S. Gassel and J. Pirvics (SKF Industries, Inc., King of Prussia, Pa.). *American Society of Mechanical Engineers and American Society of Lubrication Engineers, Lubrication Conference, Dayton, Ohio, Oct. 16-18, 1979, ASME Paper 79-Lub-34*, 10 p. 15 refs. Members \$1.50; nonmembers, \$3.00. Contract No. NAS3-20839.

An analysis and a series of computerized calculations were carried out to explore competing prototype design concepts of a shaft and two taper-roller bearings systems to support the high-speed input pinion of an advanced commercial helicopter transmission. The results were used to evaluate designs both for a straddle arrangement where the pinion gear is located between the bearings and for a cantilever arrangement where the pinion is outboard of the two bearings. Effects of varying parameters including applied gear load, preload, wall thickness, interference fits, bearing spacing and pinion gear location on system rigidity, load distribution and bearing rating life were assessed. A comparison of the bearing load distributions for these designs demonstrated that the straddle more equally distributes both radial and axial loads. The performance of these designs over a range of shaft rotational speeds, with lubrication and friction effects included, is also discussed.

S.D.

A80-14761 * # High speed cylindrical rolling element bearing analysis 'CYBEAN' - Analytic formulation. R. J. Kleckner, J. Pirvics (SKF Industries, Inc., King of Prussia, Pa.), and V. Castelli (Xerox Corp., El Segundo, Calif.). *American Society of Mechanical Engineers and American Society of Lubrication Engineers, Lubrication Conference, Dayton, Ohio, Oct. 16-18, 1979, ASME Paper 79-Lub-35*, 9 p. 24 refs. Members, \$1.50; nonmembers, \$3.00. Contract No. NAS3-20068.

This paper documents the analytic foundation and software architecture for the computerized mathematical simulation of high speed cylindrical rolling element bearing behavior. The software, CYBEAN (CYlindrical BEaring ANalysis), considers a flexible, variable geometry outer ring, EHD films, roller centrifugal and quasidynamic loads, roller tilt and skew, mounting fits, cage and flange interactions. The representation includes both steady state and time transient simulation of thermal interactions internal to and coupled with the surroundings of the bearing. A sample problem illustrating program use is presented.

(Author)

A80-35574 * # Advanced Gas Turbine Powertrain System Development Project. H. E. Helms (General Motors Corp., Detroit Diesel Allison Div., Detroit, Mich.). *U.S. Department of Energy and NASA, International Automotive Propulsion Systems Symposium, 5th, Dearborn, Mich., Apr. 14-18, 1980, Paper*, 27 p. Contract No. DEN3-168.

A progress report on the Advanced Gas Turbine Powertrain System Development Project being performed under contract from NASA Lewis is presented. The goals and objectives of the project are described noting that funds from the DOE, Office of Transportation Programs are used to sponsor the project. Among the demonstration objectives are attaining a fuel economy of 42.5 miles per gallon in a 1985 Pontiac Phoenix, multifuel capability, and emission levels within the federal standards. Design objectives examined include competitive reliability and life as well as competitive initial and life cycle costs. Finally, it is stressed that high risk and key elements in this advanced powertrain project are the development of ceramic turbine engine components and the aerodynamic development of small size turbine components.

M.E.P.

38 QUALITY ASSURANCE AND RELIABILITY

Includes product sampling procedures and techniques, and quality control.

N80-15422* National Aeronautics and Space Administration, Lewis Research Center, Cleveland, Ohio.
PHOTOVOLTAIC POWER SYSTEM RELIABILITY CONSIDERATIONS

Vincent R Lalli 1980 9 p refs Presented at the Ann. Reliability and Maintainability Symp., San Francisco, 22-24 Jan. 1980 (Contract DE-AB29-76EI-20370) (NASA-TM-79291, DOE/NASA/20370-79/19; E-235) Avail NTIS HC A02/MF A01 CSCL 14D

An example of how modern engineering and safety techniques can be used to assure the reliable and safe operation of photovoltaic power systems is presented. This particular application is for a solar cell power system demonstration project designed to provide electric power requirements for remote villages. The techniques utilized involve a definition of the power system natural and operating environment, use of design criteria and analysis techniques, an awareness of potential problems via the inherent reliability and FMEA methods, and use of fail-safe and planned spare parts engineering philosophy. J.M.S

N80-22714* National Aeronautics and Space Administration, Lewis Research Center, Cleveland, Ohio.
SIMULATION OF TRANSDUCER-COUPPLANT EFFECTS ON BROADBAND ULTRASONIC SIGNALS

Alex Vary 1980 36 p refs Presented at Spring Meeting of the Am. Soc of Nondestructive Testing, Philadelphia, 24-27 Mar. 1980 (NASA-TM-81489; E-427) Avail: NTIS HC A03/MF A01 CSCL 14D

The increasing use of broadband, pulse-echo ultrasonics in nondestructive evaluation of flaws and material properties has generated a need for improved understanding of the way signals are modified by coupled and bonded thin-layer interfaces associated with transducers. This understanding is most important when using frequency spectrum analyses for characterizing material properties. In this type of application, signals emanating from material specimens can be strongly influenced by couplant and bond-layers in the acoustic path. Computer synthesized waveforms were used to simulate a range of interface conditions encountered in ultrasonic transducer systems operating in the 20 to 80 MHz regime. The adverse effects of thin-layer multiple reflections associated with various acoustic impedance conditions are demonstrated. The information presented is relevant to ultrasonic transducer design, specimen preparation, and couplant selection. Author

N80-24634* National Aeronautics and Space Administration, Lewis Research Center, Cleveland, Ohio.
CONCEPTS AND TECHNIQUES FOR ULTRASONIC EVALUATION OF MATERIAL MECHANICAL PROPERTIES
Alex Vary 1980 21 p refs To be presented at the Conf. on Mech. of Nondestructive Testing, Blacksburg, Va., 10-12 Sep. 1980 (NASA-TM-81523; E-467) Avail: NTIS HC A02/MF A01 CSCL 14D

Ultrasonic methods that can be used for material strength are reviewed. Emergency technology involving advanced ultrasonic techniques and associated measurements is described. It is shown that ultrasonic NDE is particularly useful in this area because it involves mechanical elastic waves that are strongly modulated by morphological factors that govern mechanical strength and also dynamic failure modes. These aspects of ultrasonic NDE are described in conjunction with advanced approaches and theoretical concepts for signal acquisition and analysis for materials characterization. It is emphasized that the technology is in its infancy and that much effort is still required before the techniques

and concepts can be transferred from laboratory to field conditions. A.R.H.

N80-26682* National Aeronautics and Space Administration, Lewis Research Center, Cleveland, Ohio.
QUANTITATIVE ULTRASONIC EVALUATION OF ENGINEERING PROPERTIES IN METALS, COMPOSITES AND CERAMICS

Alex Vary 1980 18 p refs Presented at First Seminar on Advanced Ultrasonic Tech., Longueuil, Quebec, 9-10 Jun. 1980; sponsored by National Research Council of Canada (NASA-TM-81530; E-482) Avail: NTIS HC A02/MF A01 CSCL 14D

Ultrasonic technology from the perspective of nondestructive evaluation approaches to material strength prediction and property verification is reviewed. Emergent advanced technology involving quantitative ultrasonic techniques for materials characterization is described. Ultrasonic methods are particularly useful in this area because they involve mechanical elastic waves that are strongly modulated by the same morphological factors that govern mechanical strength and dynamic failure processes. It is emphasized that the technology is in its infancy and that much effort is still required before all the available techniques can be transferred from laboratory to industrial environments. E.D.K.

A80-51575 * Concepts and techniques for ultrasonic evaluation of material mechanical properties. A. Vary (NASA, Lewis Research Center, Cleveland, Ohio). *Virginia Polytechnic Institute and State University, Conference on Mechanics of Nondestructive Testing, Virginia Polytechnic Institute and State University, Blacksburg, Va., Sept. 10-12, 1980, Paper*. 19 p. 37 refs.

The ultrasonic nondestructive evaluation techniques discussed in the present paper indicate potentials for material characterization and property prediction. Stress wave interaction and material transfer function concepts are examined as a basis for explaining correlations between material mechanical behavior and ultrasonically measured quantities. It is observed that the effect and criticality of any discrete flaw, such as crack, inclusion, or any other stress raiser, is definable only in terms of its material microstructural environment. This underscores the importance of ultrasonic techniques capable of characterizing the stress wave energy transfer properties of a material. V.P.

A80-39641 * Quantitative ultrasonic evaluation of engineering properties in metals, composites, and ceramics. A. Vary (NASA, Lewis Research Center, Cleveland, Ohio). *National Research Council of Canada, Seminar on Advanced Ultrasonic Technology, 1st, Longueuil, Quebec, Canada, June 9, 10, 1980, Paper*. 16 p. 84 refs.

Ultrasonic techniques that have demonstrated potential for material characterization are reviewed. These techniques rely on physical acoustic properties of materials and the interaction of elastic stress waves with morphological factors in the ultrasonic regime. The speed of wave propagation and energy loss by interaction with material microstructure and geometrical factors underlie ultrasonic determination of material properties. Two categories of ultrasonic measurements are discussed: those related to material strengths (e.g., elastic moduli, tensile strength, and fracture toughness) and those related to morphology and material conditions that govern strength and performance (e.g., microstructure, void content, residual stress, fatigue damage). It is shown that large-scale industrial application of ultrasonic NDE will depend on advancement in such areas as theory development, instrumentation, system automation, standardization, and coordination with design. V.L.

N80-13503 Syracuse Univ., N. Y.
MODELLING OF CRACK TIP DEFORMATION WITH FINITE ELEMENT METHOD AND ITS APPLICATIONS Ph.D. Thesis
Chuang-Yeh Yang 1979 125 p
Avail: Univ. Microfilms Order No. 7925610
A finite element computer program using the initial stress

approach of elastic-plastic analysis was developed. Crack closure stresses were calculated for three different models. It was concluded that (1) the closure stress is highest in the strip necking model, lowest in the plane strain model, and intermediate in the plane stress model, and (2) the crack closure stress decreases if the separation occurs before the stress reaches the maximum value. Nonpropagating fatigue cracks in the two phase martensitic-ferritic steels were also investigated. Unzipping increments were calculated for different crack lengths. At a prescribed stress intensity level, the shorter the crack length, the greater the unzipping increment is. This means that the shorter crack will grow faster than the longer one if both are subjected to the same K-level.

Dissert. Abstr.

39 STRUCTURAL MECHANICS

Includes structural element design and weight analysis, fatigue, and thermal stress

For applications see 05 Aircraft Design, Testing and Performance and 18 Spacecraft Design, Testing and Performance.

N80-13513* National Aeronautics and Space Administration, Lewis Research Center, Cleveland, Ohio.

COMPARISON TESTS AND EXPERIMENTAL COMPLIANCE CALIBRATION OF THE PROPOSED STANDARD ROUND COMPACT PLANE STRAIN FRACTURE TOUGHNESS SPECIMEN

D. M. Fisher and R. J. Buzzard. Nov. 1979. 21 p. refs. (NASA-TM-81379; E-284) Avail: NTIS HC A02/MF A01 CSCL 20K

Standard round specimen fracture test results compared satisfactorily with results from standard rectangular compact specimens machined from the same material. The location of the loading pin holes was found to provide adequate strength in the load bearing region for plane strain fracture toughness testing. Excellent agreement was found between the stress intensity coefficient values obtained from compliance measurements and the analytic solution proposed for inclusion in the standard test method. Load displacement measurements were made using long armed displacement gages and hollow loading cylinders. Gage points registered on the loading hole surfaces through small holes in the walls of the loading cylinders. Author

N80-15428* National Aeronautics and Space Administration, Lewis Research Center, Cleveland, Ohio.

A RELATION BETWEEN SEMIEMPIRICAL FRACTURE ANALYSES AND R-CURVES

Thomas W. Orange. Jan. 1980. 45 p. refs. (NASA-TP-1600; E-9963) Avail: NTIS HC A03/MF A01 CSCL 20K

The relations between several semiempirical fracture analyses (SEFA) and the R-curve concept of fracture mechanics are examined and the conditions for equivalence between a SEFA and an R-curve are derived. A hypothetical material is employed to study the relation analytically. Equivalent R-curves are developed for several real materials using data from the literature. For each SEFA there is an equivalent R-curve whose magnitude and shape are determined by the SEFA formulation and its empirical parameters. If the R-curve is indeed unique, then the various empirical parameters cannot be constant, and vice versa. However, for one SEFA the differences are small enough that they may be within the range of normal data scatter for real materials. Author

N80-22734* National Aeronautics and Space Administration, Lewis Research Center, Cleveland, Ohio.

NONLINEAR, THREE-DIMENSIONAL FINITE-ELEMENT ANALYSIS OF AIR-COOLED GAS TURBINE BLADES

Albert Kaufman and Raymond E. Gaugler. Apr. 1980. 22 p. refs. (NASA-TP-1669; E-074) Avail: NTIS HC A02/MF A01 CSCL 21E

Cyclic stress-strain states in cooled turbine blades were calculated for a simulated mission of an advanced-technology commercial aircraft engine. The MARC, nonlinear, finite-element computer program was used for the analysis of impingement-cooled airfoils, with and without leading-edge film cooling. Creep was the predominant damage mode (ignoring hot corrosion), particularly around film-cooling holes. Radially angled holes exhibited less creep than holes with axes normal to the surface. Beam-theory analyses of all-impingement-cooled airfoils gave fair agreement with MARC results for initial creep. Author

N80-23678* National Aeronautics and Space Administration, Lewis Research Center, Cleveland, Ohio.

STATUS OF NASA FULL-SCALE ENGINE AEROELASTICITY RESEARCH

Joseph F. Lubomski. 1980. 21 p. refs. Presented at the 21st Struct., Structural Dyn., and Mater. Conf., Seattle, 12-14 May 1980, sponsored by AIAA, ASME, ASCE and AHS (NASA-TM-81500; E-437) Avail: NTIS HC A02/MF A01 CSCL 20K

Data relevant to several types of aeroelastic instabilities were obtained using several types of turbojet and turbofan engines. In particular, data relative to separated flow (stall) flutter, choke flutter, and system mode instabilities are presented. The unique characteristics of these instabilities are discussed, and a number of correlations are presented that help identify the nature of the phenomena. R.E.S.

N80-23684* National Aeronautics and Space Administration, Lewis Research Center, Cleveland, Ohio.

PRACTICAL IMPLEMENTATION OF THE DOUBLE LINEAR DAMAGE RULE AND DAMAGE CURVE APPROACH FOR TREATING CUMULATIVE FATIGUE DAMAGE

S. S. Manson (Case Western Reserve Univ) and G. R. Halford. Apr. 1980. 50 p. refs. (NASA-TM-81517; E-387) Avail: NTIS HC A03/MF A01 CSCL 20K

Simple procedures are presented for treating cumulative fatigue damage under complex loading history using either the damage curve concept or the double linear damage rule. A single equation is provided for use with the damage curve approach; each loading event providing a fraction of damage until failure is presumed to occur when the damage sum becomes unity. For the double linear damage rule, analytical expressions are provided for determining the two phases of life. The procedure involves two steps, each similar to the conventional application of the commonly used linear damage rule. When the sum of cycle ratios based on phase 1 lives reaches unity, phase 1 is presumed complete, and further loadings are summed as cycle ratios on phase 2 lives. When the phase 2 sum reaches unity, failure is presumed to occur. No other physical properties or material constants than those normally used in a conventional linear damage rule analysis are required for application of either of the two cumulative damage methods described. Illustrations and comparisons of both methods are discussed. Author

N80-27719* National Aeronautics and Space Administration, Lewis Research Center, Cleveland, Ohio.

COMPARISON OF ELASTIC AND ELASTIC-PLASTIC STRUCTURAL ANALYSES FOR COOLED TURBINE BLADE AIRFOILS

Albert Kaufman. Jul. 1980. 15 p. refs. (NASA-TP-1679; E-241) Avail: NTIS HC A02/MF A01 CSCL 20K

Elastic plastic stress strain states in cooled turbine blade airfoils were calculated by three methods for the initial takeoff transient of an advanced technology aircraft engine. The three analytical methods compared were a three dimensional elastic plastic, finite element analysis, a three dimensional, elastic, finite element analysis, and a one dimensional, elastic plastic, beam theory analysis. Structural analyses were performed for eight cases involving different combinations of mechanical and thermal loading on impingement cooled airfoils with and without leading edge film cooling holes. The von Mises effective total strains at maximum takeoff computed from the elastic and elastic plastic finite element analyses agreed with 9 percent for rotating airfoils and 28 percent for stationary airfoils with the elastic results on the conservative side. Author

N80-32753* National Aeronautics and Space Administration, Lewis Research Center, Cleveland, Ohio.

THE METHOD OF LINES IN THREE DIMENSIONAL FRACTURE MECHANICS

John Gyekenyesi and Laszlo Berke. Washington 1980. 19 p. refs. Presented at the Intern. Symp. on Absorbed Specific Energy and/or Strain Energy Density Criterion, Budapest, 17-19 Sep.

1980, sponsored by Lehigh Univ and the Hungarian Acad of Sci (NASA-TM-81593, E-576) Avail NTIS HC A02/MF A01 CSCL 20K

A review of recent developments in the calculation of design parameters for fracture mechanics by the method of lines (MOL) is presented. Three dimensional elastic and elasto-plastic formulations are examined and results from previous and current research activities are reported. The application of MOL to the appropriate partial differential equations of equilibrium leads to coupled sets of simultaneous ordinary differential equations. Solutions of these equations are obtained by the Peano-Baker and by the recurrence relations methods. The advantages and limitations of both solution methods from the computational standpoint are summarized. R.K.G.

A80-10832 * Simple spline-function equations for fracture mechanics calculations. T. W. Orange (NASA, Lewis Research Center, Cleveland, Ohio). *International Journal of Fracture*, vol. 15, Oct. 1979, p. R161-R163, 8 refs.

The paper presents simple spline-function equations for fracture mechanics calculations. A spline function is a sequence of piecewise polynomials of degree n greater than 1 whose coefficients are such that the function and its first $n-1$ derivatives are continuous. Second-degree spline equations are presented for the compact, three point bend, and crack-line wedge-loaded specimens. Some expressions can be used directly, so that for a cyclic crack propagation test using a compact specimen, the equation given allows the cracklength to be calculated from the slope of the load-displacement curve. For an R-curve test, equations allow the crack length and stress intensity factor to be calculated from the displacement and the displacement ratio. A.T.

A80-20149 * Buckling of rotating beams. W. F. White, Jr. (U.S. Army, Structures Laboratory, Hampton, Va.), R. G. Kvaternik (NASA, Langley Research Center, Hampton, Va.), and K. R. V. Kaza (NASA, Lewis Research Center, Cleveland; Toledo, University, Toledo, Ohio). *International Journal of Mechanical Sciences*, vol. 21, no. 12, 1979, p. 739-745, 12 refs.

The stability of a beam subjected to compressive centrifugal forces arising from steady rotation about an axis which does not pass through the clamped end of the beam is analyzed to determine the critical rotational speeds for buckling in the inplane and out-of-plane directions. The differential equations of motion are solved numerically using an integrating matrix method in combination with an eigenanalysis to determine the eigenvalues from which stability is assessed. The results clarify several differences which have been identified in the literature relating to the proper behavior of the critical rotational speed for buckling as the radius of rotation of the clamped end of the beam is reduced. (Author)

A80-27958 * Strainrange partitioning life predictions of the long time Metal Properties Council creep-fatigue tests. J. F. Saltzman and G. R. Halford (NASA, Lewis Research Center, Cleveland, Ohio). In: *Methods for predicting material life in fatigue; Proceedings of the Winter Annual Meeting, New York, N.Y., December 2-7, 1979*. (A80-27951 10-39) New York, American Society of Mechanical Engineers, 1979, p. 101-132, 23 refs.

The method of Strainrange Partitioning is used to predict the cyclic lives of the Metal Properties Council's long time creep-fatigue interspersed tests of several steel alloys. Comparisons are made with predictions based upon the Time- and Cycle-Fraction approach. The method of Strainrange Partitioning is shown to give consistently more accurate predictions of cyclic life than is given by the Time- and Cycle-Fraction approach. (Author)

A80-32067 * Prediction of fiber composite mechanical behavior made simple. C. C. Chamis (NASA, Lewis Research Center, Materials and Structures Div., Cleveland, Ohio). In: *Rising to the*

challenge of the '80s; Annual Conference and Exhibit, 35th, New Orleans, La., February 4-8, 1980, Preprints. (A80-32058 12-24) New York, Society of the Plastics Industry, Inc., 1980, p. 12 A 1 to 12 A 10.

A convenient procedure is described for the determination of the mechanical behavior (elastic properties and failure stresses of angleply fiber composite laminates using a pocket calculator. The procedure consists of simple equations and appropriate graphs of (plus or minus theta) ply combinations. The procedure can handle all types of fiber composites including hybrids. The versatility and generality of the procedure is illustrated using several step-by-step numerical examples. (Author)

A80-35906 * Status of NASA full-scale engine aeroelasticity research. J. F. Lubomski (NASA, Lewis Research Center, Cleveland, Ohio). In: *Structures, Structural Dynamics, and Materials Conference, 21st, Seattle, Wash., May 12-14, 1980, Technical Papers*. Conference sponsored by AIAA, ASME, ASCE, and AHS. New York, American Institute of Aeronautics and Astronautics, Inc., 1980, 18 p. 14 refs.

The paper presents data relevant to several types of aeroelastic instabilities which have been obtained using several types of turbojet and turbofan engines. Special attention is given to data relative to separated flow (stall) flutter, choke flutter, and system mode instabilities. The discussion covers the characteristics of these instabilities, and a number of correlations are presented that help identify the nature of the phenomena. M.E.P.

A80-38142 * A quarter-century of progress in the development of correlation and extrapolation methods for creep rupture data. S. S. Manson (Case Western Reserve University, Cleveland, Ohio) and C. R. Ensign (NASA, Lewis Research Center, Cleveland, Ohio). *ASME, Transactions, Journal of Engineering Materials and Technology*, vol. 101, Oct. 1979, p. 317-325, 32 refs.

Developments in the analysis of creep-rupture data are reviewed with particular reference to time temperature relations for the correlation and extrapolation of creep and stress rupture data, the minimum commitment method, and successive regression methods. Some contributions to the development of time-temperature parameters are noted. V.P.

A80-45364 * Vibration and buckling of rectangular plates under in-plane hydrostatic loading. R. E. Kiehl (NASA, Lewis Research Center, Cleveland, Ohio) and L. S. Han (Ohio State University, Columbus, Ohio). *Journal of Sound and Vibration*, vol. 70, June 22, 1980, p. 543-555, 15 refs.

Numerical solutions are presented for the fundamental natural frequency and mode shape of a rectangular plate loaded by in-plane hydrostatic forces for a wide variety of aspect ratios, boundary conditions, and load magnitudes. All six possible combinations of simply supported and clamped edges are considered. The limiting conditions of unloaded vibration and buckling are discussed in detail, with emphasis on the preferred mode shape. Design curves and approximate formulae are presented which provide a simple means of determining the fundamental frequency parameter. (Author)

A80-46032 * Compliance and stress intensity coefficients for short bar specimens with chevron notches. D. Munz (NASA, Lewis Research Center, Cleveland, Ohio; Deutsche Forschungs- und Versuchsanstalt für Luft- und Raumfahrt, Cologne, West Germany), R. T. Bubsey, and J. E. Srawley (NASA, Lewis Research Center, Cleveland, Ohio). *International Journal of Fracture*, vol. 16, Aug. 1980, p. 359-374, 15 refs. Contract No. EC-77-A-31-1040.

For the determination of fracture toughness especially with brittle materials, a short bar specimen with rectangular cross section and chevron notch can be used. As the crack propagates from the tip of the triangular notch, the load increases to a maximum then decreases. To obtain the relation between the fracture toughness and

maximum load, calculations of Srawley and Gross for specimens with a straight-through crack were applied to the specimens with chevron notches. For the specimens with a straight-through crack, an analytical expression was obtained. This expression was used for the calculation of the fracture toughness versus maximum load relation under the assumption that the change of the compliance with crack length for the specimen with a chevron notch is the same as for a specimen with a straight-through crack. (Author)

N80-10615* Pratt and Whitney Aircraft Group, East Hartford, Conn Commercial Products Div.
EFFECT OF TIME DEPENDENT FLIGHT LOADS ON JT9D-7 PERFORMANCE DETERIORATION

A Jay and B L Lewis 21 Aug 1979 73 p refs
 (Contract NAS3-20632)
 (NASA-CR-159681; PWA-5512-45) Avail: NTIS
 HC A04/MF A01 CSCL 01C

The results of a modal transient analysis of the engine/aircraft system are presented. The response of the JT9D to analytically simulated vertical gusts and landings was predicted using a NASTRAN finite element mathematical model of the JT9D/747 propulsion system. The NASTRAN finite element model of the propulsion system included engine structural models of the fan, low/high pressure compressors, diffuser/turbine cases, and high/low pressure rotors, as well as nacelle models of the inlet cowl, tailcone, and wing pylon. The analysis conducted predicts that an insignificant level of JT9D-7 performance deterioration would occur due to a typical vertical gust encounter or a typical revenue service landing. Analysis of a high sink rate landing with a heavy fuel load indicates the possibility of local wear, however, the lack of an accurate dynamic rotor/seal interference model precludes an accurate quantitative evaluation of performance change for this once-per-airframe-life event. J.M.S.

N80-22733* Mechanical Technology, Inc., Latham, N. Y.
DEVELOPMENT OF PROCEDURES FOR CALCULATING STIFFNESS AND DAMPING OF ELASTOMERS IN ENGINEERING APPLICATIONS, PART 6

A Rieger, G Burgess, and E Zorzi Apr 1980 157 p refs
 (Contract NAS3-18546)
 (NASA-CR-159838; MTI-80TR29) Avail: NTIS
 HC A08/MF A01 CSCL 20K

An elastomer damper was designed, tested, and compared with the performance of a hydraulic damper for a power transmission shaft. The six button Viton-70 damper was designed so that the elastomer damper or the hydraulic damper could be activated without upsetting the imbalance condition of the assembly. This permitted a direct comparison of damper effectiveness. The elastomer damper consistently performed better than the hydraulic mount and permitted stable operation of the power transmission shaft to speeds higher than obtained with the squeeze film damper. Tests were performed on shear specimens of Viton-79, Buna-N, EPDM, and Neoprene to determine performance limitations imposed by strain, temperature, and frequency. Frequencies of between 110 Hz and 1100 Hz were surveyed with imposed strains between 0.0005 and 0.08 at temperatures of 32 C, 66 C, and 80 C. A set of design curves was generated in a unified format for each of the elastomer materials. E.D.K.

N80-27720* Massachusetts Inst. of Tech., Cambridge. Aeroelastic and Structures Research Lab.
INSTRUCTIONS FOR THE USE OF THE CIVM-JET 4C FINITE-STRAIN COMPUTER CODE TO CALCULATE THE TRANSIENT STRUCTURAL RESPONSES OF PARTIAL AND/OR COMPLETE ARBITRARILY-CURVED RINGS SUBJECTED TO FRAGMENT IMPACT

Jose J. A. Rodal, Susan E. French, Emmett A. Witmer, and Thomas R. Stagliano Dec. 1979 38 p refs
 (Grant NGR-22-009-339)
 (NASA-CR-159873; ASTL-MR-154-1) Avail: NTIS
 HC A03/MF A01

The CIVM-JET 4C computer program for the 'finite strain' analysis of 2 d transient structural responses of complete or partial rings and beams subjected to fragment impact stored on

tape as a series of individual files. Which subroutines are found in these files are described in detail. All references to the CIVM-JET 4C program are made assuming that the user has a copy of NASA CR-134907 (ASRL TR 154-9) which serves as a user's guide to (1) the CIVM-JET 4B computer code and (2) the CIVM-JET 4C computer code 'with the use of the modified input instructions' attached hereto. L.F.M.

N80-29762* Massachusetts Inst. of Tech., Cambridge.
FINITE-STRAIN LARGE-DEFLECTION ELASTIC-VISCOPLASTIC FINITE-ELEMENT TRANSIENT RESPONSE ANALYSIS OF STRUCTURES

Jose J. A. Rodal and Emmett A. Witmer Jul. 1979 567 p refs

(Grant NGR-22-009-339)
 (NASA-CR-159874; ASRL-TR-154-15) Avail: NTIS
 HC A24/MF A01 CSCL 20K

A method of analysis for thin structures that incorporates finite strain, elastic-plastic, strain hardening, time dependent material behavior implemented with respect to a fixed configuration and is consistently valid for finite strains and finite rotations is developed. The theory is formulated systematically in a body fixed system of convected coordinates with materially embedded vectors that deform in common with continuum. Tensors are considered as linear vector functions and use is made of the dyadic representation. The kinematics of a deformable continuum is treated in detail, carefully defining precisely all quantities necessary for the analysis. The finite strain theory developed gives much better predictions and agreement with experiment than does the traditional small strain theory, and at practically no additional cost. This represents a very significant advance in the capability for the reliable prediction of nonlinear transient structural responses, including the reliable prediction of strains large enough to produce ductile metal rupture. E.D.K.

42 GEOSCIENCES (GENERAL)

N80-18880* National Aeronautics and Space Administration.
Lewis Research Center, Cleveland, Ohio.

**INTRA-OCULAR PRESSURE NORMALIZATION TECHNIQUE
AND EQUIPMENT Patent**

William J. McGannon, inventor (to NASA) Issued 22 Jan. 1980
6 p Filed 31 Aug. 1977 Supersedes N77-30727 (15 - 21,
p 2839)

(NASA-Case-LEW-12723-1; US-Patent-4,184,491;
US-Patent-Appl-SN-829317; US-Patent-Class-128-276;
US-Patent-Class-128-760) Avail: US Patent and Trademark
Office CSCL 06B

A method and apparatus for safely reducing abnormally high intraocular pressure in an eye during a predetermined time interval is presented. This allows maintenance of normal intraocular pressure during glaucoma surgery. According to the invention, a pressure regulator of the spring biased diaphragm type is provided with additional bias by a column of liquid. The height of the column of liquid is selected such that the pressure at a hypodermic needle connected to the output of the pressure regulator is equal to the measured pressure of the eye. The hypodermic needle can then be safely inserted into the anterior chamber of the eye. Liquid is then bled out of the column to reduce the bias on the diaphragm of the pressure regulator and, consequently, the output pressure of the regulator. This lowering pressure of the regulator also occurs in the eye by means of a small second bleed path provided between the pressure regulator and the hypodermic needle. Alternately, a second hypodermic needle may be inserted into the eye to provide a controlled leak off path for excessive pressure and clouded fluid from the anterior chamber.

Official Gazette of the U.S. Patent and Trademark Office

43 EARTH RESOURCES

Includes remote sensing of earth resources by aircraft and spacecraft, photogrammetry, and aerial photography. For instrumentation see 35 *Instrumentation and Photography*.

N80-15538*# National Aeronautics and Space Administration, Lewis Research Center, Cleveland, Ohio.

POSSIBLE METHODS FOR DISTINGUISHING ICEBERGS FROM SHIPS BY AERIAL REMOTE SENSING

Walton L. Howes Dec. 1979 36 p refs (NASA-TM-79310; E-266) Avail: NTIS HC A03/MF A01 CSCL 08L

The simplest methods for aerial remote sensing which are least affected by atmospheric opacities are summarized. Radar is preferred for targets off the flight path, and microwave radiometry for targets along the flight path. Radar methods are classified by ability to resolve targets. Techniques which do not require target resolution are preferred. Among these techniques, polarization methods appear most promising, specifically those which differentiate the expected relatively greater depolarization by icebergs from that by ships or which detect doubly-reversed circular polarization. R.C.T.

N80-18497*# National Aeronautics and Space Administration, Lewis Research Center, Cleveland, Ohio.

NUMERICAL CALCULATION OF STEADY INVISCID FULL POTENTIAL COMPRESSIBLE FLOW ABOUT WIND TURBINE BLADES

Djordje S. Dulikravich 1980 11 p refs Presented at the Wind Energy Conf., Boulder, Colo., 9-11 Apr. 1980; sponsored by AIAA and Midwest Energy Research Inst. (NASA-TM-81438; E-361; AIAA-Paper-80-0607) Avail: NTIS HC A02/MF A01 CSCL 10B

An exact nonlinear mathematical model that accounts for three-dimensional cascade effects about the inner portions of the rotor blades and compressibility effects about the tip regions of the blades was derived. An artificially time dependent version was iteratively solved by a finite volume technique involving an artificial viscosity and a three-level consecutive mesh refinement. The exact boundary conditions were applied by generating a boundary conforming periodic computation mesh. K.L.

N80-20787*# National Aeronautics and Space Administration, Lewis Research Center, Cleveland, Ohio.

ASSESSMENT OF SATELLITE AND AIRCRAFT MULTISPECTRAL SCANNER DATA FOR STRIP-MINE MONITORING

Ernie W. Spisz and Joyce T. Dooley Washington Mar. 1980 39 p Original contains color illustrations (NASA-TM-79268; E-187) Avail: NTIS HC A03/MF A01 CSCL 08I

The application of LANDSAT multispectral scanner data to describe the mining and reclamation changes of a hilltop surface coal mine in the rugged, mountainous area of eastern Kentucky is presented. Original single band satellite imagery, computer enhanced single band imagery, and computer classified imagery are presented for four different data sets in order to demonstrate the land cover changes that can be detected. Data obtained with an 11 band multispectral scanner on board a C-47 aircraft at an altitude of 3000 meters are also presented. Comparing the satellite data with color, infrared aerial photography, and ground survey data shows that significant changes in the disrupted area can be detected from LANDSAT band 5 satellite imagery for mines with more than 100 acres of disturbed area. However, band-ratio (bands 5/6) imagery provides greater contrast than single band imagery and can provide a qualitative level 1 classification of the land cover that may be useful for monitoring either the disturbed mining area or the revegetation progress. However, if a quantitative, accurate classification of the barren or revegetated classes is required, it is necessary to perform a detailed, four band computer classification of the data. J.M.S.

44 ENERGY PRODUCTION AND CONVERSION

Includes specific energy conversion systems, e.g., fuel cells and batteries; global sources of energy; fossil fuels; geophysical conversion; hydroelectric power; and wind power.

For related information see also 07 Aircraft Propulsion and Power, 20 Spacecraft Propulsion and Power, 28 Propellants and Fuels, and 85 Urban Technology and Transportation.

N80-10594* National Aeronautics and Space Administration, Lewis Research Center, Cleveland, Ohio.

SOME TECHNIQUES FOR REDUCING THE TOWER SHADOW OF THE DOE/NASA MOD-0 WIND TURBINE TOWER Final Report

Richard R. Burley, Joseph M. Savino, Lee H. Wagner, and James H. Diedrich Sep. 1979 129 p refs

(Contract DE AB29-76-ET20370)

(NASA-TM-79202; DOE/NASA/20370-79/17; E-087) Avail: NTIS HC A07/MF A01 CSCL 10B

Wind speed profile measurements to measure the effect of a wind turbine tower on the wind velocity are presented. Measurements were made in the wake of scale models of the tower and in the wake of certain full scale components to determine the magnitude of the speed reduction (tower shadow). Shadow abatement techniques tested on the towers included the removal of diagonals, replacement of diagonals and horizontals with round cross section members, installation of elliptical shapes on horizontal members, installation of airfoils on vertical members, and application of surface roughness to vertical members.

A.W.H.

N80-10595* National Aeronautics and Space Administration, Lewis Research Center, Cleveland, Ohio.

NASA-LEWIS CLOSED-CYCLE MAGNETOHYDRODYNAMICS PLANT ANALYSIS

Paul F. Penko 1979 13 p refs Presented at Closed-Cycle Magnetohydrodynamics Specialists Meeting, Bozeman, Montana, 21 Jun. 1979

(Contract EF-77-A-01-2674)

(NASA-TM-79249; DOE/NASA-2674-79/7; E-159) Avail: NTIS HC A02/MF A01 CSCL 10A

A brief review of preliminary analyses of coal fired closed cycle MHD power plants is presented. The performance of three power plants with differing combustion systems were compared. The combustion systems considered were (1) a direct coal-fired combustor, (2) a coal gasifier with in-bed desulfurization and (3) a coal gasifier requiring external fuel gas cleanup. Power plant efficiencies (auxiliary power excluded) were 44.5, 43, and 41 percent for the three plants, respectively.

R.E.S.

N80-12552* National Aeronautics and Space Administration, Lewis Research Center, Cleveland, Ohio.

A PHOTOVOLTAIC POWER SYSTEM IN THE REMOTE AFRICAN VILLAGE OF TANGAYE, UPPER VOLTA

William J. Bifano, Anthony F. Ratajczak, and James E. Martz 1979 17 p refs Presented at UNITAR Conf. on Long-Term Energy Resources, Montreal, 26 Nov. - 7 Dec. 1979 Sponsored in part by AID

(NASA-TM-79318; E-274) Avail: NTIS HC A02/MF A01 CSCL 10B

A photovoltaic (PV) system powering a grain mill and a water pump was installed in the remote West African village of Tangaye, Upper Volta. Village characteristics as well as system design, hardware, installation and operation to date are described. The PV system cost is discussed. A baseline socio-economic study performed and a follow-up study is planned to determine the impact of the system on the villagers.

R.E.S.

N80-13623* National Aeronautics and Space Administration, Lewis Research Center, Cleveland, Ohio.

MODIFIED POWER LAW EQUATIONS FOR VERTICAL WIND PROFILES

D. A. Spera and T. R. Richards 1979 13 p refs Presented at the Wind Characteristics and Wind Energy Siting Conf., Portland, Oreg., 19-21 Jun. 1979 Sponsored by DOE, American Meteorological Soc., Pacific Northwest Lab.

(E49-26)-1059

(NASA-TM-79275; DOE/NASA/1059-79/4) Avail: NTIS HC A02/MF A01 CSCL 10A

Equations are presented for calculating power law exponents from wind speed and surface roughness data. Results are evaluated by comparison with wind profile data measured at a variety of sites.

Author

N80-13624* National Aeronautics and Space Administration, Lewis Research Center, Cleveland, Ohio.

LOW NO(X) HEAVY FUEL COMBUSTOR PROGRAM

Eric Lister (DOE, Germantown, Md.), Richard W. Niedzwiecki, and Lester Nichols [1979] 15 p To be presented at 25th Ann. Intern. Gas Turbine Conf., New Orleans, 9-13 Mar. 1980; sponsored by ASME

(Contract EC-77-A-31-1062)

(NASA-TM-79313; E-269; DOE/NASA/1062-79/3) Avail: NTIS HC A02/MF A01 CSCL 10B

The 'low nitrogen oxides heavy fuel combustor' program is described. Main program objectives are to generate and demonstrate the technology required to develop durable gas turbine combustors for utility and industrial applications, which are capable of sustained, environmentally acceptable operation with minimally processed petroleum residual fuels. The program will focus on 'dry' reductions of oxides of nitrogen, improved combustor durability, and satisfactory combustion of minimally processed petroleum residual fuels. Other technology advancements sought include: fuel flexibility for operation with petroleum distillates, blends of petroleum distillates and residual fuels, and synfuels (fuel oils derived from coal or shale); acceptable exhaust emissions of carbon monoxide, unburned hydrocarbons, sulfur oxides and smoke; and retrofit capability to existing engines.

R.E.S.

N80-14472* National Aeronautics and Space Administration, Lewis Research Center, Cleveland, Ohio.

SELF-RECONFIGURING SOLAR CELL SYSTEM Patent

Robert P. Gruber, inventor (to NASA) Issued 20 Nov. 1979 10 p filed 19 Jun. 1978 Supersedes N78-27520 (16 - 18, p 2408)

(NASA-Case-LEW-12586-1; US-Patent-4,175,249;

US-Patent-Appl-SN-916655; US-Patent-Class-323-15;

US-Patent-Class-307-63; US-Patent-Class-307-66;

US-Patent-Class-323-19) Avail: US Patent and Trademark Office CSCL 10A

A self-reconfiguring solar cell array is disclosed wherein some of the cells are switched so that they can be either in series or in shunt within the array. This feature of series or parallel switching of cells allows the array to match the load to achieve maximum power transfer. Automatic control is used to determine the conditions for maximum power operation and to switch the array into the appropriate configuration necessary to transfer maximum power to the load.

Official Gazette of the U.S. Patent and Trademark Office

N80-14493* National Aeronautics and Space Administration, Lewis Research Center, Cleveland, Ohio.

STATUS OF THE DOE/NASA CRITICAL GAS TURBINE RESEARCH AND TECHNOLOGY PROJECT

John S. Clark 1980 21 p refs Proposed for presentation the 25th Annual Gas Turbine Conf., New Orleans, 9-13 Mar. 1980; sponsored by the Am. Soc. of Mech. Engineers

(Contract EF-77-A-01-2593)

(NASA-TM-79307; DOE/NASA/2593-79/11; E-263) Avail: NTIS HC A02/MF A01 CSCL 10B

Activities performed in order to provide an R&T data base for utility gas turbine systems burning coal-derived fuels are

described. Experiments were run to determine the corrosivity effects of trace metal contaminants (and potential fuel additives) on gas turbine materials and these results were correlated in a corrosion-life prediction model. Actual fuels were burned in a burner rig hot corrosion test to verify the model. A deposition prediction model was assembled and compared with results of actual coal-derived fuel deposition tests. Thermal barrier coatings were tested to determine their potential for protecting gas turbine hardware from the corrosive contaminants. Several coatings were identified with significantly improved spallation-resistance (and, hence, corrosion resistance). A.R.H.

N80-15554* National Aeronautics and Space Administration. Lewis Research Center, Cleveland, Ohio.

SPACE SOLAR CELLS: HIGH EFFICIENCY AND RADIATION DAMAGE

Henry W. Brandhorst, Jr. and Daniel T. Bernatowicz 1980 12 p refs Presented at 14th Photovoltaic Specialists Conf., San Diego, Calif., 7-10 Jan. 1980; sponsored by IEEE (NASA-TM-81387, E-297) Avail. NTIS HC A02/MF A01 CSCL 10A

The progress and status of efforts to increase the end-of-life efficiency of solar cells for space use is assessed. High efficiency silicon solar cells, silicon solar cell radiation damage, GaAs solar cell performance and radiation damage and 30 percent devices are discussed R.E.S.

N80-15555* National Aeronautics and Space Administration. Lewis Research Center, Cleveland, Ohio.

OPEN-CIRCUIT VOLTAGE IMPROVEMENTS IN LOW RESISTIVITY SOLAR CELLS

M. P. Godlewski, T. M. Klucher, G. A. Mazaris, and V. G. Weizer 1980 11 p refs Presented at 14th Photovoltaic Specialists Conf., San Diego, Calif., 7-10 Jan. 1980; sponsored by IEEE (NASA-TM-81388, E-298) Avail. NTIS HC A02/MF A01 CSCL 10A

Improvements in the open circuit voltage of 0.1 ohm-cm silicon solar cells were achieved using a multistep diffusion technique. Experimental details are given along with the results of an analysis that indicate that anomalous behavior of the electron mobility in the cell base limits attainment of higher voltages. Author

N80-15556* National Aeronautics and Space Administration. Lewis Research Center, Cleveland, Ohio.

BACK SURFACE REFLECTORS FOR SOLAR CELLS

An-Ti Chai Chai 1980 10 p refs Presented at 14th Photovoltaic Specialists Conf., San Diego, Calif., 7-10 Jan. 1980; sponsored by IEEE (NASA-TM-81390, E-300) Avail. NTIS HC A02/MF A01 CSCL 10A

Sample solar cells were fabricated to study the effects of various back surface reflectors on the device performance. They are typical 50 micrometers thick, space quality, silicon solar cells except for variations of the back contact configuration. The back surfaces of the sample cells are polished to a mirror like finish, and have either conventional full contacts or grid finger contacts. Measurements and evaluation of various metallic back surface reflectors, as well as cells with total internal reflection, are presented. Results indicate that back surface reflectors formed using a grid finger back contact are more effective reflectors than cells with full back metallization and that Au, Ag, or Cu are better back surface reflector metals than Al. R.C.T.

N80-15557* National Aeronautics and Space Administration. Lewis Research Center, Cleveland, Ohio.

RADIATION DAMAGE IN LITHIUM-COUNTERDOPED N/P SILICON SOLAR CELLS

A. M. Hermann (Tulane Univ.), C. K. Swartz, H. W. Brandhorst, Jr., and I. Weinberg 1980 13 p refs Presented at the 14th Photovoltaic Specialists Conf., San Diego, Calif., 7-10 Jan. 1980; sponsored by IEEE (NASA-TM-81391, E-301) Avail. NTIS HC A02/MF A01 CSCL 10A

Lithium counterdoped n+/p silicon solar cells were irradiated with 1 MV electrons and their post irradiation performance and low temperature annealing properties were compared to that of the 0.35 ohm cm control cells. Cells fabricated from float zone and Czochralski grown silicon were investigated. It was found that the float zone cells exhibited superior radiation resistance compared to the control cells, while no improvement was noted for the Czochralski grown cells. Room temperature and 60 C annealing studies were conducted. The annealing was found to be a combination of first and second order kinetics for short times. It was suggested that the principal annealing mechanism was migration of lithium to a radiation induced defect with subsequent neutralization of the defect by combination with lithium. The effects of base lithium gradient were investigated. It was found that cells with negative base lithium gradients exhibited poor radiation resistance and performance compared to those with positive or no lithium gradients, the latter being preferred for overall performance and radiation resistance. M.G.

N80-15558* National Aeronautics and Space Administration. Lewis Research Center, Cleveland, Ohio.

RADIATION DAMAGE ANNEALING MECHANISMS AND POSSIBLE LOW TEMPERATURE ANNEALING IN SILICON SOLAR CELLS

Irving Weinberg and Clifford K. Swartz 1980 10 p refs Presented at 14th Photovoltaic Specialists Conf., San Diego, Calif., 7-10 Jan. 1980; sponsored by IEEE (NASA-TM-81392, E-302) Avail. NTIS HC A02/MF A01 CSCL 10A

The defect responsible for reverse annealing in 2 ohm/cm n(+)/p silicon solar cells was identified. This defect, with energy level at $e_{\text{sub}} v + 0.30$ eV was tentatively identified as a boron oxygen-vacancy complex. Results indicate that its removal could result in significant annealing for 2 ohm/cm and lower resistivity cells at temperatures as low as 200 C. These results were obtained by use of an expression derived from the Shockley-Read-Hall recombination theory which relates measured diffusion length ratios to relative defect concentrations and electron capture cross sections. The relative defect concentrations and one of the required capture cross sections are obtained from Deep Level Transient Spectroscopy. Four additional capture cross sections are obtained using diffusion length data and data from temperature dependent lifetime studied. These calculated results are in reasonable agreement with experimental data. M.G.

N80-15560* National Aeronautics and Space Administration. Lewis Research Center, Cleveland, Ohio.

CANDIDATE THERMAL ENERGY STORAGE TECHNOLOGIES FOR SOLAR INDUSTRIAL PROCESS HEAT APPLICATIONS

Edward R. Furman 1979 12 p refs Presented at Solar Industrial Process Heat Conf., Oakland, Calif., 31 Oct. - 2 Nov. 1979; sponsored by Solar Energy Res. Inst. (Contract EC-77-A-31-1034) (NASA-TM-81380; DOE/NASA/1034-79/6; E-285) Avail. NTIS HC A02/MF A01 CSCL 10A

A number of candidate thermal energy storage system elements were identified as having the potential for the successful application of solar industrial process heat. These elements which include storage media, containment and heat exchange are shown. R.C.T.

N80-15561* National Aeronautics and Space Administration. Lewis Research Center, Cleveland, Ohio.

GLOBAL CALIBRATION OF TERRESTRIAL REFERENCE CELLS AND ERRORS INVOLVED IN USING DIFFERENT IRRADIANCE MONITORING TECHNIQUES

Henry B. Curtis 1980 12 p refs Presented at the 14th Photovoltaic Specialists Conf., San Diego, Calif., 7-10 Jan. 1980; sponsored by IEEE (Contract DE-AI01-79ET-20485) (NASA-TM-81393; DOE/NASA/20485-79/6; E-303) Avail. NTIS HC A02/MF A01 CSCL 10A

The feasibility of global calibration of terrestrial reference

cells is discussed. A simple, accurate 'secondary' calibration technique based on ratios of test to reference cell currents measured in natural sunlight is described. Different techniques for monitoring incident irradiance during solar cell performance measurements are also examined and assessed, including the techniques of black-body detectors, calibrated reference cells, and the convolution of spectral response with solar irradiance.

M.G.

N80-16453* National Aeronautics and Space Administration, Lewis Research Center, Cleveland, Ohio.

LARGE WIND TURBINE DESIGN CHARACTERISTICS AND R AND D REQUIREMENTS

Seymour Lieblein, ed. (Technical Report Services, Rocky River, Ohio) Dec. 1979 459 p refs Conf. held at Cleveland, 24-26 Apr. 1979; sponsored in part by DOE (NASA-CP-2106; CONF-7904111) Avail. NTIS HC A20/MF A01 CSCL 10B

Detailed technical presentations on large wind turbine research and development activities sponsored by public and private organizations are presented. Both horizontal and vertical axis machines are considered with emphasis on their structural design. For individual titles, see N80-16454 through N80-16482.

N80-16455* National Aeronautics and Space Administration, Lewis Research Center, Cleveland, Ohio.

DESIGN EVOLUTION OF LARGE WIND TURBINE GENERATORS

David A. Spera. In *its Large Wind Turbine Design Characteristics and R and D Requirements* Dec. 1979 p 25-33 ref (For primary document see N80-16453 07-44) Avail. NTIS HC A20/MF A01 CSCL 10B

During the past five years, the goals of economy and reliability have led to a significant evolution in the basic design--both external and internal--of large wind turbine systems. To show the scope and nature of recent changes in wind turbine designs, development of three types are described: (1) system configuration developments; (2) computer code developments; and (3) blade technology developments. R.E.S.

N80-16469* National Aeronautics and Space Administration, Lewis Research Center, Cleveland, Ohio.

STRUCTURAL ANALYSIS CONSIDERATIONS FOR WIND TURBINE BLADES

David A. Spera. In *its Large Wind Turbine Design Characteristics and R and D Requirements* Dec. 1979 p 211-224 refs (For primary document see N80-16453 07-44) Avail. NTIS HC A20/MF A01 CSCL 10B

Approaches to the structural analysis of wind turbine blade designs are reviewed. Specifications and materials data are discussed along with the analysis of vibrations, loads, stresses, and failure modes. K.L.

N80-16470* National Aeronautics and Space Administration, Lewis Research Center, Cleveland, Ohio.

BLADE DESIGN AND OPERATING EXPERIENCE ON THE MOD-0A 200 kW WIND TURBINE AT CLAYTON, NEW MEXICO

Bradford S. Linscott and Richard K. Shaltens. In *its Large Wind Turbine Design Characteristics and R and D Requirements* Dec. 1979 p 225-238 refs (For primary document see N80-16453 07-44) Avail. NTIS HC A20/MF A01 CSCL 10B

Two 60 foot long aluminum wind turbine blades were operated for over 3000 hours on the MOD-0A wind turbine. The first signs of blade structural damage were observed after 400 hours of operation. Details of the blade design, loads, cost, structural damage, and repair are discussed. K.L.

N80-16472* National Aeronautics and Space Administration, Lewis Research Center, Cleveland, Ohio.

DESIGN, FABRICATION, AND TEST OF A STEEL SPAR WIND TURBINE BLADE

Timothy L. Sullivan, Paul J. Sirocky, Jr., and Larry A. Viterna. In *its Large Wind Turbine Design Characteristics and R and D Requirements* Dec. 1979 p 267-284 refs (For primary document see N80-16453 07-44)

Avail. NTIS HC A20/MF A01 CSCL 10B

The design and fabrication of wind turbine blades based on 60 foot steel spars are discussed. Performance and blade load information is given and compared to analytical prediction. In addition, performance is compared to that of the original MOD-0 aluminum blades. Costs for building the two blades are given, and a projection is made for the cost in mass production. Design improvements to reduce weight and improve fatigue life are suggested. K.L.

N80-16480* National Aeronautics and Space Administration, Lewis Research Center, Cleveland, Ohio.

SIMULATION STUDIES OF MULTIPLE LARGE WIND TURBINE GENERATORS ON A UTILITY NETWORK

Leonard J. Gilbert and David M. Triesenberg (Purdue Univ.) In *its Large Wind Turbine Design Characteristics and R and D Requirements* Dec. 1979 p 375-384 refs (For primary document see N80-16453 07-44)

Avail. NTIS HC A20/MF A01 CSCL 10B

The potential electrical problems that may be inherent in the inertia of clusters of wind turbine generators and an electric utility network were investigated. Preliminary and limited results of an analog simulation of two MOD-2 wind generators tied to an infinite bus indicate little interaction between the generators and between the generators and the bus. The system demonstrated transient stability for the conditions considered. A.R.H.

N80-16490* National Aeronautics and Space Administration, Lewis Research Center, Cleveland, Ohio.

POTENTIAL PERFORMANCE IMPROVEMENT USING A REACTING GAS (NITROGEN TETROXIDE) AS THE WORKING FLUID IN A CLOSED BRAYTON CYCLE Final Report

Robert J. Stochl Dec. 1979 23 p refs

(Contract EX-76-A-29-1060)

(NASA-TM-79322; DOE/NASA/1060-79/3) Avail. NTIS HC A02/MF A01 CSCL 10B

The results of an analysis to estimate the performance that could be obtained by using a chemically reacting gas (nitrogen tetroxide) as the working fluid in a closed Brayton cycle are presented. Compared with data for helium as the working fluid, these results indicate efficiency improvements from 4 to 90 percent, depending on turbine inlet temperature, pressures, and gas residence time in heat transfer equipment. Author

N80-16494* National Aeronautics and Space Administration, Lewis Research Center, Cleveland, Ohio.

PRELIMINARY ANALYSIS OF PERFORMANCE AND LOADS DATA FROM THE 2-MEGAWATT MOD-1 WIND TURBINE GENERATOR

D. A. Spera, L. A. Viterna, T. R. Richardson, and C. Neustadter. 1979 16 p refs Presented at 4th Battery Conf. and Workshop on Wind Energy Conversion Systems, Washington, D.C., 29-31 Oct. 1979; sponsored by DOE

(Contract EX-77-A-29-1010)

(NASA-TM-81408; DOE/NASA/1010-79/3; E-12) Avail. NTIS HC A02/MF A01 CSCL 10A

Preliminary test data on output power versus wind speed, rotor blade loads, system dynamic behavior, and start-stop characteristics on the Mod-1 wind turbine generator are presented. These data were analyzed statistically and are compared with design predictions of system performance and loads. To date, the Mod-1 wind turbine generator has produced up to 1.5 MW of power, with a measured power versus wind speed curve which agrees closely with design. Blade loads were measured at wind speeds up to 14 m/s and also during rapid shutdowns. Peak transient loads during the most severe shutdowns are less than the design limit loads. On the inboard blade sections, fatigue loads are approximately equal to the design cyclic loads. On the outboard blade sections, however, measured cyclic loads

cells is discussed. A simple, accurate 'secondary' calibration technique based on ratios of test to reference cell currents measured in natural sunlight is described. Different techniques for monitoring incident irradiance during solar cell performance measurements are also examined and assessed, including the techniques of black-body detectors, calibrated reference cells, and the convolution of spectral response with solar irradiance.

M.G.

N80-16453* National Aeronautics and Space Administration. Lewis Research Center, Cleveland, Ohio.

LARGE WIND-TURBINE DESIGN CHARACTERISTICS AND R AND D REQUIREMENTS

Seymour Lieblein, ed. (Technical Report Services, Rocky River, Ohio) Dec. 1979 459 p refs Conf. held at Cleveland, 24-26 Apr. 1979; sponsored in part by DOE

(NASA-CP-2106; CONF-7904111)

Avail: NTIS

HC A20/MF A01 CSCL 10B

Detailed technical presentations on large wind turbine research and development activities sponsored by public and private organizations are presented. Both horizontal and vertical axis machines are considered with emphasis on their structural design. For individual titles, see N80-16454 through N80-16482.

N80-16455* National Aeronautics and Space Administration. Lewis Research Center, Cleveland, Ohio.

DESIGN EVOLUTION OF LARGE WIND TURBINE GENERATORS

David A. Spera *In its Large Wind Turbine Design Characteristics and R and D Requirements* Dec. 1979 p 25-33 ref (For primary document see N80-16453 07-44)

Avail: NTIS HC A20/MF A01 CSCL 10B

During the past five years, the goals of economy and reliability have led to a significant evolution in the basic design--both external and internal--of large wind turbine systems. To show the scope and nature of recent changes in wind turbine designs, development of three types are described: (1) system configuration developments; (2) computer code developments; and (3) blade technology developments.

R.E.S.

N80-16469* National Aeronautics and Space Administration. Lewis Research Center, Cleveland, Ohio.

STRUCTURAL ANALYSIS CONSIDERATIONS FOR WIND TURBINE BLADES

David A. Spera *In its Large Wind Turbine Design Characteristics and R and D Requirements* Dec. 1979 p 211-224 refs (For primary document see N80-16453 07-44)

Avail: NTIS HC A20/MF A01 CSCL 10B

Approaches to the structural analysis of wind turbine blade designs are reviewed. Specifications and materials data are discussed along with the analysis of vibrations, loads, stresses, and failure modes.

K.L.

N80-16470* National Aeronautics and Space Administration. Lewis Research Center, Cleveland, Ohio.

BLADE DESIGN AND OPERATING EXPERIENCE ON THE MOD-OA 200 kW WIND TURBINE AT CLAYTON, NEW MEXICO

Bradford S. Linscott and Richard K. Shaltens *In its Large Wind Turbine Design Characteristics and R and D Requirements* Dec. 1979 p 225-238 refs (For primary document see N80-16453 07-44)

Avail: NTIS HC A20/MF A01 CSCL 10B

Two 60 foot long aluminum wind turbine blades were operated for over 3000 hours on the MOD-OA wind turbine. The first signs of blade structural damage were observed after 400 hours of operation. Details of the blade design, loads, cost, structural damage, and repair are discussed.

K.L.

N80-16472* National Aeronautics and Space Administration. Lewis Research Center, Cleveland, Ohio.

DESIGN, FABRICATION, AND TEST OF A STEEL SPAR WIND TURBINE BLADE

Timothy L. Sullivan, Paul J. Sirocky, Jr., and Larry A. Viterna *In its Large Wind Turbine Design Characteristics and R and D Requirements* Dec. 1979 p 267-284 refs (For primary document see N80-16453 07-44)

Avail: NTIS HC A20/MF A01 CSCL 10B

The design and fabrication of wind turbine blades based on 60 foot steel spars are discussed. Performance and blade load information is given and compared to analytical prediction. In addition, performance is compared to that of the original MOD-O aluminum blades. Costs for building the two blades are given, and a projection is made for the cost in mass production. Design improvements to reduce weight and improve fatigue life are suggested.

K.L.

N80-16480* National Aeronautics and Space Administration. Lewis Research Center, Cleveland, Ohio.

SIMULATION STUDIES OF MULTIPLE LARGE WIND TURBINE GENERATORS ON A UTILITY NETWORK

Leonard J. Gilbert and David M. Triesenberg (Purdue Univ.) *In its Large Wind Turbine Design Characteristics and R and D Requirements* Dec. 1979 p 375-384 refs (For primary document see N80-16453 07-44)

Avail: NTIS HC A20/MF A01 CSCL 10B

The potential electrical problems that may be inherent in the inertia of clusters of wind turbine generators and an electric utility network were investigated. Preliminary and limited results of an analog simulation of two MOD-2 wind generators tied to an infinite bus indicate little interaction between the generators and between the generators and the bus. The system demonstrated transient stability for the conditions considered.

A.R.H.

N80-16490* National Aeronautics and Space Administration. Lewis Research Center, Cleveland, Ohio.

POTENTIAL PERFORMANCE IMPROVEMENT USING A REACTING GAS (NITROGEN TETROXIDE) AS THE WORKING FLUID IN A CLOSED BRAYTON CYCLE Final Report

Robert J. Stochl Dec. 1979 23 p refs

(Contract EX-76-A-29-1060)

(NASA-TM-79322; DOE/NASA/1060-79/3) Avail: NTIS

HC A02/MF A01 CSCL 10B

The results of an analysis to estimate the performance that could be obtained by using a chemically reacting gas (nitrogen tetroxide) as the working fluid in a closed Brayton cycle are presented. Compared with data for helium as the working fluid, these results indicate efficiency improvements from 4 to 90 percent, depending on turbine inlet temperature, pressures, and gas residence time in heat transfer equipment.

Author

N80-16494* National Aeronautics and Space Administration. Lewis Research Center, Cleveland, Ohio.

PRELIMINARY ANALYSIS OF PERFORMANCE AND LOADS DATA FROM THE 2-MEGAWATT MOD-1 WIND TURBINE GENERATOR

D. A. Spera, L. A. Viterna, T. R. Richards, and H. E. Neustadter 1979 16 p refs Presented at 4th Biennial Conf. and Workshop on Wind Energy Conversion Systems, Washington, D.C., 29-31 Oct. 1979; sponsored by DOE

(Contract EX-77-A-29-1010)

(NASA-TM-81408; DOE/NASA/1010-79/5; E-322) Avail:

NTIS HC A02/MF A01 CSCL 10A

Preliminary test data on output power versus wind speed, rotor blade loads, system dynamic behavior, and start-stop characteristics on the Mod-1 wind turbine generator are presented. These data were analyzed statistically and are compared with design predictions of system performance and loads. To date, the Mod-1 wind turbine generator has produced up to 1.5 MW of power, with a measured power versus wind speed curve which agrees closely with design. Blade loads were measured at wind speeds up to 14 m/s and also during rapid shutdowns. Peak transient loads during the most severe shutdowns are less than the design limit loads. On the inboard blade sections, fatigue loads are approximately equal to the design cyclic loads. On the outboard blade sections, however, measured cyclic loads

are significantly larger than design values, but they do not appear to exceed fatigue allowable loads as yet. R.E.S.

N80-18564* National Aeronautics and Space Administration. Lewis Research Center, Cleveland, Ohio.

OVERVIEW OF A STIRLING ENGINE TEST PROJECT

Jack G. Slaby 1980 27 p refs Proposed for presentation at 5th Intern. Automotive Propulsion Systems Symp., Dearborn, Mich., 14-18 Apr. 1980

(Contract EC-77-A-31-1040)

(NASA-TM-81442; DOE/NASA/1040-80/12; E-362) Avail: NTIS HC A03/MF A01 CSCL 10B

Tests were conducted on three Stirling engines ranging in size from 1.33 to 53 horsepower (1 to 40 kW). The tests were directed toward developing alternative, backup component concepts to improve engine efficiency and performance or to reduce costs. Some of the activities included investigating attractive concepts and materials for cooler-regenerator units, installing a jet impingement device on a Stirling engine to determine its potential for improved engine performance, and presenting performance maps for initial characterization of Stirling engines. The experiment results of the tests are presented along with predictions of results of future tests to be conducted on the Stirling engines. R.E.S.

N80-18555* National Aeronautics and Space Administration. Lewis Research Center, Cleveland, Ohio.

FLEXIBLE FORMULATED PLASTIC SEPARATORS FOR ALKALINE BATTERIES Patent Application

D. W. Scheibley, J. M. Bozek, and D. G. Soltis, inventors (to NASA) Filed 28 Sep. 1979 10 p

(NASA-Case-LEW-12363-4; US-Patent-Appl-SN-079914) Avail: NTIS HC A02/MF A01 CSCL 10C

A flexible separator for alkaline batteries is disclosed. The separator is comprised of a coating which is applied to a nonwoven porous substrate such as sheets or mats of asbestos or other materials which are inert with respect to the alkaline electrolyte of the battery. The coating material comprises a polyphenylene oxide polymer, an organic additive and inorganic and organic fillers which comprise 55% by volume or less of the coating material. Preferably, at least one inorganic filler material which is reactive with the electrolyte is included to produce desirable pores in the coating. The organic additive is a polymeric polyester material which is hydrolyzed by the alkaline electrolyte to improve conductivity of the coating. NASA

N80-18556* National Aeronautics and Space Administration. Lewis Research Center, Cleveland, Ohio.

FLEXIBLE FORMULATED PLASTIC SEPARATORS FOR ALKALINE BATTERIES Patent Application

D. W. Scheibley, J. M. Bozek, and D. G. Soltis, inventors (to NASA) Filed 19 Jul. 1979 10 p

(NASA-Case-LEW-12363-3; US-Patent-Appl-SN-058658) Avail: NTIS HC A02/MF A01 CSCL 10C

A flexible separator for alkaline batteries is disclosed. The separator is comprised of a coating which is applied to a nonwoven porous substrate such as sheets or mats of asbestos or other materials which are inert with respect to the alkaline electrolyte of the battery. The coating material is comprised of a polyphenylene oxide polymer, an organic additive and inorganic, and organic fillers which comprise 55% by volume or less of the coating material. Preferably, at least one inorganic filler material which is reactive with the electrolyte is included to produce desirable pores in the coating. The organic additive is a polymeric polyester material which is hydrolyzed by the alkaline electrolyte to improve conductivity of the coating. NASA

N80-18557* National Aeronautics and Space Administration. Lewis Research Center, Cleveland, Ohio.

CATALYST SURFACES FOR THE CHROMOUS/CHROMIC REDOX COUPLE Patent Application

Jose D. Giner (Giner, Inc.) and Kathleen J. Cahill, inventors (to NASA) (Giner, Inc.) Filed 27 Jul. 1979 15 p Sponsored by

NASA

(NASA-Case-Lew-13148-2; US-Patent-Appl-SN-061555) Avail: NTIS HC A02/MF A01 CSCL 10A

An electricity producing cell of the reduction-oxidation type is disclosed. The cell is divided into two compartments by a membrane and each compartment contains a solid inert electrode. A ferrous/ferric couple in a chloride solution serves as a cathode fluid which is circulated through one of the compartments to produce a positive electric potential disposed therein. A chromic/chromous couple in a chloride solution serves as an anode fluid which is circulated through the second compartment to produce a negative potential on an electrode disposed therein. The electrode is an electrically conductive, inert material plated with copper, silver or gold. A thin layer of lead plates onto the copper, silver or gold layer when the cell is being charged, the lead ions being available from lead chloride which has been added to the anode fluid. If the REDOX cell is then discharged, the current flows between the electrodes causing the lead to deplate from the negative electrode and the metal coating on the electrode will act as a catalyst to cause increased current density. NASA

N80-18563* National Aeronautics and Space Administration. Lewis Research Center, Cleveland, Ohio.

ENGINEERING EVALUATION OF A SODIUM HYDROXIDE THERMAL ENERGY STORAGE MODULE Final Report

Donald G. Perdue and Larry H. Gordon Feb. 1980 22 p refs (Contract EC-77-A-31-1034)

(NASA-TM-81417; DOE/NASA/1034-80/7; E-338) Avail: NTIS HC A02/MF A01 CSCL 10A

An engineering evaluation of thermal energy storage prototypes was performed in order to assess the development status of latent heat storage media. The testing and the evaluation of a prototype sodium hydroxide module is described. This module stored off-peak electrical energy as heat for later conversion to domestic hot water needs. R.E.S.

N80-19613* National Aeronautics and Space Administration. Lewis Research Center, Cleveland, Ohio.

TEETERED, TIP-CONTROLLED ROTOR: PRELIMINARY TEST RESULTS FROM MOD-0 100-KW EXPERIMENTAL WIND TURBINE

J. C. Glasgow and D. R. Miller 1980 16 p refs Presented at Wind Energy Conf., Boulder, Colo., 9-11 Apr. 1980; sponsored by Am. Inst. of Aeron. and Astronautics and the Midwest Res. Inst.

(Contract EX-76-I-01-1028)

(NASA-TM-81445; DOE/NASA/1028-80/26; E-365) Avail: NTIS HC A02/MF A01 CSCL 10B

Results of tests conducted using the MOD-0 100 kW experimental wind turbine are evaluated. The teetered rotor significantly decreased loads on the yaw drive mechanism and reduced blade cyclic flapwise bending moments by 25 percent at the 20 percent span location when compared to the rigid hub rotor. The teetered hub performed well, but impacted the teeter stops on occasion as wind speed and/or direction varied rapidly. The tip-controlled rotor performed satisfactorily with some expected loss of control when compared to the full span pitchable blade. The performance results indicate that a review of techniques used to calculate rotor power is in order. K.L.

N80-19614* National Aeronautics and Space Administration. Lewis Research Center, Cleveland, Ohio.

INSTALLATION AND CHECKOUT OF THE DOE/NASA MOD-1 2000-KW WIND TURBINE GENERATOR

Richard L. Puthoff and John L. Collins 1980 25 p refs Presented at Wind Energy Conf., Boulder, Colo. 9-11 Apr. 1980; sponsored by Am. Inst. of Aeron. and Astronautics and the Midwest Res. Inst.

(Contract EX-77-A-29-1010)

(NASA-TM-81444; DOE/NASA/1010-80/6; E-364) Avail: NTIS HC A02/MF A01 CSCL 10B

The Mod-1 machine was assembled without the blades, tested, and sent to the site at Boone, North Carolina for erection. The blades were transported directly to the site. A series of

checkout tests were then conducted to evaluate performance and loads. The results of these tests compared well with the design data. K.L.

N80-19626* National Aeronautics and Space Administration. Lewis Research Center, Cleveland, Ohio.

COGENERATION TECHNOLOGY ALTERNATIVES STUDY (CTAS), VOLUME 1: SUMMARY

Gerald J. Barna, Raymond K. Burns, and Gary D. Sagerman Jan. 1980 89 p

(Contract EC-77-A-31-1062)

(NASA-TM-81400; DOE/NASA/1062-80/4; E-312) Avail: NTIS HC A05/MF A01 CSCL 10B

Various advanced energy conversion systems that can use coal or coal-derived fuels for industrial cogeneration applications were compared to provide information needed by DOE to establish research and development funding priorities for advanced-technology systems that could significantly advance the use of coal or coal-derived fuels in industrial cogeneration. Steam turbines, diesel engines, open-cycle gas turbines, combined cycles, closed-cycle gas turbines, Stirling engines, phosphoric acid fuel cells, molten carbonate fuel cells, and thermionics were studied with technology advancements appropriate for the 1985-2000 time period. The various advanced systems were compared and evaluated for wide diversity of representative industrial plants on the basis of fuel energy savings, annual energy cost savings, emissions savings, and rate of return on investment as compared with purchasing electricity from a utility and providing process heat with an on-site boiler. Also included in the comparisons and evaluations are results extrapolated to the national level.

F.O.S.

N80-21837* National Aeronautics and Space Administration. Lewis Research Center, Cleveland, Ohio.

FLAME TUBE PARAMETRIC STUDIES FOR CONTROL OF FUEL BOUND NITROGEN USING RICH-LEAN TWO-STAGE COMBUSTION

Donald F. Schultz and Gary Wolfbrandt 1980 25 p refs Presented at Western States Sect. of the Combust. Inst. of Spring Meeting, Irvine, Calif., 21-22 Apr. 1980

(Contract EF-77-A-01-2593)

(NASA-TM-81472; DOE/NASA/2593-80/15; E-405) Avail: NTIS HC A02/MF A01 CSCL 21B

An experimental parametric study of rich-lean two-stage combustion in a flame tube is described and approaches for minimizing the conversion of fuel-bound nitrogen to nitrogen oxides in a premixed, homogeneous combustion system are evaluated. Air at 672 K and 0.48 MPa was premixed with fuel blends of propane, toluene, and pyridine at primary equivalence ratios ranging from 0.5 to 2.0 and secondary equivalence ratios of 0.5 to 0.7. Distillates of SRC-II, a coal syncrude, were also tested. The blended fuels were proportioned to vary fuel hydrogen composition from 9.0 to 18.3 weight percent and fuel nitrogen composition from zero to 1.5 weight percent. Rich-lean combustion proved effective in reducing fuel nitrogen to NO sub x conversion; conversion rates up to 10 times lower than those normally produced by single-stage combustion were achieved. The optimum primary equivalence ratio, where the least NO sub x was produced and combustion efficiency was acceptable, shifted between 1.4 and 1.7 with changes in fuel nitrogen content and fuel hydrogen content. Increasing levels of fuel nitrogen content lowered the conversion rate, but not enough to avoid higher NO sub x emissions as fuel nitrogen increased. M.G.

N80-22776* National Aeronautics and Space Administration. Lewis Research Center, Cleveland, Ohio.

LITERATURE SURVEY OF PROPERTIES OF SYNFUELS DERIVED FROM COAL Interim Report

Thaine W. Reynolds, Richard W. Niedzwiecki, and John S. Clark Feb. 1980 162 p refs

(Contract EF-77-A-01-2593)

(NASA-TM-79243; DOE/NASA/2593-79/8; E-150) Avail: NTIS HC A08/MF A01 CSCL 21D

A literature survey of the properties of synfuels for ground-based gas turbine applications is presented. Four major concepts

for converting coal into liquid fuels are described: solvent extraction, catalytic liquefaction, pyrolysis, and indirect liquefaction. Data on full range syncrudes, various distillate cuts, and upgraded products are presented for fuels derived from various processes, including H-coal, synthoil, solvent-refined coal, donor solvent, zinc chloride hydrocracking, co-steam, and flash pyrolysis. Some typical ranges of data for coal-derived low Btu gases are also presented. R.E.S.

N80-22777* National Aeronautics and Space Administration. Lewis Research Center, Cleveland, Ohio.

ADVANCED SCREENING OF ELECTRODE COUPLES

J. Giner and K. Cahill Feb. 1980 56 p refs

(Contract NAS3-20794; EC-77-A-31-1002)

(NASA-CR-159738; DOE/NASA/0794-80/1) Avail: NTIS HC A04/MF A01 CSCL 10B

The chromium (Cr(3+)/Cr(2+)) redox couple (electrolyte and electrode) was investigated to determine its suitability as negative electrode for the iron (Fe(3+)/Fe(2+))-chromium (Cr(3+)/Cr(2+)) redox flow battery. Literature search and laboratory investigation established that the solubility and stability of aqueous acidic solutions of chromium(3) chloride and chromium(2) chloride are sufficient for redox battery application. Four categories of electrode materials were tested; namely, metals and metalloid materials (elements and compounds), alloys, plated materials, and Teflon-bonded materials. In all, the relative performance of 26 candidate electrode materials was evaluated on the basis of slow scan rate linear sweep voltammetry in stirred solution. No single material tested gave both acceptable anodic and acceptable cathodic performance. However, the identification of lead as a good cathodic electrocatalyst and gold as a good anodic electrocatalyst led to the invention of the lead/gold combination electrocatalyst. This type of catalyst can be fabricated in several ways and appears to offer the advantages of each metal without the disadvantages associated with their use as single materials. This lead/gold electrocatalyst was tested by NASA-Lewis Research Center in complete, flowing, redox batteries comprising a stack of several cells. A large improvement in the battery's coulombic and energy efficiency was observed. F.O.S.

N80-22788* National Aeronautics and Space Administration. Lewis Research Center, Cleveland, Ohio.

THERMAL ENERGY STORAGE: FOURTH ANNUAL REVIEW MEETING

Mar. 1980 650 p refs Meeting held at Tysons Corner, Va., 3-4 Dec. 1979; sponsored by DOE

(NASA-CP-2125; E-428; CONF-791232) Avail: NTIS HC A99/MF A01 CSCL 10C

The development of low cost thermal energy storage technologies is discussed in terms of near term oil savings, solar energy applications, and dispersed energy systems for energy conservation policies. Program definition and assessment and research and technology development are considered along with industrial storage, solar thermal power storage, building heating and cooling, and seasonal thermal storage. A bibliography on seasonal thermal energy storage emphasizing aquifer thermal energy is included. For individual titles, see N80-22789 through N80-22829.

N80-22790* National Aeronautics and Space Administration. Lewis Research Center, Cleveland, Ohio.

PROGRAM DEFINITION AND ASSESSMENT OVERVIEW

Larry H. Gordon In *its Thermal Energy Storage* Mar. 1980 p 38-41 refs (For primary document see N80-22788 13-44)

Avail: NTIS HC A99/MF A01 CSCL 10B

The implementation of a program level assessment of thermal energy storage technology thrusts for the near and far term to assure overall coherent energy storage program is considered. The identification and definition of potential thermal energy storage applications, definition of technology requirements, and appropriate market sectors are discussed along with the necessary coordination, planning, and preparation associated with program reviews, workshops, multi-year plans and annual operating plans for the major laboratory tasks. J.M.S.

N80-22795* National Aeronautics and Space Administration. Lewis Research Center, Cleveland, Ohio.

INDUSTRIAL STORAGE APPLICATIONS OVERVIEW

Rudolph A. Duschka. *In its Thermal Energy Storage*. Mar. 1980 p 85-94. refs (For primary document see N80-22788 13-44) Avail: NTIS HC A99/MF A01 CSCL 10B

The implementation of a technology demonstration for the food processing industry, development and technology demonstrations for selected near-term, in-plant applications and advanced industrial applications of thermal energy storage are overviewed.

R.E.S.

N80-22797* National Aeronautics and Space Administration. Lewis Research Center, Cleveland, Ohio.

COLLECTION AND DISSEMINATION OF TES SYSTEM INFORMATION FOR THE PAPER AND PULP INDUSTRY

M. W. Dietrich and Howard Edde (Edde (Howard), Inc., Bellevue, Wash.) *In its Thermal Energy Storage*. Mar. 1980 p 105-111 (For primary document see N80-22788 13-44) (Contract DEN3-190)

Avail: NTIS HC A99/MF A01 CSCL 10B

A survey of U.S. and international paper and pulp mills using thermal energy storage (TES) systems as a part of their production processes was conducted to obtain sufficient operating data to conduct a benefits analysis encompassing: (1) an energy conservation assessment, (2) an economic benefits analysis, and (3) an environmental impact assessment. An information dissemination plan was then proposed to effectively present the benefits of TES to the U.S. paper and pulp industry.

R.E.S.

N80-23769* National Aeronautics and Space Administration. Lewis Research Center, Cleveland, Ohio.

CELL MODULE AND FUEL CONDITIONER Quarterly Report, Jan. Mar. 1980

D. Q. Hoover, Jr. Apr. 1980 87 p

(Contracts DEN3-161; DE-AI03-79ET-11272)

(NASA-CR-159875; DOE/NASA/O161-2; QR-2) Avail: NTIS HC A05/MF A01 CSCL 10A

Stack tests indicate that the discrepancies between calculated and measured temperature profiles are due to reactant cross-over and a lower than expected thermal conductivity of cells. Preliminary results indicate that acceptable contact resistance between cooling plane halves can be achieved without the use of paper. The preliminary design of the enclosure, definition of required labor and equipment for manufacturing repeating components, and the assembly procedures for the benchmark design were developed. Fabrication of components for a second 5-cell stack of the MK-2 design and a second 23-cell stack of the MK-1 design was started. The definition of water and fuel for the reforming subsystem was developed along with a preliminary definition of the control system for the subsystem. The construction and shakedown of the differential catalytic reactor was completed and testing of the first catalyst initiated.

R.E.S.

N80-23777* National Aeronautics and Space Administration. Lewis Research Center, Cleveland, Ohio.

REDOX STORAGE SYSTEMS FOR SOLAR APPLICATIONS

Norman H. Hagedorn and Lawrence H. Thaller. 1980 28 p. Proposed for presentation at Power Sources Conf., Brighton, England, 15-18 Sep. 1980

(Contract EF-77-A-31-1002)

(NASA-TM-81464; DOE/NASA/1002-80/5; E-383) Avail: NTIS HC A03/MF A01 CSCL 10A

The NASA Redox energy storage system is described. The system is based on soluble aqueous iron and chromium chloride redox couples. The needed technology advances in the two elements (electrodes and membranes) that are key to its technological feasibility have been achieved and system development has begun. The design, construction, and test of a 1 kilowatt system integrated with a solar photovoltaic array is discussed.

R.E.S.

N80-23778* National Aeronautics and Space Administration. Lewis Research Center, Cleveland, Ohio.

THE OPTIMIZATION AIR SEPARATION PLANTS FOR

COMBINED CYCLE MHD-POWER PLANT APPLICATIONS

Albert J. Juhasz, Helmut Springmann, and Ralph Greenberg. 1980 11 p. refs. Presented at the 7th Intern. Conf. on MHD Elec. Power Generation, Cambridge, Mass., 16-20 Jun. 1980 (Contracts DEN3-165; EF-77-A-01-2674)

(NASA-TM-81510; DOE/NASA/2674-80/10) Avail: NTIS HC A02/MF A01 CSCL 10B

Some of the design approaches being employed during a current supported study directed at developing an improved air separation process for the production of oxygen enriched air for magnetohydrodynamics (MHD) combustion are outlined. The ultimate objective is to arrive at conceptual designs of air separation plants, optimized for minimum specific power consumption and capital investment costs, for integration with MHD combined cycle power plants.

R.E.S.

N80-23779* National Aeronautics and Space Administration. Lewis Research Center, Cleveland, Ohio.

THE EFFECT OF CATALYST LENGTH AND DOWNSTREAM REACTOR DISTANCE ON CATALYTIC COMBUSTOR PERFORMANCE

David Anderson. 1980 24 p. refs. Presented at the 4th Workshop on Catalytic Combust., Cincinnati, 14-15 May 1980; sponsored by EPA

(Contract EC-77-A-31-1040)

(NASA-TM-81475; DOE/NASA/1040-80/14; E-409) Avail: NTIS HC A02/MF A01 CSCL 10B

A study was made to determine the effects on catalytic combustor performance which resulted from independently varying the length of a catalytic reactor and the length available for gas-phase reactions downstream of the catalyst. Monolithic combustion catalysts from three manufacturers were tested in a combustion test rig with no. 2 diesel fuel. Catalytic reactor lengths of 2.5 and 5.4 cm, and downstream gas-phase reaction distances of 7.3, 12.4, 17.5, and 22.5 cm were evaluated. Measurements of carbon monoxide, unburned hydrocarbons, nitrogen oxides, and pressure drop were made. The catalytic-reactor pressure drop was less than 1 percent of the upstream total pressure for all test configurations and test conditions. Nitrogen oxides and unburned hydrocarbons emissions were less than 0.25 g NO₂/kg fuel and 0.6 g HC/kg fuel, respectively. The minimum operating temperature (defined as the adiabatic combustion temperature required to obtain carbon monoxide emissions below a reference level of 13.6 g CO/kg fuel) ranged from 1230 K to 1500 K for the various conditions and configurations tested. The minimum operating temperature decreased with increasing total (catalytic-reactor-plus-downstream-gas-phase-reactor-zone) residence time but was independent of the relative times spent in each region when the catalytic-reactor residence time was greater than or equal to 1.4 ms.

R.E.S.

N80-23780* National Aeronautics and Space Administration. Lewis Research Center, Cleveland, Ohio.

SUMMARY AND EVALUATION OF THE PARAMETRIC STUDY OF POTENTIAL EARLY COMMERCIAL MHD POWER PLANTS (PSPEC)

Peter J. Stagner and John M. Abbott. 1980 11 p. refs. Presented at the 7th Intern. Conf. on Magnetohydrodyn. Elec. Generation, Cambridge, Mass., 16-20 Jun. 1980; sponsored by the Symp. on the Eng. Aspects of Magnetohydrodyn., Inc. (Contract EF-77-A-31-2674)

(NASA-TM-81497; DOE/NASA/2674-80/9; E-434) Avail: NTIS HC A02/MF A01 CSCL 10B

Two parallel contracted studies were conducted. Each contractor investigated three base cases and parametric variations about these base cases. Each contractor concluded that two of the base cases (a plant using separate firing of an advanced high temperature regenerative air heater with fuel from an advanced coal gasifier and a plant using an intermediate temperature metallic recuperative heat exchanger to heat oxygen enriched combustion air) were comparable in both performance and cost of electricity. The contractors differed in the level of their cost estimates with the capital cost estimates for the MHD topping cycle and the magnet subsystem in particular accounting for a significant part of the difference. The impact of the study on the decision to pursue a course which leads to an

oxygen enriched plant as the first commercial MHD plant is described. R.E.S.

N80-24756* National Aeronautics and Space Administration. Lewis Research Center, Cleveland, Ohio.

AN ELECTRIC VEHICLE PROPULSION SYSTEM'S IMPACT ON BATTERY PERFORMANCE: AN OVERVIEW

John M. Bozek, John J. Smithrick, Robert C. Cataldo, and John G. Ewashinka 1980 10 p refs Presented at the 3d Intern. Elec. Vehicle Exposition and Conf., St. Louis, 20-22 May 1980 (Contract EC-77-A-31-1044)

(NASA-TM-81515; DOE/NASA/1044-7; E-459) Avail: NTIS HC A02/MF A01 CSCL 10B

The performance of two types of batteries, lead-acid and nickel-zinc, was measured as a function of the charging and discharging demands anticipated from electric vehicle propulsion systems. The benefits of rapid high current charging were mixed; although it allowed quick charges, the energy efficiency was reduced. For low power (overnight) charging the current wave shapes delivered by the charger to the battery tended to have no effect on the battery cycle life. The use of chopper speed controllers with series traction motors resulted in a significant reduction in the energy available from a battery whenever the motor operates at part load. The demand placed on a battery by an electric vehicle propulsion system containing electrical regenerative braking confirmed significant improvement in short term performance of the battery. R.E.S.

N80-25779* National Aeronautics and Space Administration. Lewis Research Center, Cleveland, Ohio.

THERMAL ENERGY STORAGE

Jun. 1980 77 p refs

(Contract EC-77-A-31-1034)

(NASA-TM-81514; E-457; DOE/NASA/1034-8) Avail: NTIS HC A05/MF A01 CSCL 10C

The planning and implementation of activities associated with lead center management role and the technical accomplishments pertaining to high temperature thermal energy storage subsystems are described. Major elements reported are: (1) program definition and assessment; (2) research and technology development; (3) industrial storage applications; (4) solar thermal power storage applications; and (5) building heating and cooling applications. R.E.S.

N80-25780* National Aeronautics and Space Administration. Lewis Research Center, Cleveland, Ohio.

PULSE CHARGING OF LEAD-ACID TRACTION CELLS

John J. Smithrick May 1980 22 p refs

(Contract EC-77-A-31-1044)

(NASA-TM-81513; DOE/NASA/1044-6; E-454) Avail: NTIS HC A02/MF A01 CSCL 10C

Pulse charging, as a method of rapidly and efficiently charging 300 amp-hour lead-acid traction cells for an electric vehicle application was investigated. A wide range of charge pulse current square waveforms were investigated and the results were compared to constant current charging at the time averaged pulse current values. Representative pulse current waveforms were: (1) positive waveform-peak charge pulse current of 300 amperes (amps), discharge pulse-current of zero amps, and a duty cycle of about 50%; (2) Romanov waveform-peak charge pulse current of 300 amps, peak discharge pulse current of 15 amps, and a duty of 50%; and (3) McCulloch waveform peak charge pulse current of 193 amps, peak discharge pulse current of about 575 amps, and a duty cycle of 94%. Experimental results indicate that on the basis of amp-hour efficiency, pulse charging offered no significant advantage as a method of rapidly charging 300 amp-hour lead-acid traction cells when compared to constant current charging at the time average pulse current value. There were, however, some disadvantages of pulse charging in particular a decrease in charge amp-hour and energy efficiencies and an increase in cell electrolyte temperature. The constant current charge method resulted in the best energy efficiency with no significant sacrifice of charge time or amp-hour output. Whether or not pulse charging offers an advantage over constant current charging with regard to the cell charge/discharge cycle life is unknown at this time. R.E.S.

N80-27799* National Aeronautics and Space Administration. Lewis Research Center, Cleveland, Ohio.

ENGINEERING TEST FACILITY DESIGN DEFINITION

R. W. Bercau and G. R. Seikel 20 Jun. 1980 16 p refs Presented at 7th Intern. Conf. on Magnetohydrodynamic Elect. Power Generation, Cambridge, Mass., 16-20 Jun. 1980; sponsored by Symp. on the Eng. Aspects of Magnetohydrodynamics, Inc.

(Contract EF-77-A-01-2674)

(NASA-TM-81499; DOE/NASA/2674-11; E-436) Avail: NTIS HC A02/MF A01 CSCL 10A

The Engineering Test Facility (ETF) is the major focus of the Department of Energy (DOE) Magnetohydrodynamics (MHD) Program to facilitate commercialization and to demonstrate the commercial operability of MHD/steam electric power. The ETF will be a fully integrated commercial prototype MHD power plant with a nominal output of 200 MW sub e. Performance of this plant is expected to meet or surpass existing utility standards for fuel, maintenance, and operating costs; plant availability; load following; safety; and durability. It is expected to meet all applicable environmental regulations. The current design concept conforming to the general definition, the basis for its selection, and the process which will be followed in further defining and updating the conceptual design. Author

N80-27804* National Aeronautics and Space Administration. Lewis Research Center, Cleveland, Ohio.

EFFECT ON COMBINED CYCLE EFFICIENCY OF STACK GAS TEMPERATURE CONSTRAINTS TO AVOID ACID CORROSION Final Report

Joseph J. Nainiger Jul. 1980 16 p refs

(Contract EF-77-A-01-2593)

(NASA-TM-81531; DOE/NASA/2593-17; E-483) Avail: NTIS HC A02/MF A01 CSCL 10B

To avoid condensation of sulfuric acid in the gas turbine exhaust when burning fuel oils containing sulfur, the exhaust stack temperature and cold-end heat exchanger surfaces must be kept above the condensation temperature. Raising the exhaust stack temperature, however, results in lower combined cycle efficiency compared to that achievable by a combined cycle burning a sulfur-free fuel. The maximum difference in efficiency between the use of sulfur-free and fuels containing 0.8 percent sulfur is found to be less than one percentage point. The effect of using a ceramic thermal barrier coating (TBC) and a fuel containing sulfur is also evaluated. The combined-cycle efficiency gain using a TBC with a fuel containing sulfur compared to a sulfur-free fuel without TBC is 0.6 to 1.0 percentage points with air-cooled gas turbines and 1.6 to 1.8 percentage points with water-cooled gas turbines. Author

N80-27805* National Aeronautics and Space Administration. Lewis Research Center, Cleveland, Ohio.

IMPACT OF PROPULSION SYSTEM R AND D ON ELECTRIC VEHICLE PERFORMANCE AND COST

Harvey J. Schwartz and Andrew L. Gordan 22 May 1980 16 p refs Presented at 3d Intern. Electric Vehicle Exposition and Conf., St. Louis, 20-22 May 1980

(Contract EC-77-A-31-1044)

(NASA-TM-81548; DOE/NASA/1044-9; E-504) Avail: NTIS HC A02/MF A01 CSCL 10B

The efficiency, weight, and manufacturing cost of the propulsion subsystem (motor, motor controller, transmission, and differential, but excluding the battery) are major factors in the purchase price and cost of ownership of a traffic-compatible electric vehicle. The relative impact of each was studied, and the conclusions reached are that propulsion system technology advances can result in a major reduction of the sticker price of an electric vehicle and a smaller, but significant, reduction in overall cost of ownership. L.F.M.

N80-28859* National Aeronautics and Space Administration. Lewis Research Center, Cleveland, Ohio. Energy Technology Operation.

COGENERATION TECHNOLOGY ALTERNATIVES STUDY

(CTAS). VOLUME 2: ANALYTICAL APPROACH Final Report

H. E. Gerlaugh, E. W. Hall, D. H. Brown, R. R. Priestley, and W. F. Knightly. May 1980. 106 p. refs.
(Contract DEN3-31)
(NASA-CR-159766; DOE/NASA/0031-80-2;
GE80ETO10-Vol-2) Avail. NTIS HC A06/MF A01 CSCL 10B

The use of various advanced energy conversion systems were compared with each other and with current technology systems for their savings in fuel energy, costs, and emissions in individual plants and on a national level. The ground rules established by NASA and assumptions made by the General Electric Company in performing this cogeneration technology alternatives study are presented. The analytical methodology employed is described in detail and is illustrated with numerical examples together with a description of the computer program used in calculating over 7000 energy conversion system-industrial process applications. For Vol. 1, see N80-24797. R.E.S.

N80-29862* National Aeronautics and Space Administration. Lewis Research Center, Cleveland, Ohio.

RAPPORTEUR REPORT: MHD ELECTRIC POWER PLANTS

George R. Seikel. 1980. 17 p. Presented at 7th Intern. Conf. on MHD Elec. Power Generation, Cambridge, Mass. 16-20 Jun. 1980.

(Contract EF-77-A-01-2674)
(NASA-TM-81554; DOE/NASA/2674-12; E-516) Avail. NTIS HC A02/MF A01 CSCL 10B

Five US papers from the Proceedings of the Seventh International Conference on MHD Electrical Power Generation at the Massachusetts Institute of Technology are summarized. Results of the initial parametric phase of the US effort on the study of potential early commercial MHD plants are reported and aspects of the smaller commercial prototype plant termed the Engineering Test Facility are discussed. The alternative of using a disk geometry generator rather than a linear generator in baseload MHD plants is examined. Closed-cycle as well as open-cycle MHD plants are considered. A.R.H.

N80-29863* National Aeronautics and Space Administration. Lewis Research Center, Cleveland, Ohio.

GAS PHASE OXIDATION DOWNSTREAM OF A CATALYTIC COMBUSTOR

James S. Tien (Case Western Reserve Univ.) and David N. Anderson. 1979. 13 p. refs. Presented at 13th Middle Atlantic Regional Meeting of the ACS, West Long Branch, N.J., 19-23 Mar. 1979.

(Contract EC-77-A-31-1040)
(NASA-TM-81551; DOE/NASA/1040-16; E-512) Avail. NTIS HCA02/MFA01 CSCL 10A

Effect of the length available for gas-phase reactions downstream of the catalytic reactor on the emission of CO and unburned hydrocarbons was investigated. A premixed, pre-vaporized propane/air feed to a 12/cm diameter catalytic reactor test section was used. The catalytic reactor was made of four 2.5 cm long monolithic catalyst elements. Four water cooled gas sampling probes were located at positions between 0 and 22 cm downstream of the catalytic reactor. Measurements of unburned hydrocarbon, CO, and CO₂ were made. Tests were performed with an inlet air temperature of 800 K, a reference velocity of 10 m/s, pressures of 3 and 600,000 Pa, and fuel air equivalence ratios of 0.14 to 0.24. For very lean mixtures, hydrocarbon emissions were high and CO continued to be formed downstream of the catalytic reactor. At the highest equivalence ratios tested, hydrocarbon levels were much lower and CO was oxidized to CO₂ in the gas phase downstream. To achieve acceptable emissions, a downstream region several times longer than the catalytic reactor could be required. R.K.G.

N80-32858* National Aeronautics and Space Administration. Lewis Research Center, Cleveland, Ohio.

LARGE WIND TURBINES: A UTILITY OPTION FOR THE GENERATION OF ELECTRICITY

W. H. Robbins, R. L. Thomas, and D. H. Baldwin. 1980. 18 p. refs. Presented at the Am. Power Conf., Chicago, 21-23 Apr. 1980, sponsored by Illinois Inst. of Tech.; presented at the Ann. Solar Energy Program Rev., Rockport, Maine, 26-28 Aug. 1980, sponsored by Electric Power Research Inst.
(Contract DE-AI01-79ET-23139)
(NASA-TM-81502; DOE/NASA/23139-1; E-440) Avail. NTIS HC A02/MF A01 CSCL 10B

The wind resource is such that wind energy generation has the potential to save 6-7 quads of energy nationally. Thus, the Federal Government is sponsoring and encouraging the development of cost effective and reliable wind turbines. One element of the Federal Wind Energy Programs, Large Horizontal Axis Wind Turbine Development, is managed by the NASA Lewis Research Center for the Department of Energy. There are several ongoing wind system development projects oriented primarily toward utility application within this program element. In addition, a comprehensive technology program supporting the wind turbine development projects is being conducted. An overview is presented of the NASA activities with emphasis on application of large wind turbines for generation of electricity by utility systems. Author

N80-33857* National Aeronautics and Space Administration. Lewis Research Center, Cleveland, Ohio.

TOROIDAL CELL AND BATTERY Patent Application

William J. Nagle, inventor (to NASA). Filed 28 Mar. 1980. 13 p.
(NASA-Case-LEW-12918-1; US-Patent-Appl-SN-134855) Avail. NTIS HC A02/MF A01 CSCL 10C

A toroidal cell is disclosed which includes a wound core disposed within a pair of toroidal channel shaped electrodes separated by nylon insulator. The shape of the case electrodes of this cell allows one doughnut shaped surface and the inner cylindrical case wall to be used as an electrode and a second planar doughnut shaped surface and the outer cylindrical case wall to be used as another electrode. Connectors may be used to stack two or more toroidal cells together by connecting the entire surface area of the electrode of one cell to the entire surface area of the electrode of a second cell. The central cavity of each toroidal cell may be used as a conduit for pumping a fluid through the toroidal cell to thereby cool the cell. NASA

N80-33869* National Aeronautics and Space Administration. Lewis Research Center, Cleveland, Ohio.

RADIATION DAMAGE IN HIGH VOLTAGE SILICON SOLAR CELLS

Irving Weinberg, Henry W. Brandhorst, Clifford K. Swartz, and Victor G. Weizer. In: ESA Photovoltaic Generators in Space Jun. 1980. p. 129-134. refs. (For primary document see N80-33873 24-44)

Avail. NTIS HC A12/MF A01; ESA, Paris FF 80 CSCL 10A

High open circuit voltage cell designs based on 0.1 Ohm cm p-type silicon were irradiated with 1 MeV electrons and their performance determined to fluences as high as 10 to the 15th power per sq cm. Of the three cell designs, radiation induced degradation was greatest in the high low emitter (HLE) cell. The diffused and ion implanted cells degraded approximately equally but less than the HLE cell. Degradation was greatest in an HLE cell exposed to X-rays before electron irradiation. The cell regions controlling both short circuit current and open circuit voltage degradation were defined in all three cell types. An increase in front surface recombination velocity accompanied time dependent degradation of an HLE cell after X-irradiation. It was speculated that this was indirectly due to a decrease in positive charge at the silicon oxide interface. Modifications aimed at reducing radiation induced degradation are proposed for all three cell types. Author (ESA)

A80-11972 * Survey of MHD plant applications. J. J. Lynch (U.S. Department of Energy, Washington, D.C.), G. R. Seikel (NASA, Lewis Research Center, Cleveland, Ohio), and J. C. Cutting (Gilbert/Commonwealth, Inc., Reading, Pa.). In: Energy technology VI: Achievements in perspective; Proceedings of the Sixth Conference, Washington, D.C., February 26-28, 1979. (A80-11953 02-44)

Washington, D.C., Government Institutes, Inc., 1979, p. 793-807. 24 refs.

Open-cycle MHD is one of the major R&D efforts in the Department of Energy's program to meet the national goal of reducing U.S. dependence on oil through increased utilization of coal. MHD offers an effective way to use coal to produce electric power at low cost in a highly efficient and environmentally acceptable manner. Open-cycle MHD plants are categorized by the MHD combustor oxidizer, its temperature and the method of preheat. The paper discusses MHD baseline plant design, open-cycle MHD plant in the Energy Conversion Alternatives Study (ECAS), early commercial MHD plants, conceptual studies of the engineering test facility, retrofit (addition of an MHD topping cycle to an existing steam plant), and other potential applications and concepts. Emphasis is placed on a survey of both completed and ongoing studies to define both commercial and pilot plant design, cost, and performance. S.D.

A80-28804 * # Numerical calculation of steady inviscid full potential compressible flow about wind turbine blades. D. S. Dulikravich (NASA, Lewis Research Center, Cleveland, Ohio). In: Wind Energy Conference, Boulder, Colo., April 9-11, 1980, Technical Papers. (A80-28801 10-44) New York, American Institute of Aeronautics and Astronautics, Inc., 1980, p. 14-19, 9 refs. Research sponsored by the National Research Council. (AIAA 80-0607)

The air flow through a propeller-type wind turbine rotor is characterized by three-dimensional rotating cascade effects about the inner portions of the rotor blades and compressibility effects about the tip regions of the blades. In the case of large rotor diameter and/or increased rotor angular speed, the existence of small supersonic zones terminated by weak shocks is possible. An exact nonlinear mathematical model (called a steady Full Potential Equation - FPE) that accounts for the above phenomena has been rederived. An artificially time dependent version of FPE was iteratively solved by a finite volume technique involving an artificial viscosity and a three-level consecutive mesh refinement. The exact boundary conditions were applied by generating a boundary conforming periodic computation mesh. (Author)

A80-28835 * # Installation and checkout of the DOE/NASA Mod-1 2000-kW wind turbine generator. R. L. Puthoff, J. L. Collins, and R. A. Wolf (NASA, Lewis Research Center, Cleveland, Ohio). In: Wind Energy Conference, Boulder, Colo., April 9-11, 1980, Technical Papers. (A80-28801 10-44) New York, American Institute of Aeronautics and Astronautics, Inc., 1980, p. 249-260, 5 refs. (AIAA 80-0638)

The paper describes the DOE/NASA Mod-1 wind turbine generator, its assembly and testing, and its installation at Boone, North Carolina. The paper concludes with performance data taken during the initial tests conducted on the machine. The successful installation and initial operation of the Mod-1 wind turbine generator has had the following results: (1) megawatt-size wind turbines can be operated satisfactorily on utility grids; (2) the structural loads can be predicted by existing codes; (3) assembly of the machine on top of the tower presents no major problem; (4) large blades 100 ft long can be transported long distances and over mountain roads; and (5) operating experience and performance data will contribute substantially to the design of future low-cost wind turbines. S.D.

A80-28836 * # Teetered, tip-controlled rotor - Preliminary test results from Mod-O 100-kW experimental wind turbine. J. C. Glasgow and D. R. Miller (NASA, Lewis Research Center, Cleveland, Ohio). In: Wind Energy Conference, Boulder, Colo., April 9-11, 1980, Technical Papers. (A80-28801 10-44) New York, American Institute of Aeronautics and Astronautics, Inc., 1980, p. 261-268, 5 refs. (AIAA 80-0642)

A series of tests is currently being conducted using the DOE/NASA 100 kW Experimental Wind Turbine with a two-bladed, teetered rotor with 30% span tip control. Preliminary evaluation test results indicate that the teetered rotor significantly decreases loads

on the yaw drive mechanism and reduces blade cyclic flapwise bending moments by 25% at the 20% span location when compared to rigid hub rotor. The teetered hub performed well but did impact the teeter stops on occasion as wind speed and/or direction varied rapidly. The tip-controlled rotor performed satisfactorily with some expected loss of control when compared to the full span pitchable blade. The performance results indicate that a review of techniques used to calculate rotor power is in order. (Author)

A80-35730 * # The use of wind data with an operational wind turbine in a research and development environment. H. E. Neustadter (NASA, Lewis Research Center, Cleveland, Ohio). In: Conference and Workshop on Wind Energy Characteristics and Wind Energy Siting, Portland, Ore., June 19-21, 1979, Proceedings. (A80-35716 14-44) Boston, Mass., American Meteorological Society, 1979, p. 179-188; Discussion, p. 189, 9 refs.

It is noted that in 1978, 17 candidate sites were identified for detailed evaluation as potential sites for installation of large, horizontal axis Wind Turbines (WT). Attention is given to the Mod-OA, a 200 kW WT located in Clayton, New Mexico. The discussion covers the meteorological data collected, some of the analyses based on these wind data as well as additional areas currently being investigated in relation to these data. M.E.P.

A80-39639 * # Improved PFB operations - 400-hour turbine test results. R. J. Rollbuhler, S. M. Benford, and G. R. Zellars (NASA, Lewis Research Center, Cleveland, Ohio). DOE, EPRI, EPA, and Tennessee Valley Authority, International Conference on Fluidized Bed Combustion, 6th, Atlanta, Ga., Apr. 9-11, 1980, Paper. 21 p. 14 refs.

The paper deals with a 400-hr small turbine test in the effluent of a pressurized fluidized bed (PFB) at an average temperature of 770 C, an average relative gas velocity of 300 m/sec, and average solid loadings of 200 ppm. Consideration is given to combustion parameters and operating procedure as well as to the turbine system and turbine test operating procedures. Emphasis is placed on erosion/corrosion results. V.T.

A80-39642 * # Comments on TEC trends. J. F. Morris (NASA, Lewis Research Center, Cleveland, Ohio). Institute of Electrical and Electronics Engineers, International Conference on Plasma Science, Montreal, Canada, June 4-6, 1979, Paper. 26 p. 54 refs.

The paper comments on published and projected thermionic-energy-conversion (TEC) performance trends. This commentary includes graphs and an appendix relating TEC performance parameters, plots of predicted and actual TEC trends, a figure relating projected cost of electricity to overall efficiency for TEC topping, and a discussion of the implications of these relationships. V.T.

A80-40335 * # Modified aerospace R&QA method for wind turbines. W. E. Klein (NASA, Lewis Research Center, Cleveland, Ohio). In: Annual Reliability and Maintainability Symposium, San Francisco, Calif., January 22-24, 1980, Proceedings. (A80-40301 16-38) New York, Institute of Electrical and Electronics Engineers, Inc., 1980, p. 254-258.

This paper describes the Safety, Reliability and Quality Assurance (SR&QA) approach developed for the first large wind turbine generator project, MOD-OA. The SR&QA approach to be used had to assure that the machine would not be hazardous, would operate unattended on a utility grid, would demonstrate reliable operation, and would help establish the quality assurance and maintainability requirements for wind turbine projects. The final approach consisted of a modified Failure Modes and Effects Analysis (FMEA) during the design phase, minimal hardware inspections during parts fabrication, and three documents to control activities during machine construction and operation. (Author)

A80-40338 * # Photovoltaic power system reliability considerations. V. R. Lalli (NASA, Lewis Research Center, Cleveland, Ohio). In: Annual Reliability and Maintainability Symposium, San Francisco, Calif., January 22-24, 1980, Proceedings. (A80-40301 16-38) New York, Institute of Electrical and Electronics Engineers, Inc., 1980, p. 283-286.

This paper describes an example of how modern engineering and safety techniques can be used to assure the reliable and safe operation of photovoltaic power systems. This particular application was for a solar cell power system demonstration project in Tangaye, Upper Volta, Africa. The techniques involve a definition of the power system natural and operating environment, use of design criteria and analysis techniques, an awareness of potential problems via the inherent reliability and FMEA methods, and use of a fail-safe and planned spare parts engineering philosophy. (Author)

A80-45722 * # Spectral effects on direct-insolation absorptance of five collector coatings. G. B. Hotchkiss (Texas Instruments, Inc., Dallas, Tex.), F. F. Simon (NASA, Lewis Research Center, Cleveland, Ohio), and L. C. Burmeister (Kansas, University, Lawrence, Kan.). *American Society of Mechanical Engineers and American Institute of Chemical Engineers, Joint National Heat Transfer Conference, 18th, San Diego, Calif., Aug. 6-8, 1979, ASME Paper 79-HT-18, 7 p. 16 refs. Members, \$1.50; nonmembers, \$3.00. Grant No. NSG-3087.*

Absorptances for direct insolation of black chrome, black nickel, copper oxide, and two black zinc conversion selective coatings were calculated for a number of typical solar spectrums. Measured spectral reflectances were used while the effects of atmospheric ozone density, turbidity, and air mass were incorporated in calculated direct solar spectrums. Absorptance variation for direct insolation was found to be of the order of 1 percent for a typical range of clear-sky atmospheric conditions. (Author)

A80-46414 * # Cycles till failure of silver-zinc cells with competing failure modes - Preliminary data analysis. S. M. Sidik, H. F. Leibecki, and J. M. Bozek (NASA, Lewis Research Center, Cleveland, Ohio). *American Statistical Association, Annual Meeting, Houston, Tex., Aug. 11-14, 1980, Paper, 46 p. 10 refs.*

The data analysis of cycles to failure of silver-zinc electrochemical cells with competing failure modes is presented. The test ran 129 cells through charge-discharge cycles until failure; preliminary data analysis consisted of response surface estimate of life. Batteries fail through low voltage condition and an internal shorting condition; a competing failure modes analysis was made using maximum likelihood estimation for the extreme value life distribution. Extensive residual plotting and probability plotting were used to verify data quality and selection of model. A.T.

A80-46796 * Description of photovoltaic village power systems in the United States and Africa. A. F. Ratajczak and W. J. Bifano (NASA, Lewis Research Center, Cleveland, Ohio). In: Photovoltaic Solar Energy Conference, 2nd, Berlin, West Germany, April 23-26, 1979, Proceedings. (A80-46694 20-44) Dordrecht, D. Reidel Publishing Co., 1979, p. 1087-1095.

The paper describes the designs, hardware, and installations of NASA photovoltaic power systems in the village of Schuchuli in Arizona and Tangaye in Upper Volta, Africa. The projects were designed to demonstrate that current photovoltaic system technology can provide electrical power for domestic services for small, remote communities. The Schuchuli system has a 3.5 kW peak solar array which provides power for water pumping, a refrigerator for each family, lights, and community washing and sewing machines. The 1.8 kW Tangaye system provides power for pumping, flour milling, and lights in the milling building. Both are stand-alone systems operated by local personnel, and they are monitored by NASA to measure design adequacy and refine future designs. A.T.

A80-48194 * # Energy conservation and environmental benefits of thermal energy storage systems in the pulp and paper industry. H. Edde (Howard Edde, Inc., Bellevue, Wash.) and M. W. Dietrich (NASA, Lewis Research Center, Cleveland, Ohio). In: Energy to the 21st century; Proceedings of the Fifteenth Intersociety Energy Conversion Engineering Conference, Seattle, Wash., August 18-22, 1980, Volume 1. (A80-48165 21-44) New York, American Institute of Aeronautics and Astronautics, Inc., 1980, p. 239-242. 7 refs. Contract No. DEN3-190.

A80-48205 * # The planar multijunction cell - A new solar cell for earth and space. J. C. Evans, Jr., A. T. Chai (NASA, Lewis Research Center, Cleveland, Ohio), and C. Goradia. In: Energy to the 21st century; Proceedings of the Fifteenth Intersociety Energy Conversion Engineering Conference, Seattle, Wash., August 18-22, 1980, Volume 1. (A80-48165 21-44) New York, American Institute of Aeronautics and Astronautics, Inc., 1980, p. 358-363. 7 refs.

A new family of high-voltage solar cells, called the planar multijunction (PMJ) cell is being developed. The new cells combine the attractive features of planar cells with conventional or interdigitated back contacts and the vertical multijunction (VMJ) solar cell. The PMJ solar cell is internally divided into many voltage-generating regions, called unit cells, which are internally connected in series. The key to obtaining reasonable performance from this device was the separation of top surface field regions over each active unit cell area. Using existing solar cell fabricating methods, output voltages in excess of 20 volts per linear centimeter are possible. Analysis of the new device is complex, and numerous geometries are being studied which should provide substantial benefits in both normal sunlight usage as well as with concentrators. (Author)

A80-48329 * # Effect of positive pulse charge waveforms on cycle life of nickel-zinc cells. J. J. Smithrick (NASA, Lewis Research Center, Cleveland, Ohio). In: Energy to the 21st century; Proceedings of the Fifteenth Intersociety Energy Conversion Engineering Conference, Seattle, Wash., August 18-22, 1980, Volume 2. (A80-48165 21-44) New York, American Institute of Aeronautics and Astronautics, Inc., 1980, p. 1203-1206. 7 refs. Contract No. EC-77-A-31-1044.

Five amp-hour nickel-zinc cells were life cycled to evaluate four different charge methods. Three of the four waveforms investigated were 120 Hz full wave rectified sinusoidal (FWRS), 120 Hz silicon controlled rectified (SCR), and 1 kHz square wave (SW). The fourth, a constant current method, was used as a baseline of comparison. Three sealed Ni-Zn cells connected in series were cycled. Each series string was charged at an average $c/20$ rate, and discharged at a $c/2.5$ rate to a 75% rated depth. Results indicate that the relatively inexpensive 120 Hz FWRS charger appears feasible for charging 5 amp-hour nickel-zinc cells with no significant loss in average cycle life when compared to constant current charging. The 1-kHz SW charger could also be used with no significant loss in average cycle life, and suggests the possibility of utilizing the existing electric vehicle chopper controller circuitry for an on-board charger. There was an apparent difference using the 120 Hz SCR charger compared to the others, however, this difference could be due to an inadvertent severe overcharge, which occurred prior to cell failure. The remaining two positive pulse charging waveforms, FWRS and 1 kHz, did not improve the cycle life of 5 amp-hour nickel-zinc cells over that of constant current charging. (Author)

A80-48370 * # Improvement and scale-up of the NASA Redox storage system. M. A. Reid and L. H. Thaller (NASA, Lewis Research Center, Cleveland, Ohio). In: Energy to the 21st century; Proceedings of the Fifteenth Intersociety Energy Conversion Engineering Conference, Seattle, Wash., August 18-22, 1980, Volume 2. (A80-48165 21-44) New York, American Institute of Aeronautics and Astronautics, Inc., 1980, p. 1471-1476. 9 refs.

A preprototype full-function 1.0 kW Redox system (2 kW peak) with 11 kW storage capacity has been built and integrated with the

NASA/DUE photovoltaic test facility. The system includes four substacks of 39 cells each (1/3 sq ft active area) which are connected hydraulically in parallel and electrically in series. An open circuit voltage cell and a set of rebalance cells are used to continuously monitor the system state of charge and automatically maintain the anode and cathode reactants electrochemically in balance. Technological advances in membrane and electrodes and results of multicell stack tests are reviewed. V.L.

N80-10603* Energy Research Corp., Danbury, Conn.
TECHNOLOGY DEVELOPMENT FOR PHOSPHORIC ACID FUEL CELL POWERPLANT, PHASE 2 Quarterly Report
Larry Christner Jun 1979 72 p Prepared for DOE
(Contract DEN3-67)
(NASA-CR-159705; DOE/NASA/0067-79-2; QR-3) Avail: NTIS HC A04/MF A01 CSCL 10A

A technique for producing an acid inventory control member by spraying FEP onto a partially screened carbon paper backing is discussed. Theoretical analysis of the acid management indicates that the vapor composition of 103% H₃PO₄ is approximately 1.0 ppm P₄O₁₀. An SEM evaluation of corrosion resistance of phenolic resins and graphite/phenolic resin composites in H₃PO₄ at 185 C shows specific surface etching. Carbonization of graphite/phenolic bipolar plates is achieved without blistering. K.L.

N80-10622* General Electric Co., Schenectady, N. Y.
CONCEPTUAL DESIGN OF THERMAL ENERGY STORAGE SYSTEMS FOR NEAR-TERM ELECTRIC UTILITY APPLICATIONS. VOLUME 2: APPENDICES, SCREENING OF CONCEPTS
W. Hausz, B. J. Berkowitz, and R. C. Hare Apr. 1979 151 p refs
(Contract EC-77-A-31-1034; EPRI Proj. 1082-1)
(NASA-CR-159411; EPRI-EM-1037-Vol-2) Avail: NTIS HC A08/MF A01

Volume two contains three appendices entitled: (1) Bibliography and Cross References; (2) Taxonomy: Proponents and Sources; and (3) Concept Definitions. DOE

N80-11558* General Electric Co., Philadelphia, Pa. Space Div.
EXECUTIVE SUMMARY: MOD-1 WIND TURBINE GENERATOR ANALYSIS AND DESIGN REPORT Final Report
Mar. 1979 61 p
(Contracts NAS3-20058; EC-77-A-29-1010)
(NASA-CR-159497; DOE/NASA/0058-79/3) Avail: NTIS HC A04/MF A01 CSCL 10A

Activities leading to the detail design of a wind turbine generator having a nominal rating of 1.8 megawatts are reported. Topics covered include (1) system description; (2) structural dynamics; (3) stability analysis; (4) mechanical subassemblies design; (5) power generation subsystem; and (6) control and instrumentation subsystem. A.R.H.

N80-11566* Jet Propulsion Lab., Calif. Inst. of Tech., Pasadena.
CHARACTERIZATION OF SOLAR CELLS FOR SPACE APPLICATIONS. VOLUME 10: ELECTRICAL CHARACTERISTICS OF SPECTROLAB B5F, TEXTURED, 10 OHM-CM, 300 MICRON CELLS AS A FUNCTION OF INTENSITY, TEMPERATURE AND IRRADIATION
B. E. Anspaugh, R. G. Downing, T. F. Miyahira, and R. S. Weiss 1 Oct. 1979 38 p
(Contract NAS7-100)
(NASA-CR-162422; JPL-Pub-78-15-Vol-10) Avail: NTIS HC A03/MF A01 CSCL 10A

Electrical characteristics of textured, back surface field, 10 ohm cm, 300 micron N/P silicon solar cells are presented in graphical and tabular format as a function of solar illumination intensity, and temperature. Author

N80-12551* Ionics, Inc., Watertown, Mass. Research Div.
ANTON PERMSELECTIVE MEMBRANE
Samuel S. Alexander, Russell B. Hodgdon, and Warren A. Waite Mar. 1979 52 p Sponsored by NASA
(Contract DEN3-1)
(NASA-CR-159599; DOE/NASA/0001-79/1) Avail: NTIS HC A04/MF A01 CSCL 10A

Experimental composite membranes were synthesized on a lab scale consisting of a thin layer of anion permselective resin supported by and bonded to a porous physically strong and conductive substrate film. These showed good selectivity and also substantially lower electrical resistivities than the homogenous candidate membranes optimized in the previous contract. A wide range of resin porosities were examined for three candidate membrane systems, CDIL, CP4L, and A3L to identify the formulation giving the best overall redox cell performance. Candidate anion membranes showed large increases in resistivity after a short time of immersion in concentrated FeCl₃/HCl solution. Largely on the basis of resistance stability the CDIL formulation was selected as prime candidate and about thirty-five membranes (one foot square) were produced for experimental static and dynamic evaluation. R.E.S.

N80-14490* Power Electronics Associates, Inc., Lincoln, Mass.
BI-DIRECTIONAL FOUR QUADRANT (BDQ4) POWER CONVERTER DEVELOPMENT Final Report
Francis C. Schwarz 20 Dec. 1979 249 p refs
(Contract NAS3-30363)
(NASA-CR-159660) Avail: NTIS HC A11/MF A01 CSCL 10B

The feasibility for implementation of a concept for direct ac/dc multikilowatt power conversion with bidirectional transfer of energy was investigated. A 10 kHz current carrier was derived directly from a common 60 Hz three phase power system. This carrier was modulated to remove the 360 Hz ripple inherent in the three phase power supply and then demodulated and processed by a high frequency filter. The resulting dc power was then supplied to a load. The process was implemented without the use of low frequency transformers and filters. This power conversion processes was reversible and can operate in the four quadrants as viewed from any of the two of the converter's ports. Areas of application include: power systems on air and spacecraft; terrestrial traction; integration of solar and wind powered systems with utility networks; HVDC; asynchronous coupling of polyphase networks; heat treatment; industrial machine drives; and power supplies for any use including instrumentation. R.C.T.

N80-15553* Technical Report Services, Rocky River, Ohio.
EVALUATION OF FEASIBILITY OF PRESTRESSED CONCRETE FOR USE IN WIND TURBINE BLADES
Seymour Leiblein, D. S. Londahl, Donn B. Furlong, and Mark E. Dreier Sep. 1979 119 p refs Prepared in cooperation with Tuthill Pump Co., San Rafael, Calif. and Paragon Pacific, Inc., El Segundo, Calif.
(Contracts NAS3-20596; NAS3-30813; EX-76-I-01-1028; NASA Order C-25906)
(NASA-CR-159725; DOE/NASA/5906-79/1) Avail: NTIS HC A06/MF A01 CSCL 10B

A preliminary evaluation of the feasibility of the use of prestressed concrete as a material for low cost blades for wind turbines was conducted. A baseline blade design was achieved for an experimental wind turbine that met aerodynamic and structural requirements. Significant cost reductions were indicated for volume production. Casting of a model blade section showed no fabrication problems. Coupled dynamic analysis revealed that adverse rotor tower interactions can be significant with heavy rotor blades. R.C.T.

N80-15559* Solarex Corp., Rockville, Md.
ECONOMICAL SPACE POWER SYSTEMS
Joel H. Burkholder Jan. 1980 161 p refs
(Contract NAS3-21353)
(NASA-CR-159696) Avail: NTIS HC A08/MF A01 CSCL 10B

A commercial approach to design and fabrication of an economical space power system is investigated. Cost projections are based on a 2 kW space power system conceptual design taking into consideration the capability for serviceability, constraints of operation in space, and commercial production engineering approaches. A breakdown of the system design, documentation, fabrication, and reliability and quality assurance estimated costs are detailed. M.G.

N80-16483* Energy Technology, Inc., Cleveland, Ohio
STUDY OF ADVANCED RADIAL OUTFLOW TURBINE FOR SOLAR STEAM RANKINE ENGINES

Cecil Martin and Terry Kolenc Dec. 1979 74 p refs
 (Contract DEN3-88)
 (NASA-CR-159695; DOE/NASA/0086-79/1; ETI-1279) Avail:
 NTIS HC A04/MF A01 CSCL 10B

The performance characteristics of various steam Rankine engine configurations for solar electric power generation were investigated. A radial outflow steam turbine was investigated to determine: (1) a method for predicting performance from experimental data; (2) the flexibility of a single design with regard to power output and pressure ratio, and (3) the effect of varying the number of turbine stages. All turbine designs were restricted to be compatible with commercially available gearboxes and generators. A study of several operating methods and control schemes for the steam Rankine engine shows that from an efficiency and control simplicity standpoint, the best approach is to hold turbine inlet temperature constant, vary turbine inlet pressure to match load, and allow condenser temperature to float maintaining constant heat rejection load. A.R.H.

N80-16491* Foster-Miller Associates, Inc., Waltham, Mass.
A 16kW_e (NOMINAL) SOLAR THERMAL ELECTRIC POWER CONVERSION CONCEPT DEFINITION STUDY: STEAM RANKINE REHEAT RECIPROCATOR SYSTEM Final Report

H. Fuller, R. Demler, E. Poulin, and P. Dantowitz Jun. 1979 63 p refs
 (Contracts DEN3-62; EX-76-A-29-1060)
 (NASA-CR-159590; DOE/NASA/0082-79/1; NAS-7845) Avail:
 NTIS HC A04/MF A01 CSCL 10B

An evaluation was made of the potential of a steam Rankine reheat reciprocator engine to operate at high efficiency in a point-focusing distributed receiver solar thermal-electric power system. The scope of the study included the engine system and electric generator; not included was the solar collector/mirror or the steam generator/receiver. A parametric analysis of steam conditions was completed leading to the selection of 973 K (721 MPa) as the steam temperature/pressure for a conceptual design. A conceptual design was completed for a two cylinder/opposed engine operating at 1800 rpm directly coupled to a commercially available induction generator. A unique part of the expander design is the use of carbon/graphite piston rings to eliminate the need for using oil as an upper cylinder lubricant. The evaluation included a system weight estimate of 230 kg at the mirror focal point with the condenser mounted separately on the ground. The estimated cost of the overall system is \$1932 or \$90/kW for the maximum 26 kW output. R.E.S.

N80-16493* Sundstrand Corp., Rockford, Ill.
THE 15 kW SUB_e (NOMINAL) SOLAR THERMAL ELECTRIC POWER CONVERSION CONCEPT DEFINITION STUDY: STEAM RANKINE TURBINE SYSTEM Final Report

Timothy J. Bland Oct. 1979 63 p refs
 (Contracts DEN3-61; EX-76-A-29-1060)
 (NASA-CR-159589; AER-1713; DOE/NASA/0061-79/1) Avail:
 NTIS HC A04/MF A01 CSCL 10A

A study to define the performance and cost characteristics of a solar powered, steam Rankine turbine system mounted at the focal point of a solar concentrator is presented. A two stage re-entry turbine with reheat between stages, which has an efficiency of 27% at a turbine inlet temperature of 732 C was used. System efficiency was defined as 60 Hertz electrical output divided by absorbed thermal input in the working fluid. Mass production costs were found to be approximately 364 dollars/kW. R.E.S.

N80-17543* Electro-Mechanical Research, Inc. Sarasota, Fla.
DOE/NASA WIND TURBINE DATA ACQUISITION. PART 1: EQUIPMENT

O J Strock Jan. 1980 56 p
 (Contract DEN3-98)
 (NASA-CR-159779; EMR 827053) Avail: NTIS
 HC A04/MF A01 CSCL 10B

Large quantities of data were collected, stored, and analyzed in connection with research and development programs on wind turbines. The hardware configuration of the wind energy remote data acquisition system is described along with its use on the NASA/DOE Wind Energy Program. RCT

N80-17547* Institute of Gas Technology, Chicago, Ill.
HIGH-TEMPERATURE MOLTEN SALT THERMAL ENERGY STORAGE SYSTEMS Final Report, 14 Sep. 1977 - 14 Dec. 1978

Randy J. Petri, Terry D. Claar, Ray R. Tison, and Leonard G. Marianowski Feb. 1980 175 p refs
 (Contract NAS3-20806)

(NASA-CR-159663; DOE/NASA/0806-79/1) Avail: NTIS
 HC A08/MF A01 CSCL 10A

The results of comparative screening studies of candidate molten carbonate salts as phase change materials (PCM) for advanced solar thermal energy storage applications at 540 to 870 C (1004 to 1600 F) and steam Rankine electric generation at 400 to 540 C (752 to 1004 F) are presented. Alkali carbonates are attractive as latent heat storage materials because of their relatively high storage capacity and thermal conductivity, low corrosivity, moderate cost, and safe and simple handling requirements. Salts were tested in 0.1 kWhr lab scale modules and evaluated on the basis of discharge heat flux, solidification temperature range, thermal cycling stability, and compatibility with containment materials. The feasibility of using a distributed network of high conductivity material to increase the heat flux through the layer of solidified salt was evaluated. The thermal performance of an 8 kWhr thermal energy storage (TES) module containing LiKCO₃ remained very stable throughout 5650 hours and 130 charge/discharge cycles at 480 to 535 C (896 to 995 F). A TES utilization concept of an electrical generation peaking subsystem composed of a multistage condensing steam turbine and a TES subsystem with a separate power conversion loop was defined. Conceptual designs for a 100 MW sub e TES peaking system providing steam at 316 C, 427 C, and 454 C (600 F, 800 F, and 850 F) at 3.79 million Pa (550 psia) were developed and evaluated. Areas requiring further investigation have also been identified. Author

N80-17548* Kaman Aerospace Corp., Bloomfield, Conn.
DESIGN, FABRICATION, TEST, AND EVALUATION OF A PROTOTYPE 150-FOOT LONG COMPOSITE WIND TURBINE BLADE Final Report

Herbert W. Gewehr Sep. 1979 135 p refs
 (Contracts NAS3-20600; EX-76-I-01-1028)
 (NASA-CR-159775; DOE/NASA/0600-79/1; R-1575) Avail:
 NTIS HC A07/MF A01 CSCL 10B

The design, fabrication, testing, and evaluation of a prototype 150 foot long composite wind turbine blade is described. The design approach and material selection, compatible with low cost fabrication methods and objectives, are highlighted. The operating characteristics of the blade during rotating and nonrotating conditions are presented. The tensile, compression, and shear properties of the blade are reported. The blade fabrication, tooling, and quality assurance are discussed. A.W.H.

N80-18554* Spectrolab, Inc., Sylmar, Calif.
DEVELOPMENT OF IMPROVED WRAPAROUND CONTACTS FOR SILICON Final Report

Jay W. Thornhill Dec. 1979 41 p
 (Contract NAS3-20065)
 (NASA-CR-159748) Avail: NTIS HC A03/MF A01 CSCL 10A

A developmental process for fabricating 2 X 4 cm back surface field silicon solar cells featuring wraparound contacts and screen printed dielectric isolation is described. The process

was then used to fabricate a number of cells for evaluation and study, as well as to establish the validity of the process sequence. While a number of cells exhibiting relatively good conversion efficiencies were produced, nearly all had low I-V curve factors for the level of efficiencies attained. Cells with conversion efficiencies of more than 15 percent (air mass zero and 25 C) had fill factors of only 0.76. Evidence as to the cause of this has not been conclusive, but is most probably linked to isolation failure in the wraparound dielectric and associated shunting problems. Author

N80-18558* Avco Corp., Wilmington, Mass.
PARAMETRIC STUDY OF POTENTIAL EARLY COMMERCIAL MHD POWER PLANTS Final Report
 Finn A Hals Dec 1979 246 p refs
 (Contracts DEN3-51; EF-77-A-01-2674)
 (NASA-CR-159633; DOE/NASA/0051-79/1) Avail: NTIS HC A11/MF A01 CSCL 10B

Three different reference power plant configurations were considered with parametric variations of the various design parameters for each plant. Two of the reference plant designs were based on the use of high temperature regenerative air preheaters separately fired by a low Btu gas produced from a coal gasifier which was integrated with the power plant. The third reference plant design was based on the use of oxygen enriched combustion air preheated to a more moderate temperature in a tubular type metallic recuperative heat exchanger which is part of the bottoming plant heat recovery system. Comparative information was developed on plant performance and economics. The highest net plant efficiency of about 45 percent was attained by the reference plant design with the use of a high temperature air preheater separately fired with the advanced entrained bed gasifier. The use of oxygen enrichment of the combustion air yielded the lowest cost of generating electricity at a slightly lower plant efficiency. Both of these two reference plant designs are identified as potentially attractive for early MHD power plant applications. R.E.S.

N80-18582* Grumman Aerospace Corp., Bethpage, N.Y.
ACTIVE HEAT EXCHANGE SYSTEM DEVELOPMENT FOR LATENT HEAT THERMAL ENERGY STORAGE Topical Report, Jun. 1978 - Feb. 1979

Joseph Alario, Robert Kosson, and Robert Haslett Jan. 1980 73 p refs

(Contracts DEN3-39; EC-77-A-31-1034)
 (NASA-CR-159726; DOE/NASA/0039-79/1; GAC-TR-1681-09) Avail: NTIS HC A04/MF A01 CSCL 10A

Various active heat exchange concepts were identified from among three generic categories: scrapers, agitators/vibrators and slurries. The more practical ones were given a more detailed technical evaluation and an economic comparison with a passive tube-shell design for a reference application (300 MW sub t storage for 6 hours). Two concepts were selected for hardware development: (1) a direct contact heat exchanger in which molten salt droplets are injected into a cooler counterflowing stream of liquid metal carrier fluid, and (2) a rotating drum scraper in which molten salt is sprayed onto the circumference of a rotating drum, which contains the fluid salt is sprayed onto the circumference of a rotating drum, which contains the fluid heat sink in an internal annulus near the surface. A fixed scraper blade removes the solidified salt from the surface which was nickel plated to decrease adhesion forces. In addition to improving performance by providing a nearly constant transfer rate during discharge, these active heat exchanger concepts were estimated to cost at least 25% less than the passive tube-shell design. R.E.S.

N80-18585* General Electric Co., Philadelphia, Pa. Space Div.
APPENDIX: MOD-1 WIND TURBINE GENERATOR ANALYSIS AND DESIGN REPORT, VOLUME 2 Final Report
 May 1979 425 p
 (Contracts NAS3-20058; EX-77-A-29-1010)
 (NASA-CR-159496; DOE/NASA/0058-79/2-Vol-2-App) Avail:

NTIS HC A18/MF A01 CSCL 10B

The MOD-1 detail design is appended. The supporting analyses presented include a parametric system trade study, a verification of the computer codes used for rotor loads analysis, a metal blade study, and a definition of the design loads at each principal wind turbine generator interface for critical loading conditions. Shipping and assembly requirements, composite blade development, and electrical stability are also discussed. K.L.

N80-18612* Jay - Carter Enterprises, Inc., Burkburnett, Tex.
A 15 kW_e (NOMINAL) SOLAR THERMAL-ELECTRIC POWER CONVERSION CONCEPT DEFINITION STUDY: STEAM RANKIN RECIPROCATOR SYSTEM Final Report
 W. Wingenback and J. Carter, Jr. Jun. 1979 46 p refs
 (Contracts DEN3-63; EX-76-A-29-1060)
 (NASA-CR-159591; DOE/NASA/0063-79/1) Avail: NTIS HC A03/MF A01 CSCL 10A

A conceptual design of a 3600 rpm reciprocation expander was developed for maximum thermal input power of 80 kW. The conceptual design covered two engine configurations: a single cylinder design for simple cycle operation and a two cylinder design for reheat cycle operation. The reheat expander contains a high pressure cylinder and a low pressure cylinder with steam being reheated to the initial inlet temperature after expansion in the high pressure cylinder. Power generation is accomplished with a three-phase induction motor coupled directly to the expander and connected electrically to the public utility power grid. The expander, generator, water pump and control system weigh 297 kg and are dish mounted. The steam condenser, water tank and accessory pumps are ground based. Maximum heat engine efficiency is 33 percent; maximum power conversion efficiency is 30 percent. Total cost is \$3,307 or \$138 per kW of maximum output power. R.E.S.

N80-18615* United Technologies Corp., South Windsor, Conn. Power Systems Div.
ADVANCED TECHNOLOGY LIGHT WEIGHT FUEL CELL PROGRAM Final Report, 28 Jul. 1978 - 28 Jul. 1979

R. E. Martin 1979 52 p refs

(Contract NAS3-21257)

(NASA-CR-159807; FCR-1657)

Avail: NTIS

HC A04/MF A01 CSCL 10B

The development of a long life, high performance, high efficiency, hydrogen oxygen alkaline fuel cell configuration for application to a NASA orbiting space vehicle is documented. Seven full-size 0.25 ft x 2 active area single cells were constructed and tested at cell temperatures between 140 F and 200 F, current densities out to 500 ASF, and reactant pressures up to 30 psia. Cells incorporating platinum-supported-on-carbon catalyst anodes demonstrated 8,085 cell-hours of endurance operation with virtually no change in performance and 2,995 cell-hours of operation to a cyclical load profiles with no apparent loss in cathode performance due to high voltage operation. Cell edge frame materials and heat treated polybenzimidazole (PBI) matrix samples were corrosion tested in 42 wt % aqueous potassium hydroxide at 250 F. Based upon available test data, PBI appears unsuitable for use as a fuel cell matrix material. Five semiconducting oxides were evaluated as cathode catalysts and as cathode catalyst supports. The candidate supports LaMnO₃ and LaNiO₃ appear to have development potential and merit further study. K.L.

N80-18632* Jet Propulsion Lab., California Inst. of Tech., Pasadena.

ANNUAL TECHNICAL REPORT, FISCAL YEAR 1979. VOLUME 1: EXECUTIVE SUMMARY Annual Report

John W. Lucas 15 Jan. 1980 46 p Sponsored in part by DOE

(Contract NAS7-100)

(NASA-CR-159715; JPL-Pub-79-112-Vol-1) Avail: NTIS HC A03/MF A01 CSCL 10A

Accomplishments of the Point-Focusing Distributed Receiver Technology project are presented. The following aspects of the project are discussed: information dissemination, concentrator development, receiver and heat transport network development.

power conversion, manufacturing, systems engineering, and tests and evaluations R.E.S.

N80-20864* General Electric Co., Philadelphia, Pa. Space Div

MOD 1 WIND TURBINE GENERATOR FAILURE MODES AND EFFECTS ANALYSIS

Feb 1979 95 p

(Contracts NAS3-20058; EX-77-A-29-1010)

(NASA-CR-159494; DOE/NASA/0058-79/1) Avail: NTIS HC A05/MF A01 CSCL 10B

A failure modes and effects analysis (FMEA) was directed primarily at identifying those critical failure modes that would be hazardous to life or would result in major damage to the system. Each subsystem was approached from the top down, and broken down to successive lower levels where it appeared that the criticality of the failure mode warranted more detail analysis. The results were reviewed by specialists from outside the Mod 1 program, and corrective action taken wherever recommended. A.R.H.

N80-22775* Spire Corp., Bedford, Mass.

STUDY PROGRAM TO IMPROVE THE OPEN-CIRCUIT VOLTAGE OF LOW RESISTIVITY SINGLE CRYSTAL SILICON SOLAR CELLS

J. A. Minnucci and K. W. Matthei 7 Feb. 1980 119 p refs (Contract NAS3-20823)

(NASA-CR-159833; FR-10056)

Avail: NTIS

HC A06/MF A01 CSCL 10A

The results of a 14 month program to improve the open circuit voltage of low resistivity silicon solar cells are described. The approach was based on ion implantation in 0.1- to 10.0-ohm-cm float-zone silicon. As a result of the contract effort, open circuit voltages as high as 645 mV (AMO 25 C) were attained by high dose phosphorus implantation followed by furnace annealing and simultaneous SiO₂ growth. One key element was to investigate the effects of bandgap narrowing caused by high doping concentrations in the junction layer. Considerable effort was applied to optimization of implant parameters, selection of furnace annealing techniques, and utilization of pulsed electron beam annealing to minimize thermal process-induced defects in the completed solar cells. F.O.S.

N80-22778* AirResearch Mfg. Co., Phoenix, Ariz.

CONCEPT DEFINITION STUDY OF SMALL BRAYTON CYCLE ENGINES FOR DISPERSED SOLAR ELECTRIC POWER SYSTEMS Final Report, Sep. 1978 - Jun. 1979

Lyle D. Six, Thomas L. Ashe, Frank X. Dobler, and Ron T. Elkins Jan. 1980 135 p refs

(Contracts DEN3-69; EX-76-A-29-1060)

(NASA-CR-159592; DOE/NASA/0069-79/1)

AirResearch-31-3328) Avail: NTIS HC A07/MF A01 CSCL 10B

Three first-generation Brayton cycle engine types were studied for solar application: a near-term open cycle (configuration A), a near-term closed cycle (configuration B), and a longer-term open cycle (configuration C). A parametric performance analysis was carried out to select engine designs for the three configurations. The interface requirements for the Brayton cycle engine/generator and solar receivers were determined. A technology assessment was then carried out to define production costs, durability, and growth potential for the selected engine types. R.E.S.

N80-22787* Mechanical Technology, Inc., Latham, N. Y. Stirling Engine Systems Div.

DESIGN STUDY OF A 15 kW FREE-PISTON STIRLING ENGINE-LINEAR ALTERNATOR FOR DISPERSED SOLAR ELECTRIC POWER SYSTEMS Final Report, Sep. 1978 - Aug. 1979

George R. Dochat, H. S. Chen, S. Bhate, and T. Marusak Aug. 1979 189 p refs

(Contracts DEN3-56; EX-76-A-29-1060)

(NASA-CR-159587; DOE/NASA/0056-79/1; MTI-79TR47)

Avail: NTIS HC A08/MF A01 CSCL 10B

A conceptual design of a free piston solar Stirling engine-linear alternator which can be designed and developed to meet the requirements of a near-term solar test bed engine with minimum risks was developed. The conceptual design was calculated to have an overall system efficiency of 38% and provide 15kW electric output. The free piston engine design incorporates features such as gas bearings, close clearance seals, and gas springs. This design is hermetically sealed to provide long life, reliability, and maintenance free operation. An implementation assessment study performed indicates that the free piston solar Stirling engine-linear alternator can be manufactured at a reasonable price cost (direct labor plus material) of \$2,500 per engine in production quantities of 25,000 units per year. Opportunity for significant reduction of cost was also identified. R.E.S.

N80-23768* Westinghouse Research and Development Center, Pittsburgh, Pa.

CELL MODULE AND FUEL CONDITIONER DEVELOPMENT

D. Q. Hoover, Jr. Jan. 1980 58 p

(Contracts DEN3-161; DE-AI03-79ET-1272)

(NASA-CR-159828; DOE/NASA/0161-79/3; QR-1;

Rept-80-9E8-MAREO-R1) Avail: NTIS HC A04/MF A01

Components for the first 5 cell stack (no cooling plates) of the MK-2 design were fabricated. Preliminary specifications and designs for the components of a 23 cell MK-1 stack with four DIGAS cooling plates were developed. The MK-2 was selected as a bench mark design and a preliminary design of the facilities required for high rate manufacture of fuel cell modules was developed. Two stands for testing 5 cell stacks were built and design work for modifying existing stands and building new stands for 23 and 80 cell stacks was initiated. Design and procurement of components and materials for the catalyst test stand were completed and construction initiated. Work on the specifications of pipeline gas, tap water and recovered water and definition of equipment required for treatment was initiated. An innovative geometry for the reformer was conceived and modifications of the computer program to be used in its design were stated. R.E.S.

N80-23775* General Electric Co., Philadelphia, Pa. Space Div.

MOD-1 WIND TURBINE GENERATOR ANALYSIS AND DESIGN REPORT, VOLUME 1 Final Report

Mar. 1979 320 p

(Contracts NAS3-20058; EX-77-A-29-1010)

(NASA-CR-159495; DOE/NASA/0058-79/2-Vol-1) Avail: NTIS HC A14/MF A01 CSCL 10A

The activities leading to the completion of detail design of the MOD-1 wind turbine generator are described. Emphasis is placed on the description of the design as it finally evolved. However, the steps through which the design progressed are also traced in order to understand the major design decisions. R.E.S.

N80-23842* General Electric Co., Schenectady, N. Y.

CONCEPTUAL DESIGN OF THERMAL ENERGY STORAGE SYSTEMS FOR NEAR-TERM ELECTRIC UTILITY APPLICATIONS Final Report

E. W. Hall, W. Hausz, R. Anand, N. LaMarche, J. Oplinger, and M. Katzer Nov. 1979 524 p refs Sponsored by NASA and EPRI

(Contract EC-77-A-31-1034; EPRI Proj. 1082-1)

(NASA-CR-159577; EPRI-EM-1218)

Avail: NTIS

HCA22/MF A01 CSCL 10A

Over forty concepts were examined for storage media, forms of containment, and cycle configurations for conversion to electricity. An extensive analysis and screening process resulted in selecting two coal-fired and two nuclear plants for detail conceptual design. The coal plants utilized peaking turbines and the nuclear plants varied the feedwater extraction to change power output. It was shown that the performance and costs of even the best of these systems could not compete in near-term utility applications with cycling coal plants and typical gas turbines available for peaking power. Lower electricity costs, greater

flexibility of operation, and other benefits can be provided by cycling coal plants for greater than 1500 hours of peaking or by gas turbines for less than 1500 hours if oil is available and its cost does not increase significantly. DOE

N80-24742* PRC Systems Services Co., Huntsville, Ala.
SOLAR ARRAY SUBSYSTEMS STUDY Final Report, Mar. 1979 - May 1980
P. W. Richardson, F. Q. Miller, and M. B. Badgley 6 Jun. 1980 284 p
(Contract NAS3-21926)
(NASA-CR-159857) Avail: NTIS HC A13/MF A01 CSCL 10A

The effects on life cycle costs of a number of technology areas are examined for a LEO, 500 kW solar array. A baseline system conceptual design is developed and the life cycle costs estimated in detail. The baseline system requirements and design technologies are then varied and their relationships to life cycle costs quantified. For example, the thermal characteristics of the baseline design are determined by the array materials and masses. The thermal characteristics in turn determine configuration, performance and hence life cycle cost. Author

N80-24748* Engelhard Minerals and Chemicals Corp., Edison, N. J.
DURABILITY TESTING AT 5 ATMOSPHERES OF ADVANCED CATALYSTS AND CATALYST SUPPORTS FOR GAS TURBINE ENGINE COMBUSTORS Final Report
B. A. Olson, H. C. Lee, I. T. Osgerby, R. M. Heck, and H. Hess Apr. 1980 95 p refs
(Contracts NAS3-19416; Contract EF-77-A-01-2593)
(NASA-CR-159839; DOE/NASA/9416-80/2) Avail: NTIS HC A05/MF A01 CSCL 10A

The durability of CATCOM catalysts and catalyst supports was experimentally demonstrated in a combustion environment under simulated gas turbine engine combustor operating conditions. A test of 1000 hours duration was completed with one catalyst using no. 2 diesel fuel and operating at catalytically-supported thermal combustion conditions. The performance of the catalyst was determined by monitoring emissions throughout the test, and by examining the physical condition of the catalyst core at the conclusion of the test. Tests were performed periodically to determine changes in catalytic activity of the catalyst core. Detailed parametric studies were also run at the beginning and end of the durability test, using no. 2 fuel oil. Initial and final emissions for the 1000 hours test respectively were: unburned hydrocarbons (C3 vppm):0, 146, carbon monoxide (vppm):30, 2420; nitrogen oxides (vppm):5.7, 5.6. R.E.S.

N80-24751* Jet Propulsion Lab., California Inst. of Tech., Pasadena.
SOLAR THERMAL POWER SYSTEMS POINT-FOCUSING DISTRIBUTED RECEIVER TECHNOLOGY PROJECT. VOLUME 2: DETAILED REPORT Annual Technical Report, fiscal year 1979
1 Apr. 1980 134 p refs Prepared in part by NASA, Lewis Res. Center, Cleveland, Ohio 2 Vol.
(Contracts NAS7-100; DE-AI01-79ET-20307; JPL Proj. 5104-61)
(NASA-CR-159715; DOE/JPL-1060-30-Vol-2; JPL-Pub-79-112-Vol-2) Avail: NTIS HC A07/MF A01 CSCL 10A

The accomplishments of the Point-Focusing Distributed Receiver Technology Project during fiscal year 1979 are detailed. Present studies involve designs of modular units that collect and concentrate solar energy via highly reflective, parabolic-shaped dishes. The concentrated energy is then converted to heat in a working fluid, such as hot gas. In modules designed to produce heat for industrial applications, a flexible line conveys the heated fluid from the module to a heat transfer network. In modules designed to produce electricity the fluid carries the heat directly to an engine in a power conversion unit located at the focus of the concentrator. The engine is mechanically linked to an electric generator. A Brayton-cycle engine is currently being developed as the most promising electrical energy converter to meet near-future needs. R.E.S.

N80-24758* Boeing Engineering and Construction, Seattle, Wash.

MOD-2 WIND TURBINE SYSTEM CONCEPT AND PRELIMINARY DESIGN REPORT. VOLUME 1: EXECUTIVE SUMMARY

Jul. 1979 31 p
(Contracts DEN3-2; DE-AI01-793T-20305)
(NASA-CR-159609; DOE/NASA/0002-80/2) Avail: NTIS HC A03/MF A01 CSCL 10A

The configuration development of the MOD-2 wind turbine system is presented. The MOD-2 is design optimized for commercial production rates which, in multi-unit installations, will be integrated into a utility power grid and achieve a cost of electricity at less than 4 cents per kilowatt hour. R.E.S.

N80-24759* Delaware Univ., Newark. Dept. of Chemical Engineering.

HEAT STORAGE IN ALLOY TRANSFORMATIONS

C. Ernest Birchenall Apr. 1980 29 p refs
(Grant NSG-3184; Contract EC-77-A-31-1034)
(NASA-CR-159787; DOE/NASA/3184-1) Avail: NTIS HC A03/MF A01 CSCL 10C

The feasibility of using metal alloys as thermal energy storage media was investigated. The elements selected as candidate media were limited to aluminum, copper, magnesium, silicon, zinc, calcium, and phosphorus on the basis of low cost and latent heat of transformation. Several new eutectic alloys and ternary intermetallic phases were determined. A new method employing X-ray absorption techniques was developed to determine the coefficients of thermal expansion of both the solid and liquid phases and the volume change during phase transformation. The method and apparatus are discussed and the experimental results are presented for aluminum and two aluminum-eutectic alloys. Candidate materials were evaluated to determine suitable materials for containment of the metal alloys. Graphite was used to contain the alloys during the volume change measurements. Silicon carbide was identified as a promising containment material and surface-coated iron alloys were also evaluated. System considerations that are pertinent if alloy eutectics are used as thermal energy storage media are discussed. Potential applications to solar receivers and industrial furnaces are illustrated schematically. R.E.S.

N80-24797* General Electric Co., Schenectady, N. Y. Energy Technology Operation.

COGENERATION TECHNOLOGY ALTERNATIVES STUDY (CTAS). VOLUME 1: SUMMARY REPORT Final Report

H. E. Gerlaugh, E. W. Hall, D. H. Brown, R. R. Priestley, and W. F. Knightly Jan. 1980 154 p
(Contract DEN3-31)
(NASA-CR-159765; GE79ET0102; DOE/NASA/0031-80/1) Avail: NTIS HC A08/MF A01 CSCL 10B

Large savings can be made in industry by cogenerating electric power and process heat in single energy conversion systems rather than separately in utility plants and in process boilers. About fifty industrial processes from the largest energy consuming sectors were used as a basis for matching a similar number of energy conversion systems that are considered as candidates which can be made available by the 1985 to 2000 time period. The sectors considered included food, textiles, lumber, paper, chemicals, petroleum, glass, and primary metals. The energy conversion systems included steam and gas turbines, diesels, thermionics, stirling, closed-cycle and steam injected gas turbines, and fuel cells. Fuels considered were coal, both coal and petroleum-based residual and distillate liquid fuels, and low Btu gas obtained through the on-site gasification of coal. An attempt was made to use consistent assumptions and a consistent set of ground rules for determining performance and cost in individual plants and on a national level. It was found that: (1) atmospheric and pressurized fluidized bed steam turbine systems were the most attractive of the direct coal-fired systems; and (2) open-cycle gas turbines with heat recovery steam generators and combined-cycles with NO(x) emission reduction and moderately increased firing temperatures were the most attractive of the coal-derived liquid-fired systems. R.E.S.

N80-25792* United Technologies Corp., South Windsor, Conn. Power System Div.

COGENERATION TECHNOLOGY ALTERNATIVES STUDY. VOLUME 1: SUMMARY REPORT Final Report

Jan. 1980 125 p

(Contracts DEN3-30; EC-77-A-31-1062)

(NASA-CR-159759; DOE/NASA/0030-80/1;

UTC-FCR-1333-Vol-1) Avail: NTIS HC A06/MF A01 CSCL 10A

Data and information in the area of advanced energy conversion systems for industrial cogeneration applications in the 1985-2000 time period was studied. Six current and thirty-one advanced energy conversion systems were defined and combined with appropriate balance-of-plant equipment. Twenty-six industrial processes were selected from among the high energy consuming industries to serve as a framework for the study. Each conversion system was analyzed as a cogenerator with each industrial plant. Fuel consumption, costs, and environmental intrusion were evaluated and compared to corresponding traditional values. Various cogeneration strategies were analyzed and both topping and bottoming (using industrial by-product heat) applications were included. The advanced energy conversion technologies indicated reduced fuel consumption, costs, and emissions. Typically fuel energy savings of 10 to 25 percent were predicted compared to traditional on-site furnaces and utility electricity. With the variety of industrial requirements, each advanced technology had attractive applications. Overall, fuel cells indicated the greatest fuel energy savings and emission reductions. Gas turbines and combined cycles indicated high overall annual cost savings. Steam turbines and gas turbines produced high estimated returns. In some applications, diesels were most efficient. The advanced technologies used coal-derived fuels, or coal with advanced fluid bed combustion or on-site gasification systems. R.E.S.

N80-25793* United Technologies Corp., South Windsor, Conn. Power Systems Div.

COGENERATION TECHNOLOGY ALTERNATIVES STUDY. VOLUME 2: INDUSTRIAL PROCESS CHARACTERISTICS Final Report

Jan. 1980 697 p refs

(Contracts DEN3-30; EC-77-A-31-1062)

(NASA-CR-159760; DOE/NASA/0030-80/2;

UTC-FCR-1333-Vol-2) Avail: NTIS HC A99/MF A01 CSCL 10A

Information and data for 26 industrial processes are presented. The following information is given for each process: (1) a description of the process including the annual energy consumption and product production and plant capacity; (2) the energy requirements of the process for each unit of production and the detailed data concerning electrical energy requirements and also hot water, steam, and direct fired thermal requirements; (3) anticipated trends affecting energy requirements with new process or production technologies; and (4) representative plant data including capacity and projected requirements through the year 2000. R.E.S.

N80-25794* United Technologies Corp., South Windsor, Conn. Power Systems Div.

COGENERATION TECHNOLOGY ALTERNATIVES STUDY. VOLUME 4: HEAT SOURCES, BALANCE OF PLANT AND AUXILIARY SYSTEMS Final Report

Jan. 1980 296 p

(Contracts DEN3-30; EC-77-A-31-1062)

(NASA-CR-159762; DOE/NASA/0030-80/4;

UTC-FCR-1333-Vol-4) Avail: NTIS HC A13/MF A01 CSCL 10A

Data and information established for heat sources balance of plant items, thermal energy storage, and heat pumps are presented. Design case descriptions are given along with projected performance values. Capital cost estimates for representative cogeneration plants are also presented. R.E.S.

N80-25795* United Technologies Corp., South Windsor, Conn. Power Systems Div.

COGENERATION TECHNOLOGY ALTERNATIVES STUDY. VOLUME 6: COMPUTER DATA Final Report

Jan. 1980 535 p

(Contracts DEN3-30; EC-77-A-31-1062)

(NASA-CR-159764; DOE/NASA/0030-80/6;

UTC-FCR-1333-Vol-6) Avail: NTIS HC A22/MF A01 CSCL 10A

The potential technical capabilities of energy conversion systems in the 1985 - 2000 time period were defined with emphasis on systems using coal, coal-derived fuels or alternate fuels. Industrial process data developed for the large energy consuming industries serve as a framework for the cogeneration applications. Ground rules for the study were established and other necessary equipment (balance-of-plant) was defined. This combination of technical information, energy conversion system data ground rules, industrial process information and balance-of-plant characteristics was analyzed to evaluate energy consumption, capital and operating costs and emissions. Data in the form of computer printouts developed for 3000 energy conversion system-industrial process combinations are presented. R.E.S.

N80-26774* Toledo Univ., Ohio.

NONLINEAR AEROELASTIC EQUATIONS OF MOTION OF TWISTED, NONUNIFORM, FLEXIBLE HORIZONTAL-AXIS WIND TURBINE BLADES Final Report

Krishna Rao V. Kaza Jul. 1980 70 p refs

(Grant NSG-3139; Contract EX-76-1-01-1028)

(NASA-CR-159502; DOE/NASA/3139-1) Avail: NTIS HC A04/MF A01 CSCL 10A

The second-degree nonlinear equations of motion for a flexible, twisted, nonuniform, horizontal axis wind turbine blade were developed using Hamilton's principle. A mathematical ordering scheme which was consistent with the assumption of a slender beam was used to discard some higher-order elastic and inertial terms in the second-degree nonlinear equations. The blade aerodynamic loading which was employed accounted for both wind shear and tower shadow and was obtained from strip theory based on a quasi-steady approximation of two-dimensional, incompressible, unsteady, airfoil theory. The resulting equations had periodic coefficients and were suitable for determining the aeroelastic stability and response of large horizontal-axis wind turbine blades. R.E.S.

N80-26775* Boeing Engineering and Construction, Seattle, Wash.

MOD-2 WIND TURBINE SYSTEM CONCEPT AND PRELIMINARY DESIGN REPORT. VOLUME 2: DETAILED REPORT

Jul. 1979 269 p

(Contracts DEN3-2; DE-A101-793T-20305)

(NASA-CR-159609; DOE/NASA-0002-80/2) Avail: NTIS HC A12/MF A01 CSCL 10A

The configuration development of the MOD-2 wind turbine system (WTS) is documented. The MOD-2 WTS project is a continuation of DOE programs to develop and achieve early commercialization of wind energy. The MOD-2 is design optimized for commercial production rates which, in multiunit installations, will be integrated into a utility power grid and achieve a cost of electricity at less than four cents per kilowatt hour. J.M.S.

N80-26779* General Electric Co., Philadelphia, Pa. Space Sciences Lab.

PARAMETRIC STUDY OF PROSPECTIVE EARLY COMMERCIAL MHD POWER PLANTS (PSPEC). GENERAL ELECTRIC COMPANY, TASK 1: PARAMETRIC ANALYSIS Final Report

C. H. Marston, F. N. Alyea, D. J. Bender, L. K. Davis, T. C. Dellinger, J. G. Hnat, E. H. Komito, C. A. Peterson, D. A. Rogers, A. J. Roman et al Feb. 1980 358 p refs Prepared in cooperation with Foster Wheeler Corp., Livingston, N.J., Hooker Chemical Co., Niagara Falls, N.Y. and Bechtel National, Inc., San Francisco

(Contract DEN3-52; EF-77-A01-2674)

(NASA-CR-159634; DOE/NASA/0052-79/1) Avail: NTIS

HCA16/MFA01 CSCL 10B

The performance and cost of moderate technology coal-fired open cycle MHD/steam power plant designs which can be expected to require a shorter development time and have a lower development cost than previously considered mature OCMHD/steam plants were determined. Three base cases were considered: an indirectly-fired high temperature air heater (HTAH) subsystem delivering air at 2700 F, fired by a state of the art atmospheric pressure gasifier, and the HTAH subsystem was deleted and oxygen enrichment was used to obtain requisite MHD combustion temperature. Coal pile to bus bar efficiencies in base case 1 ranged from 41.4% to 42.9%, and cost of electricity (COE) was highest of the three base cases. For base case 2 the efficiency range was 42.0% to 45.6%, and COE was lowest. For base case 3 the efficiency range was 42.9% to 44.4%, and COE was intermediate. The best parametric cases in bases cases 2 and 3 are recommended for conceptual design. Eventual choice between these approaches is dependent on further evaluation of the tradeoffs among HTAH development risk, O2 plant integration, and further refinements of comparative costs. J.M.S.

N80-27803*# Wichita State Univ., Kans.**FEASIBILITY STUDY OF AILERON AND SPOILER CONTROL SYSTEMS FOR LARGE HORIZONTAL AXIS WIND TURBINES Final Report**

W. H. Wentz, Jr., M. H. Snyder, and J. T. Calhoun May 1980 69 p refs

(Grant NsG-3277; Contract EX-76-I-01-1028)

(NASA-CR-159856; DOE/NASA/3277-1; WER-10) Avail: NTIS HC A04/MF A01 CSCL 10A

The feasibility of using aileron or spoiler controls as alternates to pitch control for large horizontal axis wind turbines was studied. The NASA Mod-0 100 kw machine was used as the basis for the study. Specific performance studies were conducted for 20% chord ailerons over the outboard 30% span, and for 10% chord spoilers over the same portion of the span. Both control systems utilized control deflections up to 60 deg. Results of the study show that either ailerons or spoilers can provide the control necessary to limit turbine power in high wind conditions. The aileron system, as designed, provides overspeed protection at hurricane wind speeds, low wind speed starting torque of 778 N-m (574 ft. lb) at 3.6 m/sec, and a 1.3 to 1.5% increase in annual energy compared to a fixed pitch rotor. The aileron control system preliminary design study includes aileron loads analysis and the design of a failsafe flyweight actuator for overspeed protection in the event of a hydraulic system failure. L.F.M.

N80-27808*# Spectrolab, Inc., Sylmar, Calif.**SCREEN PRINTING TECHNOLOGY APPLIED TO SILICON SOLAR CELL FABRICATION Final Report, Nov. 1977**

Feb. 1979

Jay W. Thornhill and William E. Sipperly Apr. 1980 64 p refs

(Contract NAS3-20826)

(NASA-CR-159789) Avail: NTIS HC A04/MF A01 CSCL 10A

The process for producing space qualified solar cells in both the conventional and wraparound configuration using screen printing techniques was investigated. Process modifications were chosen that could be easily automated or mechanized. Work was accomplished to optimize the tradeoffs associated with gridline spacing, gridline definition and junction depth. An extensive search for possible front contact metallization was completed. The back surface field structures along with the screen printed back contacts were optimized to produce open circuit voltages of at least an average of 600 millivolts. After all intended modifications on the process sequence were accomplished, the cells were exhaustively tested. Electrical tests at AMO and 28 C were made before and after boiling water immersion, thermal shock, and storage under conditions of high temperature and high humidity. L.F.M.

N80-28860*# Spectrolab, Inc., Sylmar, Calif.**COPLANAR BACK CONTACTS FOR THIN SILICON SOLAR****CELLS Final Report, Jul. 1978 Dec. 1979**

Jay W. Thornhill and W. E. Sipperly Mar 1980 36 p refs
(Contract NAS3-21251)
(NASA-CR-159811) Avail: NTIS HC A03/MF A01 CSCL 10A

A process for fabricating 2 to 3 mil wraparound solar cells was formulated. Sample thin wraparound cells were fabricated using this process. The process used a reinforced perimeter construction to reduce the breakage that occurs during handling of the wafers. A retracting piston post was designed and fabricated to help minimize the breakage that occurs during the screen printing process. Two alternative methods of applying the aluminum back surface field were investigated. In addition to the standard screen printed back surface field, both spin-on and evaporated aluminum techniques were researched. Neither spin-on nor evaporated aluminum made any noticeable improvement over the screen printing technique. A fine screen mesh was chosen for the application of the aluminum paste back surface field. The optimum time and temperature for firing the aluminum turned out to be thirty seconds at 850 C. The development work on the dielectric included looking at three dielectrics for the wraparound application. Transene 1000, Thick Film Systems 1126RCB and an in house formulation 61-2-2A were all tested. Cells with pre-dielectric thickness of 3.0-0-3.5 mils using Transene 1000 as the wraparound dielectric and the procedure outlined above showed an average efficiency of 10.7 percent. Thinner cells were fabricated, but had an unacceptable yield and efficiency. R.E.S.

N80-28862*# General Dynamics/Convair, San Diego, Calif. STUDY OF POWER MANAGEMENT TECHNOLOGY FOR ORBITAL MULTI-100KWe APPLICATIONS, VOLUME 2: STUDY RESULTS Final Report

J. W. Mildice 15 Jul. 1980 293 p 3 Vol.

(Contract NAS3-21757)

(NASA-CR-159834-Vol-2; GDC-ASP-80-015) Avail: NTIS HC A13/MF A01 CSCL 10B

The preliminary requirements and technology advances required for cost effective space power management systems for multi-100 kilowatt requirements were identified. System requirements were defined by establishing a baseline space platform in the 250 KE KWe range and examining typical user loads and interfaces. The most critical design parameters identified for detailed analysis include: increased distribution voltages and space plasma losses, the choice between ac and dc distribution systems, shuttle servicing effects on reliability, life cycle costs, and frequency impacts to power management system and payload systems for AC transmission. The first choice for a power management system for this kind of application and size range is a hybrid ac/dc combination with the following major features: modular design and construction-sized minimum weight/life cycle cost; high voltage transmission (100 Vac RMS); medium voltage array < or = 440 Vdc; resonant inversion; transformer rotary joint; high frequency power transmission line > or = 20 KHz; energy storage on array side or rotary joint; fully redundant; and 10 year life with minimal replacement and repair. J.M.S.

N80-28866*# Midwest Research Inst., Kansas City, Mo. THERMAL ENERGY STORAGE SYSTEMS USING FLUIDIZED BED HEAT EXCHANGERS Final Report, Jan. 1979 - Jan. 1980

Tom Weast and Larry Shannon Jun. 1980 209 p

(Contracts DEN3-96; EC-77-A-31-1034)

(NASA-CR-159868; DOE/NASA/0096-1) Avail: NTIS HC A10/MF A01 CSCL 10C

A rotary cement kiln and an electric arc furnace were chosen for evaluation to determine the applicability of a fluid bed heat exchanger (FBHX) for thermal energy storage (TES). Multistage shallow bed FBHX's operating with high temperature differences were identified as the most suitable for TES applications. Analysis of the two selected conceptual systems included establishing a plant process flow configuration, an operational scenario, a preliminary FBHX/TES design, and parametric analysis. A computer model was developed to determine the effects of the number of stages, gas temperatures, gas flows, bed materials, charge and discharge time, and parasitic power required for operation. The maximum national energy conservation potential

of the cement plant application with TES is 15.4 million barrels of oil or 3.9 million tons of coal per year. For the electric arc furnace application the maximum national conservation potential with TES is 4.5 million barrels of oil or 1.1 million tons of coal per year. Present time of day utility rates are near the breakeven point required for the TES system. Escalation of on-peak energy due to critical fuel shortages could make the FBHX/TES applications economically attractive in the future. E.D.K.

N80-29845* General Dynamics/Convair, San Diego, Calif.
STUDY OF POWER MANAGEMENT TECHNOLOGY FOR ORBITAL MULTI-100KW_e APPLICATIONS. VOLUME 3: REQUIREMENTS

J. W. Mildice 15 Jul. 1980 37 p refs 3 Vol.
 (Contract NAS3-21757)
 (NASA-CR-159834; GDC-ASP-80-015) Avail: NTIS HC A03/MF A01 CSCL 10B

Mid to late 1980's power management technology needs to support development of a general purpose space platform, capable of supplying 100 to 250 KWe to a variety of users in low Earth orbit are examined. A typical, shuttle assembled and supplied space platform is illustrated, along with a group of payloads which might reasonably be expected to use such a facility. Examination of platform and user power needs yields a set of power requirements used to evaluate power management options for life cycle cost effectiveness. The most cost effective ac/dc and dc systems are evaluated, specifically to develop system details which lead to technology goals, including: array and transmission voltages, best frequency for ac power transmission, and advantages and disadvantages of ac and dc systems for this application. System and component requirements are compared with the state-of-the-art to identify areas where technological development is required. Author

N80-29852* Communications Satellite Corp., Clarksburg, Md.
THIN n-i-p RADIATION-RESISTANT SOLAR CELL FEASIBILITY STUDY Final Report

J. F. Allison, R. A. Arndt, and A. Meulenber, Jr. Jun. 1980 70 p refs
 (Contract NAS3-21280)
 (NASA-CR-159871) Avail: NTIS HC A04/MF A01 CSCL 10A

Silicon solar cells were fabricated to verify the predictions that: (1) thin n(+)/pp(+) cells can provide high values of open circuit voltage even when high resistivity base material (> 1000 ohm-cm) is used; (2) cells with good p(+) back contacts will display an increase in open circuit voltage with decreasing cell thickness; and (3) high quality, thin, high resistivity, solar cells can be made using processing compatible with conventional practice. Analysis of I-V and spectral response measurements of these cells confirmed theoretical predictions and thereby pointed to voltages beyond the near 600 mV obtained in this study. Author

N80-29857* Honeywell, Inc., Minneapolis, Minn. Technology Strategy Center.

ACTIVE HEAT EXCHANGE SYSTEM DEVELOPMENT FOR LATENT HEAT THERMAL ENERGY STORAGE Final Report

R. T. LeFrois and A. K. Mathur Apr. 1980 226 p
 (Contract DEN3-38)
 (NASA-CR-159727; DOE/NASA/0038-80/2; HI-79188) Avail: NTIS HC A11/MF A01 CSCL 10C

Five tasks to select, design, fabricate, test and evaluate candidate active heat exchanger modules for future applications to solar and conventional utility power plants were discussed. Alternative mechanizations of active heat exchange concepts were analyzed for use with heat of fusion phase change materials (PCMs) in the temperature range of 250 to 350 C. Twenty-six heat exchange concepts were reviewed, and eight were selected for detailed assessment. Two candidates were selected for small-scale experimentation: a coated tube and shell heat exchanger and a direct contact reflux boiler. A dilute eutectic mixture of sodium nitrate and sodium hydroxide was selected as the PCM from over 50 candidate inorganic salt mixtures.

Based on a salt screening process, eight major component salts were selected initially for further evaluation. The most attractive major components in the temperature range of 250 to 350 C appeared to be NaNO₃, NaNO₂, and NaOH. Sketches of the two active heat exchange concepts selected for test are given. R.K.G.

N80-29860* Jet Propulsion Lab., California Inst. of Tech., Pasadena. Solar Thermal Power Systems.

HIGH TEMPERATURE THERMAL ENERGY STORAGE IN STEEL AND SAND

Robert H. Turner 15 Dec. 1979 93 p Sponsored by NASA and DOE
 (NASA-CR-159708; DOE/NASA/0100-79/1; JPL-PUB-80-35)
 Avail: NTIS HC A05/MF A01 CSCL 10C

The technical and economic potential for high temperature (343 C, 650 F) thermal energy storage in hollow steel ingots, pipes embedded in concrete, and for pipes buried in sand was evaluated. Because it was determined that concrete would separate from pipes due to thermal stresses, concrete was replaced by sand, which is free from thermal stresses. Variations of the steel ingot concept were not cost effective compared to the sand-pipe approach, therefore, the sand-pipe thermal storage unit (TSU) was evaluated in depth to assess the approximate tube spacing requirements consistent with different system performance characteristics and also attendant system costs. For large TSUs which do not require fast response times, the sand-pipe approach offers attractive possibilities. A pipe diameter about 9 cm (3.5 in) and pipe spacing of approximately 25 cm (10 in), with sand filling the interspaces, appears appropriate. Such a TSU system designed for 8 hours charge/discharge cycle has an energy unit storage cost (CE) of \$2.63/kWhr-t and a power unit storage cost (Cp) of \$42/kW-t (in 1977 dollars). A.R.H.

N80-30888* General Electric Co., Fairfield, Conn. Energy Technology Operation.

COGENERATION TECHNOLOGY ALTERNATIVES STUDY (CTAS). VOLUME 6: COMPUTER DATA. PART 1: COAL-FIRED NOCOGENERATION PROCESS BOILER. SECTION A Final Report

W. F. Knightly May 1980 469 p
 (Contract DEN3-31)
 (NASA-CR-159770-Pt-1-A; DOE/NASA/0031-80/6-Vol-6-Pt-1A; GE80ET0105-Vol-6-Pt-1A) Avail: NTIS HC A20/MF A01 CSCL 10B

About fifty industrial processes from the largest energy consuming sectors were used as a basis for matching a similar number of energy conversion systems that are considered as candidate which can be made available by the 1985 to 2000 time period. The sectors considered included food, textiles, lumber, paper, chemicals, petroleum, glass, and primary metals. The energy conversion systems included steam and gas turbines, diesels, thermionics, stirling, closed cycle and steam injected gas turbines, and fuel cells. Fuels considered were coal, both coal and petroleum based residual and distillate liquid fuels, and low Btu gas obtained through the on site gasification of coal. Computer generated reports of the fuels consumption and savings, capital costs, economics and emissions of the cogeneration energy conversion systems (ECS's) heat and power matched to the individual industrial processes are presented. National fuel and emissions savings are also reported for each ECS assuming it alone is implemented. Two nocogeneration base cases are included: coal fired and residual fired process boilers. T.M.

N80-30889* General Electric Co., Fairfield, Conn. Energy Technology Operation.

COGENERATION TECHNOLOGY ALTERNATIVES STUDY (CTAS). VOLUME 6: COMPUTER DATA. PART 1: COAL-FIRED NOCOGENERATION PROCESS BOILER. SECTION B Final Report

W. F. Knightly May 1980 480 p
 (Contract DEN3-31)
 (NASA-CR-159770-Pt-1-B; DOE/NASA/0031-80/6-Vol-6-Pt-1B; GE80ET0105-Vol-6-Pt-1B) Avail: NTIS HC A21/MF A01

CSCL 10B

About fifty industrial processes from the largest energy consuming sectors were used as a basis for matching a similar number of energy conversion systems that are considered as candidate which can be made available by the 1985 to 2000 time period. The sectors considered included food, textiles, lumber, paper, chemicals, petroleum, glass, and primary metals. The energy conversion systems included steam and gas turbines, diesels, thermionics, stirling, closed cycle and steam injected gas turbines, and fuel cells. Fuels considered were coal, both coal and petroleum based residual and distillate liquid fuels, and low Btu gas obtained through the on site gasification of coal. Computer generated reports of the fuel consumption and savings, capital costs, economics and emissions of the cogeneration energy conversion systems (ECS's) heat and power matched to the individual industrial processes are presented. National fuel and emissions savings are also reported for each ECS assuming it alone is implemented. Two nocogeneration base cases are included: coal fired and residual fired process boilers. T.M.

N80-30890* General Electric Co., Fairfield, Conn. Energy Technology Operation.

COGENERATION TECHNOLOGY ALTERNATIVES STUDY (CTAS). VOLUME 6: COMPUTER DATA. PART 2: RESIDUAL-FIRED NOCOGENERATION PROCESS BOILER Final Report

W. F. Knightly May 1980 296 p
(Contract DEN3-31)

(NASA-CR-159770-Pt-2; DOE/NASA/0031-80/6-Vol-6-Pt-2; GE80ET0105-Vol-6-Pt-2) Avail: NTIS HC A13/MF A01 CSCL 10B

About fifty industrial processes from the largest energy consuming sectors were used as a basis for matching a similar number of energy conversion systems that are considered as candidate which can be made available by the 1985 to 2000 time period. The sectors considered included food, textiles, lumber, paper, chemicals, petroleum, glass, and primary metals. The energy conversion systems included steam and gas turbines, diesels, thermionics, stirling, closed cycle and steam injected gas turbines, and fuel cells. Fuels considered were coal, both coal and petroleum based residual and distillate liquid fuels, and low Btu gas obtained through the on site gasification of coal. Computer generated reports of the fuel consumption and savings, capital costs, economics and emissions of the cogeneration energy conversion systems (ECS's) heat and power matched to the individual industrial processes are presented. National fuel and emissions savings are also reported for each ECS assuming it alone is implemented. Two nocogeneration base cases are included: coal fired and residual fired process boilers. T.M.

N80-31869* United Technologies Corp., South Windsor, Conn. Power Systems Div.

COGENERATION TECHNOLOGY ALTERNATIVES STUDY (CTAS). VOLUME 3: ENERGY CONVERSION SYSTEM CHARACTERISTICS Final Report

Jan. 1980 283 p refs
(Contracts DEN3-30; EC-77-A-31-1062)

(NASA-CR-159761; DOE/NASA/0030-80/3-Vol-3; UTC-FCR-1333-Vol-3) Avail: NTIS HC A13/MF A01 CSCL 10B

Six current and thirty-six advanced energy conversion systems were defined and combined with appropriate balance of plant equipment. Twenty-six industrial processes were selected from among the high energy consuming industries to serve as a frame work for the study. Each conversion system was analyzed as a cogenerator with each industrial plant. Fuel consumption, costs, and environmental intrusion were evaluated and compared to corresponding traditional values. The advanced energy conversion technologies indicated reduced fuel consumption, costs, and emissions. Fuel energy savings of 10 to 25 percent were predicted compared to traditional on site furnaces and utility electricity. With the variety of industrial requirements, each advanced technology had attractive applications. Fuel cells indicated the greatest fuel energy savings and emission reductions. Gas turbines and combined cycles indicated high overall annual savings. Steam turbines and gas turbines produced high estimated returns. In some applications, diesels were most efficient. The advanced

technologies used coal derived fuels, or coal with advanced fluid bed combustion or on site gasifications. Data and information for both current and advanced energy conversion technology are presented. Schematic and physical descriptions, performance data, equipment cost estimates, and predicted emissions are included. Technical developments which are needed to achieve commercialization in the 1985-2000 period are identified. R.K.G.

N80-31870* General Electric Co., Philadelphia, Pa. Thermal Power Systems Engineering.

COGENERATION TECHNOLOGY ALTERNATIVES STUDY (CTAS). VOLUME 3: INDUSTRIAL PROCESSES Final Report

W. B. Palmer, H. E. Gerlaugh, and R. R. Priestley Apr. 1980 478 p Sponsored by DOE

(Contract DEN3-31)

(NASA-CR-159767; DOE/NASA/0031-80/3-Vol-3;

GE80ET0104-Vol-3) Avail: NTIS HC A21/MF A01 CSCL 10B

Cogenerating electric power and process heat in single energy conversion systems rather than separately in utility plants and in process boilers is examined in terms of cost savings. The use of various advanced energy conversion systems are examined and compared with each other and with current technology systems for their savings in fuel energy, costs, and emissions in individual plants and on a national level. About fifty industrial processes from the target energy consuming sectors were used as a basis for matching a similar number of energy conversion systems that are considered as candidate which can be made available by the 1985 to 2000 time period. The sectors considered included food, textiles, lumber, paper, chemicals, petroleum, glass, and primary metals. The energy conversion systems included steam and gas turbines, diesels, thermionics, stirling, closed cycle and steam injected gas turbines, and fuel cells. Fuels considered were coal, both coal and petroleum based residual and distillate liquid fuels, and low Btu gas obtained through the on site gasification of coal. An attempt was made to use consistent assumptions and a consistent set of ground rules specified by NASA for determining performance and cost. Data and narrative descriptions of the industrial processes are given. R.K.G.

N80-31882* Westinghouse Research and Development Center, Pittsburgh, Pa.

CELL MODULE AND FUEL CONDITIONER Quarterly Report. Apr. - Jun. 1980

D. Q. Hoover, Jr. Jul. 1980 75 p

(Contracts DEN3-161; DE-AI 03-79ET-11272)

(NASA-CR-159888; DOE/NASA/0161-4;

Rept-80-9E6-MARED-R3; QR-3) Avail: NTIS HC A04/MF A01 CSCL 10A

The computer code for the detailed analytical model of the MK-2 stacks is described. An ERC proprietary matrix is incorporated in the stacks. The mechanical behavior of the stack during thermal cycles under compression was determined. A 5 cell stack of the MK-2 design was fabricated and tested. Designs for the next three stacks were selected and component fabrication initiated. A 3 cell stack which verified the use of wet assembly and a new acid fill procedure were fabricated and tested. Components for the 2 kW test facility were received or fabricated and construction of the facility is underway. The definition of fuel and water is used in a study of the fuel conditioning subsystem. Kinetic data on several catalysts, both crushed and pellets, was obtained in the differential reactor. A preliminary definition of the equipment requirements for treating tap and recovered water was developed. S.J.

N80-33859* General Electric Co., Schenectady, N. Y.

COGENERATION TECHNOLOGY ALTERNATIVES STUDY (CTAS). VOLUME 4: ENERGY CONVERSION SYSTEMS

D. H. Brown, H. E. Gerlaugh, and R. R. Priestley Apr. 1980 178 p refs

(Contract DEN3-31)

(NASA-CR-159768; GE80ET0103-Vol-4;

DOE/NASA/0031-80/4-Vol-4)

Avail: NTIS HC A09/MF A01 CSCL 10B

Industrial processes from the largest energy consuming sectors were used as a basis for matching a similar number of energy conversion systems that are considered as candidate which can be made available by the 1985 to 2000 time period. The sectors considered included food, textiles, lumber, paper, chemicals, petroleum, glass, and primary metals. The energy conversion systems included steam and gas turbines, diesels, thermionics, stirling, closed-cycle and steam injected gas turbines, and fuel cells. Fuels considered were coal, both coal and petroleum-based residual and distillate liquid fuels, and low Btu gas obtained through the on-site gasification of coal. An attempt was made to use consistent assumptions and a consistent set of ground rules specified by NASA for determining performance and cost. The advanced and commercially available cogeneration energy conversion systems studied in CTAS are lined together with their performance, capital costs, and the research and developments required to bring them to this level of performance.

Author

N80-33860* # General Electric Co., Schenectady, N. Y. Energy Technology Operation.

COGENERATION TECHNOLOGY ALTERNATIVES STUDY (CTAS). VOLUME 6: COMPUTER DATA. PART 1: COAL-FIRED NOCOGENERATION PROCESS BOILER, SECTION A Final Report

W. F. Knightly May 1980 481 p refs Prepared for DOE 6 Vol.

(Contract DEN3-31)

(NASA-CR-159770-Pt-1; GE80ET0105-Vol-6-Pt-1;

DOE/NASA/0031-80/6) Avail: NTIS HC A21/MF A01 CSCL 10B

Various advanced energy conversion systems (ECS) are compared with each other and with current technology systems for their savings in fuel energy, costs, and emissions in individual plants and on a national level. About fifty industrial processes from the largest energy consuming sectors were used as a basis for matching a similar number of energy conversion systems that are considered as candidates which can be made available by the 1985 to 2000 time period. The sectors considered included food, textiles, lumber, paper, chemicals, petroleum, glass, and primary metals. The energy conversion systems included steam and gas turbines, diesels, thermionics, stirling, closed cycle and steam injected gas turbines, and fuel cells. Fuels considered were coal, both coal and petroleum based residual and distillate liquid fuels, and low Btu gas obtained through the on-site gasification of coal. Computer generated reports of the fuel consumption and savings, capital costs, economics and emissions of the cogeneration energy conversion systems (ECS's) heat and power matched to the individual industrial processes are presented for coal fired process boilers. National fuel and emissions savings are also reported for each ECS assuming it alone is implemented.

Author

N80-33861* # General Electric Co., Schenectady, N. Y. **COGENERATION TECHNOLOGY ALTERNATIVES STUDY (CTAS). VOLUME 6: COMPUTER DATA. PART 2: RESIDUAL-FIRED NOCOGENERATION PROCESS BOILER Final Report**

W. F. Knightly May 1980 287 p

(Contract DEN3-31)

(NASA-CR-159770-Pt-2; GE80ET0105-Vol-6-Pt-2;

DOE/NASA/0031-80/6-Vol-6-Pt-2)

Avail: NTIS

HC A13/MF A01 CSCL 10B

Computer generated data on the performance of the cogeneration energy conversion system are presented. Performance parameters included fuel consumption and savings, capital costs, economics, and emissions of residual fired process boilers.

T.M.

N80-33862* # National Aeronautics and Space Administration. Lewis Research Center, Cleveland, Ohio.

MOD-2 WIND TURBINE FARM STABILITY STUDY Final Report

E. N. Hinrichsen Jun. 1980 170 p refs

(Contracts DEN3-134; DE-A101-79ET-20305)

(NASA-CR-165156; R35-40; DOE/NASA/0134-1) Avail: NTIS HC A08/MF A01 CSCL 10A

The dynamics of single and multiple 2.5 ME, Boeing MOD-2 wind turbine generators (WTGs) connected to utility power systems were investigated. The analysis was based on digital simulation. Both time response and frequency response methods were used. The dynamics of this type of WTG are characterized by two torsional modes, a low frequency 'shaft' mode below 1 Hz and an 'electrical' mode at 3-5 Hz. High turbine inertia and low torsional stiffness between turbine and generator are inherent features. Turbine control is based on electrical power, not turbine speed as in conventional utility turbine generators. Multi-machine dynamics differ very little from single machine dynamics. T.M.

A80-25099* # Coupled generator and combustor performance calculations for potential early commercial MHD power plants. T. C. Dellinger, J. G. Hnat, and C. H. Marston (GE Space Sciences Laboratory, King of Prussia, Pa.), In: Symposium on the Engineering Aspects of Magnetohydrodynamics, 18th, Butte, Mont., June 18-20, 1979, Preprints, (A80-25061 09-31) Bozeman, Mont., Montana State University, 1979, p. G.5.1-G.5.11, 8 refs. Contract No. DEN3-52.

A parametric study of the performance of the MHD generator and combustor components of potential early commercial open-cycle MHD/steam power plants is presented. Consideration is given to the effects of air heater system concept, MHD combustor type, coal type, thermal input power, oxygen enrichment of the combustion, subsonic and supersonic generator flow and magnetic field strength on coupled generator and combustor performance. The best performance is found to be attained with a 3000 F, indirectly fired air heater, no oxygen enrichment, Illinois no. 6 coal, a two-stage cyclone combustor with 85% slag rejection, a subsonic generator, and a magnetic field configuration yielding a constant transverse electric field of 4 kV/m. Results indicate that optimum net MHD generator power is generally compressor-power-limited rather than electric-stress-limited, with optimum net power a relatively weak function of operating pressure.

A.L.W.

45 ENVIRONMENT POLLUTION

Includes air, noise, thermal and water pollution; environment monitoring; and contamination control.

N80-13721* National Aeronautics and Space Administration. Lewis Research Center, Cleveland, Ohio.

AN ANALYTICAL STUDY OF NITROGEN OXIDES AND CARBON MONOXIDE EMISSIONS IN HYDROCARBON COMBUSTION WITH ADDED NITROGEN. PRELIMINARY RESULTS

David A. Bittker [1979] 17 p refs Proposed for presentation at the 25th Intern. Gas Turbine Conf., New Orleans, 9-13 Mar. 1980; sponsored by ASME

(Contract EF-77-A-01-2593)

(NASA-TM-79296; DOE/NASA/2593-79/10) Avail. NTIS HC A02/MF A01 CSCL 13B

The effect of combustor operating conditions on the conversion of fuel-bound nitrogen (FBN) to nitrogen oxides NO sub x was analytically determined. The effect of FBN and of operating conditions on carbon monoxide (CO) formation was also studied. For these computations, the combustor was assumed to be a two stage, adiabatic, perfectly-stirred reactor. Propane-air was used as the combustible mixture and fuel-bound nitrogen was simulated by adding nitrogen atoms to the mixture. The oxidation of propane and formation of NO sub x and CO were modeled by a fifty-seven reaction chemical mechanism. The results for NO sub x and CO formation are given as functions of primary and secondary stage equivalence ratios and residence times.

R.E.S.

N80-14581* National Aeronautics and Space Administration. Lewis Research Center, Cleveland, Ohio.

SULFATE AND NITRATE COLLECTED BY FILTER SAMPLING NEAR THE TROPOPAUSE

Francis M. Humenik, Erwin A. Lezberg, and Dumas A. Otterson Jan. 1980 30 p refs

(NASA-TP-1567; E-073) Avail. NTIS HC A03/MF A01 CSCL 13B

Filter samples collected near the tropopause with an F-106 aircraft and two Boeing 747 aircraft were analyzed for sulfate and nitrate ion content. Within the range of routine commercial flight altitudes (at or below 12.5 km), stratospheric mass mixing ratios for the winter-spring group averaged 0.26 ppbm for sulfate and 0.35 ppbm for nitrate. For the summer-fall group, stratosphere mixing ratios averaged 0.13 ppbm and 0.25 ppbm for sulfate and nitrate, respectively. Winter-spring group tropospheric mass mixing ratios averaged 0.08 ppbm for sulfate and 0.10 ppbm for nitrate, while summer-fall group tropospheric mixing ratios averaged 0.05 ppbm for sulfate and 0.08 ppbm for nitrate. Correlations of the filter data with available ozone data suggest that the sulfate and nitrate are transported from the stratosphere to the troposphere.

K.L.

N80-21892* National Aeronautics and Space Administration. Lewis Research Center, Cleveland, Ohio.

NASA GLOBAL ATMOSPHERIC SAMPLING PROGRAM (GASP) DATA REPORT FOR TAPES VLO011 AND VLO013 Progress Report, 10 Jan. - 2 Oct. 1977

J. D. Holdeman, Thomas J. Dudzinski, and Marvin W. Tiefermann Mar. 1979 63 p refs

(NASA-TM-81462; E-393) Avail. NTIS HC A04/MF A01 CSCL 13B

In-situ measurements of atmospheric ozone, carbon monoxide, clouds, and related meteorological and flight information obtained during 1122 flights of aircraft VH-EBE and N655PA from January 10 through October 2, 1977 are reported. In addition, tropopause pressures obtained from time and space interpolation of achieved data for the dates of the flights are included. R.E.S.

N80-23875* National Aeronautics and Space Administration. Lewis Research Center, Cleveland, Ohio.

ASSESSMENT OF POTENTIAL EXPOSURE TO FRIABLE INSULATION MATERIALS CONTAINING ASBESTOS

Walter S. Kim and David E. Kuivinen Apr. 1980 41 p refs (NASA-TM-81435; E-359) Avail. NTIS HC A03/MF A01 CSCL 13B

Asbestos and the procedures for assessing potential exposure hazards are discussed. Assessment includes testing a bulk sample of the suspected material for the presence of asbestos, and monitoring the air, if necessary. Based on field inspections and laboratory analyses, the health hazard is evaluated, and abatement measures are taken if a potential hazard exists. Throughout the assessment and abatement program, all applicable regulations are administered as specified by the Environmental Protection Agency and the Occupational Safety and Health Administration.

R.E.S.

N80-27832* National Aeronautics and Space Administration. Lewis Research Center, Cleveland, Ohio.

COORDINATED AIRCRAFT AND SHIP SURVEYS DETERMINING IMPACT OF RIVER INPUTS ON GREAT LAKES WATERS. REMOTE SENSING RESULTS

Charles A. Raquet, Jack A. Salzman, Thom A. Coney, Roger A. Svehla, Donald F. Shook, and Richard T. Gedney Jul. 1980 105 p refs

(NASA-TP-1694; E-172) Avail. NTIS HC A06/MF A01 CSCL 13B

The remote sensing results of aircraft and ship surveys for determining the impact of river effluents on Great Lakes waters are presented. Aircraft multi-spectral scanner data were acquired throughout the spring and early summer of 1976 at five locations: the West Basin of Lake Erie, Genesee River - Lake Ontario, Menomonee River - Lake Michigan, Grand River - Lake Michigan, and Nemadji River - Lake Superior. Multispectral scanner data and ship surface sample data are correlated resulting in 40 contour plots showing large-scale distributions of parameters such as total suspended solids, turbidity, Secchi depth, nutrients, salts, and dissolved oxygen. The imagery and data analysis are used to determine the transport and dispersion of materials from the river discharges, especially during spring runoff events, and to evaluate the relative effects of river input, resuspension, and shore erosion. Twenty-five LANDSAT satellite images of the study sites are also included in the analysis. Examples of the use of remote sensing data in quantitatively estimating total particulate loading in determining water types, in assessing transport across international boundaries, and in supporting numerical current modeling are included. The importance of coordination of aircraft and ship lake surveys is discussed, including the use of telefacsimile for the transmission of imagery.

J.M.S.

A80-45005 * Quantitative interpretation of Great Lakes remote sensing data. D. F. Shook, J. Salzman, R. A. Svehla, and R. T. Gedney (NASA, Lewis Research Center, Cleveland, Ohio). *Journal of Geophysical Research*, vol. 85, July 20, 1980, p. 3991-3996. 15 refs.

The paper discusses the quantitative interpretation of Great Lakes remote sensing water quality data. Remote sensing using color information must take into account (1) the existence of many different organic and inorganic species throughout the Great Lakes, (2) the occurrence of a mixture of species in most locations, and (3) spatial variations in types and concentration of species. The radiative transfer model provides a potential method for an orderly analysis of remote sensing data and a physical basis for developing quantitative algorithms. Predictions and field measurements of volume reflectances are presented which show the advantage of using a radiative transfer model. Spectral absorbance and backscattering coefficients for two inorganic sediments are reported.

A.T.

N80-16686* ORI, Inc., Silver Spring, Md.
**AERIAL APPLICATIONS DISPERSAL SYSTEMS CONTROL
REQUIREMENTS STUDY Final Report**
J. S. Bauchspies, W. L. Cleary, W. F. Rogers, W. Simpson, and
G. S. Sanders 15 Feb. 1980 84 p refs
(Contract NAS3-21714)
(NASA-CR-159781; ORI-TR-1686) Avail: NTIS
HC A05/MF A01 CSCL 13B

Performance deficiencies in aerial liquid and dry dispersal systems are identified. Five control system concepts are explored: (1) end of field on/off control; (2) manual control of particle size and application rate from the aircraft; (3) manual control of deposit rate on the field; (4) automatic alarm and shut-off control; and (5) fully automatic control. Operational aspects of the concepts and specifications for improved control configurations are discussed in detail. A research plan to provide the technology needed to develop the proposed improvements is presented along with a flight program to verify the benefits achieved. K.L.

47 METEOROLOGY AND CLIMATOLOGY

Includes weather forecasting and modification.

A80-35719 * // Modified power law equations for vertical wind profiles. D. A. Spera and T. R. Richards (NASA, Lewis Research Center, Cleveland, Ohio). In: Conference and Workshop on Wind Energy Characteristics and Wind Energy Siting, Portland, Ore., June 19-21, 1979, Proceedings. (A80-35716 14-44) Boston, Mass., American Meteorological Society, 1979, p. 47-56; Discussion, p. 57, 58, 14 refs.

In an investigation of windpower plant siting, equations are presented and evaluated for a wind profile model which incorporates both roughness and wind speed effects, while retaining the basic simplicity of the Hellman power law. These equations recognize the statistical nature of wind profiles and are compatible with existing analytical models and recent wind profile data. Predictions of energy output based on the proposed profile equations are 10% to 20% higher than those made with the 1/7 power law. In addition, correlation between calculated and observed blade loads is significantly better at higher wind speeds when the proposed wind profile model is used than when a constant power model is used. B.J.

A80-32520 * Comments on 'Experimental evidence for interhemispheric transport from airborne carbon monoxide measurements'. P. D. Falconer and R. W. Pratt (New York, State University, Albany, N.Y.). *Journal of Applied Meteorology*, vol. 19, Mar. 1980, p. 338, 339; Reply, p. 339, 340. 8 refs. Grant No. NSG-3138; Contract No. NAS3-21606.

51 LIFE SCIENCES (GENERAL)

Includes genetics

NSO-24983* National Aeronautics and Space Administration.
Lewis Research Center, Cleveland, Ohio.

PRELIMINARY RESULTS OF FAST NEUTRON TREATMENTS IN CARCINOMA OF THE PANCREAS

Reinhard Gahbauer, Kyee Y. Koh, Antonio Rodriguez-Antunez, Gwynn L. Jelden, Robert F. Turco, John Horton, Ronald Bukowski, Ronald Reimer, James Blue, William Roberts et al 1980 4 p
Presented at the National Pancreatic Proj., New Orleans, 18 Apr. 1980 Prepared in cooperation with Cleveland Clinic Foundation, Ohio

(NASA-TM-81516; E-460) Avail: NTIS HC A02/MF A01 CSCL 06E

A group of 30 patients with adenocarcinoma of the pancreas including some patients with very advanced disease, were treated with the so-called mixed beam modality employing photon treatments three times per week and neutron treatments twice a week. Two hundred Rads or equivalent Rads (RBE 3.3) were given in daily fractions aiming at a total dose of 6000 Rads in 6 to 8 weeks. The treatments were well tolerated and significant palliation was achieved in 26 to 30 cases. Twelve months survival was 33 percent with a median survival of 7 months or 210 days. Treatment techniques and localization procedures are discussed.

R.E.S.

52 AEROSPACE MEDICINE

Includes physiological factors, biological effects of radiation; and weightlessness

N80-14684* National Aeronautics and Space Administration.
Lewis Research Center, Cleveland, Ohio.

INTNA-OCULAR PRESSURE NORMALIZATION TECHNIQUE AND EQUIPMENT Patent

Edward F. Baehr, Inventor (to NASA) Issued 12 Jun. 1979
6 p. Filed 31 Aug. 1977 Supersedes N77-30736 (15 - 21,
p 2839)

(NASA-Case-LEW-12955-1; US-Patent-4,157,718;
US-Patent-Appl-SN-829318; US-Patent-Class-128-276) Avail:
US Patent and Trademark Office CSCL 06B

A method and apparatus is described for safely reducing abnormally high intraocular pressure in an eye during a predetermined time interval. This allows maintenance of normal intraocular pressure during glaucoma surgery. A pressure regulator of the spring-biased diaphragm type is provided with additional bias by a column of liquid. The hypodermic needle can be safely inserted into the anterior chamber of the eye. Liquid is then bled out of the column to reduce the bias on the diaphragm of the pressure regulator and, consequently, the output pressure of the regulator. This lowering pressure of the regulator also occurs in the eye by means of a small second bleed path provided between the pressure regulator and the hypodermic needle.

Official Gazette of the U.S. Patent and Trademark Office

60 COMPUTER OPERATIONS AND HARDWARE

Includes computer graphics and data processing
For components see 33 *Electronics and Electrical
Engineering*

N80 16742* National Aeronautics and Space Administration
Lewis Research Center, Cleveland, Ohio

INFORM: AN INTERACTIVE DATA COLLECTION AND DISPLAY PROGRAM WITH DEBUGGING CAPABILITY

David S. Cwynar Jan 1980 169 p refs
(NASA TP 1424 E 9810) Avail NTIS HC A08/MF A01 CSCL
09B

A computer program was developed to aid ASSEMBLY language programmers of mini and micro computers in solving the man machine communications problems that exist when scaled integers are involved. In addition to producing displays of quasi-steady state values, INFORM provides an interactive mode for debugging programs, making program patches, and modifying the displays. Auxiliary routines SAMPLE and DATAO add dynamic data acquisition and high speed dynamic display capability to the program. Programming information and flow charts to aid in implementing INFORM on various machines together with descriptions of all supportive software are provided. Program modifications to satisfy the individual user's needs are considered.

RCT.

61 COMPUTER PROGRAMMING AND SOFTWARE

Includes computer programs, routines, and algorithms.

N80-33104* National Aeronautics and Space Administration.
Lewis Research Center, Cleveland, Ohio.

NONANALYTIC FUNCTION GENERATION ROUTINES FOR 16-BIT MICROPROCESSORS

James F. Soeder and Maryrita Shaufl Washington Sep. 1980
66 p refs
(NASA-TM-81586, E-565) Avail: NTIS HC A04/MF A01 CSCL
09B

Interpolation techniques for three types (univariate, bivariate, and map) of nonanalytic functions are described. These interpolation techniques are then implemented in scaled fraction arithmetic on a representative 16 bit microprocessor. A FORTRAN program is described that facilitates the scaling, documentation, and organization of data for use by these routines. Listings of all these programs are included in an appendix. L.F.M.

N80-18863* National Aeronautics and Space Administration.
Lewis Research Center, Cleveland, Ohio.

ALGORITHM FOR CALCULATING TURBINE COOLING FLOW AND THE RESULTING DECREASE IN TURBINE EFFICIENCY

James W. Gauntner Feb. 1980 23 p refs
(NASA-TM-81453; E-384) Avail: NTIS HC A02/MF A01 CSCL
09B

An algorithm is presented for calculating both the quantity of compressor bleed flow required to cool the turbine and the decrease in turbine efficiency caused by the injection of cooling air into the gas stream. The algorithm, which is intended for an axial flow, air routine in a properly written thermodynamic cycle code. Ten different cooling configurations are available for each row of cooled airfoils in the turbine. Results from the algorithm are substantiated by comparison with flows predicted by major engine manufacturers for given bulk metal temperatures and given cooling configurations. A list of definitions for the terms in the subroutine is presented. K.L.

65 STATISTICS AND PROBABILITY

Includes data sampling and smoothing, Monte Carlo method, and stochastic processes.

N80-29088* National Aeronautics and Space Administration
Lewis Research Center, Cleveland, Ohio.

CYCLES TILL FAILURE OF SILVER-ZINC CELLS WITH COMPLETING FAILURE MODES: PRELIMINARY DATA ANALYSIS

Steven M. Sidik, Harold F. Leibeck, and John M. Bozek 1980
48 p refs Presented at Ann. Meeting of the Am. Statist.
Assoc., Houston, Tex., 11-14 Aug. 1980
(NASA-TM-81556; E-517) Avail: NTIS HC A03/MF A01 CSCL
14D

One hundred and twenty nine cells were run through charge-discharge cycles until failure. The experiment design was a variant of a central composite factorial in five factors. Preliminary data analysis consisted of response surface estimation of life. Batteries fail under two basic modes; a low voltage condition and an internal shorting condition. A competing failure modes analysis using maximum likelihood estimation for the extreme value life distribution was performed. Extensive diagnostics such as residual plotting and probability plotting were employed to verify data quality and choice of model. Auhtor

A80-40764 * 'Chain pooling' model selection for two-level fixed effects factorial experiments. A. G. Holms (NASA, Lewis Research Center, Cleveland, Ohio). *Communications in Statistics, Part B: Simulation and Computation*, vol. B9, no. 1, 1980, p. 51-71. 12 refs.

As many as three iterated statistical model deletion procedures are considered for an experiment. Population model coefficients were chosen to simulate a saturated factorial experiment having an unfavorable distribution of parameter values. Using random number studies, three model selection strategies were developed, namely, (1) a strategy to be used in anticipation of large coefficients of variation (neighborhood of 65 percent), (2) strategy to be used in anticipation of small coefficients of variation (4 percent or less), and (3) a security regret strategy to be used in the absence of such prior knowledge. (Author)

66 SYSTEMS ANALYSIS

Includes mathematical modeling; network analysis; and operations research.

N80-16824*// National Aeronautics and Space Administration
Lewis Research Center, Cleveland, Ohio.

AN AVERAGING BATTERY MODEL FOR A LEAD-ACID BATTERY OPERATING IN AN ELECTRIC CAR Final Report

John M. Bozek Dec. 1979 19 p refs

(Contract EC-77-A-31-1044)

(NASA-TM-79321; DOE/NASA/1044-79/5; E-277) Avail:
NTIS HC A02/MF A01 CSCL 12B

A battery model is developed based on time averaging the current or power, and is shown to be an effective means of predicting the performance of a lead acid battery. The effectiveness of this battery model was tested on battery discharge profiles expected during the operation of an electric vehicle following the various SAE J227a driving schedules. The averaging model predicts the performance of a battery that is periodically charged (regenerated) if the regeneration energy is assumed to be converted to retrievable electrochemical energy on a one-to-one basis.

Author

A80-10035 * // Computerized systems analysis and optimization of aircraft engine performance, weight, and life cycle costs. L. H. Fishbach (NASA, Lewis Research Center, Flight Performance Section, Cleveland, Ohio). *NATO, AGARD, Symposium on the Use of Computers as a Design Tool, Munich, West Germany, Sept. 3-6, 1979, Paper*. 20 p. 16 refs.

The paper describes the computational techniques employed in determining the optimal propulsion systems for future aircraft applications and to identify system tradeoffs and technology requirements. The computer programs used to perform calculations for all the factors that enter into the selection process of determining the optimum combinations of airplanes and engines are examined. Attention is given to the description of the computer codes including NNEP, WATE, LIFCYC, INSTAL, and POD DRG. A process is illustrated by which turbine engines can be evaluated as to fuel consumption, engine weight, cost and installation effects. Examples are shown as to the benefits of variable geometry and of the tradeoff between fuel burned and engine weights. Future plans for further improvements in the analytical modeling of engine systems are also described.

C.F.W.

67 THEORETICAL MATHEMATICS

Includes topology and number theory.

N80-24129* National Aeronautics and Space Administration.
Lewis Research Center, Cleveland, Ohio.

FAR-FIELD RADIATION OF AFT TURBOFAN NOISE

Edward J. Rice and Arthur V. Saule 1980 25 p refs Presented
at 99th Meeting of the Acoust. Soc. of Am., Atlanta, 21-25 Apr
1980

(NASA-TM-81506, e-444) Avail: NTIS HC A02/MF A01 CSCL
20A

Approximate expressions were developed for the noise radiation from the aft duct. The results of approximate aft radiation equation compare favorably to more exact Wiener-Hopf radiation results. Refraction as well as convective effects in the multiple flow streams is considered. The peak in the radiation pattern, which occurs nearly at engine sideline, is composed of modes with relatively large cut-off ratios. This implies that aft fan radiation will be inherently more difficult to suppress than the fan inlet noise. The theoretical multimodal radiation pattern is compared to experimental data for the first two harmonics of blade passage frequency for three full scale fans at two speeds. The agreement between theory and experiment is quite good.

A.R.H.

71 ACOUSTICS

Includes sound generation, transmission and attenuation.
For noise pollution see 45 Environment Pollution.

N80-12822* National Aeronautics and Space Administration, Lewis Research Center, Cleveland, Ohio.
TIME-DEPENDENT DIFFERENCE THEORY FOR NOISE PROPAGATION IN A TWO-DIMENSIONAL DUCT
Kenneth J. Baumeister 1979 13 p refs Presented at 18th Aerospace Sci. Meeting, Pasadena, Calif., 14-16 Jan. 1980; sponsored by AIAA
(NASA-TM-79298; E-249; AIAA-Paper-80-0098) Avail: NTIS HC A02/MF A01 CSCL 20A

A time dependent numerical formulation was derived for sound propagation in a two dimensional straight soft-walled duct in the absence of mean flow. The time dependent governing acoustic-difference equations and boundary conditions were developed along with the maximum stable time increment. Example calculations were presented for sound attenuation in hard and soft wall ducts. The time dependent analysis were found to be superior to the conventional steady numerical analysis because of much shorter solution times and the elimination of matrix storage requirements.
R.C.T.

N80-12823* National Aeronautics and Space Administration, Lewis Research Center, Cleveland, Ohio.
A TIME DEPENDENT DIFFERENCE THEORY FOR SOUND PROPAGATION IN DUCTS WITH FLOW
K. J. Baumeister 1979 38 p refs Presented at 98th Meeting of the Acoustical Soc. of Am., Salt Lake City, Utah, 26-30 Nov. 1979
(NASA-TM-79302; E-254) Avail: NTIS HC A03/MF A01 CSCL 20A

A time dependent numerical solution of the linearized continuity and momentum equation was developed for sound propagation in a two dimensional straight hard or soft wall duct with a sheared mean flow. The time dependent governing acoustic difference equations and boundary conditions were developed along with a numerical determination of the maximum stable time increments. A harmonic noise source radiating into a quiescent duct was analyzed. This explicit iteration method then calculated stepwise in real time to obtain the transient as well as the steady state solution of the acoustic field. Example calculations were presented for sound propagation in hard and soft wall ducts, with no flow and plug flow. Although the problem with sheared flow was formulated and programmed, sample calculations were not examined. The time dependent finite difference analysis was found to be superior to the steady state finite difference and finite element techniques because of shorter solution times and the elimination of large matrix storage requirements.
R.C.T.

N80-12824* National Aeronautics and Space Administration, Lewis Research Center, Cleveland, Ohio.
RECIPROCITY PRINCIPLE IN DUCT ACOUSTICS
Young-chung Cho 1979 23 p refs Presented at 97th Meeting of the Acoustical Soc. of Am., Cambridge, Mass., 11-15 Jun. 1979
(NASA-TM-79300; E-250) Avail: NTIS HC A02/MF A01 CSCL 20A

Various reciprocity relations in duct acoustics have been derived on the basis of the spatial reciprocity principle implied in Green's functions for linear waves. The derivation includes the reciprocity relations between mode conversion coefficients for reflection and transmission in nonuniform ducts, and the relation between the radiation of a mode from an arbitrarily terminated duct and the absorption of an externally incident plane wave by the duct. Such relations are well defined as long as the systems remain linear, regardless of acoustic properties of duct nonuniformities which cause the mode conversions.
Author

N80-13881* National Aeronautics and Space Administration, Lewis Research Center, Cleveland, Ohio.

ASSESSMENT AT FULL SCALE OF EXHAUST NOZZLE TO WING SIZE ON STOL-OTW ACOUSTIC CHARACTERISTICS

U. VonGlahn and D. Grosbeck 1979 27 p refs Presented at 98th Meeting of the Acoustical Soc. of Am., Salt Lake City, 26-30 Nov. 1979
(NASA-TM-79279; E-215) Avail: NTIS HC A03/MF A01 CSCL 20A

On the basis of static aero/acoustic data obtained at model scale, the effect of exhaust nozzle size on flyover noise is evaluated at full scale for different STOL-OTW nozzle configurations. Three types of nozzles are evaluated: a circular/deflector nozzle mounted above the wing; a slot/deflector nozzle mounted on the wing; and a slot nozzle mounted on the wing. The nozzle exhaust plane location, measured from the wing leading edge, was varied from 10 to 46 percent of the wing chord (flaps retracted). Flap angles of 20 deg (takeoff) and 60 deg (approach) are included in the study. Initially, perceived noise levels (PNL) are calculated as a function flyover distance at 152m altitude. From these plots, static EPNL values (defined as flyover relative noise levels), are obtained as functions of nozzle size for equal aerodynamic performance (lift and thrust). The acoustic benefits attributable to nozzle size relative to a given wing chord size are assessed.

A.R.H.

N80-14843* National Aeronautics and Space Administration, Lewis Research Center, Cleveland, Ohio.

ACOUSTIC CONSIDERATIONS OF FLIGHT EFFECTS ON JET NOISE SUPPRESSOR NOZZLES

U. vonGlahn 1979 26 p refs Presented at the AIAA 18th Aerospace Sci. Meeting, Pasadena, Calif., 14-16 Jan. 1980
(NASA-TM-81377; E-282; AIAA-Paper-80-0164) Avail: NTIS HC A03/MF A01 CSCL 20A

The inflight acoustic characteristics of high velocity jet noise suppressor nozzles for supersonic cruise aircraft were reviewed. The inflight effects at the peak noise level were discussed. Both single and inverted velocity profile multistream suppressor nozzles were considered. The importance of static spectral shape on the noise reduction due to inflight effects was stressed.
R.C.T.

N80-15876* National Aeronautics and Space Administration, Lewis Research Center, Cleveland, Ohio.

COMPARISON OF INLET SUPPRESSOR DATA WITH APPROXIMATE THEORY BASED ON CUTOFF RATIO

Edward J. Rice and Laurence J. Heidelberg [1979] 28 p refs Presented at the AIAA Aerospace Sci. Meeting, Pasadena, Calif., 14-16 Jan. 1980
(NASA-TM-81386; E-294) Avail: NTIS HC A03/MF A01 CSCL 20A

Inlet suppressor far-field directivity suppression was quantitatively compared with that predicted using an approximate linear design and evaluation method based upon mode cutoff ratio. The experimental data was obtained using a series of cylindrical point-reacting inlet liners on a YF102 engine. The theoretical prediction program is based upon simplified sound propagation concepts derived from exact calculations. These indicate that all of the controlling phenomenon can be approximately correlated with mode cutoff ratio which itself is intimately related to the angles of propagation within the duct. The theory-data comparisons are intended to point out possible deficiencies in the approximate theory which may be corrected. After all theoretical refinements are made, then empirical corrections can be applied.
A.R.H.

N80-16882* National Aeronautics and Space Administration, Lewis Research Center, Cleveland, Ohio.

APPLICATION OF COHERENCE IN FAN NOISE STUDIES

Joseph R. Balombin Feb. 1980 26 p refs
(NASA-TP-1630; E-157) Avail: NTIS HC A03/MF A01 CSCL 20A

A study of fan noise was made by using the coherence function to obtain far field spectra that were coherent with the

fan rotational rate. Choosing fan rotational rate as one of the two variables yielded new information about the far field noise generated during static fan testing. As a result of this coherent data processing, the inlet fan-tone noise present in static testing was determined to be mostly random when the rotor-alone and rotor-stator interaction tones were cut off. After the rotor-alone sound field was cut on, the sound pressure became coherent, and the angular extent of high coherence increased as fan speed was increased. In addition, the sound field was organized as a pattern of lobes whose amplitude varied slowly with time. Additional fan test results indicate that operating the fan with an inflow control device can partially reduce the fan-tone noise levels to those produced by coherent processing R.E.S.

N80-22045* National Aeronautics and Space Administration. Lewis Research Center, Cleveland, Ohio.

SPECTRAL STRUCTURE OF PRESSURE MEASUREMENTS MADE IN A COMBUSTION DUCT

J. H. Miles and D. D. Raftopoulos (Toledo Univ.) 1980 46 p refs Presented at 99th Meeting of the Acoust. Soc. of Am., Atlanta, 21-25 Apr. 1980 (NASA-TM-81471; E-404) Avail: NTIS HC A03/MF A01 CSCL 20A

A model for acoustic plane wave propagation in a combustion duct through a confined, flowing gas containing soot particles is presented. The model takes into account only heat transfer between the gas and soot particles. As a result, the model depends on only a single parameter which can be written as the ratio of the soot particle thermal relaxation time to the soot particle mass fraction. The model yields expressions for the attenuation and dispersion of the plane wave which depends only on this single parameter. The model was used to calculate pressure spectra in a combustion duct. The results were compared with measured spectra. For particular values of the single free parameter, the calculated spectra resemble the measured spectra. Consequently, the model, to this extent, explains the experimental measurements and provides some insight into the number and type of particles. Author

N80-22046* National Aeronautics and Space Administration. Lewis Research Center, Cleveland, Ohio.

NOISE SUPPRESSION DUE TO ANNULUS SHAPING OF AN INVERTED-VELOCITY-PROFILE COAXIAL NOZZLE

J. Goodykoontz and U. vonGlahn Apr. 1980 27 p refs Presented at 99th Meeting of the Acoust. Soc. of Am., Atlanta, 21-25 Apr. 1980 (NASA-TM-81460; E-389) Avail: NTIS HC A03/MF A01 CSCL 20A

An inverted velocity profile coaxial nozzle for use with supersonic cruise aircraft produces less jet noise than an equivalent conical nozzle. Furthermore, decreasing the annulus height (increasing radius ratio with constant flow) results in further noise reduction benefits. The annulus shape (height) was varied by an eccentric mounting of the annular nozzle with respect to a conical core nozzle. Acoustic measurements were made in the flyover plane below the narrowest portion of the annulus and at 90 deg and 180 deg from this point. The model-scale spectra are scaled up to engine size (1.07 m diameter) and the perceived noise levels for the eccentric and baseline concentric inverted velocity profile coaxial nozzles are compared over a range of operating conditions. The implications of the acoustic benefits derived with the eccentric nozzle to practical applications are discussed. A.R.H.

N80-22047* National Aeronautics and Space Administration. Lewis Research Center, Cleveland, Ohio.

NOISE SUPPRESSION DUE TO ANNULUS SHAPING OF CONVENTIONAL COAXIAL NOZZLE

U. vonGlahn and J. Goodykoontz 1980 19 p refs Prepared for the 99th Meeting of the Acoust. Soc. of Am., Atlanta, 21-25 Apr. 1980 (NASA-TM-81461; E-390) Avail: NTIS HC A02/MF A01 CSCL 20A

A method which shows that increasing the annulus width

of a conventional coaxial nozzle with constant bypass velocity will lower the noise level is described. The method entails modifying a concentric coaxial nozzle to provide an eccentric outer stream annulus while maintaining approximately the same through flow as that for the original concentric bypass nozzle. Acoustical tests to determine the noise generating characteristics of the nozzle over a range of flow conditions are described. The tests involved sequentially analyzing the noise signals and digitally recording the 1/3 octave band sound pressure levels. The measurements were made in a plane passing through the minimum and maximum annulus width points, as well as at 90 degrees in this plane, by rotating the outer nozzle about its axis. Representative measured spectral data in the flyover plane for the concentric nozzle obtained at model scale are discussed. Representative spectra for several engine cycles are presented for both the eccentric and concentric nozzles at engine size. A.W.H.

N80-22048* National Aeronautics and Space Administration. Lewis Research Center, Cleveland, Ohio.

AN IMPROVED PREDICTION METHOD FOR THE NOISE GENERATED IN FLIGHT BY CIRCULAR JETS

James R. Stone and Francis J. Montegani 1980 33 p refs Prepared for the 99th Meeting of the Acoust. Soc. of Am., Atlanta, 21-25 Apr. 1980 (NASA-TM-81470; E-403) Avail: NTIS HC A03/MF A01 CSCL 20A

A semi-empirical model for predicting the noise generated by jets exhausting from circular nozzles is presented and compared with small-scale static and simulated-flight data. The present method is an updated version of that part of the original NASA aircraft noise prediction program relating to circular jet noise. The earlier method agreed reasonably well with experimental static and flight data for jet velocities up to approximately 520 m/sec. The poorer agreement at higher jet velocities appeared to be due primarily to the manner in which supersonic convection effects were formulated. The purely empirical supersonic convection formulation is replaced in the present method by one based on theoretical considerations. Other improvements of an empirical nature were included based on model-jet/free-jet simulated-flight tests. The effects of nozzle size, jet velocity, jet temperature, and flight are included. A.R.H.

N80-23096* National Aeronautics and Space Administration. Lewis Research Center, Cleveland, Ohio.

TIME DEPENDENT DIFFERENCE THEORY FOR SOUND PROPAGATION IN AXISYMMETRIC DUCTS WITH PLUG FLOW

K. J. Baumeister 1980 12 p refs Presented at 6th Aeroacoustics Conf., Hartford, Conn. 4-6 Jun. 1980; sponsored by AIAA (NASA-TM-81501; E-438) Avail: NTIS HC A02/MF A01 CSCL 20A

The time dependent governing acoustic-difference equations and boundary conditions are developed and solved for sound propagation in an axisymmetric (cylindrical) hard wall duct with a plug mean flow and spinning acoustic modes. The analysis begins with a harmonic sound source radiating into a quiescent duct. This explicit iteration method then calculates stepwise in real time to obtain the transient as well as the 'steady' state solutions of the acoustic field. The time dependent finite difference analysis has two advantages over the steady state finite difference and finite element techniques: (1) the elimination of large matrix storage requirements, and (2) shorter solution times under most conditions. Author

N80-23097* National Aeronautics and Space Administration. Lewis Research Center, Cleveland, Ohio.

PRESSURE SPECTRA AND CROSS SPECTRA AT AN AREA CONTRACTION IN A DUCTED COMBUSTION SYSTEM

J. H. Miles and D. D. Raftopoulos 1980 12 p refs Presented at 1980 ASME Aerospace Conf., San Francisco, 13-15 Aug. 1980 (NASA-TM-81477; E-411) Avail: NTIS HC A02/MF A01 CSCL 20A

Pressure spectra and cross-spectra at an area contraction in

a liquid fuel, ducted, combustion noise test facility are analyzed. Measurements made over a range of air and fuel flows are discussed. Measured spectra are compared with spectra calculated using a simple analytical model. Author

N80-23098*# National Aeronautics and Space Administration. Lewis Research Center, Cleveland, Ohio.
EFFECT OF INFLOW CONTROL ON INLET NOISE OF A CUT-ON FAN

Richard P. Woodward and Frederick W. Glaser 1980 13 p refs Presented at 6th Aeroacoustics Conf., Hartford, Conn., 4-6 Jun. 1980; sponsored by AIAA (NASA-TM-81487) Avail: NTIS HC A02/MF A01 CSCL 20A

The control of turbulence and other inflow disturbances in anechoic chambers for static turbofan noise studies was studied. A cut-on, high tip speed fan stage was acoustically tested with three configurations of an inflow control device in an anechoic chamber. Although this was a cut-on design, rotor inflow interaction appeared to be a much stronger source of blade passing tone radiated from the inlet than rotor stator interaction for the 1.6 mean rotor chord separation. Aft external suction applied to the area where the inflow control device joined the inlet produced a further reduction in blade passing tone, suggesting that disturbances in the forward flow on the outside of the inlet were superimposed on the inlet boundary layer and were a significant source of tone noise. M.G.

N80-23100*# National Aeronautics and Space Administration. Lewis Research Center, Cleveland, Ohio.

FORWARD ACOUSTIC PERFORMANCE OF A SHOCK-SWALLOWING HIGH-TIP-SPEED FAN (QF-13)

James G. Lucas, Richard P. Woodward, and Michael J. MacKinnon May 1980 20 p refs (NASA-TP-1668; E-202) Avail: NTIS HC A02/MF A01 CSCL 20A

Forward noise and overall aerodynamic performance data are presented for a high-tip-speed fan having rotor blade airfoils designed to alter the conventional leading-edge bow shocks to weak, oblique shocks which are swallowed within the interblade channels. It was anticipated that the swallowed shocks would minimize the generation of multiple-pure-tone noise. In the speed range where the shocks presumably were swallowed, the multiple-tone noise was lowered only about 3 decibels. Comparison with several high-speed fans on a thrust-corrected basis indicates that the present fan was the quietest in total forward noise at low speeds but offered no advantage at high speeds. Author

N80-23101*# National Aeronautics and Space Administration. Lewis Research Center, Cleveland, Ohio.

HIGHER ORDER MODE PROPAGATION IN NONUNIFORM CIRCULAR DUCTS

Y. C. Cho and K. U. Ingard 1980 11 p refs Presented at the 6th Aeroacoustics Conf., Hartford, 4-6 Jun. 1980; sponsored by AIAA Prepared in cooperation with MIT, Cambridge (NASA-TM-81481; E-418) Avail: NTIS HC A02/MF A01 CSCL 20A

Higher order mode propagation in a nonuniform circular duct without mean flow was investigated. An approximate wave equation is derived on the assumptions that the duct cross section varies slowly and that mode conversion is negligible. Exact closed form solutions are obtained for a particular class of converging-diverging circular duct which referred to as 'circular cosh duct.' Numerical results are presented in terms of the transmission loss for the various duct shapes and frequencies. The results are applicable to multimodal propagation, single mode propagation, and sound radiation from certain types of contoured inlet ducts, or of sound propagation in a converging-diverging duct of somewhat different shape from a cosh duct. F.O.S.

N80-23102*# National Aeronautics and Space Administration. Lewis Research Center, Cleveland, Ohio.

AN EXPLORATORY SURVEY OF NOISE LEVELS ASSOCIATED WITH A 100kW WIND TURBINE

J. R. Balombin 1980 20 p refs Presented at the 99th Meeting of the Acoustical Soc. of Am., Atlanta, 21-25 Apr. 1980 (NASA-TM-81486; E-424) Avail: NTIS HC A02/MF A01 CSCL 20A

Noise measurements of a 125-foot diameter, 100 kW wind turbine are presented. The data include measurements as functions of distance from the turbine and directivity angle and cover a frequency range from 1 Hz to several kHz. Potential community impact is discussed in terms of A-weighted noise levels relative to background levels, and the intrasonic spectral content. Finally, the change in the sound power spectrum associated with a change in the rotor speed is described. The acoustic impact of this size wind turbine is judged to be minimal. M.G.

N80-25101*# National Aeronautics and Space Administration. Lewis Research Center, Cleveland, Ohio.

A COMPARISON BETWEEN AN EXISTING PROPELLER NOISE THEORY AND WIND TUNNEL DATA

James H. Dittmar May 1980 41 p refs (NASA-TM-81519; E-464) Avail: NTIS HC A03/MF A01 CSCL 20A

The noise of three supersonic helical tip speed propellers was compared with the noise predicted by an existing noise theory. Comparisons of the peak blade passage tones showed fairly good agreement between theory and experiment at the lowest helical tip Mach numbers tested, 0.86 and 1.00, while at higher numbers, the theory predicted higher noise levels than measured. When the differences among the propellers were considered the theory and measurement showed fairly good agreement. Directivity measurements in general showed that the measured blade passage tone data peaked further downstream than the theory predicted. At the cruise design condition the harmonics appeared to fall off faster in the data than the theory indicated. E.D.K.

N80-26115*# National Aeronautics and Space Administration. Lewis Research Center, Cleveland, Ohio.

MEASURED AND PREDICTED IMPINGEMENT NOISE FOR A MODEL-SCALE UNDER THE WING EXTERNALLY BLOWN FLAP CONFIGURATION WITH A QCSEE TYPE NOZZLE

D. J. McKinzie, Jr Jun. 1980 63 p refs (NASA-TM-81494; E-432) Avail: NTIS HC A04/MF A01 CSCL 20A

Jet/flap interaction noise was measured and predicted for a small-scale model two-flap, under-the-wing, externally blown flap configuration equipped with and without noise suppression devices. The devices consisted of short spanwise fairings centered in relationship to the jet axis and positioned in the slots between the wing and flaps. The nozzle approximated that of the Quiet Clean Short-haul Experimental Engine (QCSEE). Takeoff noise reductions of 6 dB in the flyover and 5 dB in the sideline plane were obtained over a wide range of radiation angles. Approach noise reductions of about 5 dB were obtained only in the forward quadrant of the flyover plane; no reductions were obtained in the sideline plane. Models of several noise sources were combined analytically to form an overall noise prediction, the results from which compared favorably with the measured data. The aerodynamic performance characteristics for these configurations were substantially the same in the takeoff attitude. However, in the approach attitude, the suppressed configuration produced a 6 percent reduction in the flow turning efficiency. Author

N80-29132*# National Aeronautics and Space Administration. Lewis Research Center, Cleveland, Ohio.

PREDICTION OF UNSUPPRESSED JET ENGINE EXHAUST NOISE IN FLIGHT FROM STATIC DATA

James R. Stone 1980 26 p refs Presented at 6th Aeroacoustics Conf., Hartford, Conn., 4-6 Jun. 1980; sponsored by AIAA (NASA-TM-81537; E-491) Avail: NTIS HC A03/MF A01 CSCL 20A

A methodology developed for predicting in-flight exhaust noise from static data is presented and compared with experimental

data for several unsuppressed turbojet engines. For each engine, static data over a range of jet velocities are compared with the predicted jet mixing noise and shock-cell noise. The static engine noise over and above the jet and shock noises is identified as excess noise. The excess noise data are then empirically correlated to smooth the spectral and directivity relations and account for variations in test conditions. This excess noise is then projected to flight based on the assumption that the only effects of flight are a Doppler frequency shift and a level change given by $40 \log (1 - M \sin \theta \cos \theta)$, where $M \sin \theta$ is the flight Mach number and θ is the observer angle relative to the jet axis.

M.G.

N80-30154 // National Aeronautics and Space Administration. Lewis Research Center, Cleveland, Ohio.

NUMERICAL TECHNIQUES IN LINEAR DUCT ACOUSTICS Status Report

K. J. Baumeister 1980 23 p refs. Proposed for presentation at Winter Ann. Meeting of ASME Chicago, 17-21 Nov. 1980 (NASA-TM-81553; E-513). Avail: NTIS HC A02/MF A01 CSCL 20A

Both finite difference and finite element analyses of small amplitude (linear) sound propagation in straight and variable area ducts with flow, as might be found in a typical turbojet engine duct, muffler, or industrial ventilation system, are reviewed. Both steady state and transient theories are discussed. Emphasis is placed on the advantages and limitations associated with the various numerical techniques. Examples of practical problems are given for which the numerical techniques have been applied.

A.R.H.

A80-18269 * // Time-dependent difference theory for noise propagation in a two-dimensional duct. K. J. Baumeister (NASA, Lewis Research Center, Cleveland, Ohio), *American Institute of Aeronautics and Astronautics, Aerospace Sciences Meeting, 18th, Pasadena, Calif., Jan. 14-16, 1980, Paper 80-0098*, 10 p. 36 refs.

A time-dependent numerical formulation is derived for sound propagation in a two-dimensional straight soft-walled duct in the absence of mean flow. The time-dependent governing acoustic-difference equations and boundary conditions are developed along with the maximum stable time increment. Example calculations are presented for sound attenuation in hard- and soft-wall ducts. The time-dependent analysis has been found to be superior to the conventional steady numerical analysis because of much shorter solution times and the elimination of matrix storage requirements.

(Author)

A80-20951 * // A time dependent difference theory for sound propagation in ducts with flow. K. J. Baumeister (NASA, Lewis Research Center, Cleveland, Ohio), *Acoustical Society of America, Meeting, 98th, Salt Lake City, Utah, Nov. 26-30, 1979, Paper*, 36 p. 38 refs.

A time dependent numerical solution of the linearized continuity and momentum equation is developed for sound propagation in a two-dimensional straight hard or soft wall duct with a sheared mean flow. The time dependent governing acoustic-difference equations and boundary conditions are developed along with a numerical determination of the maximum stable time increments. The analysis begins with a harmonic noise source radiating into a quiescent duct. This explicit iteration method then calculates stepwise in real time to obtain the transient as well as the 'steady' state solution of the acoustic field. Example calculations are presented for sound propagation in hard and soft wall ducts, with no flow and with plug flow. Although the problem with sheared flow has been formulated and programmed, sample calculations have not yet been examined. So far, the time dependent finite difference analysis has been found to be superior to the steady state finite difference and finite element techniques because of shorter solution times and the elimination of large matrix storage requirements.

(Author)

A80-20952 * // Assessment at full scale of exhaust nozzle-to-wing size on STOL-OTW acoustic characteristics. U. von Glahn and D. Groesbeck (NASA, Lewis Research Center, Cleveland, Ohio), *Acoustical Society of America, Meeting, 98th, Salt Lake City, Utah, Nov. 26-30, 1979, Paper*, 25 p. 5 refs.

On the basis of static zero/acoustic data obtained at model scale, the effect of exhaust nozzle size on flyover noise is evaluated at full scale for different STOL-OTW nozzle configurations. Three types of nozzles are evaluated: a circular/deflector nozzle mounted above the wing, a slot/deflector nozzle mounted on the wing, and a slot nozzle mounted on the wing. The nozzle exhaust plane location, measured from the wing leading edge was varied from 10 to 48 percent of the wing chord (flaps retracted). Flap angles of 20 deg (takeoff) and 60 deg (approach) are included in the study. Initially, perceived noise levels (PNL) are calculated as a function of flyover distance at 152 m altitude. From these plots static EPNL values, defined as flyover relative noise levels, then are obtained as functions of nozzle size for equal aerodynamic performance (lift and thrust). On the basis of these calculations, the acoustic benefits attributable to nozzle size relative to a given wing chord size are assessed.

(Author)

A80-20953 * // Dispersion of sound in a combustion duct by fuel droplets and soot particles. J. H. Miles (NASA, Lewis Research Center, Cleveland, Ohio) and D. D. Raftopoulos (Toledo, University, Toledo, Ohio), *Acoustical Society of America, Meeting, 98th, Salt Lake City, Utah, Nov. 26-30, 1979, Paper*, 27 p. 22 refs.

Dispersion and attenuation of acoustic plane wave disturbances propagating in a ducted combustion system are studied. The dispersion and attenuation are caused by fuel droplet and soot emissions from a jet engine combustor. The attenuation and dispersion are due to heat transfer and mass transfer and viscous drag forces between the emissions and the ambient gas. Theoretical calculations show sound propagation at speeds below the isentropic speed of sound at low frequencies. Experimental results are in good agreement with the theory.

(Author)

A80-20956 * // Reciprocity principle in duct acoustics. Y.-C. Cho (NASA, Lewis Research Center, Cleveland, Ohio), *Acoustical Society of America, Meeting, 97th, Cambridge, Mass., June 11-15, 1979, Paper*, 21 p. 10 refs.

Various reciprocity relations in duct acoustics have been derived on the basis of the spatial reciprocity principle implied in Green's functions for linear waves. The derivation includes the reciprocity relations between mode conversion coefficients for reflection and transmission in nonuniform ducts, and the relation between the radiation of a mode from an arbitrarily terminated duct and the absorption of an externally incident plane wave by the duct. Such relations are well defined as long as the systems remain linear, regardless of acoustic properties of duct nonuniformities which cause the mode conversions.

(Author)

A80-20964 * // Comparison of inlet suppressor data with approximate theory based on cutoff ratio. E. J. Rice and L. J. Heidelberg (NASA, Lewis Research Center, Cleveland, Ohio), *American Institute of Aeronautics and Astronautics, Aerospace Sciences Meeting, 18th, Pasadena, Calif., Jan. 14-16, 1980, Paper 80-0100*, 26 p. 21 refs.

This paper represents the initial quantitative comparison of inlet suppressor far-field directivity suppression with that predicted using an approximate liner design and evaluation method based upon mode cutoff ratio. The experimental data was obtained using a series of cylindrical point-reacting inlet liners on an Avco-Lycoming YF102 engine. The theoretical prediction program is based upon simplified sound propagation concepts derived from exact calculations. These indicate that all of the controlling phenomenon can be approximately correlated with mode cutoff ratio which itself is intimately related to the angles of propagation within the duct. The objective of the theory-data comparisons is to point out possible deficiencies in the approximate theory which may be corrected. After all theoretical

refinements have been made, then empirical corrections can be applied. (Author)

A80-20965 * # Acoustic considerations of flight effects on jet noise suppressor nozzles. U. von Glahn (NASA, Lewis Research Center, Cleveland, Ohio). *American Institute of Aeronautics and Astronautics, Aerospace Sciences Meeting, 18th, Pasadena, Calif., Jan. 14-16, 1980, Paper 80-0164*, 24 p, 14 refs.

Insight into the inflight acoustic characteristics of high-velocity jet noise suppressor nozzles for supersonic cruise aircraft (SCA) is provided. Although the suppression of jet noise over the entire range of directivity angles is of interest, the suppression of the peak noise level in the rear quadrant is frequently of the most interest. Consequently, the paper is directed primarily to the inflight effects at the peak noise level. Both single and inverted-velocity-profile multistream suppressor nozzles are considered. The importance of static spectral shape on the noise reduction due to inflight effects is stressed. (Author)

A80-35496 * # Spectral structure of pressure measurements made in a combustion duct. J. H. Miles (NASA, Lewis Research Center, Cleveland, Ohio) and D. D. Raftopoulos (Toledo, University, Toledo, Ohio). *Acoustical Society of America, Meeting, 99th, Atlanta, Ga., Apr. 21-25, 1980, Paper, 44 p, 43 refs.*

The spectral structure of pressure measurements made in a ducted combustion test facility are studied. Dispersion and attenuation of acoustic plane waves may occur in the duct at low frequencies due to combustor emissions and affect the spectral structure. A model that considers the propagation of plane waves through a cloud of particles in a flowing gas and which includes heat transfer between soot particles and the gas is discussed. Experimental results are compared with theory. (Author)

A80-35497 * # Noise suppression due to annulus shaping of a conventional coaxial nozzle. U. von Glahn and J. Goodykoontz (NASA, Lewis Research Center, Cleveland, Ohio). *Acoustical Society of America, Meeting, 99th, Atlanta, Ga., Apr. 21-25, 1980, Paper, 17 p, 5 refs.*

Previous studies have shown that increasing the annulus width of a conventional coaxial nozzle with constant bypass velocity will lower the noise level. In the present model-scale study, the annulus was shaped by an eccentric mounting of the annular nozzle with respect to the conical core nozzle. Acoustic measurements were made in the flyover plane below the widest portion of the annulus and at 90 deg and 180 deg from this point. The model-scale spectra are scaled up to engine size (1.07 m diameter) and the perceived noise levels for the eccentric and concentric coaxial nozzles are compared over a limited range of operating conditions. The implications of the acoustic benefits derived from the eccentric nozzle to practical applications are discussed. (Author)

A80-35498 * # Noise suppression due to annulus shaping of an inverted-velocity-profile coaxial nozzle. J. Goodykoontz and U. von Glahn (NASA, Lewis Research Center, Cleveland, Ohio). *Acoustical Society of America, Meeting, 99th, Atlanta, Ga., Apr. 21-25, 1980, Paper, 25 p, 8 refs.*

Previous studies have shown that an inverted-velocity-profile coaxial nozzle for use with supersonic cruise aircraft produces less jet noise than an equivalent conical nozzle. Furthermore, decreasing the annulus height (increasing radius ratio with constant flow) results in further noise reduction benefits. In the present model-scale study, the annulus shape, that is, height, was varied by an eccentric mounting of the annular nozzle with respect to a conical core nozzle. Acoustic measurements were made in the flyover plane below the narrowest portion of the annulus and at 90 deg and 180 deg from this point. The model-scale spectra are scaled up to engine size (1.07 m diameter) and the perceived noise levels for the eccentric and baseline concentric inverted-velocity-profile coaxial nozzles are com-

pared over a range of operating conditions. The implications of the acoustic benefits derived with the eccentric nozzle to practical applications are discussed. (Author)

A80-35499 * # An exploratory survey of noise levels associated with a 100 kW wind turbine. J. R. Balombin (NASA, Lewis Research Center, Cleveland, Ohio). *Acoustical Society of America, Meeting, 99th, Atlanta, Ga., Apr. 21-25, 1980, Paper, 18 p.*

During performance tests of a 125-foot diameter, 100 kW wind turbine at the NASA Plum Brook Station near Sandusky, Ohio, the opportunity arose to make exploratory noise measurements and results of those surveys are presented. The data include measurements as functions of distance from the turbine, and directivity angle, and cover a frequency range from 1 Hz to several kHz. Potential community impact is discussed in terms of A-weighted noise levels relative to background levels, and the infrasonic spectral content. Finally, the change in the sound power spectrum associated with a change in the rotor speed is described. The acoustic impact of this size wind turbine is judged to be minimal. (Author)

A80-35974 * # Higher order mode propagation in nonuniform circular ducts. Y. C. Cho (NASA, Lewis Research Center, Cleveland, Ohio) and K. U. Ingard (MIT, Cambridge, Mass.). *American Institute of Aeronautics and Astronautics, Aeroacoustics Conference, 6th, Hartford, Conn., June 4-6, 1980, Paper 80-1018*, 8 p, 10 refs.

This paper presents an analytical investigation of higher order mode propagation in a nonuniform circular duct without mean flow. An approximate wave equation is derived on the assumptions that the duct cross section varies slowly and that mode conversion is negligible. Exact closed form solutions are obtained for a particular class of converging-diverging circular duct which is here referred to as 'circular cosh duct'. Numerical results are presented in terms of the transmission loss for the various duct shapes and frequencies. The results are applicable to studies of multimodal propagation as well as single mode propagation. The results are also applicable to studies of sound radiation from certain types of contoured inlet ducts, or of sound propagation in a converging-diverging duct of somewhat different shape from a cosh duct. (Author)

A80-35993 * # Effect of inflow control on inlet noise of a cut-on fan. R. P. Woodward and F. W. Glaser (NASA, Lewis Research Center, Cleveland, Ohio). *American Institute of Aeronautics and Astronautics, Aeroacoustics Conference, 6th, Hartford, Conn., June 4-6, 1980, Paper 80-1049*, 9 p, 12 refs.

A cut-on, high tip speed fan stage was acoustically tested with three configurations of an inflow control device in the NASA Lewis anechoic chamber. Although this was a cut-on design, rotor-inflow interaction appeared to be a much stronger source of blade passing tone radiated from the inlet than rotor-stator interaction for the 1.6 mean rotor chord separation. Aft external suction applied to the area where the inflow control device joined the inlet produced a further reduction in blade passing tone suggesting that disturbances in the forward flow on the outside of the inlet were superimposed on the inlet boundary layer and were a significant source of tone noise. (Author)

A80-37895 * Rigorous solutions for sound radiation from circular ducts with hyperbolic horns or infinite plane baffle. Y. C. Cho (NASA, Lewis Research Center, Cleveland, Ohio). *Journal of Sound and Vibration*, vol. 69, Apr. 8, 1980, p. 405-425. 20 refs. Grant No. NGR-09-010-085.

A rigorous treatment is presented of sound radiation from circular ducts with either a hyperbolic horn or an infinite plane baffle. In the analysis hyperboloidal wave functions are used, which are defined here, for the first time, as a class of eigensolutions of the wave equation for oblate spheroidal co-ordinates. The numerical results include the complex conversion (or reflection) coefficients and the radiation directivity for various incident wave modes,

spinning modes as well as axisymmetric modes. The solutions are valid for the whole frequency range including frequencies above and below the cut-off frequencies of the duct modes involved. (Author)

A80-41156 * # Workshop report for the AIAA 5th Aeroacoustics Conference, M. E. Goldstein (NASA, Lewis Research Center, Cleveland, Ohio). *Journal of Aircraft*, vol. 17, July 1980, p. 473-478.

Summaries of current understandings, technological tools and remaining controversies in the field of aeroacoustics are presented, with attention also given to developments in means of noise suppression to comply with proposed and projected regulations. Topics include jet noise mechanisms and their suppression; turbo-machinery noise, including noise sources, noise prediction by the modal approach and experimental methods; duct acoustics, with discussion of sound attenuation and propagation, the application of finite element methods, and the radiation of sound from inlets; helicopter rotor, airplane propeller and V/STOL noise; aircraft interior noise; and general acoustics, atmospheric propagation and the sonic boom. A.L.W.

N80-11870 * # Lockheed-Georgia Co., Marietta.
STUDIES OF THE ACOUSTIC TRANSMISSION CHARACTERISTICS OF COAXIAL NOZZLES WITH INVERTED VELOCITY PROFILES, VOLUME 1 Final Report
P. D. Dean, M. Salikuddin, K. K. Ahuja, H. E. Plumbee, and P. Mungur Cleveland, Ohio NASA May 1979 186 p refs (Contract NAS3-20797)

(NASA-CR-159698; LG79ER0178-Vol-1) Avail: NTIS HC A09/MF A01 CSDL 20A

The efficiency of internal noise radiation through coannular exhaust nozzle with an inverted velocity profile was studied. A preliminary investigation was first undertaken to: (1) define the test parameters which influence the internal noise radiation; (2) develop a test methodology which could realistically be used to examine the effects of the test parameters; (3) and to validate this methodology. The result was the choice of an acoustic impulse as the internal noise source in the jet nozzles. Noise transmission characteristics of a nozzle system were then investigated. In particular, the effects of fan nozzle convergence angle, core extension length to annulus height ratio, and flow Mach number and temperatures were studied. The results are presented as normalized directivity plots. R.C.T.

N80-13882 * # Hamilton Standard, Windsor Locks, Conn.
ADVANCED TURBO-PROP AIRPLANE INTERIOR NOISE REDUCTION-SOURCE DEFINITION Final Report
B. Magliozzi and Bennett M. Brooks Oct. 1979 90 p refs (Contract NAS3-20614)
(NASA-CR-159668) Avail: NTIS HC A05/MF A01 CSDL 20A

Acoustic pressure amplitudes and phases were measured in model scale on the surface of a rigid semicylinder mounted in an acoustically treated wind tunnel near a prop-fan (an advanced turboprop with many swept blades) model. Operating conditions during the test simulated those of a prop-fan at 0.8 Mach number cruise. Acoustic pressure amplitude and phase contours were defined on the semicylinder surface. Measurements obtained without the semi-cylinder in place were used to establish the magnitude of pressure doubling for an aircraft fuselage located near a prop-fan. Pressure doubling effects were found to be 9dB at 90 deg incidence decreasing to no effect at grazing incidence. Comparisons of measurements with predictions made using a recently developed prop-fan noise prediction theory which includes linear and non-linear source terms showed good agreement in phase and in peak noise amplitude. Predictions of noise amplitude and phase contours, including pressure doubling effects derived from test, are included for a full scale prop-fan installation. Author

N80-32186 * # Lockheed-Georgia Co., Marietta.

A STUDY OF THE TRANSMISSION CHARACTERISTICS OF SUPPRESSOR NOZZLES

K. K. Ahuja, M. Salikuddin, R. H. Burrin, and H. E. Plumbee, Jr. Jun. 1980 263 p refs
(Contract NAS3-20797)
(NASA-CR-165133) Avail: NTIS HC A12/MF A01 CSDL 20A

The internal noise radiation characteristics for a single stream 12 lobe 24 tube suppressor nozzle, and for a dual stream 36 chute suppressor nozzle were investigated. An equivalent single round conical nozzle and an equivalent coannular nozzle system were also tested to provide a reference for the two suppressors. The technique utilized a high voltage spark discharge as a noise source within the test duct which permitted separation of the incident, reflected and transmitted signals in the time domain. These signals were then Fourier transformed to obtain the nozzle transmission coefficient and the power transfer function. These transmission parameters for the 12 lobe, 24 tube suppressor nozzle and the reference conical nozzle are presented as a function of jet Mach number, duct Mach number polar angle and temperature. Effects of simulated forward flight are also considered for this nozzle. For the dual stream, 36 chute suppressor, the transmission parameters are presented as a function of velocity ratios and temperature ratios. Possible data for the equivalent coaxial nozzle is also presented. Jet noise suppression by these nozzles is also discussed. A.R.H.

A80-35951 * # Acoustic behavior of fibrous bulk materials. A. S. Hersh and B. Walker (Hersh Acoustical Engineering, Chatsworth, Calif.). *American Institute of Aeronautics and Astronautics, Aeroacoustics Conference, 6th, Hartford, Conn., June 4-6, 1980, Paper 80-0986*, 14 p. 16 refs. Contract No. NAS3-21975.

A semiempirical model of the acoustic behavior of fibrously constructed bulk materials of Hersh and Walker (1979) is generalized to take into account the filtration or removal of particles by fibrous mats and heat conduction between the material fibers and the surrounding fluid. Equations governing the propagation and attenuation of sound waves in a fibrous material are derived on the basis of a solution of the Navier Stokes equation for momentum conservation and a one-dimensional model of heat transfer between the sound field and the fibers. A comparison of the two propagation constants and material impedance specified by the model and experimental measurements for Kevlar 29 indicates the accuracy of the model over a wide range of sound frequencies, material porosities and specimen thickness. It is also found that heat transfer effects are relatively unimportant, while the attenuation constants and material characteristic impedance are a function of fiber orientation relative to sound field propagation direction. A.L.W.

A80-35965 * # Acoustic pressures on a prop-fan aircraft fuselage surface. B. Magliozzi (United Technologies Corp., Hamilton Standard Div., Windsor Locks, Conn.). *American Institute of Aeronautics and Astronautics, Aeroacoustics Conference, 6th, Hartford, Conn., June 4-6, 1980, Paper 80-1002*, 11 p. 9 refs. Contract No. NAS3-20614.

Acoustic pressure amplitude and phase distributions on the surface of a simulated fuselage (a rigid semi-cylinder) installed in an acoustically treated wind tunnel near a Prop-Fan model were measured. The test conditions simulated the relative tip Mach number and blade loading of a full scale Prop-Fan at high altitude 0.8 Mach number cruise. Measurements were also made at equivalent microphone locations without the semi-cylinder to establish the effects of the presence of a fuselage on the sound pressure amplitudes. These effects were found to be 6 dB at 90 degrees incidence, decreasing to no effect at grazing incidence. Comparison of measurements and calculations using a Hamilton Standard Prop-Fan noise calculation computer program showed good agreement in peak level and in phase distribution. Continuous recordings were also made of a Prop-Fan RPM sweep at constant simulated flight speed and a simulated flight speed sweep at constant Prop-Fan RPM. These showed smooth variations in noise level over the tip Mach number range 0.878 to 1.143. (Author)

A80-38642 * # Characteristics of internal- and jet-noise radiation from a multi-lobe, multi-tube suppressor nozzle tested statically and under flight simulation. K. K. Ahuja, M. Salikuddin, and H. E. Plumblee, Jr. (Lockheed-Georgia Co., Marietta, Ga.). *American Institute of Aeronautics and Astronautics, Aeroacoustics Conference, 6th, Hartford, Conn., June 4-6, 1980, Paper 80-1027*. 15 p. 23 refs. Research sponsored by the Lockheed-Georgia Co.; Contract No. NAS3-20797.

Nozzle transmission coefficient (NTC) for a 12-lobe, 24-tube suppressor nozzle and a reference round convergent nozzle of equal area are obtained by an impulse test technique. This technique utilizes a high voltage spark discharge as a noise source within the test duct. Effects of nozzle geometry, jet Mach number, jet temperature and flight velocity on the radiation characteristics of the two nozzles are presented. Likewise, the jet mixing noise measured in the absence of internal noise for both nozzles at static and also simulated flight conditions are discussed. (Author)

A80-45844 * A comparison of experiment and theory for sound propagation in variable area ducts. A. H. Nayfeh, J. E. Kaiser, R. L. Marshall, and C. J. Hurst (Virginia Polytechnic Institute and State University, Blacksburg, Va.). *Journal of Sound and Vibration*, vol. 71, July 22, 1980, p. 241-259. 20 refs. Contract No. NAS3-18553.

An experimental and analytical program has been carried out to evaluate sound suppression techniques in ducts that produce refraction effects due to axial velocity gradients. The analytical program employs a computer code based on the method of multiple scales to calculate the influence of axial variations due to slow changes in the cross-sectional area as well as transverse gradients due to the wall boundary layers. Detailed comparisons between the analytical predictions and the experimental measurements have been made. The circumferential variations of pressure amplitudes and phases at several axial positions have been examined in straight and variable area ducts, with hard walls and lined sections, and with and without a mean flow. Reasonable agreement between the theoretical and experimental results has been found. (Author)

72 ATOMIC AND MOLECULAR PHYSICS

Includes atomic structure and molecular spectra

N80-33188* National Aeronautics and Space Administration
Lewis Research Center, Cleveland, Ohio
HYDROGEN HOLLOW CATHODE ION SOURCE Patent
Michael J. Mirtich, Jr., James S. Sovey, and Robert F. Roman,
inventors (to NASA) Issued 19 Aug 1980 4 p Filed 23 Oct
1978 Supersedes N79-10894 (17 - 01, p 0118)
(NASA Case LEW-12940-1, US Patent 4,218,633.
US Patent Appl SN-953391, US Patent Class 313-362,
US Patent Class 313-231 4) Avail US Patent and Trademark
Office CSCL 20H

A source of hydrogen ions is disclosed and includes a chamber having at one end a cathode which provides electrons and through which hydrogen gas flows into the chamber. Screen and accelerator grids are provided at the other end of the chamber. A baffle plate is disposed between the cathode and the grids and a cylindrical baffle is disposed coaxially with the cathode at the one end of the chamber. The cylindrical baffle is of greater diameter than the baffle plate to provide discharge impedance and also to protect the cathode from ion flux. An anode electrode draws the electrons away from the cathode. The hollow cathode includes a tubular insert of tungsten impregnated with a low work function material to provide ample electrons. A heater is provided around the hollow cathode to initiate electron emission from the low work function material.

Official Gazette of the U S Patent and Trademark Office

A80-34048 * Comments on Auger electron production by Ne+/ bombardment of surfaces. S. V. Pepper and J. Ferrante (NASA, Lewis Research Center, Cleveland, Ohio). *Surface Science*, vol. 88, no. 1, Oct. 3, 1979, p. L1-L5. 5 refs.

A80-34049 * Strengthening of tough iron-12% nickel-reactive metal alloys at 77 K by copper additions. J. R. Stephens and W. R. Witzke (NASA, Lewis Research Center, Cleveland, Ohio). *Cryogenics*, vol. 20, Jan. 1980, p. 18-24. 13 refs.

75 PLASMA PHYSICS

Includes magnetohydrodynamics and plasma fusion.
For ionospheric plasmas see 46 *Geophysics*. For space plasmas see 50 *Astrophysics*.

N80-12881* National Aeronautics and Space Administration. Lewis Research Center, Cleveland, Ohio.
RESULTS OF DUCT AREA RATIO CHANGES IN THE NASA LEWIS H₂-O₂ COMBUSTION MHD EXPERIMENT
J. Marlin Smith 1979 12 p refs Presented at 18th Aerospace Sci. Meeting, Pasadena, Calif., 14-16 Jan. 1980; sponsored by AIAA
(NASA-TM-79308; E-264) Avail: NTIS HC A02/MF A01 CSCL 201

MHD power generation experiments utilizing a cesium-seeded H₂-O₂ working fluid were carried out using a diverging area Hall duct having an entrance Mach number of 2. The experiments were conducted in a high field strength cryomagnet facility at field strengths up to 5 tesla. The effects of power takeoff location, generator loading B field strength, and electrode breakdown voltage were investigated. The effect of area ratio, multiple loading of the duct, and duct location within the magnetic field are considered. R.C.T.

N80-14922* National Aeronautics and Space Administration. Lewis Research Center, Cleveland, Ohio.
EFFECT OF VELOCITY OVERSHOOT ON THE PERFORMANCE OF MAGNETOHYDRODYNAMIC SUBSONIC DIFFUSERS
Mahesh S. Greywall (Wichita State Univ.) and J. Marlin Smith 1980 10 p refs Presented at Aerospace Sci. Meeting, Pasadena, Calif., 14-16 Jan. 1980; Sponsored by AIAA
(Contract EF-77-A-01-2674)
(NASA-TM-79305; DOE/NASA/2674-79/6; E-257) Avail: NTIS HC A02/MF A01 CSCL 201

The evolution of an overshoot velocity distribution was studied in a plane two dimensional diffuser as a function of diffuser divergence angle. The diffuser performance for velocity overshoot was compared to that for a fully developed inlet velocity profile. Results indicate that the ratio of peak-to-center line velocity increases along the diffuser for a diffuser half angle greater than some critical value. It was also found that irrespective of the accompanying inlet temperature distribution, the wall shear stress and the wall heat flux is substantially larger when the inlet velocity profile has an overshoot than that for a fully developed inlet velocity profile. R.C.T.

N80-16885* National Aeronautics and Space Administration. Lewis Research Center, Cleveland, Ohio.
COMMENTS ON TEC TRENDS
James F. Morris 1979 28 p refs Presented at Intern. Conf. on Plasma Sci., Montreal, 4-6 Jun. 1979; sponsored by IEEE
(NASA-TM-79317; E-273) Avail: NTIS HC A03/MF A01 CSCL 201

A technology assessment of thermionic energy conversion research and technology is presented. R.E.S.

N80-16886* National Aeronautics and Space Administration. Lewis Research Center, Cleveland, Ohio.
EXPERIMENTS ON H₂-O₂MHD POWER GENERATION
J. Marlin Smith 1980 18 p refs Proposed for presentation at the 3d World Hydrogen Energy Conf., Tokyo, 23 - 26 Jun. 1980
(NASA-TM-81424) Avail: NTIS HCA02/MFA01 CSCL 201

Magnetohydrodynamic power generation experiments utilizing a cesium-seeded H₂-O₂ working fluid were carried out using a diverging area Hall duct having an entrance Mach number of 2. The experiments were conducted in a high-field strength cryomagnet facility at field strengths up to 5 tesla. The effects of power takeoff location, axial duct location within the magnetic

field, generator loading, B-field strength, and electrode breakdown voltage were investigated. For the operating conditions of these experiments, it is found that the power output increases with the square of the B-field and can be limited by choking of the channel or interelectrode voltage breakdown which occurs at Hall fields greater than 50 volts/insulator. Peak power densities of greater than 100 MW/cu M were achieved. A.R.H.

N80-18946* National Aeronautics and Space Administration. Lewis Research Center, Cleveland, Ohio.
EXPERIMENTAL RESULTS ON PLASMA INTERACTIONS WITH LARGE SURFACES AT HIGH VOLTAGES
Norman T. Grier 1980 12 p refs Presented at 18th Aerospace Sci. Meeting, Pasadena, Calif., 14-16 Jan. 1980; sponsored by AIAA
(NASA-TM-81423; E-346) Avail: NTIS HC A02/MF A01 CSCL 201

Multikilowatt power levels for future payloads can be more efficiently generated using solar arrays operating in the kilovolt range. This implies that large areas of the array at high operating voltages will be exposed to the space plasma environment. The resulting interactions of these high voltage surfaces with space plasma environments can seriously impact the performance of the satellite system. The plasma-surface interaction phenomena were studied in tests performed in two separate vacuum chambers, a 4.6 m diameter by 19.2 long chamber and a 2.0 m diameter by 27.4 m long chamber. The generated plasma density was approximately 1x10 to the 4th power/cm³. Ten solar array panels, each with areas of 1400 sq cm were used in the tests. Nine of the solar panels were tested as a composite unit in the form of a 3x3 solar panel matrix. The results from all the tests confirmed small sample tests results. Insulators were found to enhance the plasma coupling current for high positive bias and arcing was found to occur at high negative bias. A.R.H.

N80-22083* National Aeronautics and Space Administration. Lewis Research Center, Cleveland, Ohio.
POTENTIALITIES OF TEC TOPPING: A SIMPLIFIED VIEW OF PARAMETRIC EFFECTS
James F. Morris 1980 21 p refs Presented at Intern. Conf. on Plasma Sci., Madison, Wisc., 19-21 May 1980; sponsored by IEEE
(Contract EC-77-A-31-1062)
(NASA-TM-81468; DOE/NASA/1062-80/5; E-399) Avail: NTIS HC A02/MF A01 CSCL 10A

An examination of the benefits of thermionic-energy-conversion (TEC)-topped power plants and methods of increasing conversion efficiency are discussed. Reductions in the cost of TEC modules yield direct decreases in the cost of electricity (COE) from TEC-topped central station power plants. Simplified COE, overall-efficiency charts presented illustrate this trend. Additional capital-cost diminution results from designing more compact furnaces with considerably increased heat transfer rates allowable and desirable for high temperature TEC and heat pipes. Such improvements can evolve of the protection from hot corrosion and slag as well as the thermal expansion compatibilities offered by silicon-carbide clads on TEC-heating surfaces. Greater efficiencies and far fewer modules are possible with high-temperature, high-power-density TEC. This decreases capital and fuel costs much more and substantially increases electric power outputs for fixed fuel inputs. In addition to more electricity, less pollution, and lower costs, TEC topping used directly in coal-combustion products contributes balance-of-payment gains. M.G.

N80-33221* National Aeronautics and Space Administration. Lewis Research Center, Cleveland, Ohio.
OPTIMAL THERMIONIC ENERGY CONVERSION WITH ESTABLISHED ELECTRODES FOR HIGH-TEMPERATURE TOPPING AND PROCESS HEATING Final Report
James F. Morris Jul. 1980 33 p refs
(Contract EC-77-A-31-1062)
(NASA-TM-81555; DOE/NASA/1062-6; E-514) Avail: NTIS HC A03/MF A01 CSCL 201

Applied research-and-technology (ART) work reveals that optimal thermionic energy conversion (TEC) with approximately

1000 K to approximately 1100 K collectors is possible using well established tungsten electrodes. Such TEC with 1800 K emitters could approach 26.6% efficiency at 27.4 W/sq cm with approximately 1000 K collectors and 21.7% at 22.6 W/sq cm with approximately 1100 K collectors. These performances require 1.5 and 1.7 eV collector work functions (not the 1 eV ultimate) with nearly negligible interelectrode losses. Such collectors correspond to tungsten electrode systems in approximately 0.9 to approximately 6 torr cesium pressures with 1800 K to 1900 K emitters. Because higher heat-rejection temperatures for TEC allow greater collector work functions, interelectrode loss reduction becomes an increasingly important target for applications aimed at elevated temperatures. Studies of intragap modifications and new electrodes that will allow better electron emission and collection with lower cesium pressures are among the TEC-ART approaches to reduced interelectrode losses. These solutions will provide very effective TEC to serve directly in coal-combustion products for high-temperature topping and process heating. In turn this will help to use coal and to use it well. A.R.H.

A80-11366 * Study of a rare-gas transverse fast discharge. D. L. Chubb and C. J. Michels (NASA, Lewis Research Center, Cleveland, Ohio). *Journal of Applied Physics*, vol. 50, Oct. 1979, p. 6230-6240. 34 refs.

An experimental and analytical study of a Blumlein-type transverse fast discharge operating with He and Xe are presented. An electro-optical voltage probe was used to measure the discharge voltage, and the measured voltages were in agreement with the computed voltages. The analytical model was used to predict the dependences of the discharge efficiency for producing metastables and ions on the important plasma and external circuit parameters. In He the ion efficiency is greater than the metastable efficiency, while in Xe it is the opposite; the He ion efficiencies are much larger than in Xe, while Xe metastable efficiencies are much larger than in He. These differences between Xe and He are accounted by the large dissociative recombination rate of Xe compared with He. A.T.

A80-18243 * # Results of duct area ratio changes in the NASA Lewis H₂-O₂ combustion MHD experiment. J. M. Smith (NASA, Lewis Research Center, Cleveland, Ohio). *American Institute of Aeronautics and Astronautics, Aerospace Sciences Meeting, 18th, Pasadena, Calif., Jan. 14-16, 1980, Paper 80-0023*. 7 p.

MHD power generation experiments utilizing a cesium-seeded H₂-O₂ working fluid have been carried out using a diverging area Hall duct having an entrance Mach number of 2. The experiments are conducted in a high-field strength cryomagnet facility at field strengths up to 5 tesla. The effects of power takeoff location, generator loading, B-field strength, and electrode breakdown voltage have been investigated. In this paper the effect of area ratio, multiple loading of the duct, and duct location within the magnetic field are considered. (Author)

A80-25476 * The effect of a weak vertical magnetic field on fluctuation-induced transport in a Bumpy-Torus plasma. Y. C. Kim, E. J. Powers, J. Y. Hong (Texas, University, Austin, Tex.), J. R. Roth, and W. M. Krawczonok (NASA, Lewis Research Center, Cleveland, Ohio). *Nuclear Fusion*, vol. 20, Feb. 1980, p. 171-176. 11 refs. Research supported by the Texas Atomic Energy Research Foundation; Grant No. NSG-3089.

A80-44239 * # Experiments on H₂-O₂ MHD power generation. J. M. Smith (NASA, Lewis Research Center, Cleveland, Ohio). *International Association for Hydrogen Energy, World Hydrogen Energy Conference, 3rd, Tokyo, Japan, June 23-26, 1980, Paper. 16*.

MHD power generation experiments utilizing a cesium-seeded H₂-O₂ working fluid have been carried out using a diverging area Hall duct having an entrance Mach number of 2. The experiments are conducted in a high-field strength cryomagnet facility at field

strengths up to 5 tesla. The effects of power takeoff location, axial duct location within the magnetic field, generator loading, B field strength, and electrode breakdown voltage were investigated. For the operating conditions of these experiments it is found that the power output increases with the square of the B field and can be limited by choking of the channel or interelectrode voltage breakdown which occurs at Hall fields greater than 60 volts/insulator. (Author)

A80-46265 * Parametric dependence of ion temperature and electron density in the SUMMA hot-ion plasma using laser light scattering and emission spectroscopy. A. Snyder, R. W. Patch, and M. R. Lauver (NASA, Lewis Research Center, Cleveland, Ohio). *Journal of Quantitative Spectroscopy and Radiative Transfer*, vol. 24, Aug. 1980, p. 167-177. 16 refs.

Hot-ion plasma experiments were conducted in the NASA Lewis SUMMA facility. A steady-state modified Penning discharge was formed by applying a radially inward dc electric field of several kilovolts near the magnetic mirror maxima. Results are reported for a hydrogen plasma covering a wide range in midplane magnetic flux densities from 0.5 to 3.37 T. Input power greater than 45 kW was obtained with water-cooled cathodes. Steady-state plasmas with ion kinetic temperatures from 18 to 830 eV were produced and measured spectroscopically. These ion temperatures were correlated with current, voltage, and magnetic flux density as the independent variables. Electron density measurements were made using an unusually sensitive Thomson scattering apparatus. The measured electron densities range from 2.1×10^{18} to the 11^{th} to 6.8×10^{18} to the 12^{th} per cu cm. (Author)

N80-12880* # State Univ of New York at Buffalo. Lab. for Power and Environmental Studies
EXPERIMENTAL AND THEORETICAL INVESTIGATION FOR THE SUPPRESSION OF THE PLANAR ARC DROP IN THE THERMIONIC CONVERTER Final Report, 1 Jul. 1974 - 16 Apr. 1978

David T. Shaw Apr 1979 41 p refs

(Grant NSG-7071)

(NASA-CR-159611; LAPES-79-003)

Avail: NTIS

HC A03/MF A01 CSCL 201

The possibility of using N₂ as a gas additive for the development of thermionic topping generators was investigated. The experiment is described and observations are discussed. The potential of applying microwave power in the interelectrode spacing of the converter as an ion generation source was also assessed. A.R.H.

N80-14923* # Colorado State Univ., Fort Collins. Dept. of Physics.

INTERACTION OF HIGH VOLTAGE SURFACES WITH THE SPACE PLASMA Annual Report

Harold R. Kaufman and Raymond S. Robinson May 1979 81 p refs

(Grant NSG-3196)

(NASA-CR-159731) Avail: NTIS HC A05/MF A01 CSCL 201

Tests were conducted using plasma densities of approximately 10 to the 5th power - 10 to the 6th power/cu cm. Insulating materials tested were polyimide (Dapton), mica and glass. Surface-area effects were found to be substantially reduced from those previously reported at lower plasma densities. The difference in typical plasma density was felt to be the major cause of this change, although a saturation effect may also be involved. At the 10 to the 5th power/cu cm plasma density range, surface effects on collection current appear limited to roughly 1 cm from the hole. A factor of several reduction of collected current was obtained with both surface scribing and a 2 x 2 cm conducting mesh. It appears possible that the effects of surface treatment might be more significant at lower plasma densities. Effects of repeated tests were also noted, with current collection decreasing with successive tests. Depending on the materials involved, the effect appeared due to either the smoothing of the inside of the insulator hole or the sputtering of insulator on the exposed conductor. A general conclusion was made from a variety of

observations, that the generation of vapor is a major factor in the enhancement of collected current. A.R.H.

N80-26161* Colorado State Univ., Fort Collins. Dept. of Mechanical Engineering.
ION EXTRACTION FROM A PLASMA Ph.D. Thesis, Progress Report, 1 Dec. 1979 - 1 Dec. 1980
Graeme Aston Jun. 1980 93 p refs
(Grant NGR-06-002-112)
(NASA-CR-159849) Avail: NTIS HC A05/MF A01 CSCL 201

An experimental investigation of the physical processes governing ion extraction from a plasma is presented. The screen hole plasma sheath of a multiaperture ion accelerator system is defined by equipotential plots for a variety of accelerator system geometries and operating conditions. A sheath thickness of at least fifteen Debye lengths is shown to be typical. The electron density variation within the sheath satisfies a Maxwell Boltzmann density distribution at an effective electron temperature dependent on the discharge plasma primary to Maxwellian electron density ratio. Plasma ion flow up to and through the sheath is predominately one dimensional and the ions enter the sheath with a modified Bohm velocity. Low values of the screen grid thickness to screen hole diameter ratio give good ion focusing and high extracted ion currents because of the effect of screen webbing on ion focusing. Author

were chosen for their extreme difference in vacuum qualifications. Neither adhesive types nor configuration made a significant difference in current collection. The temperature of the insulating material was also varied. It was found that current collection decreased with increasing temperature. Tests were conducted to see if pinhole current collection decreased with time, as was indicated by the effects of several short tests. Current was collected for over four hours while the conductor potential was held constant at 1000 volts. A smooth decrease with time was not observed, but rather a roughly constant current collection with brief surges to high values. Tests were also conducted with the simulated solar cell biased negative. The current was found to be proportional to pinhole area. R.K.G.

N80-27189* Colorado State Univ., Fort Collins. Dept. of Mechanical Engineering.
PLASMA PHYSICS ANALYSIS OF SERT-2 OPERATION
Harold R. Kaufman Jan. 1980 59 p refs
(Grant NSG-3011)
(NASA-CR-159814) Avail: NTIS HC A04/MF A01 CSCL 201

An analysis of the major plasma processes involved in the SERT 2 spacecraft experiments was conducted to aid in the interpretation of recent data. A plume penetration model was developed for neutralization electron conduction to the ion beam and showed qualitative agreement with flight data. In the SERT 2 configuration conduction of neutralization electrons between thrusters was experimentally demonstrated in space. The analysis of this configuration suggests that the relative orientation of the two magnetic fields was an important factor in the observed results. Specifically, the opposed field orientation appeared to provide a high conductivity channel between thrusters and a barrier to the ambient low energy electrons in space. The SERT 2 neutralizer currents with negative neutralizer biases were up to about twice the theoretical prediction for electron collection by the ground screen. An explanation for the higher experimental values was a possible conductive path from the neutralizer plume to a nearby part of the ground screen. Plasma probe measurements of SERT 2 gave the clearest indication of plasma electron temperature, with normal operation being near 5 eV and discharge only operation near 2 eV. E.D.K.

N80-32223* Colorado State Univ., Fort Collins. Dept. of Physics.
INTERACTION OF HIGH VOLTAGE SURFACES WITH THE SPACE PLASMA Annual Report
Harold R. Kaufman and Raymond S. Robinson May 1980 50 p refs
(Grant NSG-3196)
(NASA-CR-165131) Avail: NTIS HC A03/MF A01 CSCL 201

High voltage solar arrays provide spacecraft power while optimizing mass and power efficiency. Operating such arrays in the space plasma environment can result in anomalously large currents being collected through insulation defects. Two thicknesses of the insulating material were tested, with no effect found due to insulator thickness. In these tests the polyimide thickness was always much less than the pinhole diameter. The pinhole area was varied over an area range of more than 30:1. It was found that the current collected was independent of the pinhole area for hole diameters from 0.35 to 2.0 mm. Two types of adhesives were tried in two different configurations. The adhesives

76 SOLID-STATE PHYSICS

Includes superconductivity.

For related information, see also 33 *Electronics and Electrical Engineering* and 36 *Lasers and Masers*.

N80-16914* National Aeronautics and Space Administration. Lewis Research Center, Cleveland, Ohio.

PLANAR MULTI-JUNCTION HIGH VOLTAGE SOLAR CELLS
John C. Evans, Jr., An-Ti Chai, and Chandra Goradia (Cleveland State Univ., Ohio) 1980 10 p refs Presented at 14th Photovoltaic Specialists Conf., San Diego, Calif., 7-10 Jan 1980; sponsored by IEEE (NASA-TM-81389, E-299) Avail NTIS HC A02/MF A01 CSCL 20L

Technical considerations, preliminary results, and fabrication details are discussed for a family of high-voltage planar multi-junction (PMJ) solar cells which combine the attractive features of planar cells with conventional or interdigitated back contacts and the vertical multi-junction (VMJ) solar cell. The PMJ solar cell is internally divided into many voltage-generating regions, called unit cells, which are internally connected in series. The key to obtaining reasonable performance from this device was the separation of top surface field regions over each active unit cell. Using existing solar cell fabricating methods, output voltages in excess of 20 volts per linear centimeter are possible. Analysis of the new device is complex, and numerous geometries are being studied which should provide substantial benefits in both normal sunlight usage as well as with concentrators. A.R.H.

N80-23180* National Aeronautics and Space Administration. Lewis Research Center, Cleveland, Ohio.

RADIATION DAMAGE IN HIGH VOLTAGE SILICON SOLAR CELLS
Irving Weinberg, Henry Brandhorst, Jr., Clifford K. Swartz, and Victor G. Weizer 1980 11 p refs Presented at 2nd European Symp. on Photovoltaic Generators in Space, Heidelberg, 15-17 Apr 1980 (NASA-TM-81478, E-412) Avail NTIS HC A02/MF A01 CSCL 20L

Three high open-circuit voltage cell designs based on 0.1 ohm-cm p-type silicon were irradiated with 1 MeV electrons and their performance determined to fluences as high as 10 to the 15th power/sq cm. Of the three cell designs, radiation induced degradation was greatest in the high-low emitter (HLE cell). The diffused and ion implanted cells degraded approximately equally but less than the HLE cell. Degradation was greatest in an HLE cell exposed to X-rays before electron irradiation. The cell regions controlling both short-circuit current and open-circuit voltage degradation were defined in all three cell types. An increase in front surface recombination velocity accompanied time dependent degradation of an HLE cell after X-irradiation. It was speculated that this was indirectly due to a decrease in positive charge at the silicon-oxide interface. Modifications aimed at reducing radiation induced degradation are proposed for all three cell types. Author

N80-26182* National Aeronautics and Space Administration. Lewis Research Center, Cleveland, Ohio.

THE PLANAR MULTI-JUNCTION CELL: A NEW SOLAR CELL FOR EARTH AND SPACE
John C. Evans, An-Ti Chai, and Chandra Goradia 1980 8 p refs Proposed for presentation at 15th Intern. Energy Conversion Engr. Conf., Seattle, Wash., 18-22 Aug. 1980; sponsored by AIAA, presented at 14th IEEE Photovoltaic Specialists Conf., San Diego, Calif., 7-10 Jan. 1980 (NASA-TM-81526) Avail: NTIS HC A02/MF A01 CSCL 20L

A family of high-voltage solar cells, called the planar multi-junction (PMJ) cell is being developed. The new cells combine the attractive features of planar cells with conventional or interdigitated back contacts and the vertical multi-junction solar cell. The PMJ solar cell is internally divided into many voltage-

generating regions, called unit cells, which are internally connected in series. The key to obtaining reasonable performance from this device was the separation of top surface field regions over each active unit cell area. Using existing solar cell fabricating methods, output voltages in excess of 20 volts per linear centimeter are possible. Analysis of the new device is complex, and numerous geometries are being studied which should provide substantial benefits in both normal sunlight usage as well as with concentrators. Author

A80-16843* Hyperfine magnetic field at Cd impurity site in L2/1/ Heusler alloys Rh₂MnGe and Rh₂MnPb by TDPAC technique. S. Jha (Cincinnati, University, Cincinnati, Ohio), R. D. Black, G. M. Julian (Miami University, Oxford, Ohio), J. W. Blue, and D. C. Liu (NASA, Lewis Research Center, Cleveland, Ohio). (Institute of Electrical and Electronics Engineers and American Institute of Physics, Joint International Magnetism Conference and Conference on Magnetism and Magnetic Materials, 2nd, New York, N.Y., July 17-20, 1979.) *Journal of Applied Physics*, vol. 50, Nov. 1979, pt. 2, p. 7507-7509, Grant No. NSG-3091.

A80-21120* Some dynamic and time-averaged flow measurements in a turbine rig. L. N. Krause and G. C. Fralick (NASA, Lewis Research Center, Cleveland, Ohio). *ASME, Transactions, Journal of Engineering for Power*, vol. 102, Jan. 1980, p. 223, 224, 5 refs.

Four types of sensors were used to make both dynamic and time-averaged flow measurements in a cold turbine rig to determine the magnitude of errors in time-averaged total-pressure measurement at a station 5 1/2 blade cords downstream from the rotor. The errors turned out to be negligible. The sensors and their intended use are discussed. (Author)

A80-22250* Anodic polarization behavior of austenitic stainless steel alloys with lower chromium content. W. Y. C. Chen (Purdue University, Hammond, Ind.) and J. R. Stephens (NASA, Lewis Research Center, Cleveland, Ohio). *Corrosion*, vol. 35, Oct. 1979, p. 443-451, 17 refs.

A80-22300* Effect of interfacial species on shear strength of metal-sapphire contacts. S. V. Pepper (NASA, Lewis Research Center, Cleveland, Ohio). *Journal of Applied Physics*, vol. 50, Dec. 1979, p. 8062-8065, 26 refs.

The interfacial shear strength of the metal-insulator system has been studied by means of the coefficient of static friction of copper, nickel, or gold contacts on sapphire in ultrahigh vacuum. The effect on contact strength of adsorbed oxygen, nitrogen, chlorine, and carbon monoxide on the metal surfaces is reported. It was found that exposures as low as 1 L of O₂ on Ni produced observable increases in contact strength, whereas exposures of 3 L of Cl₂ lead to a decrease in contact strength. These results imply that submonolayer concentrations of these species at the interface of a thin Ni film on Al₂O₃ should affect film adhesion similarly. The atomic mechanism by which these surface or interface phases affect interfacial strength is not yet understood. (Author)

A80-26007* Homogeneous alignment of nematic liquid crystals by ion beam etched surfaces. E. G. Wintucky (NASA, Lewis Research Center, Cleveland, Ohio), R. Mahmood, and D. L. Johnson (Kent State University, Kent, Ohio). *Electrochemical Society, Meeting, 156th, Los Angeles, Calif., Oct. 15-19, 1979, Paper, 17 p. 7 refs.*

A wide range of the ion beam etch parameters are capable of producing uniform homogeneous alignment of nematic liquid crystals on SiO₂ films. The alignment surfaces were generated by obliquely incident argon ions; a smaller range of ion beam parameters was also investigated with ZrO₂ films and found suitable for

homogeneous alignment. Extinction ratios were very high, and twist and tilt-bias angles were very small. The SEM results indicate a parallel oriented surface structure on the ion beam etched surfaces which may determine alignment. (Author)

A80-33853 * Critical currents in A-15 structure Nb₃Al converted from cold-worked bcc structure. J. A. Woollam, S. A. Alterovitz, E. Haugland (NASA, Lewis Research Center, Cleveland, Ohio), and G. W. Webb (California, University, La Jolla, Calif.). *Applied Physics Letters*, vol. 36, Apr. 15, 1980, p. 706-708, 12 refs. NASA-NSF-supported research.

The paper considers critical currents in A-15 structure Nb₃Al converted from a cold-worked bcc structure. Nb₃Al prepared in the ductile phase by quenching and mechanical working followed by conversion to the A-15 structure could carry currents above 10 to the 9th power A/sq m in fields near 20 T. These critical currents are comparable to those of Nb₃Ge and V₃Ga which are closest competing materials for use in high fields; further enhancement of the critical current is possible if thermal treatments are optimized.

A.T.

A80-44234 * // Radiation damage in high voltage silicon solar cells. I. Weinberg, H. W. Brandhorst, Jr., C. K. Swartz, and V. G. Weizer (NASA, Lewis Research Center, Cleveland, Ohio). *European Space Agency and Deutsche Gesellschaft für Luft- und Raumfahrt, European Symposium on Photovoltaic Generators in Space, 2nd, Heidelberg, West Germany, Apr. 15-17, 1980, Paper. 9 p. 12 refs.*

Three high open-circuit voltage cell designs based on 0.1 ohm-cm p-type silicon were irradiated with 1 MeV electrons and their performance determined to fluences as high as 10 to the 15th/sq cm. Of the three cell designs, radiation induced degradation was greatest in the high-low emitter (HLE) cell. The diffused and ion implanted cells degraded approximately equally but less than the HLE cell. Degradation was greatest in an HLE cell exposed to X-rays before electron irradiation. The cell regions controlling both short-circuit current and open-circuit voltage degradation were defined in all three cell types. An increase in front surface recombination velocity accompanied time dependent degradation of a HLE cell after X-irradiation. It was speculated that this was indirectly due to a decrease in positive charge at the silicon-oxide interface. Modifications aimed at reducing radiation induced degradation are proposed for all three cell types. (Author)

A80-19776 * Negative streamer development in FEP teflon. B. L. Beers, V. W. Pine, H. C. Hwang, and H. W. Bloomberg (Science Applications, Inc., Radiation and Electromagnetics Div., Vienna, Va.). (IEEE, U.S. Defense Nuclear Agency, and Jet Propulsion Laboratory, Annual Conference on Nuclear and Space Radiation Effects, 16th, Santa Cruz, Calif., July 17-20, 1979.) *IEEE Transactions on Nuclear Science*, vol. NS-26, Dec. 1979, p. 5127-5133. 12 refs. Contract No. NAS3-21378.

A computational model is developed which describes the evolution and propagation of an ionizing front (negative streamer) in solid materials. The ionization front consists of drifting avalanching electrons moving self-consistently under the influence of their own space-charge field together with an applied external field. The required input information for the model consists of the functional dependence of the macroscopic transport coefficients on the local electric field, the initial conditions for beginning the calculation, and the strength of the applied field. A computational approach for specifying the transport coefficients and initial conditions is also described. The approach has been implemented by constructing three computer codes which sequentially interface, beginning with single electron scattering, and ending with streamer development. Computational results are presented for model calculations in Teflon. The overall model is perceived to provide a picture of the initiation phase of a propagating discharge in electron-irradiated dielectrics. (Author)

77 THERMODYNAMICS AND STATISTICAL PHYSICS

Includes quantum mechanics, and Bose and Fermi statistics

For related information see also 25 *Inorganic and Physical Chemistry* and 34 *Fluid Mechanics and Heat Transfer*.

A80-18630 * # Thermophysical property data - Who needs them. R. C. Hendricks (NASA, Lewis Research Center, Cleveland, Ohio). *American Society of Mechanical Engineers, Winter Annual Meeting, New York, N.Y., Dec. 2-7, 1979, Paper 79-WA/HT-17*. 9 p. 72 refs. Members, \$1.50, nonmembers, \$3.00.

Specific examples are cited herein to illustrate the universal needs and demands for thermophysical property data. Applications of the principle of similarity in fluid mechanics and heat transfer and extensions of the principle to fluid mixtures are discussed. It becomes quite clear that no matter how eloquent theories or experiments in fluid mechanics or heat transfer are, the results of their application can be no more accurate than the thermophysical properties required to transform these theories into practice, or in the case of an experiment, to reduce the data. Present-day projects take place on such a scale that the need for international standards and mutual cooperation is evident. (Author)

81 ADMINISTRATION AND MANAGEMENT

Includes management planning and research.

N80-24200* # National Aeronautics and Space Administration, Lewis Research Center, Cleveland, Ohio.

MATRIX MANAGEMENT FOR AEROSPACE 2000

John F. McCarthy, Jr. May 1980 16 p refs Presented at the Intern. Meeting and Techn. Display: Global Technol. 2000, Baltimore, 5-11 May 1980 (NASA-TM-81509, E-447) Avail: NTIS HC A02/MF A01 CSCL 05A

The matrix management approach to program management is an organized effort for attaining program objectives by defining and structuring all elements so as to form a single system whose parts are united by interaction. The objective of the systems approach is uncompromisingly complete coverage of the program management endeavor. Starting with an analysis of the functions necessary to carry out a given program, a model must be defined; a matrix of responsibility assignment must be prepared; and each operational process must be examined to establish how it is to be carried out and how it relates to all other processes.

A.R.H.

A80-40700 * # **Matrix management for aerospace 2000.** J. F. McCarthy, Jr. (NASA, Lewis Research Center, Cleveland, Ohio). *American Institute of Aeronautics and Astronautics, International Meeting and Technical Display on Global Technology 2000, Baltimore, Md., May 6-8, 1980, Paper 80-0946.* 14 p. 8 refs.

The matrix management approach to program management is described, showing that it is an organized approach to attaining program objectives by defining and structuring all elements so as to form a single system whose parts are united by interaction. The objective of the systems approach is to attain an uncompromised complete coverage of the program management effort. It is demonstrated that beginning with an analysis of the functions necessary to carry out a given program, a model must be defined; a matrix of responsibility assignment must be prepared; and each operational process is examined to establish how it is to be implemented and how it relates to all other processes.

M.E.P.

83 ECONOMICS AND COST ANALYSIS

Includes cost effectiveness studies.

N80-11950* National Aeronautics and Space Administration, Lewis Research Center, Cleveland, Ohio.

COST-EFFECTIVE TECHNOLOGY ADVANCEMENT DIRECTIONS FOR ELECTRIC PROPULSION TRANSPORTATION SYSTEMS IN EARTH-ORBITAL MISSIONS

John D. Regetz, Jr. and C. H. Terwilliger (Boeing Aerospace Co., Seattle, Wash.) 1979 21 p ref Presented at the Fourteenth Intern. Conf. on Electric Propulsion, Princeton, N. J., 30 Oct. - 1 Nov. 1979, sponsored by AIAA and Deut. Ges. für Luft und Raumfahrt

(NASA-TM-79289) Avail NTIS HC A02/MF A01 CSCL 05C

The directions that electric propulsion technology should take to meet the primary propulsion requirements for earth-orbital missions in the most cost effective manner are determined. The mission set requirements, state of the art electric propulsion technology and the baseline system characterized by it, adequacy of the baseline system to meet the mission set requirements, cost optimum electric propulsion system characteristics for the mission set, and sensitivities of mission costs and design points to system level electric propulsion parameters are discussed. The impact on overall costs than specific masses or costs of propulsion and power systems is evaluated.

A.W.H.

85 URBAN TECHNOLOGY AND TRANSPORTATION

Includes applications of space technology to urban problems; technology transfer; technology assessment; and surface and mass transportation.

For related information see 03 Air Transportation and Safety, 16 Space Transportation, and 44 Energy Production and Conversion.

N80-21200* National Aeronautics and Space Administration. Lewis Research Center, Cleveland, Ohio.

SUPPORTING RESEARCH AND TECHNOLOGY FOR AUTOMOTIVE STIRLING ENGINE DEVELOPMENT

William A. Tomazic 1980 20 p Presented at 5th Intern. Automotive Propulsion System Symp., Dearborn, Mich., 14-18 Apr. 1980

(NASA-TM-81495; E-400; DOE/NASA/1040-80/13) Avail: NTIS HC A02/MF A01 CSCL 13F

The technology advancement topics described are a part of the supporting research and technology (SRT) program conducted to support the major Stirling engine development program. This support focuses on developing alternatives or backups to the engine development in critical areas. These areas are materials, seals control, combustors and system analysis. Specific objectives and planned milestone schedules for future activities as now envisioned are described. These planned SRT activities are related to the timeline of the engine development program that they must support. A.M.S.

N80-21201* National Aeronautics and Space Administration. Lewis Research Center, Cleveland, Ohio.

FUEL ECONOMY SCREENING STUDY OF ADVANCED AUTOMOTIVE GAS TURBINE ENGINES

John L. Klann Mar. 1980 57 p (Contract EC-77-A-31-1040)

(NASA-TM-81433; E-357; DOE/NASA/1040-80/11) Avail: NTIS HC A04/MF A01 CSCL 13F

Fuel economy potentials were calculated and compared among ten turbomachinery configurations. All gas turbine engines were evaluated with a continuously variable transmission in a 1978 compact car. A reference fuel economy was calculated for the car with its conventional spark ignition piston engine and three speed automatic transmission. Two promising engine/transmission combinations, using gasoline, had 55 to 60 percent gains over the reference fuel economy. Fuel economy sensitivities to engine design parameter changes were also calculated for these two combinations. Author

N80-28254* National Aeronautics and Space Administration. Lewis Research Center, Cleveland, Ohio.

PRELIMINARY RESULTS OF STEADY STATE CHARACTERIZATION OF NEAR TERM ELECTRIC VEHICLE BREADBOARD PROPULSION SYSTEM

Noel B. Sargent Jul. 1980 10 p (Contract EC-77-A-31-1011)

(NASA-TM-81546; DOE/NASA/1011-31; E-502) Avail: NTIS HC A02/MF A01 CSCL 13F

The steady state test results on a breadboard version of the General Electric Near Term Electric Vehicle (ETV-1) are discussed. The breadboard was built using exact duplicate vehicle propulsion system components with few exceptions. Full instrumentation was provided to measure individual component efficiencies. Tests were conducted on a 50 hp dynamometer in a road load simulator facility. Characterization of the propulsion system over the lower half of the speed-torque operating range has shown the system efficiency to be composed of a predominant motor loss plus a speed dependent transaxle loss. At the lower speeds with normal road loads the armature chopper loss is also a significant factor. At the conditions corresponding to a cycle for which the vehicle system was specifically designed, the efficiencies are near optimum. M.G.

N80-30229* National Aeronautics and Space Administration. Lewis Research Center, Cleveland, Ohio.

LABORATORY FACILITY FOR ELECTRIC VEHICLE PROPULSION SYSTEM TESTING

Noel B. Sargent 1980 11 p refs Presented at Intern. Congr. of Transportation, Dearborn, Mich., 15-17 Sep. 1980; sponsored in cooperation with Vehicle Technology Society and IEEE, Society of Automotive Engineers, and Inst. of Electrical Engineers (NASA-TM-81574; DOE/NASA/1011-32; E-544) Avail: NTIS HC A02/MF A01 CSCL 13F

The road load simulator facility located at the NASA Lewis Research Center enables a propulsion system or any of its components to be evaluated under a realistic vehicle inertia and road loads. The load is applied to the system under test according to the road load equation: $F(\text{net}) = K1F1 + K2F2V + K3 \sin V + K4(dv/dt) + K5 \sin \theta$. The coefficient of each term in the equation can be varied over a wide range with vehicle inertial representative of vehicles up to 7500 pounds simulated by means of flywheels. The required torque is applied by the flywheels, a hydroviscous absorber and clutch, and a drive motor integrated by a closed loop control system to produce a smooth, continuous load up to 150 horsepower. A.R.H.

A80-14841 * A new traffic control design method for large networks with signalized intersections. G. G. Leininger, D. C. Colony (Toledo, University, Toledo, Ohio), and K. Seldner (NASA, Lewis Research Center, Cleveland, Ohio). In: A link between science and applications of automatic control; Proceedings of the Seventh Triennial World Congress, Helsinki, Finland, June 12-16, 1978. Volume 2. (A80-14794 03-63) Oxford and New York, Pergamon Press, 1979, p. 1567-1573. 9 refs.

The paper presents a traffic control design technique for application to large traffic networks with signalized intersections. It is shown that the design method adopts a macroscopic viewpoint to establish a new traffic modelling procedure in which vehicle platoons are subdivided into main stream queues and turning queues. Optimization of the signal splits minimizes queue lengths in the steady state condition and improves traffic flow conditions, from the viewpoint of the traveling public. Finally, an application of the design method to a traffic network with thirty-three signalized intersections is used to demonstrate the effectiveness of the proposed technique. M.E.P.

N80-13989* Mechanical Technology, Inc., Latham, N. Y. Stirling Engine Systems Div.

ASSESSMENT OF THE STATE OF TECHNOLOGY OF AUTOMOTIVE STIRLING ENGINES

Sep. 1979 329 p refs

(Contracts DEN3-32; EC-77-A-31-10040)

(NASA-CR-159631; DOE/NASA/0032-79/4;

MTI-79ASE77RE2) Avail: NTIS HC A15/MF A01 CSCL 13F

The current status of automotive Stirling engine technology is considered. The energy is described and the history of its evolution is reviewed. Overall engine, component, subsystem and material problem areas are identified and recommendations are made for further development and testing. Potential improvements are also identified. Projected Stirling engine/vehicle performance is compared to that of vehicles using current internal combustion engine in terms of performance, fuel consumption, multifuel capability, emissions, and noise level. It is concluded that the potential for achieving 1984 program goals is clearly discernible. The program goals require at least a 30 percent reduction in fuel consumption, acceptable emissions, and the capability of satisfactorily operating with a variety of alternate fuels. A.R.H.

N80-17916* Garrett Corp., Torrance, Calif.

ADVANCED ELECTRIC PROPULSION SYSTEM CONCEPT FOR ELECTRIC VEHICLES

A. E. Raynard and F. E. Forbes Aug. 1979 157 p refs (Contracts EC-77-A-31-1044; DEN3-81)

(NASA-CR-159651; DOE/NASA/0081-79/1;

AiResearch 79-16182) Avail NTIS HC A08/MF A01 CSCL 13F

Seventeen propulsion system concepts for electric vehicles were compared to determine the differences in components and battery pack to achieve the basic performance level. Design tradeoffs were made for selected configurations to find the optimum component characteristics required to meet all performance goals. The anticipated performance when using nickel-zinc batteries rather than the standard lead-acid batteries was also evaluated. The two systems selected for the final conceptual design studies included a system with a flywheel energy storage unit and a basic system that did not have a flywheel. The flywheel system meets the range requirement with either lead-acid or nickel-zinc batteries and also the acceleration of zero to 89 km/hr in 15 s. The basic system can also meet the required performance with a fully charged battery, but, when the battery approaches 20 to 30 percent depth of discharge, maximum acceleration capability gradually degrades. The flywheel system has an estimated life-cycle cost of \$0.041/km using lead-acid batteries. The basic system has a life-cycle cost of \$0.06/km. The basic system, using batteries meeting ISOA goals, would have a life-cycle cost of \$0.043/km. A.R.H.

N80-18991* Brobeck (William M.) and Associates, Berkeley, Calif.

STUDY OF ADVANCED ELECTRIC PROPULSION SYSTEM CONCEPT USING A FLYWHEEL FOR ELECTRIC VEHICLES Final Report

Francis C. Younger and Heinz Lackner. Dec. 1979. 231 p. refs (Contracts DEN3-78; EC-77-A-31-1011) (NASA-CR-159650; DOE/NASA/0078-79/1; WMB/A-4500-131-3-R1) Avail. NTIS HC A11/MF A01 CSCL 10B

Advanced electric propulsion system concepts with flywheels for electric vehicles are evaluated and it is predicted that advanced systems can provide considerable performance improvement over existing electric propulsion systems with little or no cost penalty. Using components specifically designed for an integrated electric propulsion system avoids the compromises that frequently lead to a loss of efficiency and to inefficient utilization of space and weight. A propulsion system using a flywheel power energy storage device can provide excellent acceleration under adverse conditions of battery degradation due either to very low temperatures or high degrees of discharge. Both electrical and mechanical means of transfer of energy to and from the flywheel appear attractive; however, development work is required to establish the safe limits of speed and energy storage for advanced flywheel designs and to achieve the optimum efficiency of energy transfer. Brushless traction motor designs using either electronic commutation schemes or dc-to-ac inverters appear to provide a practical approach to a mass producible motor, with excellent efficiency and light weight. No comparisons were made with advanced system concepts which do not incorporate a flywheel. M.G.

N80-18992* Brobeck (William M.) and Associates, Berkeley, Calif.

AN AUTOMATICALLY-SHIFTED TWO-SPEED TRANSAXLE SYSTEM FOR AN ELECTRIC VEHICLE Final Report, Dec. 1978 - Dec. 1979

Hayden S. Gordon and Gregory V. Hassman. Jan. 1980. 34 p. refs (Contracts DEN3-84; EC-77-A-31-1044) (NASA-CR-159746; DOE/NASA/0084-79/1; WMB/A-131-4-R2) Avail. NTIS HC A03/MF A01 CSCL 13F

An automatic shifting scheme for a two speed transaxle for use with an electric vehicle propulsion system is described. The transaxle system was to be installed in an instrumented laboratory propulsion system of an ac electric vehicle drive train. The transaxle which had been fabricated is also described. J.M.S.

N80-21202* Cleveland State Univ., Ohio.
ERROR ANALYSIS IN THE MEASUREMENT OF AVERAGE POWER WITH APPLICATION TO SWITCHING CONTROLLERS Contractor Report, Oct. 1978 - Oct. 1979

James E. Maisel. Mar. 1980. 84 p. refs. Sponsored by NASA (Contract EC 77-A-31-1044) (NASA-CR-159792; DOE/NASA/3222-80/1) Avail. NTIS HC A05/MF A01 CSCL 10B

Power measurement errors due to the bandwidth of a power meter and the sampling of the input voltage and current of a power meter were investigated assuming sinusoidal excitation and periodic signals generated by a model of a simple chopper system. Errors incurred in measuring power using a microcomputer with limited data storage were also considered. The behavior of the power measurement error due to the frequency responses of first order transfer functions between the input sinusoidal voltage, input sinusoidal current, and the signal multiplier was studied. Results indicate that this power measurement error can be minimized if the frequency responses of the first order transfer functions are identical. The power error analysis was extended to include the power measurement error for a model of a simple chopper system with a power source and an ideal shunt motor acting as an electrical load for the chopper. The behavior of the power measurement error was determined as a function of the chopper's duty cycle and back EMF of the shunt motor. Results indicate that the error is large when the duty cycle or back EMF is small. Theoretical and experimental results indicate that the power measurement error due to sampling of sinusoidal voltages and currents becomes excessively large when the number of observation periods approaches one-half the size of the microcomputer data memory allocated to the storage of either the input sinusoidal voltage or current. M.G.

N80-23216* Honeywell, Inc., St. Paul, Minn. Technology Strategy Center.

ASSESSMENT AND PRELIMINARY DESIGN OF AN ENERGY BUFFER FOR REGENERATIVE BRAKING IN ELECTRIC VEHICLES Final Report

R. Buchholz and Anoop K. Mathur. Dec. 1979. 138 p. (Contracts DEN3-48; EC-77-C-31-1044) (NASA-CR-159756; DOE/NASA/0048-79/1; TSCI0082-FR) Avail. NTIS HC A07/MF A01 CSCL 13F

Energy buffer systems, capable of storing the vehicle energy during braking and reusing this stored energy during acceleration, were examined. Some of these buffer systems when incorporated in an electric vehicle would result in an improvement in the performance and range under stop and go driving conditions. Buffer systems considered included flywheels, hydropneumatic, pneumatic, spring, and regenerative braking. Buffer ranking and rating criteria were established. Buffer systems were rated based on predicted range improvements, consumer acceptance, driveability, safety, reliability and durability, and initial and life cycle costs. A hydropneumatic buffer system was selected.

Author

N80-25209* Ford Motor Co., Dearborn, Mich. Research Staff.

FEASIBILITY STUDY OF SILICON NITRIDE REGENERATORS

C. A. Fucinari and V. D. N. Rao. Oct. 1979. 58 p. refs (Contract DEN3-8) (NASA-CR-159713; DOE/NASA/0008-79/10) Avail. NTIS HC A04/MF A01 CSCL 13F

The feasibility of silicon nitride as a regenerator matrix material for applications requiring inlet temperatures above 1000 C is examined. The present generation oxide ceramics are used as a reference to examine silicon nitride from a material characteristics, manufacturing, thermal stress and aerothermodynamic viewpoint. E.D.K.

N80-26212* AiResearch Mfg. Co., Torrance, Calif.
ADVANCED PROPULSION SYSTEM FOR HYBRID VEHICLES Final Report

L. V. Norrup and A. T. Lintz. Jan. 1980. 213 p. refs (Contracts DEN3-91; EC-77-A-31-1044) (NASA-CR-159771; DOE/NASA/0091-80/1; AiResearch-79-16430) Avail. NTIS HC A10/MF A01 CSCL 13F

A number of hybrid propulsion systems were evaluated for

application in several different vehicle sizes. A conceptual design was prepared for the most promising configuration. Various system configurations were parametrically evaluated and compared, design tradeoffs performed, and a conceptual design produced. Fifteen vehicle/propulsion systems concepts were parametrically evaluated to select two systems and one vehicle for detailed design tradeoff studies. A single hybrid propulsion system concept and vehicle (five passenger family sedan) were selected for optimization based on the results of the tradeoff studies. The final propulsion system consists of a 65 kW spark-ignition heat engine, a mechanical continuously variable traction transmission, a 20 kW permanent magnet axial-gap traction motor, a variable frequency inverter, a 386 kg lead-acid improved state-of-the-art battery, and a transaxle. The system was configured with a parallel power path between the heat engine and battery. It has two automatic operational modes: electric mode and heat engine mode. Power is always shared between the heat engine and battery during acceleration periods. In both modes, regenerative braking energy is absorbed by the battery.

Author

requirements were that the CVT accommodate flywheel speeds from 14,000 to 28,000 rpm and driveline speeds of 850 to 5000 rpm without slipping. Below 850 rpm a slipping clutch was used between the CVT and the driveline. The CVT was required to accommodate 330 ft-lb maximum torque and 100 hp maximum transient. The weighted average power was 22 hp, the maximum allowable full range shift time was 2 seconds and the required life was 2600 hours. The resulting design utilized two steel V-belts in series to accommodate the required wide speed ratio. The size of the CVT, including the slipping clutch, was 20.6 inches long, 9.8 inches high and 13.8 inches wide. The estimated weight was 155 lb. An overall potential efficiency of 95 percent was projected for the average power condition.

Author

N80-28255* # Eaton Engineering and Research Center, Southfield, Mich.

SMALL PASSENGER CAR TRANSMISSION TEST-CHEVROLET 200 TRANSMISSION Final Report

M. P. Bujold Mar. 1980 381 p

(Contracts DEN3-124; EC-77-A-31-1044)

(NASA-CR-159835; DOE/NASA/O124-1; ERC-L1B-79168)

Avail: NTIS HC A17/MF A01 CSCL 13F

The small passenger car transmission was tested to supply electric vehicle manufacturers with technical information regarding the performance of commercially available transmissions which would enable them to design a more energy efficient vehicle. With this information the manufacturers could estimate vehicle driving range as well as speed and torque requirements for specific road load performance characteristics. A 1979 Chevrolet Model 200 automatic transmission was tested per a passenger car automatic transmission test code (SAE J651b) which required drive performance, coast performance, and no load test conditions. The transmission attained maximum efficiencies in the mid-eighty percent range for both drive performance tests and coast performance tests. Torque, speed and efficiency curves map the complete performance characteristics for Chevrolet Model 200 transmission.

L.F.M.

N80-30228* # Ford Motor Co., Dearborn, Mich.

REGENERATOR MATRIX PHYSICAL PROPERTY DATA

C. A. Fucinari May 1980 51 p refs

(Contracts DEN3-8; EC-77-A-31-1044)

(NASA-CR-159854; DOE/NASA/0008-80/11) Avail: NTIS HC A04/MF A01 CSCL 05A

Among several cellular ceramic structures manufactured by various suppliers for regenerator application in a gas turbine engine, three have the best potential for achieving durability and performance objectives for use in gas turbines, Stirling engines, and waste heat recovery systems: (1) an aluminum-silicate sinusoidal flow passage made from a corrugated wate paper process; (2) an extruded isosceles triangle flow passage; and (3) a second generation matrix incorporating a square flow passage formed by an embossing process. Key physical and thermal property data for these configurations presented include: heat transfer and pressure drop characteristics, compressive strength, tensile strength and elasticity, thermal expansion characteristics, chemical attack, and thermal stability.

A.R.H.

N80-32299* # Battelle Columbus Labs., Ohio.

DESIGN STUDY OF STEEL V-BELT CVT FOR ELECTRIC VEHICLES Final Report

J. C. Swain, T. A. Klausung, and J. P. Wilcox Jun. 1980 131 p refs

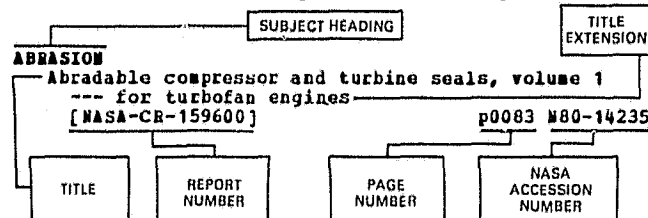
(Contracts DEN3-116; EC-77-A-31-1044)

(NASA-CR-159845; DOE/NASA/O116-80/1) Avail: NTIS HC A07/MF A01 CSCL 13F

A continuously variable transmission (CVT) design layout was completed. The intended application was for coupling the flywheel to the driveline of a flywheel battery hybrid electric vehicle. The

SUBJECT INDEX

Typical Subject Index Listing



The title is used to provide a description of the subject matter. When the title is insufficiently descriptive of the document content, a title extension is added, separated from the title by three hyphens. The *STAR* or *IAA* accession number is included in each entry to assist the user in locating the abstract in the abstract section. If applicable a report number is also included as an aid in identifying the document. The page and accession numbers are located beneath and to the right of the title. Under any one subject heading the accession numbers are arranged in sequence with the *IAA* accession numbers appearing first.

A

ABLATION
Plasma-sprayed dual density ceramic turbine seal system
[NASA-CR-159739] p0123 N80-15411

ABRASION
Abradable compressor and turbine seals, volume 1
--- for turbofan engines
[NASA-CR-159600] p0083 N80-14235
An investigation into the role of adhesion in the erosion of ductile metals
[NASA-TM-81458] p0078 N80-21489

ABRASION RESISTANCE
Friction and wear of plasma-sprayed coatings containing cobalt alloys from 25 deg to 650 deg in air
[ASLE PREPRINT 80-AH-6C-2] p0122 A80-43176
Development of improved high pressure turbine outer gas path seal components --- abradability and thermal cycling test results
[NASA-CR-159801] p0038 N80-21332

ABSORBERS (MATERIALS)
NT SOLAR ENERGY ABSORBERS

ABSORPTANCE
Spectral effects on direct-insolation absorptance of five collector coatings
[ASME PAPER 79-HT-18] p0146 A80-45722

ACCELERATED LIFE TESTS
Cycles till failure of silver-zinc cells with completing failures modes: Preliminary data analysis
[NASA-TM-81556] p0164 N80-29088

ACCELERATION STRESSES (PHYSIOLOGY)
NT CENTRIFUGING STRESS

ACCIDENTS
NT BIRD-AIRCRAFT COLLISIONS

ACCRETION
U DEPOSITION

ACCUMLATORS
NT SOLAR COLLECTORS
NT SOLAR REFLECTORS

ACIDS
NT PHOSPHORIC ACID
NT SULFURIC ACID

ACOUSTIC ATTENUATION
NT SHOCK WAVE ATTENUATION
Comparison of inlet suppressor data with approximate theory based on cutoff ratio
[AIAA PAPER 80-0100] p0170 A80-20964
Comparison of inlet suppressor data with approximate theory based on cutoff ratio
[NASA-TM-81386] p0167 N80-15876

Experimental evaluation of a spinning-mode acoustic-treatment design concept for aircraft inlets --- suppression of YF-102 engine fan noise
[NASA-TP-1613] p0016 N80-21323
Spectral structure of pressure measurements made in a combustion duct --- jet engine noise
[NASA-TM-81471] p0168 N80-22045
Pressure spectra and cross spectra at an area contraction in a ducted combustion system
[NASA-TM-81477] p0168 N80-23097

ACOUSTIC COMBUSTION
U COMBUSTION STABILITY

ACOUSTIC DUCTS
Reciprocity principle in duct acoustics
p0170 A80-20956
Spectral structure of pressure measurements made in a combustion duct
p0171 A80-35496
Higher order mode propagation in nonuniform circular ducts
[AIAA PAPER 80-1018] p0171 A80-35974
Rigorous solutions for sound radiation from circular ducts with hyperbolic horns or infinite plane baffle
p0171 A80-37895
Reciprocity principle in duct acoustics
[NASA-TM-79300] p0167 N80-12824
Pressure spectra and cross spectra at an area contraction in a ducted combustion system
[NASA-TM-81477] p0168 N80-23097
Far-field radiation of aft turbofan noise
[NASA-TM-81506] p0166 N80-24129
Numerical techniques in linear duct acoustics --- finite difference and finite element analyses
[NASA-TM-81553] p0170 N80-30154
A study of the transmission characteristics of suppressor nozzles
[NASA-CR-165133] p0172 N80-32186

ACOUSTIC EMISSION
Studies of the acoustic transmission characteristics of coaxial nozzles with inverted velocity profiles, volume 1 --- jet engine noise radiation through coannular exhaust nozzles
[NASA-CR-159698] p0172 N80-11870

ACOUSTIC IMPEDANCE
Effect of grazing flow on the nonlinear acoustic behavior of helmholtz resonators
p0095 N80-31619

ACOUSTIC MEASUREMENTS
NT NOISE MEASUREMENT
Noise suppression due to annulus shaping of a conventional coaxial nozzle
p0171 A80-35497
Acoustic measurements of three Prop-Fan models
[AIAA PAPER 80-0995] p0045 A80-35958
Advanced turbo-prop airplane interior noise reduction-source definition
[NASA-CR-159668] p0172 N80-13882
Forward acoustic performance of a shock-swallowing high-tip-speed fan (QF-13)
[NASA-TP-1668] p0169 N80-23100
Measured and predicted impingement noise for a model-scale under the wing externally blown flap configuration with a QCSEE type nozzle
[NASA-TM-81494] p0169 N80-26115
Experimental aerodynamic and acoustic model testing of the Variable Cycle Engine (VCE) testbed coannular exhaust nozzle system
[NASA-CR-159710] p0040 N80-26300
Experimental aerodynamic and acoustic model testing of the Variable Cycle Engine (VCE) testbed coannular exhaust nozzle system: Comprehensive data report
[NASA-CR-159711] p0040 N80-26301

ACOUSTIC PROPAGATION

Quiet Clean Short-haul Experimental Engine (QCSEE)
Under-The-Wing (UTW) composite Macelle test
report. Volume 2: Acoustic performance
[NASA-CR-159472] p0044 N80-29297

ACOUSTIC PROPAGATION

Rigorous solutions for sound radiation from
circular ducts with hyperbolic horns or infinite
plane baffle p0171 A80-37895

Higher order mode propagation in nonuniform
circular ducts [NASA-TM-81481] p0169 N80-23101

ACOUSTIC PROPERTIES

NT ACOUSTIC IMPEDANCE

NT ACOUSTIC VELOCITY

Higher order mode propagation in nonuniform
circular ducts [AIAA PAPER 80-1018] p0171 A80-35974

An acoustic sensitivity study of general aviation
propellers [AIAA PAPER 80-1871] p0045 A80-50191

Acoustic considerations of flight effects on jet
noise suppressor nozzles [NASA-TM-81377] p0167 N80-14843

ACOUSTIC RADIATION

U SOUND WAVES

ACOUSTIC RETROFITTING

Quiet Clean Short-Haul Experimental Engine
(QCSEE): Acoustic treatment development and
design [NASA-CR-135266] p0033 N80-15122

ACOUSTIC SIMULATION

Comparison of several inflow control devices for
flight simulation of fan tone noise using a
JT15D-1 engine [NASA-TM-81505] p0019 N80-24314

ACOUSTIC VELOCITY

Studies of the acoustic transmission
characteristics of coaxial nozzles with inverted
velocity profiles, volume 1 --- jet engine noise
radiation through coannular exhaust nozzles
[NASA-CR-159698] p0172 N80-11870

ACOUSTIC VIBRATIONS

U SOUND WAVES

ACOUSTICS

NT AEROACOUSTICS

Acoustic behavior of fibrous bulk materials
[AIAA PAPER 80-0986] p0172 A80-35951

Quiet Clean Short-haul Experimental Engine (QCSEE)
Over-The-Wing (OTW) propulsion systems test
report. Volume 4: Acoustic performance
[NASA-CR-135326] p0032 N80-15118

Core noise investigation of the CF6-50 turbofan
engine [NASA-CR-159598] p0036 N80-16061

Core noise investigation of the CF6-50 turbofan
engine [NASA-CR-159749] p0036 N80-16062

Application of coherence in fan noise studies
[NASA-TP-1630] p0167 N80-18882

ACQUISITION

NT DATA ACQUISITION

ACTUATORS

Quiet Clean Short-haul Experimental Engine
(QCSEE). Ball spline pitch change mechanism
design report [NASA-CR-134873] p0030 N80-15101

Quiet Clean Short-haul Experimental Engine
(QCSEE). Ball spline pitch change mechanism
design report [NASA-CR-134873] p0030 N80-15101

Quiet Clean Short-haul Experimental Engine (QCSEE)
whirl test of cam/harmonic pitch change
actuation system [NASA-CR-135140] p0032 N80-15117

Durability tests of solenoid valves for digital
actuators [NASA-TM-81522] p0020 N80-26299

Single-stage electrohydraulic servosystem for
actuating on airflow valve with frequencies to
500 hertz [NASA-TP-1678] p0046 N80-29369

ADAPTIVE CONTROL

Identification and dual adaptive control of a
turbojet engine p0023 A80-10033

An adaptive-control switching buck regulator -
implementation, analysis, and design p0103 A80-28167

SUBJECT INDEX

ADAPTIVE CONTROL SYSTEMS

U ADAPTIVE CONTROL

ADDITIVES

Improving the stress rupture and creep of silicon
nitride --- turbine materials [NASA-CR-159585] p0072 N80-10310

Radiation damage in lithium-counterdoped n/p
silicon solar cells [NASA-TM-81391] p0130 N80-15557

Antimisting kerosene --- reduced flammability
during aircraft accident circumstances p0021 N80-29319

ADHESION

Metal-dielectric interactions p0081 A80-13067

Improved adhesion of sputtered refractory carbides
to metal substrates p0081 A80-25274

Investigation into the effect of plasma
pretreatment on the adhesion of parylene to
various substrates p0066 A80-25900

An investigation into the role of adhesion in the
erosion of ductile metals [ASLE PREPRINT 80-AM-3E-3] p0122 A80-43159

Adhesion and friction of iron-base binary alloys
in contact with silicon carbide in vacuum [NASA-TP-1604] p0076 N80-15234

Comparison of the weight loss and adherence of
nine different polyimide films thermally aged at
315 C and 350 C in air --- high temperature
lubricants [NASA-TM-81381] p0086 N80-18183

An investigation into the role of adhesion in the
erosion of ductile metals [NASA-TM-81458] p0078 N80-21489

ADHESIVE BONDING

Effect of interfacial species on shear strength of
metal-sapphire contacts p0178 A80-22300

Investigation into the effect of plasma
pretreatment on the adhesion of parylene to
various substrates [NASA-TM-79224] p0114 N80-13473

Improved bond coatings for use with thermal
barrier coatings [NASA-TM-81567] p0080 N80-33556

ADIABATIC CONDITIONS

Phase change in liquid face seals. II - Isothermal
and adiabatic bounds with real fluids [ASME PAPER 79-LUB-4] p0129 A80-14739

AEROACOUSTICS

Assessment at full scale of exhaust nozzle-to-wing
size on STOL-OTW acoustic characteristics p0170 A80-20952

Acoustic considerations of flight effects on jet
noise suppressor nozzles [AIAA PAPER 80-0164] p0171 A80-20965

Effect of temperature on surface noise p0107 A80-28419

Effect of inflow control on inlet noise of a
cut-on fan [AIAA PAPER 80-1049] p0171 A80-35993

Workshop report for the AIAA 5th Aeroacoustics
Conference p0172 A80-41156

Assessment at full scale of exhaust nozzle to wing
size on STOL-OTW acoustic characteristics [NASA-TM-79279] p0167 N80-13881

High-speed-propeller wind-tunnel aeroacoustic
results p0018 N80-22344

Pressure spectra and cross spectra at an area
contraction in a ducted combustion system [NASA-TM-81477] p0168 N80-23097

Quiet Clean Short-haul Experimental Engine (QCSEE)
Under-The-Wing (UTW) composite Macelle test
report. Volume 2: Acoustic performance [NASA-CR-159472] p0044 N80-29297

Acoustic performance of a 50.8-cm (20-inch)
diameter variable-pitch fan and inlet. Volume
2: Acoustic data [NASA-CR-135118] p0044 N80-29299

AERODYNAMIC BUZZ

U FLUTTER

AERODYNAMIC CHARACTERISTICS

NT AERODYNAMIC DRAG

NT AERODYNAMIC STABILITY

- Scale model performance test investigation of exhaust system mixers for an Energy Efficient Engine /E3/ propulsion system
[AIAA PAPER 80-0229] p0024 A80-20968
- Numerical calculation of steady inviscid full potential compressible flow about wind turbine blades
[AIAA 80-0607] p0145 A80-28804
- Zero-length, slotted-lip inlet for subsonic military aircraft
[AIAA PAPER 80-1245] p0004 A80-41203
- Prediction method for two-dimensional aerodynamic losses of cooled vanes using integral boundary-layer parameters
[NASA-TP-1623] p0002 N80-17030
- Core compressor exit stage study. 1: Aerodynamic and mechanical design
[NASA-CR-159714] p0037 N80-19113
- Advanced propeller aerodynamic analysis
p0018 N80-22345
- Forward acoustic performance of a shock-swallowing high-tip-speed fan (QF-13)
[NASA-TP-1668] p0169 N80-23100
- CF6 jet engine performance improvement program: High pressure turbine aerodynamic performance improvement
[NASA-CR-159832] p0040 N80-26302
- AERODYNAMIC CONFIGURATIONS**
- WT WING MACELLE CONFIGURATIONS**
- Quiet Clean Short-haul Experimental Engine (QCSEE): The aerodynamic and mechanical design of the QCSEE under-the-wing fan
[NASA-CR-135009] p0031 N80-15109
- An analytical and experimental study of a short s-shaped subsonic diffuser of a supersonic inlet
[NASA-TM-81406] p0015 N80-15134
- High-speed-propeller wind-tunnel aeroacoustic results
p0018 N80-22344
- Measured and predicted impingement noise for a model-scale under the wing externally blown flap configuration with a QCSEE type nozzle
[NASA-TM-81494] p0169 N80-26115
- AERODYNAMIC DRAG**
- Dynamic behavior of a beam drag-force anemometer
[NASA-TP-1687] p0110 N80-24595
- AERODYNAMIC FORCES**
- WT AERODYNAMIC DRAG**
- WT AERODYNAMIC LOADS**
- AERODYNAMIC LOADS**
- Effect of time dependent flight loads on JT9D-7 performance deterioration
[NASA-CR-159681] p0134 N80-10515
- Expanded study of feasibility of measuring in-flight 747/JT9D loads, performance, clearance, and thermal data
[NASA-CR-159717] p0036 N80-16063
- AERODYNAMIC NOISE**
- Workshop report for the AIAA 5th Aeroacoustics Conference
p0172 A80-41156
- AERODYNAMIC STABILITY**
- Measuring unsteady pressure on rotating compressor blades --- with semiconductor strain gages under gas turbine engine operating conditions
p0110 A80-12630
- Examination of the flap-lag stability of rigid articulated rotor blades
p0010 A80-15123
- Dynamic response of a Mach 2.5 axisymmetric inlet and turbojet engine with a poppet-valve controlled inlet stability bypass system when subjected to internal and external airflow transients
[NASA-TP-1531] p0014 N80-14123
- Stabilization of aerodynamically excited turbomachinery with hydrodynamic journal bearings and supports
p0128 N80-29731
- AERODYNAMIC STALLING**
- A phenomenological model of the dynamic stall of a helicopter blade profile
[ONERA, TP NO. 1979-149] p0006 A80-20086
- AERODYNAMICS**
- WT AEROTHERMODYNAMICS**
- WT ROTOR AERODYNAMICS**
- Modification of axial compressor streamline program for analysis of engine test data
[NASA-TM-79312] p0002 N80-14051
- An experimental evaluation of the performance deficit of an aircraft engine starter turbine
[NASA-TM-81571] p0022 N80-31400
- Experimental performance and analysis of 15.04-centimeter-tip-diameter, radial-inflow turbine with work factor of 1.126 and thick blading
[NASA-TP-1730] p0023 N80-33410
- AEROELASTICITY**
- Status of NASA full-scale engine aeroelasticity research
p0133 N80-35906
- Status of NASA full-scale engine aeroelasticity research
[NASA-TM-81500] p0132 N80-23678
- Experimental determination of unsteady blade element aerodynamics in cascades. Volume 1: Torsion mode cascade
[NASA-CR-159831] p0040 N80-25335
- Nonlinear aeroelastic equations of motion of twisted, nonuniform, flexible horizontal-axis wind turbine blades
[NASA-CR-159502] p0152 N80-26774
- AEROMAGNETO FLUTTER**
- U FLUTTER**
- AERONAUTICAL ENGINEERING**
- The impact of fuels on aircraft technology through the year 2000
[NASA-TM-81492] p0093 N80-23472
- AEROSPACE ENGINEERING**
- WT AERONAUTICAL ENGINEERING**
- Optical sensors for aeronautics and space
[NASA-TM-81407] p0110 N80-17423
- AEROSPACE ENVIRONMENTS**
- First results of material charging in the space environment
p0055 A80-45609
- Interaction of high voltage surfaces with the space plasma --- solar arrays
[NASA-CR-159731] p0176 N80-14923
- Experimental results on plasma interactions with large surfaces at high voltages
[NASA-TM-81423] p0175 N80-18946
- AEROSPACE INDUSTRY**
- WT AIRCRAFT INDUSTRY**
- AEROSPACE SYSTEMS**
- Matrix management for aerospace 2000
[AIAA PAPER 80-0946] p0181 A80-40700
- AEROTHERMODYNAMICS**
- Feasibility study of silicon nitride regenerators
[NASA-CR-159713] p0184 N80-25209
- Regenerator matrix physical property data
[NASA-CR-159854] p0185 N80-30228
- AGE HARDENING**
- U PRECIPITATION HARDENING**
- AGING (MATERIALS)**
- WT AGING (METALLURGY)**
- AGING (METALLURGY)**
- Creep-rupture behavior of seven iron-base alloys after long term aging at 760 deg in low pressure hydrogen
[NASA-TM-81534] p0080 N80-32488
- AGRICULTURAL AIRCRAFT**
- Spray nozzle designs for agricultural aviation applications --- relation of drop size to spray characteristics and nozzle efficiency
[NASA-CR-159702] p0108 N80-10460
- Aerial applications dispersal systems control requirements study --- agriculture
[NASA-CR-159781] p0158 N80-18586
- Monodisperse atomizers for agricultural aviation applications
[NASA-CR-159777] p0108 N80-19450
- AILERONS**
- Feasibility study of aileron and spoiler control systems for large horizontal axis wind turbines
[NASA-CR-159456] p0153 N80-27803
- AIR BREATHING ENGINES**
- WT DUCTED FAN ENGINES**
- WT GAS TURBINE ENGINES**
- WT JET ENGINES**
- WT SUPERSONIC COMBUSTION RAMJET ENGINES**
- WT TURBOFAN ENGINES**
- WT TURBOJET ENGINES**
- WT TURBOPROP ENGINES**
- Airbreathing propulsion component technologies
p0024 A80-37482
- Fiber optic sensors for measuring angular position and rotational speed --- air breathing engines

AIR CONDITIONING

[NASA-TN-81454] p0110 N80-18368
Durability tests of solenoid valves for digital actuators

[NASA-TN-81522] p0320 N80-26299
AIR CONDITIONING
Reduced bleed air extraction for DC-10 cabin air conditioning

[AIAA PAPER 80-1197] p0010 A80-41194
AIR COOLING
Computer program for generating input for analysis of impingement-cooled, axial-flow turbine blade

[NASA-TP-1603] p0104 N80-15361
Effects of a ceramic coating on metal temperatures of an air-cooled turbine vane

[NASA-TP-1598] p0105 N80-17397
Algorithm for calculating turbine cooling flow and the resulting decrease in turbine efficiency

[NASA-TN-81453] p0163 N80-19863
Nonlinear, three-dimensional finite-element analysis of air-cooled gas turbine blades

[NASA-TP-1669] p0132 N80-22734
Extension of similarity test procedures to cooled engine components with insulating ceramic coatings

[NASA-TP-1615] p0105 N80-24577
AIR FLOW
Turbojet-exhaust-nozzle secondary-airflow pumping as an exit control of an inlet-stability bypass system for a Mach 2.5 axisymmetric mixed-compression inlet --- Lewis 10- by 10-ft. supersonic wind tunnel test

[NASA-TP-1532] p0014 N80-14124
Single-stage electrohydraulic servosystem for actuating on airflow valve with frequencies to 500 hertz

[NASA-TP-1678] p0146 N80-29369
AIR INLETS
U AIR INTAKES
AIR INTAKES
NT ENGINE INLETS
NT SUPERSONIC INLETS
Experimental investigation of a 0.15 scale model of a conformal variable-ramp inlet for the P-16 airplane

[NASA-CR-159640] p0005 N80-24263
AIR POLLUTION
Emission reduction

p0012 N80-10207
Sulfate and nitrate collected by filter sampling near the tropopause

[NASA-TP-1567] p0157 N80-14581
Quiet Clean Short-haul Experimental Engine (QCSEE) clean combustor test report

[NASA-CR-134916] p0030 N80-15104
Air pollution from aircraft

[NASA-CR-159712] p0010 N80-16060
Assessment of potential exposure to trihalogen insulation materials containing asbestos

[NASA-TN-81435] p0157 N80-23675
AIR QUALITY
NASA Global Atmospheric Sampling Program (GASP) data report for tapes VL0011 and VL0013

[NASA-TN-81462] p0157 N80-21892
AIR SAMPLING
Sulfate and nitrate collected by filter sampling near the tropopause

[NASA-TP-1567] p0157 N80-14581
AIR TRANSPORTATION
A methodology for long-range prediction of air transportation

p0041 N80-29305
AIRBORNE SURVEILLANCE RADAR
Possible methods for distinguishing icebergs from ships by aerial remote sensing

[NASA-TN-79310] p0136 N80-15538
AIRCRAFT ACCIDENTS
NT BIRD-AIRCRAFT COLLISIONS
Antismoking kerosene --- reduced flammability during aircraft accident circumstances

p0021 N80-29319
Potential release of fibers from burning carbon composites --- aircraft fires

[NASA-TN-80214] p0069 N80-29431
AIRCRAFT ANTENNAS
UHF coplanar-slot antenna for aircraft-to-satellite data communications

p0009 A80-13064
AIRCRAFT CABINS
U AIRCRAFT COMPARTMENTS

SUBJECT INDEX

AIRCRAFT COMPARTMENTS
Measurements of cabin and ambient ozone on B747 airplanes

p0010 A80-20853
Simultaneous cabin and ambient ozone measurements on two Boeing 747 airplanes, volume 1

[NASA-TN-79166] p0008 N80-15059
AIRCRAFT CONSTRUCTION MATERIALS
Fire test method for graphite fiber reinforced plastics

p0070 A80-31169
Hybrid composites that retain graphite fibers on burning

p0073 A80-32064
Endurance and failure characteristics of modified Vansco X-2, CBS 600 and AISI 9310 spur gears --- aircraft construction materials

[NASA-TN-81421] p0116 N80-18405
AIRCRAFT DESIGN
NT HELICOPTER DESIGN
Computer simulation of engine systems --- for aircraft design

[AIAA PAPER 80-0051] p0024 A80-18253
High-freezing-point fuel studies

p0043 N80-29329
AIRCRAFT ENGINES
NT T-63 ENGINE
NT VARIABLE CYCLE ENGINES
Computerized systems analysis and optimization of aircraft engine performance, weight, and life cycle costs

p0165 A80-10035
Preparing aircraft propulsion for a new era in energy and the environment

p0024 A80-17737
Thermal barrier coatings for aircraft gas turbines

[AIAA PAPER 80-0302] p0089 A80-18303
Engine component improvement program - Performance improvement

[AIAA PAPER 80-0223] p0024 A80-19300
Use of seal materials used in aircraft propulsion systems

p0121 A80-28010
Impact of new instrumentation on advanced turbine research

p0112 A80-36155
QCSEE UTM engine powered-lift acoustic performance --- Quiet Clean Short-haul Experimental Engine Under The Wing

[AIAA PAPER 80-1065] p0025 A80-38651
Advanced component technologies for energy-efficient turbofan engines

[AIAA PAPER 80-1086] p0025 A80-38902
An experimental investigation of endwall profiling in a turbine vane cascade

[AIAA PAPER 80-1089] p0004 A80-38904
Development of improved-durability plasma sprayed ceramic coatings for gas turbine engines

[AIAA PAPER 80-1193] p0089 A80-38963
Multifuel rotary aircraft engine

[AIAA PAPER 80-1237] p0045 A80-38982
Fuel conservation through active control of rotor clearances

[AIAA PAPER 80-1087] p0045 A80-41506
Analytical and experimental evaluations of the effect of broad property fuels on combustors for commercial aircraft gas turbine engines

[AIAA PAPER 80-1204] p0094 A80-41516
NASA Broad-Specification Fuels Combustion Technology Program - Status and description

[ASME PAPER 80-GT-65] p0094 A80-42195
Results from tests on a high work transonic turbine for an energy efficient engine

[ASME PAPER 80-GT-146] p0026 A80-42258
CF6 fan performance improvement

[ASME PAPER 80-GT-178] p0026 A80-42284
JT9D-7A /SP/ jet engine performance deterioration trends

p0026 A80-44230
Application of superalloy powder metallurgy for aircraft engines

p0122 A80-44240
Aeropropulsion 1979 --- conferences

[NASA-CP-2092] p0012 N80-10205
Aircraft Energy Efficiency (ACEE) status report

p0012 N80-10206
Emission reduction

p0012 N80-10207

SUBJECT INDEX

AIRCRAFT FUELS

Noise reduction p0012 N80-10208

Materials and structures technology p0012 N80-10210

Turbomachinery technology p0012 N80-10212

Mechanical components p0013 N80-10213

Effect of time dependent flight loads on JT9D-7 performance deterioration [NASA-CR-159681] p0134 N80-10515

Engine component improvement program: Performance improvement --- fuel consumption [NASA-TN-79304] p0013 N80-12092

Exhaust emission reduction for intermittent combustion aircraft engines [NASA-CR-159687] p0022 N80-14130

Quiet Clean Short-Haul Experimental Engine (QCSSE). Double-annular clean combustor technology development report [NASA-CR-159483] p0022 N80-15121

Computer simulation of engine systems [NASA-TN-79290] p0015 N80-15132

Air pollution from aircraft [NASA-CR-159711] p0010 N80-16060

Some considerations of the performance of the high-bypass ratio turbofan engines [NASA-TN-81390] p0077 N80-16143

Aeropropulsion in year 2000 [NASA-TN-81416] p0016 N80-18043

A 150 and 300 kW lightweight diesel aircraft engine design study [NASA-CR-31501] p0037 N80-20271

JT9D-7A (52) jet engine performance deterioration trends [NASA-TN-81459] p0016 N80-20274

Computerized systems analysis and optimization of aircraft engine performance, weight, and life cycle costs p0001 N80-21251

Steady-state performance of J85-21 compressor at 100 percent of design speed with and without intermediate stage blockage [NASA-TN-81451] p0017 N80-21333

Application of superalloy powder metallurgy for aircraft engines [NASA-TN-81466] p0078 N80-21408

Two-dimensional finite-element analyses of simulated rotor-fragment impacts against rings and beams compared with experiments [NASA-CR-159645] p0038 N80-22323

Performance deterioration based on existing (historical) data: JT9D jet engine diagnostics program [NASA-CR-135448] p0038 N80-22324

Design study: A 186 kW lightweight diesel aircraft engine [NASA-CR-3261] p0038 N80-22326

General Aviation Propulsion [NASA-CP-2126] p0017 N80-22327

An overview of NASA research on positive displacement general-aviation engines p0017 N80-22336

Positive displacement type general-aviation engines: Summary and concluding remarks p0018 N80-22340

Preliminary study of advanced turboprop and turboshaft engines for light aircraft --- cost effectiveness [NASA-TN-81467] p0018 N80-22350

Development of improved-durability plasma sprayed ceramic coatings for gas turbine engines [NASA-TN-81512] p0018 N80-23313

Advanced component technologies for energy-efficient turbofan engines [NASA-TN-81507] p0019 N80-24316

Engine component improvement: Performance improvement, JT9D-7 3.0 AR fan [NASA-CR-159806] p0039 N80-25332

Cold-air investigation of a 4 1/2 stage turbine with stage-loading factor of 4.66 and high specific work output. 2: Stage group performance [NASA-TP-1688] p0019 N80-25338

Performance deterioration based on in-service engine data: JT9D jet engine diagnostics program [NASA-CR-159525] p0040 N80-25340

CF6 jet engine performance improvement program: High pressure turbine aerodynamic performance improvement

[NASA-CR-159832] p0040 N80-26302

Performance, emissions, and physical characteristics of a rotating combustion aircraft engine, supplement A [NASA-CR-135119] p0041 N80-27361

Fuel/engine/airframe tradeoff study, phase 1 p0042 N80-29307

Combustion technology overview --- the use of broadened property aircraft fuels p0021 N80-29310

Experimental combustor study program p0042 N80-29311

Air Force fuel mainburner/turbine effects program p0042 N80-29314

Investigation of performance deterioration of the CF6/JT9D, high-bypass ratio turbofan engines [NASA-TN-81552] p0022 N80-29332

Some advantages of methane in an aircraft gas turbine [NASA-TN-81559] p0094 N80-29502

Reverse thrust performance of the QCSSE variable pitch turbofan engine [NASA-TN-81558] p0022 N80-31399

An experimental evaluation of the performance deficit of an aircraft engine after turbine [NASA-TN-81571] p0022 N80-31400

AIRCRAFT EQUIPMENT

NT AIRCRAFT TYPES

AIRCRAFT FUEL SYSTEMS

Advanced fuel system technology for utilizing broadened property aircraft fuels [NASA-TN-81538] p0094 N80-27510

Fuel system technology overview p0022 N80-29328

High-freezing-point fuel studies p0043 N80-29329

AIRCRAFT FUELS

Analytical and experimental evaluations of the effect of broad property fuels on combustors for commercial aircraft gas turbine engines [AIAA PAPER 80-1204] p0094 N80-41516

Temperature and flow measurements on near-freezing aviation fuels in a wing-tank model [ASME PAPER 80-GT-63] p0094 N80-42193

NASA Broad-Specification Fuels Combustion Technology Program - Status and Acceptance [ASME PAPER 80-GT-65] p0094 N80-42195

Alternative jet aircraft fuels p0012 N80-10209

Temperature and flow measurements on near-freezing aviation fuels in a wing-tank model [NASA-TN-79285] p0093 N80-13266

Initial characterization of an Experimental Referee Broadened-Specification (ERBS) aviation turbine fuel [NASA-TN-81440] p0093 N80-18205

Advanced fuel system technology for utilizing broadened property aircraft fuels [NASA-TN-81538] p0094 N80-27510

Aircraft Research and Technology for Future Fuels [NASA-CP-2146] p0022 N80-29300

Future aviation fuels overview p0021 N80-29301

Future aviation fuels overview p0021 N80-29301

Outlook for alternative energy sources --- aviation fuels p0041 N80-29302

Current jet fuel trends p0041 N80-29303

Aviation fuels outlook p0041 N80-29304

A methodology for long-range prediction of air transportation p0041 N80-29305

Effect of refining variables on the properties and composition of JP-5 p0041 N80-29306

Fuel/engine/airframe tradeoff study, phase 1 p0042 N80-29307

Military jet fuel from shale oil p0042 N80-29308

Fuels characterization studies --- jet fuels p0021 N80-29309

Combustion technology overview --- the use of broadened property aircraft fuels p0021 N80-29310

Experimental combustor study program p0042 N80-29311

- Air Force fuel mainburner/turbine effects programs
p0042 N80-29314
- The broadened-specification fuels combustion
technology program at Pratt and Whitney Aircraft
p0042 N80-29315
- Fuels research: Combustion effects overview
p0021 N80-29317
- Atomization of broad specification aircraft fuels
p0043 N80-29318
- Fuel property effects in stirred combustors
p0043 N80-29321
- Preliminary studies of combustor sensitivity to
alternative fuels
p0021 N80-29323
- Fuels research: Fuel thermal stability overview
p0021 N80-29324
- Experimental study of turbine fuel thermal
stability in an aircraft fuel system simulator
p0043 N80-29325
- Low temperature fuel behavior studies
p0044 N80-29330
- Some advantages of methane in an aircraft gas
turbine
[NASA-TM-81559] p0094 N80-29502
- Autoignition characteristics of aircraft-type fuels
[NASA-CR-159886] p0095 N80-30535
- AIRCRAFT HAZARDS**
- Simultaneous cabin and ambient ozone measurements
on two Boeing 747 airplanes, volume 1
[NASA-TM-79166] p0008 N80-15059
- AIRCRAFT INDUSTRY**
- Aeropropulsion in year 2000
[AIAA PAPER 80-0914] p0024 N80-32887
- AIRCRAFT INSTRUMENTS**
- NT ANEMOMETERS
- NT RADIO ALTIMETERS
- AIRCRAFT MAINTENANCE**
- JT9D-7A /SP/ jet engine performance deterioration
trends
p0026 N80-44230
- Study of turboprop systems reliability and
maintenance costs
[NASA-CR-135192] p0029 N80-14129
- AIRCRAFT MODELS**
- Quiet Clean Short-Haul Experimental Engine (QCSEE)
acoustic and aerodynamic tests on a scale model
over-the-wing thrust reverser and forward thrust
nozzle
[NASA-CR-135254] p0028 N80-14115
- Experimental investigation of a 0.15 scale model
of a conformal variable-ramp inlet for the F-16
airplane
[NASA-CR-159640] p0005 N80-24263
- Experimental aerodynamic and acoustic model
testing of the Variable Cycle Engine (VCE)
testbed coannular exhaust nozzle system
[NASA-CR-159710] p0040 N80-26300
- Experimental aerodynamic and acoustic model
testing of the Variable Cycle Engine (VCE)
testbed coannular exhaust nozzle system:
Comprehensive data report
[NASA-CR-159711] p0040 N80-26301
- AIRCRAFT NOISE**
- NT JET AIRCRAFT NOISE
- Assessment at full scale of exhaust nozzle-to-wing
size on STOL-OTW acoustic characteristics
p0170 N80-20952
- Comparison of inlet suppressor data with
approximate theory based on cutoff ratio
[AIAA PAPER 80-0100] p0170 N80-20964
- An acoustic sensitivity study of general aviation
propellers
[AIAA PAPER 80-1871] p0045 N80-50191
- Advanced turbo-prop airplane interior noise
reduction-source definition
[NASA-CR-159668] p0172 N80-13882
- Acoustic analysis of aft noise reduction
techniques measured on a subsonic tip speed 50.8
cm (twenty inch) diameter fan --- quiet engine
program
[NASA-CR-134891] p0030 N80-15102
- General Aviation Propulsion
[NASA-CR-2126] p0017 N80-22327
- QCSEE UTW engine powered-lift acoustic performance
[NASA-TM-81504] p0019 N80-24315
- AIRCRAFT NOISE PREDICTION**
- U NOISE PREDICTION (AIRCRAFT)
- AIRCRAFT PERFORMANCE**
- A theoretical and experimental investigation of
propeller performance methodologies
[AIAA PAPER 80-1240] p0026 N80-43283
- Optimum subsonic, high-angle-of-attack nacelles
[NASA-TM-81491] p0016 N80-20275
- Fuel/engine/airframe tradeoff study, phase 1
p0042 N80-29307
- AIRCRAFT POWER SOURCES**
- U AIRCRAFT ENGINES
- AIRCRAFT STABILITY**
- NT HOVERING STABILITY
- AIRCRAFT STRUCTURES**
- NT AIRFRAMES
- NT FUSELAGES
- AIRCRAFT TIRES**
- Improved tire/wheel concept --- pneumatic aircraft
tire
[NASA-CASE-LAR-11695-2] p0124 N80-18402
- AIRFOIL CHARACTERISTICS**
- U AIRFOILS
- AIRFOILS**
- NT ALLERONS
- NT EXTERNALLY BLOWN FLAPS
- NT PROPELLER BLADES
- NT ROTARY WINGS
- NT SPOILERS
- Advanced propeller aerodynamic analysis
p0018 N80-22345
- Core compressor exit stage study, 2
[NASA-CR-159812] p0039 N80-23312
- Diffusion bonded boron/aluminum spar-shell fan blade
[NASA-CR-159571] p0072 N80-25382
- Comparison of elastic and elastic-plastic
structural analyses for cooled turbine blade
airfoils
[NASA-TP-1679] p0132 N80-27719
- Quiet Clean Short-haul Experimental Engine (QCSEE)
under-the-wing engine composite fan blade:
Preliminary design test report
[NASA-CR-134846] p0044 N80-29298
- AIRFRAMES**
- Fuel/engine/airframe tradeoff study, phase 1
p0042 N80-29307
- ALCOHOLS**
- NT POLYVINYL ALCOHOL
- ALGEBRA**
- NT LINEAR EQUATIONS
- NT MATRICES (MATHEMATICS)
- NT NONLINEAR EQUATIONS
- ALGORITHMS**
- Algorithm for calculating turbine cooling flow and
the resulting decrease in turbine efficiency
[NASA-TM-81453] p0163 N80-19863
- ALIGNMENT**
- NT SELF ALIGNMENT
- Dynamic response to rotating-seat runout in
non-contacting face seals
[NASA-TM-81490] p0117 N80-22701
- ALIPHATIC COMPOUNDS**
- NT CETANE
- NT METHANE
- ALKALI HALIDES**
- NT SODIUM CHLORIDES
- ALKALI METALS**
- NT SODIUM
- ALKALIES**
- NT SODIUM HYDROXIDES
- ALKALINE BATTERIES**
- Decay of the zincate concentration gradient at an
alkaline zinc cathode after charging
p0074 N80-13070
- Flexible formulated plastic separators for
alkaline batteries
[NASA-CASE-LEW-12363-4] p0140 N80-18555
- Pulse charging of lead-acid traction
cells
[NASA-TM-81513] p0143 N80-25780
- ALKALINE EARTH OXIDES**
- NT MAGNESIUM OXIDES
- ALKANES**
- NT CETANE
- NT METHANE
- ALLOYS**
- NT ALUMINUM ALLOYS
- NT ASTROLOY (TRADEMARK)
- NT AUSTENITIC STAINLESS STEELS
- NT BINARY ALLOYS
- NT CARBON STEELS
- NT CAST ALLOYS
- NT CHROMIUM ALLOYS
- NT CHROMIUM STEELS

SUBJECT INDEX

ANNULAR DUCTS

- NT COBALT ALLOYS
 NT EUTECTIC ALLOYS
 NT HEAT RESISTANT ALLOYS
 NT HIGH STRENGTH ALLOYS
 NT HIGH STRENGTH STEELS
 NT IRON ALLOYS
 NT MANGANESE ALLOYS
 NT MARTENSITIC STAINLESS STEELS
 NT NICKEL ALLOYS
 NT NICKEL STEELS
 NT NIOBIUM ALLOYS
 NT REFRACTORY METAL ALLOYS
 NT RHODIUM ALLOYS
 NT STAINLESS STEELS
 NT STEELS
 NT TANTALUM ALLOYS
 NT TERNARY ALLOYS
 NT TITANIUM ALLOYS
 Heat storage in alloy transformations
 [NASA-CR-159787] p0151 N80-24759
- ALTIMETERS
 NT RADIO ALTIMETERS
- ALUMINA
 U ALUMINUM OXIDES
- ALUMINIZING
 U ALUMINUM COATINGS
- ALUMINUM
 Scanning-electron-microscope study of
 normal-impingement erosion of ductile metals
 [NASA-TP-1609] p0077 N80-16141
 Dynamic modulus and damping of boron, silicon
 carbide, and alumina fibers
 [NASA-TM-81422] p0068 N80-20313
 Predicting the time-temperature dependent axial
 failure of B/A1 composites
 [NASA-TM-81474] p0069 N80-21452
 Mechanical impact tests of materials in oxygen
 effects of contamination --- Teflon, stainless
 steel, and aluminum
 [NASA-TP-1571] p0093 N80-21551
 Effects of yttrium, aluminum and chromium
 concentrations in bond coatings on the
 performance of zirconia-yttria thermal barriers
 [NASA-TM-81485] p0079 N80-22464
- ALUMINUM ALLOYS
 The effect of zirconium on the isothermal
 oxidation of nominal Ni-14Cr-24Al alloys
 p0082 A80-26465
 Preparation of cast aluminum alloy-mica particle
 composites
 p0071 A80-32632
 An investigation into the role of adhesion in the
 erosion of ductile metals
 [ASLE PREPRINT 80-AM-3E-3] p0122 A80-43159
 Diffusion bonded boron/aluminum spar-shell fan blade
 [NASA-CR-159571] p0072 N80-25382
- ALUMINUM BORON COMPOSITES
 Predicting the time-temperature dependent axial
 failure of B/A1 composites
 p0071 A80-35494
- ALUMINUM COATINGS
 An experimental, low-cost, silicon-aluminide
 high-temperature coating for superalloys
 p0082 A80-35501
 An experimental, low-cost, silicon-aluminide
 high-temperature coating for superalloys
 [NASA-TM-81455] p0078 N80-20370
 A silicon-slurry/aluminide coating --- protects
 aircraft and land-based gas turbine engines
 [NASA-CASE-LEW-13343-1] p0069 N80-26389
- ALUMINUM COMPOUNDS
 NT ALUMINUM OXIDES
 NT SAPPHIRE
 Critical currents in A-15 structure Nb3Al
 converted from cold-worked bcc structure
 p0179 A80-33853
 Fabrication and evaluation of low fiber content
 alumina fiber/aluminum composites
 [NASA-CR-159517] p0073 N80-29430
- ALUMINUM OXIDES
 NT SAPPHIRE
 State-of-the-art of SiAlON materials
 p0009 A80-13066
 Some TEM observations of Al2O3 scales formed on
 NiCrAl alloys
 p0081 A80-13071
 Fracture toughness determination of Al2O3 using
 four-point-bend specimens with straight-through
 and chevron notches
- Dynamic modulus and damping of boron, silicon
 carbide, and alumina fibers
 p0090 A80-42085
 Performance of Chevron-notch short bar specimen in
 determining the fracture toughness of silicon
 nitride and aluminum oxide
 p0071 A80-44236
 p0090 A80-50696
- AMIDES
 NT POLYIMIDES
- AMINES
 NT DIAMINES
- AMORPHOUS MATERIALS
 Sliding friction of some metallic glasses
 p0090 A80-46153
- ASPERAGE
 U ELECTRIC CURRENT
- AMPLIFIER DESIGN
 Improved traveling wave tubes --- for ECM systems
 p0102 A80-44235
- AMPLIFIERS
 NT BEAM PLASMA AMPLIFIERS
 NT LINEAR AMPLIFIERS
 NT MICROWAVE AMPLIFIERS
- ANALOG SIMULATION
 Simulation studies of multiple large wind turbine
 generators on a utility network
 p0139 N80-16480
- ANALOGIES
 Similarity tests of turbine vanes, effects of
 ceramic thermal barrier coatings
 [NASA-TM-81473] p0105 N80-21706
- ANALYSIS (MATHEMATICS)
 NT COMPUTATIONAL FLUID DYNAMICS
 NT FINITE DIFFERENCE THEORY
 NT FINITE ELEMENT METHOD
 NT GREEN FUNCTION
 NT HELMHOLTZ VORTICITY EQUATION
 NT INTERPOLATION
 NT LINEAR EQUATIONS
 NT NONLINEAR EQUATIONS
 NT NUMERICAL ANALYSIS
 NT NUMERICAL INTEGRATION
 NT PARTIAL DIFFERENTIAL EQUATIONS
 NT POWER SERIES
- ANALYZERS
 NT ENGINE ANALYZERS
- ANATOMY
 NT EYE (ANATOMY)
 NT PANCREAS
- ANECHOIC CHAMBERS
 Effect of inflow control on inlet noise of a
 cut-on fan --- in an anechoic chamber
 [NASA-TM-81487] p0169 N80-23098
- ANEMOMETERS
 NT LASER ANEMOMETERS
 Dynamic behavior of a beam drag-force anemometer
 [NASA-TP-1687] p0110 N80-24595
- ANEMOMETRY
 U VELOCITY MEASUREMENT
- ANGLE OF ATTACK
 Wind-tunnel investigation of the flow correction
 for a model-mounted angle of attack sensor at
 angles of attack from -10 deg to 110 deg ---
 Langley 12-foot low speed wind tunnel test
 [NASA-TM-80189] p0011 N80-14110
- ANGLES (GEOMETRY)
 NT ANGLE OF ATTACK
- ANGULAR MOTION
 U ANGULAR VELOCITY
- ANGULAR VELOCITY
 Fiber optic sensors for measuring angular position
 and rotational speed --- air breathing engines
 [NASA-TM-81454] p0110 N80-18368
- ANISOTROPY
 NT PLASTIC ANISOTROPY
 Anisotropy of nickel-base superalloy single crystals
 [NASA-TM-81437] p0077 N80-17200
- ANNEALING
 Origin of reverse annealing in radiation-damaged
 silicon solar cells
 p0059 A80-33850
 Radiation damage annealing mechanisms and possible
 low temperature annealing in silicon solar cells
 [NASA-TM-81392] p0138 N80-15558
- ANNULAR DUCTS
 Performance of annular prediffuser-combustor systems
 [ASME PAPER 80-GT-15] p0026 A80-42154

- A comparison of experiment and theory for sound propagation in variable area ducts p0173 A80-45844
- ANNULAR FLOW**
Hydraulic forces caused by annular pressure seals in centrifugal pumps p0126 N80-29718
- ANNULAR NOZZLES**
Noise suppression due to annulus shaping of a conventional coaxial nozzle p0171 A80-35497
Noise suppression due to annulus shaping of an inverted-velocity-profile coaxial nozzle p0171 A80-35498
Coannular supersonic ejector nozzles p0002 N80-10128
Noise suppression due to annulus shaping of an inverted-velocity-profile coaxial nozzle --- supersonic cruise aircraft [NASA-TM-81460] p0168 N80-22046
Noise suppression due to annulus shaping of conventional coaxial nozzle [NASA-TM-81461] p0168 N80-22047
Experimental aerodynamic and acoustic model testing of the Variable Cycle Engine (VCE) testbed coannular exhaust nozzle system [NASA-CR-159710] p0040 N80-26300
Experimental aerodynamic and acoustic model testing of the Variable Cycle Engine (VCE) testbed coannular exhaust nozzle system: Comprehensive data report [NASA-CR-159711] p0040 N80-26301
- ANTENNA ARRAYS**
Ka-band, multibeam, contiguous coverage satellite antenna for the USA [AIAA 80-0557] p0099 A80-29588
- ANTENNA COMPONENTS**
NT ANTENNA FEEDS
- ANTENNA FEEDS**
Low sidelobe level low-cost earth station antennas for the 12 GHz broadcasting satellite service [NASA-CR-159703] p0098 N80-12259
- ANTENNAS**
NT AIRCRAFT ANTENNAS
NT MULTIPLE BEAM INTERVAL SCANNERS
NT PARABOLIC ANTENNAS
NT SATELLITE ANTENNAS
NT SLOT ANTENNAS
- ANTI-FRICTION BEARINGS**
NT BALL BEARINGS
NT ROLLER BEARINGS
Method of making bearing material [NASA-CASE-LEW-11930-3] p0070 N80-33482
- ANTIREFLECTION COATINGS**
Preliminary study of a solar selective coating system using black cobalt oxide for high temperature solar collectors [NASA-TM-81385] p0077 N80-18156
- APPROXIMATION**
NT FINITE DIFFERENCE THEORY
NT FINITE ELEMENT METHOD
- AQUEOUS SOLUTIONS**
Method of cross-linking polyvinyl alcohol and other water soluble resins [NASA-CASE-LEW-13103-1] p0088 N80-32516
- ARCHIPELAGOES**
A quantitative analysis of inter-island telephony traffic in the Pacific Basin Region (PBR) [NASA-TM-81587] p0097 N80-32610
- ARCHITECTURE**
An advanced mixed user domestic satellite system architecture [AIAA 80-0494] p0099 A80-29544
- ARCHITECTURE (COMPUTERS)**
High speed cylindrical rolling element bearing analysis 'CYBEAN' - Analytic formulation [ASME PAPER 79-LUB-35] p0129 A80-14761
- ARGON**
Adherence of ion beam sputter deposited metal films on H-13 steel [NASA-TM-81585] p0079 N80-31527
- ARGON PLASMA**
Investigation into the effect of plasma pretreatment on the adhesion of parylene to various substrates p0066 A80-25900
- ARIP (IMPACT PREDICTION)**
U COMPUTERIZED SIMULATION
- ARRAYS**
NT ANTENNA ARRAYS
NT SOLAR ARRAYS
- ARSENIC COMPOUNDS**
NT GALLIUM ARSENIDES
ARSENIDES
NT GALLIUM ARSENIDES
- ARTIFICIAL SATELLITES**
NT ATS 5
NT ATS 6
NT COMMUNICATION SATELLITES
NT COMMUNICATIONS TECHNOLOGY SATELLITE
NT ORBITAL SPACE STATIONS
NT SCATHA SATELLITE
NT SYNCHRONOUS SATELLITES
- ASBESTOS**
Assessment of potential exposure to friable insulation materials containing asbestos [NASA-TM-81435] p0157 N80-23875
- ASPECT RATIO**
NT LOW ASPECT RATIO
Core compressor exit stage study. 1: Aerodynamic and mechanical design [NASA-CR-159714] p0037 N80-19113
Core compressor exit stage study, 2 [NASA-CR-159812] p0039 N80-23312
- ASSESSMENTS**
NT TECHNOLOGY ASSESSMENT
- ASTROLOGY (TRADEMARK)**
Effects of thermally induced porosity on an as-HIP powder metallurgy superalloy p0082 A80-29990
Effects of fine porosity on the fatigue behavior of a powder metallurgy superalloy p0082 A80-35495
Effect of thermally induced porosity on an as-HIP powder metallurgy superalloy [NASA-TM-79263] p0076 N80-11189
Manufacture of low carbon astrology turbine disk shapes by hot isostatic pressing. Volume 2, project 1 [NASA-CR-135410] p0037 N80-21329
- ATMOSPHERIC ABSORPTION**
U ATMOSPHERIC ATTENUATION
- ATMOSPHERIC ATTENUATION**
Concepts for 18/30 GHz satellite communication system, volume 1 [NASA-CR-159625-VOL-1] p0098 N80-11277
- ATMOSPHERIC CIRCULATION**
Modified power law equations for vertical wind profiles [NASA-TM-79275] p0137 N80-13623
- ATMOSPHERIC COMPOSITION**
NT ATMOSPHERIC MOISTURE
- ATMOSPHERIC IMPURITIES**
U AIR POLLUTION
- ATMOSPHERIC MODELS**
NT DYNAMIC MODELS
- ATMOSPHERIC MOISTURE**
Calculation of water drop trajectories to and about arbitrary three-dimensional bodies in potential airflow [NASA-CR-32911] p0005 N80-28302
- ATOMIC GASES**
U MONATOMIC GASES
- ATOMIZATION**
U ATOMIZING
- ATOMIZERS**
Monodisperse atomizers for agricultural aviation applications [NASA-CR-159777] p0108 N80-19450
- ATOMIZING**
NT LIQUID ATOMIZATION
Atomizing characteristics of swirl can combustor modules with swirl blast fuel injectors [ASME PAPER 80-GT-30] p0026 A80-42164
Atomizing characteristics of swirl can combustor modules with swirl blast fuel injectors --- in terms of NOX emission rate [NASA-TM-79297] p0014 N80-13047
Monodisperse atomizers for agricultural aviation applications [NASA-CR-159777] p0108 N80-19450
- ATOMS**
NT HYDROGEN ATOMS
- ATS**
NT ATS 5
NT ATS 6

- ATS 5**
Active control of spacecraft charging p0055 A80-46890
- ATS 6**
Active control of spacecraft charging p0055 A80-46890
- ATTACK AIRCRAFT**
NT F-16 AIRCRAFT
NT F-102 AIRCRAFT
NT FIGHTER AIRCRAFT
- ATTENUATION**
NT ACOUSTIC ATTENUATION
NT ATMOSPHERIC ATTENUATION
NT SHOCK WAVE ATTENUATION
NT SIDELOBE REDUCTION
- ATTENUATION COEFFICIENTS**
A study of the transmission characteristics of suppressor nozzles [NASA-CR-165133] p0172 N80-32186
- ATTITUDE (INCLINATION)**
NT PITCH (INCLINATION)
- ATTITUDE CONTROL**
Auxiliary control of LSS p0063 N80-31459
- ATTENTION (MATERIALS)**
U COMMUNITION
- AUGER SPECTROSCOPY**
Comments on Auger electron production by Ne⁺/bombardment of surfaces p0174 A80-34048
- AUGMENTATION**
NT THRUST AUGMENTATION
- AUSTENITIC STAINLESS STEELS**
Anodic polarization behavior of austenitic stainless steel alloys with lower chromium content p0178 A80-22250
- AUTOMATIC CONTROL**
NT ADAPTIVE CONTROL
NT FEEDBACK CONTROL
NT NUMERICAL CONTROL
NT OPTIMAL CONTROL
NT SELF ALIGNMENT
An interactive modular design for computerized photometry in spectrochemical analysis p0074 A80-39640
An interactive modular design for computerized photometry in spectrochemical analysis [NASA-TM-81521] p0074 N80-24386
- AUTOMATIC CONTROL VALVES**
NT PRESSURE REGULATORS
- AUTOMATIC ROCKET IMPACT PREDICTORS**
U COMPUTERIZED SIMULATION
- AUTOMOBILE ENGINES**
Advanced Gas Turbine Powertrain System Development Project p0129 A80-35574
Assessment of the state of technology of automotive Stirling engines [NASA-CR-159631] p0183 N80-13989
Performance sensitivity analysis of Department of Energy-Chrysler upgraded automotive gas turbine engine, S/N 5-4 [NASA-TM-79242] p0115 N80-17467
Materials review for improved automotive gas turbine engine --- superalloys, refractory alloys, and ceramics p0123 N80-17470
Effect of water injection and off scheduling of variable inlet guide vanes, gas generator speed and power turbine nozzle angle on the performance of an automotive gas turbine engine [NASA-TM-81415] p0016 N80-20272
Supporting research and technology for automotive Stirling engine development [NASA-TM-81495] p0183 N80-21200
Fuel economy screening study of advanced automotive gas turbine engines [NASA-TM-81433] p0183 N80-21201
Parametric tests of a traction drive retrofitted to an automotive gas turbine [NASA-TM-81457] p0117 N80-21754
Baseline automotive gas turbine engine development program [NASA-CR-159670] p0124 N80-24620
Conceptual design study of an improved automotive gas turbine powertrain [NASA-CR-159672] p0124 N80-24621
High temperature self-lubricating coatings for air lubricated foil bearings for the automotive gas turbine engine [NASA-CR-159848] p0091 N80-26448
- AUTOMOBILES**
NT ELECTRIC AUTOMOBILES
- AVAILANCES**
NT ELECTRON AVALANCHE
- AVIONICS**
Flight test of navigation and guidance sensor errors measured on STOL approaches [NASA-TM-81154] p0028 N80-13041
- AXIAL COMPRESSORS**
U TURBOCOMPRESSORS
AXIAL FLOW COMPRESSORS
U TURBOCOMPRESSORS
AXIAL FLOW PUMPS
NT TURBINE PUMPS
AXIAL FLOW TURBINES
Efficient laser anemometer for intra-rotor flow mapping in turbomachinery p0111 A80-36140
Experimental study of low aspect ratio compressor blading [ASME PAPER 80-GT-6] p0025 A80-42147
Numerical calculation of transonic axial turbomachinery flows p0004 A80-44229
Computer program for generating input for analysis of impingement-cooled, axial-flow turbine blade [NASA-TP-1603] p0104 N80-15361
Algorithm for calculating turbine cooling flow and the resulting decrease in turbine efficiency [NASA-TM-81453] p0163 N80-19863
Small, high pressure liquid hydrogen turbopump [NASA-CR-159821] p0125 N80-26662
Numerical calculation of transonic axial turbomachinery flows [NASA-TM-81544] p0020 N80-27363
An experimental evaluation of the performance deficit of an aircraft engine starter turbine [NASA-TM-81571] p0022 N80-31400
- AXIAL LOADS**
Predicting the time-temperature dependent axial failure of B/AI composites p0071 A80-35494
- AXIAL STRAIN**
Effects of axisymmetric contractions on turbulence of various scales [NASA-CR-165136] p0006 N80-32328
- AXISYMMETRIC BODIES**
Time dependent difference theory for sound propagation in axisymmetric ducts with plug flow [NASA-TM-81501] p0168 N80-23096
- AXISYMMETRIC DEFORMATION**
U AXIAL STRAIN
- AXISYMMETRIC FLOW**
NT ANNULAR FLOW
- AXLES**
U SHAFTS (MACHINE ELEMENTS)

B

- B-A-W DEVICES**
U BULK ACOUSTIC WAVE DEVICES
- BAFFLES**
Baffle aperture design study of hollow cathode equipped ion thrusters [NASA-CR-165164] p0064 N80-33476
- BALANCING**
Development of flexible rotor balancing criteria [NASA-CR-159506] p0129 N80-32720
- BALL BEARINGS**
Rolling-element bearings --- contact sliding friction study of solid bodies p0121 A80-31961
Analysis of wear debris from full-scale bearing fatigue tests using the Ferrograph [ASLE PREPRINT 80-AM-3E-2] p0122 A80-43167
Analysis of wear-debris from full-scale bearing fatigue tests using the ferrograph [NASA-TM-81403] p0114 N80-16341
Some limitations in applying classical EHD film-thickness formulae to a high-speed bearing [NASA-TM-81431] p0116 N80-18409
Operating characteristics of high-speed, jet-lubricated 35-millimeter-bore ball bearing with a single-outer-land-guided cage [NASA-TP-1657] p0117 N80-21753
Stresses and deformations in elliptical contacts [NASA-TM-81535] p0118 N80-27697

BALLISTICS

SUBJECT INDEX

Effect of cage design on characteristics of
high-speed-jet-lubricated 35-millimeter-bore
ball bearing --- turbojet engines
[NASA-TP-1732] p0120 N80-33749

BALLISTICS
Prediction of fragment velocities and trajectories
p0096 N80-16210

BANDWIDTH
30/20 GHz wideband technology verification program
p0097 N80-25917

BARRIER APPROXIMATION
U ELECTRICAL PROPERTIES
U SURFACE PROPERTIES

BARIUM COMPOUNDS
NT BARIUM ZIRCONATES
BARIUM ZIRCONATES
Reactions of calcium orthosilicate and barium
zirconate with oxides and sulfates of various
elements
[NASA-TM-79272] p0085 N80-13256

BARS
Compliance and stress intensity coefficients for
short bar specimens with chevron notches
p0133 N80-46032

BATTERIES
U ELECTRIC BATTERIES
BATTERY CHARGERS
Effect of positive pulse charge waveforms on cycle
life of nickel-zinc cells
p0146 N80-48329
[NASA-TM-81513] p0143 N80-25780

BATTERY SEPARATORS
U SEPARATORS

BEAM PLASMA AMPLIFIERS
Barfile aperture design study of hollow cathode
equipped ion thrusters
[NASA-CR-165164] p0064 N80-33476

BEAMS (RADIATION)
NT ELECTRON BEAMS
NT ION BEAMS
Ka-band, multibeam, contiguous coverage satellite
antenna for the USA
[AIAA 80-0557] p0099 N80-29588

BEAMS (SUPPORTS)
NT CANTILEVER BEAMS
Buckling of rotating beams
p0133 N80-20149
Two-dimensional finite-element analyses of
simulated rotor-fragment impacts against rings
and beams compared with experiments
[NASA-CR-159645] p0038 N80-22323
Instructions for the use of the CIVM-Jet 4C
finite-strain computer code to calculate the
transient structural responses of partial and/or
complete arbitrarily-curved rings subjected to
fragment impact
[NASA-CR-159873] p0134 N80-27720

BEARING
Limit cycles of a flexible shaft with hydrodynamic
journal bearings in unstable regimes
p0127 N80-29725

BEARINGS
NT ANTIFRICTION BEARINGS
NT BALL BEARINGS
NT FOIL BEARINGS
NT JOURNAL BEARINGS
NT ROLLER BEARINGS
On the role of oil-film bearings in promoting
shaft instability: Some experimental observations
p0127 N80-29726
Instability thresholds for flexible rotors in
hydrodynamic bearings
p0128 N80-29730
Stabilization of aerodynamically excited
turbomachinery with hydrodynamic journal
bearings and supports
p0128 N80-29731
Method of making bearing material
[NASA-CASE-LEW-11930-3] p0070 N80-33482

BENDING MOMENTS
Fracture toughness determination of Al203 using
four-point-bend specimens with straight-through
and chevron notches
p0090 N80-42085

BIBLIOGRAPHIES
Application of advanced on-board processing
concepts to future satellite communications
systems: Bibliography

[NASA-CR-159684] p0098 N80-12261

BINARY ALLOYS
Adhesion and friction of iron-base binary alloys
in contact with silicon carbide in vacuum
[NASA-TP-1604] p0076 N80-15234
Adhesion, friction, and wear of binary alloys in
contact with single-crystal silicon carbide
[NASA-TM-79282] p0086 N80-21534

BINARY MIXTURES
NT EUTECTIC ALLOYS
BINARY SYSTEMS (DIGITAL)
U DIGITAL SYSTEMS
BINARY SYSTEMS (MATERIALS)
NT BINARY ALLOYS
NT EUTECTIC ALLOYS
BIOLOGICAL MODELS
U BIONICS
BIONICS
Mechanical and chemical effects of ion-texturing
biomedical polymers
p0089 N80-13065

BIOPHYSICS
NT PUBLIC HEALTH

BIOSIMULATION
U BIONICS

BIPROPELLANTS
U LIQUID ROCKET PROPELLANTS

BIRD-AIRCRAFT COLLISIONS
Program for impact testing of spar-shell fan
blades, test report
[NASA-CR-135393] p0037 N80-21328

BLADE TIPS
Teetered, tip-controlled rotor - Preliminary test
results from Mod-O 100-kW experimental wind
turbine
[AIAA 80-0642] p0145 N80-28836
Laser-optical blade tip clearance measurement system
p0111 N80-36137
Laser-optical blade tip clearance measurement system
[NASA-TM-81376] p0015 N80-14128
Advanced ceramic material for high temperature
turbine tip seals
[NASA-CR-159774] p0038 N80-22325
Forward acoustic performance of a shock-swallowing
high-tip-speed fan (QF-13)
[NASA-TP-1668] p0169 N80-23100
Study of blade aspect ratio on a compressor front
stage
[NASA-CR-159556] p0040 N80-25333

BLEED-OFF
U PRESSURE REDUCTION

BLOWN FLAPS
U EXTERNALLY BLOWN FLAPS

BODIES OF REVOLUTION
NT ROTATING CYLINDERS

BODY-WING CONFIGURATIONS
Quiet Clean Short-haul Experimental Engine (QCSEE)
Under-The-Wing (UTW) composite Macelle test
report. Volume 2: Acoustic performance
[NASA-CR-159472] p0044 N80-29297

BOEING AIRCRAFT
NT BOEING 747 AIRCRAFT
BOEING MILITARY AIRCRAFT
U MILITARY AIRCRAFT
BOEING 747 AIRCRAFT
Measurements of cabin and ambient ozone on B747
airplanes
p0010 N80-28853
Simultaneous cabin and ambient ozone measurements
on two Boeing 747 airplanes, volume 1
[NASA-TM-79166] p0008 N80-15059
Expanded study of feasibility of measuring
in-flight 747/JT9D loads, performance,
clearance, and thermal data
[NASA-CR-159717] p0036 N80-16063
JT9D-7A (SP) jet engine performance deterioration
trends
[NASA-TM-81459] p0016 N80-20274

BOILER PLATE
Quiet Clean Short-Haul Experimental Engine
(QCSEE). Under-the-wing (UTW) engine
boilerplate Macelle test report. Volume 2:
Aerodynamics and performance
[NASA-CR-135250] p0028 N80-14116

BOILERS
Coupled generator and combustor performance
calculations for potential early commercial MHD
power plants
p0156 N80-25099

- Parametric study of prospective early commercial
MHD power plants (PSPEC). General Electric
Company, task 1: Parametric analysis
[NASA-CR-159634] p0152 N80-26779
Rapporteur report: MHD electric power plants
[NASA-TM-81554] p0144 N80-29862
Cogeneration Technology Alternatives Study (CTAS).
Volume 6: Computer data. Part 1: Coal-fired
nucogeneration process boiler, section A
[NASA-CR-159770-PT-1-A] p0154 N80-30888
Cogeneration Technology Alternatives Study (CTAS).
Volume 6: Computer data. Part 1: Coal-fired
nucogeneration process boiler, section B
[NASA-CR-159770-PT-1-B] p0154 N80-30889
Cogeneration Technology Alternatives Study (CTAS).
Volume 6: Computer data. Part 2:
Residual-fired nucogeneration process boiler
[NASA-CR-159770-PT-2] p0155 N80-30890
Cogeneration Technology Alternatives Study (CTAS).
Volume 6: Computer data. Part 2:
Residual-fired nucogeneration process boiler
[NASA-CR-159770-PT-2] p0156 N80-33861
- BONDING**
NT ADHESIVE BONDING
NT METAL BONDING
NT REACTION BONDING
Reaction bonded silicon nitride prepared from wet
attrition-milled silicon p0089 A80-32828
Mechanisms of lubrication and wear of a bonded
solid lubricant film p0085 N80-16165
[NASA-TM-81396]
Reaction bonded silicon nitride prepared from wet
attrition-milled silicon --- fractography p0086 N80-18181
[NASA-TM-81428]
Effects of yttrium, aluminum and chromium
concentrations in bond coatings on the
performance of zirconia-yttria thermal barriers
[NASA-TM-81485] p0079 N80-22464
- BORON**
NT BORON FIBERS
BORON FIBERS
Dynamic modulus and damping of boron, silicon
carbide, and alumina fibers p0071 A80-44236
Dynamic modulus and damping of boron, silicon
carbide, and alumina fibers p0068 N80-20313
[NASA-TM-81422]
Calculation of residual principal stresses in CVD
boron on carbon filaments p0068 N80-20314
[NASA-TM-81456]
Predicting the time-temperature dependent axial
failure of B/A1 composites p0069 N80-21452
[NASA-TM-81474]
BORON REINFORCED MATERIALS
Calculation of residual principal stresses in CVD
boron on carbon filaments p0072 A80-44237
Diffusion bonded boron/aluminum spar-shell fan blade
[NASA-CR-159574] p0072 N80-25382
- BOUNDARIES**
NT GRAIN BOUNDARIES
BOUNDARY LAYER CONTROL
Griffith diffusers p0006 A80-20748
Static and transient performance of YF-102 engine
with up to 14 percent core airbleed for the
quiet short-haul research aircraft p0020 N80-25339
[NASA-TP-1692]
BOUNDARY LAYER FLOW
NT BOUNDARY LAYER SEPARATION
NT SECONDARY FLOW
NT SEPARATED FLOW
BOUNDARY LAYER NOISE
U AERODYNAMIC NOISE
U BOUNDARY LAYERS
BOUNDARY LAYER SEPARATION
The effect of finite turbulence spatial scale on
the amplification of turbulence by a contracting
stream p0004 A80-44862
- BOUNDARY LAYERS**
Prediction method for two-dimensional aerodynamic
losses of cooled vanes using integral
boundary-layer parameters p0002 N80-17030
[NASA-TP-1623]
Three dimensional mean flow and turbulence
characteristics of the near wake of a compressor
rotor blade
- [NASA-CR-159518] p0005 N80-27288
BOUNDARY LUBRICATION
Boundary lubrication, thermal and oxidative
stability of a fluorinated polyether and a
perfluoropolyether triazine p0088 A80-12089
[ASLE PREPRINT 79-AM-1B-1]
Steady-state wear and friction in boundary
lubrication studies p0087 N80-22493
[NASA-TP-1658]
BOUNDARY VALUE PROBLEMS
Two-dimensional representations of axisymmetric
fields for computer calculations --- in modeling
microwave tubes p0102 A80-18232
- BRAKING**
Assessment and preliminary design of an energy
buffer for regenerative braking in electric
vehicles p0184 N80-23216
[NASA-CR-159756]
BRAYTON CYCLE
Potential performance improvement using a reacting
gas (nitrogen tetroxide) as the working fluid in
a closed Brayton cycle p0139 N80-16490
[NASA-TM-79322]
Concept definition study of small Brayton cycle
engines for dispersed solar electric power systems
[NASA-CR-159592] p0150 N80-22778
- BREAKAWAY**
U BOUNDARY LAYER SEPARATION
BRITTLE MATERIALS
Compliance and stress intensity coefficients for
short bar specimens with chevron notches p0133 A80-46032
Fracture toughness of brittle materials determined
with chevron notch specimens p0079 N80-32486
[NASA-TM-81607]
BUBBLES
Marangoni bubble motion in zero gravity p0107 A80-20958
Marangoni bubble motion in zero gravity --- Lewis
zero gravity drop tower p0104 N80-13403
[NASA-TM-79250]
BUCKLING
Buckling of rotating beams p0133 A80-20149
Vibration and buckling of rectangular plates under
in-plane hydrostatic loading p0133 A80-45364
- BULK ACOUSTIC WAVE DEVICES**
OSCEE fan exhaust bulk absorber treatment evaluation
[NASA-TM-81498] p0019 N80-23314
BURNERS
Laboratory measurements in a turbulent, swirling
flow --- measurement of soot inside a flame-tube
burner p0095 N80-22509
[NASA-CR-159723]
BURNING
U COMBUSTION
BURNING PROCESS
U COMBUSTION
BURNING RATE
Fire test method for graphite fiber reinforced
plastics p0070 A80-31169
Investigation of critical burning of fuel droplets
[NASA-CR-159697] p0075 N80-12142
BURNOUT
Soot formation and burnout in flames p0043 N80-29320
- BUTTERFLY VALVES**
NT DAMPERS (VALVES)
BYPASSES
Dynamic response of a Mach 2.5 axisymmetric inlet
and turbojet engine with a poppet-valve
controlled inlet stability bypass system when
subjected to internal and external airflow
transients p0014 N80-14123
[NASA-TP-1531]
- C**
C-15 AIRCRAFT
Quiet powered-lift propulsion p0015 N80-15127
[NASA-CR-2077]
CABIN ATMOSPHERES
Measurements of cabin and ambient ozone on B747
airplanes p0010 A80-28853

CADMIUM

SUBJECT INDEX

Reduced bleed air extraction for DC-10 cabin air conditioning
[AIAA PAPER 80-1197] p0010 A80-41194

CADMIUM

Hyperfine magnetic field at Cd impurity site in $\text{Zn}_{1-x}\text{Cd}_x\text{Te}$ alloys Rh_2MnGe and Rh_2MnPb by TDPAC technique --- Time Differential Perturbed Angular Correlation
p0178 A80-16843

CALCIUM COMPOUNDS

NT CALCIUM FLUORIDES

NT CALCIUM SILICATES

CALCIUM FLUORIDES

Friction and wear of plasma-sprayed coatings containing cobalt alloys from 25 deg to 650 deg in air
[NASA-TM-79316] p0085 N80-14249

CALCIUM SILICATES

Analysis of the response of a thermal barrier coating to sodium and vanadium doped combustion gases
[NASA-TM-79205] p0076 N80-10344
Reactions of calcium orthosilicate and barium zirconate with oxides and sulfates of various elements
[NASA-TM-79272] p0085 N80-13256

CALCULATORS

Prediction of fiber composite mechanical behavior made simple --- using a rocket calculator
[NASA-TM-81404] p0068 N80-16107

CALCULUS

NT POWER SERIES

CALIBRATING

Wind-tunnel investigation of the flow correction for a model-mounted angle of attack sensor at angles of attack from -10 deg to 110 deg --- Langley 12-foot low speed wind tunnel test
[NASA-TM-80189] p0011 N80-14110
Global calibration of terrestrial reference cells and errors involved in using different irradiance monitoring techniques
[NASA-TM-81393] p0138 N80-15561

CANCER

Preliminary results of fast neutron treatments in carcinoma of the pancreas
[NASA-TM-81516] p0160 N80-24983

CANTILEVER BEAMS

Dynamic behavior of a beam drag-force anemometer
[NASA-TM-1687] p0110 N80-24595

CANTILEVER MEMBERS

NT CANTILEVER BEAMS

CAPILLARY CIRCULATION

U CAPILLARY FLOW

CAPILLARY FLOW

Capillary acquisition devices for high-performance vehicles: Executive summary --- evaluation of cryogenic propellant management techniques using the centaur launch vehicle
[NASA-CR-159658] p0062 N80-19185

CAPILLARY TUBES

Capillary acquisition devices for high-performance vehicles: Executive summary --- evaluation of cryogenic propellant management techniques using the centaur launch vehicle
[NASA-CR-159658] p0062 N80-19185

CAPTIVE TESTS

NT STATIC FIRING

NT STATIC TESTS

CARBIDES

NT SILICON CARBIDES

NT TITANIUM CARBIDES

NT TUNGSTEN CARBIDES

Improved adhesion of sputtered refractory carbides to metal substrates
p0081 A80-25274

An investigation of the initiation stage of hot corrosion in Ni-base alloys
[NASA-CR-159718] p0083 N80-15233

CARBON

Combustion of solid carbon rods in zero and normal gravity
p0074 A80-20955

Combustion of solid carbon rods in zero and normal gravity
[NASA-TM-79303] p0104 N80-13404

CARBON COMPOUNDS

NT CARBIDES

NT FLUOROPOLYMERS

NT SILICON CARBIDES

NT TITANIUM CARBIDES

NT TUNGSTEN CARBIDES

CARBON DIOXIDE LASERS

A cesium TELEC experiment at Lewis Research Center
[NASA-CR-159729] p0113 N80-14386

CARBON FIBER REINFORCED PLASTICS

Fire test method for graphite fiber reinforced plastics
p0070 A80-31169

Burning characteristics and fiber retention of graphite/resin matrix composites
p0070 A80-32062

Hybrid composites that retain graphite fibers on burning
p0073 A80-32064

Improved fiber retention by the use of fillers in graphite fiber/resin matrix composites
p0071 A80-32066

Burning characteristics and fiber retention of graphite/resin matrix composites
[NASA-TM-79314] p0067 N80-14196

Fire test method for graphite fiber reinforced plastics
[NASA-TM-81436] p0068 N80-18107

Circumferential shaft seal
[NASA-CASE-LEW-12119-1] p0119 N80-28711

CARBON FIBERS

Fiber release characteristics of graphite hybrid composites
p0073 A80-32063

High char imide-modified epoxy matrix resins
p0071 A80-34789

Calculation of residual principal stresses in CVD boron on carbon filaments
p0072 A80-44237

Calculation of residual principal stresses in CVD boron on carbon filaments
[NASA-TM-81456] p0068 N80-20314

Potential release of fibers from burning carbon composites --- aircraft fires
[NASA-TM-80214] p0069 N80-29431

Statistical aspects of carbon fiber risk assessment modeling --- fire accidents involving aircraft
[NASA-CR-159318] p0073 N80-29432

CARBON MONOXIDE

Comments on 'Experimental evidence for interhemispheric transport from airborne carbon monoxide measurements'
p0159 A80-32520

An analytical study of nitrogen oxides and carbon monoxide emissions in hydrocarbon combustion with added nitrogen - Preliminary results
[ASME PAPER 80-GT-60] p0074 A80-42190

An analytical study of nitrogen oxides and carbon monoxide emissions in hydrocarbon combustion with added nitrogen, preliminary results
[NASA-TM-79296] p0157 N80-13721

CARBON STEELS

Manufacture of low carbon astrology turbine disk shapes by hot isostatic pressing. Volume 2, project 1
[NASA-CR-135410] p0037 N80-21329

CARBONACEOUS ROCKS

NT COAL

CARCINOMA

U CANCER

CARGO AIRCRAFT

NT YC-14 AIRCRAFT

CARTRIDGE ACTUATED DEVICES

U ACTUATORS

CARTRIDGES

Dynamic properties of elastomer cartridge specimens under a rotating load
p0121 A80-24002

CASCADE FLOW

An experimental investigation of endwall profiling in a turbine vane cascade
[AIAA PAPER 80-1089] p0004 A80-38904

Streakline flow visualization study of a horseshoe vortex in a large-scale, two-dimensional turbine stator cascade
[ASME PAPER 80-GT-4] p0004 A80-42145

An implicit finite-difference code for inviscid and viscous cascade flow
[AIAA PAPER 80-1427] p0007 A80-44128

Aerodynamic analysis of a supersonic cascade vibrating in a complex mode
p0007 A80-45841

- Streakline flow visualization study of a horseshoe vortex in a large-scale, two-dimensional turbine stator cascade
[NASA-TM-79274] p0104 N80-11376
- Experimental determination of unsteady blade element aerodynamic in cascades. Volume 1: Torsion mode cascade
[NASA-CR-159831] p0040 N80-25335
- A calculation procedure for viscous flow in turbomachines, volume 3 --- computer programs
[NASA-CR-159864] p0005 N80-26274
- CAS2D: FORTRAN program for nonrotating blade-to-blade, steady, potential transonic cascade flows
[NASA-TP-1705] p0003 N80-27284
- CASCADES (FLUID DYNAMICS)**
U FLUID DYNAMICS
- CAST ALLOYS**
Development of exothermically cast single-crystal Mar-M 247 and derivative alloys
[AIRESEARCH-21-3469] p0084 A80-45825
- CASTING**
Preparation of cast aluminum alloy-mica particle composites
p0071 A80-32632
- Adherence of ion beam sputter deposited metal films on H-13 steel
[NASA-TM-81585] p0079 N80-31527
- CASTINGS**
NT INGOTS
Castable high temperature refractory materials
[NASA-CASE-LEW-13080-1] p0088 N80-29496
- CATALYSIS**
Advanced catalytic combustors for low pollutant emissions, phase 1
[NASA-CR-159535] p0028 N80-13048
- Diesel engine catalytic combustor system --- turbocharging
[NASA-CASE-LEW-12995-1] p0118 N80-26659
- CATALYSTS**
NT ELECTROCATALYSTS
Durability testing of advanced catalysts and catalyst supports for gas turbine engine combustors
p0074 A80-35881
- The effect of catalyst length and downstream reactor distance on catalytic combustor performance
[NASA-TM-81475] p0142 N80-23779
- Durability testing at 5 atmospheres of advanced catalysts and catalyst supports for gas turbine engine combustors
[NASA-CR-159839] p0151 N80-24748
- Gas phase oxidation downstream of a catalytic combustor
[NASA-TM-81551] p0144 N80-29863
- CATALYTIC ACTIVITY**
CATCOM catalyst 5 atm 1000 hour aging study using No. 2 fuel oil
p0075 A80-35908
- CATHODES**
NT CELL CATHODES
NT HOLLOW CATHODES
Life test studies on tungsten impregnated cathodes
Thermionic cathode life test studies
[NASA-TM-81441] p0103 A80-45122
- p0101 N80-18302
- CAVITATION**
U CAVITATION FLOW
CAVITATION FLOW
Marangoni bubble motion in zero gravity
p0107 A80-20958
- Observation of pressure variation in the cavitation region of submerged journal bearings
[NASA-TM-81582] p0120 N80-31798
- CELL CATHODES**
Decay of the zincate concentration gradient at an alkaline zinc cathode after charging
p0074 A80-13070
- CENTAUR LAUNCH VEHICLE**
Capillary acquisition devices for high-performance vehicles: Executive summary --- evaluation of cryogenic propellant management techniques using the centaur launch vehicle
[NASA-CR-159658] p0062 N80-19185
- CENTAUR VEHICLE**
U CENTAUR LAUNCH VEHICLE
- CENTRIFUGAL COMPRESSORS**
Field verification of lateral-torsional coupling effects on rotor instabilities in centrifugal compressors
p0125 N80-29708
- Analysis and identification of subsynchronous vibration for a high pressure parallel flow centrifugal compressor
p0125 N80-29710
- Subsynchronous instability of a geared centrifugal compressor of overhung design
p0125 N80-29711
- Asynchronous vibration problem of centrifugal compressor
p0125 N80-29713
- Effect of fluid forces on rotor stability of centrifugal compressors and pumps
p0126 N80-29720
- Experimental results concerning centrifugal impeller excitations
p0127 N80-29727
- CENTRIFUGAL PUMPS**
Hydraulic forces caused by annular pressure seals in centrifugal pumps
p0126 N80-29718
- A test program to measure fluid mechanical whirl-excitation forces in centrifugal pumps
p0126 N80-29719
- Effect of fluid forces on rotor stability of centrifugal compressors and pumps
p0126 N80-29720
- Fluid forces on rotating centrifugal impeller with whirling motion
p0127 N80-29724
- CENTRIFUGING STRESS**
Buckling of rotating beams
p0133 A80-20149
- CERAMAL PROTECTIVE COATINGS**
U PROTECTIVE COATINGS
- CERAMIC COATINGS**
Thick ceramic coating development for industrial gas turbines - A program plan
[SR79-M-4702-05] p0091 A80-10042
- Thermal barrier coatings for aircraft gas turbines
[AIAA PAPER 80-0302] p0089 A80-18303
- Preliminary study of a solar selective coating system using black cobalt oxide for high temperature solar collectors
p0082 A80-35500
- Effect of thermal cycling on ZrO₂-Y₂O₃ thermal barrier coatings
p0089 A80-35899
- Effects of yttrium, aluminum and chromium concentrations in bond coatings on the performance of zirconia-yttria thermal barriers
p0082 A80-35900
- Development of improved-durability plasma sprayed ceramic coatings for gas turbine engines
[AIAA PAPER 80-1193] p0089 A80-38963
- Similarity tests of turbine vanes - Effects of ceramic thermal barrier coatings
[ASME PAPER 80-HT-24] p0027 A80-48013
- Plasma-sprayed dual density ceramic turbine seal system
[NASA-CR-159739] p0123 N80-15411
- Similarity tests of turbine vanes, effects of ceramic thermal barrier coatings
[NASA-TM-81473] p0105 N80-21706
- Significance of thermal contact resistance in two-layer thermal-barrier-coated turbine vanes
[NASA-TM-81483] p0018 N80-23310
- Development of improved-durability plasma sprayed ceramic coatings for gas turbine engines
[NASA-TM-81512] p0018 N80-23313
- Extension of similarity test procedures to cooled engine components with insulating ceramic coatings
[NASA-TP-1615] p0105 N80-24577
- Composite wall concept for high temperature turbine shrouds: Heat transfer analysis
[NASA-TM-81539] p0020 N80-27362
- Effect on combined cycle efficiency of stack gas temperature constraints to avoid acid corrosion
[NASA-TM-81531] p0143 N80-27804
- CERAMICS**
State-of-the-art of Sialon materials
p0009 A80-13066
- 3500-hour durability testing of ceramic materials for automotive gas turbine engines
[AIRESEARCH-31-3542] p0092 A80-35575
- Significance of thermal contact resistance in two-layer, thermal-barrier-coated turbine vanes

CESIUM COMPOUNDS

SUBJECT INDEX

Quantitative ultrasonic evaluation of engineering properties in metals, composites, and ceramics
 [NASA-CR-159585] p0024 A80-39635
 Fracture toughness determination of Al2O3 using four-point-bend specimens with straight-through and chevron notches
 [NASA-CR-159676] p0130 A80-39641
 Improving the stress rupture and creep of silicon nitride --- turbine materials
 [NASA-CR-159676] p0090 A80-42065
 Development of silicon nitride of improved toughness
 [NASA-CR-159676] p0072 N80-10318
 Reactions of calcium orthosilicate and barium zirconate with oxides and sulfates of various elements
 [NASA-TM-79272] p0085 N80-13256
 Effects of a ceramic coating on metal temperatures of an air-cooled turbine vane
 [NASA-TP-1598] p0105 N80-17397
 Materials review for improved automotive gas turbine engine --- superalloys, refractory alloys, and ceramics
 [NASA-CR-159673] p0123 N80-17470
 Composite wall concept for high temperature turbine shrouds: Survey of low modulus strain isolator materials
 [NASA-TM-81443] p0086 N80-20398
 Advanced ceramic material for high temperature turbine tip seals
 [NASA-CR-159774] p0038 N80-22325
 Effect of thermal cycling on ZrO2-Y2O3 thermal barrier coatings
 [NASA-TM-81480] p0018 N80-22349
 Fully plasma-sprayed compliant backed ceramic turbine seal
 [NASA-CASE-LEW-13268-1] p0117 N80-24619
 Feasibility study of silicon nitride regenerators
 [NASA-CR-159713] p0194 N80-25209
 Effect of starting powder characteristics on density, microstructure and low temperature oxidation behavior of a Si3N48w/o Y2O3 ceramic
 [NASA-TM-81536] p0088 N80-27484
 Castable high temperature refractory materials
 [NASA-CASE-LEW-13080-1] p0088 N80-29496
 Regenerator matrix physical property data
 [NASA-CR-159854] p0185 N80-30228
 The 3500 hour durability testing of commercial ceramic materials
 [NASA-CR-159785] p0091 N80-31552
CESIUM COMPOUNDS
NT CESIUM OXIDES
CESIUM OXIDES
 Effects of oxide additions and temperature on sinterability of milled silicon nitride
 [NASA-TP-1644] p0086 N80-21532
CESSEA MILITARY AIRCRAFT
U MILITARY AIRCRAFT
CETANE
 Autoignition characteristics of aircraft-type fuels
 [NASA-CR-159886] p0095 N80-30535
CFRP
U CARBON FIBER REINFORCED PLASTICS
CHALCOGENIDES
NT ALUMINUM OXIDES
NT CARBON MONOXIDE
NT CESIUM OXIDES
NT COBALT OXIDES
NT MAGNESIUM OXIDES
NT METAL OXIDES
NT MOLYBDENUM DISULFIDES
NT MOLYBDENUM SULFIDES
NT NITRIC OXIDE
NT NITROGEN OXIDES
NT OXIDES
NT SAPPHIRE
NT YTTRIUM OXIDES
NT ZINC OXIDES
NT ZIRCONIUM OXIDES
CHANCE-VOUGHT MILITARY AIRCRAFT
U MILITARY AIRCRAFT
CHAPMAN-JOUGET FLAME
U FLAME PROPAGATION
CHARGED PARTICLES
NT ARGON PLASMA
NT HELIUM PLASMA
NT HIGH TEMPERATURE PLASMAS
NT HYDROGEN PLASMA
NT LASER PLASMAS

NT MAGNETICALLY TRAPPED PARTICLES
NT PHOTOELECTRONS
NT PLASMA SHEATHS
NT PLASMAS (PHYSICS)
NT TOROIDAL PLASMAS
 Specific spacecraft evaluation: Special report --- charged particle transport from a mercury ion thruster to spacecraft surfaces
 [NASA-CR-159420] p0060 N80-11137
CHARGING
 Decay of the zincate concentration gradient at an alkaline zinc cathode after charging
 p0074 A80-13070
CHARTS
NT GRAPHS (CHARTS)
CHECKOUT
 Installation and checkout of the DOE/NASA Mod-1 2000-kW wind turbine generator
 [NASA-TM-81444] p0140 N80-19614
CHECKOUT EQUIPMENT
U TEST EQUIPMENT
CHEMICAL ANALYSIS
NT GAS ANALYSIS
NT OZONOMETRY
NT SPECTROSCOPIC ANALYSIS
NT VOLUMETRIC ANALYSIS
 An interactive modular design for computerized photometry in spectrochemical analysis
 p0074 A80-39640
 Formation of porous surface layers in reaction bonded silicon nitride during processing
 p0090 A80-51574
 Effect of starting powder characteristics on density, microstructure and low temperature oxidation behavior of a Si3N48w/o Y2O3 ceramic
 [NASA-TM-81536] p0088 N80-27484
 Fuels characterization studies --- jet fuels
 p0021 N80-29309
CHEMICAL ATTACK
 The chemistry of sodium chloride involvement in processes related to hot corrosion
 p0074 A80-10041
 The erosion/corrosion of small superalloy turbine rotors operating in the effluent of a PFB coal combustor
 p0080 A80-10043
CHEMICAL COMPOSITION
 Initial characterization of an Experimental Referee Broadened-Specification (ERBS) aviation turbine fuel
 [NASA-TM-81440] p0093 N80-18205
 Fuel character effects on the J79 and F101 engine combustion systems
 p0042 N80-29312
CHEMICAL EFFECTS
 Mechanical and chemical effects of ion-texturing biomedical polymers
 p0089 A80-13065
CHEMICAL ELEMENTS
NT ALUMINUM
NT ARGON
NT CADMIUM
NT CARBON
NT CHROMIUM
NT COPPER
NT EUROPIUM
NT GALLIUM
NT HYDROGEN
NT HYDROGEN ATOMS
NT HYDROGEN IONS
NT HYDROGEN PLASMA
NT IRON
NT LIQUID HYDROGEN
NT NEON
NT OXYGEN
NT RARE GASES
NT SILICON
NT SODIUM
NT TRACE ELEMENTS
NT TUNGSTEN
NT VANADIUM
NT XENON
NT YTTRIUM
NT ZIRCONIUM
CHEMICAL FUELS
NT AIRCRAFT FUELS
NT DIESEL FUELS
NT HYDROCARBON FUELS
NT HYDROGEN FUELS

SUBJECT INDEX

COAL UTILIZATION

NT JET ENGINE FUELS
 NT JP-5 JET FUEL
 NT SYNTHETIC FUELS
CHEMICAL KINETICS
 U REACTION KINETICS
CHEMICAL PROPERTIES
 NT HEAT OF COMBUSTION
 NT HEAT OF FUSION
 NT THERMOCHEMICAL PROPERTIES
 Fuel character effects on the J79 and F101 engine combustion systems
 State-of-the-art SiAlON materials p0042 N80-29312
 p0022 N80-29358
CHEMICAL PROPULSION
 NT HYBRID PROPULSION
 Analytical investigation of two hydrogen-oxygen rocket engine systems for low-thrust application p0060 A80-35503
 Analytical investigation of two hydrogen-oxygen rocket engine systems for low-thrust application --- for orbital transfer p0057 N80-30382
 LEO-to-GEO low thrust chemical propulsion p0063 N80-30384
 Chemical propulsion technology p0058 N80-31453
 Low-thrust vehicles concept studies p0063 N80-31456
 Auxiliary control of LSS p0063 N80-31459
 Low-thrust chemical rocket engine study p0063 N80-31467
 Low-thrust chemical propulsion p0063 N80-31468
 Low-thrust chemical orbit to orbit propulsion system propellant management study p0064 N80-31469
CHEMICAL REACTION CONTROL
 Status of nickel-hydrogen cell technology p0064 N80-33474
CHEMICAL REACTIONS
 NT OXIDATION
 NT OXIDATION-REDUCTION REACTIONS
 Reactions of calcium orthosilicate and barium zirconate with oxides and sulfates of various elements [NASA-TN-79272] p0085 N80-13256
 Synthesis of improved polyester resins [NASA-CR-159665] p0090 N80-13257
 Reaction bonded silicon nitride prepared from wet attrition-milled silicon --- fractography [NASA-TN-81428] p0086 N80-18181
 Formation of porous surface layers in reaction bonded silicon nitride during processing [NASA-TN-81493] p0087 N80-23456
 Thermal fatigue and oxidation data of oxide dispersion-strengthened alloys [NASA-CR-159842] p0084 N80-25415
 Low temperature cross linking polyimides [NASA-CASE-LEW-12876-1] p0087 N80-26447
 Gas phase oxidation downstream of a catalytic combustor [NASA-TN-81551] p0144 N80-29863
CHEMICAL TESTS
 NT CHEMICAL ANALYSIS
 NT GAS ANALYSIS
 NT OZONOMETRY
 NT SPECTROSCOPIC ANALYSIS
 NT VOLUMETRIC ANALYSIS
CHEMONUCLEAR PROPULSION
 U CHEMICAL PROPULSION
CHILLING
 U COOLING
CHLORIDES
 NT SODIUM CHLORIDES
CHLORINE COMPOUNDS
 NT SODIUM CHLORIDES
CHOKES (RESTRICTIONS)
 Toward the use of similarity theory in two-phase choked flows [NASA-TN-81568] p0106 N80-29623
CHOPPERS (ELECTRIC)
 U ELECTRIC CHOPPERS
CHROMATOGRAPHY
 NT LIQUID CHROMATOGRAPHY
CHROME
 U CHROMIUM

CHROMIUM
 Effects of yttrium, aluminum and chromium concentrations in bond coatings on the performance of zirconia-yttria thermal barriers [NASA-TN-81485] p0079 N80-22464
CHROMIUM ALLOYS
 NT ASTROLOY (TRADEMARK)
 NT CHROMIUM STEELS
 The effect of zirconium on the isothermal oxidation of nominal Ni-14Cr-24Al alloys p0082 A80-26465
 Mechanical properties and oxidation and corrosion resistance of reduced-chromium 304 stainless steel alloys [NASA-TP-1557] p0076 N80-11188
CHROMIUM COMPOUNDS
 Catalyst surfaces for the chromous/chromic redox couple [NASA-CASE-LEW-13148-2] p0140 N80-18557
CHROMIUM STEELS
 Anodic polarization behavior of austenitic stainless steel alloys with lower chromium content p0178 A80-22250
CHUGGING
 U COMBUSTION STABILITY
CIRCUITS
 NT SWITCHING CIRCUITS
CIRCULATION
 NT ATMOSPHERIC CIRCULATION
CIVIL AVIATION
 Aeropropulsion in year 2000 [NASA-TN-81416] p0016 N80-18043
CLEAN FUELS
 NT FUEL OILS
CLEANING
 Evaluation of cleaners for photovoltaic modules exposed in an outdoor environment [NASA-TN-79248] p0096 N80-13317
 Investigation into the effect of plasma pretreatment on the adhesion of parylene to various substrates [NASA-TN-79224] p0114 N80-13473
CLEARANCES
 Laser-optical blade tip clearance measurement system p0111 A80-36137
 Fuel conservation through active control of rotor clearances [AIAA PAPER 80-1087] p0045 A80-41506
CLINICAL MEDICINE
 Preliminary results of fast neutron treatments in carcinoma of the pancreas [NASA-TN-81516] p0160 N80-24983
CLOSED LOOP SYSTEMS
 U FEEDBACK CONTROL
COAL
 Cogeneration Technology Alternatives Study (CTAS). Volume 1: Summary [NASA-TN-81400] p0141 N80-19626
 Assessment of satellite and aircraft multispectral scanner data for strip-mine monitoring [NASA-TN-79268] p0136 N80-20787
 Literature survey of properties of synfuels derived from coal [NASA-TN-79243] p0141 N80-22776
 Cogeneration Technology Alternatives Study (CTAS). Volume 3: Industrial processes [NASA-CR-159767] p0155 N80-31870
COAL LIQUEFACTION
 Effects of impurities in coal-derived liquids on accelerated hot corrosion of superalloys [NASA-TN-81384] p0077 N80-18157
 Use of petroleum-based correlations and estimation methods for synthetic fuels [NASA-TN-81533] p0093 N80-27509
COAL UTILIZATION
 The erosion/corrosion of small superalloy turbine rotors operating in the effluent of a PFB coal combustor p0080 A80-10043
 Survey of MHD plant applications p0144 A80-11972
 Oxygen-enriched air for MHD power plants p0096 A80-25096
 NASA-Lewis closed-cycle magnetohydrodynamics plant analysis [NASA-TN-79249] p0137 N80-10595
 Status of the DOE/NASA critical gas turbine research and technology project [NASA-TN-79307] p0137 N80-14493

COATINGS

Factors affecting cleanup of exhaust gases from a pressurized, fluidized-bed coal combustor [NASA-TM-81439] p0105 N80-20532
Improved PFB operations: 400-hour turbine test results --- coal combustion products and hot corrosion in gas turbines [NASA-TM-81511] p0079 N80-26426
Parametric study of prospective early commercial MHD power plants (PSPEC). General Electric Company, task 1: Parametric analysis [NASA-CR-159634] p0152 N80-26779
Optimal thermionic energy conversion with established electrodes for high-temperature topping and process heating --- coal combustion product environments [NASA-TM-81555] p0175 N80-33221
Cogeneration Technology Alternatives Study (CTAS). Volume 4: Energy conversion systems [NASA-CR-159768] p0155 N80-33859

COATINGS

NT ALUMINUM COATINGS
NT ANTIREFLECTION COATINGS
NT CERAMIC COATINGS
NT METAL COATINGS
NT NICKEL COATINGS
NT PLASTIC COATINGS
NT PROTECTIVE COATINGS
NT SPRAYED COATINGS
NT THERMAL CONTROL COATINGS

Abradable compressor and turbine seals, volume 1 --- for turbofan engines [NASA-CR-159600] p0083 N80-14235

COAXIAL FLOW

Noise suppression due to annulus shaping of a conventional coaxial nozzle p0171 A80-35497

COAXIAL NOZZLES

Noise suppression due to annulus shaping of an inverted-velocity-profile coaxial nozzle p0171 A80-35498
Noise suppression due to annulus shaping of an inverted-velocity-profile coaxial nozzle --- supersonic cruise aircraft [NASA-TM-81460] p0168 N80-22046
Noise suppression due to annulus shaping of conventional coaxial nozzle [NASA-TM-81461] p0168 N80-22047

COBALT ALLOYS

NT ASTROLOY (TRADEMARK)
Friction and wear of plasma-sprayed coatings containing cobalt alloys from 25 deg to 650 deg in air [ASLE PREPRINT 80-AM-6C-2] p0122 A80-43176
Corrosion resistance of sodium sulfate coated cobalt-chromium-aluminum alloys at 900 C, 1000 C, and 1100 C [NASA-TM-79311] p0076 N80-14234
Friction and wear of plasma-sprayed coatings containing cobalt alloys from 25 deg to 650 deg in air [NASA-TM-79316] p0085 N80-14249
Hot corrosion of Co-Cr, Co-Cr-Al, and Ni-Cr alloys in the temperature range of 700-750 deg C [NASA-CR-159689] p0084 N80-26427

COBALT COMPOUNDS

NT COBALT OXIDES

COBALT OXIDES

Preliminary study of a solar selective coating system using black cobalt oxide for high temperature solar collectors p0082 A80-35500
Preliminary study of a solar selective coating system using black cobalt oxide for high temperature solar collectors [NASA-TM-81385] p0077 N80-18156

COEFFICIENT OF FRICTION

Friction and wear of plasma-sprayed coatings containing cobalt alloys from 25 deg to 650 deg in air [ASLE PREPRINT 80-AM-6C-2] p0122 A80-43176
Sliding friction of some metallic glasses p0090 A80-46153
Friction and wear of plasma-sprayed coatings containing cobalt alloys from 25 deg to 650 deg in air [NASA-TM-79316] p0085 N80-14249
Adhesion and friction of iron-base binary alloys in contact with silicon carbide in vacuum [NASA-TP-1624] p0076 N80-15234

SUBJECT INDEX

Tribological properties of sputtered MoS sub 2 films in relation to film morphology [NASA-TM-81465] p0078 N80-21490
The response of turbine engine rotors to interfacial rubs [NASA-TM-81518] p0118 N80-27696

COEFFICIENTS

NT ATTENUATION COEFFICIENTS
NT COEFFICIENT OF FRICTION
NT FLOW COEFFICIENTS
NT HEAT TRANSFER COEFFICIENTS

COGENERATION

Cogeneration Technology Alternatives Study (CTAS). Volume 1: Summary [NASA-TM-81400] p0141 N80-19626
Cogeneration Technology Alternatives Study (CTAS). Volume 1: Summary report [NASA-CR-159715] p0151 N80-24797
Cogeneration technology alternatives study. Volume 1: Summary report [NASA-CR-159759] p0152 N80-25792
Cogeneration technology alternatives study. Volume 2: Industrial process characteristics [NASA-CR-159760] p0152 N80-25793
Cogeneration technology alternatives study. Volume 4: Heat Sources, balance of plant and auxiliary systems [NASA-CR-159762] p0152 N80-25794
Cogeneration technology alternatives study. Volume 6: Computer data [NASA-CR-159764] p0152 N80-25795
Cogeneration Technology Alternatives Study (CTAS). Volume 2: Analytical approach [NASA-CR-159766] p0143 N80-28859
Cogeneration Technology Alternatives Study (CTAS). Volume 6: Computer data. Part 1: Coal-fired nocogeneration process boiler, section A [NASA-CR-159770-PT-1-A] p0154 N80-30888
Cogeneration Technology Alternatives Study (CTAS). Volume 6: Computer data. Part 1: Coal-fired nocogeneration process boiler, section B [NASA-CR-159770-PT-1-B] p0154 N80-30889
Cogeneration Technology Alternatives Study (CTAS). Volume 6: Computer data. Part 2: Residual-fired nocogeneration process boiler [NASA-CR-159770-PT-2] p0155 N80-30890
Cogeneration Technology Alternatives Study (CTAS). Volume 3: Energy conversion system characteristics [NASA-CR-159761] p0155 N80-31869
Cogeneration Technology Alternatives Study (CTAS). Volume 3: Industrial processes [NASA-CR-159767] p0155 N80-31870
Optimal thermionic energy conversion with established electrodes for high-temperature topping and process heating --- coal combustion product environments [NASA-TM-81555] p0175 N80-33221
Cogeneration Technology Alternatives Study (CTAS). Volume 4: Energy conversion systems [NASA-CR-159768] p0155 N80-33859
Cogeneration Technology Alternatives Study (CTAS). Volume 6: Computer data. Part 1: Coal-fired nocogeneration process boiler, section A [NASA-CR-159770-PT-1] p0156 N80-33860
Cogeneration Technology Alternatives Study (CTAS). Volume 6: Computer data. Part 2: Residual-fired nocogeneration process boiler [NASA-CR-159770-PT-2] p0156 N80-33861

COHERENT RADIATION

Application of coherence in fan noise studies [NASA-TP-1630] p0167 N80-18882

COHERENT SOURCES

U COHERENT RADIATION

COHERENT TRANSMISSION

U COHERENT RADIATION

COLD FLOW TESTS

Design and cold-air test of single-stage uncooled turbine with high work output [NASA-TP-1680] p0019 N80-25337
Cold-air investigation of a 4 1/2 stage turbine with stage-loading factor of 4.66 and high specific work output. 2: Stage group performance [NASA-TP-1688] p0019 N80-25338

COLD FORMING

U COLD WORKING

COLD WORKING

Critical currents in A-15 structure Nb3Al converted from cold-worked bcc structure

- COLLISIONS
 NT BIRD-AIRCRAFT COLLISIONS
 NT PARTICLE COLLISIONS
 COLUMNS (PROCESS ENGINEERING)
 The optimization air separation plants for
 combined cycle MHD-power plant applications
 [NASA-TM-81510] p0179 A80-33853
- COMBUSTIBILITY
 U FLAMMABILITY
 COMBUSTIBLE FLOW
 Dispersion of sound in a combustion duct by fuel
 droplets and soot particles p0142 N80-23778
- COMBUSTION
 NT FUEL COMBUSTION
 NT HYDROCARBON COMBUSTION
 Burning characteristics and fiber retention of
 graphite/resin matrix composites p0070 A80-32062
 Investigation of critical burning of fuel droplets
 [NASA-CR-159697] p0075 N80-12142
 Combustion of solid carbon rods in zero and normal
 gravity p0104 N80-13404
 Gas phase oxidation downstream of a catalytic
 combustor [NASA-TM-81551] p0144 N80-29863
- COMBUSTION CHAMBERS
 Coupled generator and combustor performance
 calculations for potential early commercial MHD
 power plants p0156 A80-25099
 Durability testing of advanced catalysts and
 catalyst supports for gas turbine engine
 combustors p0074 A80-35881
 Cooling of high pressure rocket thrust chambers
 with liquid oxygen p0060 A80-38992
 Analytical and experimental evaluations of the
 effect of broad property fuels on combustors for
 commercial aircraft gas turbine engines
 [AIAA PAPER 80-1260] p0094 A80-41516
 Performance of annular prediffuser-combustor systems
 [ASME PAPER 80-GT-15] p0026 A80-42154
 Atomizing characteristics of swirl can combustor
 modules with swirl blast fuel injectors
 [ASME PAPER 80-GT-30] p0026 A80-42164
 Low NO_x/heavy fuel combustor program
 [ASME PAPER 80-GT-69] p0026 A80-42199
 Advanced catalytic combustors for low pollutant
 emissions, phase 1 p0028 N80-13048
 Stability analysis of a liquid fuel annular
 combustion chamber [NASA-CR-159734] p0061 N80-13165
 Effect of degree of fuel vaporization upon
 emissions for a premixed partially vaporized
 combustion system --- for gas turbine engines
 [NASA-TP-1582] p0014 N80-14125
 Quiet Clean Short-haul Experimental Engine
 (QCSEE). Double-annular clean combustor
 technology development report p0032 N80-15121
 Core noise investigation of the CF6-50 turbofan
 engine [NASA-CR-159598] p0036 N80-16061
 Core noise investigation of the CF6-50 turbofan
 engine [NASA-CR-159749] p0036 N80-16062
 Study of research and development requirements of
 small gas-turbine combustors [NASA-CR-159796] p0036 N80-18040
 Factors affecting cleanup of exhaust gases from a
 pressurized, fluidized-bed coal combustor
 [NASA-TM-81439] p0105 N80-20532
 The effect of catalyst length and downstream
 reactor distance on catalytic combustor
 performance [NASA-TM-81475] p0142 N80-23779
 Durability testing at 5 atmospheres of advanced
 catalysts and catalyst supports for gas turbine
 engine combustors [NASA-CR-159839] p0151 N80-24748
 Analytical and experimental evaluations of the
 effect of broad property fuels on combustors for
 commercial aircraft gas turbine engines
 [NASA-TM-81496] p0093 N80-25454
- Diesel engine catalytic combustor system ---
 turbocharging [NASA-CASE-LEW-12995-1] p0118 N80-26659
 Experimental combustor study program p0042 N80-29311
 NASA broadened-specification fuels combustion
 technology program p0021 N80-29313
 The broadened-specification fuels combustion
 technology program at Pratt and Whitney Aircraft
 p0042 N80-29315
 Fuel property effects in stirred combustors
 p0043 N80-29321
 Preliminary studies of combustor sensitivity to
 alternative fuels p0021 N80-29323
 Low-pressure performance of annular, high-pressure
 (40 atm) high-temperature (2480 K) combustion
 system [NASA-TP-1713] p0023 N80-32396
 Energy efficient engine [NASA-CR-159685] p0045 N80-33408
- COMBUSTION CONTROL
 Flame tube parametric studies for control of fuel
 bound nitrogen using rich-lean two-stage
 combustion [NASA-TM-81472] p0141 N80-21837
- COMBUSTION EFFICIENCY
 Results of duct area ratio changes in the NASA
 Lewis H2-O2 combustion MHD experiment
 [NASA-TM-79308] p0175 N80-12881
 Design and evaluation of high performance rocket
 engine injectors for use with hydrocarbon fuels
 [NASA-TM-79319] p0056 N80-13163
 Fuel quality combustion analysis [NASA-CR-159721] p0094 N80-19284
 The broadened-specification fuels combustion
 technology program at Pratt and Whitney Aircraft
 p0042 N80-29315
 NASA/General Electric broad-specification fuels
 combustion technology program, phase 1 p0042 N80-29316
 Fuels research: Combustion effects overview
 p0021 N80-29317
 Fuel property effects in stirred combustors
 p0043 N80-29321
 Performance deterioration of commercial
 high-bypass ratio turbofan engines
 [NASA-TM-81552-REV] p0023 N80-32394
 The energy efficient engine project
 [NASA-TM-81566] p0023 N80-32395
- COMBUSTION HEAT
 U HEAT OF COMBUSTION
 COMBUSTION INSTABILITY
 U COMBUSTION STABILITY
 COMBUSTION PHYSICS
 Symposium /International/ on Combustion, 17th,
 Leeds University, Leeds, England, August 20-25,
 1978, Proceedings p0075 A80-11754
 Combustion of solid carbon rods in zero and normal
 gravity p0074 A80-20955
 CATCOM catalyst 5 atm 1000 hour aging study using
 No. 2 fuel oil p0075 A80-35908
- COMBUSTION PRODUCTS
 The chemistry of sodium chloride involvement in
 processes related to hot corrosion p0074 A80-10041
 Combustion of solid carbon rods in zero and normal
 gravity p0074 A80-20955
 An analytical study of nitrogen oxides and carbon
 monoxide emissions in hydrocarbon combustion
 with added nitrogen - Preliminary results
 [ASME PAPER 80-GT-60] p0074 A80-42190
 Effect of fuel molecular structure on soot
 formation in gas turbine engines
 [ASME PAPER 80-GT-62] p0095 A80-42192
 Burning characteristics and fiber retention of
 graphite/resin matrix composites [NASA-TM-79314] p0067 N80-14196
 Quiet Clean Short-haul Experimental Engine (QCSEE)
 clean combustor test report [NASA-CR-134916] p0030 N80-15104
 Theory of deposition of condensable impurities on
 surfaces immersed in combustion gases
 [NASA-CR-159716] p0033 N80-15130

COMBUSTION STABILITY

SUBJECT INDEX

Experimental studies of the formation/deposition of sodium sulfate in/from combustion gases --- hot corrosion of gas turbine engine components [NASA-CR-159753] p0033 N80-15131
 Synthesis of improved phenolic resins [NASA-CR-159724] p0091 N80-17221
 Fire test method for graphite fiber reinforced plastics [NASA-TM-81436] p0068 N80-18107
 Fuel quality combustion analysis [NASA-CR-159721] p0094 N80-19284
 Improved PFB operations: 400-hour turbine test results --- coal combustion products and hot corrosion in gas turbines [NASA-TM-81511] p0079 N80-26426
 Performance, emissions, and physical characteristics of a rotating combustion aircraft engine, supplement A [NASA-CR-135119] p0041 N80-27361
 Soot formation and burnout in flames p0043 N80-29320
 Effect of fuel molecular structure on soot formation in gas turbine combustion p0043 N80-29322

Potential release of fibers from burning carbon composites --- aircraft fires [NASA-TM-80214] p0069 N80-29431

COMBUSTION STABILITY

CATCOM catalyst 5 atm 1000 hour aging study using No. 2 fuel oil p0075 A80-35908
 Analysis of combustion instability in liquid fuel rocket motors [NASA-CR-159733] p0061 N80-13164
 Stability analysis of a liquid fuel annular combustion chamber [NASA-CR-159734] p0061 N80-13165
 Amplification of Reynolds number dependent processes by wave distortion --- liquid fuel combustor stability [NASA-CR-159732] p0075 N80-13193
 Design and evaluation of high performance rocket engine injectors for use with hydrocarbon fuels p0094 N80-31621

COMBUSTION WAVES

U FLAME PROPAGATION

COMBUSTORS

U COMBUSTION CHAMBERS

COMMERCIAL AIRCRAFT

NT BOEING 747 AIRCRAFT

NT DC 9 AIRCRAFT

NT DC 10 AIRCRAFT

NT LIGHT TRANSPORT AIRCRAFT

NT SUPERSONIC COMMERCIAL AIR TRANSPORT

Aircraft Energy Efficiency (ACEE) status report p0012 N80-10206
 The NASA high-speed turboprop program [NASA-TM-81561] p0022 N80-31401

COMMERCIAL AVIATION

U CIVIL AVIATION

U COMMERCIAL AIRCRAFT

COMMERCIAL ENERGY

Coupled generator and combustor performance calculations for potential early commercial MHD power plants p0156 A80-25099
 MOD-2 wind turbine system concept and preliminary design report. Volume 2: Detailed report [DOE/NASA/0002-80/2] p0152 N80-26775

COMBINATION

Reaction bonded silicon nitride prepared from wet attrition-milled silicon --- fractography [NASA-TM-81428] p0086 N80-18181

COMMUNICATION EQUIPMENT

NASA communications technology research and development p0097 A80-25920

COMMUNICATION NETWORKS

Packet communications in satellites with multiple-beam antennas and signal processing [AIAA 80-0537] p0099 A80-29574
 Concepts for 20/30 GHz satcom systems for direct-to-user applications [AIAA 80-0582] p0050 A80-35329
 The 30/20 GHz mixed user architecture development study [NASA-CR-159686] p0097 N80-10415
 The 30/20 GHz mixed user architecture development study: Executive summary

[NASA-CR-159687] p0097 N80-10416
 Concepts for 18/30 GHz satellite communication system, volume 1 [NASA-CR-159625-VOL-1] p0098 N80-11277
 Concepts for 18/30 GHz satellite communication system, volume 1A: Appendix [NASA-CR-159625-VOL-1A] p0098 N80-11278
 Concepts for 18/30 GHz satellite communication system study. Executive summary [NASA-CR-159680] p0098 N80-11279
 The 18/30 GHz fixed communications system service demand assessment. Volume 1: Executive summary [NASA-CR-159546] p0099 N80-22547
 The 18/30 GHz fixed communications system service demand assessment. Volume 2: Main text [NASA-CR-159547] p0099 N80-22548
 The 30/20 GHz fixed communications systems service demand assessment. Volume 3: Appendices [NASA-CR-159548] p0099 N80-22549

COMMUNICATION SATELLITES

NT COMMUNICATIONS TECHNOLOGY SATELLITE

NASCAF modelling of environmental-charging-induced discharges in satellites p0054 A80-19774

NASA advanced communications systems analysis p0097 A80-25916

30/20 GHz wideband technology verification program p0097 A80-25917

NASA communications technology research and development p0097 A80-25920

National Aeronautics and Space Administration plans for space communication technology p0097 A80-26795

NASA's program in communication satellites [AAS 79-247] p0097 A80-28712

Packet communications in satellites with multiple-beam antennas and signal processing [AIAA 80-0537] p0099 A80-29574

Ka-band, multibeam, contiguous coverage satellite antenna for the USA [AIAA 80-0557] p0099 A80-29588

Multigigabit satellite on-board signal processing [AIAA 80-0583] p0100 A80-29605

Concepts for 20/30 GHz satcom systems for direct-to-user applications [AIAA 80-0582] p0050 A80-35329

System analysis for millimeter-wave communication satellites p0100 A80-52479

Concepts for 18/30 GHz satellite communication system, volume 1 [NASA-CR-159625-VOL-1] p0098 N80-11277

Concepts for 18/30 GHz satellite communication system, volume 1A: Appendix [NASA-CR-159625-VOL-1A] p0098 N80-11278

Concepts for 18/30 GHz satellite communication system study. Executive summary [NASA-CR-159680] p0098 N80-11279

The 30/20 GHz fixed communications systems service demand assessment. Volume 1: Executive summary [NASA-CR-159619] p0098 N80-18262

The 30/20 GHz fixed communications systems service demand assessment. Volume 2: Main report [NASA-CR-159620] p0098 N80-18263

The 30/20 GHz fixed communications systems service demand assessment. Volume 3: Annex [NASA-CR-159621] p0099 N80-18264

A digitally implemented communications experiment utilizing the communications technology satellite, Hermes [NASA-TM-81452] p0052 N80-21412

The 18/30 GHz fixed communications system service demand assessment. Volume 1: Executive summary [NASA-CR-159546] p0099 N80-22547

The 18/30 GHz fixed communications system service demand assessment. Volume 2: Main text [NASA-CR-159547] p0099 N80-22548

The 30/20 GHz fixed communications systems service demand assessment. Volume 3: Appendices [NASA-CR-159548] p0099 N80-22549

Study of advanced communications satellite systems based on SS-PDMA [NASA-CR-159778] p0050 N80-25357

A quantitative analysis of inter-island telephony traffic in the Pacific Basin Region (PBR) [NASA-TM-81587] p0097 N80-32610

COMMUNICATION SYSTEMS

U TELECOMMUNICATION

SUBJECT INDEX

COMPRESSOR MOTORS

COMMUNICATIONS TECHNOLOGY SATELLITE

Communications technology satellite - United States experiments and disaster communications applications

p0051 A80-10032

NASA's program in communication satellites [AAS 79-247]

p0097 A80-28712

Depriming of arterial heat pipes: An investigation of CTS thermal excursions [NASA-CR-165153]

p0108 M80-32688

COMPARTMENTS

NT AIRCRAFT COMPARTMENTS

NT ANECHOIC CHAMBERS

NT PRESSURE CHAMBERS

NT VACUUM CHAMBERS

COMPLIANCE (ELASTICITY)

U MODULUS OF ELASTICITY

COMPONENT RELIABILITY

Hg ion thruster component testing

[AIAA PAPER 79-2116]

p0059 A80-20959

The CP6 jet engine performance improvement: New front mount

p0029 M80-14127

COMPOSITE MATERIALS

NT ALUMINUM BORON COMPOSITES

NT BORON REINFORCED MATERIALS

NT CARBON FIBER REINFORCED PLASTICS

NT FIBER COMPOSITES

NT GLASS FIBER REINFORCED PLASTICS

NT GRAPHITE-EPOXY COMPOSITE MATERIALS

NT LAMINATES

NT METAL MATRIX COMPOSITES

NT POLYMER MATRIX COMPOSITE MATERIALS

NT RESIN MATRIX COMPOSITES

Engine environmental effects on composite behavior

--- moisture and temperature effects on

mechanical properties

[AIAA 80-0695]

p0024 A80-35101

Quantitative ultrasonic evaluation of engineering

properties in metals, composites, and ceramics

p0130 A80-39641

Materials and structures technology

p0012 M80-10210

Quiet Clean Short-haul Experimental Engine (QCSE)

Under-The-Wing (UTW) composite nacelle subsystem

test report --- to verify strength of selected

composite materials

[NASA-CR-135075]

p0034 M80-15100

Quiet Clean Short-haul Experimental Engine (QCSE)

Under-The-Wing (UTW) composite nacelle subsystem

test report --- to verify strength of selected

composite materials

[NASA-CR-135075]

p0034 M80-15100

Quiet Clean Short-haul Experimental Engine (QCSE)

Under-The-Wing (UTW) composite nacelle

test report --- to verify strength of selected

composite materials

[NASA-CR-135352]

p0032 M80-15119

Synthesis of improved phenolic resins

[NASA-CR-159724]

p0091 M80-17221

Feasibility of Kevlar 49/PMS-15 polyimide for high

temperature applications

[NASA-TN-81560]

p0069 M80-27429

Tungsten wire/FcCrAlY matrix turbine blade

fabrication study

[NASA-CR-159788]

p0044 M80-29331

Fabrication and evaluation of low fiber content

alumina fiber/aluminum composites

[NASA-CR-159517]

p0073 M80-29430

Method of making bearing material

[NASA-CASE-LEW-11930-3]

p0070 M80-33482

COMPOSITE STRUCTURES

NT LAMINATES

Feasibility of SiC composite structures for 1644

deg gas turbine seal applications

[NASA-CR-159597]

p0123 M80-13474

Quiet Clean Short-haul Experimental Engine (QCSE)

under-the-wing engine composite fan blade design

report

[NASA-CR-135046]

p0031 M80-15108

Composite wall concept for high temperature

turbine shrouds: Survey of low modulus strain

isolator materials

[NASA-TN-81443]

p0086 M80-20398

Sudden stretching of a four layered composite plate

[NASA-CR-159870]

p0073 M80-25383

Quiet Clean Short-haul Experimental Engine (QCSE)

under-the-wing engine composite fan blade:

Preliminary design test report

[NASA-CR-134846]

p0044 M80-29298

Cost analysis of composite fan blade manufacturing processes

[NASA-CR-159876]

p0044 M80-31398

COMPOSITES

U COMPOSITE MATERIALS

COMPOSITION (PROPERTY):

NT ATMOSPHERIC MOISTURE

NT CHEMICAL COMPOSITION

NT MOISTURE CONTENT

COMPOUNDING

Reaction bonded silicon nitride prepared from wet

attrition-milled silicon

p0089 A80-32828

COMPRESSED GAS

NT HIGH PRESSURE OXYGEN

COMPRESSIBLE FLOW

NT TRANSONIC FLOW

A three-dimensional turbulent compressible

subsonic duct flow analysis for use with

constructed coordinate systems

[AIAA PAPER 80-1398]

p0006 A80-41601

An efficient user-oriented method for calculating

compressible flow in an about three-dimensional

inlets --- panel method

[NASA-CR-159578]

p0004 M80-10134

Numerical calculation of steady inviscid full

potential compressible flow about wind turbine

blades

[NASA-TN-81438]

p0136 M80-18497

WIND: Computer program for calculation of three

dimensional potential compressible flow about

wind turbine rotor blades

[NASA-TN-1729]

p0003 M80-33357

COMPRESSIBLE FLUIDS

Damping in ring seals for compressible fluids

p0119 M80-29716

COMPRESSION LOADS

NT IMPACT LOADS

COMPRESSION TESTERS

U COMPRESSION TESTS

COMPRESSION TESTS

Buckling of rotating beams

p0133 A80-20149

COMPRESSOR BLADES

Measuring unsteady pressure on rotating compressor

blades --- with semiconductor strain gages under

gas turbine engine operating conditions

p0110 A80-12630

Experimental study of low aspect ratio compressor

blading

[ASME PAPER 80-GT-6]

p0025 A80-42147

Aerodynamic analysis of a supersonic cascade

vibrating in a complex mode

p0007 A80-45841

Experimental study of low aspect ratio compressor

blading

[NASA-TN-79280]

p0002 M80-11037

Core compressor exit stage study. 1: Aerodynamic

and mechanical design

[NASA-CR-159714]

p0037 M80-19113

COMPRESSOR EFFICIENCY

Experimental study of low aspect ratio compressor

blading

[NASA-TN-79280]

p0002 M80-11037

Steady-state performance of J85-21 compressor at

100 percent of design speed with and without

interstage rake blockage

[NASA-TN-81451]

p0017 M80-21333

Core compressor exit stage study. 2

[NASA-CR-159812]

p0039 M80-23312

Off-design correlation for losses due to part-span

dampers on transonic rotors

[NASA-TN-1693]

p0020 M80-28352

Practical experience with unstable compressors

p0125 M80-29709

COMPRESSOR MOTORS

Efficient laser anemometer for intra-rotor flow

mapping in turbomachinery

p0111 A80-36140

Laser anemometer measurements in a transonic axial

flow compressor rotor

p0111 A80-36141

Comparison between optical measurements and a

numerical solution of the flow field within a

transonic axial-flow compressor rotor

[AIAA PAPER 80-1078]

p0003 A80-38897

Laser anemometer measurements in a transonic axial

flow compressor rotor

[NASA-TN-79323]

p0002 M80-14050

COMPRESSORS

SUBJECT INDEX

Efficient laser anemometer for intra-rotor flow mapping in turbomachinery
[NASA-TM-79320] p0112 N80-14375

Three dimensional mean flow and turbulence characteristics of the near wake of a compressor rotor blade
[NASA-CR-159518] p0005 N80-27288

Evaluation of the cyclic behavior of aircraft turbine disk alloys, part 2
[NASA-CR-165123] p0084 N80-30482

COMPRESSORS

NT CENTRIFUGAL COMPRESSORS

NT SUPERCHARGERS

NT SUPERSONIC COMPRESSORS

NT TRANSONIC COMPRESSORS

NT TURBOCOMPRESSORS

Abradable compressor and turbine seals, volume 1 --- for turbofan engines
[NASA-CR-159600] p0083 N80-14235

Program to develop sprayed, plastically deformable compressor shroud seal materials
[NASA-CR-159741] p0123 N80-16338

Study of blade aspect ratio on a compressor front stage
[NASA-CR-159556] p0040 N80-25333

Composite seal for turbomachinery
[NASA-CASE-LEW-12131-2] p0118 N80-26658

Practical experience with unstable compressors
p0125 N80-29709

Evaluation of instability forces of labyrinth seals in turbines or compressors
p0126 N80-29715

COMPUTATIONAL FLUID DYNAMICS

Application of the principle of similarity fluid mechanics
p0107 A80-10039

Computation of three-dimensional flow in turbofan mixers and comparison with experimental data
[AIAA PAPER 80-0227] p0003 A80-20967

Computation of three-dimensional viscous supersonic flow in inlets
[AIAA PAPER 80-0194] p0065 A80-23941

Numerical calculation of steady inviscid full potential compressible flow about wind turbine blades
[AIAA 80-0607] p0145 A80-28804

Comparison between optical measurements and a numerical solution of the flow field within a transonic axial-flow compressor rotor
[AIAA PAPER 80-1078] p0003 A80-38897

A three-dimensional turbulent compressible subsonic duct flow analysis for use with constructed coordinate systems
[AIAA PAPER 80-1398] p0006 A80-41601

An implicit finite-difference code for inviscid and viscous cascade flow
[AIAA PAPER 80-1427] p0007 A80-44128

Numerical calculation of transonic axial turbomachinery flows
p0004 A80-44229

Computational fluid mechanics of internal flow
p0012 N80-10211

COMPUTER GRAPHICS

INFORM: An interactive data collection and display program with debugging capability
[NASA-TP-1424] p0162 N80-16742

COMPUTER METHODS

U COMPUTER PROGRAMS

COMPUTER PROGRAMMING

NT LANGUAGE PROGRAMMING

An interactive modular design for computerized photometry in spectrochemical analysis
[NASA-TM-81521] p0074 N80-24386

COMPUTER PROGRAMS

NT COMPUTER SYSTEMS PROGRAMS

NT NASTRAN

Analytical prediction and experimental verification of TWT and depressed collector performance using multidimensional computer programs
p0102 A80-13902

A matrix solution for the simulation of magnetic fields with ideal current loops
p0102 A80-13903

High speed cylindrical rolling element bearing analysis 'CYBEAN' - Analytic formulation
[ASME PAPER 79-LUB-35] p0129 A80-14761

NASCAP modelling computations on large optics spacecraft in geosynchronous substorm environments

Efficient user-oriented method for calculating compressible flow in an about three-dimensional inlets --- panel method
[NASA-CR-159578] p0004 N80-10134

Computer code for estimating installed performance of aircraft gas turbine engines. Volume 1: Final report
[NASA-CR-159691] p0028 N80-13043

Computer code for estimating installed performance of aircraft gas turbine engines. Volume 2: Users manual
[NASA-CR-159692] p0028 N80-13044

Modification of axial compressor streakline program for analysis of engine test data
[NASA-TM-79312] p0002 N80-14051

Development of a three-dimensional supersonic inlet flow analysis
[NASA-CR-3218] p0108 N80-14356

Computer program for generating input for analysis of impingement-cooled, axial-flow turbine blade
[NASA-TP-1603] p0104 N80-15361

A calculation procedure for viscous flow in turbomachines, volume 3 --- computer programs
[NASA-CR-159864] p0005 N80-26274

CAS2D: FORTRAN program for nonrotating blade-to-blade, steady, potential transonic cascade flows
[NASA-TP-1705] p0003 N80-27284

Instructions for the use of the CIVM-Jet 4C finite-strain computer code to calculate the transient structural responses of partial and/or complete arbitrarily-curved rings subjected to fragment impact
[NASA-CR-159873] p0134 N80-27720

Calculation of water drop trajectories to and about arbitrary three-dimensional bodies in potential airflow
[NASA-CR-3291] p0005 N80-28302

High-freezing-point fuel studies
p0043 N80-29329

Development of flexible rotor balancing criteria
[NASA-CR-159506] p0129 N80-3277

Nonanalytic function generation routines for 16-bit microprocessors
[NASA-TM-81586] p0163 N80-33104

WIND: Computer program for calculation of three dimensional potential compressible flow about wind turbine rotor blades
[NASA-TP-1729] p0003 N80-33357

COMPUTER SIMULATION

U COMPUTERIZED SIMULATION

COMPUTER STORAGE DEVICES

NT MAGNETIC CORES

COMPUTER SYSTEMS DESIGN

An interactive modular design for computerized photometry in spectrochemical analysis
p0074 A80-39640

COMPUTER SYSTEMS PROGRAMS

INFORM: An interactive data collection and display program with debugging capability
[NASA-TP-1424] p0162 N80-16742

COMPUTER TECHNIQUES

Modeling and analysis of Power Processing Systems
p0066 A80-28894

Computer code for estimating installed performance of aircraft gas turbine engines. Volume 1: Final report
[NASA-CR-159691] p0028 N80-13043

Computer code for estimating installed performance of aircraft gas turbine engines. Volume 2: Users manual
[NASA-CR-159692] p0028 N80-13044

Computerized systems analysis and optimization of aircraft engine performance, weight, and life cycle costs
p0001 N80-21271

COMPUTERIZED CONTROL

U NUMERICAL CONTROL

COMPUTERIZED DESIGN

Computerized systems analysis and optimization of aircraft engine performance, weight, and life cycle costs
p0165 A80-10035

Design of elastomer dampers for a high-speed flexible rotor
[ASME PAPER 79-DET-88] p0121 A80-15736

How to quickly predict the overall TWT and the multistage depressed collector efficiency

SUBJECT INDEX

CONTROLLERS

Lubrication of optimized-design tapered-roller bearings to 2.4 million DN [NASA-TP-1714] p0102 A80-31759

Simulation and visualization of face seal motion stability by means of computer generated movies [NASA-TM-81581] p0119 N80-29734

COMPUTERIZED SIMULATION p0120 N80-31797

NT ANALOG SIMULATION

NT DIGITAL SIMULATION

A matrix solution for the simulation of magnetic fields with ideal current loops p0102 A80-13903

High speed cylindrical rolling element bearing analysis 'CYBEAN' - Analytic formulation [ASME PAPER 79-LUB-35] p0129 A80-14761

Two-dimensional representations of axisymmetric fields for computer calculations --- in modeling microwave tubes p0102 A80-18232

Computer simulation of engine systems --- for aircraft design [AIAA PAPER 80-0051] p0024 A80-18253

Numerical simulation of supersonic inlets using a three-dimensional viscous flow analysis [AIAA PAPER 80-0384] p0003 A80-20969

Capillary device refilling --- liquid rocket propellant tank tests [AIAA PAPER 80-1095] p0060 A80-38908

Simulation of transducer-couplant effects on broadband ultrasonic signals --- in nondestructive flaw evaluation and materials tests p0112 A80-44233

A three-dimensional spacecraft-charging computer code p0055 A80-46891

Quiet Clean Short-haul Experimental Engine (QCSEE) under-the-wing engine simulation report [NASA-CR-134914] p0034 N80-15091

Computer simulation of engine systems [NASA-TM-79290] p0015 N80-15132

Numerical simulation of supersonic inlets using a three-dimensional viscous flow analysis [NASA-TM-81411] p0104 N80-15365

Effects of secondary yield parameter variation on predicted equilibrium potential of an object in a charging environment --- using computerized simulation [NASA-TM-79299] p0053 N80-16093

Advanced electric propulsion system concept for electric vehicles [NASA-CR-159651] p0183 N80-17916

NASCAP modelling computations on large optics spacecraft in geosynchronous substorm environments [NASA-TM-81395] p0053 N80-18095

Simulation of transducer-couplant effects on broadband ultrasonic signals [NASA-TM-81489] p0130 N80-22714

An alternative approach to the numerical simulation of steady inviscid flow [NASA-TM-81542] p0003 N80-27286

Thermal energy storage system using fluidized bed heat exchangers [NASA-CR-159868] p0153 N80-28866

Simulation and visualization of face seal motion stability by means of computer generated movies [NASA-TM-81581] p0120 N80-31797

Modelling of environmentally induced discharges in geosynchronous satellites [NASA-TM-81598] p0053 N80-32428

COMPUTERS

NT MICROCOMPUTERS

NT SITE DATA PROCESSORS

CONCENTRATION (COMPOSITION)

NT ATMOSPHERIC MOISTURE

NT MOISTURE CONTENT

CONCRETES

Evaluation of feasibility of prestressed concrete for use in wind turbine blades [NASA-CR-159725] p0147 N80-15553

CONDENSING

Synthesis of improved polyester resins [NASA-CR-159665] p0090 N80-13257

CONDITIONS

NT ADIABATIC CONDITIONS

NT NONADIABATIC CONDITIONS

CONDUCTORS

NT SUPERCONDUCTORS

CONFERENCES

Symposium /International/ on Combustion, 17th, Leeds University, Leeds, England, August 20-25, 1978, Proceedings p0075 A80-11754

Aeropropulsion 1979 --- conferences [NASA-CR-2092] p0012 N80-10205

Quiet powered-lift propulsion [NASA-CR-2077] p0015 N80-15127

General Aviation Propulsion [NASA-CR-2126] p0017 N80-22327

Thermal Energy Storage: Fourth Annual Review Meeting [NASA-CR-2125] p0141 N80-22788

Aircraft Research and Technology for Future Fuels [NASA-CR-2146] p0022 N80-29300

Rotorodynamic Instability Problems in high-performance turbomachinery [NASA-CR-2133] p0119 N80-29706

Large Space Systems/Low-Thrust Propulsion Technology [NASA-CR-2144] p0057 N80-31449

Synchronous Energy Technology [NASA-CR-2154] p0058 N80-33465

CONICAL NOZZLES

Acoustic considerations of flight effects on jet noise suppressor nozzles [NASA-TM-81377] p0167 N80-14843

CONSERVATION

NT ENERGY CONSERVATION

CONSTRAINTS

NT METEOROLOGICAL PARAMETERS

CONSUMABLES (SPACECRAFT)

NT PROPELLANT STORAGE

NT WORKING FLUIDS

CONSUMPTION

NT FUEL CONSUMPTION

CONTACT RESISTANCE

Significance of thermal contact resistance in two-layer thermal-barrier-coated turbine vanes [NASA-TM-81483] p0018 N80-23310

CONTACTS (ELECTRIC)

U ELECTRIC CONTACTS

CONTAMINATION

NT FUEL CONTAMINATION

NT SPACECRAFT CONTAMINATION

Mechanical impact tests of materials in oxygen effects of contamination --- Teflon, stainless steel, and aluminum [NASA-TP-1571] p0093 N80-21551

CONTINENTS

NT NORTH AMERICA

CONTROL DEVICES

U CONTROL EQUIPMENT

CONTROL EQUIPMENT

NT PRESSURE REGULATORS

Comparison of several inflow control devices for flight simulation of fan tone noise using a JT15D-1 engine [AIAA PAPER 80-1025] p0025 A80-38640

Aerial applications dispersal systems control requirements study --- agriculture [NASA-CR-159781] p0158 N80-18586

CONTROL SIMULATION

Quiet Clean Short-haul Experimental Engine (QCSEE) over-the-wing engine and control simulation results [NASA-CR-135049] p0031 N80-15114

CONTROL SURFACES

NT AILERONS

NT EXTERNALLY BLOWN FLAPS

NT GUIDE VANES

NT JET VANES

NT SPOILERS

Effect of temperature on surface noise p0107 A80-28419

Teetered, tip-controlled rotor - Preliminary test results from Mod-C 100-kW experimental wind turbine [AIAA 80-0642] p0145 A80-28836

CONTROL THEORY

A new traffic control design method for large networks with signalized intersections p0183 A80-14841

CONTROLLED ATMOSPHERES

NT CABIN ATMOSPHERES

CONTROLLERS

NT SERVOMECHANISMS

Performance of 22.4-kW nonlaminated-frame dc series motor with chopper controller --- a dc to

CONVAIR MILITARY AIRCRAFT

SUBJECT INDEX

dc voltage converter
[NASA-TM-79252] p0101 N80-13361

CONVAIR MILITARY AIRCRAFT
U MILITARY AIRCRAFT
CONVERTIBLES
U V/STOL AIRCRAFT
COOLANTS
Coolant tube curvature effects on film cooling as detected by infrared imagery
[ASME PAPER 79-WA/GT-7] p0107 A80-18638
Influence of coolant tube curvature on film cooling effectiveness as detected by infrared imagery
[NASA-TP-1546] p0013 N80-11087

COOLING
NT AIR COOLING
NT FILM COOLING
NT LIQUID COOLING
NT REGENERATIVE COOLING
NT SURFACE COOLING
NT SWEAT COOLING
Influence of coolant tube curvature on film cooling effectiveness as detected by infrared imagery
[NASA-TP-1546] p0013 N80-11087
Heat pipe cooled power magnetics
[NASA-CR-159659] p0103 N80-13362
Depripping of arterial heat pipes: An investigation of CTS thermal excursions
[NASA-CR-165153] p0108 N80-32688

COOLING SYSTEMS
Heat pipe cooling of power processing magnetics
[AIAA PAPER 79-2082] p0107 A80-20960
Advanced cooling techniques for high-pressure, hydrocarbon-fueled rocket engines
[AIAA PAPER 80-1266] p0060 A80-38994
Advanced cooling techniques for high-pressure hydrocarbon-fueled engines
[NASA-CR-159790] p0061 N80-17141
Some advantages of methane in an aircraft gas turbine
[NASA-TM-81559] p0094 N80-29502

COPPER
Strengthening of tough iron-12% nickel-reactive metal alloys at 77 K by copper additions
p0174 A80-34049
Scanning-electron-microscope study of normal-impingement erosion of ductile metals
[NASA-TP-1609] p0077 N80-16141

CORE FLOW
Experimental study of low aspect ratio compressor blading
[ASME PAPER 80-GT-6] p0025 A80-42147

CORES
NT MAGNETIC CORES

CORPUSCULAR RADIATION
NT ELECTRON BEAMS

CORRECTION
Wind-tunnel investigation of the flow correction for a model-mounted angle of attack sensor at angles of attack from -10 deg to 110 deg --- Langley 12-foot low speed wind tunnel test
[NASA-TM-80189] p0011 N80-14110

CORRELATION
NT SIGNAL ANALYSIS
A quarter-century of progress in the development of correlation and extrapolation methods for creep rupture data
p0133 A80-38142
Use of petroleum-based correlations and estimation methods for synthetic fuels
[NASA-TM-81533] p0093 N80-27509

CORRELATION FUNCTIONS
U CORRELATION

CORROSION
NT ELECTROCHEMICAL CORROSION
NT FUEL CORROSION
NT HOT CORROSION
NT SCALE (CORROSION)
Chemical processes involved in the initiation of hot corrosion of B-1900 and NASA-TBW VIA
[NASA-TM-81399] p0077 N80-17199

CORROSION PREVENTION
Fouling and the inhibition of salt corrosion --- hot corrosion of superalloys
[NASA-TM-81469] p0078 N80-21492

CORROSION RESISTANCE
NT OXIDATION RESISTANCE

Anodic polarization behavior of austenitic stainless steel alloys with lower chromium content
p0178 A80-22250

Evaluation of present-day thermal barrier coatings for industrial/utility applications
p0092 A80-39637

Corrosion resistant thermal barrier coating --- protecting gas turbines and other heat engine parts
[NASA-CASE-LEW-13088-1] p0067 N80-11142

Mechanical properties and oxidation and corrosion resistance of reduced-chromium 304 stainless steel alloys
[NASA-TP-1557] p0076 N80-11188

Corrosion resistance of sodium sulfate coated cobalt-chromium-aluminum alloys at 900 C, 1000 C, and 1100 C
[NASA-TM-79311] p0076 N80-14234

Effect of sodium, potassium, magnesium, calcium, and chlorine on the high temperature corrosion of IN-100, U-700, IN-792, and Mar M-509 --- coal-derived liquid fuel combustion in turbines
[NASA-TM-79309] p0076 N80-15235

Stress corrosion cracking evaluation of martensitic precipitation hardening stainless steels
[NASA-TM-78257] p0083 N80-16142

Method of making bearing material
[NASA-CASE-LEW-11930-3] p0070 N80-33482

CORROSION TESTS
An experimental, low-cost, silicon-aluminide high-temperature coating for superalloys
p0082 A80-35501
Improved PFB operations - 400-hour turbine test results --- Pressurized Fluidized Bed
p0145 A80-39639
Effect of sodium, potassium, magnesium, calcium, and chlorine on the high temperature corrosion of IN-100, U-700, IN-792, and MAR M-509
[ASME PAPER 80-GT-150] p0083 A80-42262

CORUNDUM
U ALUMINUM OXIDES

COST ANALYSIS
Economic analysis of the design and fabrication of a space qualified power system
[NASA-TM-81418] p0056 N80-18098
CF6-6D engine performance deterioration
[NASA-CR-159786] p0041 N80-27364
Impact of propulsion system R and D on electric vehicle performance and cost
[NASA-TM-81548] p0143 N80-27805
Cost analysis of composite fan blade manufacturing processes
[NASA-CR-159876] p0044 N80-31398

COST EFFECTIVENESS
Cost-effective technology advancement directions for electric propulsion transportation systems in earth-orbital missions
[AIAA PAPER 79-2043] p0048 A80-20961
Cost-effective technology advancement directions for electric propulsion transportation systems in earth-orbital missions
[NASA-TM-79289] p0182 N80-11950
Preliminary study of advanced turboprop and turboshaft engines for light aircraft --- cost effectiveness
[NASA-TM-81467] p0018 N80-22350

COST ESTIMATES
Design, performance and life cycle cost relationships for a 500kW space solar array
p0065 A80-48356
Study of turboprop systems reliability and maintenance costs
[NASA-CR-135192] p0029 N80-14129
Cogeneration Technology Alternatives Study (CTAS). Volume 3: Energy conversion system characteristics
[NASA-CR-159761] p0155 N80-31869

COUNTERMEASURES
NT ELECTRONIC COUNTERMEASURES

CONELL METHOD
U NUMERICAL INTEGRATION

COYLINGS
Quiet Clean Short-Haul Experimental Engine (QCSEE)
Under-The-Wing (UTW) graphite/PMR cowl development
[NASA-CR-135279] p0029 N80-14119

CRACK FORMATION
U CRACK INITIATION

SUBJECT INDEX

CURRENT DENSITY

CRACK INITIATION

Practical implementation of the double linear damage rule and damage curve approach for treating cumulative fatigue damage
[NASA-TM-81517] p0132 N80-23684

CRACK PROPAGATION

Simple spline-function equations for fracture mechanics calculations p0133 A80-10832
Characterization and properties of controlled nucleation thermochemical deposited /CMTD/ silicon carbide p0089 A80-13063

Fracture toughness determination of Al203 using four-point-bend specimens with straight-through and chevron notches p0090 A80-42085

Performance of Chevron-notch short bar specimen in determining the fracture toughness of silicon nitride and aluminum oxide p0090 A80-50696

Comparison tests and experimental compliance calibration of the proposed standard round compact plane strain fracture toughness specimen [NASA-TM-81379] p0132 N80-13513

Sudden bending of cracked laminates [NASA-CR-159860] p0073 N80-25384

Evaluation of the cyclic behavior of aircraft turbine disk alloys, part 2 [NASA-CR-165123] p0084 N80-30482

CRACKING (FRACTURING)

NT STRESS CORROSION CRACKING

CRACKS

Modelling of crack tip deformation with finite element method and its applications p0130 N80-13503

CREEP ANALYSIS

Long-time creep behavior of the tantalum alloy Astar 811C --- as a function of stress, temperature, and grain size [NASA-TP-1691] p0080 N80-32489

CREEP PROPERTIES

Long-time creep behavior of the niobium alloy C-103 [NASA-TP-1727] p0080 N80-33555

CREEP RESISTANCE

U CREEP STRENGTH

CREEP RUPTURE STRENGTH

A quarter-century of progress in the development of correlation and extrapolation methods for creep rupture data p0133 A80-38142

Anisotropy of nickel-base superalloy single crystals p0083 A80-51573

Improving the stress rupture and creep of silicon nitride --- turbine materials [NASA-CR-159585] p0072 N80-10318

Creep-rupture behavior of seven iron-base alloys after long term aging at 760 deg in low pressure hydrogen [NASA-TM-81534] p0080 N80-32488

CREEP STRENGTH

Elevated temperature flow strength, creep resistance and diffusion welding characteristics of Ti-6Al-2Nb-1Ta-0.8Mo p0081 A80-13277

CREEP TESTS

Strainrange partitioning life predictions of the long time Metal Properties Council creep-fatigue tests p0133 A80-27958

CRESTATIONS

U TRAVELING WAVE TUBES

CREVICES

U CRACKS

CRITERIA

NT STRUCTURAL DESIGN CRITERIA

Development of flexible rotor balancing criteria [NASA-CR-159506] p0129 N80-32720

CRITICAL REYNOLDS NUMBER

U REYNOLDS NUMBER

CROP DUSTING

Aerial applications dispersal systems control requirements study --- agriculture [NASA-CR-159781] p0158 N80-18586

CROSSLINKING

Method of cross-linking polyvinyl alcohol and other water soluble resins [NASA-CASE-LEW-13103-1] p0088 N80-32516

CRUDE OIL

Low NO/x/ heavy fuel combustor program [ASME PAPER 80-GT-69] p0026 A80-42199
Alternative jet aircraft fuels p0012 N80-10209

CRYOGENIC EQUIPMENT

Capillary acquisition devices for high-performance vehicles: Executive summary --- evaluation of cryogenic propellant management techniques using the centaur launch vehicle [NASA-CR-159658] p0062 N80-19185

CRYOGENIC FLUID STORAGE

A liquid hydrogen experiment as a Shuttle payload [AIAA PAPER 80-1096] p0054 A80-38909
LeRC reduced gravity fluid management technology program [NASA-TM-81450] p0051 N80-20304

CRYOGENIC FLUIDS

NT LIQUID HYDROGEN

NT LIQUID OXYGEN

Comparative thermal analysis of alternate Cryogenic Fluid Management Experiment (CFME) configurations [NASA-CR-165151] p0048 N80-32412

CRYOGENIC MAGNETS

Experiments on H2-O2 MHD power generation p0176 A80-44239
Experiments on H2-O2MHD power generation [NASA-TM-81424] p0175 N80-16886

CRYOGENIC ROCKET PROPELLANTS

LeRC reduced gravity fluid management technology program p0048 A80-35504

Capillary acquisition devices for high-performance vehicles: Executive summary --- evaluation of cryogenic propellant management techniques using the centaur launch vehicle [NASA-CR-159658] p0062 N80-19185

LeRC reduced gravity fluid management technology program [NASA-TM-81450] p0051 N80-20304

Conceptual design of an orbital propellant transfer experiment. Volume 2: Study results [NASA-CR-165150] p0048 N80-31423

CRYOGENICS

Oxygen-enriched air for MHD power plants p0096 A80-25096
High toughness-high strength iron alloy [NASA-CASE-LEW-12542-3] p0079 N80-32484

CRYOTRAPPING

Atomic hydrogen storage --- cryotrapping and magnetic field strength [NASA-CASE-LEW-12081-2] p0093 N80-20402

CRYSTAL GROWTH

NT DIRECTIONAL SOLIDIFICATION (CRYSTALS)
Some TEM observations of Al203 scales formed on NiCrAl alloys p0081 A80-13071

CRYSTAL STRUCTURE

State-of-the-art SiAlON materials p0022 N80-29358

CRYSTALLIZATION

NT DIRECTIONAL SOLIDIFICATION (CRYSTALS)

NT RECRYSTALLIZATION

CRYSTALS

NT LIQUID CRYSTALS

NT METAL CRYSTALS

NT SINGLE CRYSTALS

CUMULATIVE DAMAGE

Practical implementation of the double linear damage rule and damage curve approach for treating cumulative fatigue damage [NASA-TM-81517] p0132 N80-23684

CURING

Low temperature cross linking polyimides [NASA-CASE-LEW-12876-1] p0087 N80-26447

CURRENT CONVERTERS (AC TO DC)

Bi-directional four quadrant (BDQ4) power converter development [NASA-CR-159660] p0147 N80-14480

CURRENT DENSITY

Photoelectron charge density and transport near differentially charged spacecraft p0053 A80-19773

Open-circuit voltage improvements in low resistivity solar cells [NASA-TM-81388] p0138 N80-15555

Thin n-i-p radiation-resistant solar cell feasibility study

[NASA-CR-159871] p0154 N80-29852
CURTISS-WRIGHT MILITARY AIRCRAFT
 U MILITARY AIRCRAFT
CYCLES
 NT BRAYTON CYCLE
 NT RANKINE CYCLE
 NT STIRLING CYCLE
CYCLIC LOADS
 Strainrange partitioning life predictions of the
 long time Metal Properties Council creep-fatigue
 tests p0133 A80-27958
CYLINDRICAL BODIES
 NT ROTATING CYLINDERS
CYTOLOGY
 Tissue response to peritoneal implants
 [NASA-CR-159817] p0066 N80-33478

D

DAEMO (DATA ANALYSIS)
 U DATA REDUCTION
 U DATA TRANSMISSION
DAMAGE
 NT CUMULATIVE DAMAGE
 NT FIRE DAMAGE
 NT IMPACT DAMAGE
 NT RADIATION DAMAGE
 Dynamic response of damaged angleplied fiber
 composites
 [NASA-TM-79281] p0067 N80-11145
DAMPERS (VALVES)
 Off-design correlation for losses due to part-span
 dampers on transonic rotors
 [NASA-TF-1693] p0020 N80-28352
DAMPING
 NT ELASTIC DAMPING
 NT VIBRATION DAMPING
 Damping in tapered annular seals for an
 incompressible fluid
 [NASA-TF-1646] p0116 N80-19495
 Damping in ring seals for compressible fluids
 p0119 N80-29716
 Development of procedures for calculating
 stiffness and damping of elastomers in
 engineering applications, part 7
 [NASA-CR-165138] p0128 N80-32718
DAMPING FACTOR
 U DAMPING
DAMPING IN PITCH
 U DAMPING
 U PITCH (INCLINATION)
DAMPING IN ROLL
 U DAMPING
DAMPING IN YAW
 U DAMPING
DAMPNESS
 U MOISTURE CONTENT
DANGER
 U HAZARDS
DART TURBOPROP ENGINES
 U TURBOPROP ENGINES
DATA ACQUISITION
 Efficient laser anemometer for intra-rotor flow
 mapping in turbomachinery p0111 A80-36140
DATA ADAPTIVE EVALUATOR/MONITOR
 U DATA REDUCTION
 U DATA TRANSMISSION
DATA ANALYSIS
 U DATA REDUCTION
DATA CORRELATION
 NT SIGNAL ANALYSIS
DATA LINKS
 A digitally implemented communications experiment
 utilizing the communications technology
 satellite, Hermes
 [NASA-TM-81452] p0052 N80-21412
DATA PROCESSING
 NT DATA REDUCTION
 NT SIGNAL ANALYSIS
 NT SIGNAL PROCESSING
DATA PROCESSING EQUIPMENT
 NT MICROCOMPUTERS
 NT MICROPROCESSORS
 NT SITE DATA PROCESSORS
DATA REDUCTION
 Cycles till failure of silver-zinc cells with
 completing failures modes: Preliminary data

analysis
 [NASA-TM-81556] p0164 N80-29088
DATA TRANSMISSION
 NT FREQUENCY DIVISION MULTIPLE ACCESS
 UHF coplanar-slot antenna for
 aircraft-to-satellite data communications
 p0099 A80-13064
 Concepts for 18/30 GHz satellite communication
 system, volume 1
 [NASA-CR-159625-VOL-1] p0098 N80-11277
 Concepts for 18/30 GHz satellite communication
 system, volume 1A: Appendix
 [NASA-CR-159625-VOL-1A] p0098 N80-11278
 Concepts for 18/30 GHz satellite communication
 system study. Executive summary
 [NASA-CR-159680] p0098 N80-11279
 Phase-locked telemetry system for rotary
 instrumentation of turbomachinery, phase 1
 [NASA-CR-159453] p0029 N80-14182
DC (CURRENT)
 U DIRECT CURRENT
DC 9 AIRCRAFT
 Development of a Kevlar/PMR-15 reduced drag DC-9
 nacelle fairing
 [AIAA PAPER 80-1194] p0010 A80-41193
DC 10 AIRCRAFT
 Reduced bleed air extraction for DC-10 cabin air
 conditioning
 [AIAA PAPER 80-1197] p0010 A80-41194
 Engine bleed air reduction in DC-10
 [NASA-CR-159846] p0010 N80-32378
DEBUGGING
 U CHECKOUT
DECAY
 NT ACOUSTIC EMISSION
 NT ELECTRON EMISSION
 NT EXHAUST EMISSION
 NT SECONDARY EMISSION
 Decay of the zincate concentration gradient at an
 alkaline zinc cathode after charging
 p0074 A80-13070
DECISION MAKING
 Matrix management for aerospace 2000
 [NASA-TM-81509] p0181 N80-24200
DECISION THEORY
 NT STATISTICAL DECISION THEORY
DECOMPRESSION
 U PRESSURE REDUCTION
DEFENSE PROGRAM
 DOD low-thrust mission studies
 p0063 N80-31455
DEFLATING
 U PRESSURE REDUCTION
DEFLECTION
 Two-dimensional finite-element analyses of
 simulated rotor-fragment impacts against rings
 and beams compared with experiments
 [NASA-CR-159645] p0038 N80-22323
DEFORMATION
 NT AXIAL STRAIN
 NT ELASTIC DEFORMATION
 NT PLASTIC DEFORMATION
DEGRADATION
 NT THERMAL DEGRADATION
DELIVERY
 NT PAYLOAD DELIVERY (STS)
DELTA DAGGER AIRCRAFT
 U F-102 AIRCRAFT
DEMAND (ECONOMICS)
 The 30/20 GHz fixed communications systems service
 demand assessment. Volume 1: Executive summary
 [NASA-CR-159619] p0098 N80-18262
 The 30/20 GHz fixed communications systems service
 demand assessment. Volume 2: Main report
 [NASA-CR-159620] p0098 N80-18263
 The 30/20 GHz fixed communications systems service
 demand assessment. Volume 3: Annex
 [NASA-CR-159621] p0099 N80-18264
 The 18/30 GHz fixed communications system service
 demand assessment. Volume 1: Executive summary
 [NASA-CR-159546] p0099 N80-22547
 The 18/30 GHz fixed communications system service
 demand assessment. Volume 2: Main text
 [NASA-CR-159547] p0099 N80-22548
 The 30/20 GHz fixed communications systems service
 demand assessment. Volume 3: Appendices
 [NASA-CR-159548] p0099 N80-22549
DENSITOMETERS
 NT MICRODENSITOMETERS

SUBJECT INDEX

DIRECT POWER GENERATORS

DENSITY (NUMBER/VOLUME)
NT ELECTRON DENSITY (CONCENTRATION)
DENSITY DISTRIBUTION
 Volume-energy parameters and turbulent-flow density fluctuations
 [NASA-TP-1585] p0105 N80-17398
DENSITY MEASUREMENT
 Computerized video densitometry method for rapid analysis of infrared photographic images --- temperature distribution across a turbine blade
 [NASA-TP-1686] p0110 N80-25635
DEPENDENCE
NT TEMPERATURE DEPENDENCE
NT TIME DEPENDENCE
DEPOSITION
NT ELECTRODEPOSITION
NT VAPOR DEPOSITION
 Characterization and properties of controlled nucleation thermochemical deposited /CNTD/ silicon carbide
 p0089 A80-13063
 Experimental studies of the formation/deposition of sodium sulfate in/from combustion gases --- hot corrosion of gas turbine engine components
 [NASA-CR-159753] p0033 N80-15131
DEPRESSURIZATION
U PRESSURE REDUCTION
DESIGN ANALYSIS
 Advanced catalytic combustors for low pollutant emissions, phase 1
 [NASA-CR-159535] p0028 N80-13048
 Design evolution of large wind turbine generators
 p0139 N80-16455
 Parametric study of potential early commercial MHD power plants
 [NASA-CR-159633] p0149 N80-18559
 Lubrication of rolling-element bearings
 [NASA-TM-81449] p0117 N80-20591
 Development of procedures for calculating stiffness and damping of elastomers in engineering applications, part 6
 [NASA-CR-159838] p0134 N80-22733
 Assessment and preliminary design of an energy buffer for regenerative braking in electric vehicles
 [NASA-CR-159756] p0184 N80-23216
 Small, high pressure liquid hydrogen turbopump
 [NASA-CR-159821] p0125 N80-26662
 Composite wall concept for high temperature turbine shrouds: Heat transfer analysis
 [NASA-TM-81539] p0020 N80-27362
 General design method for three-dimensional potential flow fields. 1: Theory
 [NASA-CR-3288] p0005 N80-29251
 Experimental performance and analysis of 15.04-centimeter-tip-diameter, radial-inflow turbine with work factor of 1.126 and thick blading
 [NASA-TP-1730] p0023 N80-33410
DESIGN OF EXPERIMENTS
U EXPERIMENTAL DESIGN
DETECTION
NT TARGET RECOGNITION
NT ULTRASONIC FLAW DETECTION
DEVELOPING NATIONS
 A photovoltaic power system in the remote African village of Tangaye, Upper Volta
 [NASA-TM-79318] p0137 N80-12552
DEWAR SYSTEMS
U CRYOGENIC EQUIPMENT
DIAGRAMS
NT STRESS-STRAIN DIAGRAMS
DIAPHRAGMS
 Influence of excess diamine on properties of PMR polyimide resins and composites
 [NASA-TM-81580] p0069 N80-29433
DIELECTRIC MATERIALS
U DIELECTRICS
DIELECTRICS
 Metal-dielectric interactions
 p0081 A80-13067
 Initial comparison of SSPM ground test results and flight data to NASCAP simulations --- Satellite Surface Potential Monitor NASA Charging Analyzer Program
 [AIAA PAPER 80-0336] p0054 A80-29751
 Development of improved wraparound contacts for silicon
 [NASA-CR-159748] p0148 N80-18554

DIES
 Adherence of ion beam sputter deposited metal films on H-13 steel
 [NASA-TM-81585] p0079 N80-31527
DIESEL ENGINES
 A 150 and 300 kw lightweight diesel aircraft engine design study
 [NASA-CR-3260] p0037 N80-20271
 Design study: A 186 kw lightweight diesel aircraft engine
 [NASA-CR-3261] p0038 N80-22326
 Diesel engine catalytic combustor system --- turbocharging
 [NASA-CASE-LEN-12995-1] p0118 N80-26659
DIESEL FUELS
 Autoignition characteristics of aircraft-type fuels
 [NASA-CR-159886] p0095 N80-30535
 Cogeneration Technology Alternatives Study (CTAS). Volume 3: Energy conversion system characteristics
 [NASA-CR-159761] p0155 N80-31869
DIFFERENTIAL ALGEBRA
U MATRICES (MATHEMATICS)
DIFFERENTIAL EQUATIONS
NT HELMHOLTZ VORTICITY EQUATION
NT PARTIAL DIFFERENTIAL EQUATIONS
DIFFUSERS
 Griffith diffusers
 p0006 A80-20748
DIFFUSION
NT ELECTRON DIFFUSION
NT PARTICLE DIFFUSION
NT PLASMA DIFFUSION
DIFFUSION BONDING
U DIFFUSION WELDING
DIFFUSION WELDING
 Elevated temperature flow strength, creep resistance and diffusion welding characteristics of Ti-6Al-2Nb-1Ta-0.8Mo
 p0081 A80-13277
 Diffusion bonded boron/aluminum spar-shell fan blade
 [NASA-CR-159571] p0072 N80-25382
DIFLUORIDES
NT CALCIUM FLUORIDES
DIGESTIVE SYSTEM
NT PANCREAS
DIGITAL COMMUNICATION
U PULSE COMMUNICATION
DIGITAL COMPUTERS
NT MICROCOMPUTERS
DIGITAL SIMULATION
 Full-coverage film cooling. II - Heat transfer data and numerical simulation
 [ASME PAPER 80-GT-44] p0109 A80-42177
 MOD-2 wind turbine farm stability study
 [NASA-CR-165156] p0156 N80-33862
DIGITAL SYSTEMS
 Digital system for dynamic turbine engine blade displacement measurements
 p0111 A80-36151
 Quiet Clean Short-haul Experimental Engine (QCSE) under-the-wing engine digital control system design report
 [NASA-CR-134920] p0034 N80-15090
 Quiet Clean Short-haul Experimental Engine (QCSE) over-the-wing control system design report
 [NASA-CR-135337] p0035 N80-15092
DIGITAL TECHNIQUES
 A digitally implemented communications experiment utilizing the communications technology satellite, Hermes
 [NASA-TM-81452] p0052 N80-21412
DIMENSIONLESS NUMBERS
NT REYNOLDS NUMBER
 Film thickness for different regimes of fluid-film lubrication
 [NASA-TM-81550] p0119 N80-29735
DIMENSIONS
NT FILM THICKNESS
DIRECT CURRENT
 Performance of 22.4-kw nonlaminated-frame dc series motor with chopper controller --- a dc to dc voltage converter
 [NASA-TM-79252] p0101 N80-13361
DIRECT POWER GENERATORS
NT ALKALINE BATTERIES
NT FUEL CELLS
NT HYDROGEN OXYGEN FUEL CELLS
NT MAGNETOHYDRODYNAMIC GENERATORS

DIRECTIONAL ANTENNAS

SUBJECT INDEX

NT NICKEL ZINC BATTERIES
 NT SOLAR CELLS
 NT THERMIONIC CONVERTERS
 NT THERMOELECTRIC GENERATORS
 DIRECTIONAL ANTENNAS
 NT PARABOLIC ANTENNAS
 NT SLOT ANTENNAS
 DIRECTIONAL SOLIDIFICATION (CRYSTALS)
 Stability of several oxide dispersion strengthened alloys and a directionally solidified gamma/gamma prime-alpha eutectic alloy in a thermal gradient p0082 A80-40962
 Development of exothermically cast single-crystal Mar-M 247 and derivative alloys [AIRESEARCH-21-3469] p0084 A80-45825
 Directional solidification at ultra-high thermal gradient [NASA-CR-159797] p0096 N80-15300
 Thermal fatigue and oxidation data for directionally solidified MAR-M 246 turbine blades [NASA-CR-159798] p0037 N80-21330
 Performance of two-layer thermal barrier systems on directionally solidified Ni-Al-Mo and comparative effects of alloy thermal expansion on system life [NASA-TN-81604] p0080 N80-32487
 DISASTERS
 Communications technology satellite - United States experiments and disaster communications applications p0051 A80-10032
 DISEASES
 NT CANCER
 NT GLAUCOMA
 DISPERSING
 Aerial applications dispersal systems control requirements study --- agriculture [NASA-CR-159781] p0158 N80-18586
 DISPERSION PRECIPITATION HARDENING
 U PRECIPITATION HARDENING
 DISPLACEMENT MEASUREMENT
 Digital system for dynamic turbine engine blade displacement measurements p0111 A80-36151
 DISPLAY DEVICES
 NT ANEMOMETERS
 DISSIPATION
 NT ENERGY DISSIPATION
 DISSOCIATION
 NT GAS DISSOCIATION
 DISTANCE MEASURING EQUIPMENT
 NT RADIO ALTIMETERS
 DISTORTION
 NT FLOW DISTORTION
 DISTRIBUTION (PROPERTY)
 NT FLOW DISTRIBUTION
 NT ION DISTRIBUTION
 NT PRESSURE DISTRIBUTION
 NT STRESS CONCENTRATION
 NT TEMPERATURE DISTRIBUTION
 NT VELOCITY DISTRIBUTION
 DISTURBANCE THEORY
 U PERTURBATION THEORY
 DOCUMENTS
 NT BIBLIOGRAPHIES
 NT USER MANUALS (COMPUTER PROGRAMS)
 DOMESTIC SATELLITE COMMUNICATIONS SYSTEMS
 An advanced mixed user domestic satellite system architecture [AIAA 80-0494] p0099 A80-29544
 On-board processing concepts for future satellite communications systems [NASA-CR-159683] p0099 N80-24514
 DOPING (ADDITIVES)
 U ADDITIVES
 DOUGLAS AIRCRAFT
 NT DC 9 AIRCRAFT
 NT DC 10 AIRCRAFT
 DOUGLAS DC-9 AIRCRAFT
 U DC 9 AIRCRAFT
 DOUGLAS MILITARY AIRCRAFT
 U MILITARY AIRCRAFT
 DRAG
 NT AERODYNAMIC DRAG
 DRAG COEFFICIENT
 U AERODYNAMIC DRAG
 DRAG DEVICES
 NT SPOILERS

DRAG REDUCTION
 Development of a Kevlar/FHR-15 reduced drag DC-9 nacelle fairing [AIAA PAPER 80-1194] p0010 A80-41193
 DRONE HELICOPTERS
 U HELICOPTERS
 DROP SIZE
 Spray nozzle designs for agricultural aviation applications --- relation of drop size to spray characteristics and nozzle efficiency [NASA-CR-159702] p0108 N80-10460
 DROPS (LIQUIDS)
 NT RAINDROPS
 Dispersion of sound in a combustion duct by fuel droplets and soot particles p0170 A80-20953
 Investigation of critical burning of fuel droplets [NASA-CR-159697] p0075 N80-12142
 DRY CELLS
 NT NICKEL ZINC BATTERIES
 DUAL MODE PROPULSION
 U HYBRID PROPULSION
 DUCT GEOMETRY
 Higher order mode propagation in nonuniform circular ducts [AIAA PAPER 80-1018] p0171 A80-35974
 A comparison of experiment and theory for sound propagation in variable area ducts p0173 A80-45844
 Reciprocity principle in duct acoustics [NASA-TN-79300] p0167 N80-12824
 Numerical techniques in linear duct acoustics --- finite difference and finite element analyses [NASA-TN-81553] p0170 N80-30154
 DUCTED FAN ENGINES
 Experimental evaluation of a low emissions high performance duct burner for Variable Cycle Engines (VCE) [NASA-CR-159694] p0036 N80-17074
 DUCTED FANS
 Acoustic analysis of aft noise reduction techniques measured on a subsonic tip speed 50.8 cm (twenty inch) diameter fan --- quiet engine program [NASA-CR-134891] p0030 N80-15102
 DUCTED FLOW
 Some aspects of a free jet phenomena to 105 L/D in a constant area duct p0106 A80-10030
 Results of duct area ratio changes in the NASA Lewis H2-O2 combustion MHD experiment [AIAA PAPER 80-0023] p0176 A80-18243
 Time-dependent difference theory for noise propagation in a two-dimensional duct [AIAA PAPER 80-0098] p0170 A80-18269
 A time dependent difference theory for sound propagation in ducts with flow p0170 A80-20951
 Dispersion of sound in a combustion duct by fuel droplets and soot particles p0170 A80-20953
 A three-dimensional turbulent compressible subsonic duct flow analysis for use with constructed coordinate systems [AIAA PAPER 80-1398] p0006 A80-41601
 DUCTILITY
 An investigation into the role of adhesion in the erosion of ductile metals [ASLE PREPRINT 80-AM-3E-3] p0122 A80-43159
 An investigation into the role of adhesion in the erosion of ductile metals [NASA-TN-81458] p0078 N80-21489
 DUCTS
 NT ACOUSTIC DUCTS
 NT ANNULAR DUCTS
 Time dependent difference theory for sound propagation in axisymmetric ducts with plug flow [NASA-TN-81501] p0168 N80-23096
 Higher order mode propagation in nonuniform circular ducts [NASA-TN-81481] p0169 N80-23101
 DURABILITY
 Development of improved-durability plasma sprayed ceramic coatings for gas turbine engines [NASA-TN-81512] p0018 N80-23313
 Durability tests of solenoid valves for digital actuators [NASA-TN-81522] p0020 N80-26299

SUBJECT INDEX

ELASTIC PROPERTIES

Improved bond coatings for use with thermal
barrier coatings
[NASA-TM-81567] p0080 N80-33556

DYNAMIC CHARACTERISTICS
 NT AERODYNAMIC DRAG
 NT AERODYNAMIC STABILITY
 NT COMBUSTION STABILITY
 NT DYNAMIC STABILITY
 NT FLOW CHARACTERISTICS
 NT FLOW DISTRIBUTION
 NT FLOW STABILITY
 NT FLOW VELOCITY
 NT HOVERING STABILITY
 NT MAGNETOHYDRODYNAMIC STABILITY
 NT ROTARY STABILITY
 NT TRANSIENT RESPONSE
 The effects of strain and temperature on the
dynamic properties of elastomers
[ASME PAPER 79-DET-57] p0092 A80-15720
 Dynamic properties of elastomer cartridge
specimens under a rotating load
p0121 A80-24002

Micromechanics of intraply hybrid composites:
Elastic and thermal properties
[NASA-TM-79253] p0067 N80-11143

DYNAMIC LOADS
 NT AERODYNAMIC LOADS
 NT CYCLIC LOADS
 NT IMPACT LOADS
 NT ROLLING CONTACT LOADS
 Dynamic properties of elastomer cartridge
specimens under a rotating load
p0121 A80-24002

A laboratory facility for electric vehicle
propulsion system testing
[NASA-TM-81574] p0183 N80-30229

DYNAMIC MODELS
 Preliminary results from a four-working space,
double-acting piston, Stirling engine controls
model
[NASA-TM-81569] p0106 N80-29624

DYNAMIC MODULUS OF ELASTICITY
 Dynamic modulus and damping of boron, silicon
carbide, and alumina fibers
p0071 A80-44236
 Dynamic modulus and damping of boron, silicon
carbide, and alumina fibers
[NASA-TM-81422] p0068 N80-20313

DYNAMIC PROPERTIES
 U DYNAMIC CHARACTERISTICS
DYNAMIC RESPONSE
 NT TRANSIENT RESPONSE
 Dynamic response of damaged angleplied fiber
composites
p0070 A80-27982
 Dynamic response of damaged angleplied fiber
composites
[NASA-TM-79281] p0067 N80-11145
 Damping in tapered annular seals for an
incompressible fluid
[NASA-TP-1646] p0116 N80-19495
 Dynamic response to rotating-seat runout in
non-contacting face seals
[NASA-TM-81490] p0117 N80-22701
 Dynamic behavior of a beam drag-force anemometer
[NASA-TP-1687] p0110 N80-24595
 Flow induced spring coefficients of labyrinth
seals for application in rotor dynamics
p0126 N80-29717

DYNAMIC STABILITY
 NT AERODYNAMIC STABILITY
 NT COMBUSTION STABILITY
 NT FLOW STABILITY
 NT HOVERING STABILITY
 NT MAGNETOHYDRODYNAMIC STABILITY
 NT ROTARY STABILITY
 On the role of oil-film bearings in promoting
shaft instability: Some experimental observations
p0127 N80-29726
 MOD-2 wind turbine farm stability study
[NASA-CR-165156] p0156 N80-33862

DYNAMIC STRUCTURAL ANALYSIS
 Vibration and buckling of rectangular plates under
in-plane hydrostatic loading
p0133 A80-45364
 Executive summary, Mod-1 wind turbine generator
analysis and design report
[NASA-CR-159497] p0147 N80-11558

Primary propulsion/large space system interactions
p0063 N80-31456

E

EARTH ATMOSPHERE
 NT TROPOPAUSE
EARTH ORBITS
 Plasma collection by high voltage spacecraft at
low earth orbit
[AIAA PAPER 80-0042] p0055 A80-18249
 Cost-effective technology advancement directions
for electric propulsion transportation systems
in earth-orbital missions
[AIAA PAPER 79-2043] p0048 A80-20961
 Analysis of GaAs and Si solar cell arrays for
earth orbital and orbit transfer missions
[NASA-TM-81383] p0056 N80-15204
 Electric propulsion for near-Earth space missions
[NASA-CR-159735] p0062 N80-16096

EARTH RESOURCES
 NT COAL
 NT CRUDE OIL
 NT FOSSIL FUELS
 NT GEOTHERMAL RESOURCES
 NT ICEBERGS

EARTH SATELLITES
 NT ATS 5
 NT ATS 6
 NT COMMUNICATION SATELLITES
 NT COMMUNICATIONS TECHNOLOGY SATELLITE
 NT SCATHA SATELLITE
 NT SYNCHRONOUS SATELLITES

EBF
 U EXTERNALLY BLOWN FLAPS

ECONOMIC ANALYSIS
 Economical space power systems
[NASA-CR-159696] p0147 N80-15559

ECONOMICS
 NT DEMAND (ECONOMICS)

EDDIES
 U VORTICES

EDGES
 NT LEADING EDGES

EFFECTIVENESS
 NT COST EFFECTIVENESS

EFFECTORS
 U CONTROL EQUIPMENT

EFFICIENCY
 NT COMBUSTION EFFICIENCY
 NT COMPRESSOR EFFICIENCY
 NT ENERGY CONVERSION EFFICIENCY
 NT NOZZLE EFFICIENCY
 NT POWER EFFICIENCY
 NT PROPELLER EFFICIENCY
 NT PROPULSIVE EFFICIENCY
 NT THERMODYNAMIC EFFICIENCY
 NT TRANSMISSION EFFICIENCY

EFFLUENTS
 Coordinated aircraft and ship surveys for
determining impact of river inputs on great
lakes waters. Remote sensing results
[NASA-TP-1694] p0157 N80-27832

ELASTIC CONSTANTS
 U ELASTIC PROPERTIES

ELASTIC DAMPING
 Dynamic modulus and damping of boron, silicon
carbide, and alumina fibers
p0071 A80-44236
 Dynamic modulus and damping of boron, silicon
carbide, and alumina fibers
[NASA-TM-81422] p0068 N80-20313

ELASTIC DEFORMATION
 The effects of strain and temperature on the
dynamic properties of elastomers
[ASME PAPER 79-DET-57] p0092 A80-15720

ELASTIC MODULUS
 U MODULUS OF ELASTICITY

ELASTIC PROPERTIES
 NT AEROELASTICITY
 NT DYNAMIC MODULUS OF ELASTICITY
 NT ELASTOPLASTICITY
 NT MODULUS OF ELASTICITY
 NT THERMOELASTICITY
 Micromechanics of intraply hybrid composites:
Elastic and thermal properties
p0070 A80-27994
 Prediction of fiber composite mechanical behavior
made simple

ELASTIC STABILITY

SUBJECT INDEX

- Micromechanics of intraply hybrid composites: p0133 A80-32067
 Elastic and thermal properties
 [NASA-TM-79253] p0067 N80-11143
 Prediction of fiber composite mechanical behavior
 made simple --- using a rocket calculator
 [NASA-TM-81404] p0068 N80-16107
 Three dimensional finite-element elastic analysis
 of a thermally cycled double-edge wedge geometry
 specimen --- nickel alloy turbine parts
 [NASA-TM-80980] p0079 N80-26433
- ELASTIC STABILITY**
 U DAMPING
- ELASTIC WAVES**
 NT AERODYNAMIC NOISE
 NT AIRCRAFT NOISE
 NT ENGINE NOISE
 NT JET AIRCRAFT NOISE
 NT SOUND WAVES
- ELASTICITY**
 U ELASTIC PROPERTIES
- ELASTODYNAMICS**
 NT ELASTIC DAMPING
 NT ELASTOHYDRODYNAMICS
- Sudden stretching of a four layered composite plate
 [NASA-CR-159870] p0073 N80-25383
 Sudden bending of cracked laminates
 [NASA-CR-159860] p0073 N80-25384
 Film thickness for different regimes of fluid-film
 lubrication
 [NASA-TM-81550] p0119 N80-29735
- ELASTOHYDRODYNAMICS**
 Elastohydrodynamic film thickness measurements of
 artificially-produced nonsmooth surfaces
 [ASLE PREPRINT 79-LC-1A-3] p0103 A80-14720
 Some limitations in applying classical EHD
 film-thickness formulae to a high-speed bearing
 [NASA-TM-81431] p0116 N80-18409
 Fully flooded elastohydrodynamic lubricated
 elliptical contacts
 [NASA-TM-81543] p0118 N80-27698
 Starved elastohydrodynamic lubricated elliptical
 contacts
 [NASA-TM-81549] p0118 N80-27699
- ELASTOMERS**
 The effects of strain and temperature on the
 dynamic properties of elastomers
 [ASME PAPER 79-DET-57] p0092 A80-15720
 Design of elastomer dampers for a high-speed
 flexible rotor
 [ASME PAPER 79-DET-88] p0121 A80-15736
 Dynamic properties of elastomer cartridge
 specimens under a rotating load
 p0121 A80-24002
 Elastomer damper performance - A comparison with a
 squeeze film for a supercritical power
 transmission shaft
 [ASME PAPER 80-GT-162] p0121 A80-42272
 Development of procedures for calculating
 stiffness and damping of elastomers in
 engineering applications, part 6
 [NASA-CR-159838] p0134 N80-22733
 Use of elastomeric elements in control of rotor
 instability
 p0128 N80-29732
 Development of procedures for calculating
 stiffness and damping of elastomers in
 engineering applications, part 7
 [NASA-CR-165138] p0128 N80-32718
- ELASTOPLASTICITY**
 Two-dimensional finite-element analyses of
 simulated rotor-fragment impacts against rings
 and beams compared with experiments
 [NASA-CR-159645] p0038 N80-22323
 Comparison of elastic and elastic-plastic
 structural analyses for cooled turbine blade
 airfoils
 [NASA-TP-1679] p0132 N80-27719
 Finite-strain large-deflection
 elastic-viscoplastic finite-element transient
 response analysis of structures
 [NASA-CR-159874] p0134 N80-29762
- ELECTRIC AUTOMOBILES**
 Study of advanced electric propulsion system
 concept using a flywheel for electric vehicles
 [NASA-CR-159650] p0184 N80-18991
 The performance and efficiency of four
 motor/controller/battery systems for the simpler
 electric vehicles
- [NASA-CR-159776] p0103 N80-24550
 Impact of propulsion system R and D on electric
 vehicle performance and cost
 [NASA-TM-81548] p0143 N80-27805
 Small passenger car transmission test-Chevrolet
 200 transmission
 [NASA-CR-159835] p0185 N80-20255
 Small passenger car transmission test; Ford C4
 transmission
 [NASA-CR-159881] p0128 N80-31795
 Small passenger car transmission test; Chevrolet
 LUV transmission
 [NASA-CR-159882] p0128 N80-31796
- ELECTRIC BATTERIES**
 NT ALKALINE BATTERIES
 NT LEAD ACID BATTERIES
 NT NICKEL HYDROGEN BATTERIES
 NT NICKEL ZINC BATTERIES
 NT SILVER ZINC BATTERIES
 NT STORAGE BATTERIES
- Advanced screening of electrode couples
 [NASA-CR-159738] p0141 N80-22777
 Toroidal cell and battery --- energy storage for
 orbital space applications or power cells for
 electric vehicles
 [NASA-CASE-LEW-12918-1] p0144 N80-33857
- ELECTRIC CHARGE**
 NT SPACE CHARGE
 Configuration effects on satellite charging response
 [NASA-TM-81397] p0053 N80-15200
- ELECTRIC CHOPPERS**
 Error analysis in the measurement of average power
 with application to switching controllers
 [NASA-CR-159792] p0184 N80-21202
- ELECTRIC CONTACTS**
 Liquid metal slip ring --- aerospace environments
 [NASA-CASE-LEW-12277-3] p0101 N80-18300
- ELECTRIC CONTROL**
 Single-stage electrohydraulic servosystem for
 actuating an airflow valve with frequencies to
 500 hertz
 [NASA-TP-1678] p0046 N80-29369
- ELECTRIC CURRENT**
 NT DIRECT CURRENT
 NT GAS DISCHARGES
 NT GLOW DISCHARGES
- Critical currents in A-15 structure Nb3Al
 converted from cold-worked bcc structure
 p0179 A80-33853
 Bi-directional four quadrant (BDQ4) power
 converter development
 [NASA-CR-159660] p0147 N80-14480
 Interaction of high voltage surfaces with the
 space plasma
 [NASA-CR-165131] p0177 N80-32223
- ELECTRIC DISCHARGES**
 NT GAS DISCHARGES
 NT GLOW DISCHARGES
- ELECTRIC ENERGY STORAGE**
 Improvement and scale-up of the NASA Redox storage
 system
 p0146 A80-48370
 Assessment and preliminary design of an energy
 buffer for regenerative braking in electric
 vehicles
 [NASA-CR-159756] p0184 N80-23216
- ELECTRIC GENERATORS**
 NT ALKALINE BATTERIES
 NT FUEL CELLS
 NT HYDROGEN OXYGEN FUEL CELLS
 NT MAGNETOHYDRODYNAMIC GENERATORS
 NT NICKEL ZINC BATTERIES
 NT SOLAR CELLS
 NT SOLAR GENERATORS
 NT THERMIONIC CONVERTERS
 NT THERMOELECTRIC GENERATORS
 NT TURBOGENERATORS
- Bi-directional four quadrant (BDQ4) power
 converter development
 [NASA-CR-159660] p0147 N80-14480
 Large Wind Turbine Design Characteristics and R
 and D Requirements
 [NASA-CP-2106] p0139 N80-16453
 Simulation studies of multiple large wind turbine
 generators on a utility network
 p0139 N80-16480
 Engineering test facility design definition
 [NASA-TM-81499] p0143 N80-27799

SUBJECT INDEX

ELECTRIC POWER SUPPLIES

Cogeneration Technology Alternatives Study (CTAS).
 Volume 3: Energy conversion system characteristics
 [NASA-CR-159761] p0155 N80-31860

ELECTRIC HYBRID VEHICLES
 Performance of 22.4-kW nonlaminated-frame dc series motor with chopper controller --- a dc to dc voltage converter
 [NASA-TM-79252] p0101 N80-13361

Design study of toroidal traction CVT for electric vehicles
 [NASA-CR-159803] p0124 N80-25661

Advanced propulsion system for hybrid vehicles
 [NASA-CR-159771] p0184 N80-26212

A laboratory facility for electric vehicle propulsion system testing
 [NASA-TM-81574] p0183 N80-30229

Small passenger car transmission test; Ford C4 transmission
 [NASA-CR-159881] p0128 N80-31795

Small passenger car transmission test; Chevrolet LUV transmission
 [NASA-CR-159882] p0128 N80-31796

Design study of steel V-Belt CVT for electric vehicles
 [NASA-CR-159845] p0185 N80-32299

ELECTRIC IMPULSES
 U ELECTRIC PULSES

ELECTRIC MOTOR VEHICLES
 Performance of 22.4-kW nonlaminated-frame dc series motor with chopper controller --- a dc to dc voltage converter
 [NASA-TM-79252] p0101 N80-13361

An averaging battery model for a lead-acid battery operating in an electric car
 [NASA-TM-79321] p0165 N80-16824

Advanced electric propulsion system concept for electric vehicles
 [NASA-CR-159651] p0183 N80-17916

An automatically-shifted two-speed transaxle system for an electric vehicle
 [NASA-CR-159746] p0184 N80-18992

Design study of flat belt CVT for electric vehicles
 [NASA-CR-159822] p0124 N80-22702

Assessment and preliminary design of an energy buffer for regenerative braking in electric vehicles
 [NASA-CR-159756] p0184 N80-23216

The performance and efficiency of four motor/controller/battery systems for the simpler electric vehicles
 [NASA-CR-159776] p0103 N80-24550

An electric vehicle propulsion system's impact on battery performance: An overview
 [NASA-TM-81515] p0143 N80-24756

Design study of toroidal traction CVT for electric vehicles
 [NASA-CR-159803] p0124 N80-25661

Pulse charging of lead-acid traction cells
 [NASA-TM-81513] p0143 N80-25780

Impact of propulsion system R and D on electric vehicle performance and cost
 [NASA-TM-81548] p0143 N80-27805

Preliminary results of steady state characterization of near term electric vehicle breadboard propulsion system
 [NASA-TM-81546] p0183 N80-28254

A laboratory facility for electric vehicle propulsion system testing
 [NASA-TM-81574] p0183 N80-30229

Toroidal cell and battery --- energy storage for orbital space applications or power cells for electric vehicles
 [NASA-CR-159770-1] p0144 N80-33857

ELECTRIC MOTORS
 Performance of 22.4-kW nonlaminated-frame dc series motor with chopper controller --- a dc to dc voltage converter
 [NASA-TM-79252] p0101 N80-13361

Study of advanced electric propulsion system concept using a flywheel for electric vehicles
 [NASA-CR-159650] p0184 N80-18991

Preliminary results of steady state characterization of near term electric vehicle breadboard propulsion system
 [NASA-TM-81546] p0183 N80-28254

ELECTRIC NETWORKS
 Simulation studies of multiple large wind turbine generators on a utility network

p0139 N80-16480

ELECTRIC POTENTIAL
 Study of a rare-gas transverse fast discharge
 [NASA-TM-81388] p0176 A80-11366

Initial comparison of SSPM ground test results and flight data to WASCAP simulations --- Satellite Surface Potential Monitor NASA Charging Analyzer Program
 [AIAA PAPER 80-0336] p0054 A80-29751

Open-circuit voltage improvements in low resistivity solar cells
 [NASA-TM-81388] p0138 N80-15555

Study program to improve the open-circuit voltage of low resistivity single crystal silicon solar cells
 [NASA-CR-159833] p0150 N80-22775

Study of power management technology for orbital multi-100KWe applications. Volume 3: Requirements
 [NASA-CR-159834] p0154 N80-29845

ELECTRIC POWER CONVERSION
 U ELECTRIC GENERATORS

ELECTRIC POWER PLANTS
 Survey of MHD plant applications
 [NASA-TM-81400] p0144 A80-11972

Oxygen-enriched air for MHD power plants
 [NASA-TM-81400] p0096 A80-25096

Coupled generator and combustor performance calculations for potential early commercial MHD power plants
 [NASA-TM-81400] p0156 A80-25099

Modified power law equations for vertical wind profiles --- in investigation of windpower plant siting
 [NASA-TM-81400] p0159 A80-35719

Experiments on H2-O2 MHD power generation
 [NASA-TM-81400] p0176 A80-44239

NASA-Lewis closed-cycle magnetohydrodynamics plant analysis
 [NASA-TM-79249] p0137 N80-10595

Photovoltaic power system reliability considerations
 [NASA-TM-79291] p0130 N80-15422

Parametric study of potential early commercial MHD power plants
 [NASA-CR-159633] p0149 N80-18559

Cogeneration Technology Alternatives Study (CTAS). Volume 1: Summary
 [NASA-TM-81400] p0141 N80-19626

Concept definition study of small Brayton cycle engines for dispersed solar electric power systems
 [NASA-CR-159592] p0150 N80-22778

The optimization air separation plants for combined cycle MHD-power plant applications
 [NASA-TM-81510] p0142 N80-23778

Summary and evaluation of the parametric study of potential early commercial MHD power plants (PSPEC)
 [NASA-TM-81497] p0142 N80-23780

Rapporteur report: MHD electric power plants
 [NASA-TM-81554] p0144 N80-29862

Cogeneration Technology Alternatives Study (CTAS). Volume 6: Computer data. Part 1: Coal-fired nocogeneration process boiler, section A
 [NASA-CR-159770-PT-1-A] p0154 N80-30888

Cogeneration Technology Alternatives Study (CTAS). Volume 6: Computer data. Part 1: Coal-fired nocogeneration process boiler, section B
 [NASA-CR-159770-PT-1-B] p0154 N80-30889

Cogeneration Technology Alternatives Study (CTAS). Volume 6: Computer data. Part 2: Residual-fired nocogeneration process boiler
 [NASA-CR-159770-PT-2] p0155 N80-30890

Cogeneration Technology Alternatives Study (CTAS). Volume 3: Industrial processes
 [NASA-CR-159767] p0155 N80-31870

ELECTRIC POWER SUPPLIES
 NT SPACECRAFT POWER SUPPLIES

8-cm Engineering Model Thruster technology - A review of recent developments
 [AIAA PAPER 79-2103] p0064 A80-13311

An adaptive-control switching buck regulator - Implementation, analysis, and design
 [NASA-TM-81400] p0103 A80-28167

Modeling and analysis of Power Processing Systems
 [NASA-TM-81400] p0066 A80-28894

Cycles till failure of silver-zinc cells with competing failure modes - Preliminary data analysis
 [NASA-TM-81400] p0146 A80-46414

- Description of photovoltaic village power systems in the United States and Africa p0146 A80-46796
- Effect of positive pulse charge waveforms on cycle life of nickel-zinc cells p0146 A80-48329
- ELECTRIC POWER TRANSMISSION**
- Study of power management technology for orbital multi-100Kw applications. Volume 3: Requirements [NASA-CR-159834] p0154 M80-29845
- ELECTRIC PROPULSION**
- NT ELECTROMAGNETIC PROPULSION**
- NT ION PROPULSION**
- NT PLASMA PROPULSION**
- NT SOLAR ELECTRIC PROPULSION**
- Characteristics of primary electric propulsion systems [AIAA PAPER 79-2041] p0058 A80-10376
- Preliminary results of the mission profile life test of a 30 cm Hg bombardment thruster [AIAA PAPER 79-2078] p0081 A80-10391
- An electric propulsion long term test facility [AIAA PAPER 79-2080] p0049 A80-13308
- Cost-effective technology advancement directions for electric propulsion transportation systems in earth-orbital missions [AIAA PAPER 79-2043] p0048 A80-20961
- Upper stages utilizing electric propulsion p0059 A80-29989
- Electric propulsion, circa 2000 [AIAA PAPER 80-0912] p0059 A80-32886
- Cost-effective technology advancement directions for electric propulsion transportation systems in earth-orbital missions [NASA-TN-79269] p0182 M80-11950
- Primary electric propulsion technology study --- for thruster wear-out mechanisms [NASA-CR-159688] p0061 M80-13158
- Upper stages utilizing electric propulsion [NASA-TN-81412] p0056 M80-16097
- Upper stages utilizing electric propulsion p0057 M80-30386
- Electric propulsion technology p0057 M80-31452
- Auxiliary control of LSS p0063 M80-31459
- ELECTRIC PULSES**
- Effect of positive pulse charge waveforms on cycle life of nickel-zinc cells p0146 A80-48329
- ELECTRIC ROCKET ENGINES**
- NT ION ENGINES**
- NT MERCURY ION ENGINES**
- Characteristics of primary electric propulsion systems [AIAA PAPER 79-2041] p0058 A80-10376
- SENT II 1979 extended flight thruster system performance [AIAA PAPER 79-2063] p0059 A80-10386
- Orbital transfer of large space structures with nuclear electric rockets [AAS PAPER 80-083] p0054 A80-41897
- Electric propulsion for near-Earth space missions [NASA-CR-159735] p0062 M80-16096
- ELECTRICAL CONDUCTIVITY**
- U ELECTRICAL RESISTIVITY**
- ELECTRICAL ENGINEERING**
- MOD-2 wind turbine farm stability study [NASA-CR-165156] p0156 M80-33862
- ELECTRICAL IMPEDANCE**
- NT CONTACT RESISTANCE**
- NT ELECTRICAL RESISTANCE**
- ELECTRICAL MEASUREMENT**
- Study of a rare-gas transverse fast discharge p0176 A80-11366
- Initial comparison of SSPM ground test results and flight data to NASCAP simulations --- Satellite Surface Potential Monitor NASA Charging Analyzer Program [AIAA PAPER 80-0336] p0054 A80-29751
- Error analysis in the measurement of average power with application to switching controllers [NASA-CR-159792] p0184 M80-21202
- ELECTRICAL PROPERTIES**
- NT CONTACT RESISTANCE**
- NT ELECTRICAL RESISTANCE**
- NT ELECTRICAL RESISTIVITY**
- NT POLARIZATION CHARACTERISTICS**
- Characterization of solar cells for space applications. Volume 10: Electrical characteristics of Spectrolab BSF, textured, 10 ohm-cm, 300 micron cells as a function of intensity, temperature and irradiation [NASA-CR-162422] p0147 M80-11566
- Modification of the electrical and optical properties of polymers --- ion irradiation to create texture [NASA-CASE-LEW-13027-1] p0087 M80-24437
- ELECTRICAL RESISTANCE**
- NT CONTACT RESISTANCE**
- Open-circuit voltage improvements in low resistivity solar cells [NASA-TN-81388] p0138 M80-15555
- ELECTRICAL RESISTIVITY**
- Potential release of fibers from burning carbon composites --- aircraft fires [NASA-TN-80214] p0069 M80-29431
- Thin n-i-p radiation-resistant solar cell feasibility study [NASA-CR-159871] p0154 M80-29852
- ELECTRO-OPTICS**
- Study of a rare-gas transverse fast discharge p0176 A80-11366
- ELECTROCATALYSTS**
- Catalyst surfaces for the chromous/chromic redox couple [NASA-CASE-LEW-13148-1] p0101 M80-20487
- Cell module and fuel conditioner [NASA-CR-159888] p0155 M80-31882
- ELECTROCHEMICAL CELLS**
- NT ALKALINE BATTERIES**
- NT ELECTRIC BATTERIES**
- NT FUEL CELLS**
- NT HYDROGEN OXYGEN FUEL CELLS**
- NT LEAD ACID BATTERIES**
- NT NICKEL HYDROGEN BATTERIES**
- NT NICKEL ZINC BATTERIES**
- NT SILVER ZINC BATTERIES**
- NT STORAGE BATTERIES**
- Catalyst surfaces for the chromous/chromic redox couple [NASA-CASE-LEW-13148-1] p0101 M80-20487
- Redox storage systems for solar applications [NASA-TN-81464] p0142 M80-23777
- ELECTROCHEMICAL CORROSION**
- Anodic polarization behavior of austenitic stainless steel alloys with lower chromium content p0178 A80-22250
- ELECTROCHEMISTRY**
- Catalyst surfaces for the chromous/chromic redox couple [NASA-CASE-LEW-13148-2] p0140 M80-18557
- ELECTRODEPOSITION**
- Decay of the zincate concentration gradient at an alkaline zinc cathode after charging p0074 A80-13070
- Improved refractory coatings and method of producing the same [NASA-CASE-LEW-13169-1] p0076 M80-14232
- ELECTRODES**
- NT CATHODES**
- NT CELL CATHODES**
- NT HOLLOW CATHODES**
- Advanced screening of electrode couples [NASA-CR-159738] p0141 M80-22777
- Optimal thermionic energy conversion with established electrodes for high-temperature topping and process heating --- coal combustion product environments [NASA-TN-81555] p0175 M80-33221
- Status of nickel-hydrogen cell technology p0064 M80-33474
- Toroidal cell and battery --- energy storage for orbital space applications or power cells for electric vehicles [NASA-CASE-LEW-12918-1] p0144 M80-33857
- ELECTROGENERATORS**
- U ELECTRIC GENERATORS**
- ELECTROHYDRAULIC CONTROL**
- U ELECTRIC CONTROL**
- ELECTROLYTIC CELLS**
- Catalyst surfaces for the chromous/chromic redox couple [NASA-CASE-LEW-13148-1] p0101 M80-20487
- Toroidal cell and battery --- energy storage for orbital space applications or power cells for electric vehicles

- [NASA-CASE-LEW-12918-1] p0144 N80-33857
ELECTROMAGNETIC FIELDS
 NT FAR FIELDS
ELECTROMAGNETIC INTERACTIONS
 NT PLASMA-ELECTROMAGNETIC INTERACTION
ELECTROMAGNETIC PROPERTIES
 NT ABSORPTANCE
 NT ELECTRICAL PROPERTIES
 NT OPTICAL PROPERTIES
 NT REFLECTANCE
ELECTROMAGNETIC PROPULSION
 NT MASS DRIVERS (PAYLOAD DELIVERY)
 Advanced concepts --- specific impulse, mass drivers, electromagnetic launchers, and the rail gun p0058 N80-31471
ELECTROMAGNETIC RADIATION
 NT MILLIMETER WAVES
 NT X RAYS
ELECTROMAGNETIC WAVE TRANSMISSION
 NT MICROWAVE TRANSMISSION
ELECTROMAGNETS
 NT SUPERCONDUCTING MAGNETS
ELECTROMOTIVE FORCES
 Flexible formulated plastic separators for alkaline batteries [NASA-CASE-LEW-12363-4] p0140 N80-18555
ELECTRON AVALANCHES
 Negative streamer development in FEP teflon p0179 A80-19776
ELECTRON BEAMS
 90- to 93-percent efficient collector for operation of a dual-mode traveling-wave tube in the linear region p0102 A80-13909
 Coupled cavity traveling wave tube with velocity tapering [NASA-CASE-LEW-12296-1] p0101 N80-19425
 Multistage depressed collector with efficiency of 90 to 94 percent for operation of a dual-mode traveling wave tube in the linear region [NASA-TP-1670] p0101 N80-21669
 Baffle aperture design study of hollow cathode equipped ion thrusters [NASA-CR-165164] p0064 N80-33476
ELECTRON COMPOUNDS
 U INTERMETALLICS
ELECTRON DENSITY (CONCENTRATION)
 Parametric dependence of ion temperature and electron density in the SUMMA hot-ion plasma using laser light scattering and emission spectroscopy p0176 A80-46265
ELECTRON DIFFUSION
 Baffle aperture design study of hollow cathode equipped ion thrusters [NASA-CR-165164] p0064 N80-33476
ELECTRON EMISSION
 NT SECONDARY EMISSION
 Active control of spacecraft charging p0055 A80-46890
ELECTRON ENERGY
 Multistage depressed collector with efficiency of 90 to 94 percent for operation of a dual-mode traveling wave tube in the linear region [NASA-TP-1670] p0101 N80-21669
 Improved traveling wave tubes [NASA-TH-81479] p0102 N80-22598
ELECTRON IONIZATION
 U IONIZATION
ELECTRON IRRADIATION
 Radiation damage in high voltage silicon solar cells p0179 A80-44234
 Radiation damage in high voltage silicon solar cells [NASA-TH-81478] p0178 N80-23180
ELECTRON MICROSCOPY
 Some TEM observations of Al₂O₃ scales formed on NiCrAl alloys p0081 A80-13071
 Scanning-electron-microscope study of normal-impingement erosion of ductile metals [NASA-TP-1609] p0077 N80-16141
ELECTRON OPTICS
 90- to 93-percent efficient collector for operation of a dual-mode traveling-wave tube in the linear region p0102 A80-13909
ELECTRON PATHS
 U ELECTRON TRAJECTORIES
ELECTRON RADIATION
 NT ELECTRON BEAMS
ELECTRON TEMPERATURE
 U ELECTRON ENERGY
ELECTRON TRAJECTORIES
 Analytical prediction and experimental verification of TWT and depressed collector performance using multidimensional computer programs p0102 A80-13902
 A matrix solution for the simulation of magnetic fields with ideal current loops p0102 A80-13903
ELECTRON TUBES
 NT MICROWAVE TUBES
 NT TRAVELING WAVE TUBES
ELECTRONIC COUNTERMEASURES
 Improved traveling wave tubes --- for ECM systems p0102 A80-44235
ELECTRONIC EQUIPMENT
 NT PHOTOVOLTAIC CELLS
 NT SOLID STATE DEVICES
ELECTRONIC LEVELS
 U ELECTRON ENERGY
ELECTRONIC SWITCHES
 U SWITCHING CIRCUITS
ELECTRONS
 NT PHOTOELECTRONS
ELECTROPHYSICS
 NT ELECTRO-OPTICS
ELECTROSHOCK EFFECT
 U ELECTRIC CURRENT
ELECTROSTATIC PLASMA
 U PLASMAS (PHYSICS)
ELECTROSTATIC PROPULSION
 NT ION PROPULSION
ELECTROSTATICS
 Torquing and electrostatic deformation of the solar sail p0065 A80-46901
 Ion extraction from a plasma [NASA-CR-159849] p0177 N80-26161
ELEMENTARY PARTICLES
 NT PHOTOELECTRONS
ELLIPTICAL ORBITS
 NT TRANSFER ORBITS
EMISSION
 NT ACOUSTIC EMISSION
 NT ELECTRON EMISSION
 NT EXHAUST EMISSION
 NT SECONDARY EMISSION
ENDOCRINE GLANDS
 NT PANCREAS
ENERGETIC PARTICLES
 NT PLASMAS (PHYSICS)
ENERGY ABSORPTION FILMS
 Preliminary study of a solar selective coating system using black cobalt oxide for high temperature solar collectors p0082 A80-35500
ENERGY CONSERVATION
 Energy conservation and environmental benefits of thermal energy storage systems in the pulp and paper industry p0146 A80-48194
 Aircraft Energy Efficiency (ACEE) status report p0012 N80-10206
 NASA broad-specification fuels combustion technology program: Status and description [NASA-TH-79315] p0014 N80-14126
 Impact of new instrumentation on advanced turbine research [NASA-TH-79301] p0015 N80-15133
 CF6 jet engine performance improvement: New fan [NASA-CR-159699] p0039 N80-23309
 Advanced component technologies for energy-efficient turbofan engines [NASA-TH-81507] p0019 N80-24316
 CF6-6D engine performance deterioration [NASA-CR-159786] p0041 N80-27364
ENERGY CONVERSION
 NT SOLAR ENERGY CONVERSION
 Survey of MHD plant applications p0144 A80-11972
 Comments on TEC trends --- Thermionic Energy Conversion p0145 A80-39642
 A cesium TELEC experiment at Lewis Research Center [NASA-CR-159729] p0113 N80-14386

ENERGY CONVERSION EFFICIENCY

SUBJECT INDEX

Large Wind Turbine Design Characteristics and R and D Requirements [NASA-CP-2106] p0139 N80-16453
Preliminary analysis of performance and loads data from the 2-megawatt mod-1 wind turbine generator [NASA-TN-81408] p0139 N80-16494
Comments on TEC trends [NASA-TN-79317] p0175 N80-16885
Literature survey of properties of synfuels derived from coal [NASA-TN-79243] p0141 N80-22776
Cell module and fuel conditioner development [NASA-CR-159828] p0150 N80-23768
Cell module and fuel conditioner [NASA-CR-159875] p0142 N80-23769
Mod-2 wind turbine system concept and preliminary design report. Volume 1: Executive summary [DOE/NASA/0002-80/2] p0151 N80-24758
Cogeneration Technology Alternatives Study (CTAS). Volume 1: Summary report [NASA-CR-159765] p0151 N80-24797
Cogeneration technology alternatives study. Volume 1: Summary report [NASA-CR-159759] p0152 N80-25792
Cogeneration technology alternatives study. Volume 2: Industrial process characteristics [NASA-CR-159760] p0152 N80-25793
Cogeneration technology alternatives study. Volume 4: Heat Sources, balance of plant and auxiliary systems [NASA-CR-159762] p0152 N80-25794
Cogeneration technology alternatives study. Volume 6: Computer data [NASA-CR-159764] p0152 N80-25795
Parametric study of prospective early commercial MHD power plants (PSPEC). General Electric Company, task 1: Parametric analysis [NASA-CR-159634] p0152 N80-26779
Cogeneration Technology Alternatives Study (CTAS). Volume 2: Analytical approach [NASA-CR-159766] p0143 N80-28859
Cogeneration Technology Alternatives Study (CTAS). Volume 6: Computer data. Part 1: Coal-fired nocogeneration process boiler, section A [NASA-CR-159770-PT-1-A] p0154 N80-30888
Cogeneration Technology Alternatives Study (CTAS). Volume 6: Computer data. Part 1: Coal-fired nocogeneration process boiler, section B [NASA-CR-159770-PT-1-B] p0154 N80-30889
Cogeneration Technology Alternatives Study (CTAS). Volume 6: Computer data. Part 2: Residual-fired nocogeneration process boiler [NASA-CR-159770-PT-2] p0155 N80-30890
Cogeneration Technology Alternatives Study (CTAS). Volume 3: Energy conversion system characteristics [NASA-CR-159761] p0155 N80-31869
Cogeneration Technology Alternatives Study (CTAS). Volume 3: Industrial processes [NASA-CR-159767] p0155 N80-31870
Cogeneration Technology Alternatives Study (CTAS). Volume 4: Energy conversion systems [NASA-CR-159768] p0155 N80-33859
Cogeneration Technology Alternatives Study (CTAS). Volume 6: Computer data. Part 1: Coal-fired nocogeneration process boiler, section A [NASA-CR-159770-PT-1] p0156 N80-33860
ENERGY CONVERSION EFFICIENCY
90- to 93-percent efficient collector for operation of a dual-mode traveling-wave tube in the linear region p0102 A80-13909
Results of duct area ratio changes in the NASA Lewis H2-O2 combustion MHD experiment [AIAA PAPER 80-0023] p0176 A80-18243
Results from tests on a high work transonic turbine for an energy efficient engine [ASME PAPER 80-GT-146] p0028 A80-42258
The planar multijunction cell - A new solar cell for earth and space p0146 A80-48205
NASA-Lewis closed-cycle magnetohydrodynamics plant analysis [NASA-TN-79249] p0137 N80-10595
Self-reconfiguring solar cell system [NASA-CASE-LEW-12586-1] p0137 N80-14472
Space solar cells: High efficiency and radiation damage [NASA-TN-81387] p0138 N80-15554

Study of advanced radial outflow turbine for solar steam Rankine engines [NASA-CR-159695] p0148 N80-16483
DOE/NASA wind turbine data acquisition. Part 1: Equipment [NASA-CR-159779] p0148 N80-17543
Multistage depressed collector with efficiency of 90 to 94 percent for operation of a dual-mode traveling wave tube in the linear region [NASA-TP-1670] p0101 N80-21669
Potentialities of TEC topping: A simplified view of parametric effects [NASA-TN-81468] p0175 N80-22083
Photovoltaic technology development for synchronous orbit p0058 N80-33470
ENERGY DISSIPATION
How to quickly predict the overall TWT and the multistage depressed collector efficiency p0102 A80-31759
Effect of geometry and operating conditions on spur gear system power loss p0122 A80-46409
ENERGY EXCHANGE
U ENERGY TRANSFER
ENERGY LOSSES
U ENERGY DISSIPATION
ENERGY POLICY
Appendix: MOD-1 wind turbine generator analysis and design report, volume 2 [NASA-CR-159496] p0149 N80-18565
Teetered, tip-controlled rotor: Preliminary test results from Mod-0 100-kW experimental wind turbine [NASA-TN-81445] p0140 N80-19613
Installation and checkout of the DOE/NASA Mod-1 2000-kW wind turbine generator [NASA-TN-81444] p0140 N80-19614
Annual technical report, fiscal year 1979. Volume 1: Executive summary [NASA-CR-159715-VOL-1] p0149 N80-19632
Design study of a 15 kW free-piston Stirling engine-linear alternator for dispersed solar electric power systems [NASA-CR-159587] p0150 N80-22787
Thermal Energy Storage: Fourth Annual Review Meeting [NASA-CP-2125] p0141 N80-22788
Mod-1 wind turbine generator analysis and design report, volume 1 [NASA-CR-159495] p0150 N80-23775
Redox storage systems for solar applications [NASA-TN-81464] p0142 N80-23777
The optimization air separation plants for combined cycle MHD-power plant applications [NASA-TN-81510] p0142 N80-23778
Summary and evaluation of the parametric study of potential early commercial MHD power plants (PSPEC) [NASA-TN-81497] p0142 N80-23780
Solar thermal power systems point-focusing distributed receiver technology project. Volume 2: Detailed report [NASA-CR-159715-VOL-2] p0151 N80-24751
Cogeneration Technology Alternatives Study (CTAS). Volume 1: Summary report [NASA-CR-159765] p0151 N80-24797
Thermal energy storage [NASA-TN-81514] p0143 N80-25779
Cogeneration technology alternatives study. Volume 1: Summary report [NASA-CR-159759] p0152 N80-25792
Cogeneration technology alternatives study. Volume 2: Industrial process characteristics [NASA-CR-159760] p0152 N80-25793
Cogeneration technology alternatives study. Volume 4: Heat Sources, balance of plant and auxiliary systems [NASA-CR-159762] p0152 N80-25794
Cogeneration technology alternatives study. Volume 6: Computer data [NASA-CR-159764] p0152 N80-25795
CF6-6D engine performance deterioration [NASA-CR-159786] p0041 N80-27364
Use of petroleum-based correlations and estimation methods for synthetic fuels [NASA-TN-81533] p0093 N80-27509
Feasibility study of aileron and spoiler control systems for large horizontal axis wind turbines

[NASA-CR-159856] p0153 N80-27803
Impact of propulsion system R and D on electric
vehicle performance and cost
[NASA-TM-81548] p0143 N80-27805
Small passenger car transmission test-Chevrolet
200 transmission
[NASA-CR-159835] p0185 N80-28255
Cogeneration Technology Alternatives Study (CTAS).
Volume 2: Analytical approach
[NASA-CR-159766] p0143 N80-28859
Outlook for alternative energy sources ---
aviation fuels
p0041 N80-29302
Small passenger car transmission test; Ford C4
transmission
[NASA-CR-159881] p0128 N80-31795
Small passenger car transmission test; Chevrolet
LUV transmission
[NASA-CR-159882] p0128 N80-31796
Large wind turbines: A utility option for the
generation of electricity
[NASA-TM-81502] p0144 N80-32858
Optimal thermionic energy conversion with
established electrodes for high-temperature
topping and process heating --- coal combustion
product environments
[NASA-TM-81555] p0175 N80-33221
Cogeneration Technology Alternatives Study (CTAS).
Volume 6: Computer data. Part 1: Coal-fired
necogeneration process boiler, section A
[NASA-CR-159770-PT-1] p0156 N80-33860
Cogeneration Technology Alternatives Study (CTAS).
Volume 6: Computer data. Part 2:
Residual-fired necogeneration process boiler
[NASA-CR-159770-PT-2] p0156 N80-33861

ENERGY STORAGE
NT ELECTRIC ENERGY STORAGE
NT HEAT STORAGE
Anton permselective membrane
[NASA-CR-159599] p0147 N80-12551
Catalyst surfaces for the chromous/chroic redox
couple
[NASA-CASE-LEW-13148-2] p0140 N80-18557
Study of advanced electric propulsion system
concept using a flywheel for electric vehicles
[NASA-CR-159650] p0184 N80-18991
Design study of flat belt CVT for electric vehicles
[NASA-CR-159822] p0124 N80-22702
Advanced screening of electrode couples
[NASA-CR-159738] p0141 N80-22777
Redox storage systems for solar applications
[NASA-TM-81464] p0142 N80-23777

ENERGY STORAGE DEVICES
U ENERGY STORAGE
ENERGY TECHNOLOGY
The use of wind data with an operational wind
turbine in a research and development environment
p0145 A80-35730
Description of photovoltaic village power systems
in the United States and Africa
p0146 A80-46796
Power management for multi-100 KWe space systems
p0060 A80-48357
Technology development for phosphoric acid fuel
cell powerplant, phase 2
[NASA-CR-159705] p0147 N80-10603
Status of the DOE/NASA critical gas turbine
research and technology project
[NASA-TM-79307] p0137 N80-14493
Candidate thermal energy storage technologies for
solar industrial process heat applications
[NASA-TM-81380] p0138 N80-15560
Large Wind Turbine Design Characteristics and R
and D Requirements
[NASA-CP-2106] p0139 N80-16453
Structural analysis considerations for wind
turbine blades
p0139 N80-16469
Blade design and operating experience on the
N80-CA 200 kW wind turbine at Clayton, New Mexico
p0139 N80-16470
Design, fabrication, and test of a steel spar wind
turbine blade
p0139 N80-16472
Preliminary analysis of performance and loads data
from the 2-megawatt mod-1 wind turbine generator
[NASA-TM-81408] p0139 N80-16494
Experiments on H₂-O₂MHD power generation
[NASA-TM-81424] p0175 N80-16886

Parametric study of potential early commercial MHD
power plants
[NASA-CR-159633] p0149 N80-18559
Appendix: MHD-1 wind turbine generator analysis
and design report, volume 2
[NASA-CR-159496] p0149 N80-18565
Advanced technology light weight fuel cell program
--- orbiting space vehicle long-life hydrogen
oxygen fuel cell
[NASA-CR-159807] p0149 N80-19615
Cogeneration Technology Alternatives Study (CTAS).
Volume 1: Summary
[NASA-TM-81400] p0141 N80-19626
Thermal Energy Storage: Fourth Annual Review
Meeting
[NASA-CP-2125] p0141 N80-22788
Program definition and assessment overview --- for
thermal energy storage project management
p0141 N80-22790
The effect of catalyst length and downstream
reactor distance on catalytic combustor
performance
[NASA-TM-81475] p0142 N80-23779
An electric vehicle propulsion system's impact on
battery performance: An overview
[NASA-TM-81515] p0143 N80-24756
Cogeneration Technology Alternatives Study (CTAS).
Volume 1: Summary report
[NASA-CR-159765] p0151 N80-24797
Thermal energy storage
[NASA-TM-81514] p0143 N80-25779
High temperature thermal energy storage in steel
and sand
[NASA-CR-159708] p0154 N80-29860
Rapporteur report: MHD electric power plants
[NASA-TM-81554] p0144 N80-29862
Synchronous energy technology program
p0058 N80-33466

ENERGY TRANSFER
Experimental and theoretical investigation for the
suppression of the planar arc drop in the
thermionic converter
[NASA-CR-159611] p0176 N80-12880

ENGINE ANALYZERS
Computer code for estimating installed performance
of aircraft gas turbine engines. Volume 1:
Final report
[NASA-CR-159691] p0028 N80-13043
Computer code for estimating installed performance
of aircraft gas turbine engines. Volume 2:
Users manual
[NASA-CR-159692] p0028 N80-13044

ENGINE CONTROL
Identification and dual adaptive control of a
turbojet engine
p0023 A80-10033
Control technology
p0013 N80-10215
Quiet Clean Short-haul Experimental Engine (QCSEB)
under-the-wing engine digital control system
design report
[NASA-CR-134920] p0034 N80-15090
Quiet Clean Short-haul Experimental Engine (QCSEB)
under-the-wing engine simulation report
[NASA-CR-134914] p0034 N80-15091
Quiet Clean Short-haul Experimental Engine (QCSEB)
over-the-wing control system design report
[NASA-CR-135337] p0035 N80-15092
Data analysis of P sub T/P sub S noseboom probe
testing on F100 engine P680072 at NASA Lewis
Research Center
[NASA-CR-159816] p0038 N80-21334

ENGINE DESIGN
NT ROCKET ENGINE DESIGN
Computerized systems analysis and optimization of
aircraft engine performance, weight, and life
cycle costs
p0165 A80-10035
Preparing aircraft propulsion for a new era in
energy and the environment
p0024 A80-17737
Computer simulation of engine systems --- for
aircraft design
[AIAA PAPER 80-0051] p0024 A80-18253
Advanced component technologies for
energy-efficient turboprop engines
[AIAA PAPER 80-1086] p0025 A80-38902
Multifuel rotary aircraft engine
[AIAA PAPER 80-1237] p0045 A80-38982

Zero-length, slotted-lip inlet for subsonic military aircraft
[AIAA PAPER 80-1245] p0004 A80-41203

Fuel conservation through active control of rotor clearances
[AIAA PAPER 80-1087] p0045 A80-41506

NASA Broad-Specification Fuels Combustion Technology Program - Status and description
[ASME PAPER 80-GT-65] p0094 A80-42195

CF6 fan performance improvement
[ASME PAPER 80-GT-178] p0026 A80-42284

Aeropropulsion 1979 --- conferences
[NASA-CP-2092] p0012 N80-10205

VSCF technology definition study
[NASA-CR-159730] p0027 N80-10222

Design, durability and low cost processing technology for composite fan exit guide vanes
[NASA-CR-159677] p0027 N80-12091

Quiet, Clean, Short-Haul, Experimental Engine (QCSEE) Under-The-Wing (UTW) engine acoustic design
[NASA-CR-135267] p0028 N80-14117

Quiet, Clean, Short-Haul Experimental Engine (QCSEE) Over-The-Wing (OTW) engine acoustic design
[NASA-CR-135268] p0028 N80-14118

Quiet Clean Short-Haul Experimental Engine (QCSEE) Under-The-Wing (UTW) graphite/PFR cowl development
[NASA-CR-135279] p0029 N80-14119

NASA broad-specification fuels combustion technology program: Status and description
[NASA-TM-79315] p0014 N80-14126

Quiet Clean Short-haul Experimental Engine (QCSEE) Over The Wing (OTW) design report
[NASA-CR-134848] p0034 N80-15086

Quiet Clean Short-haul Experimental Engine (QCSEE). Core engine noise measurements
[NASA-CR-135160] p0035 N80-15093

Quiet Clean Short-haul Experimental Engine (QCSEE) Under-The-Wing (UTW) engine composite nacelle test report. Volume 1: Summary, aerodynamic and mechanical performance
[NASA-CR-159471] p0035 N80-15094

Quiet Clean Short-haul Experimental Engine (QCSEE) preliminary over-the-wing flight propulsion system analysis report
[NASA-CR-135296] p0035 N80-15095

Quiet Clean Short-haul Experimental Engine (QCSEE). Composite fan frame subsystem test report
[NASA-CR-135010] p0035 N80-15098

Quiet Clean Short-haul Experimental Engine (QCSEE) main reduction gears test program
[NASA-CR-134669] p0030 N80-15103

Quiet Clean Short-haul Experimental Engine (QCSEE) clean combustor test report
[NASA-CR-134916] p0030 N80-15104

Quiet Clean Short-haul Experimental Engine (QCSEE) main reduction gears detailed design report
[NASA-CR-134872] p0030 N80-15106

Quiet Clean Short-haul Experimental Engine (QCSEE): Hamilton Standard cam/harmonic drive variable pitch fan actuation system detail design report
[NASA-CR-134852] p0030 N80-15107

Quiet Clean Short-haul Experimental Engine (QCSEE): The aerodynamic and mechanical design of the QCSEE under-the-wing fan
[NASA-CR-135009] p0031 N80-15109

Quiet Clean Short-haul Experimental Engine (QCSEE) UTW fan preliminary design
[NASA-CR-134842] p0031 N80-15111

Quiet Clean Short-haul Experimental Engine (QCSEE): The aerodynamic and preliminary mechanical design of the QCSEE OTW fan
[NASA-CR-134841] p0031 N80-15112

Quiet Clean Short-haul Experimental Engine (QCSEE) under-the-wing engine composite fan blade design
[NASA-CR-134840] p0031 N80-15113

Quiet Clean Short-haul Experimental Engine (QCSEE) over-the-wing engine and control simulation results
[NASA-CR-135049] p0031 N80-15114

Quiet Clean Short-Haul Experimental Engine (QCSEE) ball spline pitch-change mechanism whirligig test report
[NASA-CR-135354] p0032 N80-15115

Quiet Clean Short-haul Experimental Engine (QCSEE) Under-The-Wing (UTW) boiler plate nacelle and core exhaust nozzle design report
[NASA-CR-135008] p0032 N80-15116

Quiet Clean Short-haul Experimental Engine (QCSEE) whirl test of cam/harmonic pitch change actuation system
[NASA-CR-135140] p0032 N80-15117

Quiet Clean Short-haul Experimental Engine (QCSEE). Double-annular clean combustor technology development report
[NASA-CR-159483] p0032 N80-15121

Quiet Clean Short-Haul Experimental Engine (QCSEE). Preliminary analyses and design report, volume 1
[NASA-CR-134838] p0033 N80-15123

Quiet Clean Short-Haul Experimental Engine (QCSEE). Preliminary analyses and design report, volume 2
[NASA-CR-134839] p0033 N80-15124

Quiet Clean Short-Haul Experimental Engine (QCSEE) Over-The-Wing (OTW) propulsion system test report. Volume 1: Summary report
[NASA-CR-135323] p0033 N80-15125

Quiet Clean Short-Haul Experimental Engine (QCSEE) Over-The Wing (OTW) propulsion system test report. Volume 3: Mechanical performance
[NASA-CR-135325] p0033 N80-15126

Method and apparatus for rapid thrust increases in a turbofan engine
[NASA-CASE-LEW-12971-1] p0016 N80-18039

Analysis and design of a uniform-clearance, pumping-ring rod seal for the Stirling engine
[NASA-TM-81463] p0116 N80-18408

A 15 kWe (nominal) solar thermal-electric power conversion concept definition study: Steam Rankin reciprocator system
[NASA-CR-159591] p0149 N80-19612

A 150 and 300 kW lightweight diesel aircraft engine design study
[NASA-CR-3260] p0037 N80-20271

Supporting research and technology for automotive Stirling engine development
[NASA-TM-81495] p0183 N80-21200

Fuel economy screening study of advanced automotive gas turbine engines
[NASA-TM-81433] p0183 N80-21201

Airesearch QCGAT program --- quiet clean general aviation turbofan engines
[NASA-CR-159758] p0037 N80-21331

Design study: A 186 kW lightweight diesel aircraft engine
[NASA-CR-3261] p0038 N80-22326

General Aviation Propulsion
[NASA-CP-2126] p0017 N80-22327

Positive displacement type general-aviation engines: Summary and concluding remarks
[NASA-CR-159822] p0018 N80-22340

Testing of reciprocating seals for application in a Stirling cycle engine
[NASA-CR-159820] p0124 N80-22700

Design study of flat belt CVT for electric vehicles
[NASA-CR-159822] p0124 N80-22702

Design study of a 15 kW free-piston Stirling engine-linear alternator for dispersed solar electric power systems
[NASA-CR-159587] p0150 N80-22787

Conceptual design study of an improved gas turbine powertrain
[NASA-CR-159852] p0039 N80-23315

Baseline automotive gas turbine engine development program
[NASA-CR-159670] p0124 N80-24620

Conceptual design study of an improved automotive gas turbine powertrain
[NASA-CR-159672] p0124 N80-24621

Design and cold-air test of single-stage uncooled turbine with high work output
[NASA-TP-1680] p0019 N80-25337

Cold-air investigation of a 4 1/2 stage turbine with stage-loading factor of 4.66 and high specific work output. 2: Stage group performance
[NASA-TP-1688] p0019 N80-25338

Loss model for off-design performance analysis of radial turbines with pivoting-vane, variable-area stators
[NASA-TM-81532] p0020 N80-27365

NASA broadened-specification fuels combustion technology program
[NASA-CR-159822] p0021 N80-29313

Improved components for engine fuel savings
[NASA-TM-81577] p0023 N80-31402

SUBJECT INDEX

ENGINE TESTS

- Free-piston regenerative hot gas hydraulic engine
[NASA-CASE-LEW-12274-1] p0119 N80-31790
- The energy efficient engine project
[NASA-TM-81566] p0023 N80-32395
- Upgraded automotive gas turbine engine design and development program, volume 2
[NASA-CR-159671] p0128 N80-32719
- ENGINE FAILURE**
Perrographic and spectrographic analysis of oil sampled before and after failure of a jet engine
[NASA-TM-81430] p0117 N80-19497
- ENGINE INLETS**
Zero-length, slotted-lip inlet for subsonic military aircraft
[AIAA PAPER 80-1245] p0004 A80-41203
- An efficient user-oriented method for calculating compressible flow in an about three-dimensional inlets --- panel method
[NASA-CR-159578] p0004 N80-10134
- Comparison of inlet suppressor data with approximate theory based on cutoff ratio
[NASA-TM-81386] p0167 N80-15876
- Distribution analysis for F100(3) engine
[NASA-CR-159754] p0036 N80-17073
- Optimum subsonic, high-angle-of-attack nacelles
[NASA-TM-81491] p0016 N80-20275
- Experimental evaluation of a spinning-mode acoustic-treatment design concept for aircraft inlets --- suppression of YF-102 engine fan noise
[NASA-TP-1613] p0016 N80-21323
- ENGINE MONITORING INSTRUMENTS**
Fatigue strength testing employed for evaluation and acceptance of jet-engine instrumentation probes
[NASA-TM-81402] p0110 N80-17422
- ENGINE NOISE**
Comparison of inlet suppressor data with approximate theory based on cutoff ratio
[AIAA PAPER 80-0100] p0170 A80-20964
- Acoustic measurements of three Prop-Fan models
[AIAA PAPER 80-0995] p0045 A80-35958
- Acoustic pressures on a prop-fan aircraft fuselage surface
[AIAA PAPER 80-1002] p0172 A80-35965
- Effect of inflow control on inlet noise of a cut-on fan
[AIAA PAPER 80-1049] p0171 A80-35993
- Prediction of unsuppressed jet engine exhaust noise in flight from static data
[AIAA PAPER 80-1008] p0027 A80-44491
- Noise reduction
p0012 N80-10208
- Quiet, Clean, Short-Haul, Experimental Engine (QCSSE) Under-The-Wing (UTW) engine acoustic design
[NASA-CR-135267] p0028 N80-14117
- Quiet, Clean, Short-Haul Experimental Engine (QCSSE) Over-The-Wing (OTW) engine acoustic design
[NASA-CR-135268] p0028 N80-14118
- Quiet Clean Short-haul Experimental Engine (QCSSE). Core engine noise measurements
[NASA-CR-135160] p0035 N80-15093
- Core noise investigation of the CF6-50 turbofan engine
[NASA-CR-159598] p0036 N80-16061
- Core noise investigation of the CF6-50 turbofan engine
[NASA-CR-159749] p0036 N80-16062
- Spectral structure of pressure measurements made in a combustion duct --- jet engine noise
[NASA-TM-81471] p0168 N80-22045
- Avco Lycoming quiet clean general aviation turbofan engine
p0039 N80-22333
- Summary of NASA QCGAT program
p0017 N80-22334
- Prediction of unsuppressed jet engine exhaust noise in flight from static data
[NASA-TM-81537] p0169 N80-29132
- Quiet Clean Short-haul Experimental Engine (QCSSE) Under-The-Wing (UTW) composite Macelle test report. Volume 2: Acoustic performance
[NASA-CR-159472] p0044 N80-29297
- Acoustic performance of a 50.8-cm (20-inch) diameter variable-pitch fan and inlet. Volume 2: Acoustic data
[NASA-CR-135118] p0044 N80-29299
- ENGINE PARTS**
Engine component improvement program - Performance improvement
[AIAA PAPER 80-0223] p0024 A80-19300
- Hg ion thruster component testing
[AIAA PAPER 79-2116] p0059 A80-20959
- Wear of seal materials used in aircraft propulsion systems
p0121 A80-28010
- Airbreathing propulsion component technologies
p0024 A80-37482
- Advanced component technologies for energy-efficient turbofan engines
[AIAA PAPER 80-1086] p0025 A80-38902
- Materials and structures technology
p0012 N80-10210
- Engine component improvement program: Performance improvement --- fuel consumption
[NASA-TM-79304] p0013 N80-12092
- Hg ion thruster component testing
[NASA-TM-79287] p0056 N80-13159
- Quiet Clean Short-haul Experimental Engine (QCSSE) under-the-wing engine composite fan blade design report
[NASA-CR-135046] p0031 N80-15108
- Gas path seal
[NASA-CASE-WPO-12131-3] p0115 N80-18400
- Development of improved high pressure turbine outer gas path seal components --- abrasability and thermal cycling test results
[NASA-CR-159801] p0038 N80-21332
- Application of superalloy powder metallurgy for aircraft engines
[NASA-TM-81466] p0078 N80-21488
- Performance deterioration based on existing (historical) data; JT9D jet engine diagnostics program
[NASA-CR-135448] p0038 N80-22324
- Extension of similarity test procedures to cooled engine components with insulating ceramic coatings
[NASA-TP-1615] p0105 N80-24577
- Engine component improvement: Performance improvement, JT9D-7 3.8 AR fan
[NASA-CR-159806] p0039 N80-25332
- Materials for advanced turbine engines. Volume 1: Power metallurgy Rene 95 rotating turbine engine parts
[NASA-CR-159802] p0084 N80-28499
- Improved components for engine fuel savings
[NASA-TM-81577] p0023 N80-31402
- Energy efficient engine
[NASA-CR-159685] p0045 N80-33408
- ENGINE STARTERS**
An experimental evaluation of the performance deficit of an aircraft engine starter turbine
[NASA-TM-81571] p0022 N80-31400
- ENGINE TESTS**
NT COLD FLOW TESTS
NT SPACE ELECTRIC ROCKET TESTS
NT STATIC FIRING
Turbine engine altitude chamber and flight testing with liquid hydrogen
p0023 A80-10034
- 8-cm Engineering Model Thruster technology - A review of recent developments
[AIAA PAPER 79-2103] p0064 A80-13311
- Scale model performance test investigation of exhaust system mixers for an Energy Efficient Engine /E3/ propulsion system
[AIAA PAPER 80-0229] p0024 A80-20968
- Status of NASA full-scale engine aeroelasticity research
p0133 A80-35906
- The measuring and growing of advanced gas turbines
p0111 A80-36127
- Flutter spectral measurements using stationary pressure transducers
p0111 A80-36147
- Temperature and pressure measurement techniques for an advanced turbine test facility
p0112 A80-36157
- QCSSE UTW engine powered-lift acoustic performance --- Quiet Clean Short-haul Experimental Engine Under The Wing
[AIAA PAPER 80-1065] p0025 A80-38651
- Experimental evaluation of exhaust mixers for an Energy Efficient Engine
[AIAA PAPER 80-1088] p0025 A80-38903
- CF6-50 Short Core Exhaust Nozzle
[AIAA PAPER 80-1196] p0025 A80-41514

- NASA Broad-Specification Fuels Combustion Technology Program - Status and description
[ASME PAPER 80-GT-65] p0094 A80-42195
Results from tests on a high work transonic turbine for an energy efficient engine
[ASME PAPER 80-GT-146] p0026 A80-42258
CP6 fan performance improvement
[ASME PAPER 80-GT-178] p0026 A80-42284
Fatigue strength testing employed for evaluation and acceptance of jet-engine instrumentation probes p0112 A80-42291
JT9D-7A /SP/ jet engine performance deterioration trends p0026 A80-44230
Computer code for estimating installed performance of aircraft gas turbine engines. Volume 1: Final report
[NASA-CR-159691] p0028 N80-13043
Hg ion thruster component testing
[NASA-TM-79287] p0056 N80-13159
Modification of axial compressor streamline program for analysis of engine test data
[NASA-TM-79312] p0002 N80-14051
Quiet Clean Short-Haul Experimental Engine (QCSEE) Over-The-Wing (OTW) propulsion system test report. Volume 2: Aerodynamics and performance --- engine performance tests to define propulsion system performance on turbofan engines
[NASA-CR-135324] p0029 N80-14120
Quiet Clean Short-Haul Experimental Engine (QCSEE) Over-The-Wing (OTW) propulsion system test report. Volume 1: Summary report
[NASA-CR-135323] p0033 N80-15125
Expanded study of feasibility of measuring in-flight 747/JT9D loads, performance, clearance, and thermal data
[NASA-CR-159717] p0036 N80-16063
Experimental evaluation of a low emissions high performance duct burner for Variable Cycle Engines (VCE)
[NASA-CR-159694] p0036 N80-17074
Analytical investigation of two hydrogen oxygen rocket engine systems for low-thrust application
[NASA-TM-81420] p0056 N80-17138
Performance sensitivity analysis of Department of Energy-Chrysler upgraded automotive gas turbine engine, S/N 5-4
[NASA-TM-79242] p0115 N80-17467
Overview of a stirling engine test project
[NASA-TM-81442] p0140 N80-18564
JT9D-7A (SP) jet engine performance deterioration trends
[NASA-TM-81459] p0016 N80-20274
CP6-6D engine short-term performance deterioration
[NASA-CR-159830] p0039 N80-23316
Engine component improvement: Performance improvement, JT9D-7 3.8 AR fan
[NASA-CR-159806] p0039 N80-25332
Static and transient performance of YF-102 engine with up to 14 percent core airbleed for the quiet short-haul research aircraft
[NASA-TP-1692] p0020 N80-25339
CP6 jet engine performance improvement program: High pressure turbine aerodynamic performance improvement
[NASA-CR-159832] p0040 N80-26302
Inert gas ion thruster development
[NASA-CR-159805] p0062 N80-27424
Air Force fuel mainburner/turbine effects programs p0042 N80-29314
Investigation of performance deterioration of the CP6/JT9D, high-bypass ratio turbofan engines
[NASA-TM-81552] p0022 N80-29332
Description of the warm core turbine facility recently installed at NASA Lewis Research Center
[NASA-TM-81562] p0022 N80-29333
Performance deterioration of commercial high-bypass ratio turbofan engines
[NASA-TM-81552-REV] p0023 N80-32394
- ENGINEERING DEVELOPMENT**
U PRODUCT DEVELOPMENT
ENGINES
NT AIR BREATHING ENGINES
NT DIESEL ENGINES
NT DUCTED FAN ENGINES
NT ELECTRIC ROCKET ENGINES
NT GAS TURBINE ENGINES
NT HYBRID PROPELLANT ROCKET ENGINES
NT HYDROGEN OXYGEN ENGINES
NT INTERNAL COMBUSTION ENGINES
NT ION ENGINES
NT JET ENGINES
NT LIQUID PROPELLANT ROCKET ENGINES
NT MERCURY ION ENGINES
NT NUCLEAR ENGINE FOR ROCKET VEHICLES
NT PISTON ENGINES
NT ROCKET ENGINES
NT SUPERSONIC COMBUSTION RAMJET ENGINES
NT T-63 ENGINE
NT TURBINE ENGINES
NT TURBOFAN ENGINES
NT TURBOJET ENGINES
NT TURBOPROP ENGINES
NT UPPER STAGE ROCKET ENGINES
NT VARIABLE CYCLE ENGINES
NT WANKEL ENGINES
ENVIRONMENT EFFECTS
Engine environmental effects on composite behavior
[NASA-TM-81508] p0069 N80-23370
ENVIRONMENT POLLUTION
NT AIR POLLUTION
ENVIRONMENT PROTECTION
Preparing aircraft propulsion for a new era in energy and the environment p0024 A80-17737
Energy conservation and environmental benefits of thermal energy storage systems in the pulp and paper industry p0146 A80-48194
Aerial applications dispersal systems control requirements study --- agriculture
[NASA-CN-159781] p0158 N80-18586
Assessment of potential exposure to friable insulation materials containing asbestos
[NASA-TM-81435] p0157 N80-23875
ENVIRONMENT SIMULATION
NT ACOUSTIC SIMULATION
NT SPACE ENVIRONMENT SIMULATION
ENVIRONMENTAL MONITORING
Assessment of satellite and aircraft multispectral scanner data for strip-mine monitoring
[NASA-TM-79268] p0136 N80-20787
ENVIRONMENTAL QUALITY
NT AIR QUALITY
NT WATER QUALITY
ENVIRONMENTAL TESTS
NT CORROSION TESTS
NT HIGH TEMPERATURE TESTS
NT LOW TEMPERATURE TESTS
Engine environmental effects on composite behavior --- moisture and temperature effects on mechanical properties
[AIAA 80-0695] p0024 A80-35101
ENVIRONMENTS
NT AEROSPACE ENVIRONMENTS
NT HIGH TEMPERATURE ENVIRONMENTS
NT SPACECRAFT ENVIRONMENTS
EPOXY RESINS
Improved fiber retention by the use of fillers in graphite fiber/resin matrix composites p0071 A80-32066
High char imide-modified epoxy matrix resins p0071 A80-34789
Tensile and flexural strength of non-graphitic superhybrid composites: Predictions and comparisons
[NASA-TM-79276] p0067 N80-11144
EQUATIONS OF MOTION
NT HELMHOLTZ VORTICITY EQUATION
Nonlinear aeroelastic equations of motion of twisted, nonuniform, flexible horizontal-axis wind turbine blades
[NASA-CR-159502] p0152 N80-26774
EROSION
The erosion/corrosion of small superalloy turbine rotors operating in the effluent of a PFB coal combustor p0080 A80-10043
An investigation into the role of adhesion in the erosion of ductile metals
[ASLE PREPRINT 80-AM-3E-3] p0122 A80-43159
Scanning-electron-microscope study of normal-impingement erosion of ductile metals
[NASA-TP-1609] p0077 N80-16741
An investigation into the role of adhesion in the erosion of ductile metals
[NASA-TM-81458] p0078 N80-21489

SUBJECT INDEX

EXTERNALLY BLOWN FLAPS

ERRORS

NT INSTRUMENT ERRORS

ESTIMATES

NT COST ESTIMATES

ETCHING

Mechanical and chemical effects of ion-texturing
biomedical polymers

p0089 A80-13065

Homogeneous alignment of nematic liquid crystals
by ion beam etched surfaces

p0178 A80-26007

Homogeneous alignment of nematic liquid crystals
by ion beam etched surfaces
[NASA-TM-81378]

p0096 N80-16232

ETHERS

NT POLYPHENYL ETHER

EUCLIDEAN GEOMETRY

NT ANGLE OF ATTACK

EUROPIUM

Design, fabrication and testing of an optical
temperature sensor

p0112 N80-31777

EUTECTIC ALLOYS

Stability of several oxide dispersion strengthened
alloys and a directionally solidified
gamma/gamma prime-alpha eutectic alloy in a
thermal gradient

p0082 A80-40962

Performance of two-layer thermal barrier systems
on directionally solidified Ni-Al-Mo and
comparative effects of alloy thermal expansion
on system life
[NASA-TM-81604]

p0080 N80-32487

EUTECTICS

NT EUTECTIC ALLOYS

EVAPORATIVE COOLING

NT FILM COOLING

NT SWEAT COOLING

EXECUTIVE AIRCRAFT

U GENERAL AVIATION AIRCRAFT

EXHAUST DIFFUSERS

Effect of velocity overshoot on the performance of
magnetohydrodynamic subsonic diffusers
[NASA-TM-79305]

p0175 N80-14922

EXHAUST EMISSION

Emission reduction

p0012 N80-10207

Atomizing characteristics of swirl can combustor
modules with swirl blast fuel injectors --- in
terms of NOx emission rate
[NASA-TM-79297]

p0014 N80-13047

Low NO(x) heavy fuel combustor program

p0137 N80-13624

An analytical study of nitrogen oxides and carbon
monoxide emissions in hydrocarbon combustion
with added nitrogen, preliminary results
[NASA-TM-79296]

p0157 N80-13721

Exhaust emission reduction for intermittent
combustion aircraft engines

p0029 N80-14130

Air pollution from aircraft

p0010 N80-16060

Experimental evaluation of a low emissions high
performance duct burner for Variable Cycle
Engines (VCE)

p0036 N80-17074

The effect of catalyst length and downstream
reactor distance on catalytic combustor
performance

p0142 N80-23779

EXHAUST FLOW SIMULATION

NT FLIGHT SIMULATION

Scale model performance test investigation of
exhaust system mixers for an Energy Efficient
Engine /E3/ propulsion system
[AIAA PAPER 80-0229]

p0024 A80-20968

EXHAUST GASES

Dispersion of sound in a combustion duct by fuel
droplets and soot particles

p0170 A80-20953

Advanced catalytic combustors for low pollutant
emissions, phase 1

p0028 N80-13048

Effect of degree of fuel vaporization upon
emissions for a premixed partially vaporized
combustion system --- for gas turbine engines
[NASA-TP-1582]

p0014 N80-14125

Quiet Clean Short-haul Experimental Engine (QCSEE)
clean combustor test report

[NASA-CR-134916]

p0030 N80-15104

Quiet Clean Short-haul Experimental Engine (QCSEE)

p0032 N80-15120

Factors affecting cleanup of exhaust gases from a
pressurized, fluidized-bed coal combustor

p0105 N80-20532

[NASA-TM-81439]

Low-pressure performance of annular, high-pressure
(40 atm) high-temperature (2480 K) combustion
system

p0023 N80-32396

[NASA-TP-1713]

Energy efficient engine

p0045 N80-33408

[NASA-CR-159685]

EXHAUST JETS

U EXHAUST GASES

EXHAUST NOZZLES

Assessment at full scale of exhaust nozzle-to-wing
size on STOL-OTW acoustic characteristics

p0170 A80-20952

Computation of three-dimensional flow in turbofan
mixers and comparison with experimental data
[AIAA PAPER 80-0227]

p0003 A80-20967

Scale model performance test investigation of
exhaust system mixers for an Energy Efficient
Engine /E3/ propulsion system

p0024 A80-20968

[AIAA PAPER 80-0229]

CF6-50 Short Core Exhaust Nozzle

p0025 A80-41514

[AIAA PAPER 80-1196]

Coannular supersonic ejector nozzles

p0002 N80-10128

Studies of the acoustic transmission
characteristics of coaxial nozzles with inverted
velocity profiles, volume 1 --- jet engine noise
radiation through coannular exhaust nozzles

p0172 N80-11870

[NASA-CR-159698]

Assessment at full scale of exhaust nozzle to wing
size on STOL-OTW acoustic characteristics

p0167 N80-13881

[NASA-TM-79279]

Turbojet-exhaust-nozzle secondary-airflow pumping
as an exit control of an inlet-stability bypass
system for a Mach 2.5 axisymmetric
mixed-compression inlet --- Lewis 10- by 10-ft.
supersonic wind tunnel test

p0014 N80-14124

[NASA-TP-1532]

Quiet Clean Short-haul Experimental Engine (QCSEE)
Under-The-Wing (UTW) boiler plate nacelle and
core exhaust nozzle design report

p0032 N80-15116

[NASA-CR-135008]

EXHAUST SYSTEMS

Experimental evaluation of exhaust mixers for an
Energy Efficient Engine

p0025 A80-38903

[AIAA PAPER 80-1088]

Far-field radiation of APT turbofan noise

p0025 A80-39638

[NASA-TP-1532]

Prediction of unsuppressed jet engine exhaust
noise in flight from static data

p0027 A80-44491

[AIAA PAPER 80-1008]

Static test-stand performance of the YF-102
turbofan engine with several exhaust
configurations for the Quiet Short-Haul Research
Aircraft (QSRA)

p0014 N80-14121

[NASA-TP-1556]

Experimental aerodynamic and acoustic model
testing of the Variable Cycle Engine (VCE)

p0040 N80-26300

[NASA-CR-159710]

Experimental aerodynamic and acoustic model
testing of the Variable Cycle Engine (VCE)

p0040 N80-26300

[NASA-TP-1556]

testbed coannular exhaust nozzle system:
Comprehensive data report

p0040 N80-26301

[NASA-CR-159711]

EXPANSION

NT THERMAL EXPANSION

EXPERIMENTAL DESIGN

NT FACTORIAL DESIGN

Experimental studies of the formation/deposition
of sodium sulfate in/from combustion gases ---
hot corrosion of gas turbine engine components
[NASA-CR-159753]

p0033 N80-15131

Conceptual design of two-phase fluid mechanics and
heat transfer facility for spacelab

p0049 N80-27403

[NASA-CR-159810]

EXPLOSIONS

Prediction of fragment velocities and trajectories

p0096 N80-16210

EXTERNALLY BLOWN FLAPS

Measured and predicted impingement noise for a
model-scale under the wing externally blown flap
configuration with a QCSEE type nozzle

p0169 N80-26115

[NASA-TM-81494]

EXTRACTION

SUBJECT INDEX

EXTRACTION

NT ION EXTRACTION

EXTRAGALACTIC LIGHT

U EXTRATERRESTRIAL RADIATION

EXTRAPOLATION

A quarter-century of progress in the development of correlation and extrapolation methods for creep rupture data

p0133 A80-38142

EXTRATERRESTRIAL RADIATION

Origin of reverse annealing in radiation-damaged silicon solar cells

p0059 A80-33850

EXTREMELY HIGH FREQUENCIES

Ka-band, multibeam, contiguous coverage satellite antenna for the USA
[AIAA 80-0557]

p0099 A80-29588

EYE (ANATOMY)

Intra-ocular pressure normalization technique and equipment

p0135 N80-18690

EYE DISEASES

NT GLAUCOMA

F

F-16 AIRCRAFT

Experimental investigation of a 0.15 scale model of a conformal variable-ramp inlet for the F-16 airplane

p0005 N80-24263

F-102 AIRCRAFT

Experimental evaluation of a spinning-mode acoustic-treatment design concept for aircraft inlets --- suppression of YF-102 engine fan noise
[NASA-TP-1613]

p0016 N80-21323

FABRICATION

Screen printing technology applied to silicon solar cell fabrication
[NASA-CR-159789]

p0153 N80-27808

State-of-the-art SiAlON materials

p0022 N80-29358

Fabrication and evaluation of low fiber content alumina fiber/aluminum composites

p0073 N80-29430

Castable high temperature refractory materials
[NASA-CASE-LEW-13080-1]

p0088 N80-29496

Cost analysis of composite fan blade manufacturing processes
[NASA-CR-159876]

p0044 N80-31398

Design, fabrication and testing of an optical temperature sensor
[NASA-CR-165125]

p0112 N80-31777

FACETS

U FLAT SURFACES

FACTORIAL DESIGN

'Chain pooling' model selection for two-level fixed effects factorial experiments

p0164 A80-40764

FAILURE

NT ENGINE FAILURE

NT SYSTEM FAILURES

FAILURE ANALYSIS

Rolling-element bearings --- contact sliding friction study of solid bodies

p0121 A80-31961

Prediction of fiber composite mechanical behavior made simple

p0133 A80-32067

A relation between semiempirical fracture analyses and K-curves
[NASA-TP-1600]

p0132 N80-15428

Endurance and failure characteristics of modified Vasco X-2, CBS 600 and AISI 9310 spur gears --- aircraft construction materials
[NASA-TM-81421]

p0116 N80-18405

Perrographic and spectrographic analysis of oil sampled before and after failure of a jet engine
[NASA-TM-81430]

p0117 N80-19497

Testing of reciprocating seals for application in a Stirling cycle engine
[NASA-CR-159820]

p0124 N80-22700

Cycles till failure of silver-zinc cells with competing failures modes: Preliminary data analysis
[NASA-TM-81556]

p0164 N80-29088

Depriving of arterial heat pipes: An investigation of CTS thermal excursions
[NASA-CR-165153]

p0108 N80-32688

FAILURE MODES

Fracture modes of high modulus graphite/epoxy angleplied laminates subjected to off-axis tensile loads

p0071 A80-32069

Predicting the time-temperature dependent axial failure of B/A1 composites

p0071 A80-35494

Cycles till failure of silver-zinc cells with competing failure modes - Preliminary data analysis

p0146 A80-46414

Fracture modes of high modulus graphite/epoxy angleplied laminates subjected to off-axis tensile loads
[NASA-TM-81405]

p0068 N80-16102

Mod 1 wind turbine generator failure modes and effects analysis
[NASA-CR-159494]

p0150 N80-20864

Predicting the time-temperature dependent axial failure of B/A1 composites
[NASA-TM-81474]

p0069 N80-21452

FAIRCHILD MILITARY AIRCRAFT

U MILITARY AIRCRAFT

FAIRINGS

Development of a Kevlar/PMR-15 reduced drag DC-9 nacelle fairing
[AIAA PAPER 80-1194]

p0010 A80-41193

FAN BLADES

Influence of mistuning on blade torsional flutter
[NASA-CR-165137]

p0005 N80-31351

Cost analysis of composite fan blade manufacturing processes
[NASA-CR-159876]

p0044 N80-31398

FANS

Engine component improvement: Performance improvement, JT9D-7 3.8 AR fan
[NASA-CR-159806]

p0039 N80-25332

FAR FIELDS

Comparison of inlet suppressor data with approximate theory based on cutoff ratio
[AIAA PAPER 80-0100]

p0170 A80-26964

Far-field radiation of APT turbofan noise
[NASA-TM-81506]

p0025 A80-39638

Far-field radiation of aft turbofan noise
[NASA-TM-81506]

p0166 N80-24129

FATIGUE (MATERIALS)

NT METAL FATIGUE

NT STRUCTURAL STRAIN

NT THERMAL FATIGUE

Effect of thermal cycling on ZrO₂-Y₂O₃ thermal barrier coatings
[NASA-TM-81480]

p0018 N80-22349

FATIGUE LIFE

Strainrange partitioning life predictions of the long time Metal Properties Council creep-fatigue tests

p0133 A80-27958

Fatigue strength testing employed for evaluation and acceptance of jet-engine instrumentation probes

p0112 A80-42291

Constrained fatigue life optimization of a NASVYTIS multiroller traction drive

p0122 A80-46407

Endurance and failure characteristics of modified Vasco X-2, CBS 600 and AISI 9310 spur gears

p0123 A80-46411

Simplified fatigue life analysis for traction drive contacts

p0123 A80-46413

Simplified fatigue life analysis for traction drive contacts
[NASA-TM-79199]

p0115 N80-17469

Constrained fatigue life optimization of a NASVYTIS multiroller traction drive
[NASA-TM-81447]

p0116 N80-18407

FATIGUE TESTS

Strainrange partitioning life predictions of the long time Metal Properties Council creep-fatigue tests

p0133 A80-27958

Fatigue strength testing employed for evaluation and acceptance of jet-engine instrumentation probes

p0112 A80-42291

Analysis of wear debris from full-scale bearing fatigue tests using the Ferrograph
[ASLE PREPRINT 80-AM-3E-2]

p0122 A80-43167

SUBJECT INDEX

FINITE DIFFERENCE THEORY

- Endurance and failure characteristics of modified
Vasco X-2, CBS 600 and AISI 9310 spur gears
[NASA-TM-81403] p0123 N80-46411
- Analysis of wear-debris from full-scale bearing
fatigue tests using the ferrograph
[NASA-TM-81403] p0114 N80-16341
- Application of composite materials to turbofan
engine fan exit guide vanes
[NASA-TM-81432] p0068 N80-18106
- Endurance and failure characteristics of modified
Vasco X-2, CBS 600 and AISI 9310 spur gears ---
aircraft construction materials
[NASA-TM-81421] p0116 N80-18405
- Evaluation of the cyclic behavior of aircraft
turbine disk alloys, part 2
[NASA-CR-165123] p0084 N80-30482
- The 3500 hour durability testing of commercial
ceramic materials
[NASA-CR-159785] p0091 N80-31552
- FAULT MECHANICS**
U FRACTURE MECHANICS
- FDMA**
U FREQUENCY DIVISION MULTIPLE ACCESS
- FEASIBILITY ANALYSIS**
Engine component improvement program: Performance
improvement --- fuel consumption
[NASA-TM-79304] p0013 N80-12092
- Evaluation of feasibility of prestressed concrete
for use in wind turbine blades
[NASA-CR-159725] p0147 N80-15553
- Thermal energy storage systems using fluidized bed
heat exchangers
[NASA-CR-159868] p0153 N80-28866
- Energy efficient engine
[NASA-CR-159685] p0045 N80-33408
- FEED SYSTEMS**
Supercharged topping rocket propellant feed system
[NASA-CASE-XLE-02062-1] p0056 N80-14188
- FEEDBACK CONTROL**
Identification and dual adaptive control of a
turbojet engine
[NASA-TM-79276] p0023 A80-10033
- An adaptive-control switching buck regulator -
Implementation, analysis, and design
[NASA-TM-79276] p0103 A80-28167
- Feasibility of active feedback control of
rotordynamic instability
[NASA-TM-79276] p0128 N80-29733
- FIBER COMPOSITES**
NT CARBON FIBER REINFORCED PLASTICS
NT GLASS FIBER REINFORCED PLASTICS
Micromechanics of intraply hybrid composites:
Elastic and thermal properties
[NASA-TM-79276] p0070 A80-27994
- Prediction of fiber composite mechanical behavior
made simple
[NASA-TM-79281] p0133 A80-32067
- A review of issues and strategies in
nondestructive evaluation of fiber reinforced
structural composites
[NASA-TM-79281] p0071 A80-34764
- High char imide-modified epoxy matrix resins
[NASA-TM-79281] p0071 A80-34789
- Micromechanics of intraply hybrid composites:
Elastic and thermal properties
[NASA-TM-79253] p0067 N80-11143
- Tensile and flexural strength of non-graphitic
superhybrid composites: Predictions and
comparisons
[NASA-TM-79276] p0067 N80-11144
- Dynamic response of damaged angleplied fiber
composites
[NASA-TM-79281] p0067 N80-11145
- Second generation PMR polyimide/fiber composites
[NASA-CR-159666] p0072 N80-12118
- Mechanical property characterization of intraply
hybrid composites
[NASA-TM-79306] p0067 N80-12120
- Burning characteristics and fiber retention of
graphite/resin matrix composites
[NASA-TM-79314] p0067 N80-14196
- Prediction of fiber composite mechanical behavior
made simple --- using a rocket calculator
[NASA-TM-81404] p0068 N80-16107
- Synthesis of improved phenolic resins
[NASA-CR-159724] p0091 N80-17221
- Application of composite materials to turbofan
engine fan exit guide vanes
[NASA-TM-81432] p0068 N80-18106
- Silicone modified resins for graphite fiber
laminates
[NASA-CR-159750] p0072 N80-22407
- Engine environmental effects on composite behavior
[NASA-TM-81508] p0069 N80-23370
- Properties of PMR Polyimide composites made with
improved high strength graphite fibers
[NASA-TM-81557] p0069 N80-28444
- Characterization of PMR-15 polyimide composition
in thermo-oxidatively exposed graphite fiber
composites
[NASA-TM-81565] p0088 N80-28524
- FIBER OPTICS**
Optical sensors for aeronautics and space
[NASA-TM-81407] p0110 N80-17423
- Fiber optic sensors for measuring angular position
and rotational speed --- air breathing engines
[NASA-TM-81454] p0110 N80-18368
- Design, fabrication and testing of an optical
temperature sensor
[NASA-CR-165125] p0112 N80-31777
- FIBER ORIENTATION**
Improved fiber retention by the use of fillers in
graphite fiber/resin matrix composites
[NASA-TM-79288] p0071 A80-32066
- FIBERGLASS**
U GLASS FIBERS
- FIBERS**
NT BORON FIBERS
NT CARBON FIBERS
NT GLASS FIBERS
NT REINFORCING FIBERS
Acoustic behavior of fibrous bulk materials
[ATAA PAPER 80-0986] p0172 A80-35951
- Fabrication and evaluation of low fiber content
alumina fiber/aluminum composites
[NASA-CR-159517] p0073 N80-29430
- FIBROUS MATERIALS**
U FIBERS
- FIGHTER AIRCRAFT**
NT F-16 AIRCRAFT
NT F-102 AIRCRAFT
High-performance-vehicle technology --- fighter
aircraft propulsion
[NASA-TM-79288] p0013 N80-10219
- FILLERS**
Improved fiber retention by the use of fillers in
graphite fiber/resin matrix composites
[NASA-TM-79288] p0071 A80-32066
- Improved fiber retention by the use of fillers in
graphite fiber/resin matrix composites
[NASA-TM-79288] p0067 N80-13171
- FILLING**
NT REFILLING
- FILM COOLING**
Coolant tube curvature effects on film cooling as
detected by infrared imagery
[ASME PAPER 79-WA/GT-7] p0107 A80-18638
- Full-coverage film cooling. I - Comparison of heat
transfer data for three injection angles
[ASME PAPER 80-GT-43] p0108 A80-42176
- Full-coverage film cooling. II - Heat transfer
data and numerical simulation
[ASME PAPER 80-GT-44] p0109 A80-42177
- Influence of coolant tube curvature on film
cooling effectiveness as detected by infrared
imagery
[NASA-TP-1546] p0013 N80-11087
- FILM THICKNESS**
Elastohydrodynamic film thickness measurements of
artificially-produced nonsmooth surfaces
[ASLE PREPRINT 79-LC-1A-3] p0102 A80-14720
- Mechanisms of lubrication and wear of a bonded
solid-lubricant film
[ASLE PREPRINT 80-AM-3E-1] p0122 A80-43163
- Some limitations in applying classical EHD
film-thickness formulae to a high-speed bearing
[NASA-TM-81431] p0116 N80-18409
- Fully flooded elastohydrodynamic lubricated
elliptical contacts
[NASA-TM-81543] p0118 N80-27698
- Starved elastohydrodynamic lubricated elliptical
contacts
[NASA-TM-81549] p0118 N80-27699
- Film thickness for different regimes of fluid-film
lubrication
[NASA-TM-81550] p0119 N80-29735
- FINITE DIFFERENCE THEORY**
Time-dependent difference theory for noise

- propagation in a two-dimensional duct
[AIAA PAPER 80-0098] p0170 A80-18269
- A time dependent difference theory for sound
propagation in ducts with flow p0170 A80-20951
- Summary of advanced methods for predicting high
speed propeller performance p0003 A80-20966
- An implicit finite-difference code for inviscid
and viscous cascade flow [AIAA PAPER 80-1427] p0007 A80-44128
- Time-dependent difference theory for noise
propagation in a two-dimensional duct --- of a
turbofan engine [NASA-TM-79298] p0167 A80-12822
- A time dependent difference theory for sound
propagation in ducts with flow ---
characteristic of inlet and exhaust ducts of
turbofan engines [NASA-TM-79302] p0167 A80-12823
- Time dependent difference theory for sound
propagation in axisymmetric ducts with plug flow
[NASA-TM-81501] p0168 A80-23096
- An alternative approach to the numerical
simulation of steady inviscid flow [NASA-TM-81542] p0003 A80-27286
- Influence of pressure driven secondary flows on
the behavior of turbofan forced mixers
[NASA-TM-81541] p0105 A80-27632
- Numerical techniques in linear duct acoustics ---
finite difference and finite element analyses
[NASA-TM-81553] p0170 A80-30154
- FINITE ELEMENT METHOD**
- Analytical and experimental spur gear tooth
temperature as affected by operating variables
p0123 A80-46412
- A three-dimensional spacecraft-charging computer
code p0055 A80-46891
- Modeling of crack tip deformation with finite
element method and its applications p0130 A80-13503
- Two-dimensional finite-element analyses of
simulated rotor-fragment impacts against rings
and beams compared with experiments
[NASA-CR-159645] p0038 A80-22323
- Nonlinear, three-dimensional finite-element
analysis of air-cooled gas turbine blades
[NASA-TP-1669] p0132 A80-22734
- Three dimensional finite-element elastic analysis
of a thermally cycled double-edge wedge geometry
specimen --- nickel alloy turbine parts
[NASA-TM-80980] p0079 A80-26433
- Finite-strain large-deflection
elastic-viscoplastic finite-element transient
response analysis of structures [NASA-CR-159874] p0134 A80-29762
- Numerical techniques in linear duct acoustics ---
finite difference and finite element analyses
[NASA-TM-81553] p0170 A80-30154
- FIRE DAMAGE**
- Fiber release characteristics of graphite hybrid
composites p0073 A80-32063
- FIRE PREVENTION**
- Hybrid composites that retain graphite fibers on
burning p0073 A80-32064
- FIRES**
- Fire test method for graphite fiber reinforced
plastics [NASA-TM-81436] p0068 A80-18107
- Potential release of fibers from burning carbon
composites --- aircraft fires [NASA-TM-80214] p0069 A80-29431
- Statistical aspects of carbon fiber risk
assessment modeling --- fire accidents involving
aircraft [NASA-CR-159318] p0073 A80-29432
- FIRING (IGNITING)**
- NT STATIC FIRING
- NT TEST FIRING
- FLAME FRONTS**
- U FLAME PROPAGATION
- FLAME INTERACTION**
- U CHEMICAL REACTIONS
- U FLAME PROPAGATION
- FLAME PROPAGATION**
- Combustion of solid carbon rods in zero and normal
gravity p0074 A80-20955
- FLAMES**
- Soot formation and burnout in flames p0043 A80-29320
- FLAMMABILITY**
- Antimisting kerosene --- reduced flammability
during aircraft accident circumstances p0021 A80-29319
- FLAMMABLE GASES**
- NT LIQUEFIED NATURAL GAS
- FLAPPING HINGES**
- Examination of the flap-lag stability of rigid
articulated rotor blades p0010 A80-15123
- FLAPS (CONTROL SURFACES)**
- NT EXTERNALLY BLOWN FLAPS
- FLAT SURFACES**
- Evolution of a rotating flow in the vicinity of a
surface p0107 A80-14660
- FLAW DETECTION**
- U NONDESTRUCTIVE TESTS
- FLEXIBILITY**
- Limit cycles of a flexible shaft with hydrodynamic
journal bearings in unstable regimes p0127 A80-29725
- FLEXIBLE BODIES**
- Development of flexible rotor balancing criteria
[NASA-CR-159506] p0129 A80-32720
- FLEXING**
- Tensile and flexural strength of non-graphitic
superhybrid composites: Predictions and
comparisons [NASA-TM-79276] p0067 A80-11144
- FLEXURE**
- U FLEXING
- FLIGHT CHARACTERISTICS**
- Acoustic considerations of flight effects on jet
noise suppressor nozzles [AIAA PAPER 80-0164] p0171 A80-20965
- FLIGHT INSTRUMENTS**
- NT RADIO ALTIMETERS
- FLIGHT LOAD RECORDERS**
- Expanded study of feasibility of measuring
in-flight 747/JT9D loads, performance,
clearance, and thermal data [NASA-CR-159717] p0036 A80-16063
- FLIGHT PERFORMANCE**
- U FLIGHT CHARACTERISTICS
- FLIGHT SIMULATION**
- Computer simulation of engine systems --- for
aircraft design [AIAA PAPER 80-0051] p0024 A80-18253
- Comparison of several inflow control devices for
flight simulation of fan tone noise using a
JT15D-1 engine [AIAA PAPER 80-1025] p0025 A80-38640
- Characteristics of internal- and jet-noise
radiation from a multi-lobe, multi-tube
suppressor nozzle tested statically and under
flight simulation [AIAA PAPER 80-1027] p0173 A80-38642
- An improved prediction method for the noise
generated in flight by circular jets
[NASA-TM-81470] p0168 A80-22048
- FLIGHT TESTS**
- Prediction of unsuppressed jet engine exhaust
noise in flight from static data [AIAA PAPER 80-1008] p0027 A80-44491
- Flight test of navigation and guidance sensor
errors measured on STOL approaches [NASA-TM-81154] p0028 A80-13041
- FLOW CHARACTERISTICS**
- NT FLOW DISTRIBUTION
- NT FLOW STABILITY
- NT FLOW VELOCITY
- NT MAGNETOHYDRODYNAMIC STABILITY
- Elevated temperature flow strength, creep
resistance and diffusion welding characteristics
of Ti-6Al-2Nb-1Ta-0.8Mo p0081 A80-13277
- Evolution of a rotating flow in the vicinity of a
surface p0107 A80-14660
- Some flow characteristics of conventional and
tapered high-pressure-drop simulated seals
[ASLE PREPRINT 79-LC-38-2] p0120 A80-14727

FLOW COEFFICIENTS

Vibration exciting mechanisms induced by flow in turbomachine stages

p0127 N80-29722

FLOW DISTORTION

Inlet flow distortion in turbomachinery. I -

Comparison of theory and experiment in a

transonic fan stage. II - A parameter study

[AIAA PAPER 80-1076] p0006 A80-38895

The effect of finite turbulence spatial scale on the amplification of turbulence by a contracting stream

p0004 A80-44862

Distribution analysis for F100(3) engine

[NASA-CR-159754]

p0036 N80-17073

FLOW DISTRIBUTION

Comparison between optical measurements and a

numerical solution of the flow field within a

transonic axial-flow compressor rotor

[AIAA PAPER 80-1078] p0003 A80-38897

General design method for three-dimensional

potential flow fields. 1: Theory

[NASA-CR-3288] p0005 N80-29251

FLOW EQUATIONS

NT HELMHOLTZ VORTICITY EQUATION

An alternative approach to the numerical

simulation of steady inviscid flow

p0107 A80-44228

FLOW FIELDS

U FLOW DISTRIBUTION

FLOW GEOMETRY

Some aspects of a free jet phenomena to 105 L/D in a constant area duct

p0106 A80-10030

An experimental investigation of endwall profiling

in a turbine vane cascade

[AIAA PAPER 80-1089] p0004 A80-38904

Computation of three-dimensional flow in turbomachinery

mixers and comparison with experimental data

[NASA-TM-81410] p0104 N80-15364

FLOW MEASUREMENT

Critical mass flux through short Borda type inlets of various cross sections

p0106 A80-10031

Some dynamic and time-averaged flow measurements

in a turbine rig

p0178 A80-21120

Laser anemometer measurements at the exit of a T63 combustor

p0045 A80-27737

Efficient laser anemometer for intra-rotor flow

mapping in turbomachinery

p0111 A80-36140

Laser anemometer measurements in a transonic axial flow compressor rotor

p0111 A80-36141

Fluid and structural measurements to advance gas turbine technology

p0111 A80-36145

Impact of new instrumentation on advanced turbine research

p0112 A80-36155

Temperature and flow measurements on near-freezing aviation fuels in a wing-tank model

[ASME PAPER 80-GT-63] p0094 A80-42193

Temperature and flow measurements on near-freezing aviation fuels in a wing-tank model

[NASA-TM-79285] p0093 N80-13268

Wind-tunnel investigation of the flow correction for a model-mounted angle of attack sensor at

angles of attack from -10 deg to 110 deg ---

Langley 12-foot low speed wind tunnel test

[NASA-TM-80189] p0011 N80-14110

Efficient laser anemometer for intra-rotor flow

mapping in turbomachinery

[NASA-TM-79320] p0112 N80-14375

FLOW PATTERNS

U FLOW DISTRIBUTION

FLOW RATE

U FLOW VELOCITY

FLOW RESISTANCE

NT AERODYNAMIC DRAG

FLOW SEPARATION

U BOUNDARY LAYER SEPARATION

U SEPARATED FLOW

FLOW STABILITY

NT MAGNETOHYDRODYNAMIC STABILITY

Comparison of several inflow control devices for flight simulation of fan tone noise using a

JT15D-1 engine

[NASA-TM-81505]

p0019 N80-24314

FLOW THEORY

Marangoni bubble motion in zero gravity --- Lewis

zero gravity drop tower

[NASA-TM-79250]

p0104 N80-13403

FLOW VELOCITY

Laser anemometer measurements at the exit of a T63

combustor

p0045 A80-27737

Noise suppression due to annulus shaping of an

inverted-velocity-profile coaxial nozzle

p0171 A80-35498

The effect of finite turbulence spatial scale on

the amplification of turbulence by a contracting

stream

p0004 A80-44862

Laser anemometer measurements in a transonic axial

flow compressor rotor

[NASA-TM-79323]

p0002 N80-14050

Lubrication of optimized-design tapered-roller

bearings to 2.4 million DN

[NASA-TF-1714]

p0119 N80-29734

Autoignition characteristics of aircraft-type fuels

[NASA-CR-159886]

p0095 N80-30535

FLOW VISUALIZATION

NT NUMERICAL FLOW VISUALIZATION

Streakline flow visualization study of a horseshoe

vortex in a large-scale, two-dimensional turbine

stator cascade

[ASME PAPER 80-GT-4]

p0004 A80-42145

Streakline flow visualization study of a horseshoe

vortex in a large-scale, two-dimensional turbine

stator cascade

[NASA-TM-79274]

p0104 N80-11376

FLOWMETERS

NT HOT-WIRE FLOWMETERS

FLUID DYNAMICS

NT AERODYNAMICS

NT AEROTHERMODYNAMICS

NT COMPUTATIONAL FLUID DYNAMICS

NT ELASTOHYDRODYNAMICS

NT HYDRODYNAMICS

NT MAGNETOHYDRODYNAMICS

NT ROTOR AERODYNAMICS

Free jet phenomena in a 90 deg-sharp edge inlet

geometry

p0106 A80-10037

Thermophysical property data - Who needs them ---

similarity principle applications in fluid

mechanics and heat transfer

[ASME PAPER 79-WA/HT-17]

p0180 A80-18630

LeRC reduced gravity fluid management technology

program

p0048 A80-35504

Preliminary results from a four-working space,

double-acting piston, Stirling engine controls

model

[NASA-TM-81569]

p0106 N80-29624

Non-synchronous whirling due to fluid-dynamic

forces in axial turbo-machinery rotors

p0126 N80-29721

Vibration exciting mechanisms induced by flow in

turbomachine stages

p0127 N80-29722

Fluid forces on rotating centrifugal impeller with

whirling motion

p0127 N80-29724

Experimental results concerning centrifugal

impeller excitations

p0127 N80-29727

LeRC reduced gravity fluid management technology

program

p0057 N80-30383

FLUID FILMS

NT SQUEEZE FILMS

Dynamic analysis of noncontacting face seals

[NASA-TM-79294]

p0118 N80-27695

Film thickness for different regimes of fluid-film

lubrication

[NASA-TM-81550]

p0119 N80-29735

FLUID FLOW

NT AIR FLOW

NT ANNULAR FLOW

NT BOUNDARY LAYER SEPARATION

NT CAPILLARY FLOW

NT CASCADE FLOW

NT CAVITATION FLOW

NT COAXIAL FLOW

FLUID INJECTION

SUBJECT INDEX

NT COMBUSTIBLE FLOW
 NT COMPRESSIBLE FLOW
 NT CORE FLOW
 NT DUCTED FLOW
 NT FREE FLOW
 NT FUEL FLOW
 NT GAS FLOW
 NT INLET FLOW
 NT INVISCID FLOW
 NT JET FLOW
 NT JET MIXING FLOW
 NT MASS FLOW
 NT NOZZLE FLOW
 NT ORIFICE FLOW
 NT OUTLET FLOW
 NT POTENTIAL FLOW
 NT PROPELLANT TRANSFER
 NT RADIAL FLOW
 NT SECONDARY FLOW
 NT SEPARATED FLOW
 NT SHEAR FLOW
 NT STEADY FLOW
 NT SUBCRITICAL FLOW
 NT SUBSONIC FLOW
 NT SUPERCRITICAL FLOW
 NT SUPERSONIC FLOW
 NT THREE DIMENSIONAL FLOW
 NT TRANSONIC FLOW
 NT TURBULENT FLOW
 NT TWO DIMENSIONAL FLOW
 NT TWO PHASE FLOW
 NT UNSTEADY FLOW
 NT VISCOUS FLOW
 NT WALL FLOW
 Phase change in liquid face seals. II - Isothermal and adiabatic bounds with real fluids
 [ASME PAPER 79-LUB-4] p0129 A80-14739

FLUID INJECTION
 NT WATER INJECTION
 Full-coverage film cooling. I - Comparison of heat transfer data for three injection angles
 [ASME PAPER 80-GT-43] p0108 A80-42176
 Full-coverage film cooling. II - Heat transfer data and numerical simulation
 [ASME PAPER 80-GT-44] p0109 A80-42177

FLUID JETS
 NT FREE JETS

FLUID MECHANICS
 NT AERODYNAMICS
 NT AEROTHERMODYNAMICS
 NT COMPUTATIONAL FLUID DYNAMICS
 NT ELASTOHYDRODYNAMICS
 NT FLUID DYNAMICS
 NT HYDRODYNAMICS
 NT MAGNETOHYDRODYNAMICS
 NT ROTOR AERODYNAMICS
 A reduced volumetric expansion factor plot
 p0107 A80-10038
 Conceptual design of two-phase fluid mechanics and heat transfer facility for spacelab
 [NASA-CR-159810] p0049 A80-27403
 A test program to measure fluid mechanical whirl-excitation forces in centrifugal pumps
 p0126 A80-29719
 Effect of grazing flow on the nonlinear acoustic behavior of helmholtz resonators
 p0095 A80-31619

FLUIDIZED BED PROCESSORS
 The erosion/corrosion of small superalloy turbine rotors operating in the effluent of a PFB coal combustor
 p0080 A80-10043
 Improved PFB operations - 400-hour turbine test results --- Pressurized Fluidized Bed
 p0145 A80-39639
 Factors affecting cleanup of exhaust gases from a pressurized, fluidized-bed coal combustor
 [NASA-TM-81439] p0105 A80-20532
 Improved PFB operations: 400-hour turbine test results --- coal combustion products and not corrosion in gas turbines
 [NASA-TM-81511] p0079 A80-26426
 Thermal energy storage systems using fluidized bed heat exchangers
 [NASA-CR-159868] p0153 A80-28866

FLUORIDES
 NT CALCIUM FLUORIDES
 Mechanisms of lubrication and wear of a bonded solid-lubricant film

[ASLE PREPRINT 80-AM-3E-1] p0122 A80-43163

FLUORINE COMPOUNDS
 NT CALCIUM FLUORIDES
 NT FLUORIDES
 NT FLUOROCARBONS
 NT FLUOROPOLYMERS
 Boundary lubrication, thermal and oxidative stability of a fluorinated polyether and a perfluoropolyether triazine
 [ASLE PREPRINT 79-AM-1B-1] p0088 A80-12089

FLUORINE ORGANIC COMPOUNDS
 NT FLUOROCARBONS
 NT FLUOROPOLYMERS

FLUORO COMPOUNDS
 NT FLUOROCARBONS
 NT FLUOROPOLYMERS

FLUOROCARBONS
 Effect of thermal aging on the tribological properties of polyimide films and polyimide-bonded graphite fluoride films
 [ASLE PREPRINT 79-AM-3B-1] p0088 A80-12094

FLUORONICA
 U MICA

FLUOROPOLYMERS
 NT TEFLON (TRADEMARK)
 Negative streamer development in PEP teflon
 p0179 A80-19776

FLUTTER
 NT SUPERSONIC FLUTTER
 Flutter spectral measurements using stationary pressure transducers
 [NASA-TN-79293] p0013 A80-13046
 Status of NASA full-scale engine aeroelasticity research
 [NASA-TN-81500] p0132 A80-23678
 Experimental determination of unsteady blade element aerodynamics in cascades. Volume 1: Torsion mode cascade
 [NASA-CR-159831] p0040 A80-25335

FLUTTER ANALYSIS
 Flutter spectral measurements using stationary pressure transducers
 p0111 A80-36147
 Influence of mistuning on blade torsional flutter
 [NASA-CR-165137] p0005 A80-31351

FLUX (RATE)
 NT HEAT FLUX

FLUX DENSITY
 NT CURRENT DENSITY
 NT IRRADIANCE

FLUXMETERS
 U MAGNETIC MEASUREMENT
 U MEASURING INSTRUMENTS

FLYING PLATFORM STABILITY
 U AERODYNAMIC STABILITY

FLYING QUALITIES
 U FLIGHT CHARACTERISTICS

FLYWHEELS
 Study of advanced electric propulsion system concept using a flywheel for electric vehicles
 [NASA-CR-159650] p0184 A80-18991
 Design study of flat belt CVT for electric vehicles
 [NASA-CR-159822] p0124 A80-22702
 Design study of steel V-Belt CVT for electric vehicles
 [NASA-CR-159845] p0185 A80-32299

FOIL BEARINGS
 High temperature self-lubricating coatings for air lubricated foil bearings for the automotive gas turbine engine
 [NASA-CR-159848] p0091 A80-26448

FORECASTING
 NT PERFORMANCE PREDICTION
 NT PREDICTION ANALYSIS TECHNIQUES
 NT TECHNOLOGICAL FORECASTING

FORMING TECHNIQUES
 NT CASTING
 NT COLD WORKING
 Characterization and properties of controlled nucleation thermochemical deposited (CNTD) silicon carbide
 [NASA-TM-79277] p0085 A80-13254

FOSSIL FUELS
 NT COAL
 NT CRUDE OIL
 Low NO(x) heavy fuel combustor program
 [NASA-TM-79313] p0137 A80-13624

FOULING
 Fouling and the inhibition of salt corrosion ---

- hot corrosion of superalloys
[NASA-TM-81469] p0078 N80-21492
- FRACTOGRAPHY**
Reaction bonded silicon nitride prepared from wet
attrition-milled silicon --- fractography
[NASA-TM-81428] p0086 N80-18181
- FRACTURE MECHANICS**
Simple spline-function equations for fracture
mechanics calculations p0133 A80-10832
- Fracture modes of high modulus graphite/epoxy
angleplied laminates subjected to off-axis
tensile loads p0071 A80-32069
- A relation between semiempirical fracture analyses
and R-curves p0132 N80-15428
[NASA-TP-1600]
- Fracture modes of high modulus graphite/epoxy
angleplied laminates subjected to off-axis
tensile loads p0068 N80-16102
[NASA-TM-81405]
- The method of lines in three dimensional fracture
mechanics p0132 N80-32753
[NASA-TM-81593]
- FRACTURE RESISTANCE**
U FRACTURE STRENGTH
- FRACTURE STRENGTH**
Quantitative ultrasonic evaluation of engineering
properties in metals, composites, and ceramics
p0130 A80-39641
- Fracture toughness determination of Al203 using
four-point-bend specimens with straight-through
and chevron notches p0090 A80-42085
- Compliance and stress intensity coefficients for
short bar specimens with chevron notches p0133 A80-46032
- Endurance and failure characteristics of modified
Vasco K-2, CBS 600 and AISI 9310 spur gears
p0123 A80-46411
- Performance of Chevron-notch short bar specimen in
determining the fracture toughness of silicon
nitride and aluminum oxide p0090 A80-50696
- Comparison tests and experimental compliance
calibration of the proposed standard round
compact plane strain fracture toughness specimen
[NASA-TM-81379] p0132 N80-13513
- A relation between semiempirical fracture analyses
and R-curves p0132 N80-15428
[NASA-TP-1600]
- Prediction of fiber composite mechanical behavior
made simple --- using a rocket calculator
[NASA-TM-81404] p0068 N80-16107
- High toughness-high strength iron alloy
[NASA-CASE-LEW-12542-3] p0079 N80-32484
- Fracture toughness of brittle materials determined
with chevron notch specimens p0079 N80-32486
[NASA-TM-81607]
- FRACTURE TOUGHNESS**
U FRACTURE STRENGTH
- FRAMES**
NT AIRFRAMES
- FRAUNHOFER REGION**
U FAR FIELDS
- FREE ENERGY**
NT GIBBS FREE ENERGY
- FREE FLOW**
The effect of finite turbulence spatial scale on
the amplification of turbulence by a contracting
stream p0004 A80-44862
- FREE JETS**
Some aspects of a free jet phenomena to 105 L/D in
a constant area duct p0106 A80-10030
- Free jet phenomena in a 90 deg-sharp edge inlet
geometry p0106 A80-10037
- FREE STREAM EFFECTS**
U FREE FLOW
- FREE STREAMS**
U FREE FLOW
- FREEZING**
Temperature and flow measurements on near-freezing
aviation fuels in a wing-tank model
[NASA-TM-79285] p0093 N80-13268
- FREQUENCIES**
NT EXTREMELY HIGH FREQUENCIES
- NT INTERMEDIATE FREQUENCIES
NT RESONANT FREQUENCIES
NT SUPERHIGH FREQUENCIES
NT ULTRAHIGH FREQUENCIES
- FREQUENCY ASSIGNMENT**
30/20 GHz wideband technology verification program
p0097 A80-25917
- FREQUENCY DIVISION MULTIPLE ACCESS**
An advanced mixed user domestic satellite system
architecture p0099 A80-29544
[ATAA 80-0494]
Study of advanced communications satellite systems
based on SS-FDMA p0050 N80-25357
[NASA-CR-159778]
- FRICTION**
NT AERODYNAMIC DRAG
NT SLIDING FRICTION
NT STATIC FRICTION
- Program to develop sprayed, plastically deformable
compressor shroud seal materials p0123 N80-16338
[NASA-CR-159741]
- Tribological properties of silicon carbide in
metal removal process p0114 N80-16340
[NASA-TM-79238]
- Practical applications of surface analytic tools
in tribology p0079 N80-23430
[NASA-TM-81484]
- FRICTION COEFFICIENT**
U COEFFICIENT OF FRICTION
- FRICTION DRAG**
NT AERODYNAMIC DRAG
- FUEL CELL CATALYSTS**
U ELECTROCATALYSTS
- FUEL CELLS**
NT HYDROGEN OXYGEN FUEL CELLS
- Technology development for phosphoric acid fuel
cell powerplant, phase 2 p0147 N80-10603
[NASA-CR-159705]
- Anton permselective membrane p0147 N80-12551
[NASA-CR-159599]
- Catalyst surfaces for the chromous/chromic redox
couple p0140 N80-18557
[NASA-CASE-LEW-13148-2]
- Cell module and fuel conditioner development
[NASA-CR-159828] p0150 N80-23768
- Cell module and fuel conditioner p0142 N80-23769
[NASA-CR-159875]
- Cell module and fuel conditioner p0155 N80-31882
[NASA-CR-159888]
- FUEL COMBUSTION**
The chemistry of sodium chloride involvement in
processes related to hot corrosion p0074 A80-10041
- Symposium /International/ on Combustion, 17th,
Leeds University, Leeds, England, August 20-25,
1978, Proceedings p0075 A80-11754
- Results of duct area ratio changes in the NASA
Lewis H2-O2 combustion MHD experiment
[AIAA PAPER 80-0023] p0176 A80-18243
- CATCOM catalyst 5 atm 1000 hour aging study using
No. 2 fuel oil p0075 A80-35908
- Effect of fuel molecular structure on soot
formation in gas turbine engines p0095 A80-42192
[ASME PAPER 80-GT-62]
- NASA Broad-Specification Fuels Combustion
Technology Program - Status and description
[ASME PAPER 80-GT-65] p0094 A80-42195
- Low NO_x/ heavy fuel combustor program
[ASME PAPER 80-GT-69] p0026 A80-42199
- Analysis of combustion instability in liquid fuel
rocket motors p0061 N80-13164
[NASA-CR-159733]
- Amplification of Reynolds number dependent
processes by wave distortion --- liquid fuel
combustor stability p0075 N80-13193
[NASA-CR-159732]
- NASA broad-specification fuels combustion
technology program: Status and description
[NASA-TM-79315] p0014 N80-14126
- Exhaust emission reduction for intermittent
combustion aircraft engines p0029 N80-14130
[NASA-CR-159757]
- Status of the DOE/NASA critical gas turbine
research and technology project p0137 N80-14493
[NASA-TM-79307]
- Effect of sodium, potassium, magnesium, calcium,
and chlorine on the high temperature corrosion

of IN-100, U-700, IN-792, and Mar M-509 ---
coal-derived liquid fuel combustion in turbines
[NASA-TM-79309] p0076 N80-15235

Air pollution from aircraft
[NASA-CR-159712] p0010 N80-16060

Fuel quality combustion analysis
[NASA-CR-159721] p0094 N80-19284

Aircraft Research and Technology for Future Fuels
[NASA-CR-2146] p0022 N80-29300

Combustion technology overview --- the use of
broadened property aircraft fuels p0021 N80-29310

NASA/General Electric broad-specification fuels
combustion technology program, phase 1 p0042 N80-29316

Fuels research: Combustion effects overview
p0021 N80-29317

Effect of fuel molecular structure on soot
formation in gas turbine combustion p0043 N80-29322

Preliminary studies of combustor sensitivity to
alternative fuels p0021 N80-29323

FUEL CONSUMPTION

Preparing aircraft propulsion for a new era in
energy and the environment p0024 A80-17737

Engine component improvement program - Performance
improvement [ATAA PAPER 80-0223] p0024 A80-19300

Advanced Gas Turbine Powertrain System Development
Project p0129 A80-35574

Reduced bleed air extraction for DC-10 cabin air
conditioning [ATAA PAPER 80-1197] p0010 A80-41194

Fuel conservation through active control of rotor
clearances [ATAA PAPER 80-1087] p0045 A80-41506

JT9D-7A /SR/ jet engine performance deterioration
trends p0026 A80-44230

Aircraft Energy Efficiency (ACEE) status report
p0012 N80-10206

Engine component improvement program: Performance
improvement --- fuel consumption [NASA-TM-79304] p0013 N80-12092

JT9D-7A (SR) jet engine performance deterioration
trends [NASA-TM-81459] p0016 N80-20274

Fuel economy screening study of advanced
automotive gas turbine engines [NASA-TM-81433] p0183 N80-21201

CF6 jet engine performance improvement: New fan
[NASA-CR-159699] p0039 N80-23309

Advanced component technologies for
energy-efficient turbofan engines [NASA-TM-81507] p0019 N80-24316

Performance, emissions, and physical
characteristics of a rotating combustion
aircraft engine, supplement A [NASA-CR-135119] p0041 N80-27361

CF6-6D engine performance deterioration
[NASA-CR-159786] p0041 N80-27364

Investigation of performance deterioration of the
CF6/JT9D, high-bypass ratio turbofan engines
[NASA-TM-81552] p0022 N80-29332

Improved components for engine fuel savings
[NASA-TM-81577] p0023 N80-31402

The energy efficient engine project
[NASA-TM-81566] p0023 N80-32395

Cogeneration Technology Alternatives Study (CTAS).
Volume 6: Computer data. Part 2:
Residual-fired nocogeneration process boiler
[NASA-CR-159770-PT-2] p0156 N80-33861

FUEL CONTAMINATION

Effects of impurities in coal-derived liquids on
accelerated hot corrosion of superalloys
[NASA-TM-81384] p0077 N80-18157

FUEL CORROSION

Effect of sodium, potassium, magnesium, calcium,
and chlorine on the high temperature corrosion
of IN-100, U-700, IN-792, and MAR M-509
[ASME PAPER 80-GT-150] p0083 A80-42262

Effects of impurities in coal-derived liquids on
accelerated hot corrosion of superalloys
[NASA-TM-81384] p0077 N80-18157

FUEL FLOW

NT PROPELLANT TRANSFER

Temperature and flow measurements on near-freezing
aviation fuels in a wing-tank model
[ASME PAPER 80-GT-63] p0094 A80-42193

FUEL INJECTION

Design and evaluation of high performance rocket
engine injectors for use with hydrocarbon fuels
p0059 A80-20957

Atomizing characteristics of swirl can combustor
modules with swirl blast fuel injectors
[ASME PAPER 80-GT-30] p0026 A80-42164

Atomizing characteristics of swirl can combustor
modules with swirl blast fuel injectors --- in
terms of NOX emission rate [NASA-TM-79297] p0014 N80-13047

Analytical and experimental evaluations of the
effect of broad property fuels on combustors for
commercial aircraft gas turbine engines
[NASA-TM-81496] p0093 N80-25454

Low-pressure performance of annular, high-pressure
(40 atm) high-temperature (2480 K) combustion
system [NASA-TP-1713] p0023 N80-32396

FUEL OILS

CATCON catalyst 5 atm 1000 hour aging study using
No. 2 fuel oil p0075 A80-35908

Effect on combined cycle efficiency of stack gas
temperature constraints to avoid acid corrosion
[NASA-TM-81531] p0143 N80-27804

FUEL PRODUCTION

Aircraft Research and Technology for Future Fuels
[NASA-CR-2146] p0022 N80-29300

Future aviation fuels overview p0021 N80-29301

Future aviation fuels overview p0021 N80-29301

Outlook for alternative energy sources ---
aviation fuels p0041 N80-29302

Current jet fuel trends p0041 N80-29303

Aviation fuels outlook p0041 N80-29304

Effect of refining variables on the properties and
composition of JP-5 p0041 N80-29306

Military jet fuel from shale oil p0042 N80-29308

FUEL SPRAYS

Atomizing characteristics of swirl can combustor
modules with swirl blast fuel injectors
[ASME PAPER 80-GT-30] p0026 A80-42164

FUEL SYSTEMS

NT AIRCRAFT FUEL SYSTEMS

Analytical and experimental evaluations of the
effect of broad property fuels on combustors for
commercial aircraft gas turbine engines
[NASA-TM-81496] p0093 N80-25454

FUEL TANK PRESSURIZATION

External fuel vaporization study, phase 1
[NASA-CR-159850] p0095 N80-25453

FUEL TANKS

NT WING TANKS

Temperature and flow measurements on near-freezing
aviation fuels in a wing-tank model
[ASME PAPER 80-GT-63] p0094 A80-42193

FUEL TESTS

Effect of fuel molecular structure on soot
formation in gas turbine engines
[ASME PAPER 80-GT-62] p0095 A80-42192

Effect of sodium, potassium, magnesium, calcium,
and chlorine on the high temperature corrosion
of IN-100, U-700, IN-792, and MAR M-509
[ASME PAPER 80-GT-150] p0083 A80-42262

NASA broadened-specification fuels combustion
technology program p0021 N80-29313

Air Force fuel mainburner/turbine effects programs
p0042 N80-29314

Fuel system technology overview p0022 N80-29328

Design and evaluation of high performance rocket
engine injectors for use with hydrocarbon fuels
p0094 N80-31621

FUEL-AIR RATIO

Effect of degree of fuel vaporization upon
emissions for a premixed partially vaporized
combustion system --- for gas turbine engines
[NASA-TP-1582] p0014 N80-14125

Flame tube parametric studies for control of fuel bound nitrogen using rich-lean two-stage combustion
[NASA-TM-81472] p0141 N80-21837

Low-pressure performance of annular, high-pressure (40 atm) high-temperature (2480 K) combustion system
[NASA-TP-1713] p0023 N80-32396

FUELING
U REFUELING

FUELS
NT AIRCRAFT FUELS
NT COAL
NT CRYOGENIC ROCKET PROPELLANTS
NT DIESEL FUELS
NT FOSSIL FUELS
NT FUEL OILS
NT HYDROCARBON FUELS
NT HYDROGEN FUELS
NT JET ENGINE FUELS
NT JP-5 JET FUEL
NT KEROSENE
NT LIQUEFIED NATURAL GAS
NT LIQUID ROCKET PROPELLANTS
NT SYNTHETIC FUELS
Analytical and experimental evaluations of the effect of broad property fuels on combustors for commercial aircraft gas turbine engines
[NASA-TM-81496] p0093 N80-25454

FULL SCALE TESTS
Assessment at full scale of exhaust nozzle-to-wing size on STOL-OTW acoustic characteristics
p0170 A80-20952
Analysis of wear debris from full-scale bearing fatigue tests using the Ferrograph
[ASLE PREPRINT 80-AM-3E-2] p0122 A80-43167

FUNCTIONS (MATHEMATICS)
NT GREEN FUNCTION
NT SELINE FUNCTIONS
Nonanalytical function generation routines for 16-bit microprocessors
[NASA-TM-81586] p0163 N80-33104

FURAN RESINS
NT KEVLAR (TRADEMARK)

FURNACES
Directional solidification at ultra-high thermal gradient
[NASA-CR-159797] p0096 N80-15300

FUSELAGES
Acoustic pressures on a prop-fan aircraft fuselage surface
[AIAA PAPER 80-1002] p0172 A80-35965

G

GAGES
U MEASURING INSTRUMENTS

GALLIUM
Liquid metal slip ring --- aerospace environments
[NASA-CASE-LEW-12277-3] p0101 N80-18300

GALLIUM ARSENIDES
Analysis of GaAs and Si solar cell arrays for earth orbital and orbit transfer missions
[NASA-TM-81383] p0056 N80-15204

GALLIUM COMPOUNDS
NT GALLIUM ARSENIDES

GALVANIC CELLS
U ELECTROLYTIC CELLS

GARP
U GLOBAL ATMOSPHERIC RESEARCH PROGRAM

GAS ANALYSIS
NT OZONOMETRY
An analytical study of nitrogen oxides and carbon monoxide emissions in hydrocarbon combustion with added nitrogen - Preliminary results
[ASME PAPER 80-GT-60] p0074 A80-42190

GAS DISCHARGES
Study of a rare-gas transverse fast discharge
p0176 A80-11366

GAS DISSOCIATION
Potential performance improvement using a reacting gas (nitrogen tetroxide) as the working fluid in a closed Brayton cycle
[NASA-TM-79322] p0139 N80-16490

GAS DYNAMICS
NT AERODYNAMICS
NT AEROTHERMODYNAMICS
NT ROTOR AERODYNAMICS

GAS FLOW**NT AIR FLOW**

Spectral structure of pressure measurements made in a combustion duct

p0171 A80-35496

Some considerations of the performance of two honeycomb gas path seal material systems
[NASA-TM-81398] p0077 N80-16143

Program to develop sprayed, plastically deformable compressor shroud seal materials
[NASA-CR-159741] p0123 N80-16338

GAS IONIZATION

Hydrogen hollow cathode ion source
[NASA-CASE-LEW-12940-1] p0174 N80-33186

GAS LASERS

NT CARBON DIOXIDE LASERS

GAS LIQUEFACTION**U CONDENSING****GAS MIXTURES**

Effect of degree of fuel vaporization upon emissions for a premixed partially vaporized combustion system --- for gas turbine engines
[NASA-TP-1582] p0014 N80-14125

GAS PRESSURE

Low-pressure performance of annular, high-pressure (40 atm) high-temperature (2480 K) combustion system
[NASA-TP-1713] p0023 N80-32396

GAS TURBINE ENGINES**NT DUCTED FAN ENGINES****NT JET ENGINES****NT SUPERSONIC COMBUSTION RAMJET ENGINES****NT T-63 ENGINE****NT TURBOFAN ENGINES****NT TURBOJET ENGINES****NT TURBOPROP ENGINES**

The chemistry of sodium chloride involvement in processes related to hot corrosion

p0074 A80-10041

Measuring unsteady pressure on rotating compressor blades --- with semiconductor strain gages under gas turbine engine operating conditions

p0110 A80-12630

Thermal barrier coatings for aircraft gas turbines
[AIAA PAPER 80-0302] p0089 A80-18303

Some dynamic and time-averaged flow measurements in a turbine rig

p0178 A80-21120

Wear of seal materials used in aircraft propulsion systems

p0121 A80-28010

An experimental, low-cost, silicon-aluminide high-temperature coating for superalloys

p0082 A80-35501

Advanced Gas Turbine Powertrain System Development Project

p0129 A80-35574

3500-hour durability testing of ceramic materials for automotive gas turbine engines

p0092 A80-35575

Durability testing of advanced catalysts and catalyst supports for gas turbine engine combustors

p0074 A80-35881

Laser-optical blade tip clearance measurement system

p0111 A80-36137

Fluid and structural measurements to advance gas turbine technology

p0111 A80-36145

Digital system for dynamic turbine engine blade displacement measurements

p0111 A80-36151

Impact of new instrumentation on advanced turbine research

p0112 A80-36155

Airbreathing propulsion component technologies

p0024 A80-37482

Development of improved-durability plasma sprayed ceramic coatings for gas turbine engines

p0089 A80-38963

CF6-50 Short Core Exhaust Nozzle

p0025 A80-41514

Analytical and experimental evaluations of the effect of broad property fuels on combustors for commercial aircraft gas turbine engines
[AIAA PAPER 80-1204] p0094 A80-41516

Streakline flow visualization study of a horseshoe vortex in a large-scale, two-dimensional turbine stator cascade

[ASME PAPER 80-GT-4] p0004 A80-42145
Experimental study of low aspect ratio compressor
blading
[ASME PAPER 80-GT-6] p0025 A80-42147
Performance of annular prediffuser-combustor systems
[ASME PAPER 80-GT-15] p0026 A80-42154
An analytical study of nitrogen oxides and carbon
monoxide emissions in hydrocarbon combustion
with added nitrogen - Preliminary results
[ASME PAPER 80-GT-60] p0074 A80-42190
Effect of fuel molecular structure on soot
formation in gas turbine engines
[ASME PAPER 80-GT-62] p0095 A80-42192
NASA Broad-Specification Fuels Combustion
Technology Program - Status and description
[ASME PAPER 80-GT-65] p0094 A80-42195
Low NO_x/ heavy fuel combustor program
[ASME PAPER 80-GT-69] p0026 A80-42199
Evaluation of a high performance fixed-ratio
traction drive
p0122 A80-46410
Similarity tests of turbine vanes - Effects of
ceramic thermal barrier coatings
[ASME PAPER 80-HT-24] p0027 A80-48013
Control technology
p0013 N80-10215
Analysis of the response of a thermal barrier
coating to sodium and vanadium doped combustion
gases
[NASA-TM-79205] p0076 N80-10344
Computer code for estimating installed performance
of aircraft gas turbine engines. Volume 1:
Final report
[NASA-CR-159691] p0028 N80-13043
Computer code for estimating installed performance
of aircraft gas turbine engines. Volume 2:
Users manual
[NASA-CR-159692] p0028 N80-13044
Advanced catalytic combustors for low pollutant
emissions, phase 1
[NASA-CR-159535] p0028 N80-13048
Effect of degree of fuel vaporization upon
emissions for a premixed partially vaporized
combustion system --- for gas turbine engines
[NASA-TP-1582] p0014 N80-14125
NASA broad-specification fuels combustion
technology program: Status and description
[NASA-TM-79315] p0014 N80-14126
Laser-optical blade tip clearance measurement system
[NASA-TM-81376] p0015 N80-14128
Temperature and pressure measurement techniques
for an advanced turbine test facility
[NASA-TM-79278] p0110 N80-14374
Theory of deposition of condensible impurities on
surfaces immersed in combustion gases
[NASA-CR-159716] p0033 N80-15130
Experimental studies of the formation/deposition
of sodium sulfate in/from combustion gases ---
hot corrosion of gas turbine engine components
[NASA-CR-159753] p0033 N80-15131
Impact of new instrumentation on advanced turbine
research
[NASA-TM-79301] p0015 N80-15133
Sintered silicon nitride recuperator fabrication
[NASA-CR-159706] p0090 N80-15263
Plasma-sprayed dual density ceramic turbine seal
system
[NASA-CR-159739] p0123 N80-15411
Air pollution from aircraft
[NASA-CR-159712] p0010 N80-16060
Some considerations of the performance of two
honeycomb gas path seal material systems
[NASA-TM-81398] p0077 N80-16143
Performance sensitivity analysis of Department of
Energy-Chrysler upgraded automotive gas turbine
engine, S/N 5-4
[NASA-TM-79242] p0115 N80-17467
Materials review for improved automotive gas
turbine engine --- superalloys, refractory
alloys, and ceramics
[NASA-CR-159673] p0123 N80-17470
Study of research and development requirements of
small gas-turbine combustors
[NASA-CR-159796] p0036 N80-18040
Effect of water injection and off scheduling of
variable inlet guide vanes, gas generator speed
and power turbine nozzle angle on the
performance of an automotive gas turbine engine
[NASA-TM-81415] p0016 N80-20272

Composite wall concept for high temperature
turbine shrouds; Survey of low modulus strain
isolator materials
[NASA-TM-81443] p0086 N80-20398
Fuel economy screening study of advanced
automotive gas turbine engines
[NASA-TM-81433] p0183 N80-21201
Operating characteristics of high-speed,
jet-lubricated 35-millimeter-bore ball bearing
with a single-outer-land-guided cage
[NASA-TP-1657] p0117 N80-21753
Parametric tests of a traction drive retrofitted
to an automotive gas turbine
[NASA-TM-81457] p0117 N80-21754
Development of improved-durability plasma sprayed
ceramic coatings for gas turbine engines
[NASA-TM-81512] p0018 N80-23313
Extension of similarity test procedures to cooled
engine components with insulating ceramic coatings
[NASA-TP-1615] p0105 N80-24577
Baseline automotive gas turbine engine development
program
[NASA-CR-159670] p0124 N80-24620
Conceptual design study of an improved automotive
gas turbine powertrain
[NASA-CR-159672] p0124 N80-24621
Durability testing at 5 atmospheres of advanced
catalysts and catalyst supports for gas turbine
engine combustors
[NASA-CR-159839] p0151 N80-24748
External fuel vaporization study, phase 1
[NASA-CR-159850] p0095 N80-25453
Analytical and experimental evaluations of the
effect of broad property fuels on combustors for
commercial aircraft gas turbine engines
[NASA-TM-81496] p0093 N80-25454
A silicon-slurry/aluminide coating --- protects
aircraft and land-based gas turbine engines
[NASA-CASE-LEW-13343-1] p0069 N80-26389
High temperature self-lubricating coatings for air
lubricated foil bearings for the automotive gas
turbine engine
[NASA-CR-159848] p0091 N80-26448
CF6-8D engine performance deterioration
[NASA-CR-159786] p0041 N80-27364
Loss model for off-design performance analysis of
radial turbines with pivoting-vane,
variable-area stators
[NASA-TM-81532] p0020 N80-27365
Air Force fuel mainburner/turbine effects programs
p0042 N80-29314
Atomization of broad specification aircraft fuels
p0043 N80-29318
Effect of fuel molecular structure on soot
formation in gas turbine combustion
p0043 N80-29322
State-of-the-art SiAlON materials
p0022 N80-29358
Some advantages of methane in an aircraft gas
turbine
[NASA-TM-81559] p0094 N80-29502
The 3500 hour durability testing of commercial
ceramic materials
[NASA-CR-159785] p0091 N80-31552
Upgraded automotive gas turbine engine design and
development program, volume 2
[NASA-CR-159671] p0128 N80-32719
GAS TURBINES
Thick ceramic coating development for industrial
gas turbines - A program plan
[SR79-M-4702-05] p0091 A80-10042
The measuring and growing of advanced gas turbines
p0111 A80-36127
Improved PFB operations - 400-hour turbine test
results --- Pressurized Fluidized Bed
p0145 A80-39639
Results from tests on a high work transonic
turbine for an energy efficient engine
[ASME PAPER 80-GT-146] p0026 A80-42258
Development of silicon nitride of improved toughness
[NASA-CR-159676] p0072 N80-10319
Corrosion resistant thermal barrier coating ---
protecting gas turbines and other heat engine
parts
[NASA-CASE-LEW-13088-1] p0067 N80-11142
Feasibility of SiC composite structures for 1644
deg gas turbine seal applications
[NASA-CR-159597] p0123 N80-13474

Low NO(x) heavy fuel combustor program
[NASA-TM-79313] p0137 N80-13624

Status of the DOE/NASA critical gas turbine
research and technology project
[NASA-TM-79307] p0137 N80-14493

Potential performance improvement using a reacting
gas (nitrogen tetroxide) as the working fluid in
a closed Brayton cycle
[NASA-TM-79322] p0139 N80-16490

Internal coating of air cooled gas turbine blades
[NASA-CR-159701] p0036 N80-18041

Nonlinear, three-dimensional finite-element
analysis of air-cooled gas turbine blades
[NASA-TP-1669] p0132 N80-22734

Literature survey of properties of synfuels
derived from coal
[NASA-TM-79243] p0141 N80-22776

Concept definition study of small Brayton cycle
engines for dispersed solar electric power systems
[NASA-CR-159592] p0150 N80-22778

Conceptual design study of an improved gas turbine
powertrain
[NASA-CR-159852] p0039 N80-23315

The effect of catalyst length and downstream
reactor distance on catalytic combustor
performance
[NASA-TM-81475] p0142 N80-23779

Improved PPB operations: 400-hour turbine test
results --- coal combustion products and hot
corrosion in gas turbines
[NASA-TM-81511] p0079 N80-26426

Effect on combined cycle efficiency of stack gas
temperature constraints to avoid acid corrosion
[NASA-TM-81531] p0143 N80-27804

Cogeneration Technology Alternatives Study (CTAS).
Volume 3: Energy conversion system
characteristics
[NASA-CR-159761] p0155 N80-31869

GAS-LIQUID INTERACTIONS
Marangoni bubble motion in zero gravity
p0107 A80-20958

GAS-METAL INTERACTIONS
Sputtering in mercury ion thrusters
[AIAA PAPER 79-2061] p0058 A80-10384

GAS-SOLID INTERACTIONS
NT GAS-METAL INTERACTIONS

GASEOUS CAVITATION
U CAVITATION FLOW
U GAS FLOW

GASHS
NT ARGON
NT ARGON PLASMA
NT CARBON MONOXIDE
NT CHARGED PARTICLES
NT EXHAUST GASES
NT GAS MIXTURES
NT HIGH PRESSURE OXYGEN
NT HIGH TEMPERATURE GASES
NT HYDROGEN
NT HYDROGEN ATOMS
NT HYDROGEN IONS
NT HYDROGEN PLASMA
NT LASER PLASMAS
NT LIQUEFIED GASES
NT LIQUEFIED NATURAL GAS
NT LIQUID HYDROGEN
NT LIQUID OXYGEN
NT MONATOMIC GASES
NT NEON
NT OXYGEN
NT OZONE
NT RARE GASES
NT RESIDUAL GAS
NT XENON

GASP
U GLOBAL AIR SAMPLING PROGRAM

GEAR TEETH
NASA gear research and its probable effect on
rotorcraft transmission design
p0120 A80-13068

Endurance and failure characteristics of modified
Vasco X-2, CBS 600 and AISI 9310 spur gears
p0123 A80-46411

Analytical and experimental spur gear tooth
temperature as affected by operating variables
p0123 A80-46412

Spur-gear-system efficiency at part and full load
[NASA-TP-1622] p0115 N80-17466

Analytical and experimental spur gear tooth
temperature as affected by operating variables
[NASA-TM-81419] p0115 N80-18403

Ideal spiral bevel gears: A new approach to
surface geometry
[NASA-TM-81446] p0117 N80-19498

GEARS
NASA gear research and its probable effect on
rotorcraft transmission design
p0120 A80-13068

Effect of geometry and operating conditions on
spur gear system power loss
p0122 A80-46409

Quiet Clean Short-haul Experimental Engine (QCSEE)
main reduction gears test program
[NASA-CR-134669] p0030 N80-15103

Quiet Clean Short-haul Experimental Engine (QCSEE)
main reduction gears bearing development program
[NASA-CR-134890] p0030 N80-15105

Quiet Clean Short-haul Experimental Engine (QCSEE)
main reduction gears detailed design report
[NASA-CR-134872] p0030 N80-15106

Spur-gear-system efficiency at part and full load
[NASA-TP-1622] p0115 N80-17466

Endurance and failure characteristics of modified
Vasco X-2, CBS 600 and AISI 9310 spur gears ---
aircraft construction materials
[NASA-TM-81421] p0116 N80-18405

Effect of geometry and operating conditions on
spur gear system power loss
[NASA-TM-81426] p0116 N80-18406

Ideal spiral bevel gears: A new approach to
surface geometry
[NASA-TM-81446] p0117 N80-19498

GENERAL AVIATION AIRCRAFT
NT AGRICULTURAL AIRCRAFT

A theoretical and experimental investigation of
propeller performance methodologies
[AIAA PAPER 80-1240] p0026 A80-43283

An acoustic sensitivity study of general aviation
propellers
[AIAA PAPER 80-1871] p0045 A80-50191

Study of research and development requirements of
small gas-turbine combustors
[NASA-CR-159796] p0036 N80-18040

A 150 and 300 kW lightweight diesel aircraft
engine design study
[NASA-CR-3260] p0037 N80-20271

High speed turboprops for executive aircraft,
potential and recent test results
[NASA-TM-81482] p0002 N80-21285

Airesearch QCGAT program --- quiet clean general
aviation turbofan engines
[NASA-CR-159758] p0037 N80-21331

General Aviation Propulsion
[NASA-CP-2126] p0017 N80-22327

Avco Lycoming quiet clean general aviation
turbofan engine
p0039 N80-22333

Summary of NASA QCGAT program
p0017 N80-22334

New opportunities for future, small,
General-Aviation Turbine Engines (GATE)
p0017 N80-22335

An overview of NASA research on positive
displacement general-aviation engines
p0017 N80-22336

GENERAL DYNAMICS AIRCRAFT
NT F-102 AIRCRAFT

GENERAL DYNAMICS MILITARY AIRCRAFT
U MILITARY AIRCRAFT

GEOMAGNETIC EFFECTS
U MAGNETIC EFFECTS

GEOMAGNETIC STORMS
U MAGNETIC STORMS

GEOMETRICAL HYDROMAGNETICS
U MAGNETOHYDRODYNAMICS

GEOMETRY
NT ANGLE OF ATTACK
NT DUCT GEOMETRY
NT FLOW GEOMETRY
NT NOZZLE GEOMETRY
NT SPECIMEN GEOMETRY

GEOSTATIONARY SATELLITES
U SYNCHRONOUS SATELLITES

GEOSYNCHRONOUS ORBITS
NASCAP modelling of environmental-charging-induced
discharges in satellites
p0054 A80-19774

GEO THERMAL RESOURCES

SUBJECT INDEX

MASCAP modelling computations on large optics spacecraft in geosynchronous substorm environments p0054 A80-32829

Analysis of GaAs and Si solar cell arrays for earth orbital and orbit transfer missions [NASA-TM-81383] p0056 N80-15204

Computed voltage distributions around solar electric propulsion spacecraft [NASA-TM-79286] p0053 N80-16094

Synchronous Energy Technology [NASA-CR-2154] p0058 N80-33465

Synchronous energy technology program p0058 N80-33466

Photovoltaic technology development for synchronous orbit p0058 N80-33470

GEO THERMAL RESOURCES

Cogeneration Technology Alternatives Study (CTAS). Volume 6: Computer data. Part 1: Coal-fired nocoeneration process boiler, section A [NASA-CR-159770-PT-1-A] p0154 N80-30888

Cogeneration Technology Alternatives Study (CTAS). Volume 6: Computer data. Part 1: Coal-fired nocoeneration process boiler, section B [NASA-CR-159770-PT-1-B] p0154 N80-30889

Cogeneration Technology Alternatives Study (CTAS). Volume 6: Computer data. Part 2: Residual-fired nocoeneration process boiler [NASA-CR-159770-PT-2] p0155 N80-30890

GERDIEN ARC HEATERS

U HEATING EQUIPMENT

GIBBS FREE ENERGY

Volume-energy parameters and turbulent-flow density fluctuations [NASA-TP-1585] p0105 N80-17398

GLANDS (ANATOMY)

NT PANCREAS

GLANDS (SEALS)

Circumferential shaft seal [NASA-CASE-LEW-12119-2] p0115 N80-18401

GLASS

NT GLASS FIBERS

NT METALLIC GLASSES

NT S GLASS

Evaluation of cleaners for photovoltaic modules exposed in an outdoor environment [NASA-TM-79248] p0096 N80-13317

GLASS FIBER REINFORCED PLASTICS

Dynamic response of damaged angleplied fiber composites p0070 A80-27982

Dynamic response of damaged angleplied fiber composites [NASA-TM-79281] p0067 N80-11145

Application of composite materials to turbofan engine fan exit guide vanes [NASA-TM-81432] p0068 N80-18106

GLASS FIBERS

Mechanical property characterization of intraply hybrid composites p0070 A80-20954

GLAUCOMA

Intra-ocular pressure normalization technique and equipment [NASA-CASE-LEW-12955-1] p0161 N80-14684

GLOBAL AIR SAMPLING PROGRAM

Measurements of cabin and ambient ozone on B747 airplanes p0010 A80-28853

NASA Global Atmospheric Sampling Program (GASP) data report for tapes VL0011 and VL0013 [NASA-TM-81462] p0157 N80-21892

GLOBAL ATMOSPHERIC RESEARCH PROGRAM

Simultaneous cabin and ambient ozone measurements on two Boeing 747 airplanes, volume 1 [NASA-TM-79166] p0008 N80-15059

GLOW DISCHARGES

Survey of ion plating sources p0120 A80-10040

GRADIENTS

NT PRESSURE GRADIENTS

NT TEMPERATURE GRADIENTS

GRADUATION

U CALIBRATING

GRAIN BOUNDARIES

Long-time creep behavior of the tantalum alloy Astar 811C --- as a function of stress, temperature, and grain size [NASA-TP-1691] p0080 N80-32489

GRAPHITE

Effect of thermal aging on the tribological properties of polyimide films and polyimide-bonded graphite fluoride films [ASLE PREPRINT 79-AM-3B-1] p0088 A80-12094

Mechanisms of lubrication and wear of a bonded solid-lubricant film [ASLE PREPRINT 80-AM-3E-1] p0122 A80-43163

Lubrication and wear mechanisms of polyimide-bonded graphite fluoride films subjected to low contact stress [NASA-TP-1584] p0085 N80-17220

Silicone modified resins for graphite fiber laminates [NASA-CR-159750] p0072 N80-22407

Properties of PMR Polyimide composites made with improved high strength graphite fibers [NASA-TM-81557] p0069 N80-28444

Characterization of PMR-15 polyimide composition in thermo-oxidatively exposed graphite fiber composites [NASA-TM-81565] p0088 N80-28524

GRAPHITE-EPOXY COMPOSITE MATERIALS

Mechanical property characterization of intraply hybrid composites p0070 A80-20954

Dynamic response of damaged angleplied fiber composites p0070 A80-27982

Fire test method for graphite fiber reinforced plastics p0070 A80-31169

Burning characteristics and fiber retention of graphite/resin matrix composites p0070 A80-32062

Fiber release characteristics of graphite hybrid composites p0073 A80-32063

Hybrid composites that retain graphite fibers on burning p0073 A80-32064

Improved fiber retention by the use of fillers in graphite fiber/resin matrix composites p0071 A80-32066

Fracture modes of high modulus graphite/epoxy angleplied laminates subjected to off-axis tensile loads p0071 A80-32069

High char imide-modified epoxy matrix resins p0071 A80-34789

Dynamic response of damaged angleplied fiber composites [NASA-TM-79281] p0067 N80-11145

Second generation PMR polyimide/fiber composites [NASA-CR-159666] p0072 N80-12118

Mechanical property characterization of intraply hybrid composites [NASA-TM-79306] p0067 N80-12120

Improved fiber retention by the use of fillers in graphite fiber/resin matrix composites [NASA-TM-79288] p0067 N80-13171

Quiet Clean Short-Haul Experimental Engine (QCSEE) Under-The-Wing (UTW) graphite/PMR cowl development [NASA-CR-135279] p0029 N80-14119

Burning characteristics and fiber retention of graphite/resin matrix composites [NASA-TM-79314] p0067 N80-14196

Quiet Clean Short-haul Experimental Engine (QCSEE). Composite fan frame subsystem test report [NASA-CR-135010] p0035 N80-15098

Quiet Clean Short-haul Experimental Engine (QCSEE) composite fan frame design report [NASA-CR-135278] p0031 N80-15110

Analyses of moisture in polymers and composites [NASA-CR-159745] p0091 N80-15264

Fracture modes of high modulus graphite/epoxy angleplied laminates subjected to off-axis tensile loads [NASA-TM-81405] p0068 N80-16102

Application of composite materials to turbofan engine fan exit guide vanes [NASA-TM-81432] p0068 N80-18106

Fire test method for graphite fiber reinforced plastics [NASA-TM-81436] p0068 N80-18107

GRAPHS (CHARTS)

A reduced volumetric expansion factor plot p0107 A80-10038

SUBJECT INDEX

HEAT RESISTANT ALLOYS

GRAVITATION
 NT REDUCED GRAVITY
GRAVITATIONAL EFFECTS
 LeRC reduced gravity fluid management technology program
 [NASA-TM-81450] p0051 N80-20304
GRAVITY GRADIENT SATELLITES
 NT ATS 5
 NT ATS 6
GREAT LAKES (NORTH AMERICA)
 NT LAKE ERIE
 NT LAKE MICHIGAN
 NT LAKE ONTARIO
 NT LAKE SUPERIOR
 Quantitative interpretation of Great Lakes remote sensing data
 p0157 A80-45005
GREEN FUNCTION
 Reciprocity principle in duct acoustics
 p0170 A80-20956
GREEN THEOREM
 U GREEN FUNCTION
GRINDING
 Tribological properties of silicon carbide in metal removal process
 [NASA-TM-79238] p0114 N80-16340
GROUND STATIONS
 Low sidelobe level low-cost earth station antennas for the 12 GHz broadcasting satellite service
 [NASA-CR-159703] p0098 N80-12259
GROUND TESTS
 NT COLD FLOW TESTS
 NT STATIC FIRING
 Initial comparison of SSPM ground test results and flight data to NASCAP simulations --- Satellite Surface Potential Monitor NASA Charging Analyzer Program
 [AIAA PAPER 80-0336] p0054 A80-29751
 CF6-50 Short Core Exhaust Nozzle
 [AIAA PAPER 80-1196] p0025 A80-41514
GROWTH
 NT CRYSTAL GROWTH
 NT DIRECTIONAL SOLIDIFICATION (CRYSTALS)
GUIDANCE SENSORS
 Flight test of navigation and guidance sensor errors measured on STOL approaches
 [NASA-TM-81154] p0028 N80-13041
GUIDE VANES
 NT JET VANES
 Design, durability and low cost processing technology for composite fan exit guide vanes
 [NASA-CR-159677] p0027 N80-12091
 Application of composite materials to turbofan engine fan exit guide vanes
 [NASA-TM-81432] p0068 N80-18106
GYROPLANES
 U HELICOPTERS

H

HALIDES
 NT CALCIUM FLUORIDES
 NT FLUORIDES
 NT SODIUM CHLORIDES
HALL CURRENTS
 U ELECTRIC CURRENT
HALOCARBONS
 NT FLUOROCARBONS
HALOGEN COMPOUNDS
 NT CALCIUM FLUORIDES
 NT FLUORIDES
 NT FLUORINE COMPOUNDS
 NT FLUOROCARBONS
 NT FLUOROPOLYMERS
 NT SODIUM CHLORIDES
HANDBOOKS
 NT USER MANUALS (COMPUTER PROGRAMS)
HARDENING (MATERIALS)
 NT HOT PRESSING
 NT PRECIPITATION HARDENING
 NT STRAIN HARDENING
HAZARDS
 NT AIRCRAFT HAZARDS
 NT TOXIC HAZARDS
 Mod 1 wind turbine generator failure modes and effects analysis
 [NASA-CR-159494] p0150 N80-20864
 Potential release of fibers from burning carbon composites --- aircraft fires

[NASA-TM-80214] p0069 N80-29431
HEALTH
 NT PUBLIC HEALTH
HEALTH PHYSICS
 NT PUBLIC HEALTH
HEAT DISSIPATION
 U COOLING
HEAT DISSIPATION CHILLING
 U COOLING
HEAT EFFECTS
 U TEMPERATURE EFFECTS
HEAT EQUATIONS
 U THERMODYNAMICS
HEAT EXCHANGERS
 Active heat exchange system development for latent heat thermal energy storage
 [NASA-CR-159726] p0149 N80-18562
 Heat exchanger and method of making --- rocket lining
 [NASA-CASE-LEW-12441-2] p0105 N80-24573
 Feasibility study of silicon nitride regenerators
 [NASA-CR-159713] p0184 N80-25209
 Thermal energy storage systems using fluidized bed heat exchangers
 [NASA-CR-159868] p0153 N80-28866
 Active heat exchange system development for latent heat thermal energy storage
 [NASA-CR-159727] p0154 N80-29857
 Regenerator matrix physical property data
 [NASA-CR-159854] p0185 N80-30228
HEAT FLUX
 Analytical and experimental spur gear tooth temperature as affected by operating variables
 p0123 A80-46412
HEAT GENERATION
 Cogeneration Technology Alternatives Study (CTAS). Volume 6: Computer data. Part 1: Coal-fired nocogeneration process boiler, section A
 [NASA-CR-159770-PT-1-A] p0154 N80-30888
 Cogeneration Technology Alternatives Study (CTAS). Volume 6: Computer data. Part 1: Coal-fired nocogeneration process boiler, section B
 [NASA-CR-159770-PT-1-B] p0154 N80-30889
 Cogeneration Technology Alternatives Study (CTAS). Volume 6: Computer data. Part 2: Residual-fired nocogeneration process boiler
 [NASA-CR-159770-PT-2] p0155 N80-30890
HEAT OF COMBUSTION
 Sintered silicon nitride recuperator fabrication
 [NASA-CR-159706] p0090 N80-15263
HEAT OF FUSION
 Active heat exchange system development for latent heat thermal energy storage
 [NASA-CR-159727] p0154 N80-29857
HEAT PIPES
 Heat pipe cooling of power processing magnetics
 [AIAA PAPER 79-2082] p0107 A80-20960
 Heat pipe cooling of power processing magnetics
 [NASA-TM-79270] p0101 N80-11327
 Heat pipe cooled power magnetics
 [NASA-CR-159659] p0103 N80-13362
 Depriming of arterial heat pipes: An investigation of CTS thermal excursions
 [NASA-CR-165153] p0108 N80-32688
HEAT RESISTANCE
 U THERMAL RESISTANCE
HEAT RESISTANT ALLOYS
 NT NIOBIUM ALLOYS
 NT REFRACTORY METAL ALLOYS
 NT TANTALUM ALLOYS
 The erosion/corrosion of small superalloy turbine rotors operating in the effluent of a PFB coal combustor
 p0080 A80-10043
 Hot corrosion of four superalloys - HA-188, S-57, IN-617, and TD-NiCrAl
 p0081 A80-14445
 Effects of thermally induced porosity on an as-HIP powder metallurgy superalloy
 p0082 A80-29990
 Effects of fine porosity on the fatigue behavior of a powder metallurgy superalloy
 p0082 A80-35495
 An experimental, low-cost, silicon-aluminide high-temperature coating for superalloys
 p0082 A80-35501
 Application of superalloy powder metallurgy for aircraft engines
 p0122 A80-44240

HEAT SOURCES

SUBJECT INDEX

Anisotropy of nickel-base superalloy single crystals
p0083 A80-51573

Materials and structures technology
p0012 N80-10210

Effect of thermally induced porosity on an as-HIP
powder metallurgy superalloy
[NASA-TM-79263] p0076 N80-11189

Characterization of an oxide dispersion
strengthened superalloy, MA-6000E, for turbine
blade applications --- turbine blade
[NASA-CR-159493] p0083 N80-13218

Effect of sodium, potassium, magnesium, calcium,
and chlorine on the high temperature corrosion
of IN-100, U-700, IN-792, and Mar M-509 ---
coal-derived liquid fuel combustion in turbines
[NASA-TM-79309] p0076 N80-15235

Chemical processes involved in the initiation of
hot corrosion of B-1900 and NASA-TRW VIA
[NASA-TM-81399] p0077 N80-17199

Anisotropy of nickel-base superalloy single crystals
[NASA-TM-81437] p0077 N80-17200

Study of the effects of gaseous environments on
the hot corrosion of superalloy materials
[NASA-CR-159747] p0083 N80-18155

Effects of impurities in coal-derived liquids on
accelerated hot corrosion of superalloys
[NASA-TM-81384] p0077 N80-18157

An experimental, low-cost, silicon-aluminate
high-temperature coating for superalloys
[NASA-TM-81455] p0078 N80-20370

Application of superalloy powder metallurgy for
aircraft engines
[NASA-TM-81466] p0078 N80-21488

Fouling and the inhibition of salt corrosion ---
hot corrosion of superalloys
[NASA-TM-81469] p0078 N80-21492

Effects of fine porosity on the fatigue behavior
of a powder metallurgy superalloy
[NASA-TM-81448] p0078 N80-21493

Performance of two-layer thermal barrier systems
on directionally solidified Ni-Al-Mo and
comparative effects of alloy thermal expansion
on system life
[NASA-TM-81604] p0080 N80-32487

HEAT SOURCES
NT GEOTHERMAL RESOURCES

HEAT STORAGE
Energy conservation and environmental benefits of
thermal energy storage systems in the pulp and
paper industry
p0146 A80-48194

Candidate thermal energy storage technologies for
solar industrial process heat applications
[NASA-TM-81380] p0138 N80-15560

High-temperature molten salt thermal energy
storage systems
[NASA-CR-159663] p0148 N80-17547

Active heat exchange system development for latent
heat thermal energy storage
[NASA-CR-159726] p0149 N80-18562

Engineering evaluation of a sodium hydroxide
thermal energy storage module
[NASA-TM-81417] p0140 N80-18563

Thermal Energy Storage: Fourth Annual Review
Meeting
[NASA-CR-2125] p0141 N80-22788

Program definition and assessment overview --- for
thermal energy storage project management
p0141 N80-22790

Industrial storage applications overview
p0142 N80-22795

Collection and dissemination of TES system
information for the paper and pulp industry
p0142 N80-22797

Heat storage in alloy transformations
[NASA-CR-159787] p0151 N80-24759

Thermal energy storage
[NASA-TM-81514] p0143 N80-25779

Thermal energy storage systems using fluidized bed
heat exchangers
[NASA-CR-159868] p0153 N80-28866

Active heat exchange system development for latent
heat thermal energy storage
[NASA-CR-159727] p0154 N80-29857

High temperature thermal energy storage in steel
and sand
[NASA-CR-159708] p0154 N80-29860

HEAT TESTS
U HIGH TEMPERATURE TESTS

HEAT TRANSFER
A reduced volumetric expansion factor plot
p0107 A80-10038

Thermophysical property data - Who needs them ---
similarity principle applications in fluid
mechanics and heat transfer
[ASME PAPER 79-WA/HT-17] p0180 A80-18630

Full-coverage film cooling. II - Heat transfer
data and numerical simulation
[ASME PAPER 80-GT-44] p0109 A80-42177

Impact of new instrumentation on advanced turbine
research
[NASA-TM-79301] p0015 N80-15133

Comparison of predicted and experimental
performance of large-bore roller bearing
operating to 3.0 million DN
[NASA-TP-1599] p0114 N80-15410

Prediction method for two-dimensional aerodynamic
losses of cooled vanes using integral
boundary-layer parameters
[NASA-TP-1623] p0002 N80-17030

Analytical and experimental spur gear tooth
temperature as affected by operating variables
[NASA-TM-81419] p0115 N80-16403

Engineering evaluation of a sodium hydroxide
thermal energy storage module
[NASA-TM-81417] p0140 N80-18563

Similarity tests of turbine vanes, effects of
ceramic thermal barrier coatings
[NASA-TM-81473] p0105 N80-21706

Significance of thermal contact resistance in
two-layer thermal-barrier-coated turbine vanes
[NASA-TM-81483] p0018 N80-23310

Two-phase working fluids for the temperature range
of 50 to 350 deg, phase 2
[NASA-CR-159847] p0108 N80-23599

Extension of similarity test procedures to cooled
engine components with insulating ceramic coatings
[NASA-TP-1615] p0105 N80-24577

Conceptual design of two-phase fluid mechanics and
heat transfer facility for spacelab
[NASA-CR-159810] p0049 N80-27403

HEAT TRANSFER COEFFICIENTS
Full-coverage film cooling. I - Comparison of heat
transfer data for three injection angles
[ASME PAPER 80-GT-43] p0108 A80-42176

HEAT TRANSMISSION
NT HEAT TRANSFER

HEAT TREATMENT
NT ANNEALING

Characterization and properties of controlled
nucleation thermochemical deposited (CNTD)
silicon carbide
[NASA-TM-79277] p0085 N80-13254

HEATING
NT SOLAR HEATING

HEATING EQUIPMENT
NT BOILERS
NT FURNACES

Engineering evaluation of a sodium hydroxide
thermal energy storage module
[NASA-TM-81417] p0140 N80-18563

HELICOPTER ATTITUDE INDICATORS
U HELICOPTERS

HELICOPTER DESIGN
NASA gear research and its probable effect on
rotorcraft transmission design
p0120 A80-13068

HELICOPTER ROTORS
U ROTARY WINGS

HELICOPTER TAIL ROTORS
Balancing of a power-transmission shaft with the
application of axial torque
[ASME PAPER 80-GT-143] p0121 A80-2256

HELICOPTERS
NT RIGID ROTOR HELICOPTERS
NT TANDEM ROTOR HELICOPTERS

A phenomenological model of the dynamic stall of a
helicopter blade profile
[ONERA, TP NO. 1979-149] p0006 A80-20086

Mechanical components
p0013 N80-10213

HELIUM PLASMA
Study of a rare-gas transverse fast discharge
p0176 A80-11366

HELIX TUBES
U TRAVELING WAVE TUBES

HELMHOLTZ VORTICITY EQUATION
Effect of grazing flow on the nonlinear acoustic

SUBJECT INDEX

NILSCH TUBES

behavior of helmholtz resonators p0095 N80-31619

HERMES SATELLITE
 U COMMUNICATIONS TECHNOLOGY SATELLITE

HIGH MELTING COMPOUNDS
 U REFRACTORY MATERIALS

HIGH PRESSURE
 Some flow characteristics of conventional and tapered high-pressure-drop simulated seals [ASLE PREPRINT 79-LC-3B-2] p0120 A80-14727
 Advanced cooling techniques for high-pressure, hydrocarbon-fueled rocket engines [AIAA PAPER 80-1266] p0060 A80-38994
 Advanced cooling techniques for high-pressure hydrocarbon-fueled engines [NASA-CR-159790] p0061 N80-17141
 Cooling of high pressure rocket thrust chambers with liquid oxygen [NASA-TM-81503] p0057 N80-23365
 CF6 jet engine performance improvement program: High pressure turbine aerodynamic performance improvement [NASA-CR-159832] p0040 N80-26302

HIGH PRESSURE OXYGEN
 Mechanical impact tests of materials in oxygen effects of contamination --- Teflon, stainless steel, and aluminum [NASA-TP-1571] p0093 N80-21551

HIGH SPEED
 Design of elastomer dampers for a high-speed flexible rotor [ASME PAPER 79-DET-88] p0121 A80-15736
 Comparison of predicted and experimental performance of large-bore roller bearing operating to 3.0 million DN [NASA-TP-1599] p0114 N80-15410
 Performance of computer-optimized tapered-roller bearings to 2.4 million DN [NASA-TM-81414] p0114 N80-16342
 Calculated and experimental data for a 118-mm bore roller bearing to 3 million DN [NASA-TM-81427] p0116 N80-19496
 Lubrication of optimized-design tapered-roller bearings to 2.4 million DN [NASA-TP-1714] p0119 N80-29734
 Effect of cage design on characteristics of high-speed-jet-lubricated 35-millimeter-bore ball bearing --- turbojet engines [NASA-TP-1732] p0120 N80-33749

HIGH SPEED FLIGHT
 U HIGH SPEED

HIGH STRENGTH
 Properties of PMR Polyimide composites made with improved high strength graphite fibers [NASA-TM-81557] p0069 N80-28444

HIGH STRENGTH ALLOYS
 NT ASTROLOY (TRADEMARK)
 NT HIGH STRENGTH STEELS
 Strengthening of tough iron-12% nickel-reactive metal alloys at 77 K by copper additions p0174 A80-34049
 Quantitative ultrasonic evaluation of engineering properties in metals, composites, and ceramics p0130 A80-39641
 Development of a high strength hot isostatically pressed /HIP/ disk alloy, MERL 76 p0084 A80-44108
 High toughness-high strength iron alloy [NASA-CASE-LEW-12542-3] p0079 N80-32484

HIGH STRENGTH STEELS
 Endurance and failure characteristics of modified Vasco X-2, CBS 600 and AISI 9310 spur gears --- aircraft construction materials [NASA-TM-81421] p0116 N80-18405

HIGH TEMPERATURE
 High-temperature molten salt thermal energy storage systems [NASA-CR-159663] p0148 N80-17547
 Composite wall concept for high temperature turbine shrouds: Survey of low modulus strain isolator materials [NASA-TM-81443] p0086 N80-20398
 High temperature self-lubricating coatings for air lubricated foil bearings for the automotive gas turbine engine [NASA-CR-159848] p0091 N80-26448
 High temperature thermal energy storage in steel and sand [NASA-CR-159708] p0154 N80-29860

Autoignition characteristics of aircraft-type fuels [NASA-CR-159886] p0095 N80-30535

HIGH TEMPERATURE ALLOYS
 U HEAT RESISTANT ALLOYS

HIGH TEMPERATURE ENVIRONMENTS
 Preliminary study of a solar selective coating system using black cobalt oxide for high temperature solar collectors p0082 A80-35500
 Development of exothermically cast single-crystal Mar-M 247 and derivative alloys [AIRESEARCH-21-3469] p0084 A80-45825
 Corrosion resistant thermal barrier coating --- protecting gas turbines and other heat engine parts [NASA-CASE-LEW-13088-1] p0067 N80-11142
 Optimal thermionic energy conversion with established electrodes for high-temperature topping and process heating --- coal combustion product environments [NASA-TM-81555] p0175 N80-33221

HIGH TEMPERATURE FLUIDS
 NT HIGH TEMPERATURE GASES

HIGH TEMPERATURE GASES
 Free-piston regenerative hot gas hydraulic engine [NASA-CASE-LEW-12274-1] p0119 N80-31790

HIGH TEMPERATURE LUBRICANTS
 Comparison of the weight loss and adherence of nine different polyimide films thermally aged at 315 C and 350 C in air --- high temperature lubricants [NASA-TM-81381] p0086 N80-18183

HIGH TEMPERATURE MATERIALS
 U REFRACTORY MATERIALS

HIGH TEMPERATURE PLASMAS
 Parametric dependence of ion temperature and electron density in the SUMMA hot-ion plasma using laser light scattering and emission spectroscopy p0176 A80-46265

HIGH TEMPERATURE RESEARCH
 Improving the stress rupture and creep of silicon nitride --- turbine materials [NASA-CR-159585] p0072 N80-10318
 Feasibility of Kevlar 49/PMR-15 polyimide for high temperature applications [NASA-TM-81560] p0069 N80-27429

HIGH TEMPERATURE TESTS
 Thick ceramic coating development for industrial gas turbines - A program plan [SR79-M-4702-05] p0091 A80-10042
 Hot corrosion of four superalloys - HA-188, S-57, IM-617, and TD-NiCrAl p0081 A80-14445
 Creep-rupture behavior of seven iron-base alloys after long term aging at 760 deg in low pressure hydrogen [NASA-TM-81534] p0080 N80-32488

HIGH VOLTAGES
 Plasma collection by high voltage spacecraft at low earth orbit [AIAA PAPER 80-0042] p0055 A80-18249
 Radiation damage in high voltage silicon solar cells p0179 A80-44234
 Space environmental interactions with biased spacecraft surfaces p0055 A80-46897
 The planar multijunction cell - A new solar cell for earth and space p0146 A80-48205
 Interaction of high voltage surfaces with the space plasma --- solar arrays [NASA-CR-159731] p0176 N80-14923
 Planar multijunction high voltage solar cells [NASA-TM-81389] p0178 N80-16914
 Experimental results on plasma interactions with large surfaces at high voltages [NASA-TM-81423] p0175 N80-18946
 Radiation damage in high voltage silicon solar cells [NASA-TM-81478] p0178 N80-23180
 Interaction of high voltage surfaces with the space plasma [NASA-CR-165131] p0177 N80-32223

HILLER MILITARY AIRCRAFT
 U MILITARY AIRCRAFT

NILSCH TUBES
 Influence of coolant tube curvature on film cooling effectiveness as detected by infrared imagery

HINGE MOMENTS

SUBJECT INDEX

[NASA-TP-1546] p0013 N80-11087
HINGE MOMENTS
 U TORQUE
HINGED ROTOR BLADES
 U ROTARY WINGS
HINGES
 NT FLAPPING HINGES
HOHMANN TRAJECTORIES
 U TRANSFER ORBITS
HOHMANN TRANSFER ORBITS
 U TRANSFER ORBITS
HOLLOW CATHODES
 Primary electric propulsion technology study ---
 for thruster wear-out mechanisms
 [NASA-CR-159688] p0061 N80-13158
 Hydrogen hollow cathode ion source
 [NASA-CASE-LEW-12940-1] p0174 N80-33186
 Baffle aperture design study of hollow cathode
 equipped ion thrusters
 [NASA-CR-165164] p0064 N80-33476
HONEYCOMB STRUCTURES
 Some considerations of the performance of two
 honeycomb gas path seal material systems
 [NASA-TM-81398] p0077 N80-16143
HOT CORROSION
 NT TEMPERATURE DEPENDENCE
 The chemistry of sodium chloride involvement in
 processes related to hot corrosion p0074 A80-10041
 Hot corrosion of four superalloys - HA-188, S-57,
 IN-617, and TD-NiCrAl p0081 A80-14445
 An experimental, low-cost, silicon-aluminide
 high-temperature coating for superalloys p0082 A80-35501
 Effect of sodium, potassium, magnesium, calcium,
 and chlorine on the high temperature corrosion
 of IN-100, U-700, IN-792, and MAR M-509 p0083 A80-42262
 [ASME PAPER 80-GT-150]
 Theory of deposition of condensable impurities on
 surfaces immersed in combustion gases p0033 N80-15130
 [NASA-CR-159716]
 Experimental studies of the formation/deposition
 of sodium sulfate in/from combustion gases ---
 hot corrosion of gas turbine engine components
 [NASA-CR-159753] p0033 N80-15131
 An investigation of the initiation stage of hot
 corrosion in Ni-base alloys p0083 N80-15233
 [NASA-CR-159718]
 Effect of sodium, potassium, magnesium, calcium,
 and chlorine on the high temperature corrosion
 of IN-100, U-700, IN-792, and MAR M-509 ---
 coal-derived liquid fuel combustion in turbines
 [NASA-TM-79309] p0076 N80-15235
 Study of the effects of gaseous environments on
 the hot corrosion of superalloy materials
 [NASA-CR-159747] p0083 N80-18155
 Fouling and the inhibition of salt corrosion ---
 hot corrosion of superalloys p0078 N80-21492
 [NASA-TM-81469]
 Improved PFB operations: 400-hour turbine test
 results --- coal combustion products and hot
 corrosion in gas turbines p0079 N80-26426
 [NASA-TM-81511]
 Hot corrosion of Co-Cr, Co-Cr-Al, and Ni-Cr alloys
 in the temperature range of 700-750 deg C
 [NASA-CR-159689] p0084 N80-26427
HOT GAS SYSTEMS
 U HIGH TEMPERATURE GASES
HOT GASES
 U HIGH TEMPERATURE GASES
HOT JET EXHAUST
 U HIGH TEMPERATURE GASES
 U JET EXHAUST
HOT JETS
 U JET FLOW
HOT PLASMAS
 U HIGH TEMPERATURE PLASMAS
HOT PRESSING
 Effects of thermally induced porosity on an as-HIP
 powder metallurgy superalloy p0082 A80-29990
 Development of a high strength hot isostatically
 pressed /HIP/ disk alloy, MERL 76 p0084 A80-44108
 Application of superalloy powder metallurgy for
 aircraft engines p0122 A80-44240

Effect of starting powder characteristics on
 density, microstructure and low temperature
 oxidation behavior of a Si3N4 - 8 w/o Y2O3 ceramic
 p0090 A80-46100
 Effect of thermally induced porosity on an as-HIP
 powder metallurgy superalloy p0076 N80-11189
 [NASA-TM-79263]
 Application of superalloy powder metallurgy for
 aircraft engines p0078 N80-21488
 [NASA-TM-81466]
HOT-WIRE FLOWMETERS
 Three dimensional mean flow and turbulence
 characteristics of the near wake of a compressor
 rotor blade p0005 N80-27288
 [NASA-CR-159518]
HOT-WIRE TURBULENCE METERS
 U HOT-WIRE FLOWMETERS
HOUSINGS
 NT COWLINGS
HOVERING STABILITY
 Examination of the flap-lag stability of rigid
 articulated rotor blades p0010 A80-15123
HUGHES MILITARY AIRCRAFT
 U MILITARY AIRCRAFT
HYBRID COMBUSTION
 U HYBRID PROPELLANT ROCKET ENGINES
HYBRID PROPELLANT ROCKET ENGINES
 Cooling of high pressure rocket thrust chambers
 with liquid oxygen p0060 A80-38992
 [AIAA PAPER 80-1260]
HYBRID PROPULSION
 Advanced propulsion system for hybrid vehicles
 [NASA-CR-159771] p0184 N80-26212
HYBRID STRUCTURES
 Mechanical property characterization of intraply
 hybrid composites p0070 A80-20954
HYDRAULIC ACTUATORS
 U ACTUATORS
 U HYDRAULIC EQUIPMENT
HYDRAULIC EQUIPMENT
 Single-stage electrohydraulic servosystem for
 actuating on airflow valve with frequencies to
 500 hertz p0046 N80-29369
 [NASA-TP-1678]
HYDRAULIC FLUIDS
 Free-piston regenerative hot gas hydraulic engine
 [NASA-CASE-LEW-12274-1] p0119 N80-31790
HYDRAULIC HEATING SOURCES
 U HYDRAULIC EQUIPMENT
HYDRAULIC PUMPS
 U HYDRAULIC EQUIPMENT
HYDRAULIC SYSTEMS
 U HYDRAULIC EQUIPMENT
HYDRAULIC VALVES
 U HYDRAULIC EQUIPMENT
 U VALVES
HYDRAULICS
 Hydraulic forces caused by annular pressure seals
 in centrifugal pumps p0126 N80-29718
HYDROAEROMECHANICS
 U AERODYNAMICS
HYDROCARBON COMBUSTION
 An analytical study of nitrogen oxides and carbon
 monoxide emissions in hydrocarbon combustion
 with added nitrogen - Preliminary results
 [ASME PAPER 80-GT-60] p0074 A80-42190
 Low NO(x) heavy fuel combustor program
 [NASA-TM-79313] p0137 N80-13624
 An analytical study of nitrogen oxides and carbon
 monoxide emissions in hydrocarbon combustion
 with added nitrogen, preliminary results
 [NASA-TM-79296] p0157 N80-13721
 Flame tube parametric studies for control of fuel
 bound nitrogen using rich-lean two-stage
 combustion p0141 N80-21837
 [NASA-TM-81472]
HYDROCARBON FUELS
 NT DIESEL FUELS
 NT FOSSIL FUELS
 NT JET ENGINE FUELS
 NT JP-5 JET FUEL
 Design and evaluation of high performance rocket
 engine injectors for use with hydrocarbon fuels
 p0059 A80-20957
 Advanced cooling techniques for high-pressure,
 hydrocarbon-fueled rocket engines

SUBJECT INDEX

IMPACT LOADS

[AIAA PAPER 80-1266] p0060 A80-38994
Design and evaluation of high performance rocket engine injectors for use with hydrocarbon fuels [NASA-TM-79319] p0056 N80-13163
Advanced cooling techniques for high-pressure hydrocarbon-fueled engines [NASA-CR-159790] p0061 N80-17141
Design and evaluation of high performance rocket engine injectors for use with hydrocarbon fuels p0094 N80-31621

HYDROCARBONS
NT CETANE
NT LIQUEFIED NATURAL GAS
NT METHANE
Performance, emissions, and physical characteristics of a rotating combustion aircraft engine, supplement A [NASA-CR-135119] p0041 N80-27361
Gas phase oxidation downstream of a catalytic combustor [NASA-TM-81551] p0144 N80-29863
Energy efficient engine [NASA-CR-159685] p0045 N80-33408

HYDRODYNAMIC EQUATIONS
NT HELMHOLTZ VORTICITY EQUATION
HYDRODYNAMIC STABILITY
U FLOW STABILITY
HYDRODYNAMICS
NT ELASTOHYDRODYNAMICS
NT MAGNETOHYDRODYNAMICS
Self-acting lift-pad geometry for circumferential seals: A noncontacting concept --- performance tests on hydrodynamic seals [NASA-TP-1583] p0114 N80-14403
Limit cycles of a flexible shaft with hydrodynamic journal bearings in unstable regimes p0127 N80-29725
Instability thresholds for flexible rotors in hydrodynamic bearings p0128 N80-29730
Stabilization of aerodynamically excited turbomachinery with hydrodynamic journal bearings and supports p0128 N80-29731

HYDROGEN
NT HYDROGEN ATOMS
NT HYDROGEN IONS
NT HYDROGEN PLASMA
NT LIQUID HYDROGEN
Results of duct area ratio changes in the NASA Lewis H2-O2 combustion MHD experiment [NASA-TM-79308] p0175 N80-12881
Method of cross-linking polyvinyl alcohol and other water soluble resins [NASA-CASE-LEW-13103-1] p0088 N80-32516

HYDROGEN AIR FUEL CELLS
U HYDROGEN OXYGEN FUEL CELLS
HYDROGEN ATOMS
Apparatus for trapping and thermal detection of atomic hydrogen in high magnetic fields at low temperatures p0111 A80-34546
Atomic hydrogen storage --- cryotrapping and magnetic field strength [NASA-CASE-LEW-12081-2] p0093 N80-20402

HYDROGEN FUELS
Turbine engine altitude chamber and flight testing with liquid hydrogen p0023 A80-10034
Results of duct area ratio changes in the NASA Lewis H2-O2 combustion MHD experiment [AIAA PAPER 80-0023] p0176 A80-18243
Cooling of high pressure rocket thrust chambers with liquid oxygen [AIAA PAPER 80-1260] p0060 A80-38992
Experiments on H2-O2 MHD power generation p0176 A80-44239
Experiments on H2-O2MHD power generation [NASA-TM-81424] p0175 N80-16886

HYDROGEN IONS
Hydrogen hollow cathode ion source [NASA-CASE-LEW-12940-1] p0174 N80-33186

HYDROGEN OXYGEN ENGINES
Analytical investigation of two hydrogen-oxygen rocket engine systems for low-thrust application p0060 A80-35503
Experiments on H2-O2 MHD power generation p0176 A80-44239

Performance of a transpiration-regenerative cooled rocket thrust chamber [NASA-CR-159742] p0061 N80-14189
Liquid oxygen/liquid hydrogen auxiliary power system thruster investigation [NASA-CR-159674] p0062 N80-15202
Analytical investigation of two hydrogen oxygen rocket engine systems for low-thrust application [NASA-TM-81420] p0056 N80-17138
Analytical investigation of two hydrogen-oxygen rocket engine systems for low-thrust application --- for orbital transfer p0057 N80-30382

HYDROGEN OXYGEN FUEL CELLS
Advanced technology light weight fuel cell program --- orbiting space vehicle long-life hydrogen oxygen fuel cell [NASA-CR-159807] p0149 N80-19615

HYDROGEN PLASMA
Parametric dependence of ion temperature and electron density in the SUMMA hot-ion plasma using laser light scattering and emission spectroscopy p0176 A80-46265

HYDROMAGNETIC STABILITY
U MAGNETOHYDRODYNAMIC STABILITY
HYDROMAGNETICS
U MAGNETOHYDRODYNAMICS
HYDROMAGNETISM
U MAGNETOHYDRODYNAMICS
HYDROMECHANICS
NT ELASTOHYDRODYNAMICS
NT HYDRODYNAMICS
NT MAGNETOHYDRODYNAMICS
HYDROSTATIC PRESSURE
Vibration and buckling of rectangular plates under in-plane hydrostatic loading p0133 A80-45364

HYDROX ENGINES
U HYDROGEN OXYGEN ENGINES
HYDROXIDES
NT SODIUM HYDROXIDES
HYDROXYL COMPOUNDS
NT POLYVINYL ALCOHOL
HYPERFINE STRUCTURE
Hyperfine magnetic field at Cd impurity site in L2/1/ Heusler alloys Rh2MnGe and Rh2MnPt by TDPAC technique --- Time Differential Perturbed Angular Correlation p0178 A80-16843

HYPERSONIC FLIGHT
Hypersonic propulsion --- supersonic combustion ramjet engines p0013 N80-10217

ICE
NT ICEBERGS
ICEBERGS
Possible methods for distinguishing icebergs from ships by aerial remote sensing [NASA-TM-79310] p0136 N80-15538

IGNITION
Autoignition characteristics of aircraft-type fuels [NASA-CR-159886] p0095 N80-30535

IGNITION SYSTEMS
8-cm Engineering Model Thruster technology - A review of recent developments [AIAA PAPER 79-2103] p0064 A80-13311

IMAGE PROCESSING
Computerized video densitometry method for rapid analysis of infrared photographic images --- temperature distribution across a turbine blade [NASA-TP-1686] p0110 N80-25635

IMAGERY
NT INFRARED IMAGERY
NT INFRARED PHOTOGRAPHY
IMPACT DAMAGE
Scanning-electron-microscope study of normal-impingement erosion of ductile metals [NASA-TP-1609] p0077 N80-16141
Two-dimensional finite-element analyses of simulated rotor-fragment impacts against rings and beams compared with experiments [NASA-CR-159645] p0038 N80-22323

IMPACT LOADS
Dynamic response of damaged angleply fiber composites

IMPACT PRESSURES

SUBJECT INDEX

IMPACT PRESSURES p0070 A80-27982
 U IMPACT LOADS
 IMPACT TESTS
 Program for impact testing of spar-shell fan blades, test report [NASA-CR-135393] p0037 N80-21328
 An investigation into the role of adhesion in the erosion of ductile metals [NASA-TN-81458] p0078 N80-21489
 Mechanical impact tests of materials in oxygen effects of contamination --- Teflon, stainless steel, and aluminum [NASA-TP-1571] p0093 N80-21551
 IMPEDANCE
 NT ACOUSTIC IMPEDANCE
 NT CONTACT RESISTANCE
 NT ELECTRICAL RESISTANCE
 IMPELLER BLADES
 U ROTOR BLADES (TURBOMACHINERY)
 IMPINGEMENT
 NT JET IMPINGEMENT
 IMPLANTATION
 NT ION IMPLANTATION
 IMPREGNATING
 Life test studies on tungsten impregnated cathodes p0103 A80-45122
 IMPURITIES
 Effect of sodium, potassium, magnesium, calcium, and chlorine on the high temperature corrosion of IN-100, U-700, IN-792, and MAR M-509 [ASME PAPER 80-GT-150] p0083 A80-42262
 Effect of sodium, potassium, magnesium, calcium, and chlorine on the high temperature corrosion of IN-100, U-700, IN-792, and MAR M-509 --- coal-derived liquid fuel combustion in turbines [NASA-TN-79309] p0076 N80-15235
 IN-FLIGHT MONITORING
 Expanded study of feasibility of measuring in-flight 747/JT9D loads, performance, clearance, and thermal data [NASA-CR-159717] p0036 N80-16063
 INCOMPRESSIBLE FLUIDS
 Damping in tapered annular seals for an incompressible fluid [NASA-TP-1646] p0116 N80-19495
 INDICATING INSTRUMENTS
 NT ANEMOMETERS
 NT LASER ANEMOMETERS
 INDUCED FLUID FLOW
 U FLUID FLOW
 INDUCTION SYSTEMS
 U INTAKE SYSTEMS
 INDUSTRIAL ENERGY
 Energy conservation and environmental benefits of thermal energy storage systems in the pulp and paper industry p0146 A80-48194
 Candidate thermal energy storage technologies for solar industrial process heat applications [NASA-TN-81380] p0138 N80-15560
 Industrial storage applications overview p0142 N80-22795
 Collection and dissemination of TES system information for the paper and pulp industry p0142 N80-22797
 Cogeneration Technology Alternatives Study (CTAS).
 Volume 1: Summary report [NASA-CR-159765] p0151 N80-24797
 Cogeneration technology alternatives study.
 Volume 1: Summary report [NASA-CR-159759] p0152 N80-25792
 Cogeneration technology alternatives study.
 Volume 2: Industrial process characteristics [NASA-CR-159760] p0152 N80-25793
 Cogeneration technology alternatives study.
 Volume 4: Heat Sources, balance of plant and auxiliary systems [NASA-CR-159762] p0152 N80-25794
 Cogeneration technology alternatives study.
 Volume 6: Computer data [NASA-CR-159764] p0152 N80-25795
 Cogeneration Technology Alternatives Study (CTAS).
 Volume 2: Analytical approach [NASA-CR-159766] p0143 N80-28859
 Cogeneration Technology Alternatives Study (CTAS).
 Volume 3: Energy conversion system characteristics [NASA-CR-159761] p0155 N80-31869

Cogeneration Technology Alternatives Study (CTAS).
 Volume 3: Industrial processes [NASA-CR-159767] p0155 N80-31870
 Cogeneration Technology Alternatives Study (CTAS).
 Volume 4: Energy conversion systems [NASA-CR-159768] p0155 N80-33859
 Cogeneration Technology Alternatives Study (CTAS).
 Volume 6: Computer data. Part 2: Residual-fired nocogeneration process boiler [NASA-CR-159770-PT-2] p0156 N80-33861
 INDUSTRIES
 NT AIRCRAFT INDUSTRY
 INERT GASES
 U RARE GASES
 INFORMATION TRANSMISSION
 U DATA TRANSMISSION
 INFRARED IMAGERY
 Coolant tube curvature effects on film cooling as detected by infrared imagery [ASME PAPER 79-WA/GT-7] p0107 A80-18638
 Influence of coolant tube curvature on film cooling effectiveness as detected by infrared imagery [NASA-TP-1546] p0013 N80-11087
 Assessment of satellite and aircraft multispectral scanner data for strip-mine monitoring [NASA-TN-79268] p0136 N80-20787
 INFRARED PHOTOGRAPHY
 Computerized video densitometry method for rapid analysis of infrared photographic images --- temperature distribution across a turbine blade [NASA-TP-1686] p0110 N80-25635
 INGOTS
 High temperature thermal energy storage in steel and sand [NASA-CR-159708] p0154 N80-29860
 INITIAL VALUE PROBLEMS
 U BOUNDARY VALUE PROBLEMS
 INJECTION
 NT FLUID INJECTION
 NT FUEL INJECTION
 NT WATER INJECTION
 INJECTION CARBURIZERS
 U FUEL INJECTION
 INJECTORS
 Design and evaluation of high performance rocket engine injectors for use with hydrocarbon fuels p0059 A80-20957
 Atomizing characteristics of swirl can combustor modules with swirl blast fuel injectors --- in terms of NOX emission rate [NASA-TN-79297] p0014 N80-13047
 Design and evaluation of high performance rocket engine injectors for use with hydrocarbon fuels [NASA-TN-79319] p0056 N80-13163
 Design and evaluation of high performance rocket engine injectors for use with hydrocarbon fuels p0094 N80-31621
 INLET FLOW
 Some aspects of a free jet phenomena to 105 L/D in a constant area duct p0106 A80-10030
 Critical mass flux through short Borda type inlets of various cross sections p0106 A80-10031
 Numerical simulation of supersonic inlets using a three-dimensional viscous flow analysis [AIAA PAPER 80-0384] p0003 A80-20969
 Computation of three-dimensional viscous supersonic flow in inlets [AIAA PAPER 80-0194] p0065 A80-23941
 Effect of inflow control on inlet noise of a cut-on fan [AIAA PAPER 80-1049] p0171 A80-35993
 Comparison of several inflow control devices for flight simulation of fan tone noise using a JT15B-1 engine [AIAA PAPER 80-1025] p0025 A80-38640
 Inlet flow distortion in turbomachinery. I - Comparison of theory and experiment in a transonic fan stage. II - A parameter study [AIAA PAPER 80-1076] p0006 A80-38895
 Experimental study of low aspect ratio compressor blading [ASME PAPER 80-GT-6] p0025 A80-42147
 Performance of annular prediffuser-combustor systems [ASME PAPER 80-GT-15] p0026 A80-42154
 The effect of finite turbulence spatial scale on the amplification of turbulence by a contracting

- stream
p0004 A80-44862
An efficient user-oriented method for calculating compressible flow in an about three-dimensional inlets --- panel method
[NASA-CR-159578] p0004 N80-10134
Computational fluid mechanics of internal flow
p0012 N80-10211
An analytical and experimental study of a short s-shaped subsonic diffuser of a supersonic inlet
[NASA-TN-81406] p0015 N80-15134
Distribution analysis for F100(3) engine
[NASA-CR-159754] p0036 N80-17073
Comparison of several inflow control devices for flight simulation of fan tone noise using a JT15D-1 engine
[NASA-TN-81505] p0019 N80-24314
- INLET NOZZLES**
Critical mass flux through short Borda type inlets of various cross sections
p0106 A80-10031
Free jet phenomena in a 90 deg-sharp edge inlet geometry
p0106 A80-10037
- INLET TEMPERATURE**
Low-pressure performance of annular, high-pressure (40 atm) high-temperature (2480 K) combustion system
[NASA-TP-1713] p0023 N80-32396
- INLETS (DEVICES)**
U INTAKE SYSTEMS
INORGANIC COATINGS
NT CERAMIC COATINGS
INORGANIC COMPOUNDS
Active heat exchange system development for latent heat thermal energy storage
[NASA-CR-159727] p0154 N80-29857
- INORGANIC SULFIDES**
NT MOLYBDENUM DISULFIDES
NT MOLYBDENUM SULFIDES
- INSTALLATION**
U INSTALLING
Installation and checkout of the DOE/NASA Mod-1 2000-kw wind turbine generator
[NASA-TN-81444] p0140 N80-19614
- INSTRUMENT ERRORS**
Flight test of navigation and guidance sensor errors measured on STOL approaches
[NASA-TN-81154] p0028 N80-13041
- INSULATING MATERIALS**
U INSULATION
INSULATION
NT THERMAL INSULATION
Assessment of potential exposure to friable insulation materials containing asbestos
[NASA-TN-81435] p0157 N80-23875
- INTAKE SYSTEMS**
NT AIR INTAKES
NT ENGINE INLETS
NT SUPERSONIC INLETS
Free jet phenomena in a 90 deg-sharp edge inlet geometry
p0106 A80-10037
Low speed test of the aft inlet designed for a tandem fan V/STOL nacelle
[NASA-CR-159752] p0037 N80-18042
Application of coherence in fan noise studies
[NASA-TP-1630] p0167 N80-18882
Acoustic performance of a 50.8-cm (20-inch) diameter variable-pitch fan and inlet. Volume 2: Acoustic data
[NASA-CR-135118] p0044 N80-29299
- INTEGRATED ENERGY SYSTEMS**
Cell module and fuel conditioner development
[NASA-CR-159828] p0150 N80-23768
Cell module and fuel conditioner
[NASA-CR-159875] p0142 N80-23769
- INTERACTIVE GRAPHICS**
U COMPUTER GRAPHICS
INTERCEPTOR AIRCRAFT
U FIGHTER AIRCRAFT
INTERFACE STABILITY
Dynamic analysis of noncontacting face seals
[NASA-TN-79294] p0118 N80-27695
- INTERFACES**
NT SOLID-SOLID INTERFACES
LSS/propulsion interactions studies
p0058 N80-31454
- INTERFACIAL STRAIN**
U INTERFACIAL TENSION
INTERFACIAL TENSION
Effect of interfacial species on shear strength of metal-sapphire contacts
p0178 A80-22300
Marangoni bubble motion in zero gravity --- Lewis zero gravity drop tower
[NASA-TN-79250] p0104 N80-13403
Liquid metal slip ring --- aerospace environments
[NASA-CASE-LEW-12277-3] p0101 N80-18300
Two-phase working fluids for the temperature range of 50 to 350 deg, phase 2
[NASA-CR-159847] p0108 N80-23599
- INTERMEDIATE FREQUENCIES**
Application of advanced on-board processing concepts to future satellite communications systems
[NASA-CR-159682] p0098 N80-12260
Application of advanced on-board processing concepts to future satellite communications systems: Bibliography
[NASA-CR-159684] p0098 N80-12261
- INTERMETALLICS**
Hyperfine magnetic field at Cd impurity site in L2/1/ Heusler alloys Rb_2MnGe and Rb_2MnPb by TDPAC technique --- Time Differential Perturbed Angular Correlation
p0178 A80-16843
Critical currents in A-15 structure Nb3Al converted from cold-worked bcc structure
p0179 A80-33853
- INTERNAL COMBUSTION ENGINES**
NT DIESEL ENGINES
NT DUCTED FAN ENGINES
NT GAS TURBINE ENGINES
NT JET ENGINES
NT SUPERSONIC COMBUSTION RAMJET ENGINES
NT T-63 ENGINE
NT TURBOPAN ENGINES
NT TURBOJET ENGINES
NT TURBOPROP ENGINES
NT WANKEL ENGINES
Multifuel rotary aircraft engine
[AIAA PAPER 80-1237] p0045 A80-38982
Overview of a stirling engine test project
[NASA-TN-81442] p0140 N80-18564
Positive displacement type general-aviation engines: Summary and concluding remarks
p0018 N80-22340
- INTERNAL STRESS**
U RESIDUAL STRESS
INTERPLANETARY PROPULSION
U ROCKET ENGINES
INTERPOLATION
Nonanalytic function generation routines for 16-bit microprocessors
[NASA-TN-81586] p0163 N80-33104
- INTRAOCULAR PRESSURE**
Intra-ocular pressure normalization technique and equipment
[NASA-CASE-LEW-12955-1] p0161 N80-14684
Intra-ocular pressure normalization technique and equipment
[NASA-CASE-LEW-12723-1] p0135 N80-18690
- INVERSIONS**
NT CENTRIFUGING STRESS
INVERTERS
NT STATIC INVERTERS
INVISCID FLOW
An implicit finite-difference code for inviscid and viscous cascade flow
[AIAA PAPER 80-1427] p0007 A80-44128
An alternative approach to the numerical simulation of steady inviscid flow
p0107 A80-44228
Numerical calculation of steady inviscid full potential compressible flow about wind turbine blades
[NASA-TN-81438] p0136 N80-18497
An alternative approach to the numerical simulation of steady inviscid flow
[NASA-TN-81542] p0003 N80-27286
- ION ACCELERATORS**
Ion extraction from a plasma
[NASA-CR-159849] p0177 N80-26161
- ION BEAMS**
Neutralization tests on the SERT II spacecraft --- of ion beams

ION CONCENTRATION

- [AIAA PAPER 79-2064] p0059 A80-10387
Homogeneous alignment of nematic liquid crystals
by ion beam etched surfaces p0178 A80-26007
- Primary electric propulsion technology study ---
for thruster wear-out mechanisms p0061 N80-13158
[NASA-CR-159688] p0096 N80-16232
Homogeneous alignment of nematic liquid crystals
by ion beam etched surfaces p0177 N80-27189
[NASA-TN-81378]
- Plasma physics analysis of SERT-2 operation
[NASA-CR-159814]
- ION CONCENTRATION**
Decay of the zincate concentration gradient at an
alkaline zinc cathode after charging p0074 A80-13070

ION CURRENTS

NT ION BEAMS

- Baffle aperture design study of hollow cathode
equipped ion thrusters p0064 N80-33476
[NASA-CR-165164]

ION DISTRIBUTION

- Specific spacecraft evaluation: Special report
--- charged particle transport from a mercury
ion thruster to spacecraft surfaces p0060 N80-11137
[NASA-CR-159420]

ION ENGINES

NT MERCURY ION ENGINES

- 8-cm Engineering Model Thruster technology - A
review of recent developments p0064 A80-13311
[AIAA PAPER 79-2103]
- Heat pipe cooling of power processing magnetics
[NASA-TN-79270] p0101 N80-11327
- Primary electric propulsion technology study ---
for thruster wear-out mechanisms p0061 N80-13158
[NASA-CR-159688]
- Baffle aperture design study of hollow cathode
equipped ion thrusters p0064 N80-33476
[NASA-CR-165164]

ION EXTRACTION

- Ion extraction from a plasma p0177 N80-26161
[NASA-CR-159849]

ION IMPLANTATION

- Mechanical and chemical effects of ion-texturing
biomedical polymers p0089 A80-13065
- Photovoltaic technology development for
synchronous orbit p0058 N80-33470

ION IRRADIATION

- Comments on Auger electron production by Ne⁺/₊
bombardment of surfaces p0174 A80-34048
- Modification of the electrical and optical
properties of polymers --- ion irradiation to
create texture p0087 N80-24437
[NASA-CASE-LEW-13027-1]

ION PLATING

- Survey of ion plating sources p0120 A80-10040

ION PRODUCTION RATES

- Study of a rare-gas transverse fast discharge
p0176 A80-11366

ION PROPULSION

- Neutralization tests on the SERT II spacecraft ---
of ion beams p0059 A80-10387
[AIAA PAPER 79-2064]
- Reduced power processor requirements for the 30-cm
diameter HG ion thruster p0059 A80-10392
[AIAA PAPER 79-2081]
- Evaluation of particle transport for the P80-1
spacecraft --- mercury ion thruster and
spacecraft surfaces interactive effects p0055 A80-13301
[AIAA PAPER 79-2047]
- A model for predicting the wearout lifetime of the
LeRC/Hughes 30-cm mercury ion thruster p0064 A80-20962
[AIAA PAPER 79-2079]
- Power processing technology for spacecraft primary
ion propulsion p0065 A80-48265
- Heat pipe cooled power magnetics
[NASA-CR-159659] p0103 N80-13362
- Electric propulsion for near-Earth space missions
[NASA-CR-159735] p0062 N80-16096
- Inert gas thrusters p0052 N80-24362
[NASA-CR-159813]
- Inert gas ion thruster development
[NASA-CR-159805] p0062 N80-27424

SUBJECT INDEX

ION SOURCES

- Survey of ion plating sources p0120 A80-10040
- Adherence of ion beam sputter deposited metal
films on H-13 steel p0079 N80-31527
[NASA-TN-81585]
- Hydrogen hollow cathode ion source p0174 N80-33186
[NASA-CASE-LEW-12940-1]

ION TEMPERATURE

- Parametric dependence of ion temperature and
electron density in the SUMMA hot-ion plasma
using laser light scattering and emission
spectroscopy p0176 A80-46265

IONIC CONDUCTIVITY

U ION CURRENTS

IONIC MOBILITY

- Evaluation of particle transport for the P80-1
spacecraft --- mercury ion thruster and
spacecraft surfaces interactive effects p0055 A80-13301
[AIAA PAPER 79-2047]

IONIC PROPELLANTS

U ION ENGINES

IONIZATION

NT GAS IONIZATION

NT ION PRODUCTION RATES

- Negative streamer development in FEP teflon
p0179 A80-19776

IONIZED GASES

- NT ARGON PLASMA
- NT CHARGED PARTICLES
- NT LASER PLASMAS
- NT PLASMA JETS
- NT PLASMA SHEATHS
- NT PLASMAS (PHYSICS)
- NT TOROIDAL PLASMAS

IONIZED PLASMAS

U PLASMAS (PHYSICS)

IONIZERS

- Physical phenomena in mercury ion thrusters
[NASA-CR-159784] p0061 N80-17137

IONIZING RADIATION

NT X RAYS

IONS

NT HYDROGEN IONS

IP (IMPACT PREDICTION)

U COMPUTERIZED SIMULATION

IRON

- Adhesion and friction of iron-base binary alloys
in contact with silicon carbide in vacuum p0076 N80-15234
[NASA-TP-1604]

IRON ALLOYS

- NT AUSTENITIC STAINLESS STEELS
- NT CARBON STEELS
- NT CHROMIUM STEELS
- NT HIGH STRENGTH STEELS
- NT MARTENSITIC STAINLESS STEELS
- NT NICKEL STEELS
- NT STAINLESS STEELS
- NT STEELS

- Strengthening of tough iron-12% nickel-reactive
metal alloys at 77 K by copper additions p0174 A80-34049

- Friction and wear of iron-base binary alloys in
sliding contact with silicon carbide in vacuum p0087 N80-22494
[NASA-TP-1612]

- High toughness-high strength iron alloy p0079 N80-32484
[NASA-CASE-LEW-12542-3]

- Creep-rupture behavior of seven iron-base alloys
after long term aging at 760 deg in low pressure
hydrogen p0080 N80-32488
[NASA-TN-81534]

IRRADIANCE

- Global calibration of terrestrial reference cells
and errors involved in using different
irradiance monitoring techniques p0138 N80-15561
[NASA-TN-81393]

IRRADIATION

NT ELECTRON IRRADIATION

NT ION IRRADIATION

NT NEUTRON IRRADIATION

NT X RAY IRRADIATION

IRROTATIONAL FLOW

U POTENTIAL FLOW

ISING MODEL

U MATHEMATICAL MODELS

ISOLATORS

NT VIBRATION ISOLATORS

ISOSTATIC PRESSURE

Effects of thermally induced porosity on an as-HIP powder metallurgy superalloy
p0082 A80-29990

ISOTHERMAL PROCESSES

Phase change in liquid face seals. II - Isothermal and adiabatic bounds with real fluids
[ASME PAPER 79-LUB-4] p0129 A80-14739
The effect of zirconium on the isothermal oxidation of nominal Ni-14Cr-24Al alloys
p0082 A80-26465
Low-pressure performance of annular, high-pressure (40 atm) high-temperature (2480 K) combustion system
[NASA-TP-1713] p0023 A80-32396

ISOTROPIC TURBULENCE

Effects of axisymmetric contractions on turbulence of various scales
[NASA-CR-165136] p0006 A80-32328

JET AIRCRAFT

NT BOEING 747 AIRCRAFT
NT DC 9 AIRCRAFT
NT DC 10 AIRCRAFT
NT F-16 AIRCRAFT
NT F-102 AIRCRAFT
NT TURBOFAN AIRCRAFT

Analysis of the response of a thermal barrier coating to sodium and vanadium doped combustion gases
[NASA-TM-79205] p0076 A80-10344

JET AIRCRAFT NOISE

Acoustic considerations of flight effects on jet noise suppressor nozzles
[AIAA PAPER 80-0164] p0171 A80-20965
Effect of temperature on surface noise
p0107 A80-28419
Noise suppression due to annulus shaping of a conventional coaxial nozzle
p0171 A80-35497
Noise suppression due to annulus shaping of an inverted-velocity-profile coaxial nozzle
p0171 A80-35498
Effect of inflow control on inlet noise of a cut-on fan
[AIAA PAPER 80-1049] p0171 A80-35993
Characteristics of internal- and jet-noise radiation from a multi-lobe, multi-tube suppressor nozzle tested statically and under flight simulation
[AIAA PAPER 80-1027] p0173 A80-38642
QCSEE UTW engine powered-lift acoustic performance --- Quiet Clean Short-haul Experimental Engine Under The Wing
[AIAA PAPER 80-1065] p0025 A80-38651
Prediction of unsuppressed jet engine exhaust noise in flight from static data
[AIAA PAPER 80-1008] p0027 A80-44491
Quiet Clean Short-Haul Experimental Engine (QCSEE) acoustic and aerodynamic tests on a scale model over-the-wing thrust reverser and forward thrust nozzle
[NASA-CR-135254] p0028 A80-14115
Acoustic considerations of flight effects on jet noise suppressor nozzles
[NASA-TM-81377] p0167 A80-14843
Quiet Clean Short-haul Experimental Engine (QCSEE) Over-The-Wing (OTW) propulsion systems test report. Volume 4: Acoustic performance
[NASA-CR-135326] p0032 A80-15118
Experimental evaluation of a spinning-mode acoustic-treatment design concept for aircraft inlets --- suppression of YF-102 engine fan noise
[NASA-TP-1613] p0016 A80-21323
Spectral structure of pressure measurements made in a combustion duct --- jet engine noise
[NASA-TM-81471] p0168 A80-22045
Noise suppression due to annulus shaping of an inverted-velocity-profile coaxial nozzle --- supersonic cruise aircraft
[NASA-TM-81460] p0168 A80-22046
Noise suppression due to annulus shaping of conventional coaxial nozzle
[NASA-TM-81461] p0168 A80-22047
An improved prediction method for the noise generated in flight by circular jets
[NASA-TM-81470] p0168 A80-22048

Prediction of unsuppressed jet engine exhaust noise in flight from static data

[NASA-TM-81537] p0169 A80-29132
A study of the transmission characteristics of suppressor nozzles
[NASA-CR-165133] p0172 A80-32186
JET BLAST EFFECTS
Free jet phenomena in a 90 deg-sharp edge inlet geometry
p0106 A80-10037

JET DAMPING

U DAMPING

JET ENGINE FUELS

NT JP-5 JET FUEL

NASA Broad-Specification Fuels Combustion Technology Program - Status and description
[ASME PAPER 80-GT-65] p0094 A80-42195
Alternative jet aircraft fuels
p0012 A80-10209

Initial characterization of an Experimental Referee Broadened-Specification (ERBS) aviation turbine fuel
[NASA-TM-81440] p0093 A80-18205
The impact of fuels on aircraft technology through the year 2000
[NASA-TM-81492] p0093 A80-23472
Aircraft Research and Technology for Future Fuels
[NASA-CR-2146] p0022 A80-29300
Future aviation fuels overview
p0021 A80-29301

Future aviation fuels overview
p0021 A80-29301
Current jet fuel trends
p0041 A80-29303

Aviation fuels outlook
p0041 A80-29304
Fuel/engine/airframe tradeoff study, phase 1
p0042 A80-29307

Military jet fuel from shale oil
p0042 A80-29308
Fuels characterization studies --- jet fuels
p0021 A80-29309

Fuel character effects on the J79 and F101 engine combustion systems
p0042 A80-29312

Antimisting kerosene --- reduced flammability during aircraft accident circumstances
p0021 A80-29319

Determination of jet fuel thermal deposit rate using a modified JPTOT
p0043 A80-29326

JET ENGINES

NT DUCTED FAN ENGINES

NT SUPERSONIC COMBUSTION RAMJET ENGINES

NT T-63 ENGINE

NT TURBOFAN ENGINES

NT TURBOJET ENGINES

NT TURBOPROP ENGINES

Fatigue strength testing employed for evaluation and acceptance of jet-engine instrumentation probes
p0112 A80-42291

JT9D-7A /SP/ jet engine performance deterioration trends
p0026 A80-44230

VSCE technology definition study
[NASA-CR-159730] p0027 A80-10222

Computer simulation of engine systems
[NASA-TM-79290] p0015 A80-15132
Expanded study of feasibility of measuring in-flight 747/JT9D loads, performance, clearance, and thermal data
[NASA-CR-159717] p0036 A80-16063

Fatigue strength testing employed for evaluation and acceptance of jet-engine instrumentation probes
[NASA-TM-81402] p0110 A80-17422

Ferrographic and spectrographic analysis of oil sampled before and after failure of a jet engine
[NASA-TM-81430] p0117 A80-19497

Data analysis of P sub T/P sub S noseboom probe testing on F100 engine P680072 at NASA Lewis Research Center
[NASA-CR-159816] p0038 A80-21334

CF6-6D engine short-term performance deterioration
[NASA-CR-159830] p0039 A80-23316

Performance deterioration based on in-service engine data: JT9D jet engine diagnostics program
[NASA-CR-159525] p0040 A80-25340

JET EXHAUST

Engine bleed air reduction in DC-10
[NASA-CR-159846] p0010 N80-32378

JET EXHAUST
Prediction of unsuppressed jet engine exhaust
noise in flight from static data
[AIAA PAPER 80-1008] p0027 A80-44491
Air pollution from aircraft
[NASA-CR-159712] p0010 N80-16060

JET FLAMES
U FLAMES
U JET FLOW
JET FLIGHT
U JET AIRCRAFT
JET FLOW
Effect of temperature on surface noise
p0107 A80-28419

JET FUELS
U JET ENGINE FUELS
JET IMPINGEMENT
Analytical and experimental spur gear tooth
temperature as affected by operating variables
p0123 A80-46412
Computer program for generating input for analysis
of impingement-cooled, axial-flow turbine blade
[NASA-TP-1603] p0104 N80-15361
Measured and predicted impingement noise for a
model-scale under the wing externally blown flap
configuration with a QCSEE type nozzle
[NASA-TM-81494] p0169 N80-26115

JET MIXING FLOW
Scale model performance test investigation of
exhaust system mixers for an Energy Efficient
Engine /E3/ propulsion system
[AIAA PAPER 80-0229] p0024 A80-20968

JET NOISE
U JET AIRCRAFT NOISE
JET THRUST
Method and apparatus for rapid thrust increases in
a turbofan engine
[NASA-CASE-LEW-12971-1] p0016 N80-18039

JET VANES
Significance of thermal contact resistance in
two-layer, thermal-barrier-coated turbine vanes
p0024 A80-39635

JETAVATORS
U GUIDE VANES
JITTER
U VIBRATION
JOURNAL BEARINGS
Observation of pressure variation in the
cavitation region of submerged journal bearings
[NASA-TM-81582] p0120 N80-31798

JOURNALS (SHAFTS)
U SHAFTS (MACHINE ELEMENTS)
JP-5 JET FUEL
Effect of refining variables on the properties and
composition of JP-5
p0041 N80-29306

K

K BAND
U EXTREMELY HIGH FREQUENCIES
KA BAND
U EXTREMELY HIGH FREQUENCIES
KENTUCKY
Assessment of satellite and aircraft multispectral
scanner data for strip-mine monitoring
[NASA-TM-79268] p0136 N80-20787

KEROSENE
Antismisting kerosene --- reduced flammability
during aircraft accident circumstances
p0021 N80-29319

KEVLAR (TRADEMARK)
Acoustic behavior of fibrous bulk materials
[AIAA PAPER 80-0986] p0172 A80-35951
Development of a Kevlar/PMR-15 reduced drag DC-9
nacelle fairing
[AIAA PAPER 80-1194] p0010 A80-41193
Feasibility of Kevlar 49/PMR-15 polyimide for high
temperature applications
[NASA-TM-81560] p0069 N80-27429

KINEMATICS
Kinematic correction for roller skewing
[NASA-TM-81564] p0119 N80-28716

KINETIC EQUATIONS
NT HELMHOLTZ VORTICITY EQUATION
KINETIC FRICTION
NT SLIDING FRICTION

SUBJECT INDEX

KINETICS
NT REACTION KINETICS
KIRCHHOFF-HUYGENS PRINCIPLE
U WAVE PROPAGATION
KU BAND
U SUPERHIGH FREQUENCIES

L

L BAND
U ULTRAHIGH FREQUENCIES
LAKE ERIE
Coordinated aircraft and ship surveys for
determining impact of river inputs on great
lakes waters. Remote sensing results
[NASA-TP-1694] p0157 N80-27832

LAKE MICHIGAN
Coordinated aircraft and ship surveys for
determining impact of river inputs on great
lakes waters. Remote sensing results
[NASA-TP-1694] p0157 N80-27832

LAKE ONTARIO
Coordinated aircraft and ship surveys for
determining impact of river inputs on great
lakes waters. Remote sensing results
[NASA-TP-1694] p0157 N80-27832

LAKE SUPERIOR
Coordinated aircraft and ship surveys for
determining impact of river inputs on great
lakes waters. Remote sensing results
[NASA-TP-1694] p0157 N80-27832

LAKES
NT GREAT LAKES (NORTH AMERICA)
NT LAKE ERIE
NT LAKE MICHIGAN
NT LAKE ONTARIO
NT LAKE SUPERIOR
LAMINAR FLAMES
U FLAMES
LAMINAR FLOW CONTROL
U BOUNDARY LAYER CONTROL
LAMINAR JETS
U JET FLOW
LAMINATED MATERIALS
U LAMINATES
LAMINATES
Mechanical property characterization of intraply
hybrid composites
p0070 A80-20954
Dynamic response of damaged angleplied fiber
composites
p0070 A80-27982
Burning characteristics and fiber retention of
graphite/resin matrix composites
p0070 A80-32062
Fracture modes of high modulus graphite/epoxy
angleplied laminates subjected to off-axis
tensile loads
p0071 A80-32069
Micromechanics of intraply hybrid composites:
Elastic and thermal properties
[NASA-TM-79253] p0067 N80-11143
Dynamic response of damaged angleplied fiber
composites
[NASA-TM-79281] p0067 N80-11145
Fracture modes of high modulus graphite/epoxy
angleplied laminates subjected to off-axis
tensile loads
[NASA-TM-81405] p0068 N80-16102
Silicone modified resins for graphite fiber
laminates
[NASA-CR-159750] p0072 N80-22407
Sudden bending of cracked laminates
[NASA-CR-159860] p0073 N80-25384
Feasibility of Kevlar 49/PMR-15 polyimide for high
temperature applications
[NASA-TM-81560] p0069 N80-27429

LAMINATIONS
U LAMINATES
LANDING
NT VERTICAL LANDING
LANGUAGE PROGRAMMING
INFORM: An interactive data collection and
display program with debugging capability
[NASA-TP-1424] p0162 N80-16742

LARGE SPACE STRUCTURES
Nuclear electric propulsion system utilization for
earth orbit transfer of large spacecraft
structures

SUBJECT INDEX

LIQUIDIFIED GASES

- [AIAA PAPER 80-1223] p0060 A80-38975
Orbital transfer of large space structures with
nuclear electric rockets
[AAS PAPER 80-083] p0054 A80-41897
Space environmental interactions with biased
spacecraft surfaces p0055 A80-46897
Large Space Systems/Low-Thrust Propulsion Technology
[NASA-CR-2144] p0057 N80-31449
Electric propulsion technology p0057 N80-31452
Chemical propulsion technology p0058 N80-31453
LSS/propulsion interactions studies p0058 N80-31454
DOD low-thrust mission studies p0063 N80-31455
Low-thrust vehicles concept studies p0063 N80-31456
Low-thrust vehicle concept studies p0058 N80-31457
Primary propulsion/large space system interactions
p0063 N80-31458
Auxiliary control of LSS p0063 N80-31459
Solar rocket system concept analysis p0064 N80-31470
Synchronous energy technology program p0058 N80-33466
- LASER ANEMOMETERS**
Laser anemometer measurements in a transonic axial
flow compressor rotor p0111 A80-36141
Laser anemometer measurements in a transonic axial
flow compressor rotor
[NASA-TM-79323] p0002 N80-14050
Efficient laser anemometer for intra-rotor flow
mapping in turbomachinery
[NASA-TM-79320] p0112 N80-14375
- LASER APPLICATIONS**
Laser-optical blade tip clearance measurement system
p0111 A80-36137
Laser-optical blade tip clearance measurement system
[NASA-TM-81376] p0015 N80-14128
- LASER DOPPLER VELOCIMETERS**
Laser anemometer measurements at the exit of a T63
combustor p0045 A80-27737
Efficient laser anemometer for intra-rotor flow
mapping in turbomachinery p0111 A80-36140
Efficient laser anemometer for intra-rotor flow
mapping in turbomachinery
[NASA-TM-79320] p0112 N80-14375
- LASER OUTPUTS**
A cesium TELEC experiment at Lewis Research Center
[NASA-CR-159729] p0113 N80-14386
- LASER FLASHES**
Parametric dependence of ion temperature and
electron density in the SUMMA hot-ion plasma
using laser light scattering and emission
spectroscopy p0176 A80-46265
- LASERS**
NT CARBON DIOXIDE LASERS
LATENT HEAT OF FUSION
U HEAT OF FUSION
LATERAL OSCILLATION
Field verification of lateral-torsional coupling
effects on rotor instabilities in centrifugal
compressors p0125 N80-29708
- LAUNCH VEHICLES**
NT CENTAUR LAUNCH VEHICLE
NT TITAN CENTAUR LAUNCH VEHICLE
LEAD ACID BATTERIES
An averaging battery model for a lead-acid battery
operating in an electric car p0165 N80-16824
An electric vehicle propulsion system's impact on
battery performance: An overview p0143 N80-24756
- LEADING EDGES**
Streakline flow visualization study of a horseshoe
vortex in a large-scale, two-dimensional turbine
stator cascade
[ASME PAPER 80-GT-4] p0004 A80-42145
- LEAKAGE**
Some flow characteristics of conventional and
tapered high-pressure-drop simulated seals
[ASLE PREPRINT 79-LC-3B-2] p0120 A80-14727
Phase change in liquid face seals. XI - Isothermal
and adiabatic bounds with real fluids
[ASME PAPER 79-LUB-4] p0129 A80-14739
Self-excited rotor whirl due to tip-seal leakage
forces p0127 N80-29723
- LEGEND CODE**
U COMPUTER PROGRAMMING
LIFE (DURABILITY)
NT FATIGUE LIFE
NT SERVICE LIFE
Preliminary results of the mission profile life
test of a 30 cm Hg bombardment thruster
[AIAA PAPER 79-2078] p0081 A80-10391
3500-hour durability testing of ceramic materials
for automotive gas turbine engines
[AIRESEARCH-31-3542] p0092 A80-35575
Durability testing of advanced catalysts and
catalyst supports for gas turbine engine
combustors p0074 A80-35881
Design, durability and low cost processing
technology for composite fan exit guide vanes
[NASA-CR-159677] p0027 N80-12091
Primary electric propulsion technology study ---
for thruster wear-out mechanisms p0061 N80-13158
Thermionic cathode life test studies
[NASA-TM-81441] p0101 N80-18302
Advanced technology light weight fuel cell program
--- orbiting space vehicle long-life hydrogen
oxygen fuel cell
[NASA-CR-159807] p0149 N80-19615
Quantitative ultrasonic evaluation of engineering
properties in metals, composites and ceramics
[NASA-TM-81530] p0130 N80-26682
- LIFE CYCLE COSTS**
Computerized systems analysis and optimization of
aircraft engine performance, weight, and life
cycle costs p0165 A80-10035
Design, performance and life cycle cost
relationships for a 500kW space solar array
p0065 A80-48356
Solar array subsystems study
[NASA-CR-159857] p0151 N80-24742
- LIFETIME (DURABILITY)**
U LIFE (DURABILITY)
LIGHT AIRCRAFT
Preliminary study of advanced turboprop and
turboshaft engines for light aircraft --- cost
effectiveness
[NASA-TM-81467] p0018 N80-22350
- LIGHT ALLOYS**
NT ALUMINUM ALLOYS
LIGHT TRANSPORT AIRCRAFT
Design study: A 186 kW lightweight diesel
aircraft engine
[NASA-CR-3261] p0038 N80-22326
- LIMNOLOGY**
Quantitative interpretation of Great Lakes remote
sensing data p0157 A80-45005
- LINEAR AMPLIFIERS**
Improved traveling wave tubes --- for ECM systems
p0102 A80-44235
Improved traveling wave tubes
[NASA-TM-81479] p0102 N80-22598
- LINEAR EQUATIONS**
Numerical techniques in linear duct acoustics ---
finite difference and finite element analyses
[NASA-TM-81553] p0170 N80-30154
- LINING PROCESSES**
Fully plasma-sprayed compliant backed ceramic
turbine seal
[NASA-CASE-LEW-13268-1] p0117 N80-24619
- LININGS**
NT ROCKET LININGS
LIQUEFACTION
NT COAL LIQUEFACTION
LIQUEFIED GASES
NT LIQUEFIED NATURAL GAS
NT LIQUID HYDROGEN
NT LIQUID OXYGEN
A reduced volumetric expansion factor plot
p0107 A80-10038

LIQUEFIED NATURAL GAS

SUBJECT INDEX

LIQUEFIED NATURAL GAS

Toward the use of similarity theory in two-phase
choked flows
[NASA-TN-81568] p0106 N80-29623

LIQUID ATOMIZATION

Atomization of broad specification aircraft fuels
p0043 N80-29318

LIQUID CHROMATOGRAPHY

Liquid chromatographic characterization of PMR-15
resin and prepreg
p0089 A80-32086

LIQUID COOLING

MT FILM COOLING

Cooling of high pressure rocket thrust chambers
with liquid oxygen
[AIAA PAPER 80-1260] p0060 A80-38992

LIQUID CRYSTALS

Homogeneous alignment of nematic liquid crystals
by ion beam etched surfaces
p0178 A80-26007

Homogeneous alignment of nematic liquid crystals
by ion beam etched surfaces
[NASA-TN-81378] p0096 N80-16232

LIQUID DROPS

U DROPS (LIQUIDS)

LIQUID HYDROGEN

Turbine engine altitude chamber and flight testing
with liquid hydrogen
p0023 A80-10034

A liquid hydrogen experiment as a Shuttle payload
[AIAA PAPER 80-1096] p0054 A80-38909

Liquid oxygen/liquid hydrogen auxiliary power
system thruster investigation
[NASA-CR-159674] p0062 N80-15202

Small, high pressure liquid hydrogen turbopump
[NASA-CR-159821] p0125 N80-26662

LIQUID INJECTION

MT WATER INJECTION

LIQUID METALS

Liquid metal slip ring --- aerospace environments
[NASA-CASE-LEW-12277-3] p0101 N80-18300

LIQUID OXYGEN

Cooling of high pressure rocket thrust chambers
with liquid oxygen
[AIAA PAPER 80-1260] p0060 A80-38992

Liquid oxygen/liquid hydrogen auxiliary power
system thruster investigation
[NASA-CR-159674] p0062 N80-15202

Cooling of high pressure rocket thrust chambers
with liquid oxygen
[NASA-TN-81503] p0057 N80-23365

LIQUID PROPELLANT ROCKET ENGINES

MT HYDROGEN OXYGEN ENGINES

Design and evaluation of high performance rocket
engine injectors for use with hydrocarbon fuels
p0059 A80-20957

Analysis of combustion instability in liquid fuel
rocket motors
[NASA-CR-159733] p0061 N80-13164

Amplification of Reynolds number dependent
processes by wave distortion --- liquid fuel
combustor stability
[NASA-CR-159732] p0075 N80-13193

Performance of a transpiration-regenerative cooled
rocket thrust chamber
[NASA-CR-159742] p0061 N80-14189

LIQUID ROCKET PROPELLANTS

MT CRYOGENIC ROCKET PROPELLANTS

LeRC reduced gravity fluid management technology
program
p0048 A80-35504

Capillary device refilling --- liquid rocket
propellant tank tests
[AIAA PAPER 80-1095] p0060 A80-38908

Investigation of critical burning of fuel droplets
[NASA-CR-159697] p0075 N80-12142

Analysis of combustion instability in liquid fuel
rocket motors
[NASA-CR-159733] p0061 N80-13164

Stability analysis of a liquid fuel annular
combustion chamber
[NASA-CR-159734] p0061 N80-14189

Supercharged topping rocket propellant feed system
[NASA-CASE-XLE-02062-1] p0056 N80-14188

LIQUIDS

MT CRYOGENIC FLUIDS

MT CRYOGENIC ROCKET PROPELLANTS

MT HYDRAULIC FLUIDS

MT LIQUEFIED GASES

MT LIQUID HYDROGEN

MT LIQUID METALS

MT LIQUID OXYGEN

MT LIQUID ROCKET PROPELLANTS

LNG

U LIQUEFIED NATURAL GAS

LOAD FACTORS

U LOADS (FORCES)

LOAD TESTS

Dynamic properties of elastomer cartridge
specimens under a rotating load
p0121 A80-24002

Comparison tests and experimental compliance
calibration of the proposed standard round
compact plane strain fracture toughness specimen
[NASA-TN-81379] p0132 N80-13513

Fracture modes of high modulus graphite/epoxy
angleplied laminates subjected to off-axis
tensile loads
[NASA-TN-81405] p0068 N80-16102

The method of lines in three dimensional fracture
mechanics
[NASA-TN-81593] p0132 N80-32753

LOADING FORCES

U LOADS (FORCES)

LOADING WAVES

U LOADS (FORCES)

LOADS (FORCES)

MT AERODYNAMIC LOADS

MT AXIAL LOADS

MT CYCLIC LOADS

MT DYNAMIC LOADS

MT IMPACT LOADS

MT ROLLING CONTACT LOADS

Analytical and experimental spur gear tooth
temperature as affected by operating variables
[NASA-TN-81419] p0115 N80-18403

Dynamic behavior of a beam drag-force anemometer
[NASA-TN-1687] p0110 N80-24595

Cold-air investigation of a 4 1/2 stage turbine
with stage-loading factor of 4.66 and high
specific work output. 2: Stage group performance
[NASA-TN-1688] p0019 N80-25338

Stresses and deformations in elliptical contacts
[NASA-TN-81535] p0118 N80-27697

Hydraulic forces caused by annular pressure seals
in centrifugal pumps
p0126 N80-29718

Limit cycles of a flexible shaft with hydrodynamic
journal bearings in unstable regimes
p0127 N80-29725

Limit cycles of a flexible shaft with hydrodynamic
journal bearings in unstable regimes
p0127 N80-29725

Limit cycles of a flexible shaft with hydrodynamic
journal bearings in unstable regimes
p0127 N80-29725

Limit cycles of a flexible shaft with hydrodynamic
journal bearings in unstable regimes
p0127 N80-29725

Limit cycles of a flexible shaft with hydrodynamic
journal bearings in unstable regimes
p0127 N80-29725

Limit cycles of a flexible shaft with hydrodynamic
journal bearings in unstable regimes
p0127 N80-29725

Limit cycles of a flexible shaft with hydrodynamic
journal bearings in unstable regimes
p0127 N80-29725

Limit cycles of a flexible shaft with hydrodynamic
journal bearings in unstable regimes
p0127 N80-29725

Limit cycles of a flexible shaft with hydrodynamic
journal bearings in unstable regimes
p0127 N80-29725

Limit cycles of a flexible shaft with hydrodynamic
journal bearings in unstable regimes
p0127 N80-29725

Limit cycles of a flexible shaft with hydrodynamic
journal bearings in unstable regimes
p0127 N80-29725

Limit cycles of a flexible shaft with hydrodynamic
journal bearings in unstable regimes
p0127 N80-29725

Limit cycles of a flexible shaft with hydrodynamic
journal bearings in unstable regimes
p0127 N80-29725

Limit cycles of a flexible shaft with hydrodynamic
journal bearings in unstable regimes
p0127 N80-29725

Limit cycles of a flexible shaft with hydrodynamic
journal bearings in unstable regimes
p0127 N80-29725

Limit cycles of a flexible shaft with hydrodynamic
journal bearings in unstable regimes
p0127 N80-29725

- oxidation behavior of a Si3N4/Al2O3 ceramic
[NASA-TN-81536] p0088 N80-27484
Low temperature fuel behavior studies p0044 N80-29330
- LOW TEMPERATURE TESTS**
Temperature and flow measurements on near-freezing aviation fuels in a wing-tank model
[ASME PAPER 80-GT-63] p0094 A80-42193
Hot corrosion of Co-Cr, Co-Cr-Al, and Ni-Cr alloys in the temperature range of 700-750 deg C
[NASA-CR-159689] p0084 N80-26427
- LOW THRUST**
Analytical investigation of two hydrogen oxygen rocket engine systems for low-thrust application
[NASA-TN-81420] p0056 N80-17138
LSS/propulsion interactions studies p0050 N80-31454
- LOW THRUST PROPULSION**
NT ELECTROMAGNETIC PROPULSION
NT ION PROPULSION
NT PLASMA PROPULSION
NT SOLAR ELECTRIC PROPULSION
NT SOLAR PROPULSION
Analytical investigation of two hydrogen-oxygen rocket engine systems for low-thrust application
p0060 A80-35503
Analytical investigation of two hydrogen-oxygen rocket engine systems for low-thrust application --- for orbital transfer p0057 N80-30382
LEO-to-GEO low thrust chemical propulsion p0063 N80-30384
Large Space Systems/Low-Thrust Propulsion Technology [NASA-CP-2144] p0057 N80-31449
Chemical propulsion technology p0058 N80-31453
DOD low-thrust mission studies p0063 N80-31455
Low-thrust vehicles concept studies p0063 N80-31456
Low-thrust vehicle concept studies p0058 N80-31457
Low-thrust chemical rocket engine study p0063 N80-31467
Low-thrust chemical propulsion p0063 N80-31468
Low-thrust chemical orbit to orbit propulsion system propellant management study p0064 N80-31469
Advanced concepts --- specific impulse, mass drivers, electromagnetic launchers, and the rail gun p0058 N80-31471
- LOW VELOCITY**
U LOW SPEED
LOX (OXYGEN)
U LIQUID OXYGEN
LOX-HYDROGEN ENGINES
U HYDROGEN OXYGEN ENGINES
- LUBRICANT TESTS**
Boundary lubrication, thermal and oxidative stability of a fluorinated polyether and a perfluoropolyether triazine
[ASLE PREPRINT 79-AH-1B-1] p0088 A80-12089
Effect of thermal aging on the tribological properties of polyimide films and polyimide-bonded graphite fluoride films
[ASLE PREPRINT 79-AH-3B-1] p0088 A80-12094
- LUBRICANTS**
NT HIGH TEMPERATURE LUBRICANTS
NT LUBRICATING OILS
NT SOLID LUBRICANTS
Tribological properties of sputtered MoS2 films in relation to film morphology p0089 A80-35502
Mechanisms of lubrication and wear of a bonded solid lubricant film
[NASA-TN-81396] p0085 N80-16165
- LUBRICATING OILS**
Ferrographic and spectrographic analysis of oil sampled before and after failure of a jet engine
[NASA-TN-81430] p0117 N80-19497
- LUBRICATION**
NT BOUNDARY LUBRICATION
Elastohydrodynamic film thickness measurements of artificially-produced nonsmooth surfaces
[ASLE PREPRINT 79-LC-1A-3] p0102 A80-14720
Lubrication and wear mechanisms of polyimide-bonded graphite fluoride films subjected to low contact stress
[NASA-TP-1584] p0085 N80-17220
Analytical and experimental spur gear tooth temperature as affected by operating variables
[NASA-TN-81419] p0115 N80-18403
Lubrication of rolling-element bearings
[NASA-TN-81449] p0117 N80-20591
Operating characteristics of high-speed, jet-lubricated 35-millimeter-bore ball bearing with a single-outer-land-guided cage
[NASA-TP-1657] p0117 N80-21753
Fully flooded elastohydrodynamic lubricated elliptical contacts
[NASA-TN-81543] p0118 N80-27698
Starved elastohydrodynamic lubricated elliptical contacts
[NASA-TN-81549] p0118 N80-27699
Lubrication of optimized-design tapered-roller bearings to 2.4 million DM
[NASA-TP-1714] p0119 N80-29734
Film thickness for different regimes of fluid-film lubrication
[NASA-TN-81550] p0119 N80-29735
Effect of cage design on characteristics of high-speed-jet-lubricated 35-millimeter-bore ball bearing --- turbojet engines
[NASA-TP-1732] p0120 N80-33749
- LUBRICATION SYSTEMS**
Comparison of predicted and experimental performance of large-bore roller bearing operating to 3.0 million DM
[NASA-TP-1599] p0114 N80-15410
- LUDER BANDS**
U PLASTIC DEFORMATION
- M**
- MACHINE LIFE**
U SERVICE LIFE
MAGNESIUM COMPOUNDS
NT MAGNESIUM OXIDES
MAGNESIUM OXIDES
Effects of oxide additions and temperature on sinterability of milled silicon nitride
[NASA-TP-1644] p0086 N80-21532
- MAGNETIC CORES**
Heat pipe cooled power magnetics
[NASA-CR-159659] p0103 N80-13362
- MAGNETIC DISTURBANCES**
NT MAGNETIC STORMS
MAGNETIC EFFECTS
The effect of a weak vertical magnetic field on fluctuation-induced transport in a Bumpy-Torus plasma p0176 A80-25476
- MAGNETIC FIELD CONFIGURATIONS**
A matrix solution for the simulation of magnetic fields with ideal current loops p0102 A80-13903
The effect of a weak vertical magnetic field on fluctuation-induced transport in a Bumpy-Torus plasma p0176 A80-25476
- MAGNETIC FIELDS**
Two-dimensional representations of axisymmetric fields for computer calculations --- in modeling microwave tubes p0102 A80-18232
Atomic hydrogen storage --- cryotrapping and magnetic field strength
[NASA-CASE-LEW-12081-2] p0093 N80-20402
- MAGNETIC MEASUREMENT**
Hyperfine magnetic field at Cd impurity site in L2/1/ Heusler alloys Rh2MnGe and Rh2MnPt by TDPAC technique --- Time Differential Perturbed Angular Correlation p0178 A80-16843
- MAGNETIC PROPERTIES**
NT MAGNETIC EFFECTS
NT POLARIZATION CHARACTERISTICS
MAGNETIC RESONANCE
NT PARAMAGNETIC RESONANCE
MAGNETIC STORMS
Computed voltage distributions around solar electric propulsion spacecraft
[NASA-TN-79286] p0053 N80-16094
- MAGNETIC SUBSTANCES**
U MAGNETIC STORMS

MAGNETICALLY TRAPPED PARTICLES

Apparatus for trapping and thermal detection of atomic hydrogen in high magnetic fields at low temperatures

p0111 A80-34546

MAGNETOGASDYNAMICS

U MAGNETOHYDRODYNAMICS

MAGNETOHYDRODYNAMIC GENERATORS

Survey of MHD plant applications

p0144 A80-11972

Results of duct area ratio changes in the NASA

Lewis H2-O2 combustion MHD experiment

[AIAA PAPER 80-0023]

p0176 A80-18243

Oxygen-enriched air for MHD power plants

p0096 A80-25096

Coupled generator and combustor performance

calculations for potential early commercial MHD power plants

p0156 A80-25099

Experiments on H2-O2 MHD power generation

p0176 A80-44239

Results of duct area ratio changes in the NASA

Lewis H2-O2 combustion MHD experiment

[NASA-TM-79308]

p0175 A80-12881

Effect of velocity overshoot on the performance of

magnetohydrodynamic subsonic diffusers

[NASA-TM-79305]

p0175 A80-14922

Experiments on H2-O2 MHD power generation

[NASA-TM-81424]

p0175 A80-16886

The optimization air separation plants for

combined cycle MHD-power plant applications

[NASA-TM-81510]

p0142 A80-23778

Summary and evaluation of the parametric study of

potential early commercial MHD power plants

(PSPEC)

[NASA-TM-81497]

p0142 A80-23780

Parametric study of prospective early commercial

MHD power plants (PSPEC). General Electric

Company, task 1: Parametric analysis

[NASA-CR-159634]

p0152 A80-26779

MAGNETOHYDRODYNAMIC STABILITY

Experimental and theoretical investigation for the

suppression of the planar arc drop in the

thermionic converter

[NASA-CR-159611]

p0176 A80-12880

MAGNETOHYDRODYNAMICS

NASA-Lewis closed-cycle magnetohydrodynamics plant

analysis

[NASA-TM-79249]

p0137 A80-10595

Parametric study of potential early commercial MHD

power plants

[NASA-CR-159633]

p0149 A80-18559

Engineering test facility design definition

[NASA-TM-81499]

p0143 A80-27799

Rapporteur report: MHD electric power plants

[NASA-TM-81554]

p0144 A80-29862

DOD low-thrust mission studies

p0063 A80-31455

MAGNETOIONIC PLASMA

U PLASMAS (PHYSICS)

MAGNETOMETRY

U MAGNETIC MEASUREMENT

MAGNETOPLASMAS

U PLASMAS (PHYSICS)

MAGNETS

NT CRYOGENIC MAGNETS

NT SUPERCONDUCTING MAGNETS

Heat pipe cooling of power processing magnetics

[AIAA PAPER 79-2082]

p0107 A80-20960

MAINTAINABILITY

Modified aerospace R&QA method for wind turbines

p0145 A80-40335

Performance deterioration based on existing

(historical) data; JT9D jet engine diagnostics

program

[NASA-CR-135448]

p0038 A80-22324

MAINTENANCE

NT AIRCRAFT MAINTENANCE

MAN MACHINE SYSTEMS

An interactive modular design for computerized

photometry in spectrochemical analysis

[NASA-TM-81521]

p0074 A80-24386

MANAGEMENT

NT PROJECT MANAGEMENT

NT RESEARCH MANAGEMENT

NT RESOURCES MANAGEMENT

MANAGEMENT METHODS

Matrix management for aerospace 2000

[NASA-TM-81509]

p0181 A80-24200

MANAGEMENT PLANNING

NT PROJECT PLANNING

Thermal energy storage

[NASA-TM-81514]

p0143 A80-25779

MANGANESE ALLOYS

Hyperfine magnetic field at α impurity site in

L2/1/ Heusler alloys Rh_2MnGe and Rh_2MnPt by

TDPAC technique --- Time Differential Perturbed

Angular Correlation

p0178 A80-16843

MANNED ORBITAL SPACE STATIONS

U ORBITAL SPACE STATIONS

MANNED SPACECRAFT

NT ORBITAL SPACE STATIONS

NT SPACE SHUTTLES

NT SPACE STATIONS

MANUALS

NT USER MANUALS (COMPUTER PROGRAMS)

MARKET RESEARCH

The 18/30 GHz fixed communications system service

demand assessment. Volume 1: Executive summary

[NASA-CR-159546]

p0099 A80-22547

The 18/30 GHz fixed communications system service

demand assessment. Volume 2: Main text

[NASA-CR-159547]

p0099 A80-22548

The 30/20 GHz fixed communications systems service

demand assessment. Volume 3: Appendices

[NASA-CR-159548]

p0099 A80-22549

Summary and evaluation of the parametric study of

potential early commercial MHD power plants

(PSPEC)

[NASA-TM-81497]

p0142 A80-23780

MARTENSITIC STAINLESS STEELS

Stress corrosion cracking evaluation of

martensitic precipitation hardening stainless

steels

[NASA-TM-78257]

p0083 A80-16142

MASS DRIVERS (PAYLOAD DELIVERY)

Advanced concepts --- specific impulse, mass

drivers, electromagnetic launchers, and the rail

gun

p0058 A80-31471

MASS FLOW

Application of the principle of similarity fluid

mechanics

p0107 A80-10039

Design and cold-air test of single-stage uncooled

turbine with high work output

[NASA-TF-1680]

p0019 A80-25337

MASS FLOW RATE

Some aspects of a free jet phenomena to 105 L/D in

a constant area duct

p0106 A80-10030

Critical mass flux through short Borda type inlets

of various cross sections

p0106 A80-10031

MATERIALS HANDLING

NT PROPELLANT TRANSFER

MATERIALS TESTS

Fire test method for graphite fiber reinforced

plastics

p0070 A80-31169

Fiber release characteristics of graphite hybrid

composites

p0073 A80-32063

A review of issues and strategies in

nondestructive evaluation of fiber reinforced

structural composites

p0071 A80-34764

Simulation of transducer-couplant effects on

broadband ultrasonic signals --- in

nondestructive flaw evaluation and materials tests

First results of material charging in the space

environment

p0112 A80-44233

p0055 A80-45609

Concepts and techniques for ultrasonic evaluation

of material mechanical properties

p0130 A80-51575

MATHEMATICAL LOGIC

NT ALGORITHMS

MATHEMATICAL MODELS

NT ANALOG SIMULATION

NT DIGITAL SIMULATION

Two-dimensional representations of axisymmetric

fields for computer calculations --- in modeling

microwave tubes

p0102 A80-18232

SUBJECT INDEX

MECHANICAL PROPERTIES

- Initial comparison of SSPM ground test results and flight data to NASCAP simulations --- Satellite Surface Potential Monitor NASA Charging Analyzer Program [AIAA PAPER 80-0336] p0054 A80-29751
- Modified power law equations for vertical wind profiles --- in investigation of windpower plant siting p0159 A80-35719
- 'Chain pooling' model selection for two-level fixed effects factorial experiments p0164 A80-40764
- Analysis of combustion instability in liquid fuel rocket motors [NASA-CR-159733] p0061 A80-13164
- Modelling of crack tip deformation with finite element method and its applications p0130 A80-13503
- CAS2D: FORTRAN program for nonrotating blade-to-blade, steady, potential transonic cascade flows [NASA-TP-1705] p0003 A80-27284
- Statistical aspects of carbon fiber risk assessment modeling --- fire accidents involving aircraft [NASA-CR-159318] p0073 A80-29432
- MATRICES (MATHEMATICS)
A matrix solution for the simulation of magnetic fields with ideal current loops p0102 A80-13903
- MATRIX ANALYSIS
U MATRICES (MATHEMATICS)
MATRIX METHODS
Feasibility of Kevlar 49/PBR-15 polyimide for high temperature applications [NASA-TM-81560] p0069 A80-27429
- MATRIX STRESS CALCULATION
U MATRIX METHODS
MAXIMUM LIKELIHOOD ESTIMATES
Cycles till failure of silver-zinc cells with completing failures modes: Preliminary data analysis [NASA-TM-81556] p0164 A80-29088
- MCDONNELL AIRCRAFT
NT DC 10 AIRCRAFT
MCDONNELL DOUGLAS AIRCRAFT
NT DC 9 AIRCRAFT
NT DC 10 AIRCRAFT
MEASURE AND INTEGRATION
NT NUMERICAL INTEGRATION
MEASURING INSTRUMENTS
NT ANEMOMETERS
NT ENGINE ANALYZERS
NT ENGINE MONITORING INSTRUMENTS
NT FLIGHT LOAD RECORDERS
NT HOT-WIRE FLOWMETERS
NT LASER ANEMOMETERS
NT LASER DOPPLER VELOCIMETERS
NT MICRODENSITOMETERS
NT OPTICAL MEASURING INSTRUMENTS
NT RADIO ALTIMETERS
NT STRAIN GAGES
NT TEMPERATURE MEASURING INSTRUMENTS
NT VISCOMETERS
NT WATTMETERS
The measuring and growing of advanced gas turbines p0111 A80-36127
Instrumentation technology p0013 A80-10214
- MECHANICAL DRIVES
NT TRANSMISSIONS (MACHINE ELEMENTS)
Load support system analysis high speed input pinion configuration [ASME PAPER 79-LUB-34] p0129 A80-14760
Balancing of a power-transmission shaft with the application of axial torque [ASME PAPER 80-GT-143] p0121 A80-42256
Elastomer damper performance - A comparison with a squeeze film for a supercritical power transmission shaft [ASME PAPER 80-GT-162] p0121 A80-42272
Constrained fatigue life optimization of a NASVITIS multiroller traction drive p0122 A80-46407
Effect of geometry and operating conditions on spur gear system power loss p0122 A80-46409
Evaluation of a high performance fixed-ratio traction drive p0122 A80-46410
- Simplified fatigue life analysis for traction drive contacts p0123 A80-46413
- Mechanical components p0013 A80-10213
- Simplified fatigue life analysis for traction drive contacts [NASA-TM-79199] p0115 A80-17469
- Evaluation of a high performance fixed-ratio traction drive [NASA-TM-81425] p0115 A80-18404
- Effect of geometry and operating conditions on spur gear system power loss [NASA-TM-81426] p0116 A80-18406
- Constrained fatigue life optimization of a NASVITIS multiroller traction drive [NASA-TM-81447] p0116 A80-18407
- Ideal spiral bevel gears: A new approach to surface geometry [NASA-TM-81446] p0117 A80-19498
- Parametric tests of a traction drive retrofitted to an automotive gas turbine [NASA-TM-81457] p0117 A80-21754
- Design study of flat belt CVT for electric vehicles [NASA-CR-159822] p0124 A80-22702
- Design study of steel V-Belt CVT for electric vehicles [NASA-CR-159845] p0185 A80-32299
- MECHANICAL ENGINEERING
Load support system analysis high speed input pinion configuration [ASME PAPER 79-LUB-34] p0129 A80-14760
- MECHANICAL MEASUREMENT
NT DISPLACEMENT MEASUREMENT
NT FLOW MEASUREMENT
NT PRESSURE MEASUREMENTS
NT VELOCITY MEASUREMENT
NT VIBRATION MEASUREMENT
NT WIND MEASUREMENT
NT WIND VELOCITY MEASUREMENT
- MECHANICAL PROPERTIES
NT ABRASION RESISTANCE
NT AEROELASTICITY
NT CREEP PROPERTIES
NT CREEP RUPTURE STRENGTH
NT CREEP STRENGTH
NT DUCTILITY
NT DYNAMIC MODULUS OF ELASTICITY
NT ELASTIC PROPERTIES
NT ELASTOPLASTICITY
NT FATIGUE LIFE
NT FLEXIBILITY
NT FRACTURE STRENGTH
NT HIGH STRENGTH
NT MODULUS OF ELASTICITY
NT SHEAR STRENGTH
NT STIFFNESS
NT STRESS RATIO
NT TENSILE PROPERTIES
NT TENSILE STRENGTH
NT THERMAL RESISTANCE
NT THERMOELASTICITY
NT YIELD STRENGTH
Mechanical property characterization of intraply hybrid composites p0070 A80-20954
Effects of thermally induced porosity on an as-HIP powder metallurgy superalloy p0082 A80-29990
Improved fiber retention by the use of fillers in graphite fiber/resin matrix composites p0071 A80-32066
Strengthening of tough iron-12% nickel-reactive metal alloys at 77 K by copper additions p0174 A80-34049
A review of issues and strategies in nondestructive evaluation of fiber reinforced structural composites p0071 A80-34764
Engine environmental effects on composite behavior --- moisture and temperature effects on mechanical properties [AIAA 80-0695] p0024 A80-35101
Application of superalloy powder metallurgy for aircraft engines p0122 A80-44240
Concepts and techniques for ultrasonic evaluation of material mechanical properties

MECHANICAL RESONANCE

SUBJECT INDEX

Effect of thermally induced porosity on an as-HIP powder metallurgy superalloy p0130 A80-51575
 [NASA-TM-79263] p0076 N80-11189
 Mechanical property characterization of intraply hybrid composites p0067 N80-12120
 [NASA-TM-79306]
 Characterization of an oxide dispersion strengthened superalloy, MA-6000E, for turbine blade applications --- turbine blade [NASA-CR-159493] p0083 N80-13218
 Synthesis of improved phenolic resins [NASA-CR-159724] p0091 N80-17221
 Concepts and techniques for ultrasonic evaluation of material mechanical properties [NASA-TM-81523] p0130 N80-24634
 Quantitative ultrasonic evaluation of engineering properties in metals, composites and ceramics [NASA-TM-81530] p0130 N80-26682
 Influence of excess diamine on properties of PMR polyimide resins and composites [NASA-TM-81580] p0069 N80-29433
 Regenerator matrix physical property data [NASA-CR-159854] p0185 N80-30228
METAL FLUORIDES
 U RESONANT VIBRATION
MEDICAL EQUIPMENT
 Intra-ocular pressure normalization technique and equipment [NASA-CASE-LEW-12723-1] p0135 N80-18690
MEETINGS
 U CONFERENCES
MEMBRANE ANALOGY
 U STRUCTURAL ANALYSIS
MEMBRANE THEORY
 U STRUCTURAL ANALYSIS
MEMBRANES
 Anton permselective membrane [NASA-CR-159599] p0147 N80-12551
MERCURY ION ENGINES
 Sputtering in mercury ion thrusters [AIAA PAPER 79-2061] p0058 A80-10384
 Preliminary results of the mission profile life test of a 30 cm Hg bombardment thruster [AIAA PAPER 79-2078] p0081 A80-10391
 Reduced power processor requirements for the 30-cm diameter Hg ion thruster [AIAA PAPER 79-2081] p0059 A80-10392
 Evaluation of particle transport for the P80-1 spacecraft --- mercury ion thruster and spacecraft surfaces interactive effects [AIAA PAPER 79-2047] p0055 A80-13301
 HG ion thruster component testing [AIAA PAPER 79-2116] p0059 A80-20959
 A model for predicting the wearout lifetime of the LeRC/Hughes 30-cm mercury ion thruster [AIAA PAPER 79-2079] p0064 A80-20962
 Specific spacecraft evaluation: Special report --- charged particle transport from a mercury ion thruster to spacecraft surfaces [NASA-CR-159420] p0060 N80-11137
 Hg ion thruster component testing [NASA-TM-79287] p0056 N80-13159
 Physical phenomena in mercury ion thrusters [NASA-CR-159784] p0061 N80-17137
METAL BONDING
 Effects of yttrium, aluminum and chromium concentrations in bond coatings on the performance of zirconia-yttria thermal barriers p0082 A80-35900
 Heat exchanger and method of making --- rocket lining [NASA-CASE-LEW-12441-2] p0105 N80-24573
METAL COATINGS
 NT ALUMINUM COATINGS
 NT NICKEL COATINGS
 Spectral effects on direct-insolation absorptance of five collector coatings [ASME PAPER 79-HT-18] p0146 A80-45722
 Effect of thermal cycling on ZrO₂-Y₂O₃ thermal barrier coatings [NASA-TM-81480] p0018 N80-22349
 Adherence of ion beam sputter deposited metal films on H-13 steel [NASA-TM-81585] p0079 N80-31527
METAL CORROSION
 U CORROSION
METAL CRYSTALS
 Development of exothermically cast single-crystal

Mar-M 247 and derivative alloys [AIRESEARCH-21-3469] p0084 A80-45825
METAL FATIGUE
 Strainrange partitioning life predictions of the long time Metal Properties Council creep-fatigue tests p0133 A80-27958
 Effects of fine porosity on the fatigue behavior of a powder metallurgy superalloy p0082 A80-35495
 Constrained fatigue life optimization of a NASVYTIS multiroller traction drive p0122 A80-46407
 Effects of fine porosity on the fatigue behavior of a powder metallurgy superalloy [NASA-TM-81448] p0078 N80-21493
 Practical implementation of the double linear damage rule and damage curve approach for treating cumulative fatigue damage [NASA-TM-81517] p0132 N80-23684
METAL FILMS
 Tribological properties of sputtered MoS₂ sub 2 films in relation to film morphology [NASA-TM-81465] p0078 N80-21490
METAL FLUORIDES
 NT CALCIUM FLUORIDES
METAL FORMING
 U FORMING TECHNIQUES
METAL HALIDES
 NT CALCIUM FLUORIDES
 NT SODIUM CHLORIDES
METAL MATRIX COMPOSITES
 Fatigue behavior of SiC reinforced titanium composites p0070 A80-10036
 Preparation of cast aluminum alloy-mica particle composites p0071 A80-32632
 A review of issues and strategies in nondestructive evaluation of fiber reinforced structural composites p0071 A80-34764
 Tensile and flexural strength of non-graphitic superhybrid composites: Predictions and comparisons [NASA-TM-79276] p0067 N80-11144
 Predicting the time-temperature dependent axial failure of B/A1 composites [NASA-TM-81474] p0069 N80-21452
 Heat exchanger and method of making --- rocket lining [NASA-CASE-LEW-12441-2] p0105 N80-24573
 Diffusion bonded boron/aluminum spar-shell fan blade [NASA-CR-159571] p0072 N80-25382
 Cost analysis of composite fan blade manufacturing processes [NASA-CR-159876] p0044 N80-31396
METAL OXIDES
 NT ALUMINUM OXIDES
 NT CESIUM OXIDES
 NT COBALT OXIDES
 NT MAGNESIUM OXIDES
 NT SAPPHIRE
 NT YTTRIUM OXIDES
 NT ZINC OXIDES
 NT ZIRCONIUM OXIDES
 Characterization of an oxide dispersion strengthened superalloy, MA-6000E, for turbine blade applications --- turbine blade [NASA-CR-159493] p0083 N80-13218
 Performance of two-layer thermal barrier systems on directionally solidified Ni-Al-Mo and comparative effects of alloy thermal expansion on system life [NASA-TM-81604] p0080 N80-32487
METAL PARTICLES
 NT METAL POWDER
 An investigation into the role of adhesion in the erosion of ductile metals [ASLE PREPRINT 80-AM-3E-3] p0122 A80-43159
 Analysis of wear debris from full-scale bearing fatigue tests using the Ferrograph [ASLE PREPRINT 80-AM-3E-2] p0122 A80-43167
METAL PLATES
 NT BOILER PLATE
METAL POWDER
 Development of a high strength hot isostatically pressed /HIP/ disk alloy, MERL 76 p0084 A80-44108

SUBJECT INDEX

MIXERS

- Application of superalloy powder metallurgy for aircraft engines p0122 A80-44240
- METAL SURFACES**
- Metal-dielectric interactions p0081 A80-13067
- The friction and wear of metals and binary alloys in contact with an abrasive grit of single-crystal silicon carbide [ASLE PREPRINT 79-1C-5C-1] p0120 A80-14734
- Comments on Auger electron production by Ne⁺/ bombardment of surfaces p0174 A80-34048
- An investigation into the role of adhesion in the erosion of ductile metals [ASLE PREPRINT 80-AH-3E-3] p0122 A80-43159
- Uncertainties in predicting turbine blade metal temperatures [ASME PAPER 80-HT-25] p0027 A80-48014
- Corrosion resistant thermal barrier coating --- protecting gas turbines and other heat engine parts [NASA-CASE-LEW-13088-1] p0067 N80-11142
- Back surface reflectors for solar cells [NASA-TM-81390] p0138 N80-15556
- Tribological properties of silicon carbide in metal removal process [NASA-TM-79238] p0114 N80-16340
- An investigation into the role of adhesion in the erosion of ductile metals [NASA-TM-81458] p0078 N80-21489
- Practical applications of surface analytic tools in tribology [NASA-TM-81484] p0079 N80-23430
- METALLIC GLASSES**
- Sliding friction of some metallic glasses p0090 A80-46153
- METALLOGRAPHY**
- Analysis of wear debris from full-scale bearing fatigue tests using the Ferrograph [ASLE PREPRINT 80-AH-3E-2] p0122 A80-43167
- METALLOIDS**
- NT SILICON
- METALS**
- NT ALUMINUM
- NT ALUMINUM COATINGS
- NT CADMIUM
- NT CHROMIUM
- NT EUROPIUM
- NT GALLIUM
- NT IRON
- NT LIQUID METALS
- NT METAL COATINGS
- NT METAL CRYSTALS
- NT METAL FILMS
- NT METAL MATRIX COMPOSITES
- NT METAL POWDER
- NT NICKEL COATINGS
- NT SODIUM
- NT TUNGSTEN
- NT VANADIUM
- NT YTTRIUM
- NT ZIRCONIUM
- METEORITE COMPRESSION TESTS**
- U COMPRESSION TESTS
- U MECHANICAL PROPERTIES
- METEOROLOGICAL PARAMETERS**
- The use of wind data with an operational wind turbine in a research and development environment p0145 A80-35730
- METERS**
- U MEASURING INSTRUMENTS
- METHANE**
- Some advantages of methane in an aircraft gas turbine [NASA-TM-81559] p0094 N80-29502
- MICA**
- Preparation of cast aluminum alloy-mica particle composites p0071 A80-32632
- MICROCOMPUTERS**
- Digital system for dynamic turbine engine blade displacement measurements p0111 A80-36151
- MICRODENSITOMETERS**
- Computerized video densitometry method for rapid analysis of infrared photographic images --- temperature distribution across a turbine blade [NASA-TP-1686] p0110 N80-25635
- MICROPROCESSORS**
- Nonanalytic function generation routines for 16-bit microprocessors [NASA-TM-81586] p0163 N80-33104
- MICROSCOPY**
- NT ELECTRON MICROSCOPY
- MICROSTRUCTURE**
- Some TEM observations of Al₂O₃ scales formed on NiCrAl alloys p0081 A80-13071
- Quantitative ultrasonic evaluation of engineering properties in metals, composites and ceramics [NASA-TM-81530] p0130 N80-26682
- Effect of starting powder characteristics on density, microstructure and low temperature oxidation behavior of a Si₃N₄/w/o Y₂O₃ ceramic [NASA-TM-81536] p0088 N80-27484
- State-of-the-art SiAlON materials p0022 N80-29358
- MICROWAVE AMPLIFIERS**
- Solid-state X-band combiner study [NASA-CR-162432] p0103 N80-11328
- MICROWAVE ANTENNAS**
- NT SLOT ANTENNAS
- MICROWAVE EQUIPMENT**
- NT MICROWAVE AMPLIFIERS
- NT MICROWAVE TUBES
- NT SLOT ANTENNAS
- NT TRAVELING WAVE TUBES
- MICROWAVE FREQUENCIES**
- NT EXTREMELY HIGH FREQUENCIES
- NT SUPERHIGH FREQUENCIES
- MICROWAVE SWITCHING**
- Study of advanced communications satellite systems based on SS-FDMA [NASA-CR-159778] p0050 N80-25357
- MICROWAVE TRANSMISSION**
- Communications technology satellite - United States experiments and disaster communications applications p0051 A80-10032
- Concepts for 20/30 GHz satcom systems for direct-to-user applications [AIAA 80-0582] p0050 A80-35329
- MICROWAVE TUBES**
- NT TRAVELING WAVE TUBES
- Two-dimensional representations of axisymmetric fields for computer calculations --- in modeling microwave tubes p0102 A80-18232
- MICROWAVES**
- NT MILLIMETER WAVES
- MIDAIR COLLISIONS**
- NT BIRD-AIRCRAFT COLLISIONS
- MILITARY AIRCRAFT**
- Zero-length, slotted-lip inlet for subsonic military aircraft [AIAA PAPER 80-1245] p0004 A80-41203
- MILLIMETER WAVES**
- System analysis for millimeter-wave communication satellites p0100 A80-52479
- MILLING (MIXING)**
- U COMPOUNDING
- MINERALS**
- NT ASBESTOS
- NT GRAPHITE
- NT MICA
- MINES (EXCAVATIONS)**
- Assessment of satellite and aircraft multispectral scanner data for strip-mine monitoring [NASA-TM-79268] p0136 N80-20787
- MINIMIZATION**
- U OPTIMIZATION
- MINING**
- NT STRIP MINING
- MISSILE STABILIZATION**
- U STABILIZATION
- MISSION PLANNING**
- Characteristics of primary electric propulsion systems [AIAA PAPER 79-2041] p0058 A80-10376
- Electric propulsion for near-Earth space missions [NASA-CR-159735] p0062 N80-16096
- MIXERS**
- Experimental evaluation of exhaust mixers for an Energy Efficient Engine [AIAA PAPER 80-1088] p0025 A80-38903

- Influence of pressure driven secondary flows on the behavior of turbofan forced mixers
[AIAA PAPER 80-1198] p0025 A80-41515
- Influence of pressure driven secondary flows on the behavior of turbofan forced mixers
[NASA-TM-81541] p0105 N80-27632
- MIXING**
- NT COMPOUNDING
- NT TURBULENT MIXING
- Computation of three-dimensional flow in turbofan mixers and comparison with experimental data
[AIAA PAPER 80-0227] p0003 A80-20967
- MIXTURES**
- NT AQUEOUS SOLUTIONS
- NT EUTECTIC ALLOYS
- NT GAS MIXTURES
- NT METAL MATRIX COMPOSITES
- NT SOLID SOLUTIONS
- MOBILITY**
- NT IONIC MOBILITY
- MODE OF VIBRATION**
- U VIBRATION MODE
- MODELS**
- NT AIRCRAFT MODELS
- NT ANALOG SIMULATION
- NT DIGITAL SIMULATION
- NT DYNAMIC MODELS
- NT MATHEMATICAL MODELS
- NT SCALE MODELS
- Acoustic test and analyses of three advanced turboprop models
[NASA-CR-159667] p0039 N80-23311
- MODES**
- NT FAILURE MODES
- NT PROPAGATION MODES
- NT VIBRATION MODE
- MODULATION**
- NT VELOCITY MODULATION
- MODULUS OF ELASTICITY**
- NT DYNAMIC MODULUS OF ELASTICITY
- Compliance and stress intensity coefficients for short bar specimens with chevron notches
p0133 A80-46032
- Composite wall concept for high temperature turbine shrouds: Survey of low modulus strain isolator materials
[NASA-TM-81443] p0086 N80-20398
- Fully plasma-sprayed compliant backed ceramic turbine seal
[NASA-CASE-LEW-13268-1] p0117 N80-24619
- Fully flooded elastohydrodynamic lubricated elliptical contacts
[NASA-TM-81543] p0118 N80-27698
- Starved elastohydrodynamic lubricated elliptical contacts
[NASA-TM-81549] p0118 N80-27699
- MOHR CIRCLES**
- U FRACTURE MECHANICS
- MOISTURE CONTENT**
- NT ATMOSPHERIC MOISTURE
- Engine environmental effects on composite behavior --- moisture and temperature effects on mechanical properties
[AIAA 80-0695] p0024 A80-35101
- Analyses of moisture in polymers and composites
[NASA-CR-159745] p0091 N80-15264
- MOLECULAR STRUCTURE**
- Effect of fuel molecular structure on soot formation in gas turbine engines
[ASME PAPER 80-GT-62] p0095 A80-42192
- Effect of fuel molecular structure on soot formation in gas turbine combustion
p0043 N80-29322
- MOLECULAR WEIGHT**
- Influence of excess diamine on properties of PMR polyimide resins and composites
[NASA-TM-81580] p0069 N80-29433
- MOLTEN SALTS**
- High-temperature molten salt thermal energy storage systems
[NASA-CR-159663] p0148 N80-17547
- Active heat exchange system development for latent heat thermal energy storage
[NASA-CR-159726] p0149 N80-18562
- MOLYBDENUM COMPOUNDS**
- NT MOLYBDENUM DISULFIDES
- MOLYBDENUM DISULFIDES**
- Tribological properties of sputtered MoS sub 2 films in relation to film morphology
[NASA-TM-81465] p0078 N80-21490
- MOLYBDENUM SULFIDES**
- NT MOLYBDENUM DISULFIDES
- Tribological properties of sputtered MoS2 films in relation to film morphology
p0089 A80-35502
- MOMENTS**
- NT BENDING MOMENTS
- NT TORQUE
- MONATOMIC GASES**
- Atomic hydrogen storage --- cryotrapping and magnetic field strength
[NASA-CASE-LEW-12081-2] p0093 N80-20402
- MONOCRYSTALS**
- U SINGLE CRYSTALS
- MONOPLANES**
- NT F-102 AIRCRAFT
- MOSS (SPACE STATIONS)**
- U ORBITAL SPACE STATIONS
- MOTION EQUATIONS**
- U EQUATIONS OF MOTION
- MOTION STABILITY**
- NT AERODYNAMIC STABILITY
- NT FLOW STABILITY
- NT HOVERING STABILITY
- NT MAGNETOHYDRODYNAMIC STABILITY
- NT ROTARY STABILITY
- MOTOR VEHICLES**
- NT ELECTRIC AUTOMOBILES
- NT ELECTRIC MOTOR VEHICLES
- MOTORS**
- NT ELECTRIC MOTORS
- MOUNTS**
- U SUPPORTS
- MUBIS (SCANNERS)**
- U MULTIPLE BEAM INTERVAL SCANNERS
- MULTILAYER STRUCTURES**
- U LAMINATES
- MULTIPHASE FLOW**
- NT TWO PHASE FLOW
- MULTIPLE ACCESS**
- NT FREQUENCY DIVISION MULTIPLE ACCESS
- NT TIME DIVISION MULTIPLE ACCESS
- MULTIPLE BEAM INTERVAL SCANNERS**
- Packet communications in satellites with multiple-beam antennas and signal processing
[AIAA 80-0537] p0099 A80-29574
- Concepts for 18/30 GHz satellite communication system, volume 1
[NASA-CR-159625-VOL-1] p0098 N80-11277
- Concepts for 18/30 GHz satellite communication system, volume 1A: Appendix
[NASA-CR-159625-VOL-1A] p0098 N80-11278
- Concepts for 18/30 GHz satellite communication system study. Executive summary
[NASA-CR-159680] p0098 N80-11279
- MULTIPLEX TRANSMISSION**
- U MULTIPLEXING
- MULTIPLEXERS**
- U MULTIPLEXING
- MULTIPLEXING**
- On-board processing concepts for future satellite communications systems
[NASA-CR-159683] p0099 N80-24514
- MULTIPROPELLANTS**
- U ROCKET PROPELLANTS
- MULTISPECTRAL PHOTOGRAPHY**
- NT INFRARED PHOTOGRAPHY
- MULTISTAGE COMPRESSORS**
- U TURBOCOMPRESSORS
- MULTIVARIATE STATISTICAL ANALYSIS**
- NT REGRESSION ANALYSIS

N

NACELLES

- Development of a Kevlar/PMR-15 reduced drag DC-9 nacelle fairing
[AIAA PAPER 80-1194] p0010 A80-41193
- CF6-50 Short Core Exhaust Nozzle
[AIAA PAPER 80-1196] p0025 A80-41514
- Quiet Clean Short-haul Experimental Engine (QCSSE) preliminary under the wing flight propulsion system analysis report
[NASA-CR-134868] p0034 N80-15088
- Quiet Clean Short-haul Experimental Engine (QCSSE). Under-The-Wing (UTW) engine boilerplate nacelle test report, volume 1
[NASA-CR-135249] p0035 N80-15096

SUBJECT INDEX

NICKEL ALLOYS

Quiet Clean Short-haul Experimental Engine (QCSEE). Under-The-Wing (UTW) engine boilerplate nacelle test report. Volume 3: Mechanical performance [NASA-CR-135251] p0035 N80-15097

Quiet Clean Short-haul Experimental Engine (QCSEE) Over-The-Wing (OTW) boilerplate nacelle design report [NASA-CR-135168] p0035 N80-15099

Quiet Clean Short-haul Experimental Engine (QCSEE) Under-The-Wing (UTW) composite nacelle subsystem test report --- to verify strength of selected composite materials [NASA-CR-135075] p0034 N80-15100

Quiet Clean Short-haul Experimental Engine (QCSEE) Under-The-Wing (UTW) composite nacelle subsystem test report --- to verify strength of selected composite materials [NASA-CR-135075] p0034 N80-15100

Quiet Clean Short-haul Experimental Engine (QCSEE) Under-The-Wing (UTW) boiler plate nacelle and core exhaust nozzle design report [NASA-CR-135008] p0032 N80-15116

Quiet Clean Short-haul Experimental Engine (QCSEE) Under-The-Wing (UTW) composite nacelle [NASA-CR-135352] p0032 N80-15119

Optimum subsonic, high-angle-of-attack nacelles [NASA-TM-81491] p0016 N80-20275

Quiet Clean Short-haul Experimental Engine (QCSEE) Under-The-Wing (UTW) composite nacelle test report. Volume 2: Acoustic performance [NASA-CR-159472] p0044 N80-29297

NASA PROGRAMS

NT GLOBAL ATMOSPHERIC RESEARCH PROGRAM

NT QUIET ENGINE PROGRAM

NT SUPERSONIC CRUISE AIRCRAFT RESEARCH

NASA gear research and its probable effect on rotorcraft transmission design p0120 A80-13068

Engine component improvement program - Performance improvement [AIAA PAPER 80-0223] p0024 A80-19300

MASCAP modelling of environmental-charging-induced discharges in satellites p0054 A80-19774

NASA advanced communications systems analysis p0097 A80-25916

30/20 GHz wideband technology verification program p0097 A80-25917

NASA communications technology research and development p0097 A80-25920

National Aeronautics and Space Administration plans for space communication technology p0097 A80-26795

NASA's program in communication satellites [AAS 79-247] p0097 A80-28712

Initial comparison of SSPM ground test results and flight data to MASCAP simulations --- Satellite Surface Potential Monitor NASA Charging Analyzer Program [AIAA PAPER 80-0336] p0054 A80-29751

MASCAP modelling computations on large optics spacecraft in geosynchronous substorm environments p0054 A80-32829

Status of NASA full-scale engine aeroelasticity research p0133 A80-35906

Experimental evaluation of exhaust mixers for an Energy Efficient Engine [AIAA PAPER 80-1088] p0025 A80-38903

Matrix management for aerospace 2000 [AIAA PAPER 80-0946] p0181 A80-40700

NASA broad-specification fuels combustion technology program: Status and description [NASA-TM-79315] p0014 N80-14126

Status of the DOE/NASA critical gas turbine research and technology project [NASA-TM-79307] p0137 N80-14493

Quiet powered-lift propulsion [NASA-CR-2077] p0015 N80-15127

NASA propeller technology program p0018 N80-22341

Redox storage systems for solar applications [NASA-TM-81464] p0142 N80-23777

NASA STRUCTURAL ANALYSIS PROGRAM

U NASTRAN

NASTRAN

Effect of time dependent flight loads on JT9D-7 performance deterioration [NASA-CR-159681] p0134 N80-10515

NATIONS

NT DEVELOPING NATIONS

NATURAL FREQUENCIES

U RESONANT FREQUENCIES

NATURAL GAS

NT LIQUEFIED NATURAL GAS

NAVIGATION AIDS

NT NAVIGATION INSTRUMENTS

NAVIGATION INSTRUMENTS

NT RADIO ALTIMETERS

Flight test of navigation and guidance sensor errors measured on STOL approaches [NASA-TM-81154] p0028 N80-13041

NEAR WAKES

Three dimensional mean flow and turbulence characteristics of the near wake of a compressor rotor blade [NASA-CR-159518] p0005 N80-27288

NEON

Comments on Auger electron production by Ne+/ bombardment of surfaces p0174 A80-34048

NEOPLASMS

NT CANCER

NERVA (ENGINE)

U NUCLEAR ENGINE FOR ROCKET VEHICLES

NEUTRALIZERS

Plasma physics analysis of SERT-2 operation [NASA-CR-159814] p0177 N80-27189

NEUTRON IRRADIATION

Preliminary results of fast neutron treatments in carcinoma of the pancreas [NASA-TM-81516] p0160 N80-24983

NEW MEXICO

Blade design and operating experience on the MOD-OA 200 kW wind turbine at Clayton, New Mexico p0139 N80-16470

NICKEL ALLOYS

NT ASTROLOY (TRADEMARK)

Some TEM observations of Al2O3 scales formed on NiCrAl alloys p0081 A80-13071

The effect of zirconium on the isothermal oxidation of nominal Ni-14Cr-24Al alloys p0082 A80-26465

Strengthening of tough iron-12% nickel-reactive metal alloys at 77 K by copper additions p0174 A80-34049

Stability of several oxide dispersion strengthened alloys and a directionally solidified gamma/gamma prime-alpha eutectic alloy in a thermal gradient p0082 A80-40962

Development of a high strength hot isostatically pressed /HIP/ disk alloy, MREL 76 p0084 A80-44108

Anisotropy of nickel-base superalloy single crystals p0083 A80-51573

Characterization of an oxide dispersion strengthened superalloy, MA-6000E, for turbine blade applications --- turbine blade [NASA-CR-159493] p0083 N80-13218

An investigation of the initiation stage of hot corrosion in Ni-base alloys [NASA-CR-159718] p0083 N80-15233

Chemical processes involved in the initiation of hot corrosion of B-1900 and NASA-TM VIA [NASA-TM-81399] p0077 N80-17199

Anisotropy of nickel-base superalloy single crystals [NASA-TM-81437] p0077 N80-17200

Thermal fatigue and oxidation data for directionally solidified MAR-M 246 turbine blades [NASA-CR-159798] p0037 N80-21330

Thermal fatigue and oxidation data of oxide dispersion-strengthened alloys [NASA-CR-159842] p0084 N80-25415

Hot corrosion of Co-Cr, Co-Cr-Al, and Ni-Cr alloys in the temperature range of 700-750 deg C [NASA-CR-159689] p0084 N80-26427

Three dimensional finite-element elastic analysis of a thermally cycled double-edge wedge geometry specimen --- nickel alloy turbine parts [NASA-TM-80980] p0079 N80-26433

Evaluation of the cyclic behavior of aircraft turbine disk alloys, part 2 [NASA-CR-165123] p0084 N80-30482

NICKEL COATINGS

SUBJECT INDEX

NICKEL COATINGS

Internal coating of air cooled gas turbine blades
[NASA-CR-159701] p0036 N80-18041

NICKEL HYDROGEN BATTERIES

Status of nickel-hydrogen cell technology
p0064 N80-33474

NICKEL STEELS

Comparison tests and experimental compliance
calibration of the proposed standard round
compact plane strain fracture toughness specimen
[NASA-TM-81379] p0132 N80-13513

NICKEL ZINC BATTERIES

Effect of positive pulse charge waveforms on cycle
life of nickel-zinc cells
p0146 N80-48329

An electric vehicle propulsion system's impact on
battery performance: An overview
[NASA-TM-81515] p0143 N80-24756

Pulse charging of lead-acid traction
cells
[NASA-TM-81513] p0143 N80-25780

NIOBIUM ALLOYS

Long-time creep behavior of the niobium alloy C-103
[NASA-TP-1727] p0080 N80-33555

NIOBIUM COMPOUNDS

Critical currents in A-15 structure Nb3Al
converted from cold-worked bcc structure
p0179 N80-33853

NITRATES

Sulfate and nitrate collected by filter sampling
near the tropopause
[NASA-TP-1567] p0157 N80-14581

NITRIC OXIDE

Flame tube parametric studies for control of fuel
bound nitrogen using rich-lean two-stage
combustion
[NASA-TM-81472] p0141 N80-21837

NITRIDES

NT OXYNITRIDES
NT SILICON NITRIDES

NITROGEN COMPOUNDS

NT NITRATES
NT NITRIC OXIDE
NT NITROGEN OXIDES
NT OXYNITRIDES
NT POLYIMIDES
NT SILICON NITRIDES

Mechanisms of nitrogen heterocycle influence on
turbine fuel stability
p0043 N80-29327

NITROGEN OXIDES

NT NITRIC OXIDE
An analytical study of nitrogen oxides and carbon
monoxide emissions in hydrocarbon combustion
with added nitrogen - Preliminary results
[ASME PAPER 80-GT-60] p0074 N80-42190

Low NO_x/heavy fuel combustor program
[ASME PAPER 80-GT-69] p0026 N80-42199

Atomizing characteristics of swirl can combustor
modules with swirl blast fuel injectors --- in
terms of NO_x emission rate
[NASA-TM-79297] p0014 N80-13047

An analytical study of nitrogen oxides and carbon
monoxide emissions in hydrocarbon combustion
with added nitrogen, preliminary results
[NASA-TM-79296] p0157 N80-13721

Energy efficient engine
[NASA-CR-159685] p0045 N80-33408

NOBLE GASES

U RARE GASES

NOISE

Comparison of several inflow control devices for
flight simulation of fan tone noise using a
JT15D-1 engine
[NASA-TM-81505] p0019 N80-24314

NOISE (SOUND)

NT AERODYNAMIC NOISE
NT AIRCRAFT NOISE
NT ENGINE NOISE
NT JET AIRCRAFT NOISE

NOISE ATTENUATION

U NOISE REDUCTION

NOISE ELIMINATION

U NOISE REDUCTION

NOISE HAZARDS

U HAZARDS

NOISE INTENSITY

An exploratory survey of noise levels associated
with a 100 kW wind turbine
p0171 N80-35499

NOISE MEASUREMENT

Acoustic pressures on a prop-fan aircraft fuselage
surface
[AIAA PAPER 80-1002] p0172 N80-35965

Quiet Clean Short-haul Experimental Engine
(QCSEE). Core engine noise measurements
[NASA-CR-135160] p0035 N80-15093

An exploratory survey of noise levels associated
with a 100kW wind turbine
[NASA-TM-81486] p0169 N80-23102

Acoustic test and analyses of three advanced
turbo-prop models
[NASA-CR-159667] p0039 N80-23311

A comparison between an existing propeller noise
theory and wind tunnel data
[NASA-TM-81519] p0169 N80-25101

NOISE PREDICTION (AIRCRAFT)

Acoustic considerations of flight effects on jet
noise suppressor nozzles
[AIAA PAPER 80-0164] p0171 N80-20965

Prediction of unsuppressed jet engine exhaust
noise in flight from static data
[AIAA PAPER 80-1008] p0027 N80-44491

An improved prediction method for the noise
generated in flight by circular jets
[NASA-TM-81470] p0168 N80-22048

A comparison between an existing propeller noise
theory and wind tunnel data
[NASA-TM-81519] p0169 N80-25101

Measured and predicted impingement noise for a
model-scale under the wing externally blown flap
configuration with a QCSEE type nozzle
[NASA-TM-81494] p0169 N80-26115

Prediction of unsuppressed jet engine exhaust
noise in flight from static data
[NASA-TM-81537] p0169 N80-29132

NOISE PROPAGATION

Time-dependent difference theory for noise
propagation in a two-dimensional duct
[AIAA PAPER 80-0098] p0170 N80-18269

Comparison of inlet suppressor data with
approximate theory based on cutoff ratio
[AIAA PAPER 80-0100] p0170 N80-20964

Spectral structure of pressure measurements made
in a combustion duct
p0171 N80-35496

Comparison of several inflow control devices for
flight simulation of fan tone noise using a
JT15D-1 engine
[AIAA PAPER 80-1025] p0025 N80-38640

Far-field radiation of APT turbofan noise
p0025 N80-39638

Time-dependent difference theory for noise
propagation in a two-dimensional duct --- of a
turbofan engine
[NASA-TM-79298] p0167 N80-12822

Core noise investigation of the CF6-50 turbofan
engine
[NASA-CR-159598] p0036 N80-16061

Core noise investigation of the CF6-50 turbofan
engine
[NASA-CR-159749] p0036 N80-16062

Far-field radiation of aft turbofan noise
[NASA-TM-81506] p0166 N80-24129

NOISE REDUCTION

Comparison of inlet suppressor data with
approximate theory based on cutoff ratio
[AIAA PAPER 80-0100] p0170 N80-20964

Acoustic considerations of flight effects on jet
noise suppressor nozzles
[AIAA PAPER 80-0164] p0171 N80-20965

Noise suppression due to annulus shaping of a
conventional coaxial nozzle
p0171 N80-35497

Noise suppression due to annulus shaping of an
inverted-velocity-profile coaxial nozzle
p0171 N80-35498

Acoustic measurements of three Prop-Fan models
[AIAA PAPER 80-0995] p0045 N80-35958

Effect of inflow control on inlet noise of a
cut-on fan
[AIAA PAPER 80-1049] p0171 N80-35993

Rigorous solutions for sound radiation from
circular ducts with hyperbolic horns or infinite
plane baffle
p0171 N80-37895

Comparison of several inflow control devices for
flight simulation of fan tone noise using a
JT15D-1 engine

SUBJECT INDEX

NOZZLE FLOW

[AIAA PAPER 80-1025] p0025 A80-38640
 Characteristics of internal- and jet-noise
 radiation from a multi-lobe, multi-tube
 suppressor nozzle tested statically and under
 flight simulation
 [AIAA PAPER 80-1027] p0173 A80-38642
 Far-field radiation of APT turbofan noise
 p0025 A80-39638
 A comparison of experiment and theory for sound
 propagation in variable area ducts
 p0173 A80-45844
 An acoustic sensitivity study of general aviation
 propellers
 [AIAA PAPER 80-1871] p0045 A80-50191
 Noise reduction
 p0012 A80-10208
 Advanced turbo-prop airplane interior noise
 reduction-source definition
 [NASA-CR-159668] p0172 A80-13882
 Acoustic considerations of flight effects on jet
 noise suppressor nozzles
 [NASA-TM-81377] p0167 A80-14843
 Demonstration of short-haul aircraft aft noise
 reduction techniques on a twenty inch (50.8 cm)
 diameter fan, volume 1
 [NASA-CR-134849] p0033 A80-15083
 Demonstration of short-haul aircraft aft noise
 reduction techniques on a twenty inch (50.8)
 diameter fan, volume 2
 [NASA-CR-134850] p0034 A80-15084
 Demonstration of short haul aircraft aft noise
 reduction techniques on a twenty inch (50.8 cm)
 diameter fan, volume 3
 [NASA-CR-134851] p0034 A80-15085
 Acoustic analysis of aft noise reduction
 techniques measured on a subsonic tip speed 50.8
 cm (twenty inch) diameter fan --- quiet engine
 program
 [NASA-CR-134891] p0030 A80-15102
 Quiet Clean Short-haul Experimental Engine
 (QCSEE): Acoustic treatment development and
 design
 [NASA-CR-135266] p0033 A80-15122
 Experimental evaluation of a spinning-mode
 acoustic-treatment design concept for aircraft
 inlets --- suppression of YF-102 engine fan noise
 [NASA-TP-1613] p0016 A80-21323
 Aircsearch QCGAT program --- quiet clean general
 aviation turbofan engines
 [NASA-CR-159758] p0037 A80-21331
 Noise suppression due to annulus shaping of an
 inverted-velocity-profile coaxial nozzle ---
 supersonic cruise aircraft
 [NASA-TM-81460] p0168 A80-22046
 Noise suppression due to annulus shaping of
 conventional coaxial nozzle
 [NASA-TM-81461] p0168 A80-22047
 Avco Lycoming quiet clean general aviation
 turbofan engine
 p0039 A80-22333
 Summary of NASA QCGAT program
 p0017 A80-22334
 Effect of inflow control on inlet noise of a
 cut-on fan --- in an anechoic chamber
 [NASA-TM-81487] p0169 A80-23098
 Forward acoustic performance of a shock-swallowing
 high-tip-speed fan (QF-13)
 [NASA-TP-1668] p0169 A80-23100
 OSCEE fan exhaust bulk absorber treatment evaluation
 [NASA-TM-81498] p0019 A80-23314
 Measured and predicted impingement noise for a
 model-scale under the wing externally blown flap
 configuration with a QCSEE type nozzle
 [NASA-TM-81494] p0169 A80-26115
 A study of the transmission characteristics of
 suppressor nozzles
 [NASA-CR-165133] p0172 A80-32186
NOISE SPECTRA
 Effect of temperature on surface noise
 p0107 A80-28419
 An exploratory survey of noise levels associated
 with a 100 kw wind turbine
 p0171 A80-35499
NOISE SUPPRESSORS
U NOISE REDUCTION
NONADIABATIC CONDITIONS
 A calculation procedure for viscous flow in
 turbomachines, volume 3 --- computer programs
 [NASA-CR-159864] p0005 A80-26274

NONADIABATIC PROCESSES

U HEAT TRANSFER

NONDESTRUCTIVE TESTS

U STATIC FINING

A review of issues and strategies in
 nondestructive evaluation of fiber reinforced
 structural composites
 p0071 A80-34764
 Quantitative ultrasonic evaluation of engineering
 properties in metals, composites, and ceramics
 p0130 A80-39641
 Simulation of transducer-couplant effects on
 broadband ultrasonic signals --- in
 nondestructive flaw evaluation and materials tests
 p0112 A80-44233
 Concepts and techniques for ultrasonic evaluation
 of material mechanical properties
 p0130 A80-51575
 Simulation of transducer-couplant effects on
 broadband ultrasonic signals
 [NASA-TM-81489] p0130 A80-22714
 Concepts and techniques for ultrasonic evaluation
 of material mechanical properties
 [NASA-TM-81523] p0130 A80-24634
 Quantitative ultrasonic evaluation of engineering
 properties in metals, composites and ceramics
 [NASA-TM-81530] p0130 A80-26682

NONISOTROPY

U ANISOTROPY

NONLINEAR EQUATIONS

Evaluation of a strained-coordinate perturbation
 procedure - Nonlinear subsonic and transonic flows
 [AIAA PAPER 80-0339] p0006 A80-18324

NONRIGIDITY

U FLEXIBILITY

NONVISCOUS FLOW

U TURBULENT FLOW

NORTH AMERICA

Quantitative interpretation of Great Lakes remote
 sensing data
 p0157 A80-45005

NORTHERN HEMISPHERE

Comments on 'Experimental evidence for
 interhemispheric transport from airborne carbon
 monoxide measurements'
 p0159 A80-32520

NOTCH TESTS

Fracture toughness determination of Al203 using
 four-point-bend specimens with straight-through
 and chevron notches
 p0090 A80-42085
 Compliance and stress intensity coefficients for
 short bar specimens with chevron notches
 p0133 A80-46032
 Performance of Chevron-notch short bar specimen in
 determining the fracture toughness of silicon
 nitride and alumina oxide
 p0090 A80-50696
 Fracture toughness of brittle materials determined
 with chevron notch specimens
 [NASA-TM-81607] p0079 A80-32486

NOTCHED METALS

U NOTCH TESTS

NOZZLE COEFFICIENT

U NOZZLE FLOW

NOZZLE DESIGN

Critical mass flow through short Borda type inlets
 of various cross sections
 p0106 A80-10031
 Acoustic considerations of flight effects on jet
 noise suppressor nozzles
 [AIAA PAPER 80-0164] p0171 A80-20965
 Spray nozzle designs for agricultural aviation
 applications --- relation of drop size to spray
 characteristics and nozzle efficiency
 [NASA-CR-159702] p0108 A80-10460
NOZZLE EFFICIENCY
 Spray nozzle designs for agricultural aviation
 applications --- relation of drop size to spray
 characteristics and nozzle efficiency
 [NASA-CR-159702] p0108 A80-10460

NOZZLE FLOW

Application of the principle of similarity fluid
 mechanics
 p0107 A80-10039
 Computation of three-dimensional flow in turbofan
 mixers and comparison with experimental data
 [AIAA PAPER 80-0227] p0003 A80-20967

- Characteristics of internal- and jet-noise radiation from a multi-lobe, multi-tube suppressor nozzle tested statically and under flight simulation
[AIAA PAPER 80-1027] p0173 A80-38642
- Influence of pressure driven secondary flows on the behavior of turbofan forced mixers
[AIAA PAPER 80-1190] p0025 A80-41515
- Time-dependent difference theory for noise propagation in a two-dimensional duct --- of a turbofan engine
[NASA-TM-79298] p0167 A80-12822
- A time dependent difference theory for sound propagation in ducts with flow --- characteristic of inlet and exhaust ducts of turbofan engines
[NASA-TM-79302] p0167 A80-12823
- Computation of three-dimensional flow in turbofan mixers and comparison with experimental data
[NASA-TM-81410] p0104 A80-15364
- Influence of pressure driven secondary flows on the behavior of turbofan forced mixers
[NASA-TM-81541] p0105 A80-27632
- Toward the use of similarity theory in two-phase choked flows
[NASA-TM-81568] p0106 A80-29623
- NOZZLE GEOMETRY**
- Critical mass flux through short Borda type inlets of various cross sections
p0106 A80-10031
- Noise suppression due to annulus shaping of a conventional coaxial nozzle
p0171 A80-35497
- Noise suppression due to annulus shaping of an inverted-velocity-profile coaxial nozzle
p0171 A80-35498
- Coannular supersonic ejector nozzles
p0002 A80-10128
- Static test-stand performance of the YF-102 turbofan engine with several exhaust configurations for the Quiet Short-Haul Research Aircraft (QSRA)
[NASA-TP-1556] p0014 A80-14121
- Noise suppression due to annulus shaping of an inverted-velocity-profile coaxial nozzle --- supersonic cruise aircraft
[NASA-TM-81460] p0168 A80-22046
- An improved prediction method for the noise generated in flight by circular jets
[NASA-TM-81470] p0168 A80-22048
- A study of the transmission characteristics of suppressor nozzles
[NASA-CR-165133] p0172 A80-32186
- NUCLEAR ELECTRIC PROPULSION**
- Nuclear electric propulsion system utilization for earth orbit transfer of large spacecraft structures
[AIAA PAPER 80-1223] p0060 A80-38975
- Orbital transfer of large space structures with nuclear electric rockets
[AAS PAPER 80-083] p0054 A80-41897
- NUCLEAR ENGINE FOR ROCKET VEHICLES**
- Orbital transfer of large space structures with nuclear electric rockets
[AAS PAPER 80-083] p0054 A80-41897
- NUCLEAR PARTICLES**
- NT PHOTOELECTRONS
- NUCLEAR PROPULSION**
- NT NUCLEAR ELECTRIC PROPULSION
- NUCLEAR SHIELDING**
- U RADIATION SHIELDING
- NUCLEATION**
- Characterization and properties of controlled nucleation thermochemical deposited /CMTD/ silicon carbide
p0089 A80-13063
- Characterization and properties of controlled nucleation thermochemical deposited (CMTD) silicon carbide
[NASA-TM-79277] p0085 A80-13254
- NUMERICAL ANALYSIS**
- NT COMPUTATIONAL FLUID DYNAMICS
- NT FINITE DIFFERENCE THEORY
- NT FINITE ELEMENT METHOD
- NT INTERPOLATION
- NT NUMERICAL INTEGRATION
- Prediction of fragment velocities and trajectories
p0096 A80-16210
- Numerical calculation of transonic axial turbomachinery flows
[NASA-TM-81544] p0020 A80-27363
- Dynamic analysis of noncontacting face seals
[NASA-TM-79294] p0118 A80-27695
- NUMERICAL CONTROL**
- An interactive modular design for computerized photometry in spectrochemical analysis
p0074 A80-39640
- NUMERICAL FLOW VISUALIZATION**
- Numerical simulation of supersonic inlets using a three-dimensional viscous flow analysis
[AIAA PAPER 80-0384] p0003 A80-20969
- An alternative approach to the numerical simulation of steady inviscid flow
p0107 A80-44228
- Aerodynamic analysis of a supersonic cascade vibrating in a complex mode
p0007 A80-45841
- WIND: Computer program for calculation of three dimensional potential compressible flow about wind turbine rotor blades**
[NASA-TP-1729] p0003 A80-33357
- NUMERICAL INTEGRATION**
- Direct integration of transient rotor dynamics
[NASA-TP-1597] p0015 A80-15128
- The response of turbine engine rotors to interference rubs
[NASA-TM-81518] p0118 A80-27696
- O**
- O RING SEALS**
- Circumferential shaft seal
[NASA-CASE-LEN-12119-2] p0115 A80-18401
- Damping in tapered annular seals for an incompressible fluid
[NASA-TP-1646] p0116 A80-19495
- Damping in ring seals for compressible fluids
p0119 A80-29716
- OCEANS**
- NT PACIFIC OCEAN
- OIL RECOVERY**
- Field experiences with rotordynamic instability in high-performance turbomachinery --- oil and natural gas recovery
p0125 A80-29707
- OILS**
- NT CRUDE OIL
- NT FUEL OILS
- NT LUBRICATING OILS
- NT SHALE OIL
- ONBOARD EQUIPMENT**
- Multigigabit satellite on-board signal processing
[AIAA 80-0583] p0100 A80-29605
- ONISOTROPY**
- U ANISOTROPY
- OPTICAL EQUIPMENT**
- NT LASER DOPPLER VELOCIMETERS
- NT MICRODENSITOMETERS
- NT OPTICAL MEASURING INSTRUMENTS
- MASCAP modelling computations on large optics spacecraft in geosynchronous substorm environments
p0054 A80-32829
- OPTICAL MEASUREMENT**
- NT PHOTOMETRY
- Laser-optical blade tip clearance measurement system
p0111 A80-36137
- OPTICAL MEASURING INSTRUMENTS**
- NT MICRODENSITOMETERS
- Optical sensors for aeronautics and space
[NASA-TM-81407] p0110 A80-17423
- Design, fabrication and testing of an optical temperature sensor
[NASA-CR-165125] p0112 A80-31777
- OPTICAL PROPERTIES**
- NT ABSORPTANCE
- NT REFLECTANCE
- NT SPECTRAL REFLECTANCE
- Modification of the electrical and optical properties of polymers --- ion irradiation to create texture
[NASA-CASE-LEN-13027-1] p0087 A80-24437
- OPTICAL SENSORS**
- U OPTICAL MEASURING INSTRUMENTS
- OPTIMAL CONTROL**
- A new traffic control design method for large networks with signalized intersections
p0183 A80-14841

SUBJECT INDEX

OXYGEN

- An adaptive-control switching buck regulator -
Implementation, analysis, and design
p0103 A80-28167
- Modeling and analysis of Power Processing Systems
p0066 A80-28894
- OPTIMIZATION**
- NT OPTIMAL CONTROL**
Performance of computer-optimized tapered-roller
bearings to 2.4 million DN
[NASA-TM-81414] p0114 A80-16342
- OPTIMUM CONTROL**
U OPTIMAL CONTROL
- ORBIT TRANSFER VEHICLES**
Nuclear electric propulsion system utilization for
earth orbit transfer of large spacecraft
structures
[AIAA PAPER 80-1223] p0060 A80-38975
Orbital transfer of large space structures with
nuclear electric rockets
[AAS PAPER 80-083] p0054 A80-41897
Analytical investigation of two hydrogen-oxygen
rocket engine systems for low-thrust application
--- for orbital transfer
p0057 A80-30382
LEO-to-GEO low thrust chemical propulsion
p0063 A80-30384
Upper stages utilizing electric propulsion
p0057 A80-30386
Conceptual design of an orbital propellant
transfer experiment. Volume 2: Study results
[NASA-CR-165150] p0048 A80-31423
Low-thrust vehicles concept studies
p0063 A80-31456
Low-thrust vehicle concept studies
p0058 A80-31457
Low-thrust chemical orbit to orbit propulsion
system propellant management study
p0064 A80-31469
Solar rocket system concept analysis
p0064 A80-31470
- ORBITAL SPACE STATIONS**
Power management for multi-100 KWe space systems
p0060 A80-48357
- ORBITAL TRANSFER**
U TRANSFER ORBITS
- ORBITS**
NT EARTH ORBITS
NT GEOSYNCHRONOUS ORBITS
NT SATELLITE ORBITS
NT TRANSFER ORBITS
- ORGANIC COMPOUNDS**
NT FLUOROCARBONS
- ORIFICE FLOW**
Free jet phenomena in a 90 deg-sharp edge inlet
geometry
p0106 A80-10037
- OSCILLATION DAMPERS**
Off-design correlation for losses due to part-span
dampers on transonic rotors
[NASA-TP-1693] p0020 A80-28352
- OSCILLATIONS**
NT PRESSURE OSCILLATIONS
- OSCILLATORS**
NT MICROWAVE TUBES
- OTV**
U ORBIT TRANSFER VEHICLES
- OUTLET FLOW**
Laser anemometer measurements at the exit of a T63
combustor
p0045 A80-27737
Far-field radiation of aft turbofan noise
[NASA-TM-81506] p0166 A80-24129
- OUTLETS**
NT VENTS
- OUTPUT**
NT LASER OUTPUTS
- OXIDATION**
Effect of starting powder characteristics on
density, microstructure and low temperature
oxidation behavior of a Si₃N₄ - 8 w/o Y₂O₃ ceramic
p0090 A80-46100
Combustion of solid carbon rods in zero and normal
gravity
[NASA-TM-79303] p0104 A80-13404
Chemical processes involved in the initiation of
hot corrosion of B-1900 and NASA-TRW VJA
[NASA-TM-81399] p0077 A80-17199
Thermal fatigue and oxidation data for
directionally solidified MAR-M 246 turbine blades
[NASA-CR-159798] p0037 A80-21330
Effect of starting powder characteristics on
density, microstructure and low temperature
oxidation behavior of a Si₃N₄ w/o Y₂O₃ ceramic
[NASA-TM-81536] p0088 A80-27484
Characterization of PMR-15 polyimide composition
in thermo-oxidatively exposed graphite fiber
composites
[NASA-TM-81565] p0088 A80-28524
Determination of jet fuel thermal deposit rate
using a modified JPTOT
p0043 A80-29326
Gas phase oxidation downstream of a catalytic
combustor
[NASA-TM-81551] p0144 A80-29863
- OXIDATION RESISTANCE**
Boundary lubrication, thermal and oxidative
stability of a fluorinated polyether and a
perfluoropolyether triazine
[ASLE PREPRINT 79-AM-18-1] p0088 A80-12089
Hot corrosion of four superalloys - HA-188, S-57,
IN-617, and TD-NiCrAl
p0081 A80-14445
The effect of zirconium on the isothermal
oxidation of nominal Ni-14Cr-24Al alloys
p0082 A80-26465
Effect of W and WC on the oxidation resistance of
yttria-doped silicon nitride
p0090 A80-46099
Study of the effects of gaseous environments on
the hot corrosion of superalloy materials
[NASA-CR-159747] p0083 A80-18155
Effect of W and WC on the oxidation resistance of
yttria-doped silicon nitride
[NASA-TM-81529] p0087 A80-27483
- OXIDATION-REDUCTION REACTIONS**
Catalyst surfaces for the chromous/chromic redox
couple
[NASA-CASE-LEW-13148-2] p0140 A80-18557
Catalyst surfaces for the chromous/chromic redox
couple
[NASA-CASE-LEW-13148-1] p0101 A80-20487
Redox storage systems for solar applications
[NASA-TM-81464] p0142 A80-23777
- OXIDE FILMS**
Homogeneous alignment of nematic liquid crystals
by ion beam etched surfaces
p0178 A80-26007
Effects of yttrium, aluminum and chromium
concentrations in bond coatings on the
performance of zirconia-yttria thermal barriers
p0082 A80-35900
Adherence of ion beam sputter deposited metal
films on H-13 steel
[NASA-TM-81585] p0079 A80-31527
- OXIDES**
NT ALUMINUM OXIDES
NT CARBON MONOXIDE
NT CESIUM OXIDES
NT COBALT OXIDES
NT MAGNESIUM OXIDES
NT METAL OXIDES
NT NITRIC OXIDE
NT NITROGEN OXIDES
NT SAPPHIRE
NT YTTRIUM OXIDES
NT ZINC OXIDES
NT ZIRCONIUM OXIDES
Stability of several oxide dispersion strengthened
alloys and a directionally solidified
gamma/gamma prime-alpha eutectic alloy in a
thermal gradient
p0082 A80-40962
Reactions of calcium orthosilicate and barium
zirconate with oxides and sulfates of various
elements
[NASA-TM-79272] p0085 A80-13256
- OXIDIZERS**
NT LIQUID OXYGEN
- OXYGEN**
NT HIGH PRESSURE OXYGEN
NT LIQUID OXYGEN
NT OZONE
Oxygen-enriched air for MHD power plants
p0096 A80-25096
Results of duct area ratio changes in the NASA
Lewis H₂-O₂ combustion MHD experiment
[NASA-TM-79308] p0175 A80-12881

OXYNITRIDES

SUBJECT INDEX

Experiments on H₂-O₂MHD power generation
[NASA-TN-81424] p0175 N80-16886

OXYNITRIDES
State-of-the-art SiAlON materials p0022 N80-29358

OZONE
Simultaneous cabin and ambient ozone measurements
on two Boeing 747 airplanes, volume 1
[NASA-TN-79166] p0008 N80-15059

OZONOMETRY
Measurements of cabin and ambient ozone on B747
airplanes p0010 A80-28853

P

PACIFIC OCEAN
A quantitative analysis of inter-island telephony
traffic in the Pacific Basin Region (PBR)
[NASA-TN-81587] p0097 N80-32610

PANCREAS
Preliminary results of fast neutron treatments in
carcinoma of the pancreas
[NASA-TN-81516] p0160 N80-24983

PANELS
An efficient user-oriented method for calculating
compressible flow in an about three-dimensional
inlets --- panel method
[NASA-CR-159578] p0004 N80-10134

PARABOLIC ANTENNAS
Low sidelobe level low-cost earth station antennas
for the 12 GHz broadcasting satellite service
[NASA-CR-159703] p0098 N80-12259

PARALLEL FLOW
NT THREE DIMENSIONAL FLOW

PARAMAGNETIC RESONANCE
Properties of PMR Polyimide composites made with
improved high strength graphite fibers
[NASA-TN-81557] p0069 N80-28444

Characterization of PMR-15 polyimide composition
in thermo-oxidatively exposed graphite fiber
composites
[NASA-TN-81565] p0088 N80-28524

PARAMETERIZATION
Effects of secondary yield parameter variation on
predicted equilibrium potential of an object in
a charging environment --- using computerized
simulation
[NASA-TN-79299] p0053 N80-16093

PARTIAL DIFFERENTIAL EQUATIONS
NT HELMHOLTZ VORTICITY EQUATION
An alternative approach to the numerical
simulation of steady inviscid flow
[NASA-TN-81542] p0003 N80-27286

PARTICLE ACCELERATORS
NT ION ACCELERATORS

PARTICLE BEAMS
NT ELECTRON BEAMS
NT ION BEAMS

PARTICLE COLLISIONS
Effects of secondary yield parameter variation on
predicted equilibrium potential of an object in
a charging environment --- for spacecraft
p0054 A80-44238

PARTICLE DENSITY (CONCENTRATION)
NT ELECTRON DENSITY (CONCENTRATION)

PARTICLE DIFFUSION
NT ELECTRON DIFFUSION
The effect of a weak vertical magnetic field on
fluctuation-induced transport in a Bumpy-Torus
plasma p0176 A80-25476

PARTICLE EMISSION
NT ELECTRON EMISSION
NT SECONDARY EMISSION

PARTICLE ENERGY
NT ELECTRON ENERGY

PARTICLE TRAJECTORIES
NT ELECTRON TRAJECTORIES

PARTICLES
NT ARGON PLASMA
NT CHARGED PARTICLES
NT DROPS (LIQUIDS)
NT ELECTRON BEAMS
NT HELIUM PLASMA
NT HIGH TEMPERATURE PLASMAS
NT HYDROGEN PLASMA
NT LASER PLASMAS
NT MAGNETICALLY TRAPPED PARTICLES

NT METAL PARTICLES
NT PHOTOELECTRONS
NT PLASMA JETS
NT PLASMA SHEATHS
NT PLASMAS (PHYSICS)
NT POWDER (PARTICLES)
NT RAINDROPS
NT SOOT
NT TOROIDAL PLASMAS
PASSENGER AIRCRAFT
NT BOEING 747 AIRCRAFT
NT DC 10 AIRCRAFT
PAYLOAD DELIVERY (STS)
Electric propulsion technology p0057 N80-31452
Chemical propulsion technology p0058 N80-31453
DOD low-thrust mission studies p0063 N80-31455
Low-thrust vehicles concept studies p0063 N80-31456
Low-thrust vehicle concept studies p0058 N80-31457
Solar rocket system concept analysis p0064 N80-31470

PAYLOADS
NT SPACE SHUTTLE PAYLOADS

PERFLUORO COMPOUNDS
Boundary lubrication, thermal and oxidative
stability of a fluorinated polyether and a
perfluoropolyether triazine
[ASLE PREPRINT 79-AM-1B-1] p0088 A80-12089

PERFORMANCE PREDICTION
NT PREDICTION ANALYSIS TECHNIQUES
Analytical prediction and experimental
verification of TWT and depressed collector
performance using multidimensional computer
programs p0102 A80-13902
Design and evaluation of high performance rocket
engine injectors for use with hydrocarbon fuels
p0059 A80-20957
Summary of advanced methods for predicting high
speed propeller performance
[AIAA PAPER 80-0225] p0003 A80-20966
How to quickly predict the overall TWT and the
multistage depressed collector efficiency
p0102 A80-31759
Predicting the time-temperature dependent axial
failure of B/A1 composites p0071 A80-35494
A theoretical and experimental investigation of
propeller performance methodologies
[AIAA PAPER 80-1240] p0026 A80-43283
Improved traveling wave tubes --- for ECM systems
p0102 A80-44235
Uncertainties in predicting turbine blade metal
temperatures p0027 A80-48014
Effect of time dependent flight loads on JT9D-7
performance deterioration p0134 N80-10515
Engine component improvement program: Performance
improvement --- fuel consumption
[NASA-TN-79304] p0013 N80-12092
Summary of advanced methods for predicting high
speed propeller performance
[NASA-TN-81409] p0002 N80-15051
Comparison of predicted and experimental
performance of large-bore roller bearing
operating to 3.0 million DN p0114 N80-15410
An averaging battery model for a lead-acid battery
operating in an electric car
[NASA-TN-79321] p0165 N80-16824
Computerized systems analysis and optimization of
aircraft engine performance, weight, and life
cycle costs p0001 N80-21271
Advanced propeller aerodynamic analysis p0018 N80-22345
Improved traveling wave tubes
[NASA-TN-81479] p0102 N80-22598
Performance deterioration based on in-service
engine data: JT9D jet engine diagnostics program
[NASA-CR-159525] p0040 N80-25340
Quantitative ultrasonic evaluation of engineering
properties in metals, composites and ceramics
[NASA-TN-81530] p0130 N80-26682

SUBJECT INDEX

PHOTOVOLTAIC CELLS

- CF6-6D engine performance deterioration
[NASA-CR-159786] p0041 N80-27364
Determination of jet fuel thermal deposit rate
using a modified JPTOT p0043 N80-29326
- Experimental performance and analysis of
15.04-centimeter-tip-diameter, radial-inflow
turbine with work factor of 1.126 and thick
blading [NASA-TP-1730] p0023 N80-33410
- PERFORMANCE TESTS**
- 8-cm Engineering Model Thruster technology - A
review of recent developments [AIAA PAPER 79-2103] p0064 A80-13311
90- to 93-percent efficient collector for
operation of a dual-mode traveling-wave tube in
the linear region p0102 N80-13909
- Installation and checkout of the DOE/NASA Mod-1
2000-kW wind turbine generator [AIAA 80-0638] p0145 A80-28835
- Tested, tip-controlled rotor - Preliminary test
results from Mod-0 100-kW experimental wind
turbine [AIAA 80-0642] p0145 A80-28836
- Evaluation of present-day thermal barrier coatings
for industrial/utility applications p0092 A80-39637
- Improved PFB operations - 400-hour turbine test
results --- Pressurized Fluidized Bed p0145 A80-39639
- CF6-50 Short Core Exhaust Nozzle
[AIAA PAPER 80-1196] p0025 A80-41514
- Performance of annular prediffuser-combustor systems
[ASME PAPER 80-GT-15] p0026 A80-42154
- Elastomer damper performance - A comparison with a
squeeze film for a supercritical power
transmission shaft [ASME PAPER 80-GT-162] p0121 A80-42272
- Life test studies on tungsten impregnated cathodes
p0103 A80-45122
- Effect of geometry and operating conditions on
spur gear system power loss p0122 A80-46409
- Evaluation of a high performance fixed-ratio
traction drive p0122 A80-46410
- Hg ion thruster component testing
[NASA-TM-79287] p0056 N80-13159
- Quiet Clean Short-Haul Experimental Engine (QCSEE)
Over-The-Wing (OTW) propulsion system test
report. Volume 2: Aerodynamics and performance
--- engine performance tests to define
propulsion system performance on turbofan engines
[NASA-CR-135324] p0029 N80-14120
- The CF6 jet engine performance improvement: New
front mount [NASA-CR-159639] p0029 N80-14127
- Self-acting lift-pad geometry for circumferential
seals: A noncontacting concept --- performance
tests on hydrodynamic seals [NASA-TP-1583] p0114 N80-14403
- Performance of computer-optimized tapered-roller
bearings to 2.4 million DN [NASA-TM-81414] p0114 N80-16342
- Experimental evaluation of a low emissions high
performance duct burner for Variable Cycle
Engines (VCE) [NASA-CR-159694] p0036 N80-17074
- Performance sensitivity analysis of Department of
Energy-Chrysler upgraded automotive gas turbine
engine, S/N 5-4 [NASA-TM-79242] p0115 N80-17467
- Testing of reciprocating seals for application in
a Stirling cycle engine [NASA-CR-159820] p0124 N80-22700
- Development of procedures for calculating
stiffness and damping of elastomers in
engineering applications, part 6 [NASA-CR-159838] p0134 N80-22733
- CF6 jet engine performance improvement: New fan
[NASA-CR-159699] p0039 N80-23309
- CF6-6D engine short-term performance deterioration
[NASA-CR-159836] p0039 N80-23316
- Durability tests of solenoid valves for digital
actuators [NASA-TM-81522] p0020 N80-26299
- Small, high pressure liquid hydrogen turbopump
[NASA-CR-159821] p0125 N80-26662
- Performance, emissions, and physical
characteristics of a rotating combustion
aircraft engine, supplement A [NASA-CR-135119] p0041 N80-27361
- Small passenger car transmission test-Chevrolet
200 transmission [NASA-CR-159835] p0185 N80-28255
- Fuel character effects on the J79 and F101 engine
combustion systems p0042 N80-29312
- Air Force fuel mainburner/turbine effects programs
p0042 N80-29314
- Investigation of performance deterioration of the
CF6/JT9D, high-bypass ratio turbofan engines
[NASA-TM-81552] p0022 N80-29332
- Performance deterioration of commercial
high-bypass ratio turbofan engines [NASA-TM-81552-REV] p0023 N80-32394
- Upgraded automotive gas turbine engine design and
development program, volume 2 [NASA-CR-159671] p0128 N80-32719
- PERITONEUM**
- Tissue response to peritoneal implants
[NASA-CR-159817] p0066 N80-33478
- PERMEABILITY**
- Anton permselective membrane
[NASA-CR-159599] p0147 N80-12551
- PERTURBATION THEORY**
- Evaluation of a strained-coordinate perturbation
procedure - Nonlinear subsonic and transonic flows
[AIAA PAPER 80-0339] p0006 A80-18324
- PETROLEUM**
- U CRUDE OIL
- PETROLEUM PRODUCTS**
- NT DIESEL FUELS
- NT LUBRICATING OILS
- PHASE LOCKED SYSTEMS**
- Phase-locked telemetry system for rotary
instrumentation of turbomachinery, phase 1
[NASA-CR-159453] p0029 N80-14182
- PHASE TRANSFORMATIONS**
- NT COAL LIQUEFACTION
- NT FREEZING
- NT VAPORIZING
- State-of-the-art of SiAlON materials p0009 A80-13066
- Phase change in liquid face seals. II - Isothermal
and adiabatic bounds with real fluids
[ASME PAPER 79-LUB-4] p0129 A80-14739
- Heat storage in alloy transformations
[NASA-CR-159787] p0151 N80-24759
- PHENOLIC RESINS**
- Synthesis of improved phenolic resins
[NASA-CR-159724] p0091 N80-17221
- PHOSPHORIC ACID**
- Technology development for phosphoric acid fuel
cell powerplant, phase 2 [NASA-CR-159705] p0147 N80-10603
- Cell module and fuel conditioner
[NASA-CR-159888] p0155 N80-31882
- PHOSPHORUS COMPOUNDS**
- NT PHOSPHORIC ACID
- PHOTOCURRENTS**
- U ELECTRIC CURRENT
- PHOTOELECTRIC CELLS**
- NT PHOTOVOLTAIC CELLS
- PHOTOELECTRONS**
- Photoelectron charge density and transport near
differentially charged spacecraft p0053 A80-19773
- PHOTOGRAPHY**
- NT FRAC TOGRAPHY
- NT INFRARED IMAGERY
- NT INFRARED PHOTOGRAPHY
- PHOTOMETRY**
- An interactive modular design for computerized
photometry in spectrochemical analysis p0074 A80-39640
- An interactive modular design for computerized
photometry in spectrochemical analysis
[NASA-TM-81521] p0074 N80-24386
- PHOTOTHERMOTROPISM**
- U ANISOTROPY
- U TEMPERATURE EFFECTS
- PHOTOVOLTAIC CELLS**
- Improvement and scale-up of the NASA Redox storage
system p0146 A80-48370

PHOTOVOLTAIC CONVERSION

SUBJECT INDEX

A photovoltaic power system in the remote African village of Tangaye, Upper Volta
[NASA-TM-79218] p0137 N80-12552

Evaluation of cleaners for photovoltaic modules exposed in an outdoor environment
[NASA-TM-79248] p0096 N80-13317

Economic analysis of the design and fabrication of a space qualified power system
[NASA-TM-81418] p0056 N80-18098

Study of power management technology for orbital multi-100Kw applications. Volume 3: Requirements
[NASA-CR-159834] p0154 N80-29845

Photovoltaic technology development for synchronous orbit
p0058 N80-33470

PHOTOVOLTAIC CONVERSION
Photovoltaic power system reliability considerations
p0146 A80-40338

Description of photovoltaic village power systems in the United States and Africa
p0146 A80-46796

Photovoltaic power system reliability considerations
[NASA-TM-79291] p0130 N80-15422

PLUGGABLE OSCILLATIONS
U PITCH (INCLINATION)

PHYSIOLOGICAL EFFECTS
NT PHYSIOLOGICAL RESPONSES

PHYSIOLOGICAL RESPONSES
Tissue response to peritoneal implants
[NASA-CR-159817] p0066 N80-33478

PINHOLES
Interaction of high voltage surfaces with the space plasma
[NASA-CR-165131] p0177 N80-32223

PIPES (TUBES)
Coolant tube curvature effects on film cooling as detected by infrared imagery
[ASME PAPER 79-WA/GT-7] p0107 A80-18638

High temperature thermal energy storage in steel and sand
[NASA-CR-159708] p0154 N80-29860

PISTON ENGINES
NT DIESEL ENGINES
Exhaust emission reduction for intermittent combustion aircraft engines
[NASA-CR-159757] p0029 N80-14130

Overview of a Stirling engine test project
[NASA-TM-81442] p0140 N80-18564

A 15 kWe (nominal) solar thermal-electric power conversion concept definition study: Steam Rankine reciprocator system
[NASA-CR-159591] p0149 N80-19612

Design study of a 15 kW free-piston Stirling engine-linear alternator for dispersed solar electric power systems
[NASA-CR-159587] p0150 N80-22787

PISTONS
Preliminary results from a four-working space, double-acting piston, Stirling engine controls model
[NASA-TM-81569] p0106 N80-29624

Free-piston regenerative hot gas hydraulic engine
[NASA-CASE-LEW-12274-1] p0119 N80-31790

PITCH (INCLINATION)
Quiet Clean Short-haul Experimental Engine (QCSEE). Ball spline pitch change mechanism design report
[NASA-CR-134873] p0030 N80-15101

Quiet Clean Short-haul Experimental Engine (QCSEE). Ball spline pitch change mechanism design report
[NASA-CR-134873] p0030 N80-15101

PITCH ANGLES
U PITCH (INCLINATION)

PLANAR STRUCTURES
The planar multijunction cell - A new solar cell for earth and space
p0146 A80-48205

Planar multijunction high voltage solar cells
[NASA-TM-81389] p0178 N80-16914

PLANFORMS
NT RECTANGULAR PLATES

PLANNING
NT MANAGEMENT PLANNING
NT MISSION PLANNING
NT PROJECT PLANNING

PLASMA ARCS
U PLASMA JETS

PLASMA CONFINEMENT
U PLASMA CONTROL
PLASMA CONTROL
The effect of a weak vertical magnetic field on fluctuation-induced transport in a Bumpy-Torus plasma
p0176 A80-25476

PLASMA DIAGNOSTICS
Study of a rare-gas transverse fast discharge
p0176 A80-11366

PLASMA DIFFUSION
The effect of a weak vertical magnetic field on fluctuation-induced transport in a Bumpy-Torus plasma
p0176 A80-25476

PLASMA DISCHARGES
U PLASMA JETS
PLASMA DISPERSION
U PLASMA DIFFUSION
PLASMA INSTABILITY
U MAGNETOHYDRODYNAMIC STABILITY
PLASMA INTERACTIONS
NT PLASMA-ELECTROMAGNETIC INTERACTION
Torquing and electrostatic deformation of the solar sail
p0065 A80-46901

PLASMA JETS
Experimental and theoretical investigation for the suppression of the planar arc drop in the thermionic converter
[NASA-CR-159611] p0176 N80-12880

Investigation into the effect of plasma pretreatment on the adhesion of parylene to various substrates
[NASA-TM-79224] p0114 N80-13473

Baffle aperture design study of hollow cathode equipped ion thrusters
[NASA-CR-165164] p0064 N80-33476

PLASMA LAYERS
NT PLASMA SHEATHS
PLASMA LOS
Experimental and theoretical investigation for the suppression of the planar arc drop in the thermionic converter
[NASA-CR-159611] p0176 N80-12880

PLASMA PHYSICS
Plasma physics analysis of SERT-2 operation
[NASA-CR-159814] p0177 N80-27169

PLASMA POTENTIALS
Neutralization tests on the SERT I spacecraft --- of ion beams
[AIAA PAPER 79-2064] p0059 A80-10387

Active control of spacecraft charging
p0055 A80-46890

PLASMA PROPULSION
A model for predicting the wearout lifetime of the LERC/Hughes 30-cm mercury ion thruster
[AIAA PAPER 79-2079] p0064 A80-20962

Inert gas thrusters
[NASA-CR-159813] p0062 N80-24362

PLASMA RINGS
U TOKOIAL PLASMAS
PLASMA SHEATHS
Plasma collection by high voltage spacecraft at low earth orbit
[AIAA PAPER 80-0042] p0055 A80-18249

Physical phenomena in mercury ion thrusters
[NASA-CR-159784] p0061 N80-17137

PLASMA SPRAYING
Investigation into the effect of plasma pretreatment on the adhesion of parylene to various substrates
p0066 A80-25900

Development of improved-durability plasma sprayed ceramic coatings for gas turbine engines
[AIAA PAPER 80-1193] p0089 A80-38963

Evaluation of present-day thermal barrier coatings for industrial/utility applications
p0092 A80-39637

Friction and wear of plasma-sprayed coatings containing cobalt alloys from 25 deg to 650 deg in air
[ASLE PREPRINT 80-AM-6C-2] p0122 A80-43176

Improved refractory coatings and method of producing the same
[NASA-CASE-LEW-13169-1] p0076 N80-14232

Friction and wear of plasma-sprayed coatings containing cobalt alloys from 25 deg to 650 deg in air

SUBJECT INDEX

POLYMER CHEMISTRY

[NASA-TM-79316] p0085 N80-14249
 Program to develop sprayed, plastically deformable
 compressor shroud seal materials
 [NASA-CR-159741] p0123 N80-16338
 Significance of thermal contact resistance in
 two-layer thermal-barrier-coated turbine vanes
 [NASA-TM-81483] p0018 N80-23310
 Preliminary study of methods for providing thermal
 shock resistance to plasma-sprayed ceramic
 gas-path seals
 [NASA-TP-1561] p0087 N80-23453
 Fully plasma-sprayed compliant backed ceramic
 turbine seal
 [NASA-CASE-LEW-13268-1] p0117 N80-24619
PLASMA STABILITY
 U MAGNETOHYDRODYNAMIC STABILITY
PLASMA THEORY
 U PLASMA PHYSICS
PLASMA-ELECTROMAGNETIC INTERACTION
 Experimental results on plasma interactions with
 large surfaces at high voltages
 [NASA-TM-81423] p0175 N80-18946
PLASMAS (PHYSICS)
 NT ARGON PLASMA
 NT HELIUM PLASMA
 NT HIGH TEMPERATURE PLASMAS
 NT HYDROGEN PLASMA
 NT LASER PLASMAS
 Interaction of high voltage surfaces with the
 space plasma --- solar arrays
 [NASA-CR-159731] p0176 N80-14923
 Ion extraction from a plasma
 [NASA-CR-159849] p0177 N80-26161
PLASMOIDS
 U PLASMAS (PHYSICS)
PLASTIC ANISOTROPY
 Anisotropy of nickel-base superalloy single crystals
 p0083 A80-51573
PLASTIC COATINGS
 Investigation into the effect of plasma
 pretreatment on the adhesion of parylene to
 various substrates
 p0066 A80-25900
 Investigation into the effect of plasma
 pretreatment on the adhesion of parylene to
 various substrates
 [NASA-TM-79224] p0114 N80-13473
 Flexible formulated plastic separators for
 alkaline batteries
 [NASA-CASE-LEW-12363-4] p0140 N80-18555
PLASTIC DEFORMATION
 Modelling of crack tip deformation with finite
 element method and its applications
 p0130 N80-13503
PLASTIC FILMS
 U POLYMERIC FILMS
PLASTIC PROPERTIES
 NT ELASTOPLASTICITY
PLASTIC YIELDING
 U PLASTIC DEFORMATION
PLASTICS
 NT CARBON FIBER REINFORCED PLASTICS
 NT EPOXY RESINS
 NT KEVLAR (TRADEMARK)
 NT PHENOLIC RESINS
 NT POLYESTER RESINS
 NT POLYVINYL ALCOHOL
 NT TEFLON (TRADEMARK)
 NT THERMOSETTING RESINS
PLATE THEORY
 Sudden stretching of a four layered composite plate
 [NASA-CR-159870] p0073 N80-25383
 Sudden bending of cracked laminates
 [NASA-CR-159860] p0073 N80-25384
PLATING
 NT ION PLATING
PLUMES
 NT ROCKET EXHAUST
PNEUMATIC EQUIPMENT
 Improved tire/wheel concept --- pneumatic aircraft
 tire
 [NASA-CASE-LAR-11695-2] p0124 N80-18402
POINT MATCHING METHOD (MATHEMATICS)
 U BOUNDARY VALUE PROBLEMS
POLARIZATION CHARACTERISTICS
 Anodic polarization behavior of austenitic
 stainless steel alloys with lower chromium content
 p0178 A80-22250

POLARIZATION CHARTS
 U GRAFHS (CHARTS)
POLICIES
 NT ENERGY POLICY
POLLUTION
 NT AIR POLLUTION
POLLUTION CONTROL
 Emission reduction
 p0012 N80-10207
 Noise reduction
 p0012 N80-10208
 Quiet Clean Short-haul Experimental Engine (QCSEE)
 [NASA-CR-159473] p0032 N80-15120
 Effect of water injection and off scheduling of
 variable inlet guide vanes, gas generator speed
 and power turbine nozzle angle on the
 performance of an automotive gas turbine engine
 [NASA-TM-81415] p0016 N80-20272
 Energy efficient engine
 [NASA-CR-159685] p0045 N80-33408
POLLUTION MONITORING
 NASA Global Atmospheric Sampling Program (GASP)
 data report for tapes VL0011 and VL0013
 [NASA-TM-81462] p0157 N80-21892
 Coordinated aircraft and ship surveys for
 determining impact of river inputs on great
 lakes waters. Remote sensing results
 [NASA-TE-1694] p0157 N80-27832
POLYAMIDE RESINS
 NT KEVLAR (TRADEMARK)
POLYESTER RESINS
 Synthesis of improved polyester resins
 [NASA-CR-159665] p0090 N80-13257
POLYIMIDE RESINS
 Liquid chromatographic characterization of PMR-15
 resin and prepreg
 p0089 A80-32086
 Second generation PMR polyimide/fiber composites
 [NASA-CR-159666] p0072 N80-12118
 Quiet Clean Short-Haul Experimental Engine (QCSEE)
 Under-The-Wing (UTW) graphite/PMR cowl development
 [NASA-CR-135279] p0029 N80-14119
 Burning characteristics and fiber retention of
 graphite/resin matrix composites
 [NASA-TM-79314] p0067 N80-14196
 Analyses of moisture in polymers and composites
 [NASA-CR-159745] p0091 N80-15264
 Fire test method for graphite fiber reinforced
 plastics
 [NASA-TM-81436] p0068 N80-18107
 Comparison of the weight loss and adherence of
 nine different polyimide films thermally aged at
 315 C and 350 C in air --- high temperature
 lubricants
 [NASA-TM-81381] p0086 N80-18183
 Characterization of PMR-15 polyimide composition
 in thermo-oxidatively exposed graphite fiber
 composites
 [NASA-TM-81565] p0088 N80-28524
 Influence of excess diamine on properties of PMR
 polyimide resins and composites
 [NASA-TM-81580] p0069 N80-29433
POLYIMIDES
 Effect of thermal aging on the tribological
 properties of polyimide films and
 polyimide-bonded graphite fluoride films
 [ASLE PREPRINT 79-AM-3E-1] p0088 A80-12094
 Mechanisms of lubrication and wear of a bonded
 solid-lubricant film
 [ASLE PREPRINT 80-AM-3E-1] p0122 A80-43163
 Lubrication and wear mechanisms of
 polyimide-bonded graphite fluoride films
 subjected to low contact stress
 [NASA-TP-1584] p0085 N80-17220
 Comparison of the tribological properties at 25 C
 of seven different polyimide films bonded to 301
 stainless steel
 [NASA-TM-81413] p0086 N80-19263
 Low temperature cross linking polyimides
 [NASA-CASE-LEW-12876-1] p0087 N80-26447
 Feasibility of Kevlar 49/PMR-15 polyimide for high
 temperature applications
 [NASA-TM-81560] p0069 N80-27429
 Properties of PMR Polyimide composites made with
 improved high strength graphite fibers
 [NASA-TM-81557] p0069 N80-28444
POLYMER CHEMISTRY
 Synthesis of improved polyester resins
 [NASA-CR-159665] p0090 N80-13257

POLYMER MATRIX COMPOSITE MATERIALS

A review of issues and strategies in
nondestructive evaluation of fiber reinforced
structural composites

High char imide-modified epoxy matrix resins
[AIAA PAPER 80-1194] p0071 A80-34764
Development of a Kevlar/PMR-15 reduced drag DC-9
nacelle fairing p0071 A80-34789

Improved fiber retention by the use of fillers in
graphite fiber/resin matrix composites
[NASA-TM-79288] p0010 A80-41193
[NASA-TM-79288] p0067 N80-13171

POLYMERIC FILMS

Effect of thermal aging on the tribological
properties of polyimide films and
polyimide-bonded graphite fluoride films
[ASLE PREPRINT 79-AM-3B-1] p0088 A80-12094

Mechanisms of lubrication and wear of a bonded
solid lubricant film
[NASA-TM-81396] p0085 N80-16165

Lubrication and wear mechanisms of
polyimide-bonded graphite fluoride films
subjected to low contact stress
[NASA-TP-1584] p0085 N80-17220

Comparison of the tribological properties at 25 C
of seven different polyimide films bonded to 301
stainless steel
[NASA-TM-81413] p0086 N80-19263

POLYMERS

Mechanical and chemical effects of ion-texturing
biomedical polymers
p0089 A80-13065

Modification of the electrical and optical
properties of polymers --- ion irradiation to
create texture
[NASA-CASE-LEW-13027-1] p0087 N80-24437

POLYPHENYL ETHER

Boundary lubrication, thermal and oxidative
stability of a fluorinated polyether and a
perfluoropolyether triazine
[ASLE PREPRINT 79-AM-1B-1] p0088 A80-12089

POLYVINYL ALCOHOL

Method of cross-linking polyvinyl alcohol and
other water soluble resins
[NASA-CASE-LEW-13103-1] p0088 N80-32516

POPULATION THEORY

'Chain pooling' model selection for two-level
fixed effects factorial experiments
p0164 A80-40764

PONES

U POROSITY

POROSITY

Effects of thermally induced porosity on an as-HIP
powder metallurgy superalloy p0082 A80-29990

Effects of fine porosity on the fatigue behavior
of a powder metallurgy superalloy p0082 A80-35495

Formation of porous surface layers in reaction
bonded silicon nitride during processing
p0090 A80-51574

Effect of thermally induced porosity on an as-HIP
powder metallurgy superalloy
[NASA-TM-79263] p0076 N80-11189

Effects of fine porosity on the fatigue behavior
of a powder metallurgy superalloy
[NASA-TM-81448] p0078 N80-21493

Formation of porous surface layers in reaction
bonded silicon nitride during processing
[NASA-TM-81493] p0087 N80-23456

POROUS MATERIALS

Castable high temperature refractory materials
[NASA-CASE-LEW-13080-1] p0088 N80-29496

POSITION (LOCATION)

Laser-optical blade tip clearance measurement system
[NASA-TM-81376] p0015 N80-14128

Fiber optic sensors for measuring angular position
and rotational speed --- air breathing engines
[NASA-TM-81454] p0110 N80-18368

POTENTIAL ENERGY

NT ELECTRIC POTENTIAL

NT PLASMA POTENTIALS

POTENTIAL FLOW

Calculation of water drop trajectories to and
about arbitrary three-dimensional bodies in
potential airflow
[NASA-CR-32911] p0005 N80-28302

POWDER (PARTICLES)

NT METAL POWDER

Reaction bonded silicon nitride prepared from wet
attrition-milled silicon p0089 A80-32828

Effect of starting powder characteristics on
density, microstructure and low temperature
oxidation behavior of a Si3N4 - 8 w/o Y2O3 ceramic
p0090 A80-46100

POWDER METALLURGY

Effects of thermally induced porosity on an as-HIP
powder metallurgy superalloy p0082 A80-29990

Effects of fine porosity on the fatigue behavior
of a powder metallurgy superalloy p0082 A80-35495

Development of a high strength hot isostatically
pressed /HIP/ disk alloy, MEEL 76 p0084 A80-44108

Application of superalloy powder metallurgy for
aircraft engines p0122 A80-44240

Effect of thermally induced porosity on an as-HIP
powder metallurgy superalloy
[NASA-TM-79263] p0076 N80-11189

Reaction bonded silicon nitride prepared from wet
attrition-milled silicon --- fractography
[NASA-TM-81428] p0086 N80-18181

Manufacture of low carbon astrology turbine disk
shapes by hot isostatic pressing. Volume 2,
project 1 p0037 N80-21329

Application of superalloy powder metallurgy for
aircraft engines
[NASA-TM-81466] p0078 N80-21488

Effects of fine porosity on the fatigue behavior
of a powder metallurgy superalloy
[NASA-TM-81448] p0078 N80-21493

Materials for advanced turbine engines. Volume 1:
Power metallurgy Rene 95 rotating turbine engine
parts p0084 N80-28499

POWDERED METALS

U METAL POWDER

POWER CONDITIONING

Reduced power processor requirements for the 30-cm
diameter HG ion thruster
[AIAA PAPER 79-2081] p0059 A80-10392

Heat pipe cooling of power processing magnetics
[AIAA PAPER 79-2082] p0107 A80-20960

Modeling and analysis of Power Processing Systems
p0066 A80-28894

Power processing technology for spacecraft primary
ion propulsion p0065 A80-48265

Heat pipe cooling of power processing magnetics
[NASA-TM-79270] p0101 N80-11327

Heat pipe cooled power magnetics
[NASA-CR-159659] p0103 N80-13362

Self-reconfiguring solar cell system
[NASA-CASE-LEW-12586-1] p0137 N80-14472

Improved traveling wave tubes
[NASA-TM-81479] p0102 N80-22598

Study of power management technology for orbital
multi-100Kwe applications. Volume 2: Study
results
[NASA-CR-159834-VOL-2] p0153 N80-28862

POWER EFFICIENCY

How to quickly predict the overall TWT and the
multistage depressed collector efficiency
p0102 A80-31759

Improved traveling wave tubes --- for ECM systems
p0102 A80-44235

Evaluation of a high performance fixed-ratio
traction drive p0122 A80-46410

Power processing technology for spacecraft primary
ion propulsion p0065 A80-48265

Effect of geometry and operating conditions on
spur gear system power loss
[NASA-TM-81426] p0116 N80-18406

Effect of water injection and off scheduling of
variable inlet guide vanes, gas generator speed
and power turbine nozzle angle on the
performance of an automotive gas turbine engine
[NASA-TM-81415] p0016 N80-20272

Effect on combined cycle efficiency of stack gas
temperature constraints to avoid acid corrosion

[NASA-TM-81531] p0143 N80-27804
 Synchronous Energy Technology
 [NASA-CP-2154] p0058 N80-33465
POWER GENERATORS
 U ELECTRIC GENERATORS
POWER PROCESSING SYSTEMS
 U POWER CONDITIONING
POWER SERIES
 Modified power law equations for vertical wind
 profiles
 [NASA-TM-79275] p0137 N80-13623
POWER SUPPLIES
 Reduced power processor requirements for the 30-cm
 diameter HG ion thruster
 [AIAA PAPER 79-2081] p0059 A80-10392
POWER TRANSMISSION
 Balancing of a power-transmission shaft with the
 application of axial torque
 [ASME PAPER 80-GT-143] p0121 A80-42256
POWERED LIFT AIRCRAFT
 QCSEE UTM engine powered-lift acoustic performance
 --- Quiet Clean Short-haul Experimental Engine
 Under The Wing
 [AIAA PAPER 80-1065] p0025 A80-38651
 Quiet Clean Short-haul Experimental Engine (QCSEE)
 [NASA-CR-159473] p0032 N80-15120
 Quiet powered-lift propulsion
 [NASA-CP-2077] p0015 N80-15127
 QCSEE UTM engine powered-lift acoustic performance
 [NASA-TM-81504] p0019 N80-24315
PRECIPITATION (METEOROLOGY)
 NT RAIN
PRECIPITATION HARDENING
 Strengthening of tough iron-12% nickel-reactive
 metal alloys at 77 K by copper additions
 p0174 A80-34049
 Stability of several oxide dispersion strengthened
 alloys and a directionally solidified
 gamma/gamma prime-alpha eutectic alloy in a
 thermal gradient
 p0082 A80-40962
 Stress corrosion cracking evaluation of
 martensitic precipitation hardening stainless
 steels
 [NASA-TM-78257] p0083 N80-16142
PREDICTION ANALYSIS TECHNIQUES
 A model for predicting the wearout lifetime of the
 LeRC/Hughes 30-cm mercury ion thruster
 [AIAA PAPER 79-2079] p0064 A80-20962
 Strainrange partitioning life predictions of the
 long time Metal Properties Council creep-fatigue
 tests
 p0133 A80-27958
 Prediction of fiber composite mechanical behavior
 made simple
 p0133 A80-32067
 Prediction of fiber composite mechanical behavior
 made simple --- using a rocket calculator
 [NASA-TM-81404] p0068 N80-16107
 Prediction method for two-dimensional aerodynamic
 losses of cooled vanes using integral
 boundary-layer parameters
 [NASA-TP-1623] p0002 N80-17030
 Analysis of uncertainties in turbine metal
 temperature predictions
 [NASA-TP-1593] p0017 N80-21326
 Concepts and techniques for ultrasonic evaluation
 of material mechanical properties
 [NASA-TM-81523] p0130 N80-24634
 Use of petroleum-based correlations and estimation
 methods for synthetic fuels
 [NASA-TM-81533] p0093 N80-27509
 Stresses and deformations in elliptical contacts
 [NASA-TM-81535] p0118 N80-27697
 Fully flooded elastohydrodynamic lubricated
 elliptical contacts
 [NASA-TM-81543] p0118 N80-27698
 Starved elastohydrodynamic lubricated elliptical
 contacts
 [NASA-TM-81549] p0118 N80-27699
 Off-design correlation for losses due to part-span
 dampers on transonic rotors
 [NASA-TP-1693] p0020 N80-28352
 A methodology for long-range prediction of air
 transportation
 p0041 N80-29305
 Toward the use of similarity theory in two-phase
 choked flows
 [NASA-TM-81568] p0106 N80-29623

Influence of mistuning on blade torsional flutter
 [NASA-CR-165137] p0005 N80-31351
PREDICTIONS
 NT NOISE PREDICTION (AIRCRAFT)
 NT PERFORMANCE PREDICTION
PREHEATERS
 U HEATING EQUIPMENT
PRELAUNCH TESTS
 NT STATIC FIRING
PRELOADING
 U PRESTRESSING
PREPARATION
 NT PRESTRESSING
PREPOLYMERS
 Synthesis of improved polyester resins
 [NASA-CR-159665] p0090 N80-13257
 Low temperature cross linking polyimides
 [NASA-CASE-LEW-12876-1] p0087 N80-26447
PRESSURIZING
 U SINTERING
PRESSURE
 NT GAS PRESSURE
 NT HIGH PRESSURE
 NT HYDROSTATIC PRESSURE
 NT IMPACT LOADS
 NT INTRAOCULAR PRESSURE
 NT ISOSTATIC PRESSURE
 NT SOUND PRESSURE
 NT STATIC PRESSURE
 NT THRUST CHAMBER PRESSURE
 NT TRANSIENT PRESSURES
 Temperature and pressure measurement techniques
 for an advanced turbine test facility
 [NASA-TM-79278] p0110 N80-14374
PRESSURE CHAMBERS
 NT VACUUM CHAMBERS
 Advanced cooling techniques for high-pressure,
 hydrocarbon-fueled rocket engines
 [AIAA PAPER 80-1266] p0060 A80-38994
PRESSURE DISTRIBUTION
 Spectral structure of pressure measurements made
 in a combustion duct
 p0171 A80-35496
PRESSURE FIELDS
 U PRESSURE DISTRIBUTION
PRESSURE GRADIENTS
 Observation of pressure variation in the
 cavitation region of submerged journal bearings
 [NASA-TM-81582] p0120 N80-31798
PRESSURE MEASUREMENTS
 Temperature and pressure measurement techniques
 for an advanced turbine test facility
 p0112 A80-36157
 Spectral structure of pressure measurements made
 in a combustion duct --- jet engine noise
 [NASA-TM-81471] p0168 N80-22045
 Pressure spectra and cross spectra at an area
 contraction in a ducted combustion system
 [NASA-TM-81477] p0168 N80-23097
PRESSURE OSCILLATIONS
 Analysis of combustion instability in liquid fuel
 rocket motors
 [NASA-CR-159733] p0061 N80-13164
PRESSURE PROBES
 U PRESSURE SENSORS
PRESSURE RECOVERY
 Griffith diffusers
 p0006 A80-20748
PRESSURE REDUCTION
 Reduced bleed air extraction for DC-10 cabin air
 conditioning
 [AIAA PAPER 80-1197] p0010 A80-41194
 Engine bleed air reduction in DC-10
 [NASA-CR-159846] p0010 N80-32378
PRESSURE REGULATORS
 Intra-ocular pressure normalization technique and
 equipment
 [NASA-CASE-LEW-12955-1] p0161 N80-14684
 Intra-ocular pressure normalization technique and
 equipment
 [NASA-CASE-LEW-12723-1] p0135 N80-18690
PRESSURE SENSORS
 Measuring unsteady pressure on rotating compressor
 blades --- with semiconductor strain gages under
 gas turbine engine operating conditions
 p0110 A80-12630
 Some dynamic and time-averaged flow measurements
 in a turbine rig
 p0178 A80-21120

PRESSURE TRANSDUCERS

SUBJECT INDEX

Flutter spectral measurements using stationary pressure transducers p0111 A80-36147

Flutter spectral measurements using stationary pressure transducers [NASA-TM-79293] p0013 N80-13046

Steady-state performance of J85-21 compressor at 100 percent of design speed with and without interstage rake blockage [NASA-TM-81451] p0017 N80-21333

Data analysis of P sub T/P sub S noseboom probe testing on F100 engine P680072 at NASA Lewis Research Center [NASA-CR-159816] p0038 N80-21334

PRESSURE TRANSDUCERS

U PRESSURE SENSORS

PRESSURE VESSELS

Prediction of fragment velocities and trajectories p0096 N80-16210

PRESSURE WELDING

NT DIFFUSION WELDING

PRESSURIZING

NT FUEL TANK PRESSURIZATION

PRESTRAINING

U PRESTRESSING

PRESTRESSING

Evaluation of feasibility of prestressed concrete for use in wind turbine blades [NASA-CR-159725] p0147 N80-15553

PRETREATMENT

NT PRESTRESSING

PRETWISTING

U PRESTRESSING

PREVENTION

NT CORROSION PREVENTION

NT FIRE PREVENTION

PRIMARY BATTERIES

NT ALKALINE BATTERIES

NT NICKEL ZINC BATTERIES

PRIVATE AIRCRAFT

U GENERAL AVIATION AIRCRAFT

PROBABILITY

U PROBABILITY THEORY

PROBABILITY THEORY

Statistical aspects of carbon fiber risk assessment modeling --- fire accidents involving aircraft [NASA-CR-159318] p0073 N80-29432

PROCEDURES

NT FINITE ELEMENT METHOD

PRODUCT DEVELOPMENT

Thick ceramic coating development for industrial gas turbines - A program plan [SR79-M-4702-05] p0091 A80-10042

Characteristics of primary electric propulsion systems [AIAA PAPER 79-2041] p0058 A80-10376

NASA gear research and its probable effect on rotorcraft transmission design p0120 A80-13068

Advanced Gas Turbine Powertrain System Development Project p0129 A80-35574

Development of improved wraparound contacts for silicon [NASA-CR-159748] p0148 N80-18554

Cell module and fuel conditioner development [NASA-CR-159828] p0150 N80-23768

Cell module and fuel conditioner [NASA-CR-159875] p0142 N80-23769

Baseline automotive gas turbine engine development program [NASA-CR-159670] p0124 N80-24620

Photovoltaic technology development for synchronous orbit p0058 N80-33470

PRODUCTION ENGINEERING

Manufacture of low carbon astrology turbine disk shapes by hot isostatic pressing. Volume 2, project 1 [NASA-CR-135410] p0037 N80-21329

Screen printing technology applied to silicon solar cell fabrication [NASA-CR-159789] p0153 N80-27808

Coplanar back contacts for thin silicon solar cells [NASA-CR-159811] p0153 N80-28860

PRODUCTION METHODS

U PRODUCTION ENGINEERING

PROGRAM MANAGEMENT

U PROJECT MANAGEMENT

PROGRAMS

NT DEFENSE PROGRAM

NT GLOBAL ATMOSPHERIC RESEARCH PROGRAM

NT NASA PROGRAMS

NT QUIET ENGINE PROGRAM

NT SUPERSONIC CRUISE AIRCRAFT RESEARCH

PROJECT MANAGEMENT

Matrix management for aerospace 2000 [AIAA PAPER 80-0946] p0181 A80-40700

Matrix management for aerospace 2000 [NASA-TM-81509] p0181 N80-24200

PROJECT PLANNING

Low NO(x) heavy fuel combustor program [NASA-TM-79313] p0137 N80-13624

PROPAGATION (EXTENSION)

NT CRACK PROPAGATION

NT FLAME PROPAGATION

PROPAGATION MODES

Reciprocity principle in duct acoustics p0170 A80-20956

Higher order mode propagation in nonuniform circular ducts [AIAA PAPER 80-1018] p0171 A80-35974

Rigorous solutions for sound radiation from circular ducts with hyperbolic horns or infinite plane baffle p0171 A80-37895

Comparison of inlet suppressor data with approximate theory based on cutoff ratio [NASA-TM-81386] p0167 N80-15876

Higher order mode propagation in nonuniform circular ducts [NASA-TM-81481] p0169 N80-23101

PROPELLANT STORAGE

LeRC reduced gravity fluid management technology program p0048 A80-35504

PROPELLANT TANKS

Capillary device refilling --- liquid rocket propellant tank tests [AIAA PAPER 80-1095] p0060 A80-38908

LeRC reduced gravity fluid management technology program p0057 N80-30383

PROPELLANT TRANSFER

Conceptual design of an orbital propellant transfer experiment. Volume 2: Study results [NASA-CR-165150] p0048 N80-31423

Comparative thermal analysis of alternate Cryogenic Fluid Management Experiment (CFME) configurations [NASA-CR-165151] p0048 N80-32412

PROPELLANTS

NT CRYOGENIC ROCKET PROPELLANTS

NT LIQUID ROCKET PROPELLANTS

NT ROCKET PROPELLANTS

PROPELLER BLADES

Summary of advanced methods for predicting high speed propeller performance [AIAA PAPER 80-0225] p0003 A80-20966

The NASA high-speed turboprop program [NASA-TM-81561] p0022 N80-31401

PROPELLER EFFICIENCY

Summary of advanced methods for predicting high speed propeller performance [AIAA PAPER 80-0225] p0003 A80-20966

Summary of advanced methods for predicting high speed propeller performance [NASA-TM-81409] p0002 N80-15051

High speed turboprops for executive aircraft, potential and recent test results [NASA-TM-81482] p0002 N80-21285

NASA propeller technology program p0018 N80-22341

PROPELLER FANS

Acoustic measurements of three Prop-Fan models [AIAA PAPER 80-0995] p0045 A80-35958

Acoustic pressures on a prop-fan aircraft fuselage surface [AIAA PAPER 80-1002] p0172 A80-35965

PROPELLERS

NT PROPELLER FANS

A theoretical and experimental investigation of propeller performance methodologies [AIAA PAPER 80-1240] p0026 A80-43283

An acoustic sensitivity study of general aviation propellers

SUBJECT INDEX

PROPULSION SYSTEM PERFORMANCE

[AIAA PAPER 80-1871] p0045 A80-50191
 NASA propeller technology program p0018 N80-22341
 High-speed-propeller wind-tunnel aeroacoustic results p0018 N80-22344
 Advanced propeller aerodynamic analysis p0018 N80-22345
 A comparison between an existing propeller noise theory and wind tunnel data [NASA-TM-81519] p0169 N80-25101

PROPULSION
 NT CHEMICAL PROPULSION
 NT ELECTRIC PROPULSION
 NT ELECTROMAGNETIC PROPULSION
 NT HYBRID PROPULSION
 NT ION PROPULSION
 NT LOW THRUST PROPULSION
 NT MASS DRIVERS (PAYLOAD DELIVERY)
 NT NUCLEAR ELECTRIC PROPULSION
 NT PLASMA PROPULSION
 NT SOLAR ELECTRIC PROPULSION
 NT SOLAR PROPULSION
 NT SPACECRAFT PROPULSION
 Computational fluid mechanics of internal flow p0012 N80-10211
 Instrumentation technology p0013 N80-10214
 Control technology p0013 N80-10215

PROPULSION SYSTEM CONFIGURATIONS
 Aeropropulsion in year 2000 [AIAA PAPER 80-0914] p0024 A80-32887
 Supersonic propulsion technology --- variable cycle engines p0013 N80-10216
 Hypersonic propulsion --- supersonic combustion ramjet engines p0013 N80-10217
 Vertical Takeoff and Landing (VTOL) propulsion technology p0013 N80-10218
 High-performance-vehicle technology --- fighter aircraft propulsion p0013 N80-10219
 Quiet Clean Short-haul Experimental Engine (QCSEE) Over The Wing (OTW) design report [NASA-CR-134848] p0034 N80-15086
 Quiet Clean Short-haul Experimental Engine (QCSEE) preliminary over-the-wing flight propulsion system analysis report [NASA-CR-135296] p0035 N80-15095
 Quiet Clean Short-haul Experimental Engine (QCSEE) Over-The-Wing (OTW) boilerplate nacelle design report [NASA-CR-135168] p0035 N80-15099
 Quiet Clean Short-haul Experimental Engine (QCSEE): The aerodynamic and mechanical design of the QCSEE under-the-wing fan [NASA-CR-135009] p0031 N80-15109
 Quiet Clean Short-haul Experimental Engine (QCSEE) [NASA-CR-159473] p0032 N80-15120
 Quiet Clean Short-Haul Experimental Engine (QCSEE). Preliminary analyses and design report, volume 1 [NASA-CR-134838] p0033 N80-15123
 Quiet Clean Short-Haul Experimental Engine (QCSEE). Preliminary analyses and design report, volume 2 [NASA-CR-134839] p0033 N80-15124
 Liquid oxygen/liquid hydrogen auxiliary power system thruster investigation [NASA-CR-159674] p0062 N80-15202
 Advanced electric propulsion system concept for electric vehicles [NASA-CR-159651] p0183 N80-17916
 An automatically-shifted two-speed transaxle system for an electric vehicle [NASA-CR-159746] p0184 N80-18992
 Fuel economy screening study of advanced automotive gas turbine engines [NASA-TM-81433] p0183 N80-21201
 General Aviation Propulsion [NASA-CP-2126] p0017 N80-22327
 The impact of fuels on aircraft technology through the year 2000 [NASA-TM-81492] p0093 N80-23472
 The NASA high-speed turboprop program [NASA-TM-81561] p0022 N80-31401

Large Space Systems/Low-Thrust Propulsion Technology [NASA-CP-2144] p0057 N80-31449
 Electric propulsion technology p0057 N80-31452
 Chemical propulsion technology p0058 N80-31453
 LSS/propulsion interactions studies p0058 N80-31454
 Low-thrust vehicles concept studies p0063 N80-31456

PROPULSION SYSTEM PERFORMANCE
 Turbine engine altitude chamber and flight testing with liquid hydrogen p0023 A80-10034
 Computerized systems analysis and optimization of aircraft engine performance, weight, and life cycle costs p0165 A80-10035
 Characteristics of primary electric propulsion systems [AIAA PAPER 79-2041] p0058 A80-10376
 SERT II 1979 extended flight thruster system performance [AIAA PAPER 79-2063] p0059 A80-10386
 Preliminary results of the mission profile life test of a 30 cm Hg bombardment thruster [AIAA PAPER 79-2078] p0081 A80-10391
 Preparing aircraft propulsion for a new era in energy and the environment p0024 A80-17737
 HG ion thruster component testing [AIAA PAPER 79-2116] p0059 A80-20359
 QCSEE UTW engine powered-lift acoustic performance --- Quiet Clean Short-haul Experimental Engine Under The Wing [AIAA PAPER 80-1065] p0025 A80-38651
 CF6 fan performance improvement [ASME PAPER 80-GT-178] p0026 A80-42284
 Aeropropulsion 1979 --- conferences [NASA-CP-2092] p0012 N80-10205
 Supersonic propulsion technology --- variable cycle engines p0013 N80-10216
 Hypersonic propulsion --- supersonic combustion ramjet engines p0013 N80-10217
 Vertical Takeoff and Landing (VTOL) propulsion technology p0013 N80-10218
 High-performance-vehicle technology --- fighter aircraft propulsion p0013 N80-10219
 Effect of time dependent flight loads on JT9D-7 performance deterioration [NASA-CR-159681] p0134 N80-10515
 Quiet Clean Short-Haul Experimental Engine (QCSEE) Over-The-Wing (OTW) propulsion system test report. Volume 2: Aerodynamics and performance --- engine performance tests to define propulsion system performance on turbofan engines [NASA-CR-135324] p0029 N80-14120
 Dynamic response of a Mach 2.5 axisymmetric inlet and turbojet engine with a poppet-valve controlled inlet stability bypass system when subjected to internal and external airflow transients [NASA-TP-1531] p0014 N80-14123
 Quiet Clean Short-haul Experimental Engine (QCSEE) preliminary under the wing flight propulsion system analysis report [NASA-CR-134868] p0034 N80-15088
 Quiet Clean Short-haul Experimental Engine (QCSEE) Under-The-Wing (UTW) engine composite nacelle test report. Volume 1: Summary, aerodynamic and mechanical performance [NASA-CR-159471] p0035 N80-15094
 Quiet Clean Short-haul Experimental Engine (QCSEE). Under-The-Wing (UTW) engine boilerplate nacelle test report, volume 1 [NASA-CR-135249] p0035 N80-15096
 Quiet Clean Short-haul Experimental Engine (QCSEE). Under-The-Wing (UTW) engine boilerplate nacelle test report. Volume 3: Mechanical performance [NASA-CR-135251] p0035 N80-15097
 Quiet Clean Short-haul Experimental Engine (QCSEE) main reduction gears bearing development program [NASA-CR-134890] p0030 N80-15105

PROPULSIVE EFFICIENCY

SUBJECT INDEX

Quiet Clean Short-haul Experimental Engine (QCSEE)
main reduction gears detailed design report
[NASA-CR-134872] p0030 N80-15106

Quiet Clean Short-Haul Experimental Engine (QCSEE)
Over-The-Wing (OTW) propulsion system test
report. Volume 1: Summary report
[NASA-CR-135323] p0033 N80-15125

Quiet Clean Short-Haul Experimental Engine (QCSEE)
Over-The Wing (OTW) propulsion system test
report. Volume 3: Mechanical performance
[NASA-CR-135325] p0033 N80-15126

Potential performance improvement using a reacting
gas (nitrogen tetroxide) as the working fluid in
a closed Brayton cycle
[NASA-TM-79322] p0139 N80-16490

Preliminary study of VTO thrust requirements for a
V/STOL aircraft with lift plus lift/cruise
propulsion
[NASA-TM-81429] p0016 N80-19110

JT9D-7A (SP) jet engine performance deterioration
trends
[NASA-TM-81459] p0016 N80-20274

The performance and efficiency of four
motor/controller/battery systems for the simpler
electric vehicles
[NASA-CR-159776] p0103 N80-24550

Engine component improvement: Performance
improvement, JT9D-7 3.8 AR fan
[NASA-CR-159806] p0039 N80-25332

Preliminary results of steady state
characterization of near term electric vehicle
breadboard propulsion system
[NASA-TM-81546] p0183 N80-28254

A laboratory facility for electric vehicle
propulsion system testing
[NASA-TM-81574] p0183 N80-30229

Primary propulsion/large space system interactions
p0063 N80-31458

PROPULSIVE EFFICIENCY

NT PROPELLER EFFICIENCY

Engine component improvement program - Performance
improvement
[AIAA PAPER 80-0223] p0024 A80-19300

Fuel conservation through active control of rotor
clearances
[AIAA PAPER 80-1087] p0045 A80-41506

Quiet Clean Short-Haul Experimental Engine
(QCSEE). Under-the-wing (UTW) engine
boilerplate nacelle test report. Volume 2:
Aerodynamics and performance
[NASA-CR-135250] p0028 N80-14116

LSS/propulsion interactions studies
p0058 N80-31454

Advanced concepts --- specific impulse, mass
drivers, electromagnetic launchers, and the rail
gun
p0058 N80-31471

PROTECTION

NT CORROSION PREVENTION
NT ENVIRONMENT PROTECTION
NT RADIATION SHIELDING
NT THERMAL PROTECTION

PROTECTIVE COATINGS

NT CERAMIC COATINGS
An experimental, low-cost, silicon-aluminide
high-temperature coating for superalloys
p0082 A80-35501

Similarity tests of turbine vanes - Effects of
ceramic thermal barrier coatings
[ASME PAPER 80-HT-24] p0027 A80-48013

Corrosion resistant thermal barrier coating ---
protecting gas turbines and other heat engine
parts
[NASA-CASE-LEW-13088-1] p0067 N80-11142

Investigation into the effect of plasma
pretreatment on the adhesion of parylene to
various substrates
[NASA-TM-79224] p0114 N80-13473

Improved refractory coatings and method of
producing the same
[NASA-CASE-LEW-13169-1] p0076 N80-14232

Corrosion resistance of sodium sulfate coated
cobalt-chromium-aluminum alloys at 900 C, 1000
C, and 1100 C
[NASA-TM-79311] p0076 N80-14234

Friction and wear of plasma-sprayed coatings
containing cobalt alloys from 25 deg to 650 deg
in air
[NASA-TM-79316] p0085 N80-14249

Internal coating of air cooled gas turbine blades
[NASA-CR-159701] p0036 N80-18041

Effect of thermal cycling on ZrO₂-Y₂O₃ thermal
barrier coatings
[NASA-TM-81480] p0018 N80-22349

A silicon-slurry/aluminide coating --- protects
aircraft and land-based gas turbine engines
[NASA-CASE-LEW-13343-1] p0069 N80-26389

High temperature self-lubricating coatings for air
lubricated foil bearings for the automotive gas
turbine engine
[NASA-CR-159848] p0091 N80-26448

Performance of two-layer thermal barrier systems
on directionally solidified Ni-Al-Mo and
comparative effects of alloy thermal expansion
on system life
[NASA-TM-81604] p0080 N80-32487

Improved bond coatings for use with thermal
barrier coatings
[NASA-TM-81567] p0080 N80-33556

PUBLIC HEALTH
Assessment of potential exposure to friable
insulation materials containing asbestos
[NASA-TM-81435] p0157 N80-23875

PULLEYS
Design study of steel V-Belt CVT for electric
vehicles
[NASA-CR-159845] p0185 N80-32299

PULSATING FLOW
U UNSTEADY FLOW
PULSE COMMUNICATION
The 30/20 GHz mixed user architecture development
study
[NASA-CR-159686] p0097 N80-10415

The 30/20 GHz mixed user architecture development
study: Executive summary
[NASA-CR-159687] p0097 N80-10416

A digitally implemented communications experiment
utilizing the communications technology
satellite, Hermes
[NASA-TM-81452] p0052 N80-21412

PULSES

NT ELECTRIC PULSES

PUMP SEALS

Analysis and design of a uniform-clearance,
pumping-ring rod seal for the Stirling engine
[NASA-TM-81463] p0116 N80-18408

PUMPS

NT CENTRIFUGAL PUMPS
NT TURBINE PUMPS

PYROGRAPHALLOY

U COMPOSITE MATERIALS
U REFRACTORY MATERIALS

PYROMETRY

U TEMPERATURE MEASUREMENT

Q

QUALITY

NT AIR QUALITY
NT WATER QUALITY

QUALITY CONTROL

Modified aerospace BEQA method for wind turbines
p0145 A80-40335

Alternative jet aircraft fuels
p0012 N80-10209

Fatigue strength testing employed for evaluation
and acceptance of jet-engine instrumentation
probes
[NASA-TM-81402] p0110 N80-17422

QUARRIES

U MINES (EXCAVATIONS)

QUIET ENGINE PROGRAM

QCSEE UTW engine powered-lift acoustic performance
--- Quiet Clean Short-haul Experimental Engine
Under The Wing
[AIAA PAPER 80-1065] p0025 A80-38651

Quiet Clean Short-Haul Experimental Engine (QCSEE)
acoustic and aerodynamic tests on a scale model
over-the-wing thrust reverser and forward thrust
nozzle
[NASA-CR-135254] p0028 N80-14115

Quiet Clean Short-Haul Experimental Engine
(QCSEE). Under-the-wing (UTW) engine
boilerplate nacelle test report. Volume 2:
Aerodynamics and performance
[NASA-CR-135250] p0028 N80-14116

Quiet, Clean, Short-Haul, Experimental Engine
(QCSEE) Under-The-Wing (UTW) engine acoustic

SUBJECT INDEX

QUIET ENGINE PROGRAM CONTD

design
 [NASA-CR-135267] p0028 N80-14117
 Quiet, Clean, Short-Haul Experimental Engine
 (QCSEE) Over-The-Wing (OTW) engine acoustic design
 [NASA-CR-135268] p0028 N80-14118
 Static test-stand performance of the YF-102
 turbofan engine with several exhaust
 configurations for the Quiet Short-Haul Research
 Aircraft (QSRA)
 [NASA-TP-1556] p0014 N80-14121
 Demonstration of short-haul aircraft aft noise
 reduction techniques on a twenty inch (50.8 cm)
 diameter fan, volume 1
 [NASA-CR-134849] p0033 N80-15083
 Demonstration of short haul aircraft aft noise
 reduction techniques on a twenty inch (50.8 cm)
 diameter fan, volume 3
 [NASA-CR-134851] p0034 N80-15085
 Quiet Clean Short-haul Experimental Engine (QCSEE)
 Over The Wing (OTW) design report
 [NASA-CR-134848] p0034 N80-15086
 Quiet Clean Short-haul Experimental Engine (QCSEE)
 preliminary under the wing flight propulsion
 system analysis report
 [NASA-CR-134868] p0034 N80-15088
 Quiet Clean Short-haul Experimental Engine
 (QCSEE). The aerodynamic and mechanical design
 of the QCSEE over-the-wing fan
 [NASA-CR-134915] p0034 N80-15089
 Quiet Clean Short-haul Experimental Engine (QCSEE)
 under-the-wing engine digital control system
 design report
 [NASA-CR-134920] p0034 N80-15090
 Quiet Clean Short-haul Experimental Engine (QCSEE)
 under-the-wing engine simulation report
 [NASA-CR-134914] p0034 N80-15091
 Quiet Clean Short-haul Experimental Engine (QCSEE)
 over-the-wing control system design report
 [NASA-CR-135337] p0035 N80-15092
 Quiet Clean Short-haul Experimental Engine
 (QCSEE). Core engine noise measurements
 [NASA-CR-135160] p0035 N80-15093
 Quiet Clean Short-haul Experimental Engine (QCSEE)
 Under-The-Wing (UTW) engine composite nacelle
 test report. Volume 1: Summary, aerodynamic
 and mechanical performance
 [NASA-CR-159471] p0035 N80-15094
 Quiet Clean Short-haul Experimental Engine (QCSEE)
 preliminary over-the-wing flight propulsion
 system analysis report
 [NASA-CR-135296] p0035 N80-15095
 Quiet Clean Short-haul Experimental Engine
 (QCSEE). Under-The-Wing (UTW) engine boilerplate
 nacelle test report, volume 1
 [NASA-CR-135249] p0035 N80-15096
 Quiet Clean Short-haul Experimental Engine
 (QCSEE). Under-The-Wing (UTW) engine boilerplate
 nacelle test report. Volume 3: Mechanical
 performance
 [NASA-CR-135251] p0035 N80-15097
 Quiet Clean Short-haul Experimental Engine
 (QCSEE). Composite fan frame subsystem test
 report
 [NASA-CR-135010] p0035 N80-15098
 Quiet Clean Short-haul Experimental Engine (QCSEE)
 Over-The-Wing (OTW) boilerplate nacelle design
 report
 [NASA-CR-135168] p0035 N80-15099
 Quiet Clean Short-haul Experimental Engine (QCSEE)
 Under-The-Wing (UTW) composite nacelle subsystem
 test report --- to verify strength of selected
 composite materials
 [NASA-CR-135075] p0034 N80-15100
 Quiet Clean Short-haul Experimental Engine (QCSEE)
 Under-The-Wing (UTW) composite nacelle subsystem
 test report --- to verify strength of selected
 composite materials
 [NASA-CR-135075] p0034 N80-15100
 Quiet Clean Short-haul Experimental Engine
 (QCSEE). Ball spline pitch change mechanism
 design report
 [NASA-CR-134873] p0030 N80-15101
 Quiet Clean Short-haul Experimental Engine
 (QCSEE). Ball spline pitch change mechanism
 design report
 [NASA-CR-134873] p0030 N80-15101
 Acoustic analysis of aft noise reduction
 techniques measured on a subsonic tip speed 50.8
 cm (twenty inch) diameter fan --- quiet engine

program
 [NASA-CR-134891] p0030 N80-15102
 Quiet Clean Short-haul Experimental Engine (QCSEE)
 main reduction gears test program
 [NASA-CR-134669] p0030 N80-15103
 Quiet Clean Short-haul Experimental Engine (QCSEE)
 clean combustor test report
 [NASA-CR-134916] p0030 N80-15104
 Quiet Clean Short-haul Experimental Engine (QCSEE)
 main reduction gears bearing development program
 [NASA-CR-134890] p0030 N80-15105
 Quiet Clean Short-haul Experimental Engine (QCSEE)
 main reduction gears detailed design report
 [NASA-CR-134872] p0030 N80-15106
 Quiet Clean Short-haul Experimental Engine
 (QCSEE): Hamilton Standard cam/harmonic drive
 variable pitch fan actuation system detail
 design report
 [NASA-CR-134852] p0030 N80-15107
 Quiet Clean Short-haul Experimental Engine (QCSEE)
 under-the-wing engine composite fan blade design
 report
 [NASA-CR-135046] p0031 N80-15108
 Quiet Clean Short-haul Experimental Engine
 (QCSEE): The aerodynamic and mechanical design
 of the QCSEE under-the-wing fan
 [NASA-CR-135009] p0031 N80-15109
 Quiet Clean Short-haul Experimental Engine (QCSEE)
 composite fan frame design report
 [NASA-CR-135278] p0031 N80-15110
 Quiet Clean Short-haul Experimental Engine (QCSEE)
 UTW fan preliminary design
 [NASA-CR-134842] p0031 N80-15111
 Quiet Clean Short-haul Experimental Engine
 (QCSEE): The aerodynamic and preliminary
 mechanical design of the QCSEE OTW fan
 [NASA-CR-134841] p0031 N80-15112
 Quiet Clean Short-haul Experimental Engine (QCSEE)
 under-the-wing engine composite fan blade design
 [NASA-CR-134840] p0031 N80-15113
 Quiet Clean Short-haul Experimental Engine (QCSEE)
 over-the-wing engine and control simulation
 results
 [NASA-CR-135049] p0031 N80-15114
 Quiet Clean Short-Haul Experimental Engine (QCSEE)
 ball spline pitch-change mechanism whirligig
 test report
 [NASA-CR-135354] p0032 N80-15115
 Quiet Clean Short-haul Experimental Engine (QCSEE)
 Under-The-Wing (UTW) boiler plate nacelle and
 core exhaust nozzle design report
 [NASA-CR-135008] p0032 N80-15116
 Quiet Clean Short-haul Experimental Engine (QCSEE)
 whirl test of cam/harmonic pitch change
 actuation system
 [NASA-CR-135140] p0032 N80-15117
 Quiet Clean Short-haul Experimental Engine (QCSEE)
 Over-The-Wing (OTW) propulsion systems test
 report. Volume 4: Acoustic performance
 [NASA-CR-135326] p0032 N80-15118
 Quiet Clean Short-haul Experimental Engine (QCSEE)
 Under-The-Wing (UTW) composite nacelle
 [NASA-CR-135352] p0032 N80-15119
 Quiet Clean Short-haul Experimental Engine (QCSEE)
 [NASA-CR-159473] p0032 N80-15120
 Quiet Clean Short-haul Experimental Engine
 (QCSEE). Double-annular clean combustor
 technology development report
 [NASA-CR-159483] p0032 N80-15121
 Quiet Clean Short-Haul Experimental Engine
 (QCSEE): Acoustic treatment development and
 design
 [NASA-CR-135266] p0033 N80-15122
 Quiet Clean Short-Haul Experimental Engine
 (QCSEE). Preliminary analyses and design
 report, volume 1
 [NASA-CR-134838] p0033 N80-15123
 Quiet Clean Short-Haul Experimental Engine
 (QCSEE). Preliminary analyses and design
 report, volume 2
 [NASA-CR-134839] p0033 N80-15124
 Quiet Clean Short-Haul Experimental Engine (QCSEE)
 Over-The-Wing (OTW) propulsion system test
 report. Volume 1: Summary report
 [NASA-CR-135323] p0033 N80-15125
 Quiet Clean Short-Haul Experimental Engine (QCSEE)
 Over-The Wing (OTW) propulsion system test
 report. Volume 3: Mechanical performance
 [NASA-CR-135325] p0033 N80-15126

Quiet powered-lift propulsion
[NASA-CR-2077] p0015 N80-15127
Program for impact testing of spar-shell fan
blades, test report
[NASA-CR-135393] p0037 N80-21328
Airesearch QCGAT program --- quiet clean general
aviation turbofan engines
[NASA-CR-159758] p0037 N80-21331
Avco Lycoming quiet clean general aviation
turbofan engine
p0039 N80-22333
Summary of NASA QCGAT program
p0017 N80-22334
OSCEE fan exhaust bulk absorber treatment evaluation
[NASA-TM-81498] p0019 N80-23314
QCSSE UTM engine powered-lift acoustic performance
[NASA-TM-81504] p0019 N80-24315
Quiet Clean Short-haul Experimental Engine (QCSEE)
Under-The-Wing (UTW) composite Macelle test
report. Volume 2: Acoustic performance
[NASA-CR-159472] p0044 N80-29297
Quiet Clean Short-haul Experimental Engine (QCSEE)
under-the-wing engine composite fan blade:
Preliminary design test report
[NASA-CR-134846] p0044 N80-29298
Acoustic performance of a 50.8-cm (20-inch)
diameter variable-pitch fan and inlet. Volume
2: Acoustic data
[NASA-CR-135118] p0044 N80-29299

R

RADAR

NT AIRBORNE SURVEILLANCE RADAR

RADAR ALTIMETERS

U RADIO ALTIMETERS

RADIAL FLOW

Evolution of a rotating flow in the vicinity of a
surface

p0107 A80-14660

Study of advanced radial outflow turbine for solar
steam Rankine engines

[NASA-CR-159695] p0148 N80-16483

Loss model for off-design performance analysis of
radial turbines with pivoting-vane,
variable-area stators

[NASA-TM-81532] p0020 N80-27365

RADIANT FLUX DENSITY

NT IRRADIANCE

RADIATION ABSORPTION

NT ATMOSPHERIC ATTENUATION

RADIATION DAMAGE

Origin of reverse annealing in radiation-damaged
silicon solar cells

p0059 A80-33850

Radiation damage in high voltage silicon solar cells
p0179 A80-44234Space solar cells: High efficiency and radiation
damage

[NASA-TM-81387] p0138 N80-15554

Radiation damage in lithium-counterdoped n/p
silicon solar cells

[NASA-TM-81391] p0138 N80-15557

Radiation damage annealing mechanisms and possible
low temperature annealing in silicon solar cells

[NASA-TM-81392] p0138 N80-15558

Radiation damage in high voltage silicon solar cells
[NASA-TM-81478] p0178 N80-23180Radiation damage in high voltage silicon solar cells
p0144 N80-33889

RADIATION EFFECTS

NT RADIATION DAMAGE

RADIATION MEASUREMENT

Global calibration of terrestrial reference cells
and errors involved in using different
irradiance monitoring techniques

[NASA-TM-81393] p0138 N80-15561

RADIATION PRESSURE

NT SOUND PRESSURE

RADIATION PROTECTION

NT RADIATION SHIELDING

RADIATION RESISTANCE

U RADIATION TOLERANCE

RADIATION SHIELDING

Interaction of high voltage surfaces with the
space plasma

[NASA-CR-165131] p0177 N80-32223

RADIATION THERAPY

Preliminary results of fast neutron treatments in

carcinoma of the pancreas

[NASA-TM-81516] p0160 N80-24983

RADIATION TOLERANCE

Radiation damage in lithium-counterdoped n/p

silicon solar cells

[NASA-TM-81391] p0138 N80-15557

Thin n-i-p radiation-resistant solar cell

feasibility study

[NASA-CR-159871] p0154 N80-29852

RADIO ALTIMETERS

Solid-state X-band combiner study

[NASA-CR-162432] p0103 N80-11328

RADIO COMMUNICATION

NT TIME DIVISION MULTIPLE ACCESS

The 30/20 GHz fixed communications systems service

demand assessment. Volume 1: Executive summary

[NASA-CR-159619] p0098 N80-18262

The 30/20 GHz fixed communications systems service

demand assessment. Volume 2: Main report

[NASA-CR-159620] p0098 N80-18263

The 30/20 GHz fixed communications systems service

demand assessment. Volume 3: Annex

[NASA-CR-159621] p0099 N80-18264

RADIO FREQUENCIES

NT EXTREMELY HIGH FREQUENCIES

NT SUPERHIGH FREQUENCIES

NT ULTRAHIGH FREQUENCIES

RADIO RELAY SYSTEMS

NT TIME DIVISION MULTIPLE ACCESS

RADIO TRANSMISSION

NT MICROWAVE TRANSMISSION

RADIO WAVES

NT MILLIMETER WAVES

RADIOSENSITIVITY

U RADIATION TOLERANCE

RADIOTHERAPY

U RADIATION THERAPY

RAIN

Concepts for 18/30 GHz satellite communication
system, volume 1

[NASA-CR-159625-VOL-1] p0098 N80-11277

Concepts for 18/30 GHz satellite communication

system, volume 1A: Appendix

[NASA-CR-159625-VOL-1A] p0098 N80-11278

Concepts for 18/30 GHz satellite communication

system study. Executive summary

[NASA-CR-159680] p0098 N80-11279

RAINDROPS

Calculation of water drop trajectories to and
about arbitrary three-dimensional bodies in
potential airflow

[NASA-CR-3291] p0005 N80-28302

RAMJET ENGINES

NT SUPERSONIC COMBUSTION RAMJET ENGINES

RANKINE CYCLE

Study of advanced radial outflow turbine for solar
steam Rankine engines

[NASA-CR-159695] p0148 N80-16483

A 15kWe (nominal) solar thermal electric power

conversion concept definition study: Steam

Rankine reheat reciprocator system

[NASA-CR-159590] p0148 N80-16491

The 15 kW sub e (nominal) solar thermal electric

power conversion concept definition study:

Steam Rankine turbine system

[NASA-CR-159589] p0148 N80-16493

A 15 kWe (nominal) solar thermal-electric power

conversion concept definition study: Steam

Rankin reciprocator system

[NASA-CR-159591] p0149 N80-19612

RARE EARTH ELEMENTS

NT EUROFIUM

NT YTTRIUM

RARE GASES

NT ARGON

NT NEON

NT XENON

Inert gas thrusters

[NASA-CR-159813] p0062 N80-24362

Inert gas ion thruster development

[NASA-CR-159805] p0062 N80-27424

RATE METERS

U MEASURING INSTRUMENTS

RATES (PER TIME)

NT ACOUSTIC VELOCITY

NT ANGULAR VELOCITY

NT BURNING RATE

NT CURRENT DENSITY

NT FLOW VELOCITY

SUBJECT INDEX

REGULATORS

NT HEAT FLUX
 NT HIGH SPEED
 NT ION PRODUCTION RATES
 NT IRRADIANCE
 NT LOW SPEED
 NT MASS FLOW RATE
 NT ROTOR SPEED
 NT WIND VELOCITY
RATIOS
 NT ASPECT RATIO
 NT DIMENSIONLESS NUMBERS
 NT FUEL-AIR RATIO
 NT LOW ASPECT RATIO
 NT REYNOLDS NUMBER
 NT STRESS RATIO
 NT THICKNESS RATIO
 NT THRUST-WEIGHT RATIO
REACTION BONDING
 Formation of porous surface layers in reaction
 bonded silicon nitride during processing
 p0090 A80-51574
REACTION JETS
 U JET FLOW
 U JET THRUST
REACTION KINETICS
 Symposium /International/ on Combustion, 17th,
 Leeds University, Leeds, England, August 20-25,
 1978, Proceedings
 p0075 A80-11754
 The effect of catalyst length and downstream
 reactor distance on catalytic combustor
 performance
 [NASA-TM-81475] p0142 A80-23779
REAL VARIABLES
 NT GREEN FUNCTION
 NT HELMHOLTZ VORTICITY EQUATION
 NT LINEAR EQUATIONS
 NT NONLINEAR EQUATIONS
 NT NUMERICAL INTEGRATION
 NT PARTIAL DIFFERENTIAL EQUATIONS
 NT POWER SERIES
RECIPROCAL THEOREMS
 Reciprocity principle in duct acoustics
 p0170 A80-20956
 Reciprocity principle in duct acoustics
 [NASA-TM-79300] p0167 A80-12824
RECIPROCATING ENGINES
 U PISTON ENGINES
RECLAMATION
 Assessment of satellite and aircraft multispectral
 scanner data for strip-mine monitoring
 [NASA-TM-79268] p0136 A80-20787
RECOGNITION
 NT TARGET RECOGNITION
RECORDING INSTRUMENTS
 NT FLIGHT LOAD RECORDERS
RECOVERABLE SPACECRAFT
 NT SPACE SHUTTLES
RECRYSTALLIZATION
 Characterization and properties of controlled
 nucleation thermochemical deposited (CNTD)
 silicon carbide
 [NASA-TM-79277] p0085 A80-13254
RECTANGULAR PLANKFORMS
 NT RECTANGULAR PLATES
RECTANGULAR PLATES
 Vibration and buckling of rectangular plates under
 in-plane hydrostatic loading
 p0133 A80-45364
RECUPERATORS
 U REGENERATORS
REDUCED GRAVITY
 LeRC reduced gravity fluid management technology
 program
 p0048 A80-35504
 LeRC reduced gravity fluid management technology
 program
 [NASA-TM-81450] p0051 A80-20304
 Conceptual design of two-phase fluid mechanics and
 heat transfer facility for spacelab
 [NASA-CR-159810] p0049 A80-27403
 LeRC reduced gravity fluid management technology
 program
 p0057 A80-30383
REDUCTION (MATHEMATICS)
 U OPTIMIZATION
REFILLING
 Capillary device refilling --- liquid rocket
 propellant tank tests

[AIAA PAPER 80-1095] p0060 A80-38908
REFLECTANCE
 NT SPECTRAL REFLECTANCE
 Quantitative interpretation of Great Lakes remote
 sensing data
 p0157 A80-45005
REFLECTION
 NT WAVE REFLECTION
REFLECTION COEFFICIENT
 U REFLECTANCE
REFLECTIVITY
 U REFLECTANCE
REFLECTORS
 NT SOLAR REFLECTORS
 Back surface reflectors for solar cells
 [NASA-TM-81390] p0138 A80-15556
REFRACTORY MATERIALS
 NT CHROMIUM
 NT NIOBIUM ALLOYS
 NT REFRACTORY METAL ALLOYS
 NT TANTALUM ALLOYS
 NT TUNGSTEN
 Thick ceramic coating development for industrial
 gas turbines - A program plan
 [SR79-M-4702-05] p0091 A80-10042
 State-of-the-art of SiAlON materials
 p0009 A80-13066
 Improved adhesion of sputtered refractory carbides
 to metal substrates
 p0081 A80-25274
 Effect of W and WC on the oxidation resistance of
 yttria-doped silicon nitride
 p0090 A80-46099
 Effect of starting powder characteristics on
 density, microstructure and low temperature
 oxidation behavior of a Si₃N₄ - 8 w/o Y₂O₃ ceramic
 p0090 A80-46100
 Improved refractory coatings and method of
 producing the same
 [NASA-CASE-LEW-13169-1] p0076 A80-14232
 Castable high temperature refractory materials
 [NASA-CASE-LEW-13080-1] p0088 A80-29496
REFRACTORY METAL ALLOYS
 NT NIOBIUM ALLOYS
 NT TANTALUM ALLOYS
 Materials review for improved automotive gas
 turbine engine --- superalloys, refractory
 alloys, and ceramics
 [NASA-CR-159673] p0123 A80-17470
REFRACTORY METALS
 NT CHROMIUM
 NT TUNGSTEN
REFRASIL (TRADEMARK)
 U FIBERS
REFUELING
 Conceptual design of an orbital propellant
 transfer experiment. Volume 2: Study results
 [NASA-CR-165150] p0048 A80-31423
REGENERATION (ENGINEERING)
 Assessment and preliminary design of an energy
 buffer for regenerative braking in electric
 vehicles
 [NASA-CR-159756] p0184 A80-23216
 Free-piston regenerative hot gas hydraulic engine
 [NASA-CASE-LEW-12274-1] p0119 A80-31790
REGENERATIVE COOLING
 Advanced cooling techniques for high-pressure,
 hydrocarbon-fueled rocket engines
 [AIAA PAPER 80-1266] p0060 A80-38994
 Performance of a transpiration-regenerative cooled
 rocket thrust chamber
 [NASA-CR-159742] p0061 A80-14189
REGENERATIVE CYCLES
 U REGENERATION (ENGINEERING)
REGENERATORS
 Sintered silicon nitride recuperator fabrication
 [NASA-CR-159706] p0090 A80-15263
 Feasibility study of silicon nitride
 regenerators
 [NASA-CR-159713] p0184 A80-25209
 Regenerator matrix physical property
 data
 [NASA-CR-159854] p0185 A80-30228
REGRESSION (STATISTICS)
 U REGRESSION ANALYSIS
REGRESSION ANALYSIS
 'Chain pooling' model selection for two-level
 fixed effects factorial experiments
 p0164 A80-40764
REGULATORS
 NT PRESSURE REGULATORS

IGNITION

SUBJECT INDEX

NT VOLTAGE REGULATORS
IGNITION
U IGNITION
REINFORCED MATERIALS
U COMPOSITE MATERIALS
REINFORCED PLASTICS
NT GLASS FIBER REINFORCED PLASTICS
REINFORCING FIBERS
NT BORON FIBERS
NT CARBON FIBERS
Fatigue behavior of SiC reinforced titanium composites
p0070 A80-10036
Dynamic modulus and damping of boron, silicon carbide, and alumina fibers
p0071 A80-44236
Improved fiber retention by the use of fillers in graphite fiber/resin matrix composites
[NASA-TM-79288] p0067 N80-13171
RELATIONSHIPS
NT STRESS-STRAIN RELATIONSHIPS
RELIABILITY
NT COMPONENT RELIABILITY
RELIABILITY ANALYSIS
Study of turboprop systems reliability and maintenance costs
[NASA-CR-135192] p0029 N80-14129
RELIABILITY CONTROL
U QUALITY CONTROL
U RELIABILITY ENGINEERING
RELIABILITY ENGINEERING
Modified aerospace REQA method for wind turbines
p0145 A80-40335
Photovoltaic power system reliability considerations
p0146 A80-40338
Photovoltaic power system reliability considerations
[NASA-TM-79291] p0130 N80-15422
Fatigue strength testing employed for evaluation and acceptance of jet-engine instrumentation probes
[NASA-TM-81402] p0110 N80-17422
REMOTE SENSORS
Possible methods for distinguishing icebergs from ships by aerial remote sensing
[NASA-TM-79310] p0136 N80-15538
Optical sensors for aeronautics and space
[NASA-TM-81407] p0110 N80-17423
Fiber optic sensors for measuring angular position and rotational speed --- air breathing engines
[NASA-TM-81454] p0110 N80-18368
REPORTS
Workshop report for the AIAA 5th Aeroacoustics Conference
p0172 A80-41156
REPUBLIC MILITARY AIRCRAFT
U MILITARY AIRCRAFT
RESEARCH
NT HIGH TEMPERATURE RESEARCH
NT MARKET RESEARCH
RESEARCH AND DEVELOPMENT
NASA communications technology research and development
p0097 A80-25920
Aeropropulsion in year 2000
[AIAA PAPER 80-0914] p0024 A80-32887
The use of wind data with an operational wind turbine in a research and development environment
p0145 A80-35730
Airbreathing propulsion component technologies
p0024 A80-37482
Comments on TEC trends --- Thermionic Energy Conversion
p0145 A80-39642
Modified aerospace REQA method for wind turbines
p0145 A80-40335
System analysis for millimeter-wave communication satellites
p0100 A80-52479
Status of the DOE/NASA critical gas turbine research and technology project
[NASA-TM-79307] p0137 N80-14493
Study of research and development requirements of small gas-turbine combustors
[NASA-CR-159796] p0036 N80-18040
An overview of NASA research on positive displacement general-aviation engines
p0017 N80-22336
RESEARCH FACILITIES
Description of the warm core turbine facility

recently installed at NASA Lewis Research Center
[NASA-TM-81562] p0022 N80-29333
RESEARCH MANAGEMENT
National Aeronautics and Space Administration plans for space communication technology
p0097 A80-26795
NASA broad-specification fuels combustion technology program: Status and description
[NASA-TM-79315] p0014 N80-14126
Program definition and assessment overview --- for thermal energy storage project management
p0141 N80-22790
RESIDUAL GAS
Cogeneration Technology Alternatives Study (CTAS). Volume 6: Computer data. Part 2: Residual-fired nocogeneration process boiler
[NASA-CR-159770-PT-2] p0156 N80-33861
RESIDUAL STRESS
Calculation of residual principal stresses in CVD boron on carbon filaments
p0072 A80-44237
Calculation of residual principal stresses in CVD boron on carbon filaments
[NASA-TM-81456] p0068 N80-20314
RESIN MATRIX COMPOSITES
Cost analysis of composite fan blade manufacturing processes
[NASA-CR-159876] p0044 N80-31398
RESINS
NT EPOXY RESINS
NT KEVLAR (TRADEMARK)
NT PHENOLIC RESINS
NT POLYESTER RESINS
NT POLYIMIDE RESINS
NT SILICONE RESINS
NT THERMOSETTING RESINS
Burning characteristics and fiber retention of graphite/resin matrix composites
p0070 A80-32062
RESISTIVITY
U ELECTRICAL RESISTIVITY
RESONANCE
NT PARAMAGNETIC RESONANCE
NT RESONANT VIBRATION
RESONANT FREQUENCIES
Vibration and buckling of rectangular plates under in-plane hydrostatic loading
p0133 A80-45364
RESONANT VIBRATION
Design of elastomer dampers for a high-speed flexible rotor
[ASME PAPER 79-DET-88] p0121 A80-15736
RESONATORS
Effect of grazing flow on the nonlinear acoustic behavior of helmholtz resonators
p0095 N80-31619
RESOURCES
NT COAL
NT CRUDE OIL
NT FOSSIL FUELS
NT GEOTHERMAL RESOURCES
NT ICEBERGS
RESOURCES MANAGEMENT
Fuels research: Fuel thermal stability overview
p0021 N80-29324
RESPONSES
NT DYNAMIC RESPONSE
NT PHYSIOLOGICAL RESPONSES
NT TRANSIENT RESPONSE
RETROFITTING
NT ACOUSTIC RETROFITTING
REUSABLE SPACECRAFT
NT SPACE SHUTTLES
REYNOLDS NUMBER
Amplification of Reynolds number dependent processes by wave distortion --- liquid fuel combustor stability
[NASA-CR-159732] p0075 N80-13193
RENOLOGY
Influence of excess diamine on properties of PNB polyimide resins and composites
[NASA-TM-81580] p0069 N80-29433
RHODIUM ALLOYS
Hyperfine magnetic field at Cd impurity site in L2/1/ Heusler alloys Rh2MnGe and Rh2MnPt by TDPAC technique --- Time Differential Perturbed Angular Correlation
p0178 A80-16843

SUBJECT INDEX

NOTARY STABILITY

RICHARDSON-DUSMAN EQUATION U TEMPERATURE EFFECTS RIGID ROTOR HELICOPTERS

Examination of the flap-lag stability of rigid articulated rotor blades p0010 A80-15123

RING STRUCTURES

Two-dimensional finite-element analyses of simulated rotor-fragment impacts against rings and beams compared with experiments [NASA-CR-159645] p0038 A80-22323
Dynamic response to rotating-seat runout in non-contacting face seals [NASA-TM-81490] p0117 A80-22701
Instructions for the use of the CIVM-Jet 4C finite-strain computer code to calculate the transient structural responses of partial and/or complete arbitrarily-curved rings subjected to fragment impact [NASA-CR-159873] p0134 A80-27720

RISK

Statistical aspects of carbon fiber risk assessment modeling --- fire accidents involving aircraft [NASA-CR-159318] p0073 A80-29432

ROCKET CHAMBERS

U THRUST CHAMBERS

ROCKET ENGINE DESIGN

8-cm Engineering Model Thruster technology - A review of recent developments [AIAA PAPER 79-2103] p0064 A80-13311
A model for predicting the wearout lifetime of the LeRC/Hughes 30-cm mercury ion thruster [AIAA PAPER 79-2079] p0064 A80-20962
Liquid oxygen/liquid hydrogen auxiliary power system thruster investigation [NASA-CR-159674] p0062 A80-15202
Inert gas thrusters [NASA-CR-159813] p0062 A80-24362
Analytical investigation of two hydrogen-oxygen rocket engine systems for low-thrust application --- for orbital transfer p0057 A80-30382
LEO-to-GEO low thrust chemical propulsion p0063 A80-30384

ROCKET ENGINES

NT ELECTRIC ROCKET ENGINES
NT HYBRID PROPELLANT ROCKET ENGINES
NT HYDROGEN OXYGEN ENGINES
NT ION ENGINES
NT LIQUID PROPELLANT ROCKET ENGINES
NT MERCURY ION ENGINES
NT NUCLEAR ENGINE FOR ROCKET VEHICLES
NT UPPER STAGE ROCKET ENGINES

Preliminary results of the mission profile life test of a 30 cm Hg bombardment thruster [AIAA PAPER 79-2078] p0081 A80-10391
An electric propulsion long term test facility [AIAA PAPER 79-2080] p0049 A80-13308
Advanced cooling techniques for high-pressure, hydrocarbon-fueled rocket engines [AIAA PAPER 80-1266] p0060 A80-38994
Advanced cooling techniques for high-pressure hydrocarbon-fueled engines [NASA-CR-159790] p0061 A80-17141
Plasma physics analysis of SERT-2 operation [NASA-CR-159814] p0177 A80-27189
Low-thrust chemical rocket engine study p0063 A80-31467
Low-thrust chemical propulsion p0063 A80-31468
Solar rocket system concept analysis p0064 A80-31470

ROCKET EXHAUST

Specific spacecraft evaluation: Special report --- charged particle transport from a mercury ion thruster to spacecraft surfaces [NASA-CR-159420] p0060 A80-11137

ROCKET LININGS

Heat exchanger and method of making --- rocket lining [NASA-CASE-LEW-12441-2] p0105 A80-24573

ROCKET PROPELLANT TANKS

U PROPELLANT TANKS

ROCKET PROPELLANTS

NT CRYOGENIC ROCKET PROPELLANTS
NT LIQUID ROCKET PROPELLANTS
Design and evaluation of high performance rocket engine injectors for use with hydrocarbon fuels

[NASA-TM-79319] p0056 A80-13163
Low-thrust chemical orbit to orbit propulsion system propellant management study p0064 A80-31469
Design and evaluation of high performance rocket engine injectors for use with hydrocarbon fuels p0094 A80-31621

ROCKET THRUST

Cooling of high pressure rocket thrust chambers with liquid oxygen [NASA-TM-81503] p0057 A80-23365

ROCKET VEHICLES

NT CENTAUR LAUNCH VEHICLE
NT TITAN CENTAUR LAUNCH VEHICLE

ROCKS

NT COAL

ROLLER BEARINGS

Load support system analysis high speed input pinion configuration [ASME PAPER 79-LUB-34] p0129 A80-14760
High speed cylindrical rolling element bearing analysis 'CYBEAN' - Analytic formulation [ASME PAPER 79-LUB-35] p0129 A80-14761
Rolling-element bearings --- contact sliding friction study of solid bodies p0121 A80-31961
Constrained fatigue life optimization of a NASVYTIS multiroller traction drive p0122 A80-46407
Endurance and failure characteristics of modified Vasco X-2, CBS 600 and AISI 9310 spur gears p0123 A80-46411
Simplified fatigue life analysis for traction drive contacts p0123 A80-46413
Quiet Clean Short-haul Experimental Engine (QCSSE) main reduction gears bearing development program [NASA-CR-134890] p0030 A80-15105
Comparison of predicted and experimental performance of large-bore roller bearing operating to 3.0 million DM [NASA-TF-1599] p0114 A80-15410
Performance of computer-optimized tapered-roller bearings to 2.4 million DM [NASA-TM-81414] p0114 A80-16342
Constrained fatigue life optimization of a NASVYTIS multiroller traction drive [NASA-TM-81447] p0116 A80-18407
Calculated and experimental data for a 118-mm bore roller bearing to 3 million DM [NASA-TM-81427] p0116 A80-19496
Lubrication of rolling-element bearings [NASA-TM-81449] p0117 A80-20591
Stresses and deformations in elliptical contacts [NASA-TM-81535] p0118 A80-27697
Kinematic correction for roller skewing [NASA-TM-81564] p0119 A80-28716
Lubrication of optimized-design tapered-roller bearings to 2.4 million DM [NASA-TF-1714] p0119 A80-29734
Effect of cage design on characteristics of high-speed-jet-lubricated 35-millimeter-bore ball bearing --- turbojet engines [NASA-TF-1732] p0120 A80-33749

ROLLING CONTACT LOADS

Load support system analysis high speed input pinion configuration [ASME PAPER 79-LUB-34] p0129 A80-14760
High speed cylindrical rolling element bearing analysis 'CYBEAN' - Analytic formulation [ASME PAPER 79-LUB-35] p0129 A80-14761
Rolling-element bearings --- contact sliding friction study of solid bodies p0121 A80-31961
Constrained fatigue life optimization of a NASVYTIS multiroller traction drive p0122 A80-46407
Spur-gear-system efficiency at part and full load [NASA-TF-1622] p0115 A80-17466
Endurance and failure characteristics of modified Vasco X-2, CBS 600 and AISI 9310 spur gears --- aircraft construction materials [NASA-TM-81421] p0116 A80-18405

ROLLUP SOLAR ARRAYS

U SOLAR ARRAYS

NOTARY DRIVES

U MECHANICAL DRIVES

NOTARY STABILITY

The response of turbine engine rotors to

ROTARY WING AIRCRAFT

SUBJECT INDEX

interference rubs
[NASA-TN-81518] p0118 N80-27696

Rotordynamic Instability Problems in
high-performance turbomachinery
[NASA-CP-2133] p0119 N80-29706

Field experiences with rotordynamic instability in
high-performance turbomachinery --- oil and
natural gas recovery p0125 N80-29707

Field verification of lateral-torsional coupling
effects on rotor instabilities in centrifugal
compressors p0125 N80-29708

Practical experience with unstable compressors
p0125 N80-29709

Analysis and identification of subsynchronous
vibration for a high pressure parallel flow
centrifugal compressor p0125 N80-29710

Subsynchronous instability of a geared centrifugal
compressor of overhung design p0125 N80-29711

The parameters and measurements of the
destabilizing actions of rotating machines, and
the assumptions of the 1950's p0125 N80-29712

Asynchronous vibration problem of centrifugal
compressor p0125 N80-29713

Testing of turbulent seals for rotodynamic
coefficients p0126 N80-29714

Evaluation of instability forces of labyrinth
seals in turbines or compressors p0126 N80-29715

Damping in ring seals for compressible fluids
p0119 N80-29716

Flow induced spring coefficients of labyrinth
seals for application in rotor dynamics p0126 N80-29717

A test program to measure fluid mechanical
whirl-excitation forces in centrifugal pumps
p0126 N80-29719

Effect of fluid forces on rotor stability of
centrifugal compressors and pumps p0126 N80-29720

Non-synchronous whirling due to fluid-dynamic
forces in axial turbo-machinery rotors
p0126 N80-29721

Self-excited rotor whirl due to tip-seal leakage
forces p0127 N80-29723

Fluid forces on rotating centrifugal impeller with
whirling motion p0127 N80-29724

Experimental results concerning centrifugal
impeller excitations p0127 N80-29727

Physical explanations of the destabilizing effect
of damping in rotating parts p0127 N80-29728

Parametric instabilities of rotor-support systems
with application to industrial ventilators
p0127 N80-29729

Instability thresholds for flexible rotors in
hydrodynamic bearings p0128 N80-29730

Use of elastomeric elements in control of rotor
instability p0128 N80-29732

Feasibility of active feedback control of
rotordynamic instability p0128 N80-29733

ROTARY WING AIRCRAFT

NT HELICOPTERS

NT RIGID ROTOR HELICOPTERS

NT TANDEM ROTOR HELICOPTERS

NT TILT ROTOR AIRCRAFT

ROTARY WINGS

Examination of the flap-lag stability of rigid
articulated rotor blades p0010 A80-15123

ROTATING BODIES

NT COMPRESSOR ROTORS

NT FLYWHEELS

NT HELICOPTER TAIL ROTORS

NT ROTARY WINGS

NT ROTATING CYLINDERS

NT ROTORS

NT TURBINE WHEELS

Temperature and pressure measurement techniques
for an advanced turbine test facility
[NASA-TN-79278] p0110 N80-14374

Dynamic response to rotating-seal runout in
non-contacting face seals
[NASA-TN-81490] p0117 N80-22701

ROTATING CYLINDERS

Calculated and experimental data for a 118-mm bore
roller bearing to 3 million DN
[NASA-TN-81427] p0116 N80-19496

Kinematic correction for roller skewing
[NASA-TN-81564] p0119 N80-28716

ROTATING FLUIDS

Evolution of a rotating flow in the vicinity of a
surface p0107 A80-14660

ROTATING GENERATORS

NT TURBOGENERATORS

ROTATING SHAFTS

NT SHAFTS (MACHINE ELEMENTS)

NT TURBOSHAFTS

Balancing of a power-transmission shaft with the
application of axial torque
[ASME PAPER 80-GT-143] p0121 A80-42256

Direct integration of transient rotor dynamics
[NASA-TP-1597] p0015 N80-15128

Development of procedures for calculating
stiffness and damping of elastomers in
engineering applications, part 6
[NASA-CR-159838] p0134 N 0-22733

Circumferential shaft seal
[NASA-CASE-LEW-12119-1] p0119 N80-28711

ROTATING STALLS

A phenomenological model of the dynamic stall of a
helicopter blade profile
[ONERA, TP NO. 1979-149] p0006 A80-20086

ROTATING VEHICLES

U ROTATING BODIES

ROTATIONAL FLOW

U FLUID FLOW

U VORTICES

ROTOR AERODYNAMICS

A phenomenological model of the dynamic stall of a
helicopter blade profile
[ONERA, TP NO. 1979-149] p0006 A80-20086

Numerical calculation of steady inviscid full
potential compressible flow about wind turbine
blades
[AIAA 80-0607] p0145 A80-28804

Comparison between optical measurements and a
numerical solution of the flow field within a
transonic axial-flow compressor rotor
[AIAA PAPER 80-1078] p0003 A80-38897

Aerodynamic analysis of a supersonic cascade
vibrating in a complex mode p0007 A80-45841

Aerodynamic performances of three fan stator
designs operating with rotor having tip speed of
337 meters per second and pressure ratio of
1.54: 1: Experimental performance
[NASA-TP-1610] p0015 N80-17071

Numerical calculation of steady inviscid full
potential compressible flow about wind turbine
blades
[NASA-TN-81438] p0136 N80-18497

Forward acoustic performance of a shock-swallowing
high-tip-speed fan (QF-13)
[NASA-TP-1668] p0169 N80-23100

Development of flexible rotor balancing criteria
[NASA-CR-159506] p0129 N80-32720

ROTOR BLADES

Teetered, tip-controlled rotor - Preliminary test
results from Mod-O 100-kW experimental wind
turbine
[AIAA 80-0642] p0145 A80-28836

ROTOR BLADES (TURBOMACHINERY)

The erosion/corrosion of small superalloy turbine
rotors operating in the effluent of a PFB coal
combustor p0080 A80-10043

Instrumentation technology p0013 N80-10214

Flutter spectral measurements using stationary
pressure transducers
[NASA-TN-79293] p0013 N80-13046

The response of turbine engine rotors to
interference rubs
[NASA-TN-81518] p0118 N80-27696

SUBJECT INDEX

SCALE MODELS

Feasibility study of aileron and spoiler control systems for large horizontal axis wind turbines [NASA-CR-159856] p0153 N80-27803
 Off-design correlation for losses due to part-span dampers on transonic rotors [NASA-TP-1693] p0020 N80-28352
 Effect of fluid forces on rotor stability of centrifugal compressors and pumps p0126 N80-29720
 Non-synchronous whirling due to fluid-dynamic forces in axial turbo-machinery rotors p0126 N80-29721
 Self-excited rotor whirl due to tip-seal leakage forces p0127 N80-29723
 Fluid forces on rotating centrifugal impeller with whirling motion p0127 N80-29724
 Physical explanations of the destabilizing effect of damping in rotating parts p0127 N80-29728
 Parametric instabilities of rotor-support systems with application to industrial ventilators p0127 N80-29729
 Instability thresholds for flexible rotors in hydrodynamic bearings p0128 N80-29730
 Stabilization of aerodynamically excited turbomachinery with hydrodynamic journal bearings and supports p0128 N80-29731
 Use of elastomeric elements in control of rotor instability p0128 N80-29732
 Feasibility of active feedback control of rotordynamic instability p0128 N80-29733

ROTOR DISKS
 U TURBINE WHEELS
ROTOR HUBS
 U ROTORS
ROTOR SPEED
 CP6 jet engine performance improvement: New fan [NASA-CR-159699] p0039 N80-23309

ROTORS
 NT COMPRESSOR ROTORS
 NT FLYWHEELS
 NT HELICOPTER TAIL ROTORS
 NT ROTARY WINGS
 NT TURBINE WHEELS
 Design of elastomer dampers for a high-speed flexible rotor [ASME PAPER 79-DET-88] p0121 A80-15736
 Dynamic properties of elastomer cartridge specimens under a rotating load p0121 A80-24002
 Direct integration of transient rotor dynamics [NASA-TP-1597] p0015 N80-15128
 Liquid metal slip ring --- aerospace environments [NASA-CASE-LEW-12277-3] p0101 N80-18300
 Teetered, tip-controlled rotor: Preliminary test results from Mod-0 100-kw experimental wind turbine [NASA-TN-81445] p0140 N80-19613
 The parameters and measurements of the destabilizing actions of rotating machines, and the assumptions of the 1950's p0125 N80-29712

ROUGHNESS
 NT SURFACE ROUGHNESS
RUBBER
 NT ELASTOMERS

S

S BAND
 U SUPERHIGH FREQUENCIES
 U ULTRAHIGH FREQUENCIES
S GLASS
 Mechanical property characterization of intraply hybrid composites [NASA-TN-79306] p0067 N80-12120

SAFETY FACTORS
 Photovoltaic power system reliability considerations p0146 A80-40338

SAILS
 NT SOLAR SAILS
SAMPLING
 NT AIR SAMPLING

SANDS
 High temperature thermal energy storage in steel and sand [NASA-CR-159708] p0154 N80-29860

SAPPHIRE
 Effect of interfacial species on shear strength of metal-sapphire contacts p0178 A80-22300

SARCOMA
 U CANCER
SATELLITE ANTENNAS
 UHF coplanar-slot antenna for aircraft-to-satellite data communications p0009 A80-13064
 Packet communications in satellites with multiple-beam antennas and signal processing [AIAA 80-0537] p0099 A80-29574
 Ka-band, multibeam, contiguous coverage satellite antenna for the USA [AIAA 80-0557] p0099 A80-29588

SATELLITE COMMUNICATIONS
 U SPACECRAFT COMMUNICATION
SATELLITE CONFIGURATIONS
 Configuration effects on satellite charging response [NASA-TN-81397] p0053 N80-15200

SATELLITE DESIGN
 An advanced mixed user domestic satellite system architecture [AIAA 80-0494] p0099 A80-29544
 A three-dimensional spacecraft-charging computer code p0055 A80-46891

SATELLITE NETWORKS
 UHF coplanar-slot antenna for aircraft-to-satellite data communications p0009 A80-13064
 NASA's program in communication satellites [AAS 79-247] p0097 A80-28712
 Packet communications in satellites with multiple-beam antennas and signal processing [AIAA 80-0537] p0099 A80-29574
 Concepts for 20/30 GHz satcom systems for direct-to-user applications [AIAA 80-0582] p0050 A80-35329

SATELLITE ORBITS
 NT GEOSYNCHRONOUS ORBITS
 Plasma collection by high voltage spacecraft at low earth orbit [AIAA PAPER 80-0042] p0055 A80-18249

SATELLITE TRANSMISSION
 The 30/20 GHz mixed user architecture development study [NASA-CR-159686] p0097 N80-10415
 The 30/20 GHz mixed user architecture development study: Executive summary [NASA-CR-159687] p0097 N80-10416
 Low sidelobe level low-cost earth station antennas for the 12 GHz broadcasting satellite service [NASA-CR-159703] p0098 N80-12259
 A digitally implemented communications experiment utilizing the communications technology satellite, Hermes [NASA-TN-81452] p0052 N80-21412
 On-board processing concepts for future satellite communications systems [NASA-CR-159683] p0099 N80-24514
 Study of advanced communications satellite systems based on SS-FDMA [NASA-CR-159778] p0050 N80-25357

SATELLITES
 NT ATS 5
 NT ATS 6
 NT COMMUNICATION SATELLITES
 NT COMMUNICATIONS TECHNOLOGY SATELLITE
 NT ORBITAL SPACE STATIONS
 NT SCATHA SATELLITE
 NT SYNCHRONOUS SATELLITES

SCALE (CORROSION)
 Some TEM observations of Al2O3 scales formed on NiCrAl alloys p0081 A80-13071

SCALE MODELS
 Scale model performance test investigation of exhaust system mixers for an Energy Efficient Engine /E3/ propulsion system [AIAA PAPER 80-0229] p0024 A80-20968
 Acoustic measurements of three Prop-Fan models [AIAA PAPER 80-0995] p0045 A80-35958

SCAR PROGRAM

SUBJECT INDEX

Low speed test of the aft inlet designed for a tandem fan V/STOL nacelle
[NASA-CR-159752] p0037 N80-18042

SCAR PROGRAM
U SUPERSONIC CRUISE AIRCRAFT RESEARCH
SCARS (GEOLOGY)
U EROSION
SCAT
U SUPERSONIC COMMERCIAL AIR TRANSPORT
SCATHA SATELLITE
A three-dimensional spacecraft-charging computer code
p0055 A80-46891

SCHEDULING
NT PREDICTION ANALYSIS TECHNIQUES
SCIENTIFIC SATELLITES
NT ATS 5
NT ATS 6
SCRAMJET ENGINES
U SUPERSONIC COMBUSTION RAMJET ENGINES
SCRAMJETS
U SUPERSONIC COMBUSTION RAMJET ENGINES
SDP (COMPUTERS)
U SITE DATA PROCESSORS
SEA ICE
NT ICEBERGS
SEALING
Plasma-sprayed dual density ceramic turbine seal system
[NASA-CR-159739] p0123 N80-15411
SEALS (STOPPERS)
NT GLANDS (SEALS)
NT O RING SEALS
NT PUMP SEALS
Some flow characteristics of conventional and tapered high-pressure-drop simulated seals
[ASLE PREPRINT 79-1C-3B-2] p0120 A80-14727
Phase change in liquid face seals. II - Isothermal and adiabatic bounds with real fluids
[ASME PAPER 79-LUB-4] p0129 A80-14739
Wear of seal materials used in aircraft propulsion systems
p0121 A80-28010
Modified face seal for positive film stiffness
[NASA-CASE-LEW-12989-1] p0114 N80-12414
Feasibility of SiC composite structures for 1644 deg gas turbine seal applications
[NASA-CR-159597] p0123 N80-13474
Abradable compressor and turbine seals, volume 1 --- for turbofan engines
[NASA-CR-159600] p0083 N80-14235
Self-acting lift-pad geometry for circumferential seals: A noncontacting concept --- performance tests on hydrodynamic seals
[NASA-TP-1583] p0114 N80-14403
Some considerations of the performance of two honeycomb gas path seal material systems
[NASA-TM-81398] p0077 N80-16143
Program to develop sprayed, plastically deformable compressor shroud seal materials
[NASA-CR-159741] p0123 N80-16338
Gas path seal
[NASA-CASE-NPO-12131-3] p0115 N80-18400
Development of improved high pressure turbine outer gas path seal components --- abradability and thermal cycling test results
[NASA-CR-159801] p0038 N80-21332
Advanced ceramic material for high temperature turbine tip seals
[NASA-CR-159774] p0038 N80-22325
Testing of reciprocating seals for application in a Stirling cycle engine
[NASA-CR-159820] p0124 N80-22700
Dynamic response to rotating-seat runoff in non-contacting face seals
[NASA-TM-81490] p0117 N80-22701
Fully plasma-sprayed compliant backed ceramic turbine seal
[NASA-CASE-LEW-13268-1] p0117 N80-24619
Composite seal for turbomachinery
[NASA-CASE-LEW-12131-2] p0118 N80-26658
Dynamic analysis of noncontacting face seals
[NASA-TM-79294] p0118 N80-27695
Circumferential shaft seal
[NASA-CASE-LEW-12119-1] p0119 N80-28711
Testing of turbulent seals for rotodynamic coefficients
p0126 N80-29714

Evaluation of instability forces of labyrinth seals in turbines or compressors
p0126 N80-29715
Flow induced spring coefficients of labyrinth seals for application in rotor dynamics
p0126 N80-29717
Simulation and visualization of face seal motion stability by means of computer generated movies
[NASA-TM-81581] p0120 N80-31797
SECONDARY BATTERIES
U STORAGE BATTERIES
SECONDARY EMISSION
Effects of secondary yield parameter variation on predicted equilibrium potential of an object in a charging environment --- for spacecraft
p0054 A80-44238
SECONDARY FLOW
Influence of pressure driven secondary flows on the behavior of turbofan forced mixers
[AIAA PAPER 80-1198] p0025 A80-41515
Streakline flow visualization study of a horseshoe vortex in a large-scale, two-dimensional turbine stator cascade
[NASA-TM-79274] p0104 N80-11376
Influence of pressure driven secondary flows on the behavior of turbofan forced mixers
[NASA-TM-81541] p0105 N80-27632
SEDIMENTARY ROCKS
NT COAL
SEDIMENTS
NT SANDS
Quantitative interpretation of Great Lakes remote sensing data
p0157 A80-45005
SELF ALIGNMENT
Homogeneous alignment of nematic liquid crystals by ion beam etched surfaces
p0178 A80-26007
SELF DEPLOYING SPACE STATIONS
U SPACE STATIONS
SELF INDUCED VIBRATION
NT SUPERSONIC FLUTTER
SELF LUBRICATING MATERIALS
Method of making bearing material
[NASA-CASE-LEW-11930-3] p0070 N80-33482
SELF REGULATING
U AUTOMATIC CONTROL
SEMICONDUCTOR DEVICES
NT PHOTOVOLTAIC CELLS
SEMICONDUCTOR JUNCTIONS
NT SILICON JUNCTIONS
Planar multijunction high voltage solar cells
[NASA-TM-81389] p0178 N80-16914
SENSE ORGANS
NT EYE (ANATOMY)
SENSITIVITY
NT RADIATION TOLERANCE
NT SPECTRAL SENSITIVITY
SEPARATED FLOW
NT BOUNDARY LAYER SEPARATION
An analytical and experimental study of a short s-shaped subsonic diffuser of a supersonic inlet
[NASA-TM-81406] p0015 N80-15134
SEPARATORS
Flexible formulated plastic separators for alkaline batteries
[NASA-CASE-LEW-12363-4] p0140 N80-18555
Status of nickel-hydrogen cell technology
p0064 N80-33474
SERIES (MATHEMATICS)
NT POWER SERIES
SERT (ROCKET TESTS)
U SPACE ELECTRIC ROCKET TESTS
SERT 2 SPACECRAFT
SERT II 1979 extended flight thruster system performance
[AIAA PAPER 79-2063] p0059 A80-10386
Neutralization tests on the SERT II spacecraft --- of ion beams
[AIAA PAPER 79-2064] p0059 A80-10387
Plasma physics analysis of SERT-2 operation
[NASA-CR-159814] p0177 N80-27189
SERVICE LIFE
HG ion thruster component testing
[AIAA PAPER 79-2116] p0059 A80-20959
A model for predicting the wearout lifetime of the LeRC/Hughes 30-cm mercury ion thruster
[AIAA PAPER 79-2079] p0064 A80-20962

- Life test studies on tungsten impregnated cathodes
p0103 A80-45122
- Cycles till failure of silver-zinc cells with
competing failure modes - Preliminary data
analysis
p0146 A80-46414
- Effect of positive pulse charge waveforms on cycle
life of nickel-zinc cells
p0146 A80-48329
- Design, performance and life cycle cost
relationships for a 500kW space solar array
p0065 A80-48356
- JT9D-7A (SP) jet engine performance deterioration
trends
[NASA-TN-81459] p0016 N80-20274
- Performance deterioration based on existing
(historical) data; JT9D jet engine diagnostics
program
[NASA-CR-135448] p0038 N80-22324
- Performance deterioration based on in-service
engine data; JT9D jet engine diagnostics program
[NASA-CR-159525] p0040 N80-25340
- SERVO MECHANISMS**
- Single-stage electrohydraulic servosystem for
actuating an airflow valve with frequencies to
500 hertz
[NASA-TP-1678] p0046 N80-29369
- SHAFTS (MACHINE ELEMENTS)**
- NT TURBO SHAFTS**
- Some flow characteristics of conventional and
tapered high-pressure-drop simulated seals
[ASLE PREPRINT 79-LC-3D-2] p0120 A80-14727
- Load support system analysis high speed input
pinion configuration
[ASME PAPER 79-LUB-34] p0129 A80-14760
- Elastomer damper performance - A comparison with a
squeeze film for a supercritical power
transmission shaft
[ASME PAPER 80-GT-162] p0121 A80-42272
- Circumferential shaft seal
[NASA-CASE-LEW-12119-2] p0115 N80-18401
- Operating characteristics of high-speed,
jet-lubricated 35-millimeter-bore ball bearing
with a single-outer-land-guided cage
[NASA-TP-1657] p0117 N80-21753
- Limit cycles of a flexible shaft with hydrodynamic
journal bearings in unstable regimes
p0127 N80-29725
- On the role of oil-film bearings in promoting
shaft instability: Some experimental observations
p0127 N80-29726
- Stabilization of aerodynamically excited
turbomachinery with hydrodynamic journal
bearings and supports
p0128 N80-29731
- Effect of cage design on characteristics of
high-speed-jet-lubricated 35-millimeter-bore
ball bearing --- turbojet engines
[NASA-TP-1732] p0120 N80-33749
- SHALE OIL**
- Alternative jet aircraft fuels
p0012 N80-10209
- Use of petroleum-based correlations and estimation
methods for synthetic fuels
[NASA-TN-81533] p0093 N80-27509
- Military jet fuel from shale oil
p0042 N80-29308
- SHEAR FLOW**
- A time dependent difference theory for sound
propagation in ducts with flow
p0170 A80-20951
- SHEAR PROPERTIES**
- NT SHEAR STRENGTH**
- SHEAR STRENGTH**
- Effect of interfacial species on shear strength of
metal-sapphire contacts
p0178 A80-22300
- SHEATHS**
- NT PLASMA SHEATHS**
- SHIELDING**
- NT RADIATION SHIELDING**
- SHOCK DIFFUSERS**
- U DIFFUSERS**
- U SHOCK WAVE ATTENUATION**
- SHOCK RESISTANCE**
- Preliminary study of methods for providing thermal
shock resistance to plasma-sprayed ceramic
gas-path seals
[NASA-TP-1561] p0087 N80-23453
- SHOCK WAVE ATTENUATION**
- Forward acoustic performance of a shock-swallowing
high-tip-speed fan (QF-13)
[NASA-TP-1668] p0169 N80-23100
- SHOCK WAVE CONTROL**
- Turbojet-exhaust-nozzle secondary-airflow pumping
as an exit control of an inlet-stability bypass
system for a Mach 2.5 axisymmetric
mixed-compression inlet --- Lewis 10- by 10-ft.
supersonic wind tunnel test
[NASA-TP-1532] p0014 N80-14124
- SHORT HAUL AIRCRAFT**
- QCSEE UTM engine powered-lift acoustic performance
--- Quiet Clean Short-haul Experimental Engine
Under The Wing
[AIAA PAPER 80-1065] p0025 A80-38651
- Quiet Clean Short-Haul Experimental Engine (QCSEE)
acoustic and aerodynamic tests on a scale model
over-the-wing thrust reverser and forward thrust
nozzle
[NASA-CR-135254] p0028 N80-14115
- Quiet Clean Short-Haul Experimental Engine
(QCSEE). Under-the-wing (UTW) engine
boilerplate nacelle test report. Volume 2:
Aerodynamics and performance
[NASA-CR-135250] p0028 N80-14116
- Quiet, Clean, Short-Haul, Experimental Engine
(QCSEE) Under-The-Wing (UTW) engine acoustic
design
[NASA-CR-135267] p0028 N80-14117
- Quiet, Clean, Short-Haul Experimental Engine
(QCSEE) Over-The-Wing (OTW) engine acoustic design
[NASA-CR-135268] p0028 N80-14118
- Quiet Clean Short-Haul Experimental Engine (QCSEE)
Under-The-Wing (UTW) graphite/PBR cowl development
[NASA-CR-135279] p0029 N80-14119
- Static test-stand performance of the YF-102
turbofan engine with several exhaust
configurations for the Quiet Short-Haul Research
Aircraft (QSRA)
[NASA-TP-1556] p0014 N80-14121
- Demonstration of short-haul aircraft aft noise
reduction techniques on a twenty inch (50.8 cm)
diameter fan, volume 1
[NASA-CR-134849] p0033 N80-15083
- Demonstration of short-haul aircraft aft noise
reduction techniques on a twenty inch (50.8 cm)
diameter fan, volume 2
[NASA-CR-134850] p0034 N80-15084
- Demonstration of short haul aircraft aft noise
reduction techniques on a twenty inch (50.8 cm)
diameter fan, volume 3
[NASA-CR-134851] p0034 N80-15085
- Quiet Clean Short-haul Experimental Engine (QCSEE)
Over The Wing (OTW) design report
[NASA-CR-134848] p0034 N80-15086
- Quiet Clean Short-haul Experimental Engine (QCSEE)
preliminary under the wing flight propulsion
system analysis report
[NASA-CR-134868] p0034 N80-15088
- Quiet Clean Short-haul Experimental Engine
(QCSEE). The aerodynamic and mechanical design
of the QCSEE over-the-wing fan
[NASA-CR-134915] p0034 N80-15089
- Quiet Clean Short-haul Experimental Engine (QCSEE)
under-the-wing engine digital control system
design report
[NASA-CR-134920] p0034 N80-15090
- Quiet Clean Short-haul Experimental Engine (QCSEE)
over-the-wing control system design report
[NASA-CR-135337] p0035 N80-15092
- Quiet Clean Short-haul Experimental Engine
(QCSEE). Core engine noise measurements
[NASA-CR-135160] p0035 N80-15093
- Quiet Clean Short-haul Experimental Engine (QCSEE)
Under-The-Wing (UTW) engine composite nacelle
test report. Volume 1: Summary, aerodynamic
and mechanical performance
[NASA-CR-159471] p0035 N80-15094
- Quiet Clean Short-haul Experimental Engine (QCSEE)
preliminary over-the-wing flight propulsion
system analysis report
[NASA-CR-135296] p0035 N80-15095
- Quiet Clean Short-haul Experimental Engine
(QCSEE). Under-The-Wing (UTW) engine boilerplate
nacelle test report, volume 1
[NASA-CR-135249] p0035 N80-15096
- Quiet Clean Short-haul Experimental Engine
(QCSEE). Under-The-Wing (UTW) engine boilerplate

- nacelle test report. Volume 3: Mechanical performance
 [NASA-CR-135251] p0035 N80-15097
 Quiet Clean Short-haul Experimental Engine (QCSEE)
 Under-The-Wing (UTW) composite nacelle subsystem
 test report --- to verify strength of selected
 composite materials [NASA-CR-135075] p0034 N80-15100
 Quiet Clean Short-haul Experimental Engine (QCSEE)
 Under-The-Wing (UTW) composite nacelle subsystem
 test report --- to verify strength of selected
 composite materials [NASA-CR-135075] p0034 N80-15100
 Quiet Clean Short-haul Experimental Engine
 (QCSEE). Ball spline pitch change mechanism
 design report [NASA-CR-134673] p0030 N80-15101
 Quiet Clean Short-haul Experimental Engine
 (QCSEE). Ball spline pitch change mechanism
 design report [NASA-CR-134673] p0030 N80-15101
 Acoustic analysis of aft noise reduction
 techniques measured on a subsonic tip speed 50.8
 cm (twenty inch) diameter fan --- quiet engine
 program [NASA-CR-134891] p0030 N80-15102
 Quiet Clean Short-haul Experimental Engine (QCSEE)
 main reduction gears test program [NASA-CR-134669] p0030 N80-15103
 Quiet Clean Short-haul Experimental Engine (QCSEE)
 clean combustor test report [NASA-CR-134916] p0030 N80-15104
 Quiet Clean Short-haul Experimental Engine (QCSEE)
 main reduction gears bearing development program
 [NASA-CR-134890] p0030 N80-15105
 Quiet Clean Short-haul Experimental Engine
 (QCSEE): Hamilton Standard cam/harmonic drive
 variable pitch fan actuation system detail
 design report [NASA-CR-134852] p0030 N80-15107
 Quiet Clean Short-haul Experimental Engine (QCSEE)
 under-the-wing engine composite fan blade design
 report [NASA-CR-135046] p0031 N80-15108
 Quiet Clean Short-haul Experimental Engine
 (QCSEE): The aerodynamic and mechanical design
 of the QCSEE under-the-wing fan [NASA-CR-135009] p0031 N80-15109
 Quiet Clean Short-haul Experimental Engine (QCSEE)
 composite fan frame design report [NASA-CR-135278] p0031 N80-15110
 Quiet Clean Short-haul Experimental Engine (QCSEE)
 UTW fan preliminary design [NASA-CR-134842] p0031 N80-15111
 Quiet Clean Short-haul Experimental Engine
 (QCSEE): The aerodynamic and preliminary
 mechanical design of the QCSEE OTW fan [NASA-CR-134841] p0031 N80-15112
 Quiet Clean Short-haul Experimental Engine (QCSEE)
 under-the-wing engine composite fan blade design
 [NASA-CR-134840] p0031 N80-15113
 Quiet Clean Short-haul Experimental Engine (QCSEE)
 over-the-wing engine and control simulation
 results [NASA-CR-135049] p0031 N80-15114
 Quiet Clean Short-Haul Experimental Engine (QCSEE)
 ball spline pitch-change mechanism whirligig
 test report [NASA-CR-135354] p0032 N80-15115
 Quiet Clean Short-haul Experimental Engine (QCSEE)
 Under-The-Wing (UTW) boiler plate nacelle and
 core exhaust nozzle design report [NASA-CR-135008] p0032 N80-15116
 Quiet Clean Short-haul Experimental Engine (QCSEE)
 whirl test of cam/harmonic pitch change
 actuation system [NASA-CR-135140] p0032 N80-15117
 Quiet Clean Short-haul Experimental Engine (QCSEE)
 Over-The-Wing (OTW) propulsion systems test
 report. Volume 4: Acoustic performance
 [NASA-CR-135326] p0032 N80-15118
 Quiet Clean Short-haul Experimental Engine (QCSEE)
 Under-The-Wing (UTW) composite nacelle
 [NASA-CR-135352] p0032 N80-15119
 Quiet Clean Short-haul Experimental Engine (QCSEE)
 [NASA-CR-159473] p0032 N80-15120
 Quiet Clean Short-haul Experimental Engine
 (QCSEE). Double-annular clean combustor
 technology development report
- [NASA-CR-159483] p0032 N80-15121
 Quiet Clean Short-Haul Experimental Engine
 (QCSEE): Acoustic treatment development and
 design [NASA-CR-135266] p0033 N80-15122
 Quiet Clean Short-Haul Experimental Engine
 (QCSEE). Preliminary analyses and design
 report, volume 1 [NASA-CR-134838] p0033 N80-15123
 Quiet Clean Short-Haul Experimental Engine
 (QCSEE). Preliminary analyses and design
 report, volume 2 [NASA-CR-134839] p0033 N80-15124
 QCSEE UTW engine powered-lift acoustic performance
 [NASA-TN-81504] p0019 N80-24315
 Static and transient performance of YF-102 engine
 with up to 14 percent core airbleed for the
 quiet short-haul research aircraft [NASA-TN-1692] p0020 N80-25339
 Quiet Clean Short-haul Experimental Engine (QCSEE)
 under-the-wing engine composite fan blade:
 Preliminary design test report [NASA-CR-134846] p0044 N80-29298
 Reverse thrust performance of the QCSEE variable
 pitch turbofan engine [NASA-TN-81558] p0022 N80-31399
- SHORT TAKEOFF AIRCRAFT**
NT C-15 AIRCRAFT
 Assessment at full scale of exhaust nozzle-to-wing
 size on STOL-OTW acoustic characteristics p0170 A80-20952
 Flight test of navigation and guidance sensor
 errors measured on STOL approaches [NASA-TN-81154] p0028 N80-13041
 Assessment at full scale of exhaust nozzle to wing
 size on STOL-OTW acoustic characteristics [NASA-TN-79279] p0167 N80-13881
- SHORT WAVE RADIATION**
NT MILLIMETER WAVES
SHROUDED TURBINES
 Abradable compressor and turbine seals, volume 1
 --- for turbofan engines [NASA-CR-159600] p0083 N80-14235
 Gas path seal [NASA-CASE-NPO-12131-3] p0115 N80-18400
 Composite seal for turbomachinery [NASA-CASE-LEW-12131-2] p0118 N80-26658
 Composite wall concept for high temperature
 turbine shrouds: Heat transfer analysis [NASA-TN-81539] p0020 N80-27362
 The response of turbine engine rotors to
 interference rubs [NASA-TN-81518] p0118 N80-27696
- SHUNTS**
U BYPASSES
SIDELobe REDUCTION
 Low sidelobe level low-cost earth station antennas
 for the 12 GHz broadcasting satellite service
 [NASA-CR-159703] p0098 N80-12259
- SIGNAL ANALYSIS**
 Simulation of transducer-couplant effects on
 broadband ultrasonic signals --- in
 nondestructive flaw evaluation and materials tests
 p0112 A80-44233
- SIGNAL PROCESSING**
 Packet communications in satellites with
 multiple-beam antennas and signal processing
 [AIAA 80-0537] p0099 A80-29574
 Multigigabit satellite on-board signal processing
 [AIAA 80-0583] p0100 A80-29605
 Application of coherence in fan noise studies
 [NASA-TP-1630] p0167 N80-18682
 On-board processing concepts for future satellite
 communications systems [NASA-CR-159683] p0099 N80-24514
- SIGNAL TRANSMISSION**
NT DATA TRANSMISSION
NT FREQUENCY DIVISION MULTIPLE ACCESS
NT MICROWAVE TRANSMISSION
NT SATELLITE TRANSMISSION
NT TELEMETRY
SIGNATURES
NT SPECTRAL SIGNATURES
SILICATES
NT CALCIUM SILICATES
SILICON
 Characterization of solar cells for space
 applications. Volume 10: Electrical
 characteristics of Spectrolab BSF, textured, 10

- ohm-cm, 300 micron cells as a function of intensity, temperature and irradiation
[NASA-CR-162422] p0147 N80-11566
- Analysis of GaAs and Si solar cell arrays for earth orbital and orbit transfer missions
[NASA-TM-81383] p0056 N80-15204
- Study program to improve the open-circuit voltage of low resistivity single crystal silicon solar cells
[NASA-CR-159833] p0150 N80-22775
- A silicon-slurry/aluminide coating --- protects aircraft and land-based gas turbine engines
[NASA-CASE-LEN-13343-1] p0069 N80-26389
- Screen printing technology applied to silicon solar cell fabrication
[NASA-CR-159789] p0153 N80-27808
- Radiation damage in high voltage silicon solar cells
p0144 N80-33889
- SILICON CARBIDES**
- Fatigue behavior of SiC reinforced titanium composites
p0070 A80-10036
- Characterization and properties of controlled nucleation thermochemical deposited /CMTD/ silicon carbide
p0089 A80-13063
- The friction and wear of metals and binary alloys in contact with an abrasive grit of single-crystal silicon carbide
[ASLE PREPRINT 79-LC-5C-1] p0120 A80-14734
- 3500-hour durability testing of ceramic materials for automotive gas turbine engines
[AIRESEARCH-31-3542] p0092 A80-35575
- Dynamic modulus and damping of boron, silicon carbide, and alumina fibers
p0071 A80-44236
- Characterization and properties of controlled nucleation thermochemical deposited (CMTD) silicon carbide
[NASA-TM-79277] p0085 N80-13254
- Feasibility of SiC composite structures for 1644 deg gas turbine seal applications
[NASA-CR-159597] p0123 N80-13474
- Adhesion and friction of iron-base binary alloys in contact with silicon carbide in vacuum
[NASA-TP-1604] p0076 N80-15234
- Tribological properties of silicon carbide in metal removal process
[NASA-TM-79238] p0114 N80-16340
- Wear particles of single-crystal silicon carbide in vacuum
[NASA-TP-1624] p0085 N80-18178
- Dynamic modulus and damping of boron, silicon carbide, and alumina fibers
[NASA-TM-81422] p0068 N80-20313
- Adhesion, friction, and wear of binary alloys in contact with single-crystal silicon carbide
[NASA-TM-79282] p0086 N80-21534
- Friction and wear of iron-base binary alloys in sliding contact with silicon carbide in vacuum
[NASA-TP-1612] p0087 N80-22494
- The 3500 hour durability testing of commercial ceramic materials
[NASA-CR-159785] p0091 N80-31552
- SILICON COMPOUNDS**
- NT CALCIUM SILICATES
- NT SILICON CARBIDES
- NT SILICON NITRIDES
- An experimental, low-cost, silicon-aluminide high-temperature coating for superalloys
[NASA-TM-81455] p0078 N80-20370
- State-of-the-art SiALON materials
p0022 N80-29358
- SILICON JUNCTIONS**
- Radiation damage in high voltage silicon solar cells
p0179 A80-44234
- SILICON NITRIDES**
- State-of-the-art of SiALON materials
p0009 A80-13066
- Reaction bonded silicon nitride prepared from wet attrition-milled silicon
p0089 A80-32828
- 3500-hour durability testing of ceramic materials for automotive gas turbine engines
[AIRESEARCH-31-3542] p0092 A80-35575
- Effect of W and WC on the oxidation resistance of yttria-doped silicon nitride
p0090 A80-46099
- Effect of starting powder characteristics on density, microstructure and low temperature oxidation behavior of a Si3N4 - 8 w/o Y2O3 ceramic
p0090 A80-46100
- Performance of Chevron-notch short bar specimen in determining the fracture toughness of silicon nitride and aluminum oxide
p0090 A80-50696
- Formation of porous surface layers in reaction bonded silicon nitride during processing
p0090 A80-51574
- Improving the stress rupture and creep of silicon nitride --- turbine materials
[NASA-CR-159585] p0072 N80-10318
- Development of silicon nitride of improved toughness
[NASA-CR-159676] p0072 N80-10319
- Sintered silicon nitride recuperator fabrication
[NASA-CR-159706] p0090 N80-15263
- Reaction bonded silicon nitride prepared from wet attrition-milled silicon --- fractography
[NASA-TM-81428] p0086 N80-18181
- Effects of oxide additions and temperature on sinterability of milled silicon nitride
[NASA-TP-1644] p0086 N80-21532
- Formation of porous surface layers in reaction bonded silicon nitride during processing
[NASA-TM-81493] p0087 N80-23456
- Feasibility study of silicon nitride regenerators
[NASA-CR-159713] p0184 N80-25209
- Effect of W and WC on the oxidation resistance of yttria-doped silicon nitride
[NASA-TM-81529] p0087 N80-27483
- Effect of starting powder characteristics on density, microstructure and low temperature oxidation behavior of a Si3N4-8w/o Y2O3 ceramic
[NASA-TM-81536] p0088 N80-27484
- The 3500 hour durability testing of commercial ceramic materials
[NASA-CR-159785] p0091 N80-31552
- SILICON POLYMERS**
- NT SILICONE RESINS
- NT SILICONES
- SILICON SOLAR CELLS**
- U SOLAR CELLS
- SILICONE RESINS**
- Silicone modified resins for graphite fiber laminates
[NASA-CR-159750] p0072 N80-22407
- SILICONES**
- Evaluation of cleaners for photovoltaic modules exposed in an outdoor environment
[NASA-TM-79248] p0096 N80-13317
- SILTS**
- U SEDIMENTS
- SILVER OXIDE ZINC BATTERIES**
- U SILVER ZINC BATTERIES
- SILVER ZINC BATTERIES**
- Cycles till failure of silver-zinc cells with competing failure modes - Preliminary data analysis
p0146 A80-46414
- Cycles till failure of silver-zinc cells with completing failures modes: Preliminary data analysis
[NASA-TM-81556] p0164 N80-29088
- SIMILARITIES**
- U ANALOGIES
- SIMILARITY THEOREM**
- Application of the principle of similarity fluid mechanics
p0107 A80-10039
- Extension of similarity test procedures to cooled engine components with insulating ceramic coatings
[NASA-TP-1615] p0105 N80-24577
- Toward the use of similarity theory in two-phase choked flows
[NASA-TM-81568] p0106 N80-29623
- SIMULATION**
- NT ACOUSTIC SIMULATION
- NT ANALOG SIMULATION
- NT COMPUTERIZED SIMULATION
- NT CONTROL SIMULATION
- NT DIGITAL SIMULATION
- NT EXHAUST FLOW SIMULATION
- NT FLIGHT SIMULATION
- NT SPACE ENVIRONMENT SIMULATION
- SIMULATORS**
- NT CONTROL SIMULATION

SINGLE CRYSTALS

SUBJECT INDEX

Preliminary results from a four-working space, double-acting piston, Stirling engine controls model
[NASA-TM-81569] p0106 N80-29624

A laboratory facility for electric vehicle propulsion system testing
[NASA-TM-81574] p0183 N80-30229

SINGLE CRYSTALS

The friction and wear of metals and binary alloys in contact with an abrasive grit of single-crystal silicon carbide
[ASLE PREPRINT 79-IC-5C-1] p0120 A80-14734

Development of exothermically cast single-crystal Mar-M 247 and derivative alloys
[AIRESEARCH-21-3469] p0084 A80-45825

Anisotropy of nickel-base superalloy single crystals
p0083 A80-51573

Anisotropy of nickel-base superalloy single crystals
[NASA-TM-81437] p0077 N80-17200

Study program to improve the open-circuit voltage of low resistivity single crystal silicon solar cells
[NASA-CR-159833] p0150 N80-22775

SINTERING

Effect of starting powder characteristics on density, microstructure and low temperature oxidation behavior of a Si₃N₄ - 8 w/o Y₂O₃ ceramic
p0090 A80-46100

Effects of oxide additions and temperature on sinterability of milled silicon nitride
[NASA-TP-1644] p0086 N80-21532

Formation of porous surface layers in reaction bonded silicon nitride during processing
[NASA-TM-81493] p0087 N80-23456

SITE DATA PROCESSORS

Modified power law equations for vertical wind profiles --- in investigation of windpower plant siting
p0159 A80-35719

SKENNESS

Kinematic correction for roller skewing
[NASA-TM-81564] p0119 N80-28716

SKIN FRICTION

NT AERODYNAMIC DRAG

SLIDING FRICTION

The friction and wear of metals and binary alloys in contact with an abrasive grit of single-crystal silicon carbide
[ASLE PREPRINT 79-IC-5C-1] p0120 A80-14734

Rolling-element bearings --- contact sliding friction study of solid bodies
p0121 A80-31961

Sliding friction of some metallic glasses
p0090 A80-46153

Adhesion, friction, and wear of binary alloys in contact with single-crystal silicon carbide
[NASA-TM-79282] p0086 N80-21534

Friction and wear of iron-base binary alloys in sliding contact with silicon carbide in vacuum
[NASA-TP-1612] p0087 N80-22494

SLOT ANTENNAS

UHF coplanar-slot antenna for aircraft-to-satellite data communications
p0009 A80-13064

SLOTTED ANTENNAS

U SLOT ANTENNAS

SNAILING

U LATERAL OSCILLATION

SODIUM

Analysis of the response of a thermal barrier coating to sodium and vanadium doped combustion gases
[NASA-TM-79205] p0076 N80-10344

SODIUM CHLORIDES

The chemistry of sodium chloride involvement in processes related to hot corrosion
p0074 A80-10041

SODIUM COMPOUNDS

NT SODIUM CHLORIDES

NT SODIUM HYDROXIDES

NT SODIUM SULFATES

SODIUM HYDROXIDES

Engineering evaluation of a sodium hydroxide thermal energy storage module
[NASA-TM-81417] p0140 N80-18563

SODIUM SULFATES

Experimental studies of the formation/deposition of sodium sulfate in/from combustion gases --- hot corrosion of gas turbine engine components

[NASA-CR-159753] p0033 N80-15131

SOFTWARE (COMPUTERS)

U COMPUTER PROGRAMS

U COMPUTER SYSTEMS PROGRAMS

SOILS

NT SANDS

SOLAR ARRAYS

Description of photovoltaic village power systems in the United States and Africa
p0146 A80-46796

Design, performance and life cycle cost relationships for a 500kW space solar array
p0065 A80-48356

Interaction of high voltage surfaces with the space plasma --- solar arrays
[NASA-CR-159731] p0176 N80-14923

Analysis of GaAs and Si solar cell arrays for earth orbital and orbit transfer missions
[NASA-TM-81383] p0056 N80-15204

Economic analysis of the design and fabrication of a space qualified power system
[NASA-TM-81418] p0056 N80-18098

Experimental results on plasma interactions with large surfaces at high voltages
[NASA-TM-81423] p0175 N80-18946

Solar array subsystems study
[NASA-CR-159857] p0151 N80-24742

Interaction of high voltage surfaces with the space plasma
[NASA-CR-165131] p0177 N80-32223

SOLAR CELLS

Origin of reverse annealing in radiation-damaged silicon solar cells
p0059 A80-33850

Radiation damage in high voltage silicon solar cells
p0179 A80-44234

The planar multijunction cell - A new solar cell for earth and space
p0146 A80-48205

Characterization of solar cells for space applications. Volume 10: Electrical characteristics of Spectrolab BSF, textured, 10 ohm-cm, 300 micron cells as a function of intensity, temperature and irradiation
[NASA-CR-162422] p0147 N80-11566

Self-reconfiguring solar cell system
[NASA-CASE-LEW-12586-1] p0137 N80-14472

Analysis of GaAs and Si solar cell arrays for earth orbital and orbit transfer missions
[NASA-TM-81383] p0056 N80-15204

Space solar cells: High efficiency and radiation damage
[NASA-TM-81387] p0138 N80-15554

Open-circuit voltage improvements in low resistivity solar cells
[NASA-TM-81388] p0138 N80-15555

Back surface reflectors for solar cells
[NASA-TM-81390] p0138 N80-15556

Radiation damage in lithium-counterdoped n/p silicon solar cells
[NASA-TM-81391] p0138 N80-15557

Radiation damage annealing mechanisms and possible low temperature annealing in silicon solar cells
[NASA-TM-81392] p0138 N80-15558

Global calibration of terrestrial reference cells and errors involved in using different irradiance monitoring techniques
[NASA-TM-81393] p0138 N80-15561

Planar multijunction high voltage solar cells
[NASA-TM-81389] p0178 N80-16914

Development of improved wraparound contacts for silicon
[NASA-CR-159748] p0148 N80-18554

Study program to improve the open-circuit voltage of low resistivity single crystal silicon solar cells
[NASA-CR-159833] p0150 N80-22775

Radiation damage in high voltage silicon solar cells
[NASA-TM-81478] p0178 N80-23180

Screen printing technology applied to silicon solar cell fabrication
[NASA-CR-159789] p0153 N80-27808

Coplanar back contacts for thin silicon solar cells
[NASA-CR-159811] p0153 N80-28860

Thin n-i-p radiation-resistant solar cell feasibility study
[NASA-CR-159871] p0154 N80-29852

Photovoltaic technology development for synchronous orbit

SUBJECT INDEX

SOUND

- Radiation damage in high voltage silicon solar cells
p0058 N80-33470
p0144 N80-33889
- SOLAR COLLECTORS**
NT SOLAR REFLECTORS
Preliminary study of a solar selective coating system using black cobalt oxide for high temperature solar collectors
p0082 A80-35500
- Spectral effects on direct-insolation absorptance of five collector coatings
[ASME PAPER 79-HT-18]
p0146 A80-45722
- Preliminary study of a solar selective coating system using black cobalt oxide for high temperature solar collectors
[NASA-TM-81385]
p0077 N80-18156
- Annual technical report, fiscal year 1979. Volume 1: Executive summary
[NASA-CR-159715-VOL-1]
p0149 N80-19632
- SOLAR CONVERTERS**
U SOLAR GENERATORS
SOLAR ELECTRIC PROPULSION
SERT II 1979 extended flight thruster system performance
[AIAA PAPER 79-2063]
p0059 A80-10386
- Computed voltage distribution around Solar Electric Propulsion spacecraft
[AIAA PAPER 79-2104]
p0054 A80-29750
- Computed voltage distributions around solar electric propulsion spacecraft
[NASA-TM-79286]
p0053 N80-16094
- SOLAR ENERGY**
Photovoltaic power system reliability considerations
[NASA-TM-79291]
p0130 N80-15422
- MOD-2 wind turbine system concept and preliminary design report. Volume 2: Detailed report
[DOE/NASA/0002-80/2]
p0152 N80-26775
- SOLAR ENERGY ABSORBERS**
Preliminary study of a solar selective coating system using black cobalt oxide for high temperature solar collectors
p0082 A80-35500
- Spectral effects on direct-insolation absorptance of five collector coatings
[ASME PAPER 79-HT-18]
p0146 A80-45722
- SOLAR ENERGY CONVERSION**
A photovoltaic power system in the remote African village of Tangaye, Upper Volta
[NASA-TM-79318]
p0137 N80-12552
- A 15kWe (nominal) solar thermal electric power conversion concept definition study: Steam Rankine reheat reciprocator system
[NASA-CR-159590]
p0148 N80-16491
- The 15 kW sub e (nominal) solar thermal electric power conversion concept definition study: Steam Rankine turbine system
[NASA-CR-159589]
p0148 N80-16493
- A 15 kWe (nominal) solar thermal-electric power conversion concept definition study: Steam Rankin reciprocator system
[NASA-CR-159591]
p0149 N80-19612
- Annual technical report, fiscal year 1979. Volume 1: Executive summary
[NASA-CR-159715-VOL-1]
p0149 N80-19632
- Redox storage systems for solar applications
[NASA-TM-81464]
p0142 N80-23777
- Solar thermal power systems point-focusing distributed receiver technology project. Volume 2: Detailed report
[NASA-CR-159715-VOL-2]
p0151 N80-24751
- SOLAR GENERATORS**
NT SOLAR CELLS
Photovoltaic power system reliability considerations
p0146 A80-40338
- Study of advanced radial outflow turbine for solar steam Rankine engines
[NASA-CR-159695]
p0148 N80-16483
- A 15kWe (nominal) solar thermal electric power conversion concept definition study: Steam Rankine reheat reciprocator system
[NASA-CR-159590]
p0148 N80-16491
- Concept definition study of small Brayton cycle engines for dispersed solar electric power systems
[NASA-CR-159592]
p0150 N80-22778
- Design study of a 15 kW free-piston Stirling engine-linear alternator for dispersed solar electric power systems
[NASA-CR-159587]
p0150 N80-22787
- Solar thermal power systems point-focusing distributed receiver technology project. Volume 2: Detailed report
[NASA-CR-159715-VOL-2]
p0151 N80-24751
- SOLAR HEATING**
Candidate thermal energy storage technologies for solar industrial process heat applications
[NASA-TM-81380]
p0138 N80-15560
- SOLAR POWER GENERATION**
U SOLAR GENERATORS
SOLAR POWER SOURCES
U SOLAR GENERATORS
SOLAR PROPULSION
NT SOLAR ELECTRIC PROPULSION
Solar rocket system concept analysis
p0064 N80-31470
- SOLAR REFLECTORS**
Solar thermal power systems point-focusing distributed receiver technology project. Volume 2: Detailed report
[NASA-CR-159715-VOL-2]
p0151 N80-24751
- SOLAR SAILS**
Torquing and electrostatic deformation of the solar sail
p0065 A80-46901
- SOLENOID VALVES**
Durability tests of solenoid valves for digital actuators
[NASA-TM-81522]
p0020 N80-26299
- SOLID LUBRICANTS**
Effect of thermal aging on the tribological properties of polyimide films and polyimide-bonded graphite fluoride films
[ASLE PREPRINT 79-AM-3B-1]
p0088 A80-12094
- Preparation of cast aluminum alloy-mica particle composites
p0071 A80-32632
- Mechanisms of lubrication and wear of a bonded solid-lubricant film
[ASLE PREPRINT 80-AM-3E-1]
p0122 A80-43163
- SOLID ROTATION**
U ROTATING BODIES
SOLID SOLUTIONS
State-of-the-art of SIALON materials
p0009 A80-13066
- SOLID STATE DEVICES**
NT PHOTOVOLTAIC CELLS
Solid-state X-band combiner study
[NASA-CR-162432]
p0103 N80-11328
- SOLID-SOLID INTERFACES**
Metal-dielectric interactions
p0081 A80-13067
- Effect of interfacial species on shear strength of metal-sapphire contacts
p0178 A80-22300
- Rolling-element bearings --- contact sliding friction study of solid bodies
p0121 A80-31961
- SOLUTIONS**
NT AQUEOUS SOLUTIONS
NT GAS MIXTURES
NT SOLID SOLUTIONS
SONIC FLOW
U TRANSONIC FLOW
SONIC SPEED
U ACOUSTIC VELOCITY
SOOT
Dispersion of sound in a combustion duct by fuel droplets and soot particles
p0170 A80-20953
- Effect of fuel molecular structure on soot formation in gas turbine engines
[ASME PAPER 80-GT-62]
p0095 A80-42192
- Laboratory measurements in a turbulent, swirling flow --- measurement of soot inside a flame-tube burner
[NASA-CR-159723]
p0095 N80-22509
- Soot formation and burnout in flames
p0043 N80-29320
- Effect of fuel molecular structure on soot formation in gas turbine combustion
p0043 N80-29322
- SORTIE CAN**
U SPACELAB
SORTIE LAB
U SPACELAB
SOUND
U ACOUSTICS

SOUND ABSORPTION

SUBJECT INDEX

SOUND ABSORPTION

U SOUND TRANSMISSION

SOUND BARRIER

U ACOUSTIC VELOCITY

SOUND MEASUREMENT

U ACOUSTIC MEASUREMENTS

SOUND PRESSURE

Acoustic pressures on a prop-fan aircraft fuselage

surface

[AIAA PAPER 80-1002]

p0172 A80-35965

Advanced turbo-prop airplane interior noise

reduction-source definition

[NASA-CR-159668]

p0172 N80-13882

SOUND PROPAGATION

A time dependent difference theory for sound

propagation in ducts with flow

p0170 A80-20951

Dispersion of sound in a combustion duct by fuel

droplets and soot particles

p0170 A80-20953

Acoustic behavior of fibrous bulk materials

[AIAA PAPER 80-0986]

p0172 A80-35951

Higher order mode propagation in nonuniform

circular ducts

[AIAA PAPER 80-1018]

p0171 A80-35974

A comparison of experiment and theory for sound

propagation in variable area ducts

p0173 A80-45844

A time dependent difference theory for sound

propagation in ducts with flow ---

characteristic of inlet and exhaust ducts of

turbofan engines

[NASA-TM-79302]

p0167 N80-12823

Comparison of inlet suppressor data with

approximate theory based on cutoff ratio

[NASA-TM-81386]

p0167 N80-15876

Spectral structure of pressure measurements made

in a combustion duct --- jet engine noise

[NASA-TM-81471]

p0168 N80-22045

Time dependent difference theory for sound

propagation in axisymmetric ducts with plug flow

[NASA-TM-81501]

p0168 N80-23096

Numerical techniques in linear duct acoustics ---

finite difference and finite element analyses

[NASA-TM-81553]

p0170 N80-30154

A study of the transmission characteristics of

suppressor nozzles

[NASA-CR-165133]

p0172 N80-32186

SOUND TRANSMISSION

Studies of the acoustic transmission

characteristics of coaxial nozzles with inverted

velocity profiles, volume 1 --- jet engine noise

radiation through coannular exhaust nozzles

[NASA-CR-159698]

p0172 N80-11870

Reciprocity principle in duct acoustics

[NASA-TM-79300]

p0167 N80-12824

SOUND VELOCITY

U ACOUSTIC VELOCITY

SOUND WAVES

NT AERODYNAMIC NOISE

NT AIRCRAFT NOISE

NT ENGINE NOISE

NT JET AIRCRAFT NOISE

Spectral structure of pressure measurements made

in a combustion duct

p0171 A80-35496

Rigorous solutions for sound radiation from

circular ducts with hyperbolic horns or infinite

plane baffle

p0171 A80-37895

SOUTHERN HEMISPHERE

Comments on 'Experimental evidence for

interhemispheric transport from airborne carbon

monoxide measurements'

p0159 A80-32520

SPACE CHARGE

Photoelectron charge density and transport near

differentially charged spacecraft

p0053 A80-19773

SPACE COMMUNICATION

NT SPACECRAFT COMMUNICATION

National Aeronautics and Space Administration

plans for space communication technology

p0097 A80-26795

SPACE ELECTRIC ROCKET TESTS

Neutralization tests on the SERT II spacecraft ---

of ion beams

[AIAA PAPER 79-2064]

p0059 A80-10387

SPACE ENVIRONMENT

U AEROSPACE ENVIRONMENTS

SPACE ENVIRONMENT SIMULATION

NASCAP modelling of environmental-charging-induced

discharges in satellites

p0054 A80-19774

A three-dimensional spacecraft-charging computer

code

p0055 A80-46891

Space environmental interactions with biased

spacecraft surfaces

p0055 A80-46897

SPACE MISSIONS

Cost-effective technology advancement directions

for electric propulsion transportation systems

in earth-orbital missions

[NASA-TM-79289]

p0182 N80-11950

SPACE PLASMAS

Interaction of high voltage surfaces with the

space plasma

[NASA-CR-165131]

p0177 N80-32223

SPACE RADIATION

U EXTRATERRESTRIAL RADIATION

SPACE SHUTTLE PAYLOADS

NT SPACEBORNE EXPERIMENTS

NT SPACELAB

A liquid hydrogen experiment as a Shuttle payload

[AIAA PAPER 80-1096]

p0054 A80-38909

SPACE SHUTTLES

Upper stages utilizing electric propulsion

p0059 A80-29989

SPACE STATIONS

NT ORBITAL SPACE STATIONS

Study of power management technology for orbital

multi-100Kwe applications. Volume 2: Study

results

[NASA-CR-159834-VOL-2]

p0153 N80-28862

Study of power management technology for orbital

multi-100Kwe applications. Volume 3:

Requirements

[NASA-CR-159834]

p0154 N80-29845

SPACE STORAGE

LeRC reduced gravity fluid management technology

program

p0048 A80-35504

SPACE SYSTEMS ENGINEERING

U AEROSPACE ENGINEERING

SPACE TRANSPORTATION

NT SPACE TRANSPORTATION SYSTEM

SPACE TRANSPORTATION SYSTEM

NT SPACE SHUTTLES

Cost-effective technology advancement directions

for electric propulsion transportation systems

in earth-orbital missions

[AIAA PAPER 79-2043]

p0048 A80-20961

Orbital transfer of large space structures with

nuclear electric rockets

[AAS PAPER 80-083]

p0054 A80-41897

Large Space Systems/Low-Thrust Propulsion Technology

[NASA-CP-2144]

p0057 N80-31449

DOD low-thrust mission studies

p0063 N80-31455

Low-thrust vehicle concept studies

p0058 N80-31457

SPACEBORNE EXPERIMENTS

A liquid hydrogen experiment as a Shuttle payload

[AIAA PAPER 80-1096]

p0054 A80-38909

First results of material charging in the space

environment

p0055 A80-45609

Plasma physics analysis of SERT-2 operation

[NASA-CR-159814]

p0177 N80-27189

Conceptual design of two-phase fluid mechanics and

heat transfer facility for spacelab

[NASA-CR-159810]

p0049 N80-27403

SPACECRAFT CHARGING

Neutralization tests on the SERT II spacecraft ---

of ion beams

[AIAA PAPER 79-2064]

p0059 A80-10387

Plasma collection by high voltage spacecraft at

low earth orbit

[AIAA PAPER 80-0042]

p0055 A80-18249

Photoelectron charge density and transport near

differentially charged spacecraft

p0053 A80-19773

NASCAP modelling of environmental-charging-induced

discharges in satellites

p0054 A80-19774

SUBJECT INDEX

SPACECRAFT STRUCTURES

Computed voltage distribution around Solar
Electric Propulsion spacecraft
[AIAA PAPER 79-2104] p0054 A80-29750

Initial comparison of SSPM ground test results and
flight data to NASCAP simulations --- Satellite
Surface Potential Monitor NASA Charging Analyzer
Program
[AIAA PAPER 80-0336] p0054 A80-29751

NASCAP modelling computations on large optics
spacecraft in geosynchronous substorm environments
p0054 A80-32829

Effects of secondary yield parameter variation on
predicted equilibrium potential of an object in
a charging environment --- for spacecraft
p0054 A80-44238

First results of material charging in the space
environment
p0055 A80-45609

Active control of spacecraft charging
p0055 A80-46890

A three-dimensional spacecraft-charging computer
code
p0055 A80-46891

Space environmental interactions with biased
spacecraft surfaces
p0055 A80-46897

Torquing and electrostatic deformation of the
solar sail
p0065 A80-46901

Specific spacecraft evaluation: Special report
--- charged particle transport from a mercury
ion thruster to spacecraft surfaces
[NASA-CR-159420] p0060 N80-11137

Configuration effects on satellite charging response
[NASA-TM-81397] p0053 N80-15200

Effects of secondary yield parameter variation on
predicted equilibrium potential of an object in
a charging environment --- using computerized
simulation
[NASA-TM-79299] p0053 N80-16093

Computed voltage distributions around solar
electric propulsion spacecraft
[NASA-TM-79286] p0053 N80-16094

NASCAP modelling computations on large optics
spacecraft in geosynchronous substorm environments
[NASA-TM-81395] p0053 N80-18095

Modelling of environmentally induced discharges in
geosynchronous satellites
[NASA-TM-81598] p0053 N80-32428

SPACECRAFT COMMUNICATION

UHF coplanar-slot antenna for
aircraft-to-satellite data communications
p0009 A80-13064

NASA's program in communication satellites
[AAS 79-247] p0097 A80-28712

Multigigabit satellite on-board signal processing
[AIAA 80-0583] p0100 A80-29605

Application of advanced on-board processing
concepts to future satellite communications
systems
[NASA-CR-159682] p0098 N80-12260

Application of advanced on-board processing
concepts to future satellite communications
systems: Bibliography
[NASA-CR-159684] p0098 N80-12261

Study of advanced communications satellite systems
based on SS-PDMA
[NASA-CR-159778] p0050 N80-25357

SPACECRAFT CONFIGURATIONS

NT SATELLITE CONFIGURATIONS

Primary propulsion/large space system interactions
p0063 N80-31458

SPACECRAFT CONSTRUCTION MATERIALS

First results of material charging in the space
environment
p0055 A80-45609

SPACECRAFT CONTAMINATION

NASCAP modelling computations on large optics
spacecraft in geosynchronous substorm environments
[NASA-TM-81395] p0053 N80-18095

SPACECRAFT DESIGN

NT SATELLITE DESIGN

Computed voltage distribution around Solar
Electric Propulsion spacecraft
[AIAA PAPER 79-2104] p0054 A80-29750

Economical space power systems
[NASA-CR-159696] p0147 N80-15559

SPACECRAFT ENVIRONMENTS

Computed voltage distribution around Solar

Electric Propulsion spacecraft
[AIAA PAPER 79-2104] p0054 A80-29750

SPACECRAFT ORBITS

NT GEOSYNCHRONOUS ORBITS

NT SATELLITE ORBITS

NT TRANSFER ORBITS

SPACECRAFT POWER SUPPLIES

Cycles till failure of silver-zinc cells with
competing failure modes - Preliminary data
analysis
p0146 A80-46414

Space environmental interactions with biased
spacecraft surfaces
p0055 A80-46897

Power processing technology for spacecraft primary
ion propulsion
p0065 A80-48265

Power management for multi-100 KWe space systems
p0060 A80-48357

Heat pipe cooling of power processing magnetics
[NASA-TM-79270] p0101 N80-11327

Economical space power systems
[NASA-CR-159696] p0147 N80-15559

Economic analysis of the design and fabrication of
a space qualified power system
[NASA-TM-81418] p0056 N80-18098

Advanced technology light weight fuel cell program
--- orbiting space vehicle long-life hydrogen
oxygen fuel cell
[NASA-CR-159807] p0149 N80-19615

Solar array subsystems study
[NASA-CR-159857] p0151 N80-24742

Study of power management technology for orbital
multi-100KWe applications. Volume 2: Study
results
[NASA-CR-159834-VOL-2] p0153 N80-28862

Synchronous Energy Technology
[NASA-CR-2154] p0058 N80-33465

Toroidal cell and battery --- energy storage for
orbital space applications or power cells for
electric vehicles
[NASA-CASE-LEW-12918-1] p0144 N80-33857

SPACECRAFT PROPULSION

NT ELECTROMAGNETIC PROPULSION

NT ION PROPULSION

NT MASS DRIVERS (PAYLOAD DELIVERY)

NT PLASMA PROPULSION

NT SOLAR ELECTRIC PROPULSION

NT SOLAR PROPULSION

Characteristics of primary electric propulsion
systems
[AIAA PAPER 79-2041] p0058 A80-10376

Preliminary results of the mission profile life
test of a 30 cm Hg bombardment thruster
[AIAA PAPER 79-2078] p0081 A80-10391

Cost-effective technology advancement directions
for electric propulsion transportation systems
in earth-orbital missions
[AIAA PAPER 79-2043] p0048 A80-20961

Upper stages utilizing electric propulsion
p0059 A80-29989

Analytical investigation of two hydrogen-oxygen
rocket engine systems for low-thrust application
p0060 A80-35503

Upper stages utilizing electric propulsion
[NASA-TM-81412] p0056 N80-16097

Analytical investigation of two hydrogen-oxygen
rocket engine systems for low-thrust application
--- for orbital transfer
p0057 N80-30382

Upper stages utilizing electric propulsion
p0057 N80-30386

Large Space Systems/Low-Thrust Propulsion Technology
[NASA-CR-2144] p0057 N80-31449

Electric propulsion technology
p0057 N80-31452

Chemical propulsion technology
p0058 N80-31453

Auxiliary control of LSS
p0063 N80-31459

Low-thrust chemical rocket engine study
p0063 N80-31467

Low-thrust chemical propulsion
p0063 N80-31468

SPACECRAFT STRUCTURES

Evaluation of particle transport for the P80-1
spacecraft --- mercury ion thruster and
spacecraft surfaces interactive effects
[AIAA PAPER 79-2047] p0055 A80-13301

SPACELAB

SUBJECT INDEX

SPACELAB

Conceptual design of two-phase fluid mechanics and heat transfer facility for spacelab
[NASA-CR-159810] p0049 N80-27403

SPALLING

Wear particles of single-crystal silicon carbide in vacuum
[NASA-TP-1624] p0085 N80-18178

SPECIFIC IMPULSE

Electric propulsion technology p0057 N80-31452
Advanced concepts --- specific impulse, mass drivers, electromagnetic launchers, and the rail gun p0058 N80-31471

SPECIFIC GEOMETRY

Effect of geometry and operating conditions on spur gear system power loss p0122 A80-46409

Comparison tests and experimental compliance calibration of the proposed standard round compact plane strain fracture toughness specimen [NASA-TM-81379] p0132 N80-13513
Fracture toughness of brittle materials determined with chevron notch specimens [NASA-TM-81607] p0079 N80-32486

SPECTRA

NT NOISE SPECTRA

SPECTRAL ANALYSIS

U SPECTRUM ANALYSIS

SPECTRAL REFLECTANCE

Spectral effects on direct-insolation absorptance of five collector coatings [ASME PAPER 79-HT-18] p0146 A80-45722

SPECTRAL SENSITIVITY

Preliminary study of a solar selective coating system using black cobalt oxide for high temperature solar collectors p0082 A80-35500

Spectral effects on direct-insolation absorptance of five collector coatings [ASME PAPER 79-HT-18] p0146 A80-45722

SPECTRAL SIGNATURES

Assessment of satellite and aircraft multispectral scanner data for strip-mine monitoring [NASA-TM-79268] p0136 N80-20787

SPECTROSCOPIC ANALYSIS

An interactive modular design for computerized photometry in spectrochemical analysis p0074 A80-39640
An interactive modular design for computerized photometry in spectrochemical analysis [NASA-TM-81521] p0074 N80-24386

SPECTROSCOPY

NT AUGER SPECTROSCOPY

NT SPECTROSCOPIC ANALYSIS

Ferrographic and spectrographic analysis of oil sampled before and after failure of a jet engine [NASA-TM-81430] p0117 N80-19897

SPECTRUM ANALYSIS

Spectral structure of pressure measurements made in a combustion duct --- jet engine noise [NASA-TM-81471] p0168 N80-22045

SPEED INDICATORS

NT ANEMOMETERS

NT LASER ANEMOMETERS

SPLINE FUNCTIONS

Simple spline-function equations for fracture mechanics calculations p0133 A80-10832

SPOILERS

Feasibility study of aileron and spoiler control systems for large horizontal axis wind turbines [NASA-CR-159856] p0153 N80-27803

SPRAY CHARACTERISTICS

Spray nozzle designs for agricultural aviation applications --- relation of drop size to spray characteristics and nozzle efficiency [NASA-CR-159702] p0108 N80-10460

SPRAY NOZZLES

Spray nozzle designs for agricultural aviation applications --- relation of drop size to spray characteristics and nozzle efficiency [NASA-CR-159702] p0108 N80-10460

Monodisperse atomizers for agricultural aviation applications [NASA-CR-159777] p0108 N80-19450

SPRAYED COATINGS

Tribological properties of sputtered MoS₂ films in

relation to film morphology

Development of improved-durability plasma sprayed ceramic coatings for gas turbine engines [AIAA PAPER 80-1193] p0089 A80-35502
Evaluation of present-day thermal barrier coatings for industrial/utility applications p0092 A80-39637

Friction and wear of plasma-sprayed coatings containing cobalt alloys from 25 deg to 650 deg in air [ASLE PREPRINT 80-AM-6C-2] p0122 A80-43176
Development of improved-durability plasma sprayed ceramic coatings for gas turbine engines [NASA-TM-81512] p0018 N80-23313

SPRAYED PROTECTIVE COATINGS

U PROTECTIVE COATINGS

U SPRAYED COATINGS

SPRAYING

NT CHOP DUSTING

NT PLASMA SPRAYING

SPUTTERING

Survey of ion plating sources p0120 A80-10040

Sputtering in mercury ion thrusters [AIAA PAPER 79-2061] p0058 A80-10384
Mechanical and chemical effects of ion-texturing biomedical polymers p0089 A80-13065

Improved adhesion of sputtered refractory carbides to metal substrates p0081 A80-25274

Primary electric propulsion technology study --- for thruster wear-out mechanisms [NASA-CR-159688] p0061 N80-13159

Tribological properties of sputtered MoS₂ sub 2 films in relation to film morphology [NASA-TM-81465] p0078 N80-21490

Adherence of ion beam sputter deposited metal films on H-13 steel [NASA-TM-81585] p0079 N80-31527

SQUEEZE FILMS

Tribological properties of sputtered MoS₂ films in relation to film morphology p0089 A80-35502

Elastomer damper performance - A comparison with a squeeze film for a supercritical power transmission shaft [ASME PAPER 80-GT-162] p0121 A80-42272

STABILITY

NT AERODYNAMIC STABILITY

NT COMBUSTION STABILITY

NT DYNAMIC STABILITY

NT FLOW STABILITY

NT HOVERING STABILITY

NT MAGNETOHYDRODYNAMIC STABILITY

NT ROTARY STABILITY

NT THERMAL STABILITY

STABILIZATION

Kinematic correction for roller skewing [NASA-TM-81564] p0119 N80-28716

STAINLESS STEELS

NT AUSTENITIC STAINLESS STEELS

NT MARTENSITIC STAINLESS STEELS

Mechanical properties and oxidation and corrosion resistance of reduced-chromium 304 stainless steel alloys [NASA-TP-1557] p0076 N80-11188

Comparison of the tribological properties at 25 C of seven different polyimide films bonded to 301 stainless steel [NASA-TM-81413] p0086 N80-19263

Mechanical impact tests of materials in oxygen effects of contamination --- Teflon, stainless steel, and aluminum [NASA-TP-1571] p0093 N80-21551

STANDS

U SUPPORTS

STARTERS

NT ENGINE STARTERS

STATIC FIRING

Static test-stand performance of the YF-102 turbofan engine with several exhaust configurations for the Quiet Short-Haul Research Aircraft (QSRA) [NASA-TP-1556] p0014 N80-14121

STATIC FRICTION

Steady-state wear and friction in boundary lubrication studies

[NASA-TP-1658] p0087 N80-22493
STATIC INVENTERS
 Power processing technology for spacecraft primary ion propulsion p0065 A80-48265

STATIC PRESSURE
NT HYDROSTATIC PRESSURE
 An experimental investigation of endwall profiling in a turbine vane cascade [AIAA PAPER 80-1089] p0004 A80-38904
 Wind tunnel investigation of the Titan Forward Skirt compartment vent from a free-stream Mach number of 0.80 to 1.96 --- conducted in the Lewis Research Center 8 by 6 foot supersonic wind tunnel [NASA-TM-81572] p0106 N80-32689

STATIC TESTS
NT STATIC FIRING
 An improved prediction method for the noise generated in flight by circular jets [NASA-TM-81470] p0168 N80-22048
 Effect of inflow control on inlet noise of a cut-on fan --- in an anechoic chamber [NASA-TM-81487] p0169 N80-23098
 Static and transient performance of YF-102 engine with up to 14 percent core airbleed for the quiet short-haul research aircraft [NASA-TR-1692] p0020 N80-25339

STATICS
NT ELECTROSTATICS

STATIONS
NT GROUND STATIONS
NT ORBITAL SPACE STATIONS
NT SPACE STATIONS

STATISTICAL ANALYSIS
NT REGRESSION ANALYSIS
NT STATISTICAL DECISION THEORY
 Statistical aspects of carbon fiber risk assessment modeling --- fire accidents involving aircraft [NASA-CR-159318] p0073 N80-29432

STATISTICAL DECISION THEORY
 'Chain pooling' model selection for two-level fixed effects factorial experiments p0164 A80-40764

STATISTICAL PROBABILITY
U PROBABILITY THEORY

STATOR BLADES
 Aerodynamic performances of three fan stator designs operating with rotor having tip speed of 337 meters per second and pressure ratio of 1.54. 1: Experimental performance [NASA-TP-1610] p0015 N80-17071

STATIONS
 Streakline flow visualization study of a horseshoe vortex in a large-scale, two-dimensional turbine stator cascade [ASME PAPER 80-GT-4] p0004 A80-42145
 Streakline flow visualization study of a horseshoe vortex in a large-scale, two-dimensional turbine stator cascade [NASA-TM-79274] p0104 N80-11376
 Liquid metal slip ring --- aerospace environments [NASA-CASE-LEW-12277-3] p0101 N80-18300
 Dynamic response to rotating-seat runout in non-contacting face seals [NASA-TM-81490] p0117 N80-22701

STEADY FLOW
 An alternative approach to the numerical simulation of steady inviscid flow p0107 A80-44228
 Experimental determination of unsteady blade element aerodynamics in cascades. Volume 1: Torsion mode cascade [NASA-CR-159831] p0040 N80-25335
 An alternative approach to the numerical simulation of steady inviscid flow [NASA-TM-81542] p0003 N80-27286

STEAM GENERATORS
U BOILERS

STEAM TURBINES
 Study of advanced radial outflow turbine for solar steam Rankine engines [NASA-CR-159695] p0148 N80-16483
 The 15 kW sub e (nominal) solar thermal electric power conversion concept definition study: Steam Rankine turbine system [NASA-CR-159589] p0148 N80-16493

Cogeneration Technology Alternatives Study (CTAS). Volume 3: Energy conversion system characteristics [NASA-CR-159761] p0155 N80-31869

STEEL STRUCTURES
 Design, fabrication, and test of a steel spar wind turbine blade p0139 N80-16472

STEELS
NT AUSTENITIC STAINLESS STEELS
NT CARBON STEELS
NT CHROMIUM STEELS
NT HIGH STRENGTH STEELS
NT MARTENSITIC STAINLESS STEELS
NT NICKEL STEELS
NT STAINLESS STEELS
 High temperature thermal energy storage in steel and sand [NASA-CR-159708] p0154 N80-29860
 Adherence of ion beam sputter deposited metal films on H-13 steel [NASA-TM-81585] p0079 N80-31527

STEEP GRADIENT AIRCRAFT
U V/STOL AIRCRAFT

STELLAR DOPPLER SHIFT
U EXTRATERRESTRIAL RADIATION

STENCIL PROCESSES
 Screen printing technology applied to silicon solar cell fabrication [NASA-CR-159789] p0153 N80-27808

STERILIZATION EFFECTS
NT CHEMICAL EFFECTS
NT THERMAL DEGRADATION

STIFFNESS
 Modified face seal for positive film stiffness [NASA-CASE-LEW-12989-1] p0114 N80-12414
 Development of procedures for calculating stiffness and damping of elastomers in engineering applications, part 7 [NASA-CR-165138] p0128 N80-32718

STIMULATED EMISSION DEVICES
NT CARBON DIOXIDE LASERS

STIRLING CYCLE
 Assessment of the state of technology of automotive Stirling engines [NASA-CR-159631] p0183 N80-13989
 Sintered silicon nitride recuperator fabrication [NASA-CR-159706] p0090 N80-15263
 Analysis and design of a uniform-clearance, pumping-ring rod seal for the Stirling engine [NASA-TM-81463] p0116 N80-18408
 Overview of a Stirling engine test project [NASA-TM-81442] p0140 N80-18564
 Supporting research and technology for automotive Stirling engine development [NASA-TM-81495] p0183 N80-21200
 Testing of reciprocating seals for application in a Stirling cycle engine [NASA-CR-159820] p0124 N80-22700
 Design study of a 15 kW free-piston Stirling engine-linear alternator for dispersed solar electric power systems [NASA-CR-159587] p0150 N80-22787
 Preliminary results from a four-working space, double-acting piston, Stirling engine controls model [NASA-TM-81569] p0106 N80-29624
 Creep-rupture behavior of seven iron-base alloys after long term aging at 760 deg in low pressure hydrogen [NASA-TM-81534] p0080 N80-32488

STOL AIRCRAFT
U SHORT TAKEOFF AIRCRAFT

STORABLE PROPELLANTS
NT AIRCRAFT FUELS

STORAGE BATTERIES
NT LEAD ACID BATTERIES
NT NICKEL HYDROGEN BATTERIES
NT NICKEL ZINC BATTERIES
NT SILVER ZINC BATTERIES
 Decay of the zincate concentration gradient at an alkaline zinc cathode after charging p0074 A80-13070
 Improvement and scale-up of the NASA Redox storage system p0146 A80-40370

STORMS
NT MAGNETIC STORMS

STRAIN AGING

SUBJECT INDEX

STRAIN AGING

U PRECIPITATION HARDENING

STRAIN DISTRIBUTION

U STRESS CONCENTRATION

STRAIN FATIGUE

U FATIGUE (MATERIALS)

STRAIN GAGES

Measuring unsteady pressure on rotating compressor blades --- with semiconductor strain gages under gas turbine engine operating conditions

p0110 A80-12630

STRAIN HARDENING

Finite-strain large-deflection

elastic-viscoplastic finite-element transient response analysis of structures

[NASA-CR-159874]

p0134 A80-29762

STRAIN SOFTENING

U PLASTIC DEFORMATION

STRATA

NT SUBSTRATES

STREAMLINED BODIES

NT PAIRINGS

STREAMLINING

Selected data from a transonic flexible walled test section

[NASA-CR-159360]

p0047 A80-32404

STRENGTH OF MATERIALS

U MECHANICAL PROPERTIES

STRESS (PHYSIOLOGY)

NT CENTRIFUGING STRESS

STRESS ANALYSIS

Calculation of residual principal stresses in CVD boron on carbon filaments

p0072 A80-44237

Simplified fatigue life analysis for traction drive contacts

p0123 A80-46413

Prediction of fiber composite mechanical behavior made simple --- using a rocket calculator

[NASA-TM-81404]

p0068 A80-16107

Simplified fatigue life analysis for traction drive contacts

[NASA-TM-79199]

p0115 A80-17469

Calculation of residual principal stresses in CVD boron on carbon filaments

[NASA-TM-81456]

p0068 A80-20314

Mod 1 wind turbine generator failure modes and effects analysis

[NASA-CR-159494]

p0150 A80-20864

Sudden stretching of a four layered composite plate

[NASA-CR-159870]

p0073 A80-25383

Sudden bending of cracked laminates

[NASA-CR-159860]

p0073 A80-25384

Stresses and deformations in elliptical contacts

[NASA-TM-81535]

p0118 A80-27697

Instructions for the use of the CIVM-Jet 4C finite-strain computer code to calculate the transient structural responses of partial and/or complete arbitrarily-curved rings subjected to fragment impact

[NASA-CR-159873]

p0134 A80-27720

STRESS CALCULATIONS

U STRESS ANALYSIS

STRESS CONCENTRATION

Prediction of fiber composite mechanical behavior made simple

p0133 A80-32067

Comparison tests and experimental compliance calibration of the proposed standard round compact plane strain fracture toughness specimen

[NASA-TM-81379]

p0132 A80-13513

The method of lines in three dimensional fracture mechanics

[NASA-TM-81593]

p0132 A80-32753

STRESS CORROSION

NT STRESS CORROSION CRACKING

STRESS CORROSION CRACKING

Stress corrosion cracking evaluation of martensitic precipitation hardening stainless steels

[NASA-TM-78257]

p0083 A80-16142

STRESS DISTRIBUTION

U STRESS CONCENTRATION

STRESS INTENSITY FACTORS

Compliance and stress intensity coefficients for short bar specimens with chevron notches

p0133 A80-46032

STRESS RATIO

Practical implementation of the double linear

damage rule and damage curve approach for treating cumulative fatigue damage

[NASA-TM-81517]

p0132 A80-23684

STRESS RUPTURE STRENGTH

U CREEP RUPTURE STRENGTH

STRESS-STRAIN DIAGRAMS

Tensile and flexural strength of non-graphitic superhybrid composites: Predictions and comparisons

[NASA-TM-79276]

p0067 A80-11144

STRESS-STRAIN DISTRIBUTION

U STRESS CONCENTRATION

STRESS-STRAIN RELATIONSHIPS

Mechanical property characterization of intraply hybrid composites

p0070 A80-20954

Comparison of elastic and elastic-plastic structural analyses for cooled turbine blade airfoils

[NASA-TP-1679]

p0132 A80-27719

STRESS-STRAIN-TIME RELATIONS

Long-time creep behavior of the tantalum alloy Astar 811C --- as a function of stress, temperature, and grain size

[NASA-TP-1691]

p0080 A80-32489

STRESSES

NT RESIDUAL STRESS

NT THERMAL STRESSES

STRIP MINING

Assessment of satellite and aircraft multispectral scanner data for strip-mine monitoring

[NASA-TM-79268]

p0136 A80-20787

STRUCTURAL ANALYSIS

NT DYNAMIC STRUCTURAL ANALYSIS

NT FLUTTER ANALYSIS

NT MATRIX METHODS

Fluid and structural measurements to advance gas turbine technology

p0111 A80-36145

Calculation of residual principal stresses in CVD boron on carbon filaments

p0072 A80-44237

Effect of time dependent flight loads on JT9D-7 performance deterioration

[NASA-CR-159681]

p0134 A80-10515

Some techniques for reducing the tower shadow of the DOE/NASA mod-0 wind turbine tower --- wind tunnel tests to measure effects of tower structure on wind velocity

[NASA-TM-79202]

p0137 A80-10594

Computer simulation of engine systems

[NASA-TM-79290]

p0015 A80-15132

Structural analysis considerations for wind turbine blades

p0139 A80-16469

Comparison of elastic and elastic-plastic structural analyses for cooled turbine blade airfoils

[NASA-TP-1679]

p0132 A80-27719

STRUCTURAL BEAMS

U BEAMS (SUPPORTS)

STRUCTURAL DESIGN

Installation and checkout of the DOE/NASA Mod-1 2000-kW wind turbine generator

[AIAA 80-0638]

p0145 A80-28835

Quiet Clean Short-haul Experimental Engine (QCSEE). The aerodynamic and mechanical design of the QCSEE over-the-wing fan

[NASA-TM-134915]

p0034 A80-15089

Quiet Clean Short-haul Experimental Engine (QCSEE) Over-The-Wing (OTW) boilerplate nacelle design report

[NASA-CR-135168]

p0035 A80-15099

Design evolution of large wind turbine generators

p0139 A80-16455

Structural analysis considerations for wind turbine blades

p0139 A80-16469

Design, fabrication, and test of a steel spar wind turbine blade

p0139 A80-16472

Design, fabrication, test, and evaluation of a prototype 150-foot long composite wind turbine blade

[NASA-CR-159775]

p0148 A80-17548

Study of power management technology for orbital multi-100Kw applications. Volume 3: Requirements

[NASA-CR-159834]

p0154 A80-29845

STRUCTURAL DESIGN CRITERIA

Executive summary: Mod-1 wind turbine generator
analysis and design report
[NASA-CR-159497] p0147 N80-11558
Computer simulation of engine systems
[NASA-TN-79290] p0015 N80-15132

STRUCTURAL DYNAMICS

U DYNAMIC STRUCTURAL ANALYSIS

STRUCTURAL ENGINEERING

Coannular supersonic ejector nozzles p0002 N80-10128
Quiet Clean Short-haul Experimental Engine (QCSEE)
Under-The-Wing (UTW) composite nacelle
[NASA-CR-135352] p0032 N80-15119

STRUCTURAL FATIGUE

U FATIGUE (MATERIALS)

STRUCTURAL MEMBERS

NT BEAMS (SUPPORTS)

NT CANTILEVER BEAMS

STRUCTURAL STRAIN

Development of silicon nitride of improved toughness
[NASA-CR-159676] p0072 N80-10319
Effects of axisymmetric contractions on turbulence
of various scales
[NASA-CR-165136] p0006 N80-32328

STRUCTURAL VIBRATION

NT FLUTTER

NT SUPERSONIC FLUTTER

NT TORSIONAL VIBRATION

Vibration and buckling of rectangular plates under
in-plane hydrostatic loading p0133 A80-45364

STS

U SPACE TRANSPORTATION SYSTEM

STYRENES

Low temperature cross linking polyimides
[NASA-CASE-LEW-12876-1] p0087 N80-26447

SUBCRITICAL FLOW

Evaluation of a strained-coordinate perturbation
procedure - Nonlinear subsonic and transonic flows
[AIAA PAPER 80-0339] p0006 A80-18324

SUBGRAVITY

U REDUCED GRAVITY

SUBLAYERS

U SUBSTRATES

SUBSONIC AIRCRAFT

Zero-length, slotted-lip inlet for subsonic
military aircraft
[AIAA PAPER 80-1245] p0004 A80-41203

SUBSONIC FLOW

Evaluation of a strained-coordinate perturbation
procedure - Nonlinear subsonic and transonic flows
[AIAA PAPER 80-0339] p0006 A80-18324

Summary of advanced methods for predicting high
speed propeller performance
[AIAA PAPER 80-0225] p0003 A80-20966

A three-dimensional turbulent compressible
subsonic duct flow analysis for use with
constructed coordinate systems
[AIAA PAPER 80-1398] p0006 A80-41601

Summary of advanced methods for predicting high
speed propeller performance
[NASA-TN-81409] p0002 N80-15051

Influence of pressure driven secondary flows on
the behavior of turbofan forced mixers
[NASA-TN-81541] p0105 N80-27632

SUBSTRATES

Investigation into the effect of plasma
pretreatment on the adhesion of parylene to
various substrates p0066 A80-25900

Investigation into the effect of plasma
pretreatment on the adhesion of parylene to
various substrates
[NASA-TN-79224] p0114 N80-13473

SUCTION

Small, high pressure liquid hydrogen turbopump
[NASA-CR-159821] p0125 N80-26662

SULFATES

NT SODIUM SULFATES

Reactions of calcium orthosilicate and barium
zirconate with oxides and sulfates of various
elements
[NASA-TN-79272] p0085 N80-13256
Sulfate and nitrate collected by filter sampling
near the tropopause
[NASA-TP-1567] p0157 N80-14581
Fouling and the inhibition of salt corrosion ---
hot corrosion of superalloys

[NASA-TN-81469]

p0078 N80-21492

SULFIDES

NT MOLYBDENUM DISULFIDES

NT MOLYBDENUM SULFIDES

SULFUR COMPOUNDS

NT MOLYBDENUM DISULFIDES

NT MOLYBDENUM SULFIDES

NT SODIUM SULFATES

NT SULFATES

NT SULFURIC ACID

SULFURIC ACID

Effect on combined cycle efficiency of stack gas
temperature constraints to avoid acid corrosion
[NASA-TN-81531] p0143 N80-27804

SUPERALLOYS

U HEAT RESISTANT ALLOYS

SUPERCHARGERS

Supercharged topping rocket propellant feed system
[NASA-CASE-XLE-02062-1] p0056 N80-14188
Diesel engine catalytic combustor system ---
turbocharging
[NASA-CASE-LEW-12995-1] p0118 N80-26659

SUPERCHARGING

U SUPERCHARGERS

SUPERCONDUCTING MAGNETS

Apparatus for trapping and thermal detection of
atomic hydrogen in high magnetic fields at low
temperatures p0111 A80-34546

SUPERCONDUCTORS

Critical currents in A-15 structure Nb3Al
converted from cold-worked bcc structure
p0179 A80-33853

SUPERCRITICAL FLOW

Evaluation of a strained-coordinate perturbation
procedure - Nonlinear subsonic and transonic flows
[AIAA PAPER 80-0339] p0006 A80-18324

SUPERHIGH FREQUENCIES

Concepts for 18/30 GHz satellite communication
system, volume 1
[NASA-CR-159625-VOL-1] p0098 N80-11277

Concepts for 18/30 GHz satellite communication
system, volume 1A: Appendix
[NASA-CR-159625-VOL-1A] p0098 N80-11278

Concepts for 18/30 GHz satellite communication
system study. Executive summary
[NASA-CR-159680] p0098 N80-11279

Solid-state X-band combiner study
[NASA-CR-162432] p0103 N80-11328

SUPERHYBRID MATERIALS

NT GRAPHITE-EPOXY COMPOSITE MATERIALS

SUPERSONIC AIRCRAFT

NT F-16 AIRCRAFT

NT F-102 AIRCRAFT

NT SUPERSONIC COMMERCIAL AIR TRANSPORT

NT SUPERSONIC TRANSPORTS

SUPERSONIC COMBUSTION RAMJET ENGINES

Hypersonic propulsion --- supersonic combustion
ramjet engines p0013 N80-10217

SUPERSONIC COMMERCIAL AIR TRANSPORT

Supersonic propulsion technology --- variable
cycle engines p0013 N80-10216

SUPERSONIC COMPRESSORS

Inlet flow distortion in turbomachinery. I -
Comparison of theory and experiment in a
transonic fan stage. II - A parameter study
[AIAA PAPER 80-1076] p0006 A80-38895
Aerodynamic analysis of a supersonic cascade
vibrating in a complex mode p0007 A80-45841

SUPERSONIC CRUISE AIRCRAFT RESEARCH

Noise suppression due to annulus shaping of an
inverted-velocity-profile coaxial nozzle ---
supersonic cruise aircraft
[NASA-TN-81460] p0168 N80-22046

SUPERSONIC FLOW

Numerical simulation of supersonic inlets using a
three-dimensional viscous flow analysis
[AIAA PAPER 80-0384] p0003 A80-20969

Computation of three-dimensional viscous
supersonic flow in inlets
[AIAA PAPER 80-0194] p0065 A80-23941

Coannular supersonic ejector nozzles
p0002 N80-10128

Summary of advanced methods for predicting high
speed propeller performance
[NASA-TN-81409] p0002 N80-15051

SUPERSONIC FLOW INLETS

U SUPERSONIC INLETS

SUPERSONIC FLUTTER

Aerodynamic analysis of a supersonic cascade vibrating in a complex mode

p0007 A80-45841

SUPERSONIC INLETS

Inlet flow distortion in turbomachinery. I -

Comparison of theory and experiment in a transonic fan stage. II - A parameter study [AIAA PAPER 80-1076]

p0006 A80-38895

Dynamic response of a Mach 2.5 axisymmetric inlet and turbojet engine with a poppet-valve controlled inlet stability bypass system when subjected to internal and external airflow transients

[NASA-TP-1531] p0014 N80-14123

Turbojet-exhaust-nozzle secondary-airflow pumping as an exit control of an inlet-stability bypass system for a Mach 2.5 axisymmetric mixed-compression inlet --- Lewis 10- by 10-ft. supersonic wind tunnel test

[NASA-TP-1532] p0014 N80-14124

Development of a three-dimensional supersonic inlet flow analysis

[NASA-CR-3218] p0108 N80-14356

An analytical and experimental study of a short s-shaped subsonic diffuser of a supersonic inlet [NASA-TN-81406]

p0015 N80-15134

Numerical simulation of supersonic inlets using a three-dimensional viscous flow analysis

[NASA-TN-81411] p0104 N80-15365

SUPERSONIC TRANSPORTS

NT SUPERSONIC COMMERCIAL AIR TRANSPORT

VSCF technology definition study

[NASA-CR-159730] p0027 N80-10222

SUPERSONIC TURBINES

VSCF technology definition study

[NASA-CR-159730] p0027 N80-10222

SUPPORTS

The CP6 jet engine performance improvement: New

front mount [NASA-CR-159639] p0029 N80-14127

SUPPRESSORS

Comparison of inlet suppressor data with approximate theory based on cutoff ratio

[NASA-TN-81386] p0167 N80-15876

SURFACE COOLING

Full-coverage film cooling. I - Comparison of heat transfer data for three injection angles [ASME PAPER 80-GT-43]

p0108 A80-42176

SURFACE ENERGY

Interaction of high voltage surfaces with the space plasma --- solar arrays

[NASA-CR-159731] p0176 N80-14923

SURFACE FINISHING

Investigation into the effect of plasma pretreatment on the adhesion of parylene to various substrates

p0066 A80-25900

Tribological properties of silicon carbide in metal removal process

[NASA-TN-79238] p0114 N80-16340

Modification of the electrical and optical properties of polymers --- ion irradiation to create texture

[NASA-CASE-LEW-13027-1] p0087 N80-24437

SURFACE GEOMETRY

Full-coverage film cooling. II - Heat transfer data and numerical simulation

[ASME PAPER 80-GT-44] p0109 A80-42177

SURFACE INTERACTIONS

U SURFACE REACTIONS

SURFACE LAYERS

Significance of thermal contact resistance in two-layer, thermal-barrier-coated turbine vanes

p0024 A80-39635

Formation of porous surface layers in reaction bonded silicon nitride during processing

[NASA-TN-81493] p0087 N80-23456

SURFACE PRESSURE

U PRESSURE

SURFACE PROPERTIES

NT ADHESION

NT COEFFICIENT OF FRICTION

NT INTERFACIAL TENSION

NT SPECTRAL REFLECTANCE

NT SURFACE ENERGY

NT SURFACE ROUGHNESS

NT SURFACE TEMPERATURE

NT WALL TEMPERATURE

A time dependent difference theory for sound propagation in ducts with flow

p0170 A80-20951

Practical applications of surface analytic tools in tribology

[NASA-TN-81484] p0079 N80-23430

SURFACE REACTIONS

Homogeneous alignment of nematic liquid crystals by ion beam etched surfaces

p0178 A80-26007

Interaction of high voltage surfaces with the space plasma --- solar arrays

[NASA-CR-159731] p0176 N80-14923

Experimental results on plasma interactions with large surfaces at high voltages

[NASA-TN-81423] p0175 N80-18946

SURFACE ROUGHNESS

Elastohydrodynamic film thickness measurements of artificially-produced nonsmooth surfaces

[ASLE PREPRINT 79-LC-1A-3] p0102 A80-14720

SURFACE ROUGHNESS EFFECTS

Modified power law equations for vertical wind profiles --- in investigation of windpower plant siting

p0159 A80-35719

SURFACE TEMPERATURE

NT WALL TEMPERATURE

Analytical and experimental spur gear tooth temperature as affected by operating variables

[NASA-TN-81419] p0123 A80-46412

Uncertainties in predicting turbine blade metal temperatures

[ASME PAPER 80-HT-25] p0027 A80-48014

Effects of a ceramic coating on metal temperatures of an air-cooled turbine vane

[NASA-TP-1598] p0105 N80-17397

Analytical and experimental spur gear tooth temperature as affected by operating variables

[NASA-TN-81419] p0115 N80-18403

Analysis of uncertainties in turbine metal temperature predictions

[NASA-TP-1593] p0017 N80-21326

SURFACE TENSION

U INTERFACIAL TENSION

SURFACE TREATMENT

U SURFACE FINISHING

SURFACE VEHICLES

NT ELECTRIC AUTOMOBILES

NT ELECTRIC HYBRID VEHICLES

NT ELECTRIC MOTOR VEHICLES

SURGERY

Intra-ocular pressure normalization technique and equipment

[NASA-CASE-LEW-12955-1] p0161 N80-14684

SURVEILLANCE RADAR

NT AIRBORNE SURVEILLANCE RADAR

SWEAT COOLING

Performance of a transpiration-regenerative cooled rocket thrust chamber

[NASA-CR-159742] p0061 N80-14189

SWITCHES

NT SWITCHING CIRCUITS

SWITCHING

NT MICROWAVE SWITCHING

SWITCHING CIRCUITS

An adaptive-control switching buck regulator - implementation, analysis, and design

[NASA-CASE-LEW-12586-1] p0103 A80-28167

Self-reconfiguring solar cell system

[NASA-CASE-LEW-12586-1] p0137 N80-14472

SWITCHING ELEMENTS

U SWITCHING CIRCUITS

SYMMETRICAL BODIES

NT AXISYMMETRIC BODIES

NT FAIRINGS

NT ROTATING CYLINDERS

SYNCHRONOUS SATELLITES

Ka-band, multibeam, contiguous coverage satellite antenna for the USA

[AIAA 80-0557] p0099 A80-29588

Effects of secondary yield parameter variation on predicted equilibrium potential of an object in a charging environment --- for spacecraft

p0054 A80-44238

Modelling of environmentally induced discharges in geosynchronous satellites

[NASA-TN-81398] p0053 N80-32428

SUBJECT INDEX

TECHNOLOGY ASSESSMENT

SYNTHETIC FIBERS		
NT GLASS FIBERS		
SYNTHETIC FUELS		
Literature survey of properties of synfuels derived from coal		
[NASA-TN-79243]	p0141	N80-22776
Use of petroleum-based correlations and estimation methods for synthetic fuels		
[NASA-TN-81533]	p0093	N80-27509
SYNTHETIC RESINS		
NT EPOXY RESINS		
NT KEVLAR (TRADEMARK)		
NT PHENOLIC RESINS		
NT POLYESTER RESINS		
NT THERMOSETTING RESINS		
SYNTHETIC RUBBERS		
NT ELASTOMERS		
SYSTEM FAILURES		
Mod 1 wind turbine generator failure modes and effects analysis		
[NASA-CR-159494]	p0150	N80-20864
SYSTEMS ANALYSIS		
NASA advanced communications systems analysis		
	p0097	A80-25916
Modeling and analysis of Power Processing Systems		
	p0066	A80-28894
Upper stages utilizing electric propulsion		
	p0059	A80-29989
System analysis for millimeter-wave communication satellites		
	p0100	A80-52479
Analytical investigation of two hydrogen oxygen rocket engine systems for low-thrust application		
[NASA-TN-81420]	p0056	N80-17138
Computerized systems analysis and optimization of aircraft engine performance, weight, and life cycle costs		
	p0001	N80-21271
Matrix management for aerospace 2000		
[NASA-TN-81509]	p0181	N80-24200
SYSTEMS DESIGN		
U SYSTEMS ENGINEERING		
SYSTEMS ENGINEERING		
NT COMPUTER SYSTEMS DESIGN		
SERT II 1979 extended flight thruster system performance		
[AIAA PAPER 79-2063]	p0059	A80-10386
A new traffic control design method for large networks with signalized intersections		
	p0183	A80-14841
An advanced mixed user domestic satellite system architecture		
[AIAA 80-0494]	p0099	A80-29544
Photovoltaic power system reliability considerations		
	p0146	A80-40338
Design, performance and life cycle cost relationships for a 500kW space solar array		
	p0065	A80-48356
Executive summary: Mod-1 wind turbine generator analysis and design report		
[NASA-CR-159497]	p0147	N80-11558
Phase-locked telemetry system for rotary instrumentation of turbomachinery, phase 1		
[NASA-CR-159453]	p0029	N80-14182
Mod-1 wind turbine generator analysis and design report, volume 1		
[NASA-CR-159495]	p0150	N80-23775
On-board processing concepts for future satellite communications systems		
[NASA-CR-159683]	p0099	N80-24514
T		
T-63 ENGINE		
Laser anemometer measurements at the exit of a T63 combustor		
	p0045	A80-27737
TABLES (DATA)		
Cogeneration Technology Alternatives Study (CTAS). Volume 6: Computer data. Part 1: Coal-fired nocogeneration process boiler, section A		
[NASA-CR-159770-PT-1-A]	p0154	N80-30888
Cogeneration Technology Alternatives Study (CTAS). Volume 6: Computer data. Part 1: Coal-fired nocogeneration process boiler, section B		
[NASA-CR-159770-PT-1-B]	p0154	N80-30889
Cogeneration Technology Alternatives Study (CTAS). Volume 6: Computer data. Part 2: Residual-fired nocogeneration process boiler		
[NASA-CR-159770-PT-2]	p0155	N80-30890
Selected data from a transonic flexible walled test section		
[NASA-CR-159360]	p0047	N80-32404
TAIL ROTORS		
NT HELICOPTER TAIL ROTORS		
TAILLESS AIRCRAFT		
NT F-102 AIRCRAFT		
TAKEOFF		
NT VERTICAL TAKEOFF		
TANDEN MOTOR HELICOPTERS		
Low speed test of the aft inlet designed for a tandem fan V/STOL nacelle		
[NASA-CR-159752]	p0037	N80-18042
TANKS (CONTAINERS)		
NT FUEL TANKS		
NT PROPELLANT TANKS		
NT WING TANKS		
TANTALUM ALLOYS		
Long-time creep behavior of the tantalum alloy Astar 811C --- as a function of stress, temperature, and grain size		
[NASA-TF-1691]	p0080	N80-32460
TAPER		
U TAPERING		
TAPERING		
Lubrication of optimized-design tapered-roller bearings to 2.4 million DN		
[NASA-TF-1714]	p0119	N80-29734
TARE (DATA REDUCTION)		
U DATA REDUCTION		
TARGET RECOGNITION		
Possible methods for distinguishing icebergs from ships by aerial remote sensing		
[NASA-TN-79310]	p0136	N80-15538
TDMA		
U TIME DIVISION MULTIPLE ACCESS		
TECHNOLOGICAL FORECASTING		
Electric propulsion, circa 2000		
[AIAA PAPER 80-0912]	p0059	A80-32886
Matrix management for aerospace 2000		
[AIAA PAPER 80-0946]	p0181	A80-40700
Aeropropulsion in year 2000		
[NASA-TN-81416]	p0016	N80-18043
New opportunities for future, small, General-Aviation Turbine Engines (GATE)		
	p0017	N80-22335
Cogeneration technology alternatives study. Volume 1: Summary report		
[NASA-CR-159759]	p0152	N80-25792
Cogeneration technology alternatives study. Volume 2: Industrial process characteristics		
[NASA-CR-159760]	p0152	N80-25793
Cogeneration technology alternatives study. Volume 4: Heat Sources, balance of plant and auxiliary systems		
[NASA-CR-159762]	p0152	N80-25794
Cogeneration technology alternatives study. Volume 6: Computer data		
[NASA-CR-159764]	p0152	N80-25795
TECHNOLOGIES		
NT ENERGY TECHNOLOGY		
TECHNOLOGY ASSESSMENT		
8-cm Engineering Model Thruster technology - A review of recent developments		
[AIAA PAPER 79-2103]	p0064	A80-13311
Preparing aircraft propulsion for a new era in energy and the environment		
	p0024	A80-17737
30/20 GHz wideband technology verification program		
	p0097	A80-25917
Aeropropulsion in year 2000		
[AIAA PAPER 80-0914]	p0024	A80-32887
The measuring and growing of advanced gas turbines		
	p0111	A80-36127
Fluid and structural measurements to advance gas turbine technology		
	p0111	A80-36145
A quarter-century of progress in the development of correlation and extrapolation methods for creep rupture data		
	p0133	A80-38142
System analysis for millimeter-wave communication satellites		
	p0100	A80-52479
Turbomachinery technology		
	p0012	N80-10212
Control technology		
	p0013	N80-10215

- VSCE technology definition study
[NASA-CR-159730] p0027 N80-10222
- Cost-effective technology advancement directions
for electric propulsion transportation systems
in earth-orbital missions
[NASA-TM-79289] p0182 N80-11950
- Assessment of the state of technology of
automotive Stirling engines
[NASA-CR-159631] p0183 N80-13989
- Comments on TEC trends
[NASA-TM-79317] p0175 N80-16885
- An overview of NASA research on positive
displacement general aviation engines
p0017 N80-22336
- Assessment and preliminary design of an energy
buffer for regenerative braking in electric
vehicles
[NASA-CR-159756] p0184 N80-23216
- Concepts and techniques for ultrasonic evaluation
of material mechanical properties
[NASA-TM-81523] p0130 N80-24634
- Solar array subsystems study
[NASA-CR-110857] p0151 N80-24742
- Advanced fuel system technology for utilizing
broadened property aircraft fuels
[NASA-TM-81538] p0094 N80-27510
- Impact of propulsion system R and D on electric
vehicle performance and cost
[NASA-TM-81548] p0143 N80-27805
- Synchronous energy technology program
p0058 N80-33466
- Status of nickel-hydrogen cell technology
p0064 N80-33474
- TECHNOLOGY TRANSFER**
Energy conservation and environmental benefits of
thermal energy storage systems in the pulp and
paper industry
p0146 A80-48194
- Collection and dissemination of TES system
information for the paper and pulp industry
p0142 N80-22797
- TECHNOLOGY UTILIZATION**
NASA communications technology research and
development
p0097 A80-25920
- Evaluation of present-day thermal barrier coatings
for industrial/utility applications
p0092 A80-39647
- Instrumentation technology
p0013 N80-10214
- The 30/20 GHz fixed communications systems service
demand assessment. Volume 1: Executive summary
[NASA-CR-159619] p0098 N80-18262
- The 30/20 GHz fixed communications systems service
demand assessment. Volume 2: Main report
[NASA-CR-159620] p0098 N80-18263
- The 30/20 GHz fixed communications systems service
demand assessment. Volume 3: Annex
[NASA-CR-159621] p0099 N80-18264
- Industrial storage applications overview
p0142 N80-22795
- Collection and dissemination of TES system
information for the paper and pulp industry
p0142 N80-22797
- TESTING**
Teetered, tip-controlled rotor: Preliminary test
results from Mod-0 100-kW experimental wind
turbine
[NASA-TM-81445] p0140 N80-19613
- TEFLON (TRADEMARK)**
Negative streamer development in FEP teflon
p0179 A80-19776
- Mechanical impact tests of materials in oxygen
effects of contamination --- Teflon, stainless
steel, and aluminum
[NASA-TP-1571] p0093 N80-21551
- TELECOMMUNICATION**
NT DATA LINKS
NT FREQUENCY DIVISION MULTIPLE ACCESS
NT PULSE COMMUNICATION
NT RADIO COMMUNICATION
NT SPACE COMMUNICATION
NT SPACECRAFT COMMUNICATION
NT TELEMETRY
NT TIME DIVISION MULTIPLE ACCESS
NT VOICE COMMUNICATION
NT WIDEBAND COMMUNICATION
NASA advanced communications systems analysis
p0097 A80-25916
- Multigigabit satellite on-board signal processing
[AIAA 89-0583] p0100 A80-29605
- On-board processing concepts for future satellite
communications systems
[NASA-CR-159683] p0099 N80-24514
- A quantitative analysis of inter-island telephony
traffic in the Pacific Basin Region (PER)
[NASA-TM-81587] p0097 N80-32610
- TELEMETRIES**
U TELEMETRY
TELEMETRY
Phase-locked telemetry system for rotary
instrumentation of turbomachinery, phase 1
[NASA-CR-159453] p0029 N80-14182
- TEMPERATURE**
NT HIGH TEMPERATURE
NT INLET TEMPERATURE
NT ION TEMPERATURE
NT LOW TEMPERATURE
NT SURFACE TEMPERATURE
NT WALL TEMPERATURE
TEMPERATURE DEPENDENCE
Predicting the time-temperature dependent axial
failure of B/A1 composites
p0071 A80-35494
- Predicting the time-temperature dependent axial
failure of B/A1 composites
[NASA-TM-81474] p0069 N80-21452
- Long-time creep behavior of the tantalum alloy
Astar 811C --- as a function of stress,
temperature, and grain size
[NASA-TP-1691] p0080 N80-32489
- TEMPERATURE DIFFERENCES**
U TEMPERATURE GRADIENTS
TEMPERATURE DISTRIBUTION
Computerized video densitometry method for rapid
analysis of infrared photographic images ---
temperature distribution across a turbine blade
[NASA-TP-1686] p0110 N80-25635
- TEMPERATURE EFFECTS**
Elevated temperature flow strength, creep
resistance and diffusion welding characteristics
of Ti-6Al-2Nb-1Ta-0.8Mo
p0081 A80-13277
- The effects of strain and temperature on the
dynamic properties of elastomers
[SME PAPER 79-DET-57] p0572 A80-15720
- Effect of temperature on surface noise
p0107 A80-28419
- Apparatus for trapping and thermal detection of
atomic hydrogen in high magnetic fields at low
temperatures
p0111 A80-34546
- Engine environmental effects on composite behavior
--- moisture and temperature effects on
mechanical properties
[AIAA 80-0695] p0024 A80-35101
- Effect of thermal cycling on ZrO₂-Y₂O₃ thermal
barrier coatings
p0089 A80-35899
- Effects of oxide additions and temperature on
sinterability of silled silicon nitride
[NASA-TP-1644] p0086 N80-21532
- Feasibility study of silicon nitride regenerators
[NASA-CR-159713] p0184 N80-25209
- Fuel system technology overview
p0022 N80-29328
- Long-time creep behavior of the niobium alloy C-103
[NASA-TP-1727] p0080 N80-33555
- TEMPERATURE FIELDS**
U TEMPERATURE DISTRIBUTION
TEMPERATURE GRADIENTS
Stability of several oxide dispersion strengthened
alloys and a directionally solidified
gamma/gamma prime-alpha eutectic alloy in a
thermal gradient
p0082 A80-40962
- Directional solidification at ultra-high thermal
gradient
[NASA-CR-159797] p0096 N80-15300
- TEMPERATURE INDICATORS**
U TEMPERATURE MEASURING INSTRUMENTS
TEMPERATURE INSTRUMENTS
U TEMPERATURE MEASURING INSTRUMENTS
TEMPERATURE INVERSIONS
NT CENTRIFUGING STRESS
NT INTERFACIAL TENSION
TEMPERATURE MEASUREMENT
Impact of new instrumentation on advanced turbine

research p0112 A80-36155
 Temperature and pressure measurement techniques for an advanced turbine test facility p0112 A80-36157
 Temperature and flow measurements on near-freezing aviation fuels in a wing-tank model [ASME PAPER 80-GT-63] p0094 A80-42193
 Temperature and pressure measurement techniques for an advanced turbine test facility [NASA-TN-79278] p0110 A80-14374
TEMPERATURE MEASURING INSTRUMENTS
 Design, fabrication and testing of an optical temperature sensor [NASA-CR-165125] p0112 A80-31777
TEMPERATURE PROFILES
 Temperature and flow measurements on near-freezing aviation fuels in a wing-tank model [NASA-TN-79285] p0093 A80-13268
TEMPERATURE SENSORS
 Thin film temperature sensor [NASA-CR-159782] p0112 A80-17425
TENSILE PROPERTIES
 Mechanical properties and oxidation and corrosion resistance of reduced-chromium 304 stainless steel alloys [NASA-TP-1557] p0076 A80-11188
 Creep-rupture behavior of seven iron-base alloys after long term aging at 760 deg in low pressure hydrogen [NASA-TN-81534] p0080 A80-32488
TENSILE STRENGTH
 Tensile and flexural strength of non-graphitic superhybrid composites: Predictions and comparisons [NASA-TN-79276] p0067 A80-11144
TENSILE TESTS
 Fracture modes of high modulus graphite/epoxy angleplied laminates subjected to off-axis tensile loads p0071 A80-32069
 Anisotropy of nickel-base superalloy single crystals p0083 A80-51573
 Fracture modes of high modulus graphite/epoxy angleplied laminates subjected to off-axis tensile loads [NASA-TN-81405] p0068 A80-16102
THERMALLY ALLOYS
 NO. 1 (TRADEMARK)
 hyperfine magnetic field at Cd impurity site in L2/1/ Heusler alloys Rh₂MnGe and Rh₂MnPb by TDPAC technique --- Time Differential Perturbed Angular Correlation p0178 A80-16843
THERMAL SYSTEMS (DIGITAL)
 U DIGITAL SYSTEMS
TEST BEDS
 U TEST EQUIPMENT
TEST CHAMBERS
 NT ANECHOIC CHAMBERS
 NT PRESSURE CHAMBERS
 NT VACUUM CHAMBERS
TEST EQUIPMENT
 Fatigue strength testing employed for evaluation and acceptance of jet-engine instrumentation probes p0112 A80-42291
 Impact of new instrumentation on advanced turbine research [NASA-TN-79301] p0015 A80-15133
TEST FACILITIES
 NT ANECHOIC CHAMBERS
 NT LOW SPEED WIND TUNNELS
 An electric propulsion long term test facility [AIAA PAPER 79-2080] p0049 A80-13308
 Temperature and pressure measurement techniques for an advanced turbine test facility p0112 A80-36157
 Improvement and scale-up of the NASA Redox storage system p0146 A80-48370
 Temperature and pressure measurement techniques for an advanced turbine test facility [NASA-TN-79278] p0110 A80-14374
 Engineering test facility design definition [NASA-TN-81499] p0143 A80-27799
TEST FIRING
 NT STATIC FIRING

Design and evaluation of high performance rocket engine injectors for use with hydrocarbon fuels p0059 A80-20957
TESTERS
 U TEST EQUIPMENT
TESTING MACHINES
 U TEST EQUIPMENT
TEXTURES
 Mechanical and chemical effects of ion-texturing biomedical polymers p0089 A80-13065
 Modification of the electrical and optical properties of polymers --- ion irradiation to create texture [NASA-CASE-LEW-13027-1] p0087 A80-24437
THEOREMS
 NT RECIPROCAL THEOREMS
 NT SIMILARITY THEOREM
THERAPY
 NT RADIATION THERAPY
THERMAL AGITATION
 U THERMAL ENERGY
THERMAL CONTROL COATINGS
 Thermal barrier coatings for aircraft gas turbines [AIAA PAPER 80-0302] p0089 A80-18303
 Effects of yttrium, aluminum and chromium concentrations in bond coatings on the performance of zirconia-yttria thermal barriers p0082 A80-35900
 Evaluation of present-day thermal barrier coatings for industrial/utility applications p0092 A80-39637
 Similarity tests of turbine vanes - Effects of ceramic thermal barrier coatings [ASME PAPER 80-HT-24] p0027 A80-48013
 Effects of a ceramic coating on metal temperatures of an air-cooled turbine vane [NASA-TP-1598] p0105 A80-17397
 An experimental, low-cost, silicon-aluminide high-temperature coating for superalloys [NASA-TN-81455] p0078 A80-20370
 Similarity tests of turbine vanes, effects of ceramic thermal barrier coatings [NASA-TN-81473] p0105 A80-21706
 Effects of yttrium, aluminum and chromium concentrations in bond coatings on the performance of zirconia-yttria thermal barriers [NASA-TN-81485] p0079 A80-22464
 Development of improved-durability plasma sprayed ceramic coatings for gas turbine engines [NASA-TN-81512] p0018 A80-23313
THERMAL CYCLING TESTS
 Hot corrosion of four superalloys - HA-188, S-57, IN-617, and TD-NiCrAl p0081 A80-14445
 3500-hour durability testing of ceramic materials for automotive gas turbine engines [AIRESARCH-31-3542] p0092 A80-35575
 Effect of thermal cycling on ZrO₂-Y₂O₃ thermal barrier coatings p0089 A80-35899
 Development of improved high pressure turbine outer gas path seal components --- abrasability and thermal cycling test results [NASA-CR-159801] p0038 A80-21332
 Three dimensional finite-element elastic analysis of a thermally cycled double-edge wedge geometry specimen --- nickel alloy turbine parts [NASA-TN-80980] p0079 A80-26433
 The 3500 hour durability testing of commercial ceramic materials [NASA-CR-159785] p0091 A80-31552
THERMAL DEGRADATION
 Effect of thermal aging on the tribological properties of polyimide films and polyimide-bonded graphite fluoride films [ASLE PREPRINT 79-AH-3B-1] p0088 A80-12094
 Evaluation of present-day thermal barrier coatings for industrial/utility applications p0092 A80-39637
 Life test studies on tungsten impregnated cathodes p0103 A80-45122
THERMAL EFFECTS
 U TEMPERATURE EFFECTS
THERMAL EFFICIENCY
 U THERMODYNAMIC EFFICIENCY
THERMAL ENERGY
 Energy conservation and environmental benefits of thermal energy storage systems in the pulp and

THERMAL ENERGY STORAGE

SUBJECT INDEX

- paper industry p0146 A80-48194
- High-temperature molten salt thermal energy storage systems p0148 N80-17547
[NASA-CR-159663]
- Thermal Energy Storage: Fourth Annual Review Meeting [NASA-CR-2125] p0141 N80-22788
- Program definition and assessment overview --- for thermal energy storage project management p0141 N80-22790
- Thermal energy storage systems using fluidized bed heat exchangers [NASA-CR-159868] p0153 N80-28866
- Active heat exchange system development for latent heat thermal energy storage [NASA-CR-159727] p0154 N80-29857
- Cogeneration Technology Alternatives Study (CTAS). Volume 3: Industrial processes [NASA-CR-159767] p0155 N80-31870
- THERMAL ENERGY STORAGE**
- U HEAT STORAGE**
- THERMAL EXPANSION**
- Performance of two-layer thermal barrier systems on directionally solidified Ni-Al-Mo and comparative effects of alloy thermal expansion on system life [NASA-TM-81604] p0080 N80-32487
- THERMAL FATIGUE**
- Analytical and experimental spur gear tooth temperature as affected by operating variables p0123 A80-46412
- Thermal fatigue and oxidation data for directionally solidified MAR-M 246 turbine blades [NASA-CR-159798] p0037 N80-21330
- Thermal fatigue and oxidation data of oxide dispersion-strengthened alloys [NASA-CR-159842] p0084 N80-25415
- THERMAL INSULATION**
- Composite wall concept for high temperature turbine shrouds: Heat transfer analysis [NASA-TM-81539] p0020 N80-27362
- THERMAL POWER**
- U TURBOGENERATORS**
- THERMAL PROPERTIES**
- U THERMODYNAMIC PROPERTIES**
- THERMAL PROTECTION**
- Significance of thermal contact resistance in two-layer, thermal-barrier-coated turbine vanes p0024 A80-39635
- Analysis of the response of a thermal barrier coating to sodium and vanadium doped combustion gases [NASA-TM-79205] p0076 N80-10344
- Corrosion resistant thermal barrier coating --- protecting gas turbines and other heat engine parts [NASA-CASE-LEW-13088-1] p0067 N80-11142
- Improved bond coatings for use with thermal barrier coatings [NASA-TM-81567] p0080 N80-33556
- THERMAL RESISTANCE**
- Significance of thermal contact resistance in two-layer, thermal-barrier-coated turbine vanes p0024 A80-39635
- Corrosion resistance of sodium sulfate coated cobalt-chromium-aluminum alloys at 900 C, 1000 C, and 1100 C [NASA-TM-79311] p0076 N80-14234
- Fire test method for graphite fiber reinforced plastics [NASA-TM-81436] p0068 N80-18107
- Significance of thermal contact resistance in two-layer thermal-barrier-coated turbine vanes [NASA-TM-81483] p0018 N80-23310
- THERMAL RESOURCES**
- NT GEOTHERMAL RESOURCES**
- THERMAL SHOCK**
- Preliminary study of methods for providing thermal shock resistance to plasma-sprayed ceramic gas-path seals [NASA-TP-1561] p0087 N80-23453
- THERMAL STABILITY**
- NT TEMPERATURE DEPENDENCE**
- Boundary lubrication, thermal and oxidative stability of a fluorinated polyether and a perfluoropolyether triazine [ASLE PREPRINT 79-AM-18-1] p0088 A80-12089
- Development of improved-durability plasma sprayed ceramic coatings for gas turbine engines [AIAA PAPER 80-1193] p0089 A80-38963
- Uncertainties in predicting turbine blade metal temperatures [ASME PAPER 80-HT-25] p0027 A80-48014
- Comparison of the weight loss and adherence of nine different polyimide films thermally aged at 315 C and 350 C in air --- high temperature lubricants [NASA-TM-81381] p0086 N80-18183
- External fuel vaporization study, phase 1 [NASA-CR-159850] p0095 N80-25453
- Fuels research: Fuel thermal stability overview p0021 N80-29324
- Experimental study of turbine fuel thermal stability in an aircraft fuel system simulator p0043 N80-29325
- Determination of jet fuel thermal deposit rate using a modified JFTOT p0043 N80-29326
- Mechanisms of nitrogen heterocycle influence on turbine fuel stability p0043 N80-29327
- Low temperature fuel behavior studies p0044 N80-29330
- Influence of excess diamine on properties of PBR polyimide resins and composites [NASA-TM-81580] p0069 N80-29433
- THERMAL STRESSES**
- Feasibility study of silicon nitride regenerators [NASA-CR-159713] p0184 N80-25209
- THERMIONIC CONVERSION SYSTEMS**
- U THERMIONIC POWER GENERATION**
- THERMIONIC CONVERTERS**
- Experimental and theoretical investigation for the suppression of the planar arc drop in the thermionic converter [NASA-CR-159611] p0176 N80-12880
- Potentialities of TEC topping: A simplified view of parametric effects [NASA-TM-81468] p0175 N80-22083
- THERMIONIC POWER GENERATION**
- Comments on TEC trends [NASA-TM-79317] p0175 N80-16885
- Potentialities of TEC topping: A simplified view of parametric effects [NASA-TM-81468] p0175 N80-22083
- Optimal thermionic energy conversion with established electrodes for high-temperature topping and process heating --- coal combustion product environments [NASA-TM-81555] p0175 N80-33221
- THERMIONIC REACTORS**
- U ION ENGINES**
- THERMIONICS**
- Comments on TEC trends --- Thermionic Energy Conversion p0145 A80-39642
- Comments on TEC trends [NASA-TM-79317] p0175 N80-16885
- Thermionic cathode life test studies [NASA-TM-81441] p0101 N80-18302
- THERMOCHEMICAL PROPERTIES**
- NT HEAT OF COMBUSTION**
- NT HEAT OF FUSION**
- Characterization and properties of controlled nucleation thermochemical deposited /CNTD/ silicon carbide p0089 A80-13063
- THERMOCOUPLES**
- Thin film temperature sensor [NASA-CR-159782] p0112 N80-17425
- THERMODYNAMIC CYCLES**
- NT BRAYTON CYCLE**
- NT RANKINE CYCLE**
- NT STIRLING CYCLE**
- THERMODYNAMIC EFFICIENCY**
- Assessment of the state of technology of automotive Stirling engines [NASA-CR-159631] p0183 N80-13989
- Algorithm for calculating turbine cooling flow and the resulting decrease in turbine efficiency [NASA-TM-81453] p0163 N80-19863
- THERMODYNAMIC PROPERTIES**
- NT GIBBS FREE ENERGY**
- NT HEAT OF COMBUSTION**
- NT HEAT OF FUSION**
- NT SURFACE ENERGY**

SUBJECT INDEX

THRUST

- NT THERMAL EXPANSION
 NT THERMAL STABILITY
 NT THERMOCHEMICAL PROPERTIES
 NT THERMOPHYSICAL PROPERTIES
 A reduced volumetric expansion factor plot
 p0107 A80-10038
 Heat pipe cooling of power processing magnetics
 [ATAA PAPER 79-2082] p0107 A80-20960
 Micromechanics of intraply hybrid composites:
 Elastic and thermal properties p0070 A80-27994
 Micromechanics of intraply hybrid composites:
 Elastic and thermal properties p0067 N80-11143
 [NASA-TM-79253]
 Advanced screening of electrode couples
 [NASA-CR-159738] p0141 N80-22777
 CPE jet engine performance improvement program:
 High pressure turbine aerodynamic performance
 improvement p0040 N80-26302
 [NASA-CR-159832]
 Regenerator matrix physical property data
 [NASA-CR-159854] p0185 N80-30228
- THERMODYNAMICS**
 NT AEROTHERMODYNAMICS
 NT COMBUSTION PHYSICS
 Thermophysical property data - Who needs them ---
 similarity principle applications in fluid
 mechanics and heat transfer p0180 A80-18630
 [ASME PAPER 79-WA/HT-17]
 Comparative thermal analysis of alternate
 Cryogenic Fluid Management Experiment (CFME)
 configurations p0048 N80-32412
 [NASA-CR-165151]
- THERMOELASTICITY**
 The effects of strain and temperature on the
 dynamic properties of elastomers p0092 A80-15720
 [ASME PAPER 79-DET-57]
- THERMOELECTRIC CONVERSION SYSTEMS**
 U THERMOELECTRIC POWER GENERATION
THERMOELECTRIC GENERATORS
 Design study of a 15 kW free-piston Stirling
 engine-linear alternator for dispersed solar
 electric power systems p0150 N80-22787
 [NASA-CR-159587]
- THERMOELECTRIC POWER GENERATION**
 A cesium TELEC experiment at Lewis Research Center
 [NASA-CR-159729] p0113 N80-14386
 A 15kWe (nominal) solar thermal electric power
 conversion concept definition study: Steam
 Rankine reheat reciprocator system p0148 N80-16491
 [NASA-CR-159590]
 The 15 kW sub e (nominal) solar thermal electric
 power conversion concept definition study:
 Steam Rankine turbine system p0148 N80-16493
 [NASA-CR-159589]
 A 15 kWe (nominal) solar thermal-electric power
 conversion concept definition study: Steam
 Rankin reciprocator system p0149 N80-19612
 [NASA-CR-159591]
 Annual technical report, fiscal year 1979. Volume
 1: Executive summary p0149 N80-19632
 [NASA-CR-159715-VOL-1]
 Solar thermal power systems point-focusing
 distributed receiver technology project. Volume
 2: Detailed report p0151 N80-24751
 [NASA-CR-159715-VOL-2]
- THERMOGRAMS**
 U TEMPERATURE MEASURING INSTRUMENTS
THERMOMECHANICS
 U THERMODYNAMICS
THERMOMETRY
 U TEMPERATURE MEASUREMENT
THERMOPHYSICAL PROPERTIES
 NT HEAT OF FUSION
 NT TEMPERATURE DEPENDENCE
 NT THERMAL STABILITY
 Application of the principle of similarity fluid
 mechanics p0107 A80-10039
 Thermophysical property data - Who needs them ---
 similarity principle applications in fluid
 mechanics and heat transfer p0180 A80-18630
 [ASME PAPER 79-WA/HT-17]
- THERMOPHYSICS**
 U THERMODYNAMICS
THERMOSETTING RESINS
 NT EPOXY RESINS
 NT KEVLAR (TRADEMARK)
 NT PHENOLIC RESINS
- Synthesis of improved polyester resins
 [NASA-CR-159665] p0090 N80-13257
- THERMOSTABILITY**
 U THERMAL STABILITY
THERMOGRAPHY
 U ANISOTROPY
 U TEMPERATURE EFFECTS
THICK FILMS
 Thick ceramic coating development for industrial
 gas turbines - A program plan p0091 A80-10042
 [SR79-A-4702-05]
- THICKNESS RATIO**
 Physical phenomena in mercury ion thrusters
 [NASA-CR-159784] p0061 N80-17137
- THIN BODIES**
 Finite-strain large-deflection
 elastic-viscoplastic finite-element transient
 response analysis of structures p0134 N80-29762
 [NASA-CR-159874]
- THIN FILMS**
 NT ENERGY ABSORPTION FILMS
 Thin film temperature sensor
 [NASA-CR-159782] p0112 N80-17425
 Tribological properties of sputtered MoS sub 2
 films in relation to film morphology p0078 N80-21490
 [NASA-TM-81465]
 Coplanar back contacts for thin silicon solar cells
 [NASA-CR-159811] p0153 N80-28860
 Thin n-i-p radiation-resistant solar cell
 feasibility study p0154 N80-29852
 [NASA-CR-159871]
- THREE DIMENSIONAL FLOW**
 NT SECONDARY FLOW
 Computation of three-dimensional flow in turbofan
 mixers and comparison with experimental data
 [ATAA PAPER 80-0227] p0003 A80-20967
 Numerical simulation of supersonic inlets using a
 three-dimensional viscous flow analysis p0003 A80-20969
 [ATAA PAPER 80-0384]
 Computation of three-dimensional viscous
 supersonic flow in inlets p0065 A80-23941
 [ATAA PAPER 80-0194]
 Impact of new instrumentation on advanced turbine
 research p0112 A80-36155
- A three-dimensional turbulent compressible
 subsonic duct flow analysis for use with
 constructed coordinate systems p0006 A80-41601
 [ATAA PAPER 80-1398]
 Numerical calculation of transonic axial
 turbomachinery flows p0004 A80-44229
- An efficient user-oriented method for calculating
 compressible flow in an about three-dimensional
 inlets --- panel method p0004 N80-10134
 [NASA-CR-159578]
 Development of a three-dimensional supersonic
 inlet flow analysis p0108 N80-14356
 [NASA-CR-3218]
 Computation of three-dimensional flow in turbofan
 mixers and comparison with experimental data
 [NASA-TM-81410] p0104 N80-15364
 Numerical simulation of supersonic inlets using a
 three-dimensional viscous flow analysis p0104 N80-15365
 [NASA-TM-81411]
 Three dimensional mean flow and turbulence
 characteristics of the near wake of a compressor
 rotor blade p0005 N80-27288
 [NASA-CR-159518]
 Influence of pressure driven secondary flows on
 the behavior of turbofan forced mixers
 [NASA-TM-81541] p0105 N80-27632
 Calculation of water drop trajectories to and
 about arbitrary three-dimensional bodies in
 potential airflow p0005 N80-28302
 [NASA-CR-3291]
 General design method for three-dimensional
 potential flow fields. 1: Theory p0005 N80-29251
 [NASA-CR-3288]
- WIND: Computer program for calculation of three
 dimensional potential compressible flow about
 wind turbine rotor blades p0003 N80-33357**
 [NASA-TP-1729]
- THREE DIMENSIONAL MOTION**
 NT SECONDARY FLOW
 NT THREE DIMENSIONAL FLOW
THRUST
 NT JET THRUST
 NT LOW THRUST

THRUST AUGMENTATION

NT ROCKET THRUST
Liquid oxygen/liquid hydrogen auxiliary power
system thruster investigation
[NASA-CR-159674] p0062 N80-15202

THRUST AUGMENTATION
Coannular supersonic ejector nozzles p0002 N80-10128
Method and apparatus for rapid thrust increases in
a turbofan engine p0016 N80-18039
[NASA-CASE-LEW-12971-1]
Effect of water injection and off scheduling of
variable inlet guide vanes, gas generator speed
and power turbine nozzle angle on the
performance of an automotive gas turbine engine
[NASA-TM-81415] p0016 N80-20272

THRUST CHAMBER PRESSURE
Cooling of high pressure rocket thrust chambers
with liquid oxygen
[AIAA PAPER 80-1260] p0060 A80-38992

THRUST CHAMBERS
Performance of a transpiration-regenerative cooled
rocket thrust chamber p0061 N80-14189
[NASA-CR-159742]
Cooling of high pressure rocket thrust chambers
with liquid oxygen
[NASA-TM-81503] p0057 N80-23365

THRUST CONTROL
Identification and dual adaptive control of a
turbojet engine p0023 A80-10033

THRUST DISTRIBUTION
Auxiliary control of LSS p0063 N80-31459

THRUST POWER
U THRUST

THRUST REVERSAL
Quiet Clean Short-Haul Experimental Engine (QCSEE)
acoustic and aerodynamic tests on a scale model
over-the-wing thrust reverser and forward thrust
nozzle
[NASA-CR-135254] p0028 N80-14115
Reverse thrust performance of the QCSEE variable
pitch turbofan engine
[NASA-TM-81558] p0022 N80-31399

THRUST-WEIGHT RATIO
Preliminary study of VTO thrust requirements for a
V/STOL aircraft with lift plus lift/cruise
propulsion
[NASA-TM-81425] p0016 N80-19110

THRUSTORS
U ROCKET ENGINES

TILT MOTOR AIRCRAFT
Quiet powered-lift propulsion
[NASA-CP-2077] p0015 N80-15127

TIME DEPENDENCE
Time-dependent difference theory for noise
propagation in a two-dimensional duct
[AIAA PAPER 80-0098] p0170 A80-18269
Predicting the time-temperature dependent axial
failure of B/AI composites p0071 A80-35494
Time-dependent difference theory for noise
propagation in a two-dimensional duct --- of a
turbofan engine
[NASA-TM-79298] p0167 N80-12822
A time dependent difference theory for sound
propagation in ducts with flow ---
characteristic of inlet and exhaust ducts of
turbofan engines
[NASA-TM-79302] p0167 N80-12823
Predicting the time-temperature dependent axial
failure of B/AI composites
[NASA-TM-81474] p0069 N80-21452
Finite-strain large-deflection
elastic-viscoplastic finite-element transient
response analysis of structures
[NASA-CR-159874] p0134 N80-29762

TIME DIVISION MULTIPLE ACCESS
An advanced mixed user domestic satellite system
architecture
[AIAA 80-0494] p0099 A80-29544
The 30/20 GHz mixed user architecture development
study
[NASA-CR-159686] p0097 N80-10415
The 30/20 GHz mixed user architecture development
study: Executive summary
[NASA-CR-159687] p0097 N80-10416

TIPS
NT BLADE TIPS

SUBJECT INDEX

TIRES
NT AIRCRAFT TIRES
TISSUES (BIOLOGY)
NT PERITONEUM
TITAN CENTAUR LAUNCH VEHICLE
Wind tunnel investigation of the Titan Forward
Skirt compartment vent from a free-stream Mach
number of 0.80 to 1.96 --- conducted in the
Lewis Research Center 8 by 6 foot supersonic
wind tunnel
[NASA-TM-81572] p0106 N80-32689

TITANIUM ALLOYS
Fatigue behavior of SiC reinforced titanium
composites p0070 A80-10036
Elevated temperature flow strength, creep
resistance and diffusion welding characteristics
of Ti-6Al-2Nb-1Ta-0.8Mo p0081 A80-13277

TITANIUM CARBIDES
Improved refractory coatings and method of
producing the same
[NASA-CASE-LEW-13169-1] p0076 N80-14232

TITANIUM COMPOUNDS
NT TITANIUM CARBIDES
TOLERANCES (PHYSIOLOGY)
NT RADIATION TOLERANCE
TONOMETRY
U INTRAOCULAR PRESSURE
U PRESSURE MEASUREMENTS
TOROIDAL PLASMAS
The effect of a weak vertical magnetic field on
fluctuation-induced transport in a Bumpy-Torus
plasma p0176 A80-25476

TOROIDS
Toroidal cell and battery --- energy storage for
orbital space applications or power cells for
electric vehicles
[NASA-CASE-LEW-12918-1] p0144 N80-33857

TORQUE
Balancing of a power-transmission shaft with the
application of axial torque
[ASME PAPER 80-GT-143] p0121 A80-42256
Torquing and electrostatic deformation of the
solar sail p0065 A80-46901

TORQUE CONVERTERS
Design study of toroidal traction CVT for electric
vehicles
[NASA-CR-159803] p0124 N80-25661
Small passenger car transmission test-Chevrolet
200 transmission
[NASA-CR-159835] p0185 N80-28255
Small passenger car transmission test; Ford C4
transmission
[NASA-CR-159881] p0128 N80-31795

TORSIONAL VIBRATION
Field verification of lateral-torsional coupling
effects on rotor instabilities in centrifugal
compressors p0125 N80-29708
Influence of mistuning on blade torsional flutter
[NASA-CR-165137] p0005 N80-31351

TOWERS
Some techniques for reducing the tower shadow of
the DOE/NASA mod-0 wind turbine tower --- wind
tunnel tests to measure effects of tower
structure on wind velocity
[NASA-TM-79202] p0137 N80-10594

TOWNSEND DISCHARGE
NT GAS DISCHARGES

TOXIC HAZARDS
Assessment of potential exposure to friable
insulation materials containing asbestos
[NASA-TM-81435] p0157 N80-23875

TRACE ELEMENTS
Effect of sodium, potassium, magnesium, calcium,
and chlorine on the high temperature corrosion
of IN-100, U-700, IN-792, and MAR M-509
[ASME PAPER 80-GT-150] p0083 A80-42262

TRACKING (POSITION)
Dynamic response to rotating-seat runout in
non-contacting face seals
[NASA-TM-81490] p0117 N80-22701

TRACKING STUDIES
U TRACKING (POSITION)

TRACTION
Constrained fatigue life optimization of a

NASVYTIS multiroller traction drive
p0122 A80-46407

Evaluation of a high performance fixed-ratio traction drive
p0122 A80-46410

Simplified fatigue life analysis for traction drive contacts
p0123 A80-46413

Simplified fatigue life analysis for traction drive contacts
[NASA-TM-79199]
p0115 N80-17469

Evaluation of a high performance fixed-ratio traction drive
[NASA-TM-81425]
p0115 N80-18404

Constrained fatigue life optimization of a NASVYTIS multiroller traction drive
[NASA-TM-81447]
p0116 N80-18407

TRAFFIC CONTROL
A new traffic control design method for large networks with signalized intersections
p0183 A80-14841

TRAJECTORIES
NT ELECTRON TRAJECTORIES

TRAJECTORY ANALYSIS
A. Analytical prediction and experimental verification of TWT and depressed collector performance using multidimensional computer programs
p0102 A80-13902

A matrix solution for the simulation of magnetic fields with ideal current loops
p0102 A80-13903

Calculation of water drop trajectories to and about arbitrary three-dimensional bodies in potential airflow
[NASA-CR-3291]
p0005 N80-28302

TRANSDUCERS
NT PRESSURE SENSORS
NT ULTRASONIC WAVE TRANSDUCERS

TRANSFER ORBITS
Upper stages utilizing electric propulsion
p0059 A80-29989

Orbital transfer of large space structures with nuclear electric rockets
[AAS PAPER 80-083]
p0054 A80-41897

Analysis of GaAs and Si solar cell arrays for earth orbital and orbit transfer missions
[NASA-TM-81383]
p0056 N80-15204

Upper stages utilizing electric propulsion
[NASA-TM-81412]
p0056 N80-16097

TRANSFORMERS
Heat pipe cooling of power processing magnetics
[AIAA PAPER 79-2082]
p0107 A80-20960

Heat pipe cooled power magnetics
[NASA-CR-159659]
p0103 N80-13362

Study of power management technology for orbital multi-100Kw applications. Volume 2: Study results
[NASA-CR-159834-VOL-2]
p0153 N80-28862

TRANSIENT LOADS
NT IMPACT LOADS

TRANSIENT PRESSURES
Measuring unsteady pressure on rotating compressor blades --- with semiconductor strain gages under gas turbine engine operating conditions
p0110 A80-12630

TRANSIENT RESPONSE
Two-dimensional finite-element analyses of simulated rotor-fragment impacts against rings and beams compared with experiments
[NASA-CR-159645]
p0038 N80-22323

Static and transient performance of YF-102 engine with up to 14 percent core airbleed for the quiet short-haul research aircraft
[NASA-TP-1692]
p0020 N80-25339

Instructions for the use of the CIVM-Jet 4C finite-strain computer code to calculate the transient structural responses of partial and/or complete arbitrarily-curved rings subjected to fragment impact
[NASA-CR-159873]
p0134 N80-27720

TRANSITION METALS
NT CADMIUM
NT CHROMIUM
NT IRON
NT TUNGSTEN
NT VANADIUM
NT YTTRIUM
NT ZIRCONIUM

TRANSLATIONAL MOTION
NT SECONDARY FLOW
NT THREE DIMENSIONAL FLOW

TRANSMISSION
NT ACOUSTIC PROPAGATION
NT DATA TRANSMISSION
NT ELECTRIC POWER TRANSMISSION
NT FREQUENCY DIVISION MULTIPLE ACCESS
NT HEAT TRANSFER
NT MICROWAVE TRANSMISSION
NT MULTIPLEXING
NT SATELLITE TRANSMISSION
NT SOUND TRANSMISSION
NT WAVE PROPAGATION

TRANSMISSION EFFICIENCY
Small passenger car transmission test; Ford C4 transmission
[NASA-CR-159881]
p0128 N80-31795

Small passenger car transmission test; Chevrolet LUV transmission
[NASA-CR-159882]
p0128 N80-31796

TRANSMISSIONS (MACHINE ELEMENTS)
NASA gear research and its probable effect on rotorcraft transmission design
p0120 A80-13068

Load support system analysis high speed input pinion configuration
[ASME PAPER 79-LUB-34]
p0129 A80-14760

Evaluation of a high performance fixed-ratio traction drive
[NASA-TM-81425]
p0115 N80-18404

An automatically-shifted two-speed transaxle system for an electric vehicle
[NASA-CR-159746]
p0184 N80-18992

Parametric tests of a traction drive retrofitted to an automotive gas turbine
[NASA-TM-81457]
p0117 N80-21754

Design study of flat belt CVT for electric vehicles
[NASA-CR-159822]
p0124 N80-22702

Conceptual design study of an improved automotive gas turbine powertrain
[NASA-CR-159672]
p0124 N80-24621

Design study of toroidal traction CVT for electric vehicles
[NASA-CR-159803]
p0124 N80-25661

Small passenger car transmission test-Chevrolet 200 transmission
[NASA-CR-159835]
p0185 N80-28255

Small passenger car transmission test; Ford C4 transmission
[NASA-CR-159881]
p0128 N80-31795

Small passenger car transmission test; Chevrolet LUV transmission
[NASA-CR-159882]
p0128 N80-31796

Design study of steel V-Belt CVT for electric vehicles
[NASA-CR-159845]
p0185 N80-32299

TRANSONIC COMPRESSORS
Comparison between optical measurements and a numerical solution of the flow field within a transonic axial-flow compressor rotor
[AIAA PAPER 80-1078]
p0003 A80-38897

Experimental study of low aspect ratio compressor blading
[NASA-TM-79280]
p0002 N80-11037

Laser anemometer measurements in a transonic axial flow compressor rotor
[NASA-TM-79323]
p0002 N80-14050

TRANSONIC FLOW
Evaluation of a strained-coordinate perturbation procedure - Nonlinear subsonic and transonic flows
[AIAA PAPER 80-0339]
p0006 A80-18324

Laser anemometer measurements in a transonic axial flow compressor rotor
p0111 A80-36141

Results from tests on a high work transonic turbine for an energy efficient engine
[ASME PAPER 80-GT-146]
p0026 A80-42258

An implicit finite-difference code for inviscid and viscous cascade flow
[AIAA PAPER 80-1427]
p0007 A80-44128

Numerical calculation of transonic axial turbomachinery flows
p0004 A80-44229

CAS2D: FORTRAN program for nonrotating blade-to-blade, steady, potential transonic cascade flows
[NASA-TP-1705]
p0003 N80-27284

TRANSONIC INLETS

Numerical calculation of transonic axial
turbomachinery flows
[NASA-TM-81544] p0020 N80-27363

TRANSONIC INLETS

U SUPERSONIC INLETS

TRANSONIC TURBINES

U SUPERSONIC TURBINES

TRANSONICS

U TRANSONIC FLOW

TRANSPIRATION COOLING

U SWEAT COOLING

TRANSPORT AIRCRAFT

NT BOEING 747 AIRCRAFT

NT DC 9 AIRCRAFT

NT DC 10 AIRCRAFT

NT LIGHT TRANSPORT AIRCRAFT

NT SHORT HAUL AIRCRAFT

NT YC-14 AIRCRAFT

TRANSPORT COEFFICIENTS

U TRANSPORT PROPERTIES

TRANSPORT PROPERTIES

NT ELECTRICAL RESISTIVITY

NT IONIC MOBILITY

NT VISCOSITY

Comments on 'Experimental evidence for
interhemispheric transport from airborne carbon
monoxide measurements'

p0159 A80-32520

TRANSPORTATION

NT AIR TRANSPORTATION

NT SPACE TRANSPORTATION SYSTEM

NT URBAN TRANSPORTATION

TRAPPED PARTICLES

NT MAGNETICALLY TRAPPED PARTICLES

TRAPPING

NT CRYOTRAPPING

TRAVELING WAVE TUBES

Analytical prediction and experimental
verification of TWT and depressed collector
performance using multidimensional computer
programs

p0102 A80-13902

90- to 93-percent efficient collector for
operation of a dual-mode traveling-wave tube in
the linear region

p0102 A80-13909

How to quickly predict the overall TWT and the
multistage depressed collector efficiency

p0102 A80-31759

Improved traveling wave tubes --- for ECM systems

p0102 A80-44235

Thermionic cathode life test studies

[NASA-TM-81441]

p0101 N80-18302

Coupled cavity traveling wave tube with velocity
tapering

[NASA-CASE-LEW-12296-1]

p0101 N80-19425

Multistage depressed collector with efficiency of
90 to 94 percent for operation of a dual-mode
traveling wave tube in the linear region

[NASA-TP-1670]

p0101 N80-21669

Improved traveling wave tubes

[NASA-TM-81479]

p0102 N80-22598

TRIBOLOGY

Effect of thermal aging on the tribological

properties of polyimide films and

polyimide-bonded graphite fluoride films

[ASLE PREPRINT 79-AM-3B-1]

p0088 A80-12094

Metal-dielectric interactions

p0081 A80-13067

Elastohydrodynamic film thickness measurements of
artificially-produced nonsmooth surfaces

[ASLE PREPRINT 79-IC-1A-3]

p0102 A80-14720

Tribological properties of sputtered MoS₂ films in
relation to film morphology

p0089 A80-35502

Mechanisms of lubrication and wear of a bonded
solid-lubricant film

[ASLE PREPRINT 80-AM-3E-1]

p0122 A80-43163

Comparison of the tribological properties at 25 C
of seven different polyimide films bonded to 301
stainless steel

[NASA-TM-81413]

p0086 N80-19263

Tribological properties of sputtered MoS₂ sub 2
films in relation to film morphology

[NASA-TM-81465]

p0078 N80-21490

Friction and wear of iron-base binary alloys in
sliding contact with silicon carbide in vacuum

[NASA-TP-1612]

p0087 N80-22494

SUBJECT INDEX

TRIGGERS

U ACTUATORS

TRIPROPELLANTS

U LIQUID ROCKET PROPELLANTS

TROPOPAUSE

Sulfate and nitrate collected by filter sampling

near the tropopause

[NASA-TP-1567]

p0157 N80-14581

TRUNNIONS

U SHAFTS (MACHINE ELEMENTS)

TUBING

U PIPES (TUBES)

TUMORS

NT CANCER

TUNGSTEN

Life test studies on tungsten impregnated cathodes

p0103 A80-45122

Effect of W and WC on the oxidation resistance of

yttria-doped silicon nitride

p0090 A80-46099

Effect of W and WC on the oxidation resistance of

yttria-doped silicon nitride

[NASA-TM-81529]

p0087 N80-27483

Tungsten wire/FeCrAl matrix turbine blade

fabrication study

[NASA-CR-159788]

p0044 N80-29331

TUNGSTEN CARBIDES

Effect of W and WC on the oxidation resistance of

yttria-doped silicon nitride

p0090 A80-46099

Effect of W and WC on the oxidation resistance of

yttria-doped silicon nitride

[NASA-TM-81529]

p0087 N80-27483

TUNGSTEN COMPOUNDS

NT TUNGSTEN CARBIDES

TUNING

Influence of mistuning on blade torsional flutter

[NASA-CR-165137]

p0005 N80-31351

TURBINE BLADES

Numerical calculation of steady inviscid full
potential compressible flow about wind turbine
blades

[AIAA 80-0607]

p0145 A80-28804

Digital system for dynamic turbine engine blade

displacement measurements

p0111 A80-36151

An experimental investigation of endwall profiling

in a turbine vane cascade

[AIAA PAPER 80-1089]

p0004 A80-38904

Development of exothermically cast single-crystal

Mar-M 247 and derivative alloys

[AIBESARCH-21-3469]

p0084 A80-45825

Uncertainties in predicting turbine blade metal

temperatures

[ASME PAPER 80-HT-25]

p0027 A80-48014

Characterization of an oxide dispersion

strengthened superalloy, MA-6000E, for turbine

blade applications --- turbine blade

[NASA-CR-159493]

p0083 N80-13218

Quiet Clean Short-haul Experimental Engine (QCSEE)

under-the-wing engine composite fan blade design

report

[NASA-CR-135046]

p0031 N80-15108

Computer program for generating input for analysis

of impingement-cooled, axial-flow turbine blade

[NASA-TP-1603]

p0104 N80-15361

Evaluation of feasibility of prestressed concrete

for use in wind turbine blades

[NASA-CR-159725]

p0147 N80-15553

Structural analysis considerations for wind

turbine blades

p0139 N80-16469

Blade design and operating experience on the

MOD-OA 200 kW wind turbine at Clayton, New Mexico

[NASA-TP-1603]

p0139 N80-16470

Design, fabrication, and test of a steel spar wind

turbine blade

p0139 N80-16472

Prediction method for two-dimensional aerodynamic

losses of cooled vanes using integral

boundary-layer parameters

[NASA-TP-1623]

p0002 N80-17030

Effects of a ceramic coating on metal temperatures

of an air-cooled turbine vane

[NASA-TP-1598]

p0105 N80-17397

Design, fabrication, test, and evaluation of a

prototype 150-foot long composite wind turbine

blade

[NASA-CR-159775]

p0148 N80-17548

SUBJECT INDEX

TURBINES

Internal coating of air cooled gas turbine blades
[NASA-CR-159701] p0036 N80-18041

Numerical calculation of steady inviscid full potential compressible flow about wind turbine blades
[NASA-TM-81438] p0136 N80-18497

Analysis of uncertainties in turbine metal temperature predictions
[NASA-TP-1593] p0017 N80-21326

Program for impact testing of spar-shell fan blades, test report
[NASA-CR-135393] p0037 N80-21328

Thermal fatigue and oxidation data for directionally solidified MAR-M 246 turbine blades
[NASA-CR-159798] p0037 N80-21330

Similarity tests of turbine vanes, effects of ceramic thermal barrier coatings
[NASA-TM-81473] p0105 N80-21706

Advanced ceramic material for high temperature turbine tip seals
[NASA-CR-159774] p0038 N80-22325

Nonlinear, three-dimensional finite-element analysis of air-cooled gas turbine blades
[NASA-TP-1669] p0132 N80-22734

Significance of thermal contact resistance in two-layer thermal-barrier-coated turbine vanes
[NASA-TM-81483] p0018 N80-23310

Fully plasma-sprayed compliant backed ceramic turbine seal
[NASA-CASE-LEW-13268-1] p0117 N80-24619

Computerized video densitometry method for rapid analysis of infrared photographic images --- temperature distribution across a turbine blade
[NASA-TP-1686] p0110 N80-25635

Nonlinear aeroelastic equations of motion of twisted, nonuniform, flexible horizontal-axis wind turbine blades
[NASA-CR-159502] p0152 N80-26774

Comparison of elastic and elastic-plastic structural analyses for cooled turbine blade airfoils
[NASA-TP-1679] p0132 N80-27719

Tungsten wire/FeCrAlY matrix turbine blade fabrication study
[NASA-CR-159788] p0044 N80-29331

WIND: Computer program for calculation of three dimensional potential compressible flow about wind turbine rotor blades
[NASA-TP-1729] p0003 N80-33357

Experimental performance and analysis of 15.04-centimeter-tip-diameter, radial-inflow turbine with work factor of 1.126 and thick blading
[NASA-TP-1730] p0023 N80-33410

TURBINE ENGINES

NT DUCTED FAN ENGINES

NT GAS TURBINE ENGINES

NT JET ENGINES

NT SUPERSONIC COMBUSTION RAMJET ENGINES

NT T-63 ENGINE

NT TURBOFAN ENGINES

NT TURBOJET ENGINES

NT TURBOPROP ENGINES

Turbine engine altitude chamber and flight testing with liquid hydrogen
p0023 N80-10034

Aeropropulsion 1979 --- conferences
[NASA-CR-2092] p0012 N80-10205

Materials and structures technology
p0012 N80-10210

Turbomachinery technology
p0012 N80-10212

Mechanical components
p0013 N80-10213

Development of improved high pressure turbine outer gas path seal components --- abrasability and thermal cycling test results
[NASA-CR-159801] p0038 N80-21332

Application of superalloy powder metallurgy for aircraft engines
[NASA-TM-81466] p0078 N80-21488

New opportunities for future, small, General-Aviation Turbine Engines (GATE)
p0017 N80-22335

CF6 jet engine performance improvement program: High pressure turbine aerodynamic performance improvement
[NASA-CR-159832] p0040 N80-26302

Composite seal for turbomachinery
[NASA-CASE-LEW-12131-2] p0118 N80-26658

Materials for advanced turbine engines. Volume 1: Power metallurgy Rene 95 rotating turbine engine parts
[NASA-CR-159802] p0084 N80-28499

NASA/General Electric broad-specification fuels combustion technology program, phase 1
p0042 N80-29316

Experimental study of turbine fuel thermal stability in an aircraft fuel system simulator
p0043 N80-29325

Mechanisms of nitrogen heterocycle influence on turbine fuel stability
p0043 N80-29327

Description of the warm core turbine facility recently installed at NASA Lewis Research Center
[NASA-TM-81562] p0022 N80-29333

TURBINE INSTRUMENTS

Laser-optical blade tip clearance measurement system
p0111 N80-36137

Impact of new instrumentation on advanced turbine research
p0112 N80-36155

Temperature and pressure measurement techniques for an advanced turbine test facility
p0112 N80-36157

Phase-locked telemetry system for rotary instrumentation of turbomachinery, phase 1
[NASA-CR-159453] p0029 N80-14182

TURBINE PUMPS

Supercharged topping rocket propellant feed system
[NASA-CASE-XLE-02062-1] p0056 N80-14188

Small, high pressure liquid hydrogen turbopump
[NASA-CR-159821] p0125 N80-26662

TURBINE WHEELS

Development of a high strength hot isostatically pressed /HIP/ disk alloy, MERL 76
p0084 N80-44108

Evaluation of the cyclic behavior of aircraft turbine disk alloys, part 2
[NASA-CR-165123] p0084 N80-30482

TURBINES

NT AXIAL FLOW TURBINES

NT GAS TURBINES

NT SHROUDED TURBINES

NT STEAM TURBINES

NT SUPERSONIC TURBINES

NT TWO STAGE TURBINES

An exploratory survey of noise levels associated with a 100 kW wind turbine
p0171 N80-35499

The use of wind data with an operational wind turbine in a research and development environment
p0145 N80-35730

Significance of thermal contact resistance in two-layer, thermal-barrier-coated turbine vanes
p0024 N80-39635

Effect of sodium, potassium, magnesium, calcium, and chlorine on the high temperature corrosion of IN-100, U-700, IN-792, and MAR M-509
[ASME PAPER 80-GT-150] p0083 N80-42262

Improving the stress rupture and creep of silicon nitride --- turbine materials
[NASA-CR-159585] p0072 N80-10318

Some techniques for reducing the tower shadow of the DOE/NASA mod-0 wind turbine tower --- wind tunnel tests to measure effects of tower structure on wind velocity
[NASA-TM-79202] p0137 N80-10594

Executive summary: Mod-1 wind turbine generator analysis and design report
[NASA-CR-159497] p0147 N80-11558

Design evolution of large wind turbine generators
p0139 N80-16455

Preliminary analysis of performance and loads data from the 2-megawatt mod-1 wind turbine generator
[NASA-TM-81408] p0139 N80-16494

An exploratory survey of noise levels associated with a 100kW wind turbine
[NASA-TM-81486] p0169 N80-23102

Mod-1 wind turbine generator analysis and design report, volume 1
[NASA-CR-159495] p0150 N80-23775

Mod-2 wind turbine system concept and preliminary design report. Volume 1: Executive summary
[DOE/NASA/0002-80/2] p0151 N80-24758

Design and cold-air test of single-stage uncooled turbine with high work output

[NASA-TP-1680] p0019 N80-25337
Cold-air investigation of a 4 1/2 stage turbine
with stage-loading factor of 4.66 and high
specific work output. 2: Stage group performance
[NASA-TP-1688] p0019 N80-25338
A calculation procedure for viscous flow in
turbomachines, volume 3 --- computer programs
[NASA-CR-159864] p0005 N80-26274
Three dimensional finite-element elastic analysis
of a thermally cycled double-edge wedge geometry
specimen --- nickel alloy turbine parts
[NASA-TN-80980] p0079 N80-26433
Nonlinear aeroelastic equations of motion of
twisted, nonuniform, flexible horizontal-axis
wind turbine blades
[NASA-CR-159502] p0152 N80-26774
MOD-2 wind turbine system concept and preliminary
design report. Volume 2: Detailed report
[DOE/NASA/0002-80/2] p0152 N80-26775
Feasibility study of aileron and spoiler control
systems for large horizontal axis wind turbines
[NASA-CR-159856] p0153 N80-27803
Evaluation of instability forces of labyrinth
seals in turbines or compressors
p0126 N80-29715
Development of procedures for calculating
stiffness and damping of elastomers in
engineering applications, part 7
[NASA-CR-165138] p0128 N80-32718

TURBOCHARGERS
U SUPERCHARGERS
U TURBOCOMPRESSORS
TURBOCOMPRESSORS
Comparison between optical measurements and a
numerical solution of the flow field within a
transonic axial-flow compressor rotor
[AIAA PAPER 80-1078] p0003 A80-38897
Experimental study of low aspect ratio compressor
blading
[NASA-TN-79280] p0002 N80-11037
Laser anemometer measurements in a transonic axial
flow compressor rotor
[NASA-TN-79323] p0002 N80-14050
Modification of axial compressor streamline
program for analysis of engine test data
[NASA-TN-79312] p0002 N80-14051
Diesel engine catalytic combustor system ---
turbocharging
[NASA-CASE-LEW-12995-1] p0118 N80-26659
Three dimensional mean flow and turbulence
characteristics of the near wake of a compressor
rotor blade
[NASA-CR-159518] p0005 N80-27288

TURBOCONVERTERS
U TURBOGENERATORS
TURBOELECTRIC CONVERSION
U TURBOGENERATORS
TURBOFAN ENGINES
Computation of three-dimensional flow in turbofan
mixers and comparison with experimental data
[AIAA PAPER 80-0227] p0003 A80-20967
Scale model performance test investigation of
exhaust system mixers for an Energy Efficient
Engine /E3/ propulsion system
[AIAA PAPER 80-0229] p0024 A80-20968
Status of NASA full-scale engine aeroelasticity
research
p0133 A80-35906
Temperature and pressure measurement techniques
for an advanced turbine test facility
p0112 A80-36157
Advanced component technologies for
energy-efficient turbofan engines
[AIAA PAPER 80-1086] p0025 A80-38902
Experimental evaluation of exhaust mixers for an
Energy Efficient Engine
[AIAA PAPER 80-1088] p0025 A80-38903
Far-field radiation of APT turbofan noise
p0025 A80-39638
Fuel conservation through active control of rotor
clearances
[AIAA PAPER 80-1087] p0045 A80-41506
Influence of pressure driven secondary flows on
the behavior of turbofan forced mixers
[AIAA PAPER 80-1198] p0025 A80-41515
Results from tests on a high work transonic
turbine for an energy efficient engine
[ASME PAPER 80-GT-146] p0026 A80-42258

CF6 fan performance improvement
[ASME PAPER 80-GT-178] p0026 A80-42284
Uncertainties in predicting turbine blade metal
temperatures
[ASME PAPER 80-HT-25] p0027 A80-48014
Design, durability and low cost processing
technology for composite fan exit guide vanes
[NASA-CR-159677] p0027 N80-12091
Time-dependent difference theory for noise
propagation in a two-dimensional duct --- of a
turbofan engine
[NASA-TN-79298] p0167 N80-12822
A time dependent difference theory for sound
propagation in ducts with flow ---
characteristic of inlet and exhaust ducts of
turbofan engines
[NASA-TN-79302] p0167 N80-12823
Quiet Clean Short-Haul Experimental Engine (QCSEE)
Over-The-Wing (OTW) propulsion system test
report. Volume 2: Aerodynamics and performance
--- engine performance tests to define
propulsion system performance on turbofan engines
[NASA-CR-135324] p0029 N80-14120
Static test-stand performance of the YF-102
turbofan engine with several exhaust
configurations for the Quiet Short-Haul Research
Aircraft (CSRA)
[NASA-TP-1556] p0014 N80-14121
The CF6 jet engine performance improvement: New
front mount
[NASA-CR-159639] p0029 N80-14127
Study of turboprop systems reliability and
maintenance costs
[NASA-CR-135192] p0029 N80-14129
Abradable compressor and turbine seals, volume 1
--- for turbofan engines
[NASA-CR-159600] p0083 N80-14235
Quiet Clean Short-haul Experimental Engine (QCSEE)
Over The Wing (OTW) design report
[NASA-CR-134848] p0034 N80-15086
Quiet Clean Short-haul Experimental Engine (QCSEE)
preliminary under the wing flight propulsion
system analysis report
[NASA-CR-134868] p0034 N80-15088
Computation of three-dimensional flow in turbofan
mixers and comparison with experimental data
[NASA-TN-81410] p0104 N80-15364
Core noise investigation of the CF6-50 turbofan
engine
[NASA-CR-159598] p0036 N80-16061
Core noise investigation of the CF6-50 turbofan
engine
[NASA-CR-159749] p0036 N80-16062
Method and apparatus for rapid thrust increases in
a turbofan engine
[NASA-CASE-LEW-12971-1] p0016 N80-18039
Application of composite materials to turbofan
engine fan exit guide vanes
[NASA-TN-81432] p0068 N80-18106
Experimental evaluation of a spinning-mode
acoustic-treatment design concept for aircraft
inlets --- suppression of YF-102 engine fan noise
[NASA-TP-1613] p0016 N80-21323
Analysis of uncertainties in turbine metal
temperature predictions
[NASA-TP-1593] p0017 N80-21326
Airsearch QCGAT program --- quiet clean general
aviation turbofan engines
[NASA-CR-159758] p0037 N80-21331
Avco Lycoming quiet clean general aviation
turbofan engine
p0039 N80-22333
Summary of NASA QCGAT program
p0017 N80-22334
CF6 jet engine performance improvement: New fan
[NASA-CR-159699] p0039 N80-23309
Status of NASA full-scale engine aeroelasticity
research
[NASA-TN-81500] p0132 N80-23678
Far-field radiation of aft turbofan noise
[NASA-TN-81506] p0166 N80-24129
Advanced component technologies for
energy-efficient turbofan engines
[NASA-TN-81507] p0019 N80-24316
Static and transient performance of YF-102 engine
with up to 14 percent core airbleed for the
quiet short-haul research aircraft
[NASA-TP-1692] p0020 N80-25339

SUBJECT INDEX

TURBOMACHINE BLADES

- Off-design correlation for losses due to part-span dampers on transonic rotors
[NASA-TP-1693] p0020 N80-28352
- Quiet Clean Short-haul Experimental Engine (QCSEE) Under-The-Wing (UTW) composite Macelle test report. Volume 2: Acoustic performance
[NASA-CR-159472] p0044 N80-29297
- Acoustic performance of a 50.8-cm (20-inch) diameter variable-pitch fan and inlet. Volume 2: Acoustic data
[NASA-CR-135118] p0044 N80-29299
- NASA broadened-specification fuels combustion technology program
p0021 N80-29313
- Investigation of performance deterioration of the CF6/JT9D, high-bypass ratio turbofan engines
[NASA-TM-81552] p0022 N80-29332
- Influence of mistuning on blade torsional flutter
[NASA-CR-165137] p0005 N80-31351
- Reverse thrust performance of the QCSEE variable pitch turbofan engine
[NASA-TM-81558] p0022 N80-31399
- Improved components for engine fuel savings
[NASA-TM-81577] p0023 N80-31402
- Effects of axisymmetric contractions on turbulence of various scales
[NASA-CR-165136] p0006 N80-32328
- Performance deterioration of commercial high-bypass ratio turbofan engines
[NASA-TM-81552-REV] p0023 N80-32394
- The energy efficient engine project
[NASA-TM-81566] p0023 N80-32395
- TURBOPANS**
- Effect of inflow control on inlet noise of a cut-on fan
[AIAA PAPER 80-1049] p0171 A80-35993
- Comparison of several inflow control devices for flight simulation of fan tone noise using a JT15D-1 engine
[AIAA PAPER 80-1025] p0025 A80-38640
- CF6 fan performance improvement
[ASME PAPER 80-GT-178] p0026 A80-42284
- Demonstration of short-haul aircraft aft noise reduction techniques on a twenty inch (50.8 cm) diameter fan, volume 1
[NASA-CR-134849] p0033 N80-15083
- Demonstration of short-haul aircraft aft noise reduction techniques on a twenty inch (50.8) diameter fan, volume 2
[NASA-CR-134850] p0034 N80-15084
- Demonstration of short haul aircraft aft noise reduction techniques on a twenty inch (50.8 cm) diameter fan, volume 3
[NASA-CR-134851] p0034 N80-15085
- Quiet Clean Short-haul Experimental Engine (QCSEE). The aerodynamic and mechanical design of the QCSEE over-the-wing fan
[NASA-CR-134915] p0034 N80-15089
- Quiet Clean Short-haul Experimental Engine (QCSEE). Composite fan frame subsystem test report
[NASA-CR-135010] p0035 N80-15098
- Quiet Clean Short-haul Experimental Engine (QCSEE): Hamilton Standard cam/harmonic drive variable pitch fan actuation system detail design report
[NASA-CR-134852] p0030 N80-15107
- Quiet Clean Short-haul Experimental Engine (QCSEE) composite fan frame design report
[NASA-CR-135278] p0031 N80-15110
- Quiet Clean Short-haul Experimental Engine (QCSEE) UTW fan preliminary design
[NASA-CR-134842] p0031 N80-15111
- Quiet Clean Short-haul Experimental Engine (QCSEE): The aerodynamic and preliminary mechanical design of the QCSEE OTW fan
[NASA-CR-134841] p0031 N80-15112
- Quiet Clean Short-haul Experimental Engine (QCSEE) under-the-wing engine composite fan blade design
[NASA-CR-134840] p0031 N80-15113
- Quiet Clean Short-haul Experimental Engine (QCSEE) whirl test of cam/harmonic pitch change actuation system
[NASA-CR-135140] p0032 N80-15117
- Effect of inflow control on inlet noise of a cut-on fan --- in an anechoic chamber
[NASA-TM-81487] p0169 N80-23098
- Forward acoustic performance of a shock-swallowing high-tip-speed fan (QF-13)
[NASA-TP-1668] p0169 N80-23100
- CF6 jet engine performance improvement: New fan
[NASA-CR-159699] p0039 N80-23309
- Comparison of several inflow control devices for flight simulation of fan tone noise using a JT15D-1 engine
[NASA-TM-81505] p0019 N80-24314
- Diffusion bonded boron/aluminum spar-shell fan blade
[NASA-CR-159571] p0072 N80-25382
- Influence of pressure driven secondary flows on the behavior of turbofan forced mixers
[NASA-TM-81541] p0105 N80-27632
- Quiet Clean Short-haul Experimental Engine (QCSEE) under-the-wing engine composite fan blade: Preliminary design test report
[NASA-CR-134846] p0044 N80-29298
- TURBOGENERATORS**
- Installation and checkout of the DOE/NASA Mod-1 2000-kW wind turbine generator
[AIAA 80-0638] p0145 A80-28835
- An exploratory survey of noise levels associated with a 100 kW wind turbine
p0171 A80-35499
- Improved PFB operations - 400-hour turbine test results --- Pressurized Fluidized Bed
p0145 A80-39639
- Modified aerospace BEQA method for wind turbines
p0145 A80-40335
- Large wind turbines: A utility option for the generation of electricity
[NASA-TM-81502] p0144 N80-32858
- MOD-2 wind turbine farm stability study
[NASA-CR-165156] p0156 N80-33862
- TURBOJET AIRCRAFT**
- U JET AIRCRAFT**
- TURBOJET ENGINES**
- NT DUCTED FAN ENGINES
- NT TURBOPAN ENGINES
- NT TURBOPROP ENGINES
- Identification and dual adaptive control of a turbojet engine
p0023 A80-10033
- Engine environmental effects on composite behavior --- moisture and temperature effects on mechanical properties
[AIAA 80-0695] p0024 A80-35101
- Status of NASA full-scale engine aeroelasticity research
p0133 A80-35906
- Dynamic response of a Mach 2.5 axisymmetric inlet and turbojet engine with a poppet-valve controlled inlet stability bypass system when subjected to internal and external airflow transients
[NASA-TP-1531] p0014 N80-14123
- Turbojet-exhaust-nozzle secondary-airflow pumping as an exit control of an inlet-stability bypass system for a Mach 2.5 axisymmetric mixed-compression inlet --- Lewis 10- by 10-ft. supersonic wind tunnel test
[NASA-TP-1532] p0014 N80-14124
- Steady-state performance of J85-21 compressor at 100 percent of design speed with and without interstage rake blockage
[NASA-TM-81451] p0017 N80-21333
- Engine environmental effects on composite behavior
[NASA-TM-81508] p0069 N80-23370
- Status of NASA full-scale engine aeroelasticity research
[NASA-TM-81500] p0132 N80-23678
- Prediction of unsuppressed jet engine exhaust noise in flight from static data
[NASA-TM-81537] p0169 N80-29132
- Effect of cage design on characteristics of high-speed-jet-lubricated 35-millimeter-bore ball bearing --- turbojet engines
[NASA-TP-1732] p0120 N80-33749
- TURBOMACHINE BLADES**
- NT COMPRESSOR BLADES
- NT ROTOR BLADES (TURBOMACHINERY)
- NT STATOR BLADES
- NT TURBINE BLADES
- Impact of new instrumentation on advanced turbine research
[NASA-TM-79301] p0015 N80-15133
- Composite seal for turbomachinery
[NASA-CASE-LEN-12131-2] p0118 N80-26658
- CAS2D: FORTRAN program for nonrotating blade-to-blade, steady, potential transonic

TURBOMACHINERY

SUBJECT INDEX

cascade flows
[NASA-TP-1705] p0003 N80-27284

TURBOMACHINERY

NT AXIAL FLOW TURBINES
NT CENTRIFUGAL COMPRESSORS
NT CENTRIFUGAL PUMPS
NT GAS TURBINES
NT SHROUDED TURBINES
NT STEAM TURBINES
NT SUPERSONIC TURBINES
NT TURBINE PUMPS
NT TURBINES
NT TURBOCOMPRESSORS
NT TURBOFANS
NT TURBOGENERATORS
NT TWO STAGE TURBINES

Efficient laser anemometer for intra-rotor flow mapping in turbomachinery p0111 A80-36140

Inlet flow distortion in turbomachinery. I - Comparison of theory and experiment in a transonic fan stage. II - A parameter study [AIAA PAPER 80-1076] p0006 A80-38895

Turbomachinery technology p0012 N80-10212

Phase-locked telemetry system for rotary instrumentation of turbomachinery, phase 1 [NASA-CR-159453] p0029 N80-14182

Aerodynamic performances of three fan stator designs operating with rotor having tip speed of 337 meters per second and pressure ratio of 1.54. 1: Experimental performance [NASA-TP-1610] p0015 N80-17071

A calculation procedure for viscous flow in turbomachines, volume 2 [NASA-CR-159636] p0004 A80-17995

Rotordynamic Instability Problems in high-performance turbomachinery [NASA-CR-2133] p0119 N80-29706

Field experiences with rotordynamic instability in high-performance turbomachinery --- oil and natural gas recovery p0125 N80-29707

The parameters and measurements of the destabilizing actions of rotating machines, and the assumptions of the 1950's p0125 N80-29712

Testing of turbulent seals for rotodynamic coefficients p0126 N80-29714

Flow induced spring coefficients of labyrinth seals for application in rotor dynamics p0126 N80-29717

Vibration exciting mechanisms induced by flow in turbomachine stages p0127 N80-29722

Development of flexible rotor balancing criteria [NASA-CR-159506] p0129 N80-32720

TURBOPROP AIRCRAFT

Acoustic pressures on a prop-fan aircraft fuselage surface [AIAA PAPER 80-1002] p0172 A80-35965

Advanced turbo-prop airplane interior noise reduction-source definition [NASA-CR-159668] p0172 N80-13882

High speed turboprops for executive aircraft, potential and recent test results [NASA-TM-81482] p0002 N80-21285

Acoustic test and analyses of three advanced turboprop models [NASA-CR-159667] p0039 N80-23311

TURBOPROP ENGINES

Acoustic measurements of three Prop-Fan models [AIAA PAPER 80-0995] p0045 A80-35958

Study of turboprop systems reliability and maintenance costs [NASA-CR-135192] p0029 N80-14129

Preliminary study of advanced turboprop and turboshaft engines for light aircraft --- cost effectiveness [NASA-TM-81467] p0018 N80-22350

The NASA high-speed turboprop program [NASA-TM-81561] p0022 N80-31401

TURBOPUMPS

U TURBINE PUMPS

TURBOROTORS

U TURBINE WHEELS

TURBOSHAFTS

Preliminary study of advanced turboprop and

turboshaft engines for light aircraft --- cost effectiveness [NASA-TM-81467] p0018 N80-22350

TURBULENCE

NT ISOTHERMIC TURBULENCE

Three dimensional mean flow and turbulence characteristics of the near wake of a compressor rotor blade [NASA-CR-159518] p0005 N80-27288

TURBULENT FLOW

NT CAVITATION FLOW

A three-dimensional turbulent compressible subsonic duct flow analysis for use with constructed coordinate systems [AIAA PAPER 80-1398] p0006 A80-41601

The effect of finite turbulence spatial scale on the amplification of turbulence by a contracting stream p0004 A80-44862

Volume-energy parameters and turbulent-flow density fluctuations [NASA-TP-1585] p0105 N80-17398

A calculation procedure for viscous flow in turbomachines, volume 2 [NASA-CR-159636] p0004 N80-17995

Laboratory measurements in a turbulent, swirling flow --- measurement of soot inside a flame-tube burner [NASA-CR-159723] p0095 N80-22509

Influence of pressure driven secondary flows on the behavior of turbofan forced mixers [NASA-TM-81541] p0105 N80-27632

Effects of axisymmetric contractions on turbulence of various scales [NASA-CR-165136] p0006 N80-32328

TURBULENT MIXING

Influence of pressure driven secondary flows on the behavior of turbofan forced mixers [AIAA PAPER 80-1198] p0025 A80-41515

Computation of three-dimensional flow in turbofan mixers and comparison with experimental data [NASA-TM-81410] p0104 N80-15364

TWO DIMENSIONAL FLOW

Time-dependent difference theory for noise propagation in a two-dimensional duct [AIAA PAPER 80-0098] p0170 A80-18269

Prediction method for two-dimensional aerodynamic losses of cooled vanes using integral boundary-layer parameters [NASA-TP-1623] p0002 N80-17030

TWO PHASE FLOW

Application of the principle of similarity fluid mechanics p0107 A80-10039

Marangoni bubble motion in zero gravity p0107 A80-20958

Two-phase working fluids for the temperature range of 50 to 350 deg, phase 2 [NASA-CR-159847] p0108 N80-23599

Conceptual design of two-phase fluid mechanics and heat transfer facility for spacelab [NASA-CR-159810] p0049 N80-27403

Toward the use of similarity theory in two-phase choked flows [NASA-TM-81568] p0106 N80-29623

TWO STAGE TURBINES

Conceptual design study of an improved gas turbine powertrain [NASA-CR-159852] p0039 N80-23315

U

ULTRAHIGH FREQUENCIES

UHF coplanar-slot antenna for aircraft-to-satellite data communications p0009 A80-13064

ULTRASONIC FLAW DETECTION

Simulation of transducer-couplant effects on broadband ultrasonic signals --- in nondestructive flaw evaluation and materials tests p0112 A80-44233

ULTRASONIC TESTS

Quantitative ultrasonic evaluation of engineering properties in metals, composites, and ceramics p0130 A80-39641

Concepts and techniques for ultrasonic evaluation of material mechanical properties p0130 A80-51575

Simulation of transducer-couplant effects on
broadband ultrasonic signals
[NASA-TM-81489] p0130 N80-22714
Concepts and techniques for ultrasonic evaluation
of material mechanical properties
[NASA-TM-81523] p0130 N80-24634
ULTRASONIC WAVE TRANSDUCERS
Simulation of transducer-couplant effects on
broadband ultrasonic signals --- in
nondestructive flaw evaluation and materials tests
p0112 A80-44233
ULTRASONICS
Quantitative ultrasonic evaluation of engineering
properties in metals, composites and ceramics
[NASA-TM-81530] p0130 N80-26682
UNIAxIAL STRAIN
U AXIAL STRAIN
UNITED STATES OF AMERICA
NT KENTUCKY
NT NEW MEXICO
UNSTEADY FLOW
Experimental determination of unsteady blade
element aerodynamics in cascades. Volume 1:
Torsion mode cascade
[NASA-CR-159831] p0040 N80-25335
UPPER STAGE ROCKET ENGINES
Upper stages utilizing electric propulsion
p0059 A80-29989
Upper stages utilizing electric propulsion
p0057 N80-30386
UPPER VOLTA
A photovoltaic power system in the remote African
village of Tangaye, Upper Volta
[NASA-TM-79318] p0137 N80-12552
URBAN TRANSPORTATION
A new traffic control design method for large
networks with signalized intersections
p0183 A80-14841
USER MANUALS (COMPUTER PROGRAMS)
Computer code for estimating installed performance
of aircraft gas turbine engines. Volume 2:
Users manual
[NASA-CR-159692] p0028 N80-13044
A calculation procedure for viscous flow in
turbomachines, volume 3 --- computer programs
[NASA-CR-159864] p0005 N80-26274
UTILITIES
Description of photovoltaic village power systems
in the United States and Africa
p0146 A80-46796
Simulation studies of multiple large wind turbine
generators on a utility network
p0139 N80-16480
Summary and evaluation of the parametric study of
potential early commercial MHD power plants
(PSPEC)
[NASA-TM-81497] p0142 N80-23780
MOD-2 wind turbine farm stability study
[NASA-CR-165156] p0156 N80-33862
UTILIZATION
NT COAL UTILIZATION
NT LASER APPLICATIONS
NT WASTE ENERGY UTILIZATION
NT WINDPOWER UTILIZATION

V

V BAND
U EXTREMELY HIGH FREQUENCIES
V/STOL AIRCRAFT
NT C-15 AIRCRAFT
NT HELICOPTERS
NT RIGID ROTOR HELICOPTERS
NT SHORT TAKEOFF AIRCRAFT
NT TANDEM ROTOR HELICOPTERS
NT TILT ROTOR AIRCRAFT
NT VERTICAL TAKEOFF AIRCRAFT
Low speed test of the aft inlet designed for a
tandem fan V/STOL nacelle
[NASA-CR-159752] p0037 N80-18042
Preliminary study of VTO thrust requirements for a
V/STOL aircraft with lift plus lift/cruise
propulsion
[NASA-TM-81429] p0016 N80-19110
VACUUM APPARATUS
NT VACUUM CHAMBERS
VACUUM CHAMBERS
Atomic hydrogen storage --- cryotrapping and
magnetic field strength

[NASA-CASE-LEW-12081-2] p0093 N80-20402
VACUUM TUBE OSCILLATORS
NT MICROWAVE TUBES
NT TRAVELING WAVE TUBES
VACUUM TUBES
NT MICROWAVE TUBES
NT TRAVELING WAVE TUBES
VALVES
NT DAMPERS (VALVES)
NT PRESSURE REGULATORS
NT SOLENOID VALVES
Single-stage electrohydraulic servosystem for
actuating on airflow valve with frequencies to
500 hertz
[NASA-TF-1678] p0046 N80-29369
VANADIUM
Analysis of the response of a thermal barrier
coating to sodium and vanadium doped combustion
gases
[NASA-TM-79201] p0076 N80-10344
VANES
NT GUIDE VANES
NT JET VANES
An experimental investigation of endwall profiling
in a turbine vane cascade
[AIAA PAPER 80-1089] p0004 A80-38904
Similarity tests of turbine vanes - Effects of
ceramic thermal barrier coatings
[ASME PAPER 80-HT-24] p0027 A80-48013
Similarity tests of turbine vanes, effects of
ceramic thermal barrier coatings
[NASA-TM-81473] p0105 N80-21706
VAPOR DEPOSITION
Survey of ion plating sources
p0120 A80-10040
Calculation of residual principal stresses in CVD
boron on carbon filaments
p0072 A80-44237
Calculation of residual principal stresses in CVD
boron on carbon filaments
[NASA-TM-81456] p0068 N80-20314
VAPORIZING
Effect of degree of fuel vaporization upon
emissions for a premixed partially vaporized
combustion system --- for gas turbine engines
[NASA-TF-1582] p0014 N80-14125
VARIABLE CYCLE ENGINES
Computational fluid mechanics of internal flow
p0012 N80-10211
Supersonic propulsion technology --- variable
cycle engines
p0013 N80-10216
Experimental evaluation of a low emissions high
performance duct burner for Variable Cycle
Engines (VCE)
[NASA-CR-159694] p0036 N80-17074
Experimental aerodynamic and acoustic model
testing of the Variable Cycle Engine (VCE)
testbed coannular exhaust nozzle system
[NASA-CR-159710] p0040 N80-26300
Experimental aerodynamic and acoustic model
testing of the Variable Cycle Engine (VCE)
testbed coannular exhaust nozzle system:
Comprehensive data report
[NASA-CR-159711] p0040 N80-26301
VARIABLE GEOMETRY STRUCTURES
A comparison of experiment and theory for sound
propagation in variable area ducts
p0173 A80-45844
Experimental investigation of a 0.15 scale model
of a conformal variable-ramp inlet for the F-16
airplane
[NASA-CR-159640] p0005 N80-24263
VARIANCE (STATISTICS)
NT REGRESSION ANALYSIS
VCE
U VARIABLE CYCLE ENGINES
VECTOR SPACES
NT MATRICES (MATHEMATICS)
VEGETATION
Assessment of satellite and aircraft multispectral
scanner data for strip-mine monitoring
[NASA-TM-79268] p0136 N80-20787
VEHICLE WHEELS
Improved tire/wheel concept --- pneumatic aircraft
tire
[NASA-CASE-LAR-11695-2] p0124 N80-18402
VELOCITY
NT ACOUSTIC VELOCITY

VELOCITY DISTRIBUTION

NT ANGULAR VELOCITY
 NT FLOW VELOCITY
 NT HIGH SPEED
 NT LOW SPEED
 NT ROTOR SPEED
 NT WIND VELOCITY
VELOCITY DISTRIBUTION
 Effect of velocity overshoot on the performance of magnetohydrodynamic subsonic diffusers
 [NASA-TN-79305] p0175 N80-14722
VELOCITY FIELDS
U VELOCITY DISTRIBUTION
VELOCITY MEASUREMENT
NT WIND VELOCITY MEASUREMENT
 Dynamic behavior of a beam drag-force anemometer
 [NASA-TP-1687] p0110 N80-24595
 Three dimensional mean flow and turbulence characteristics of the near wake of a compressor rotor blade
 [NASA-CR-159518] p0005 N80-27288
VELOCITY MODULATION
 Coupled cavity traveling wave tube with velocity tapering
 [NASA-CASE-LEW-12296-1] p0101 N80-19425
VELOCITY PROFILES
U VELOCITY DISTRIBUTION
VENTILATORS
 Parametric instabilities of rotor-support systems with application to industrial ventilators
 p0127 N80-29729
VENTS
 Wind tunnel investigation of the Titan Forward Skirt compartment vent from a free-stream Mach number of 0.80 to 1.96 --- conducted in the Lewis Research Center 8 by 6 foot supersonic wind tunnel
 [NASA-TN-81572] p0106 N80-32689
VERTICAL LANDING
 Vertical Takeoff and Landing (VTOL) propulsion technology
 p0013 N80-10218
VERTICAL TAKEOFF
 Preliminary study of VTO thrust requirements for a V/STOL aircraft with lift plus lift/cruise propulsion
 [NASA-TN-81429] p0016 N80-19110
VERTICAL TAKEOFF AIRCRAFT
 Vertical Takeoff and Landing (VTOL) propulsion technology
 p0013 N80-10218
VERTICAL TAKEOFF AND LANDING
U VERTICAL LANDING
U VERTICAL TAKEOFF
VIBRATION
NT FLUTTER
NT RESONANT VIBRATION
NT STRUCTURAL VIBRATION
NT SUPERSONIC FLUTTER
NT TORSIONAL VIBRATION
 Vibration exciting mechanisms induced by flow in turbomachine stages
 p0127 N80-29722
VIBRATION DAMPERS
U VIBRATION ISOLATORS
VIBRATION DAMPING
 Elastomer damper performance - A comparison with a squeeze film for a supercritical power transmission shaft
 [ASME PAPER 80-GT-162] p0121 A80-42272
 Development of procedures for calculating stiffness and damping of elastomers in engineering applications, part 6
 [NASA-CR-159838] p0134 N80-22733
VIBRATION EFFECTS
 Subsynchronous instability of a geared centrifugal compressor of overhung design
 p0125 N80-29711
 Asynchronous vibration problem of centrifugal compressor
 p0125 N80-29713
VIBRATION ISOLATORS
 Design of elastomer dampers for a high-speed flexible rotor
 [ASME PAPER 79-DET-88] p0121 A80-15736
 Elastomer damper performance - A comparison with a squeeze film for a supercritical power transmission shaft
 [ASME PAPER 80-GT-162] p0121 A80-42272

SUBJECT INDEX

VIBRATION MEASUREMENT
 Flutter spectral measurements using stationary pressure transducers
 p0111 A80-36147
 Digital system for dynamic turbine engine blade displacement measurements
 p0111 A80-36151
VIBRATION MODE
 Aerodynamic analysis of a supersonic cascade vibrating in a complex mode
 p0007 A80-45841
VIBRATION PROTECTION
U VIBRATION ISOLATORS
VIBRATION TESTS
 Analysis and identification of subsynchronous vibration for a high pressure parallel flow centrifugal compressor
 p0125 N80-29710
VISCERA
NT PANCHEAS
VISCOMETERS
 Two-phase working fluids for the temperature range of 50 to 350 deg, phase 2
 [NASA-CR-159847] p0108 N80-23599
VISCOSITY
 Fuel character effects on the J79 and F101 engine combustion systems
 p0042 N80-29312
VISCOUS FLOW
NT BOUNDARY LAYER SEPARATION
NT SECONDARY FLOW
NT SEPARATED FLOW
 Numerical simulation of supersonic inlets using a three-dimensional viscous flow analysis
 [AIAA PAPER 80-0384] p0003 A80-20969
 Computation of three-dimensional viscous supersonic flow in inlets
 [AIAA PAPER 80-0194] p0065 A80-23941
 An implicit finite-difference code for inviscid and viscous cascade flow
 [AIAA PAPER 80-1427] p0007 A80-44128
 Development of a three-dimensional supersonic inlet flow analysis
 [NASA-CR-3218] p0108 N80-14356
 Numerical simulation of supersonic inlets using a three-dimensional viscous flow analysis
 [NASA-TN-81411] p0104 N80-15365
 A calculation procedure for viscous flow in turbomachines, volume 2
 [NASA-CR-159636] p0004 N80-17995
 A calculation procedure for viscous flow in turbomachines, volume 3 --- computer programs
 [NASA-CR-159864] p0005 N80-26274
VISUALIZATION OF FLOW
U FLOW VISUALIZATION
VOICE COMMUNICATION
 The 30/20 GHz mixed user architecture development study
 [NASA-CR-159686] p0097 N80-10415
 The 30/20 GHz mixed user architecture development study: Executive summary
 [NASA-CR-159687] p0097 N80-10416
VOLATILIZATION
U VAPORIZING
VOLT-AMPERE CHARACTERISTICS
 Improvement and scale-up of the NASA Redox storage system
 p0146 A80-48370
VOLTAGE
U ELECTRIC POTENTIAL
VOLTAGE CONVERTERS (DC TO DC)
 Performance of 22.4-kW nonlaminated-frame dc series motor with chopper controller --- a dc to dc voltage converter
 [NASA-TN-79252] p0101 N80-13361
VOLTAGE GENERATORS
NT PHOTOVOLTAIC CELLS
VOLTAGE MEASUREMENT
U ELECTRICAL MEASUREMENT
VOLTAGE REGULATORS
 An adaptive-control switching buck regulator - Implementation, analysis, and design
 p0103 A80-28167
VOLUME
 Volume-energy parameters and turbulent-flow density fluctuations
 [NASA-TP-1585] p0105 N80-17398
VOLUMETRIC ANALYSIS
 A reduced volumetric expansion factor plot

- VORTEX COLUMNS**
U VORTICES
VORTEX DISTURBANCES
U VORTICES
VORTEX FLOW
U VORTICES
VORTEX TUBES
U HILSCH TUBES
U VORTICES
VORTICES
Evolution of a rotating flow in the vicinity of a surface p0107 A80-10038
Summary of advanced methods for predicting high speed propeller performance p0107 A80-14660
[AIAA PAPER 80-0225] p0003 A80-20966
Influence of pressure driven secondary flows on the behavior of turbofan forced mixers p0025 A80-41515
[AIAA PAPER 80-1198] p0025 A80-41515
Streakline flow visualization study of a horseshoe vortex in a large-scale, two-dimensional turbine stator cascade p0004 A80-42145
[ASME PAPER 80-GT-4]
- VTOL**
U VERTICAL LANDING
U VERTICAL TAKEOFF
VTOL AIRCRAFT
U VERTICAL TAKEOFF AIRCRAFT
- W**
- WAFERS**
Thin n-i-p radiation-resistant solar cell feasibility study p0154 M80-29852
[NASA-CR-159871]
- WAKES**
NT NEAR WAKES
- WALL FLOW**
Evolution of a rotating flow in the vicinity of a surface p0107 A80-14660
Griffith diffusers p0006 A80-20748
An experimental investigation of endwall profiling in a turbine vane cascade p0004 A80-38904
[AIAA PAPER 80-1089]
Selected data from a transonic flexible walled test section p0047 M80-32404
[NASA-CR-159360]
- WALL TEMPERATURE**
Significance of thermal contact resistance in two-layer, thermal-barrier-coated turbine vanes p0024 A80-39635
- WANKEL ENGINES**
Performance, emissions, and physical characteristics of a rotating combustion aircraft engine, supplement A p0041 M80-27361
[NASA-CR-135119]
- WASTE ENERGY UTILIZATION**
Thermal energy storage systems using fluidized bed heat exchangers p0153 M80-28866
[NASA-CR-159868]
Cogeneration Technology Alternatives Study (CTAS). Volume 4: Energy conversion systems p0155 M80-33859
[NASA-CR-159768]
Cogeneration Technology Alternatives Study (CTAS). Volume 6: Computer data. Part 1: Coal-fired noco-generation process boiler, section A p0156 M80-33860
[NASA-CR-159770-PT-1]
Cogeneration Technology Alternatives Study (CTAS). Volume 6: Computer data. Part 2: Residual-fired noco-generation process boiler p0156 M80-33861
[NASA-CR-159770-PT-2]
- WATER CONTENT**
U MOISTURE CONTENT
WATER COOLING
U LIQUID COOLING
WATER INJECTION
Effect of water injection and off scheduling of variable inlet guide vanes, gas generator speed and power turbine nozzle angle on the performance of an automotive gas turbine engine p0016 M80-20272
[NASA-TN-81415]
- WATER PURIFICATION**
U WATER TREATMENT
WATER QUALITY
Quantitative interpretation of Great Lakes remote sensing data
- WATER TREATMENT**
Cell module and fuel conditioner p0157 A80-45005
[NASA-CR-159888] p0155 M80-31882
- WATTMETERS**
Error analysis in the measurement of average power with application to switching controllers p0184 M80-21202
[NASA-CR-159792]
- WAVE ATTENUATION**
NT ACOUSTIC ATTENUATION
NT SHOCK WAVE ATTENUATION
WAVE PROPAGATION
NT ACOUSTIC PROPAGATION
Spectral structure of pressure measurements made in a combustion duct p0171 A80-35496
- WAVE REFLECTION**
Reciprocity principle in duct acoustics p0167 M80-12824
[NASA-TN-79300]
- WEAR**
Some considerations of the performance of two honeycomb gas path seal material systems p0077 M80-16143
[NASA-TN-81398]
Program to develop sprayed, plastically deformable compressor shroud seal materials p0123 M80-16338
[NASA-CR-159741]
Analysis of wear-debris from full-scale bearing fatigue tests using the ferrograph p0114 M80-16341
[NASA-TN-81403]
Blade design and operating experience on the MOD-OA 200 kW wind turbine at Clayton, New Mexico p0139 M80-16470
Lubrication and wear mechanisms of polyimide-bonded graphite fluoride films subjected to low contact stress p0085 M80-17220
[NASA-TP-1584]
Wear particles of single-crystal silicon carbide in vacuum p0085 M80-18178
[NASA-TP-1624]
Adhesion, friction, and wear of binary alloys in contact with single-crystal silicon carbide p0086 M80-21534
[NASA-TN-79282]
Steady-state wear and friction in boundary lubrication studies p0087 M80-22493
[NASA-TP-1658]
Friction and wear of iron-base binary alloys in sliding contact with silicon carbide in vacuum p0087 M80-22494
[NASA-TP-1612]
Practical applications of surface analytic tools in tribology p0079 M80-23430
[NASA-TN-81484]
- WEAR TESTS**
The friction and wear of metals and binary alloys in contact with an abrasive grit of single-crystal silicon carbide p0120 A80-14734
[ASLE PREPRINT 79-LC-5C-1]
Wear of seal materials used in aircraft propulsion systems p0121 A80-28010
Mechanisms of lubrication and wear of a bonded solid-lubricant film p0122 A80-43163
[ASLE PREPRINT 80-AM-3E-1]
Analysis of wear debris from full-scale bearing fatigue tests using the Ferrograph p0122 A80-43167
[ASLE PREPRINT 80-AM-3E-2]
Friction and wear of plasma-sprayed coatings containing cobalt alloys from 25 deg to 650 deg in air p0122 A80-43176
[ASLE PREPRINT 80-AM-6C-2]
Friction and wear of plasma-sprayed coatings containing cobalt alloys from 25 deg to 650 deg in air p0085 M80-14249
[NASA-TN-79316]
Mechanisms of lubrication and wear of a bonded solid lubricant film p0085 M80-16165
[NASA-TN-81396]
- WEBS (MEMBRANES)**
U MEMBRANES
WEDGES
Three dimensional finite-element elastic analysis of a thermally cycled double-edge wedge geometry specimen --- nickel alloy turbine parts p0079 M80-26433
[NASA-TN-80980]
- WEIGHT (NASS)**
Comparison of the weight loss and adherence of nine different polyimide films thermally aged at 315 C and 350 C in air --- high temperature lubricants p0086 M80-18183
[NASA-TN-81381]

WEIGHT FACTORS

SUBJECT INDEX

WEIGHT FACTORS

U WEIGHT (MASS)

WEIGHT REDUCTION

Computerized systems analysis and optimization of aircraft engine performance, weight, and life cycle costs

p0165 A80-10035

WEIGHTLESSNESS

Combustion of solid carbon rods in zero and normal gravity

p0074 A80-20955

Marangoni bubble motion in zero gravity

p0107 A80-20958

Marangoni bubble motion in zero gravity --- Lewis

zero gravity drop tower

[NASA-TM-79250]

p0104 A80-13403

Combustion of solid carbon rods in zero and normal gravity

[NASA-TM-79303]

p0104 A80-13404

WELDED STRUCTURES

NT STEEL STRUCTURES

WELDING

NT DIFFUSION WELDING

WETNESS

U MOISTURE CONTENT

WHEELS

NT FLYWHEELS

NT TURBINE WHEELS

NT VEHICLE WHEELS

WHIRL INSTABILITY

U ROTARY STABILITY

WIDEBAND COMMUNICATION

Communications technology satellite - United States experiments and disaster communications applications

p0051 A80-10032

30/20 GHz wideband technology verification program

p0097 A80-25917

Application of advanced on-board processing concepts to future satellite communications systems

[NASA-CR-159682]

p0098 A80-12260

Application of advanced on-board processing concepts to future satellite communications systems: Bibliography

[NASA-CR-159684]

p0098 A80-12261

WIND (METEOROLOGY)

MOD-2 wind turbine system concept and preliminary design report. Volume 2: Detailed report

[DOE/NASA/0002-80/2]

p0152 A80-26775

WIND CIRCULATION

U ATMOSPHERIC CIRCULATION

WIND MEASUREMENT

NT WIND VELOCITY MEASUREMENT

The use of wind data with an operational wind turbine in a research and development environment

p0145 A80-35730

WIND PROFILES

Modified power law equations for vertical wind profiles --- in investigation of windpower plant siting

p0159 A80-35719

Modified power law equations for vertical wind profiles

[NASA-TM-79275]

p0137 A80-13623

WIND TUNNEL TESTS

Full-coverage film cooling. I - Comparison of heat transfer data for three injection angles

[ASME PAPER 80-GT-43]

p0108 A80-42176

A theoretical and experimental investigation of propeller performance methodologies

[AIAA PAPER 80-1240]

p0026 A80-43283

Some techniques for reducing the tower shadow of the DOE/NASA mod-0 wind turbine tower --- wind tunnel tests to measure effects of tower structure on wind velocity

[NASA-TM-79202]

p0137 A80-10594

Wind-tunnel investigation of the flow correction for a model-mounted angle of attack sensor at angles of attack from -10 deg to 110 deg --- Langley 12-foot low speed wind tunnel test

[NASA-TM-80189]

p0011 A80-14110

Turbomachinery exhaust-nozzle secondary-airflow pumping as an exit control of an inlet-stability bypass system for a Mach 2.5 axisymmetric

mixed-compression inlet --- Lewis 10- by 10-ft. supersonic wind tunnel test

[NASA-TP-1532]

p0014 A80-14124

High-speed-propeller wind-tunnel aeroacoustic results

p0018 A80-22344

A comparison between an existing propeller noise theory and wind tunnel data

[NASA-TM-81519]

p0169 A80-25101

Selected data from a transonic flexible walled test section

[NASA-CR-159360]

p0047 A80-32404

Wind tunnel investigation of the Titan Forward Skirt compartment vent from a free-stream Mach number of 0.80 to 1.96 --- conducted in the Lewis Research Center 8 by 6 foot supersonic wind tunnel

[NASA-TM-81572]

p0106 A80-32689

WIND TUNNELS

NT LOW SPEED WIND TUNNELS

WIND VELOCITY

Some techniques for reducing the tower shadow of the DOE/NASA mod-0 wind turbine tower --- wind tunnel tests to measure effects of tower structure on wind velocity

[NASA-TM-79202]

p0137 A80-10594

WIND VELOCITY MEASUREMENT

Some techniques for reducing the tower shadow of the DOE/NASA mod-0 wind turbine tower --- wind tunnel tests to measure effects of tower structure on wind velocity

[NASA-TM-79202]

p0137 A80-10594

WINDMILLS (WINDPOWERED MACHINES)

Numerical calculation of steady inviscid full potential compressible flow about wind turbine blades

[AIAA 80-0607]

p0145 A80-28804

Evaluation of feasibility of prestressed concrete for use in wind turbine blades

[NASA-CR-159725]

p0147 A80-15553

DOE/NASA wind turbine data acquisition. Part 1:

Equipment

[NASA-CR-159779]

p0148 A80-17543

Feasibility study of aileron and spoiler control systems for large horizontal axis wind turbines

[NASA-CR-159856]

p0153 A80-27803

WIND: Computer program for calculation of three dimensional potential compressible flow about wind turbine rotor blades

[NASA-TP-1729]

p0003 A80-33357

WINDPOWER UTILIZATION

Modified power law equations for vertical wind profiles --- in investigation of windpower plant siting

p0159 A80-35719

Modified power law equations for vertical wind profiles

[NASA-TM-79275]

p0137 A80-13623

Large Wind Turbine Design Characteristics and R and D Requirements

[NASA-CR-2106]

p0139 A80-16453

Structural analysis considerations for wind turbine blades

p0139 A80-16469

Blade design and operating experience on the MOD-OA 200 kW wind turbine at Clayton, New Mexico

[NASA-TM-81408]

p0139 A80-16470

Design, fabrication, and test of a steel spar wind turbine blade

p0139 A80-16472

Preliminary analysis of performance and loads data from the 2-megawatt mod-1 wind turbine generator

[NASA-TM-81408]

p0139 A80-16494

DOE/NASA wind turbine data acquisition. Part 1:

Equipment

[NASA-CR-159779]

p0148 A80-17543

Design, fabrication, test, and evaluation of a prototype 150-foot long composite wind turbine blade

[NASA-CR-159775]

p0148 A80-17548

Appendix: MOD-1 wind turbine generator analysis and design report, volume 2

[NASA-CR-159496]

p0149 A80-18565

Teetered, tip-controlled rotor: Preliminary test results from Mod-0 100-kW experimental wind turbine

[NASA-TM-81445]

p0140 A80-19613

Installation and checkout of the DOE/NASA Mod-1 2000-kW wind turbine generator

[NASA-TM-81444]

p0140 A80-19614

Mod-2 wind turbine system concept and preliminary design report. Volume 1: Executive summary

SUBJECT INDEX

ZINC SILVER BATTERIES

[DOE/NASA/0002-80/2] p0151 N80-24758
WINDPOWERED GENERATORS
 Installation and checkout of the DOE/NASA Mod-1
 2000-kW wind turbine generator p0145 A80-28835
 [AIAA 80-0638]
 Teetered, tip-controlled rotor - Preliminary test
 results from Mod-0 100-kW experimental wind
 turbine p0145 A80-28836
 [AIAA 80-0642]
 An exploratory survey of noise levels associated
 with a 100 kW wind turbine p0171 A80-35499
 The use of wind data with an operational wind
 turbine in a research and development environment p0145 A80-35730
 Modified aerospace REQA method for wind turbines p0145 A80-40335
 Executive summary: Mod-1 wind turbine generator
 analysis and design report p0147 N80-11558
 [NASA-CR-159497]
 Large Wind Turbine Design Characteristics and R
 and D Requirements p0139 N80-16453
 [NASA-CP-2106]
 Design evolution of large wind turbine generators p0139 N80-16455
 Simulation studies of multiple large wind turbine
 generators on a utility network p0139 N80-16480
 Preliminary analysis of performance and loads data
 from the 2-megawatt mod-1 wind turbine generator p0139 N80-16494
 [NASA-TM-81408]
 Design, fabrication, test, and evaluation of a
 prototype 150-foot long composite wind turbine
 blade p0148 N80-17548
 [NASA-CR-159775]
 Numerical calculation of steady inviscid full
 potential compressible flow about wind turbine
 blades p0136 N80-18497
 [NASA-TM-81438]
 Appendix: MOD-1 wind turbine generator analysis
 and design report, volume 2 p0149 N80-18565
 [NASA-CR-159496]
 Teetered, tip-controlled rotor: Preliminary test
 results from Mod-0 100-kW experimental wind
 turbine p0140 N80-19613
 [NASA-TM-81445]
 Installation and checkout of the DOE/NASA Mod-1
 2000-kW wind turbine generator p0140 N80-19614
 [NASA-TM-81444]
 Mod 1 wind turbine generator failure modes and
 effects analysis p0150 N80-20864
 [NASA-CR-159494]
 An exploratory survey of noise levels associated
 with a 100kW wind turbine p0169 N80-23102
 [NASA-TM-81486]
 Mod-1 wind turbine generator analysis and design
 report, volume 1 p0150 N80-23775
 [NASA-CR-159495]
 Mod-2 wind turbine system concept and preliminary
 design report. Volume 1: Executive summary p0151 N80-24758
 [DOE/NASA/0002-80/2]
 Nonlinear aeroelastic equations of motion of
 twisted, nonuniform, flexible horizontal-axis
 wind turbine blades p0152 N80-26774
 [NASA-CR-159502]
 MOD-2 wind turbine system concept and preliminary
 design report. Volume 2: Detailed report p0152 N80-26775
 [DOE/NASA/0002-80/2]
 Large wind turbines: A utility option for the
 generation of electricity p0144 N80-32858
 [NASA-TM-81502]
 MOD-2 wind turbine farm stability study p0156 N80-33862
 [NASA-CR-165156]
WING MACELLE CONFIGURATIONS
 Assessment at full scale of exhaust nozzle to wing
 size on STOL-OTW acoustic characteristics p0167 N80-13881
 [NASA-TM-79279]
 Quiet Clean Short-Haul Experimental Engine
 (QCSEE). Under-the-wing (UTW) engine
 boilerplate Macelle test report. Volume 2:
 Aerodynamics and performance p0028 N80-14116
 [NASA-CR-135250]
WING TANKS
 Temperature and flow measurements on near-freezing
 aviation fuels in a wing-tank model p0094 A80-42193
 [ASHE PAPER 80-GT-63]
 Temperature and flow measurements on near-freezing
 aviation fuels in a wing-tank model p0093 N80-13268
 [NASA-TM-79285]

WINGS

NT ROTARY WINGS

WORK HARDENING

NT STRAIN HARDENING

WORKING FLUIDS

Two-phase working fluids for the temperature range
 of 50 to 350 deg, phase 2

[NASA-CR-159847]

p0108 N80-23599

WRAPAROUND CONTACT SOLAR CELLS

U SOLAR CELLS

X

X BAND

U SUPERHIGH FREQUENCIES

X RAY IRRADIATION

Radiation damage in high voltage silicon solar cells
 [NASA-TM-81478]

p0178 N80-23180

X RAYS

Radiation damage in high voltage silicon solar cells
 p0144 A80-33889

XENON

Study of a rare-gas transverse fast discharge

p0176 A80-11366

Y

YC-15 AIRCRAFT

U C-15 AIRCRAFT

YC-14 AIRCRAFT

Quiet powered-lift propulsion

[NASA-CR-2077]

p0015 N80-15127

YF-102 AIRCRAFT

U F-102 AIRCRAFT

YIELD STRENGTH

High toughness-high strength iron alloy

[NASA-CASE-LEW-12542-3]

p0079 N80-32484

YOUNG MODULUS

U MODULUS OF ELASTICITY

YTTRIUM

Effects of yttrium, aluminum and chromium
 concentrations in bond coatings on the
 performance of zirconia-yttria thermal barriers

[NASA-TM-81485]

p0079 N80-22464

Composite wall concept for high temperature
 turbine shrouds: Heat transfer analysis

[NASA-TM-81539]

p0020 N80-27362

Effect of W and WC on the oxidation resis of
 yttria-doped silicon nitride

[NASA-TM-81529]

p0087 N80-27483

YTTRIUM COMPOUNDS

NT YTTRIUM OXIDES

YTTRIUM OXIDES

Effect of thermal cycling on ZrO₂-Y₂O₃ thermal
 barrier coatings

p0089 A80-35899

Effects of yttrium, aluminum and chromium
 concentrations in bond coatings on the
 performance of zirconia-yttria thermal barriers

[NASA-TM-81485]

p0082 A80-35900

Effect of W and WC on the oxidation resistance of
 yttria-doped silicon nitride

[NASA-TM-81529]

p0090 A80-46099

Effect of starting powder characteristics on
 density, microstructure and low temperature
 oxidation behavior of a Si₃N₄ - 8 w/o Y₂O₃ ceramic

[NASA-TM-81536]

p0090 A80-46100

Effects of oxide additions and temperature on
 sinterability of milled silicon nitride

[NASA-TP-1644]

p0086 N80-21532

Effect of starting powder characteristics on
 density, microstructure and low temperature
 oxidation behavior of a Si₃N₄w/o Y₂O₃ ceramic

[NASA-TM-81536]

p0088 N80-27484

Z

ZERO GRAVITY

U WEIGHTLESSNESS

ZINC COMPOUNDS

NT ZINC OXIDES

ZINC NICKEL BATTERIES

U NICKEL ZINC BATTERIES

ZINC OXIDES

Decay of the zincate concentration gradient at an
 alkaline zinc cathode after charging

[NASA-TM-81536]

p0074 A80-13070

ZINC SILVER BATTERIES

U SILVER ZINC BATTERIES

ZINC SILVER OXIDE BATTERIES

SUBJECT INDEX

ZINC SILVER OXIDE BATTERIES

U SILVER ZINC BATTERIES

ZIRCONATES

NT BARIUM ZIRCONATES

ZIRCONIUM

The effect of zirconium on the isothermal
oxidation of nominal Ni-14Cr-24Al alloys
p0082 A80-26465

Composite wall concept for high temperature
turbine shrouds: Heat transfer analysis
[NASA-TM-81539] p0020 N80-27362

ZIRCONIUM COMPOUNDS

NT BARIUM ZIRCONATES

NT ZIRCONIUM OXIDES

ZIRCONIUM OXIDES

Effect of thermal cycling on ZrO₂-Y₂O₃ thermal
barrier coatings
p0089 A80-35899

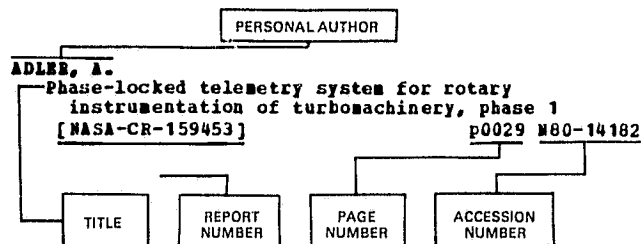
Effects of yttrium, aluminum and chromium
concentrations in bond coatings on the
performance of zirconia-yttria thermal barriers
p0082 A80-35900

Analysis of the response of a thermal barrier
coating to sodium and vanadium doped combustion
gases
[NASA-TM-79205] p0076 N80-10344

Effects of yttrium, aluminum and chromium
concentrations in bond coatings on the
performance of zirconia-yttria thermal barriers
[NASA-TM-81485] p0079 N80-22464

PERSONAL AUTHOR INDEX

Typical Personal Author Index Listing



Listings in this index are arranged alphabetically by personal author. The title of the document provides the user with a brief description of the subject matter. The report number helps to indicate the type of document listed (e.g., NASA report, translation, NASA contractor report). The page and accession numbers are located beneath and to the right of the title. Under any one author's name the accession numbers are arranged in sequence with the IAA accession numbers appearing first.

A

- ABBOTT, J. H.**
Vertical Takeoff and Landing (VTOL) propulsion technology
p0013 N80-10218
Summary and evaluation of the parametric study of potential early commercial MHD power plants (PSPEC)
[NASA-TN-81497] p0142 N80-23780
- ACOSTA, A. J.**
A test program to measure fluid mechanical whirl-excitation forces in centrifugal pumps
p0126 N80-29719
- ADAMCZYK, J. J.**
Inlet flow distortion in turbomachinery. I - Comparison of theory and experiment in a transonic fan stage. II - A parameter study
[AIAA PAPER 80-1076] p0006 A80-38895
Computational fluid mechanics of internal flow
p0012 N80-10211
- ADLER, A.**
Phase-locked telemetry system for rotary instrumentation of turbomachinery, phase 1
[NASA-CR-159453] p0029 N80-14182
- AHUJA, K. K.**
Characteristics of internal- and jet-noise radiation from a multi-lobe, multi-tube suppressor nozzle tested statically and under flight simulation
[AIAA PAPER 80-1027] p0173 A80-38642
Studies of the acoustic transmission characteristics of coaxial nozzles with inverted velocity profiles, volume 1
[NASA-CR-159698] p0172 N80-11870
A study of the transmission characteristics of suppressor nozzles
[NASA-CR-165133] p0172 N80-32186
- AHUJA, P. L.**
Internal coating of air cooled gas turbine blades
[NASA-CR-159701] p0036 N80-18041
- AKIN, L. S.**
Analytical and experimental spur gear tooth temperature as affected by operating variables
p0123 A80-46412
Analytical and experimental spur gear tooth temperature as affected by operating variables
[NASA-TN-81419] p0115 N80-18403
- ALARIO, J.**
Active heat exchange system development for latent heat thermal energy storage
[NASA-CR-159726] p0149 N80-18562
- ALEXANDER, J.**
Optical sensors for aeronautics and space
[NASA-TN-81407] p0110 N80-17423
- ALEXANDER, S. S.**
Antion permeable membrane
[NASA-CR-159599] p0147 N80-12551
- ALEXOVICH, R. E.**
National Aeronautics and Space Administration plans for space communication technology
p0097 A80-26795
- ALLAINE, P. E.**
Instability thresholds for flexible rotors in hydrodynamic bearings
p0128 N80-29730
- ALLEN, G. P.**
Self-acting lift-pad geometry for circumferential seals: A noncontacting concept
[NASA-TP-1583] p0114 N80-14403
Composite wall concept for high temperature turbine shrouds: Survey of low modulus strain isolator materials
[NASA-TN-81443] p0086 N80-20398
- ALLEN, J. L.**
Preliminary study of VTO thrust requirements for a V/STOL aircraft with lift plus lift/cruise propulsion
[NASA-TN-81429] p0016 N80-19110
- ALLISON, J. F.**
Thin n-i-p radiation-resistant solar cell feasibility study
[NASA-CR-159871] p0154 N80-29852
- ALSTON, W. B.**
Characterization of PMR-15 polyimide composition in thermo-oxidatively exposed graphite fiber composites
[NASA-TN-81565] p0088 N80-28524
- ALTEROVITZ, S. A.**
Critical currents in A-15 structure Nb3Al converted from cold-worked bcc structure
p0179 A80-33853
- ALYEA, F. M.**
Parametric study of prospective early commercial MHD power plants (PSPEC). General Electric Company, task 1: Parametric analysis
[NASA-CR-159634] p0152 N80-26779
- AMUZU, J. K. A.**
Sliding friction of some metallic glasses
p0090 A80-46153
- ANDERSEN, H. B.**
JT9D-7A /SP/ jet engine performance deterioration trends
p0026 A80-44230
JT9D-7A (SP) jet engine performance deterioration trends
[NASA-TN-81459] p0016 N80-20274
- ANDERSON, B.**
Influence of pressure driven secondary flows on the behavior of turbofan forced mixers
[AIAA PAPER 80-1198] p0025 A80-41515
Influence of pressure driven secondary flows on the behavior of turbofan forced mixers
[NASA-TN-81541] p0105 N80-27632
- ANDERSON, B. B.**
Computation of three-dimensional flow in turbofan mixers and comparison with experimental data
[AIAA PAPER 80-0227] p0003 A80-20967
Numerical simulation of supersonic inlets using a three-dimensional viscous flow analysis
[AIAA PAPER 80-0384] p0003 A80-20969
Computational fluid mechanics of internal flow
p0012 N80-10211
Computation of three-dimensional flow in turbofan mixers and comparison with experimental data
[NASA-TN-81410] p0104 N80-15364

- Numerical simulation of supersonic inlets using a three-dimensional viscous flow analysis
[NASA-TN-81411] p0104 N80-15365
- ANDERSON, D.
The effect of catalyst length and downstream reactor distance on catalytic combustor performance
[NASA-TN-81475] p0142 N80-23779
- ANDERSON, D. E.
Gas phase oxidation downstream of a catalytic combustor
[NASA-TN-81551] p0144 N80-29863
- ANDERSON, W. E.
Effect of geometry and operating conditions on spur gear system power loss
p0122 A80-46409
Evaluation of a high performance fixed-ratio traction drive
p0122 A80-46410
Spur-gear-system efficiency at part and full load
[NASA-TP-1622] p0115 N80-17466
Evaluation of a high performance fixed-ratio traction drive
[NASA-TN-81425] p0115 N80-18404
Effect of geometry and operating conditions on spur gear system power loss
[NASA-TN-81426] p0116 N80-18406
Parametric tests of a traction drive retrofitted to an automotive gas turbine
[NASA-TN-81457] p0117 N80-21754
- ANDERSON, W. J.
Rolling-element bearings
p0121 A80-31961
Mechanical components
p0013 N80-10213
- ANSPAUGH, B. E.
Characterization of solar cells for space applications. Volume 10: Electrical characteristics of Spectrolab BSF, textured, 10 ohm-cm, 300 micron cells as a function of intensity, temperature and irradiation
[NASA-CR-162422] p0147 N80-11566
- ANTL, R. J.
Improved components for engine fuel savings
[NASA-TN-81577] p0023 N80-31402
- ANTOINE, A. C.
Use of petroleum-based correlations and estimation methods for synthetic fuels
[NASA-TN-81533] p0093 N80-27509
Fuels characterization studies
p0021 N80-29309
- ANTONIUK, D.
Depriming of arterial heat pipes: An investigation of CTS thermal excursions
[NASA-CR-165153] p0108 N80-32688
- ARIAS, A.
Effects of oxide additions and temperature on sinterability of milled silicon nitride
[NASA-TP-1644] p0086 N80-21532
- ARNENTROUT, E. C.
Fatigue strength testing employed for evaluation and acceptance of jet-engine instrumentation probes
p0112 A80-42291
Fatigue strength testing employed for evaluation and acceptance of jet-engine instrumentation probes
[NASA-TN-81402] p0110 N80-17422
- ARNOLD, E. A.
Thin n-i-p radiation-resistant solar cell feasibility study
[NASA-CR-159871] p0154 N80-29852
- ARTH, C. H.
A quantitative analysis of inter-island telephony traffic in the Pacific Basin Region (PBR)
[NASA-TN-81587] p0097 N80-32610
- ASHE, T. L.
Concept definition study of small Brayton cycle engines for dispersed solar electric power systems
[NASA-CR-159592] p0150 N80-22778
- ASTON, G.
Ion extraction from a plasma
[NASA-CR-159849] p0177 N80-26161
- AUER, B. H.
Simulation and visualization of face seal motion stability by means of computer generated movies
[NASA-TN-81581] p0120 N80-31797
- AUGLER, E. E.
Prediction method for two-dimensional aerodynamic losses of cooled vanes using integral boundary-layer parameters
[NASA-TP-1623] p0002 N80-17030
- AYATI, H. B.
A methodology for long-range prediction of air transportation
p0041 N80-29305
- AYDELOTT, J. C.
LeRC reduced gravity fluid management technology program
p0048 A80-35504
A liquid hydrogen experiment as a Shuttle payload
[AIAA PAPER 80-1096] p0054 A80-38909
LeRC reduced gravity fluid management technology program
[NASA-TN-81450] p0051 N80-20304
LeRC reduced gravity fluid management technology program
p0057 N80-30383
- B**
- BADGLEY, H. B.
Solar array subsystems study
[NASA-CR-159857] p0151 N80-24742
- BAEHR, E. F.
Intra-ocular pressure normalization technique and equipment
[NASA-CASE-LEW-12955-1] p0161 N80-14684
- BAEZ, A. M.
Durability tests of solenoid valves for digital actuators
[NASA-TN-81522] p0020 N80-26299
- BAER, D. W.
Quiet Clean Short-haul Experimental Engine (QCSEE). Double-annular clean combustor technology development report
[NASA-CR-159483] p0032 N80-15121
Energy efficient engine
[NASA-CR-159685] p0045 N80-33408
- BAIR, V. L.
An interactive modular design for computerized photometry in spectrochemical analysis
p0074 A80-39640
An interactive modular design for computerized photometry in spectrochemical analysis
[NASA-TN-81521] p0074 N80-24386
- BAKER, H.
Concepts for 20/30 GHz satcom systems for direct-to-user applications
[AIAA 80-0582] p0050 A80-35329
Concepts for 18/30 GHz satellite communication system, volume 1
[NASA-CR-159625-VOL-1] p0098 N80-11277
Concepts for 18/30 GHz satellite communication system, volume 1A: Appendix
[NASA-CR-159625-VOL-1A] p0098 N80-11278
Concepts for 18/30 GHz satellite communication system study. Executive summary
[NASA-CR-159680] p0098 N80-11279
- BALDWIN, D. H.
Large wind turbines: A utility option for the generation of electricity
[NASA-TN-81502] p0144 N80-32858
- BALOMBIN, J. E.
An exploratory survey of noise levels associated with a 100 kW wind turbine
p0171 A80-35499
Application of coherence in fan noise studies
[NASA-TP-1630] p0167 N80-18882
An exploratory survey of noise levels associated with a 100kW wind turbine
[NASA-TN-81486] p0169 N80-23102
- BANKS, B. A.
Advanced concepts
p0058 N80-31471
- BARNA, G. J.
Cogeneration Technology Alternatives Study (CTAS). Volume 1: Summary
[NASA-TN-81400] p0141 N80-19626
- BARRANGER, J. P.
Laser-optical blade tip clearance measurement system
p0111 A80-36137
Laser-optical blade tip clearance measurement system
[NASA-TN-81376] p0015 N80-14128
- BARRETT, C. A.
The effect of zirconium on the isothermal oxidation of nominal Ni-14Cr-24Al alloys
p0082 A80-26465

- Mechanical properties and oxidation and corrosion resistance of reduced-chromium 304 stainless steel alloys
[NASA-TP-1557] p0076 N80-11188
- BARNETT, L. E.**
Stabilization of aerodynamically excited turbomachinery with hydrodynamic journal bearings and supports p0128 N80-29731
- BARTH, C. F.**
Cost analysis of composite fan blade manufacturing processes
[NASA-CR-159876] p0044 N80-31398
- BARTLETT, R. O.**
Active control of spacecraft charging p0055 A80-46890
- BASSETT, C. E.**
Conceptual design of an orbital propellant transfer experiment. Volume 2: Study results
[NASA-CR-165150] p0048 N80-31423
- BAUCHSPIES, J. S.**
Aerial applications dispersal systems control requirements study
[NASA-CR-159781] p0158 N80-18586
- BAUMBICK, R. J.**
Optical sensors for aeronautics and space
[NASA-TM-81407] p0110 N80-17423
Fiber optic sensors for measuring angular position and rotational speed
[NASA-TM-81454] p0110 N80-18368
- BAUMHISTE, K. J.**
Time-dependent difference theory for noise propagation in a two-dimensional duct
[AIAA PAPER 80-0098] p0170 A80-18269
A time dependent difference theory for sound propagation in ducts with flow p0170 A80-20951
Time-dependent difference theory for noise propagation in a two-dimensional duct
[NASA-TM-79298] p0167 N80-12822
A time dependent difference theory for sound propagation in ducts with flow
[NASA-TM-79302] p0167 N80-12823
Time dependent difference theory for sound propagation in axisymmetric ducts with plug flow
[NASA-TM-81501] p0168 N80-23096
Numerical techniques in linear duct acoustics
[NASA-TM-81553] p0170 N80-30154
- BAYLESS, J. R.**
8-cm Engineering Model Thruster technology - A review of recent developments
[AIAA PAPER 79-2103] p0064 A80-13311
- BEACH, R. L., JR.**
Hypersonic propulsion p0013 N80-10217
- BEATTIE, J. R.**
A model for predicting the wearout lifetime of the LeRC/Hughes 30-cm mercury ion thruster
[AIAA PAPER 79-2079] p0064 A80-20962
Primary electric propulsion technology study
[NASA-CR-159688] p0061 N80-13158
- BECHTEL, R.**
An electric propulsion long term test facility
[AIAA PAPER 79-2080] p0049 A80-13308
- BECHTEL, R. T.**
Preliminary results of the mission profile life test of a 30 cm Hg bombardment thruster
[AIAA PAPER 79-2078] p0081 A80-10391
- BECK, T. L.**
Testing of reciprocating seals for application in a Stirling cycle engine
[NASA-CR-159820] p0124 N80-22700
- BECK, W. E.**
Zero-length, slotted-lip inlet for subsonic military aircraft
[AIAA PAPER 80-1245] p0004 A80-41203
- BEERS, B. L.**
Negative streamer development in FEP teflon p0179 A80-19776
- BEHLKE, R. F.**
Core compressor exit stage study, 2
[NASA-CR-159812] p0039 N80-23312
Study of blade aspect ratio on a compressor front stage
[NASA-CR-159556] p0040 N80-25333
- BENNING, F. P.**
Design and cold-air test of single-stage uncooled turbine with high work output
[NASA-TP-1680] p0019 N80-25337
- Cold-air investigation of a 4 1/2 stage turbine with stage-loading factor of 4.66 and high specific work output. 2: Stage group performance
[NASA-TP-1688] p0019 N80-25338
- BENRENDT, D. E.**
Calculation of residual principal stresses in CVD boron on carbon filaments p0072 A80-44237
Calculation of residual principal stresses in CVD boron on carbon filaments
[NASA-TM-81456] p0068 N80-20314
- BEITLER, R. S.**
Fuel conservation through active control of rotor clearances
[AIAA PAPER 80-1087] p0045 A80-41506
- BELL, D. D.**
Design study of toroidal traction CVT for electric vehicles
[NASA-CR-159803] p0124 N80-25661
- BELL, V. L.**
Potential release of fibers from burning carbon composites
[NASA-TM-80214] p0069 N80-29431
- BELEAU, C.**
Materials review for improved automotive gas turbine engine
[NASA-CR-159673] p0123 N80-17470
- BENCKERT, H.**
Flow induced spring coefficients of labyrinth seals for application in rotor dynamics p0126 N80-29717
- BENDER, D. J.**
Parametric study of prospective early commercial MHD power plants (PSPEC). General Electric Company, task 1: Parametric analysis
[NASA-CR-159634] p0152 N80-26779
- BENFORD, S. H.**
The erosion/corrosion of small superalloy turbine rotors operating in the effluent of a PFB coal combustor p0080 A80-10043
Improved PFB operations - 400-hour turbine test results p0145 A80-39639
Improved PFB operations: 400-hour turbine test results
[NASA-TM-81511] p0079 N80-26426
- BENN, K. W.**
3500-hour durability testing of ceramic materials for automotive gas turbine engines
[AERESEARCH-31-3542] p0092 A80-35575
The 3500 hour durability testing of commercial ceramic materials
[NASA-CR-159785] p0091 N80-31552
- BENTLY, D. E.**
The parameters and measurements of the destabilizing actions of rotating machines, and the assumptions of the 1950's p0125 N80-29712
- BERCAN, R. W.**
Engineering test facility design definition
[NASA-TM-81499] p0143 N80-27799
- BERNHARD, D. G.**
Free-piston regenerative hot gas hydraulic engine
[NASA-CASE-LEW-12274-1] p0119 N80-31790
- BERKE, L.**
The method of lines in three dimensional fracture mechanics
[NASA-TM-81593] p0132 N80-32753
- BERKOPEC, F.**
First results of material charging in the space environment p0055 A80-45609
- BERKOPEC, F. D.**
Liquid metal slip ring
[NASA-CASE-LEW-12277-3] p0101 N80-18300
- BERKOWITZ, M.**
Multifuel rotary aircraft engine
[AIAA PAPER 80-1237] p0045 A80-38982
- BERNATOWICZ, D. T.**
Space solar cells: High efficiency and radiation damage
[NASA-TM-81387] p0138 N80-15554
- BHAT, R. T.**
Preparation of cast aluminum alloy-mica particle composites p0071 A80-32632
- BHATH, S.**
Design study of a 15 kW free-piston Stirling

- engine-linear alternator for dispersed solar electric power systems
[NASA-CR-159587] p0150 N80-22787
- SHATT, R. T.**
Fatigue behavior of SiC reinforced titanium composites p0070 A80-10036
- BHUSHAN, B.**
High temperature self-lubricating coatings for air lubricated foil bearings for the automotive gas turbine engine
[NASA-CR-159848] p0091 N80-26448
- BIESS, J. J.**
Power processing technology for spacecraft primary ion propulsion p0065 A80-48265
- BIFANO, W. J.**
Description of photovoltaic village power systems in the United States and Africa p0146 A80-46796
- A photovoltaic power system in the remote African village of Tangaye, Upper Volta
[NASA-TM-79318] p0137 N80-12552
- BILL, R. C.**
Wear of seal materials used in aircraft propulsion systems p0121 A80-28010
- Mechanical components p0013 N80-10213
- Some considerations of the performance of two honeycomb gas path seal material systems
[NASA-TM-81398] p0077 N80-16143
- Gas path seal
[NASA-CASE-NPO-12131-3] p0115 N80-18400
- Composite wall concept for high temperature turbine shrouds: Survey of low modulus strain isolator materials
[NASA-TM-81443] p0086 N80-20398
- Preliminary study of methods for providing thermal shock resistance to plasma-sprayed ceramic gas-path seals
[NASA-TP-1561] p0087 N80-23453
- Fully plasma-sprayed compliant backed ceramic turbine seal
[NASA-CASE-LEN-13268-1] p0117 N80-24619
- Composite seal for turbomachinery
[NASA-CASE-LEN-12131-2] p0118 N80-26658
- BILWAKESH, K. R.**
Acoustic performance of a 50.8-cm (20-inch) diameter variable-pitch fan and inlet. Volume 2: Acoustic data
[NASA-CR-135118] p0044 N80-29299
- BIRCHENALL, C. R.**
Heat storage in alloy transformations
[NASA-CR-159787] p0151 N80-24759
- BISHOP, A. R.**
Coannular supersonic ejector nozzles p0002 N80-10128
- BITTNER, D. A.**
An analytical study of nitrogen oxides and carbon monoxide emissions in hydrocarbon combustion with added nitrogen - Preliminary results
[ASME PAPER 80-GT-60] p0074 A80-42190
- An analytical study of nitrogen oxides and carbon monoxide emissions in hydrocarbon combustion with added nitrogen, preliminary results
[NASA-TM-79296] p0157 N80-13721
- BITTNER, J. D.**
Soot formation and burnout in flames p0043 N80-29320
- BIZON, P. T.**
Three dimensional finite-element elastic analysis of a thermally cycled double-edge wedge geometry specimen
[NASA-TM-80980] p0079 N80-26433
- BLACK, H. F.**
Limit cycles of a flexible shaft with hydrodynamic journal bearings in unstable regimes p0127 N80-29725
- BLACK, R. D.**
Hyperfine magnetic field at Cd impurity site in L2/1/ Heusler alloys Rh₂MnGe and Rh₂MnPb by TDPAC technique p0178 A80-16843
- BLAND, T. J.**
The 15 kW sub e (nominal) solar thermal electric power conversion concept definition study: Steam Rankine turbine system
[NASA-CR-159589] p0148 N80-16493
- BLATT, M. H.**
Capillary device refilling
[AIAA PAPER 80-1095] p0060 A80-38908
- Capillary acquisition devices for high-performance vehicles: Executive summary
[NASA-CR-159658] p0062 N80-19185
- BLECHERMAN, S. S.**
Design, durability and low cost processing technology for composite fan exit guide vanes
[NASA-CR-159677] p0027 N80-12091
- BLODNER, H. E.**
Reverse thrust performance of the QCSEE variable pitch turbofan engine
[NASA-TM-81558] p0022 N80-31399
- BLOOMBERG, H. W.**
Negative streamer development in FEP teflon p0179 A80-19776
- BLOOMER, M. E.**
QCSEE UTM engine powered-lift acoustic performance
[AIAA PAPER 80-1065] p0025 A80-38651
- QCSEE fan exhaust bulk absorber treatment evaluation
[NASA-TM-81498] p0019 N80-23314
- QCSEE UTM engine powered-lift acoustic performance
[NASA-TM-81504] p0019 N80-24315
- BLUE, J.**
Preliminary results of fast neutron treatments in carcinoma of the pancreas
[NASA-TM-81516] p0160 N80-24983
- BLUE, J. W.**
Hyperfine magnetic field at Cd impurity site in L2/1/ Heusler alloys Rh₂MnGe and Rh₂MnPb by TDPAC technique p0178 A80-16843
- BOBER, L. A.**
Summary of advanced methods for predicting high speed propeller performance
[NASA-TM-81409] p0002 N80-15051
- BOBER, L. J.**
Summary of advanced methods for predicting high speed propeller performance
[AIAA PAPER 80-0225] p0003 A80-20966
- Advanced propeller aerodynamic analysis p0018 N80-22345
- BODDY, J. A.**
Solar rocket system concept analysis p0064 N80-31470
- BORNSTEIN, M. S.**
Study of the effects of gaseous environments on the hot corrosion of superalloy materials
[NASA-CR-159747] p0083 N80-18155
- BOWDEN, J. H.**
Quiet Clean Short-haul Experimental Engine (QCSEE). Composite fan frame subsystem test report
[NASA-CR-135010] p0035 N80-15098
- BOWDITCH, D. M.**
Computational fluid mechanics of internal flow p0012 N80-10211
- BOWER, G. M.**
Silicone modified resins for graphite fiber laminates
[NASA-CR-159750] p0072 N80-22407
- BOWLES, K. J.**
Fire test method for graphite fiber reinforced plastics p0070 A80-31169
- Burning characteristics and fiber retention of graphite/resin matrix composites p0070 A80-32062
- Improved fiber retention by the use of fillers in graphite fiber/resin matrix composites p0071 A80-32066
- Improved fiber retention by the use of fillers in graphite fiber/resin matrix composites
[NASA-TM-79288] p0067 N80-13171
- Burning characteristics and fiber retention of graphite/resin matrix composites
[NASA-TM-79314] p0067 N80-14196
- Fire test method for graphite fiber reinforced plastics
[NASA-TM-81436] p0068 N80-18107
- BOZEK, J. M.**
Cycles till failure of silver-zinc cells with competing failure modes - Preliminary data analysis p0146 A80-46414
- An averaging battery model for a lead-acid battery operating in an electric car
[NASA-TM-79321] p0165 N80-16824

- Flexible formulated plastic separators for alkaline batteries
[NASA-CASE-LEN-12363-4] p0140 N80-18555
- An electric vehicle propulsion system's impact on battery performance: An overview
[NASA-TM-81515] p0143 N80-24756
- Cycles till failure of silver-zinc cells with completing failures modes: Preliminary data analysis
[NASA-TM-81556] p0164 N80-29088
- BRADLEY, E. E.
Conceptual design of an orbital propellant transfer experiment. Volume 2: Study results
[NASA-CR-165150] p0048 N80-31423
- BRADSHAW, E. D.
Capillary acquisition devices for high-performance vehicles: Executive summary
[NASA-CR-159658] p0062 N80-19185
- BRAINARD, W. A.
Improved adhesion of sputtered refractory carbides to metal substrates
p0081 A80-25274
- An investigation into the role of adhesion in the erosion of ductile metals
[ASLE PREPRINT 80-AM-3E-3] p0122 A80-43159
- Improved refractory coatings and method of producing the same
[NASA-CASE-LEN-13169-1] p0076 N80-14232
- Scanning-electron-microscope study of normal-impingement erosion of ductile metals
[NASA-TP-1609] p0077 N80-16141
- An investigation into the role of adhesion in the erosion of ductile metals
[NASA-TM-81458] p0078 N80-21489
- BRANDHORST, H. W.
Photovoltaic technology development for synchronous orbit
p0058 N80-33470
- Radiation damage in high voltage silicon solar cells
p0144 N80-33889
- BRANDHORST, H. W., JR.
Radiation damage in high voltage silicon solar cells
p0179 A80-44234
- Radiation damage in lithium-counterdoped n/p silicon solar cells
[NASA-TM-81391] p0138 N80-15557
- BRANDHORST, H., JR.
Space solar cells: High efficiency and radiation damage
[NASA-TM-81387] p0138 N80-15554
- Radiation damage in high voltage silicon solar cells
[NASA-TM-81478] p0178 N80-23180
- BRANDON, W. T.
On-board processing concepts for future satellite communications systems
[NASA-CR-159683] p0099 N80-24514
- BRATTON, E. J.
Evaluation of present-day thermal barrier coatings for industrial/utility applications
p0092 A80-39637
- BRENNAN, J. J.
Development of silicon nitride of improved toughness
[NASA-CR-159676] p0072 N80-10319
- BRENNEN, C. E.
A test program to measure fluid mechanical whirl-excitation forces in centrifugal pumps
p0126 N80-29719
- BREVE, D. E.
Preliminary study of methods for providing thermal shock resistance to plasma-sprayed ceramic gas-path seals
[NASA-TP-1561] p0087 N80-23453
- BRILEY, W. E.
A three-dimensional turbulent compressible subsonic duct flow analysis for use with constructed coordinate systems
[AIAA PAPER 80-1398] p0006 A80-41601
- BRITT, E. J.
A cesium TELEC experiment at Lewis Research Center
[NASA-CR-159729] p0113 N80-14386
- BROOKS, B. H.
Acoustic measurements of three Prop-Fan models
[AIAA PAPER 80-0995] p0045 A80-35958
- Advanced turbo-prop airplane interior noise reduction-source definition
[NASA-CR-159668] p0172 N80-13882
- Acoustic test and analyses of three advanced turboprop models
[NASA-CR-159667] p0039 N80-23311
- BROOKY, J. D.
Study of blade aspect ratio on a compressor front stage
[NASA-CR-159556] p0040 N80-25333
- BROPHY, J. E., JR.
Baffle aperture design study of hollow cathode equipped ion thrusters
[NASA-CR-165164] p0064 N80-33476
- BROUWERS, A. P.
A 150 and 300 kw lightweight diesel aircraft engine design study
[NASA-CR-3260] p0037 N80-20271
- Design study: A 186 kw lightweight diesel aircraft engine
[NASA-CR-3261] p0038 N80-22326
- BROWN, D. H.
Cogeneration Technology Alternatives Study (CTAS). Volume 1: Summary report
[NASA-CR-159765] p0151 N80-24797
- Cogeneration Technology Alternatives Study (CTAS). Volume 2: Analytical approach
[NASA-CR-159766] p0143 N80-28859
- Cogeneration Technology Alternatives Study (CTAS). Volume 4: Energy conversion systems
[NASA-CR-159768] p0155 N80-33859
- BROWN, R. D.
Limit cycles of a flexible shaft with hydrodynamic journal bearings in unstable regimes
p0127 N80-29725
- BURNEY, R. T.
Fracture toughness determination of Al203 using four-point-bend specimens with straight-through and chevron notches
p0090 A80-42085
- Compliance and stress intensity coefficients for short bar specimens with chevron notches
p0133 A80-46032
- Performance of Chevron-notch short bar specimen in determining the fracture toughness of silicon nitride and aluminum oxide
p0090 A80-50696
- BUCHHOLZ, R.
Assessment and preliminary design of an energy buffer for regenerative braking in electric vehicles
[NASA-CR-159756] p0184 N80-23216
- BUCK, R.
Improved traveling wave tubes
p0102 A80-44235
- Improved traveling wave tubes
[NASA-TM-81479] p0102 N80-22598
- BUCKLEY, D. H.
Metal-dielectric interactions
p0081 A80-13067
- The friction and wear of metals and binary alloys in contact with an abrasive grit of single-crystal silicon carbide
[ASLE PREPRINT 79-LC-5C-1] p0120 A80-14734
- Adhesion and friction of iron-base binary alloys in contact with silicon carbide in vacuum
[NASA-TP-1604] p0076 N80-15234
- Tribological properties of silicon carbide in metal removal process
[NASA-TM-79238] p0114 N80-16340
- Wear particles of single-crystal silicon carbide in vacuum
[NASA-TP-1624] p0085 N80-18178
- Adhesion, friction, and wear of binary alloys in contact with single-crystal silicon carbide
[NASA-TM-79202] p0086 N80-21534
- Friction and wear of iron-base binary alloys in sliding contact with silicon carbide in vacuum
[NASA-TP-1612] p0087 N80-22494
- BUGGELN, R. C.
Computation of three-dimensional viscous supersonic flow in inlets
[AIAA PAPER 80-0194] p0065 A80-23941
- Development of a three-dimensional supersonic inlet flow analysis
[NASA-CR-3218] p0108 N80-14356
- BUJOLD, M. P.
Small passenger car transmission test-Chevrolet 200 transmission
[NASA-CR-159835] p0185 N80-28255
- Small passenger car transmission test; Ford C4 transmission
[NASA-CR-159881] p0128 N80-31795
- Small passenger car transmission test; Chevrolet LUV transmission

- [NASA-CR-159882] p0128 N80-31796
BUKOWSKI, R.
 Preliminary results of fast neutron treatments in carcinoma of the pancreas
 [NASA-TN-81516] p0160 N80-24983
- BURDSALL, E. A.**
 Core compressor exit stage study. 1: Aerodynamic and mechanical design
 [NASA-CR-159714] p0037 N80-19113
 Core compressor exit stage study, 2
 [NASA-CR-159812] p0039 N80-23312
- BURGESS, G.**
 Elastomer damper performance - A comparison with a squeeze film for a supercritical power transmission shaft
 [ASME PAPER 80-GT-162] p0121 A80-42272
 Development of procedures for calculating stiffness and damping of elastomers in engineering applications, part 6
 [NASA-CR-159838] p0134 N80-22733
- BURKHART, J. A.**
 Oxygen-enriched air for MHD power plants
 p0096 A80-25096
- BURKHOLDER, J. H.**
 Economical space power systems
 [NASA-CR-159696] p0147 N80-15559
- BURLIN, R. E.**
 Some techniques for reducing the tower shadow of the DOE/NASA mod-0 wind turbine tower
 [NASA-TN-79202] p0137 N80-10594
- BURMEISTER, L. C.**
 Spectral effects on direct-insolation absorptance of five collector coatings
 [ASME PAPER 79-HT-18] p0146 A80-45722
- BURNS, R. K.**
 Cogeneration Technology Alternatives Study (CTAS). Volume 1: Summary
 [NASA-TN-81400] p0141 N80-19626
- BURRIN, R. H.**
 A study of the transmission characteristics of suppressor nozzles
 [NASA-CR-165133] p0172 N80-32186
- BURRUS, D.**
 Energy efficient engine
 [NASA-CR-159685] p0045 N80-33408
- BURRUS, D. L.**
 Quiet Clean Short-haul Experimental Engine (QCSEE). Double-annular clean combustor technology development report
 [NASA-CR-159483] p0032 N80-15121
- BURSEY, R. T.**
 Fracture toughness of brittle materials determined with chevron notch specimens
 [NASA-TN-81607] p0079 N80-32486
- BUZZARD, E. J.**
 Comparison tests and experimental compliance calibration of the proposed standard round compact plane strain fracture toughness specimen
 [NASA-TN-81379] p0132 N80-13513
- BYERS, D. C.**
 Characteristics of primary electric propulsion systems
 [AIAA PAPER 79-2041] p0058 A80-10376
 Upper stages utilizing electric propulsion
 p0059 A80-29989
 Nuclear electric propulsion system utilization for earth orbit transfer of large spacecraft structures
 [AIAA PAPER 80-1223] p0060 A80-38975
 Orbital transfer of large space structures with nuclear electric rockets
 [AAS PAPER 80-083] p0054 A80-41897
 Upper stages utilizing electric propulsion
 [NASA-TN-81412] p0056 N80-16097
 Upper stages utilizing electric propulsion
 p0057 N80-30386
- C**
- CAGEAO, R. P.**
 Influence of coolant tube curvature on film cooling effectiveness as detected by infrared imagery
 [NASA-TP-1546] p0013 N80-11087
- CAHILL, K.**
 Advanced screening of electrode couples
 [NASA-TP-159738] p0141 N80-22777
- CAHILL, K.**
 Catalyst surfaces for the chromous/chromic redox couple
 [NASA-CASE-LEW-13148-2] p0140 N80-18557
 Catalyst surfaces for the chromous/chromic redox couple
 [NASA-CASE-LEW-13148-1] p0101 N80-20487
- CALPO, P. D.**
 Computerized video densitometry method for rapid analysis of infrared photographic images
 [NASA-TP-1686] p0110 N80-25635
- CALHOUN, J. T.**
 Feasibility study of aileron and spoiler control systems for large horizontal axis wind turbines
 [NASA-CR-159856] p0153 N80-27803
- CAMPBELL, P. P.**
 Current jet fuel trends
 p0041 N80-29303
- CANAL, R., JR.**
 Core compressor exit stage study. 1: Aerodynamic and mechanical design
 [NASA-CR-159714] p0037 N80-19113
 Core compressor exit stage study, 2
 [NASA-CR-159812] p0039 N80-23312
 Study of blade aspect ratio on a compressor front stage
 [NASA-CR-159556] p0040 N80-25333
- CANNON, E. H., JR.**
 Improving the stress rupture and creep of silicon nitride
 [NASA-CR-159585] p0072 N80-10318
- CARD, E. E.**
 Outlook for alternative energy sources
 p0041 N80-29302
- CARLSON, C. E. K.**
 Diffusion bonded boron/aluminum spar-shell fan blade
 [NASA-CR-159571] p0072 N80-25382
- CARR, E. J.**
 Conceptual design of an orbital propellant transfer experiment. Volume 2: Study results
 [NASA-CR-165150] p0048 N80-31423
- CARRUTHERS, H. D.**
 3500-hour durability testing of ceramic materials for automotive gas turbine engines
 [AIAA-SEARCH-31-3542] p0092 A80-35575
 The 3500 hour durability testing of commercial ceramic materials
 [NASA-CR-159785] p0091 N80-31552
- CARTER, J., JR.**
 A 15 kWe (nominal) solar thermal-electric power conversion concept definition study: Steam Rankin reciprocator system
 [NASA-CR-159591] p0149 N80-19612
- CARUTHERS, J. E.**
 Aerodynamic analysis of a supersonic cascade vibrating in a complex mode
 p0007 A80-45841
- CASSIDY, J.**
 A three-dimensional spacecraft-charging computer code
 p0055 A80-46891
- CASTELLI, V.**
 High speed cylindrical rolling element bearing analysis 'CYBEAN' - Analytic formulation
 [ASME PAPER 79-LUB-35] p0129 A80-14761
- CATALDO, R. C.**
 An electric vehicle propulsion system's impact on battery performance: An overview
 [NASA-TN-81515] p0143 N80-24756
- CAUGHEY, T. K.**
 A test program to measure fluid mechanical whirl-excitation forces in centrifugal pumps
 p0126 N80-29719
- CAVANAGH, J. E.**
 Plasma-sprayed dual density ceramic turbine seal system
 [NASA-CR-159739] p0123 N80-15411
- CAVANO, P. J.**
 Second generation PMR polyimide/fiber composites
 [NASA-CR-159666] p0072 N80-12118
- CENKUS, H. A.**
 Mechanical and chemical effects of ion-texturing biomedical polymers
 p0089 A80-13065
- CHAI, A. T.**
 Back surface reflectors for solar cells
 [NASA-TN-81390] p0138 N80-15556
 Planar multijunction high voltage solar cells
 [NASA-TN-81389] p0178 N80-16914
- CHAI, A.-T.**
 The planar multijunction cell - A new solar cell

- for earth and space p0146 A80-48205
- CHAMBERLIN, R.
Scale model performance test investigation of
exhaust system mixers for an Energy Efficient
Engine /E3/ propulsion system
[AIAA PAPER 80-0229] p0024 A80-20968
- CHAMIS, C. C.
Mechanical property characterization of intraply
hybrid composites p0070 A80-20954
Dynamic response of damaged angleplied fiber
composites p0070 A80-27982
Micromechanics of intraply hybrid composites:
Elastic and thermal properties p0070 A80-27994
Prediction of fiber composite mechanical behavior
made simple p0133 A80-32067
Engine environmental effects on composite behavior
[AIAA 80-0695] p0024 A80-35101
Micromechanics of intraply hybrid composites:
Elastic and thermal properties p0067 N80-11143
Tensile and flexural strength of non-graphitic
superhybrid composites: Predictions and
comparisons p0067 N80-11144
Dynamic response of damaged angleplied fiber
composites p0067 N80-11145
Mechanical property characterization of intraply
hybrid composites p0067 N80-12120
Prediction of fiber composite mechanical behavior
made simple p0068 N80-16107
Engine environmental effects on composite behavior
[NASA-TM-81508] p0069 N80-23370
- CHANG, M.
Durability testing of advanced catalysts and
catalyst supports for gas turbine engine
combustors p0074 A80-35881
- CHAO, M. H.
Phase change in liquid face seals. II - Isothermal
and adiabatic bounds with real fluids
[ASME PAPER 79-LUB-4] p0129 A80-14739
- CHAPMAN, W. I.
Conceptual design study of an improved gas turbine
powertrain p0039 N80-23315
[NASA-CR-159852]
- CHEN, E. P.
Sudden stretching of a four layered composit. plate
[NASA-CR-159870] p0073 N80-25383
Sudden bending of cracked laminates
[NASA-CR-159860] p0073 N80-25384
- CHEN, H. S.
Design study of a 15 kW free-piston Stirling
engine-linear alternator for dispersed solar
electric power systems p0150 N80-22787
[NASA-CR-159587]
- CHEN, W. Y. C.
Anodic polarization behavior of austenitic
stainless steel alloys with lower chromium content
p0178 A80-22250
- CHESTER, H.
Heat pipe cooling of power processing magnetics
[AIAA PAPER 79-2082] p0107 A80-20960
- CHESTER, H. S.
Heat pipe cooling of power processing magnetics
[NASA-TM-79270] p0101 N80-11327
Heat pipe cooled power magnetics
[NASA-CR-159659] p0103 N80-12362
- CHETNIK, F.
Packet communications in satellites with
multiple-beam antennas and signal processing
[AIAA 80-0537] p0099 A80-29574
- CHIANG, K. T.
Hot corrosion of Co-Cr, Co-Cr-Al, and Ni-Cr alloys
in the temperature range of 700-750 deg C
[NASA-CR-159689] p0084 N80-26427
- CHIAPPETTA, L.
External fuel vaporization study, phase 1
[NASA-CR-159850] p0095 N80-25453
- CHIGIER, M. A.
Air pollution from aircraft
[NASA-CR-159712] p0010 N80-16060
- CHILDS, D. W.
Testing of turbulent seals for rotodynamic
coefficients p0126 N80-29714
- CHILDS, S. B.
Testing of turbulent seals for rotodynamic
coefficients p0126 N80-29714
- CHINA, B. V.
Comparison between optical measurements and a
numerical solution of the flow field within a
transonic axial-flow compressor rotor
[AIAA PAPER 80-1078] p0003 A80-38897
An implicit finite-difference code for inviscid
and viscous cascade flow
[AIAA PAPER 80-1427] p0007 A80-44128
- CHIU, W. S.
Sintered silicon nitride recuperator fabrication
[NASA-CR-159706] p0090 N80-15263
- CHO, Y. C.
Higher order mode propagation in nonuniform
circular ducts p0171 A80-35974
[AIAA PAPER 80-1018]
Rigorous solutions for sound radiation from
circular ducts with hyperbolic horns or infinite
plane baffle p0171 A80-37895
Reciprocity principle in duct acoustics
[NASA-TM-79300] p0167 N80-12824
Higher order mode propagation in nonuniform
circular ducts p0169 N80-23101
[NASA-TM-81481]
- CHO, Y.-C.
Reciprocity principle in duct acoustics
p0170 A80-20956
- CHRISTENSEN, L. S.
Monodisperse atomizers for agricultural aviation
applications p0108 N80-19450
[NASA-CR-159777]
- CHRISTNER, L.
Technology development for phosphoric acid fuel
cell powerplant, phase 2
[NASA-CR-159705] p0147 N80-10603
- CHUBB, D. L.
Study of a rare-gas transverse fast discharge
p0176 A80-11366
- CIEPLUCH, C. C.
Vertical Takeoff and Landing (VTOL) propulsion
technology p0013 N80-10218
- CLAAR, T. D.
High-temperature molten salt thermal energy
storage systems p0148 N80-17547
[NASA-CR-159663]
- CLARK, J. S.
Status of the DOE/NASA critical gas turbine
research and technology project p0137 N80-14493
[NASA-TM-79307]
Literature survey of properties of syngas
derived from coal p0141 N80-22776
[NASA-TM-79243]
- CLARY, W. L.
Aerial applications dispersal systems control
requirements study p0158 N80-18586
[NASA-CR-159781]
- CLEMONS, A.
Acoustic analysis of aft noise reduction
techniques measured on a subsonic tip speed 50.8
cm (twenty inch) diameter fan p0030 N80-15102
[NASA-CR-134891]
Quiet Clean Short-Haul Experimental Engine
(QCSSE): Acoustic treatment development and
design p0033 N80-15122
[NASA-CR-135266]
Acoustic performance of a 50.8-cm (20-inch)
diameter variable-pitch fan and inlet. Volume
2: Acoustic data p0044 N80-29299
[NASA-CR-135118]
- CLINGMAN, D. L.
Plasma-sprayed dual density ceramic turbine seal
system p0123 N80-15411
[NASA-CR-159739]
- COCHMAN, R. P.
Temperature and pressure measurement techniques
for an advanced turbine test facility p0112 A80-36157
Temperature and pressure measurement techniques
for an advanced turbine test facility p0110 N80-14374
[NASA-TM-79278]

- COB, M. H.
Comparison of predicted and experimental performance of large-bore roller bearing operating to 3.0 million DM
[NASA-TP-1599] p0114 N80-15410
Calculated and experimental data for a 118-mm bore roller bearing to 3 million DM
[NASA-TM-81427] p0116 N80-19496
- COHEN, S. M.
Fuels research: Fuel thermal stability overview
p0021 N80-29324
- COLDING-JORGENSEN, J.
Effect of fluid forces on rotor stability of centrifugal compressors and pumps
p0126 N80-29720
- COLLIN, B. E.
Low sidelobe level low-cost earth station antennas for the 12 GHz broadcasting satellite service
[NASA-CR-159703] p0098 N80-12259
- COLLINS, J. L.
Installation and checkout of the DOE/NASA Mod-1 2000-kW wind turbine generator
[AIAA 80-0638] p0145 A80-28835
Installation and checkout of the DOE/NASA Mod-1 2000-kW wind turbine generator
[NASA-TM-81444] p0140 N80-19614
- COLONY, D. C.
A new traffic control design method for large networks with signalized intersections
p0183 A80-14841
- COLTSON, R. E.
Supersonic propulsion technology
p0013 N80-10216
An analytical and experimental study of a short s-shaped subsonic diffuser of a supersonic inlet
[NASA-TM-81406] p0015 N80-15134
- CORRY, T. A.
Coordinated aircraft and ship surveys for determining impact of river inputs on great lakes waters. Remote sensing results
[NASA-TP-1694] p0157 N80-27832
- CONNOLLY, D. J.
Coupled cavity traveling wave tube with velocity tapering
[NASA-CASE-LEW-12296-1] p0101 N80-19425
- CONRAD, E. W.
Turbine engine altitude chamber and flight testing with liquid hydrogen
p0023 A80-10034
- COOK, R. T.
Advanced cooling techniques for high-pressure, hydrocarbon-fueled rocket engines
[AIAA PAPER 80-1266] p0060 A80-38994
Advanced cooling techniques for high-pressure hydrocarbon-fueled engines
[NASA-CR-159790] p0061 N80-17147
- COOPER, L. P.
Effect of degree of fuel vaporization upon emissions for a premixed partially vaporized combustion system
[NASA-TP-1582] p0014 N80-14125
- COPPOLA, E. M.
Military jet fuel from shale oil
p0042 N80-29308
- CORLEY, R. C.
Method and apparatus for rapid thrust increases in a turbofan engine
[NASA-CASE-LEW-12971-1] p0016 N80-18039
- CONNETT, J. E.
Method and apparatus for rapid thrust increases in a turbofan engine
[NASA-CASE-LEW-12971-1] p0016 N80-18039
- COWARD, W. E.
Quiet, Clean, Short-Haul, Experimental Engine (QCSEE) Under-The-Wing (UTW) engine acoustic design
[NASA-CR-135267] p0028 N80-14117
Quiet, Clean, Short-Haul Experimental Engine (QCSEE) Over-The-Wing (OTW) engine acoustic design
[NASA-CR-135268] p0028 N80-14118
Quiet Clean Short-haul Experimental Engine (QCSEE). Core engine noise measurements
[NASA-CR-135160] p0035 N80-15093
- COWLES, B. A.
Evaluation of the cyclic behavior of aircraft turbine disk alloys, part 2
[NASA-CR-165123] p0084 N80-30482
- COY, J. J.
NASA gear research and its probable effect on rotorcraft transmission design
p0120 A80-13068
- Constrained fatigue life optimization of a NASVYTIS multiroller traction drive
p0122 A80-46407
- Simplified fatigue life analysis for traction drive contacts
p0123 A80-46413
- Mechanical components
p0013 N80-10213
- Simplified fatigue life analysis for traction drive contacts
[NASA-TM-79199] p0115 N80-17469
- Constrained fatigue life optimization of a NASVYTIS multiroller traction drive
[NASA-TM-81447] p0116 N80-18407
- Some limitations in applying classical EHD film-thickness formulae to a high-speed bearing
[NASA-TM-81431] p0116 N80-18409
- Ideal spiral bevel gears: A new approach to surface geometry
[NASA-TM-81446] p0117 N80-19498
- CRANDALL, S. H.
Physical explanations of the destabilizing effect of damping in rotating parts
p0127 N80-29728
- CRAWFORD, M. E.
Full-coverage film cooling. I - Comparison of heat transfer data for three injection angles
[ASME PAPER 80-GT-43] p0108 A80-42176
Full-coverage film cooling. II - Heat transfer data and numerical simulation
[ASME PAPER 80-GT-44] p0109 A80-42177
- CRISALLI, A. J.
Evaluation of a strained-coordinate perturbation procedure - Nonlinear subsonic and transonic flows
[AIAA PAPER 80-0339] p0006 A80-18324
- CROLEY, D. E., JR.
First results of material charging in the space environment
p0055 A80-45609
- CROSS, K. E.
Plasma-sprayed dual density ceramic turbine seal system
[NASA-CR-159739] p0123 N80-15411
- CROUSE, J. E.
Off-design correlation for losses due to part-span dampers on transonic rotors
[NASA-TP-1693] p0020 N80-28352
- CROW, D. E.
Results from tests on a high work transonic turbine for an energy efficient engine
[ASME PAPER 80-GT-146] p0026 A80-42258
- CSOMOR, A.
Small, high pressure liquid hydrogen turbopump
[NASA-CR-159821] p0125 N80-26662
- CUCCIA, L.
Concepts for 18/30 GHz satellite communication system, volume 1
[NASA-CR-159625-VOL-1] p0098 N80-11277
Concepts for 18/30 GHz satellite communication system, volume 1A: Appendix
[NASA-CR-159625-VOL-1A] p0098 N80-11278
Concepts for 18/30 GHz satellite communication system study. Executive summary
[NASA-CR-159680] p0098 N80-11279
- CULP, D. H.
Liquid metal slip ring
[NASA-CASE-LEW-12277-3] p0101 N80-18300
- CUNNINGHAM, R.
Elastomer damper performance - A comparison with a squeeze film for a supercritical power transmission shaft
[ASME PAPER 80-GT-162] p0121 A80-42272
- CUNNINGHAM, R. E.
Design of elastomer dampers for a high-speed flexible rotor
[ASME PAPER 79-DET-88] p0121 A80-15736
Dynamic properties of elastomer cartridge specimens under a rotating load
p0121 A80-24002
- CURTIS, H. B.
Global calibration of terrestrial reference cells and errors involved in using different irradiance monitoring techniques
[NASA-TM-81393] p0138 N80-15561
- CURULLA, J. F.
Testing of reciprocating seals for application in a Stirling cycle engine

- [NASA-CR-159820] p0124 N80-22700
CUSANO, C.
 Elastohydrodynamic film thickness measurements of
 artificially-produced nonsmooth surfaces
 [ASLE PREPRINT 79-LC-1A-3] p0102 A80-14720
CUTLER, J. L.
 Diffusion bonded boron/aluminum spar-shell fan blade
 [NASA-CR-159571] p0072 N80-25382
CUTTING, J. C.
 Survey of MHD plant applications p0144 A80-11972
 Oxygen-enriched air for MHD power plants p0096 A80-25096
CHYNAB, D. S.
 INFORM: An interactive data collection and
 display program with debugging capability
 [NASA-TF-1424] p0162 N80-16742

D

- DANIEL, S. R.**
 Mechanisms of nitrogen heterocycle influence on
 turbine fuel stability p0043 N80-29327
DANIELLE, C. J.
 Preliminary results from a four-working space,
 double-acting piston, Stirling engine controls
 model [NASA-TM-81569] p0106 N80-29624
DANTONITZ, P.
 A 15kWe (nominal) solar thermal electric power
 conversion concept definition study: Steam
 Rankine reheat reciprocator system
 [NASA-CR-159590] p0148 N80-16491
DARLOW, M. S.
 The effects of strain and temperature on the
 dynamic properties of elastomers
 [ASME PAPER 79-DET-57] p0092 A80-15720
 Design of elastomer dampers for a high-speed
 flexible rotor [ASME PAPER 79-DET-88] p0121 A80-15736
 Dynamic properties of elastomer cartridge
 specimens under a rotating load p0121 A80-24002
DAROLIA, R.
 Feasibility of SiC composite structures for 1644
 deg gas turbine seal applications [NASA-CR-159597] p0123 N80-13474
DAT, B.
 A phenomenological model of the dynamic stall of a
 helicopter blade profile [ONERA, TP No. 1979-149] p0006 A80-20086
DAVIES, R.
 Packet communications in satellites with
 multiple-beam antennas and signal processing
 [AIAA 80-0537] p0099 A80-29574
 Concepts for 20/30 GHz satcom systems for
 direct-to-user applications [AIAA 80-0582] p0050 A80-35329
 Concepts for 18/30 GHz satellite communication
 system, volume 1 [NASA-CR-159625-VOL-1] p0098 N80-11277
 Concepts for 18/30 GHz satellite communication
 system, volume 1A: Appendix [NASA-CR-159625-VOL-1A] p0098 N80-11278
 Concepts for 18/30 GHz satellite communication
 system study. Executive summary [NASA-CR-159680] p0098 N80-11279
DAVIS, L. K.
 Parametric study of prospective early commercial
 MHD power plants (PSPEC). General Electric
 Company, task 1: Parametric analysis
 [NASA-CR-159634] p0152 N80-26779
DAYTON, J. A., JR.
 Analytical prediction and experimental
 verification of TWT and depressed collector
 performance using multidimensional computer
 programs p0102 A80-13902
DE WITT, K. J.
 Combustion of solid carbon rods in zero and normal
 gravity p0074 A80-20955
 Marangoni bubble motion in zero gravity p0107 A80-20958
DEADMORE, D. L.
 An experimental, low-cost, silicon-aluminide
 high-temperature coating for superalloys p0082 A80-35501

- Effect of sodium, potassium, magnesium, calcium,
 and chlorine on the high temperature corrosion
 of IN-100, U-700, IN-792, and MAR M-509
 [ASME PAPER 80-GT-150] p0083 A80-42262
 Effect of sodium, potassium, magnesium, calcium,
 and chlorine on the high temperature corrosion
 of IN-100, U-700, IN-792, and MAR M-509
 [NASA-TM-79309] p0076 N80-15235
 Effects of impurities in coal-derived liquids on
 accelerated hot corrosion of superalloys
 [NASA-TM-81384] p0077 N80-18157
 An experimental, low-cost, silicon-aluminide
 high-temperature coating for superalloys
 [NASA-TM-81455] p0078 N80-20370
 Fouling and the inhibition of salt corrosion
 [NASA-TM-81469] p0078 N80-21492
 A silicon-slurry/aluminide coating
 [NASA-CASE-LEW-13343-1] p0069 N80-26389
DEAN, P. D.
 Studies of the acoustic transmission
 characteristics of coaxial nozzles with inverted
 velocity profiles, volume 1 [NASA-CR-159698] p0172 N80-11670
DECKER, M. O.
 Design, fabrication and testing of an optical
 temperature sensor [NASA-CR-165125] p0112 N80-31777
DEFFO, A.
 Quiet Clean Short-haul Experimental Engine (QCSSE)
 main reduction gears detailed design report
 [NASA-CR-134872] p0030 N80-15106
DEFOREST, S. E.
 Torquing and electrostatic deformation of the
 solar sail p0065 A80-46901
DEISSLER, M. G.
 Evolution of a rotating flow in the vicinity of a
 surface p0107 A80-14660
DELANO, C. B.
 Synthesis of improved polyester resins
 [NASA-CR-159665] p0090 N80-13257
 Synthesis of improved phenolic resins
 [NASA-CR-159724] p0091 N80-17221
DELFOSE, A. J.
 Determination of jet fuel thermal deposit rate
 using a modified JFTOT p0043 N80-29326
DELLINGER, T. C.
 Coupled generator and combustor performance
 calculations for potential early commercial MHD
 power plants p0156 A80-25099
 Parametric study of prospective early commercial
 MHD power plants (PSPEC). General Electric
 Company, task 1: Parametric analysis
 [NASA-CR-159634] p0152 N80-26779
DELVIGS, P.
 High char imide-modified epoxy matrix resins
 p0071 A80-34789
DELVISS, P.
 Low temperature cross linking polyimides
 [NASA-CASE-LEW-12876-1] p0087 N80-26447
DEMERTSI, R. P.
 Study of research and development requirements of
 small gas-turbine combustors [NASA-CR-159796] p0036 N80-18040
DEMLER, R.
 A 15kWe (nominal) solar thermal electric power
 conversion concept definition study: Steam
 Rankine reheat reciprocator system
 [NASA-CR-159590] p0148 N80-16491
DENNIS, R. E.
 Abradable compressor and turbine seals, volume 1
 [NASA-CR-159600] p0083 N80-14235
DEONATH, M.
 Preparation of cast aluminum alloy-mica particle
 composites p0071 A80-32632
DERGANCE, R. H.
 Primary propulsion/large space system interactions
 p0063 N80-31458
 Low-thrust chemical orbit to orbit propulsion
 system propellant management study p0064 N80-31469
DEWITT, E. J.
 Marangoni bubble motion in zero gravity
 [NASA-TM-79250] p0104 N80-13403

Combustion of solid carbon rods in zero and normal gravity
[NASA-TM-79303] p0104 N80-13404

DICARLO, J. A.
Predicting the time-temperature dependent axial failure of B/AI composites p0071 A80-35494

Dynamic modulus and damping of boron, silicon carbide, and alumina fibers p0071 A80-44236

Dynamic modulus and damping of boron, silicon carbide, and alumina fibers
[NASA-TM-81422] p0068 N80-20313

Predicting the time-temperature dependent axial failure of B/AI composites
[NASA-TM-81474] p0069 N80-21452

DINDRICH, J. W.
Some techniques for reducing the tower shadow of the DOE/NASA mod-0 wind turbine tower
[NASA-TM-79202] p0137 N80-10594

Optimum subsonic, high-angle-of-attack nacelles
[NASA-TM-81491] p0016 N80-20275

DINHL, L. A.
Emission reduction p0012 N80-10207

DITTRICH, M. W.
Energy conservation and environmental benefits of thermal energy storage systems in the pulp and paper industry p0146 A80-48194

Collection and dissemination of TES system information for the paper and pulp industry p0142 N80-22797

DITTMAN, J. W.
High-speed-propeller wind-tunnel aeroacoustic results p0018 N80-22344

A comparison between an existing propeller noise theory and wind tunnel data
[NASA-TM-81519] p0169 N80-25101

DOBLER, F. X.
Concept definition study of small Brayton cycle engines for dispersed solar electric power systems
[NASA-CR-159592] p0150 N80-22778

DOCHAT, G. E.
Design study of a 15 kW free-piston Stirling engine-linear alternator for dispersed solar electric power systems
[NASA-CR-159587] p0150 N80-22787

DODDS, W. J.
Advanced catalytic combustors for low pollutant emissions, phase 1
[NASA-CR-159535] p0028 N80-13048

NASA/General Electric broad-specification fuels combustion technology program, phase 1 p0042 N80-29316

DONITZ, S.
Neutralization tests on the SERT II spacecraft
[AIAA PAPER 79-2064] p0059 A80-10387

DONALD, G. H.
Analysis and identification of subsynchronous vibration for a high pressure parallel flow centrifugal compressor p0125 N80-29710

DONOUGHE, P. L.
Communications technology satellite - United States experiments and disaster communications applications p0051 A80-10032

DOOLBY, J. T.
Assessment of satellite and aircraft multispectral scanner data for strip-mine monitoring
[NASA-TM-79268] p0136 N80-20787

DOUGLAS, M.
Torquing and electrostatic deformation of the solar sail p0065 A80-46901

DOWNING, R. G.
Characterization of solar cells for space applications. Volume 10: Electrical characteristics of Spectrolab BSF, textured, 10 ohm-cm, 300 micron cells as a function of intensity, temperature and irradiation
[NASA-CR-162422] p0147 N80-11566

DOYLE, M. E.
Field experiences with rotordynamic instability in high-performance turbomachinery p0125 N80-29707

DOYLE, V. L.
Core noise investigation of the CF6-50 turbofan engine
[NASA-CR-159598] p0036 N80-16061

Core noise investigation of the CF6-50 turbofan engine
[NASA-CR-159749] p0036 N80-16062

DRAKE, G. L.
Conceptual design of an orbital propellant transfer experiment. Volume 2: Study results
[NASA-CR-165150] p0048 N80-31423

DRAKE, S. E.
Three dimensional finite-element elastic analysis of a thermally cycled double-edge wedge geometry specimen
[NASA-TM-80980] p0079 N80-26433

DRENNER, M. E.
Evaluation of feasibility of prestressed concrete for use in wind turbine blades
[NASA-CR-159725] p0147 N80-15553

DRENNFIELD, M. L.
Effects of thermally induced porosity on an as-HIP powder metallurgy superalloy p0082 A80-29990

Effects of fine porosity on the fatigue behavior of a powder metallurgy superalloy p0082 A80-35495

Application of superalloy powder metallurgy for aircraft engines p0122 A80-44240

Anisotropy of nickel-base superalloy single crystals p0083 A80-51573

Effect of thermally induced porosity on an as-HIP powder metallurgy superalloy
[NASA-TM-79263] p0076 N80-11189

Anisotropy of nickel-base superalloy single crystals
[NASA-TM-81437] p0077 N80-17200

Application of superalloy powder metallurgy for aircraft engines
[NASA-TM-81466] p0078 N80-21488

Effects of fine porosity on the fatigue behavior of a powder metallurgy superalloy
[NASA-TM-81448] p0078 N80-21493

DRESSMAN, J. B.
Testing of turbulent seals for rotodynamic coefficients p0126 N80-29714

DRUBKA, R. E.
Effects of axisymmetric contractions on turbulence of various scales
[NASA-CR-165136] p0006 N80-32328

DUDEKINSKI, T. J.
NASA Global Atmospheric Sampling Program (GASP) data report for tapes VL0011 and VL0013
[NASA-TM-81462] p0157 N80-21892

DUGAN, J. F.
The NASA high-speed turboprop program
[NASA-TM-81561] p0022 N80-31401

DUGAN, J. F., JR.
Aircraft Energy Efficiency (ACEE) status report p0012 N80-10206

DULGHEROFF, C. E.
8-cm Engineering Model Thruster technology - A review of recent developments
[AIAA PAPER 79-2103] p0064 A80-13311

DULIKRAVICH, D. S.
Numerical calculation of steady inviscid full potential compressible flow about wind turbine blades
[AIAA 80-0607] p0145 A80-28804

Numerical calculation of transonic axial turbomachinery flows p0004 A80-44229

Numerical calculation of steady inviscid full potential compressible flow about wind turbine blades
[NASA-TM-81438] p0136 N80-18497

CAS2D: FORTRAN program for nonrotating blade-to-blade, steady, potential transonic cascade flows
[NASA-TP-1705] p0003 N80-27284

Numerical calculation of transonic axial turbomachinery flows
[NASA-TM-81544] p0020 N80-27363

WIND: Computer program for calculation of three dimensional potential compressible flow about wind turbine rotor blades
[NASA-TP-1729] p0003 N80-33357

- DURBIN, P. A.**
The effect of finite turbulence spatial scale on the amplification of turbulence by a contracting stream
p0004 A80-44862
- DURNAN, A. P.**
NASA communications technology research and development
p0097 A80-25920
- DUSA, D. J.**
CF6-50 Short Core Exhaust Nozzle
[AIAA PAPER 80-1196]
p0025 A80-41514
- DUSCHNA, E. A.**
Industrial storage applications overview
p0142 N80-22795
- DUTTA, S.**
Characterization and properties of controlled nucleation thermochemical deposited /CMTD/ silicon carbide
p0089 A80-13063
- State-of-the-art of SiALON materials
p0009 A80-13066
- Effect of starting powder characteristics on density, microstructure and low temperature oxidation behavior of a Si3N4 - 8 w/o Y2O3 ceramic
p0090 A80-46100
- Characterization and properties of controlled nucleation thermochemical deposited (CMTD) silicon carbide
[NASA-TM-79277]
p0085 N80-13254
- Effect of starting powder characteristics on density, microstructure and low temperature oxidation behavior of a Si3N4-8w/o Y2O3 ceramic
[NASA-TM-81536]
p0088 N80-27484
- State-of-the-art SiALON materials
p0022 N80-29358

E

- EBELING, R. W., JR.**
Oxygen-enriched air for MHD power plants
p0096 A80-25096
- EBERHARDT, R. W.**
A liquid hydrogen experiment as a Shuttle payload
[AIAA PAPER 80-1096]
p0054 A80-38909
- EBERLE, E. E.**
Liquid oxygen/liquid hydrogen auxiliary power system thruster investigation
[NASA-CR-159674]
p0062 N80-15202
- EDDER, E.**
Energy conservation and environmental benefits of thermal energy storage systems in the pulp and paper industry
p0146 A80-48194
- Collection and dissemination of TES system information for the paper and pulp industry
p0142 N80-22797
- EDRLMAN, R. L.**
Application of advanced on-board processing concepts to future satellite communications systems: Bibliography
[NASA-CR-159684]
p0098 N80-12264
- EDWARDS, D. K.**
Depriming of arterial heat pipes: An investigation of CTS thermal excursions
[NASA-CR-165153]
p0108 N80-32688
- ENLERS, W. L.**
Materials review for improved automotive gas turbine engine
[NASA-CR-159673]
p0123 N80-17470
- EISENBERG, J. D.**
Preliminary study of advanced turboprop and turboshaft engines for light aircraft
[NASA-TM-81467]
p0018 N80-22350
- EXSTEDT, E. E.**
Experimental combustor study program
p0042 N80-29311
- ELKINS, R. T.**
Concept definition study of small Brayton cycle engines for dispersed solar electric power systems
[NASA-CR-159592]
p0150 N80-22778
- ELNER, P.**
Life test studies on tungsten impregnated cathodes
p0103 A80-45122
- Thermionic cathode life test studies
[NASA-TM-81441]
p0101 N80-18302
- ENG, E. D.**
Development of a high strength hot isostatically pressed /HIP/ disk alloy, MERL 76
p0084 A80-44108
- Manufacture of low carbon astrology turbine disk shapes by hot isostatic pressing. Volume 2, project 1
[NASA-CR-135410]
p0037 N80-21329
- ENGLISH, J. M.**
A methodology for long-range prediction of air transportation
p0041 N80-29305
- ENGLUND, D. E.**
Measuring unsteady pressure on rotating compressor blades
p0110 A80-12630
- ENGLUND, D. E., JR.**
Instrumentation technology
p0013 N80-10214
- ENGLISH, C. M.**
A quarter-century of progress in the development of correlation and extrapolation methods for creep rupture data
p0133 A80-38142
- ENTSON, I.**
Modified face seal for positive film stiffness
[NASA-CASX-LEM-12989-1]
p0114 N80-12414
- Analysis and design of a uniform-clearance, pumping-ring rod seal for the Stirling engine
[NASA-TM-81463]
p0116 N80-18408
- Dynamic response to rotating-seat runout in non-contacting face seals
[NASA-TM-81490]
p0117 N80-22701
- Dynamic analysis of noncontacting face seals
[NASA-TM-79294]
p0118 N80-27695
- Simulation and visualization of face seal motion stability by means of computer generated movies
[NASA-TM-81581]
p0120 N80-31797
- Observation of pressure variation in the cavitation region of submerged journal bearings
[NASA-TM-81582]
p0120 N80-31798
- EVANS, D. D.**
A quantitative analysis of inter-island telephony traffic in the Pacific Basin Region (PBR)
[NASA-TM-81587]
p0097 N80-32610
- EVANS, D. J.**
Development of a high strength hot isostatically pressed /HIP/ disk alloy, MERL 76
p0084 A80-44108
- Manufacture of low carbon astrology turbine disk shapes by hot isostatic pressing. Volume 2, project 1
[NASA-CR-135410]
p0037 N80-21329
- EVANS, J. C., JR.**
The planar multijunction cell - A new solar cell for earth and space
p0146 A80-48205
- Planar multijunction high voltage solar cells
[NASA-TM-81389]
p0178 N80-16914
- EVASHINKA, J. G.**
An electric vehicle propulsion system's impact on battery performance: An overview
[NASA-TM-81515]
p0143 N80-24756

F

- FABTH, G. M.**
Investigation of critical burning of fuel droplets
[NASA-CR-159697]
p0075 N80-12142
- FALCONER, P. D.**
Comments on 'Experimental evidence for interhemispheric transport from airborne carbon monoxide measurements'
p0159 A80-32520
- FASCHING, W. A.**
The CF6 jet engine performance improvement: New front mount
[NASA-CR-159639]
p0029 N80-14127
- CF6 jet engine performance improvement: New fan
[NASA-CR-159699]
p0039 N80-23309
- CF6 jet engine performance improvement program: High pressure turbine aerodynamic performance improvement
[NASA-CR-159832]
p0040 N80-26302
- FAY, J. A.**
Air pollution from aircraft
[NASA-CR-159712]
p0010 N80-16060
- FEAR, J. S.**
NASA Broad-Specification Fuels Combustion Technology Program - Status and description
[ASME PAPER 80-GT-65]
p0094 A80-42195

- NASA broad-specification fuels combustion technology program: Status and description
[NASA-TN-79315] p0014 N80-14126
NASA broadened-specification fuels combustion technology program p0021 N80-29313
- FEILER, C. E.**
Preparing aircraft propulsion for a new era in energy and the environment p0024 A80-17737
Noise reduction p0012 N80-10208
- FERRANTE, J.**
Comments on Auger electron production by He⁺/ bombardment of surfaces p0174 A80-34048
Practical applications of surface analytic tools in tribology [NASA-TN-81484] p0079 N80-23430
- FESTER, D. A.**
A liquid hydrogen experiment as a Shuttle payload [AIAA PAPER 80-1096] p0054 A80-38909
- FIALA, J.**
A digitally implemented communications experiment utilizing the communications technology satellite, Hermes [NASA-TN-81452] p0052 N80-21412
- FINK, R. C.**
Electric propulsion, circa 2000 [AIAA PAPER 80-0912] p0059 A80-32886
Electric propulsion technology p0057 N80-31452
Synchronous energy technology program p0058 N80-33466
- FISHBACH, L. H.**
Computerized systems analysis and optimization of aircraft engine performance, weight, and life cycle costs p0165 A80-10035
Computer simulation of engine systems [AIAA PAPER 80-0051] p0024 A80-18253
Computer simulation of engine systems [NASA-TN-79290] p0015 N80-35132
Computerized systems analysis and optimization of aircraft engine performance, weight, and life cycle costs p0001 N80-21271
- FISHER, D. M.**
Comparison tests and experimental compliance calibration of the proposed standard round compact plane strain fracture toughness specimen [NASA-TN-81379] p0132 N80-13513
- FISHER, M. J.**
Diffusion bonded boron/aluminum spar-shell fan blade [NASA-CR-159571] p0072 N80-25382
- FLACK, R. D.**
Instability thresholds for flexible rotors in hydrodynamic bearings p0128 N80-29730
- PLECK, J. M.**
Tungsten wire/FcCrAlY matrix turbine blade fabrication study [NASA-CR-159788] p0044 N80-29331
- FLINING, D. P.**
Mechanical components p0013 N80-10213
Damping in tapered annular seals for an incompressible fluid [NASA-TP-1646] p0116 N80-19495
Damping in ring seals for compressible fluids p0119 N80-29716
- FLININGS, M. C.**
Directional solidification at ultra-high thermal gradient [NASA-CR-159797] p0096 N80-15300
- FLINING, D.**
Balancing of a power-transmission shaft with the application of axial torque [ASME PAPER 80-GT-143] p0121 A80-42256
- FLORES, F. J.**
Fuels characterization studies p0021 N80-29309
- FOLDES, P.**
Ka-band, multibeam, contiguous coverage satellite antenna for the USA [AIAA 80-0557] p0099 A80-29588
- FOOTE, C. E.**
Data analysis of P sub T/P sub S noseboom probe testing on F100 engine P680072 at NASA Lewis Research Center [NASA-CR-159816] p0038 N80-21334
- FOLDES, P. E.**
Advanced electric propulsion system concept for electric vehicles [NASA-CR-159651] p0183 N80-17916
- FORD, M. J.**
Laser-optical blade tip clearance measurement system p0111 A80-36137
Laser-optical blade tip clearance measurement system [NASA-TN-81376] p0015 N80-14128
- FORNAB, E.**
Life test studies on tungsten impregnated cathodes p0103 A80-45122
Thermionic cathode life test studies [NASA-TN-81441] p0101 N80-18302
- FORTINI, A.**
Heat exchanger and method of making [NASA-CASE-LEW-12441-2] p0105 N80-24573
- FOX, T. A.**
90- to 93-percent efficient collector for operation of a dual-mode traveling-wave tube in the linear region p0102 A80-13909
Multistage depressed collector with efficiency of 90 to 94 percent for operation of a dual-mode traveling wave tube in the linear region [NASA-TP-1670] p0101 N80-21669
- FRALBY, T. O.**
Method and apparatus for rapid thrust increases in a turbofan engine [NASA-CASE-LEW-12971-1] p0016 N80-18039
- FRALICK, G. C.**
Some dynamic and time-averaged flow measurements in a turbine rig p0178 A80-21120
Dynamic behavior of a beam drag-force anemometer [NASA-TP-1687] p0110 N80-24595
- FREEMAN, D. S.**
Quiet Clean Short-haul Experimental Engine (QCSEE) Under-The-Wing (UTW) composite nacelle subsystem test report [NASA-CR-135075] p0034 N80-15100
Quiet Clean Short-haul Experimental Engine (QCSEE) Under-The-Wing (UTW) composite nacelle subsystem test report [NASA-CR-135075] p0034 N80-15100
- FRENCH, S. E.**
Instructions for the use of the CIVM-Jet 4C finite-strain computer code to calculate the transient structural responses of partial and/or complete arbitrarily-curved rings subjected to fragment impact [NASA-CR-159873] p0134 N80-27720
- FRIEDMAN, R.**
Temperature and flow measurements on near-freezing aviation fuels in a wing-tank model [ASME PAPER 80-GT-63] p0094 A80-42193
Temperature and flow measurements on near-freezing aviation fuels in a wing-tank model [NASA-TN-79285] p0093 N80-13268
Fuel system technology overview p0022 N80-29328
- FROST, L. W.**
Silicone modified resins for graphite fiber laminates [NASA-CR-159750] p0072 N80-22407
- FRYBURG, G. C.**
The chemistry of sodium chloride involvement in processes related to hot corrosion p0074 A80-10041
Chemical processes involved in the initiation of hot corrosion of B-1900 and NASA-TRW VIA [NASA-TN-81399] p0077 N80-17199
- FRYE, R. J.**
Power processing technology for spacecraft primary ion propulsion p0065 A80-48265
- FUCINARI, C. A.**
Feasibility study of silicon nitride regenerators [NASA-CR-159713] p0184 N80-25209
Regenerator matrix physical property data [NASA-CR-159854] p0185 N80-30228
- FUJIKAWA, T.**
Asynchronous vibration problem of centrifugal compressor p0125 N80-29713
- FULLER, H.**
A 15kWe (nominal) solar thermal electric power

- conversion concept definition study: Steam
Rankine reheat reciprocator system
[NASA-CR-159590] p0148 N80-16491
- FURLONG, D. B.
Evaluation of feasibility of prestressed concrete
for use in wind turbine blades
[NASA-CR-159725] p0147 N80-15553
- FURNAN, E. R.
Candidate thermal energy storage technologies for
solar industrial process heat applications
[NASA-TM-81380] p0138 N80-15560
- FUSARO, R. L.
Effect of thermal aging on the tribological
properties of polyimide films and
polyimide-bonded graphite fluoride films
[ASLE PREPRINT 79-AM-3B-1] p0088 A80-12094
Mechanisms of lubrication and wear of a bonded
solid-lubricant film
[ASLE PREPRINT 80-AM-3E-1] p0122 A80-43163
Mechanisms of lubrication and wear of a bonded
solid lubricant film
[NASA-TM-81396] p0085 N80-16165
Lubrication and wear mechanisms of
polyimide-bonded graphite fluoride films
subjected to low contact stress
[NASA-TP-1584] p0085 N80-17220
Comparison of the weight loss and adherence of
nine different polyimide films thermally aged at
315 C and 350 C in air
[NASA-TM-81381] p0086 N80-18183
Comparison of the tribological properties at 25 C
of seven different polyimide films bonded to 301
stainless steel
[NASA-TM-81413] p0086 N80-19263
- G**
- GADEL, L. R.
Low sidelobe level low-cost earth station antennas
for the 12 GHz broadcasting satellite service
[NASA-CR-159703] p0098 N80-12259
- GABRISZESKI, T.
The 18/30 GHz fixed communications system service
demand assessment. Volume 1: Executive summary
[NASA-CR-159546] p0099 N80-22547
The 18/30 GHz fixed communications system service
demand assessment. Volume 2: Main text
[NASA-CR-159547] p0099 N80-22548
The 30/20 GHz fixed communications systems service
demand assessment. Volume 3: Appendices
[NASA-CR-159548] p0099 N80-22549
- GAFFIN, W. O.
Engine component improvement: Performance
improvement, JT9D-7 3.8 AR fan
[NASA-CR-159806] p0039 N80-25332
- GAHBAUER, R.
Preliminary results of fast neutron treatments in
carcinoma of the pancreas
[NASA-TM-81516] p0160 N80-24983
- GALLAGHER, J. J.
System analysis for millimeter-wave communication
satellites
p0100 A80-52479
- GAMBLE, R. B.
The 30/20 GHz fixed communications systems service
demand assessment. Volume 1: Executive summary
[NASA-CR-159619] p0098 N80-18262
The 30/20 GHz fixed communications systems service
demand assessment. Volume 2: Main report
[NASA-CR-159620] p0098 N80-18263
The 30/20 GHz fixed communications systems service
demand assessment. Volume 3: Annex
[NASA-CR-159621] p0099 N80-18264
- GASSEL, S. S.
Load support system analysis high speed input
pinion configuration
[ASME PAPER 79-LUB-34] p0129 A80-14760
- GATTI, A.
Sintered silicon nitride recuperator fabrication
[NASA-CR-159706] p0090 N80-15263
- GAUGLER, E.
Significance of thermal contact resistance in
two-layer, thermal-barrier-coated turbine vanes
p0024 A80-39635
- GAUGLER, R. E.
Streakline flow visualization study of a horseshoe
vortex in a large-scale, two-dimensional turbine
stator cascade
[ASME PAPER 80-GT-4] p0004 A80-42145
- Streakline flow visualization study of a horseshoe
vortex in a large-scale, two-dimensional turbine
stator cascade
[NASA-TM-79274] p0104 N80-11376
Nonlinear, three-dimensional finite-element
analysis of air-cooled gas turbine blades
[NASA-TP-1669] p0132 N80-22734
Significance of thermal contact resistance in
two-layer thermal-barrier-coated turbine vanes
[NASA-TM-81483] p0018 N80-23310
- GAUTHER, J. W.
Algorithm for calculating turbine cooling flow and
the resulting decrease in turbine efficiency
[NASA-TM-81453] p0163 N80-19863
- GEENEY, R. T.
Quantitative interpretation of Great Lakes remote
sensing data
p0157 A80-45005
Coordinated aircraft and ship surveys for
determining impact of river inputs on great
lakes waters. Remote sensing results
[NASA-TP-1694] p0157 N80-27832
- GRDUILL, H. A.
Improved bond coatings for use with thermal
barrier coatings
[NASA-TM-81567] p0080 N80-33556
- GRIDER, T. F.
Aerodynamic performances of three fan stator
designs operating with rotor having tip speed of
337 meters per second and pressure ratio of
1.54. 1: Experimental performance
[NASA-TP-1610] p0015 N80-17071
- GERLAUGH, H. E.
Cogeneration Technology Alternatives Study (CTAS).
Volume 1: Summary report
[NASA-CR-159765] p0151 N80-24797
Cogeneration Technology Alternatives Study (CTAS).
Volume 2: Analytical approach
[NASA-CR-159766] p0143 N80-28859
Cogeneration Technology Alternatives Study (CTAS).
Volume 3: Industrial processes
[NASA-CR-159767] p0155 N80-31870
Cogeneration Technology Alternatives Study (CTAS).
Volume 4: Energy conversion systems
[NASA-CR-159768] p0155 N80-33859
- GERSTENMAIER, H.
Computation of three-dimensional flow in turbobfan
mixers and comparison with experimental data
[AIAA PAPER 80-0227] p0003 A80-20967
Influence of pressure driven secondary flows on
the behavior of turbobfan forced mixers
[AIAA PAPER 80-1198] p0025 A80-41515
Computation of three-dimensional flow in turbobfan
mixers and comparison with experimental data
[NASA-TM-81410] p0104 N80-15364
Influence of pressure driven secondary flows on
the behavior of turbobfan forced mixers
[NASA-TM-81541] p0105 N80-27632
- GEYER, H. W.
Design, fabrication, test, and evaluation of a
prototype 150-foot long composite wind turbine
blade
[NASA-CR-159775] p0148 N80-17548
- GIBALA, R.
Some TEM observations of Al2O3 scales formed on
NiCrAl alloys
p0081 A80-13071
- GINSKE, J. A.
Spray nozzle designs for agricultural aviation
applications
[NASA-CR-159702] p0108 N80-10460
- GILBERT, L. J.
Simulation studies of multiple large wind turbine
generators on a utility network
p0139 N80-16480
- GIMER, J. D.
Catalyst surfaces for the chromous/chromic redox
couple
[NASA-CASE-LEW-13148-2] p0140 N80-18557
Catalyst surfaces for the chromous/chromic redox
couple
[NASA-CASE-LEW-13148-1] p0101 N80-20487
Advanced screening of electrode couples
[NASA-CR-159738] p0141 N80-22777
- GINSBURG, A.
Supercharged topping rocket propellant feed system
[NASA-CASE-XLE-02062-1] p0056 N80-14188
- GLADDEN, H. J.
Similarity tests of turbine vanes - Effects of

- ceramic thermal barrier coatings
[ASME PAPER 80-HT-24] p0027 A80-48013
- Effects of a ceramic coating on metal temperatures
of an air-cooled turbine vane
[NASA-TP-1598] p0105 N80-17397
- Similarity tests of turbine vanes, effects of
ceramic thermal barrier coatings
[NASA-TM-81473] p0105 N80-21706
- Extension of similarity test procedures to cooled
engine components with insulating ceramic coatings
[NASA-TP-1615] p0105 N80-24577
- GLASPER, P. W.**
- Effect of inflow control on inlet noise of a
cut-on fan
[AIAA PAPER 80-1049] p0171 A80-35993
- Effect of inflow control on inlet noise of a
cut-on fan
[NASA-TM-81487] p0169 N80-23098
- GLASGOW, E. R.**
- Zero-length, slotted-lip inlet for subsonic
military aircraft
[AIAA PAPER 80-1245] p0004 A80-41203
- GLASGOW, J. C.**
- Teetered, tip-controlled rotor - Preliminary test
results from Mod-0 100-kW experimental wind
turbine
[AIAA 80-0642] p0145 A80-28836
- Teetered, tip-controlled rotor: Preliminary test
results from Mod-0 100-kW experimental wind
turbine
[NASA-TM-81445] p0140 N80-19613
- GLASGOW, T. K.**
- Reaction bonded silicon nitride prepared from wet
attrition-milled silicon
p0089 A80-32828
- Formation of porous surface layers in reaction
bonded silicon nitride during processing
p0090 A80-51574
- Materials and structures technology
p0012 N80-10210
- Reaction bonded silicon nitride prepared from wet
attrition-milled silicon
[NASA-TM-81428] p0086 N80-18181
- Formation of porous surface layers in reaction
bonded silicon nitride during processing
[NASA-TM-81493] p0087 N80-23456
- GLASSMAN, A. J.**
- Loss model for off-design performance analysis of
radial turbines with pivoting-vane,
variable-area stators
[NASA-TM-81532] p0020 N80-27365
- Some advantages of methane in an aircraft gas
turbine
[NASA-TM-81559] p0094 N80-29502
- GLAVE, G. E.**
- Instrumentation technology
p0013 N80-10214
- GLENN, R. E.**
- Design, fabrication and testing of an optical
temperature sensor
[NASA-CR-165125] p0112 N80-31777
- GLUYAS, R. E.**
- Improved fiber retention by the use of fillers in
graphite fiber/resin matrix composites
p0071 A80-32066
- Improved fiber retention by the use of fillers in
graphite fiber/resin matrix composites
[NASA-TM-79288] p0067 N80-13171
- GODLEWSKI, M. P.**
- Open-circuit voltage improvements in low
resistivity solar cells
[NASA-TM-81388] p0138 N80-15555
- GOLDMAN, L. J.**
- Prediction method for two-dimensional aerodynamic
losses of cooled vanes using integral
boundary-layer parameters
[NASA-TP-1623] p0002 N80-17030
- GOLDSTEIN, M. E.**
- Workshop report for the AIAA 5th Aeroacoustics
Conference
p0172 A80-41156
- The effect of finite turbulence spatial scale on
the amplification of turbulence by a contracting
stream
p0004 A80-44862
- GOLOVIN, M. N.**
- Spray nozzle designs for agricultural aviation
applications
[NASA-CR-159702] p0108 N80-10460
- GOODYKOONTS, J.**
- Noise suppression due to annulus shaping of a
conventional coaxial nozzle
p0171 A80-35497
- Noise suppression due to annulus shaping of an
inverted-velocity-profile coaxial nozzle
p0171 A80-35498
- Noise suppression due to annulus shaping of an
inverted-velocity-profile coaxial nozzle
[NASA-TM-81460] p0168 N80-22046
- Noise suppression due to annulus shaping of
conventional coaxial nozzle
[NASA-TM-81461] p0168 N80-22047
- GONADIA, C.**
- The planar multijunction cell - A new solar cell
for earth and space
p0146 A80-48205
- Planar multijunction high voltage solar cells
[NASA-TM-81389] p0178 N80-16914
- GORDAN, A. L.**
- Impact of propulsion system R and D on electric
vehicle performance and cost
[NASA-TM-81548] p0143 N80-27805
- GORDON, H. S.**
- An automatically-shifted two-speed transaxle
system for an electric vehicle
[NASA-CR-159746] p0184 N80-18992
- GORDON, L. H.**
- Engineering evaluation of a sodium hydroxide
thermal energy storage module
[NASA-TM-81417] p0140 N80-18563
- Program definition and assessment overview
p0141 N80-22790
- GORSLER, R. W.**
- Materials for advanced turbine engines. Volume 1:
Power metallurgy Rene 95 rotating turbine engine
parts
[NASA-CR-159802] p0084 N80-28499
- GRABER, E. J.**
- The NASA high-speed turboprop program
[NASA-TM-81561] p0022 N80-31401
- GRAHAM, H. C.**
- Characterization and properties of controlled
nucleation thermochemical deposited /CMTD/
silicon carbide
p0089 A80-13063
- Characterization and properties of controlled
nucleation thermochemical deposited (CMTD)
silicon carbide
[NASA-TM-79277] p0085 N80-13254
- GRAHAM, R. W.**
- Coolant tube curvature effects on film cooling as
detected by infrared imagery
[ASME PAPER 79-WA/GT-7] p0107 A80-18638
- Impact of new instrumentation on advanced turbine
research
p0112 A80-36155
- Influence of coolant tube curvature on film
cooling effectiveness as detected by infrared
imagery
[NASA-TP-1546] p0013 N80-11087
- Impact of new instrumentation on advanced turbine
research
[NASA-TM-79301] p0015 N80-15133
- Some advantages of methane in an aircraft gas
turbine
[NASA-TM-81559] p0094 N80-29502
- GRANT, H. P.**
- Measuring unsteady pressure on rotating compressor
blades
p0110 A80-12630
- Thin film temperature sensor
[NASA-CR-159782] p0112 N80-17425
- GREENBERG, R.**
- The optimization air separation plants for
combined cycle MHD-power plant applications
[NASA-TM-81510] p0142 N80-23778
- GREGG, G. H.**
- A theoretical and experimental investigation of
propeller performance methodologies
[AIAA PAPER 80-1240] p0026 A80-43283
- An acoustic sensitivity study of general aviation
propellers
[AIAA PAPER 80-1871] p0045 A80-50191
- GREYWALL, H. S.**
- Effect of velocity overshoot on the performance of
magnetohydrodynamic subsonic diffusers
[NASA-TM-79305] p0175 N80-14922

- GRINN, M. T.**
Experimental results on plasma interactions with large surfaces at high voltages
[NASA-TM-81423] p0175 N80-18946
- GRINNS, E. H.**
Fatigue behavior of SiC reinforced titanium composites p0070 A80-10036
- GROBMAN, J.**
Alternative jet aircraft fuels p0012 N80-10209
The impact of fuels on aircraft technology through the year 2000
[NASA-TM-81492] p0093 N80-23472
- GROBMAN, J. S.**
Preparing aircraft propulsion for a new era in energy and the environment p0024 A80-17737
- GROENBERG, J. P.**
Noise reduction p0012 N80-10208
- GROESBECK, D.**
Assessment at full scale of exhaust nozzle-to-wing size on STOL-OTW acoustic characteristics p0170 A80-20952
- GROESBECK, D.**
Assessment at full scale of exhaust nozzle to wing size on STOL-OTW acoustic characteristics
[NASA-TM-79279] p0167 N80-13881
- GROSS, D.**
Statistical aspects of carbon fiber risk assessment modeling
[NASA-CR-159318] p0073 N80-29432
- GRUBER, E. F.**
Self-reconfiguring solar cell system
[NASA-CASE-LEW-12586-1] p0137 N80-14472
- GUILLIAMS, B. F.**
Three dimensional finite-element elastic analysis of a thermally cycled double-edge wedge geometry specimen
[NASA-TM-80980] p0079 N80-26433
- GUNTER, E. J.**
Stabilization of aerodynamically excited turbomachinery with hydrodynamic journal bearings and supports p0128 N80-29731
- GURSKI, G. S.**
Communications technology satellite - United States experiments and disaster communications applications p0051 A80-10032
- GYEKHYESI, J.**
The method of lines in three dimensional fracture mechanics
[NASA-TM-81593] p0132 N80-32753
- GYORGAK, C. A.**
Mechanical properties and oxidation and corrosion resistance of reduced-chromium 304 stainless steel alloys
[NASA-TP-1557] p0076 N80-11188
- H**
- HAAS, J. E.**
Turbomachinery technology p0012 N80-10212
Experimental performance and analysis of 15.04-centimeter-tip-diameter, radial-inflow turbine with work factor of 1.126 and thick blading
[NASA-TP-1730] p0023 N80-33410
- HACK, J. E.**
Fabrication and evaluation of low fiber content alumina fiber/aluminum composites
[NASA-CR-159517] p0073 N80-29430
- HAGEDORN, M. H.**
Redox storage systems for solar applications
[NASA-TM-81464] p0142 N80-23777
- HAGEN, P. A.**
Materials review for improved automotive gas turbine engine
[NASA-CR-159673] p0123 N80-17470
- HAGGARD, J. B., JR.**
Fuels research: Combustion effects overview p0021 N80-29317
- HALE, J. A.**
Spray nozzle designs for agricultural aviation applications
[NASA-CR-159702] p0108 N80-10460
- HALFORD, G. E.**
Strainrange partitioning life predictions of the long time Metal Properties Council creep-fatigue tests p0133 A80-27958
Materials and structures technology p0012 N80-10210
Practical implementation of the double linear damage rule and damage curve approach for treating cumulative fatigue damage
[NASA-TM-81517] p0132 N80-23684
- HALL, E. W.**
Cogeneration Technology Alternatives Study (CTAS). Volume 1: Summary report p0151 N80-24797
Cogeneration Technology Alternatives Study (CTAS). Volume 2: Analytical approach p0143 N80-28859
- HALLS, P. A.**
Parametric study of potential early commercial MHD power plants
[NASA-CR-159633] p0149 N80-18559
- HANCOCK, B. J.**
Stresses and deformations in elliptical contacts
[NASA-TM-81535] p0118 N80-27697
Fully flooded elastohydrodynamic lubricated elliptical contacts p0118 N80-27698
Starved elastohydrodynamic lubricated elliptical contacts p0118 N80-27699
Film thickness for different regimes of fluid-film lubrication p0119 N80-29735
[NASA-TM-81550]
- HAN, L. S.**
Vibration and buckling of rectangular plates under in-plane hydrostatic loading p0133 A80-45364
- HANSEN, I. G.**
Heat pipe cooling of power processing magnetics
[AIAA PAPER 79-2082] p0107 A80-20960
Heat pipe cooling of power processing magnetics
[NASA-TM-79270] p0101 N80-11327
- HANSON, E. P.**
Feasibility of Kevlar 49/PMR-15 polyimide for high temperature applications
[NASA-TM-81560] p0069 N80-27429
- HARPER, P. M., SR.**
Improved tire/wheel concept
[NASA-CASE-LAR-11695-2] p0124 N80-18402
- HARRIS, E.**
Development of exothermically cast single-crystal Mar-M 247 and derivative alloys
[AIRESEARCH-21-3469] p0084 A80-45825
- HARTL, J. H.**
Two-phase working fluids for the temperature range of 50 to 350 deg, phase 2
[NASA-CR-159847] p0108 N80-23599
- HARTMAN, E.**
Airbreathing propulsion component technologies p0024 A80-37482
- HARTMAN, M. J.**
The measuring and growing of advanced gas turbines p0111 A80-36127
Fluid and structural measurements to advance gas turbine technology p0111 A80-36145
Supercharged topping rocket propellant feed system
[NASA-CASE-XLE-02062-1] p0056 N80-14188
- HASLETT, E.**
Active heat exchange system development for latent heat thermal energy storage
[NASA-CR-159726] p0149 N80-18562
- HASS, J. E.**
An experimental evaluation of the performance deficit of an aircraft engine starter turbine
[NASA-TM-81571] p0022 N80-31400
- HASSMAN, G. V.**
An automatically-shifted two-speed transaxle system for an electric vehicle
[NASA-CR-159746] p0184 N80-18992
- HAUGLAND, E.**
Critical currents in A-15 structure Nb3Al converted from cold-worked bcc structure p0179 A80-33853
- HAUSER, C. E.**
Turbomachinery technology p0012 N80-10212

- MAWKINS, J. E.**
Experimental investigation of a 0.15 scale model of a conformal variable-ramp inlet for the F-16 airplane
[NASA-CR-159640] p0005 N80-24263
- MECK, E. E.**
Durability testing of advanced catalysts and catalyst supports for gas turbine engine combustors
p0074 A80-35881
- Durability testing at 5 atmospheres of advanced catalysts and catalyst supports for gas turbine engine combustors
[NASA-CR-159839] p0151 N80-24748
- MEIDELSBEC, L. J.**
Comparison of inlet suppressor data with approximate theory based on cutoff ratio
[AIAA PAPER 80-0100] p0170 A80-20964
- Comparison of several inflow control devices for flight simulation of fan tone noise using a JT15D-1 engine
[AIAA PAPER 80-1025] p0025 A80-38640
- Comparison of inlet suppressor data with approximate theory based on cutoff ratio
[NASA-TM-81386] p0167 N80-15876
- Experimental evaluation of a spinning-mode acoustic-treatment design concept for aircraft inlets
[NASA-TP-1613] p0016 N80-21323
- Comparison of several inflow control devices for flight simulation of fan tone noise using a JT15D-1 engine
[NASA-TM-81505] p0019 N80-24314
- MEINZMAN, J.**
Feasibility of active feedback control of rotorodynamic instability
p0128 N80-29733
- MELDENBRAND, R. W.**
Airesearch QCGAT program
[NASA-CR-159758] p0037 N80-21331
- MELMS, R. E.**
Advanced Gas Turbine Powertrain System Development Project
p0129 A80-35574
- MENDRICKS, R. C.**
Toward the use of similarity theory in two-phase choked flows
[NASA-TM-81568] p0106 N80-29623
- MENDRICKS, R. C.**
Some aspects of a free jet phenomena to 105 L/D in a constant area duct
p0106 A80-10030
- Critical mass flux through short Borda type inlets of various cross sections
p0106 A80-10031
- Free jet phenomena in a 90 deg-sharp edge inlet geometry
p0106 A80-10037
- A reduced volumetric expansion factor plot
p0107 A80-10038
- Application of the principle of similarity fluid mechanics
p0107 A80-10039
- Some flow characteristics of conventional and tapered high-pressure-drop simulated seals
[ASLE PREPRINT 79-LC-3B-2] p0120 A80-14727
- Thermophysical property data - Who needs them
[ASME PAPER 79-WA/HT-17] p0180 A80-18630
- Effect of thermal cycling on ZrO₂-Y₂O₃ thermal barrier coatings
p0089 A80-35899
- Volume-energy parameters and turbulent-flow density fluctuations
[NASA-TP-1585] p0105 N80-17398
- Effect of thermal cycling on ZrO₂-Y₂O₃ thermal barrier coatings
[NASA-TM-81480] p0018 N80-22349
- MENSHAW, J.**
Fiber release characteristics of graphite hybrid composites
p0073 A80-32063
- MERBALL, T. P.**
Reaction bonded silicon nitride prepared from wet attrition-milled silicon
[NASA-TM-81428] p0086 N80-18181
- MERBELL, T. P.**
Reaction bonded silicon nitride prepared from wet attrition-milled silicon
p0089 A80-32828

- MERNANN, A. M.**
Radiation damage in lithium-counterdoped n/p silicon solar cells
[NASA-TM-81391] p0138 N80-15557
- MERNANN, P.**
An experimental evaluation of the performance deficit of an aircraft engine starter turbine
[NASA-TM-81571] p0022 N80-31400
- MERSH, A. S.**
Acoustic behavior of fibrous bulk materials
[AIAA PAPER 80-0986] p0172 A80-35951
- Effect of grazing flow on the nonlinear acoustic behavior of helmholtz resonators
p0095 N80-31619
- MESS, H.**
Durability testing at 5 atmospheres of advanced catalysts and catalyst supports for gas turbine engine combustors
[NASA-CR-159839] p0151 N80-24748
- MESS, H. W.**
Durability testing of advanced catalysts and catalyst supports for gas turbine engine combustors
p0074 A80-35881
- MESS, J. L.**
An efficient user-oriented method for calculating compressible flow in an about three-dimensional inlets
[NASA-CR-159578] p0004 N80-10134
- MEYWOOD, J. E.**
Air pollution from aircraft
[NASA-CR-159712] p0010 N80-16060
- MILL, M. E.**
Conceptual design of two-phase fluid mechanics and heat transfer facility for spacelab
[NASA-CR-159810] p0049 N80-27403
- MILL, R. J.**
Three dimensional finite-element elastic analysis of a thermally cycled double-edge wedge geometry specimen
[NASA-TM-80980] p0079 N80-26433
- MILL, V. L.**
Thermal fatigue and oxidation data for directionally solidified MAR-M 246 turbine blades
[NASA-CR-159798] p0037 N80-21330
- Thermal fatigue and oxidation data of oxide dispersion-strengthened alloys
[NASA-CR-159842] p0084 N80-25415
- MILSEN, M. B.**
System analysis for millimeter-wave communication satellites
p0100 A80-52479
- MIMBICHSEN, E. W.**
MOD-2 wind turbine farm stability study
[NASA-CR-165156] p0156 N80-33862
- MNAT, J. G.**
Coupled generator and combustor performance calculations for potential early commercial MHD power plants
p0156 A80-25099
- Parametric study of prospective early commercial MHD power plants (PSPEC). General Electric Company, task 1: Parametric analysis
[NASA-CR-159634] p0152 N80-26779
- MODGDON, R. B.**
Anton permselective membrane
[NASA-CR-159599] p0147 N80-12551
- MUDGE, F. E.**
Corrosion resistant thermal barrier coating
[NASA-CASE-LEW-13088-1] p0067 N80-11142
- MOEKS, B.**
Phase-locked telemetry system for rotary instrumentation of turbomachinery, phase 1
[NASA-CR-159453] p0029 N80-14182
- MOFFER, K. E.**
Thermal fatigue and oxidation data of oxide dispersion-strengthened alloys
[NASA-CR-159842] p0084 N80-25415
- MOFFMAN, H.**
Application of advanced on-board processing concepts to future satellite communications systems
[NASA-CR-159682] p0098 N80-12260
- MOLDENAU, J. D.**
Measurements of cabin and ambient ozone on B747 airplanes
p0010 A80-28853
- Simultaneous cabin and ambient ozone measurements on two Boeing 747 airplanes, volume 1

- [NASA-TM-79166] p0008 N80-15059
NASA Global Atmospheric Sampling Program (GASP)
data report for tapes V10011 and V10013
[NASA-TM-81462] p0157 N80-21892
- HOLLAND, L. D.
System analysis for millimeter-wave communication
satellites p0100 A80-52479
- HOLMES, R.
On the role of oil-film bearings in promoting
shaft instability: Some experimental observations p0127 N80-29726
- HOLMES, W. H., JR.
An advanced mixed user domestic satellite system
architecture [AIAA 80-0494] p0099 A80-29544
Multigigabit satellite on-board signal processing
[AIAA 80-0583] p0100 A80-29605
- HOLMS, A. G.
'Chain pooling' model selection for two-level
fixed effects factorial experiments p0164 A80-40764
- HONYAK, L.
Comparison of several inflow control devices for
flight simulation of fan tone noise using a
JT15D-1 engine [AIAA PAPER 80-1025] p0025 A80-38640
Static test-stand performance of the YF-102
turbofan engine with several exhaust
configurations for the Quiet Short-Haul Research
Aircraft (QSRA) [NASA-TP-1556] p0014 N80-14121
Experimental evaluation of a spinning-mode
acoustic-treatment design concept for aircraft
inlets [NASA-TP-1613] p0016 N80-21323
Comparison of several inflow control devices for
flight simulation of fan tone noise using a
JT15D-1 engine [NASA-TM-81505] p0019 N80-24314
Static and transient performance of YF-102 engine
with up to 14 percent core airbleed for the
quiet short-haul research aircraft [NASA-TP-1692] p0020 N80-25339
- HONG, J. Y.
The effect of a weak vertical magnetic field on
fluctuation-induced transport in a Bumpy-Torus
plasma p0176 A80-25476
- HOOVER, D. Q., JR.
Cell module and fuel conditioner development
[NASA-CR-159828] p0150 N80-23768
Cell module and fuel conditioner
[NASA-CR-159875] p0142 N80-23769
Cell module and fuel conditioner
[NASA-CR-159888] p0155 N80-31882
- HOPPIN, G. S., III
Development of exothermically cast single-crystal
Mar-M 247 and derivative alloys [AIAA-ARCH-21-3469] p0084 A80-45825
- HORTON, J.
Preliminary results of fast neutron treatments in
carcinoma of the pancreas [NASA-TM-81516] p0160 N80-24983
- HOTCHKISS, G. B.
Spectral effects on direct-insolation absorptance
of five collector coatings [ASME PAPER 79-HT-18] p0146 A80-45722
- HOTZ, G. H.
Cold-air investigation of a 4 1/2 stage turbine
with stage-loading factor of 4.66 and high
specific work output. 2: Stage group performance
[NASA-TP-1688] p0019 N80-25338
- HOULT, D. P.
Laboratory measurements in a turbulent, swirling
flow [NASA-CR-159723] p0095 N80-22509
- HOUSE, E. E.
Hybrid composites that retain graphite fibers on
burning p0073 A80-32064
- HOWARD, D. F.
Quiet Clean Short-haul Experimental Engine (QCSEE)
preliminary under the wing flight propulsion
system analysis report [NASA-CR-134868] p0034 N80-15088
Quiet Clean Short-haul Experimental Engine (QCSEE)
preliminary over-the-wing flight propulsion
system analysis report
- [NASA-CR-135296] p0035 N80-15095
HOWARD, J. B.
Soot formation and burnout in flames p0043 N80-29320
- HOWES, W. L.
Possible methods for distinguishing icebergs from
ships by aerial remote sensing [NASA-TM-79310] p0136 N80-15538
- HOWLETT, R. A.
VSCE technology definition study
[NASA-CR-159730] p0027 N80-10222
- HRACH, P. J.
Development of a Kevlar/PFR-15 reduced drag DC-9
nacelle fairing [AIAA PAPER 80-1194] p0010 A80-41193
Reduced bleed air extraction for DC-10 cabin air
conditioning [AIAA PAPER 80-1197] p0010 A80-41194
CF6-50 Short Core Exhaust Nozzle
[AIAA PAPER 80-1196] p0025 A80-41514
- HSU, L. C.
Method of cross-linking polyvinyl alcohol and
other water soluble resins [NASA-CASE-LEW-13103-1] p0088 N80-32516
- HUANG, T. T.
An investigation of the initiation stage of hot
corrosion in Ni-base alloys [NASA-CR-159718] p0083 N80-15233
- HUDSON, J. H.
Subsynchronous instability of a geared centrifugal
compressor of overhung design p0125 N80-29711
- HUDSON, W. R.
Electric propulsion, circa 2000
[AIAA PAPER 80-0912] p0059 A80-32886
- HUGHES, W. P.
Phase change in liquid face seals. II - Isothermal
and adiabatic bounds with real fluids
[ASME PAPER 79-LUB-4] p0129 A80-14739
- HULLER, F. T.
Comparison of predicted and experimental
performance of large-bore roller bearing
operating to 3.0 million DN [NASA-TP-1599] p0114 N80-15410
- HUMENIK, F. M.
Sulfate and nitrate collected by filter sampling
near the tropopause [NASA-TP-1567] p0157 N80-14581
Preliminary studies of combustor sensitivity to
alternative fuels p0021 N80-29323
- HUMPHREYS, V. E.
Thermal fatigue and oxidation data for
directionally solidified MAR-M 246 turbine blades
[NASA-CR-159798] p0037 N80-21330
Thermal fatigue and oxidation data of oxide
dispersion-strengthened alloys [NASA-CR-159842] p0084 N80-25415
- HUMPHRIES, T. S.
Stress corrosion cracking evaluation of
martensitic precipitation hardening stainless
steels [NASA-TM-78257] p0083 N80-16142
- HUNCZAK, H. E.
Communications technology satellite - United
States experiments and disaster communications
applications p0051 A80-10032
- HUNT, R. B.
VSCE technology definition study
[NASA-CR-159730] p0027 N80-10222
- HURST, C. J.
A comparison of experiment and theory for sound
propagation in variable area ducts p0173 A80-45844
- HURST, L. G.
Abradable compressor and turbine seals, volume 1
[NASA-CR-159600] p0083 N80-14235
- HURNITZ, F. I.
Influence of excess diamine on properties of PFR
polyimide resins and composites [NASA-TM-81580] p0069 N80-29433
- HUSTON, R. L.
Ideal spiral bevel gears: A new approach to
surface geometry [NASA-TM-81446] p0117 N80-19498
- HUANG, H. C.
Negative streamer development in FEP teflon
p0179 A80-19776

- IGNACZAK, L. R.**
SENT II 1979 extended flight thruster system performance
[AIAA PAPER 79-2063] p0059 A80-10386
- IINO, T.**
Hydraulic forces caused by annular pressure seals in centrifugal pumps
p0126 N80-29718
- INGARD, K. U.**
Higher order mode propagation in nonuniform circular ducts
[AIAA PAPER 80-1018] p0171 A80-35974
Higher order mode propagation in nonuniform circular ducts
[NASA-TM-81481] p0169 N80-23101
- INGERSO, R. D.**
Atomizing characteristics of swirl can combustor modules with swirl blast fuel injectors
[ASME PAPER 80-GT-30] p0026 A80-42164
Atomizing characteristics of swirl can combustor modules with swirl blast fuel injectors
[NASA-TM-79297] p0014 N80-13047
- INOUE, L. Y.**
Power processing technology for spacecraft primary ion propulsion
p0065 A80-48265
- ISHIGURO, M.**
Asynchronous vibration problem of centrifugal compressor
p0125 N80-29713
- ITO, M.**
Asynchronous vibration problem of centrifugal compressor
p0125 N80-29713
- IWATSUBO, T.**
Evaluation of instability forces of labyrinth seals in turbines or compressors
p0126 N80-29715
- JACKSON, H. D.**
A digitally implemented communications experiment utilizing the communications technology satellite, Hermes
[NASA-TM-81452] p0052 N80-21412
- JACKSON, T. A.**
Fuel character effects on the J79 and F101 engine combustion systems
p0042 N80-29312
Air Force fuel mainburner/turbine effects programs
p0042 N80-29314
- JACOBSON, T. P.**
Friction and wear of plasma-sprayed coatings containing cobalt alloys from 25 deg to 650 deg in air
[ASLE PREPRINT 80-AM-6C-2] p0122 A80-43176
Friction and wear of plasma-sprayed coatings containing cobalt alloys from 25 deg to 650 deg in air
[NASA-TM-79316] p0085 N80-14249
- JAMES, R.**
An electric propulsion long term test facility
[AIAA PAPER 79-2080] p0049 A80-13308
- JAMES, E. L.**
Preliminary results of the mission profile life test of a 30 cm Hg bombardment thruster
[AIAA PAPER 79-2078] p0081 A80-10391
- JAY, A.**
Effect of time dependent flight loads on JT9D-7 performance deterioration
[NASA-CR-159681] p0134 N80-10515
- JEFFRIES, K. D.**
Analysis of GaAs and Si solar cell arrays for earth orbital and orbit transfer missions
[NASA-TM-81383] p0056 N80-15204
- JELDEN, G. L.**
Preliminary results of fast neutron treatments in carcinoma of the pancreas
[NASA-TM-81516] p0160 N80-24983
- JERACKI, R. J.**
High-speed-propeller wind-tunnel aeroacoustic results
p0018 N80-22344
- JHA, S.**
Hyperfine magnetic field at Cd impurity site in

- L2/1/ Heusler alloys Rh₂MnGe and Rh₂MnPb by TDPAC technique
p0178 A80-16843
- JOHNS, A. L.**
Wind tunnel investigation of the Titan Forward Skirt compartment vent from a free-stream Mach number of 0.80 to 1.96
[NASA-TM-81572] p0106 N80-32689
- JOHNSON, R. L.**
Performance sensitivity analysis of Department of Energy-Chrysler upgraded automotive gas turbine engine, S/N 5-4
[NASA-TM-79242] p0115 N80-17467
- JOHNSON, D. L.**
Homogeneous alignment of nematic liquid crystals by ion beam etched surfaces
p0178 A80-26007
Homogeneous alignment of nematic liquid crystals by ion beam etched surfaces
[NASA-TM-81378] p0096 N80-16232
- JOHNSON, G. M.**
An alternative approach to the numerical simulation of steady inviscid flow
p0107 A80-44228
An alternative approach to the numerical simulation of steady inviscid flow
[NASA-TM-81542] p0003 N80-27286
- JOHNSON, R. D.**
Gas path seal
[NASA-CASE-NPO-12131-3] p0115 N80-18400
- JOHNSTON, E. A.**
Quiet Clean Short-haul Experimental Engine (QCSEE) Under-The-Wing (UTW) composite nacelle subsystem test report
[NASA-CR-135075] p0034 N80-15100
Quiet Clean Short-haul Experimental Engine (QCSEE) Under-The-Wing (UTW) composite nacelle subsystem test report
[NASA-CR-135075] p0034 N80-15100
Quiet Clean Short-haul Experimental Engine (QCSEE) Under-The-Wing (UTW) composite nacelle
[NASA-CR-135352] p0032 N80-15119
- JONES, C.**
Multifuel rotary aircraft engine
[AIAA PAPER 80-1237] p0045 A80-38982
- JONES, R. E.**
Emission reduction
p0012 N80-10207
- JONES, W. L.**
Comparison of several inflow control devices for flight simulation of fan tone noise using a JT15D-1 engine
[AIAA PAPER 80-1025] p0025 A80-38640
Comparison of several inflow control devices for flight simulation of fan tone noise using a JT15D-1 engine
[NASA-TM-81505] p0019 N80-24314
- JONES, W. R.**
Analysis of wear-debris from full-scale bearing fatigue tests using the ferrograph
[NASA-TM-81403] p0114 N80-16341
- JONES, W. R., JR.**
Boundary lubrication, thermal and oxidative stability of a fluorinated polyether and a perfluoropolyether triazine
[ASLE PREPRINT 79-AM-1B-1] p0088 A80-12089
Analysis of wear debris from full-scale bearing fatigue tests using the Ferrograph
[ASLE PREPRINT 80-AM-3E-2] p0122 A80-43167
Ferrographic and spectrographic analysis of oil sampled before and after failure of a jet engine
[NASA-TM-81430] p0117 N80-19497
Steady-state wear and friction in boundary lubrication studies
[NASA-TP-1658] p0087 N80-22493
- JORASCH, R.**
Concepts for 20/30 GHz satcom systems for direct-to-user applications
[AIAA 80-0582] p0050 A80-35329
Concepts for 18/30 GHz satellite communication system, volume 1
[NASA-CR-159625-VOL-1] p0098 N80-11277
Concepts for 18/30 GHz satellite communication system, volume 1A: Appendix
[NASA-CR-159625-VOL-1A] p0098 N80-11278
- JUHASZ, A. J.**
The optimization air separation plants for combined cycle MHD-power plant applications
[NASA-TM-81510] p0142 N80-23778

- JULIAN, G. H.
Hyperfine magnetic field at Cd impurity site in
L2/1/ Heusler alloys Rh_2MnGe and Rh_2MnPt by
TDPAC technique p0178 A80-16843

K

- KAHN, A. S.
The effect of zirconium on the isothermal
oxidation of nominal Ni-14Cr-24Al alloys p0082 A80-26465
- KAISER, J. H.
A comparison of experiment and theory for sound
propagation in variable area ducts p0173 A80-45844
- KAN, H. K. A.
First results of material charging in the space
environment p0055 A80-45609
- KANEKO, H.
Hydraulic forces caused by annular pressure seals
in centrifugal pumps p0126 N80-29718
- KASCAN, A. F.
Direct integration of transient rotor dynamics
[NASA-TP-1597] p0015 N80-15128
The response of turbine engine rotors to
interference rums p0118 N80-27696
[NASA-TN-81518]
- KASPER, J. H.
Experimental combustor study program p0042 N80-29311
- KATZ, I.
Plasma collection by high voltage spacecraft at
low earth orbit p0055 A80-18249
[AIAA PAPER 80-0042]
Photoelectron charge density and transport near
differentially charged spacecraft p0053 A80-19773
A three-dimensional spacecraft-charging computer
code p0055 A80-46891
- KATZ, J. L.
Application of advanced on-board processing
concepts to future satellite communications
systems p0098 N80-12260
[NASA-CR-159682]
Application of advanced on-board processing
concepts to future satellite communications
systems: Bibliography p0098 N80-12261
[NASA-CR-159684]
- KATZ, R.
Optical sensors for aeronautics and space
[NASA-TN-81407] p0110 N80-17423
- KAUFMAN, A.
Nonlinear, three-dimensional finite-element
analysis of air-cooled gas turbine blades
[NASA-TP-1669] p0132 N80-22734
Comparison of elastic and elastic-plastic
structural analyses for cooled turbine blade
airfoils p0132 N80-27719
[NASA-TP-1679]
- KAUFMAN, H. E.
Interaction of high voltage surfaces with the
space plasma p0176 N80-14923
[NASA-CR-159731]
Inert gas thrusters p0062 N80-24362
[NASA-CR-159813]
Plasma physics analysis of SERT-2 operation
[NASA-CR-159814] p0177 N80-27189
Interaction of high voltage surfaces with the
space plasma p0177 N80-32223
[NASA-CR-165131]
- KAUTZ, H. E.
Decay of the zincate concentration gradient at an
alkaline zinc cathode after charging p0074 A80-13070
- KAWAI, R. T.
Development of a Kevlar/PME-15 reduced drag DC-9
nacelle fairing p0010 A80-41193
[AIAA PAPER 80-1194]
- KAYS, W. H.
Full-coverage film cooling. I - Comparison of heat
transfer data for three injection angles p0108 A80-42176
[ASME PAPER 80-GT-43]
Full-coverage film cooling. II - Heat transfer
data and numerical simulation p0109 A80-42177
[ASME PAPER 80-GT-44]
- KAZA, H. R. V.
Examination of the flap-lag stability of rigid
articulated rotor blades p0010 A80-15123
- Buckling of rotating beams p0133 A80-20149
- Nonlinear aeroelastic equations of motion of
twisted, nonuniform, flexible horizontal-axis
wind turbine blades p0152 N80-26774
[NASA-CR-159502]
- KAZAROFF, J. H.
Heat exchanger and method of making p0105 N80-24573
[NASA-CASE-LEN-12441-2]
- KEITNER, I.
An acoustic sensitivity study of general aviation
propellers p0045 A80-50191
[AIAA PAPER 80-1871]
- KEMPER, R. E., JR.
An overview of NASA research on positive
displacement general-aviation engines p0017 N80-22336
Positive displacement type general-aviation
engines: Summary and concluding remarks p0018 N80-22340
- KERSLAKH, V. R.
SERT II 1979 extended flight thruster system
performance p0059 A80-10386
[AIAA PAPER 79-2063]
Neutralization tests on the SERT II spacecraft
[AIAA PAPER 79-2064] p0059 A80-10387
- KETCHUM, W. J.
Low-thrust vehicles concept studies p0063 N80-31456
- KHALIL, I.
A calculation procedure for viscous flow in
turbomachines, volume 3 p0005 N80-26274
[NASA-CR-159864]
- KHALIL, J.
A calculation procedure for viscous flow in
turbomachines, volume 2 p0004 N80-17995
[NASA-CR-159636]
- KIELE, R. E.
Vibration and buckling of rectangular plates under
in-plane hydrostatic loading p0133 A80-45364
- KINSLING, J.
Study of advanced communications satellite systems
based on SS-FDMA p0050 N80-25357
[NASA-CR-159778]
- KIN, W. S.
Assessment of potential exposure to friable
insulation materials containing asbestos p0157 N80-23875
[NASA-TN-81435]
- KIN, Y. C.
The effect of a weak vertical magnetic field on
fluctuation-induced transport in a Bumpy-Torus
plasma p0176 A80-25476
- KIN, Y. G.
Characterization of an oxide dispersion
strengthened superalloy, MA-6000E, for turbine
blade applications p0083 N80-13218
[NASA-CR-159493]
- KIRALY, L. J.
Digital system for dynamic turbine engine blade
displacement measurements p0111 A80-36151
- KIRK, R. G.
Analysis and identification of subsynchronous
vibration for a high pressure parallel flow
centrifugal compressor p0125 N80-29710
- KLADDER, J. L.
Three dimensional finite-element elastic analysis
of a thermally cycled double-edge wedge geometry
specimen p0079 N80-26433
[NASA-TN-80980]
- KLANN, J. L.
Fuel economy screening study of advanced
automotive gas turbine engines p0183 N80-21201
[NASA-TN-81433]
- KLAUSING, T. A.
Design study of steel V-Belt CVT for electric
vehicles p0185 N80-32299
[NASA-CR-159845]
- KLECKNER, R. J.
High speed cylindrical rolling element bearing
analysis 'CYBEAN' - Analytic formulation p0129 A80-14761
[ASME PAPER 79-LUB-35]

- KLEIN, W. E.**
Modified aerospace REQA method for wind turbines
p0145 A80-40335
- KLOPP, W. D.**
Long-time creep behavior of the tantalum alloy
Astar 811C
[NASA-TP-1691] p0080 M80-32489
Long-time creep behavior of the niobium alloy C-103
[NASA-TP-1727] p0080 M80-33555
- KLUCHER, T. M.**
Open-circuit voltage improvements in low
resistivity solar cells
[NASA-TN-81388] p0138 M80-15555
- KNAPE, W. D.**
Evaluation of cleaners for photovoltaic modules
exposed in an outdoor environment
[NASA-TN-79248] p0096 M80-13317
- KNIGHTLY, W. F.**
Cogeneration Technology Alternatives Study (CTAS).
Volume 1: Summary report
[NASA-CR-159765] p0151 M80-24797
Cogeneration Technology Alternatives Study (CTAS).
Volume 2: Analytical approach
[NASA-CR-159766] p0143 M80-28859
Cogeneration Technology Alternatives Study (CTAS).
Volume 6: Computer data. Part 1: Coal-fired
nucogeneration process boiler, section A
[NASA-CR-159770-PT-1-A] p0154 M80-30888
Cogeneration Technology Alternatives Study (CTAS).
Volume 6: Computer data. Part 1: Coal-fired
nucogeneration process boiler, section B
[NASA-CR-159770-PT-1-B] p0154 M80-30889
Cogeneration Technology Alternatives Study (CTAS).
Volume 6: Computer data. Part 2:
Residual-fired nucogeneration process boiler
[NASA-CR-159770-PT-2] p0155 M80-30890
Cogeneration Technology Alternatives Study (CTAS).
Volume 6: Computer data. Part 1: Coal-fired
nucogeneration process boiler, section A
[NASA-CR-159770-PT-1] p0156 M80-33860
Cogeneration Technology Alternatives Study (CTAS).
Volume 6: Computer data. Part 2:
Residual-fired nucogeneration process boiler
[NASA-CR-159770-PT-2] p0156 M80-33861
- KNIP, G.**
Preliminary study of advanced turboprop and
turboshaft engines for light aircraft
[NASA-TN-81467] p0018 M80-22350
- KOBAR, J. A.**
Factors affecting cleanup of exhaust gases from a
pressurized, fluidized-bed coal combustor
[NASA-TN-81439] p0105 M80-20532
- KOFF, B.**
Airbreathing propulsion component technologies
p0024 A80-37482
- KOH, K. Y.**
Preliminary results of fast neutron treatments in
carcinoma of the pancreas
[NASA-TN-81516] p0160 M80-24983
- KOHL, P. J.**
The chemistry of sodium chloride involvement in
processes related to hot corrosion
p0074 A80-10041
Combustion of solid carbon rods in zero and normal
gravity
p0074 A80-20955
Combustion of solid carbon rods in zero and normal
gravity
[NASA-TN-79303] p0104 M80-13404
Chemical processes involved in the initiation of
hot corrosion of B-1900 and NASA-TRW VIA
[NASA-TN-81399] p0077 M80-17199
- KOLECKI, J.**
Modeling and analysis of Power Processing Systems
p0066 A80-28894
- KOLEMC, T.**
Study of advanced radial outflow turbine for solar
steam Rankine engines
[NASA-CR-159695] p0148 M80-16483
- KONATSU, G. K.**
Evaluation of particle transport for the P80-1
spacecraft
[AIAA PAPER 79-2047] p0055 A80-13301
- KONITO, E. H.**
Parametric study of prospective early commercial
MHD power plants (PSPC). General Electric
Company, task 1: Parametric analysis
[NASA-CR-159634] p0152 M80-26779
- KOONS, M. C.**
First results of material charging in the space
environment
p0055 A80-45609
- KOPPER, F. C.**
An experimental investigation of endwall profiling
in a turbine vane cascade
[AIAA PAPER 80-1089] p0004 A80-38904
- KORKAN, K. D.**
A theoretical and experimental investigation of
propeller performance methodologies
[AIAA PAPER 80-1240] p0026 A80-43283
An acoustic sensitivity study of general aviation
propellers
[AIAA PAPER 80-1871] p0045 A80-50191
- KORN, M. D.**
Core compressor exit stage study, 2
[NASA-CR-159812] p0039 M80-23312
- KOSMAHL, H. G.**
Analytical prediction and experimental
verification of TWT and depressed collector
performance using multidimensional computer
programs
p0102 A80-13902
How to quickly predict the overall TWT and the
multistage depressed collector efficiency
p0102 A80-31759
- KOSSON, H.**
Active heat exchange system development for latent
heat thermal energy storage
[NASA-CR-159726] p0149 M80-18562
- KOTA, S. L.**
Application of advanced on-board processing
concepts to future satellite communications
systems
[NASA-CR-159682] p0098 M80-12260
- KONALSKI, E. J.**
Computer code for estimating installed performance
of aircraft gas turbine engines. Volume 1:
Final report
[NASA-CR-159691] p0028 M80-13043
Computer code for estimating installed performance
of aircraft gas turbine engines. Volume 2:
Users manual
[NASA-CR-159692] p0028 M80-13044
- KOZLOWSKI, H.**
Experimental evaluation of exhaust mixers for an
Energy Efficient Engine
[AIAA PAPER 80-1088] p0025 A80-38903
- KRAFT, G.**
Experimental evaluation of exhaust mixers for an
Energy Efficient Engine
[AIAA PAPER 80-1088] p0025 A80-38903
- KRAMER, W. H.**
CP6-6D engine short-term performance deterioration
[NASA-CR-159830] p0039 M80-23316
CP6-6D engine performance deterioration
[NASA-CR-159786] p0041 M80-27364
- KRAUS, J.**
Design study of toroidal traction CVT for electric
vehicles
[NASA-CR-159803] p0124 M80-25661
- KRAUSE, L. M.**
Some dynamic and time-averaged flow measurements
in a turbine rig
p0178 A80-21120
- KRANCZONEK, W. H.**
The effect of a weak vertical magnetic field on
fluctuation-induced transport in a Bumpy-Torus
plasma
p0176 A80-25476
- KRESKOVSKI, J. P.**
Computation of three-dimensional viscous
supersonic flow in inlets
[AIAA PAPER 80-0194] p0065 A80-23941
A three-dimensional turbulent compressible
subsonic duct flow analysis for use with
constructed coordinate systems
[AIAA PAPER 80-1398] p0006 A80-41601
Development of a three-dimensional supersonic
inlet flow analysis
[NASA-CR-3218] p0108 M80-14356
- KRODKIENSKI, T.**
Parametric instabilities of rotor-support systems
with application to industrial ventilators
p0127 M80-29729
- KUCIAR, A. P.**
Scale model performance test investigation of
exhaust system mixers for an Energy Efficient

Engine /E3/ propulsion system
[AIAA PAPER 80-0229] p0024 A80-20968

KUUVINEN, D. E.
Assessment of potential exposure to friable
insulation materials containing asbestos
[NASA-TM-81435] p0157 M80-23875

KULCSZ, J. J.
Prediction of fragment velocities and trajectories
p0096 M80-16210

KULINA, M.
Quiet Clean Short-haul Experimental Engine (QCSSE)
main reduction gears detailed design report
[NASA-CR-134872] p0030 M80-15106

KUMM, E. L.
Design study of flat belt CVT for electric vehicles
[NASA-CR-159822] p0124 M80-22702

KURKOV, A. P.
Flutter spectral measurements using stationary
pressure transducers p0111 A80-36147

Flutter spectral measurements using stationary
pressure transducers
[NASA-TM-79293] p0013 M80-13046

KUSAK, L.
Liquid oxygen/liquid hydrogen auxiliary power
system thruster investigation
[NASA-CR-159674] p0062 M80-15202

KVATERNIK, E. G.
Examination of the flap-lag stability of rigid
articulated rotor blades p0010 A80-15123

Buckling of rotating beams p0133 A80-20149

L

LACKNER, H.
Study of advanced electric propulsion system
concept using a flywheel for electric vehicles
[NASA-CR-159650] p0184 M80-18991

LAKSHMINARAYANA, B.
Three dimensional mean flow and turbulence
characteristics of the near wake of a compressor
rotor blade
[NASA-CR-159518] p0005 M80-27288

LALLI, V. R.
Photovoltaic power system reliability considerations
p0146 A80-40338

Photovoltaic power system reliability considerations
[NASA-TM-79291] p0130 M80-15422

LAMPING, R. K.
Performance, emissions, and physical
characteristics of a rotating combustion
aircraft engine, supplement A
[NASA-CR-135119] p0041 M80-27361

LANATI, G. A.
Measuring unsteady pressure on rotating compressor
blades p0110 A80-12630

LANDADIO, F. J.
Experimental results concerning centrifugal
impeller excitations p0127 M80-29727

LAQUEY, R. E.
Torquing and electrostatic deformation of the
solar sail p0065 A80-46901

LARK, R. F.
Mechanical property characterization of intraply
hybrid composites p0070 A80-20954

Dynamic response of damaged angleplied fiber
composites p0070 A80-27982

Tensile and flexural strength of non-graphitic
superhybrid composites: Predictions and
comparisons
[NASA-TM-79276] p0067 M80-11144

Dynamic response of damaged angleplied fiber
composites
[NASA-TM-79281] p0067 M80-11145

Mechanical property characterization of intraply
hybrid composites
[NASA-TM-79306] p0067 M80-12120

LAU, S. K.
Evaluation of present-day thermal barrier coatings
for industrial/utility applications p0092 A80-39637

LAUVER, M. E.
Parametric dependence of ion temperature and
electron density in the SUNMA hot-ion plasma
using laser light scattering and emission
spectroscopy p0176 A80-46265

LEE, D. S.
Directional solidification at ultra-high thermal
gradient
[NASA-CR-159797] p0096 M80-15300

LEE, F. C.
An adaptive-control switching buck regulator -
Implementation, analysis, and design p0103 A80-28167

LEE, F. C. Y.
Modeling and analysis of Power Processing Systems
p0066 A80-28894

LEE, M. C.
CATCON catalyst 5 atm 1000 hour aging study using
No. 2 fuel oil p0075 A80-35908

Durability testing at 5 atmospheres of advanced
catalysts and catalyst supports for gas turbine
engine combustors
[NASA-CR-159839] p0151 M80-24748

LEE, K. W.
Spray nozzle designs for agricultural aviation
applications
[NASA-CR-159702] p0108 M80-10460

LEE, S. Y.
Evaluation of present-day thermal barrier coatings
for industrial/utility applications p0092 A80-39637

LEFEBVRE, A. H.
Atomization of broad specification aircraft fuels
p0043 M80-29318

LEPROIS, M. T.
Active heat exchange system development for latent
heat thermal energy storage
[NASA-CR-159727] p0154 M80-29857

LENN, W. L.
First results of material charging in the space
environment p0055 A80-45609

LEIBCKI, H. P.
Cycles till failure of silver-zinc cells with
competing failure modes - Preliminary data
analysis p0146 A80-46414

Cycles till failure of silver-zinc cells with
completing failures modes: Preliminary data
analysis
[NASA-TM-81556] p0164 M80-29088

LEIBLIEB, S.
Evaluation of feasibility of prestressed concrete
for use in wind turbine blades
[NASA-CR-159725] p0147 M80-15553

LEIE, B.
Self-excited rotor whirl due to tip-seal leakage
forces p0127 M80-29723

LEININGER, G.
Identification and dual adaptive control of a
turbojet engine p0023 A80-10033

LEININGER, G. G.
A new traffic control design method for large
networks with signalized intersections p0183 A80-14841

LEUNG, M. S.
First results of material charging in the space
environment p0055 A80-45609

LEVINE, S. E.
Thermal barrier coatings for aircraft gas turbines
[AIAA PAPER 80-0302] p0089 A80-18303

Materials and structures technology p0012 M80-10210

Corrosion resistant thermal barrier coating
[NASA-CASE-LEW-13088-1] p0067 M80-11142

LEVY, R.
Computation of three-dimensional viscous
supersonic flow in inlets
[AIAA PAPER 80-0194] p0065 A80-23941

A three-dimensional turbulent compressible
subsonic duct flow analysis for use with
constructed coordinate systems
[AIAA PAPER 80-1398] p0006 A80-41601

- Development of a three-dimensional supersonic inlet flow analysis
[NASA-CN-3218] p0108 N80-14356
- LEWIS, B. L.
Effect of time dependent flight loads on JT9D-7 performance deterioration
[NASA-CR-159681] p0134 N80-10515
- LEWIS, D. W.
Feasibility of active feedback control of rotordynamic instability
p0128 N80-29733
- LEWIS, E. A.
Sulfate and nitrate collected by filter sampling near the tropopause
[NASA-TP-1567] p0157 N80-14581
- LIEBMAN, M.
Effect of refining variables on the properties and composition of JP-5
p0041 N80-29306
- LIEBENT, C. H.
Significance of thermal contact resistance in two-layer, thermal-barrier-coated turbine vanes
p0024 A80-39635
Effects of a ceramic coating on metal temperatures of an air-cooled turbine vane
[NASA-TP-1598] p0105 N80-17397
Significance of thermal contact resistance in two-layer thermal-barrier-coated turbine vanes
[NASA-TN-81483] p0018 N80-23310
- LIEBLEIN, S.
Large Wind Turbine Design Characteristics and R and D Requirements
[NASA-CP-2106] p0139 N80-16453
- LIMSCOTT, B. S.
Blade design and operating experience on the MOD-OA 200 kW wind turbine at Clayton, New Mexico
p0139 N80-16470
- LINTZ, A. T.
Advanced propulsion system for hybrid vehicles
[NASA-CR-159771] p0184 N80-26212
- LIPSHITZ, A.
Modified face seal for positive film stiffness
[NASA-CASE-LEN-12989-1] p0114 N80-12414
- LISTER, E.
Low NO_x/ heavy fuel combustor program
[ASME PAPER 80-GT-69] p0026 A80-42199
Low NO_x/ heavy fuel combustor program
[NASA-TN-79313] p0137 N80-13624
- LIU, D. C.
Hyperfine magnetic field at Cd impurity site in L2/1/ Heusler alloys Rh₂MnGe and Rh₂MnPb by TDPAC technique
p0178 A80-16843
- LOEFFLER, I. J.
QCSE engine powered-lift acoustic performance
[AIAA PAPER 80-1065] p0025 A80-38651
QCSE UTM engine powered-lift acoustic performance
[NASA-TN-81504] p0019 N80-24315
- LORENTHAL, S. H.
Analysis of wear debris from full-scale bearing fatigue tests using the Ferrograph
[ASLE PREPRINT 80-AM-3E-2] p0122 A80-43167
Constrained fatigue life optimization of a NASVYTIS multiroller traction drive
p0122 A80-46407
Effect of geometry and operating conditions on spur gear system power loss
p0122 A80-46409
Evaluation of a high performance fixed-ratio traction drive
p0122 A80-46410
Simplified fatigue life analysis for traction drive contacts
p0123 A80-46413
Analysis of wear-debris from full-scale bearing fatigue tests using the ferrograph
[NASA-TN-81403] p0114 N80-16341
Spur-gear-system efficiency at part and full load
[NASA-TP-1622] p0115 N80-17466
Simplified fatigue life analysis for traction drive contacts
[NASA-TN-79199] p0115 N80-17469
Evaluation of a high performance fixed-ratio traction drive
[NASA-TN-81425] p0115 N80-18404
Effect of geometry and operating conditions on spur gear system power loss
[NASA-TN-81426] p0116 N80-18406
- Constrained fatigue life optimization of a NASVYTIS multiroller traction drive
[NASA-TN-81447] p0116 N80-18407
Kinematic correction for roller skewing
[NASA-TN-81564] p0119 N80-28716
- LOHMEYER, R. F.
Experimental evaluation of a low emissions high performance duct burner for Variable Cycle Engines (VCE)
[NASA-CR-159694] p0036 N80-17074
The broadened-specification fuels combustion technology program at Pratt and Whitney Aircraft
p0042 N80-29315
- LONDAN, D. S.
Evaluation of feasibility of prestressed concrete for use in wind turbine blades
[NASA-CR-159725] p0147 N80-15553
- LOONIS, W. E.
Steady-state wear and friction in boundary lubrication studies
[NASA-TP-1658] p0087 N80-22493
- LORENZO, C. F.
Single-stage electrohydraulic servosystem for actuating on airflow valve with frequencies to 500 hertz
[NASA-TP-1678] p0046 N80-29369
Preliminary results from a four-working space, double-acting piston, Stirling engine controls model
[NASA-TN-81569] p0106 N80-29624
- LOVELL, E. E.
Liquid metal slip ring
[NASA-CASE-LEN-12277-3] p0101 N80-18300
- LOVELL, C. E.
The erosion/corrosion of small superalloy turbine rotors operating in the effluent of a PFB coal combustor
p0080 A80-10043
The effect of zirconium on the isothermal oxidation of nominal Ni-14Cr-24Al alloys
p0082 A80-26465
Effect of sodium, potassium, magnesium, calcium, and chlorine on the high temperature corrosion of IN-100, U-700, IN-792, and MAR M-509
[ASME PAPER 80-GT-150] p0083 A80-42262
Effect of sodium, potassium, magnesium, calcium, and chlorine on the high temperature corrosion of IN-100, U-700, IN-792, and MAR M-509
[NASA-TN-79309] p0076 N80-15235
Effects of impurities in coal-derived liquids on accelerated hot corrosion of superalloys
[NASA-TN-81384] p0077 N80-18157
Fouling and the inhibition of salt corrosion
[NASA-TN-81469] p0078 N80-21492
- LOVENTHAL, S. H.
Parametric tests of a traction drive retrofitted to an automotive gas turbine
[NASA-TN-81457] p0117 N80-21754
- LUBOMSKI, J. F.
Status of NASA full-scale engine aeroelasticity research
p0133 A80-35906
Status of NASA full-scale engine aeroelasticity research
[NASA-TN-81500] p0132 N80-23678
- LUCAS, J. G.
Forward acoustic performance of a shock-swallowing high-tip-speed fan (QF-13)
[NASA-TP-1668] p0169 N80-23100
- LUCAS, J. W.
Annual technical report, fiscal year 1979. Volume 1: Executive summary
[NASA-CR-159715-VOL-1] p0149 N80-19632
- LUDWIG, L. P.
Wear of seal materials used in aircraft propulsion systems
p0121 A80-28010
Circumferential shaft seal
[NASA-CASE-LEN-12119-2] p0115 N80-18401
Composite seal for turbomachinery
[NASA-CASE-LEN-12131-2] p0118 N80-26658
Composite wall concept for high temperature turbine shrouds: Heat transfer analysis
[NASA-TN-81539] p0020 N80-27362
Circumferential shaft seal
[NASA-CASE-LEN-12119-1] p0119 N80-28711
Observation of pressure variation in the cavitation region of submerged journal bearings
[NASA-TN-81582] p0120 N80-31798

- LUXEMBURG, R. W.
Optimum subsonic, high-angle-of-attack nacelles
[NASA-TN-81491] p0016 N80-20275
- LYNCH, J. J.
Survey of MHD plant applications p0144 A80-11972
- LYONS, K. A.
Core compressor exit stage study. 1: Aerodynamic
and mechanical design
[NASA-CR-159714] p0037 N80-19113

M

- MACIOCH, L. E.
The energy efficient engine project
[NASA-TN-81566] p0023 N80-32395
- MACK, D. P.
An efficient user-oriented method for calculating
compressible flow in an about three-dimensional
inlets
[NASA-CR-159578] p0004 N80-10134
- MACKAY, R. A.
Anisotropy of nickel-base superalloy single crystals
p0083 A80-51573
Anisotropy of nickel-base superalloy single crystals
[NASA-TN-81437] p0077 N80-17200
- MACKINNON, M. J.
Forward acoustic performance of a shock-swallowing
high-tip-speed fan (QF-13)
[NASA-TP-1668] p0169 N80-23100
- MADON, E. J.
Experimental evaluation of a low emissions high
performance duct burner for Variable Cycle
Engines (VCE)
[NASA-CR-159694] p0036 N80-17074
- MAGLIOZZI, B.
Acoustic pressures on a prop-fan aircraft fuselage
surface
[AIAA PAPER 80-1002] p0172 A80-35965
Advanced turbo-prop airplane interior noise
reduction-source definition
[NASA-CR-159668] p0172 N80-13882
- MAHMOOD, R.
Homogeneous alignment of nematic liquid crystals
by ion beam etched surfaces p0178 A80-26007
Homogeneous alignment of nematic liquid crystals
by ion beam etched surfaces
[NASA-TN-81378] p0096 N80-16232
- MAHUSON, T. C.
Investigation into the effect of plasma
pretreatment on the adhesion of parylene to
various substrates p0066 A80-25900
Investigation into the effect of plasma
pretreatment on the adhesion of parylene to
various substrates
[NASA-TN-79224] p0114 N80-13473
- MAIER, R. D.
Anisotropy of nickel-base superalloy single crystals
p0083 A80-51573
Anisotropy of nickel-base superalloy single crystals
[NASA-TN-81437] p0077 N80-17200
- MAISEL, J. E.
Error analysis in the measurement of average power
with application to switching controllers
[NASA-CR-159792] p0184 N80-21202
- MALANOSKI, S. B.
Practical experience with unstable compressors
p0125 N80-29709
- MANDELL, M.
A three-dimensional spacecraft-charging computer
code p0055 A80-46891
- MANDELL, M. J.
Plasma collection by high voltage spacecraft at
low earth orbit
[AIAA PAPER 80-0042] p0055 A80-18249
Photoelectron charge density and transport near
differentially charged spacecraft p0053 A80-19773
- MANNING, I.
Performance, emissions, and physical
characteristics of a rotating combustion
aircraft engine, supplement A
[NASA-CR-135119] p0041 N80-27361
- MANSON, S. S.
A quarter-century of progress in the development
of correlation and extrapolation methods for

- creep rupture data p0133 A80-38142
- Practical implementation of the double linear
damage rule and damage curve approach for
treating cumulative fatigue damage
[NASA-TN-81517] p0132 N80-23684
- MANTHINI, M. A.
Sputtering in mercury ion thrusters
[AIAA PAPER 79-2061] p0058 A80-10384
Hg ion thruster component testing
[AIAA PAPER 79-2116] p0059 A80-20959
Hg ion thruster component testing
[NASA-TN-79287] p0056 N80-13159
- MARIANOSKI, L. G.
High-temperature molten salt thermal energy
storage systems
[NASA-CR-159663] p0148 N80-17547
- MARSHALL, R. L.
A comparison of experiment and theory for sound
propagation in variable area ducts p0173 A80-45844
- MARTIN, C. M.
Coupled generator and combustor performance
calculations for potential early commercial MHD
power plants p0156 A80-25099
Parametric study of prospective early commercial
MHD power plants (PSPRC). General Electric
Company, task 1: Parametric analysis
[NASA-CR-159634] p0152 N80-26779
- MARTINEY, P. J.
Experimental study of turbine fuel thermal
stability in an aircraft fuel system simulator
p0043 N80-29325
- MARTIN, C.
Study of advanced radial outflow turbine for solar
steam Rankine engines
[NASA-CR-159695] p0148 N80-16483
- MARTIN, R. E.
Advanced technology light weight fuel cell program
[NASA-CR-159807] p0149 N80-19615
- MARTIN, R. L.
Expanded study of feasibility of measuring
in-flight 747/JT9D loads, performance,
clearance, and thermal data
[NASA-CR-159717] p0036 N80-16063
- MARTZ, J. E.
A photovoltaic power system in the remote African
village of Tangaye, Upper Volta
[NASA-TN-79318] p0137 N80-12552
- MARUSAK, T.
Design study of a 15 kW free-piston Stirling
engine-linear alternator for dispersed solar
electric power systems
[NASA-CR-159587] p0150 N80-22787
- MARYNOWSKI, K.
Parametric instabilities of rotor-support systems
with application to industrial ventilators
p0127 N80-29729
- MATHUR, A. K.
Assessment and preliminary design of an energy
buffer for regenerative braking in electric
vehicles
[NASA-CR-159756] p0184 N80-23216
Active heat exchange system development for latent
heat thermal energy storage
[NASA-CR-159727] p0154 N80-29857
- MATTHEI, K. W.
Study program to improve the open-circuit voltage
of low resistivity single crystal silicon solar
cells
[NASA-CR-159833] p0150 N80-22775
- MATTHEI, M. D.
Inlet flow distortion in turbomachinery. I -
Comparison of theory and experiment in a
transonic fan stage. II - A parameter study
[AIAA PAPER 80-1076] p0006 A80-38895
- MAY, C. E.
Decay of the zincate concentration gradient at an
alkaline zinc cathode after charging
p0074 A80-13070
Method of cross-linking polyvinyl alcohol and
other water soluble resins
[NASA-CASE-LEW-13103-1] p0088 N80-32516
- HAZABIS, G. A.
Open-circuit voltage improvements in low
resistivity solar cells
[NASA-TN-81388] p0138 N80-15555

- MCARDIN, J. G.
Comparison of several inflow control devices for flight simulation of fan tone noise using a JT15D-1 engine
[AIAA PAPER 80-1025] p0025 A80-38640
- MCARDIN, J. G.
Static test-stand performance of the YF-102 turbofan engine with several exhaust configurations for the Quiet Short-Haul Research Aircraft (QSHA)
[NASA-TP-1556] p0014 N80-14121
Comparison of several inflow control devices for flight simulation of fan tone noise using a JT15D-1 engine
[NASA-TM-81505] p0019 N80-24314
Static and transient performance of YF-102 engine with up to 14 percent core airbleed for the quiet short-haul research aircraft
[NASA-TP-1692] p0020 N80-25339
- MCAULAY, J. E.
Engine component improvement program - Performance improvement
[AIAA PAPER 80-0223] p0024 A80-19300
Engine component improvement program: Performance improvement
[NASA-TM-79304] p0013 N80-12092
Improved components for engine fuel savings
[NASA-TM-81577] p0023 N80-31402
- MCCARTHY, J. F., JR.
Matrix management for aerospace 2000
[AIAA PAPER 80-0946] p0181 A80-40700
Matrix management for aerospace 2000
[NASA-TM-81509] p0181 N80-24200
- MCCLEUNG, W. C.
Design, fabrication and testing of an optical temperature sensor
[NASA-CR-165125] p0112 N80-31777
- MCCREIGHT, L. R.
Sintered silicon nitride recuperator fabrication
[NASA-CR-159706] p0090 N80-15263
- MCDONALD, G.
Preliminary study of a solar selective coating system using black cobalt oxide for high temperature solar collectors
p0082 A80-35500
Effect of thermal cycling on ZrO₂-Y₂O₃ thermal barrier coatings
p0089 A80-35899
Preliminary study of a solar selective coating system using black cobalt oxide for high temperature solar collectors
[NASA-TM-81385] p0077 N80-18156
Effect of thermal cycling on ZrO₂-Y₂O₃ thermal barrier coatings
[NASA-TM-81480] p0018 N80-22349
- MCDONALD, G. H.
Stability analysis of a liquid fuel annular combustion chamber
[NASA-CR-159734] p0061 N80-13165
- MCDONALD, H.
Computation of three-dimensional viscous supersonic flow in inlets
[AIAA PAPER 80-0194] p0065 A80-23941
A three-dimensional turbulent compressible subsonic duct flow analysis for use with constructed coordinate systems
[AIAA PAPER 80-1398] p0006 A80-41601
Development of a three-dimensional supersonic inlet flow analysis
[NASA-CR-3218] p0108 N80-14356
- MCFALLS, R. A.
Demonstration of short-haul aircraft aft noise reduction techniques on a twenty inch (50.8 cm) diameter fan, volume 1
[NASA-CR-134849] p0033 N80-15083
- MCGANNON, W. J.
Intra-ocular pressure normalization technique and equipment
[NASA-CASE-LEN-12723-1] p0135 N80-18690
- MCKENZIE, D. J., JR.
Measured and predicted impingement noise for a model-scale under the wing externally blown flap configuration with a QCSEE type nozzle
[NASA-TM-81494] p0169 N80-26115
- MCLALLIN, K. L.
Experimental performance and analysis of 15.04-centimeter-tip-diameter, radial-inflow turbine with work factor of 1.126 and thick blading
[NASA-TP-1730] p0023 N80-33410
- MCLERO, A. M.
Synthesis of improved polyester resins
[NASA-CR-159665] p0090 N80-13257
Synthesis of improved phenolic resins
[NASA-CR-159724] p0091 N80-17221
- MCHALLY, W. D.
Computational fluid mechanics of internal flow
p0012 N80-10211
- MENALIC, C. M.
Investigation of performance deterioration of the CF6/JT9D, high-bypass ratio turbofan engines
[NASA-TM-81552] p0022 N80-29332
Performance deterioration of commercial high-bypass ratio turbofan engines
[NASA-TM-81552-REV] p0023 N80-32394
- MENNEID, O.
Single-stage electrohydraulic servosystem for actuating on airflow valve with frequencies to 500 hertz
[NASA-TP-1678] p0046 N80-29369
- MENIN, G. M.
An investigation of the initiation stage of hot corrosion in Ni-base alloys
[NASA-CR-159718] p0083 N80-15233
Hot corrosion of Co-Cr, Co-Cr-Al, and Ni-Cr alloys in the temperature range of 700-750 deg C
[NASA-CR-159689] p0084 N80-26427
- MEITNER, P. L.
Loss model for off-design performance analysis of radial turbines with pivoting-vane, variable-area stators
[NASA-TM-81532] p0020 N80-27365
- MELLISH, J. A.
Low-thrust chemical rocket engine study
p0063 N80-31467
- MELNYK, P.
Tungsten wire/FeCrAlY matrix turbine blade fabrication study
[NASA-CR-159788] p0044 N80-29331
- MENHOTT, J. V. W.
Diffusion bonded boron/aluminum spar-shell fan blade
[NASA-CR-159571] p0072 N80-25382
- MENDIRATTA, M. C.
Characterization and properties of controlled nucleation thermochemical deposited (CNTD)/silicon carbide
p0089 A80-13063
Characterization and properties of controlled nucleation thermochemical deposited (CNTD) silicon carbide
[NASA-TM-79277] p0085 N80-13254
- MENGLE, V. G.
Non-synchronous whirling due to fluid-dynamic forces in axial turbo-machinery rotors
p0126 N80-29721
- MERINO, F.
Capillary device refilling
[AIAA PAPER 80-1095] p0060 A80-38908
Conceptual design of an orbital propellant transfer experiment. Volume 2: Study results
[NASA-CR-165150] p0048 N80-31423
Comparative thermal analysis of alternate Cryogenic Fluid Management Experiment (CFME) configurations
[NASA-CR-165151] p0048 N80-32412
- MERRICK, H. F.
Characterization of an oxide dispersion strengthened superalloy, MA-6000E, for turbine blade applications
[NASA-CR-159493] p0083 N80-13218
- MERRILL, W.
Identification and dual adaptive control of a turbojet engine
p0023 A80-10033
- METZGER, F. B.
Acoustic test and analyses of three advanced turboprop models
[NASA-CR-159667] p0039 N80-23311
- MEULENBERG, A., JR.
Thin n-i-p radiation-resistant solar cell feasibility study
[NASA-CR-159871] p0154 N80-29852
- MICHELS, C. J.
Study of a rare-gas transverse fast discharge
p0176 A80-11366
- MIKELSON, D. C.
A theoretical and experimental investigation of propeller performance methodologies

- [AIAA PAPER 80-1240] p0026 A80-43283
High speed turboprops for executive aircraft,
potential and recent test results
[NASA-TN-81482] p0002 A80-21285
NASA propeller technology program p0018 A80-22341
- MILANO, E.
An experimental investigation of endwall profiling
in a turbine vane cascade
[AIAA PAPER 80-1089] p0004 A80-38904
- MILDICH, J. W.
Power management for multi-100 KWe space systems
p0060 A80-48357
Study of power management technology for orbital
multi-100KWe applications. Volume 2: Study
results
[NASA-CR-159834-VOL-2] p0153 A80-28862
Study of power management technology for orbital
multi-100KWe applications. Volume 3:
Requirements
[NASA-CR-159834] p0154 A80-29845
- MILES, J. M.
Dispersion of sound in a combustion duct by fuel
droplets and soot particles p0170 A80-20953
Spectral structure of pressure measurements made
in a combustion duct p0171 A80-35496
Spectral structure of pressure measurements made
in a combustion duct
[NASA-TN-81471] p0168 A80-22045
Pressure spectra and cross spectra at an area
contraction in a ducted combustion system
[NASA-TN-81477] p0168 A80-23097
- MILLER, B. A.
The NASA high-speed turboprop program
[NASA-TN-81561] p0022 A80-31401
- MILLER, D. B.
Tested, tip-controlled rotor - Preliminary test
results from Mod-O 100-kW experimental wind
turbine
[AIAA 80-0642] p0145 A80-28836
Tested, tip-controlled rotor: Preliminary test
results from Mod-O 100-kW experimental wind
turbine
[NASA-TN-81445] p0140 A80-19613
Statistical aspects of carbon fiber risk
assessment modeling
[NASA-CR-159318] p0073 A80-29432
- MILLER, F. O.
Design, performance and life cycle cost
relationships for a 500kW space solar array
p0065 A80-48356
Solar array subsystems study
[NASA-CR-159857] p0151 A80-24742
- MILLER, R. A.
Thermal barrier coatings for aircraft gas turbines
[AIAA PAPER 80-0302] p0089 A80-18303
Combustion of solid carbon rods in zero and normal
gravity p0074 A80-20955
Analysis of the response of a thermal barrier
coating to sodium and vanadium doped combustion
gases
[NASA-TN-79205] p0076 A80-10344
Corrosion resistant thermal barrier coating
[NASA-CASE-LEW-13088-1] p0067 A80-11142
Combustion of solid carbon rods in zero and normal
gravity
[NASA-TN-79303] p0104 A80-13404
- MISER, R. V.
Effects of fine porosity on the fatigue behavior
of a powder metallurgy superalloy p0082 A80-35495
- MISER, R. V., JR.
Effects of thermally induced porosity on an as-HIP
powder metallurgy superalloy p0082 A80-29990
Application of superalloy powder metallurgy for
aircraft engines p0122 A80-44240
Effect of thermally induced porosity on an as-HIP
powder metallurgy superalloy
[NASA-TN-79263] p0076 A80-11189
Application of superalloy powder metallurgy for
aircraft engines
[NASA-TN-81466] p0078 A80-21488
Effects of fine porosity on the fatigue behavior
of a powder metallurgy superalloy
- [NASA-TN-81448] p0078 A80-21493
MINNUCCI, J. A.
Study program to improve the open-circuit voltage
of low resistivity single crystal silicon solar
cells
[NASA-CR-159833] p0150 A80-22775
- MISTICH, M. J.
Modification of the electrical and optical
properties of polymers
[NASA-CASE-LEW-13027-1] p0087 A80-24437
Adherence of ion beam sputter deposited metal
films on H-13 steel
[NASA-TN-81585] p0079 A80-31527
- MISTICH, M. J., JR.
Hydrogen hollow cathode ion source
[NASA-CASE-LEW-12940-1] p0174 A80-33186
- MISSEL, O. M.
Quiet Clean Short-haul Experimental Engine (QCSSE)
main reduction gears test program
[NASA-CR-134669] p0030 A80-15103
- MITCHELL, C.
Concepts for 18/30 GHz satellite communication
system, volume 1
[NASA-CR-159625-VOL-1] p0098 A80-11277
Concepts for 18/30 GHz satellite communication
system, volume 1A: Appendix
[NASA-CR-159625-VOL-1A] p0098 A80-11278
Concepts for 18/30 GHz satellite communication
system study. Executive summary
[NASA-CR-159680] p0098 A80-11279
- MITCHELL, G. A.
Summary of advanced methods for predicting high
speed propeller performance
[AIAA PAPER 80-0225] p0003 A80-20966
High speed turboprops for executive aircraft,
potential and recent test results
[NASA-TN-81482] p0002 A80-21285
- MITCHELL, S. C.
Quiet Clean Short-haul Experimental Engine (QCSSE)
composite fan frame design report
[NASA-CR-135278] p0031 A80-15110
- MIYAMURA, T. F.
Characterization of solar cells for space
applications. Volume 10: Electrical
characteristics of Spectrolab BSP, textured, 10
ohm-cm, 300 micron cells as a function of
intensity, temperature and irradiation
[NASA-CR-162422] p0147 A80-11566
- MIYOSHI, E.
The friction and wear of metals and binary alloys
in contact with an abrasive grit of
single-crystal silicon carbide
[ASLE PREPRINT 79-1C-5C-1] p0120 A80-14734
Adhesion and friction of iron-base binary alloys
in contact with silicon carbide in vacuum
[NASA-TP-1604] p0076 A80-15234
Tribological properties of silicon carbide in
metal removal process
[NASA-TN-79238] p0114 A80-16340
Wear particles of single-crystal silicon carbide
in vacuum
[NASA-TP-1624] p0085 A80-18178
Adhesion, friction, and wear of binary alloys in
contact with single-crystal silicon carbide
[NASA-TN-79282] p0086 A80-21534
Friction and wear of iron-base binary alloys in
sliding contact with silicon carbide in vacuum
[NASA-TP-1612] p0087 A80-22494
- MIZERA, P. F.
Initial comparison of SSPM ground test results and
flight data to NASCAP simulations
[AIAA PAPER 80-0336] p0054 A80-29751
First results of material charging in the space
environment p0055 A80-45609
- HOFFAT, E. J.
Full-coverage film cooling. I - Comparison of heat
transfer data for three injection angles
[ASME PAPER 80-GT-43] p0108 A80-42176
Full-coverage film cooling. II - Heat transfer
data and numerical simulation
[ASME PAPER 80-GT-44] p0109 A80-42177
- HOFFETT, E. E.
Exhaust emission reduction for intermittent
combustion aircraft engines
[NASA-CR-159757] p0029 A80-14130
- HOFFITT, T. P.
Design and cold-air test of single-stage uncooled
turbine with high work output

[NASA-TP-1680] p0019 N80-25337
Cold-air investigation of a 4 1/2 stage turbine
with stage-loading factor of 4.66 and high
specific work output. 2: Stage group performance
[NASA-TP-1688] p0019 N80-25338
Description of the warm core turbine facility
recently installed at NASA Lewis Research Center
[NASA-TM-81562] p0022 N80-29333

SOMENTNY, A. M.
Aviation fuels outlook p0041 N80-29304

MONTGOMERY, P. J.
Noise reduction p0012 N80-10208
An improved prediction method for the noise
generated in flight by circular jets
[NASA-TM-81470] p0168 N80-22048

MOORE, A. S.
Static test-stand performance of the YF-102
turbofan engine with several exhaust
configurations for the Quiet Short-Haul Research
Aircraft (QSRA) p0014 N80-14121
Static and transient performance of YF-102 engine
with up to 14 percent core airbleed for the
quiet short-haul research aircraft
[NASA-TP-1692] p0020 N80-25339

MOORE, J. W.
Feasibility of active feedback control of
rotordynamic instability p0128 N80-29733

MOORE, M. T.
Core noise investigation of the CF6-50 turbofan
engine p0036 N80-16062
[NASA-CR-159749]

MOORE, B. D.
Experimental study of low aspect ratio compressor
blading p0025 A80-42147
[ASME PAPER 80-GT-6]
Vertical Takeoff and Landing (VTOL) propulsion
technology p0013 N80-10218
Experimental study of low aspect ratio compressor
blading p0002 N80-11037
[NASA-TM-79280]

MOORE, T. J.
Elevated temperature flow strength, creep
resistance and diffusion welding characteristics
of Ti-6Al-2Nb-1Ta-0.8Mo p0081 A80-13277

MORAN, P. J.
Flight test of navigation and guidance sensor
errors measured on STOL approaches p0028 N80-13041
[NASA-TM-81154]

MORREY, W. H.
Design, fabrication and testing of an optical
temperature sensor p0112 N80-31777
[NASA-CR-165125]

MORRIS, J. P.
Comments on TEC trends p0145 A80-39642
Comments on TEC trends p0175 N80-16885
[NASA-TM-79317]
Potentialities of TEC topping: A simplified view
of parametric effects p0175 N80-22083
[NASA-TM-81468]
Optimal thermionic energy conversion with
established electrodes for high-temperature
topping and process heating p0175 N80-33221
[NASA-TM-81555]

MORRIS, P. H.
Experimental aerodynamic and acoustic model
testing of the Variable Cycle Engine (VCE)
testbed coannular exhaust nozzle system p0040 N80-26300
[NASA-CR-159710]
Experimental aerodynamic and acoustic model
testing of the Variable Cycle Engine (VCE)
testbed coannular exhaust nozzle system:
Comprehensive data report p0040 N80-26301
[NASA-CR-159711]

MOSLEY, P. K.
Prediction of fragment velocities and trajectories p0096 N80-16210

MOSER, C. A.
Effect of fuel molecular structure on soot
formation in gas turbine engines p0095 A80-42192
[ASME PAPER 80-GT-62]
Fuel quality combustion analysis p0094 N80-19284
[NASA-CR-159721]

Effect of fuel molecular structure on soot
formation in gas turbine combustion p0043 N80-29322

MOSIER, J. S.
Materials for advanced turbine engines. Volume 1:
Power metallurgy Bene 95 rotating turbine engine
parts p0084 N80-28499
[NASA-CR-159802]

MOUL, T. M.
Wind-tunnel investigation of the flow correction
for a model-mounted angle of attack sensor at
angles of attack from -10 deg to 110 deg
[NASA-TM-80189] p0011 N80-14110

MROZ, T. S.
Durability testing of advanced catalysts and
catalyst supports for gas turbine engine
combustors p0074 A80-35881

MULLEN, E. J.
Emission reduction p0012 N80-10207

MUMFORD, P.
Studies of the acoustic transmission
characteristics of coaxial nozzles with inverted
velocity profiles, volume 1 p0172 N80-11870
[NASA-CR-159698]

MUNZ, D.
Fracture toughness determination of Al203 using
four-point-bend specimens with straight-through
and chevron notches p0090 A80-42085

Compliance and stress intensity coefficients for
short bar specimens with chevron notches p0133 A80-46032

Performance of Chevron-notch short bar specimen in
determining the fracture toughness of silicon
nitride and aluminum oxide p0090 A80-50696

Fracture toughness of brittle materials determined
with chevron notch specimens p0079 N80-32486
[NASA-TM-81607]

MURPHY, E. C.
Analysis and identification of subsynchronous
vibration for a high pressure parallel flow
centrifugal compressor p0125 N80-29710

MYERS, D.
Performance, emissions, and physical
characteristics of a rotating combustion
aircraft engine, supplement A p0041 N80-27361
[NASA-CR-135119]

MYHRE, E. W.
UHF coplanar-slot antenna for
aircraft-to-satellite data communications p0009 A80-13064

N

NANGELI, D. W.
Effect of fuel molecular structure on soot
formation in gas turbine engines p0095 A80-42192
[ASME PAPER 80-GT-62]
Fuel quality combustion analysis p0094 N80-19284
[NASA-CR-159721]
Effect of fuel molecular structure on soot
formation in gas turbine combustion p0043 N80-29322

NAGIB, H. H.
Effects of axisymmetric contractions on turbulence
of various scales p0006 N80-32328
[NASA-CR-165136]

NAGLE, W. J.
Toroidal cell and battery p0144 N80-33857
[NASA-CASE-LEN-12918-1]

NAJMBER, J. J.
Effect on combined cycle efficiency of stack gas
temperature constraints to avoid acid corrosion
[NASA-TM-81531] p0143 N80-27804

NASTRON, G. D.
Measurements of cabin and ambient ozone on B747
airplanes p0010 A80-28853

Simultaneous cabin and ambient ozone
measurements on two Boeing 747 airplanes, volume 1
[NASA-TM-79166] p0008 N80-15059

NAYFER, A. H.
A comparison of experiment and theory for sound
propagation in variable area ducts p0173 A80-45844

- NEFF, H. A.
Directional solidification at ultra-high thermal gradient
[NASA-CR-159797] p0096 N80-15300
- NELSON, C. D.
Griffith diffusers p0006 A80-20748
- NELSON, D. P.
Experimental aerodynamic and acoustic model testing of the Variable Cycle Engine (VCE) testbed coannular exhaust nozzle system
[NASA-CR-159710] p0040 N80-26300
Experimental aerodynamic and acoustic model testing of the Variable Cycle Engine (VCE) testbed coannular exhaust nozzle system: Comprehensive data report
[NASA-CR-159711] p0040 N80-26301
- NELSON, E. E.
Stress corrosion cracking evaluation of martensitic precipitation hardening stainless steels
[NASA-TM-78257] p0083 N80-16142
- NEON, K.
Soot formation and burnout in flames p0043 N80-29320
- NEUMANN, H. E.
An analytical and experimental study of a short s-shaped subsonic diffuser of a supersonic inlet
[NASA-TM-81406] p0015 N80-15134
- NEUSTADTER, E. E.
The use of wind data with an operational wind turbine in a research and development environment
p0145 A80-35730
Preliminary analysis of performance and loads data from the 2-megawatt mod-1 wind turbine generator
[NASA-TM-81408] p0139 N80-16494
- NEWMAN, W. H.
Reduced bleed air extraction for DC-10 cabin air conditioning
[AIAA PAPER 80-1197] p0010 A80-41194
Engine bleed air reduction in DC-10
[NASA-CR-159846] p0010 N80-32378
- NICHOLAS, J. C.
Analysis and identification of subsynchronous vibration for a high pressure parallel flow centrifugal compressor p0125 N80-29710
- NICHOLS, L.
Low NO_x/ heavy fuel combustor program
[ASME PAPER 80-GT-69] p0026 A80-42199
Low NO(x) heavy fuel combustor program
[NASA-TM-79313] p0137 N80-13624
- NIMBRING, W. C.
Instrumentation technology p0013 N80-10214
- NIEDZWIECKI, R. W.
Low NO_x/ heavy fuel combustor program
[ASME PAPER 80-GT-69] p0026 A80-42199
Low NO(x) heavy fuel combustor program
[NASA-TM-79313] p0137 N80-13624
Literature survey of properties of synfuels derived from coal
[NASA-TM-79243] p0141 N80-22776
Combustion technology overview p0021 N80-29310
- NORED, D. L.
Preparing aircraft propulsion for a new era in energy and the environment p0024 A80-17737
Aircraft Energy Efficiency (ACEE) status report p0012 N80-10206
- NORGREN, W. H.
Airesearch QCGAT program
[NASA-CR-159758] p0037 N80-21331
- NORMENT, H. G.
Calculation of water drop trajectories to and about arbitrary three-dimensional bodies in potential airflow
[NASA-CR-3291] p0005 N80-28302
- NORRUP, L. V.
Advanced propulsion system for hybrid vehicles
[NASA-CR-159771] p0184 N80-26212
- NORTH, B. F.
Conceptual design of two-phase fluid mechanics and heat transfer facility for spacelab
[NASA-CR-159810] p0049 N80-27403
- NOBACK, C. J.
Determination of jet fuel thermal deposit rate using a modified JPTOT
- ONASHI, H.
Fluid forces on rotating centrifugal impeller with whirling motion p0127 N80-29724
- OLSEN, W.
Effect of temperature on surface noise p0107 A80-28419
- OLSON, B. A.
CATCOM catalyst 5 atm 1000 hour aging study using No. 2 fuel oil p0075 A80-35908
Durability testing at 5 atmospheres of advanced catalysts and catalyst supports for gas turbine engine combustors
[NASA-CR-159839] p0151 N80-24748
- OLSSON, W. J.
JT9D-7A /SP/ jet engine performance deterioration trends p0026 A80-44230
JT9D-7A (SP) jet engine performance deterioration trends
[NASA-TM-81459] p0016 N80-20274
- ONEILL, R. F.
Comparative thermal analysis of alternate Cryogenic Fluid Management Experiment (CFME) configurations
[NASA-CR-165151] p0048 N80-32412
- ORANGE, T. W.
Simple spline-function equations for fracture mechanics calculations p0133 A80-10832
A relation between semiempirical fracture analyses and R-curves
[NASA-TP-1600] p0132 N80-15428
- ORDIN, P. H.
Mechanical impact tests of materials in oxygen effects of contamination
[NASA-TP-1571] p0093 N80-21551
- OSGEBY, I. T.
CATCOM catalyst 5 atm 1000 hour aging study using No. 2 fuel oil p0075 A80-35908
Durability testing at 5 atmospheres of advanced catalysts and catalyst supports for gas turbine engine combustors
[NASA-CR-159839] p0151 N80-24748
- OTTENSON, D. A.
Sulfate and nitrate collected by filter sampling near the tropopause
[NASA-TP-1567] p0157 N80-14581
- PAAS, J. E.
CF6-60 engine short-term performance deterioration
[NASA-CR-159830] p0039 N80-23316
- PALMER, W. B.
Cogeneration Technology Alternatives Study (CTAS). Volume 3: Industrial processes
[NASA-CR-159767] p0155 N80-31870
- PAMPREU, R. C.
Baseline automotive gas turbine engine development program
[NASA-CR-159670] p0124 N80-24620
Conceptual design study of an improved automotive gas turbine powertrain
[NASA-CR-159672] p0124 N80-24621
Upgraded automotive gas turbine engine design and development program, volume 2
[NASA-CR-159671] p0128 N80-32719
- PAPELL, S. S.
Coolant tube curvature effects on film cooling as detected by infrared imagery
[ASME PAPER 79-WA/GT-7] p0107 A80-18638
Influence of coolant tube curvature on film cooling effectiveness as detected by infrared imagery
[NASA-TP-1546] p0013 N80-11087
- PARKER, R. E.
Conceptual design of an orbital propellant transfer experiment. Volume 2: Study results
[NASA-CR-165150] p0048 N80-31423
- PARKER, R. J.
Performance of computer-optimized tapered-roller bearings to 2.4 million DN

- [NASA-TM-81414] p0114 N80-16342
 Lubrication of rolling-element bearings
 [NASA-TM-81449] p0117 N80-20591
 Lubrication of optimized-design tapered-roller bearings to 2.4 million DN
 [NASA-TP-1714] p0119 N80-29734
- PARKS, D.**
 A three-dimensional spacecraft-charging computer code p0055 A80-46891
- PARKS, D. E.**
 Plasma collection by high voltage spacecraft at low earth orbit
 [AIAA PAPER 80-0042] p0055 A80-18249
- PARSZKUSKI, Z.**
 Parametric instabilities of rotor-support systems with application to industrial ventilators p0127 N80-29729
- PASS, J. E.**
 CF6-60 engine performance deterioration
 [NASA-CR-159786] p0041 N80-27364
- PATCH, R. W.**
 Parametric dependence of ion temperature and electron density in the SUMMA hot-ion plasma using laser light scattering and emission spectroscopy p0176 A80-46265
- PATT, R. P.**
 CF6 fan performance improvement
 [ASME PAPER 80-GT-178] p0026 A80-42284
- PAVLI, A. J.**
 Design and evaluation of high performance rocket engine injectors for use with hydrocarbon fuels p0059 A80-20957
 Design and evaluation of high performance rocket engine injectors for use with hydrocarbon fuels [NASA-TM-79319] p0056 N80-13163
 Design and evaluation of high performance rocket engine injectors for use with hydrocarbon fuels p0094 N80-31621
- PEACOCK, A. T.**
 Fuel/engine/airframe tradeoff study, phase 1 p0042 N80-29307
- PEEBLES, R. E.**
 Materials for advanced turbine engines. Volume 1: Power metallurgy Rene 95 rotating turbine engine parts [NASA-CR-159802] p0084 N80-28499
- PEENICK, M.**
 Packet communications in satellites with multiple-beam antennas and signal processing [AIAA 80-0537] p0099 A80-29574
- PENKO, P. P.**
 NASA-Lewis closed-cycle magnetohydrodynamics plant analysis [NASA-TM-79249] p0137 N80-10595
- PEPPER, S. V.**
 Effect of interfacial species on shear strength of metal-sapphire contacts p0178 A80-22300
 Comments on Auger electron production by He⁺⁺ bombardment of surfaces p0174 A80-34048
- PERDUE, D. G.**
 Engineering evaluation of a sodium hydroxide thermal energy storage module [NASA-TM-81417] p0140 N80-18563
- PERKINS, P. J.**
 Measurements of cabin and ambient ozone on B747 airplanes p0010 A80-28853
 Simultaneous cabin and ambient ozone measurements on two Boeing 747 airplanes, volume 1 [NASA-TM-79166] p0008 N80-15059
- PETERSON, C. A.**
 Parametric study of prospective early commercial MHD power plants (PSPEC). General Electric Company, task 1: Parametric analysis [NASA-CR-159634] p0152 N80-26779
- PETOT, D.**
 A phenomenological model of the dynamic stall of a helicopter blade profile [ONERA, TP NO. 1979-149] p0006 A80-20086
- PETRASH, D. A.**
 Preparing aircraft propulsion for a new era in energy and the environment p0024 A80-17737
 Emission reduction p0012 N80-10207
- PETRI, R. J.**
 High-temperature molten salt thermal energy storage systems [NASA-CR-159663] p0148 N80-17547
- PFOOTS, W. R.**
 Materials for advanced turbine engines. Volume 1: Power metallurgy Rene 95 rotating turbine engine parts [NASA-CR-159802] p0084 N80-28499
- PHILLIPP, W. W.**
 Method of cross-linking polyvinyl alcohol and other water soluble resins [NASA-CASE-LEW-13103-1] p0088 N80-32516
- PHIPPS, C. M.**
 Development of exothermically cast single-crystal Mar-M 247 and derivative alloys [AIRESEARCH-21-3469] p0084 A80-45825
- PICHA, G. J.**
 Tissue response to peritoneal implants [NASA-CR-159817] p0066 N80-33478
- PIERCE, W. S.**
 Fracture toughness of brittle materials determined with chevron notch specimens [NASA-TM-81607] p0079 N80-32486
- PINE, V. W.**
 Negative streamer development in FEP teflon p0179 A80-19776
- PINEL, S. I.**
 Performance of computer-optimized tapered-roller bearings to 2.4 million DN [NASA-TM-81414] p0114 N80-16342
 Operating characteristics of high-speed, jet-lubricated 35-millimeter-bore ball bearing with a single-outer-land-guided cage [NASA-TP-1657] p0117 N80-21753
 Lubrication of optimized-design tapered-roller bearings to 2.4 million DN [NASA-TP-1714] p0119 N80-29734
 Effect of cage design on characteristics of high-speed-jet-lubricated 35-millimeter-bore ball bearing [NASA-TP-1732] p0120 N80-33749
- PIPES, W. E.**
 DOD low-thrust mission studies p0063 N80-31455
- PIRVICS, J.**
 Load support system analysis high speed input pinion configuration [ASME PAPER 79-LUB-34] p0129 A80-14760
 High speed cylindrical rolling element bearing analysis 'CYBEAN' - Analytic formulation [ASME PAPER 79-LUB-35] p0129 A80-14761
- PITZALIS, G., JR.**
 Solid-state X-band combiner study [NASA-CR-162432] p0103 N80-11328
- PLENCHER, R. M.**
 Preliminary study of advanced turboprop and turboshaft engines for light aircraft [NASA-TM-81467] p0018 N80-22350
- PLUMBEE, H. E., JR.**
 A study of the transmission characteristics of suppressor nozzles [NASA-CR-165133] p0172 N80-32186
- PLUMBEE, H. E.**
 Studies of the acoustic transmission characteristics of coaxial nozzles with inverted velocity profiles, volume 1 [NASA-CR-159698] p0172 N80-11870
- PLUMBEE, H. E., JR.**
 Characteristics of internal- and jet-noise radiation from a multi-lobe, multi-tube suppressor nozzle tested statically and under flight simulation [AIAA PAPER 80-1027] p0173 A80-38642
- PONSCHER, R. L.**
 Primary electric propulsion technology study [NASA-CR-159688] p0061 N80-13158
- POLLACK, F. G.**
 Temperature and pressure measurement techniques for an advanced turbine test facility p0112 A80-36157
 Temperature and pressure measurement techniques for an advanced turbine test facility [NASA-TM-79278] p0110 N80-14374
 Computerized video densitometry method for rapid analysis of infrared photographic images [NASA-TP-1686] p0110 N80-25635
- POOLOS, R. P.**
 Critical mass flux through short Borda type inlets

- of various cross sections p0106 A80-10031
- FOULIN, E.**
A 15kWe (nominal) solar thermal electric power conversion concept definition study: Steam Rankine reheat reciprocator system [NASA-CR-159590] p0148 N80-16491
- FOVINELLI, L.**
Influence of pressure driven secondary flows on the behavior of turbofan forced mixers [AIAA PAPER 80-1198] p0025 A80-41515
Influence of pressure driven secondary flows on the behavior of turbofan forced mixers [NASA-TN-81541] p0105 N80-27632
- FOVINELLI, L. A.**
Computation of three-dimensional flow in turbofan mixers and comparison with experimental data [AIAA PAPER 80-0227] p0003 A80-20967
High-performance-vehicle technology p0013 N80-10219
- An analytical and experimental study of a short s-shaped subsonic diffuser of a supersonic inlet [NASA-TN-81406] p0015 N80-15134
Computation of three-dimensional flow in turbofan mixers and comparison with experimental data [NASA-TN-81410] p0104 N80-15364
- FOWELL, J. A.**
Efficient laser anemometer for intra-rotor flow mapping in turbomachinery p0111 A80-36140
Laser anemometer measurements in a transonic axial flow compressor rotor p0111 A80-36141
Laser anemometer measurements in a transonic axial flow compressor rotor [NASA-TN-79323] p0002 N80-14050
Efficient laser anemometer for intra-rotor flow mapping in turbomachinery [NASA-TN-79320] p0112 N80-14375
- FOWERS, A. G.**
Supersonic propulsion technology p0013 N80-10216
- FOWERS, E. J.**
The effect of a weak vertical magnetic field on fluctuation-induced transport in a Bumpy-Torus plasma p0176 A80-25476
- FRADO, B.**
Soot formation and burnout in flames p0043 N80-29320
- FRATT, R. W.**
Comments on 'Experimental evidence for interhemispheric transport from airborne carbon monoxide measurements' p0159 A80-32520
- PRICE, H. G.**
Cooling of high pressure rocket thrust chambers with liquid oxygen [AIAA PAPER 80-1260] p0060 A80-38992
Cooling of high pressure rocket thrust chambers with liquid oxygen [NASA-TN-81503] p0057 N80-23365
- PRINN, R. J.**
Chemical propulsion technology p0058 N80-31453
- PRINSTEY, R. R.**
Cogeneration Technology Alternatives Study (CTAS). Volume 1: Summary report [NASA-CR-159765] p0151 N80-24797
Cogeneration Technology Alternatives Study (CTAS). Volume 2: Analytical approach [NASA-CR-159766] p0143 N80-28859
Cogeneration Technology Alternatives Study (CTAS). Volume 3: Industrial processes [NASA-CR-159767] p0155 N80-31870
Cogeneration Technology Alternatives Study (CTAS). Volume 4: Energy conversion systems [NASA-CR-159768] p0155 N80-33859
- PROK, G. M.**
Initial characterization of an Experimental Referee Broadened-Specification (ERBS) aviation turbine fuel [NASA-TN-81440] p0093 N80-18205
- PRZYBYLSKI, J. S.**
Thin film temperature sensor [NASA-CR-159782] p0112 N80-17425
- PULLIAM, T. H.**
An implicit finite-difference code for inviscid and viscous cascade flow
- [AIAA PAPER 80-1427] p0007 A80-44128
- PURVIS, C. E.**
NASCAP modelling computations on large optics spacecraft in geosynchronous substorm environments p0054 A80-32829
Effects of secondary yield parameter variation on predicted equilibrium potential of an object in a charging environment p0054 A80-44230
Active control of spacecraft charging p0055 A80-46890
Configuration effects on satellite charging response [NASA-TN-81397] p0053 N80-15200
Effects of secondary yield parameter variation on predicted equilibrium potential of an object in a charging environment [NASA-TN-79299] p0053 N80-16093
NASCAP modelling computations on large optics spacecraft in geosynchronous substorm environments [NASA-TN-81395] p0053 N80-18095
- PUTHOFF, E. L.**
Installation and checkout of the DOE/NASA Mod-1 2000-kW wind turbine generator [AIAA 80-0638] p0145 A80-28835
Installation and checkout of the DOE/NASA Mod-1 2000-kW wind turbine generator [NASA-TN-81444] p0140 N80-19614
- PUTHAN, A. A.**
Spray nozzle designs for agricultural aviation applications [NASA-CR-159702] p0108 N80-10460
- Q**
- QUENTENBERG, R. J.**
Advanced cooling techniques for high-pressure, hydrocarbon-fueled rocket engines [AIAA PAPER 80-1266] p0060 A80-38994
- R**
- RAFTOPOULOS, D. D.**
Dispersion of sound in a combustion duct by fuel droplets and soot particles p0170 A80-20953
Spectral structure of pressure measurements made in a combustion duct p0171 A80-35496
Spectral structure of pressure measurements made in a combustion duct [NASA-TN-81471] p0168 N80-22045
Pressure spectra and cross spectra at an area contraction in a ducted combustion system [NASA-TN-81477] p0168 N80-23097
- RABINS, R.**
Analytical prediction and experimental verification of TWT and depressed collector performance using multidimensional computer programs p0102 A80-13902
90- to 93-percent efficient collector for operation of a dual-mode traveling-wave tube in the linear region p0102 A80-13909
Multistage depressed collector with efficiency of 90 to 94 percent for operation of a dual-mode traveling wave tube in the linear region [NASA-TP-1670] p0101 N80-21669
- RANSBY, W. D.**
Inert gas ion thruster development [NASA-CR-159805] p0062 N80-27424
- RANSBY, J. P.**
Noise reduction p0012 N80-10208
- RAO, V. D. N.**
Feasibility study of silicon nitride regenerators [NASA-CR-159713] p0184 N80-25209
- RAQUET, C. A.**
Coordinated aircraft and ship surveys for determining impact of river inputs on great lakes waters. Remote sensing results [NASA-TP-1694] p0157 N80-27832
- BATAJCHAK, A. P.**
Description of photovoltaic village power systems in the United States and Africa p0146 A80-46796
A photovoltaic power system in the remote African village of Tangaye, Upper Volta [NASA-TN-79318] p0137 N80-12552

- RAVENHALL, R.
Quiet Clean Short-haul Experimental Engine (QCSEE)
under-the-wing engine composite fan blade design
report
[NASA-CR-135046] p0031 N80-15108
Program for impact testing of spar-shell fan
blades, test report
[NASA-CR-135393] p0037 N80-21328
- RAVINDRANATH, A.
Three dimensional mean flow and turbulence
characteristics of the near wake of a compressor
rotor blade
[NASA-CR-159518] p0005 N80-27288
- RAWLIN, V. K.
Sputtering in mercury ion thrusters
[AIAA PAPER 79-2061] p0058 A80-10384
Reduced power processor requirements for the 30-cm
diameter HG ion thruster
[AIAA PAPER 79-2081] p0059 A80-10392
- RAYMOND, H. G.
An advanced mixed user domestic satellite system
architecture
[AIAA 80-0494] p0099 A80-29544
- RAYWARD, A. E.
Advanced electric propulsion system concept for
electric vehicles
[NASA-CR-159651] p0183 N80-17916
Design study of toroidal traction CVT for electric
vehicles
[NASA-CR-159803] p0124 N80-25661
- REAN, L. E.
Diesel engine catalytic combustor system
[NASA-CASE-LEW-12995-1] p0118 N80-26659
- RECK, G. M.
The impact of fuels on aircraft technology through
the year 2000
[NASA-TM-81492] p0093 N80-23472
Advanced fuel system technology for utilizing
broadened property aircraft fuels
[NASA-TM-81538] p0094 N80-27510
Future aviation fuels overview
p0021 N80-29301
Future aviation fuels overview
p0021 N80-29301
- REED, K. E.
Liquid chromatographic characterization of PMR-15
resin and prepreg
p0089 A80-32086
- REHNSMYDER, D. C.
CF6 fan performance improvement
[ASME PAPER 80-GT-178] p0026 A80-42284
Reverse thrust performance of the QCSEE variable
pitch turbofan engine
[NASA-TM-81558] p0022 N80-31399
- RECHTZ, J. D., JR.
Cost-effective technology advancement directions
for electric propulsion transportation systems
in earth-orbital missions
[AIAA PAPER 79-2043] p0048 A80-20961
Cost-effective technology advancement directions
for electric propulsion transportation systems
in earth-orbital missions
[NASA-TM-79289] p0182 N80-11950
- REID, L.
Experimental study of low aspect ratio compressor
blading
[ASME PAPER 80-GT-6] p0025 A80-42147
Turbomachinery technology
p0012 N80-10212
Experimental study of low aspect ratio compressor
blading
[NASA-TM-79280] p0002 N80-11037
- REID, M. A.
Improvement and scale-up of the NASA Redox storage
system
p0146 A80-48370
- REIMER, R.
Preliminary results of fast neutron treatments in
carcinoma of the pancreas
[NASA-TM-81516] p0160 N80-24983
- REIMER, R.
The 18/30 GHz fixed communications system service
demand assessment. Volume 1: Executive summary
[NASA-CR-159546] p0099 N80-22547
The 18/30 GHz fixed communications system service
demand assessment. Volume 2: Main text
[NASA-CR-159547] p0099 N80-22548
The 30/20 GHz fixed communications systems service
demand assessment. Volume 3: Appendices
- [NASA-CR-159548] p0099 N80-22549
- REYNOLDS, T. W.
Literature survey of properties of synfuels
derived from coal
[NASA-TM-79243] p0141 N80-22776
- RHOADES, W. W.
Low speed test of the aft inlet designed for a
tandem fan V/STOL nacelle
[NASA-CR-159752] p0037 N80-18042
- RICH, E. J.
Comparison of inlet suppressor data with
approximate theory based on cutoff ratio
[AIAA PAPER 80-0100] p0170 A80-20964
Far-field radiation of APT turbofan noise
p0025 A80-39638
Noise reduction
p0012 N80-10208
Comparison of inlet suppressor data with
approximate theory based on cutoff ratio
[NASA-TM-81386] p0167 N80-15876
Experimental evaluation of a spinning-mode
acoustic-treatment design concept for aircraft
inlets
[NASA-TP-1613] p0016 N80-21323
Far-field radiation of aft turbofan noise
[NASA-TM-81506] p0166 N80-24129
- RICH, E. W.
Characterization and properties of controlled
nucleation thermochemical deposited /CNTD/
silicon carbide
p0089 A80-13063
Characterization and properties of controlled
nucleation thermochemical deposited (CNTD)
silicon carbide
[NASA-TM-79277] p0085 N80-13254
- RICHARDS, T. E.
Modified power law equations for vertical wind
profiles
p0159 A80-35719
Modified power law equations for vertical wind
profiles
[NASA-TM-79275] p0137 N80-13623
Preliminary analysis of performance and loads data
from the 2-megawatt mod-1 wind turbine generator
[NASA-TM-81408] p0139 N80-16494
- RICHARDSON, P. W.
Design, performance and life cycle cost
relationships for a 500kW space solar array
p0065 A80-48356
Solar array subsystems study
[NASA-CR-159857] p0151 N80-24742
- RICHMOND, D. W.
3500-hour durability testing of ceramic materials
for automotive gas turbine engines
[AIRESEARCH-31-3542] p0092 A80-35575
The 3500 hour durability testing of commercial
ceramic materials
[NASA-CR-159785] p0091 N80-31552
- RICHTER, G. P.
JT9D-7A /SP/ jet engine performance deterioration
trends
p0026 A80-44230
JT9D-7A (SP) jet engine performance deterioration
trends
[NASA-TM-81459] p0016 N80-20274
- RINGER, A.
Development of procedures for calculating
stiffness and damping of elastomers in
engineering applications, part 6
[NASA-CR-159838] p0134 N80-22733
Development of procedures for calculating
stiffness and damping of elastomers in
engineering applications, part 7
[NASA-CR-165138] p0128 N80-32718
- RIEGER, M. F.
Development of flexible rotor balancing criteria
[NASA-CR-159506] p0129 N80-32720
- RIPPEL, R. E.
Aerodynamic analysis of a supersonic cascade
vibrating in a complex mode
p0007 A80-45841
Experimental determination of unsteady blade
element aerodynamics in cascades. Volume 1:
Torsion mode cascade
[NASA-CR-159831] p0040 N80-25335
- RILEY, T.
Investigation into the effect of plasma
pretreatment on the adhesion of parylene to
various substrates

- Investigation into the effect of plasma pretreatment on the adhesion of parylene to various substrates
[NASA-TM-79224] p0066 A80-25900
- RISBERG, J. A.
Capillary acquisition devices for high-performance vehicles: Executive summary
[NASA-CR-159658] p0114 N80-13473
- ROBBINS, W. M.
Large wind turbines: A utility option for the generation of electricity
[NASA-TM-81502] p0062 N80-19185
- ROBBINS, E., JR.
Computerized video densitometry method for rapid analysis of infrared photographic images
[NASA-TP-1686] p0144 N80-32858
- ROBERTS, W.
Preliminary results of fast neutron treatments in carcinoma of the pancreas
[NASA-TM-81516] p0110 N80-25635
- ROBERTS, W. B.
Off-design correlation for losses due to part-span dampers on transonic rotors
[NASA-TP-1693] p0160 N80-24983
- ROBINSON, R. S.
Interaction of high voltage surfaces with the space plasma
[NASA-CR-159731] p0020 N80-28352
- Inert gas thrusters
[NASA-CR-159813] p0176 N80-14923
- Interaction of high voltage surfaces with the space plasma
[NASA-CR-165131] p0062 N80-24362
- ROCHE, J.
A three-dimensional spacecraft-charging computer code
[NASA-TP-1693] p0177 N80-32223
- ROCHE, J. C.
Photoelectron charge density and transport near differentially charged spacecraft
[NASA-TP-1693] p0055 A80-46891
- NASCAP modelling of environmental-charging-induced discharges in satellites
[NASA-TP-1693] p0053 A80-19773
- Initial comparison of SSPM ground test results and flight data to NASCAP simulations
[AIAA PAPER 80-0336] p0054 A80-19774
- RODAL, J. J. A.
Two-dimensional finite-element analyses of simulated rotor-fragment impacts against rings and beams compared with experiments
[NASA-CR-159645] p0054 A80-29751
- Instructions for the use of the CIVM-Jet 4C finite-strain computer code to calculate the transient structural responses of partial and/or complete arbitrarily-curved rings subjected to fragment impact
[NASA-CR-159873] p0038 N80-22323
- Finite-strain large-deflection elastic-viscoplastic finite-element transient response analysis of structures
[NASA-CR-159874] p0134 N80-27720
- RODRIGUEZ-ANTUNEZ, A.
Preliminary results of fast neutron treatments in carcinoma of the pancreas
[NASA-TM-81516] p0134 N80-29762
- ROELKE, R. J.
An experimental evaluation of the performance deficit of an aircraft engine starter turbine
[NASA-TM-81571] p0160 N80-24983
- ROGERS, D. A.
Parametric study of prospective early commercial MHD power plants (PSPEC). General Electric Company, task 1: Parametric analysis
[NASA-CR-159634] p0022 N80-31400
- ROGERS, J.
The 18/30 GHz fixed communications system service demand assessment. Volume 1: Executive summary
[NASA-CR-159546] p0152 N80-26779
- The 18/30 GHz fixed communications system service demand assessment. Volume 2: Main text
[NASA-CR-159547] p0099 N80-22548
- The 30/20 GHz fixed communications systems service demand assessment. Volume 3: Appendices
[NASA-CR-159548] p0099 N80-22549
- ROGERS, W. F.
Aerial applications dispersal systems control requirements study
- [NASA-CR-159781] p0158 N80-18586
- ROMATGI, P. E.
Preparation of cast aluminum alloy-mica particle composites
[NASA-CR-159781] p0071 A80-32632
- ROMM, D. A.
Constrained fatigue life optimization of a NASVYTIS multiroller traction drive
[NASA-TM-81425] p0122 A80-46407
- Evaluation of a high performance fixed-ratio traction drive
[NASA-TM-81425] p0122 A80-46410
- Simplified fatigue life analysis for traction drive contacts
[NASA-TM-81425] p0123 A80-46413
- Simplified fatigue life analysis for traction drive contacts
[NASA-TM-81425] p0115 N80-17469
- Evaluation of a high performance fixed-ratio traction drive
[NASA-TM-81425] p0115 N80-18404
- Constrained fatigue life optimization of a NASVYTIS multiroller traction drive
[NASA-TM-81447] p0116 N80-18407
- Parametric tests of a traction drive retrofitted to an automotive gas turbine
[NASA-TM-81457] p0117 N80-21754
- ROLLBUHLER, R. J.
Improved PFB operations - 400-hour turbine test results
[NASA-TM-81511] p0145 A80-39639
- Factors affecting cleanup of exhaust gases from a pressurized, fluidized-bed coal combustor
[NASA-TM-81439] p0105 N80-20532
- Improved PFB operations: 400-hour turbine test results
[NASA-TM-81511] p0079 N80-26426
- ROMAN, A. J.
Parametric study of prospective early commercial MHD power plants (PSPEC). General Electric Company, task 1: Parametric analysis
[NASA-CR-159634] p0152 N80-26779
- ROMAN, R. F.
Hydrogen hollow cathode ion source
[NASA-CR-159634] p0174 N80-33186
- ROSEN, C.
Airbreathing propulsion component technologies
[NASA-CR-159634] p0024 A80-37482
- ROSENBAUM, D.
Computer program for generating input for analysis of impingement-cooled, axial-flow turbine blade
[NASA-TP-1603] p0104 N80-15361
- ROSENBERG, D. E.
Theory of deposition of condensable impurities on surfaces immersed in combustion gases
[NASA-CR-159716] p0033 N80-15130
- Experimental studies of the formation/deposition of sodium sulfate in/from combustion gases
[NASA-CR-159753] p0033 N80-15131
- ROTH, J. R.
The effect of a weak vertical magnetic field on fluctuation-induced transport in a Bumpy-Torus plasma
[NASA-CR-159753] p0176 A80-25476
- ROTHROCK, M. D.
Experimental determination of unsteady blade element aerodynamics in cascades. Volume 1: Torsion mode cascade
[NASA-CR-159831] p0040 N80-25335
- ROWE, A. P.
The erosion/corrosion of small superalloy turbine rotors operating in the effluent of a PFB coal combustor
[NASA-CR-159831] p0080 A80-10043
- RUBIN, A. G.
A three-dimensional spacecraft-charging computer code
[NASA-TP-1693] p0055 A80-46891
- RUCKLE, D. L.
Development of improved-durability plasma sprayed ceramic coatings for gas turbine engines
[AIAA PAPER 80-1193] p0089 A80-38963
- Development of improved-durability plasma sprayed ceramic coatings for gas turbine engines
[NASA-TM-81512] p0018 N80-23313
- RUDDY, J. M.
Application of advanced on-board processing concepts to future satellite communications systems

- [NASA-CR-159682] p0098 N80-12260
RUGGLES, C. L.
 Quiet Clean Short-Haul Experimental Engine (QCSEE)
 Under-The-Wing (UTW) graphite/PFR cowl development
 [NASA-CR-135279] p0029 N80-14119
RUSKOWSKI, G.
 Economic analysis of the design and fabrication of
 a space qualified power system
 [NASA-TM-81418] p0056 N80-18098
RUSSELL, K. J.
 Solid-state X-band combiner study
 [NASA-CR-162432] p0103 N80-11328
RUSSELL, L. M.
 Streakline flow visualization study of a horseshoe
 vortex in a large-scale, two-dimensional turbine
 stator cascade
 [ASME PAPER 80-GT-4] p0004 A80-42145
 Streakline flow visualization study of a horseshoe
 vortex in a large-scale, two-dimensional turbine
 stator cascade
 [NASA-TM-79274] p0104 N80-11376
RYAN, L. E.
 Analyses of moisture in polymers and composites
 [NASA-CR-159745] p0091 N80-15264

S

- SAASEN, E. W.**
 Two-phase working fluids for the temperature range
 of 50 to 350 deg, phase 2
 [NASA-CR-159847] p0108 N80-23599
SABLA, P. E.
 Quiet Clean Short-haul Experimental Engine
 (QCSEE). Double-annular clean combustor
 technology development report
 [NASA-CR-159483] p0032 N80-15121
 Energy efficient engine
 [NASA-CR-159685] p0045 N80-33408
SAGERMAN, G. D.
 Cogeneration Technology Alternatives Study (CTAS).
 Volume 1: Summary
 [NASA-TM-81400] p0141 N80-19626
SAGERSEER, D. A.
 The NASA high-speed turboprop program
 [NASA-TM-81561] p0022 N80-31401
SALEH, C. T.
 Quiet Clean Short-haul Experimental Engine (QCSEE)
 under-the-wing engine composite fan blade design
 report
 [NASA-CR-135046] p0031 N80-15108
 Program for impact testing of spar-shell fan
 blades, test report
 [NASA-CR-135393] p0037 N80-21328
SALIK, J.
 An investigation into the role of adhesion in the
 erosion of ductile metals
 [ASLE PREPRINT 80-AM-3E-3] p0122 A80-43159
 Scanning-electron-microscope study of
 normal-impingement erosion of ductile metals
 [NASA-TP-1609] p0077 N80-16141
 An investigation into the role of adhesion in the
 erosion of ductile metals
 [NASA-TM-81458] p0078 N80-21489
SALIKUDDIN, M.
 Characteristics of internal- and jet-noise
 radiation from a multi-lobe, multi-tube
 suppressor nozzle tested statically and under
 flight simulation
 [AIAA PAPER 80-1027] p0173 A80-38642
 Studies of the acoustic transmission
 characteristics of coaxial nozzles with inverted
 velocity profiles, volume 1
 [NASA-CR-159698] p0172 N80-11870
 A study of the transmission characteristics of
 suppressor nozzles
 [NASA-CR-165133] p0172 N80-32186
SALLER, G. P.
 Expanded study of feasibility of measuring
 in-flight 747/JT9D loads, performance,
 clearance, and thermal data
 [NASA-CR-159717] p0036 N80-16063
 Performance deterioration based on existing
 (historical) data; JT9D jet engine diagnostics
 program
 [NASA-CR-135448] p0038 N80-22324
 Performance deterioration based on in-service
 engine data: JT9D jet engine diagnostics program
 [NASA-CR-159525] p0040 N80-25340

- SALTSMAN, J. F.**
 Strainrange partitioning life predictions of the
 long time Metal Properties Council creep-fatigue
 tests
 p0133 A80-27958
SALZMAN, J.
 Quantitative interpretation of Great Lakes remote
 sensing data
 p0157 A80-45005
SALZMAN, J. A.
 Coordinated aircraft and ship surveys for
 determining impact of river inputs on great
 lakes waters. Remote sensing results
 [NASA-TP-1694] p0157 N80-27832
SAMANICH, M. E.
 QCSEE UTM engine powered-lift acoustic performance
 [AIAA PAPER 80-1065] p0025 A80-38651
 QCSEE fan exhaust bulk absorber treatment evaluation
 [NASA-TM-81498] p0019 N80-23314
 QCSEE UTM engine powered-lift acoustic performance
 [NASA-TM-81504] p0019 N80-24315
 Reverse thrust performance of the QCSEE variable
 pitch turbofan engine
 [NASA-TM-81558] p0022 N80-31399
SANDERCOCK, D. F.
 Off-design correlation for losses due to part-span
 dampers on transonic rotors
 [NASA-TP-1693] p0020 N80-28352
SANDERS, B. W.
 Dynamic response of a Mach 2.5 axisymmetric inlet
 and turbojet engine with a poppet-valve
 controlled inlet stability bypass system when
 subjected to internal and external airflow
 transients
 [NASA-TP-1531] p0014 N80-14123
 Turbojet-exhaust-nozzle secondary-airflow pumping
 as an exit control of an inlet-stability bypass
 system for a Mach 2.5 axisymmetric
 mixed-compression inlet
 [NASA-TP-1532] p0014 N80-14124
SANDERS, G. S.
 Aerial applications dispersal systems control
 requirements study
 [NASA-CR-159781] p0158 N80-18586
SANTORO, G. J.
 Hot corrosion of four superalloys - HA-188, S-57,
 IN-617, and TD-NiCrAl
 p0081 A80-14445
 Corrosion resistance of sodium sulfate coated
 cobalt-chromium-aluminum alloys at 900 C, 1000
 C, and 1100 C
 [NASA-TM-79311] p0076 N80-14234
SARGENT, M. B.
 Preliminary results of steady state
 characterization of near term electric vehicle
 breadboard propulsion system
 [NASA-TM-81546] p0183 N80-28254
 A laboratory facility for electric vehicle
 propulsion system testing
 [NASA-TM-81574] p0183 N80-30229
SAULE, A. V.
 Far-field radiation of APT turbofan noise
 p0025 A80-39638
 Far-field radiation of aft turbofan noise
 [NASA-TM-81506] p0166 N80-24129
SAUNDERS, A. A.
 Fuel conservation through active control of rotor
 clearances
 [AIAA PAPER 80-1087] p0045 A80-41506
SAUNDERS, A. A., JR.
 Method and apparatus for rapid thrust increases in
 a turbofan engine
 [NASA-CASE-LEW-12971-1] p0016 N80-18039
SAUNDERS, M. T.
 Advanced component technologies for
 energy-efficient turbofan engines
 [AIAA PAPER 80-1086] p0025 A80-38902
 Aircraft Energy Efficiency (ACEE) status report
 p0012 N80-10206
 Advanced component technologies for
 energy-efficient turbofan engines
 [NASA-TM-81507] p0019 N80-24316
 The energy efficient engine project
 [NASA-TM-81566] p0023 N80-32395
SAVAGE, E.
 Kinematic correction for roller skewing
 [NASA-TM-81564] p0119 N80-28716
SAVINO, J. M.
 Some techniques for reducing the tower shadow of

- the DOE/NASA mod-0 wind turbine tower
[NASA-TM-79202] p0137 N80-10594
- SCHAEFER, J. W.
The energy efficient engine project
[NASA-TM-81566] p0023 N80-32395
- SCHNECHTER, B.
Plasma-sprayed dual density ceramic turbine seal
system
[NASA-CR-159739] p0123 N80-15411
- SCHNEER, D. D.
Analytical investigation of two hydrogen-oxygen
rocket engine systems for low-thrust application
p0060 A80-35503
Analytical investigation of two hydrogen oxygen
rocket engine systems for low-thrust application
[NASA-TM-81420] p0056 N80-17138
Analytical investigation of two hydrogen-oxygen
rocket engine systems for low-thrust application
p0057 N80-30382
- SCHNEIBLY, D. W.
Flexible formulated plastic separators for
alkaline batteries
[NASA-CASE-LEW-12363-4] p0140 N80-18555
- SCHMIDT, H. W.
Antimisting kerosene
p0021 N80-29319
- SCHNAUSS, E. R.
First results of material charging in the space
environment
p0055 A80-45609
- SCHMUELLER, G.
A three-dimensional spacecraft-charging computer
code
p0055 A80-46891
- SCHMUELLER, G. W.
Plasma collection by high voltage spacecraft at
low earth orbit
[AIAA PAPER 80-0042] p0055 A80-18249
Photoelectron charge density and transport near
differentially charged spacecraft
p0053 A80-19773
- SCHULLER, F. T.
Calculated and experimental data for a 118-mm bore
roller bearing to 3 million DM
[NASA-TM-81427] p0116 N80-19496
Operating characteristics of high-speed,
jet-lubricated 35-millimeter-bore ball bearing
with a single-outer-land-guided cage
[NASA-TP-1657] p0117 N80-21753
Effect of cage design on characteristics of
high-speed-jet-lubricated 35-millimeter-bore
ball bearing
[NASA-TP-1732] p0120 N80-33749
- SCHULTZ, D. F.
Flame tube parametric studies for control of fuel
bound nitrogen using rich-lean two-stage
combustion
[NASA-TM-81472] p0141 N80-21837
- SCHUON, S.
Effect of W and WC on the oxidation resistance of
yttria-doped silicon nitride
p0090 A80-46099
Effect of starting powder characteristics on
density, microstructure and low temperature
oxidation behavior of a Si₃N₄ - 8 w/o Y₂O₃ ceramic
p0090 A80-46100
Effect of W and WC on the oxidation resistance of
yttria-doped silicon nitride
[NASA-TM-81529] p0087 N80-27483
Effect of starting powder characteristics on
density, microstructure and low temperature
oxidation behavior of a Si₃N₄8w/o Y₂O₃ ceramic
[NASA-TM-81536] p0088 N80-27484
- SCHWAB, J. R.
Performance of 22.4-kW nonlaminated-frame dc
series motor with chopper controller
[NASA-TM-79252] p0101 N80-13361
- SCHWAB, R. C.
Program to develop sprayed, plastically deformable
compressor shroud seal materials
[NASA-CR-159741] p0123 N80-16338
- SCHWARTZ, H. J.
Impact of propulsion system R and D on electric
vehicle performance and cost
[NASA-TM-81548] p0143 N80-27805
- SCHWARTZ, P. C.
Bi-directional four quadrant (BDQ4) power
converter development
[NASA-CR-159660] p0147 N80-14480
- SCHWEN, E. E.
Development of exothermically cast single-crystal
Mar-M 247 and derivative alloys
[AIRESEARCH-21-3469] p0084 A80-45825
- SEASHOLTZ, E. G.
Efficient laser anemometer for intra-rotor flow
mapping in turbomachinery
p0111 A80-36140
Efficient laser anemometer for intra-rotor flow
mapping in turbomachinery
[NASA-TM-79320] p0112 N80-14375
- SEIBERT, K.
Investigation into the effect of plasma
pretreatment on the adhesion of parylene to
various substrates
p0066 A80-25900
Investigation into the effect of plasma
pretreatment on the adhesion of parylene to
various substrates
[NASA-TM-79224] p0114 N80-13473
- SEIDEL, B. S.
Inlet flow distortion in turbomachinery. I -
Comparison of theory and experiment in a
transonic fan stage. II - A parameter study
[AIAA PAPER 80-1076] p0006 A80-38895
- SEIKEL, G. E.
Survey of MHD plant applications
p0144 A80-11972
Engineering test facility design definition
[NASA-TM-81499] p0143 N80-27799
Rapporteur report: MHD electric power plants
[NASA-TM-81554] p0144 N80-29862
- SELDNER, K.
A new traffic control design method for large
networks with signalized intersections
p0183 A80-14841
- SELLEN, J. M., JR.
Evaluation of particle transport for the P80-1
spacecraft
[AIAA PAPER 79-2047] p0055 A80-13301
Specific spacecraft evaluation: Special report
[NASA-CR-159420] p0060 N80-11137
- SELLERS, J. F.
Vertical Takeoff and Landing (VTOL) propulsion
technology
p0013 N80-10218
- SELTER, H. E.
The 30/20 GHz fixed communications systems service
demand assessment. Volume 1: Executive summary
[NASA-CR-159619] p0098 N80-18262
The 30/20 GHz fixed communications systems service
demand assessment. Volume 2: Main report
[NASA-CR-159620] p0098 N80-18263
The 30/20 GHz fixed communications systems service
demand assessment. Volume 3: Annex
[NASA-CR-159621] p0099 N80-18264
- SENG, G. T.
Initial characterization of an Experimental
Referee Broadened-Specification (ERBS) aviation
turbine fuel
[NASA-TM-81440] p0093 N80-18205
Fuels characterization studies
p0021 N80-29309
- SENGERS, J. V.
Application of the principle of similarity fluid
mechanics
p0107 A80-10039
Toward the use of similarity theory in two-phase
choked flows
[NASA-TM-81568] p0106 N80-29623
- SERAFINI, T. T.
High char inside-modified epoxy matrix resins
p0071 A80-34789
Low temperature cross linking polyimides
[NASA-CASE-LEW-12876-1] p0087 N80-26447
- SHALTENS, R. E.
Blade design and operating experience on the
MOD-OA 200 kW wind turbine at Clayton, New Mexico
p0139 N80-16470
- SHAMBLIN, C. E.
Materials for advanced turbine engines. Volume 1:
Power metallurgy Rene 95 rotating turbine engine
parts
[NASA-CR-159802] p0084 N80-28499
- SHANNON, J. L., JR.
Fracture toughness determination of Al₂O₃ using
four-point-bend specimens with straight-through
and chevron notches
p0090 A80-42085

- Performance of Chevron-notch short bar specimen in determining the fracture toughness of silicon nitride and aluminum oxide p0090 A80-50696
- Fracture toughness of brittle materials determined with chevron notch specimens [NASA-TM-81607] p0079 N80-32486
- SHANNON, L.
Thermal energy storage systems using fluidized bed heat exchangers [NASA-CR-159868] p0153 N80-28866
- SHAUFEL, M.
Nonanalytic function generation routines for 16-bit microprocessors [NASA-TM-81586] p0163 N80-33104
- SHAW, D. T.
Experimental and theoretical investigation for the suppression of the planar arc drop in the thermionic converter [NASA-CR-159611] p0176 N80-12880
- SHAW, M.
Distribution analysis for F100(3) engine [NASA-CR-159754] p0036 N80-17073
- SHAW, M. J.
Reaction bonded silicon nitride prepared from wet attrition-milled silicon p0089 A80-32828
- Formation of porous surface layers in reaction bonded silicon nitride during processing p0090 A80-51574
- Reaction bonded silicon nitride prepared from wet attrition-milled silicon [NASA-TM-81428] p0086 N80-18181
- Formation of porous surface layers in reaction bonded silicon nitride during processing [NASA-TM-81493] p0087 N80-23456
- SHEFFLER, K. D.
Long-time creep behavior of the tantalum alloy Astar 811C [NASA-TP-1691] p0080 N80-32489
- SHIBLEY, D. W.
Method of cross-linking polyvinyl alcohol and other water soluble resins [NASA-CASE-LEW-13103-1] p0088 N80-32516
- SHEW, S. F.
Non-synchronous whirling due to fluid-dynamic forces in axial turbo-machinery rotors p0126 N80-29721
- SHORAN, Y.
A calculation procedure for viscous flow in turbomachines, volume 3 [NASA-CR-159864] p0005 N80-26274
- SHREBBOB, L. T.
Some considerations of the performance of two honeycomb gas path seal material systems [NASA-TM-81398] p0077 N80-16143
- Development of improved high pressure turbine outer gas path seal components [NASA-CR-159801] p0038 N80-21332
- SHIFFS, P. E.
The performance and efficiency of four motor/controller/battery systems for the simpler electric vehicles [NASA-CR-159776] p0103 N80-24550
- SHOJI, H.
Fluid forces on rotating centrifugal impeller with whirling motion p0127 N80-29724
- SHOJI, J. M.
LEO-to-GEO low thrust chemical propulsion p0063 N80-30384
- Low-thrust chemical propulsion p0063 N80-31468
- SHOOK, D. F.
Quantitative interpretation of Great Lakes remote sensing data p0157 A80-45005
- Coordinated aircraft and ship surveys for determining impact of river inputs on great lakes waters. Remote sensing results [NASA-TP-1694] p0157 N80-27832
- SIDEN, L. E.
Conceptual design of an orbital propellant transfer experiment. Volume 2: Study results [NASA-CR-165150] p0048 N80-31423
- SIDIK, S. M.
Effect of sodium, potassium, magnesium, calcium, and chlorine on the high temperature corrosion of IN-100, U-700, IN-792, and MAR M-509 [ASME PAPER 80-GT-150] p0083 A80-42262
- Cycles till failure of silver-zinc cells with competing failure modes - Preliminary data analysis p0146 A80-46414
- Effect of sodium, potassium, magnesium, calcium, and chlorine on the high temperature corrosion of IN-100, U-700, IN-792, and MAR M-509 [NASA-TM-79309] p0076 N80-15235
- Cycles till failure of silver-zinc cells with competing failure modes: Preliminary data analysis [NASA-TM-81556] p0164 N80-29088
- SIEVENS, G. E.
Summary of NASA QCGAT program p0017 N80-22334
- SIGHER, M. E.
Performance of computer-optimized tapered-roller bearings to 2.4 million DM [NASA-TM-81414] p0114 N80-16342
- Operating characteristics of high-speed, jet-lubricated 35-millimeter-bore ball bearing with a single-outer-land-guided cage [NASA-TP-1657] p0117 N80-21753
- Effect of cage design on characteristics of high-speed-jet-lubricated 35-millimeter-bore ball bearing [NASA-TP-1732] p0120 N80-33749
- SIGNORIELLI, B. A.
Materials and structures technology p0012 N80-10210
- SIN, G. C.
Sudden stretching of a four layered composite plate [NASA-CR-159870] p0073 N80-25383
- Sudden bending of cracked laminates [NASA-CR-159860] p0073 N80-25384
- SILVA, T. H.
Nuclear electric propulsion system utilization for earth orbit transfer of large spacecraft structures [AIAA PAPER 80-1223] p0060 A80-38975
- Orbital transfer of large space structures with nuclear electric rockets [AAS PAPER 80-083] p0054 A80-41897
- SIMON, P. F.
Spectral effects on direct-insolation absorptance of five collector coatings [ASME PAPER 79-HT-18] p0146 A80-45722
- SIMONEAU, R. J.
Toward the use of similarity theory in two-phase choked flows [NASA-TM-81568] p0106 N80-29623
- SIMPSON, W.
Aerial applications dispersal systems control requirements study [NASA-CR-159781] p0158 N80-18586
- SINCLAIR, J. H.
Mechanical property characterization of intraply hybrid composites p0070 A80-20954
- Dynamic response of damaged angleplied fiber composites p0070 A80-27982
- Micromechanics of intraply hybrid composites: Elastic and thermal properties p0070 A80-27994
- Fracture modes of high modulus graphite/epoxy angleplied laminates subjected to off-axis tensile loads p0071 A80-32069
- Micromechanics of intraply hybrid composites: Elastic and thermal properties [NASA-TM-79253] p0067 N80-11143
- Tensile and flexural strength of non-graphitic superhybrid composites: Predictions and comparisons [NASA-TM-79276] p0067 N80-11144
- Dynamic response of damaged angleplied fiber composites [NASA-TM-79281] p0067 N80-11145
- Mechanical property characterization of intraply hybrid composites [NASA-TM-79306] p0067 N80-12120
- Fracture modes of high modulus graphite/epoxy angleplied laminates subjected to off-axis tensile loads [NASA-TM-81405] p0068 N80-16102
- SINGER, I. D.
Results from tests on a high work transonic

- turbine for an energy efficient engine
[ASME PAPER 80-GT-146] p0026 A80-42258
- SIPPENLY, W. E.
Screen printing technology applied to silicon
solar cell fabrication
[NASA-CR-159789] p0153 N80-27808
Coplanar back contacts for thin silicon solar cells
[NASA-CR-159811] p0153 N80-28860
- SIROCKY, P. J., JR.
Design, fabrication, and test of a steel spar wind
turbine blade
p0139 N80-16472
- SIVO, J. M.
NASA's program in communication satellites
[AAS 79-247] p0097 A80-28712
- SIX, L. D.
Concept definition study of small Brayton cycle
engines for dispersed solar electric power systems
[NASA-CR-159592] p0150 N80-22778
- SKIPSTAD, J. G.
Atomization of broad specification aircraft fuels
p0043 N80-29318
- SLADY, J. G.
Overview of a stirling engine test project
[NASA-TM-81442] p0140 N80-18564
- SLINBY, E. E.
Friction and wear of plasma-sprayed coatings
containing cobalt alloys from 25 deg to 650 deg
in air
[ASLE PREPRINT 80-AM-6C-2] p0122 A80-43176
Friction and wear of plasma-sprayed coatings
containing cobalt alloys from 25 deg to 650 deg
in air
[NASA-TM-79316] p0085 N80-14249
Method of making bearing material
[NASA-CASE-LEW-11930-3] p0070 N80-33482
- SMALLEY, A. J.
The effects of strain and temperature on the
dynamic properties of elastomers
[ASME PAPER 79-DET-57] p0092 A80-15720
Design of elastomer dampers for a high-speed
flexible rotor
[ASME PAPER 79-DET-88] p0121 A80-15736
Dynamic properties of elastomer cartridge
specimens under a rotating load
p0121 A80-24002
Use of elastomeric elements in control of rotor
instability
p0128 N80-29732
- SMEGGIL, J. G.
Study of the effects of gaseous environments on
the hot corrosion of superalloy materials
[NASA-CR-159747] p0083 N80-18155
- SMIALSK, J.
Some TEM observations of Al₂O₃ scales formed on
NiCrAl alloys
p0081 A80-13071
- SMITH, A. L.
Analytical and experimental evaluations of the
effect of broad property fuels on combustors for
commercial aircraft gas turbine engines
[AIAA PAPER 80-1204] p0094 A80-41516
Analytical and experimental evaluations of the
effect of broad property fuels on combustors for
commercial aircraft gas turbine engines
[NASA-TM-81496] p0093 N80-25454
- SMITH, G. T.
Engine environmental effects on composite behavior
[AIAA 80-0695] p0024 A80-35101
Application of composite materials to turbofan
engine fan exit guide vanes
[NASA-TM-81432] p0068 N80-18106
Engine environmental effects on composite behavior
[NASA-TM-81508] p0069 N80-23370
- SMITH, J. J.
CF6-6D engine short-term performance deterioration
[NASA-CR-159830] p0039 N80-23316
CF6-6D engine performance deterioration
[NASA-CR-159786] p0041 N80-27364
- SMITH, J. M.
Results of duct area ratio changes in the NASA
Lewis H2-O2 combustion MHD experiment
[AIAA PAPER 80-0023] p0176 A80-18243
Experiments on H2-O2 MHD power generation
p0176 A80-44239
Results of duct area ratio changes in the NASA
Lewis H2-O2 combustion MHD experiment
[NASA-TM-79308] p0175 N80-12881
- Effect of velocity overshoot on the performance of
magnetohydrodynamic subsonic diffusers
[NASA-TM-79305] p0175 N80-14922
Experiments on H2-O2 MHD power generation
[NASA-TM-81424] p0175 N80-16886
- SMITH, U.
Auxiliary control of LSS
p0063 N80-31459
- SMITH, W. U.
Electric propulsion for near-Earth space missions
[NASA-CR-159735] p0062 N80-16096
- SMITHWICK, J. J.
Effect of positive pulse charge waveforms on cycle
life of nickel-zinc cells
p0146 A80-48329
An electric vehicle propulsion system's impact on
battery performance: An overview
[NASA-TM-81515] p0143 N80-24756
Pulse charging of lead-acid traction
cells
[NASA-TM-81513] p0143 N80-25780
- SMOLAK, G. E.
Low-thrust vehicle concept studies
p0058 N80-31457
- SNYDER, A.
Parametric dependence of ion temperature and
electron density in the SUMMA hot-ion plasma
using laser light scattering and emission
spectroscopy
p0176 A80-46265
- SNYDER, C. E., JR.
Boundary lubrication, thermal and oxidative
stability of a fluorinated polyether and a
perfluoropolyether triazine
[ASLE PREPRINT 79-AM-1B-1] p0088 A80-12089
- SNYDER, M. H.
Feasibility study of aileron and spoiler control
systems for large horizontal axis wind turbines
[NASA-CR-159856] p0153 N80-27803
- SOCKOL, P. M.
Computational fluid mechanics of internal flow
p0012 N80-10211
- SOMMER, J. F.
Nonanalytic function generation routines for
16-bit microprocessors
[NASA-TM-81586] p0163 N80-33104
- SOKOLOWSKI, D. E.
Performance of annular prediffuser-combustor systems
[ASME PAPER 80-GT-15] p0026 A80-42154
- SOLAND, R. E.
Statistical aspects of carbon fiber risk
assessment modeling
[NASA-CR-159318] p0073 N80-29432
- SOLOMON, M. G.
Advanced ceramic material for high temperature
turbine tip seals
[NASA-CR-159774] p0038 N80-22325
- SOLTIS, D. G.
Flexible formulated plastic separators for
alkaline batteries
[NASA-CASE-LEW-12363-4] p0140 N80-18555
- SOVEY, J. S.
Modification of the electrical and optical
properties of polymers
[NASA-CASE-LEW-13027-1] p0087 N80-24437
Hydrogen hollow cathode ion source
[NASA-CASE-LEW-12940-1] p0174 N80-33186
- SONERS, M. D.
Quiet, Clean, Short-Haul, Experimental Engine
(QCSEE) Under-The-Wing (UTW) engine acoustic
design
[NASA-CR-135267] p0028 N80-14117
Quiet, Clean, Short-Haul Experimental Engine
(QCSEE) Over-The-Wing (OTW) engine acoustic design
[NASA-CR-135268] p0028 N80-14118
Quiet Clean Short-haul Experimental Engine
(QCSEE). Core engine noise measurements
[NASA-CR-135160] p0035 N80-15093
- SPADACCINI, L. J.
Autoignition characteristics of aircraft-type fuels
[NASA-CR-159886] p0095 N80-30535
- SPALVINS, T.
Survey of ion plating sources
p0120 A80-10040
Tribological properties of sputtered MoS₂ films in
relation to film morphology
p0089 A80-35502
Tribological properties of sputtered
MoS sub 2
films in relation to film morphology
[NASA-TM-81465] p0078 N80-21490

- SPERA, D. A.**
Modified power law equations for vertical wind profiles p0159 A80-35719
Modified power law equations for vertical wind profiles [NASA-TN-79275] p0137 M80-13623
Design evolution of large wind turbine generators p0139 M80-16455
Structural analysis considerations for wind turbine blades p0139 M80-16469
Preliminary analysis of performance and loads data from the 2-megawatt mod-1 wind turbine generator [NASA-TN-81408] p0139 M80-16494
- SPETEN, K. M.**
The 30/20 GHz fixed communications systems service demand assessment. Volume 1: Executive summary [NASA-CR-159619] p0098 M80-18262
The 30/20 GHz fixed communications systems service demand assessment. Volume 2: Main report [NASA-CR-159620] p0098 M80-18263
The 30/20 GHz fixed communications systems service demand assessment. Volume 3: Annex [NASA-CR-159621] p0099 M80-18264
- SPISZ, E. W.**
Assessment of satellite and aircraft multispectral scanner data for strip-mine monitoring [NASA-TN-79268] p0136 M80-20787
- SPREITER, J. E.**
Evaluation of a strained-coordinate perturbation procedure - Nonlinear subsonic and transonic flows [AIAA PAPER 80-0339] p0006 A80-18324
- SPRINGMAN, H.**
The optimization air separation plants for combined cycle MHD-power plant applications [NASA-TN-81510] p0142 M80-23778
- SPOCKLER, C. M.**
Combustion of solid carbon rods in zero and normal gravity p0074 A80-20955
Combustion of solid carbon rods in zero and normal gravity [NASA-TN-79303] p0104 M80-13404
- SPOELOCK, O. F.**
LSS/propulsion interactions studies p0058 M80-31454
- SPURLIN, J. E.**
Compliance and stress intensity coefficients for short bar specimens with chevron notches p0133 A80-46032
- SRINIVASAN, A. V.**
Influence of mistuning on blade torsional flutter [NASA-CR-165137] p0005 M80-31351
- STABE, E. G.**
Description of the warm core turbine facility recently installed at NASA Lewis Research Center [NASA-TN-81562] p0022 M80-29333
- STACLIANO, T. E.**
Two-dimensional finite-element analyses of simulated rotor-fragment impacts against rings and beams compared with experiments [NASA-CR-159645] p0038 M80-22323
Instructions for the use of the CIVM-Jet 4C finite-strain computer code to calculate the transient structural responses of partial and/or complete arbitrarily-curved rings subjected to fragment impact [NASA-CR-159873] p0134 M80-27720
- STANARA, S. S.**
Evaluation of a strained-coordinate perturbation procedure - Nonlinear subsonic and transonic flows [AIAA PAPER 80-0339] p0006 A80-18324
- STALGNER, P. J.**
Summary and evaluation of the parametric study of potential early commercial MHD power plants (PSPEC) [NASA-TN-81497] p0142 M80-23780
- STANIEK, G.**
Stability of several oxide dispersion strengthened alloys and a directionally solidified gamma/gamma prime-alpha eutectic alloy in a thermal gradient p0082 A80-40962
- STANITZ, J. D.**
General design method for three-dimensional potential flow fields. 1: Theory [NASA-CR-3288] p0005 M80-29251
- STANNIENICK, B.**
Analytical prediction and experimental verification of TWT and depressed collector performance using multidimensional computer programs p0102 A80-13902
A matrix solution for the simulation of magnetic fields with ideal current loops p0102 A80-13903
Two-dimensional representations of axisymmetric fields for computer calculations p0102 A80-18232
NASA communications technology research and development p0097 A80-25920
- STASKUS, J.**
First results of material charging in the space environment p0055 A80-45609
- STASKUS, J. V.**
Initial comparison of SSPM ground test results and flight data to NASCAP simulations [AIAA PAPER 80-0336] p0054 A80-29751
- STARRIS, C. A.**
The chemistry of sodium chloride involvement in processes related to hot corrosion p0074 A80-10041
Combustion of solid carbon rods in zero and normal gravity p0074 A80-20955
Combustion of solid carbon rods in zero and normal gravity [NASA-TN-79303] p0104 M80-13404
Chemical processes involved in the initiation of hot corrosion of B-1900 and NASA-TN VIA [NASA-TN-81399] p0077 M80-17199
- STECORA, S.**
Thermal barrier coatings for aircraft gas turbines [AIAA PAPER 80-0302] p0089 A80-18303
Effects of yttrium, aluminum and chromium concentrations in bond coatings on the performance of zirconia-yttria thermal barriers p0082 A80-35900
Effects of yttrium, aluminum and chromium concentrations in bond coatings on the performance of zirconia-yttria thermal barriers [NASA-TN-81485] p0079 M80-22464
Performance of two-layer thermal barrier systems on directionally solidified Ni-Al-Mo and comparative effects of alloy thermal expansion on system life [NASA-TN-81604] p0080 M80-32487
- STEELY, S. L.**
Monodisperse atomizers for agricultural aviation applications [NASA-CR-159777] p0108 M80-19450
- STEEN, P.**
A three-dimensional spacecraft-charging computer code p0055 A80-46891
- STEIN, P. G.**
Plasma collection by high voltage spacecraft at low earth orbit [AIAA PAPER 80-0042] p0055 A80-18249
- STEGER, J. L.**
An implicit finite-difference code for inviscid and viscous cascade flow [AIAA PAPER 80-1427] p0007 A80-44128
- STELSON, T. S.**
Cost analysis of composite fan blade manufacturing processes [NASA-CR-159876] p0044 M80-31398
- STEPHENS, J. E.**
Anodic polarization behavior of austenitic stainless steel alloys with lower chromium content p0178 A80-22250
Strengthening of tough iron-12% nickel-reactive metal alloys at 77 K by copper additions p0174 A80-34049
Mechanical properties and oxidation and corrosion resistance of reduced-chromium 304 stainless steel alloys [NASA-TP-1557] p0076 M80-11188
High toughness-high strength iron alloy [NASA-CASE-LEW-12542-3] p0079 M80-32484
Creep-rupture behavior of seven iron-base alloys after long term aging at 760 deg in low pressure hydrogen [NASA-TN-81534] p0080 M80-32488

- STEPHA, P. S.**
Uncertainties in predicting turbine blade metal temperatures
[ASME PAPER 80-HT-25] p0027 A80-48014
Turbomachinery technology p0012 M80-10212
Analysis of uncertainties in turbine metal temperature predictions
[NASA-TP-1593] p0017 M80-21326
Composite wall concept for high temperature turbine shrouds: Heat transfer analysis
[NASA-TM-81539] p0020 M80-27362
- STETSON, A. B.**
Thick ceramic coating development for industrial gas turbines - A program plan
[SR79-M-4702-05] p0091 A80-10042
Advanced ceramic material for high temperature turbine tip seals
[NASA-CR-159774] p0038 M80-22325
- STEVENS, G.**
System analysis for millimeter-wave communication satellites p0100 A80-52479
- STEVENS, M. J.**
MASCAP modelling of environmental-charging-induced discharges in satellites p0054 A80-19774
Computed voltage distribution around Solar Electric Propulsion spacecraft
[AIAA PAPER 79-2104] p0054 A80-29750
Initial comparison of SSPM ground test results and flight data to MASCAP simulations
[AIAA PAPER 80-0336] p0054 A80-29751
MASCAP modelling computations on large optics spacecraft in geosynchronous substorm environments p0054 A80-32829
First results of material charging in the space environment p0055 A80-45609
Space environmental interactions with biased spacecraft surfaces p0055 A80-46897
Computed voltage distributions around solar electric propulsion spacecraft
[NASA-TM-79286] p0053 M80-16094
MASCAP modelling computations on large optics spacecraft in geosynchronous substorm environments
[NASA-TM-81395] p0053 M80-18095
Modelling of environmentally induced discharges in geosynchronous satellites
[NASA-TM-81598] p0053 M80-32428
- STEWART, W. L.**
Preparing aircraft propulsion for a new era in energy and the environment p0024 A80-17737
Supercharged topping rocket propellant feed system
[NASA-CASE-XLE-02062-1] p0056 M80-14188
- STIMPENT, D. L.**
Quiet Clean Short-Haul Experimental Engine (QCSEE) acoustic and aerodynamic tests on a scale model over-the-wing thrust reverser and forward thrust nozzle
[NASA-CR-135254] p0028 M80-14115
Demonstration of short-haul aircraft aft noise reduction techniques on a twenty inch (50.8 cm) diameter fan, volume 1
[NASA-CR-134849] p0033 M80-15083
Demonstration of short-haul aircraft aft noise reduction techniques on a twenty inch (50.8 cm) diameter fan, volume 2
[NASA-CR-134850] p0034 M80-15084
Demonstration of short haul aircraft aft noise reduction techniques on a twenty inch (50.8 cm) diameter fan, volume 3
[NASA-CR-134851] p0034 M80-15085
Acoustic analysis of aft noise reduction techniques measured on a subsonic tip speed 50.8 cm (twenty inch) diameter fan
[NASA-CR-134891] p0030 M80-15102
Quiet Clean Short-haul Experimental Engine (QCSEE) Over-The-Wing (OTW) propulsion systems test report. Volume 4: Acoustic performance
[NASA-CR-135326] p0032 M80-15118
Quiet Clean Short-haul Experimental Engine (QCSEE) Under-The-Wing (UTW) composite nacelle test report. Volume 2: Acoustic performance
[NASA-CR-159472] p0044 M80-29297
Acoustic performance of a 50.8-cm (20-inch) diameter variable-pitch fan and inlet. Volume 2: Acoustic data
[NASA-CR-135118] p0044 M80-29299
- STITT, L. B.**
Supersonic propulsion technology p0013 M80-10216
- STOCHEL, M. J.**
Potential performance improvement using a reacting gas (nitrogen tetroxide) as the working fluid in a closed Brayton cycle
[NASA-TM-79322] p0139 M80-16490
- STOCKENBER, F. J.**
Temperature and flow measurements on near-freezing aviation fuels in a wing-tank model
[ASME PAPER 80-GT-63] p0094 A80-42193
Temperature and flow measurements on near-freezing aviation fuels in a wing-tank model
[NASA-TM-79285] p0093 M80-13268
Low temperature fuel behavior studies p0044 M80-29330
- STOCKMAN, M. O.**
An efficient user-oriented method for calculating compressible flow in an about three-dimensional inlets
[NASA-CR-159578] p0004 A80-10134
Optimum subsonic, high-angle-of-attack nacelles
[NASA-TM-81491] p0016 M80-20275
- STONE, J. B.**
Prediction of unsuppressed jet engine exhaust noise in flight from static data
[AIAA PAPER 80-1008] p0027 A80-44491
Noise reduction p0012 M80-10208
An improved prediction method for the noise generated in flight by circular jets
[NASA-TM-81470] p0168 M80-22048
Prediction of unsuppressed jet engine exhaust noise in flight from static data
[NASA-TM-81537] p0169 M80-29132
- STOTLER, C. L., JR.**
Quiet Clean Short-haul Experimental Engine (QCSEE). Composite fan frame subsystem test report
[NASA-CR-135010] p0035 M80-15098
Quiet Clean Short-haul Experimental Engine (QCSEE) Under-The-Wing (UTW) composite nacelle subsystem test report
[NASA-CR-135075] p0034 M80-15100
Quiet Clean Short-haul Experimental Engine (QCSEE) Under-The-Wing (UTW) composite nacelle subsystem test report
[NASA-CR-135075] p0034 M80-15100
- STRACK, W. C.**
New opportunities for future, small, General-Aviation Turbine Engines (GATE) p0017 M80-22335
- STRANAHAN, T. E.**
Development of exothermically cast single-crystal Mar-M 247 and derivative alloys
[AIRESARCH-21-3469] p0084 A80-45825
- STRATISMAN, A. J.**
Efficient laser anemometer for intra-rotor flow mapping in turbomachinery p0111 A80-36140
Laser anemometer measurements in a transonic axial flow compressor rotor p0111 A80-36141
Comparison between optical measurements and a numerical solution of the flow field within a transonic axial-flow compressor rotor
[AIAA PAPER 80-1078] p0003 A80-38897
Laser anemometer measurements in a transonic axial flow compressor rotor
[NASA-TM-79323] p0002 M80-14050
Efficient laser anemometer for intra-rotor flow mapping in turbomachinery
[NASA-TM-79320] p0112 M80-14375
- STREMPER, G. C.**
Fabrication and evaluation of low fiber content alumina fiber/aluminum composites
[NASA-CR-159517] p0073 M80-29430
- STROCK, O. J.**
DOE/NASA wind turbine data acquisition. Part 1: Equipment
[NASA-CR-159779] p0148 M80-17543
- SULLIVAN, T. L.**
Design, fabrication, and test of a steel spar wind turbine blade p0139 M80-16472

- SUMNER, I. E.**
Development of improved-durability plasma sprayed ceramic coatings for gas turbine engines [AIAA PAPER 80-1193] p0089 A80-38963
Development of improved-durability plasma sprayed ceramic coatings for gas turbine engines [NASA-TM-81512] p0018 N80-23313
- SUNDBERG, D. V.**
Abradable compressor and turbine seals, volume 1 [NASA-CR-159600] p0083 N80-14235
- SVENILA, B. A.**
Quantitative interpretation of Great Lakes remote sensing data p0157 A80-45005
Coordinated aircraft and ship surveys for determining impact of river inputs on great lakes waters. Remote sensing results [NASA-TP-1694] p0157 N80-27832
- SWAIN, J. C.**
Design study of steel V-Belt CVT for electric vehicles [NASA-CR-159845] p0185 N80-32299
- SWARTZ, C. E.**
Origin of reverse annealing in radiation-damaged silicon solar cells p0059 A80-33850
Radiation damage in high voltage silicon solar cells p0179 A80-44234
Radiation damage in lithium-counterdoped n/p silicon solar cells [NASA-TM-81391] p0138 N80-15557
Radiation damage annealing mechanisms and possible low temperature annealing in silicon solar cells [NASA-TM-81392] p0138 N80-15558
Radiation damage in high voltage silicon solar cells [NASA-TM-81478] p0178 N80-23180
Radiation damage in high voltage silicon solar cells p0144 N80-33889
- SYMONS, E. P.**
LeRC reduced gravity fluid management technology program p0048 A80-35504
Capillary device refilling [AIAA PAPER 80-1095] p0060 A80-38908
LeRC reduced gravity fluid management technology program [NASA-TM-81450] p0051 N80-20304
LeRC reduced gravity fluid management technology program p0057 N80-30383
- SZANCA, E. M.**
Design and cold-air test of single-stage uncooled turbine with high work output [NASA-TP-1680] p0019 N80-25337
- SZENASZ, F. E.**
Field verification of lateral-torsional coupling effects on rotor instabilities in centrifugal compressors p0125 N80-29708
- SENTELA, E. J.**
External fuel vaporization study, phase 1 [NASA-CR-159850] p0095 N80-25453
- SZUCH, J. E.**
Control technology p0013 N80-10215
- T**
- TADAKOFF, W.**
A calculation procedure for viscous flow in turbomachines, volume 2 [NASA-CR-159636] p0004 N80-17995
A calculation procedure for viscous flow in turbomachines, volume 3 [NASA-CR-159864] p0005 N80-26274
- TAN-ATICHAT, J.**
Effects of axisymmetric contractions on turbulence of various scales [NASA-CR-165136] p0006 N80-32328
- TANRIKUT, S.**
Performance of annular prediffuser-combustor systems [ASME PAPER 80-GT-15] p0026 A80-42154
- TAYLOR, W. F.**
Effect of refining variables on the properties and composition of JP-5 p0041 N80-29306
- TECZA, J. A.**
Design of elastomer dampers for a high-speed flexible rotor [ASME PAPER 79-DGT-88] p0121 A80-15736
- TERBO, W.**
The 18/30 GHz fixed communications system service demand assessment. Volume 1: Executive summary [NASA-CR-159546] p0099 N80-22547
The 18/30 GHz fixed communications system service demand assessment. Volume 2: Main text [NASA-CR-159547] p0099 N80-22548
The 30/20 GHz fixed communications system service demand assessment. Volume 3: Appendices [NASA-CR-159548] p0099 N80-22549
- TERRY, J.**
Optical sensors for aeronautics and space [NASA-TM-81407] p0110 N80-17423
- TERVILLIGER, C. H.**
Cost-effective technology advancement directions for electric propulsion transportation systems in earth-orbital missions [NASA-TM-79289] p0182 N80-11950
Electric propulsion for near-Earth space missions [NASA-CR-159735] p0062 N80-16096
- TERVILLIGER, C. H., JR.**
Cost-effective technology advancement directions for electric propulsion transportation systems in earth-orbital missions [AIAA PAPER 79-2043] p0048 A80-20961
- THEVELDE, J. A.**
Autoignition characteristics of aircraft-type fuels [NASA-CR-159886] p0095 N80-30535
- THALLER, L. H.**
Improvement and scale-up of the NASA Redox storage system p0146 A80-48370
Redox storage systems for solar applications [NASA-TM-81464] p0142 N80-23777
- THOMAS, H. J.**
Self-excited rotor whirl due to tip-seal leakage forces p0127 N80-29723
- THOMAS, R. L.**
Large wind turbines: A utility option for the generation of electricity [NASA-TM-81502] p0144 N80-32858
- THOMPSON, E. L.**
Marangoni bubble motion in zero gravity p0107 A80-20958
Marangoni bubble motion in zero gravity [NASA-TM-79250] p0104 N80-13403
- THOMPSON, W. E.**
Vibration exciting mechanisms induced by flow in turbomachine stages p0127 N80-29722
- THORNHILL, J. W.**
Development of improved wraparound contacts for silicon [NASA-CR-159748] p0148 N80-18554
Screen printing technology applied to silicon solar cell fabrication [NASA-CR-159789] p0153 N80-27808
Coplanar back contacts for thin silicon solar cells [NASA-CR-159811] p0153 N80-28860
- TIERPNERMAN, E. W.**
NASA Global Atmospheric Sampling Program (GASP) data report for tapes VL0011 and VL0013 [NASA-TM-81462] p0157 N80-21892
- TIEN, J. S.**
Gas phase oxidation downstream of a catalytic combustor [NASA-TM-81551] p0144 N80-29863
- TISON, E. E.**
High-temperature molten salt thermal energy storage systems [NASA-CR-159663] p0148 N80-17547
- TITMAN, E. H.**
Long-time creep behavior of the tantalum alloy Astar 811C [NASA-TP-1691] p0080 N80-32489
Long-time creep behavior of the niobium alloy C-103 [NASA-TP-1727] p0080 N80-33555
- TJOA, B.**
Performance, emissions, and physical characteristics of a rotating combustion aircraft engine, supplement A [NASA-CR-135119] p0041 N80-27361
- TOLLE, P. P.**
High-freezing-point fuel studies p0043 N80-29329
- TOHAZIC, W. A.**
Supporting research and technology for automotive

Stirling engine development
[NASA-TM-81495] p0183 N80-21200

TOPPING, R. F.
Study of research and development requirements of
small gas-turbine combustors
[NASA-CR-159796] p0036 N80-18040

TOWNE, C. E.
Numerical simulation of supersonic inlets using a
three-dimensional viscous flow analysis
[AIAA PAPER 80-0384] p0003 A80-20969
Numerical simulation of supersonic inlets using a
three-dimensional viscous flow analysis
[NASA-TM-81411] p0104 N80-15365

TOUNSHEND, D. E.
NASA gear research and its probable effect on
rotorcraft transmission design p0120 A80-13068
Endurance and failure characteristics of modified
Vasco X-2, CBS 600 and AISI 9310 spur gears
p0123 A80-46411
Analytical and experimental spur gear tooth
temperature as affected by operating variables
p0123 A80-46412
Analytical and experimental spur gear tooth
temperature as affected by operating variables
[NASA-TM-81419] p0115 N80-18403
Endurance and failure characteristics of modified
Vasco X-2, CBS 600 and AISI 9310 spur gears
[NASA-TM-81421] p0116 N80-18405

TRAN, C. T.
A phenomenological model of the dynamic stall of a
helicopter blade profile
[ONERA, TP NO. 1979-149] p0006 A80-20086

TRIEZENBERG, D. M.
Simulation studies of multiple large wind turbine
generators on a utility network p0139 N80-16480

TRUMP, G.
An electric propulsion long term test facility
[AIAA PAPER 79-2080] p0049 A80-13308

TURCO, R. F.
Preliminary results of fast neutron treatments in
carcinoma of the pancreas
[NASA-TM-81516] p0160 N80-24983

TURNER, R. H.
High temperature thermal energy storage in steel
and sand
[NASA-CR-159708] p0154 N80-29860

TURNER, G. E.
Preliminary study of VTO thrust requirements for a
V/STOL aircraft with lift plus lift/cruise
propulsion
[NASA-TM-81429] p0016 N80-19110

V

VALGORA, M. E.
Power management for multi-100 Kwe space systems
p0060 A80-46357

VALLER, M. W.
Performance of a transpiration-regenerative cooled
rocket thrust chamber
[NASA-CR-159742] p0061 N80-14189

VANCE, J. H.
Experimental results concerning centrifugal
impeller excitations p0127 N80-29727

VANCO, M.
An experimental investigation of endwall profiling
in a turbine vane cascade
[AIAA PAPER 80-1089] p0004 A80-38904

VANCO, M. E.
Results from tests on a high work transonic
turbine for an energy efficient engine
[ASME PAPER 80-GT-146] p0026 A80-42258

VANNUCCI, R. D.
High char imide-modified epoxy matrix resins
p0071 A80-34789
Properties of PHE Polyimide composites made with
improved high strength graphite fibers
[NASA-TM-81557] p0069 N80-25444

VARGAS, L. M.
Prediction of fragment velocities and trajectories
p0096 N80-16210

VARY, A.
A review of issues and strategies in
nondestructive evaluation of fiber reinforced
structural composites p0071 A80-34764

Quantitative ultrasonic evaluation of engineering
properties in metals, composites, and ceramics
p0130 A80-39641

Simulation of transducer-couplant effects on
broadband ultrasonic signals p0112 A80-44233

Concepts and techniques for ultrasonic evaluation
of material mechanical properties p0130 A80-51575

Simulation of transducer-couplant effects on
broadband ultrasonic signals
[NASA-TM-81489] p0130 N80-22714

Concepts and techniques for ultrasonic evaluation
of material mechanical properties
[NASA-TM-81523] p0130 N80-24634

Quantitative ultrasonic evaluation of engineering
properties in metals, composites and ceramics
[NASA-TM-81530] p0130 N80-26682

VASILIOS, T.
Improving the stress rupture and creep of silicon
nitride
[NASA-CR-159585] p0072 N80-10318

VAUGHAN, R. W.
Analyses of moisture in polymers and composites
[NASA-CR-159745] p0091 N80-15264

VESTRICH, M.
Analysis of combustion instability in liquid fuel
rocket motors
[NASA-CR-159733] p0061 N80-13164
Amplification of Reynolds number dependent
processes by wave distortion
[NASA-CR-159732] p0075 N80-13193

VETROME, R.
An electric propulsion long term test facility
[AIAA PAPER 79-2080] p0049 A80-13308

VIELE, M. E.
Reduced bleed air extraction for DC-10 cabin air
conditioning
[AIAA PAPER 80-1197] p0010 A80-41194
Engine bleed air reduction in DC-10
[NASA-CR-159846] p0010 N80-32378

VITENNA, L. A.
Design, fabrication, and test of a steel spar wind
turbine blade p0139 N80-16472
Preliminary analysis of performance and loads data
from the 2-megawatt mod-1 wind turbine generator
[NASA-TM-81408] p0139 N80-16494

VOGAN, J. W.
Thick ceramic coating development for industrial
gas turbines - A program plan
[SR79-M-4702-05] p0091 A80-10042
Advanced ceramic material for high temperature
turbine tip seals
[NASA-CR-159774] p0038 N80-22325

VON GLAHN, U.
Assessment at full scale of exhaust nozzle-to-wing
size on STOL-OTW acoustic characteristics
p0170 A80-20952
Acoustic considerations of flight effects on jet
noise suppressor nozzles
[AIAA PAPER 80-0164] p0171 A80-20965
Noise suppression due to annulus shaping of a
conventional coaxial nozzle p0171 A80-35497
Noise suppression due to annulus shaping of an
inverted-velocity-profile coaxial nozzle p0171 A80-35498

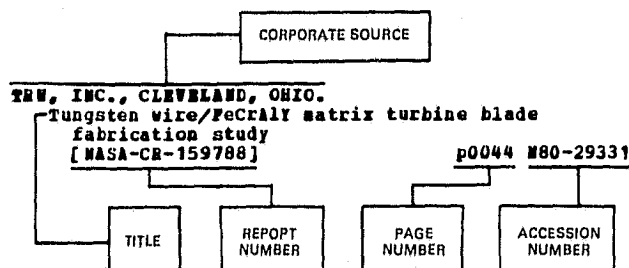
VONGLAHN, U.
Assessment at full scale of exhaust nozzle to wing
size on STOL-OTW acoustic characteristics
[NASA-TM-79279] p0167 N80-13281
Acoustic considerations of flight effects on jet
noise suppressor nozzles
[NASA-TM-81377] p0167 N80-14843
Noise suppression due to annulus shaping of an
inverted-velocity-profile coaxial nozzle
[NASA-TM-81460] p0168 N80-22046
Noise suppression due to annulus shaping of
conventional coaxial nozzle
[NASA-TM-81461] p0166 N80-22047

VRANOS, A.
Experimental study of turbine fuel thermal
stability in an aircraft fuel system simulator
p0043 N80-29325

- relationships for a 500kW space solar array
p0065 A80-40356
- WHITE, W. F., JR.
Buckling of rotating beams
p0133 A80-20149
- WHITLOW, J. B., JR.
Supersonic propulsion technology
p0013 N80-10216
- WHITNEY, W. J.
Design and cold-air test of single-stage uncooled turbine with high work output
[NASA-TP-1680] p0019 N80-25337
Cold-air investigation of a 4 1/2 stage turbine with stage-loading factor of 4.66 and high specific work output. 2: Stage group performance
[NASA-TP-1688] p0019 N80-25338
Description of the warm core turbine facility recently installed at NASA Lewis Research Center
[NASA-TN-81562] p0022 N80-29333
- WHITTEMBERGER, J. D.
Elevated temperature flow strength, creep resistance and diffusion welding characteristics of Ti-6Al-2Nb-1Ta-0.8Mo
p0081 A80-13277
Stability of several oxide dispersion strengthened alloys and a directionally solidified gamma/gamma prime-alpha eutectic alloy in a thermal gradient
p0082 A80-40962
- WILBUR, P. J.
Physical phenomena in mercury ion thrusters
[NASA-CR-159784] p0061 N80-17137
Baffle aperture design study of hollow cathode equipped ion thrusters
[NASA-CR-165164] p0064 N80-33476
- WILCOX, J. P.
Design study of steel V-Belt CVT for electric vehicles
[NASA-CR-159845] p0185 N80-32299
- WILLIAMS, J. C.
Modification of axial compressor streamline program for analysis of engine test data
[NASA-TN-79312] p0002 N80-14051
- WILLIAMS, R. L.
8-cm Engineering Model Thruster technology - A review of recent developments
[AIAA PAPER 79-2103] p0064 A80-13311
- WILLIAMS, W.
Dynamic modulus and damping of boron, silicon carbide, and alumina fibers
p0071 A80-44236
Dynamic modulus and damping of boron, silicon carbide, and alumina fibers
[NASA-TN-81422] p0068 N80-20313
- WILLIAMSON, W. S.
8-cm Engineering Model Thruster technology - A review of recent developments
[AIAA PAPER 79-2103] p0064 A80-13311
- WILLIS, W. S.
Quiet Clean Short-haul Experimental Engine (QCSEE)
[NASA-CR-159473] p0032 N80-15120
- WILSON, C. A.
Avco Lycoming quiet clean general aviation turbofan engine
p0039 N80-22333
- WILSON, B. P., JR.
Study of research and development requirements of small gas-turbine combustors
[NASA-CR-159796] p0036 N80-18040
- WINGENBACK, W.
A 15 kWe (nominal) solar thermal-electric power conversion concept definition study: Steam Rankine reciprocator system
[NASA-CR-159591] p0149 N80-19612
- WINTUCKY, R. G.
Homogeneous alignment of nematic liquid crystals by ion beam etched surfaces
p0178 A80-26007
Homogeneous alignment of nematic liquid crystals by ion beam etched surfaces
[NASA-TN-81378] p0096 N80-16232
- WISANDER, D. W.
Composite wall concept for high temperature turbine shrouds: Survey of low modulus strain isolator materials
[NASA-TN-81443] p0086 N80-20398
Preliminary study of methods for providing thermal shock resistance to plasma-sprayed ceramic gas-path seals
- [NASA-TP-1561] p0087 N80-23453
- WITTEK, R. A.
Two-dimensional finite-element analyses of simulated rotor-fragment impacts against rings and beams compared with experiments
[NASA-CR-159645] p0038 N80-22323
Instructions for the use of the CIVM-Jet 4C finite-strain computer code to calculate the transient structural responses of partial and/or complete arbitrarily-curved rings subjected to fragment impact
[NASA-CR-159873] p0134 N80-27720
Finite-strain large-deflection elastic-viscoplastic finite-element transient response analysis of structures
[NASA-CR-159874] p0134 N80-22762
- WITTEK, L. J.
Subsynchronous instability of a geared centrifugal compressor of overhung design
p0125 N80-29711
- WITTEK, W. E.
Strengthening of tough iron-12% nickel-reactive metal alloys at 77 K by copper additions
p0174 A80-34049
High toughness-high strength iron alloy
[NASA-CASE-LEW-12542-3] p0079 N80-32484
Creep-rupture behavior of seven iron-base alloys after long term aging at 760 deg in low pressure hydrogen
[NASA-TN-81534] p0080 N80-32488
- WOLF, R. A.
Installation and checkout of the DOE/NASA Mod-1 2000-kW wind turbine generator
[AIAA 80-0638] p0145 A80-28835
- WOLF, S. W. D.
Selected data from a transonic flexible walled test section
[NASA-CR-159360] p0047 N80-32404
- WOLFSBRANDT, G.
Flame tube parametric studies for control of fuel bound nitrogen using rich-lean two-stage combustion
[NASA-TN-81472] p0141 N80-21837
- WONG, K. W.
Analysis of combustion instability in liquid fuel rocket motors
[NASA-CR-159733] p0061 N80-13164
- WOODWARD, R. P.
Effect of inflow control on inlet noise of a cut-on fan
[AIAA PAPER 80-1049] p0171 A80-35993
Effect of inflow control on inlet noise of a cut-on fan
[NASA-TN-81487] p0169 N80-23098
Forward acoustic performance of a shock-swallowing high-tip-speed fan (QF-13)
[NASA-TP-1668] p0169 N80-23100
- WOOLLAN, J. A.
Critical currents in A-15 structure Nb3Al converted from cold-worked bcc structure
p0179 A80-33853
Apparatus for trapping and thermal detection of atomic hydrogen in high magnetic fields at low temperatures
p0111 A80-34546
Atomic hydrogen storage
[NASA-CASE-LEW-12081-2] p0093 N80-20402
- WOOLLETT, R. E.
Zero-length, slotted-lip inlet for subsonic military aircraft
[AIAA PAPER 80-1245] p0004 A80-41203
- WONSTELL, J. E.
Mechanisms of nitrogen heterocycle influence on turbine fuel stability
p0043 N80-29327
- WRIGHT, D. L.
30/20 GHz wideband technology verification program
p0097 A80-25917
- WUENSCHE, B. J.
Improving the stress rupture and creep of silicon nitride
[NASA-CR-159585] p0072 N80-10318
- WULF, R. H.
CF6-6D engine short-term performance deterioration
[NASA-CR-159830] p0039 N80-23316
CF6-6D engine performance deterioration
[NASA-CR-159786] p0041 N80-27364

CORPORATE SOURCE INDEX

Typical Corporate Source Index Listing



The title of the document is used to provide a brief description of the subject matter. The page number and NASA or AIAA accession number are included in each entry to assist the user in locating the abstract in the abstract section. If applicable, a report number is also included as an aid in identifying the document.

A

ACUREX CORP., MOUNTAIN VIEW, CALIF.
 Synthesis of improved polyester resins
 [NASA-CR-159665] p0090 N80-13257
 Phase-locked telemetry system for rotary
 instrumentation of turbomachinery, phase 1
 [NASA-CR-159453] p0029 N80-14182

AEROJET LIQUID ROCKET CO., SACRAMENTO, CALIF.
 Performance of a transpiration-regenerative
 cooled rocket thrust chamber
 [NASA-CR-159742] p0061 N80-14189
 Low-thrust chemical rocket engine study
 p0063 N80-31467

AEROSPACE CORP., EL SEGUNDO, CALIF.
 Nuclear electric propulsion system utilization
 for earth orbit transfer of large spacecraft
 structures
 [AIAA PAPER 80-1223] p0060 A80-38975
 Orbital transfer of large space structures with
 nuclear electric rockets
 [AAS PAPER 80-083] p0054 A80-41897
 First results of material charging in the space
 environment
 p0055 A80-45609

AEROSPACE CORP., LOS ANGELES, CALIF.
 Initial comparison of SSPM ground test results
 and flight data to NASCAP simulations
 [AIAA PAPER 80-0336] p0054 A80-29751

AEROTHERM ACUREX CORP., MOUNTAIN VIEW, CALIF.
 Synthesis of improved phenolic resins
 [NASA-CR-159724] p0091 N80-17221

**AIR FORCE AERO PROPULSION LAB., WRIGHT-PATTERSON
 AFB, OHIO.**
 Military jet fuel from shale oil
 p0042 N80-29308
 Fuel character effects on the J79 and F101
 engine combustion systems
 p0042 N80-29312
 Air Force fuel mainburner/turbine effects programs
 p0042 N80-29314
 Status of nickel-hydrogen cell technology
 p0064 N80-33474

AIR FORCE GEOPHYSICS LAB., HANSCOM AFB, MASS.
 A three-dimensional spacecraft-charging computer
 code
 p0055 A80-46891

AIR FORCE MATERIALS LAB., WRIGHT-PATTERSON AFB, OHIO.
 Boundary lubrication, thermal and oxidative
 stability of a fluorinated polyether and a
 perfluoropolyether triazine
 [ASLE PREPRINT 79-AM-1B-1] p0088 A80-12089

Characterization and properties of controlled
 nucleation thermochemical deposited /CMTD/
 silicon carbide
 p0089 A80-13063

First results of material charging in the space
 environment
 p0055 A80-45609

**AIR FORCE WRIGHT AERONAUTICAL LABS.,
 WRIGHT-PATTERSON AFB, OHIO.**
 Three dimensional finite-element elastic
 analysis of a thermally cycled double-edge
 wedge geometry specimen
 [NASA-TN-80980] p0079 N80-26433

AIRESEARCH MFG. CO., PHOENIX, ARIZ.
 3500-hour durability testing of ceramic
 materials for automotive gas turbine engines
 [AIRESEARCH-31-3542] p0092 A80-35575
 Development of exothermically cast
 single-crystal Mar-M 247 and derivative alloys
 [AIRESEARCH-21-3469] p0084 A80-45825
 Abradable compressor and turbine seals, volume 1
 [NASA-CR-159600] p0083 N80-14235

Airesearch QCGAT program
 [NASA-CR-159758] p0037 N80-21331
 Concept definition study of small Brayton cycle
 engines for dispersed solar electric power
 systems
 [NASA-CR-159592] p0150 N80-22778
 The 3500 hour durability testing of commercial
 ceramic materials
 [NASA-CR-159785] p0091 N80-31552

AIRESEARCH MFG. CO., TORRANCE, CALIF.
 Design study of toroidal traction CVT for
 electric vehicles
 [NASA-CR-159803] p0124 N80-25661
 Advanced propulsion system for hybrid vehicles
 [NASA-CR-159771] p0184 N80-26212

ALLIS-CHALMERS MFG. CO., MILWAUKEE, WIS.
 Subsynchronous instability of a geared
 centrifugal compressor of overhung design
 p0125 N80-29711

APPLIED MEDICAL TECHNOLOGY, CLEVELAND HEIGHTS, OHIO.
 Tissue response to peritoneal implants
 [NASA-CR-159817] p0066 N80-33478

**ARMY AVIATION RESEARCH AND DEVELOPMENT COMMAND,
 CLEVELAND, OHIO.**
 Constrained fatigue life optimization of a
 NASVITIS multiroller traction drive
 p0122 A80-46407
 Effect of geometry and operating conditions on
 spur gear system power loss
 p0122 A80-46409
 Evaluation of a high performance fixed-ratio
 traction drive
 p0122 A80-46410
 Computer program for generating input for
 analysis of impingement-cooled, axial-flow
 turbine blade
 [NASA-TP-1603] p0104 N80-15361
 Some considerations of the performance of two
 honeycomb gas path seal material systems
 [NASA-TN-81398] p0077 N80-16143
 Spur-gear-system efficiency at part and full load
 [NASA-TP-1622] p0115 N80-17466
 Simplified fatigue life analysis for traction
 drive contacts
 [NASA-TN-79199] p0115 N80-17469
 Composite wall concept for high temperature
 turbine shrouds: Survey of low modulus strain
 isolator materials
 [NASA-TN-81443] p0086 N80-20398
 Parametric tests of a traction drive retrofitted
 to an automotive gas turbine
 [NASA-TN-81457] p0117 N80-21754

Loss model for off-design performance analysis of radial turbines with pivoting-vane, variable-area stator
[NASA-TN-81532] p0020 N80-27365
ARMY AVIATION RESEARCH AND DEVELOPMENT COMMAND, ST. LOUIS, MO.

Experimental performance and analysis of 15.04-centimeter-tip-diameter, radial-inflow turbine with work factor of 1.126 and thick blading
[NASA-TP-1730] p0023 N80-33410
ARMY PROPULSION LAB., CLEVELAND, OHIO.

Wear of seal materials used in aircraft propulsion systems
p0121 N80-28010

Simplified fatigue life analysis for traction drive contacts
p0123 N80-46413

ARMY STRUCTURES LAB., HAMPTON, VA.
Buckling of rotating beams
p0133 N80-20149

ATMOSPHERIC SCIENCE ASSOCIATES, BEDFORD, MASS.
Calculation of water drop trajectories to and about arbitrary three-dimensional bodies in potential airflow
[NASA-CR-3291] p0005 N80-28302

AVCO CORP., LOWELL, MASS.
Fiber release characteristics of graphite hybrid composites
p0073 N80-32063

AVCO CORP., WILMINGTON, MASS.
Parametric study of potential early commercial MHD power plants
[NASA-CR-159633] p0149 N80-18559

AVCO LYCOMING DIV., STRATFORD, CONN.
Avco Lycoming quiet clean general aviation turbofan engine
p0039 N80-22333

AVCO LYCOMING DIV., WILLIAMSPORT, PA.
Exhaust emission reduction for intermittent combustion aircraft engines
[NASA-CR-159757] p0029 N80-14130

AVCO SYSTEMS DIV., WILMINGTON, MASS.
Improving the stress rupture and creep of silicon nitride
[NASA-CR-159585] p0072 N80-10318

B

BANARAS HINDU UNIV., VARANASI (INDIA).
Preparation of cast aluminum alloy-mica particle composites
p0071 N80-32632

BATTELLE COLUMBUS LABS., OHIO.
Spray nozzle designs for agricultural aviation applications
[NASA-CR-159702] p0108 N80-10460
Design study of steel V-Belt CVT for electric vehicles
[NASA-CR-159845] p0185 N80-32299

BECHTEL NATIONAL, INC., SAN FRANCISCO, CALIF.
Parametric study of prospective early commercial MHD power plants (PSPEC). General Electric Company, task 1: Parametric analysis
[NASA-CR-159634] p0152 N80-26779

BENTLY NEVADA CORP., RINDEN.
The parameters and measurements of the destabilizing actions of rotating machines, and the assumptions of the 1950's
p0125 N80-29712

BOEING AEROSPACE CO., KENNEDY SPACE CENTER, FLA.
Cost-effective technology advancement directions for electric propulsion transportation systems in earth-orbital missions
[AIAA PAPER 79-2043] p0048 N80-20961

BOEING AEROSPACE CO., SEATTLE, WASH.
Hybrid composites that retain graphite fibers on burning
p0073 N80-32064

Electric propulsion for near-Earth space missions
[NASA-CR-159735] p0062 N80-16096

Auxiliary control of LSS
p0063 N80-31459

BOEING CO., SEATTLE, WASH.
Computer code for estimating installed performance of aircraft gas turbine engines. Volume 1: Final report
[NASA-CR-159691] p0028 N80-13043

Computer code for estimating installed performance of aircraft gas turbine engines. Volume 2: Users manual
[NASA-CR-159692] p0028 N80-13044
BOEING COMMERCIAL AIRPLANE CO., SEATTLE, WASH.

Improved tire/wheel concept
[NASA-CASE-LAR-11695-2] p0124 N80-18402
Testing of reciprocating seals for application in a Stirling cycle engine
[NASA-CR-159820] p0124 N80-22700

Aviation fuels outlook
p0041 N80-29304

BOEING ENGINEERING AND CONSTRUCTION, SEATTLE, WASH.
Mod-2 wind turbine system concept and preliminary design report. Volume 1: Executive summary
[DOE/NASA/0002-80/2] p0151 N80-24758

Mod-2 wind turbine system concept and preliminary design report. Volume 2: Detailed report
[DOE/NASA/0002-80/2] p0152 N80-26775

BOEING MILITARY AIRPLANE DEVELOPMENT, SEATTLE, WASH.
High-freezing-point fuel studies
p0043 N80-29329

BROBECK (WILLIAM M.) AND ASSOCIATES, BERKELEY, CALIF.
Study of advanced electric propulsion system concept using a flywheel for electric vehicles
[NASA-CR-159650] p0184 N80-18991
An automatically-shifted two-speed transaxle system for an electric vehicle
[NASA-CR-159746] p0184 N80-18992

C

CALIFORNIA INST. OF TECH., PASADENA.
A test program to measure fluid mechanical whirl-excitation forces in centrifugal pumps
p0126 N80-29719

CALIFORNIA UNIV., LA JOLLA.
Critical currents in A-15 structure Nb3Al converted from cold-worked bcc structure
p0179 N80-33853

CALIFORNIA UNIV. AT LOS ANGELES.
A methodology for long-range prediction of air transportation
p0041 N80-29305

CAMBRIDGE UNIV. (ENGLAND).
The effect of finite turbulence spatial scale on the amplification of turbulence by a contracting stream
p0004 N80-44862

CARNEGIE-MELLON UNIV., PITTSBURGH, PA.
Phase change in liquid face seals. II - Isothermal and adiabatic bounds with real fluids
[ASME PAPER 79-LUB-4] p0129 N80-14739

CASE WESTERN RESERVE UNIV., CLEVELAND, OHIO.
Some TEM observations of Al2O3 scales formed on NiCrAl alloys
p0081 N80-13071

A quarter-century of progress in the development of correlation and extrapolation methods for creep rupture data
p0133 N80-38142

Anisotropy of nickel-base superalloy single crystals
p0083 N80-51573

Low sidelobe level low-cost earth station antennas for the 12 GHz broadcasting satellite service
[NASA-CR-159703] p0098 N80-12259

CHRYSLER CORP., DETROIT, MICH.
Materials review for improved automotive gas turbine engine
[NASA-CR-159673] p0123 N80-17470

Baseline automotive gas turbine engine development program
[NASA-CR-159670] p0124 N80-24620

Conceptual design study of an improved automotive gas turbine powertrain
[NASA-CR-159672] p0124 N80-24621

Upgraded automotive gas turbine engine design and development program, volume 2
[NASA-CR-159671] p0128 N80-32719

CINCINNATI UNIV., OHIO.
Hyperfine magnetic field at Cd impurity site in L2/1 Heusler alloys Rh2MnGe and Rh2MnPt by TDPAC technique
p0178 N80-16843

A calculation procedure for viscous flow in turbomachines, volume 2
[NASA-CR-159636] p0004 N80-17995

A calculation procedure for viscous flow in turbomachines, volume 3
[NASA-CR-159864] p0005 N80-26274

CLEMSON UNIV., S.C.
Griffith diffusers p0006 A80-20748

CLEVELAND CLINIC FOUNDATION, OHIO.
Preliminary results of fast neutron treatments in carcinoma of the pancreas
[NASA-TM-81516] p0160 N80-24983

CLEVELAND STATE UNIV., OHIO.
Error analysis in the measurement of average power with application to switching controllers
[NASA-CR-159792] p0184 N80-21202

COLORADO SCHOOL OF MINES, GOLDEN.
Mechanisms of nitrogen heterocycle influence on turbine fuel stability p0043 N80-29327

COLORADO STATE UNIV., FORT COLLINS.
Interaction of high voltage surfaces with the space plasma
[NASA-CR-159731] p0176 N80-14923

Physical phenomena in mercury ion thrusters
[NASA-CR-159784] p0061 N80-17137

Inert gas thrusters
[NASA-CR-159813] p0062 N80-24362

Ion extraction from a plasma
[NASA-CR-159849] p0177 N80-26161

Plasma physics analysis of SENT-2 operation
[NASA-CR-159814] p0177 N80-27189

Interaction of high voltage surfaces with the space plasma
[NASA-CR-165131] p0177 N80-32223

Baffle aperture design study of hollow cathode equipped ion thrusters
[NASA-CR-165164] p0064 N80-33476

COMMUNICATIONS SATELLITE CORP., CLARKSBURG, MD.
Thin n-i-p radiation-resistant solar cell feasibility study
[NASA-CR-159871] p0154 N80-29852

CONTROL DATA CORP., MINNEAPOLIS, MINN.
Measurements of cabin and ambient ozone on B747 airplanes p0010 A80-28853

CORNELL UNIV., ITHACA, N. Y.
Non-synchronous whirling due to fluid-dynamic forces in axial turbo-machinery rotors
p0126 N80-29721

CURTIS-WRIGHT CORP., WOOD-RIDGE, N.J.
Multifuel rotary aircraft engine
[AIAA PAPER 80-1237] p0045 A80-38982

Quiet Clean Short-haul Experimental Engine (QCSE) main reduction gears test program
[NASA-CR-134669] p0030 N80-15103

Quiet Clean Short-haul Experimental Engine (QCSE) main reduction gears bearing development program
[NASA-CR-134890] p0030 N80-15105

Quiet Clean Short-haul Experimental Engine (QCSE) main reduction gears detailed design report
[NASA-CR-134872] p0030 N80-15106

Performance, emissions, and physical characteristics of a rotating combustion aircraft engine, supplement A
[NASA-CR-135119] p0041 N80-27361

D

DELAWARE UNIV., NEWARK.
Inlet flow distortion in turbomachinery. I - Comparison of theory and experiment in a transonic fan stage. II - A parameter study
[AIAA PAPER 80-1076] p0006 A80-38895

Heat storage in alloy transformations
[NASA-CR-159787] p0151 N80-24759

DEPARTMENT OF ENERGY, GERMANTOWN, MD.
Low NO_x/heavy fuel combustor program
[ASME PAPER 80-GT-69] p0026 A80-42199

DEPARTMENT OF ENERGY, WASHINGTON, D. C.
Survey of MHD plant applications p0144 A80-11972

Outlook for alternative energy sources p0041 N80-29302

Cogeneration Technology Alternatives Study (CTAS). Volume 6: Computer data. Part 1:

Coal-fired nocogeneration process boiler, section A
[NASA-CR-159770-PT-1] p0156 N80-33860

DETROIT DIESEL ALLISON, INDIANAPOLIS, IND.
Laser anemometer measurements at the exit of a T63 combustor p0045 A80-27737

Study of turboprop systems reliability and maintenance costs
[NASA-CR-135192] p0029 N80-14129

Plasma-sprayed dual density ceramic turbine seal system
[NASA-CR-159739] p0123 N80-15411

Experimental determination of unsteady blade element aerodynamics in cascades. Volume 1: Torsion mode cascade
[NASA-CR-159831] p0040 N80-25335

DEUTSCHE FORSCHUNGS- UND VERSUCHSANSTALT FÜR LUFT- UND RAUMFAHRT, COLOGNE (WEST GERMANY).
Stability of several oxide dispersion strengthened alloys and a directionally solidified gamma/gamma prime-alpha eutectic alloy in a thermal gradient p0082 A80-40962

Compliance and stress intensity coefficients for short bar specimens with chevron notches p0133 A80-46032

Performance of Chevron-notch short bar specimen in determining the fracture toughness of silicon nitride and alumina oxide p0090 A80-50696

DOUGLAS AIRCRAFT CO., INC., LONG BEACH, CALIF.
Development of a Kevlar/PFR-15 reduced drag DC-9 nacelle fairing
[AIAA PAPER 80-1194] p0010 A80-41193

Reduced bleed air extraction for DC-10 cabin air conditioning
[AIAA PAPER 80-1197] p0010 A80-41194

An efficient user-oriented method for calculating compressible flow in an about three-dimensional inlets
[NASA-CR-159578] p0004 N80-10134

Engine bleed air reduction in DC-10
[NASA-CR-159846] p0010 N80-32378

DOUGLAS AIRCRAFT CO., INC., SANTA MONICA, CALIF.
Fuel/engine/airframe tradeoff study, phase 1 p0042 N80-29307

E

EATON CORP., SOUTHFIELD, MICH.
Small passenger car transmission test; Ford C4 transmission
[NASA-CR-159881] p0128 N80-31795

Small passenger car transmission test; Chevrolet LUV transmission
[NASA-CR-159882] p0128 N80-31796

EATON ENGINEERING AND RESEARCH CENTER, SOUTHFIELD, MICH.
Small passenger car transmission test-Chevrolet 200 transmission
[NASA-CR-159835] p0185 N80-28255

EDDE (HOWARD), INC., BELLEVUE, WASH.
Energy conservation and environmental benefits of thermal energy storage systems in the pulp and paper industry p0146 A80-48194

ELECTRO-MECHANICAL RESEARCH, INC., SARASOTA, FLA.
DOE/NASA wind turbine data acquisition. Part 1: Equipment
[NASA-CR-159779] p0148 N80-17543

ENERGY RESEARCH CORP., DANBURY, CONN.
Technology development for phosphoric acid fuel cell powerplant, phase 2
[NASA-CR-159705] p0147 N80-10603

ENERGY TECHNOLOGY, INC., CLEVELAND, OHIO.
Study of advanced radial outflow turbine for solar steam Rankine engines
[NASA-CR-159695] p0148 N80-16483

ENGELHARD MINERALS AND CHEMICALS CORP., EDISON, N. J.
CATCON catalyst 5 atm 1000 hour aging study using No. 2 fuel oil p0075 A80-35908

Durability testing at 5 atmospheres of advanced catalysts and catalyst supports for gas turbine engine combustors
[NASA-CR-159839] p0151 N80-24748

EXION RESEARCH AND ENGINEERING CO., LINDEN, N.J.
Effect of refining variables on the properties

and composition of JP-5

Fuel property effects in stirred combustors p0041 N80-29306
p0043 N80-29321

F**FIBER MATERIALS, INC., BIDDEFORD, MAINE.**

Fabrication and evaluation of low fiber content
alumina fiber/aluminum composites p0073 N80-29430
[NASA-CR-159517]

FLOW SIMULATIONS, INC., SUNNYVILLE, CALIF.

An implicit finite-difference code for inviscid
and viscous cascade flow p0007 A80-44128
[AIAA PAPER 80-1427]

FORD AEROSPACE AND COMMUNICATIONS CORP., PALO ALTO, CALIF.

Packet communications in satellites with
multiple-beam antennas and signal processing
[AIAA 80-0537] p0099 A80-29574

Concepts for 20/30 GHz satcom systems for
direct-to-user applications p0050 A80-35329
[AIAA 80-0582]

Concepts for 18/30 GHz satellite communication
system, volume 1 p0098 N80-11277
[NASA-CR-159625-VOL-1]

Concepts for 18/30 GHz satellite communication
system, volume 1A: Appendix p0098 N80-11278
[NASA-CR-159625-VOL-1A]

Concepts for 18/30 GHz satellite communication
system study. Executive summary p0098 N80-11279
[NASA-CR-159680]

FORD MOTOR CO., DEARBORN, MICH.

Feasibility study of silicon nitride regenerators
[NASA-CR-159713] p0184 N80-25209

Regenerator matrix physical property data
[NASA-CR-159854] p0185 N80-30228

POSTER-MILLER ASSOCIATES, INC., WALTHAM, MASS.

A 15kWe (nominal) solar thermal electric power
conversion concept definition study: Steam
Rankine reheat reciprocator system p0148 N80-16491
[NASA-CR-159590]

POSTER WHEELER CORP., LIVINGSTON, N.J.

Parametric study of prospective early commercial
MHD power plants (PSPEC). General Electric
Company, task 1: Parametric analysis p0152 N80-26779
[NASA-CR-159634]

PWG ASSOCIATES, INC., TULLAHOA, TENN.

Monodisperse atomizers for agricultural aviation
applications p0108 N80-19450
[NASA-CR-159777]

G**GARRETT CORP., TORRANCE, CALIF.**

Advanced electric propulsion system concept for
electric vehicles p0183 N80-17916
[NASA-CR-159651]

GENERAL DYNAMICS/CONVAIR, SAN DIEGO, CALIF.

Capillary device refilling p0060 A80-38908
[AIAA PAPER 80-1095]
Power management for multi-100 KWe space systems p0060 A80-48357

Capillary acquisition devices for
high-performance vehicles: Executive summary
[NASA-CR-159658] p0062 N80-19185

Conceptual design of two-phase fluid mechanics
and heat transfer facility for spacelab p0049 N80-27403
[NASA-CR-159810]

Study of power management technology for orbital
multi-100KWe applications. Volume 2: Study
results p0153 N80-28862
[NASA-CR-159834-VOL-2]

Study of power management technology for orbital
multi-100KWe applications. Volume 3:
Requirements p0154 N80-29845
[NASA-CR-159834]

Conceptual design of an orbital propellant
transfer experiment. Volume 2: Study results
[NASA-CR-165150] p0048 N80-31423

Comparative thermal analysis of alternate
Cryogenic Fluid Management Experiment (CFME)
configurations p0048 N80-32412
[NASA-CR-165151]

GENERAL DYNAMICS CORP., SAN DIEGO, CALIF.

Low-thrust vehicles concept studies p0063 N80-31456

GENERAL DYNAMICS/FORT WORTH, TEX.

Experimental investigation of a 0.15 scale model
of a conformal variable-ramp inlet for the
F-16 airplane p0005 N80-24263
[NASA-CR-159640]

GENERAL ELECTRIC CO., CINCINNATI, OHIO.

Scale model performance test investigation of
exhaust system mixers for an Energy Efficient
Engine /E3/ propulsion system p0024 A80-20960
[AIAA PAPER 80-0229]

Airbreathing propulsion component technologies
p0024 A80-37482

CF6-50 Short Core Exhaust Nozzle
[AIAA PAPER 80-1196] p0025 A80-41514

Advanced catalytic combustors for low pollutant
emissions, phase 1 p0028 N80-13048
[NASA-CR-159535]

Feasibility of SiC composite structures for 1644
deg gas turbine seal applications p0123 N80-13474
[NASA-CR-159597]

Quiet Clean Short-Haul Experimental Engine
(QCSEE) acoustic and aerodynamic tests on a
scale model over-the-wing thrust reverser and
forward thrust nozzle p0028 N80-14115
[NASA-CR-135254]

Quiet Clean Short-Haul Experimental Engine
(QCSEE). Under-the-wing (UTW) engine
boilerplate nacelle test report. Volume 2:
Aerodynamics and performance p0028 N80-14116
[NASA-CR-135250]

Quiet, Clean, Short-Haul, Experimental Engine
(QCSEE) Under-The-Wing (UTW) engine acoustic
design p0028 N80-14117
[NASA-CR-135267]

Quiet, Clean, Short-Haul Experimental Engine
(QCSEE) Over-The-Wing (OTW) engine acoustic
design p0028 N80-14118
[NASA-CR-135268]

Quiet Clean Short-Haul Experimental Engine
(QCSEE) Under-The-Wing (UTW) graphite/PMR cowl
development p0029 N80-14119
[NASA-CR-135279]

Quiet Clean Short-Haul Experimental Engine
(QCSEE) Over-The-Wing (OTW) propulsion system
test report. Volume 2: Aerodynamics and
performance p0029 N80-14120
[NASA-CR-135324]

The CF6 jet engine performance improvement: New
front mount p0029 N80-14127
[NASA-CR-159639]

Demonstration of short haul aircraft aft noise
reduction techniques on a twenty inch (50.8
cm) diameter fan, volume 3 p0034 N80-15085
[NASA-CR-134851]

Quiet Clean Short-haul Experimental Engine
(QCSEE) Over The Wing (OTW) design report
[NASA-CR-134848] p0034 N80-15086

Quiet Clean Short-haul Experimental Engine
(QCSEE) preliminary under the wing flight
propulsion system analysis report p0034 N80-15088
[NASA-CR-134868]

Quiet Clean Short-haul Experimental Engine
(QCSEE). The aerodynamic and mechanical
design of the QCSEE over-the-wing fan p0034 N80-15089
[NASA-CR-134915]

Quiet Clean Short-haul Experimental Engine
(QCSEE) under-the-wing engine digital control
system design report p0034 N80-15090
[NASA-CR-134920]

Quiet Clean Short-haul Experimental Engine
(QCSEE) under-the-wing engine simulation report
[NASA-CR-134914] p0034 N80-15091

Quiet Clean Short-haul Experimental Engine
(QCSEE) over-the-wing control system design
report p0035 N80-15092
[NASA-CR-135337]

Quiet Clean Short-haul Experimental Engine
(QCSEE). Core engine noise measurements
[NASA-CR-135160] p0035 N80-15093

Quiet Clean Short-haul Experimental Engine
(QCSEE) Under-The-Wing (UTW) engine composite
nacelle test report. Volume 1: Summary,
aerodynamic and mechanical performance p0035 N80-15094
[NASA-CR-159471]

Quiet Clean Short-haul Experimental Engine
(QCSEE) preliminary over-the-wing flight
propulsion system analysis report p0035 N80-15095
[NASA-CR-135296]

Quiet Clean Short-haul Experimental Engine
(QCSEE). Under-The-Wing (UTW) engine
boilerplate nacelle test report, volume 1

[NASA-CR-135249] p0035 N80-15096
 Quiet Clean Short-haul Experimental Engine
 (QCSEE). Under-The-Wing (UTW) engine
 boilerplate nacelle test report. Volume 3:
 Mechanical performance
 [NASA-CR-135251] p0035 N80-15097
 Quiet Clean Short-haul Experimental Engine
 (QCSEE). Composite fan frame subsystem test
 report
 [NASA-CR-135010] p0035 N80-15098
 Quiet Clean Short-haul Experimental Engine
 (QCSEE) Over-The-Wing (OTW) boilerplate
 nacelle design report
 [NASA-CR-135168] p0035 N80-15099
 Quiet Clean Short-haul Experimental Engine
 (QCSEE) Under-The-Wing (UTW) composite nacelle
 subsystem test report
 [NASA-CR-135075] p0034 N80-15100
 Quiet Clean Short-haul Experimental Engine
 (QCSEE) Under-The-Wing (UTW) composite nacelle
 subsystem test report
 [NASA-CR-135075] p0034 N80-15100
 Quiet Clean Short-haul Experimental Engine
 (QCSEE). Ball spline pitch change mechanism
 design report
 [NASA-CR-134873] p0030 N80-15101
 Quiet Clean Short-haul Experimental Engine
 (QCSEE). Ball spline pitch change mechanism
 design report
 [NASA-CR-134873] p0030 N80-15101
 Acoustic analysis of aft noise reduction
 techniques measured on a subsonic tip speed
 50.8 cm (twenty inch) diameter fan
 [NASA-CR-134891] p0030 N80-15102
 Quiet Clean Short-haul Experimental Engine
 (QCSEE) clean combustor test report
 [NASA-CR-134916] p0030 N80-15104
 Quiet Clean Short-haul Experimental Engine
 (QCSEE) under-the-wing engine composite fan
 blade design report
 [NASA-CR-135046] p0031 N80-15108
 Quiet Clean Short-haul Experimental Engine
 (QCSEE): The aerodynamic and mechanical
 design of the QCSEE under-the-wing fan
 [NASA-CR-135009] p0031 N80-15109
 Quiet Clean Short-haul Experimental Engine
 (QCSEE) composite fan frame design report
 [NASA-CR-135278] p0031 N80-15110
 Quiet Clean Short-haul Experimental Engine
 (QCSEE) UTW fan preliminary design
 [NASA-CR-134842] p0031 N80-15111
 Quiet Clean Short-haul Experimental Engine
 (QCSEE): The aerodynamic and preliminary
 mechanical design of the QCSEE OTW fan
 [NASA-CR-134841] p0031 N80-15112
 Quiet Clean Short-haul Experimental Engine
 (QCSEE) under-the-wing engine composite fan
 blade design
 [NASA-CR-134840] p0031 N80-15113
 Quiet Clean Short-haul Experimental Engine
 (QCSEE) over-the-wing engine and control
 simulation results
 [NASA-CR-135049] p0031 N80-15114
 Quiet Clean Short-Haul Experimental Engine
 (QCSEE) ball spline pitch-change mechanism
 whirligig test report
 [NASA-CR-135354] p0032 N80-15115
 Quiet Clean Short-haul Experimental Engine
 (QCSEE) Under-The-Wing (UTW) boiler plate
 nacelle and core exhaust nozzle design report
 [NASA-CR-135008] p0032 N80-15116
 Quiet Clean Short-haul Experimental Engine
 (QCSEE) Over-The-Wing (OTW) propulsion systems
 test report. Volume 4: Acoustic performance
 [NASA-CR-135326] p0032 N80-15118
 Quiet Clean Short-haul Experimental Engine
 (QCSEE) Under-The-Wing (UTW) composite nacelle
 [NASA-CR-135352] p0032 N80-15119
 Quiet Clean Short-haul Experimental Engine (QCSEE)
 [NASA-CR-159473] p0032 N80-15120
 Quiet Clean Short-haul Experimental Engine
 (QCSEE). Double-annular clean combustor
 technology development report
 [NASA-CR-159483] p0032 N80-15121
 Quiet Clean Short-Haul Experimental Engine
 (QCSEE): Acoustic treatment development and
 design
 [NASA-CR-135266] p0033 N80-15122

Quiet Clean Short-Haul Experimental Engine
 (QCSEE). Preliminary analyses and design
 report, volume 1
 [NASA-CR-134838] p0033 N80-15123
 Quiet Clean Short-Haul Experimental Engine
 (QCSEE). Preliminary analyses and design
 report, volume 2
 [NASA-CR-134839] p0033 N80-15124
 Quiet Clean Short-Haul Experimental Engine
 (QCSEE) Over-The-Wing (OTW) propulsion system
 test report. Volume 1: Summary report
 [NASA-CR-135323] p0033 N80-15125
 Quiet Clean Short-Haul Experimental Engine
 (QCSEE) over-The Wing (OTW) propulsion system
 test report. Volume 3: Mechanical performance
 [NASA-CR-135325] p0033 N80-15126
 Core noise investigation of the CF6-50 turbofan
 engine
 [NASA-CR-159598] p0036 N80-16061
 Core noise investigation of the CF6-50 turbofan
 engine
 [NASA-CR-159749] p0036 N80-16062
 Program to develop sprayed, plastically
 deformable compressor shroud seal materials
 [NASA-CR-159741] p0123 N80-16338
 Method and apparatus for rapid thrust increases
 in a turbofan engine
 [NASA-CR-LEW-12971-1] p0016 N80-18039
 Internal coating of air cooled gas turbine blades
 [NASA-CR-159701] p0036 N80-18041
 Program for impact testing of spar-shell fan
 blades, test report
 [NASA-CR-135393] p0037 N80-21328
 CF6 jet engine performance improvement: New fan
 [NASA-CR-159699] p0039 N80-23309
 CF6-6D engine short-term performance deterioration
 [NASA-CR-159830] p0039 N80-23316
 CF6 jet engine performance improvement program:
 High pressure turbine aerodynamic performance
 improvement
 [NASA-CR-159832] p0040 N80-26302
 CF6-6D engine performance deterioration
 [NASA-CR-159786] p0041 N80-27364
 Materials for advanced turbine engines. Volume
 1: Power metallurgy Rene 95 rotating turbine
 engine parts
 [NASA-CR-159802] p0084 N80-28499
 Quiet Clean Short-haul Experimental Engine
 (QCSEE) Under-The-Wing (UTW) composite nacelle
 test report. Volume 2: Acoustic performance
 [NASA-CR-159472] p0044 N80-29297
 Quiet Clean Short-haul Experimental Engine
 (QCSEE) under-the-wing engine composite fan
 blade: Preliminary design test report
 [NASA-CR-134846] p0044 N80-29298
 Acoustic performance of a 50.8-cm (20-inch)
 diameter variable-pitch fan and inlet. Volume
 2: Acoustic data
 [NASA-CR-135118] p0044 N80-29299
 NASA/General Electric broad-specification fuels
 combustion technology program, phase 1
 p0042 N80-29316
 Energy efficient engine
 [NASA-CR-159685] p0045 N80-33408
 GENERAL ELECTRIC CO., EVENDALE, OHIO.
 Fuel conservation through active control of
 rotor clearances
 [AIAA PAPER 80-1087] p0045 N80-41506
 CF6 fan performance improvement
 [ASME PAPER 80-GT-178] p0026 N80-42284
 GENERAL ELECTRIC CO., FAIRFIELD, CONN.
 Experimental combustor study program
 p0042 N80-29311
 Cogeneration Technology Alternatives Study
 (CTAS). Volume 6: Computer data. Part 1:
 Coal-fired nocogeneration process boiler,
 section A
 [NASA-CR-159770-PT-1-A] p0154 N80-30888
 Cogeneration Technology Alternatives Study
 (CTAS). Volume 6: Computer data. Part 1:
 Coal-fired nocogeneration process boiler,
 section B
 [NASA-CR-159770-PT-1-B] p0154 N80-30889
 Cogeneration Technology Alternatives Study
 (CTAS). Volume 6: Computer data. Part 2:
 Residual-fired nocogeneration process boiler
 [NASA-CR-159770-PT-2] p0155 N80-30890
 GENERAL ELECTRIC CO., PHILADELPHIA, PA.
 Coupled generator and combustor performance

H

- calculations for potential early commercial
MHD power plants p0156 A80-25099
- Ka-band, multibeam, contiguous coverage
satellite antenna for the USA p0099 A80-29588
[AIAA 80-0557]
- Executive summary: Mod-1 wind turbine generator
analysis and design report p0147 N80-11558
[NASA-CR-159497]
- Sintered silicon nitride recuperator fabrication
[NASA-CR-159706] p0090 N80-15263
- Appendix: MOD-1 wind turbine generator analysis
and design report, volume 2 p0149 N80-18565
[NASA-CR-159496]
- Mod 1 wind turbine generator failure modes and
effects analysis p0150 N80-20864
[NASA-CR-159494]
- Mod-1 wind turbine generator analysis and design
report, volume 1 p0150 N80-23775
[NASA-CR-159495]
- Study of advanced communications satellite
systems based on SS-PDMA p0050 N80-25357
[NASA-CR-159778]
- Parametric study of prospective early commercial
MHD power plants (PSPEC). General Electric
Company, task 1: Parametric analysis p0152 N80-26779
[NASA-CR-159634]
- Cogeneration Technology Alternatives Study
(CTAS). Volume 3: Industrial processes p0155 N80-31870
[NASA-CR-159767]
- GENERAL ELECTRIC CO., SCHENECTADY, N. Y.
Cogeneration Technology Alternatives Study
(CTAS). Volume 1: Summary report p0151 N80-24797
[NASA-CR-159765]
- Cogeneration Technology Alternatives Study
(CTAS). Volume 4: Energy conversion systems p0155 N80-33859
[NASA-CR-159768]
- Cogeneration Technology Alternatives Study
(CTAS). Volume 6: Computer data. Part 1:
Coal-fired nocooperation process boiler,
section A p0156 N80-33860
[NASA-CR-159770-PT-1]
- Cogeneration Technology Alternatives Study
(CTAS). Volume 6: Computer data. Part 2:
Residual-fired nocooperation process boiler
[NASA-CR-159770-PT-2] p0156 N80-33861
- GENERAL ELECTRIC CO., WASHINGTON, D. C.
Demonstration of short-haul aircraft aft noise
reduction techniques on a twenty inch (50.8
cm) diameter fan, volume 1 p0033 N80-15083
[NASA-CR-134849]
- Demonstration of short-haul aircraft aft noise
reduction techniques on a twenty inch (50.8)
diameter fan, volume 2 p0034 N80-15084
[NASA-CR-134850]
- GENERAL MOTORS CORP., DETROIT, MICH.
Advanced Gas Turbine Powertrain System
Development Project p0129 A80-35574
- Aerodynamic analysis of a supersonic cascade
vibrating in a complex mode p0007 A80-45841
- GEORGE WASHINGTON UNIV., WASHINGTON, D.C.
Statistical aspects of carbon fiber risk
assessment modeling p0073 N80-29432
[NASA-CR-159318]
- GEORGIA INST. OF TECH., ATLANTA.
System analysis for millimeter-wave
communication satellites p0100 A80-52479
- GILBERT/COMMONWEALTH, READING, PA.
Survey of MHD plant applications p0144 A80-11972
- GILBERT ASSOCIATES, INC., READING, PA.
Oxygen-enriched air for MHD power plants p0096 A80-25096
- GINER, INC., WALTHAM, MASS.
Catalyst surfaces for the chromous/chromic redox
couple p0140 N80-18557
[NASA-CASE-LEW-13148-2]
- Catalyst surfaces for the chromous/chromic redox
couple p0101 N80-20487
[NASA-CASE-LEW-13148-1]
- GRUMMAN AEROSPACE CORP., BETHPAGE, N.Y.
Active heat exchange system development for
latent heat thermal energy storage p0149 N80-18562
[NASA-CR-159726]
- HAMILTON STANDARD, WINDSOR LOCKS, CONN.
Advanced turbo-prop airplane interior noise
reduction-source definition p0172 N80-13882
[NASA-CR-159668]
- Quiet Clean Short-haul Experimental Engine
(QCSEE): Hamilton Standard cam/harmonic drive
variable pitch fan actuation system detail
design report p0030 N80-15107
[NASA-CR-134852]
- Quiet Clean Short-haul Experimental Engine
(QCSEE) whirl test of cam/harmonic pitch
change actuation system p0032 N80-15117
[NASA-CR-135140]
- Acoustic test and analyses of three advanced
turbo-prop models p0039 N80-23311
[NASA-CR-159667]
- Diffusion bonded boron/aluminum spar-shell fan
blade p0072 N80-25382
[NASA-CR-159571]
- HAMILTON STANDARD DIV., UNITED AIRCRAFT CORP.,
WINDSOR LOCKS, CONN.
Acoustic measurements of three Prop-Fan models
[AIAA PAPER 80-0995] p0045 A80-35958
- Acoustic pressures on a prop-fan aircraft
fuselage surface p0172 A80-35965
[AIAA PAPER 80-1002]
- MERRIOTT-WATT UNIV., EDINBURGH (SCOTLAND).
Limit cycles of a flexible shaft with
hydrodynamic journal bearings in unstable
regimes p0127 N80-29725
- MERSH ACOUSTICAL ENGINEERING, CHATSWORTH, CALIF.
Acoustic behavior of fibrous bulk materials
[AIAA PAPER 80-0986] p0172 A80-35951
- Effect of grazing flow on the nonlinear acoustic
behavior of helmholtz resonators p0095 N80-31619
- MITACHI LTD., TSUCHIURA (JAPAN).
Hydraulic forces caused by annular pressure
seals in centrifugal pumps p0126 N80-29718
- MONEYWELL, INC., MINNEAPOLIS, MINN.
Active heat exchange system development for
latent heat thermal energy storage p0154 N80-29857
[NASA-CR-159727]
- MONEYWELL, INC., ST. PAUL, MINN.
Assessment and preliminary design of an energy
buffer for regenerative braking in electric
vehicles p0184 N80-23216
[NASA-CR-159756]
- HOOVER CHEMICAL CORP., NIAGARA FALLS, N.Y.
Parametric study of prospective early commercial
MHD power plants (PSPEC). General Electric
Company, task 1: Parametric analysis p0152 N80-26779
[NASA-CR-159634]
- HUGHES RESEARCH LABS., MALIBU, CALIF.
8-cm Engineering Model Thruster technology - A
review of recent developments p0064 A80-13311
[AIAA PAPER 79-2103]
- A model for predicting the wearout lifetime of
the LeRC/Hughes 30-cm mercury ion thruster p0064 A80-20962
[AIAA PAPER 79-2079]
- Solid-state X-band combiner study p0103 N80-11328
[NASA-CR-162432]
- Primary electric propulsion technology study
[NASA-CR-159688] p0061 N80-13158
- IIT RESEARCH INST., CHICAGO, ILL.
Thermal fatigue and oxidation data for
directionally solidified MAR-M 246 turbine
blades p0037 N80-21330
[NASA-CR-159798]
- Thermal fatigue and oxidation data of oxide
dispersion-strengthened alloys p0084 N80-25415
[NASA-CR-159842]
- ILLINOIS INST. OF TECH., CHICAGO.
Effects of axisymmetric contractions on
turbulence of various scales p0006 N80-32328
[NASA-CR-165136]
- ILLINOIS UNIV., URBANA.
Elastohydrodynamic film thickness measurements
of artificially-produced nonsmooth surfaces
[ASLE PREPRINT 79-1C-1A-3] p0102 A80-14720

INCO RESEARCH AND DEVELOPMENT CENTER, SUFFERN, N. Y.
Characterization of an oxide dispersion strengthened superalloy, MA-6000E, for turbine blade applications
[NASA-CR-159493] p0083 N80-13218

INDIAN INST. OF SCIENCE, BANGALORE.
Preparation of cast aluminum alloy-mica particle composites
p0071 A80-32632

INGERSOLL-RAND CO., EASTON, PA.
Analysis and identification of subsynchronous vibration for a high pressure parallel flow centrifugal compressor
p0125 N80-29710

INSTITUTE OF GAS TECHNOLOGY, CHICAGO, ILL.
High-temperature molten salt thermal energy storage systems
[NASA-CR-159663] p0148 N80-17547

INTERNATIONAL TELEPHONE AND TELEGRAPH CORP., NEW YORK.

The 30/20 GHz fixed communications systems service demand assessment. Volume 1: Executive summary
[NASA-CR-159619] p0098 N80-18262

The 30/20 GHz fixed communications systems service demand assessment. Volume 2: Main report
[NASA-CR-159620] p0098 N80-18263

The 30/20 GHz fixed communications systems service demand assessment. Volume 3: Annex
[NASA-CR-159621] p0099 N80-18264

IONICS, INC., WATERTOWN, MASS.
Anton permselective membrane
[NASA-CR-159599] p0147 N80-12551

J

JAY - CARTER ENTERPRISES, INC., BURKBURNETT, TEX.
A 15 kWe (nominal) solar thermal-electric power conversion concept definition study: Steam Rankin reciprocator system
[NASA-CR-159591] p0149 N80-19612

JET PROPULSION LAB., CALIFORNIA INST. OF TECH., PASADENA.

Characterization of solar cells for space applications. Volume 10: Electrical characteristics of Spectrolab BSP, textured, 10 ohm-cm, 300 micron cells as a function of intensity, temperature and irradiation
[NASA-CR-162422] p0147 N80-11566

Annual technical report, fiscal year 1979. Volume 1: Executive summary
[NASA-CR-159715-VOL-1] p0149 N80-19632

Solar thermal power systems point-focusing distributed receiver technology project. Volume 2: Detailed report
[NASA-CR-159715-VOL-2] p0151 N80-24751

High temperature thermal energy storage in steel and sand
[NASA-CR-159708] p0154 N80-29860

JETSHAPES, INC., ROCKLEIGH, N. J.
Development of exothermically cast single-crystal Mar-M 247 and derivative alloys
[AIRESEARCH-21-3469] p0084 A80-45825

K

KANAN AEROSPACE CORP., BLOOMFIELD, CONN.
Design, fabrication, test, and evaluation of a prototype 150-foot long composite wind turbine blade
[NASA-CR-159775] p0148 N80-17548

KANSAS UNIV., LAWRENCE.
Spectral effects on direct-insolation absorptance of five collector coatings
[ASME PAPER 79-HT-18] p0146 A80-45722

KENT STATE UNIV., OHIO.
Homogeneous alignment of nematic liquid crystals by ion beam etched surfaces
p0178 A80-26007

KOBE STEEL LTD. (JAPAN).
Asynchronous vibration problem of centrifugal compressor
p0125 N80-29713

KOBE UNIV. (JAPAN).
Evaluation of instability forces of labyrinth seals in turbines or compressors
p0126 N80-29715

KUMH (EMERSON L.), TEMPE, ARIZ.
Design study of flat belt CVT for electric vehicles
[NASA-CR-159822] p0124 N80-22702

L

LEHIGH UNIV., BETHLEHEM, PA.
Sudden stretching of a four layered composite plate
[NASA-CR-159870] p0073 N80-25383

Sudden bending of cracked laminates
[NASA-CR-159860] p0073 N80-25384

LINCOLN UNIV., PA.
Dynamic modulus and damping of boron, silicon carbide, and alumina fibers
p0071 A80-44236

LITTLE (ARTHUR D.), INC., CAMBRIDGE, MASS.
Study of research and development requirements of small gas-turbine combustors
[NASA-CR-159796] p0036 N80-18040

LOCKHEED-CALIFORNIA CO., BURBANK.
Zero-length, slotted-lip inlet for subsonic military aircraft
[AIAA PAPER 80-1245] p0004 A80-41203

Temperature and flow measurements on near-freezing aviation fuels in a wing-tank model
[ASME PAPER 80-GT-63] p0094 A80-42193

Low temperature fuel behavior studies
p0044 N80-29330

LOCKHEED-GEORGIA CO., MARIETTA.
Characteristics of internal- and jet-noise radiation from a multi-lobe, multi-tube suppressor nozzle tested statically and under flight simulation
[AIAA PAPER 80-1027] p0173 A80-38642

Studies of the acoustic transmission characteristics of coaxial nozzles with inverted velocity profiles, volume 1
[NASA-CR-159598] p0172 N80-11870

A study of the transmission characteristics of suppressor nozzles
[NASA-CR-165133] p0172 N80-32186

LOUISVILLE UNIV., KY.
Testing of turbulent seals for rotodynamic coefficients
p0126 N80-29714

M

MARTIN MARIETTA AEROSPACE, DENVER, COLO.
A liquid hydrogen experiment as a Shuttle payload
[AIAA PAPER 80-1096] p0054 A80-38909

MARTIN MARIETTA CORP., BETHESDA, MD.
DOD low-thrust mission studies
p0063 N80-31455

Primary propulsion/large space system interactions
p0063 N80-31458

Low-thrust chemical orbit to orbit propulsion system propellant management study
p0064 N80-31469

MARYLAND UNIV., COLLEGE PARK.
Application of the principle of similarity fluid mechanics
p0107 A80-10039

MASSACHUSETTS INST. OF TECH., CAMBRIDGE.
Higher order mode propagation in nonuniform circular ducts
[AIAA PAPER 80-1018] p0171 A80-35974

Full-coverage film cooling. I - Comparison of heat transfer data for three injection angles
[ASME PAPER 80-GT-43] p0108 A80-42176

Full-coverage film cooling. II - Heat transfer data and numerical simulation
[ASME PAPER 80-GT-44] p0109 A80-42177

Directional solidification at ultra-high thermal gradient
[NASA-CR-159797] p0096 N80-15300

Air pollution from aircraft
[NASA-CR-159712] p0010 N80-16060

Two-dimensional finite-element analyses of simulated rotor-fragment impacts against rings and beams compared with experiments
[NASA-CR-159645] p0038 N80-22323

Laboratory measurements in a turbulent, swirling flow
[NASA-CR-159723] p0095 N80-22509

N

Higher order mode propagation in nonuniform circular ducts
[NASA-TM-81481] p0169 N80-23101

Instructions for the use of the CIVM-Jet 4C finite-strain computer code to calculate the transient structural responses of partial and/or complete arbitrarily-curved rings subjected to fragment impact
[NASA-CR-159873] p0134 N80-27720

Soot formation and burnout in flames
p0043 N80-29320

Physical explanations of the destabilizing effect of damping in rotating parts
p0127 N80-29728

Finite-strain large-deflection elastic-viscoplastic finite-element transient response analysis of structures
[NASA-CR-159874] p0134 N80-29762

MAYA DEVELOPMENT CORP., SAN DIEGO, CALIF.
Torquing and electrostatic deformation of the solar sail
p0065 A80-46901

MECHANICAL TECHNOLOGY, INC., LATHAM, N. Y.
The effects of strain and temperature on the dynamic properties of elastomers
[ASME PAPER 79-DET-57] p0092 A80-15720

Design of elastomer dampers for a high-speed flexible rotor
[ASME PAPER 79-DET-88] p0121 A80-15736

Dynamic properties of elastomer cartridge specimens under a rotating load
p0121 A80-24002

Balancing of a power-transmission shaft with the application of axial torque
[ASME PAPER 80-GT-143] p0121 A80-42256

Elastomer damper performance - A comparison with a squeeze film for a supercritical power transmission shaft
[ASME PAPER 80-GT-162] p0121 A80-42272

Assessment of the state of technology of automotive Stirling engines
[NASA-CR-159631] p0183 N80-13989

Development of procedures for calculating stiffness and damping of elastomers in engineering applications, part 6
[NASA-CR-159838] p0134 N80-22733

Design study of a 15 kW free-piston Stirling engine-linear alternator for dispersed solar electric power systems
[NASA-CR-159587] p0150 N80-22787

High temperature self-lubricating coatings for air lubricated foil bearings for the automotive gas turbine engine
[NASA-CR-159848] p0091 N80-26448

Practical experience with unstable compressors
p0125 N80-29709

Use of elastomeric elements in control of rotor instability
p0128 N80-29732

Development of procedures for calculating stiffness and damping of elastomers in engineering applications, part 7
[NASA-CR-165138] p0128 N80-32718

MIAMI UNIV., OXFORD, OHIO.
Hyperfine magnetic field at Cd impurity site in 12/1 Heusler alloys Rh_2MnGe and Rh_2MnPb by TDPAC technique
p0178 A80-16843

MIDWEST RESEARCH INST., KANSAS CITY, MO.
Thermal energy storage systems using fluidized bed heat exchangers
[NASA-CR-159838] p0153 N80-28866

MITRE CORP., BEDFORD, MASS.
Application of advanced on-board processing concepts to future satellite communications systems
[NASA-CR-159682] p0098 N80-12260

Application of advanced on-board processing concepts to future satellite communications systems: Bibliography
[NASA-CR-159684] p0098 N80-12261

On-board processing concepts for future satellite communications systems
[NASA-CR-159683] p0099 N80-24514

NATIONAL AERONAUTICS AND SPACE ADMINISTRATION, WASHINGTON, D. C.
Electric propulsion, circa 2000
[AIAA PAPER 80-0912] p0059 A80-32886

Airbreathing propulsion component technologies
p0024 A80-37482

NATIONAL AERONAUTICS AND SPACE ADMINISTRATION. AMES RESEARCH CENTER, MOFFETT FIELD, CALIF.
An implicit finite-difference code for inviscid and viscous cascade flow
[AIAA PAPER 80-1427] p0007 A80-44128

Flight test of navigation and guidance sensor errors measured on STOL approaches
[NASA-TM-81154] p0028 N80-13041

NATIONAL AERONAUTICS AND SPACE ADMINISTRATION. GODDARD SPACE FLIGHT CENTER, GREENBELT, MD.
NASA communications technology research and development
p0097 A80-25920

Active control of spacecraft charging
p0055 A80-46890

NATIONAL AERONAUTICS AND SPACE ADMINISTRATION. LANGLEY RESEARCH CENTER, HAMPTON, VA.
Examination of the flap-lag stability of rigid articulated rotor blades
p0010 A80-15123

Buckling of rotating beams
p0133 A80-20149

Wind-tunnel investigation of the flow correction for a model-mounted angle of attack sensor at angles of attack from -10 deg to 110 deg
[NASA-TM-80189] p0011 N80-14110

Improved tire/wheel concept
[NASA-CASE-LAR-11695-2] p0124 N80-18402

NATIONAL AERONAUTICS AND SPACE ADMINISTRATION. MARSHALL SPACE FLIGHT CENTER, HUNTSVILLE, ALA.
Stress corrosion cracking evaluation of martensitic precipitation hardening stainless steels
[NASA-TM-78257] p0083 N80-16142

NAVAL AIR PROPULSION TEST CENTER, TRENTON, N.J.
Determination of jet fuel thermal deposit rate using a modified JFTOT
p0043 N80-29326

NAVAL RESEARCH LAB., WASHINGTON, D. C.
Characterization and properties of controlled nucleation thermochemical deposited /CNTD/ silicon carbide
p0089 A80-13063

NIELSEN ENGINEERING AND RESEARCH, INC., MOUNTAIN VIEW, CALIF.
Evaluation of a strained-coordinate perturbation procedure - Nonlinear subsonic and transonic flows
[AIAA PAPER 80-0339] p0006 A80-18324

O

OHIO STATE UNIV., COLUMBUS.
A theoretical and experimental investigation of propeller performance methodologies
[AIAA PAPER 80-1240] p0026 A80-43283

Vibration and buckling of rectangular plates under in-plane hydrostatic loading
p0133 A80-45364

An acoustic sensitivity study of general aviation propellers
[AIAA PAPER 80-1871] p0045 A80-50191

OPERATIONS RESEARCH, INC., SILVER SPRING, MD.
Aerial applications dispersal systems control requirements study
[NASA-CR-159781] p0158 N80-18586

P

PAN AMERICAN WORLD AIRWAYS, INC., JAMAICA, N. Y.
JT9D-7A /SP/ jet engine performance deterioration trends
p0026 A80-44230

JT9D-7A (SP) jet engine performance deterioration trends
[NASA-TM-81459] p0016 N80-20274

PARAGON PACIFIC, INC., EL SEGUNDO, CALIF.
Evaluation of feasibility of prestressed concrete for use in wind turbine blades
[NASA-CR-159725] p0147 N80-15553

CORPORATE SOURCE INDEX

ROCKWELL INTERNATIONAL CORP., PITTSBURGH, PA.

PENNSYLVANIA STATE UNIV., UNIVERSITY PARK.
Investigation of critical burning of fuel droplets
[NASA-CR-159697] p0075 N80-12142
Three dimensional mean flow and turbulence
characteristics of the near wake of a
compressor rotor blade
[NASA-CR-159518] p0005 N80-27288

**PHILLIPS PETROLEUM CO. EUROPE-AFRICA, LONDON
(ENGLAND).**
Field experiences with rotordynamic instability
in high-performance turbomachinery
p0125 N80-29707

PITTSBURG UNIV., PA.
An investigation of the initiation stage of hot
corrosion in Ni-base alloys
[NASA-CR-159718] p0083 N80-15233
Hot corrosion of Co-Cr, Co-Cr-Al, and Ni-Cr
alloys in the temperature range of 700-750 deg C
[NASA-CR-159689] p0084 N80-26427

POLITECHNIKA LODZKA (POLAND).
Parametric instabilities of rotor-support
systems with application to industrial
ventilators
p0127 N80-29729

POWER ELECTRONICS ASSOCIATES, INC., LINCOLN, MASS.
Bi-directional four quadrant (BDQ4) power
converter development
[NASA-CR-159660] p0147 N80-14480

PRATT AND WHITNEY AIRCRAFT, EAST HARTFORD, CONN.
Development of a high strength hot isostatically
pressed /HIP/ disk alloy, MEHL 76
p0084 A80-44108

VSCE technology definition study
[NASA-CR-159730] p0027 N80-10222
Experimental evaluation of a low emissions high
performance duct burner for Variable Cycle
Engines (VCE)
[NASA-CR-159694] p0036 N80-17074
Thin film temperature sensor
[NASA-CR-159782] p0112 N80-17425
Study of blade aspect ratio on a compressor
front stage
[NASA-CR-159556] p0040 N80-25333

**PRATT AND WHITNEY AIRCRAFT GROUP, EAST HARTFORD,
CONN.**
Measuring unsteady pressure on rotating
compressor blades
p0110 A80-12630
Experimental evaluation of exhaust mixers for an
Energy Efficient Engine
[AIAA PAPER 80-1088] p0025 A80-38903
An experimental investigation of endwall
profiling in a turbine vane cascade
[AIAA PAPER 80-1089] p0004 A80-38904
Development of improved-durability plasma
sprayed ceramic coatings for gas turbine engines
[AIAA PAPER 80-1193] p0089 A80-38963
Performance of annular prediffuser-combustor
systems
[ASME PAPER 80-GT-15] p0026 A80-42154
Results from tests on a high work transonic
turbine for an energy efficient engine
[ASME PAPER 80-GT-146] p0026 A80-42258
JT9D-7A /SP/ jet engine performance
deterioration trends
p0026 A80-44230
Effect of time dependent flight loads on JT9D-7
performance deterioration
[NASA-CR-159681] p0134 N80-10515
Design, durability and low cost processing
technology for composite fan exit guide vanes
[NASA-CR-159677] p0027 N80-12091
Expanded study of feasibility of measuring
in-flight 747/JT9D loads, performance,
clearance, and thermal data
[NASA-CR-159717] p0036 N80-16063
Some considerations of the performance of two
honeycomb gas path seal material systems
[NASA-TN-81398] p0077 N80-16143
Core compressor exit stage study. 1:
Aerodynamic and mechanical design
[NASA-CR-159714] p0037 N80-19113
JT9D-7A (SP) jet engine performance
deterioration trends
[NASA-TN-81459] p0016 N80-20274

Manufacture of low carbon astrology turbine disk
shapes by hot isostatic pressing. Volume 2,
project 1
[NASA-CR-135410] p0037 N80-21329
Development of improved high pressure turbine
outer gas path seal components
[NASA-CR-159801] p0038 N80-21332
Performance deterioration based on existing
(historical) data; JT9D jet engine diagnostics
program
[NASA-CR-135448] p0038 N80-22324
Core compressor exit stage study, 2
[NASA-CR-159812] p0039 N80-23312
Engine component improvement: Performance
improvement, JT9D-7 3.8 AR fan
[NASA-CR-159806] p0039 N80-25332
Performance deterioration based on in-service
engine data: JT9D jet engine diagnostics
program
[NASA-CR-159525] p0040 N80-25340
Experimental aerodynamic and acoustic model
testing of the Variable Cycle Engine (VCE)
testbed coannular exhaust nozzle system
[NASA-CR-159710] p0040 N80-26300
Experimental aerodynamic and acoustic model
testing of the Variable Cycle Engine (VCE)
testbed coannular exhaust nozzle system:
Comprehensive data report
[NASA-CR-159711] p0040 N80-26301
The broadened-specification fuels combustion
technology program at Pratt and Whitney Aircraft
p0042 N80-29315

**PRATT AND WHITNEY AIRCRAFT GROUP, WEST PALM BEACH,
FLA.**
Laser-optical blade tip clearance measurement
system
p0111 A80-36137
Distribution analysis for F100(3) engine
[NASA-CR-159754] p0036 N80-17073
Data analysis of P sub T/P sub S noseboom probe
testing on F100 engine P680072 at NASA Lewis
Research Center
[NASA-CR-159816] p0038 N80-21334
Evaluation of the cyclic behavior of aircraft
turbine disk alloys, part 2
[NASA-CR-165123] p0084 N80-30482

PRC SYSTEMS SERVICES CO., HUNTSVILLE, ALA.
Design, performance and life cycle cost
relationships for a 500kW space solar array
p0065 A80-48356
Solar array subsystems study
[NASA-CR-159857] p0151 N80-24742

PURDUE UNIV., LAFAYETTE, IND.
Atomization of broad specification aircraft fuels
p0043 N80-29318

R

RASON ASSOCIATES, INC., SUNNYVALE, CALIF.
A cesium TELEC experiment at Lewis Research Center
[NASA-CR-159729] p0113 N80-14386

ROCHESTER INST. OF TECH., N. Y.
Development of flexible rotor balancing criteria
[NASA-CR-159506] p0129 N80-32720

ROCKETDYNE, CANOGA PARK, CALIF.
Liquid oxygen/liquid hydrogen auxiliary power
system thruster investigation
[NASA-CR-159674] p0062 N80-15202
Advanced cooling techniques for high-pressure
hydrocarbon-fueled engines
[NASA-CR-159790] p0061 N80-17141
Small, high pressure liquid hydrogen turbopump
[NASA-CR-159821] p0125 N80-26662
LEO-to-GEO low thrust chemical propulsion
p0063 N80-30384

ROCKWELL INTERNATIONAL CORP., CANOGA PARK, CALIF.
Advanced cooling techniques for high-pressure,
hydrocarbon-fueled rocket engines
[AIAA PAPER 80-1266] p0060 A80-38994

ROCKWELL INTERNATIONAL CORP., PITTSBURGH, PA.
Low-thrust chemical propulsion
p0063 N80-31468
Solar rocket system concept analysis
p0064 N80-31470

S

SCIENCE APPLICATIONS, INC., VIENNA, VA.

Negative streamer development in PEP teflon
p0179 A80-19776

SCIENTIFIC RESEARCH ASSOCIATES, INC., GLASTONBURY, CONN.

Computation of three-dimensional viscous
supersonic flow in inlets
[AIAA PAPER 80-0194] p0065 A80-23941

A three-dimensional turbulent compressible
subsonic duct flow analysis for use with
constructed coordinate systems
[AIAA PAPER 80-1398] p0006 A80-41601

Development of a three-dimensional supersonic
inlet flow analysis
[NASA-CR-3218] p0108 A80-14356

SIGMA RESEARCH, INC., RICHLAND, WASH.

Two-phase working fluids for the temperature
range of 50 to 350 deg, phase 2
[NASA-CR-159847] p0108 A80-23599

SKP INDUSTRIES, INC., KING OF PRUSSIA, PA.

Load support system analysis high speed input
pinion configuration
[ASME PAPER 79-LUB-34] p0129 A80-14760

High speed cylindrical rolling element bearing
analysis 'CYBEAM' - Analytic formulation
[ASME PAPER 79-LUB-35] p0129 A80-14761

SOLAR TURBINES INTERNATIONAL, SAN DIEGO, CALIF.

Thick ceramic coating development for industrial
gas turbines - A program plan
[SR79-M-4702-05] p0091 A80-10042

Advanced ceramic material for high temperature
turbine tip seals
[NASA-CR-159774] p0038 A80-22325

SOLAREX CORP., ROCKVILLE, MD.

Economical space power systems
[NASA-CR-159696] p0147 A80-15559

SOUTHAMPTON UNIV. (ENGLAND).

Selected data from a transonic flexible walled
test section
[NASA-CR-159360] p0047 A80-32404

SOUTHWEST RESEARCH INST., SAN ANTONIO, TEX.

Effect of fuel molecular structure on soot
formation in gas turbine engines
[ASME PAPER 80-GT-62] p0095 A80-42192

Prediction of fragment velocities and trajectories
p0096 A80-16210

Fuel quality combustion analysis
[NASA-CR-159721] p0094 A80-19284

Effect of fuel molecular structure on soot
formation in gas turbine combustion
p0043 A80-29322

Field verification of lateral-torsional coupling
effects on rotor instabilities in centrifugal
compressors
p0125 A80-29708

SPECTROLAB, INC., SYLMAR, CALIF.

Development of improved wraparound contacts for
silicon
[NASA-CR-159748] p0148 A80-18554

Screen printing technology applied to silicon
solar cell fabrication
[NASA-CR-159789] p0153 A80-27808

Coplanar back contacts for thin silicon solar
cells
[NASA-CR-159811] p0153 A80-28860

SPIRE CORP., BEDFORD, MASS.

Study program to improve the open-circuit
voltage of low resistivity single crystal
silicon solar cells
[NASA-CR-159833] p0150 A80-22775

STANFORD UNIV., CALIF.

Evaluation of a strained-coordinate perturbation
procedure - Nonlinear subsonic and transonic
flows
[AIAA PAPER 80-0339] p0006 A80-18324

Full-coverage film cooling. I - Comparison of
heat transfer data for three injection angles
[ASME PAPER 80-GT-43] p0108 A80-42176

Full-coverage film cooling. II - Heat transfer
data and numerical simulation
[ASME PAPER 80-GT-44] p0109 A80-42177

STANITZ (JOHN D.), UNIVERSITY HEIGHTS, OHIO.

General design method for three-dimensional
potential flow fields. 1: Theory
[NASA-CR-3288] p0005 A80-29251

STATE UNIV. OF NEW YORK, ALBANY.

Comments on 'Experimental evidence for
interhemispheric transport from airborne
carbon monoxide measurements'
p0159 A80-32520

STATE UNIV. OF NEW YORK AT BUFFALO.

Experimental and theoretical investigation for
the suppression of the planar arc drop in the
thermionic converter
[NASA-CR-159611] p0176 A80-12880

STUTTGART UNIV. (WEST GERMANY).

Flow induced spring coefficients of labyrinth
seals for application in rotor dynamics
p0126 A80-29717

SUNDSTRAND CORP., ROCKFORD, ILL.

The 15 kW sub e (nominal) solar thermal electric
power conversion concept definition study:
Steam Rankine turbine system
[NASA-CR-159589] p0148 A80-16493

SUSSEX UNIV., BRIGHTON (ENGLAND).

On the role of oil-film bearings in promoting
shaft instability: Some experimental
observations
p0127 A80-29726

SYRACUSE UNIV., N. Y.

Modelling of crack tip deformation with finite
element method and its applications
p0130 A80-13503

SYSTEMS RESEARCH LABS., INC., DAYTON, OHIO.

Characterization and properties of controlled
nucleation thermochemical deposited /CMTD/
silicon carbide
p0089 A80-13063

SYSTEMS SCIENCE AND SOFTWARE, LA JOLLA, CALIF.

Plasma collection by high voltage spacecraft at
low earth orbit
[AIAA PAPER 80-0042] p0055 A80-18249

Photoelectron charge density and transport near
differentially charged spacecraft
p0053 A80-19773

A three-dimensional spacecraft-charging computer
code
p0055 A80-46891

T

TECHNICAL REPORT SERVICES, ROCKY RIVER, OHIO.

Evaluation of feasibility of prestressed
concrete for use in wind turbine blades
[NASA-CR-159725] p0147 A80-15553

TECHNICAL UNIV. OF DENMARK, COPENHAGEN.

Effect of fluid forces on rotor stability of
centrifugal compressors and pumps
p0126 A80-29720

TECHNION - ISRAEL INST. OF TECH., HAIFA.

Modified face seal for positive film stiffness
[NASA-CASE-LEW-12989-1] p0114 A80-12414

TECHNISCHE UNIVERSITAET, MUNICH (WEST GERMANY).

Self-excited rotor whirl due to tip-seal leakage
forces
p0127 A80-29723

TELEDYNE CONTINENTAL MOTORS, MUSKOGEE, MICH.

A 150 and 300 kW lightweight diesel aircraft
engine design study
[NASA-CR-3260] p0037 A80-20271

Design study: A 186 kW lightweight diesel
aircraft engine
[NASA-CR-3261] p0038 A80-22326

TENNESSEE TECHNOLOGICAL UNIV., COOKEVILLE.

Analysis of combustion instability in liquid
fuel rocket motors
[NASA-CR-159733] p0061 A80-13164

Stability analysis of a liquid fuel annular
combustion chamber
[NASA-CR-159734] p0061 A80-13165

Amplification of Reynolds number dependent
processes by wave distortion
[NASA-CR-159732] p0075 A80-13193

TENNESSEE UNIV., KNOXVILLE.

Griffith diffusers
p0006 A80-20748

TENNESSEE UNIV. SPACE INST., TULLAHOA.

Aerodynamic analysis of a supersonic cascade
vibrating in a complex mode
p0007 A80-45841

TEXAS A&M UNIV., COLLEGE STATION.

Testing of turbulent seals for rotodynamic coefficients
p0126 N80-29714
Experimental results concerning centrifugal impeller excitations
p0127 N80-29727

TEXAS INSTRUMENTS, INC., DALLAS.

Spectral effects on direct-insolation absorptance of five collector coatings
[ASME PAPER 79-HT-18]
p0146 A80-45722

TEXAS UNIV., AUSTIN.

The effect of a weak vertical magnetic field on fluctuation-induced transport in a Bumpy-Torus plasma
p0176 A80-25476

THREE E VEHICLES, SAN DIEGO, CALIF.

The performance and efficiency of four motor/controller/battery systems for the simpler electric vehicles
[NASA-CR-159776]
p0103 N80-24550

TOKYO UNIV. (JAPAN).

Fluid forces on rotating centrifugal impeller with whirling motion
p0127 N80-29724

TOLEDO UNIV., OHIO.

Identification and dual adaptive control of a turbojet engine
p0023 A80-10033

A new traffic control design method for large networks with signalized intersections
p0183 A80-14841

Examination of the flap-lag stability of rigid articulated rotor blades
p0010 A80-15123

Dispersion of sound in a combustion duct by fuel droplets and soot particles
p0170 A80-20953

Combustion of solid carbon rods in zero and normal gravity
p0074 A80-20955

Marangoni bubble motion in zero gravity
p0107 A80-20958

Spectral structure of pressure measurements made in a combustion duct
p0171 A80-35496

Nonlinear aeroelastic equations of motion of twisted, nonuniform, flexible horizontal-axis wind turbine blades
[NASA-CR-159502]
p0152 N80-26774

TRW DEFENSE AND SPACE SYSTEMS GROUP, REDONDO BEACH, CALIF.

Evaluation of particle transport for the P80-1 spacecraft
[AIAA PAPER 79-2047]
p0055 A80-13301

An adaptive-control switching buck regulator - Implementation, analysis, and design
p0103 A80-28167

Modeling and analysis of Power Processing Systems
p0066 A80-28894

An advanced mixed user domestic satellite system architecture
[AIAA 80-0494]
p0099 A80-29544

Power processing technology for spacecraft primary ion propulsion
p0065 A80-48265

Specific spacecraft evaluation: Special report
[NASA-CR-159420]
p0060 N80-11137

Heat pipe cooled power magnetics
[NASA-CR-159659]
p0103 N80-13362

Analyses of moisture in polymers and composites
[NASA-CR-159745]
p0091 N80-15264

Depriming of arterial heat pipes: An investigation of CTS thermal excursions
[NASA-CR-165153]
p0108 N80-32688

TRW EQUIPMENT LABS., CLEVELAND, OHIO.

Second generation FMR polyimide/fiber composites
[NASA-CR-159666]
p0072 N80-12118

TRW, INC., CLEVELAND, OHIO.

Tungsten wire/FcCrAlY matrix turbine blade fabrication study
[NASA-CR-159788]
p0044 N80-29331

Cost analysis of composite fan blade manufacturing processes
[NASA-CR-159876]
p0044 N80-31398

TRW, INC., REDONDO BEACH, CALIF.

Heat pipe cooling of power processing magnetics
[AIAA PAPER 79-2082]
p0107 A80-20960

Multigigabit satellite on-board signal processing
[AIAA 80-0583]
p0100 A80-29605

The 30/20 GHz mixed user architecture development study
[NASA-CR-159686]
p0097 N80-10415

The 30/20 GHz mixed user architecture development study: Executive summary
[NASA-CR-159687]
p0097 N80-10416

TURBO RESEARCH, INC., LYONVILLE, PA.

Vibration exciting mechanisms induced by flow in turbomachine stages
p0127 N80-29722

TUTNILL PUMP CO., SAN RAFAEL, CALIF.

Evaluation of feasibility of prestressed concrete for use in wind turbine blades
[NASA-CR-159725]
p0147 N80-15553

U

UNITED AIR LINES, INC., CHICAGO, ILL.

Current jet fuel trends
p0041 N80-29303

UNITED TECHNOLOGIES CORP., EAST HARTFORD, CONN.

External fuel vaporization study, phase 1
[NASA-CR-159850]
p0095 N80-25453

UNITED TECHNOLOGIES CORP., SOUTH WINDSOR, CONN.

Advanced technology light weight fuel cell program
[NASA-CR-159807]
p0149 N80-19615

Cogeneration technology alternatives study. Volume 1: Summary report
[NASA-CR-159759]
p0152 N80-25792

Cogeneration technology alternatives study. Volume 2: Industrial process characteristics
[NASA-CR-159760]
p0152 N80-25793

Cogeneration technology alternatives study. Volume 4: Heat Sources, balance of plant and auxiliary systems
[NASA-CR-159762]
p0152 N80-25794

Cogeneration technology alternatives study. Volume 6: Computer data
[NASA-CR-159764]
p0152 N80-25795

Cogeneration Technology Alternatives Study (CTAS). Volume 3: Energy conversion system characteristics
[NASA-CR-159761]
p0155 N80-31869

UNITED TECHNOLOGIES RESEARCH CENTER, EAST HARTFORD, CONN.

Development of silicon nitride of improved toughness
[NASA-CR-159676]
p0072 N80-10319

Study of the effects of gaseous environments on the hot corrosion of superalloy materials
[NASA-CR-159747]
p0083 N80-18155

Experimental study of turbine fuel thermal stability in an aircraft fuel system simulator
p0043 N80-29325

Autoignition characteristics of aircraft-type fuels
[NASA-CR-159886]
p0095 N80-30535

Influence of mistuning on blade torsional flutter
[NASA-CR-165137]
p0005 N80-31351

Design, fabrication and testing of an optical temperature sensor
[NASA-CR-165125]
p0112 N80-31777

V

VIRGINIA POLYTECHNIC INST. AND STATE UNIV., BLACKSBURG.

An adaptive-control switching buck regulator - Implementation, analysis, and design
p0103 A80-28167

Modeling and analysis of Power Processing Systems
p0066 A80-28894

A comparison of experiment and theory for sound propagation in variable area ducts
p0173 A80-45844

VIRGINIA UNIV., CHARLOTTESVILLE.

Instability thresholds for flexible rotors in hydrodynamic bearings
p0128 N80-29730

Stabilization of aerodynamically excited turbomachinery with hydrodynamic journal bearings and supports
p0128 N80-29731

Feasibility of active feedback control of
rotordynamic instability

p0128 N80-29733

VOUGHT CORP., DALLAS, TEX.

Low speed test of the aft inlet designed for a
tandem fan V/STOL nacelle
[NASA-CR-159752]

p0037 N80-18042

W

WATKINS-JOHNSON CO., PALO ALTO, CALIF.

Life test studies on tungsten impregnated cathodes
p0103 A80-45122

WESTERN GEAR CORP., LYNNWOOD, CALIF.

Analytical and experimental spur gear tooth
temperature as affected by operating variables
p0123 A80-46412

WESTERN UNION TELEGRAPH CO., UPPER SADDLE RIVER, N.J.

The 18/30 GHz fixed communications system

service demand assessment. Volume 1:

Executive summary

[NASA-CR-159546] p0099 N80-22547

The 18/30 GHz fixed communications system

service demand assessment. Volume 2: Main text

[NASA-CR-159547] p0099 N80-22548

The 30/20 GHz fixed communications systems

service demand assessment. Volume 3:

Appendices

[NASA-CR-159548] p0099 N80-22549

WESTINGHOUSE ELECTRIC CORP., PITTSBURGH, PA.

Evaluation of present-day thermal barrier
coatings for industrial/utility applications
p0092 A80-39637

WESTINGHOUSE RESEARCH AND DEVELOPMENT CENTER,
PITTSBURGH, PA.

Silicone modified resins for graphite fiber

laminates

[NASA-CR-159750] p0072 N80-22407

Cell module and fuel conditioner development

[NASA-CR-159828] p0150 N80-23768

Cell module and fuel conditioner

[NASA-CR-159888] p0155 N80-31882

WICHITA STATE UNIV., KANS.

Feasibility study of aileron and spoiler control

systems for large horizontal axis wind turbines

[NASA-CR-159856] p0153 N80-27803

WILLIAMS RESEARCH CORP., WALLED LAKE, WICH.

Conceptual design study of an improved gas

turbine powertrain

[NASA-CR-159852] p0039 N80-23315

X

XEROX CORP., EL SEGUNDO, CALIF.

High speed cylindrical rolling element bearing

analysis 'CYBEAN' - Analytic formulation

[ASME PAPER 79-LUB-35] p0129 A80-14761

XEROX ELECTRO-OPTICAL SYSTEMS, PASADENA, CALIF.

Preliminary results of the mission profile life

test of a 30 cm Hg bombardment thruster

[AIAA PAPER 79-2078] p0081 A80-10391

An electric propulsion long term test facility

[AIAA PAPER 79-2080] p0049 A80-13308

Inert gas ion thruster development

[NASA-CR-159805] p0062 N80-27424

Y

YALE UNIV., NEW HAVEN, CONN.

Theory of deposition of condensible impurities

on surfaces immersed in combustion gases

[NASA-CR-159716] p0033 N80-15130

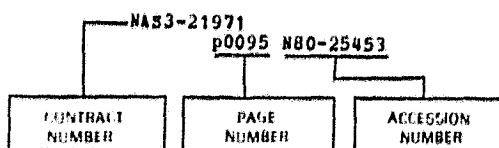
Experimental studies of the formation/deposition

of sodium sulfate in/from combustion gases

[NASA-CR-159753] p0033 N80-15131

CONTRACT NUMBER INDEX

Typical Contract Number Index Listing



Listings in this index are arranged alphabetically by contract number. Under each contract number, the accession numbers denoting documents that have been produced as a result of research done under that contract are arranged in ascending order with the FAA accession numbers appearing first. Preceding the accession number is the page number in the abstract section in which the citation may be found.

ACUREX PROJ. 6497
p0029 N80-14182
AF PROJ. 3066
p0079 N80-26433
AF PROJ. 8680
p0098 N80-12260
p0098 N80-12261
DA PROJ. 1L1-61102-AH-45
p0004 N80-17995
DAAG29-77-C-0009
p0128 N80-29731
DAAK11-78-M-0007
p0075 A80-11754
DE-AB29-76ET-20370
p0130 N80-15422
DE-AB29-76ET-20370
p0137 N80-10594
DE-AC01-79ET-13151
p0128 N80-29730
p0128 N80-29733
DE-AC02-76CS-52749
p0124 N80-24621
DE-AI01-79ET-20305
p0151 N80-24758
p0152 N80-26775
p0156 N80-33862
DE-AI01-79ET-20307
p0151 N80-24751
DE-AI01-79ET-20485
p0096 N80-13317
p0138 N80-15561
DE-AI01-79ET-23139
p0144 N80-32858
DE-AI03-79ET-11272
p0150 N80-23768
p0142 N80-23769
p0155 N80-31882
DEN3-1 p0147 N80-12551
DEN3-2 p0151 N80-24758
p0152 N80-26775
DEN3-8 p0184 N80-25209
p0185 N80-30228
DEN3-12 p0039 N80-23315
DEN3-27 p0092 A80-35575
p0091 N80-31552
DEN3-30 p0152 N80-25792
p0152 N80-25793
p0152 N80-25794
p0152 N80-25795
p0155 N80-31869
DEN3-31 p0151 N80-24797
p0143 N80-28859
p0154 N80-30888
p0154 N80-30889
p0155 N80-30890
p0155 N80-31870
p0155 N80-33859
p0156 N80-33860
p0156 N80-33861
DEN3-32 p0183 N80-13989

DEN3-38 p0154 N80-29857
DEN3-39 p0149 N80-18562
DEN3-43 p0091 N80-26448
DEN3-48 p0184 N80-23216
DEN3-51 p0149 N80-18559
DEN3-52 p0156 A80-25099
p0152 N80-26779
DEN3-54 p0090 N80-15263
DEN3-56 p0150 N80-22787
DEN3-61 p0140 N80-16493
DEN3-62 p0148 N80-16491
DEN3-63 p0149 N80-19612
DEN3-67 p0147 N80-10603
DEN3-69 p0150 N80-22778
DEN3-78 p0184 N80-18991
DEN3-81 p0184 N80-17916
DEN3-84 p0184 N80-18992
DEN3-86 p0148 N80-16483
DEN3-91 p0184 N80-26212
DEN3-96 p0153 N80-28866
DEN3-98 p0148 N80-17543
DEN3-109 p0091 A80-10042
DEN3-114 p0124 N80-22702
DEN3-116 p0185 N80-32299
DEN3-117 p0124 N80-25661
DEN3-124 p0185 N80-28255
p0128 N80-31795
p0128 N80-31796
DEN3-130 p0103 N80-24550
DEN3-134 p0156 N80-33862
DEN3-161 p0150 N80-23768
p0142 N80-23769
p0155 N80-31882
DEN3-165 p0142 N80-23778
DEN3-168 p0129 A80-35574

DEN3-190 p0146 A80-48194
p0142 N80-22797
E(49-26)-1059 p0137 N80-13623
EC-77-A-29-1010 p0147 N80-11558
EC-77-A-31-1002 p0141 N80-22777
EC-77-A-31-1011 p0184 N80-18991
p0183 N80-28254
EC-77-A-31-1034 p0138 N80-15560
p0149 N80-18562
p0140 N80-18563
p0151 N80-24759
p0143 N80-25779
p0153 N80-28866
EC-77-A-31-1040 p0133 A80-46032
p0183 N80-13989
p0115 N80-17467
p0140 N80-18564
p0016 N80-20272
p0183 N80-21201
p0039 N80-23315
p0142 N80-23779
p0124 N80-24620
p0091 N80-26448
p0106 N80-29624
p0144 N80-29863
p0091 N80-31552
p0080 N80-32488
p0128 N80-32719
EC-77-A-31-1044 p0146 A80-48329
p0101 N80-13361
p0165 N80-16824
p0184 N80-17916
p0184 N80-18992
p0184 N80-21202
p0124 N80-22702
p0103 N80-24550
p0143 N80-24756
p0124 N80-25661
p0143 N80-25780
p0184 N80-26212
p0143 N80-27805
p0185 N80-28255
p0185 N80-30228
p0128 N80-31795
p0128 N80-31796
p0185 N80-32299
EC-77-A-31-1062 p0137 N80-13624
p0141 N80-19626
p0175 N80-22083
p0152 N80-25792
p0152 N80-25793
p0152 N80-25794
p0152 N80-25795
p0155 N80-31869
p0175 N80-33221
EC-77-C-31-1044 p0184 N80-23216
EF-76-S-01-2479 p0128 N80-29731
EF-77-A-01-2593 p0076 N80-10344
p0157 N80-13721
p0137 N80-14493
p0076 N80-15235
p0077 N80-18157
p0078 N80-21492
p0141 N80-21837
p0141 N80-22776
p0151 N80-24748
p0143 N80-27804
p0080 N80-33556
EF-77-A-01-2674 p0137 N80-10595
p0175 N80-14922
p0149 N80-18559
p0142 N80-23778

p0152 N80-26779
p0143 N80-27799
p0144 N80-29862
EF-77-A-31-1002 p0142 N80-23777
EF-77-A-31-1011 p0117 N80-21754
EF-77-A-31-2674 p0142 N80-23780
ET-78-G-01-3642 p0075 A80-11754
EX-76-A-29-1060 p0139 N80-16490
p0148 N80-16491
p0148 N80-16493
p0149 N80-19612
p0150 N80-22778
p0150 N80-22787
EX-76-I-01-1028 p0147 N80-15553
p0148 N80-17548
p0140 N80-19613
p0152 N80-26774
p0153 N80-27803
EX-77-A-29-1010 p0139 N80-16494
p0149 N80-18565
p0140 N80-19614
p0150 N80-20864
p0150 N80-23775
EX-76-C-02-2749 p0123 N80-17470
p0124 N80-24620
p0128 N80-32719
F04611-79-C-0007 p0064 N80-31470
F04611-79-C-0032 p0063 N80-31455
F04701-79-C-0080 p0055 A80-45609
F19628-79-C-0001 p0098 N80-12260
p0098 N80-12261
19628-80-C-0001 p0099 N80-24514
F33615-74-C-2039 p0006 A80-20748
JPL PROJ. 5104-61 p0151 N80-24751
JPL-955223 p0103 N80-11328
NASA ORDER C-25906 p0147 N80-15553
NASA ORDER C-33350-D p0066 N80-33478
NAS3-13486 p0006 A80-20748
NAS3-14336 p0108 A80-42176
p0109 A80-42177
NAS3-14383 p0065 A80-48265
NAS3-17787 p0084 N80-25415
NAS3-18021 p0028 N80-14115
p0028 N80-14116
p0028 N80-14117
p0028 N80-14118
p0029 N80-14119
p0029 N80-14120
p0033 N80-15083
p0034 N80-15084
p0034 N80-15085
p0034 N80-15086
p0034 N80-15088
p0034 N80-15089
p0034 N80-15090
p0034 N80-15091
p0035 N80-15092
p0035 N80-15093
p0035 N80-15094
p0035 N80-15095
p0035 N80-15096
p0035 N80-15097

CONTRACT NUMBER INDEX

p0035 N80-15098
p0035 N80-15099
p0034 N80-15100
p0034 N80-15100
p0030 N80-15101
p0030 N80-15101
p0030 N80-15102
p0030 N80-15103
p0030 N80-15104
p0030 N80-15105
p0030 N80-15106
p0030 N80-15107
p0031 N80-15108
p0031 N80-15109
p0031 N80-15110
p0031 N80-15111
p0031 N80-15112
p0031 N80-15113
p0031 N80-15114
p0032 N80-15115
p0032 N80-15116
p0032 N80-15117
p0032 N80-15118
p0032 N80-15119
p0032 N80-15120
p0032 N80-15121
p0033 N80-15122
p0033 N80-15123
p0033 N80-15124
p0033 N80-15125
p0033 N80-15126
p0044 N80-29297
p0044 N80-29298
NAS3-18546
p0092 A80-15720
p0134 N80-22733
NAS3-18553
p0173 A80-45844
NAS3-18924
p0065 A80-48265
NAS3-19416
p0075 A80-35908
p0151 N80-24748
NAS3-19442
p0038 N80-21334
NAS3-19690
p0066 A80-28894
NAS3-19696
p0037 N80-21330
NAS3-19745
p0095 N80-31619
NAS3-19754
p0029 N80-14130
NAS3-20054
p0123 N80-16338
NAS3-20055
p0007 A80-45841
p0040 N80-25335
NAS3-20057
p0029 N80-14129
NAS3-20058
p0147 N80-11558
p0149 N80-18565
p0150 N80-20864
p0150 N80-23775
NAS3-20061
p0040 N80-26300
p0040 N80-26301
NAS3-20065
p0148 N80-18554
NAS3-20066
p0095 N80-30535
NAS3-20068
p0129 A80-14761
NAS3-20072
p0084 A80-44108
p0037 N80-21329
NAS3-20073
p0084 A80-45825
p0083 N80-14235
NAS3-20074
p0084 N80-28499
NAS3-20081
p0038 N80-22325
NAS3-20082
p0123 N80-13474
NAS3-20088
p0072 N80-10318
NAS3-20092
p0060 A80-38908
p0062 N80-19185

NAS3-20093
p0083 N80-13218
NAS3-20102
p0103 A80-28167
NAS3-20119
p0065 A80-46901
NAS3-20290
p0029 N80-14182
NAS3-20373
p0062 N80-15202
NAS3-20391
p0044 N80-29331
NAS3-20399
p0049 A80-13308
NAS3-20403
p0065 A80-48265
NAS3-20406
p0091 N80-15264
NAS3-20407
p0072 N80-25382
NAS3-20497
p0096 N80-16210
NAS3-20578
p0037 N80-19113
p0039 N80-23312
NAS3-20585
p0037 N80-21331
NAS3-20590
p0038 N80-21332
NAS3-20596
p0147 N80-15553
NAS3-20600
p0148 N80-17548
NAS3-20602
p0036 N80-17074
NAS3-20612
p0124 N80-22700
NAS3-20614
p0045 A80-35958
p0172 A80-35965
p0172 N80-13882
p0039 N80-23311
NAS3-20629
p0029 N80-14127
p0039 N80-23309
p0040 N80-26302
NAS3-20630
p0039 N80-25332
NAS3-20631
p0039 N80-23316
p0041 N80-27364
NAS3-20632
p0134 N80-10515
p0036 N80-16063
p0038 N80-22324
p0040 N80-25340
NAS3-20643
p0045 A80-41506
p0045 N80-33408
NAS3-20646
p0004 A80-38904
p0026 A80-42258
NAS3-20768
p0112 N80-17425
NAS3-20794
p0141 N80-22777
NAS3-20797
p0173 A80-38642
p0172 N80-11870
p0172 N80-32186
NAS3-20801
p0037 N80-21328
NAS3-20806
p0148 N80-17547
NAS3-20808
p0041 N80-27361
NAS3-20809
p0040 N80-25333
NAS3-20814
p0044 N80-29330
NAS3-20820
p0028 N80-13048
NAS3-20823
p0150 N80-22775
NAS3-20826
p0153 N80-27808
NAS3-20830
p0037 N80-20271
p0038 N80-22326
NAS3-20835
p0036 N80-17073

NAS3-20836
p0006 A80-18324
NAS3-20839
p0129 A80-14760
NAS3-21003
p0065 A80-23941
p0108 N80-14356
NAS3-21008
p0125 N80-26662
NAS3-21029
p0061 N80-14189
NAS3-21037
p0027 N80-12091
NAS3-21038
p0036 N80-18041
NAS3-21040
p0064 A80-20962
p0061 N80-13158
NAS3-21047
p0055 A80-13301
p0060 N80-11137
NAS3-21051
p0103 A80-28167
NAS3-21135
p0004 N80-10134
NAS3-21149
p0113 N80-14386
NAS3-21202
p0108 N80-23599
NAS3-21238
p0028 N80-13043
p0028 N80-13044
NAS3-21251
p0153 N80-28860
NAS3-21257
p0149 N80-19615
NAS3-21260
p0036 N80-16061
p0036 N80-16062
NAS3-21263
p0123 N80-15411
NAS3-21267
p0045 A80-27737
NAS3-21280
p0154 N80-29852
NAS3-21285
p0045 A80-38982
NAS3-21311
p0075 A80-11754
NAS3-21345
p0062 N80-27424
NAS3-21346
p0062 N80-16096
NAS3-21349
p0072 N80-12118
NAS3-21352
p0044 N80-31398
NAS3-21353
p0147 N80-15559
NAS3-21358
p0064 A80-13311
NAS3-21359
p0099 N80-22547
p0099 N80-22548
p0099 N80-22549
NAS3-21362
p0050 A80-35329
p0098 N80-11277
p0098 N80-11278
p0098 N80-11279
NAS3-21364
p0099 A80-29574
NAS3-21365
p0098 N80-12259
NAS3-21366
p0098 N80-18262
p0098 N80-18263
p0099 N80-18264
NAS3-21368
p0091 N80-17221
NAS3-21371
p0073 N80-29430
NAS3-21372
p0065 A80-48265
NAS3-21373
p0072 N80-22407
NAS3-21374
p0090 N80-13257
NAS3-21375
p0072 N80-10319

NAS3-21376
p0083 N80-18155
NAS3-21377
p0092 A80-39637
NAS3-21378
p0179 A80-19776
NAS3-21379
p0084 N80-30482
NAS3-21381
p0060 A80-38994
p0061 N80-17141
NAS3-21383
p0073 A80-32064
NAS3-21385
p0073 A80-32063
NAS3-21389
p0027 N80-10222
NAS3-21461
p0004 A80-41203
NAS3-21468
p0037 N80-18042
NAS3-21581
p0108 N80-10460
NAS3-21582
p0108 N80-19450
NAS3-21587
p0095 A80-42192
p0094 N80-19284
NAS3-21591
p0054 A80-38909
NAS3-21593
p0043 N80-29325
NAS3-21603
p0005 N80-31351
NAS3-21605
p0005 N80-29251
NAS3-21606
p0159 A80-32520
NAS3-21609
p0004 N80-17995
p0005 N80-26274
NAS3-21623
p0128 N80-32718
NAS3-21714
p0158 N80-18586
NAS3-21719
p0045 A80-50191
NAS3-21735
p0006 A80-41601
NAS3-21740
p0108 N80-32688
NAS3-21745
p0099 A80-29588
p0050 N80-25357
NAS3-21746
p0065 A80-48265
NAS3-21750
p0049 N80-27403
NAS3-21757
p0060 A80-48357
p0153 N80-28862
p0154 N80-29845
NAS3-21762
p0055 A80-18249
p0053 A80-19773
NAS3-21763
p0010 N80-32378
NAS3-21841
p0112 N80-31777
NAS3-21926
p0065 A80-48356
p0151 N80-24742
NAS3-21933
p0099 A80-29544
p0100 A80-29605
p0097 N80-10415
p0097 N80-10416
NAS3-21935
p0048 N80-31423
p0048 N80-32412
NAS3-21940
p0063 N80-31467
NAS3-21941
p0063 N80-30384
NAS3-21952
p0063 N80-31459
NAS3-21954
p0064 N80-31469
NAS3-21955
p0063 N80-31458

CONTRACT NUMBER INDEX

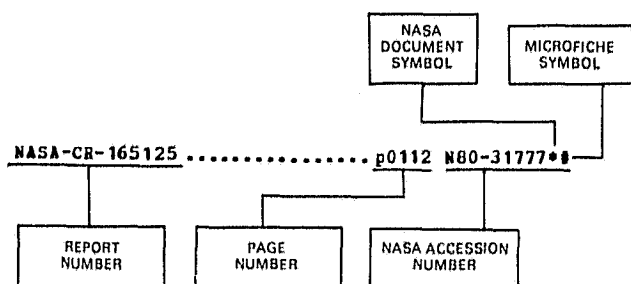
NAS3-21971
 p0095 N80-25453
 NAS3-21975
 p0172 A80-35951
 NAS3-21980
 p0036 N80-18040
 NAS3-22199
 p0005 N80-28302
 NAS3-30363
 p0147 N80-14480
 NAS3-30813
 p0147 N80-15553
 NAS7-100
 p0103 N80-11328
 p0147 N80-11566
 p0149 N80-19632
 p0151 N80-24751
 NAS8-33108
 p0126 N80-29719
 NAS12-2183
 p0065 A80-48265
 NGL-41-001-031
 p0006 A80-20748
 NGR-06-002-112
 p0061 N80-17137
 p0177 N80-26161
 p0064 N80-33476
 NGR-09-010-085
 p0171 A80-37895
 NGR-21-002-344
 p0107 A80-10039
 NGR-22-009-339
 p0038 N80-22323
 p0134 N80-27720
 p0134 N80-29762
 NGR-22-009-378
 p0010 N80-16060
 NGR-36-010-024
 p0023 A80-10033
 NGR-39-009-077
 p0075 N80-12142
 NGR-43-003-015
 p0061 N80-13164
 p0061 N80-13165
 p0075 N80-13193
 NSF ENG-78-18544
 p0075 A80-11754
 MSG-1556
 p0073 N80-29432
 MSG-3011
 p0062 N80-24362
 p0177 N80-27189
 MSG-3012
 p0005 N80-27288
 MSG-3023
 p0129 A80-14739
 MSG-3046
 p0096 N80-15300
 MSG-3072
 p0129 N80-32720
 MSG-3076
 p0095 N80-22509
 MSG-3087
 p0146 A80-45722
 MSG-3089
 p0176 A80-25476
 MSG-3091
 p0178 A80-16843
 MSG-3105
 p0128 N80-29731
 MSG-3107
 p0033 N80-15130
 MSG-3122
 p0043 N80-29327
 MSG-3138
 p0159 A80-32520
 MSG-3139
 p0152 N80-26774
 MSG-3169
 p0033 N80-15131
 MSG-3177
 p0128 N80-29730
 MSG-3184
 p0151 N80-24759
 MSG-3189
 p0006 A80-38895
 MSG-3196
 p0176 N80-14923
 p0177 N80-32223
 MSG-3197
 p0073 N80-25383

p0073 N80-25384
 MSG-3200
 p0126 N80-29714
 MSG-3214
 p0083 N80-15233
 p0084 N80-26427
 MSG-3220
 p0006 N80-32328
 MSG-3246
 p0083 A80-51573
 MSG-3247
 p0026 A80-43283
 MSG-3277
 p0153 N80-27803
 MSG-7071
 p0176 N80-12880
 MSG-7172
 p0047 N80-32404
 N00014-78-M-0053
 p0075 A80-11754
 N00140-78-C-1491
 p0041 N80-29306
 RC-A-77-6C
 p0128 N80-29730
 146-20 p0157 N80-27832
 505-01 p0086 N80-21532
 p0110 N80-25635
 p0132 N80-27719
 505-02 p0132 N80-15428
 p0132 N80-22734
 505-03 p0014 N80-14125
 p0167 N80-18882
 p0016 N80-21323
 p0169 N80-22100
 505-04 p0013 N80-11087
 p0014 N80-14124
 p0114 N80-14403
 p0015 N80-15128
 p0104 N80-15361
 p0114 N80-15410
 p0002 N80-17030
 p0015 N80-17071
 p0085 N80-17220
 p0105 N80-17397
 p0115 N80-17466
 p0116 N80-19495
 p0017 N80-21326
 p0117 N80-21753
 p0087 N80-22493
 p0105 N80-24577
 p0110 N80-24595
 p0019 N80-25337
 p0019 N80-25338
 p0020 N80-28352
 p0119 N80-29734
 p0023 N80-32396
 p0120 N80-33749
 505-04-22
 p0004 N80-17995
 505-05 p0162 N80-16742
 p0046 N80-29369
 505-05-52
 p0028 N80-13043
 p0028 N80-13044
 505-08 p0093 N80-21551
 505-32 p0003 N80-27284
 p0003 N80-33357
 p0023 N80-33410
 505-32-12
 p0005 N80-24263
 505-32-22
 p0040 N80-25333
 505-41-13-03
 p0011 N80-14110
 505-42-62
 p0037 N80-18042
 506-16 p0076 N80-11188
 p0077 N80-16141
 p0105 N80-17398
 p0085 N80-18178
 p0087 N80-22494
 p0080 N80-32489
 506-20 p0101 N80-21669
 506-21-12
 p0062 N80-15202
 506-53 p0080 N80-33555
 506-55-32
 p0062 N80-27424
 511-54-02
 p0038 N80-21332

534-03-23-01
 p0069 N80-29431
 535-01-12
 p0045 N80-33408
 650-20-16
 p0098 N80-11277
 p0098 N80-11278
 663-01 p0136 N80-20787
 769-02 p0014 N80-14121
 p0020 N80-25339
 778-17-01
 p0147 N80-10603
 778-35-03
 p0090 N80-15263

REPORT/ACCESSION NUMBER INDEX

Typical Report/Accession Number Index Listing



Listings in this index are arranged alphanumerically by report number. The page number indicates the page in the abstract section in which the citation is located. The accession number denotes the number by which the citation is identified. An asterisk (*) indicates that the item is a NASA report. A pound sign (#) indicates that the item is available on microfiche.

A-8008	p0028	N80-13041**
AAS PAPER 80-083	p0054	A80-41897**
AAS 79-247	p0097	A80-28712*
ACUREX-FR-78-284	p0029	N80-14182**
AD-A083245	p0079	N80-26433**
ADL-83381-2	p0036	N80-18040**
AER-1713	p0148	N80-16493**
AFWAL-TR-80-2013	p0079	N80-26433**
ATAA PAPER 79-2041	p0058	A80-10376**
ATAA PAPER 79-2043	p0048	A80-20961**
ATAA PAPER 79-2047	p0055	A80-13301**
ATAA PAPER 79-2061	p0058	A80-10384**
ATAA PAPER 79-2063	p0059	A80-10386**
ATAA PAPER 79-2064	p0059	A80-10387**
ATAA PAPER 79-2078	p0081	A80-10391**
ATAA PAPER 79-2079	p0064	A80-20962**
ATAA PAPER 79-2080	p0049	A80-13308**
ATAA PAPER 79-2081	p0059	A80-10392**
ATAA PAPER 79-2082	p0107	A80-20960**
ATAA PAPER 79-2103	p0064	A80-13311**
ATAA PAPER 79-2104	p0054	A80-29750**
ATAA PAPER 79-2116	p0059	A80-20959**
ATAA PAPER 80-0023	p0176	A80-18243**
ATAA PAPER 80-0042	p0055	A80-18249**
ATAA PAPER 80-0051	p0024	A80-18253**
ATAA PAPER 80-0098	p0170	A80-18269**
ATAA PAPER 80-0100	p0170	A80-20964**
ATAA PAPER 80-0164	p0171	A80-20965**
ATAA PAPER 80-0194	p0065	A80-23941**
ATAA PAPER 80-0223	p0024	A80-19300**
ATAA PAPER 80-0225	p0003	A80-20966**
ATAA PAPER 80-0227	p0003	A80-20967**
ATAA PAPER 80-0229	p0024	A80-20968**
ATAA PAPER 80-0302	p0089	A80-18303**
ATAA PAPER 80-0336	p0054	A80-29751**
ATAA PAPER 80-0339	p0006	A80-18324**
ATAA PAPER 80-0384	p0003	A80-20969**
ATAA PAPER 80-0912	p0059	A80-32886**
ATAA PAPER 80-0914	p0024	A80-32887**
ATAA PAPER 80-0946	p0181	A80-40700**
ATAA PAPER 80-0986	p0172	A80-35551**
ATAA PAPER 80-0995	p0045	A80-35958**
ATAA PAPER 80-1002	p0172	A80-35965**
ATAA PAPER 80-1008	p0027	A80-44491**
ATAA PAPER 80-1018	p0171	A80-35974**

ATAA PAPER 80-1025	p0025	A80-38640**
ATAA PAPER 80-1029	p0173	A80-38642**
ATAA PAPER 80-1042	p0171	A80-35993**
ATAA PAPER 80-1065	p0025	A80-38651**
ATAA PAPER 80-1076	p0006	A80-38895**
ATAA PAPER 80-1078	p0003	A80-38897**
ATAA PAPER 80-1086	p0025	A80-38902**
ATAA PAPER 80-1087	p0045	A80-41506**
ATAA PAPER 80-1088	p0025	A80-38903**
ATAA PAPER 80-1089	p0004	A80-38904**
ATAA PAPER 80-1095	p0060	A80-38908**
ATAA PAPER 80-1096	p0054	A80-38909**
ATAA PAPER 80-1193	p0089	A80-38963**
ATAA PAPER 80-1194	p0010	A80-41193**
ATAA PAPER 80-1196	p0025	A80-41514**
ATAA PAPER 80-1197	p0010	A80-41194**
ATAA PAPER 80-1198	p0025	A80-41515**
ATAA PAPER 80-1204	p0094	A80-41516**
ATAA PAPER 80-1223	p0060	A80-38975**
ATAA PAPER 80-1237	p0045	A80-38982**
ATAA PAPER 80-1240	p0026	A80-43283**
ATAA PAPER 80-1245	p0004	A80-41203**
ATAA PAPER 80-1260	p0060	A80-38992**
ATAA PAPER 80-1266	p0060	A80-38994**
ATAA PAPER 80-1398	p0006	A80-41601**
ATAA PAPER 80-1427	p0007	A80-44128**
ATAA PAPER 80-1871	p0045	A80-50191**
ATAA 80-0494	p0099	A80-29544**
ATAA 80-0537	p0099	A80-29574**
ATAA 80-0557	p0099	A80-29588**
ATAA 80-0582	p0050	A80-35329**
ATAA 80-0583	p0100	A80-29605**
ATAA 80-0607	p0145	A80-28804**
ATAA 80-0638	p0145	A80-28835**
ATAA 80-0642	p0145	A80-28836**
ATAA 80-0695	p0024	A80-35101**

ATAA-PAPER-80-0098	p0167	N80-12822**
ATAA-PAPER-80-0164	p0167	N80-14843**
ATAA-PAPER-80-0607	p0136	N80-18497**

AIRSEARCH-21-3071	p0037	N80-21331**
AIRSEARCH-21-3213-1	p0083	N80-14235**
AIRSEARCH-21-3469	p0084	A80-45825**
AIRSEARCH-31-3328	p0150	N80-22778**
AIRSEARCH-31-3542	p0092	A80-35575**
AIRSEARCH-31-3575A	p0091	N80-31552**
AIRSEARCH-79-16182	p0183	N80-17916**
AIRSEARCH-79-16430	p0184	N80-26212**

AMD-0001	p0073	N80-29430**
----------------	-------	-------------

ASLE PREPRINT 79-AM-1B-1	p0088	A80-12089*
ASLE PREPRINT 79-AM-3B-1	p0088	A80-12094*
ASLE PREPRINT 79-LC-1A-3	p0102	A80-14720*
ASLE PREPRINT 79-LC-3B-2	p0120	A80-14727*
ASLE PREPRINT 79-LC-5C-1	p0120	A80-14734*
ASLE PREPRINT 80-AM-3E-1	p0122	A80-43163*
ASLE PREPRINT 80-AM-3E-2	p0122	A80-43167*
ASLE PREPRINT 80-AM-3E-3	p0122	A80-43159*
ASLE PREPRINT 80-AM-6C-2	p0122	A80-43176*

ASME PAPER 79-DET-57	p0092	A80-15720**
ASME PAPER 79-DET-88	p0121	A80-15736**
ASME PAPER 79-HT-18	p0146	A80-45722**
ASME PAPER 79-LUB-4	p0129	A80-14739**
ASME PAPER 79-LUB-34	p0129	A80-14760**
ASME PAPER 79-LUB-35	p0129	A80-14761**
ASME PAPER 79-WA/GT-7	p0107	A80-18638**
ASME PAPER 79-WA/HT-17	p0180	A80-18630**
ASME PAPER 80-GT-4	p0004	A80-42145**
ASME PAPER 80-GT-6	p0025	A80-42147**
ASME PAPER 80-GT-15	p0026	A80-42154**
ASME PAPER 80-GT-30	p0026	A80-42164**
ASME PAPER 80-GT-43	p0108	A80-42176**

REPORT/ACCESSION NUMBER INDEX

ASME PAPER 80-GT-44	p0109	A80-42177*	DOE/NASA/0062-79/1	p0148	N80-16491*
ASME PAPER 80-GT-60	p0074	A80-42190*	DOE/NASA/0063-79/1	p0149	N80-19612*
ASME PAPER 80-GT-62	p0095	A80-42192*	DOE/NASA/0067-79/2	p0147	N80-10603*
ASME PAPER 80-GT-63	p0094	A80-42193*	DOE/NASA/0069-79/1	p0150	N80-22778*
ASME PAPER 80-GT-65	p0094	A80-42195*	DOE/NASA/0078-79/1	p0184	N80-18991*
ASME PAPER 80-GT-69	p0026	A80-42199*	DOE/NASA/0081-79/1	p0183	N80-17916*
ASME PAPER 80-GT-143	p0121	A80-42256*	DOE/NASA/0084-79/1	p0184	N80-18992*
ASME PAPER 80-GT-146	p0026	A80-42258*	DOE/NASA/0086-79/1	p0148	N80-16483*
ASME PAPER 80-GT-150	p0083	A80-42262*	DOE/NASA/0091-80/1	p0184	N80-26212*
ASME PAPER 80-GT-162	p0121	A80-42272*	DOE/NASA/0096-1	p0153	N80-28866*
ASME PAPER 80-GT-178	p0026	A80-42284*	DOE/NASA/0100-79/1	p0154	N80-29860*
ASME PAPER 80-HT-24	p0027	A80-46013*	DOE/NASA/0116-80/1	p0185	N80-32299*
ASME PAPER 80-HT-25	p0027	A80-46014*	DOE/NASA/0117-80/1	p0124	N80-25661*
ASNL-TR-154-13	p0038	N80-22323*	DOE/NASA/0124-1	p0185	N80-28255*
ASNL-TR-154-15	p0134	N80-29762*	DOE/NASA/0124-2	p0128	N80-31795*
ASTL-MR-154-1	p0134	N80-27720*	DOE/NASA/0124-3	p0128	N80-31796*
AVRADCOM-TR-79-28	p0087	N80-23453*	DOE/NASA/0130-80/1	p0103	N80-24550*
AVRADCOM-TR-79-33	p0077	N80-16143*	DOE/NASA/0134-1	p0156	N80-33862*
AVRADCOM-TR-79-34	p0104	N80-15361*	DOE/NASA/0161-2	p0142	N80-23769*
AVRADCOM-TR-79-42	p0015	N80-15128*	DOE/NASA/0161-4	p0155	N80-31882*
AVRADCOM-TR-79-46	p0115	N80-17466*	DOE/NASA/0161-79/3	p0150	N80-22758*
AVRADCOM-TR-80-C-2	p0116	N80-18406*	DOE/NASA/0600-79/1	p0148	N80-17548*
AVRADCOM-TR-80-C-3	p0116	N80-18409*	DOE/NASA/0612-80/1	p0124	N80-22700*
AVRADCOM-TR-80-C-4	p0115	N80-17469*	DOE/NASA/0794-80/1	p0141	N80-22777*
AVRADCOM-TR-80-C-5	p0117	N80-19498*	DOE/NASA/0806-79/1	p0148	N80-17547*
AVRADCOM-TR-80-C-6	p0116	N80-18407*	DOE/NASA/1002-80/5	p0142	N80-23777*
AVRADCOM-TR-80-C-7	p0086	N80-20398*	DOE/NASA/1010-79/5	p0139	N80-16494*
AVRADCOM-TR-80-C-10	p0088	N80-28524*	DOE/NASA/1010-80/6	p0140	N80-19614*
AVRADCOM-TR-80-C-14	p0118	N80-27696*	DOE/NASA/1011-31	p0183	N80-28254*
AVRADCOM-TR-80-C-15	p0020	N80-27365*	DOE/NASA/1011-32	p0183	N80-30229*
AVRADCOM-TR-80-8	p0117	N80-21754*	DOE/NASA/1011-80/4	p0117	N80-21754*
AVRADCOM-TR-80-09	p0023	N80-33410*	DOE/NASA/1028-80/26	p0140	N80-19613*
BCAC-D6-48915	p0124	N80-22700*	DOE/NASA/1034-8	p0143	N80-25779*
CEEDO-TR-79-03	p0028	N80-13048*	DOE/NASA/1034-79/6	p0138	N80-15560*
CONF-791232	p0141	N80-22788*	DOE/NASA/1034-80/7	p0140	N80-18563*
CONF-7904111	p0139	N80-16453*	DOE/NASA/1040-15	p0080	N80-32488*
COO-2749-40	p0124	N80-24621*	DOE/NASA/1040-16	p0144	N80-29863*
COO-2749-42	p0124	N80-24620*	DOE/NASA/1040-17	p0106	N80-29624*
COO-2749-43-VOL-2	p0128	N80-32719*	DOE/NASA/1040-79/9	p0115	N80-17467*
CW-NR-76-028.3	p0041	N80-27361*	DOE/NASA/1040-80/10	p0016	N80-20272*
CW-NR-77-008	p0030	N80-15103*	DOE/NASA/1040-80/11	p0183	N80-21201*
CW-NR-77-024	p0030	N80-15106*	DOE/NASA/1040-80/12	p0140	N80-18564*
DOC-80SDS4217	p0050	N80-25357*	DOE/NASA/1040-80/13	p0183	N80-21200*
DOE/JPL-1060-30-VOL-2	p0151	N80-24751*	DOE/NASA/1040-80/14	p0142	N80-23779*
DOE/NASA/0001-79/1	p0147	N80-12551*	DOE/NASA/1044-6	p0143	N80-25780*
DOE/NASA/0002-80/2	p0151	N80-24758*	DOE/NASA/1044-7	p0143	N80-24756*
DOE/NASA/0002-80/2	p0152	N80-26775*	DOE/NASA/1044-9	p0143	N80-27805*
DOE/NASA/0008-79/10	p0184	N80-25209*	DOE/NASA/1044-79/4	p0101	N80-13361*
DOE/NASA/0008-80/11	p0185	N80-30228*	DOE/NASA/1044-79/5	p0165	N80-16824*
DOE/NASA/0013-80/1	p0039	N80-23315*	DOE/NASA/1059-79/4	p0137	N80-13623*
DOE/NASA/0027-80/1	p0091	N80-31552*	DOE/NASA/1060-79/3	p0139	N80-16490*
DOE/NASA/0030-80/1	p0152	N80-25792*	DOE/NASA/1062-6	p0175	N80-33221*
DOE/NASA/0030-80/2	p0152	N80-25793*	DOE/NASA/1062-79/3	p0137	N80-13624*
DOE/NASA/0030-80/3-VOL-3	p0155	N80-31869*	DOE/NASA/1062-80/4	p0141	N80-19626*
DOE/NASA/0030-80/4	p0152	N80-25794*	DOE/NASA/1062-80/5	p0175	N80-22083*
DOE/NASA/0030-80/6	p0152	N80-25795*	DOE/NASA/2593-17	p0143	N80-27804*
DOE/NASA/0031-80-2	p0143	N80-28859*	DOE/NASA/2593-18	p0080	N80-33556*
DOE/NASA/0031-80/1	p0151	N80-24797*	DOE/NASA/2593-79/7	p0076	N80-10344*
DOE/NASA/0031-80/3-VOL-3	p0155	N80-31870*	DOE/NASA/2593-79/8	p0141	N80-22776*
DOE/NASA/0031-80/4-VOL-4	p0155	N80-33859*	DOE/NASA/2593-79/9	p0085	N80-13256*
DOE/NASA/0031-80/6	p0156	N80-33860*	DOE/NASA/2593-79/10	p0157	N80-13721*
DOE/NASA/0031-80/6-VOL-6-PT-1B	p0154	N80-30889*	DOE/NASA/2593-79/11	p0137	N80-14493*
DOE/NASA/0031-80/6-VOL-6-PT-2	p0155	N80-30890*	DOE/NASA/2593-79/12	p0076	N80-15235*
DOE/NASA/0031-80/6-VOL-6-PT-2	p0156	N80-33861*	DOE/NASA/2593-79/13	p0077	N80-18157*
DOE/NASA/0031-80/6-VOL-6-1A	p0154	N80-30888*	DOE/NASA/2593-80	p0078	N80-21492*
DOE/NASA/0032-79/4	p0183	N80-13989*	DOE/NASA/2593-80/15	p0141	N80-21837*
DOE/NASA/0038-80/2	p0154	N80-29857*	DOE/NASA/2674-11	p0143	N80-27799*
DOE/NASA/0039-79/1	p0149	N80-18562*	DOE/NASA/2674-12	p0144	N80-29862*
DOE/NASA/0043-2	p0091	N80-26448*	DOE/NASA/2674-79/7	p0137	N80-10595*
DOE/NASA/0048-79/1	p0184	N80-23216*	DOE/NASA/2674-79/8	p0175	N80-14922*
DOE/NASA/0051-79/1	p0149	N80-18559*	DOE/NASA/2674-80/9	p0142	N80-23780*
DOE/NASA/0052-79/1	p0152	N80-26779*	DOE/NASA/2674-80/10	p0142	N80-23778*
DOE/NASA/0054-79/1	p0090	N80-15263*	DOE/NASA/2749-79/1-VOL-1	p0124	N80-24620*
DOE/NASA/0056-79/1	p0150	N80-22787*	DOE/NASA/2749-79/2-VOL-2	p0128	N80-32719*
DOE/NASA/0058-79/1	p0150	N80-20864*	DOE/NASA/2749-79/3-VOL-3	p0124	N80-24621*
DOE/NASA/0058-79/2-VOL-1	p0150	N80-23775*	DOE/NASA/2749-79/4-VOL-4	p0123	N80-17470*
DOE/NASA/0058-79/2-VOL-2-APP	p0149	N80-18565*	DOE/NASA/3139-1	p0152	N80-26774*
DOE/NASA/0058-79/3	p0147	N80-11558*	DOE/NASA/3184-1	p0151	N80-24759*
DOE/NASA/0061-79/1	p0148	N80-16493*	DOE/NASA/3222-80/1	p0184	N80-21202*
			DOE/NASA/3277-1	p0153	N80-27803*
			DOE/NASA/5906-79/1	p0147	N80-15553*
			DOE/NASA/9416-80/2	p0151	N80-24748*
			DOE/NASA/20370-79/17	p0137	N80-10594*
			DOE/NASA/20370-79/19	p0130	N80-15422*
			DOE/NASA/20485-79/5	p0096	N80-13317*
			DOE/NASA/20485-79/6	p0138	N80-15561*
			DOE/NASA/23139-1	p0144	N80-32858*
			D180-25475-1	p0062	N80-16096*

REPORT/ACCESSION NUMBER INDEX

D180-25481-1-VOL-1	p0028	M80-13043**	E-266	p0136	M80-15538**
D180-25481-2-VOL-2	p0028	M80-13044**	E-267	p0076	M80-14234**
E-010	p0014	M80-14125**	E-268	p0002	M80-14051**
E-019	p0014	M80-14121**	E-269	p0137	M80-13624**
E-028	p0078	M80-21489**	E-270	p0119	M80-29734**
E-032	p0077	M80-16143**	E-271	p0067	M80-14196**
E-041	p0080	M80-32489**	E-272	p0014	M80-14126**
E-047	p0093	M80-21551**	E-273	p0175	M80-16885**
E-061	p0115	M80-17466**	E-274	p0137	M80-12552**
E-063	p0114	M80-15410**	E-275	p0056	M80-13163**
E-063	p0116	M80-19496**	E-276	p0112	M80-14375**
E-065	p0076	M80-11188**	E-277	p0165	M80-16824**
E-066	p0013	M80-11087**	E-279	p0002	M80-14050**
E-073	p0157	M80-14581**	E-282	p0167	M80-14843**
E-074	p0132	M80-22734**	E-283	p0096	M80-16232**
E-076	p0002	M80-17030**	E-284	p0132	M80-13513**
E-077	p0085	M80-18178**	E-285	p0138	M80-15560**
E-079	p0012	M80-10205**	E-286	p0086	M80-18183**
E-080	p0116	M80-18408**	E-289	p0120	M80-33749**
E-085	p0077	M80-16141**	E-291	p0056	M80-15204**
E-087	p0137	M80-10594**	E-292	p0077	M80-18157**
E-090	p0076	M80-10344**	E-293	p0077	M80-18156**
E-101	p0015	M80-15128**	E-294	p0167	M80-15876**
E-117	p0053	M80-16093**	E-296	p0085	M80-16165**
E-119	p0114	M80-13473**	E-297	p0138	M80-15554**
E-124	p0116	M80-19495**	E-298	p0138	M80-15555**
E-126	p0076	M80-15234**	E-299	p0178	M80-16914**
E-127	p0105	M80-17398**	E-300	p0138	M80-15556**
E-129	p0087	M80-22493**	E-301	p0138	M80-15557**
E-136	p0015	M80-17071**	E-302	p0138	M80-15558**
E-147	p0115	M80-17467**	E-303	p0138	M80-15561**
E-150	p0141	M80-22776**	E-305	p0053	M80-18095**
E-154	p0114	M80-14403**	E-307	p0053	M80-15200**
E-156	p0093	M80-13268**	E-308	p0077	M80-17199**
E-157	p0167	M80-18882**	E-309	p0020	M80-28352**
E-159	p0137	M80-10595**	E-310	p0017	M80-22327**
E-160	p0104	M80-13403**	E-312	p0141	M80-19626**
E-163	p0101	M80-13361**	E-313	p0110	M80-17422**
E-164	p0067	M80-11143**	E-315	p0019	M80-25338**
E-167	p0105	M80-17397**	E-316	p0019	M80-25337**
E-172	p0157	M80-27832**	E-317	p0101	M80-18302**
E-178	p0076	M80-11189**	E-319	p0068	M80-16102**
E-182	p0067	M80-11145**	E-320	p0015	M80-15134**
E-185	p0016	M80-21323**	E-321	p0110	M80-17423**
E-187	p0136	M80-20787**	E-322	p0139	M80-16494**
E-189	p0085	M80-14249**	E-324	p0104	M80-15364**
E-192	p0085	M80-13256**	E-325	p0104	M80-15365**
E-196	p0008	M80-15059**	E-327	p0077	M80-17200**
E-198	p0116	M80-18409**	E-328	p0086	M80-19263**
E-201	p0104	M80-11376**	E-329	p0086	M80-18181**
E-202	p0169	M80-23100**	E-330	p0056	M80-16097**
E-203	p0067	M80-11144**	E-331	p0068	M80-16107**
E-204	p0096	M80-13317**	E-332	p0114	M80-16342**
E-206	p0093	M80-18205**	E-333	p0016	M80-20272**
E-210	p0085	M80-13254**	E-335	p0016	M80-18043**
E-212	p0110	M80-14374**	E-337	p0105	M80-24577**
E-214	p0116	M80-18407**	E-338	p0140	M80-18563**
E-215	p0167	M80-13881**	E-339	p0056	M80-18098**
E-217	p0002	M80-11037**	E-340	p0110	M80-24595**
E-220	p0117	M80-21753**	E-342	p0115	M80-18403**
E-221	p0086	M80-21534**	E-343	p0056	M80-17138**
E-223	p0101	M80-11327**	E-344	p0116	M80-18405**
E-224	p0080	M80-33555**	E-345	p0068	M80-20313**
E-225	p0053	M80-16094**	E-346	p0175	M80-18946**
E-228	p0017	M80-21326**	E-349	p0115	M80-18404**
E-230	p0056	M80-13159**	E-350	p0116	M80-18406**
E-231	p0067	M80-13171**	E-351	p0016	M80-19110**
E-234	p0015	M80-15132**	E-353	p0117	M80-19497**
E-235	p0130	M80-15422**	E-354	p0110	M80-25635**
E-237	p0013	M80-13046**	E-355	p0115	M80-17469**
E-241	p0132	M80-27719**	E-356	p0068	M80-18106**
E-243	p0086	M80-21532**	E-357	p0183	M80-21201**
E-248	p0014	M80-13047**	E-359	p0157	M80-23875**
E-249	p0167	M80-12822**	E-360	p0068	M80-18107**
E-250	p0167	M80-12824**	E-361	p0136	M80-18497**
E-251	p0015	M80-15133**	E-362	p0140	M80-18564**
E-252	p0046	M80-29369**	E-363	p0086	M80-20398**
E-253	p0003	M80-27284**	E-364	p0140	M80-19614**
E-254	p0167	M80-12823**	E-365	p0140	M80-19613**
E-255	p0104	M80-13404**	E-366	p0117	M80-19498**
E-256	p0013	M80-12092**	E-367	p0078	M80-21493**
E-257	p0175	M80-14922**	E-370	p0117	M80-20591**
E-260	p0087	M80-22494**	E-371	p0051	M80-20304**
E-260	p0079	M80-26426**	E-372	p0023	M80-32396**
E-261	p0067	M80-12120**	E-377	p0017	M80-21333**
E-263	p0137	M80-14493**	E-379	p0052	M80-21412**
E-264	p0175	M80-12881**	E-381	p0110	M80-18368**
E-265	p0076	M80-15235**	E-382	p0105	M80-20532**
			E-383	p0142	M80-23777**

REPORT/ACCESSION NUMBER INDEX

E-384	p0163	N80-19863**	E-511-REV	p0023	N80-32394**
E-385	p0078	N80-20370**	E-512	p0144	N80-29863**
E-386	p0068	N80-20314**	E-513	p0170	N80-30154**
E-387	p0132	N80-23684**	E-514	p0175	N80-33221**
E-388	p0016	N80-20274**	E-516	p0144	N80-29862**
E-389	p0168	N80-22046**	E-517	p0164	N80-29088**
E-390	p0168	N80-22047**	E-518	p0069	N80-28444**
E-391	p0023	N80-33410**	E-519	p0022	N80-31399**
E-392	p0117	N80-22701**	E-520	p0094	N80-29502**
E-393	p0157	N80-21892**	E-521	p0069	N80-27429**
E-394	p0078	N80-21490**	E-524	p0022	N80-29333**
E-395	p0078	N80-21488**	E-526	p0119	N80-28716**
E-397	p0018	N80-22350**	E-527	p0088	N80-28524**
E-398	p0022	N80-29300**	E-531	p0023	N80-32395**
E-399	p0175	N80-22083**	E-532	p0080	N80-33556**
E-400	p0183	N80-21200**	E-534	p0106	N80-29624**
E-401	p0078	N80-21492**	E-539	p0022	N80-31400**
E-402	p0020	N80-27362**	E-541	p0106	N80-32689**
E-403	p0168	N80-22048**	E-544	p0183	N80-30229**
E-404	p0168	N80-22045**	E-550	p0069	N80-29433**
E-405	p0141	N80-21837**	E-554	p0120	N80-31797**
E-406	p0016	N80-20275**	E-555	p0120	N80-31798**
E-407	p0105	N80-21706**	E-562	p0079	N80-31527**
E-408	p0069	N80-21452**	E-565	p0163	N80-33104**
E-409	p0142	N80-23779**	E-566	p0097	N80-32610**
E-411	p0168	N80-23097**	E-576	p0132	N80-32753**
E-412	p0178	N80-23180**	E-581	p0053	N80-32428**
E-413	p0119	N80-29706**	E-600	p0079	N80-32486**
E-415	p0102	N80-22598**	E-9467	p0014	N80-14123**
E-416	p0018	N80-22349**	E-9468	p0014	N80-14124**
E-418	p0169	N80-23101**	E-9744	p0087	N80-27483**
E-419	p0002	N80-21285**	E-9810	p0162	N80-16742**
E-420	p0018	N80-23310**	E-9827	p0114	N80-16341**
E-422	p0079	N80-23430**	E-9906	p0015	N80-15127**
E-423	p0079	N80-22464**	E-9941	p0087	N80-23453**
E-424	p0169	N80-23102**	E-9963	p0132	N80-15428**
E-427	p0130	N80-22714**	E-9975	p0101	N80-21669**
E-428	p0141	N80-22788**	E-9996	p0085	N80-17220**
E-429	p0093	N80-23472**	EDR-9132	p0029	N80-14129**
E-431	p0087	N80-23456**	EDR-10085	p0123	N80-15411**
E-432	p0169	N80-26115**	EDR-10119-VOL-1	p0040	N80-25335**
E-433	p0093	N80-25454**	EMR-827053	p0148	N80-17543**
E-434	p0142	N80-23780**	ER-7989F	p0072	N80-12118**
E-435	p0019	N80-23314**	ERC-LIB-8060	p0128	N80-31795**
E-436	p0143	N80-27799**	ERC-LIB-79168	p0185	N80-28255**
E-437	p0132	N80-23678**	ERC-LIB-80121	p0128	N80-31796**
E-438	p0168	N80-23096**	ERR-FW-2014	p0005	N80-24263**
E-440	p0144	N80-32858**	ETI-1279	p0148	N80-16483**
E-441	p0057	N80-23365**	FAA-EE-79-05	p0008	N80-15059**
E-442	p0019	N80-24315**	FCR-1657	p0149	N80-19615**
E-443	p0019	N80-24314**	FR-79-9B7-SICOP-R1	p0072	N80-22407**
E-444	p0166	N80-24129**	FR-79-13/AS	p0090	N80-13257**
E-445	p0019	N80-24316**	FR-79-25/AS	p0091	N80-17221**
E-446	p0069	N80-23370**	FR-10056	p0150	N80-22775**
E-447	p0181	N80-24200**	FR-12087	p0036	N80-17073**
E-451	p0018	N80-23313**	GAC-TR-1681-09	p0149	N80-18562**
E-452	p0022	N80-31401**	GDC-ASP-80-013-VOL-2	p0048	N80-31423**
E-453	p0080	N80-32487**	GDC-ASP-80-015	p0153	N80-28862**
E-454	p0143	N80-25780**	GDC-ASP-80-015	p0154	N80-29845**
E-455	p0020	N80-27365**	GDC-CRAD-80-002	p0049	N80-27403**
E-457	p0143	N80-25779**	GDC-CRAD-80-003	p0062	N80-19185**
E-458	p0118	N80-27695**	GDC-CRAD-80-014	p0048	N80-32412**
E-459	p0143	N80-24756**	GE79ET0102	p0151	N80-24797**
E-460	p0160	N80-24583**	GE80ET010-VOL-2	p0143	N80-28859**
E-462	p0118	N80-27696**	GE80ET0103-VOL-4	p0155	N80-33859**
E-464	p0169	N80-25101**	GE80ET0104-VOL-3	p0155	N80-31870**
E-465	p0074	N80-24386**	GE80ET0105-VOL-6-PT-1	p0156	N80-33860**
E-466	p0020	N80-26299**	GE80ET0105-VOL-6-PT-1A	p0154	N80-30888**
E-467	p0130	N80-24634**	GE80ET0105-VOL-6-PT-1B	p0154	N80-30889**
E-469	p0058	N80-33465**	GE80ET0105-VOL-6-PT-2	p0155	N80-30890**
E-474	p0003	N80-33357**	GE80ET0105-VOL-6-PT-2	p0156	N80-33861**
E-482	p0130	N80-26682**	HI-79188	p0154	N80-29857**
E-483	p0143	N80-27804**	HSEB-7001	p0030	N80-15107**
E-485	p0093	N80-27509**	HSEB-7002	p0032	N80-15117**
E-486	p0080	N80-32488**			
E-488	p0118	N80-27697**			
E-490	p0088	N80-27484**			
E-491	p0169	N80-29132**			
E-492	p0094	N80-27510**			
E-493	p0105	N80-27632**			
E-497	p0118	N80-27698**			
E-500	p0020	N80-27363**			
E-502	p0183	N80-28254**			
E-504	p0143	N80-27805**			
E-506	p0023	N80-31402**			
E-507	p0118	N80-27699**			
E-508	p0119	N80-29735**			
E-510	p0057	N80-31449**			
E-511	p0022	N80-29332**			

REPORT/ACCESSION NUMBER INDEX

HSEB-7968	p0072	N80-25382**	NASA-CR-134840	p0031	N80-15113**
IFSM-80-102	p0073	N80-25383**	NASA-CR-134841	p0031	N80-15112**
IFSM-80-103	p0073	N80-25384**	NASA-CR-134842	p0031	N80-15111**
IITRI-M6001-82	pJ084	N80-25415**	NASA-CR-134846	p0044	N80-29298**
IITRI-M6003-53	p0037	N80-21330**	NASA-CR-134848	p0034	N80-15086**
IR-1	p0062	N80-27424**	NASA-CR-134849	p0033	N80-15083**
ITPR-1	p0123	N80-16338**	NASA-CR-134850	p0034	N80-15084**
JPL-PUB-78-15-VOL-10	p0147	N80-11566**	NASA-CR-134851	p0034	N80-15085**
JPL-PUB-79-112-VOL-1	p0149	N80-19632**	NASA-CR-134852	p0030	N80-15107**
JPL-PUB-79-112-VOL-2	p0151	N80-24751**	NASA-CR-134868	p0034	N80-15088**
JPL-PUB-80-35	p0154	N80-29860**	NASA-CR-134872	p0030	N80-15106**
LAPES-79-003	p0176	N80-12880**	NASA-CR-134873	p0030	N80-15101**
LG79ER0178-VOL-1	p0172	N80-11870**	NASA-CR-134873	p0030	N80-15101**
MDC-J7733	p0004	N80-10134**	NASA-CR-134873	p0030	N80-15101**
MED113	p0094	N80-19284**	NASA-CR-134873	p0030	N80-15101**
MTI-79ASE77RE2	p0183	N80-13989**	NASA-CR-134890	p0030	N80-15105**
MTI-79TR47	p0150	N80-22787**	NASA-CR-134891	p0030	N80-15102**
MTI-80TR29	p0134	N80-22733**	NASA-CR-134914	p0034	N80-15091**
MTR-3787-VOL-1	p0098	N80-12260**	NASA-CR-134915	p0034	N80-15089**
MTR-3787-VOL-2	p0098	N80-12261**	NASA-CR-134916	p0030	N80-15104**
MTR-3943	p0099	N80-24514**	NASA-CR-134920	p0034	N80-15090**
NAS-7845	p0148	N80-16491**	NASA-CR-135008	p0032	N80-15116**
NASA-CASE-LAR-11695-2	p0124	N80-18402**	NASA-CR-135009	p0031	N80-15109**
NASA-CASE-LEW-11930-3	p0070	N80-33482**	NASA-CR-135010	p0035	N80-15098**
NASA-CASE-LEW-12081-2	p0093	N80-20402**	NASA-CR-135046	p0031	N80-15108**
NASA-CASE-LEW-12119-1	p0119	N80-28711**	NASA-CR-135049	p0031	N80-15114**
NASA-CASE-LEW-12119-2	p0115	N80-18401**	NASA-CR-135075	p0034	N80-15100**
NASA-CASE-LEW-12131-2	p0118	N80-26658**	NASA-CR-135075	p0034	N80-15100**
NASA-CASE-LEW-12274-1	p0119	N80-31790**	NASA-CR-135118	p0044	N80-29299**
NASA-CASE-LEW-12277-3	p0101	N80-18300**	NASA-CR-135119	p0041	N80-27361**
NASA-CASE-LEW-12296-1	p0101	N80-19425**	NASA-CR-135140	p0032	N80-15117**
NASA-CASE-LEW-12363-4	p0140	N80-18555**	NASA-CR-135160	p0035	N80-15093**
NASA-CASE-LEW-12441-2	p0105	N80-24573**	NASA-CR-135168	p0035	N80-15099**
NASA-CASE-LEW-12542-3	p0079	N80-32484**	NASA-CR-135192	p0029	N80-14129**
NASA-CASE-LEW-12586-1	p0137	N80-14472**	NASA-CR-135249	p0035	N80-15096**
NASA-CASE-LEW-12723-1	p0135	N80-18690**	NASA-CR-135250	p0028	N80-14116**
NASA-CASE-LEW-12876-1	p0087	N80-26447**	NASA-CR-135251	p0035	N80-15097**
NASA-CASE-LEW-12918-1	p0144	N80-33857**	NASA-CR-135254	p0028	N80-14115**
NASA-CASE-LEW-12940-1	p0174	N80-33186**	NASA-CR-135266	p0033	N80-15122**
NASA-CASE-LEW-12955-1	p0161	N80-14684**	NASA-CR-135267	p0028	N80-14117**
NASA-CASE-LEW-12971-1	p0016	N80-18039**	NASA-CR-135268	p0028	N80-14118**
NASA-CASE-LEW-12989-1	p0114	N80-12414**	NASA-CR-135278	p0031	N80-15110**
NASA-CASE-LEW-12995-1	p0118	N80-26659**	NASA-CR-135279	p0029	N80-14119**
NASA-CASE-LEW-13027-1	p0087	N80-24437**	NASA-CR-135296	p0035	N80-15095**
NASA-CASE-LEW-13080-1	p0088	N80-29496**	NASA-CR-135323	p0033	N80-15125**
NASA-CASE-LEW-13088-1	p0067	N80-11142**	NASA-CR-135324	p0029	N80-14120**
NASA-CASE-LEW-13103-1	p0088	N80-32516**	NASA-CR-135325	p0033	N80-15126**
NASA-CASE-LEW-13148-1	p0101	N80-20487**	NASA-CR-135326	p0032	N80-15118**
NASA-CASE-LEW-13148-2	p0140	N80-18557**	NASA-CR-135337	p0035	N80-15092**
NASA-CASE-LEW-13169-1	p0076	N80-14232**	NASA-CR-135352	p0032	N80-15119**
NASA-CASE-LEW-13268-1	p0117	N80-24619**	NASA-CR-135354	p0032	N80-15115**
NASA-CASE-LEW-13343-1	p0069	N80-26389**	NASA-CR-135393	p0037	N80-21328**
NASA-CASE-MPO-12131-3	p0115	N80-18400**	NASA-CR-135410	p0037	N80-21329**
NASA-CASE-XLE-02062-1	p0056	N80-14188**	NASA-CR-135448	p0038	N80-22324**
NASA-CP-2077	p0015	N80-15127**	NASA-CR-159318	p0073	N80-29432**
NASA-CP-2092	p0012	N80-10205**	NASA-CR-159360	p0047	N80-32404**
NASA-CP-2106	p0139	N80-16453**	NASA-CR-159420	p0060	N80-11137**
NASA-CP-2125	p0141	N80-22788**	NASA-CR-159453	p0029	N80-14182**
NASA-CP-2126	p0017	N80-22327**	NASA-CR-159471	p0035	N80-15094**
NASA-CP-2133	p0119	N80-29706**	NASA-CR-159472	p0044	N80-29297**
NASA-CP-2144	p0057	N80-31443**	NASA-CR-159473	p0032	N80-15120**
NASA-CP-2146	p0022	N80-29300**	NASA-CR-159483	p0032	N80-15121**
NASA-CP-2154	p0058	N80-33465**	NASA-CR-159493	p0083	N80-13218**
NASA-CR-3218	p0108	N80-14356**	NASA-CR-159494	p0150	N80-20864**
NASA-CR-3260	p0037	N80-20271**	NASA-CR-159495	p0150	N80-23775**
NASA-CR-3261	p0038	N80-22326**	NASA-CR-159496	p0149	N80-18565**
NASA-CR-3288	p0005	N80-29251**	NASA-CR-159497	p0147	N80-11558**
NASA-CR-3291	p0005	N80-28302**	NASA-CR-159502	p0152	N80-26774**
NASA-CR-134669	p0030	N80-15103**	NASA-CR-159506	p0129	N80-32720**
NASA-CR-134838	p0033	N80-15123**	NASA-CR-159517	p0073	N80-29430**
NASA-CR-134839	p0033	N80-15124**	NASA-CR-159518	p0005	N80-27288**
NASA-CR-134840	p0033	N80-15124**	NASA-CR-159525	p0040	N80-25340**
NASA-CR-134841	p0033	N80-15124**	NASA-CR-159535	p0028	N80-13048**
NASA-CR-134842	p0033	N80-15124**	NASA-CR-159546	p0099	N80-22547**
NASA-CR-134846	p0033	N80-15124**	NASA-CR-159547	p0099	N80-22548**
NASA-CR-134848	p0033	N80-15124**	NASA-CR-159548	p0099	N80-22549**
NASA-CR-134849	p0033	N80-15124**	NASA-CR-159556	p0040	N80-25333**
NASA-CR-134850	p0033	N80-15124**	NASA-CR-159571	p0072	N80-25382**
NASA-CR-134851	p0033	N80-15124**	NASA-CR-159578	p0004	N80-10134**
NASA-CR-134852	p0033	N80-15124**	NASA-CR-159585	p0072	N80-10318**
NASA-CR-134868	p0033	N80-15124**	NASA-CR-159587	p0150	N80-22787**
NASA-CR-134872	p0033	N80-15124**	NASA-CR-159589	p0148	N80-16493**
NASA-CR-134873	p0033	N80-15124**	NASA-CR-159590	p0148	N80-16491**
NASA-CR-134873	p0033	N80-15124**	NASA-CR-159591	p0149	N80-19612**
NASA-CR-134890	p0033	N80-15124**	NASA-CR-159592	p0150	N80-22778**
NASA-CR-134891	p0033	N80-15124**	NASA-CR-159597	p0123	N80-13474**
NASA-CR-134914	p0033	N80-15124**	NASA-CR-159598	p0036	N80-16061**
NASA-CR-134915	p0033	N80-15124**	NASA-CR-159599	p0147	N80-12551**
NASA-CR-134916	p0033	N80-15124**	NASA-CR-159600	p0083	N80-14235**
NASA-CR-134920	p0033	N80-15124**	NASA-CR-159611	p0176	N80-12880**
NASA-CR-135008	p0033	N80-15124**	NASA-CR-159619	p0098	N80-18262**
NASA-CR-135009	p0033	N80-15124**			
NASA-CR-135010	p0033	N80-15124**			
NASA-CR-135046	p0033	N80-15124**			
NASA-CR-135049	p0033	N80-15124**			
NASA-CR-135075	p0033	N80-15124**			
NASA-CR-135075	p0033	N80-15124**			
NASA-CR-135118	p0033	N80-15124**			
NASA-CR-135119	p0033	N80-15124**			
NASA-CR-135140	p0033	N80-15124**			
NASA-CR-135160	p0033	N80-15124**			
NASA-CR-135168	p0033	N80-15124**			
NASA-CR-135192	p0033	N80-15124**			
NASA-CR-135249	p0033	N80-15124**			
NASA-CR-135250	p0033	N80-15124**			
NASA-CR-135251	p0033	N80-15124**			
NASA-CR-135254	p0033	N80-15124**			
NASA-CR-135266	p0033	N80-15124**			
NASA-CR-135267	p0033	N80-15124**			
NASA-CR-135268	p0033	N80-15124**			
NASA-CR-135278	p0033	N80-15124**			
NASA-CR-135279	p0033	N80-15124**			
NASA-CR-135296	p0033	N80-15124**			
NASA-CR-135323	p0033	N80-15124**			
NASA-CR-135324	p0033	N80-15124**			
NASA-CR-135325	p0033	N80-15124**			
NASA-CR-135326	p0033	N80-15124**			
NASA-CR-135337	p0033	N80-15124**			
NASA-CR-135352	p0033	N80-15124**			
NASA-CR-135354	p0033	N80-15124**			
NASA-CR-135393	p0033	N80-15124**			
NASA-CR-135410	p0033	N80-15124**			
NASA-CR-135448	p0033	N80-15124**			
NASA-CR-159318	p0033	N80-15124**			
NASA-CR-159360	p0033	N80-15124**			
NASA-CR-159420	p0033	N80-15124**			
NASA-CR-159453	p0033	N80-15124**			
NASA-CR-159471	p0033	N80-15124**			
NASA-CR-159472	p0033	N80-15124**			
NASA-CR-159473	p0033	N80-15124**			
NASA-CR-159483	p0033	N80-15124**			
NASA-CR-159493	p0033	N80-15124**			
NASA-CR-159494	p0033	N80-15124**			
NASA-CR-159495	p0033	N80-15124**			
NASA-CR-159496	p0033	N80-15124**			
NASA-CR-159497	p0033	N80-15124**			
NASA-CR-159502	p0033	N80-15124**			
NASA-CR-159506	p0033	N80-15124**			
NASA-CR-159517	p0033	N80-15124**			
NASA-CR-159518	p0033	N80-15124**			
NASA-CR-159525	p0033	N80-15124**			
NASA-CR-159535	p0033	N80-15124**			
NASA-CR-159546	p0033	N80-15124**			
NASA-CR-159547	p0033	N80-15124**			
NASA-CR-159548	p0033	N80-15124**			
NASA-CR-159556	p0033	N80-15124**			
NASA-CR-159571	p0033	N80-15124**			
NASA-CR-159578	p0033	N80-15124**			
NASA-CR-159585	p0033	N80-15124**			
NASA-CR-159587	p0033	N80-15124**			
NASA-CR-159589	p0033	N80-15124**			
NASA-CR-159590	p0033	N80-15124**			
NASA-CR-159591	p0033	N80-15124**			

REPORT/ACCESSION NUMBER INDEX

NASA-CR-159620	p0098	N80-18263**	NASA-CR-159757	p0029	N80-14130**
NASA-CR-159621	p0099	N80-18264**	NASA-CR-159758	p0037	N80-21331**
NASA-CR-159625-VOL-1	p0098	N80-11277**	NASA-CR-159759	p0152	N80-25792**
NASA-CR-159625-VOL-1A	p0098	N80-11278**	NASA-CR-159760	p0152	N80-25793**
NASA-CR-159631	p0183	N80-13989**	NASA-CR-159761	p0155	N80-31869**
NASA-CR-159633	p0149	N80-18559**	NASA-CR-159762	p0152	N80-25794**
NASA-CR-159634	p0152	N80-26779**	NASA-CR-159764	p0152	N80-25795**
NASA-CR-159636	p0004	N80-17995**	NASA-CR-159765	p0151	N80-24797**
NASA-CR-159639	p0029	N80-14127**	NASA-CR-159766	p0143	N80-28859**
NASA-CR-159640	p0005	N80-24263**	NASA-CR-159767	p0155	N80-31870**
NASA-CR-159645	p0038	N80-22323**	NASA-CR-159768	p0155	N80-33859**
NASA-CR-159650	p0184	N80-18991**	NASA-CR-159770-PT-1	p0156	N80-33860**
NASA-CR-159651	p0183	N80-17916**	NASA-CR-159770-PT-1-A	p0154	N80-30888**
NASA-CR-159658	p0062	N80-19185**	NASA-CR-159770-PT-1-B	p0154	N80-30889**
NASA-CR-159659	p0103	N80-13362**	NASA-CR-159770-PT-2	p0155	N80-30890**
NASA-CR-159660	p0147	N80-14480**	NASA-CR-159770-PT-2	p0156	N80-33861**
NASA-CR-159663	p0148	N80-17547**	NASA-CR-159771	p0184	N80-26212**
NASA-CR-159665	p0090	N80-13257**	NASA-CR-159774	p0038	N80-22325**
NASA-CR-159666	p0072	N80-12118**	NASA-CR-159775	p0148	N80-17548**
NASA-CR-159667	p0039	N80-23311**	NASA-CR-159776	p0103	N80-24550**
NASA-CR-159668	p0172	N80-13882**	NASA-CR-159777	p0108	N80-19450**
NASA-CR-159670	p0124	N80-24620**	NASA-CR-159778	p0050	N80-25357**
NASA-CR-159671	p0128	N80-32719**	NASA-CR-159779	p0148	N80-17543**
NASA-CR-159672	p0124	N80-24621**	NASA-CR-159781	p0158	N80-18588**
NASA-CR-159673	p0123	N80-17470**	NASA-CR-159782	p0112	N80-17425**
NASA-CR-159674	p0362	N80-15202**	NASA-CR-159784	p0061	N80-17137**
NASA-CR-159676	p0072	N80-10319**	NASA-CR-159785	p0091	N80-31552**
NASA-CR-159677	p0027	N80-12091**	NASA-CR-159786	p0041	N80-27364**
NASA-CR-159680	p0098	N80-11279**	NASA-CR-159787	p0151	N80-24759**
NASA-CR-159681	p0134	N80-10515**	NASA-CR-159788	p0044	N80-29331**
NASA-CR-159682	p0098	N80-12260**	NASA-CR-159789	p0153	N80-27808**
NASA-CR-159683	p0099	N80-24514**	NASA-CR-159790	p0061	N80-17141**
NASA-CR-159684	p0098	N80-12261**	NASA-CR-159792	p0184	N80-21202**
NASA-CR-159685	p0045	N80-33408**	NASA-CR-159796	p0036	N80-18040**
NASA-CR-159686	p0097	N80-10415**	NASA-CR-159797	p0096	N80-15300**
NASA-CR-159687	p0097	N80-10416**	NASA-CR-159798	p0037	N80-21330**
NASA-CR-159688	p0061	N80-13158**	NASA-CR-159801	p0038	N80-21332**
NASA-CR-159689	p0084	N80-26427**	NASA-CR-159802	p0084	N80-28499**
NASA-CR-159691	p0028	N80-13043**	NASA-CR-159803	p0124	N80-25661**
NASA-CR-159692	p0028	N80-13044**	NASA-CR-159805	p0062	N80-27424**
NASA-CR-159694	p0036	N80-17074**	NASA-CR-159806	p0039	N80-25332**
NASA-CR-159695	p0148	N80-16483**	NASA-CR-159807	p0149	N80-19615**
NASA-CR-159696	p0147	N80-15559**	NASA-CR-159810	p0049	N80-27403**
NASA-CR-159697	p0075	N80-12142**	NASA-CR-159811	p0153	N80-28860**
NASA-CR-159698	p0172	N80-11870**	NASA-CR-159812	p0039	N80-23312**
NASA-CR-159699	p0039	N80-23309**	NASA-CR-159813	p0062	N80-24362**
NASA-CR-159701	p0036	N80-18041**	NASA-CR-159814	p0177	N80-27189**
NASA-CR-159702	p0108	N80-10460**	NASA-CR-159816	p0038	N80-21334**
NASA-CR-159703	p0098	N80-12259**	NASA-CR-159817	p0066	N80-33478**
NASA-CR-159705	p0147	N80-10603**	NASA-CR-159820	p0124	N80-22700**
NASA-CR-159706	p0090	N80-15263**	NASA-CR-159821	p0125	N80-26662**
NASA-CR-159708	p0154	N80-29860**	NASA-CR-159822	p0124	N80-22702**
NASA-CR-159710	p0040	N80-26300**	NASA-CR-159828	p0150	N80-23768**
NASA-CR-159711	p0040	N80-26301**	NASA-CR-159830	p0039	N80-23316**
NASA-CR-159712	p0010	N80-16060**	NASA-CR-159831	p0040	N80-25335**
NASA-CR-159713	p0184	N80-25209**	NASA-CR-159832	p0040	N80-26302**
NASA-CR-159714	p0037	N80-19113**	NASA-CR-159833	p0150	N80-22775**
NASA-CR-159715-VOL-1	p0149	N80-19632**	NASA-CR-159834	p0154	N80-29845**
NASA-CR-159715-VOL-2	p0151	N80-24751**	NASA-CR-159835	p0153	N80-28862**
NASA-CR-159716	p0033	N80-15130**	NASA-CR-159838	p0185	N80-28255**
NASA-CR-159717	p0036	N80-16063**	NASA-CR-159839	p0134	N80-22733**
NASA-CR-159718	p0083	N80-15233**	NASA-CR-159842	p0151	N80-24748**
NASA-CR-159721	p0094	N80-19284**	NASA-CR-159845	p0084	N80-25415**
NASA-CR-159723	p0095	N80-22509**	NASA-CR-159846	p0185	N80-32299**
NASA-CR-159724	p0091	N80-17221**	NASA-CR-159847	p0010	N80-32378**
NASA-CR-159725	p0147	N80-15553**	NASA-CR-159848	p0108	N80-23599**
NASA-CR-159726	p0149	N80-18562**	NASA-CR-159849	p0091	N80-26448**
NASA-CR-159727	p0154	N80-29857**	NASA-CR-159850	p0177	N80-26161**
NASA-CR-159729	p0113	N80-14386**	NASA-CR-159852	p0095	N80-25453**
NASA-CR-159730	p0027	N80-10222**	NASA-CR-159854	p0039	N80-23315**
NASA-CR-159731	p0176	N80-14523**	NASA-CR-159856	p0185	N80-30228**
NASA-CR-159732	p0075	N80-13193**	NASA-CR-159857	p0153	N80-27803**
NASA-CR-159733	p0061	N80-13164**	NASA-CR-159860	p0151	N80-24742**
NASA-CR-159734	p0061	N80-13165**	NASA-CR-159864	p0073	N80-25384**
NASA-CR-159735	p0062	N80-16096**	NASA-CR-159870	p0005	N80-26274**
NASA-CR-159738	p0141	N80-22777**	NASA-CR-159871	p0153	N80-28866**
NASA-CR-159739	p0123	N80-15411**	NASA-CR-159874	p0073	N80-25383**
NASA-CR-159741	p0123	N80-16338**	NASA-CR-159877	p0154	N80-29852**
NASA-CR-159742	p0061	N80-14189**	NASA-CR-159878	p0134	N80-27720**
NASA-CR-159745	p0091	N80-15264**	NASA-CR-159879	p0134	N80-29762**
NASA-CR-159746	p0184	N80-18992**	NASA-CR-159882	p0142	N80-23769**
NASA-CR-159747	p0083	N80-18155**	NASA-CR-159886	p0044	N80-31398**
NASA-CR-159748	p0148	N80-18554**	NASA-CR-159888	p0128	N80-31795**
NASA-CR-159749	p0036	N80-16062**	NASA-CR-159890	p0128	N80-31796**
NASA-CR-159750	p0072	N80-22407**	NASA-CR-159892	p0095	N80-30535**
NASA-CR-159752	p0037	N80-18042**	NASA-CR-159894	p0155	N80-31882**
NASA-CR-159753	p0033	N80-15131**	NASA-CR-159896	p0147	N80-11566**
NASA-CR-159754	p0036	N80-17073**	NASA-CR-159898	p0103	N80-11328**
NASA-CR-159756	p0184	N80-23216**	NASA-CR-159900	p0084	N80-30482**

REPORT/ACCESSION NUMBER INDEX

NASA-CR-165125	p0112	N80-31777**	NASA-TM-81386	p0167	N80-15876**
NASA-CR-165131	p0177	N80-32223**	NASA-TM-81387	p0138	N80-15554**
NASA-CR-165133	p0172	N80-32186**	NASA-TM-81388	p0138	N80-15555**
NASA-CR-165136	p0006	N80-32328**	NASA-TM-81389	p0178	N80-16914**
NASA-CR-165137	p0005	N80-31351**	NASA-TM-81390	p0138	N80-15556**
NASA-CR-165138	p0128	N80-32718**	NASA-TM-81391	p0138	N80-15557**
NASA-CR-165150	p0048	N80-31423**	NASA-TM-81392	p0138	N80-15558**
NASA-CR-165151	p0048	N80-32412**	NASA-TM-81393	p0138	N80-15561**
NASA-CR-165153	p0108	N80-32688**	NASA-TM-81395	p0053	N80-18095**
NASA-CR-165156	p0156	N80-33862**	NASA-TM-81396	p0085	N80-16165**
NASA-CR-165164	p0064	N80-33476**	NASA-TM-81397	p0053	N80-15200**
				NASA-TM-81398	p0077	N80-16143**
NASA-TM-78257	p0083	N80-16142**	NASA-TM-81399	p0077	N80-17199**
NASA-TM-79166	p0008	N80-15059**	NASA-TM-81400	p0141	N80-19626**
NASA-TM-79199	p0115	N80-17469**	NASA-TM-81402	p0110	N80-17422**
NASA-TM-79202	p0137	N80-10594**	NASA-TM-81403	p0114	N80-16341**
NASA-TM-79205	p0076	N80-10344**	NASA-TM-81404	p0068	N80-16107**
NASA-TM-79224	p0114	N80-13473**	NASA-TM-81405	p0068	N80-16102**
NASA-TM-79238	p0114	N80-16340**	NASA-TM-81406	p0015	N80-15134**
NASA-TM-79242	p0115	N80-17467**	NASA-TM-81407	p0110	N80-17423**
NASA-TM-79243	p0141	N80-22776**	NASA-TM-81408	p0139	N80-16894**
NASA-TM-79248	p0096	N80-13317**	NASA-TM-81409	p0002	N80-15051**
NASA-TM-79249	p0137	N80-10595**	NASA-TM-81410	p0104	N80-15364**
NASA-TM-79250	p0104	N80-13403**	NASA-TM-81411	p0104	N80-15365**
NASA-TM-79252	p0101	N80-13361**	NASA-TM-81412	p0056	N80-16097**
NASA-TM-79253	p0067	N80-11143**	NASA-TM-81413	p0086	N80-19263**
NASA-TM-79263	p0076	N80-11189**	NASA-TM-81414	p0114	N80-16342**
NASA-TM-79268	p0136	N80-20787**	NASA-TM-81415	p0016	N80-20272**
NASA-TM-79270	p0101	N80-11327**	NASA-TM-81416	p0016	N80-18043**
NASA-TM-79272	p0085	N80-13256**	NASA-TM-81417	p0140	N80-18563**
NASA-TM-79274	p0104	N80-11376**	NASA-TM-81418	p0056	N80-18098**
NASA-TM-79275	p0137	N80-13623**	NASA-TM-81419	p0115	N80-18403**
NASA-TM-79276	p0067	N80-11144**	NASA-TM-81420	p0056	N80-17138**
NASA-TM-79277	p0085	N80-13254**	NASA-TM-81421	p0116	N80-18405**
NASA-TM-79278	p0110	N80-14374**	NASA-TM-81422	p0068	N80-20313**
NASA-TM-79279	p0167	N80-13881**	NASA-TM-81423	p0175	N80-18946**
NASA-TM-79280	p0002	N80-11037**	NASA-TM-81424	p0175	N80-16886**
NASA-TM-79281	p0067	N80-11145**	NASA-TM-81425	p0115	N80-18404**
NASA-TM-79282	p0086	N80-21534**	NASA-TM-81426	p0116	N80-18406**
NASA-TM-79285	p0093	N80-13268**	NASA-TM-81427	p0116	N80-19496**
NASA-TM-79286	p0053	N80-16094**	NASA-TM-81428	p0086	N80-18181**
NASA-TM-79287	p0056	N80-13159**	NASA-TM-81429	p0016	N80-19110**
NASA-TM-79288	p0067	N80-13171**	NASA-TM-81430	p0117	N80-19497**
NASA-TM-79289	p0182	N80-11950**	NASA-TM-81431	p0116	N80-18409**
NASA-TM-79290	p0015	N80-15132**	NASA-TM-81432	p0068	N80-18106**
NASA-TM-79291	p0130	N80-15422**	NASA-TM-81433	p0183	N80-21201**
NASA-TM-79293	p0013	N80-13046**	NASA-TM-81435	p0157	N80-23875**
NASA-TM-79294	p0118	N80-27695**	NASA-TM-81436	p0068	N80-18107**
NASA-TM-79296	p0157	N80-13721**	NASA-TM-81437	p0077	N80-17200**
NASA-TM-79297	p0014	N80-13047**	NASA-TM-81438	p0136	N80-18497**
NASA-TM-79298	p0167	N80-12822**	NASA-TM-81439	p0105	N80-20532**
NASA-TM-79299	p0053	N80-16093**	NASA-TM-81440	p0093	N80-18205**
NASA-TM-79300	p0167	N80-12824**	NASA-TM-81441	p0101	N80-18302**
NASA-TM-79301	p0015	N80-15133**	NASA-TM-81442	p0140	N80-18564**
NASA-TM-79302	p0167	N80-12823**	NASA-TM-81443	p0086	N80-20398**
NASA-TM-79303	p0104	N80-13404**	NASA-TM-81444	p0140	N80-19614**
NASA-TM-79304	p0013	N80-12092**	NASA-TM-81445	p0140	N80-19613**
NASA-TM-79305	p0175	N80-14922**	NASA-TM-81446	p0117	N80-19498**
NASA-TM-79306	p0067	N80-12120**	NASA-TM-81447	p0116	N80-18407**
NASA-TM-79307	p0137	N80-14493**	NASA-TM-81448	p0078	N80-21493**
NASA-TM-79308	p0175	N80-12881**	NASA-TM-81449	p0117	N80-20591**
NASA-TM-79309	p0076	N80-15235**	NASA-TM-81450	p0051	N80-20304**
NASA-TM-79310	p0136	N80-15538**	NASA-TM-81451	p0017	N80-21333**
NASA-TM-79311	p0076	N80-14234**	NASA-TM-81452	p0052	N80-21412**
NASA-TM-79312	p0002	N80-14051**	NASA-TM-81453	p0163	N80-19863**
NASA-TM-79313	p0137	N80-13624**	NASA-TM-81454	p0110	N80-18368**
NASA-TM-79314	p0067	N80-14196**	NASA-TM-81455	p0078	N80-20370**
NASA-TM-79315	p0014	N80-14126**	NASA-TM-81456	p0068	N80-20314**
NASA-TM-79316	p0085	N80-14249**	NASA-TM-81457	p0117	N80-21754**
NASA-TM-79317	p0175	N80-16885**	NASA-TM-81458	p0078	N80-21489**
NASA-TM-79318	p0137	N80-12552**	NASA-TM-81459	p0016	N80-20274**
NASA-TM-79319	p0056	N80-13163**	NASA-TM-81460	p0168	N80-22046**
NASA-TM-79320	p0112	N80-14375**	NASA-TM-81461	p0168	N80-22047**
NASA-TM-79321	p0165	N80-16824**	NASA-TM-81462	p0157	N80-21892**
NASA-TM-79322	p0139	N80-16450**	NASA-TM-81463	p0116	N80-18408**
NASA-TM-79323	p0002	N80-14050**	NASA-TM-81464	p0142	N80-23777**
NASA-TM-80189	p0011	N80-14110**	NASA-TM-81465	p0078	N80-21490**
NASA-TM-80214	p0069	N80-29431**	NASA-TM-81466	p0078	N80-21488**
NASA-TM-80980	p0079	N80-26433**	NASA-TM-81467	p0018	N80-22350**
NASA-TM-81154	p0028	N80-13041**	NASA-TM-81468	p0175	N80-22083**
NASA-TM-81376	p0015	N80-14128**	NASA-TM-81469	p0078	N80-21492**
NASA-TM-81377	p0167	N80-14843**	NASA-TM-81470	p0168	N80-22048**
NASA-TM-81378	p0096	N80-16232**	NASA-TM-81471	p0168	N80-22045**
NASA-TM-81379	p0132	N80-13513**	NASA-TM-81472	p0141	N80-21837**
NASA-TM-81380	p0138	N80-15560**	NASA-TM-81473	p0105	N80-21706**
NASA-TM-81381	p0086	N80-18183**	NASA-TM-81474	p0069	N80-21452**
NASA-TM-81383	p0056	N80-15204**	NASA-TM-81475	p0142	N80-23779**
NASA-TM-81384	p0077	N80-18157**	NASA-TM-81477	p0168	N80-23097**
NASA-TM-81385	p0077	N80-18156**	NASA-TM-81478	p0178	N80-23180**

REPORT/ACCESSION NUMBER INDEX

NASA-CR-165125	p0112	N80-31777**	NASA-TM-81386	p0167	N80-15876**
NASA-CR-165131	p0177	N80-32223**	NASA-TM-81387	p0138	N80-15554**
NASA-CR-165133	p0172	N80-32186**	NASA-TM-81388	p0138	N80-15555**
NASA-CR-165136	p0006	N80-32328**	NASA-TM-81389	p0178	N80-16914**
NASA-CR-165137	p0005	N80-31351**	NASA-TM-81390	p0138	N80-15556**
NASA-CR-165138	p0128	N80-32718**	NASA-TM-81391	p0138	N80-15557**
NASA-CR-165150	p0048	N80-31423**	NASA-TM-81392	p0138	N80-15558**
NASA-CR-165151	p0048	N80-32412**	NASA-TM-81393	p0138	N80-15561**
NASA-CR-165153	p0108	N80-32688**	NASA-TM-81395	p0053	N80-18095**
NASA-CR-165156	p0156	N80-33862**	NASA-TM-81396	p0085	N80-16165**
NASA-CR-165164	p0064	N80-33476**	NASA-TM-81397	p0053	N80-15200**
				NASA-TM-81398	p0077	N80-16143**
NASA-TM-78257	p0083	N80-16142**	NASA-TM-81399	p0077	N80-17199**
NASA-TM-79166	p0008	N80-15059**	NASA-TM-81400	p0141	N80-19626**
NASA-TM-79199	p0115	N80-17469**	NASA-TM-81402	p0110	N80-17422**
NASA-TM-79202	p0137	N80-10594**	NASA-TM-81403	p0114	N80-16341**
NASA-TM-79205	p0076	N80-10344**	NASA-TM-81404	p0068	N80-16107**
NASA-TM-79224	p0114	N80-13473**	NASA-TM-81405	p0068	N80-16102**
NASA-TM-79238	p0114	N80-16340**	NASA-TM-81406	p0015	N80-15134**
NASA-TM-79242	p0115	N80-17467**	NASA-TM-81407	p0110	N80-17423**
NASA-TM-79243	p0141	N80-22776**	NASA-TM-81408	p0139	N80-16494**
NASA-TM-79248	p0096	N80-13317**	NASA-TM-81409	p0002	N80-15051**
NASA-TM-79249	p0137	N80-10595**	NASA-TM-81410	p0104	N80-15364**
NASA-TM-79250	p0104	N80-13403**	NASA-TM-81411	p0104	N80-15365**
NASA-TM-79252	p0101	N80-13361**	NASA-TM-81412	p0056	N80-16097**
NASA-TM-79253	p0067	N80-11143**	NASA-TM-81413	p0086	N80-19263**
NASA-TM-79263	p0076	N80-11189**	NASA-TM-81414	p0114	N80-16342**
NASA-TM-79268	p0136	N80-20787**	NASA-TM-81415	p0016	N80-20272**
NASA-TM-79270	p0101	N80-11327**	NASA-TM-81416	p0016	N80-18043**
NASA-TM-79272	p0085	N80-13256**	NASA-TM-81417	p0140	N80-18563**
NASA-TM-79274	p0104	N80-11376**	NASA-TM-81418	p0056	N80-18098**
NASA-TM-79275	p0137	N80-13623**	NASA-TM-81419	p0115	N80-18403**
NASA-TM-79276	p0067	N80-11144**	NASA-TM-81420	p0056	N80-17138**
NASA-TM-79277	p0085	N80-13254**	NASA-TM-81421	p0116	N80-18405**
NASA-TM-79278	p0110	N80-14374**	NASA-TM-81422	p0068	N80-20313**
NASA-TM-79279	p0167	N80-13881**	NASA-TM-81423	p0175	N80-18946**
NASA-TM-79280	p0002	N80-11037**	NASA-TM-81424	p0175	N80-16886**
NASA-TM-79281	p0067	N80-11145**	NASA-TM-81425	p0115	N80-18404**
NASA-TM-79282	p0086	N80-21534**	NASA-TM-81426	p0116	N80-18406**
NASA-TM-79285	p0093	N80-13268**	NASA-TM-81427	p0116	N80-19496**
NASA-TM-79286	p0053	N80-16094**	NASA-TM-81428	p0086	N80-18181**
NASA-TM-79287	p0056	N80-13159**	NASA-TM-81429	p0016	N80-19110**
NASA-TM-79288	p0067	N80-13171**	NASA-TM-81430	p0117	N80-19497**
NASA-TM-79289	p0182	N80-11950**	NASA-TM-81431	p0116	N80-18409**
NASA-TM-79290	p0015	N80-15132**	NASA-TM-81432	p0068	N80-18106**
NASA-TM-79291	p0130	N80-15422**	NASA-TM-81433	p0183	N80-21201**
NASA-TM-79293	p0013	N80-13046**	NASA-TM-81435	p0157	N80-23875**
NASA-TM-79294	p0118	N80-27695**	NASA-TM-81436	p0068	N80-18107**
NASA-TM-79296	p0157	N80-13721**	NASA-TM-81437	p0077	N80-17200**
NASA-TM-79297	p0014	N80-13047**	NASA-TM-81438	p0136	N80-18497**
NASA-TM-79298	p0167	N80-12822**	NASA-TM-81439	p0105	N80-20532**
NASA-TM-79299	p0053	N80-16093**	NASA-TM-81440	p0093	N80-18205**
NASA-TM-79300	p0167	N80-12824**	NASA-TM-81441	p0101	N80-18302**
NASA-TM-79301	p0015	N80-15133**	NASA-TM-81442	p0140	N80-18564**
NASA-TM-79302	p0167	N80-12823**	NASA-TM-81443	p0086	N80-20398**
NASA-TM-79303	p0104	N80-13404**	NASA-TM-81444	p0140	N80-19614**
NASA-TM-79304	p0013	N80-12092**	NASA-TM-81445	p0140	N80-19613**
NASA-TM-79305	p0175	N80-14922**	NASA-TM-81446	p0117	N80-19498**
NASA-TM-79306	p0067	N80-12120**	NASA-TM-81447	p0116	N80-18407**
NASA-TM-79307	p0137	N80-14493**	NASA-TM-81448	p0078	N80-21493**
NASA-TM-79308	p0175	N80-12881**	NASA-TM-81449	p0117	N80-20591**
NASA-TM-79309	p0076	N80-15235**	NASA-TM-81450	p0051	N80-20304**
NASA-TM-79310	p0136	N80-15538**	NASA-TM-81451	p0017	N80-21333**
NASA-TM-79311	p0076	N80-14234**	NASA-TM-81452	p0052	N80-21412**
NASA-TM-79312	p0002	N80-14051**	NASA-TM-81453	p0163	N80-19863**
NASA-TM-79313	p0137	N80-13624**	NASA-TM-81454	p0110	N80-18368**
NASA-TM-79314	p0067	N80-14196**	NASA-TM-81455	p0078	N80-20370**
NASA-TM-79315	p0014	N80-14126**	NASA-TM-81456	p0068	N80-20314**
NASA-TM-79316	p0085	N80-14249**	NASA-TM-81457	p0117	N80-21754**
NASA-TM-79317	p0175	N80-16885**	NASA-TM-81458	p0078	N80-21489**
NASA-TM-79318	p0137	N80-12552**	NASA-TM-81459	p0016	N80-20274**
NASA-TM-79319	p0056	N80-13163**	NASA-TM-81460	p0168	N80-22046**
NASA-TM-79320	p0112	N80-14375**	NASA-TM-81461	p0168	N80-22047**
NASA-TM-79321	p0165	N80-16824**	NASA-TM-81462	p0157	N80-21892**
NASA-TM-79322	p0139	N80-16490**	NASA-TM-81463	p0116	N80-18408**
NASA-TM-79323	p0002	N80-14050**	NASA-TM-81464	p0142	N80-23777**
NASA-TM-80189	p0011	N80-14110**	NASA-TM-81465	p0078	N80-21490**
NASA-TM-80214	p0069	N80-29431**	NASA-TM-81466	p0078	N80-21488**
NASA-TM-80980	p0079	N80-26433**	NASA-TM-81467	p0018	N80-22350**
NASA-TM-81154	p0028	N80-13041**	NASA-TM-81468	p0175	N80-22083**
NASA-TM-81376	p0015	N80-14128**	NASA-TM-81469	p0078	N80-21492**
NASA-TM-81377	p0167	N80-14843**	NASA-TM-81470	p0168	N80-22048**
NASA-TM-81378	p0096	N80-16232**	NASA-TM-81471	p0168	N80-22045**
NASA-TM-81379	p0132	N80-13513**	NASA-TM-81472	p0141	N80-21837**
NASA-TM-81380	p0138	N80-15560**	NASA-TM-81473	p0105	N80-21706**
NASA-TM-81381	p0086	N80-18183**	NASA-TM-81474	p0069	N80-21452**
NASA-TM-81383	p0056	N80-15204**	NASA-TM-81475	p0142	N80-23779**
NASA-TM-81384	p0077	N80-18157**	NASA-TM-81477	p0168	N80-23097**
NASA-TM-81385	p0077	N80-18156**	NASA-TM-81478	p0178	N80-23180**

REPORT/ACCESSION NUMBER INDEX

PWA-5630-11 p0027 N80-10222**

QR-1 p0150 N80-23768**

QR-2 p0142 N80-23769**

QR-3 p0147 N80-10603**

QR-3 p0155 N80-31882**

R-1575 p0140 N80-17548**

RDR-1831-43 p0038 N80-22325**

REPT-80-9E6-MARE-R1 p0150 N80-23768**

REPT-80-9E6-MARE-R3 p0155 N80-31882**

REPT-80-16762 p0124 N80-25661**

REPT-80TR63 p0128 N80-32718**

REPT-756 p0037 N80-20271**

RI/RD79-217 p0062 N80-15202**

RI/RD79-310 p0061 N80-17141**

RI/RD79-322 p0125 N80-26662**

R35-40 p0156 N80-33862**

R74AEG479-VOL-1 p0033 N80-15123**

R74AEG479-VOL-2 p0033 N80-15124**

R75AEG213 p0031 N80-15111**

R75AEG252-VOL-1 p0033 N80-15083**

R75AEG252-VOL-2 p0034 N80-15084**

R75AEG252-VOL-3 p0034 N80-15085**

R75AEG278 p0031 N80-15113**

R75AEG349 p0034 N80-15088**

R75AEG368 p0030 N80-15102**

R75AEG381 p0031 N80-15112**

R75AEG411 p0044 N80-29298**

R75AEG443 p0034 N80-15086**

R75AEG444 p0034 N80-15091**

R75AEG449 p0030 N80-15104**

R75AEG483 p0034 N80-15090**

R75AEG484 p0031 N80-15109**

R75AEG504 p0038 N80-14115**

R75AEG511 p0035 N80-15093**

R76AEG195 p0038 N80-14117**

R76AEG218 p0031 N80-15114**

R76AEG222 p0032 N80-15116**

R76AEG228 p0028 N80-14118**

R76AEG233 p0035 N80-15098**

R76AEG379-1 p0033 N80-15122**

R76AEG420 p0034 N80-15100**

R76AEG420 p0034 N80-15100**

R77AEG177 p0031 N80-15108**

R77AEG212-VOL-3 p0035 N80-15097**

R77AEG229-VOL-2 p0044 N80-29299**

R77AEG300 p0035 N80-15099**

R77AEG305 p0035 N80-15095**

R77AEG327 p0030 N80-15101**

R77AEG327 p0030 N80-15101**

R77AEG394 p0032 N80-15115**

R77AEG439 p0031 N80-15110**

R77AEG473-VOL-1 p0033 N80-15125**

R77AEG474-VOL-2 p0029 N80-14120**

R77AEG475-VOL-3 p0033 N80-15126**

R77AEG476-VOL-4 p0032 N80-15118**

R77AEG588 p0032 N80-15119**

R77AEG664 p0035 N80-15092**

R77AEG2121-VOL-1 p0035 N80-15096**

R77AEG2122-VOL-2 p0028 N80-14116**

R78AEG206 p0029 N80-14119**

R78AEG444 p0037 N80-21328**

R78AEG573-VOL-1 p0035 N80-15094**

R78AEG574-VOL-2 p0044 N80-29297**

R79-914364-12 p0072 N80-10319**

R79-914387-4 p0083 N80-18155**

R79AEG247 p0036 N80-16061**

R79AEG366 p0029 N80-14127**

R79AEG395 p0036 N80-16062**

R79AEG397 p0032 N80-15121**

R79AEG413 p0039 N80-23309**

R79AEG416-VOL-1 p0084 N80-28499**

R79AEG478 p0032 N80-15120**

R79AEG562 p0045 N80-33408**

R79AEG625 p0123 N80-13474**

R80-1 p0006 N80-32328**

R80-914545-16 p0005 N80-31351**

R80-914617-1 p0095 N80-30535**

R80-924624-11 p0112 N80-31777**

R80AEG218 p0041 N80-27364**

R80AEG374 p0039 N80-23316**

SAR-2 p0083 N80-15233**

SAR-3 p0084 N80-26427**

SAR-4 p0033 N80-15131**

SAR-6 p0033 N80-15130**

SETEC-HME-79-61 p0083 N80-15233**

SR79-M-4702-05 p0091 N80-10042**

SR79-R-4482-43 p0038 N80-22325**

TR-2-30320/OR-52360 p0037 N80-18042**

TRW-ER-8064 p0044 N80-31398**

TRW-ER-8101 p0044 N80-29331**

TRW-31782-6082-RU-00 p0091 N80-15264**

TRW-33572-6001-RU-00 p0103 N80-13362**

TRW-34129-6001-UT-00 p0108 N80-32688**

TSC10082-FR p0184 N80-23216**

US-PATENT-APPL-SM-007083 p0079 N80-32484**

US-PATENT-APPL-SM-061555 p0140 N80-18557**

US-PATENT-APPL-SM-079914 p0140 N80-18555**

US-PATENT-APPL-SM-089779 p0067 N80-11142**

US-PATENT-APPL-SM-092145 p0114 N80-12414**

US-PATENT-APPL-SM-096255 p0115 N80-18400**

US-PATENT-APPL-SM-102003 p0076 N80-14232**

US-PATENT-APPL-SM-102004 p0115 N80-18401**

US-PATENT-APPL-SM-103836 p0124 N80-18402**

US-PATENT-APPL-SM-106190 p0101 N80-18300**

US-PATENT-APPL-SM-122966 p0101 N80-19425**

US-PATENT-APPL-SM-134855 p0144 N80-33857**

US-PATENT-APPL-SM-145209 p0117 N80-24619**

US-PATENT-APPL-SM-157150 p0118 N80-26659**

US-PATENT-APPL-SM-161253 p0087 N80-26447**

US-PATENT-APPL-SM-161254 p0069 N80-26389**

US-PATENT-APPL-SM-173521 p0088 N80-29496**

US-PATENT-APPL-SM-513611 p0070 N80-33482**

US-PATENT-APPL-SM-545793 p0056 N80-14188**

US-PATENT-APPL-SM-559846 p0105 N80-24573**

US-PATENT-APPL-SM-616528 p0070 N80-33482**

US-PATENT-APPL-SM-672219 p0119 N80-28711**

US-PATENT-APPL-SM-676432 p0093 N80-20402**

US-PATENT-APPL-SM-764245 p0070 N80-33482**

US-PATENT-APPL-SM-801290 p0118 N80-26658**

US-PATENT-APPL-SM-803822 p0079 N80-32484**

US-PATENT-APPL-SM-829317 p0135 N80-18690**

US-PATENT-APPL-SM-829318 p0161 N80-14684**

US-PATENT-APPL-SM-837794 p0093 N80-20402**

US-PATENT-APPL-SM-856462 p0105 N80-24573**

US-PATENT-APPL-SM-858936 p0016 N80-18039**

US-PATENT-APPL-SM-916655 p0137 N80-14472**

US-PATENT-APPL-SM-931090 p0118 N80-26658**

US-PATENT-APPL-SM-950876 p0119 N80-31790**

US-PATENT-APPL-SM-953391 p0174 N80-33186**

US-PATENT-APPL-SM-958575 p0087 N80-24437**

US-PATENT-APPL-SM-964754 p0101 N80-20487**

US-PATENT-APPL-SM-971596 p0088 N80-32516**

US-PATENT-CLASS-60-39.03 p0016 N80-18039**

US-PATENT-CLASS-60-39.27 p0016 N80-18039**

US-PATENT-CLASS-60-203 p0056 N80-14188**

US-PATENT-CLASS-60-240 p0016 N80-18039**

US-PATENT-CLASS-60-259 p0056 N80-14188**

US-PATENT-CLASS-60-267 p0105 N80-24573**

US-PATENT-CLASS-60-520 p0119 N80-31790**

US-PATENT-CLASS-75-124 p0079 N80-32484**

US-PATENT-CLASS-75-200 p0070 N80-33482**

US-PATENT-CLASS-75-222 p0070 N80-33482**

US-PATENT-CLASS-128-276 p0161 N80-14684**

US-PATENT-CLASS-128-276 p0135 N80-18690**

US-PATENT-CLASS-128-760 p0135 N80-18690**

US-PATENT-CLASS-149-1 p0093 N80-20402**

US-PATENT-CLASS-156-272 p0088 N80-32516**

US-PATENT-CLASS-156-292 p0088 N80-32516**

US-PATENT-CLASS-204-159.11 p0088 N80-32516**

US-PATENT-CLASS-204-159.14 p0088 N80-32516**

US-PATENT-CLASS-239-127.1 p0105 N80-24573**

US-PATENT-CLASS-264-22 p0088 N80-32516**

US-PATENT-CLASS-264-212 p0088 N80-32516**

US-PATENT-CLASS-277-153 p0119 N80-28711**

US-PATENT-CLASS-277-193 p0119 N80-28711**

US-PATENT-CLASS-277-224 p0119 N80-28711**

US-PATENT-CLASS-307-63 p0137 N80-14472**

US-PATENT-CLASS-307-66 p0137 N80-14472**

US-PATENT-CLASS-313-231.4 p0174 N80-33186**

US-PATENT-CLASS-313-362 p0174 N80-33186**

US-PATENT-CLASS-323-15 p0137 N80-14472**

US-PATENT-CLASS-323-19 p0137 N80-14472**

US-PATENT-CLASS-415-174 p0118 N80-26658**

REPORT/ACCESSION NUMBER INDEX

US-PATENT-CLASS-415-196	p0118	N80-26658*
US-PATENT-CLASS-417-383	p0119	N80-31790*
US-PATENT-CLASS-423-648R	p0093	N80-20402*
US-PATENT-CLASS-427-38	p0087	N80-24437*
US-PATENT-CLASS-427-40	p0087	N80-24437*
US-PATENT-CLASS-427-44	p0088	N80-32516*
US-PATENT-CLASS-427-164	p0087	N80-24437*
US-PATENT-CLASS-428-421	p0087	N80-24437*
US-PATENT-CLASS-428-474	p0087	N80-24437*
US-PATENT-CLASS-428-500	p0088	N80-32516*
US-PATENT-CLASS-429-101	p0101	N80-20487*
US-PATENT-CLASS-429-105	p0101	N80-20487*
US-PATENT-CLASS-429-107	p0101	N80-20487*
US-PATENT-CLASS-429-109	p0101	N80-20487*
US-PATENT-CLASS-429-139	p0088	N80-32516*
US-PATENT-4,135,851	p0118	N80-26658*
US-PATENT-4,157,718	p0161	N80-14684*
US-PATENT-4,171,615	p0056	N80-14188*
US-PATENT-4,175,249	p0137	N80-14472*
US-PATENT-4,184,327	p0016	N80-18039*
US-PATENT-4,184,491	p0135	N80-18690*
US-PATENT-4,192,910	p0101	N80-20487*
US-PATENT-4,193,827	p0093	N80-20402*
US-PATENT-4,199,650	p0087	N80-24437*
US-PATENT-4,199,937	p0105	N80-24573*
US-PATENT-4,207,024	p0118	N80-26658*
US-PATENT-4,212,477	p0119	N80-28711*
US-PATENT-4,214,902	p0079	N80-32484*
US-PATENT-4,214,905	p0070	N80-33482*
US-PATENT-4,215,548	p0119	N60-31790*
US-PATENT-4,218,280	p0088	N80-32516*
US-PATENT-4,218,633	p0174	N80-33186*
UTC-PCR-1333-VOL-1	p0152	N80-25792*
UTC-PCR-1333-VOL-2	p0152	N80-25793*
UTC-PCR-1333-VOL-3	p0155	N80-31869*
UTC-PCR-1333-VOL-4	p0152	N80-25794*
UTC-PCR-1333-VOL-6	p0152	N80-25795*
UTRC/B80-914607-12	p0095	N80-25453*
WDL-TR8457	p0098	N80-11279*
WDL-TR8457-VOL-1	p0098	N80-11277*
WDL-TR8457-VOL-1A	p0098	N80-11278*
WER-10	p0153	N80-27803*
WMB/A-4500-131-3-R1	p0184	N80-18991*
WMB/A-4500-131-4-R2	p0184	N80-18992*
WRC-78-182	p0039	N80-23315*
XEOS-2372	p0062	N80-27424*